

LEARNING TO SWIM: AN EXPLORATION OF THE TERRESTRIAL TO AQUATIC
TRANSITION IN ELAPIDS (SQUAMATA: ELAPIDAE)

By

JUSTIN LAWRENCE JACOBS

DISSERTATION

Submitted in partial fulfillment of the requirements for the degree of Doctor of Philosophy at
The University of Texas at Arlington

December 2021

Arlington, Texas

Supervising Committee

Eric N. Smith, Supervising Professor

Todd A. Castoe

Luke O. Frishkoff

Matthew K. Fujita

Matthew P. Loocke

ABSTRACT

LEARNING TO SWIM: AN EXPLORATION OF THE TERRESTRIAL TO AQUATIC TRANSITION IN ELAPIDS (SQUAMATA: ELAPIDAE)

Justin Lawrence Jacobs

The University of Texas at Arlington, 2021

Supervising Professor: Eric N. Smith

Elapidae is an extremely diverse family of venomous snake that have a nearly global distribution. To conquer such wide swaths of territory the initially fossorial snakes evolved many successful strategies pertaining to reproduction, locomotion, and predation techniques. Here I explore the multiple transitions of terrestrial to aquatic life through a high-density 3D geometric morphometric methodology conducted upon five large datasets of computed tomography (CT) data. This occurs primarily through the comparison of the genus of New World coralsnakes, *Micrurus*, with sea snakes of *Hydrophis* and *Laticauda* and is informed by a scale created to document and classify the disparate life history of elapids. My dissertation elucidates the morphological characters that are associated with an aquatic lifestyle and represent possibly undescribed biodiversity found within Elapidae. The CT data created for this dissertation is expected to significantly benefit future efforts into morphological analyses of the Elapidae.

Copyright© by Justin Lawrence Jacobs 2021

All Right Reserved



ACKNOWLEDGMENTS

One might assume from only my name being listed as an author, that this was a solitary effort. I can assure you that this was not the case and if it were not for the following people, I would not have made it this far.

Thank you to my wife, Evelyn, for being there with a hug and reassurance when I needed it, for your confidence in me even when I didn't have it for myself, and for all your hard work that allowed us to prosper while working on this dissertation. To my wonderful daughter, Olivia, who's smile instantly destresses me. Thank you to my family for your support and your pride in me despite not really understanding the research I've done.

If not for Vasanthy 'Vas' Narayanaswami and Mark Katayama of the MARC U-STAR program at California State University, Long Beach, I would not have known that scientific research and graduate school was a viable option for me. Thank you to James Archie for introducing me to herpetological research as an undergraduate and taking me into the field.

I am grateful for the guidance and advice from my advisor Eric N. Smith and my committee Todd A. Castoe, Luke O. Frishkoff, Matthew K. Fujita, Matthew P. Loocke. All of whom have helped my navigate through this program in a different way.

I am again appreciative of Matthew P. Loocke, who in his role at the Shimadzu Center for Environmental, Forensics, and Material Science enabled me to collect all data required for this project. Thank you to Carla Bardua, Farnaz Fouladi, Ryan N. Felice, and Stefan Schlager for their instrumental assistance with my methods and R packages used. I would like to thank all the wonderful people at the museums who loaned us many specimens for this study, with special thanks to Gregory G. Pandelis of the UTA Amphibian and Reptile Diversity Research Center.

I am indebted to James E. Titus- McQuillan for his assistance with analysis on this project and his friendship and support throughout my time at UTA. Thank you to Alexander S. Hall for initial data collection on this project and to my undergraduate researchers, Joshua D. Gregg, Dat V. Huynh, Matthew S. Leach, John L. Long, Crystal M. Mills, Walter Tunnell Wilson, who lighted the burden of segmentation and landmarking amongst other necessary tasks. Through my mentorship I was able to learn how to act as a project manager and become a better leader.

I am grateful for my labmates, Thornton R. Larson, Goutam C. Sarker, Cristian H. Morales, Utpal Smart, and Panupong “Arm” Thammachoti, and colleagues at UT Arlington, William R. Budnick, Joseph L. Mruzek, and Thomas J. Firneno Jr., all of whom have helped me directly or indirectly with this project and made my graduate school experience memorable.

DEDICATED TO MY WIFE AND DAUGHTER

TABLE OF CONTENTS

ABSTRACT	ii
ACKNOWLEDGEMENTS	iv
DEDICATION	vi
LIST OF FIGURES	ix
LIST OF TABLES.....	xlix
CHAPTER ONE: Introduction to the Family Elapidae	1
INTRODUCTION	1
TAXONOMY	2
PALEOBIOGRAPHY AND EVOLUTION OF BASAL ELAPIDS	4
TRENDS OF LIFE HISTORY	6
THE SKULL	8
VERTEBRAE.....	12
CHAPTER TWO: Materials and Methods of a Geometric Morphometric Approach to the Analysis of the Elapid Skull and Vertebrae	30
PHYLOGENY	30
ECOLOGY	30
SKULL.....	35
QUADRATUM.....	39
LOWER JAW	41
MIDBODY VERTEBRA	42
CAUDAL VERTEBRA.....	44

CHAPTER THREE: Results.....	70
SKULL.....	70
QUADRAT.....	83
LOWER JAW	84
MIDBODY VERTEBRA	86
CAUDAL VERTEBRA.....	87
CHAPTER FOUR: Discussion	155
CHAPTER FIVE: General Conclusion	162
REFERENCES	164
APPENDIX.....	184
SUPPLEMENTAL FIGURES.....	184
SUPPLEMENTAL TABLES	550

LIST OF FIGURES

Chapter 2

Figure 2.1. Bayesian phylogenetic reconstruction using Mr. Bayes 3.2.7 with <i>ND4</i> (922 bp). The phylogeny was run 90,000,000 generations. Node labels denote posterior probabilities.....	46
Figure 2.2. Steps in morphometric data preparation of the skull dataset. CT data was sharpened with CLAHE (A), segmented in DrishtiPaint (B), and landmarked in Checkpoint (C). The curves were subsampled (D), surface points were added (E), and all points were slid together (F) with <i>Morpho</i> in R. Green points are the original position and red are the position post-slide.....	47
Figure 2.3. Steps in morphometric data preparation of the quadrate dataset. CT data was sharpened with CLAHE (A), segmented in DrishtiPaint (B), and landmarked in Checkpoint (C). The curves were subsampled (D), surface points were added (E), and all points were slid together (F) with <i>Morpho</i> in R. Green points are the original position and red are the position post-slide.....	48
Figure 2.4. Steps in morphometric data preparation of the lower jaw dataset. CT data was sharpened with CLAHE (A), segmented in DrishtiPaint (B), and landmarked in Checkpoint (C). The curves were subsampled (D), surface points were added (E), and all points were slid together (F) with <i>Morpho</i> in R. Green points are the original position and red are the position post-slide.....	49
Figure 2.5. Steps in morphometric data preparation of the midbody vertebra dataset. CT data was sharpened with CLAHE (A), segmented in DrishtiPaint (B), and landmarked in Checkpoint (C). The curves were subsampled with <i>Morpho</i> in R (D).....	50

Figure 2.6. Steps in morphometric data preparation of the caudal vertebra dataset. CT	
data was sharpened with CLAHE (A), segmented in DrishtiPaint (B), and	
landmarked in Checkpoint (C). The curves were subsampled with <i>Morpho</i> in R (D).....	50
Figure 2.7. Dorsal, lateral, and ventral views (A-C, respectively) of the skull of	
<i>Hemibungarus calligaster</i> (KU 307474). Right suspensorium excluded.	
Abbreviations: bo, basioccipital; bs, basisphenoid; ecp, ectopterygoid; exo,	
exoccipital; f, frontal; f5b, foramen for maxillary branch of trigeminal; f5c, foramen	
for mandibular branch of trigeminal; mx, maxilla; na, nasal; p, parietal; pal, palatine;	
pfr, prefrontal; pmx, premaxilla; pro, prootic; pt, pterygoid; pVf, posterior Vidian	
foramen; smx, septomaxilla; so, supraoccipital; st, supratemporal; v, vomer. Adapted	
from Cundall and Irish (2008).....	51
Figure 2.8. Lateral and medial views (A-B, respectively) of the left lower jaw of	
<i>Hemibungarus calligaster</i> (KU 307474). Abbreviations: a, articular; an, angular; cf,	
compound foramen; corp, coronoid process; cp, compound; d, dentary; df, dentary	
foramen; sp, splenial. Adapted from Cundall and Irish (2008).....	52
Figure 2.9. Dorsal, lateral, anterior, and posterior views (A-D, respectively) of a midbody	
vertebra of <i>Hemibungarus calligaster</i> (KU 307474). Abbreviations: cn, condyle; ct,	
cotyle; d, diapophysis; hy, hypapophysis; ir, interzygapophyseal ridge; nc, neural	
canal; ns, neural spine; pp, parapophysial process; p, parapophysis; poa,	
postzygapophyseal articular facet; po, postzygapophysis; prp, prezygapophyseal	
accessory process; pra, prezygapophyseal articular facet; pr, prezygapophysis; sr,	
subcentral ridge; sn, synapophyses; zgf, zygantral articular facet; zg, zygantrum; zyf,	
zygosphenal articular facet; zy, zygosphene. Adapted from Ikeda (2007).	53

Figure 2.10. Dorsal, lateral, anterior, and posterior views (A-D, respectively) of a caudal vertebra of *Hemibungarus calligaster* (KU 307474). Abbreviations: cn, condyle; ct, cotyle; he, hemapophysis; ir, interzygapophyseal ridge; nc, neural canal; ns, neural spine; ple, pleurapophysis; pp, parapophysial process; poa, postzygapophyseal articular facet; po, postzygapophysis; prp, prezygapophyseal accessory process; pra, prezygapophyseal articular facet; pr, prezygapophysis; sr, subcentral ridge; zgf, zygantral articular facet; zg, zygantrum; zyf, zygosphenal articular facet; zy, zygosphene. Adapted from Ikeda (2007).54

Chapter 3

Figure 3.1. PCA of the skull, utilizing all specimens, colored by ATS (A) and genus (B). Images of the skull of specimens at the extremes of PC1 (C-D) and PC2 (D-E) in dorsal view.	89
Figure 3.2. PCA of the skull conducted on the coralsnake subset, colored by ATS (A) and genus (B). Images of the skull of specimens at the extremes of PC1 (C-D) and PC2 (E-F) in dorsal view.....	90
Figure 3.3. PCA of the skull of the semi-aquatic and aquatic subset (>5 ATS), colored by ATS (A) and genus (B). Images of the skull of specimens at the minimum of PC1 and PC2 (C) and maximum of PC1 (D) and maximum of PC2 (E) in dorsal view.	91
Figure 3.4. PCA of the premaxilla module, utilizing all specimens, colored by ATS (A) and genus (B). Images of the premaxilla of specimens at the extremes of PC1 (C-D) and PC2 (E-F) in frontal (left) and ventral (right) view.....	92

Figure 3.5. PCA of the premaxilla module conducted on the coralsnake subset, colored by ATS (A) and genus (B). Images of the premaxilla of specimens at the extremes of PC1 (C-D) and PC2 (E-F) in frontal (left) and ventral (right) view.....	93
Figure 3.6. PCA of the premaxilla module conducted on the semi-aquatic and aquatic subset (>5 ATS), colored by ATS (A) and genus (B). Images of the premaxilla of specimens at the extremes of PC1 and PC2 (C-D) in frontal (left) and ventral (right) view.....	94
Figure 3.7. PCA of the septomaxilla and vomer module, utilizing all specimens, colored by ATS (A) and genus (B). Images of the septomaxilla and vomer of specimens at the extremes of PC1 (C-D) and PC2 (E-F) in ventral (left) and anterolateral (right) view	95
Figure 3.8. PCA of the septomaxilla and vomer module conducted on the coralsnake subset, colored by ATS (A) and genus (B). Images of this module of specimens at the extremes of PC1 (C-D) and PC2 (E-F) in ventral (left) and anterolateral (right) view.....	96
Figure 3.9. PCA of the septomaxilla and vomer module conducted on the semi-aquatic and aquatic subset (>5 ATS), colored by ATS (A) and genus (B). Images of specimens at the extremes of PC1 (C-D) and PC2 (E-F) in ventral (left) and anterolateral (right) view	97
Figure 3.10. PCA of the nasal module, utilizing all specimens, colored by ATS (A) and genus (B). Images of the nasal of specimens at the extremes of PC1 (C-D) and PC2 (E-F) in dorsal view.....	98

Figure 3.11. PCA of the nasal module conducted on the coralsnake subset, colored by ATS (A) and genus (B). Images of the nasal of specimens at the extremes of PC1 (C-D) and PC2 (E-F) in dorsal view.....	99
Figure 3.12. PCA of the nasal module conducted on the semi-aquatic and aquatic subset (>5 ATS), colored by ATS (A) and genus (B). Images of the nasal of specimens at the extremes of PC1 (C-D) and PC2 (E-F) in dorsal view.....	100
Figure 3.13. PCA of the prefrontal module, utilizing all specimens, colored by ATS (A) and genus (B). Images of the prefrontal of specimens at the extremes of PC1 (C-D) and PC2 (E-F) in dorsolateral view.....	101
Figure 3.14. PCA of the prefrontal module conducted on the coralsnake subset, colored by ATS (A) and genus (B). Images of the prefrontal of specimens at the extremes of PC1 (C-D) and PC2 (E-F) in dorsolateral view.	102
Figure 3.15. PCA of the prefrontal module conducted on the semi-aquatic and aquatic subset (>5 ATS), colored by ATS (A) and genus (B). Images of the prefrontal of specimens at the extremes of PC1 (C-D) and PC2 (D-E) in dorsolateral view.....	103
Figure 3.16. PCA of the frontal module, utilizing all specimens, colored by ATS (A) and genus (B). Images of the frontal of specimens at the extremes of PC1 (C-D) and PC2 (E-F) in dorsal view.....	104
Figure 3.17. PCA of the frontal module conducted on the coralsnake subset, colored by ATS (A) and genus (B). Images of the frontal of specimens at the extremes of PC1 (C-D) and PC2 (E-F) in dorsal view.	105

Figure 3.18. PCA of the frontal module conducted on the semi-aquatic and aquatic subset (>5 ATS), colored by ATS (A) and genus (B). Images of the frontal of specimens at the extremes of PC1 (C-D) and PC2 (E-F) in dorsal view.....	106
Figure 3.19. PCA of the parietal module, utilizing all specimens, colored by ATS (A) and genus (B). Images of the parietal of specimens at the extremes of PC1 (C-D) and PC2 maximum (C) and minimum (E) in lateral view.	107
Figure 3.20. PCA of the parietal module conducted on the coralsnake subset, colored by ATS (A) and genus (B). Images of the parietal of specimens at the extremes of PC1 (C-D) and PC2 (E-F) in lateral view.	108
Figure 3.21. PCA of the parietal module conducted on the semi-aquatic and aquatic subset (>5 ATS), colored by ATS (A) and genus (B). Images of the parietal of specimens at the extremes of PC1 (C-D) and PC2 (E-F) in lateral view.	109
Figure 3.22. PCA of the supraoccipital module, utilizing all specimens, colored by ATS (A) and genus (B). Images of the supraoccipital of specimens at the extremes of PC1 (C-D) and PC2 (E-F) in dorsal view.	110
Figure 3.23. PCA of the supraoccipital module conducted on the coralsnake subset, colored by ATS (A) and genus (B). Images of the supraoccipital of specimens at the extremes of PC1 (C-D) and PC2 (E-F) in dorsal view.	111
Figure 3.24. PCA of the supraoccipital module conducted on the semi-aquatic and aquatic subset (>5 ATS), colored by ATS (A) and genus (B). Images of the supraoccipital of specimens at the extremes of PC1 (C-D) and PC2 (E-F) in dorsal view.	112

Figure 3.25. PCA of the prootic module utilizing all specimens, colored by ATS (A) and genus (B). Images of the prootic of specimens at the extremes of PC1 (C-D) and PC2 (E-F) in lateral view.	113
Figure 3.26. PCA of the prootic module conducted on the coralsnake subset, colored by ATS (A) and genus (B). Images of the prootic of specimens at the extremes of PC1 (C-D) and PC2 (E-F) in lateral view.	114
Figure 3.27. PCA of the prootic module conducted on the semi-aquatic and aquatic subset (>5 ATS), colored by ATS (A) and genus (B). Images of the supraoccipital of specimens at the extremes of PC1 (C-D) and PC2 (E-F) in lateral view.	115
Figure 3.28. PCA of the exoccipital module utilizing all specimens, colored by ATS (A) and genus (B). Images of the exoccipital of specimens at the extremes of PC1 (C-D) and PC2 (E-F) in posterolateral view.	116
Figure 3.29. PCA of the exoccipital module conducted on the coralsnake subset, colored by ATS (A) and genus (B). Images of the exoccipital of specimens at the extremes of PC1 (C-D) and PC2 (E-F) in posterolateral view.	117
Figure 3.30. PCA of the exoccipital module conducted on the semi-aquatic and aquatic subset (>5 ATS), colored by ATS (A) and genus (B). Images of the exoccipital of specimens at the extremes of PC1 (C-D) and PC2 (E-F) in posterolateral view.	118
Figure 3.31. PCA of the supratemporal module utilizing all specimens, colored by ATS (A) and genus (B). Images of the supratemporal of specimens at the extremes of PC1 (C-D) and PC2 (E-F) in dorsolateral view.	119

Figure 3.32. PCA of the supratemporal module conducted on the coralsnake subset, colored by ATS (A) and genus (B). Images of the supratemporal of specimens at the extremes of PC1 (C-D) and PC2 (E-F) in dorsolateral view.....	120
Figure 3.33. PCA of the supratemporal module conducted on the semi-aquatic and aquatic subset (>5 ATS), colored by ATS (A) and genus (B). Images of the supratemporal of specimens at the extremes of PC1 (C-D) and PC2 (E-F) in dorsolateral view.	121
Figure 3.34. PCA of the basisphenoid module utilizing all specimens, colored by ATS (A) and genus (B). Images of the basisphenoid of specimens at the extremes of PC1 (C-D) and PC2 (E-F) in lateral view.	122
Figure 3.35. PCA of the basisphenoid module conducted on the coralsnake subset, colored by ATS (A) and genus (B). Images of the basisphenoid of specimens at the extremes of PC1 (C-D) and PC2 (E-F) in lateral view.....	123
Figure 3.36. PCA of the basisphenoid module conducted on the semi-aquatic and aquatic subset (>5 ATS), colored by ATS (A) and genus (B). Images of the basisphenoid of specimens at the extremes of PC1 (C-D) and PC2 (E-F) in lateral view.	124
Figure 3.37. PCA of the basioccipital module utilizing all specimens, colored by ATS (A) and genus (B). Images of the basioccipital of specimens at the extremes of PC1 (C- D) and PC2 (E-F) in ventral view.	125
Figure 3.38. PCA of the basioccipital module conducted on the coralsnake subset, colored by ATS (A) and genus (B). Images of the basioccipital of specimens at the extremes of PC1 (C-D) and PC2 (E-F) in ventral view.	126

Figure 3.39. PCA of the basioccipital module conducted on the semi-aquatic and aquatic subset (>5 ATS), colored by ATS (A) and genus (B). Images of the basioccipital of specimens at the extremes of PC1 (C-D) and PC2 (E-F) in ventral view.....	127
Figure 3.40. PCA of the maxilla and palatine module utilizing all specimens, colored by ATS (A) and genus (B). Images oof specimens at the extremes of PC1 (C-D) and the PC2 maximum (C) and minimum (E) in lateral (top) and ventral (bottom) views.....	128
Figure 3.41. PCA of the maxilla and palatine module conducted on the coralsnake subset, colored by ATS (A) and genus (B). Images of the maxilla and palatine of specimens at the extremes of PC1 (C-D) and PC2 (E-F) in anterolateral (left) and ventral (right) views.....	129
Figure 3.42. PCA of the maxilla and palatine module conducted on the semi-aquatic and aquatic subset (>5 ATS), colored by ATS (A) and genus (B). Images of specimens at the extremes of PC1 (C-D) and PC2 (E-F) in anterolateral (left) and ventral (right) views.....	130
Figure 3.43. PCA of the ectopterygoid module, utilizing all specimens, colored by ATS (A) and genus (B). Images of the ectopterygoid of specimens at the extremes of PC1 (C-D) and PC2 (E-F) in ventral view.....	131
Figure 3.44. PCA of the ectopterygoid module conducted on the coralsnake subset, colored by ATS (A) and genus (B). Images of the ectopterygoid of specimens at the extremes of PC1 (C-D) and PC2 (E-F) in ventral view.	132
Figure 3.45. PCA of the ectopterygoid module conducted on the semi-aquatic and aquatic subset (>5 ATS), colored by ATS (A) and genus (B). Images of the ectopterygoid of specimens at the extremes of PC1 (C-D) and PC2 (E-F) in ventrolateral view.....	133

Figure 3.46. PCA of the pterygoid module utilizing all specimens, colored by ATS (A) and genus (B). Images of the pterygoid of specimens at the extremes of PC1 (C-D) and PC2 (E-F) in ventral view.....	134
Figure 3.47. PCA of the pterygoid module conducted on the coralsnake subset, colored by ATS (A) and genus (B). Images of the pterygoid of specimens at the PC1 minimum (C) and PC2 minimum (E) and PC1 and PC2 maxima (D)	135
Figure 3.48. PCA of the pterygoid module conducted on the semi-aquatic and aquatic subset (>5 ATS), colored by ATS (A) and genus (B). Images of the pterygoid of specimens at the PC1 minimum (C) and PC2 minimum (E) and PC1 and PC2 maxima (D).....	136
Figure 3.49. PCA of the quadrate dataset utilizing all specimens, colored by ATS (A) and genus (B). Images of the quadrate of specimens at the extremes of PC1 (C-D) and PC2 (E-F) in lateral (left) and medial (right) view.....	137
Figure 3.50. PCA of the quadrate dataset conducted on the coralsnake subset, colored by ATS (A) and genus (B). Images of the quadrate of specimens at the extremes of PC1 (C-D) and PC2 (E-F) in lateral (left) and medial (right) view.	138
Figure 3.51. PCA of the quadrate dataset conducted on the semi-aquatic and aquatic subset (>5 ATS), colored by ATS (A) and genus (B). Images of the quadrate of specimens at the extremes of PC1 (C-D) and PC2 (E-F) in lateral (left) and medial (right) view.....	139
Figure 3.52. PCA of the jaw utilizing all specimens, colored by ATS (A) and genus (B). Images of the jaw of specimens at the extremes of PC1 (C-D) and PC2 (E-F) in lateral view.	140

Figure 3.53. PCA of the jaw conducted on the coralsnake subset, colored by ATS (A) and genus (B). Images of the jaw of specimens at the extremes of PC1 (C-D) and PC2 (E-F) in lateral view.141

Figure 3.54. PCA of the jaw conducted on the semi-aquatic and aquatic subset (>5 ATS), colored by ATS (A) and genus (B). Images of the jaw of specimens at the extremes of PC1 (C-D) and PC2 (E-F) in lateral view.142

Figure 3.55. PCA of the compound module utilizing all specimens, colored by ATS (A) and genus (B). Images of the compound of specimens at the extremes of PC1 (C-D) and PC2 minimum (C) and maximum (E) in lateral (top) and dorsal (bottom) views.....143

Figure 3.56. PCA of the compound module conducted on the coralsnake subset, colored by ATS (A) and genus (B). Images of the compound of specimens at the extremes of PC1 (C-D) and PC2 (E-F) in lateral (top) and dorsal (bottom) views.144

Figure 3.57. PCA of the compound module conducted on the semi-aquatic and aquatic subset (>5 ATS), colored by ATS (A) and genus (B). Images 5 of specimens at the extremes of PC1 (C-D) and PC2 (D-E) in lateral (top) and dorsal (bottom) views.145

Figure 3.58. PCA of the dentary, angular, and splenial module utilizing all specimens, colored by ATS (A) and genus (B). Images of the dentary, angular, and splenial of specimens at the extremes of PC1 (C-D) and PC2 (E-F) in medial (left) and lateral (right) views.146

Figure 3.59. PCA of the dentary, angular, and splenial module conducted on the coralsnake subset, colored by ATS (A) and genus (B). Images of specimens at the extremes of PC1 (C-D) and PC2 (C, E) in medial (left) and lateral (right) views.147

Figure 3.60. PCA of the dentary, angular, and splenial module conducted on the semi-aquatic and aquatic subset (>5 ATS), colored by ATS (A) and genus (B). Images of specimens at the extremes of PC1 (C-D) and PC2 (E-F) in medial (left) and lateral (right) views.	148
Figure 3.61. PCA of the midbody vertebra dataset, utilizing all specimens, colored by ATS (A) and genus (B). Images of the midbody vertebra of specimens at the extremes of PC1 (C-D) and PC2 (E-F) in the anterior (left) and lateral (right) views.....	149
Figure 3.62. PCA of the midbody vertebra dataset conducted on the coralsnake subset, colored by ATS (A) and genus (B). Images of the midbody vertebra of specimens at the extremes of PC1 (C-D) and PC2 (E-F) in the anterior (left) and lateral (right) views.....	150
Figure 3.63. PCA of the midbody vertebra dataset conducted on the semi-aquatic and aquatic subset (>5 ATS), colored by ATS (A) and genus (B). Images at the extremes of PC1 (C-D) and PC2 (E-F) in the anterior (left) and lateral (right) views.	151
Figure 3.64. PCA of the caudal vertebra dataset, utilizing all specimens, colored by ATS (A) and genus (B). Images of the midbody vertebra of specimens at the extremes of PC1 (C-D) and PC2 (E-F) in the anterior (left) and lateral (right) views.	152
Figure 3.65. PCA of the caudal vertebra dataset conducted on the coralsnake subset, colored by ATS (A) and genus (B). Images of the midbody vertebra of specimens at the extremes of PC1 (C-D) and PC2 (E-F) in the anterior (left) and lateral (right) views.	153

Figure 3.66. PCA of the caudal vertebra dataset conducted on the semi-aquatic and aquatic subset (>5 ATS), colored by ATS (A) and genus (B). Images of specimens at the extremes of PC1 (C-D) and PC2 (E-F) in the anterior (left) and lateral (right) views.....	154
---	-----

Appendix

Supplemental Figure 1. Dorsal, lateral, ventral, anterior, and posterior views

(A-E, respectively) of the skull of the given specimen	184
1.1. <i>Acanthophis antarcticus</i> (UTA R-7623)	184
1.2. <i>Bungarus candidus</i> (UTA R-65799)	185
1.3. <i>Bungarus flaviceps</i> (UTA R-62257)	186
1.4. <i>Calliophis beddomei</i> (MNHN 46-81)	187
1.5. <i>Calliophis biliniatus</i> (KU 309511)	188
1.6. <i>Calliophis biliniatus</i> (KU 311415)	189
1.7. <i>Calliophis bivirgatus bivirgatus</i> (UTA R-63079)	190
1.8. <i>Calliophis gracilis</i> (USNM 53447)	191
1.9. <i>Calliophis intestinalis</i> (UTA R-60738)	192
1.10. <i>Calliophis cf. intestinalis</i> (NMW 27221-4)	193
1.11. <i>Calliophis intestinalis immaculata</i> (UTA R-65802)	194
1.12. <i>Calliophis intestinalis lineata</i> (UTA R-65801)	195
1.13. <i>Calliophis maculiceps</i> (MNHN 5459)	196
1.14. <i>Calliophis melanurus</i> (MNHN 46-286)	197
1.15. <i>Calliophis melanurus</i> (MNHN 48-318)	198
1.16. <i>Calliophis nigrotaeniatus</i> (NMW 27220-7)	199

1.17. <i>Calliophis philippinus</i> (KU 310369)	200
1.18. <i>Calliophis philippinus</i> (KU 314913)	201
1.19. <i>Calliophis salitan</i> (PNM 9844)	202
1.20. <i>Hemachatus haemachatus</i> (UTA R-7431)	203
1.21. <i>Hemibungarus calligaster</i> (KU 307474)	204
1.22. <i>Hydrophis platurus</i> (UTA R-41049)	205
1.23. <i>Hydrophis schistosus</i> (UTA R-63074)	206
1.24. <i>Laticauda colubrina</i> (UTA R-65800)	207
1.25. <i>Laticauda laticauda</i> (UTA R-6355)	208
1.26. <i>Micruroides euryxanthus</i> (UTA R-60734)	209
1.27. <i>Micrurus allenii</i> (UTA R-60556)	210
1.28. <i>Micrurus australis</i> (UTA R-55945)	211
1.29. <i>Micrurus apiatus</i> (UTA R-39267)	212
1.30. <i>Micrurus apiatus</i> (UTA R-39554)	213
1.31. <i>Micrurus diastema</i> (UTA R-52565)	214
1.32. <i>Micrurus diutius</i> (UTA R-54182)	215
1.33. <i>Micrurus dumerilii</i> (AMNH 35951)	216
1.34. <i>Micrurus elegans elegans</i> (MZFC 18819)	217
1.35. <i>Micrurus elegans veraepacis</i> (UTA R-58869)	218
1.36. <i>Micrurus elegans veraepacis</i> (UTA R-7072)	219
1.37. <i>Micrurus ephippifer</i> (UTA R-64863)	220
1.38. <i>Micrurus filiformis</i> (UTA R-65836)	221
1.39. <i>Micrurus filiformis</i> (UTA R-3423)	222

1.40. <i>Micrurus fulvius</i> (UTA R-61632)	223
1.41. <i>Micrurus helleri</i> (UTA R-38005)	224
1.42. <i>Micrurus helleri</i> (UTA R-65841)	225
1.43. <i>Micrurus hemprichii</i> (UTA R-9683)	226
1.44. <i>Micrurus hemprichii</i> (UTA R-29997)	227
1.45. <i>Micrurus isozonus</i> (UTA R-22589)	228
1.46. <i>Micrurus isozonus</i> (UTA R-3951)	229
1.47. <i>Micrurus laticollaris</i> (UTA R-52559)	230
1.48. <i>Micrurus laticollaris</i> (UTA R-57562)	231
1.49. <i>Micrurus lemniscatus</i> cf. <i>helleri</i> (UTA R-34563)	232
1.50. <i>Micrurus lemniscatus</i> cf. <i>helleri</i> (UTA R-65803)	233
1.51. <i>Micrurus limbatus</i> (UTA R-64852)	234
1.52. <i>Micrurus limbatus</i> (UTA R-64899)	235
1.53. <i>Micrurus melanotus</i> (UTA R-22582)	236
1.54. <i>Micrurus mipartitus</i> (UTA R-54187)	237
1.55. <i>Micrurus mosquitensis</i> (UTA R-12919)	238
1.56. <i>Micrurus nattereri</i> (UTA R-54175)	239
1.57. <i>Micrurus nattereri</i> (UTA R-55086)	240
1.58. <i>Micrurus nattereri</i> (UTA R-60727)	241
1.59. <i>Micrurus nigrocinctus zunilensis</i> (UTA R-64858)	242
1.60. <i>Micrurus obscurus</i> (UTA R-3840)	243
1.61. <i>Micrurus ornatissimus</i> (UTA R-60724)	244
1.62. <i>Micrurus pyrrhocryptus</i> (UTA R-51404)	245

1.63. <i>Micrurus renjifoi</i> (UTA R-3490)	246
1.64. <i>Micrurus serranus</i> (UTA R-34561)	247
1.65. <i>Micrurus steindachneri</i> (AMNH 28846)	248
1.66. <i>Micrurus steindachneri</i> (AMNH 35819)	249
1.67. <i>Micrurus surinamensis</i> (UTA R-15679)	250
1.68. <i>Micrurus surinamensis</i> (UTA R-50173)	251
1.69. <i>Micrurus surinamensis</i> (UTA R-54378)	252
1.70. <i>Micrurus surinamensis</i> (UTA R-65844)	253
1.71. <i>Micrurus tener</i> (FMNH 39479)	254
1.72. <i>Micrurus tener</i> (UTA R-63282)	255
1.73. <i>Naja annulata</i> (UTA R-18199)	256
1.74. <i>Naja christyi</i> (UTA R-18200)	257
1.75. <i>Naja siamensis</i> (UTA R-16872)	258
1.76. <i>Ophiophagus hannah</i> (UTA R-60836)	259
1.77. <i>Oxyuranus scutellatus</i> (UTA R-60839)	260
1.78. <i>Pseudohaje goldii</i> (UTA R-63636)	261
1.79. <i>Simoselaps bertholdi</i> (UMMZ 244197)	262
1.80. <i>Sinomicrurus annularis</i> (ROM 31158)	263
1.81. <i>Sinomicrurus boettgeri</i> (UTA R-58837)	264
1.82. <i>Sinomicrurus japonicus</i> (CAS 204979)	265
1.83. <i>Sinomicrurus kelloggi</i> (ROM 37079)	266
1.84. <i>Sinomicrurus peinani</i> (ROM 35245)	267
1.85. <i>Sinomicrurus peinani</i> (ROM 37109)	268

1.86. <i>Sinomicrurus swinhoei</i> (MVZ 23876)	269
1.87. <i>Walterinnesia aegyptia</i> (UTA R-13021)	270
Supplemental Figure 2. Lateral and medial views (A and B, respectively) of	
the quadrate of the given specimen	271
2.1. <i>Acanthophis antarcticus</i> (UTA R-7623)	271
2.2. <i>Bungarus candidus</i> (UTA R-65799)	271
2.3. <i>Bungarus flaviceps</i> (UTA R-62257)	272
2.4. <i>Calliophis beddomei</i> (MNHN 46-81)	272
2.5. <i>Calliophis biliniatus</i> (KU 309511)	273
2.6. <i>Calliophis biliniatus</i> (KU 311415)	273
2.7. <i>Calliophis bivirgatus bivirgatus</i> (UTA R-63079)	274
2.8. <i>Calliophis gracilis</i> (USNM 53447)	274
2.9. <i>Calliophis intestinalis</i> (UTA R-60738)	275
2.10. <i>Calliophis cf. intestinalis</i> (NMW 27221-4)	275
2.11. <i>Calliophis intestinalis immaculata</i> (UTA R-65802)	276
2.12. <i>Calliophis intestinalis cf. immaculata</i> (NMW 27192-1)	276
2.13. <i>Calliophis intestinalis lineata</i> (UTA R-65801)	277
2.14. <i>Calliophis maculiceps</i> (MNHN 5459)	277
2.15. <i>Calliophis melanurus</i> (MNHN 46-286)	278
2.16. <i>Calliophis nigrotaeniatus</i> (NMW 27220-7)	278
2.17. <i>Calliophis philippinus</i> (KU 310369)	279
2.18. <i>Calliophis philippinus</i> (KU 314913)	279
2.19. <i>Calliophis salitan</i> (PNM 9844)	280

2.20. <i>Dendroaspis angusticeps</i> (UTA R-34982)	280
2.21. <i>Elapsoidea nigra</i> (CAS 168978)	281
2.22. <i>Hemachatus haemachatus</i> (UTA R-7431)	281
2.23. <i>Hemibungarus calligaster</i> (KU 307474)	282
2.24. <i>Hydrophis platurus</i> (UTA R-41049)	282
2.25. <i>Hydrophis schistosus</i> (UTA R-63074)	283
2.26. <i>Laticauda colubrina</i> (UTA R-65800)	283
2.27. <i>Laticauda laticauda</i> (UTA R-6355)	284
2.28. <i>Micrelaps vaillanti</i> (CAS 169941)	284
2.29. <i>Micruroides euryxanthus</i> (UTA R-60734)	285
2.30. <i>Micrurus allenii</i> (UTA R-60556)	285
2.31. <i>Micrurus australis</i> (UTA R-55945)	286
2.32. <i>Micrurus apiyatus</i> (UTA R-39267)	286
2.33. <i>Micrurus apiyatus</i> (UTA R-39554)	287
2.34. <i>Micrurus apiyatus</i> (UTA R-53450)	287
2.35. <i>Micrurus bocourti</i> (UTA R-58145)	288
2.36. <i>Micrurus diastema</i> (UTA R-52565)	288
2.37. <i>Micrurus dissoluteucus</i> (UTA R-54184)	289
2.38. <i>Micrurus distans</i> (UTA R-14471)	289
2.39. <i>Micrurus diutius</i> (UTA R-20756)	290
2.40. <i>Micrurus diutius</i> (UTA R-54182)	290
2.41. <i>Micrurus dumerilii</i> (AMNH 35951)	291
2.42. <i>Micrurus elegans elegans</i> (MZFC 18819)	291

2.43. <i>Micrurus elegans veraepacis</i> (UTA R-7072)	292
2.44. <i>Micrurus elegans veraepacis</i> (UTA R-58869)	292
2.45. <i>Micrurus ephippifer</i> (UTA R-64863)	293
2.46. <i>Micrurus filiformis</i> (UTA R-3423)	293
2.47. <i>Micrurus filiformis</i> (UTA R-65836)	294
2.48. <i>Micrurus fulvius</i> (UTA R-61632)	294
2.49. <i>Micrurus helleri</i> (UTA R-38005)	295
2.50. <i>Micrurus helleri</i> (UTA R-55977)	295
2.51. <i>Micrurus helleri</i> (UTA R-65841)	296
2.52. <i>Micrurus hemprichii</i> (UTA R-9683)	296
2.53. <i>Micrurus hemprichii</i> (UTA R-29997)	297
2.54. <i>Micrurus isozonus</i> (UTA R-3951)	297
2.55. <i>Micrurus isozonus</i> (UTA R-22589)	298
2.56. <i>Micrurus laticollaris</i> (UTA R-52559)	298
2.57. <i>Micrurus laticollaris</i> (UTA R-57562)	299
2.58. <i>Micrurus lemniscatus</i> cf. <i>helleri</i> (UTA R-34563)	299
2.59. <i>Micrurus lemniscatus</i> cf. <i>helleri</i> (UTA R-65803)	300
2.60. <i>Micrurus limbatus</i> (UTA R-64852)	300
2.61. <i>Micrurus limbatus</i> (UTA R-64899)	301
2.62. <i>Micrurus melanotus</i> (AMNH 35934)	301
2.63. <i>Micrurus melanotus</i> (UTA R-22582)	302
2.64. <i>Micrurus mipartitus</i> (UTA R-54187)	302
2.65. <i>Micrurus mosquitensis</i> (UTA R-12919)	303

2.66. <i>Micrurus nattereri</i> (UTA R-54175)	303
2.67. <i>Micrurus nattereri</i> (UTA R-55086)	304
2.68. <i>Micrurus nattereri</i> (UTA R-60727)	304
2.69. <i>Micrurus nigrocinctus zunilensis</i> (UTA R-64858)	305
2.70. <i>Micrurus obscurus</i> (UTA R-3840)	305
2.71. <i>Micrurus oliveri</i> (UTA R-64893)	306
2.72. <i>Micrurus ornatissimus</i> (UTA R-60724)	306
2.73. <i>Micrurus pyrrhocryptus</i> (UTA R-51404)	307
2.74. <i>Micrurus renjifoi</i> (UTA R-3490)	307
2.75. <i>Micrurus serranus</i> (UTA R-34561)	308
2.76. <i>Micrurus steindachneri</i> (AMNH 28846)	308
2.77. <i>Micrurus steindachneri</i> (AMNH 35819)	309
2.78. <i>Micrurus surinamensis</i> (UTA R-15679)	309
2.79. <i>Micrurus surinamensis</i> (UTA R-50173)	310
2.80. <i>Micrurus surinamensis</i> (UTA R-54378)	310
2.81. <i>Micrurus surinamensis</i> (UTA R-5849)	311
2.82. <i>Micrurus surinamensis</i> (UTA R-65844)	311
2.83. <i>Micrurus tener</i> (FMNH 39479)	312
2.84. <i>Micrurus tener</i> (UTA R-63282)	312
2.85. <i>Micrurus sp.</i> (UTA R-6086)	313
2.86. <i>Naja annulata</i> (UTA R-18199)	313
2.87. <i>Naja christyi</i> (UTA R-18200)	314
2.88. <i>Naja siamensis</i> (UTA R-16872)	314

2.89. <i>Ophiophagus hannah</i> (UTA R-60836)	315
2.90. <i>Oxyuranus scutellatus</i> (UTA R-60839)	315
2.91. <i>Prosymna stuhlmanni</i> (UTA R-64493)	316
2.92. <i>Pseudohaje goldii</i> (UTA R-63636)	316
2.93. <i>Simoselaps bertholdi</i> (UMMZ 244197)	317
2.94. <i>Sinomicrurus annularis</i> (ROM 31158)	317
2.95. <i>Sinomicrurus boettgeri</i> (UTA R-58837)	318
2.96. <i>Sinomicrurus japonicus</i> (CAS 204979)	318
2.97. <i>Sinomicrurus kelloggi</i> (ROM 37079)	319
2.98. <i>Sinomicrurus peinani</i> (ROM 35245)	319
2.99. <i>Sinomicrurus peinani</i> (ROM 37109)	320
2.100. <i>Sinomicrurus swinhoei</i> (MVZ 23876)	320
2.101. <i>Walterinnesia aegyptia</i> (UTA R-13021)	321

Supplemental Figure 3. Medial, dorsal, and lateral views (A-C, respectively)

of the lower jaw of the given specimen.....	322
3.1. <i>Acanthophis antarcticus</i> (UTA R-7623)	322
3.2. <i>Bungarus candidus</i> (UTA R-65799)	322
3.3. <i>Bungarus flaviceps</i> (UTA R-62257)	323
3.4. <i>Calliophis beddomei</i> (MNHN 46-81)	323
3.5. <i>Calliophis biliniatus</i> (KU 309511)	324
3.6. <i>Calliophis biliniatus</i> (KU 311415)	324
3.7. <i>Calliophis bivirgatus bivirgatus</i> (UTA R-63079)	325
3.8. <i>Calliophis gracilis</i> (USNM 53447)	325

3.9. <i>Calliophis intestinalis</i> (UTA R-60738)	326
3.10. <i>Calliophis cf. intestinalis</i> (NMW 27221-4)	326
3.11. <i>Calliophis intestinalis cf. immaculata</i> (NMW 27192-1)	327
3.12. <i>Calliophis intestinalis immaculata</i> (UTA R-65802)	327
3.13. <i>Calliophis intestinalis lineata</i> (UTA R-65801)	328
3.14. <i>Calliophis maculiceps</i> (MNHN 5459)	328
3.15. <i>Calliophis melanurus</i> (MNHN 46-286)	329
3.16. <i>Calliophis melanurus</i> (MNHN 48-318)	329
3.17. <i>Calliophis nigrotaeniatus</i> (NMW 27220-7)	330
3.18. <i>Calliophis philippinus</i> (KU 310369)	330
3.19. <i>Calliophis philippinus</i> (KU 314913)	331
3.20. <i>Calliophis salitan</i> (PNM 9844)	331
3.21. <i>Dendroaspis angusticeps</i> (UTA R-34982)	332
3.22. <i>Elapsoidea nigra</i> (CAS 168978)	332
3.23. <i>Hemachatus haemachatus</i> (UTA R-7431)	333
3.24. <i>Hemibungarus calligaster</i> (KU 307474)	333
3.25. <i>Hydrophis platurus</i> (UTA R-41049)	334
3.26. <i>Hydrophis schistosus</i> (UTA R-63074)	334
3.27. <i>Laticauda colubrina</i> (UTA R-65800)	335
3.28. <i>Laticauda laticauda</i> (UTA R-6355)	335
3.29. <i>Micrelaps vaillanti</i> (CAS 169941)	336
3.30. <i>Micruroides euryxanthus</i> (UTA R-60734)	336
3.31. <i>Micrurus aleni</i> (UTA R-60556)	337

3.32. <i>Micrurus ancoralis</i> (UTA R-55945)	337
3.33. <i>Micrurus apiatus</i> (UTA R-39267)	338
3.34. <i>Micrurus apiatus</i> (UTA R-39554)	338
3.35. <i>Micrurus apiatus</i> (UTA R-53450)	339
3.36. <i>Micrurus bocourti</i> (UTA R-58145)	339
3.37. <i>Micrurus diastema</i> (UTA R-52565)	340
3.38. <i>Micrurus dissoluteucus</i> (UTA R-54184)	340
3.39. <i>Micrurus distans</i> (UTA R-14471)	341
3.40. <i>Micrurus diutius</i> (UTA R-20756)	341
3.41. <i>Micrurus diutius</i> (UTA R-54182)	342
3.42. <i>Micrurus dumerilii</i> (AMNH 35951)	342
3.43. <i>Micrurus elegans elegans</i> (MZFC 18819)	343
3.44. <i>Micrurus elegans veraepacis</i> (UTA R-7072)	343
3.45. <i>Micrurus elegans veraepacis</i> (UTA R-58869)	344
3.46. <i>Micrurus ephippifer</i> (UTA R-64863)	344
3.47. <i>Micrurus filiformis</i> (UTA R-3423)	345
3.48. <i>Micrurus filiformis</i> (UTA R-65836)	345
3.49. <i>Micrurus fulvius</i> (UTA R-61632)	346
3.50. <i>Micrurus helleri</i> (UTA R-38005)	346
3.51. <i>Micrurus helleri</i> (UTA R-65841)	347
3.52. <i>Micrurus hemprichii</i> (UTA R-9683)	347
3.53. <i>Micrurus hemprichii</i> (UTA R-29997)	348
3.54. <i>Micrurus isozonus</i> (UTA R-3951)	348

3.55. <i>Micrurus isozonus</i> (UTA R-22589)	349
3.56. <i>Micrurus laticollaris</i> (UTA R-52559)	349
3.57. <i>Micrurus laticollaris</i> (UTA R-57562)	350
3.58. <i>Micrurus latifasciatus</i> (UTA R-4606)	350
3.59. <i>Micrurus lemniscatus</i> cf. <i>helleri</i> (UTA R-34563)	351
3.60. <i>Micrurus lemniscatus</i> cf. <i>helleri</i> (UTA R-65803)	351
3.61. <i>Micrurus limbatus</i> (UTA R-64852)	352
3.62. <i>Micrurus limbatus</i> (UTA R-64899)	352
3.63. <i>Micrurus melanotus</i> (AMNH 35934)	353
3.64. <i>Micrurus melanotus</i> (UTA R-22582)	353
3.65. <i>Micrurus mipartitus</i> (UTA R-54187)	354
3.66. <i>Micrurus mosquitensis</i> (UTA R-12919)	354
3.67. <i>Micrurus nattereri</i> (UTA R-54175)	355
3.68. <i>Micrurus nattereri</i> (UTA R-55086)	355
3.69. <i>Micrurus nattereri</i> (UTA R-60727)	356
3.70. <i>Micrurus nigrocinctus zunilensis</i> (UTA R-64858)	356
3.71. <i>Micrurus obscurus</i> (UTA R-3840)	357
3.72. <i>Micrurus oliveri</i> (UTA R-64893)	357
3.73. <i>Micrurus ornatissimus</i> (UTA R-60724)	358
3.74. <i>Micrurus pyrrhocryptus</i> (UTA R-51404)	358
3.75. <i>Micrurus renjifoii</i> (UTA R-3490)	359
3.76. <i>Micrurus serranus</i> (UTA R-34561)	359
3.77. <i>Micrurus steindachneri</i> (AMNH 28846)	360

3.78. <i>Micrurus steindachneri</i> (AMNH 35819)	360
3.79. <i>Micrurus surinamensis</i> (UTA R-15679)	361
3.80. <i>Micrurus surinamensis</i> (UTA R-50173)	361
3.81. <i>Micrurus surinamensis</i> (UTA R-54378)	362
3.82. <i>Micrurus surinamensis</i> (UTA R-65844)	362
3.83. <i>Micrurus tener</i> (FMNH 39479)	363
3.84. <i>Micrurus tener</i> (UTA R-63282)	363
3.85. <i>Micrurus sp.</i> (UTA R-6086)	364
3.86. <i>Naja annulata</i> (UTA R-18199)	364
3.87. <i>Naja christyi</i> (UTA R-18200)	365
3.88. <i>Naja siamensis</i> (UTA R-16872)	365
3.89. <i>Ophiophagus hannah</i> (UTA R-60836)	366
3.90. <i>Oxyuranus scutellatus</i> (UTA R-60839)	366
3.91. <i>Prosymna stuhlmanni</i> (UTA R-64493)	367
3.92. <i>Pseudohaje goldii</i> (UTA R-63636)	367
3.93. <i>Simoselaps bertholdi</i> (UMMZ 244197)	368
3.94. <i>Sinomicrurus annularis</i> (ROM 31158)	368
3.95. <i>Sinomicrurus boettgeri</i> (UTA R-58837)	369
3.96. <i>Sinomicrurus japonicus</i> (CAS 204979)	369
3.97. <i>Sinomicrurus peinani</i> (ROM 35245)	370
3.98. <i>Sinomicrurus peinani</i> (ROM 37109)	370
3.99. <i>Sinomicrurus swinhoei</i> (MVZ 23876)	371
3.100. <i>Walterinnesia aegyptia</i> (UTA R-13021)	371

Supplemental Figure 4. Dorsal, lateral, ventral, anterior, and posterior views

(A-E, respectively) of the midbody vertebra of the given specimen.....	372
4.1. <i>Acanthophis antarcticus</i> (UTA R-7623)	372
4.2. <i>Bungarus candidus</i> (UTA R-65799)	373
4.3. <i>Bungarus flaviceps</i> (UTA R-62257)	374
4.4. <i>Calliophis beddomei</i> (MNHN 46-81)	375
4.5. <i>Calliophis biliniatus</i> (KU 309511)	376
4.6. <i>Calliophis biliniatus</i> (KU 311415)	377
4.7. <i>Calliophis bivirgatus bivirgatus</i> (UTA R-63079)	378
4.8. <i>Calliophis gracilis</i> (USNM 53447)	379
4.9. <i>Calliophis intestinalis</i> (UTA R-60738)	380
4.10. <i>Calliophis intestinalis immaculata</i> (UTA R-65802)	381
4.11. <i>Calliophis intestinalis lineata</i> (UTA R-65801)	382
4.12. <i>Calliophis maculiceps</i> (MNHN 5459)	383
4.13. <i>Calliophis melanurus</i> (MNHN 46-286)	384
4.14. <i>Calliophis philippinus</i> (KU 310369)	385
4.15. <i>Calliophis philippinus</i> (KU 314913)	386
4.16. <i>Dendroaspis angusticeps</i> (UTA R-34982)	387
4.17. <i>Elapsoidea nigra</i> (CAS 168978)	388
4.18. <i>Hemachatus haemachatus</i> (UTA R-7431)	389
4.19. <i>Hemibungarus calligaster</i> (KU 307474)	390
4.20. <i>Hydrophis platurus</i> (UTA R-41049)	391
4.21. <i>Hydrophis schistosus</i> (UTA R-63074)	392

4.22. <i>Laticauda colubrina</i> (UTA R-65800)	393
4.23. <i>Laticauda laticauda</i> (UTA R-6355)	394
4.24. <i>Micrelaps vaillanti</i> (CAS 169941)	395
4.25. <i>Micruroides euryxanthus</i> (UTA R-60734)	396
4.26. <i>Micrurus allenii</i> (UTA R-60556)	397
4.27. <i>Micrurus ancoralis</i> (UTA R-55945)	398
4.28. <i>Micrurus apiatus</i> (UTA R-39267)	399
4.29. <i>Micrurus apiatus</i> (UTA R-39554)	400
4.30. <i>Micrurus apiatus</i> (UTA R-53450)	401
4.31. <i>Micrurus bocourti</i> (UTA R-58145)	402
4.32. <i>Micrurus diastema</i> (UTA R-52565)	403
4.33. <i>Micrurus dissoluteucus</i> (UTA R-54184)	404
4.34. <i>Micrurus distans</i> (UTA R-14471)	405
4.35. <i>Micrurus diutius</i> (UTA R-20756)	406
4.36. <i>Micrurus diutius</i> (UTA R-54182)	407
4.37. <i>Micrurus dumerilii</i> (AMNH 35951)	408
4.38. <i>Micrurus elegans elegans</i> (MZFC 18819)	409
4.39. <i>Micrurus elegans veraepacis</i> (UTA R-58869)	410
4.40. <i>Micrurus ephippifer</i> (UTA R-64863)	411
4.41. <i>Micrurus filiformis</i> (UTA R-3423)	412
4.42. <i>Micrurus filiformis</i> (UTA R-65836)	413
4.43. <i>Micrurus fulvius</i> (UTA R-61632)	414
4.44. <i>Micrurus helleri</i> (UTA R-38005)	415

4.45. <i>Micrurus helleri</i> (UTA R-55977)	416
4.46. <i>Micrurus helleri</i> (UTA R-65841)	417
4.47. <i>Micrurus hemprichii</i> (UTA R-9683)	418
4.48. <i>Micrurus hemprichii</i> (UTA R-29997)	419
4.49. <i>Micrurus isozonus</i> (UTA R-3951)	420
4.50. <i>Micrurus isozonus</i> (UTA R-22589)	421
4.51. <i>Micrurus laticollaris</i> (UTA R-52559)	422
4.52. <i>Micrurus laticollaris</i> (UTA R-57562)	423
4.53. <i>Micrurus latifasciatus</i> (UTA R-4606)	424
4.54. <i>Micrurus lemniscatus</i> cf. <i>helleri</i> (UTA R-34563)	425
4.55. <i>Micrurus lemniscatus</i> cf. <i>helleri</i> (UTA R-65803)	426
4.56. <i>Micrurus limbatus</i> (UTA R-64852)	427
4.57. <i>Micrurus limbatus</i> (UTA R-64899)	428
4.58. <i>Micrurus melanotus</i> (AMNH 35934)	429
4.59. <i>Micrurus melanotus</i> (UTA R-22582)	430
4.60. <i>Micrurus mipartitus</i> (UTA R-54187)	431
4.61. <i>Micrurus mosquitensis</i> (UTA R-12919)	432
4.62. <i>Micrurus nattereri</i> (UTA R-3594)	433
4.63. <i>Micrurus nattereri</i> (UTA R-54175)	434
4.64. <i>Micrurus nattereri</i> (UTA R-55086)	435
4.65. <i>Micrurus nattereri</i> (UTA R-60727)	436
4.66. <i>Micrurus nigrocinctus zunilensis</i> (UTA R-64858)	437
4.67. <i>Micrurus obscurus</i> (UTA R-3840)	438

4.68. <i>Micrurus oliveri</i> (UTA R-64893)	439
4.69. <i>Micrurus ornatissimus</i> (UTA R-60724)	440
4.70. <i>Micrurus pyrrhocryptus</i> (UTA R-51404)	441
4.71. <i>Micrurus renjifoi</i> (UTA R-3490)	442
4.72. <i>Micrurus serranus</i> (UTA R-34561)	443
4.73. <i>Micrurus steindachneri</i> (AMNH 28846)	444
4.74. <i>Micrurus steindachneri</i> (AMNH 35819)	445
4.75. <i>Micrurus surinamensis</i> (UTA R-5849)	446
4.76. <i>Micrurus surinamensis</i> (UTA R-15679)	447
4.77. <i>Micrurus surinamensis</i> (UTA R-50173)	448
4.78. <i>Micrurus surinamensis</i> (UTA R-54378)	449
4.79. <i>Micrurus surinamensis</i> (UTA R-65798)	450
4.80. <i>Micrurus surinamensis</i> (UTA R-65844)	451
4.81. <i>Micrurus tener</i> (UTA R-63282)	452
4.82. <i>Naja annulata</i> (UTA R-18199)	453
4.83. <i>Naja christyi</i> (UTA R-18200)	454
4.84. <i>Naja siamensis</i> (UTA R-16872)	455
4.85. <i>Ophiophagus hannah</i> (UTA R-60836)	456
4.86. <i>Oxyuranus scutellatus</i> (UTA R-60839)	457
4.87. <i>Prosymna stuhlmanni</i> (UTA R-64493)	458
4.88. <i>Pseudohaje goldii</i> (UTA R-63636)	459
4.89. <i>Sinomicrurus boettgeri</i> (UTA R-58837)	460
4.90. <i>Sinomicrurus kelloggi</i> (ROM 37079)	461

4.91. <i>Sinomicrurus peinani</i> (ROM 37109)	462
4.92. <i>Sinomicrurus swinhoei</i> (MVZ 23876)	463
4.93. <i>Walterinnesia aegyptia</i> (UTA R-13021)	464
Supplemental Figure 5. Dorsal, lateral, ventral, anterior, and posterior views	
(A-E, respectively) of the caudal vertebra of the given specimen	465
5.1. <i>Acanthophis antarcticus</i> (UTA R-7623)	465
5.2. <i>Bungarus candidus</i> (UTA R-65799)	466
5.3. <i>Bungarus flaviceps</i> (UTA R-62257)	467
5.4. <i>Calliophis beddomei</i> (MNHN 46-81)	468
5.5. <i>Calliophis bibroni</i> (CAS 17268)	469
5.6. <i>Calliophis biliniatus</i> (KU 309511)	470
5.7. <i>Calliophis biliniatus</i> (KU 311415)	471
5.8. <i>Calliophis bivirgatus bivirgatus</i> (UTA R-63079)	472
5.9. <i>Calliophis intestinalis</i> (UTA R-60738)	473
5.10. <i>Calliophis intestinalis immaculata</i> (UTA R-65802)	474
5.11. <i>Calliophis intestinalis lineata</i> (UTA R-65801)	475
5.12. <i>Calliophis maculiceps</i> (MNHN 5459)	476
5.13. <i>Calliophis melanurus</i> (MNHN 46-286)	477
5.14. <i>Calliophis nigrescens</i> (CAS 17265)	478
5.15. <i>Calliophis philippinus</i> (KU 310369)	479
5.16. <i>Calliophis philippinus</i> (KU 314913)	480
5.17. <i>Dendroaspis angusticeps</i> (UTA R-34982)	481
5.18. <i>Elapsoidea nigra</i> (CAS 168978)	482

5.19. <i>Hemachatus haemachatus</i> (UTA R-7431)	483
5.20. <i>Hemibungarus calligaster</i> (KU 307474)	484
5.21. <i>Hydrophis platurus</i> (UTA R-41049)	485
5.22. <i>Hydrophis schistosus</i> (UTA R-63074)	486
5.23. <i>Laticauda colubrina</i> (UTA R-65800)	487
5.24. <i>Laticauda laticauda</i> (UTA R-6355)	488
5.25. <i>Micrelaps vaillanti</i> (CAS 169941)	489
5.26. <i>Micrurus allenii</i> (UTA R-60556)	490
5.27. <i>Micrurus ancoralis</i> (UTA R-55945)	491
5.28. <i>Micrurus apiatus</i> (UTA R-39267)	492
5.29. <i>Micrurus apiatus</i> (UTA R-39554)	493
5.30. <i>Micrurus apiatus</i> (UTA R-53450)	494
5.31. <i>Micrurus bocourti</i> (UTA R-58145)	495
5.32. <i>Micrurus diastema</i> (UTA R-52565)	496
5.33. <i>Micrurus disssoleucus</i> (UTA R-54184)	497
5.34. <i>Micrurus distans</i> (UTA R-14471)	498
5.35. <i>Micrurus diutius</i> (UTA R-20756)	499
5.36. <i>Micrurus diutius</i> (UTA R-54182)	500
5.37. <i>Micrurus dumerilii</i> (AMNH 35951)	501
5.38. <i>Micrurus elegans elegans</i> (MZFC 18819)	502
5.39. <i>Micrurus elegans veraepacis</i> (UTA R-58869)	503
5.40. <i>Micrurus ephippifer</i> (UTA R-64863)	504
5.41. <i>Micrurus filiformis</i> (UTA R-3423)	505

5.42. <i>Micrurus filiformis</i> (UTA R-65836)	506
5.43. <i>Micrurus fulvius</i> (UTA R-61632)	507
5.44. <i>Micrurus helleri</i> (UTA R-38005)	508
5.45. <i>Micrurus helleri</i> (UTA R-55977)	509
5.46. <i>Micrurus hemprichii</i> (UTA R-9683)	510
5.47. <i>Micrurus hemprichii</i> (UTA R-29997)	511
5.48. <i>Micrurus isozonus</i> (UTA R-3951)	512
5.49. <i>Micrurus isozonus</i> (UTA R-22589)	513
5.50. <i>Micrurus laticollaris</i> (UTA R-52559)	514
5.51. <i>Micrurus laticollaris</i> (UTA R-57562)	515
5.52. <i>Micrurus latifasciatus</i> (UTA R-4606)	516
5.53. <i>Micrurus lemniscatus</i> cf. <i>helleri</i> (UTA R-34563)	517
5.54. <i>Micrurus lemniscatus</i> cf. <i>helleri</i> (UTA R-65803)	518
5.55. <i>Micrurus limbatus</i> (UTA R-64852)	519
5.56. <i>Micrurus limbatus</i> (UTA R-64899)	520
5.57. <i>Micrurus melanotus</i> (AMNH 35934)	521
5.58. <i>Micrurus melanotus</i> (UTA R-22582)	522
5.59. <i>Micrurus mipartitus</i> (UTA R-54187)	523
5.60. <i>Micrurus mosquitensis</i> (UTA R-12919)	524
5.61. <i>Micrurus nattereri</i> (UTA R-3594)	525
5.62. <i>Micrurus nattereri</i> (UTA R-60727)	526
5.63. <i>Micrurus nigrocinctus zunilensis</i> (UTA R-64858)	527
5.64. <i>Micrurus obscurus</i> (UTA R-3840)	528

5.65. <i>Micrurus oliveri</i> (UTA R-64893)	529
5.66. <i>Micrurus ornatissimus</i> (UTA R-60724)	530
5.67. <i>Micrurus pyrrhocryptus</i> (UTA R-51404)	531
5.68. <i>Micrurus renjifoi</i> (UTA R-3490)	532
5.69. <i>Micrurus serranus</i> (UTA R-34561)	533
5.70. <i>Micrurus steindachneri</i> (AMNH 28846)	534
5.71. <i>Micrurus steindachneri</i> (AMNH 35819)	535
5.72. <i>Micrurus surinamensis</i> (UTA R-5849)	536
5.73. <i>Micrurus surinamensis</i> (UTA R-15679)	537
5.74. <i>Micrurus surinamensis</i> (UTA R-50173)	538
5.75. <i>Micrurus surinamensis</i> (UTA R-54378)	539
5.76. <i>Micrurus surinamensis</i> (UTA R-65798)	540
5.77. <i>Micrurus surinamensis</i> (UTA R-65844)	541
5.78. <i>Micrurus tener</i> (UTA R-63282)	542
5.79. <i>Naja annulata</i> (UTA R-18199)	543
5.80. <i>Naja christyi</i> (UTA R-18200)	544
5.81. <i>Naja siamensis</i> (UTA R-16872)	545
5.82. <i>Ophiophagus hannah</i> (UTA R-60836)	546
5.83. <i>Oxyuranus scutellatus</i> (UTA R-60839)	547
5.84. <i>Prosymna stuhlmanni</i> (UTA R-64493)	548
5.85. <i>Pseudohaje goldii</i> (UTA R-63636)	549
5.86. <i>Sinomicrurus annularis</i> (ROM 31158)	550
5.87. <i>Sinomicrurus boettgeri</i> (UTA R-58837)	551

5.88. <i>Sinomicrurus kelloggi</i> (ROM 37079)	552
5.89. <i>Sinomicrurus maccolellandi</i> (CAS 17267)	553
5.90. <i>Sinomicrurus peinani</i> (ROM 37109)	554
5.91. <i>Sinomicrurus swinhoei</i> (MVZ 23876)	555
5.92. <i>Walterinnesia aegyptia</i> (UTA R-13021)	556
Supplemental Figure 6. PCA of the skull, utilizing all specimens, colored by ATS.	
Numbering corresponds with Table 2.1.....	557
Supplemental Figure 7. PCA of the skull conducted on the coralsnake subset, colored by	
ATS. Numbering corresponds with Table 2.1.....	558
Supplemental Figure 8. PCA of the skull of the semi-aquatic and aquatic subset (>5	
ATS), colored by ATS. Numbering corresponds with Table 2.1.....	559
Supplemental Figure 9. PCA of the premaxilla module, utilizing all specimens, colored	
by ATS. Numbering corresponds with Table 2.1.....	560
Supplemental Figure 10. PCA of the premaxilla module conducted on the coralsnake	
subset, colored by ATS. Numbering corresponds with Table 2.1.....	561
Supplemental Figure 11. PCA of the premaxilla module conducted on the semi-aquatic	
and aquatic subset (>5 ATS), colored by ATS. Numbering corresponds with Table	
2.1.....	562
Supplemental Figure 12. PCA of the septomaxilla and vomer module, utilizing all	
specimens, colored by ATS. Numbering corresponds with Table 2.1.....	563
Supplemental Figure 13. PCA of the septomaxilla and vomer module conducted on the	
coralsnake subset, colored by ATS. Numbering corresponds with Table 2.1.....	564

Supplemental Figure 14. PCA of the septomaxilla and vomer module conducted on the semi-aquatic and aquatic subset (>5 ATS), colored by ATS. Numbering corresponds with Table 2.1.....	565
Supplemental Figure 15. PCA of the nasal module, utilizing all specimens, colored by ATS. Numbering corresponds with Table 2.1.....	566
Supplemental Figure 16. PCA of the nasal module conducted on the coralsnake subset, colored by ATS. Numbering corresponds with Table 2.1.....	567
Supplemental Figure 17. PCA of the nasal module conducted on the semi-aquatic and aquatic subset (>5 ATS), colored by ATS. Numbering corresponds with Table 2.1.....	568
Supplemental Figure 18. PCA of the prefrontal module, utilizing all specimens, colored by ATS. Numbering corresponds with Table 2.1.....	569
Supplemental Figure 19. PCA of the prefrontal module conducted on the coralsnake subset, colored by ATS. Numbering corresponds with Table 2.1.....	570
Supplemental Figure 20. PCA of the prefrontal module conducted on the semi-aquatic and aquatic subset (>5 ATS), colored by ATS. Numbering corresponds with Table 2.1.....	571
Supplemental Figure 21. PCA of the frontal module, utilizing all specimens, colored by ATS. Numbering corresponds with Table 2.1.....	572
Supplemental Figure 22. PCA of the frontal module conducted on the coralsnake subset, colored by ATS. Numbering corresponds with Table 2.1.....	573
Supplemental Figure 23. PCA of the frontal module conducted on the semi-aquatic and aquatic subset (>5 ATS), colored by ATS. Numbering corresponds with Table 2.1.....	574

Supplemental Figure 24. PCA of the parietal module, utilizing all specimens, colored by ATS. Numbering corresponds with Table 2.1.....	575
Supplemental Figure 25. PCA of the parietal module conducted on the coralsnake subset, colored by ATS. Numbering corresponds with Table 2.1.....	576
Supplemental Figure 26. PCA of the parietal module conducted on the semi-aquatic and aquatic subset (>5 ATS), colored by ATS. Numbering corresponds with Table 2.1.....	577
Supplemental Figure 27. PCA of the supraoccipital module, utilizing all specimens, colored by ATS. Numbering corresponds with Table 2.1.....	578
Supplemental Figure 28. PCA of the supraoccipital module conducted on the coralsnake subset, colored by ATS. Numbering corresponds with Table 2.1.....	579
Supplemental Figure 29. PCA of the supraoccipital module conducted on the semi-aquatic and aquatic subset (>5 ATS), colored by ATS. Numbering corresponds with Table 2.1.....	580
Supplemental Figure 30. PCA of the prootic module utilizing all specimens, colored by ATS. Numbering corresponds with Table 2.1.....	581
Supplemental Figure 31. PCA of the prootic module conducted on the coralsnake subset, colored by ATS. Numbering corresponds with Table 2.1.....	582
Supplemental Figure 32. PCA of the prootic module conducted on the semi-aquatic and aquatic subset (>5 ATS), colored by ATS. Numbering corresponds with Table 2.1.....	583
Supplemental Figure 33. PCA of the exoccipital module utilizing all specimens, colored by ATS. Numbering corresponds with Table 2.1.....	584
Supplemental Figure 34. PCA of the exoccipital module conducted on the coralsnake subset, colored by ATS. Numbering corresponds with Table 2.1.....	585

Supplemental Figure 35. PCA of the exoccipital module conducted on the semi-aquatic and aquatic subset (>5 ATS), colored by ATS. Numbering corresponds with Table 2.1.....	586
Supplemental Figure 36. PCA of the supratemporal module utilizing all specimens, colored by ATS. Numbering corresponds with Table 2.1.....	587
Supplemental Figure 37. PCA of the supratemporal module conducted on the coralsnake subset, colored by ATS. Numbering corresponds with Table 2.1.....	588
Supplemental Figure 38. PCA of the supratemporal module conducted on the semi-aquatic and aquatic subset (>5 ATS), colored by ATS. Numbering corresponds with Table 2.1.....	589
Supplemental Figure 39. PCA of the basisphenoid module utilizing all specimens, colored by ATS. Numbering corresponds with Table 2.1.....	590
Supplemental Figure 40. PCA of the basisphenoid module conducted on the coralsnake subset, colored by ATS. Numbering corresponds with Table 2.1.....	591
Supplemental Figure 41. PCA of the basisphenoid module conducted on the semi-aquatic and aquatic subset (>5 ATS), colored by ATS. Numbering corresponds with Table 2.1.....	592
Supplemental Figure 42. PCA of the basioccipital module utilizing all specimens, colored by ATS. Numbering corresponds with Table 2.1.....	593
Supplemental Figure 43. PCA of the basioccipital module conducted on the coralsnake subset, colored by ATS. Numbering corresponds with Table 2.1.....	594

Supplemental Figure 44. PCA of the basioccipital module conducted on the semi-aquatic and aquatic subset (>5 ATS), colored by ATS. Numbering corresponds with Table 2.1.....	595
Supplemental Figure 45. PCA of the maxilla and palatine module utilizing all specimens, colored by ATS. Numbering corresponds with Table 2.1.....	596
Supplemental Figure 46. PCA of the maxilla and palatine module conducted on the coralsnake subset, colored by ATS. Numbering corresponds with Table 2.1.....	597
Supplemental Figure 47. PCA of the maxilla and palatine module conducted on the semi-aquatic and aquatic subset (>5 ATS), colored by ATS. Numbering corresponds with Table 2.1.....	598
Supplemental Figure 48. PCA of the ectopterygoid module, utilizing all specimens, colored by ATS. Numbering corresponds with Table 2.1.....	599
Supplemental Figure 49. PCA of the ectopterygoid module conducted on the coralsnake subset, colored by ATS. Numbering corresponds with Table 2.1.....	600
Supplemental Figure 50. PCA of the ectopterygoid module conducted on the semi-aquatic and aquatic subset (>5 ATS), colored by ATS. Numbering corresponds with Table 2.1.....	601
Supplemental Figure 51. PCA of the pterygoid module utilizing all specimens, colored by ATS. Numbering corresponds with Table 2.1.....	602
Supplemental Figure 52. PCA of the pterygoid module conducted on the coralsnake subset, colored by ATS. Numbering corresponds with Table 2.1.....	603

Supplemental Figure 53. PCA of the pterygoid module conducted on the semi-aquatic and aquatic subset (>5 ATS), colored by ATS. Numbering corresponds with Table 2.1.....	604
Supplemental Figure 54. PCA of the quadrate dataset utilizing all specimens, colored by ATS. Numbering corresponds with Table 2.1.....	605
Supplemental Figure 55. PCA of the quadrate dataset conducted on the coralsnake subset, colored by ATS. Numbering corresponds with Table 2.1.....	606
Supplemental Figure 56. PCA of the quadrate dataset conducted on the semi-aquatic and aquatic subset (>5 ATS), colored by ATS. Numbering corresponds with Table 2.1.....	607
Supplemental Figure 57. PCA of the jaw utilizing all specimens, colored by ATS. Numbering corresponds with Table 2.1.....	608
Supplemental Figure 58. PCA of the jaw conducted on the coralsnake subset, colored by ATS. Numbering corresponds with Table 2.1.....	609
Supplemental Figure 59. PCA of the jaw conducted on the semi-aquatic and aquatic subset (>5 ATS), colored by ATS. Numbering corresponds with Table 2.1.....	610
Supplemental Figure 60. PCA of the compound module utilizing all specimens, colored by ATS. Numbering corresponds with Table 2.1.....	611
Supplemental Figure 61. PCA of the compound module conducted on the coralsnake subset, colored by ATS. Numbering corresponds with Table 2.1.....	612
Supplemental Figure 62. PCA of the compound module conducted on the semi-aquatic and aquatic subset (>5 ATS), colored by ATS. Numbering corresponds with Table 2.1.....	613

Supplemental Figure 63. PCA of the dentary, angular, and splenial module utilizing all specimens, colored by ATS. Numbering corresponds with Table 2.1	614
Supplemental Figure 64. PCA of the dentary, angular, and splenial module conducted on the coralsnake subset, colored by ATS. Numbering corresponds with Table 2.1.....	615
Supplemental Figure 65. PCA of the dentary, angular, and splenial module conducted on the semi-aquatic and aquatic subset (>5 ATS), colored by ATS. Numbering corresponds with Table 2.1.....	616
Supplemental Figure 66. PCA of the midbody vertebra dataset, utilizing all specimens, colored by ATS. Numbering corresponds with Table 2.1.....	617
Supplemental Figure 67. PCA of the midbody vertebra dataset conducted on the coralsnake subset, colored by ATS. Numbering corresponds with Table 2.1.....	618
Supplemental Figure 68. PCA of the midbody vertebra dataset conducted on the semi-aquatic and aquatic subset (>5 ATS), colored by ATS. Numbering corresponds with Table 2.1.....	619
Supplemental Figure 69. PCA of the caudal vertebra dataset, utilizing all specimens, colored by ATS. Numbering corresponds with Table 2.1.....	620
Supplemental Figure 70. PCA of the caudal vertebra dataset conducted on the coralsnake subset, colored by ATS. Numbering corresponds with Table 2.1.....	621
Supplemental Figure 71. PCA of the caudal vertebra dataset conducted on the semi-aquatic and aquatic subset (>5 ATS), colored by ATS. Numbering corresponds with Table 2.1.....	622

LIST OF TABLES

Chapter 1

Table 1.1. Time calibrated divergences of Elapid clades from recent studies. Asterisks denote divergences approximated from figures rather than stated by a given author. Dates given in millions of years ago.....	15
---	----

Table 1.2. Aquatic tendency score (ATS), generalized range, diet information and references for diet and habit for a selection of Elapids. Where Aus = Australia, Ind = Indonesia, SEA = South East Asia, NA = North America, CA = Central America, SA = South America, PNG = Papua New Guinea, ME = Middle East, and NC = New Caledonia.	16
--	----

Table 1.3. Description of the aquatic tendency score (ATS) ratings.	29
--	----

Chapter 2

Table 2.1. Specimens used in this study.	55
Table 2.2. Regions of the skull used in this study.	59
Table 2.3. Landmarks and semi-landmark curves of the skull.	60
Table 2.4. Model structures evaluated for modularity of the skull dataset.	62
Table 2.5. Landmarks and semi-landmark curves of the quadrate.	66
Table 2.6. Regions of the lower jaw used in this study.	66
Table 2.7. Landmarks and semi-landmark curves of the lower jaw.	66
Table 2.8. Model structures evaluated for modularity of the lower jaw.	67
Table 2.9. Landmarks and semi-landmark curves of the midbody vertebrae.	67
Table 2.10. Landmarks and semi-landmark curves of the caudal vertebrae.	68

Appendix

Supplemental Table 1. GenBank accession numbers of specimens used in phylogenetic tree creation.....	623
--	-----

CHAPTER ONE

Introduction to Family Elapidae

INTRODUCTION

Elapidae is a diverse family of venomous snakes with over 380 currently recognized species distributed among 53 genera (Uetz and Etzold 1996). It is suggested that the crown elapid diversification occurred 30-38 Mya with an initial distribution in Asia while at present, elapids are widely distributed with species naturally occurring on all continents excluding Europe and Antarctica (Smart 2016; Lee et al. 2016; Zaher et al. 2019; White 1996). Elapidae is either sister to a monophyletic (Pyron et al. 2013), or nested within a paraphyletic (Figueroa et al. 2016; Zheng and Wiens 2016; Zaher et al. 2019), Lamprophiidae.

Elapids vary in habit—from the pelagic sea snake (*Hydrophis platurus*) with the broadest distribution of any snake from the eastern shores of Africa, across the pacific to the western shores of the Americas to the desert dwelling Sonoran coral snake (*Micruroides euryxanthus*)—and in diet, with the former only eating fish and the latter eating snakes and lizards. Cannibalism has been reported in numerous species of *Micrurus* and arboreal mambas (*Dendroaspis*) typically feed on birds and other small mammals. There is a spectrum of aquatic behavior for which we have developed the aquatic tendency score (ATS) to help stratify this behavior.

This behavior is linked directly to the morphological traits of the skull, jaw, and vertebrae in Elapids. This morphologically disparate family varies from semi-fossorial Southeast Asian coralsnakes (e.g., *Sinomicrurus swinhoei*) with anteroposteriorly elongated midbody vertebrae that nearly lack a neural spine to the pelagic sea snake (*Hydrophis platurus*) with a large narrow neural spine (Supplemental Figures 4.20, 4.92).

In this study we use high density 3D geometric morphometrics on 22 bones across five datasets that make up the skull and body to explore phylogenetically informed patterns of external shape variation and modularity. Focusing on the diverse family of Elapidae, this study aims to investigate the multiple within-family aquatic origins to identify morphological similarities.

TAXONOMY

Historical higher level elapid relationships were reviewed in depth by Nock (2001). At the inception the family Elapidae, terrestrial and aquatic proteroglyphs were grouped in separate families Elapidae and Hydrophiidae, respectively (Boie 1827). Elapinae and Hydrophiinae were erected in Colubridae to delineate terrestrial proteroglyphs from aquatic proteroglyphs by Boulenger (1896). Elapidae and Hydrophiidae were elevated to family by Smith (1926), with Hydrophiidae containing two subfamilies, Hydrophiinae and Laticaudinae. Marine elapids and terrestrial elapids were placed in Elapidae as Hydrophiinae and Elapinae by Dowling (1959). This nominal organization was confirmed by McDowell (1970) but the included species in each group were no longer based on aquatic affinity. The division was based on the kinesis and shape of the palatine. Hydrophiinae, described as palatine draggers, included sea snakes excluding *Laticauda* and all Australian terrestrial elapids. Elapinae, described as palatine erectors, included *Laticauda* and all other elapids. Smith *et al.* (1977) extrapolated from McDowell and resurrected Hydrophiidae as palatine draggers with two subfamilies: Oxyurinae, terrestrial palatine draggers, and Hydrophiinae, true seasnakes. Elapidae was divided into two subfamilies: Bungarinae, cobras, and Elapinae, coralsnakes and *Laticauda*. Slowinski *et al.* (1997) reverted to Dowling's (1959) nomenclature while acknowledging the work of McDowell (1970) and Smith *et al.* (1977)

by including Australian terrestrial elapids in Hydrophiinae.: At present there are three valid subfamilies of Elapidae: paraphyletic Elapinae, which includes coralsnakes, cobras, terrestrial kraits, and their kin, Laticaudinae, solely containing *Laticauda*, and Hydrophiinae, which contains true seasnakes and Australian terrestrial elapids (ITIS 2021). In confirming the placement of *Hemibungarus* as within the cobra clade, Castoe *et al.* (2007) devised a new tribal organization for within Elapinae: Calliophini, containing all coralsnakes, and Hemibungarini, containing terrestrial kraits, cobras, and all other elapids endemic to Africa. Despite both being found to be paraphyletic in recent years (Pyron *et al.* 2013; Figueroa *et al.* 2016; Lee *et al.* 2016; Zaher *et al.* 2019), the terms are still infrequently used (e.g., Smart 2016).

The organization within Elapidae is largely consistent between five recent large-scale phylogenies (Pyron *et al.* 2013; Figueroa *et al.* 2016; Lee *et al.* 2016; Zheng and Wiens 2016; Zaher *et al.* 2019). Concordant with these studies, Elapidae can be split into seven monophyletic groups: *Calliophis*, true coralsnakes (*Micrurus*, *Micruroides*, and *Sinomicrurus*), cobras and their kin (*Naja*, *Heamachatus*, *Aspidelaps*, *Dendroaspis*, *Ophiophagus*, and *Hemibungarus*), African garter snakes (*Elapsoidea*), terrestrial kraits (*Bungarus*), sea kraits (*Laticauda*), and true sea snakes including terrestrial Australian elapids (Hydrophiinae). Australasian elapids (Hydrophiinae) have been consistently shown to be monophyletic and are the best supported clade within Elapidae (Slowinski *et al.* 1997; Keogh 1998; Slowinski and Keogh 2000; Slowinski and Lawson 2005). *Bungarus* was found to be paraphyletic by Zaher *et al.* (2019) with *Bungarus flaviceps* as sister to the American coralsnake clade whereas Pyron *et al.* (2013), Figueroa *et al.* (2016), Lee *et al.* (2016), and Zheng and Wiens (2016) all recovered *Bungarus* as monophyletic. Two samples of *Aspidelaps*, *A. lubricus* and *A. scutatus* were only used by Figueroa *et al.* (2016) and Zaher *et al.* (2019) which were recovered as paraphyletic with the

cobra clade and monophyletic, respectively. Lee *et al.* (2016) was the only to find *Calliophis* to be monophyletic. Pyron *et al.* (2013) and Zheng and Wiens (2016) included the same two species as Lee *et al.* (2016), *C. melanurus* and *C. bivirgatus*, and recovered *C. melanurus* as basal to all other elapids and *C. bivirgatus* nested within, but basal to, all other coral snakes. Figueroa *et al.* (2016) had increased sampling of *Calliophis* but did not include *C. bivirgatus*. *Calliophis* was recovered as paraphyletic with *C. sp.* being nested within *Sinomicrurus*. Zaher *et al.* (2019) included *C. bivirgatus* and four additional species of *Calliophis*. *Calliophis* was recovered as sister to all other elapids but not monophyletic. *C. bivirgatus* was more closely related to all other elapids rather than the clade formed by the remaining *Calliophis*. Monophyly of *Calliophis* was recovered with high support with increased sampling focused on Asian coralsnakes (Smart 2016).

PALEOBIOGROGRAPHY AND EVOLUTION OF BASAL ELAPIDS

Multiple attempts have been made to corroborate genetic evidence with the limited fossil evidence in existence. Despite varying methods and scope, the results are broadly congruent, and have the crown elapid radiation taking place in the late-Eocene/early-Oligocene (Table 1.1). Wüster *et al.* (2007) is the exception to the agreement with all dates of divergence being consistently older than other studies reviewed.

These time calibrated trees help support the biogeographic hypothesis of an Asian origin of Elapidae, which has been provisional due to the lack of resolution at the base of the tree (Keogh 1998; Kelly *et al.* 2009; Smart 2016). A well resolved basal elapid phylogeny is presented by Smart (2016) who goes on to describe the roughly seven million yearlong elapid dispersal as a series of events from Asia. The divergence of basal elapids (~28 mya; Kelly *et al.*

2009; Smart 2016) corresponds with estimates of the ‘hard’ collision of the Indian plate with the Laurasian (20-35 mya; Aitchison et al. 2007; Ali and Aitchison 2008; van Hinsbergen et al. 2012; van Hinsbergen et al. 2019). The source of ancestral elapids in India was likely Sundaland, assuming ancestral elapids inhabited forests like most extant *Calliophis* (Smart 2016), as both areas were megathermal monsoonal forests at the time (Morley 2011).

The divergence of Australasian elapids (~25 mya, Table 1.1) is in line with the geologic record. Tectonic reconstructions provide evidence for the first collision between the Australian continent with Southeast Asia occurring between 25 and 20 mya (Sparkman and Hall 2010; Hall 2011, 2012). This collision is the likely impetus of the dispersal to the Australian continent and rapid diversification of Australasian elapids (Tyler 1979; Cogger and Heatwole 1981; Schwaner et al. 1985; Dessauer et al. 1987; Cadle 1987, 1988; Smart 2016). This rapid radiation could explain the regional dominance of Elapids (Scanlon et al. 2003).

Environmental changes rather than tectonic events seem to be the cause of diversification and dispersal of elapids into the New World. Recent paleoclimate reconstructions based on paleobotanical evidence show bands of boreotropical and warm temperate forest stretching from the Atlantic coast of Europe to the Pacific coast of Asia and continuing to the northern latitudes of the New World from the Oligocene to the late Miocene (Boucot et al. 2013; Meseguer et al. 2015). There was an expansive arid zone south of the boreotropical band that would have cut off this East-West corridor from tropical Southeast Asia if it were not for the seasonal monsoonal rains along Asia’s Pacific coast (Crowley 2012). If the most recent common ancestor of coralsnakes had the same proclivity for temperate and tropical forests as modern, the presence of *Micrurus* in Western Europe during the Miocene (Rage and Holman 1984, Ivanov 2000) can be understood. This supports the long-discussed hypothesis that ancestral coralsnakes invaded the

New World by crossing the Bering land Strait (Hoffstetter 1939; Bogert 1943; Darlington 1957; Underwood 1967; Cadle and Sarich 1981; Slowinski et al. 2001; Smart 2016).

Following the elapid invasion of the New World, another clade of elapids dispersed into Africa during two periods of connection between Africa and Eurasia (Smart 2016). The first occurred during the late early Miocene (20-18 mya), when the Mediterranean was cut off from the Indian Ocean for the first time, the African and Arabian plates rotated clockwise and collided with the Anatolian plate (Rögl 1999). This collision formed the *Gomphotherium* landbridge, named after the extinct genus of ancestral elephants, which enabled mammal migration between Eurasia and Africa (Tassy 1990; Rögl 1998, 1999; Popov et al. 2004; Harzhauser et al. 2007). It is thought that during this time stem cobras migrated into Africa (Smart 2016). Briefly during the early middle Miocene (Langhian, 16.4-15 mya), the connection between Eurasian and Africa was severed only to be reconnected later in the middle Miocene (Serravallian, ~14 mya; Rögl 1998, 1999; Popov et al. 2004). After the reconnection, derived cobras backdispersed into Asia to gain their modern distribution (Smart 2016). It is speculated by Smart (2016) that there was a second migration of elapids from Asia into Africa (~16 mya), when the most recent common ancestor of *Dendroaspis* (mambas) diverged from the clade containing Asian lineages, *Ophiophagus* (king cobra) and *Hemibungarus* (Philippine False Coral Snakes). Due to poor resolution and inconsistent tree topologies of these nodes this cannot be stated with much certainty (Smart 2016).

TRENDS OF LIFE HISTORY

With such a widely distributed family as Elapidae, the behavior and habits are equally diverse. From the large arboreal eastern green mamba in Africa (*Dendroaspis angusticeps*) to the

widely distributed yellow-bellied sea snake (*Hydrophis platurus*) to the diminutive fossorial Indian coralsnake (*Calliophis melanurus*), elapids are broadly represented in terms of distribution, lifestyle, and diet. The information in Table 1.2 was compiled to aid in analyses in subsequent chapters and summarizes much of what is known about the diet and provides references for life history information of a selection of elapids.

Determination of habit (e.g., terrestrial, semi-aquatic, arboreal, etc.) for a given species proved to be a difficult task due to lack of information on numerous secretive snakes and conflicting or vague statements of different authors. Some texts made specific claims to the habit of species covered (Valencia et al. 2016) while others made sweeping claims pertaining to an entire genus rather than each species (Cogger 2018), and others still made no determination but provided information left up to interpretation (Campbell and Lamar 1989). In addition, habit is difficult to delineate as there are not clear distinctions between groupings as some straddle the line between two categories that the addition of ‘semi-’ to the grouping would still be insufficient. Take *Micrurus dumerilii* for example, by all accounts it is semi-fossorial (Campbell and Lamar 1989, 2004; Valencia et al. 2016) but has been documented eating synbranchid eels in addition to lizards and caecilians (Schmidt 1932; Herrera-Lopera et al. 2018).

To overcome this challenge, the terrestrial elevation (arboreal, terrestrial, fossorial) of a species was separated from its habits associated with water. We developed a 1-10 scale to classify each species by degree of aquatic affinity, dubbed the aquatic tendency score (ATS). The ATS takes the form of reproduction, diet, locomotion, general proximity to water and willingness to enter water into account. Scores range from *Acanthophis*, which lacks record of aquatic prey or association with aquatic habitats and is scored as a 1, to *Micrurus surinamensis*, which is oviparous, has terrestrial and aquatic prey, and spends much of its life in water, scored as a 7, to

Hydrophis platurus, which is ovoviviparous, spends all its life in water, and only takes aquatic prey, scored as a 10. Each species in Table 1.2 has been scored according to the scale broken down in Table 1.3. As availability of an aquatic habitat varies across the range of a species, some populations use aquatic habitats more extensively than other populations as a result (Aubret 2004). Because of this, the ATS of a given species is subject to change with more study.

THE SKULL

Origin of the Skull

The skull is a ubiquitous feature in extant vertebrates and it developed during the Cambrian Explosion (Shu et al. 1999). Over the course of the last 525 million years the skull developed through evolutionary stages. The skull was first a cartilaginous complex that facilitated feeding, followed by the cartilaginous chondrocranium, and finally the ossified dermatocranium (Kardong, 2009; Hirasawa and Kuratani 2015; Kaucka and Adameyko 2017). The long period of development has given rise to the plentiful anatomic diversity of skull pattern shapes and sizes, including those of reptiles. The path of vertebrate skull evolution begins with the development of a new head followed by cartilage and bone and continued toward limb growth and terrestriality. Dermal elements were the most plentiful in bony fishes and trends of simplification can be seen in all derived extant lineages (Westoll 1938; Herrel et al. 2007; Schoch 2014). Diversification from this simplification has yielded hyperdiversity in mammals and squamates.

Elapids within the Diversity of Reptilia

Reptiles are on the other side of the amniote tree, with respect to mammals. This group is further broken up into Eureptilia and Parareptilia. Eureptilia are diapsids (dinosaurs, Aves, and squamates) classically grouped together, while the Parareptilia include anapsids (previously including turtles, now considered diapsids; Hedges 2012). The definitions of these groups have stabilized in recent years after much revision with Parareptilia lacking extant taxa and including numerous groups like mesosaurs while Eureptilia contains all reptiles and Aves (Meyer 1857; Cope 1882; Osborn 1903; Williston 1917; Olson 1947; Romer 1956; Tsuji and Müller 2009). The past synonymous use of Parareptilia and Anapsida is erroneous as the current phylogeny includes bolosaurids, among others, which have temporal fenestrations (Reisz et al. 2007; Tsuji and Müller 2009). Under the current definition, Parareptilia is strongly supported by multiple defining characteristics that include the lack of lacrimal-narial contact, a shortened postorbital region, and the absence of a subtemporal process on the jugal (Müller and Tsuji 2007; Tsuji and Müller 2009).

Squamates are united by a plethora of characters reviewed in detail by Gauthier *et al.* (1988) but are largely characterized by their cranial kinesis. This kinesis is exemplified by the most derived skulls of snakes, the most recent common ancestor of which had a small skull adapted for fossoriality (Herrel et al. 2007; da Silva et al. 2018). The reasons for the vast majority of differences in snake skulls are due to their fossorial evolution, limblessness, and their ability to swallow large prey (Greene 1997; Cundall and Irish 2008). In lizards, the lower jaw is the edge of the facial region but in snakes this remains a kinetic and loosely connected collection of elements attached to the brain case (Evans 2008; Cundall and Irish 2008). Snakes are

characterized by the supraoccipital not forming a border with the foramen magnum and other developmental differences (Cundall and Irish 2008).

Skull morphology has been shown to be associated with the diet and ecology of the snake (xenodontine snakes: Klaczko et al. 2016; aquatic snakes: Segall et al. 2020). Where fossorial snake skulls have lateral expansions of the parietal region, a posteriorly extended braincase, and a curved, reduced quadrate (da Silva et al. 2018). Aquatic snakes have a narrower anterior head region to reduce drag during strikes and a larger posterior region of the head to accommodate large prey items, with dorsally positioned nostrils and eyes (Segall et al. 2016) and overall converge on more hydrodynamic designs (Moon et al. 2019). Hydrophiine sea snake dietary preferences drive morphology, with burrowing eel specialists being of the ‘microcephalic’ type with a very thin forebody and longer body length than the burrowing goby specialists that are short with small heads (Sherratt et al. 2018). Natricine piscivorous snakes have longer skulls than frog eating snakes (Vincent et al. 2009; Hampton 2011; Brecko et al. 2011). Long sharp teeth and an elongated lower jaw are also associated with piscivory (Britt et al. 2009). Piscivorous snakes have faster closing jaws, and frog-eating snakes have higher closing forces (Hampton 2011)

Quadrate morphology is extremely plastic regardless of phylogenetic position across the Squamata. This diversity is partly correlated with ecology and particularly fossoriality, and much of the remainder is likely due to dietary preference (Placi et al. 2020). Quadrate length contributes directly to gape size, and the mandible may as well, though it does not contribute to expanding the narrowest part of the oral cavity and may just grow along with other parts of the skull (Hampton and Moon 2012).

The Elapid Skull

Elapids are diverse in the shape of their heads and that diversity extends to the morphology of the skull. There are not many consistent differences between the skulls of the Elapidae and related families other than anterior grooved maxillary fangs (McDowell 1968; McCarthy 1985).

The snout of elapids varies greatly but in most, the nasals have contact with the frontals. This contact typically is between a narrow posterior projection from the nasals to the anteroventral surface of the frontals along the midline. This limited connection between bones facilitates kinesis (Cundall and Irish 2008). The premaxilla varies as much as the nasal frontal joint. In some species, like *Simoselaps bertholdi*, the dorsal extent of the premaxilla touches the nasal and has well developed transverse processes (Supplemental Figure 1.79). In others, as with *Hydrophis schistosus*, the premaxilla is disconnected from the rest of the snout and the transverse processes are much reduced in development (Cundall and Irish 2008; Supplemental Figure 1.23).

As with viperids and colubrids, the braincase of elapids follows a similar scheme most having connected frontals and parietals with many lacking post orbital elements (Underwood and Kochva 1993). The loss of postorbital elements or a reduction in size of the orbital margin may be related to fossoriality. The posterior braincase varies in shape but is consistent in bones present (Cundall and Irish 2008).

Morphology and function of the palatine and maxillary apparatus in hydrophiine snakes, characterized as “palatine dragging” due to the independence of the palatine and pterygoid. Other elapids are characterized as “palatine erecting,” as the maxillae move with the palato-pterygoid

bar to walk prey into the mouth, and the palato-pterygoid joint facilitates the elevation of the rostral maxilla and palatine and caudal pterygoid (Deufel and Cundall 2009).

Osteology-based Morphometric studies

There have been a few recent studies that performed geometric morphometric analyses on elapids. Silva *et al.* (2017) used a low-density 2D approach to investigate the shape variation of the skull mandible and quadrate between aquatic and terrestrial *Micrurus*. *Micrurus surinamensis* was found to have a wider head, smaller nostrils, longer supratemporals and quadrates, and a longer tail than terrestrial species in the genus. This gives it an increased gape for eating fish instead of the elongate prey that is the main diet of other congeners. This contrasts with Rhoda *et al.* (2021), who used a high-density 3D approach to investigate the modularity of the feeding systems in aquatic snakes. Their dataset included *M. surinamensis*, *M. lemniscatus*, one *Laticauda*, four *Hydrophis*, and two other elapids amongst numerous other non-elapids. Their landmark scheme excluded the braincase and snout in their entirety to focus on the suspensorium, lower jaw, quadrate and supratemporal. The most supported groupings of bones are the mandible group and the palatopterygoid arch group (palatine and pterygoid), with the maxilla and quadrate grouped with cranial or mandibular elements.

VERTEBRAE

Broadly, elapids have four types of vertebrae: cervical, trunk, cloacal and caudal. Herein we use midbody vertebrae to describe the trunk vertebrae of the middle third between base of the skull and vent. Elapid vertebrae are comparable to those of colubrids but more substantial (Rage 1984). Three characters were observed by Ikeda (2007) that are exclusive to Elapids: “the neural arch is more depressed than that of colubrids; the zygosphenal articular facets are oval in lateral

view; the subcentral ridge runs straight in lateral view.” The vertebrae of *Bungarus* have an extended neural spine and laterally elongated prezygapophysial and postzygapophysial processes (Hoffsetter 1939), where enlarged zygapophysial processes are diagnostic features of the genus (Slowinski 1994). The vertebrae of *Sinomicrurus* have an almost negligible neural spine and underdeveloped parapophyseal processes (Ikeda 2007). The vertebrae of *Micrurus* and *Micruroides* also have a low neural spine and have well developed paradiapophyses that extend beyond the condyle (Holman 1977). The neural spine is higher in *Micrurus* than in *Micruroides* (Holman 1977).

Sea snakes (Hydrophiinae) have evolved a dorsoventrally elongated cross-sectional body shape achieved by an increase in body height rather than a decrease in width, and sea kraits (*Laticauda*) and other amphibious species exhibit a shape intermediate between sea snakes and the largely circular cross section of terrestrial snakes. The tail is higher and thinner in marine snakes, but it is shorter in length (Brischoux and Shine 2006). Paddle tails may allow sea snakes to maintain position in the water column under increased buoyancy due to the salt water while probing coral reefs for food, possibly explaining the lack of such a feature in non-marine aquatic snakes. Aquatic snakes frequently have closely related fossorial taxa, suggesting that burrowing adaptations aid in colonizing aquatic habitats and/or vice versa (Murphy 2012). Aquatic snakes have variation in vertebral size, with burrowing eel specialists evolving tiny heads and a greater disparity between forebody and hindbody girth as well as possessing more numerous and smaller vertebrae in the forebody region (Sherratt et al 2019; Sherratt and Sanders 2020).

Analysis of the function of the zygosphene-zygantrum joint in snake midbody vertebrae found this as an osseous limit to the range of motion of the vertebral column, especially yaw, preventing injuries to soft tissue if this was responsible for limiting motion (Jurestovsky et al

2020). The spinalis muscle was found to have multiple vertebrae of origin in the vast majority of specimens, including all booids. Low relative segmental length of the spinalis may be indicative of flexibility, aiding in constriction and the contortion of hydrophiids for skin on skin contact to facilitate pelagic shedding (Jayne 1982).

Table 1.1. Time calibrated divergences of Elapid clades from recent studies. Asterisks denote divergences approximated from figures rather than stated by a given author. Dates given in millions of years ago.

Study	Nagy et al. 2003	Wüster et al. 2007	Sanders et al. 2008	Sanders & Lee 2008	Kelly et al. 2009	Lukoschek et al. 2012	Lee et al. 2016	Smart 2016
Scope	Alethinophidia	Alethinophidia	Hydrophiinae	Squamata	Elapoidea	Caenophidi a	Elapida	Alethinophidia
Elapidae	35*			26.2 (32.7-19.5)	37.4 (42.8-32.8)			33.00 (41.97- 27.42)
<i>Calliophis</i>					28.5 (32.5-24.7)	35-18*	38	28.38 (35.46- 23.50)
Coralsnakes		62*			28.5 (32.5-24.7)	24-15*	33*	26.57 (32.47- 21.73)
Cobras and kin	25*	56*			29.5 (33.0-25.9)	30-15*	32*	
Bungararurs					26.1 (30.6-21.4)	18-10*	31*	
<i>Elapoidea</i>		47*			26.1 (30.6-21.4)	24-14*	30*	
Hydrophinae/ <i>Laticauda</i>		46*	12.6 (15.6-10.1)	13.1(18.6-8.3)	23.0 (27.1-18.8)	25-14*	25	26.57 (32.47- 21.73)
<i>Hydrophis</i>			6.2 (7.9-4.7)			14-8*	12*	

Table 1.2. Aquatic tendency score (ATS), generalized range, diet information and references for diet and habit for a selection of Elapids.

Where Aus = Australia, Ind = Indonesia, SEA = South East Asia, NA = North America, CA = Central America, SA = South America, PNG = Papua New Guinea, ME = Middle East, and NC = New Caledonia.

Species	Range	ATS	Habit Reference(s)	Diet	Diet Reference(s)
<i>Acanthophis antarcticus</i>	Aus	1	Cogger 2018	Adults: small mammals & birds; juveniles: reptiles	Cogger 2018
<i>Acanthophis cryptamydros</i>	Aus	1	Cogger 2018		
<i>Acanthophis hawkei</i>	Aus	1	Cogger 2018		
<i>Acanthophis laevis</i>	Ind, PNG	1	Cogger 2018		
<i>Acanthophis praelongus</i>	Ind, Aus	1	Cogger 2018		
<i>Acanthophis pyrrhus</i>	Aus	1	Cogger 2018		
<i>Acanthophis rugosus</i>	Ind, Aus	1	Cogger 2018		
<i>Acanthophis wellsi</i>	Aus	1	Cogger 2018		
<i>Bungarus bungaroides</i>	SEA	2	Whitaker & Captain 2004; Das 2012	Snakes	Whitaker & Captain 2004; Das 2012
<i>Bungarus caeruleus</i>	South Asia	2	Whitaker & Captain 2004	Snakes, lizards, frogs & rodents	Whitaker & Captain 2004
<i>Bungarus candidus</i>	SEA	1	Das 2012; Chan-ard et al. 2015	Snakes, Lizards & toads	Das 2012
<i>Bungarus fasciatus</i>	SEA	4	Whitaker & Captain 2004; Das 2007; Das 2012; Ahmed et al. 2009; Stuebing et al. 2014; Chan-ard et al. 2015	Snakes, lizards, reptile eggs, frogs, rats & fishes	Whitaker & Captain 2004; Das 2007, 2012; Stuebing et al. 2014; Chan-ard et al. 2015
<i>Bungarus flaviceps</i>	SEA	1	Das 2012; Chan-ard et al. 2015	Snakes, lizards & small mammals	Ahmed et al. 2009; Das 2012; Stuebing et al. 2014
<i>Bungarus magnimaculatus</i>	Myanmar	1	Das 2010		
<i>Bungarus multicinctus</i>	SEA	4	Das 2012	Snakes, lizards, frogs, rodents & eels	Das 2012
<i>Bungarus niger</i>	South Asia	1	Whitaker & Captain 2004; Ahmed et al. 2009; Das 2012	Snakes & mammals when in captivity	Whitaker & Captain 2004; Ahmed et al. 2009; Das 2012

Species	Range	ATS	Habit Reference(s)	Diet	Diet Reference(s)
<i>Bungarus walli</i>	South Asia	1	Whitaker & Captain 2004; Das 2010	Snakes when in captivity	Whitaker & Captain 2004
<i>Calliophis beddomei</i>	India	1			
<i>Calliophis bivirgatus</i>	SEA	1	Shankar & Ganesh 2009		
<i>Calliophis biliniatus</i>	Philippines	1	Brown et al. 2018		
<i>Calliophis castoe</i>	India	1	Das 2007; Chanhome et al. 2011; Stuebing et al. 2014; Chan-ard et al. 2015; Brown et al. 2018	Snakes, lizards, frogs & rodents	Das 2007, 2012; Chanhome et al. 2011; Stuebing et al. 2014; Chan-ard et al. 2015
<i>Calliophis gracilis</i>	SEA	1	Tweedie 1983; Das 2010; Chanhome et al. 2011; Chan-ard et al. 2015	Fossorial snakes & lizards	Chanhome et al. 2011
<i>Calliophis haematoetron</i>	Sri Lanka	1	Smith et al. 2008; Silva et al. 2020		
<i>Calliophis intestinalis</i>	SEA	1	Das 2007; Chanhome et al. 2011; Das 2012; Stuebing et al. 2014; Chan-ard et al. 2015; Fukuyama et al. 2020	Fossorial snakes & lizards	Das 2007, 2012; Chanhome et al. 2011; Stuebing et al. 2014; Chan-ard et al. 2015
<i>Calliophis maculiceps</i>	SEA	1	Chanhome et al. 2011; Das 2012; Chan-ard et al. 2015	Snakes	Chanhome et al. 2011; Das 2012; Chan-ard et al. 2015
<i>Calliophis melanurus</i>	South Asia	1	Whitaker & Captain 2004		
<i>Calliophis nigrescens</i>	India	1	Kannan 2006; Lobo 2006	Snakes	Whitaker & Captain 2004; Lobo 2006
<i>Calliophis nigrotaeniatus</i>	SEA	1	EN Smith 2021, pers. comm.	Snakes	EN Smith 2021, pers. comm.
<i>Calliophis philippinus</i>	Philippines	1	Brown et al. 2018		
<i>Calliophis salitan</i>	Philippines	2	Brown et al. 2018		
<i>Calliophis suluensis</i>	Philippines	1	Brown et al. 2018		
<i>Dendroaspis angusticeps</i>	Africa	1	Marais 2004; Spawls et al. 2004, 2006	Birds, eggs, rodents, bats & chameleons	Marais 2004; Spawls et al. 2004, 2006
<i>Dendroaspis jamesoni</i>	Africa	1	Chippaux & Jackson 2019	Adults: birds; juveniles: birds, lizards & toads	Spawls et al. 2006; Chippaux & Jackson 2019
<i>Dendroaspis polylepis</i>	Africa	1	Marais 2004; Spawls et al. 2006; Chippaux & Jackson 2019	Mammals, birds & snakes	Marais 2004; Spawls et al. 2006; Chippaux & Jackson 2019

Species	Range	ATS	Habit Reference(s)	Diet	Diet Reference(s)
<i>Dendroaspis viridis</i>	Africa	1	Chippaux & Jackson 2019	birds	Fuchs et al. 2019
<i>Elapsoidea boulengeri</i>	Africa	1	Marais 2004; Spawls et al. 2004, 2006	Snakes, lizards, frogs & rodents	Marais 2004; Spawls et al. 2004, 2006
<i>Elapsoidea guentherii</i>	Africa	1	Marais 2004; Chippaux & Jackson 2019	Snakes, lizards, amphibians & termites	Marais 2004; Chippaux & Jackson 2019
<i>Elapsoidea laticincta</i>	Africa	1	Spawls et al. 2004; Chippaux & Jackson 2019	Snakes, lizards, amphibians & insects	Spawls et al. 2004; Chippaux & Jackson 2019
<i>Elapsoidea loveridgei</i>	Africa	1	Spawls et al. 2004, 2006; Chippaux & Jackson 2019	Snakes, lizards, amphibians, insects, rodents & reptile eggs	Spawls et al. 2004, 2006; Chippaux & Jackson 2019
<i>Elapsoidea nigra</i>	Tanzania	1	Spawls et al. 2004, 2006	Caecilians	Spawls et al. 2004, 2006
<i>Elapsoidea semiannulata</i>	Africa	1	Marais 2004	Snakes, lizards & amphibians	Marais 2004
<i>Elapsoidea sundevallii</i>	Africa	1	Marais 2004	Snakes, lizards & their eggs, amphibians & mammals	Marais 2004
<i>Elapsoidea trapei</i>	Africa	1	Chippaux & Jackson 2019	Snakes, lizards, amphibians &, insects	Chippaux & Jackson 2019
<i>Hemachatus haemachatus</i>	Africa	1	Marais 2004	Snakes, lizards, rodents, birds & their eggs	Marais 2004
<i>Hemibungarus calligaster</i>	Philippines	2	McLeod et al. 2011		
<i>Hydrophis annandalei</i>	SEA	10	Das 2012; Stuebing et al. 2014	Fishes	Voris 1972; Das 2012; Stuebing et al. 2014
<i>Hydrophis anomalus</i>	SEA	10	Chan-ard et al. 2015	Eels	Voris 1972
<i>Hydrophis atriceps</i>	SEA	10	Das 2010; Stuebing et al. 2014	Eels & invertebrates	Denburgh & Thompson 1908; Das 2010; Stuebing et al. 2014
<i>Hydrophis belcheri</i>	SEA	10	Cogger 1975	Eels	Voris 1972
<i>Hydrophis bituberculatus</i>	SEA	10	Chan-ard et al. 2015	Eels	Chan-ard et al. 2015

Species	Range	ATS	Habit Reference(s)	Diet	Diet Reference(s)
<i>Hydrophis brookii</i>	SEA	10	Stuebing et al. 2014; Chan-ard et al. 2015	Eels	Voris 1972
<i>Hydrophis caerulescens</i>	SEA	10	Whitaker & Captain 2004; Das 2012; Stuebing et al. 2014	Fishes & eels	Voris 1972; Whitaker & Captain 2004; Das 2012; Stuebing et al. 2014
<i>Hydrophis cantoris</i>	SEA	10	Chan-ard et al. 2015	Eels & invertebrates	Chan-ard et al. 2015
<i>Hydrophis coggeri</i>	Aus	10	Cogger 2018		
<i>Hydrophis curtus</i>	SEA	9	Whitaker & Captain 2004; Das 2012; Stuebing et al. 2014	Fishes, eels & squid	Volsøe 1939; Whitaker & Captain 2004; Das 2012; Stuebing et al. 2014
<i>Hydrophis cyanocinctus</i>	SEA	9	Goris 2004; Whitaker & Captain 2004; Das 2012	Fishes, eels & invertebrates	Smith 1935; Volsøe 1939; Voris 1972; Goris 2004; Whitaker & Captain 2004; Das 2012
<i>Hydrophis czeblukovi</i>	Aus	10	Cogger 2018		
<i>Hydrophis donaldi</i>	Aus	10	Cogger 2018		
<i>Hydrophis elegans</i>	Aus	10	Cogger 1975		
<i>Hydrophis fasciatus</i>	SEA	10	Cogger 1975; Das 2012	Eels	Voris 1972; Das 2012
<i>Hydrophis gracilis</i>	SEA	10	Cogger 1975; Das 2012; Chan-ard et al. 2015	Eels	Wall 1921; Volsøe 1939; Voris 1972; Das 2012; Chan-ard et al. 2015
<i>Hydrophis hardwickii</i>	SEA	10	Cogger 1975	Fishes & invertebrates	Smith 1935; Voris 1972
<i>Hydrophis inornatus</i>	SEA	10	Cogger 1975; Chan-ard et al. 2015	Fishes	Voris 1972; Chan-ard et al. 2015
<i>Hydrophis jerdonii</i>	SEA	9	Whitaker & Captain 2004; Chan-ard et al. 2015; Stuebing et al. 2014	Eels	Voris 1972; Whitaker & Captain 2004
<i>Hydrophis kingii</i>	Aus	10	Cogger 1975		
<i>Hydrophis klossi</i>	SEA	10	Chan-ard et al. 2015		
<i>Hydrophis laboutei</i>	NC	10	Cogger 2018		
<i>Hydrophis lamberti</i>	SEA	10	Chan-ard et al. 2015	Catfishes	Das 2010
<i>Hydrophis lapemoides</i>	SEA	10	Chan-ard et al. 2015	Fishes & eels	Volsøe 1939; Das 2010
<i>Hydrophis macdowelli</i>	Aus	10	Cogger 2018		
<i>Hydrophis major</i>	Aus	10	Cogger 1975	Fishes	Voris 1972
<i>Hydrophis melanocephalus</i>	East Asia	10	Goris 2004	Eels	Voris 1972; Goris 2004
<i>Hydrophis melanosoma</i>	SEA	10	Cogger 1975; Chan-ard et al. 2015	Eels	Voris 1972; Chan-ard et al. 2015

Species	Range	ATS	Habit Reference(s)	Diet	Diet Reference(s)
<i>Hydrophis nigroinctus</i>	SEA	10	Chan-ard et al. 2015	Eels	Voris 1972
<i>Hydrophis obscurus</i>	SEA	10	Cogger 1975; Das 2012; Chan-ard et al. 2015	Fishes	Wall 1921
<i>Hydrophis ocellatus</i>	Aus	10	Cogger 2018		
<i>Hydrophis ornatus</i>	SEA	10	Goris 2004; Whitaker & Captain 2004; Das 2012	Fishes & eels	Goris 2004; Whitaker & Captain 2004; Das 2012
<i>Hydrophis pachycercos</i>	SEA	10	Das 2010		
<i>Hydrophis pacificus</i>	SEA	10	Cogger 1975		
<i>Hydrophis parviceps</i>	SEA	10	Das 2010		
<i>Hydrophis peronii</i>	SEA	10	Cogger 1975, 2018; Das 2012	Fishes	Voris 1972; Cogger 1975; Das 2012
<i>Hydrophis platurus</i>	Pacific	10	Gasperetti 1988; Marais 2004; Whitaker & Captain 2004; Das 2012	Fishes	Klawe 1964; Visser 1967; Marais 2004; Whitaker & Captain 2004; Das 2012
<i>Hydrophis schistosus</i>	SEA	10	Cogger 1975; Whitaker & Captain 2004; Das 2012; Stuebing et al. 2014	Fishes & prawns	Volsøe 1939; Minton 1966; Voris 1972; Whitaker & Captain 2004; Das 2012; Stuebing et al. 2014
<i>Hydrophis sibauensis</i>	Ind	10	Das 2012		
<i>Hydrophis spiralis</i>	SEA	10	Das 2012	Eels	Wall 1921; Volsøe 1939; Das 2012
<i>Hydrophis stokesii</i>	SEA	10	Whitaker & Captain 2004	Fishes	Chan-ard et al. 2015
<i>Hydrophis stricticollis</i>	South Asia	10	Das 2010		
<i>Hydrophis torquatus</i>	SEA	10	Stuebing et al. 2014; Chan-ard et al. 2015	Fishes	Voris 1972
<i>Hydrophis viperinus</i>	SEA	10	Das 2012; Stuebing et al. 2014	Fishes, eels & invertebrates	Volsøe 1939; Voris 1972; Das 2012
<i>Hydrophis vorisi</i>	Aus	10	Cogger 2018		
<i>Hydrophis zweifeli</i>	PNG	10	Cogger 2018	Fishes	Cogger 2018
<i>Laticauda colubrina</i>	Pacific	8	Goris 2004; Whitaker & Captain 2004; Das 2007, 2012; Stuebing et al. 2014	Eels	Voris 1972; Whitaker & Captain 2004; Das 2007, 2012; Stuebing et al. 2014
<i>Laticauda laticauda</i>	SEA	8	Goris 2004	Fishes	Goris 2004
<i>Laticauda schistorhyncha</i>	SEA	8	Uetz & Etzold 1996	Fishes	Voris 1972
<i>Laticauda semifasciata</i>	SEA	8	Goris 2004	Fishes	Goris 2004

Species	Range	ATS	Habit Reference(s)	Diet	Diet Reference(s)
<i>Micruroides euryxanthus</i>	NA	1	Campbell & Lamar 1989, 2004; Heimes 2016; Babb & Brennan 2018	Snakes and lizards	Vitt & Hulse 1973; Lowe et al. 1986; Heimes 2016; Babb & Brennan 2018
<i>Micrurus albicinctus</i>	SA	1	Souza et al. 2011	Snakes	Souza et al. 2011
<i>Micrurus aleni</i>	CA	5	Campbell & Lamar 1989, 2004	Eels & lizards	Gaige et al. 1937; Roze 1996; Burger 1997; Solórzano 2004, 2005
<i>Micrurus altirostris</i>	SA	1	Rodriguez et al. 2018		
<i>Micrurus anchoralis</i>	SA	2	Campbell & Lamar 1989; Arteaga et al. 2013; Valencia et al. 2016	Snakes, caecilians & invertebrates	Boulenger 1913; Roze 1996; Cisneros-Heredia 2005; Valencia et al. 2016; Rodriguez et al. 2018
<i>Micrurus annellatus</i>	SA	1	Campbell & Lamar 1989	Snakes & lizards	Schmidt 1954; Roze 1996
<i>Micrurus apiatus</i>	CA	5	EN Smith 2021, pers. comm.	Snakes, lizards, caecilians & eels; cannibalistic	Greene 1973; Seib 1985; Smith 1994; Roze 1996; Campbell 1998; West et al. 2019
<i>Micrurus averyi</i>	SA	1	Campbell & Lamar 1989; Martins & Oliveira 1998	Snakes & lizards	Martins & Oliveira 1998
<i>Micrurus bernardi</i>	Mexico	1	Heimes 2016	Snakes	Roze 1996
<i>Micrurus bocourti</i>	SA	1	Campbell & Lamar 1989; Valencia et al. 2016	Caecilians	Roze 1996; Valencia et al. 2016
<i>Micrurus boicora</i>	Brazil	1	Bernarde et al. 2018		
<i>Micrurus brasiliensis</i>	Brazil	1	Freitas 2003	Snakes & amphisbaenids	Freitas 1999, 2003
<i>Micrurus browni</i>	CA	1	Blaney & Blaney 1978; Campbell & Lamar 1989	Snakes	Blaney & Blaney 1978; Casas-Andreu & Lopez-Forment 1978; Spencer et al. 1999
<i>Micrurus carvalhoi</i>	SA	5			
<i>Micrurus circinalis</i>	Trinidad	5	Campbell & Lamar 2004	Snakes, lizards, amphisbaenids & eels; cannibalistic	Mole & Ulrich 1894; Mole 1924; Schmidt 1932; Wehekind 1955; Emsley 1977; Boos 1984; Murphy 1997
<i>Micrurus clarki</i>	CA	5	Campbell & Lamar 1989	Eels & snakes	Ray 2017
<i>Micrurus collaris</i>	SA	1	Roze & Trebbau 1958; Campbell & Lamar 1989		

Species	Range	ATS	Habit Reference(s)	Diet	Diet Reference(s)
<i>Micrurus corallinus</i>	SA	1	Amaral 1978; Campbell & Lamar 1989; de Sousa et al. 2012; Freitas 2003	Snakes, lizards, aphidbaenians & caecilians; cannibalistic	Amaral 1978; Hoge & Federsoni 1981; Lema et al. 1983; Roze 1996; Marques & Sazima 1997; Freitas 2003
<i>Micrurus decoratus</i>	Brazil	1	Campbell & Lamar 1989; Freitas 2003	Snakes, lizards, amphidbaenians & caecilians	Marques 2002; Freitas 2003
<i>Micrurus diana</i>	SA	1	Campbell & Lamar 2004	Snakes	Roze 1966
<i>Micrurus diastema</i>	CA	6	Campbell & Lamar 1989, 2004; Lee 1996	Snakes and their eggs, lizards, centipedes & eels; cannibalistic	Greene 1973; Blaney & Blaney 1978; Lee 1996; Roze 1996; Campbell 1998; Rodriguez-Garcia et al. 1998; Köhler et al. 2016; Heimes 2016; West et al. 2019
<i>Micrurus dissoluteucus</i>	SA	1	Campbell & Lamar 1989	Snakes & lizards	Roze 1996; Arévalo-Páez et al. 2015
<i>Micrurus distans</i>	Mexico	1	Campbell & Lamar 1989; Suazo-Ortuño et al. 2004	Snakes, lizards & frogs	Ramírez-Bautista 1994; Heimes 2016
<i>Micrurus diutius</i>	SA	6	Jowers et al. 2019; EN Smith 2021, pers. comm.		
<i>Micrurus dumerilii</i>	SA	4	Campbell & Lamar 1989, 2004; Valencia et al. 2016	Lizards, caecilians & eels	Schmidt 1932, Valencia et al. 2016; Herrera-Lopera et al. 2018
<i>Micrurus elegans</i>	Mexico	1	Álvarez del Toro & Smith 1956; Blaney & Blaney 1978; Campbell & Lamar 1989, 2004	Snakes	Schmidt 1932; Roze 1996; Campbell & Lamar 2004
<i>Micrurus ephippifer</i>	Mexico	1	Campbell & Lamar 1989	Snakes	Greene 1973; Roze 1996
<i>Micrurus filiformis</i>	SA	3	Campbell & Lamar 1989, 2004	Snakes & amphidbaenians	Soini 1974b; Cunha & Nascimento 1993
<i>Micrurus frontalis</i>	SA	1	Campbell & Lamar 1989; Freitas 2003	Snakes, lizards & amphidbaenians; cannibalistic	Azevedo 1961; Sazima & Abe 1991; Roze 1996

Species	Range	ATS	Habit Reference(s)	Diet	Diet Reference(s)
<i>Micrurus fulvius</i>	NA	1	Campbell & Lamar 1989; Davidson & Eisner 1996; Archis et al. 2018	Snakes & lizards; cannibalistic	Loveridge 1938, 1944; Obrecht 1946; Myers 1965; Chance 1970; Greene 1973, 1984; Jackson & Franz 1981; Heinrich 1996; Roze 1996; Krysko & Abdelfattah 2002; Archis et al. 2018
<i>Micrurus helleri</i>	SA	6	EN Smith 2021, pers. comm.		
<i>Micrurus hemprichii</i>	SA	1	Cunha & Nascimento 1978; Dixon & Soini 1986; Campbell & Lamar 1989; Roze 1996; Martins & Oliveira 1998; Freitas 2003	Snakes, lizards, amphisbaenians & onychophorans	Beebe 1946; Schmidt 1953a; Greene 1973; Cunha & Nascimento 1978; Dixon & Soini 1986; Silva 1993; Roze 1996; Martins & Oliveira 1998; Freitas 2003; Valencia et al. 2016; Rojas-Morales et al. 2018
<i>Micrurus hippocrepis</i>	CA	1	Campbell & Lamar 1989; Lee 1996	Snakes, caecilians & earthworms	Greene 1973; Campbell 1998
<i>Micrurus ibiboboca</i>	Brazil	1	Campbell & Lamar 1989; Wang & Abe 1994; Freitas 2003	Snakes, caecilians & amphisbaneians; cannibalistic	Amaral 1933; Roze 1996; Freitas 2003; Cavalcanti et al. 2012
<i>Micrurus isozonus</i>	SA	1	Campbell & Lamar 1989, 2004	Snakes & lizards	Campbell & Lamar 2004
<i>Micrurus langsdorffi</i>	SA	4	Campbell & Lamar 1989, 2004; Valencia et al. 2016	Snakes	Soini 1947a; Roze 1996
<i>Micrurus laticollaris</i>	Mexico	1	Campbell & Lamar 1989	Snakes, lizards, amphisbaenians	Papenfuss 1982; Benítez Gálvez 1997
<i>Micrurus latifasciatus</i>	Mexico	1	Campbell & Lamar 1989	Snakes & caecilians	Landy et al. 1966; Greene 1973; Seib 1985
<i>Micrurus lemniscatus</i>	SA	5	Beebe 1946; Campbell & Lamar 1989, 2004; Martins & Oliveira 1998; Freitas 2003; Valencia et al. 2016	Snakes, lizards, caecilians, amphisbaenians, fish & eels; cannibalistic	Beebe 1946; Wehekind 1955; Greene 1973; Soini 1974b; Cunha & Nascimento 1978, 1982; Roze 1982, 1996; Dixon & Soini 1986; Vanzolini 1986; Sazima & Abe 1991; Martins & Oliveira 1998; Freitas 2003; Campbell & Lamar 2004; Viana et al. 2015
<i>Micrurus limbatus</i>	Mexico	1	Campbell & Lamar 1989, 2004; Heimes 2016	Snakes	Greene 1973

Species	Range	ATS	Habit Reference(s)	Diet	Diet Reference(s)
<i>Micrurus margaritiferus</i>	SA	1	Campbell & Lamar 1989		
<i>Micrurus medemi</i>	Colombia	1	Galvis-Rizo et al. 2015	Snakes	Campbell & Lamar 2004; Galvis-Rizo et al. 2015
<i>Micrurus mertensi</i>	SA	1	Campbell & Lamar 2004; Valencia et al. 2016	Snakes	Roze 1996; Valencia et al. 2016
<i>Micrurus mipartitus</i>	SA	2	Campbell & Lamar 1989; Valencia et al. 2016	Snakes, lizards, caecilians & amphisbaenians	Schmidt 1932; Roze 1996; Campbell & Lamar 2004
<i>Micrurus mosquitensis</i>	CA	5		Eels, snake eggs, snakes, caecilians, lizards	Roze 1996, Solorzano 2004, Ray 2017
<i>Micrurus multifasciatus</i>	CA	1	Campbell & Lamar 1989	Snakes & caecilians	Burger 1997; Solorzano 2004
<i>Micrurus multiscutatus</i>	SA	1	Campbell & Lamar 1989; Valencia et al. 2016		
<i>Micrurus narduccii</i>	SA	1	Soini 1974b; Campbell & Lamar 1989; Valencia et al. 2016	Snakes & lizards	Carrillo de Espinosa 1983; Roze 1996
<i>Micrurus nattereri</i>	SA	7	Passos & Fernandes 2005		
<i>Micrurus nebularis</i>	Mexico	1	Campbell & Lamar 2004	Snakes	Roze 1996
<i>Micrurus nigrocinctus</i>	CA	2	Schmidt & Smith 1943; Campbell & Lamar 1989, 2004; Urdaneta et al. 2004; Heimes 2016	Snakes, lizards & their eggs, caecilians & eels; cannibalistic	Schmidt 1932; Smith & Grant 1958; Landy et al. 1966; Seib 1985; Roze 1996; Campbell & Lamar 2004; Solorzano 2004; Urdaneta et al. 2004
<i>Micrurus obscurus</i>	SA	2	Melo-Sampaio et al. 2013; Valencia et al. 2016	Snakes & lizards	Schmidt 1953b; Dixon & Soini 1986; Cunha & Nascimento 1993; Roze 1996; Martins & Oliveira 1998; Valencia et al. 2016
<i>Micrurus oligoanellatus</i>	Colombia	1	campbell and lamar 2004		
<i>Micrurus ornatissimus</i>	SA	1	Valencia et al. 2016	Snakes	Valencia et al. 2016
<i>Micrurus pachecogili</i>	Mexico	1	Canseco-Márquez & Campbell 2003	Snakes	Canseco-Márquez & Gutiérrez-Mayén 2010
<i>Micrurus paraensis</i>	Brazil	1	Souza et al. 2011	Snakes & centipedes	Cunha & Nascimento 1993; Roze 1996; Souza et al. 2011
<i>Micrurus petersi</i>	Ecuador	2	Campbell & Lamar 1989; Valencia et al. 2016		

Species	Range	ATS	Habit Reference(s)	Diet	Diet Reference(s)
<i>Micrurus proximans</i>	Mexico	1	Campbell & Lamar 1989, 2004	Snakes	Roze 1996
<i>Micrurus psyches</i>	SA	1	Campbell & Lamar 1989	Snakes & lizards; cannibalistic	Wehekind 1955; Roze 1996
<i>Micrurus putumayensis</i>	SA	2	Campbell & Lamar 1989, 2004		
<i>Micrurus pyrrhocryptus</i>	SA	1	Leynaud et al. 2008	Snakes & amphisbaenians	Campbell & Lamar 2004; Leynaud et al. 2008; Ávila et al. 2010
<i>Micrurus renjifoi</i>	Colombia	2	Lamar 2003; Campbell & Lamar 2004		
<i>Micrurus ruatanus</i>	Honduras	1	Campbell & Lamar 1989	Lizards	Campbell & Lamar 2004
<i>Micrurus sangilensis</i>	Colombia	1	Campbell & Lamar 1989; Galvis- Rizo et al. 2015		
<i>Micrurus scutiventralis</i>	SA	1	Campbell & Lamar 1989; Valencia et al. 2016	Lizards & invertebrates	Roze 1996; Valencia et al. 2016
<i>Micrurus serranus</i>	Bolivia	1	Muñoz-Saravia et al. 2009	Snakes & amphisbaenians	Harvey et al. 2003; Sosa et al. 2013
<i>Micrurus silviae</i>	SA	1	Di-Bernardo et al. 2007; Cacciali et al. 2011		
<i>Micrurus spixii</i>	SA	1	Cunha & Nascimento 1978; Duellman 1978; Dixon & Soini 1986; Campbell & Lamar 1989, 2004; Duellman & Mendelson 1995; Raze 1996; Martins & Oliveira 1998; Freitas 2003	Snakes, lizards & amphisbaenians	Schmidt 1953b; Greene 1973; Dixon & Soini 1986; Cunha & Nascimento 1993; Silva 1993; Roze 1996; Martins & Oliveira 1998; Freitas 2003
<i>Micrurus steindachneri</i>	SA	2	Campbell & Lamar 1989; Valencia et al. 2016	Snakes	Valencia et al. 2016
<i>Micrurus surinamensis</i>	SA	7	Cunha & Nascimento 1978; Dixon & Soini 1986; Campbell & Lamar 1989, 2004; Duellman & Salas 1991; Roze 1996; Martins & Oliveira 1998; Freitas 2003; Avila et al. 2013; Valencia et al. 2016	Lizards, fishes & eels	Bean 1924; Schmidt 1952; Greene 1973; Duellman 1978; Dixon & Soini 1986; Cunha & Nascimento 1993; Roze 1996; Martins & Oliveira 1998; Valencia et al. 2016; Tavares-Pinheiro et al. 2021

Species	Range	ATS	Habit Reference(s)	Diet	Diet Reference(s)
<i>Micrurus tener</i>	NA	1	Irwin 2004	Snakes, lizards, frogs & mammals	Ruick 1948; Curtis 1952; Greene 1973; Strecker 1980; Greene 1984; Roze 1996; Reams et al. 1999
<i>Micrurus tschudii</i>	SA	2	Campbell & Lamar 1989, 2004; Valencia et al. 2016	Snakes, lizards & amphisbaenids	Roze 1996; Campbell & Lamar 2004
<i>Naja anchietae</i>	Africa	1	Marais 2004	Snakes, toads, rodents, birds & their eggs	Marais 2004
<i>Naja annulata</i>	Africa	8	Spawls et al. 2004; Spawls et al. 2006	Fishes	Spawls et al. 2004, 2006
<i>Naja annulifera</i>	Africa	1	Marais 2004	Snakes, toads, rodents, birds & their eggs	Marais 2004
<i>Naja atra</i>	SEA	4	Das 2010	Snakes, lizards, frogs, fish, rodents & birds	Das 2010
<i>Naja christyi</i>	Africa	8	Chippaux & Jackson 2019	Fishes	Chippaux & Jackson 2019
<i>Naja haje</i>	Africa, ME	1	Corkill & Cochrane 1966; Gasperetti 1988; Spawls et al. 2004; Spawls et al. 2006; Chippaux & Jackson 2019	Snakes, amphibians & their eggs, birds & mammals	Gasperetti 1988; Spawls et al. 2004, 2006
<i>Naja kaouthia</i>	SEA	5	Whitaker & Captain 2004; Ahmed et al. 2009; Das 2012; Chan-ard et al. 2015	Snakes, frogs, fish & rodents	Whitaker & Captain 2004; Ahmed et al. 2009; Das 2012; Chan-ard et al. 2015
<i>Naja katiensis</i>	Africa	1	Chippaux & Jackson 2019		
<i>Naja mandalayensis</i>	Myanmar	1	Das 2010		
<i>Naja melanoleuca</i>	Africa	5	Marais 2004; Spawls et al. 2004; Spawls et al. 2006	Snakes, lizards, amphibians, fishes, birds & their eggs & mammals	Spawls et al. 2004, 2006; Marais 2004; Chippaux & Jackson 2019
<i>Naja mossambica</i>	Africa	1	Marais 2004; Spawls et al. 2004; Spawls et al. 2006	Snakes, lizards, amphibians, mammals & insects	Marais 2004; Spawls et al. 2004, 2006
<i>Naja multifasciata</i>	Africa	1	Chippaux & Jackson 2019		

Species	Range	ATS	Habit Reference(s)	Diet	Diet Reference(s)
<i>Naja Naja</i>	South Asia	4	Whitaker & Captain 2004	Snakes, amphibians, birds & rodents	Whitaker & Captain 2004
<i>Naja nigricincta</i>	Africa	1	Chippaux & Jackson 2019		
<i>Naja nigricollis</i>	Africa	4	Marais 2004; Spawls et al. 2004; Spawls et al. 2006	Snakes, lizards, amphibians, fishes, birds & their eggs & mammals	Marais 2004; Spawls et al. 2004, 2006; Chippaux & Jackson 2019
<i>Naja nivea</i>	Africa	1	Marais 2004	Snakes, lizards, toads, birds & rodents	Marais 2004
<i>Naja nubiae</i>	Africa	1	Chippaux & Jackson 2019		
<i>Naja oxiana</i>	Asia	1	Whitaker & Captain 2004	Lizards, amphibians & rodents	Whitaker & Captain 2004
<i>Naja pallida</i>	Africa	1	Spawls et al. 2004; Spawls et al. 2006	Snakes, lizards, amphibians, birds & mammals	Spawls et al. 2004, 2006
<i>Naja sagittifera</i>	India	4	Whitaker & Captain 2004	Reptiles, amphibians & rodents	Whitaker & Captain 2004
<i>Naja senegalensis</i>	Africa	1	Chippaux & Jackson 2019		
<i>Naja siamensis</i>	SEA	1	Das 2012; Chan-ard et al. 2015	Rodents	Chan-ard et al. 2015
<i>Naja sputatrix</i>	Ind	1	Das 2012	Reptiles, toads & rodents	Das 2012
<i>Naja sumatrana</i>	SEA	1	Das 2007; Das 2010; Das 2012; Stuebing et al. 2014	Lizards, amphibians, birds & rodents	Das 2007, 2012; Stuebing et al. 2014
<i>Ophiophagus hannah</i>	Asia	4	Whitaker & Captain 2004; Das 2007; Ahmed et al. 2009; Das 2012; Stuebing et al. 2014	Snakes, lizards, fishes & rodents	Whitaker & Captain 2004; Das 2007, 2012; Ahmed et al. 2009; Stuebing et al. 2014
<i>Oxyuranus microlepidotus</i>	Aus	1	Cogger 2018	Mammals	Cogger 2018
<i>Oxyuranus scutellatus</i>	Ind, Aus	1	Cogger 2018	Mammals	Cogger 2018
<i>Oxyuranus temporalis</i>	Aus	1	Cogger 2018		
<i>Pseudohaje goldii</i>	Africa	4	Spawls et al. 2004; Spawls et al. 2006; Chippaux & Jackson 2019	Tortoises, amphibians, fishes & mammals	Spawls et al. 2004, 2006; Chippaux & Jackson 2019

Species	Range	ATS	Habit Reference(s)	Diet	Diet Reference(s)
<i>Pseudohaje nigra</i>	Africa	2	Chippaux & Jackson 2019	Amphibians	Chippaux & Jackson 2019
<i>Simoselaps anomalus</i>	Aus	1	Cogger 2018	Lizard eggs	Cogger 2018
<i>Simoselaps bertholdi</i>	Aus	1	Cogger 2018	Lizards	Cogger 2018
<i>Simoselaps littoralis</i>	Aus	1	Cogger 2018	Lizards	Cogger 2018
<i>Simoselaps minimus</i>	Aus	1	Cogger 2018		
<i>Sinomicrurus houii</i>	China	2	Peng et al. 2018	Snakes	Peng et al. 2018
<i>Sinomicrurus japonicus</i>	Japan	1	Goris 2004	Snakes, lizards & small mammals	Mori & Moriguchi 1988; Goris 2004
<i>Sinomicrurus boettgeri</i>	Japan	1		Snakes & lizards	Takahashi & Ota 1995; Matsuhashi & Kyōichi 2007; Ohara 2013; Hamanaka et al. 2014
<i>Sinomicrurus kelloggi</i>	SEA	1	Das 2010	Snakes	Das 2010
<i>Sinomicrurus maccolellandi</i>	SEA	1	Goris 2004; Ahmed et al. 2009; Chanhome et al. 2011; Das 2012; Chan-ard et al. 2015; Rahman et al. 2017	Snakes & lizards	Goris 2004; Whitaker & Captain 2004; Ahmed et al. 2009; Hamanaka et al. 2014; Ōta 2014; Chan-ard et al. 2015
<i>Sinomicrurus swinhonis</i>	Taiwan	1			
<i>Sinomicrurus annularis</i>	SEA	1			
<i>Sinomicrurus peinani</i>	SEA	1			
<i>Walterinnesia aegyptia</i>	ME	2	Gasperetti 1988; Uğurtaş et al. 2001; Nilson & Rastegar-Pouyani 2007	Lizards	Gasperetti 1988

Table 1.3. Descriptions of the aquatic tendency score (ATS) ratings.

Score	Description	Exemplifier
1	No record of aquatic prey. Not associated with aquatic habitats.	<i>Acanthophis</i>
2	No record of aquatic prey. Infrequently associated with aquatic habitats.	<i>Bungarus bungaroides</i>
3	Enters water infrequently. Poor or unknown locomotion in water.	<i>Micrurus filiformis</i>
4	Enters water infrequently. Competent locomotion in water	<i>Bungarus fasciatus</i>
5	Forages along the edges of bodies of water. Will enter water. Diet consists of terrestrial and aquatic prey items.	<i>Micrurus allenii</i>
6	Found frequently in aquatic environments but spends a smaller proportion than 7. Enters water to feed on prey. Diet consists of terrestrial and aquatic prey items.	<i>Micrurus diutius</i>
7	Spends majority of its life in aquatic environments. Capable locomotion on land. Diet consists of terrestrial and aquatic prey items.	<i>Micrurus surinamensis</i>
8	Oviparous; comes to land for a portion of its life cycle. Slow locomotion on land. Solely aquatic diet.	<i>Laticauda</i>
9	Non-egg laying; spends nearly all its life in aquatic environments. Slow locomotion on land. Solely aquatic diet.	<i>Hydrophis cyanocinctus</i>
10	Non-egg laying; spends nearly all its life in aquatic environments. Futile locomotion on land. Solely aquatic diet.	<i>Hydrophis platurus</i>

CHAPTER TWO

Materials and Methods of a Geometric Morphometric Approach to the Analysis of the Elapid Skull and Vertebrae

PHYLOGENY

Phylogenetic reconstruction was conducted with Mr. Bayes 3.2.7. (Huelsenbeck and Ronquist 2001; Ronquist and Huelsenbeck 2003) in parallel (Altekar et al., 2004). Gene tree used locus NADH: ubiquinone oxidoreductase core subunit 4 (*ND4*) and associated tRNAs (tRNA-His, tRNA-Ser, and tRNA-Leu), for a total length of 922 bp. MUSCLE (Edgar 2004) was used to align data. The data set was partitioned by codon 1, 2, 3, and each following tRNA was partitioned as well. All partitions used a Dirichlet prior with a nucleotide model set to “4x4.” The number of substitution types were all set to Nst = Mixed with a rate set to Invgamma. Sample frequency was set to 1,000 and diagnosed at 10,000 with a total number of generations of 50,000,000 across two runs with 12 chains (for parallel processing across 24 CPUs). A burn-in was set using a relative burn-in of 25.0 % for diagnostics ('relburnin=yes') and checked with Tracer 1.7 (Rambaut et al. 2018). After three independent runs for a total of 10 runs (first analysis at 4 runs, second analysis at 4 runs, and third analysis at 2 runs) for a total of 90,000,000 million generations no runs fully converged. This is a limitation of the data for the group at hand (Vidal et al. 2008; Zaher et al. 2019). Because of this we kept the most concordant phylogeny, our third analysis.

ECOLOGY

Like Elapidae as a whole, the specimens used in this study are extremely variable in their life history. They are fossorial, semi-fossorial, terrestrial, semi-aquatic, aquatic, and arboreal.

Some are egg-laying while others have live young. Specimens were evaluated on their aquatic behavior using the aquatic tendency score (ATS) to aid in graphical presentation of results and pattern identification (Table 1.3).

Asian coralsnakes, *Calliophis* and *Sinomicrurus*, are small semi-fossorial snakes that eat snakes and other small prey items. As such most have been rated 1 ATS, except for *C. salitan* and *S. houi*, both 2 ATS, due to being infrequently found near aquatic habitats (Brown et al. 2018; Peng et al. 2018). Specific references to habit and diet were not found for *C. beddomei*, *S. boettgeri*, *S. swinhoei*, *S. annularis*, and *S. peinani*. *C. beddomei* is a rare species, known from only a few specimens and has been rated under the assumption that it is similar in habit and diet to other striped Indian *Calliophis*. At times, *S. boettgeri*, is considered to be a subspecies of *S. japonicus* and has been rated with the information for *S. japonicus*. *Sinomicrurus swinhoei* and *S. annularis* are recently recognized species, formerly considered to be a subspecies and a synonym of *S. macrolellandi* (Smart et al. 2021), respectively, and as such were rated with information concerning *S. macrolellandi*. There is a lack of information on the newly described *S. peinani*, so it was rated based on the assumption that its habit and diet are similar to other *Sinomicrurus* (Liu et al. 2020).

New world coralsnakes, monotypic *Micruroides* and speciose *Micrurus*, have more diverse habits and diet in comparison to their Asian counterparts. This can be seen in the broad range of ATS, with desert dwelling *Micruroides euryxanthus* give a 1 ATS and *Micrurus surinamensis*, commonly known as the aquatic coral snake, with 7 ATS at the high end (Uetz and Etzold 1996; Heimes 2016). Most of the New World coralsnakes in Table 1.2 are semi-fossorial or terrestrial and lack aquatic prey items in their diet (57/72) and have been rated a 1 or 2 ATS where those rather 2 ATS inhabit areas close to aquatic environments. The one exception is *M.*

nigrocinctus, which Table 1.2 includes a record of eels in its diet. It is likely that these eel records are misattributed to *M. nigrocinctus* and should be associated with *M. mosquitensis* (EN Smith 2021, pers. comm.). A case can be made that the remaining 15 *Micrurus* are semi-aquatic or aquatic to varying degrees.

Micrurus can be split into two clades based on coloration which has had genetic support (Slowinski 1995; Jowers et al. 2019). The two clades consist of monadals, where a dark band, typically black, occurs per each red band and is bound by light bands, and triadals, where additional dark bands are added between the light bands, typically white or yellow, and the red bands, giving three dark bands per red band, hence the term triadal. The *M. lemniscatus* complex is a taxonomically challenging group. The complex includes taxa that until recently have been considered subspecies of *M. lemniscatus*: *M. l. lemniscatus*, *M. l. frontifasciatus*, *M. helleri*, *M. carvalhoi* and *M. diutius*. There is support to elevate them all to full species except for *M. l. frontifasciatus* and is included as *M. lemniscatus* in table 1.2 (Valencia et al. 2016; Jowers et al. 2019; Hurtado Gómez et al. 2021). Feitosa et al. (2007) and Terribile et al. (2018) have suggested that the *M. lemniscatus* complex should also include *M. filiformis*, *M. isozonus*, and *M. serranus*. Despite plethora of dietary accounts of *M. lemniscatus* and its former subspecies (Beebe 1946; Wehekind 1955; Greene 1973; Soini 1974b; Cunha and Nascimento 1978, 1982; Roze 1982, 1996; Dixon and Soini 1986; Vanzolini 1986; Sazima and Abe 1991; Martins and Oliveira 1998; Freitas 2003; Campbell and Lamar 2004) nothing can be said definitively until the specimens are reidentified due to the taxonomic flux and reassessment of distribution where there exists substantial overlap between members of the complex (Roze 1996; Campbell and Lamar 2004; Floriano et al. 2019). For that reason, the dietary information of the *M. lemniscatus* complex is under *M. lemniscatus* in Table 1.2. *Micrurus lemniscatus* was rated 5 ATS but could

potentially be lowered if it is determined that the accounts of aquatic prey items are of other members in the complex. *Micrurus diutius* and *M. helleri* were rated 6 ATS due to their tendency to go into the water to seek prey (EN Smith 2021, pers. comm.). *Micrurus carvalhoi* was conservatively rated 5 ATS based on what is known of the complex and could change based on further study. Campbell and Lamar (1989, 2004) have seen *M. filiformis* readily crossing streams, but it has not been found with aquatic prey and has therefore been rated 3 ATS. *Micrurus isozonus*, and *M. serranus* have been rated 1 ATS as they have a terrestrial diet and are not associated with aquatic environments.

Micrurus surinamensis and *M. nattereri* are sister species and part of the *M. lemniscatus* complex and are known to be aquatic with more time spent in water than on land, taking both terrestrial and aquatic prey. The 7 ATS of both *M. surinamensis* and *M. nattereri* is based also on accounts attributed to *M. surinamensis* before *M. nattereri* was elevated to full species status from being a subspecies or synonym of *M. surinamensis* (Passos and Fernandes 2005).

There are eight monadal *Micrurus* that are semi-aquatic to some degree and are included in Table 1.2. The first two are a part of the *M. diastema* complex: the eponymous *M. diastema* and *M. apiatus*, both of which are at the top end of the ATS for monadals, rated 6 and 5, respectively. West et al. (2019) conducted an in-depth review of the diet for the *M. diastema* complex, broken down by subspecies and author. Both *M. diastema* and *M. apiatus* have record of one swamp eel each and frequent aquatic habitats with *M. apiatus* to a lesser degree (EN Smith 2021, pers. comm.). *Micrurus dumerilii* and *M. langsdorffi* rated as 4 ATS with different justifications. *Micrurus dumerilii* is semi-fossorial but has taken eels on more than one occasion, likely opportunistically along stream banks while *M. langsdorffi* has been seen swimming across streams on multiple occasions but has not been recorded with aquatic prey (Campbell and Lamar

1989, 2004; Valencia et al. 2016). The remaining four semi-aquatic monads, *M. alleni*, *M. clarki*, *M. circinalis*, and *M. mosquitensis* were all given a 5 ATS due to the records of them eating eels in addition to terrestrial prey and their association with water.

Cobras and their kin are represented by seven genera in Table 1.2: *Dendroaspis*, *Hemachatus*, *Hemibungarus*, *Naja*, *Ophiophagus*, *Pseudohaje*, and *Walterinnesia*. The mambas, *Dendroaspis*, are arboreal snakes endemic to Africa that feed primarily on birds and other arboreal and terrestrial prey, they were all rated 1 ATS. The rinkhals, *Hemachatus haemachatus*, generally live in arid environments, possess a varied terrestrial diet and was also rated 1 ATS. *Hemibungarus* inhabit tropical environments associated with water, lack data on their diet and were rated 2 ATS. True cobras, *Naja*, have a wide-ranging distribution—from Africa to India to Indonesia—and varied behavior and are the most speciose genera of this clade. Of the 24 *Naja* represented in Table 1.2, 16 were rated 1 ATS as they are not associated with aquatic habitats and have not been recorded with aquatic prey. The remaining eight range from the largely terrestrial, *N. atra* and *N. nigriceps* rated 4 ATS due to taking aquatic prey, to the aquatic and oviparous *N. annulata* and *N. christyi* rated 8 ATS. The king cobra, *Ophiophagus hannah*, was rated 4 ATS due to its frequent association with aquatic habitats and taking of aquatic prey. The two tree cobras in Table 1.2, *Pseudohaje goldii* and *P. nigra*, were rated 4 and 2 ATS, respectively, due to their arboreal nature and prey choice. *Walterinnesia aegyptia* was rated 2 ATS due to its preference of being near aquatic habitats while not taking aquatic prey.

African garter snakes, *Elapsoidea*, are terrestrial snakes endemic to Africa that have not been found with aquatic prey and have all been rated 1 ATS.

There are two related, but monophyletic groups referred to as kraits, *Bungarus* and *Laticauda*, terrestrial and sea kraits, respectively. *Bungarus* can be found across South and South

East Asia. *Bungarus fasciatus* and *B. multicinctus* have both been recorded with aquatic prey and were rated 4 ATS. The remaining seven *Bungarus* covered in Table 1.2 were rated 1 or 2 ATS as they have not taken aquatic prey but have an association with aquatic habitats, assigned 2 ATS.

Laticauda can be found in rocky crevices along South East Asian shorelines by day and foraging out at sea by night. *Laticauda colubrina* has the broadest distribution, from the shores of Indonesia east to small pacific islands, and is also the most land-loving of its congeners, having been seen as high as 50 m above sea level (Goris 2004). The species of this entirely oviparous genus were rated 8 ATS.

Four genera of Hydrophiinae were included in Table 1.2, *Hydrophis*, *Acanthophis*, *Oxyuranus* and *Simoselaps*. Unsurprisingly, *Hydrophis* consistently rated 10 ATS as they are entirely aquatic, bear live young and have aquatic diets. This is with the exceptions of *H. curtus*, *H. cyanocinctus*, and *H. jerdonii*, which were all rated 9 ATS due to their ability to locomote, albeit slowly, on land (Whitaker and Captain 2004; Das 2012). Death adders and taipans, *Acanthophis* and *Oxyuranus*, which inhabit Australia, Indonesia, and Papua New Guinea, were rated 1 ATS as they are entirely terrestrial with varied but terrestrial diets (Cogger 2018). *Simoselaps* is a genus of Australia burrowing snakes found in arid regions (Cogger 2018). As such their diet is also fossorial and have been rated 1 ATS.

SKULL

Specimens

We produced and analyzed data from the skulls of 87 elapid specimens, including 46 New World coralsnakes (*Micruurus* and *Micruroides*) and 23 Asian coralsnakes (*Calliophis* and *Sinomicrurus*). This dataset includes 65 species and subspecies (Table 2.1; Appendix).

Specimens were chosen based on the condition and quality of their preservation. All specimens were preserved in 70% EtOH apart from UTA R-7072, which is dry. The skull of FMNH 39479 was scanned by The University of Texas High-Resolution X-ray CT Facility (UTCT) and is available through the Digital Morphology online library (DigiMorph; http://digimorph.org/specimens/Micrurus_fulvius). The skull of UMMZ 244197 was scanned by The University of Michigan, Museum of Zoology, Research Museums Center and is available through the online repository, MorphoSource, (Media ID: 000071019). All other specimens were scanned at the Shimadzu Center for Environmental, Forensics, and Material Science with a Shimadzu InspeXio SMX-100CT CT system. The data was produced from 960 second scans at 65 kV, 40 μ A, and 500 SID at a zoom level to minimize the voxel size while capturing the entire skull in frame.

Volumes were brightness and contrast adjusted in ImageJ (Schneider et al. 2012) by CLAHE (Reza 2004; Figure 2.2A) then digitally dissected to create 3D polygon models (.ply) of the skulls with DrishtiPaint (Limaye 2012, Yuzhi et al. 2020; Figure 2.2B). Skulls were segmented into eight regions which allowed for the export of the quadrate and lower jaw to be analyzed separately. The right suspensorium, lower jaw and quadrate were removed to simplify the model as analysis was only conducted on one side of the skull. Models were simplified down to a maximum of 1,000,000 faces to ease downstream data analysis in Avizo (Thermo Fisher Scientific, Waltham, MA, US). Models were converted from binary ply to ASCII ply at the instruction of Bardua, Felice, *et al.* (2019) in R 4.0.2 (R Core Team 2021) to alleviate potential compatibility issues with R packages.

Morphometric Data Preparation and Collection

Regions

In line with Bardua, Wilkinson, Gower, Sherratt, and Goswami (2019), regions were defined a priori to enable testing of modularity hypotheses. The 17 regions are largely based on entire bones and are defined in Table 2.2. Of all bones investigated in this study, the postorbital was the only one that was not present in all specimens and was therefore segmented out and excluded from analysis.

Landmarks and Semi-landmark Curves

Eighty-four landmarks and 86 semi-landmark curves were placed on the left side of each skull using Checkpoint (Stratovan, Davis, CA, US; Figure 2.2C). If there were broken bones on the left side while the right was complete, the skull was reflected in Checkpoint. The landmark and curve placement scheme was developed to outline the lateral edges of each bone and influenced by recent geometric morphometric studies and guides (Placi et al. 2016; Bardua, Felice, et al. 2019; Bardua, Wilkinson, et al. 2019; Rhoda et al. 2020; C Bardua 2020, pers. comm.; Table 2.3). Due to the degree of fusion of the supratemporal to the prootic and exoccipital in most specimens, the supratemporal was not segmented away from the braincase. As a result, the posterior edge of the prootic is defined by the anterior edge of the supratemporal in that curves 30 and 33 are shared by both and the anterodorsal edge of the exoccipital is defined by the exoccipital crest and the ventral edge of the supratemporal.

The number of points along each curve was increased and the points were placed equidistantly between two landmarks by the function `equidistantCurve`, which is contained within the R package *Morpho* (Schlager 2017; 2.2D).

Surface landmarks

Surface landmarks were applied to the skull of ANMH-28846 in Checkpoint. ANMH-28846 was designated the template, from which surface points were applied to all other skulls. Patching was conducted in a piecemeal fashion started with the creation of multiple atlases with ‘createAtlas,’ with which the surface points of the template are defined and subsequently applied to the rest of the skulls with ‘placePatch’ (Bardua, Felice, et al. 2019; Figure 2.2E). The functions ‘createAtlas’ and ‘placePatch’ are both found within *Morpho* (Schlager 2017). Patching the parietal, prootic, exoccipital, basisphenoid, and basioccipital while using a mesh that included the suspensorium resulted in erroneous point placement. To overcome this, patches were placed on these bones though the use of meshes with the suspensorium removed.

Surface landmarks were excluded from the septomaxilla and vomer due to the extreme variability of completeness caused by the insufficient thickness and incomplete calcification of the bone. Surface points were also excluded from the pterygoid due to the variable presence of teeth on the dorsal surface in addition to the incomplete posterior extent and from the palatine due to insuperable issues with patching.

With patching complete, the surface points were slid together with slider3d to minimize the bending energy and allow for a geometrically and biologically preferable location of the points as the initial patch placement is somewhat arbitrary (Schlager 2017; Bardua, Felice, et al. 2019; Figure 2.2F). Points were mirrored across midline with mirror2plane (Schlager 2017), aligned with ‘gpage’ from the R package *geomorph* (Adams et al. 2021; Baken et al. 2021) and finally mirrored pointed were removed before additional analyses. Mirroring across the midline prior to alignment reduces shape variation along the midline when compared with the alignment of data from just one side of a bilaterally symmetric structure (Bardua, Felice, et al. 2019).

Data Analyses

The covariance ratio (CR) through the implementation of ‘modularity.test’ from *geomorph* (Collyer and Adams 2018, 2021; Adams et al. 2021; Baken et al. 2021) was used to assess the patterns of modularity of the 87 skulls. CR evaluated the modularity of 210 different model structures that varied from the null hypothesis of one module (no modularity) to 17 modules (all regions are separate). Descriptions of which can be found in Table 2.4.

Subsequent analyses were conducted on the skull as a whole and each aligned module separately using *geomorph* (Collyer and Adams 2018, 2021; Adams et al. 2021; Baken et al. 2021) as in Bardua, Wilkinson, *et al.* (2019). Generalized Procrustes Analysis (GPA; Gower 1975) through ‘gpagen,’ was conducted on all specimens and two additional data subsets: just coralsnakes, and aquatic and semiaquatic species (5-10 ATS). From these three comparisons we can identify patterns of variation in aquatic coralsnakes associated with phylogeny or with aquatic tendency.

QUADRATATE

Specimens

We produced and analyzed data from the skulls of 101 elapid specimens, including 57 New World coralsnakes (*Micrurus* and *Micruroides*) and 23 Asian coralsnakes (*Calliophis* and *Sinomicrurus*). This dataset includes 78 species and subspecies (Table 2.1; Appendix).

The quadrate dataset was derived from the skull dataset and underwent the same initial preparation (Figure 2.3A-B). The segmented left quadrate was exported from DrishtiPaint if present and lacking any apparent deformity. If the left was missing or the right quadrate was in better shape, the right quadrate was exported and reflected using Checkpoint. Models were

converted from binary ply to ASCII ply at the instruction of Bardua, Felice, *et al.* (2019) in R 4.0.2 (R Core Team 2021) to alleviate potential compatibility issues with R packages.

Morphometric Data Preparation and Collection

Landmarks and Semi-landmark Curves

Ten landmarks and 10 semi-landmark curves were placed on each quadrate using Checkpoint (Figure 2.3C). The landmark and curve placement scheme was developed to outline dorsal edge and the quadrate/articular joint while connecting the two across the lateral face and influenced by recent geometric morphometric studies and guides (Placi et al. 2016; Bardua, Felice, et al. 2019; Bardua, Wilkinson, et al. 2019; Rhoda et al. 2020; Table 2.5).

The number of points along each curve was increased and the points were placed equidistantly between two landmarks by the function equidistantCurve (Schlager 2017; Figure 2.3D).

Surface landmarks

Surface landmarks were applied the quadrate of ANMH-28846 in Checkpoint. ANMH-28846 was designated the template, from which surface points were applied to all other quadrates. Patching sliding and alignment of the quadrate was completed with the same means as the skull (Figure 2.3E-F).

Surface landmarks were excluded from the face of the quadrate/articular joint as the fusion between the quadrate and lower jaw was variable and therefore the quality of quadrate is variable. As a single quadrate is not bilaterally symmetrical, points were not mirrored across the midline as with the skull.

Data Analyses

As the quadrate is a single bone, modularity testing was not conducted. All other analyses were performed as on the skull.

LOWER JAW

Specimens

We produced and analyzed data from the skulls of 100 elapid specimens, including 56 New World coralsnakes (*Micrurus* and *Micruroides*) and 23 Asian coralsnakes (*Calliophis* and *Sinomicrurus*). This dataset includes 78 species and subspecies (Table 2.1; Appendix).

The lower jaw dataset was derived from the skull dataset and underwent the same initial preparation (Figure 2.4A-B). The left lower jaw was exported if present and lacking any apparent deformity (e.g., breakage, growths). If the left was missing or the right lower jaw was in better condition, the right lower jaw was exported and reflected using Checkpoint. Models were simplified down to a maximum of 1,000,000 faces to ease downstream data analysis in Avizo (Thermo Fisher Scientific, Waltham, MA, US). Models were converted from binary ply to ASCII ply at the instruction of Bardua, Felice, *et al.* (2019) in R 4.0.2 (R Core Team 2021) to alleviate potential compatibility issues with R packages.

Morphometric Data Preparation and Collection

Regions

The four regions of the lower jaw data set are based on a single surface of entire bones: the lateral face of the dentary, the lateral face of the compound, the medial face of the splenial, and the medial face of the angular (Table 2.6).

Landmarks and Semi-landmark Curves

Nineteen landmarks and 20 semi-landmark curves were placed on each jaw using Checkpoint (Figure 2.4C). The landmark and curve placement scheme was developed to outline the lateral edges of each bone and influenced by recent geometric morphometric studies and guides (Placi et al. 2016; Bardua, Felice, et al. 2019; Bardua, Wilkinson, et al. 2019; Rhoda et al. 2020; Table 2.7).

The number of points along each curve was increased and the points were placed equidistantly between two landmarks by the function equidistantCurve (Schlager 2017; 2.4D).

Surface landmarks

Surface landmarks were applied to the lower jaw of ANMH-28846 in Checkpoint. ANMH-28846 was designated the template, from which surface points were applied to all other jaws. Patching, sliding and alignment of the quadrate was completed with the same means as the skull (Figure 2.4E-F). As the exported half of the lower jaw in this dataset is not bilaterally symmetrical, points were not mirrored across the midline as with the skull.

Data Analyses

Modularity and all other analyses were performed on the lower jaw dataset as on the skull dataset.

MIDBODY VERTEBRA

Specimens

We produced and analyzed data from the midbody vertebrae of 93 elapid specimens, including 57 New World coralsnakes (*Micrurus* and *Micruroides*) and 16 Asian coralsnakes

(*Calliophis* and *Sinomicrurus*). This dataset includes 71 species and subspecies (Table 2.1; Appendix). CT scans were conducted with the same settings as the skull dataset at a zoom level to minimize the voxel size and capture a minimal number of vertebrae in frame. The vertebrae scanned were at the midpoint between the base of the skull and vent.

Volumes were brightness and contrast adjusted and segmented with the same means as the skull dataset (Figure 2.5A-B).

Morphometric Data Preparation and Collection

Landmarks and Semi-landmark Curves

Twenty-seven landmarks and 35 semi-landmark curves were placed on the left side of each vertebrae using Checkpoint (Figure 2.5C). If the left side of the vertebrae was found to be deformed or otherwise abnormal, the vertebra was reflected with Checkpoint. The landmark and curve placement scheme was developed to highlight anatomically pertinent features like, the perimeter of all facets and the lateral extent of all processes and was influenced by recent geometric morphometric guides (Bardua, Felice, et al. 2019; C Bardua 2020, pers. comm.; Table 2.9).

The number of points along each curve was increased and the points were placed equidistantly between two landmarks by the function `equidistantCurve` (Schlager 2017; 2.5D). Surface points were not applied due to the variable completeness of the vertebral mesh which is a result of the small size of the specimens and the limitations of the micro-CT scanner used. Points were mirrored across midline and aligned with the same means as the skull dataset.

Data Analyses

As a vertebra is a single bone, modularity testing was not conducted. All other analyses were performed as on the skull.

CAUDAL VERTEBRA

Specimens

We produced and analyzed data from the caudal vertebrae of 92 elapid specimens, including 53 New World coralsnakes (*Micrurus*) and 19 Asian coralsnakes (*Calliophis* and *Sinomicrurus*). This dataset includes 73 species and subspecies (Table 2.1; Appendix). CT scans were conducted with the same settings as the skull dataset at a zoom level to minimize the voxel size and capture a minimal number of vertebrae in frame. The vertebrae scanned were at the midpoint between the base of the skull and vent.

Volumes were brightness and contrast adjusted and segmented with the same means as the skull dataset (Figure 2.6A-B).

Morphometric Data Preparation and Collection

Landmarks and Semi-landmark Curves

Twenty-nine landmarks and 37 semi-landmark curves were placed on the left side of each skull using Checkpoint (Figure 2.6C). The landmark and curve placement scheme was developed in the same manner as the midbody vertebra dataset (Table 2.10).

The number of points along each curve was increased and the points were placed equidistantly between two landmarks, mirrored across the midline alinged and mirror points were removed with the same means of the midbody vertebra dataset (Figure 2.6D).

Data Analyses

As a vertebra is a single bone, modularity testing was not conducted. All other analyses were performed as on the skull.

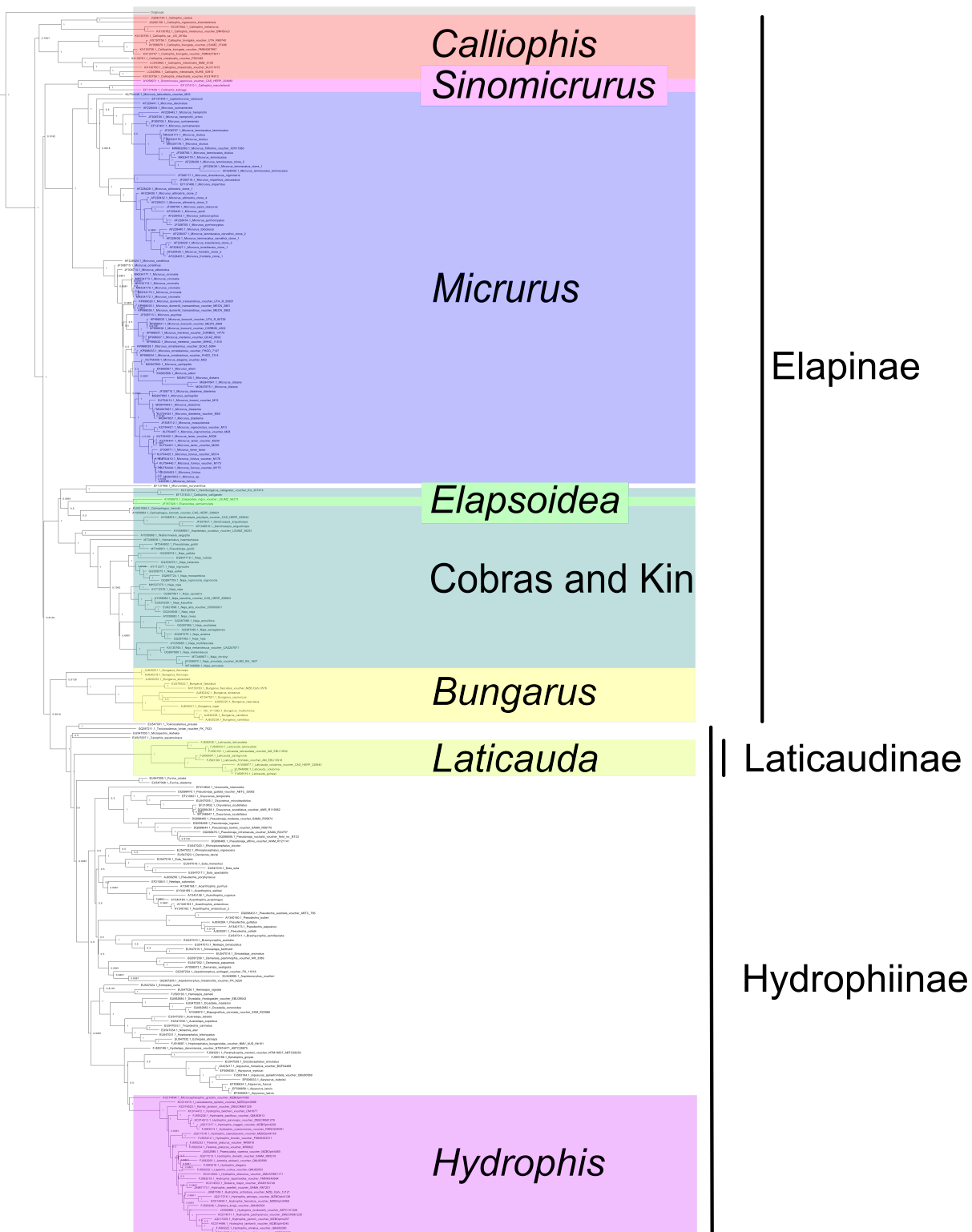


Figure 2.1. Bayesian phylogenetic reconstruction using Mr. Bayes 3.2.7 with *ND4* (922 bp). The phylogeny was run 90,000,000 generations. Node labels denote posterior probabilities.

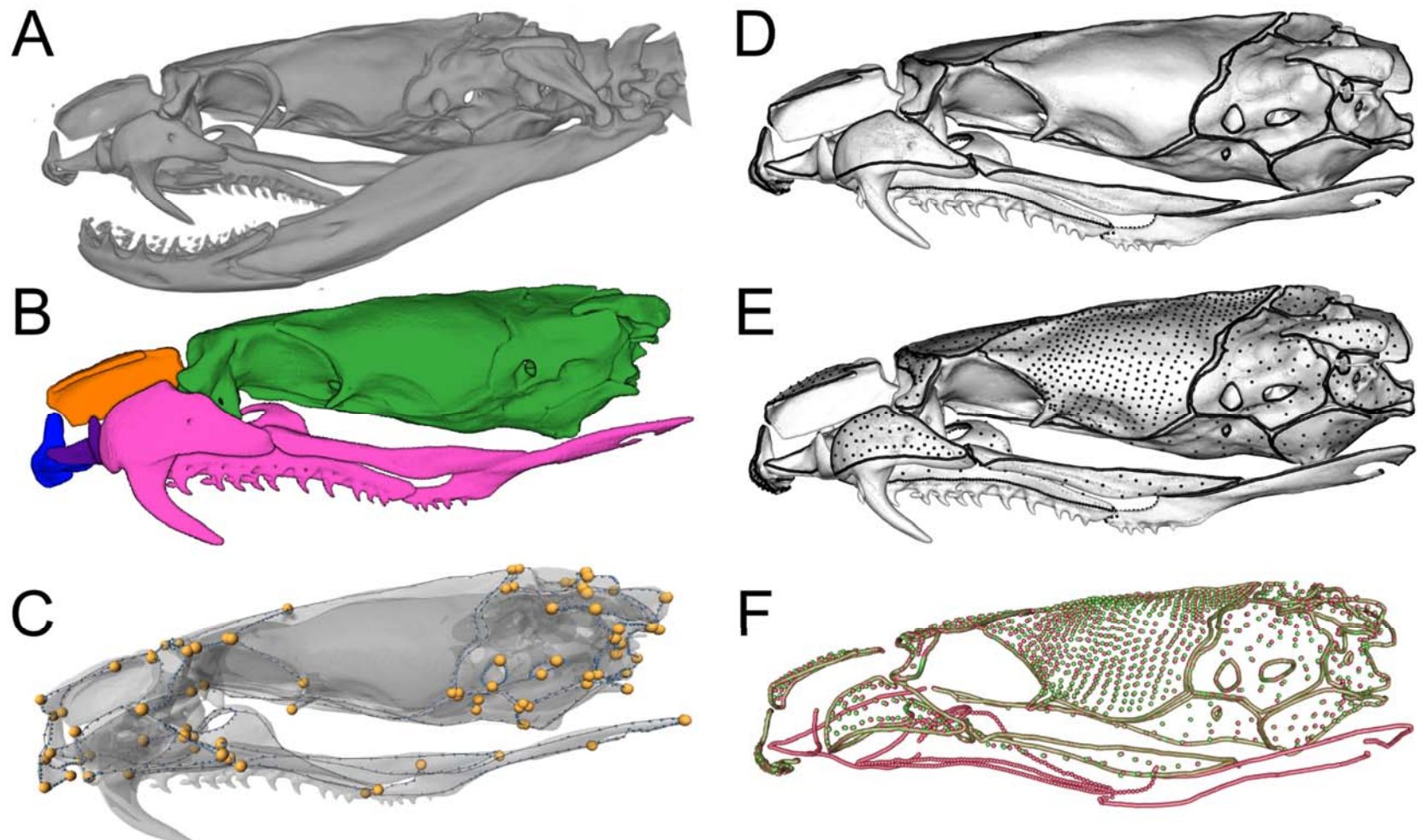


Figure 2.2. Steps in morphometric data preparation. CT data was sharpened with CLAHE (A), segmented in DrishtiPaint (B), and landmarked in Checkpoint (C). The curves were subsampled (D), surface points were added (E), and all points were slid together (F) with *Morpho* in R. Green points are the original position and red are the position post-slide.

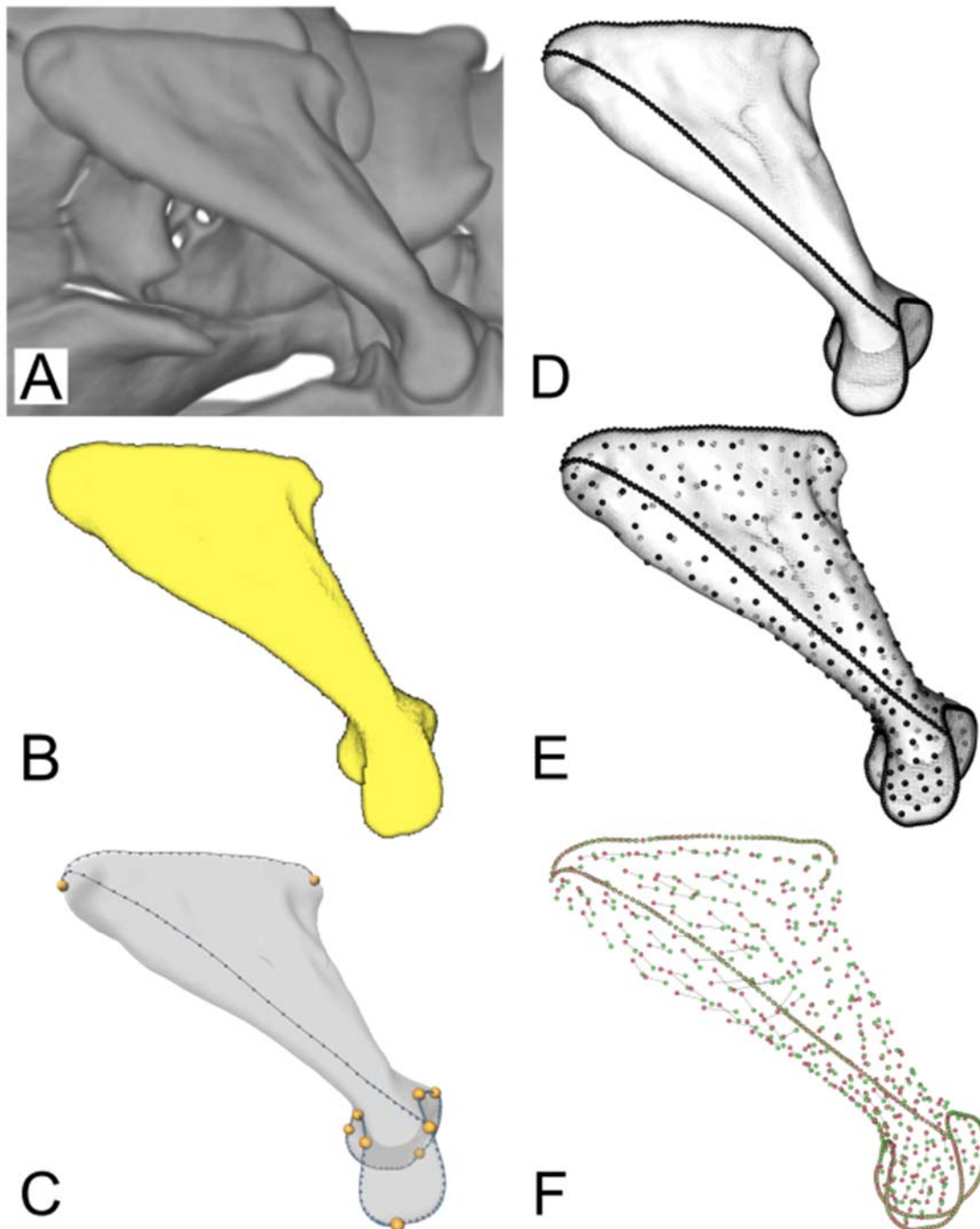


Figure 2.3. Steps in morphometric data preparation of the quadrate dataset. CT data was sharpened with CLAHE (A), segmented in DrishtiPaint (B), and landmarked in Checkpoint (C). The curves were subsampled (D), surface points were added (E), and all points were slid together (F) with *Morpho* in R. Green points are the original position and red are the position post-slide.

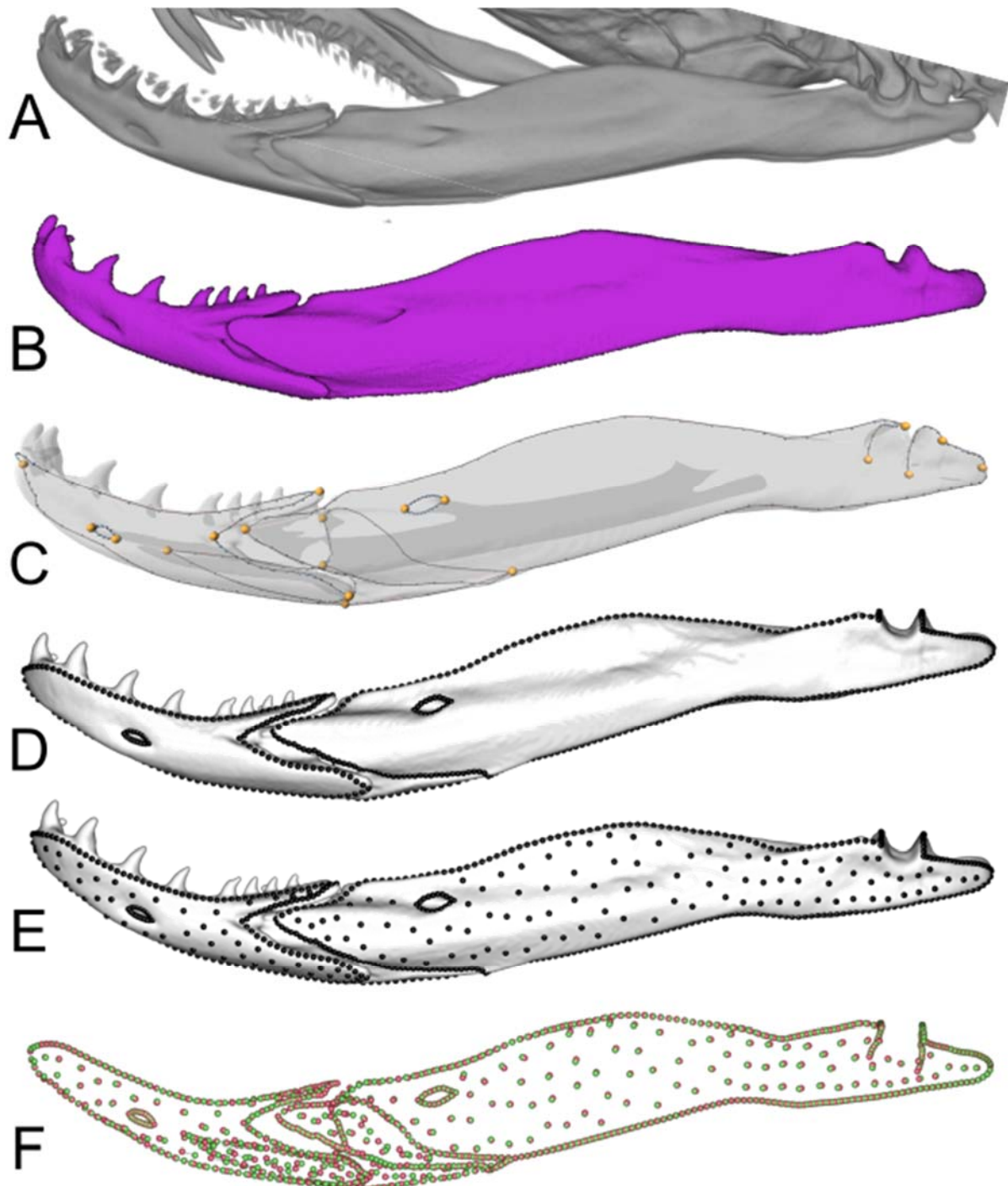


Figure 2.4. Steps in morphometric data preparation of the lower jaw dataset. CT data was sharpened with CLAHE (A), segmented in DrishtiPaint (B), and landmarked in Checkpoint (C). The curves were subsampled (D), surface points were added (E), and all points were slid together (F) with *Morpho* in R. Green points are the original position and red are the position post-slide.

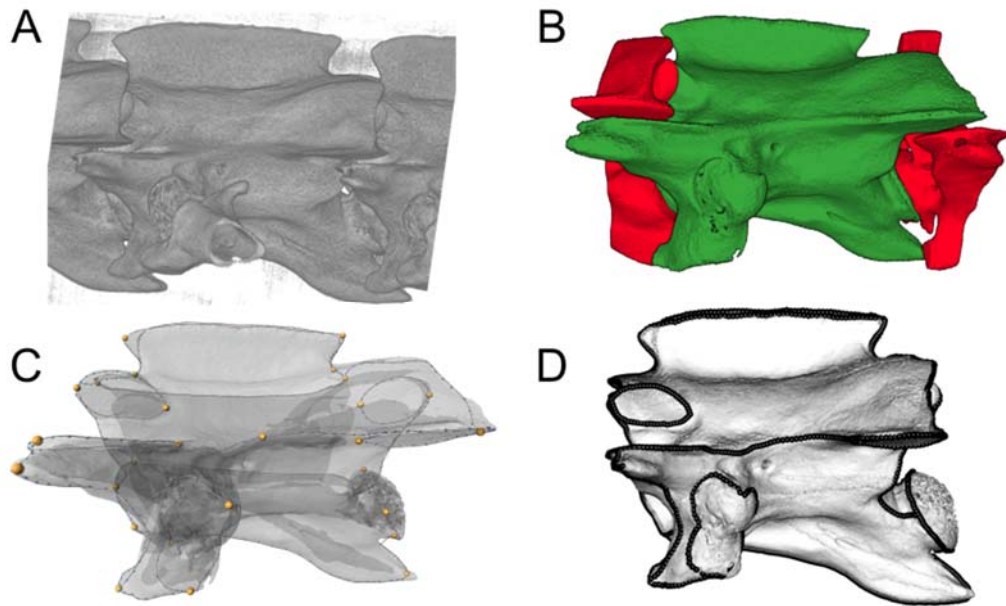


Figure 2.5. Steps in morphometric data preparation of midbody vertebra dataset. CT data was sharpened with CLAHE (A), segmented in DrishtiPaint (B), and landmarked in Checkpoint (C). The curves were subsampled with *Morpho* in R (D).

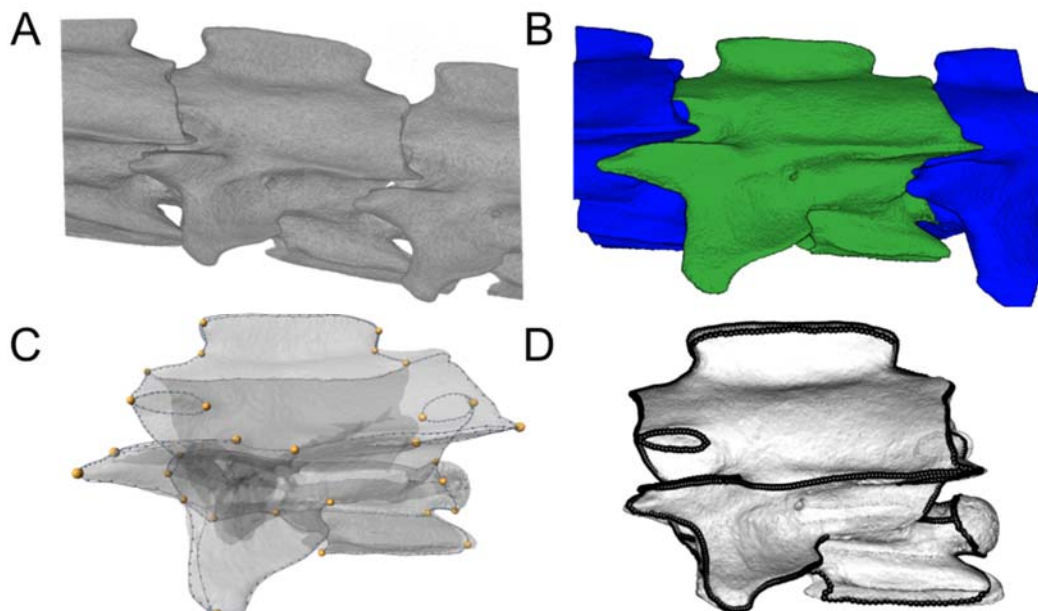


Figure 2.6. Steps in morphometric data preparation of the caudal vertebra dataset. CT data was sharpened with CLAHE (A), segmented in DrishtiPaint (B), and landmarked in Checkpoint (C). The curves were subsampled with *Morpho* in R (D).

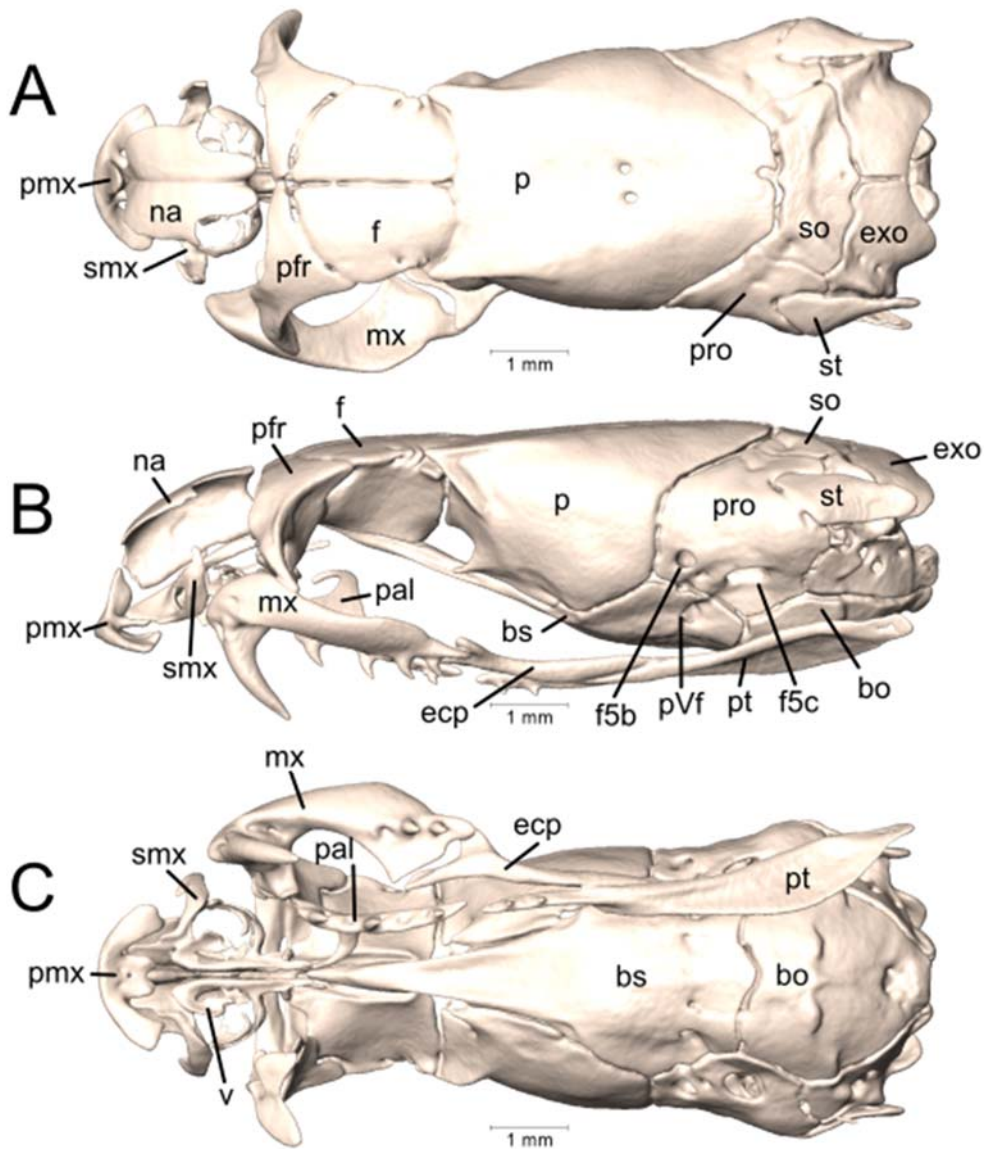


Figure 2.7. Dorsal, lateral, and ventral views (A-C, respectively) of the skull of *Hemibungarus calligaster* (KU 307474). Right suspensorium excluded. Abbreviations: bo, basioccipital; bs, basisphenoid; ecp, ectopterygoid; exo, exoccipital; f, frontal; f5b, foramen for maxillary branch of trigeminal; f5c, foramen for mandibular branch of trigeminal; mx, maxilla; na, nasal; p, parietal; pal, palatine; pfr, prefrontal; pmx, premaxilla; pro, prootic; pt, pterygoid; pVf, posterior Vidian foramen; smx, septomaxilla; so, supraoccipital; st, supratemporal; v, vomer. Adapted from Cundall and Irish (2008).

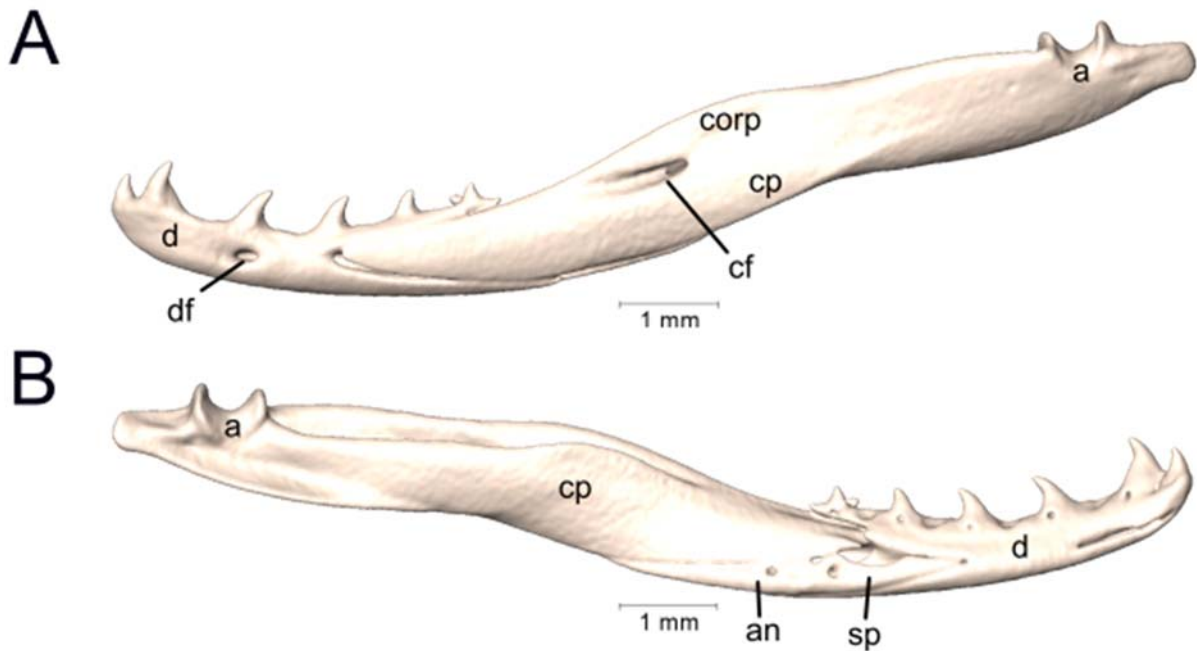


Figure 2.8. Lateral and medial views (A-B, respectively) of the left lower jaw of *Hemibungarus calligaster* (KU 307474). Abbreviations: a, articular; an, angular; cf, compound foramen; corp, coronoid process; cp, compound; d, dentary; df, dentary foramen; sp, splenial. Adapted from Cundall and Irish (2008).

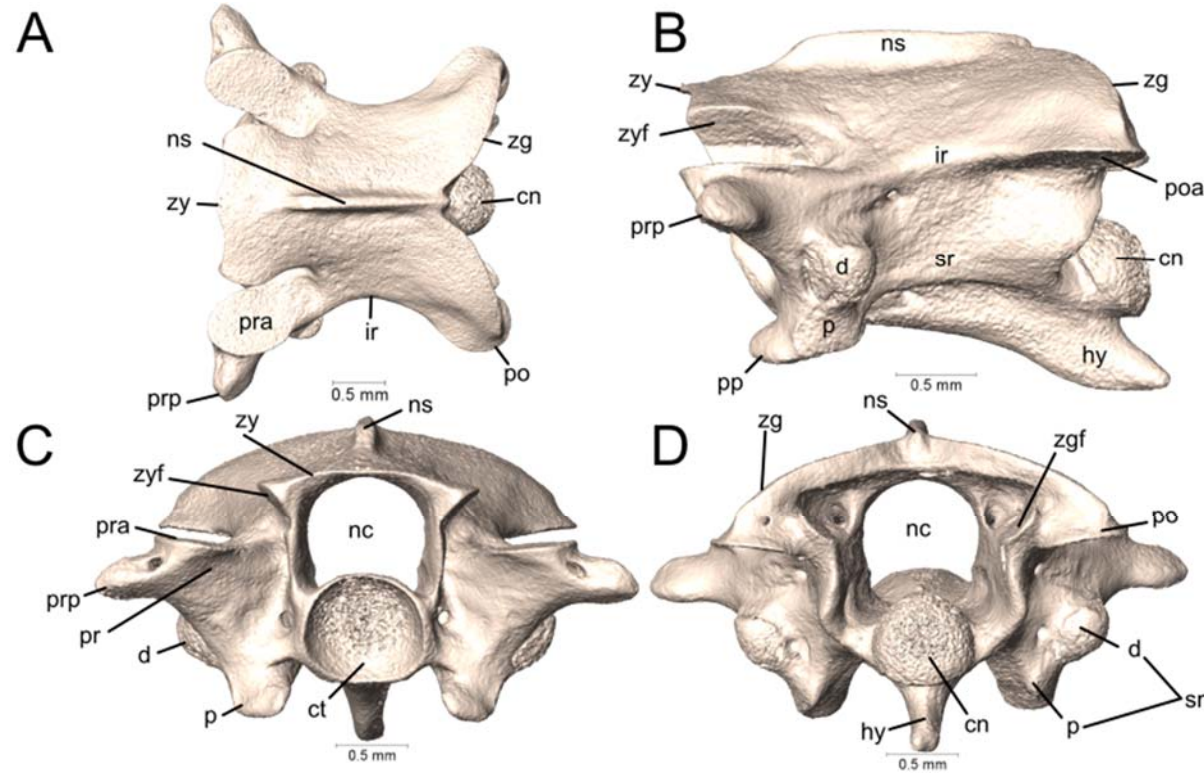


Figure 2.9. Dorsal, lateral, anterior, and posterior views (A-D, respectively) of a midbody vertebra of *Hemibungarus calligaster* (KU 307474). Abbreviations: cn, condyle; ct, cotyle; d, diapophysis; hy, hypapophysis; ir, interzygapophyseal ridge; nc, neural canal; ns, neural spine; pp, parapophysial process; p, parapophysis; poa, postzygapophyseal articular facet; po, postzygapophysis; prp, prezygapophyseal accessory process; pra, prezygapophyseal articular facet; pr, prezygapophysis; sr, subcentral ridge; sn, synapophyses; zgf, zygantral articular facet; zg, zygantrum; zyf, zygosphenal articular facet; zy, zygosphenes. Adapted from Ikeda (2007).

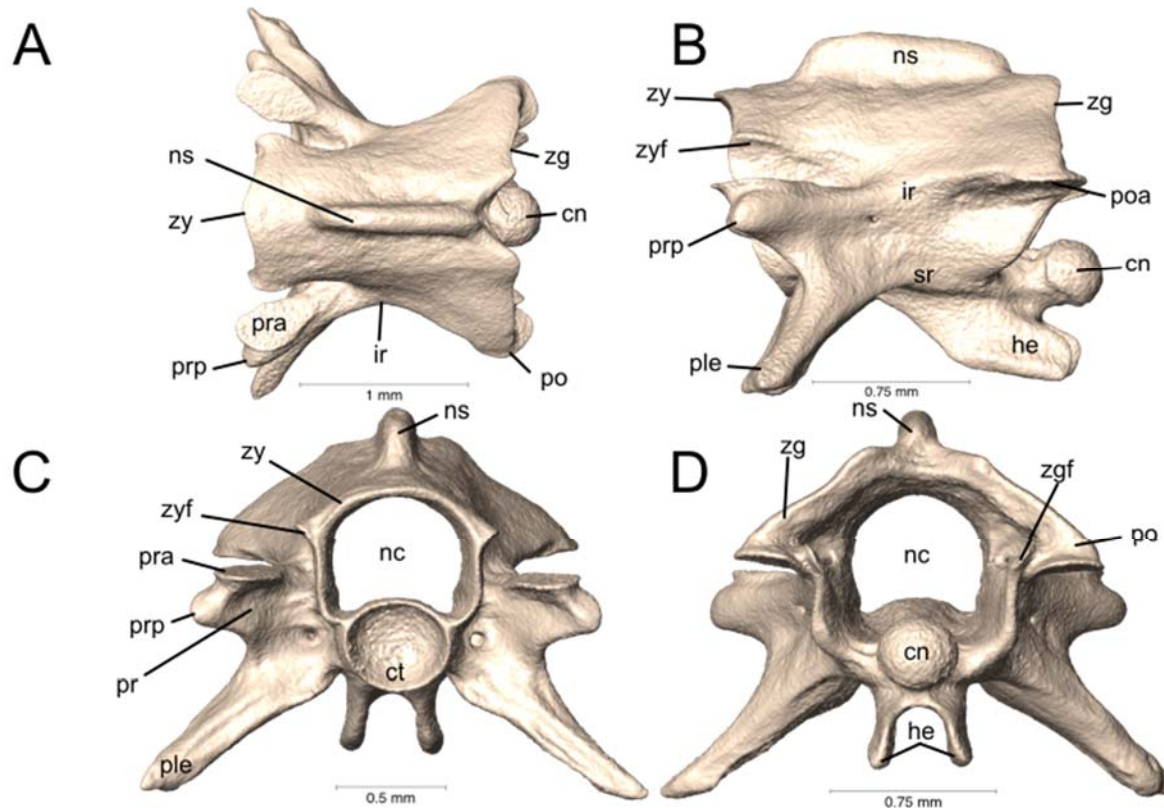


Figure 2.10. Dorsal, lateral, anterior, and posterior views (A-D, respectively) of a caudal vertebra of *Hemibungarus calligaster* (KU 307474). Abbreviations: cn, condyle; ct, cotyle; he, hemapophysis; ir, interzygapophyseal ridge; nc, neural canal; ns, neural spine; ple, pleurapophysis; pp, parapophysial process; poa, postzygapophyseal articular facet; po, postzygapophysis; prp, prezygapophyseal accessory process; pra, prezygapophyseal articular facet; pr, prezygapophysis; sr, subcentral ridge; zgf, zygantral articular facet; zg, zygantrum; zyf, zygosphenal articular facet; zy, zygosphenes. Adapted from Ikeda (2007).

Table 2.1. Specimens used in this study.

#	Species	Catalog Number	ATS	Sex	SVL	TL	V	SC	SC type	Dataset Inclusion				
										S	Q	J	M	C
1	<i>Acanthophis antarcticus</i>	UTA R-7623	1	M	467	110	123	47	Entire	X	X	X	X	X
2	<i>Bungarus candidus</i>	UTA R-65799	1	M	657	158	211	77	Divided	X	X	X	X	X
3	<i>Bungarus flaviceps</i>	UTA R-62257	1	M	835	138	219	53	Divided	X	X	X	X	X
4	<i>Calliophis beddomei</i>	MNHN 46-81	1	F	277	28	225	31	Divided	X	X	X	X	X
5	<i>Calliophis bibroni</i>	CAS 17268	1	F	402	41	222	29	Entire					X
6	<i>Calliophis biliniatus</i>	KU 309511	1	M	856	141	229	54	Divided	X	X	X	X	X
7	<i>Calliophis biliniatus</i>	KU 311415	1	M	568	52	231	30	Divided	X	X	X	X	X
8	<i>Calliophis bivirgatus bivirgatus</i>	UTA R-63079	1	M	693	59+	286	29+	Divided	X	X	X	X	X
9	<i>Calliophis cf. intestinalis</i>	NMW 27221-4	1	F	334	15	259	16	Entire	X	X	X		
10	<i>Calliophis gracilis</i>	USNM 53447	1	juv.	368	23	309	26	Divided	X	X	X	X	
11	<i>Calliophis intestinalis</i>	UTA R-60738	1	M	391	21	263	16	Divided	X	X	X	X	X
12	<i>Calliophis intestinalis cf. immaculata</i>	NMW 27192-1	1	F	393	28	218	22	Entire		X	X		
13	<i>Calliophis intestinalis immaculata</i>	UTA R-65802	1	M	276	22	212	22	Entire	X	X	X	X	X
14	<i>Calliophis intestinalis lineata</i>	UTA R-65801	1	M	478	40	231	25	Entire	X	X	X	X	X
15	<i>Calliophis maculiceps</i>	MNHN 5459	1	M	348	39	188	30	Divided	X	X	X	X	X
16	<i>Calliophis melanurus</i>	MNHN 46-286	1	F	189	13	269	26	Divided	X	X	X	X	X
17	<i>Calliophis melanurus</i>	MNHN 48-318	1	F	216	17	276	29	Divided	X		X		
18	<i>Calliophis nigrescens</i>	CAS 17265	1	M	567	72	251	40	Divided					X
19	<i>Calliophis nigrotaeniatus</i>	NMW 27220-7	1	M	504	51	211	26	Entire	X	X	X		
20	<i>Calliophis philippinus</i>	KU 310369	1	M	625	56	246	32	Divided	X	X	X	X	X
21	<i>Calliophis philippinus</i>	KU 314913	1	M	438	41	248	32	Divided	X	X	X	X	X
22	<i>Calliophis salitan</i>	PNM 9844	2	M	856	141	229	54	Divided	X	X	X		
23	<i>Dendroaspis angusticeps</i>	UTA R-34982	1	M	274	89	210	108	Divided		X	X	X	X
24	<i>Elapoidea nigra</i>	CAS 168978	1	F	355	24	160	15	Divided		X	X	X	X
25	<i>Hemachatus haemachatus</i>	UTA R-7431	1	M	725	150	132	38	Divided	X	X	X	X	X

#	Species	Catalog Number	ATS	Sex	SVL	TL	V	SC	SC type	S	Q	J	M	C
26	<i>Hemibungarus calligaster</i>	KU 307474	2	M	416	36	204	23	Divided	X	X	X	X	X
27	<i>Hydrophis platurus</i>	UTA R-41049	10	F	449	57	353	50	Entire	X	X	X	X	X
28	<i>Hydrophis schistosus</i>	UTA R-63074	10	M	713	112	256	47	Entire	X	X	X	X	X
29	<i>Laticauda colubrina</i>	UTA R-65800	8	F	425	27	240	35	Divided	X	X	X	X	X
30	<i>Laticauda laticauda</i>	UTA R-6355	8	M	770	119	236	47	Divided	X	X	X	X	X
31	<i>Micrelaps vaillanti</i>	CAS 169941	1	F	391	23	246	22	Divided		X	X	X	X
32	<i>Micruroides euryxanthus</i>	UTA R-60734	1	M	357	31	222	27	Divided	X	X	X	X	
33	<i>Micrurus allenii</i>	UTA R-60556	5	M	734	128	222	52	Divided	X	X	X	X	X
34	<i>Micrurus australis</i>	UTA R-55945	2	M	952	80	257	36	Divided	X	X	X	X	X
35	<i>Micrurus apiatus</i>	UTA R-39267	5	F	502	64	224	46	Divided	X	X	X	X	X
36	<i>Micrurus apiatus</i>	UTA R-39554	5	F	396	43	222	38	Divided	X	X	X	X	X
37	<i>Micrurus apiatus</i>	UTA R-53450	5	F	426	61	210	44	Divided		X	X	X	X
38	<i>Micrurus bocourti</i>	UTA R-58145	1	F	421	37	225	32	Divided		X	X	X	X
39	<i>Micrurus diastema</i>	UTA R-52565	6	F	717	87	215	39	Divided	X	X	X	X	X
40	<i>Micrurus dissolucus</i>	UTA R-54184	1	M	366	41	176	28	Divided		X	X	X	X
41	<i>Micrurus distans</i>	UTA R-14471	1	M	665	88	212	45	Divided		X	X	X	X
42	<i>Micrurus diutius</i>	UTA R-20756	6	M	766	66	214	27	Divided		X	X	X	X
43	<i>Micrurus diutius</i>	UTA R-54182	6	M	622	61	212	31	Divided	X	X	X	X	X
44	<i>Micrurus dumerilii</i>	AMNH 35951	4	F	254	32	212	41	Divided	X	X	X	X	X
45	<i>Micrurus elegans elegans</i>	MZFC 18819	1	M	364	86	201	50	Divided	X	X	X	X	X
46	<i>Micrurus elegans veraepacis</i>	UTA R-58869	1	M	444	73	205	44	Divided	X	X	X	X	X
47	<i>Micrurus elegans veraepacis</i>	UTA R-7072	1	F	775	64	226	30	Divided	X	X	X		
48	<i>Micrurus ephippifer</i>	UTA R-64863	1	M	603	120	213	57	Divided	X	X	X	X	X
49	<i>Micrurus filiformis</i>	UTA R-3423	3	F	247	19	289	34	Divided	X	X	X	X	X
50	<i>Micrurus filiformis</i>	UTA R-65836	3	M	344	32	267	37	Divided	X	X	X	X	X
51	<i>Micrurus fulvius</i>	UTA R-61632	1	M	430	54	210	34	Divided	X	X	X	X	X
52	<i>Micrurus helleri</i>	UTA R-38005	6	F	323	28	257	37	Divided	X	X	X	X	X

#	Species	Catalog Number	ATS	Sex	SVL	TL	V	SC	SC type	S	Q	J	M	C
53	<i>Micrurus helleri</i>	UTA R-55977	6	F	677	57	250	33	Divided	X	X	X	X	
54	<i>Micrurus helleri</i>	UTA R-65841	6	F	395	38	253	38	Divided	X	X	X	X	
55	<i>Micrurus hemprichii</i>	UTA R-29997	1	M	510	55	178	31	Divided	X	X	X	X	X
56	<i>Micrurus hemprichii</i>	UTA R-9683	1	M	735	78	194	31	Divided	X	X	X	X	X
57	<i>Micrurus isozonus</i>	UTA R-22589	4	F	557	33	216	21	Divided	X	X	X	X	X
58	<i>Micrurus isozonus</i>	UTA R-3951	4	F	648	33	217	17	Divided	X	X	X	X	X
59	<i>Micrurus laticollaris</i>	UTA R-52559	4	M	401	48	206	40	Divided	X	X	X	X	X
60	<i>Micrurus laticollaris</i>	UTA R-57562	4	F	496	67	215	40	Divided	X	X	X	X	X
61	<i>Micrurus latifasciatus</i>	UTA R-4606	4	M	344	61	193	53	Divided		X	X	X	
62	<i>Micrurus lemniscatus cf. helleri</i>	UTA R-34563	5	M	275	21	241	32	Divided	X	X	X	X	X
63	<i>Micrurus lemniscatus cf. helleri</i>	UTA R-65803	5	M	703	51	229	33	Divided	X	X	X	X	X
64	<i>Micrurus limbatus</i>	UTA R-64852	1	F	479	44	201	25	Divided	X	X	X	X	X
65	<i>Micrurus limbatus</i>	UTA R-64899	1	M	464	74	188	37	Divided	X	X	X	X	X
66	<i>Micrurus melanotus</i>	AMNH 35934	1	F	439	23	305	21	Divided		X	X	X	X
67	<i>Micrurus melanotus</i>	UTA R-22582	1	M	218	16	309	29	Divided	X	X	X	X	X
68	<i>Micrurus mipartitus</i>	UTA R-54187	2	F	539	36	262	25	Divided	X	X	X	X	X
69	<i>Micrurus mosquitensis</i>	UTA R-12919	5	F	378	42	210	36	Divided	X	X	X	X	X
70	<i>Micrurus nattereri</i>	UTA R-3594	7	M	239	33	182	40	Divided			X	X	
71	<i>Micrurus nattereri</i>	UTA R-54175	7	M	513	76	188	41	Divided	X	X	X	X	
72	<i>Micrurus nattereri</i>	UTA R-55086	7	M	248	35	189	42	Divided	X	X	X	X	
73	<i>Micrurus nattereri</i>	UTA R-60727	7	F	834	88	201	32	Divided	X	X	X	X	X
74	<i>Micrurus nigrocinctus zunilensis</i>	UTA R-64858	2	M	496	77	208	50	Divided	X	X	X	X	X
75	<i>Micrurus obscurus</i>	UTA R-3840	2	F	642	32	214	16	Divided	X	X	X	X	X
76	<i>Micrurus oliveri</i>	UTA R-64893	1	M	602	112	210	52	Divided		X	X	X	X
77	<i>Micrurus ornatissimus</i>	UTA R-60724	1	F	612	65	224	37	Divided	X	X	X	X	X
78	<i>Micrurus pyrrhocryptus</i>	UTA R-51404	1	M	317	29	224	29	Divided	X	X	X	X	X
79	<i>Micrurus renjifoi</i>	UTA R-3490	2	F	405	21	241	17	Divided	X	X	X	X	X

#	Species	Catalog Number	ATS	Sex	SVL	TL	V	SC	SC type	S	Q	J	M	C
80	<i>Micrurus serranus</i>	UTA R-34561	1	M	484	35	218	22	Divided	X	X	X	X	X
82	<i>Micrurus steindachneri</i>	AMNH 28846	2	F	499	51	227	36	Divided	X	X	X	X	X
83	<i>Micrurus steindachneri</i>	AMNH 35819	2	M	510	87	203	42	Divided	X	X	X	X	X
84	<i>Micrurus surinamensis</i>	UTA R-15679	7	F	1074	120	171	31	Divided	X	X	X	X	X
85	<i>Micrurus surinamensis</i>	UTA R-50173	7	M	620	93	171	35	Divided	X	X	X	X	X
86	<i>Micrurus surinamensis</i>	UTA R-54378	7	F	1054	125	178	32	Divided	X	X	X	X	X
87	<i>Micrurus surinamensis</i>	UTA R-5849	7	M	343	50	168	37	Divided		X		X	X
88	<i>Micrurus surinamensis</i>	UTA R-65798	7	F	217	27	183	36	Divided				X	X
89	<i>Micrurus surinamensis</i>	UTA R-65844	7	M	620	90	173	36	Divided	X	X	X	X	X
90	<i>Micrurus tener</i>	FMNH 39479	1	?	?	?	?	?	?	X	X	X		
91	<i>Micrurus tener</i>	UTA R-63282	1	M	506	76	207	41	Divided	X	X	X	X	X
81	<i>Micrurus sp.</i>	UTA R-6086	-	F	726	79	218	40	Divided		X			
92	<i>Naja annulata</i>	UTA R-18199	8	M	327	81	199	74	Divided	X	X	X	X	X
93	<i>Naja christyi</i>	UTA R-18200	8	M	386	95	206	73	Divided	X	X	X	X	X
94	<i>Naja siamensis</i>	UTA R-16872	1	F	287	50	165	48	Divided	X	X	X	X	X
95	<i>Ophiophagus hannah</i>	UTA R-60836	4	M	422	98	242	97	Divided	X	X	X	X	X
96	<i>Oxyuranus scutellatus</i>	UTA R-60839	1	M	1333	240	227	69	Divided	X	X	X	X	X
97	<i>Prosymna stuhlmanni</i>	UTA R-64493	1	M	178	33	135	30	Divided		X	X	X	X
98	<i>Pseudohaje goldii</i>	UTA R-63636	2	M	481	286	198	85	Divided	X	X	X	X	X
99	<i>Simoselaps bertholdi</i>	UMMZ 244197	1	M	153	19	109	?	Divided	X	X	X		
100	<i>Sinomicrurus annularis</i>	ROM 31158	1	M	308	40	197	36	Divided	X	X	X		X
101	<i>Sinomicrurus boettgeri</i>	UTA R-58837	1	M	408	38	195	25	Divided	X	X	X	X	X
102	<i>Sinomicrurus japonicus</i>	CAS 204979	1	M	432	40	203	28	Divided	X	X	X		
103	<i>Sinomicrurus kelloggi</i>	ROM 37079	1	M	505	72	183	40	Divided	X	X		X	X
104	<i>Sinomicrurus maclellandi</i>	CAS 17267	1	M	490	58	203	32	Divided					X
105	<i>Sinomicrurus peinani</i>	ROM 35245	1	M	524	59	210	32	Divided	X	X	X		
106	<i>Sinomicrurus peinani</i>	ROM 37109	1	M	525	59	218	30	Divided	X	X	X	X	X

#	Species	Catalog Number	ATS	Sex	SVL	TL	V	SC	SC type	S	Q	J	M	C
107	<i>Sinomicrurus swinhoei</i>	MVZ 23876	1	F	449	47	232	34	Divided	X	X	X	X	X
108	<i>Walterinnesia aegyptia</i>	UTA R-13021	2	M	848	141	185	46	Divided	X	X	X	X	X

Tail length is abbreviated as TL, ventral scale count as V, subcaudal scale count as SC, skull dataset as S, quadrate dataset as Q, lowerjaw dataset as J, mibdbody vertebra dataset as M, and caudal vertebra dataset as C. Measurements for SVL and TL are in millimeters. Numbering correlates with Supplemental Figures 6-71. Specimens are from the following institutions: American Museum of Natural History, New York, USA (AMNH), California Academy of Sciences, San Francisco, USA (CAS), Field Museum of Natural History, Chicago, USA (FMNH), University of Kansas Natural History Museum, Lawrence, USA (KU), Muséum National d'Histoire Naturelle, Paris, France (MNHN), Museum of Vertebrate Zoology, Berkeley, USA (MVZ), Museo de Zoología Alfonso L. Herrera, Ciudad de México, México (MZFC), Naturhistorisches Museum Wien, Vienna, Austria (NMW), National Museum of the Philippines, Manila, Philippines (PNM), Royal Ontario Museum, Toronto, Canada (ROM), University of Michigan Museum of Zoology, Ann Arbor, USA (UMMZ), Smithsonian National Museum of Natural History, Washington, D.C., USA (USNM), University of Texas Arlington Amphibian and Reptile Diversity Research Center, Arlington, USA (UTA).

Table 2.2. Regions of the skull used in this study.

Region	Definition
Premaxilla	Anterior and ventral faces of premaxilla.
Nasal	Dorsal surface of nasal.
Prefrontal	Extent of the dorsoanterior surface of prefrontal that can be seen in dorsal aspect.
Frontal	Dorsal surface of frontal.
Parietal	Dorsal and lateral surfaces of parietal.
Supraoccipital	Dorsal surface of supraoccipital.
Supratemporal	Lateral surface of supratemporal.
Prootic	Lateral surface of prootic. Posterior extent of the region is interrupted by, and therefore defined by, the intrusion of the supratemporal. In most specimens the supratemporal is firmly fused with the braincase at its anterior end. Segmenting it out would leave the lateral surface of the prootic altered and unfit for inclusion in analysis.
Exoccipital	Dorsal, lateral, and posterior surfaces of exoccipital. The dorsolateral extent of this region is defined by the exoccipital ridge as the complete surface is obscured by the supratemporal in most specimens.
Septomaxilla	Defined by two curves, one along the dorsal edge to capture posterior and anterior extent, and the second along the anterior edge.
Vomer	Defined by one curve to capture the posterior and anterior extent in ventral view.
Maxilla	Surface points were placed on the lateral surface from the tooth row ventrally to the dorsal ridge. Additional landmarks and curves are included to capture the depth of the complex geometry.
Palatine	Surface points were placed on the lateral surface from the tooth row ventrally to the dorsal ridge. Additional landmarks and curves are included to capture the depth of the complex geometry.
Ectopterygoid	Ventrolateral surface of ectopterygoid.
Pterygoid	Ventral surface of the pterygoid.
Basisphenoid	Ventral surface of basisphenoid.
Basioccipital	Ventral surface of basioccipital.

Table 2.3. Landmarks and semi-landmark curves of the skull.

Landmark position	
1	Premaxilla; anterior most point in dorsal view
2	Premaxilla; dorsal most point
3	Premaxilla; lateral most point
4	Premaxilla; posterior lateral projection
5	Premaxilla; most posterior point along midline in ventral view
6	Nasal; anteromedial corner in dorsal view
7	Nasal; anterolateral corner in dorsal view
8	Nasal; posterolateral corner in dorsal view
9	Nasal; posteromedial corner in dorsal view
10	Prefrontal; point of greatest medial inflection of dorsomedial flange
11	Prefrontal; anterolateral end in dorsal/lateral view
12	Prefrontal; lateral posteroventral end; ventral end
13	Prefrontal; posterolateral end of left prefrontal in dorsal (or lateral) view
14	Frontal; anteromedial corner in dorsal view
15	Frontal; end of left anterolateral process; most lateral point of contact between frontal and prefrontal in dorsal view
16	Frontal; anterolateral corner of joint/suture between parietal and frontal
17	Frontal; posteromedial corner of joint/suture between parietal and frontal
18	Parietal; most anterior point dorsal view along mid-sagittal plane
19	Parietal; anterolateral corner of joint/suture between parietal and frontal
20	Parietal; anterolateral projection at frontal junction and around orbital foramen
21	Parietal; left anteroventral corner
22	Parietal; point of contact between basisphenoid, parietal, and left pectoral
23	Parietal; most posterior point along mid-sagittal plane in dorsal view
24	Supraoccipital; most anterior point along mid-sagittal plane in dorsal view
25	Supraoccipital; anterolateral corner next to pectoral
26	Supraoccipital; posterolateral corner
27	Supraoccipital; most posterior point along mid-sagittal plane in dorsal view
28	Supratemporal; anterodorsal end
29	Supratemporal; anteroventral end
30	Supratemporal; posterior end
31	Supratemporal; point along anterior edge in line with posterior edge of pectoral
32	Pectoral; anterodorsal corner
33	Pectoral; anteroventral corner
34	Pectoral; point of contact between basisphenoid, basioccipital, and pectoral
35	Pectoral; posteroventral corner
36	Pectoral; posterodorsal corner
37	Pectoral; dorsal point of foramen for the maxillary branch of the trigeminal nerve
38	Pectoral; ventral point of foramen for the maxillary branch of the trigeminal nerve
39	Pectoral; dorsal point of foramen for the mandibular branch of the trigeminal nerve
40	Pectoral; ventral point of foramen for the mandibular branch of the trigeminal nerve
41	Exoccipital; anteromedial corner
42	Exoccipital; anterior most point of exoccipital crest at exoccipital-supraoccipital suture
43	Exoccipital; ventral most point of exoccipital crest
44	Exoccipital; anterodorsal end of opening for columella
45	Exoccipital; anteroventral end of opening for columella
46	Exoccipital; anteroventral corner
47	Exoccipital; posteroventral most point
48	Exoccipital; posterolateral corner dorsolateral to foramen magnum
49	Exoccipital; most posterior point in dorsal view along mid-sagittal plane
50	Exoccipital; dorsal point of exoccipital foramen
51	Exoccipital; ventral point of exoccipital foramen
52	Septomaxilla; end of conchal process
53	Septomaxilla; anterior most point
54	Septomaxilla; posterior most point
55	Vomer; anterior extreme in ventral view
56	Vomer; posterior extreme in ventral view
57	Maxilla; anterior most point along tooth row
58	Maxilla; posterior most point along tooth row
59	Maxilla; posterior most point of ectopterygoid process
60	Maxilla; anterior most point of ectopterygoid process
61	Maxilla; posterior most point of palatine facet
62	Maxilla; anterior most point of palatine facet
63	Palatine; anterior tip
64	Palatine; lateral end of the maxillary process
65	Palatine; medial end of choanal process
66	Palatine; posterior end
67	Ectopterygoid; anterodorsal tip of ectopterygoid
68	Ectopterygoid; posterior end of ectopterygoid
69	Ectopterygoid; anteroventral tip of ectopterygoid
70	Pterygoid; anterodorsal end of palatine process of pterygoid

Landmark position	
71	Pterygoid; posterolateral extent of pterygoid
72	Pterygoid; posteromedial extent of pterygoid
73	Pterygoid; anteromedial end of pterygoid
74	Basisphenoid; anterior end of cultriform process in ventral view
75	Basisphenoid; point of contact between basisphenoid, parietal, and prootic
76	Basisphenoid; point of contact between basisphenoid, basioccipital, and prootic
77	Basisphenoid; most posterior point along mid-sagittal plane
78	Basisphenoid; lateral edge of posterior Vidian foramen
79	Basisphenoid; medial edge of posterior Vidian foramen
80	Basioccipital; most anterior point of basioccipital along mid-sagittal plane in ventral view
81	Basioccipital; point of contact between basisphenoid, basioccipital, and left prootic; placed on basioccipital
82	Basioccipital; most posterior point of contact between left prootic and basioccipital
83	Basioccipital; tip of left posterolateral process of basioccipital
84	Basioccipital; posterior end of occipital condyle
Semi-landmark curve position	
1	Premaxilla; midline; point 1 to 2
2	Premaxilla; dorsolateral edge; point 2 to 3
3	Premaxilla; anteroventral edge; point 1 to 3
4	Premaxilla; posteroventral edge; point 3 to 4
5	Premaxilla; posteroventral edge; point 4 to 5
6	Premaxilla; midline in ventral view; point 1 to 5
7	Nasal; anterior edge; point 6 to 7
8	Nasal; lateral edge; point 7 to 8
9	Nasal; posterior edge; point 8 to 9
10	Nasal; medial edge; point 6 to 9
11	Prefrontal; anteromedial edge; point 10 to 11
12	Prefrontal; anterolateral edge; point 11 to 12
13	Prefrontal; posterolateral edge; anterior margin of orbital; point 12 to 13
14	Prefrontal; posteromedial edge along anterior edge; point 10 to 13
15	Frontal; anterior edge; point 14 to 15
16	Frontal; lateral edge; point 15 to 16
17	Frontal; posterior edge; point 16 to 17
18	Frontal; medial edge; point 14 to 17
19	Parietal; anterior edge in dorsal aspect; point 18 to 19
20	Parietal; margin; point 19 to 20
21	Parietal; margin; point 20 to 21
22	Parietal; margin, along edge of basisphenoid; point 21 to 22
23	Parietal; posterior edge; point 22 to 23
24	Parietal; midline in dorsal aspect; point 18 to 23
25	Supraoccipital; anterior edge from midline to anterolateral most point; point 24 to 25
26	Supraoccipital; lateral edge; point 25 to 26
27	Supraoccipital; posterior edge from most posterolateral point to midline; point 26 to 27
28	Supraoccipital; midline; point 24 to 27
29	Supratemporal; anterior edge; point 28 to 29
30	Supratemporal; ventrolateral edge; point 29 to 30
31	Supratemporal; posterodorsal edge; point 30 to 31
32	Supratemporal; anterodorsal edge; point 28 to 31
33	Prootic; anterior edge that connects points 32 and 33
34	Prootic; edge along prootic-basisphenoid suture; point 33 to 34
35	Prootic; edge along prootic-basioccipital suture; point 34 to 35
36	Prootic; posteroventral edge; point 29 to 35
37	Prootic; posterior edge, dorsal to the supratemporal; point 31 to 36
38	Prootic; dorsal edge that connects points 32 and 36
39	Prootic; anterior edge of foramen for the maxillary branch of the trigeminal nerve; point 37 to 38
40	Prootic; posterior edge of foramen for the maxillary branch of the trigeminal nerve; point 37 to 38
41	Prootic; anterior edge of the foramen for the mandibular branch of the trigeminal nerve; point 39 to 40
42	Prootic; posterior edge of the foramen for the mandibular branch of the trigeminal nerve; point 39 to 40
	Curves 30 and 33 of the supratemporal also define the boundary of the prootic
43	Exoccipital; anterior edge; point 41 to 42
44	Exoccipital; exoccipital crest; point 42 to 43
45	Exoccipital; the ventral extent of the exoccipital crest to the anterior edge of the exoccipital, ventral to the supratemporal; point 43 to 44
46	Exoccipital; edge of foreman which the columella passes through that connects points 44 and 45
47	Exoccipital; anteroventral edge; point 45 to 46
48	Exoccipital; ventral edge; point 46 to 47
49	Exoccipital; posterolateral edge of exoccipital; point 47 to 48
50	Exoccipital; posterodorsal edge of exoccipital; point 48 to 49

Semi-landmark curve position	
51	Exoccipital; medial edge of exoccipital along the sagittal plane; point 41 to 49
52	Exoccipital; anterior edge of exoccipital foramen; point 50 to 51
53	Exoccipital; posterior edge of exoccipital foramen; point 50 to 51
54	Septomaxilla; dorsoanterior edge; point 52 to 53
55	Septomaxilla; dorsal edge along sagittal plane; point 53 to 54
56	Vomer; medial edge in ventral view; point 55 to 56
57	Maxilla; lateral edge along tooth row; point 57 to 58
58	Maxilla; posteromedial ridge; point 58 to 59
59	Maxilla; edge of ectopterygoid process; point 59 to 60
60	Maxilla; medial edge; point 60 to 61
61	Maxilla; edge of platine facet; point 61 to 62
62	Maxilla; anterodorsal ridge; point 57 to 62
63	Maxilla; dorsal ridge; point 57 to 58
64	Palatine; anterodorsal edge; point 63 to 64
65	Palatine; dorsal edge; point 64 to 65
66	Palatine; posterodorsal edge; point 65 to 66
67	Palatine; ventrolateral edge; point 63 to 66
68	Palatine; ventromedial edge; point 63 to 66
69	Ectopterygoid; dorsal edge; point 67 to 68
70	Ectopterygoid; ventral edge; point 68 to 69
71	Ectopterygoid; anterior edge; point 67 to 69
72	Pterygoid; lateral edge; point 70 to 71
73	Pterygoid; Posterior edge; point 71 to 72
74	Pterygoid; Medial edge; point 72 to 73
75	Pterygoid; Anterior edge; point 70 to 73
76	Basisphenoid; lateral edge; point 74 to 75
77	Basisphenoid; lateral edge; point 75 to 76
78	Basisphenoid; posterior edge; point 76 to 77
79	Basisphenoid; midline; point 74 to 77
80	Basisphenoid; anterior edge of posterior Vidian foramen; point 78 to 79
81	Basisphenoid; posterior edge of posterior Vidian foramen; point 78 to 79
82	Basioccipital; anterior edge; point 80 to 81
83	Basioccipital; anterolateral edge along suture with prootic; point 81 and 82
84	Basioccipital; lateral edge; point 82 to 83
85	Basioccipital; posterolateral edge; point 83 to 84
86	Basioccipital; midline; point 80 to 84

Table 2.4. Model structures evaluated for modularity of the skull dataset.

Model	Definition
1	no modules
2A	jaw, else
2B	jaw+pmx, else
2C	jaw+pmx+pfr, else
2D	jaw+pfr, else
2E	jaw+pmx+smx+v, else
2F	braincase, else
2G	braincase+pfr, else
2H	braincase+st, else
2I	braincase+pfr+st, else
2J	jaw+bo+bs, else
2K	jaw+bs+bo+v, else
2L	jaw+bs+bo+v+smx, else
3A	braincase+st, jaw, snout+pfr
3B	jaw, braincase+snout, st
3C	braincase+pfr+st, jaw, snout
3D	braincase+st, snout, jaw+pfr
3E	braincase+st+pfr, jaw+v, snout
3F	braincase+st+pfr, jaw+v+smx, snout
3G	braincase+st, jaw+v+pfr, snout
3H	braincase+st, jaw+v+smx+pfr, snout
3I	pro+so+exo+bo, jaw, else
3J	braincase+pfr+st, ecp+pt, snout+mx+pal
4A	jaw, snout, f+p+bs+pfr, pro+so+exo+bo+st
4B	jaw+pfr, snout, f+p+bs, pro+so+exo+bo+st
4C	jaw, snout+pfr, f+p+bs, pro+so+exo+bo+st
4D	snout+pfr, jaw, braincase, st
4E	snout+pfr, f+p+pro+so+exo+st, bs+bo, jaw
4F	snout, jaw, f+p+pro+so+exo+st+pfr, bs+bo
4G	snout, jaw+pfr, f+p+pro+so+exo+st, bs+bo
4H	pmx+n+smx, jaw+v, f+p+pro+so+exo+pfr+st, bs+bo
4I	pmx+n, jaw+v+smx, f+p+pro+so+exo+pfr+st, bs+bo
4J	pmx+n, jaw+v+smx+pfr, f+p+pro+so+exo+st, bs+bo
4I	pmx, n+smx+v, pfr+braincase+st, jaw
5A	pmx, na+smx+v, braincase+pfr, st, jaw
5B	snout, braincase, pfr, st, jaw

Model	Definition	
5C	pmx, na+smx+v, jaw, braincase+pfr, st	7J pmx+na, pfr+fr, smx+v, p, bs+pro+so+exo+bo, st, jaw
5D	snout, braincase, st, pfr+mx+pal, ecp+pt	7K snout, pfr, fr, p, bs+pro+so+exo+bo, st, jaw
5E	snout, braincase+pfr, st, mx+pal, ecp+pt	8A pmx, na, smx+v, pfr braincase, st, mx+pal, ecp+pt
5F	snout, braincase, st, pfr+mx+ecp, pal+pt	8B pmx, na, smx+v, pfr braincase, st, mx+ecp, pal+pt
5G	snout, braincase+pfr, st, mx+ecp, pal+pt	8C pmx+na, smx, v, pfr braincase, st, mx+pal, ecp+pt
5H	f+p+pro+so+exo+pfr, bs+bo, st, jaw, snout	8D pmx+na, smx, v, pfr braincase, st, mx+ecp, pal+pt
5I	f+p+pro+so+exo, bs+bo, st, jaw+pfr, snout	8E pmx+na, smx+v, pfr braincase, st, mx, pal, ecp+pt
5J	f+p+pro+so+exo, bs+bo, st, jaw, snout+pfr	8F pmx+na, smx+v, pfr braincase, st, mx+pal, ecp, pt
5K	snout+pfr, frontal+p+bs, pro+so+exo+bo, st, jaw	8G snout, pfr braincase, st, mx, pal, ecp, pt
5L	snout+pfr+frontal, p+bs, pro+so+exo+bo, st, jaw	8H pmx, na+smx+v, pfr braincase, st, mx+pal, ecp, pt
5M	snout, pfr+frontal+p+bs, pro+so+exo+bo, st, jaw	8I pmx, na+smx+v, pfr braincase, st, mx, pal, ecp+pt
6A	pmx+na, smx+v, pfr, braincase, st, jaw	8J pmx+na, pfr, f+p+bs, pro+so+exo+bo, st, jaw, smx, v
6B	pmx, na+smx+v, pfr, braincase, st, jaw	8K pmx, na, pfr, f+p+bs, pro+so+exo+bo, st, jaw, smx+v
6C	pmx+na, smx+v, braincase+pfr, pal+pt, mx+ecp, st	8L pmx, na, pfr, f+p+bs, pro+so+exo+bo+st, jaw, smx, v
6D	pmx+na, smx+v, braincase+pfr, pal+mx, pt+ecp, st	8M pmx+na, smx, v, pfr, f+p+pro+so+exo, st, bs+bo, jaw
6E	pmx+na, smx+v, f+p+pro+so+exo+pfr, st, bs+bo, jaw	8N pmx, na, smx+v, pfr, f+p+pro+so+exo, st, bs+bo, jaw
6F	snout, f+p+pro+so+exo, pfr, st, bs+bo, jaw	8O pmx, na, smx, v, pfr, f+p+pro+so+exo+st, bs+bo, jaw
6G	pmx+na, smx+v, f+p+pro+so+exo, st, bs+bo, jaw+pfr	9A pmx, na, smx, v, braincase+st+pfr, mx, pal, ecp, pt
6H	snout, pfr, fr+bs+p, pro+so+exo+bo, st, jaw	9B pmx, na, smx, v, braincase+st, pfr, mx, pal, ecp+pt
6I	pmx+na, smx+v, pfr+fr+bs+p, pro+so+exo+bo, st, jaw	9C pmx, na, smx, v, braincase+pfr, mx, pal, ecp+pt, st
6J	snout, pfr, +fr, bs+p, pro+so+exo+bo, st, jaw	9D pmx, na, smx, v, braincase+pfr, mx, pal+pt, ecp, st
6K	pmx+na, smx+v, fr+bs+p, pro+so+exo+bo, st, jaw+pfr	9E pmx, na, smx, v, braincase+pfr, mx+pal, pt, ecp, st
6L	pmx+na, smx+v, pfr, fr+bs+p, pro+so+exo+bo+st, jaw	9F pmx, na, smx+v, pfr, f+p+bs, pro+so+exo+bo, st, mx+pal, ecp+pt
7A	pmx+na, pfr, smx+v, fr+p+bs, pro+so+exo+bo, st, jaw	9G pmx, na, smx+v, pfr, f+p+bs, pro+so+exo+bo, st, mx+ecp, pal+pt
7B	pmx+na, pfr, smx+v, f+p+pro+so+exo, bs+bo, st, jaw	9H pmx+na, smx, v, pfr, f+p+bs, pro+so+exo+bo, st, mx+pal, ecp+pt
7D	pmx, pfr, na+smx+v, fr+p+bs, pro+so+exo+bo, st, jaw	9I pmx+na, smx, v, pfr, f+p+bs, pro+so+exo+bo, st, mx+pal, ecp+pt
7E	pmx, na, smx+v, fr+p+bs, pro+so+exo+bo, st, jaw+pfr	9J pmx, na, smx, v, pfr, f+p+pro+so+exo, st, bs+bo, jaw
7F	pmx, na, pfr, smx+v, braincase+st, pal+pt, mx+ecp	9K pmx+na, smx+v, pfr, f+p+pro+so+exo, st, bs+bo, mx, pal, ecp+pt
7G	pmx, na, pfr, smx+v, braincase+st, ecp+pt, mx+pal	
7H	pmx+na, pfr, smx+v, braincase, st, pal+pt, mx+ecp	
7I	pmx+na, pfr, smx+v, braincase, st, ecp+pt, mx+pal	

Model	Definition		
9L	pmx+na, smx+v, pfr, f+p+pro+so+exo+st, bs+bo, mx, pal, ecp, pt	11D	pmx, na, smx, v, pfr, f+p+bs, pro+so+exo+bo, st, pal, mx, ecp+pt
9M	pmx+na, smx+v, pfr, fr+p, bs, bo, so+exo+po, st, jaw	11E	pmx, na, smx, v, pfr, f+p+bs, pro+so+exo+bo, st, pal+mx, ecp, pt
9N	pmx, na, smx+v, pfr, fr+p, bs+bo, so+exo+po, st, jaw	11F	pmx, na+v+smx, pfr+fr, p, so, po, exo, st, bs, bo, jaw
9O	pmx+na, smx, v, pfr, fr+p, bs+bo, so+exo+po, st, jaw	11G	pmx+na, v+smx, pfr+fr, p, so, po, exo, st, bs, bo, jaw
10A	pmx, na, smx, v, f+p+bs, pro+so+exo+bo, st, mx+pal, ecp+pt	11H	pmx+na, v+smx, pfr, fr+p, so, po, exo, st, bs, bo, jaw
10B	pmx, na, smx, v, f+p+bs, pro+so+exo+bo, st, mx+ecp, pal+pt	11I	pmx+na, v+smx, pfr+fr, p, so, po, exo, st, bs+bo, mx+pal, ecp+pt
10C	pmx+na, smx+v, pfr, f+p+bs, pro+so+exo+bo, st, mx, pal, ecp, pt	11J	pmx+na, v+smx, pfr+fr, p, so, po, exo, st, bs+bo, mx+ecp, pal+pt
10D	pmx, na+smx+v, pfr, f+p+bs, pro+so+exo+bo, st, mx, pal, ecp, pt	11K	pmx+na, v+smx, pfr, fr, p, so, po, exo, st, bs+bo, Jaw
10E	pmx, na, smx+v, pfr, f+p+bs, pro+so+exo+bo+st, mx, pal, ecp, pt	11L	pmx+na, smx+v, pfr, fr, p+bs, so+exo, po+bo, st, mx, pal, ecp+pt
10F	pmx, na, pfr, smx+v, fr+p, bs, bo, so+exo+po, st, jaw	11M	pmx+na, smx+v, pfr, fr, p+bs, so+exo, po+bo, st, mx+ecp, pal, pt
10G	pmx+na, pfr, smx, v, fr+p, bs, bo, so+exo+po, st, jaw	11N	pmx+na, smx+v, pfr, fr, p+bs, so, exo, po+bo, st, mx+pal, ecp+pt
10H	pmx+na, pfr, smx+v, fr+pal, bs, bo, so+exo+po, st, mx+pal, ecp+pt	11O	pmx+na, smx+v, pfr, fr, p+bs, exo, po+so, bo, st, mx+pal, ecp+pt
10I	pmx+na, pfr, smx+v, fr+pal, bs, bo, so+exo+po, st, mx+ecp, pal+pt	11P	pmx+na, smx+v, pfr, fr, p+bs, exo, po+so+bo, st, mx, pal, ecp+pt
10J	pmx+na, smx+v, pfr, fr+pal, bs+bo, so, po+exo, st, mx+pal, ecp+pt	12A	pmx, na, smx+v, fr, p, bs, bo, so, exo, po, st, jaw+pfr
10K	pmx+na, smx+v, pfr, fr+pal, bs+bo, so, po+exo, st, mx+ecp, pal+pt	12B	pmx+na, smx+v, fr, p, bs, bo, so, exo, po, st, jaw, pfr
10L	pmx+na, smx+v, pfr, fr+p, bs, bo, so, po+exo, st, jaw	12C	pmx, na, smx+v, fr, p+bs, bo, so, exo, po, st, jaw, pfr
10M	pmx, na, smx+v, pfr, fr+pal, bs+bo, so, po+exo+st, mx+pal, ecp+pt	12D	pmx, na, smx, v, fr+p+bs, bo, so, exo, po, st, jaw, pfr
10N	pmx, na, smx+v, pfr, fr+pal, bs+bo, so, po+exo+st, mx+ecp, pal+pt	12E	pmx, na, smx+v, fr, p, bs, bo+po, so, exo, st, jaw, pfr
10O	pmx+na, smx, v, pfr, fr+pal, bs+bo, so, po+exo+st, mx+pal, ecp+pt	12F	pmx, na, smx+v, fr, p, bs, bo, po+so, exo, st, jaw, pfr
10P	pmx+na, smx, v, pfr, fr+pal, bs+bo, so, po+exo+st, mx+ecp, pal+pt	12G	pmx, na, smx+v, fr, p, bs, bo, po, so+exo, st, jaw, pfr
10Q	pmx+na, smx+v, pfr, fr+p, so+exo, st, bs, po, bo, jaw	12H	pmx, na, smx+v, fr, p, bs, bo, po+exo, so, st, jaw, pfr
10R	pmx+na, smx+v, pfr, fr+pal, so+exo, st, bs, po+bo, mx+pal, ecp+pt	12I	pmx+na, pfr, fr, p, pro+so+exo+bo, st, smx+v, mx+pal, ecp, pt, bs
10S	pmx+na, smx+v, pfr, fr+pal, so+exo, st, bs, po+bo, mx+ecp, pal+pt	12J	pmx, na, pfr, fr, p, pro+so+exo+bo, st, smx+v, mx+pal, ecp, pt, bs
11A	pmx, na, smx, v, pfr, braincase, st, pal, mx, ecp, pt	12K	pmx+na, pfr, fr, p, pro+so+exo+bo, st, smx, v, mx+pal, ecp, pt, bs
11B	pmx, na, smx, v, pfr, f+p+bs, pro+so+exo+bo+st, pal, mx, ecp, pt	12L	pmx, na, pfr, fr, p, pro+so+exo+bo, st, smx+v, mx+ecp, pal, pt, bs
11C	pmx, na, smx, v, pfr, bs+bo, f+p+pro+so+exo+st, pal, mx, ecp, pt	12M	pmx+na, pfr, fr, p, pro+so+exo+bo, st, smx+v, mx+ecp, pal, pt, bs
		12N	pmx, na, pfr, fr, p, pro+so+exo+bo, st, smx+v, mx, ecp, pt+pal, bs

Model	Definition	
13A	pmx+na, pfr, smx+v, fr+p+bs, so, exo, po, st, bo, mx, pal, ecp, pt	14G pmx, na, smx, v, pfr, fr, p, bs, so, exo+po+bo, st, mx, pal, ecp+pt
13B	pmx+na, pfr, smx+v, fr, p+bs, so, exo, po, st, bo, mx+pal, ecp, pt	14H pmx, na, smx, v, pfr, fr, p, bs, so+exo+po, bo, st, mx, pal, ecp+pt
13C	pmx+na, pfr, smx+v, fr+p, bs, so, exo, po, st, bo, mx+pal, ecp, pt	14I pmx+na, smx+v, pfr, fr, p, bs+bo, so, exo, po, st, mx, pal, ecp, pt
13D	pmx+na, pfr, smx+v, fr, p+bs, so, exo, po, st, bo, mx, pal, ecp+pt	14J pmx, na, smx, v, pfr, fr, p, bs+bo, so, exo, po, st, mx+pal, ecp+pt
13E	pmx+na, pfr, smx+v, fr+p, bs, so, exo, po, st, bo, mx, pal, ecp+pt	14K pmx, na, smx, v, pfr, fr, p, bs+bo, so+exo+po, st, mx, pal, ecp, pt
13F	pmx+na, pfr, smx+v, fr, p, bs, so, exo, po, st, bo, mx+pal, ecp+pt	14L pmx, na, smx+v, pfr, fr+p, bs+bo, so, exo, po, st, mx, pal, ecp, pt
13G	pmx, na, pfr, smx, v, fr, p, bs, so, exo, po+bo, st, jaw	15A pal+ecp+pt, else separate
13H	pmx+na, pfr, smx, v, fr, p, bs, so, exo, po, bo, st, jaw	15B mx+pal, ecp+pt, else separate
13I	pmx, na, pfr, smx+v, fr, p, bs, so, exo, po, bo, st, jaw	15C mx+ecp, pal+pt, else separate
13J	pmx, na, pfr, smx, v, fr, p, bs, so+po, exo, bo, st, jaw	15D mx+pal+ecp, else separate
13K	pmx, na, pfr, smx, v, fr, p, bs, po, so+exo, bo, st, jaw	15E pmx+na, smx+v, else separate
13L	pmx, na, pfr, smx, v, fr, p, bs, so, po+exo, bo, st, jaw	15F pmx, na, smx+v, ecp+pt, else separate
13M	pmx+na, pfr, fr, p, bs+bo, so, exo, po, st, mx+pal, ecp, pt, smx+v	15G pmx+na, ecp+pt, else separate
13N	pmx+na, pfr, fr, p, bs+bo, so, exo, po, st, mx, pal, ecp+pt, smx+v	15H pmx, na, smx+v, mx+pal, else separate
13O	pmx+na, pfr, fr+p, bs+bo, so, exo, po, st, mx, pal, ecp, pt, smx+v	15I pmx+na, mx+pal, else separate
13P	pmx+na, pfr, fr, p+so, bs+bo, exo, po, st, mx, pal, ecp, pt, smx+v	15J fr+p+bs, else separate
13Q	pmx+na, pfr, fr, p+po, bs+bo, exo, so, st, mx, pal, ecp, pt, smx+v	15K p+bs, bo+po, else separate
13R	pmx, na, pfr, fr, p, bs+bo, so+exo, po, st, mx+pal, ecp, pt, smx+v	15L p+bs, so+po, else separate
13S	pmx, na, pfr, fr, p, bs+bo, so+po, exo, st, mx+pal, ecp, pt, smx+v	15M p+bs, exo+po, else separate
14A	jaw, pmx, na, smx, v, pfr, fr, p, bs, so, exo, po, st, bo	15N p+bs, exo+so, else separate
14B	snout, pfr, fr, p, bs, so, exo, po, st, bo, mx, pal, ecp, pt	15O p+bs, exo+bo, else separate
14C	pmx+na, smx, v, pfr, fr+p+bs, so, exo, po, st, bo, mx, pal, ecp, pt	16A pmx+na, else separate
14D	pmx, na, smx, v, pfr, fr, p, bs, st, pro+so+exo+bo, mx, pal, ecp, pt	16B pfr+fr, else separate
14E	pmx, na, smx, v, pfr+fr+p+bs, so, exo, po, st, bo, mx, pal, ecp, pt	16C p+bs, else separate
14F	pmx, na, smx, v, pfr, fr, pal, bs, so+exo, po+bo, st, mx, pal, ecp+pt	16D po+exo, else separate
		16E mx+ecp, else separate
		16F smx+v, else separate
		16G fr+p, else separate
		16H bo+po, else separate
		16I so+exo, else separate
		16J exo+bo, else separate
		16K pal+mx, else separate
		16L na+smx, else separate
		16M p+so, else separate
		16N bs+bo, else separate
		16O ecp+pt, else separate
		17 all separate

Single bone abbreviations are in line with Cundall and Irish (2008). jaw=ecp+mx+pal+pt, snout=pmx+na+smx+v, braincase=f+p+pro+so+exo+bo+bs

Table 2.5. Landmarks and semi-landmark curves of the quadrate.

Single Landmark Points		
1	Anterior most point along dorsal ridge	10 Ventrolateral most point of articulation with the articular
2	Posterior most point along dorsal ridge	
3	Posterolateral most point of articulation with the articular	Semi-landmark Curves
4	Dorsoaterior most point of articulation with the articular	1 Dorsal edge that connects; point 1 to 2
5	Posteromedial most point of articulation with the articular	2 Lateral edge that connects; point 1 to 3
6	Ventromedial most point of articulation with the articular	3 Edge of quadrate/articular joint; point 3 to 4
7	Anterolateral most point of articulation with the articular	4 Edge of quadrate/articular joint; point 4 to 5
8	Dorsoposterior most point of articulation with the articular	5 Edge of quadrate/articular joint; point 5 to 6
9	Anteromedial most point of articulation with the articular	6 Edge of quadrate/articular joint; point 6 to 7

Table 2.6. Regions of the lower jaw used in this study.

Region	Definition
Dentary	Lateral surface of dentary.
Compound	Lateral surface of compound.
Angular	Medial surface of angular.
Splenial	Medial surface of splenial.

Table 2.7. Landmarks and semi-landmark curves of the lower jaw.

Single Landmark Points		
1	Dentary; anterior tip	13 Most dorsal point of contact between splenial and angular in medial view
2	Dentary; posterodorsal extreme	14 Most ventral contact between angular and splenial
3	Dentary; most concave point along posterior edge in lateral aspect	15 Splenial; anterior tip
4	Dentary; end of posteroventral process	16 Anterior edge of dentary foramen seen in lateral view
5	Compound; anterior tip	17 Posterior edge of dentary foramen
6	Compound; anterolateral most point of the compound/quadrate joint	18 Anterior edge of compound foramen seen in lateral view
7	Compound; anteromedial most point of the compound/quadrate joint	19 Posterior edge of compound foramen
8	Compound; posterolateral most point of the compound/quadrate joint	
9	Compound; posteromedial most point of the compound/quadrate joint	Semi-landmark Curves
10	Compound; posterior end retroarticular process	
11	Most posteroventral contact between angular and compound	1 Dentary; dorsolateral edge, along tooth base; point 1 to 2
12	Angular; most anterodorsal point of dorsal flange	2 Dentary; posterolateral edge; point 2 to 3
		3 Dentary; posterolateral edge; point 3 to 4
		4 Dentary; ventral edge; point 1 to 4
		5 Compound; dorsolateral edge; point 5 to 6

Semi-landmark Curves	
6	Anterior ridge of compound/quadrat joint; point 6 to 7
7	Posterior ridge of compound quadrat joint; point 8 to 9
8	Compound; posterodorsal edge; point 8 to 10
9	Compound; ventral edge; point 10 to 11
10	Compound; anteroventral edge; point 5 to 11
11	Angular; dorsal edge; point 11 to 12
12	Angular; anterior edge of angular; point 12 to 13
13	Boundary of angular and splenial in medial aspect; point 13 to 14
14	Angular; ventral edge; point 11 to 14
15	Splenial; ventral edge; point 14 to 15
16	Splenial; dorsal edge of splenial; point 13 to 15
17	Dorsal edge of dentary foramen; point 16 to 17
18	Ventral edge of dentary foramen; point 16 to 17
19	Ventral edge of compound foramen; point 18 to 19
20	Dorsal edge of compound foramen; point 18 to 19

Table 2.8. Model structures evaluated for modularity of the lower jaw.

Definition	
1	no modules
2A	compound+dentary, angular+splenial
2B	dentary+splenial, compound+angular
2C	dentary+angular+splenial, compound
2D	compound+angular+splenial, dentary
2E	dentary+compound+splenial, angular
2F	dentary+compound+angular, splenial
3A	compound, dentary, angular+splenial
3B	compound+dentary, angular, splenial
3C	dentary, splenial, compound+angular
3D	dentary+splenial, compound, angular
3E	dentary, angular+splenial, compound
3F	dentary+angular, splenial, compound
4	all separate

Table 2.9. Landmarks and semi-landmark curves of the midbody vertebrae.

Single Landmark Points	
1	Posterior most point of zygosphenal articular facet
2	Anterior most point of zygosphenal articular facet
3	Anterior most point of zygosphenal along sagittal plane
4	Anterior base of neural spine
5	Anterior most point of neural spine
6	Posterior most point of neural spine
7	Posterior base of neural spine
8	Posterior most point of zygantrum along sagittal plane
9	Posterior most point of left postzygapophyseal articular facet
10	Anterior most point of left postzygapophyseal articular facet
11	Medial most point along interzygapophyseal ridge
12	Anterior most point of left prezygapophyseal articular facet
13	Posterior most point of left prezygapophyseal articular facet
14	End of prezygapophyseal accessory process
15	End of parapophysial process
16	Ventral most point of parapophysis
17	Dorsal most point of diapophysis
18	Point along cotyle margin that intersects with medial ridge of parapophysial process
19	Point along cotyle margin that intersects with ventrolateral most margin of neural canal
20	Anterodorsal extent of cotyle along sagittal plane
21	Anterodorsal extent of condyle along sagittal plane
22	Point along condyle margin that intersects with ventrolateral most margin of neural canal
23	Posterior most point of zygantral articular facet
24	Anterior most point of zygantral articular facet
25	Anteroventral extent of condyle along sagittal plane
26	Posterior extent of hypapophysis
27	Anteroventral extent of cotyle along sagittal plane

Semi-landmark Curves	
1	Dorsolateral edge of zygosphenal articular facet; point 1 to 2
2	Ventromedial edge of zygosphenal articular facet; point 1 to 2
3	Anterior edge of zygosphen; point 2 to 3
4	Dorsomedial line; point 3 to 4
5	Anterolateral edge of neural spine; point 4 to 5
6	Dorsolateral edge of neural spine; point 5 to 6
7	Posterolateral edge of neural spine; point 6 to 7
8	Dorsal edge of neural spine; point 4 to 7
9	Dorsomedial line along sagittal plane; point 7 to 8
10	Internal dorsal line of neural canal along sagittal plane; point 3 to 8
11	Posterior edge of zygantrum; point 8 to 9
12	Medial edge of postzygapophyseal articular facet; point 9 to 10
13	Lateral edge of postzygapophyseal articular facet; point 9 to 10
14	Curve along posterior half of interzygapophyseal ridge; point 9 to 11
15	Curve along anterior half of interzygapophyseal ridge; point 11 to 12
16	Lateral edge of the left prezygapophyseal articular facet; point 12 to 13
17	Medial edge of the left prezygapophyseal articular facet; point 12 to 13
18	Curve along anterior edge of the prezygapophyseal accessory process; point 12 to 14
19	Anterolateral edge that connects prezygapophyseal accessory process and parapophysial process; point 14 to 15
20	Ventrolateral edge of parapophysial process; point 15 to 16
21	Posterior margin of left synapophyses; point 16 to 17
22	Anterior margin of left synapophyses; point 16 to 17
23	Ventromedial edge of parapophysial process; point 15 to 18
24	Lateral margin of cotyle; point 18 to 19
25	Anterolateral edge of neural canal; point 2 to 19
26	Anterodorsal margin of cotyle; point 19 to 20
27	Internal ventral line of neural canal along sagittal plane; point 20 to 21
28	Dorsal margin of condyle; point 21 to 22
29	Posterolateral margin of neural canal; point 22 to 23
30	Dorsolateral margin of zygantral articular facet; point 23 to 24
31	Ventromedial margin of zygantral articular facet; point 23 to 24
32	Ventrolateral margin of condyle; point 22 to 25
33	Dorsoposterior edge of hypapophysis; point 25 to 26
34	Ventral edge of hypapophysis; point 26 to 27
35	Ventral margin of cotyle; point 18 to 27

Table 2.10. Landmarks and semi-landmark curves of the caudal vertebrae.

Single Landmark Points	
1	Posterior most point of zygosphenal articular facet
2	Anterior most point of zygosphenal articular facet
3	Anterior most point of zygosphen along sagittal plane
4	Anterior base of neural spine
5	Anterior most point of neural spine
6	Posterior most point of neural spine
7	Posterior base of neural spine
8	Posterior most point of zygantrum along sagittal plane
9	Posterior most point of left postzygapophyseal articular facet
10	Anterior most point of left postzygapophyseal articular facet
11	Medial most point along interzygapophyseal ridge
12	Anterior most point of left prezygapophyseal articular facet
13	Posterior most point of left prezygapophyseal articular facet
14	End of prezygapophyseal accessory process
15	End of pleurapophysis
16	Posterior most point of pleurapophysis
17	Point along cotyle margin that intersects with medial ridge of pleurapophysis
18	Point along cotyle margin that intersects with ventrolateral most margin of neural canal
19	Anterodorsal extent of cotyle along sagittal plane
20	Anterodorsal extent of condyle along sagittal plane
21	Point along condyle margin that intersects with ventrolateral most margin of neural canal
22	Posterior most point of zygantral articular facet

Single Landmark Points	
23	Anterior most point of zygantral articular facet
24	Anteroventral extent of condyle along sagittal plane
25	Posterior base of hemapophysis/hemal keel along sagittal plane
26	Posteroventral extent of hemapophysis/hemal keel
27	Anteroventral extent of hemapophysis/hemal keel
28	Anterior base of hemapophysis/hemal keel along sagittal plane
29	Anteroventral extent of cotyle along sagittal plane
Semi-landmark Curves	
1	Dorsolateral edge of zygosphenal articular facet; point 1 to 2
2	Ventromedial edge of zygosphenal articular facet; point 1 to 2
3	Anterior edge of zygosphene; point 2 to 3
4	Dorsomedial line; point 3 to 4
5	Anterolateral edge of neural spine; point 4 to 5
6	Dorsolateral edge of neural spine; point 5 to 6
7	Posterolateral edge of neural spine; point 6 to 7
8	Dorsal edge of neural spine along sagittal plane; point 4 to 7
9	Dorsomedial line along sagittal plane; point 7 to 8
10	Internal dorsal line of neural canal along sagittal plane; point 3 to 8
11	Posterior edge of zygantrum; point 8 to 9
12	Medial edge of postzygapophyseal articular facet; point 9 to 10
13	Lateral edge of postzygapophyseal articular facet; point 9 to 10
14	Curve along posterior half of interzygapophyseal ridge; point 9 to 11
15	Curve along anterior half of interzygapophyseal ridge; point 11 to 12
16	Lateral edge of the left prezygapophyseal articular facet; point 12 to 13
17	Medial edge of the left prezygapophyseal articular facet; point 12 to 13
18	Curve along anterior edge of the prezygapophyseal accessory process; point 12 to 14
19	Anterolateral edge that connects prezygapophyseal accessory process and parapophysial process; point 14 to 15
20	Ventrolateral edge of parapophysial process; point 15 to 16
21	Ventromedial edge of pleurapophysis; point 15 to 17
22	Lateral margin of cotyle; point 17 to 18
23	Anterolateral edge of neural canal; point 2 to 18
24	Anterodorsal margin of cotyle; point 18 to 19
25	Internal ventral line of neural canal; point 19 to 20
26	Dorsal margin of condyle; point 20 to 21
27	Posterolateral margin of neural canal; point 21 to 22
28	Dorsolateral margin of zygantral articular facet; point 22 to 23
29	Ventromedial margin of zygantral articular facet; point 22 to 23
30	Ventrolateral margin of condyle; point 21 to 24
31	Ventral edge of condyle; point 24 to 25
32	Posterolateral extent of hemapophysis/hemal keel; point 25 to 26
33	Venterolateral edge of hemapophysis/hemal keel; point 26 to 27
34	Anterolateral extent of hemapophysis/hemal keel; point 27 to 28
35	Ventral edge of hemapophysis/hemal keel along sagittal plane; point 25 to 28
36	Anteroventral edge of cotyle; point 28 to 29
37	Ventral margin of cotyle; point 17 to 29

CHAPTER THREE

Results

SKULL

Modularity

A 15-module model of the skull was the most supported by Covariance Ratio (CR) (Adams and Collyer 2019) which was phylogenetically corrected. This model, 15H, consists of the premaxilla, nasal, prefrontal, frontal, parietal, basisphenoid, basioccipital, supraoccipital, prootic, exoccipital, supratemporal, ectopterygoid and pterygoid as separate modules with the septomaxilla and vomer combined to form one module and the maxilla and palatine to form another (Table 2.4). The CR of 15H was 0.633 with a p-value of <0.01 and an associated effect size (Z) of -9.999. Disregarding the one module null hypothesis where, Z = 0, Z ranged from a maximum of -9.182 to -9.999 for models 8C and 15H, respectively.

Generalized Procrustes Analysis

Whole Skull

Principal component analysis (PCA) of the whole skull dataset which utilized all specimens showed that the first principal component (PC1) accounts for 22.5% of shape variation and PC2 accounts for 20.7% (Figure 3.1). PC1 appears to describe the overall length of skull while, PC2 is related to the robustness of the braincase. Hydrophiinae samples (*Acanthophis*, *Hydrophis Oxyurarus*, and *Simoselaps*) clustered along the maximum of PC2 (PC2+) with no trend along PC1. *Sinomicrurus* clustered along a single band of PC2 on the minimal half of PC1, while *Naja* clustered toward PC1+. There is an association of aquatic *Micrurus* clustering higher along PC2 than the remaining congeners.

A PCA of the whole skull data set conducted on the coralsnake subset (*Micruroides*, *Micrurus*, *Sinomicrurus*) showed that PC1 accounts for 27.6% of shape variation and PC2 accounts for 20.2% (Figure 3.2). PC1 appears to describe the robustness of the parietal, PC2 is related to the rugosity and size of the braincase and length of the supratemporal. PC2- and PC2+, *M. surinamensis* and *M. ephippifer*, respectively (Figure 3.2E-F), are found close along PC1. This association allows for the association with the extreme ends of PC2 to be seen. Aquatic *Micrurus* are consistently found on the lower end of PC2, while terrestrial and semi-aquatic species are found higher along PC2.

A PCA of the whole skull data set conducted on the semi-aquatic and aquatic subset (>5 ATS) showed that PC1 accounts for 32.7% of shape variation and PC2 accounts for 22.5% (Figure 3.3). PC1 appears to describe the robustness of the parietal, PC2 is related to the length of the supratemporal. There is a clear association based on phylogeny genus-based clusters do not touch.

Premaxilla

A PCA of the premaxilla module, which utilized all specimens, showed that the PC1 accounts for 30.8% of shape variation and PC2 accounts for 17.1% (Figure 3.4). PC1 appears to describe the extent of the transverse process, PC2 is related to the dorsal maximum. Coralsnakes have a close association that does not appear to have an aquatic tendency stratification. Both *Laticauda* samples can be seen within *Micrurus* and *Sinomicrurus*.

A PCA of the premaxilla module conducted on the coralsnake subset showed that PC1 accounts for 36.1% of shape variation and PC2 accounts for 11.1% (Figure 3.5). PC1 appears to describe the extent of the transverse process, PC2 is related to the prominence of the posterior

lateral projection. *Sinomicrurus* is clustered tightly while *Micrurus* has more variation. Higher ATS tend to be associated with PC2+, but the aquatic specimens are clustered within terrestrial specimens as well.

A PCA of the premaxilla module conducted on the semi-aquatic and aquatic subset (>5 ATS) showed that PC1 accounts for 29.8% of shape variation and PC2 accounts for 29.3% (Figure 3.6). PC1 appears to describe the dorsal maximum, PC2 is related to the shape of the ventral surface. *Micrurus* is clustered tightly in comparison to *Hydrophis* which runs the length of PC2.

Septomaxilla and Vomer

A PCA of the septomaxilla and vomer module, which utilized all specimens, showed that the PC1 accounts for 24.6% of shape variation and PC2 accounts for 23.4% (Figure 3.7). PC1 appears to describe angle and length of the dorsoposterior process of the septomaxilla along the midline, PC2 is related to the dorsomedial extent of the choanal process. While overall, clustering is associated with relatedness, the aquatic groups take different path. Basal *Calliophis* clustered tightly in the center. *Micrurus* increases in ATS from center toward PC2- while *Hydrophis* and aquatic *Naja* are toward the opposite end of PC2.

A PCA of the septomaxilla and vomer module conducted on the coralsnake subset showed that PC1 accounts for 26.8% of shape variation and PC2 accounts for 21% (Figure 3.8). Taken together, PC1 and PC2 appear to describe angle and length of the dorsoposterior process of the septomaxilla along the midline and the dorsomedial extent of the choanal process. *Sinomicrurus* is clustered tightly while *Micrurus* has more variation. Higher ATS tend to be

associated with PC1+ and PC2-, but the aquatic specimens are not cleanly divided from the rest of *Micrurus*.

A PCA of the septomaxilla and vomer module conducted on the semi-aquatic and aquatic subset (>5 ATS) showed that PC1 accounts for 50.9% of shape variation and PC2 accounts for 21% (Figure 3.9). PC1 appears to describe the angle of the anteroventral edge of the septomaxilla, PC2 is related to the extent of the choanal process. There appears to be more association with phylogeny than ATS.

Nasal

A PCA of the nasal module, which utilized all specimens, showed that the PC1 accounts for 63.2% of shape variation and PC2 accounts for 14.7% (Figure 3.10). PC1 appears to describe the angle and length of the anterior edge, PC2 is related to the overall length in comparison to the width and location of the lateral edge. While overall, clustering is associated with relatedness, the aquatic groups tend to be associated with PC1+. *Micrurus* increases in ATS from PC1- toward PC1+ while *Hydrophis* and *Laticauda* are still more extreme.

A PCA of the nasal module conducted on the coralsnake subset showed that PC1 accounts for 46.4% of shape variation and PC2 accounts for 20.9% (Figure 3.11). PC1 appears to describe the angle and length of the anterior edge, while the variation within PC2 is unclear. *Micrurus surinamensis* and *M. nattereri*, all 7 ATS, are grouped toward PC1- with some exception.

A PCA of the nasal module conducted on the semi-aquatic and aquatic subset (>5 ATS) showed that PC1 accounts for 66.6% of shape variation and PC2 accounts for 17.3% (Figure 3.12). PC1 appears to describe the angle and length of the anterior edge, PC2 is related to the

overall length in comparison to the width and location of the lateral edge. *Micrurus* increases in ATS from PC1- toward PC1+ while *Hydrophis* and *Laticauda* are still more extreme.

Prefrontal

A PCA of the prefrontal module, which utilized all specimens, showed that the PC1 accounts for 43.4% of shape variation and PC2 accounts for 27.2% (Figure 3.13). PC1 appears to describe the angle of attachment with the frontal along the posterior edge, PC2 is related to the change in dorsoventral width. There is a strong association with relatedness. *Calliophis* is broken into two discrete clusters along PC1, accounting for both PC1+ and PC1-.

A PCA of the prefrontal module conducted on the coralsnake subset showed that PC1 accounts for 28.6% of shape variation and PC2 accounts for 23.9% (Figure 3.14). PC1 appears to describe width at the dorsoventral midpoint compared to the dorsal edge, while the variation within PC2 is associated with the dorsoventral length. There looks to be an association with ATS and the prefrontal extending laterally rather than ventrolaterally.

A PCA of the prefrontal module conducted on the semi-aquatic and aquatic subset (>5 ATS) showed that PC1 accounts for 54.4% of shape variation and PC2 accounts for 17.6% (Figure 3.15). PC1 appears to describe the angle of attachment with the frontal along the posterior edge, PC2 is related to the width at midpoint. *Hydrophis* is more extreme while the other three genera are tightly clustered.

Frontal

A PCA of the frontal module, which utilized all specimens, showed that the PC1 accounts for 39.1% of shape variation and PC2 accounts for 31.9% (Figure 3.16). PC1 appears to describe

the angle of anterior edge, PC2 is related to the angle of the posterior edge. There is an association with relatedness more so than ATS. The three *Micrurus* specimens closest to PC1- are all *M. surinamensis* with 7 ATS.

A PCA of the prefrontal module conducted on the coralsnake subset showed that PC1 accounts for 34.4% of shape variation and PC2 accounts for 28.9% (Figure 3.17). PC1 appears to describe the angle of the posterior edge, while the variation within PC2 may be associated with the posterior edge length. Sister taxa, *Micrurus surinamensis* and *M. nattereri*, (both 7 ATS) are split across PC2.

A PCA of the prefrontal module conducted on the semi-aquatic and aquatic subset (>5 ATS) showed that PC1 accounts for 44.6% of shape variation and PC2 accounts for 30.8% (Figure 3.18). PC1 appears to describe the length of the lateral edge, PC2 is related to angle of the posterior edge. The specimens are clustered tightly by genus with *Micrurus surinamensis* extending toward PC1+.

Parietal

A PCA of the parietal module, which utilized all specimens, showed that the PC1 accounts for 47.3% of shape variation and PC2 accounts for 23.8% (Figure 3.19). PC1 appears to describe the anteroposterior length of the bone, PC2 is related to the length of the ventrolateral extent. There is a great deal of variation and spread exhibited by the PCA. Loose clustering is exhibited by genus and by ATS. Hydrophiinae is spread out across PC1 in the top half of PC2 apart from *Oxyuranus*. *Calliophis* is spread out across PC1 in the bottom half of PC2. Cobras and their kin are clustered toward and include PC1- and PC2+.

A PCA of the parietal module conducted on the coralsnake subset showed that PC1 accounts for 51.6% of shape variation and PC2 accounts for 16.4% (Figure 3.20). PC1 appears to describe overall concavity where PC1- looks like a deflated version of PC1+. The variation within PC2 is associated with the overall length. Sister taxa, *Micrurus surinamensis* and *M. nattereri*, (both 7 ATS) are downshifted along PC2 but spread across PC1.

A PCA of the parietal module conducted on the semi-aquatic and aquatic subset (>5 ATS) showed that PC1 accounts for 62.8% of shape variation and PC2 accounts for 14.4% (Figure 3.21). PC1 appears to describe the rugosity and concavity, PC2 is related to the protrusion of the parietal crest associated with the postorbital. The specimens are clustered tightly by genus.

Supraoccipital

A PCA of the supraoccipital module, which utilized all specimens, showed that the PC1 accounts for 42.5% of shape variation and PC2 accounts for 19.7% (Figure 3.22). PC1 appears to describe the rugosity and width, the variation described by PC2 is less clear. Despite significant overlap and spread, grouping is largely based on relatedness with *Calliophis* downshifted along PC2.

A PCA of the supraoccipital module conducted on the coralsnake subset showed that PC1 accounts for 52.1% of shape variation and PC2 accounts for 13.3% (Figure 3.23). PC1 appears to describe the rugosity and width, the variation described by PC2 is less clear. *Sinomicrurus* is downshifted along PC2 while the spread of *Micrurus* extends to all extremes without a pattern associated with ATS.

A PCA of the supraoccipital module conducted on the semi-aquatic and aquatic subset (>5 ATS) showed that PC1 accounts for 47.9% of shape variation and PC2 accounts for 19.9% (Figure 3.24). PC1 appears to describe the rugosity and width, the variation described by PC2 is less clear. The *Naja* is clustered tightly at the extreme end of PC1 with no clear pattern of association with the remaining specimens.

Prootic

A PCA of the prootic module, which utilized all specimens, showed that the PC1 accounts for 56.5% of shape variation and PC2 accounts for 9.27% (Figure 3.25). PC1 appears to describe amount of overlap of the prootic by the supratemporal, the variation described by PC2 may be associated with the width of the prootic along its ventral edge of the dorsoventral width of the supratemporal. There is a clear clustering by genus for all genera apart from *Micrurus*. *Micrurus surinamensis* and *M. nattereri* are found towards PC1+ while the remaining *Micrurus* overlap with *Sinomicrurus* and *Calliophis* and include PC1-.

A PCA of the prootic module conducted on the coralsnake subset showed that PC1 accounts for 56.1% of shape variation and PC2 accounts for 11% (Figure 3.26). The variation described by PC1 and PC2 are the same as in Figure 3.25 with the same trend found in *Micrurus*.

A PCA of the prootic module conducted on the semi-aquatic and aquatic subset (>5 ATS) showed that PC1 accounts for 63.4% of shape variation and PC2 accounts for 14.6% (Figure 3.27). The variation described by PC1 and PC2 are the same as in Figure 3.25 with the same trend found in *Micrurus*.

Exoccipital

A PCA of the exoccipital module, which utilized all specimens, showed that the PC1 accounts for 24.5% of shape variation and PC2 accounts for 12.6% (Figure 3.28). PC1 appears to describe the length of the suture with the basioccipital, the variation described by PC2 is less clear. There is a trend of increasing ATS along PC1 in *Micrurus*. Aquatic specimens of other genera are also found on the higher end of PC1 intermixed with their terrestrial congeners.

A PCA of the exoccipital module conducted on the coralsnake subset showed that PC1 accounts for 22.7% of shape variation and PC2 accounts for 15.9% (Figure 3.29). PC1 appears to describe the length of the suture with the basioccipital, the variation described by PC2 is less clear. All specimens are clustered together on the low end of PC1 apart from the 7 ATS *Micrurus*.

A PCA of the exoccipital module conducted on the semi-aquatic and aquatic subset (>5 ATS) showed that PC1 accounts for 27.4% of shape variation and PC2 accounts for 17.8% (Figure 3.30). PC1 appears to describe the length of the suture with the basioccipital, the variation described by PC2 is less clear. The trend visible in Figure 3.26 is still apparent with aquatic *Micrurus* split from semi-aquatic *Micrurus* across PC1 by the remaining samples.

Supratemporal

A PCA of the supratemporal module, which utilized all specimens, showed that the PC1 accounts for 57.1% of shape variation and PC2 accounts for 13.4% (Figure 3.31). PC1 appears to describe the overall length of the supratemporal, the variation described by PC2 is less clear. There is a trend of increasing ATS along PC1 in *Micrurus*. Aquatic specimens of other genera are also found on the higher end of PC1 intermixed with their terrestrial members of their clade.

Calliophis has two specimens at PC2- while the rest are clustered with terrestrial *Micrurus* and *Sinomicrurus*.

A PCA of the supratemporal module conducted on the coralsnake subset showed that PC1 accounts for 59.7% of shape variation and PC2 accounts for 12.4% (Figure 3.32). PC1 appears to describe the overall length of the supratemporal, the variation described by PC2 is less clear. All specimens are clustered together on the low end of PC1 apart from the 7 ATS *Micrurus*.

A PCA of the supratemporal module conducted on the semi-aquatic and aquatic subset (>5 ATS) showed that PC1 accounts for 77% of shape variation and PC2 accounts for 8.61% (Figure 3.33). PC1 appears to describe the overall length of the supratemporal, the variation described by PC2 is less clear. The trend visible in Figure 3.32 is still apparent with aquatic *Micrurus* split from semi-aquatic *Micrurus* across PC1 by the remaining samples.

Basisphenoid

A PCA of the basisphenoid module, which utilized all specimens, showed that the PC1 accounts for 35.7% of shape variation and PC2 accounts for 20.9% (Figure 3.34). PC1 appears to describe the overall length of the anterior half of the basisphenoid, the variation described by PC2 looks to be associated with the dorsoventral height of the anterior tip. *Calliophis* is highly variable along both axes.

A PCA of the basisphenoid module conducted on the coralsnake subset showed that PC1 accounts for 47.3% of shape variation and PC2 accounts for 11.8% (Figure 3.35). PC1 appears to describe the length and width of the anterior extent, the variation described by PC2 is less clear. A consistent trend is not readily apparent.

A PCA of the basisphenoid module conducted on the semi-aquatic and aquatic subset (>5 ATS) showed that PC1 accounts for 46.7% of shape variation and PC2 accounts for 16.2% (Figure 3.36). PC1 appears to describe the length and width of the anterior extent, the variation described by PC2 is associated with the ventral extent of the bone. *Hydrophis schistosus* has a ventral keel along the midline that is causing it to be so far away along PC2 from the remaining specimens. There is variation along PC1, but it does not appear to be related to a trend in ATS.

Basioccipital

A PCA of the basioccipital module, which utilized all specimens, showed that the PC1 accounts for 30.4% of shape variation and PC2 accounts for 20.3% (Figure 3.37). PC1 appears to describe the concavity of the bone, the variation described by PC2 looks to be associated with the shape of the suture with the exoccipital. There appears to be a trend of aquatic *Micrurus* extending toward the higher end of PC2+ albeit with exceptions.

A PCA of the basioccipital module conducted on the coralsnake subset showed that PC1 accounts for 28.7% of shape variation and PC2 accounts for 20.6% (Figure 3.38). PC1 appears to describe the rugosity of the basioccipital, PC2 looks to be associated with concavity. Some aquatic *Micrurus* cluster away from most samples but also near some terrestrial samples. The trend here is not as clear as it is with other modules.

A PCA of the basioccipital module conducted on the semi-aquatic and aquatic subset (>5 ATS) showed that PC1 accounts for 32.9% of shape variation and PC2 accounts for 20.6% (Figure 3.39). PC1 appears to describe the rugosity of the bone, the variation described by PC2 is associated with the overall length. Clustering is based on relatedness more than anything else.

Maxilla and Palatine

A PCA of the maxilla and palatine module, which utilized all specimens, showed that the PC1 accounts for 50% of shape variation and PC2 accounts for 10.9% (Figure 3.40). PC1 appears to describe the anteroposterior length of the maxilla, the variation described by PC2 is associated with the overall robustness of the maxilla. *Calliophis* has one compact cluster at PC1+ and a few more specimens of the same ATS isolated from the cluster. *Micrurus surinamensis* and *M. nattereri* and the aquatic *Naja* are found higher along PC2 than their terrestrial counterparts.

A PCA of the maxilla and palatine module conducted on the coralsnake subset showed that PC1 accounts for 44.7% of shape variation and PC2 accounts for 11.3% (Figure 3.41). PC1 appears to describe the anteroposterior length of the maxilla, the variation described by PC2 is associated with length of the maxilla in comparison to the palatine. Clusters are loosely based on genus while 7 ATS *Micrurus* is grouped tightly near PC1+, PC2+.

A PCA of the maxilla and palatine module conducted on the semi-aquatic and aquatic subset (>5 ATS) showed that PC1 accounts for 68.8% of shape variation and PC2 accounts for 10.1% (Figure 3.42). PC1 appears to describe the anteroposterior length of the maxilla, the variation described by PC2 may describe the length of the palatine. Groups are clustered tightly by genus.

Ectopterygoid

A PCA of the ectopterygoid module, which utilized all specimens, showed that the PC1 accounts for 33.2% of shape variation and PC2 accounts for 26.2% (Figure 3.43). PC1 appears to describe the lateromedial width, the variation described by PC2 is associated with the width of

the anterior edge. Clustering is largely based on genus. *Calliophis* has two specimens at PC2- while the rest are clustered with terrestrial *Micrurus* and *Sinomicrurus*.

A PCA of the ectopterygoid module conducted on the coralsnake subset showed that PC1 accounts for 36.3% of shape variation and PC2 accounts for 18.9% (Figure 3.44). PC1 appears to describe the overall length, the variation described by PC2 is less clear. Aquatic *Micrurus* are clustered toward PC1+. *Sinomicrurus japonicus* and *S. boettgeri* are isolated from their congeners toward PC1-, PC2+.

A PCA of the ectopterygoid module conducted on the semi-aquatic and aquatic subset (>5 ATS) showed that PC1 accounts for 62.9% of shape variation and PC2 accounts for 14.1% (Figure 3.45). PC1 appears to describe the lateromedial width, the variation described by PC2 is associated with the presence of an additional lateral process. Grouping is based on genus.

Pterygoid

A PCA of the pterygoid module, which utilized all specimens, showed that the PC1 accounts for 50.9% of shape variation and PC2 accounts for 24.5% (Figure 3.46). PC1 appears to describe the overall length of the pterygoid, the variation described by PC2 may be associated with the angle of the posterior extent. There is variation along PC1 but without an obvious trend associated with genus or ATS. *Calliophis* is split along PC2 with the majority near PC2-.

A PCA of the pterygoid module conducted on the coralsnake subset showed that PC1 accounts for 66.4% of shape variation and PC2 accounts for 10.1% (Figure 3.47). PC1 appears to describe the overall length of the pterygoid, the variation described by PC2 is less clear. Aquatic *Micrurus* tend to have PC values along both axes.

A PCA of the pterygoid module conducted on the semi-aquatic and aquatic subset (>5 ATS) showed that PC1 accounts for 73.3% of shape variation and PC2 accounts for 10.4% (Figure 3.48). PC1 appears to describe the overall length of the pterygoid, the variation described by PC2 is less clear. The clustering is similar to that seen in Figure 3.46.

QUADRATATE

Generalized Procrustes Analysis

A PCA of the quadrate, which utilized all specimens, showed that the PC1 accounts for 44% of shape variation and PC2 accounts for 15.9% (Figure 3.49). PC1 the dorsoventral length of the quadrate, the variation described by PC2 is less clear. Basal *Calliophis*, terrestrial coralsnakes and *Hemibungarus* are found on the lower end of PC. All other specimens are found on the higher end of PC1+ without a distinct trend.

A PCA of the quadrate conducted on the coralsnake subset showed that PC1 accounts for 41.3% of shape variation and PC2 accounts for 16.9% (Figure 3.50). PC1 the dorsoventral length of the quadrate, the variation described by PC2 is less clear but might be associated with the shape of the head. 7 ATS *Micrurus* are consistently found toward PC1+.

A PCA of the quadrate conducted on the semi-aquatic and aquatic subset (>5 ATS) showed that PC1 accounts for 43.8% of shape variation and PC2 accounts for 18.6% (Figure 3.51). PC1 the dorsoventral length of the quadrate, the variation described by PC2 is less clear. 7 ATS *Micrurus* are consistently found toward PC1+ clustered more tightly with *Hydrophis* and *Naja* than their congeners.

LOWER JAW

Modularity

A 2-module model of the skull was the most supported by CR (Adams and Collyer 2019) which was phylogenetically corrected. This model, 2C, consists of the dentary, angular and splenial combined to form one module and the compound as a separate module (Table 2.8). The CR of 2C was 0.89 with a p-value of 0.001 and an associated effect size (Z) of -26.878. Disregarding the one module null hypothesis where, Z = 0, Z ranged from a maximum of -15.744 to -26.878 for models 2F and 2C, respectively.

Generalized Procrustes Analysis

Jaw

A PCA of the entire jaw dataset, which utilized all specimens, showed that the PC1 accounts for 47.5% of shape variation and PC2 accounts for 11.3% (Figure 3.52). PC1 appears to describe the overall angle of the compound in lateral view, the variation described by PC2 is less clear. The angle of the compound is correlated with relatedness and does not show a trend associated with ATS.

A PCA of the entire jaw dataset conducted on the coralsnake subset showed that PC1 accounts for 31.6% of shape variation and PC2 accounts for 13.4% (Figure 3.53). PC1 appears to describe the ratio of the length of the dentary to length of the compound, the variation described by PC2 is associated with the height of the coronoid process of the compound. *Micrurus surinamensis* and *M. nattereri* are clustered toward PC1+, PC2+ and away from other congeners.

A PCA of the entire jaw dataset conducted on the semi-aquatic and aquatic subset (>5 ATS) showed that PC1 accounts for 58.8% of shape variation and PC2 accounts for 13.7%

(Figure 3.54). PC1 appears to describe the ratio of the length of the dentary to length of the compound, the variation described by PC2 is less clear. Aquatic *Micrurus* cluster tightly within genus but a trend along ATS can be seen. All other genera are clustered along PC1

Compound

A PCA of the compound module, which utilized all specimens, showed that the PC1 accounts for 52.3% of shape variation and PC2 accounts for 15.2% (Figure 3.55). PC1 appears to describe the overall angle of the compound in lateral view, the variation described by PC2 is less clear. Clustering is related to genus in *Micrurus*, *Calliophis* and *Sinomicrurus*, which form a tight overlapping group toward PC1+.

A PCA of the compound module conducted on the coralsnake subset showed that PC1 accounts for 28.8% of shape variation and PC2 accounts for 21.11% (Figure 3.56). PC1 appears to describe the general robustness of the compound, the variation described by PC2 is less clear but somewhat associated with the extent of the coronoid process of the compound. *Sinomicrurus* forms a much looser cluster than *Micrurus*. *Micrurus surinamensis* and *M. nattereri* cluster toward PC2+.

A PCA of the compound module conducted on the semi-aquatic and aquatic subset (>5 ATS) showed that PC1 accounts for 65.3% of shape variation and PC2 accounts for 15% (Figure 3.57). PC1 appears to describe the overall angle of the compound in lateral view, the variation described by PC2 is less clear. Clustering is associated with relatedness without an underlying trend in ATS.

Dentary, Angular and Splenial

A PCA of the dentary, angular and splenial module, which utilized all specimens, showed that the PC1 accounts for 34.2% of shape variation and PC2 accounts for 14.3% (Figure 3.58). PC1 appears to describe the posterior extent of the dentary, the variation described by PC2 is associated with the dorsal extent of the splenial dorsal process in relation to the dorsoposterior extent of the angular. Clustering is largely based on genus with significant overlap between genera. *Calliophis melanurus* is an exception which is found isolated toward PC2+.

A PCA of the dentary, angular and splenial module conducted on the coralsnake subset showed that PC1 accounts for 34.6% of shape variation and PC2 accounts for 15.4% (Figure 3.59). PC1 appears to describe the overall length of the toothrow past the point of contact between the dentary and the anterior extend to the compound. The variation described by PC2 may be associated with the comparison of curves 2 and 3 (Table 2.7). Aquatic *Micrurus* are more associated with PC1+ than the main *Micrurus* cluster.

A PCA of the dentary, angular and splenial module conducted on the semi-aquatic and aquatic subset (>5 ATS) showed that PC1 accounts for 56.3% of shape variation and PC2 accounts for 12.9% (Figure 3.60). PC1 appears to describe the posterior extent of the dentary along the toothrow, the variation described by PC2 is less clear. Clustering is largely based on genus.

MIDBODY VERTEBRA

Generalized Procrustes Analysis

A PCA of the midbody vertebra dataset, which utilized all specimens, showed that the PC1 accounts for 41% of shape variation and PC2 accounts for 18.4% (Figure 3.61). PC1

appears to describe the anteroposterior length of the vertebra, the variation described by PC2 is associated with the height of the neural spine. There is a trend of increasing ATS along PC1 in *Micrurus*. Aquatic specimens of other genera are also found on the higher end of PC1 intermixed with their terrestrial members of their clade. *Hydrophis* is at the extreme end of PC2+ isolated from other Hydrophiinae.

A PCA of the midbody vertebra dataset conducted on the coralsnake subset showed that PC1 accounts for 46.6% of shape variation and PC2 accounts for 11.2% (Figure 3.62). PC1 appears to describe the anteroposterior length of the vertebra, the variation described by PC2 is less clear. A clear trend is not apparent. Aquatic *Micrurus* are both the minimum and maximum along PC1 and scattered in between.

A PCA of the midbody vertebra dataset conducted on the semi-aquatic and aquatic subset (>5 ATS) showed that PC1 accounts for 47.5% of shape variation and PC2 accounts for 27.7% (Figure 3.63). PC1 appears to describe the anteroposterior length of the vertebra, the variation described by PC2 is associated with the height of the neural spine. Clustering looks to be more associated with relatedness than ATS.

CAUDAL VERTEBRA

Generalized Procrustes Analysis

A PCA of the caudal vertebra dataset, which utilized all specimens, showed that the PC1 accounts for 32.7% of shape variation and PC2 accounts for 23.3% (Figure 3.64). PC1 appears to describe the overall length of the vertebra in combination with the angle of the pleurapophysis, the variation described by PC2 is associated with the height of the neural spine in combination with the angle and length of the pleurapophysis. There is a trend of increasing ATS along PC2

but is overshadowed by the extreme morphology of *Hydrophis*. Specimens are clustered along PC1 largely by genus with the exception of *Micrurus* which is spread out along the axis.

A PCA of the caudal vertebra dataset conducted on the coralsnake subset showed that PC1 accounts for 42% of shape variation and PC2 accounts for 20.3% (Figure 3.65). PC1 appears to describe the anteroposterior length of the vertebra, the variation described by PC2 is associated with the length of the pleurapophysis. Specimens with a lower ATS tend to be found toward PC2+. The trend associated with PC1 is not readily apparent.

A PCA of the caudal vertebra dataset conducted on the semi-aquatic and aquatic subset (>5 ATS) showed that PC1 accounts for 36.4% of shape variation and PC2 accounts for 32.8% (Figure 3.66). PC1 and PC2 both describe the length of the neural spine and the extent of the pleurapophysis. The extreme morphology of *Hydrophis* allows the remainder of specimens to largely cluster by genus.

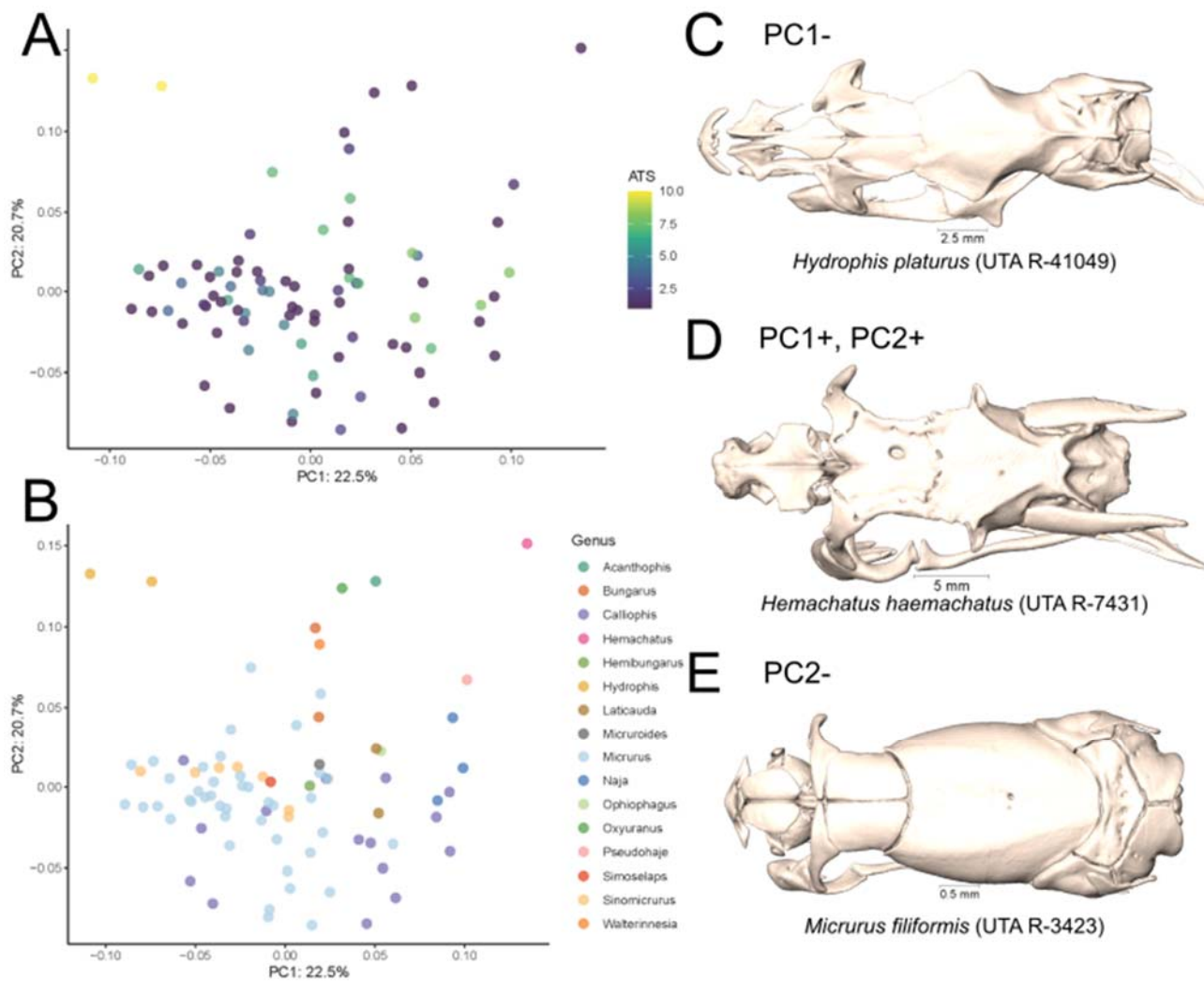


Figure 3.1. PCA of the skull, utilizing all specimens, colored by ATS (A) and genus (B). Images of the skull of specimens at the extremes of PC1 (C-D) and PC2 (D-E) in dorsal view.

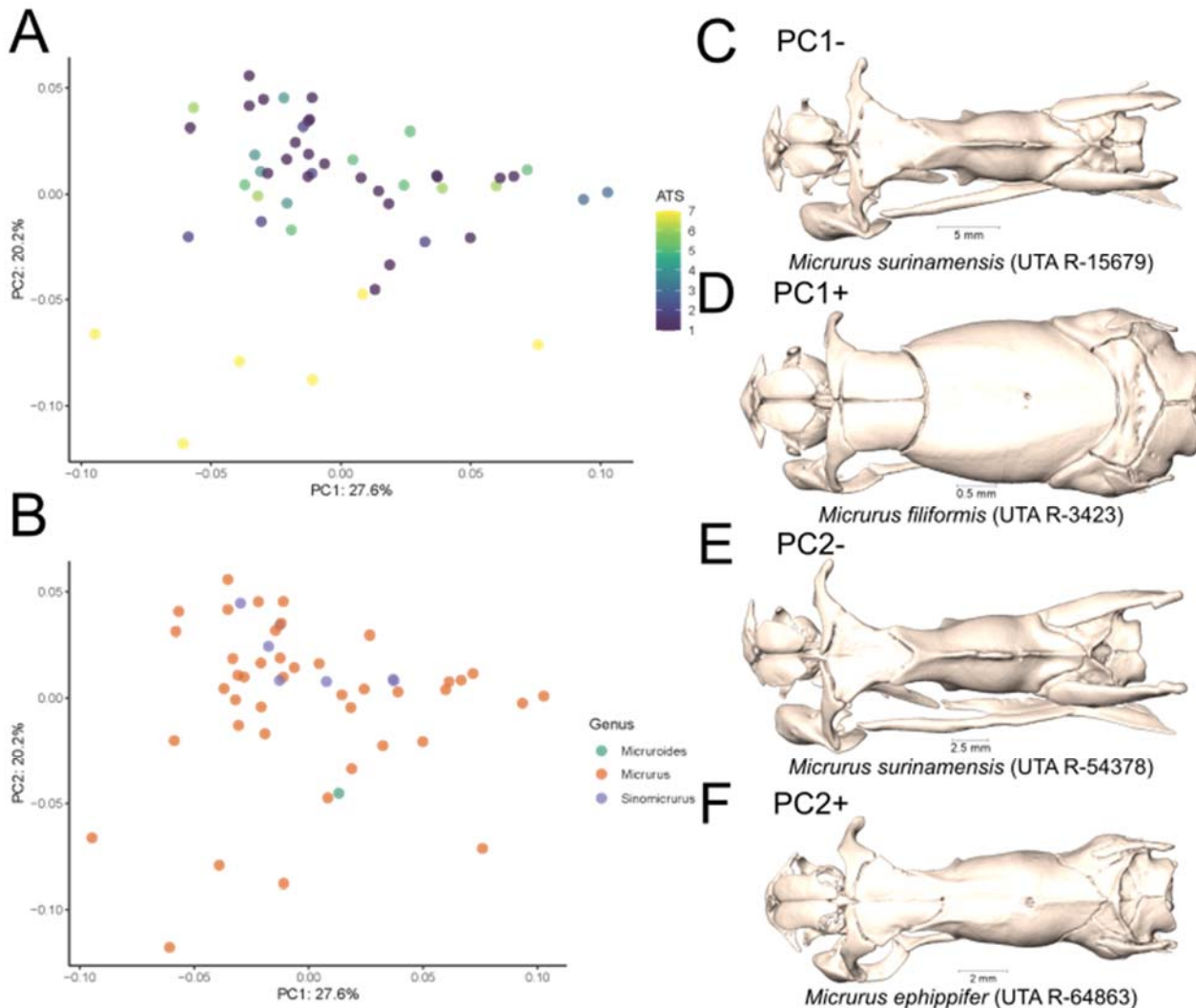


Figure 3.2. PCA of the skull conducted on the coralsnake subset, colored by ATS (A) and genus (B). Images of the skull of specimens at the extremes of PC1 (C-D) and PC2 (E-F) in dorsal view.

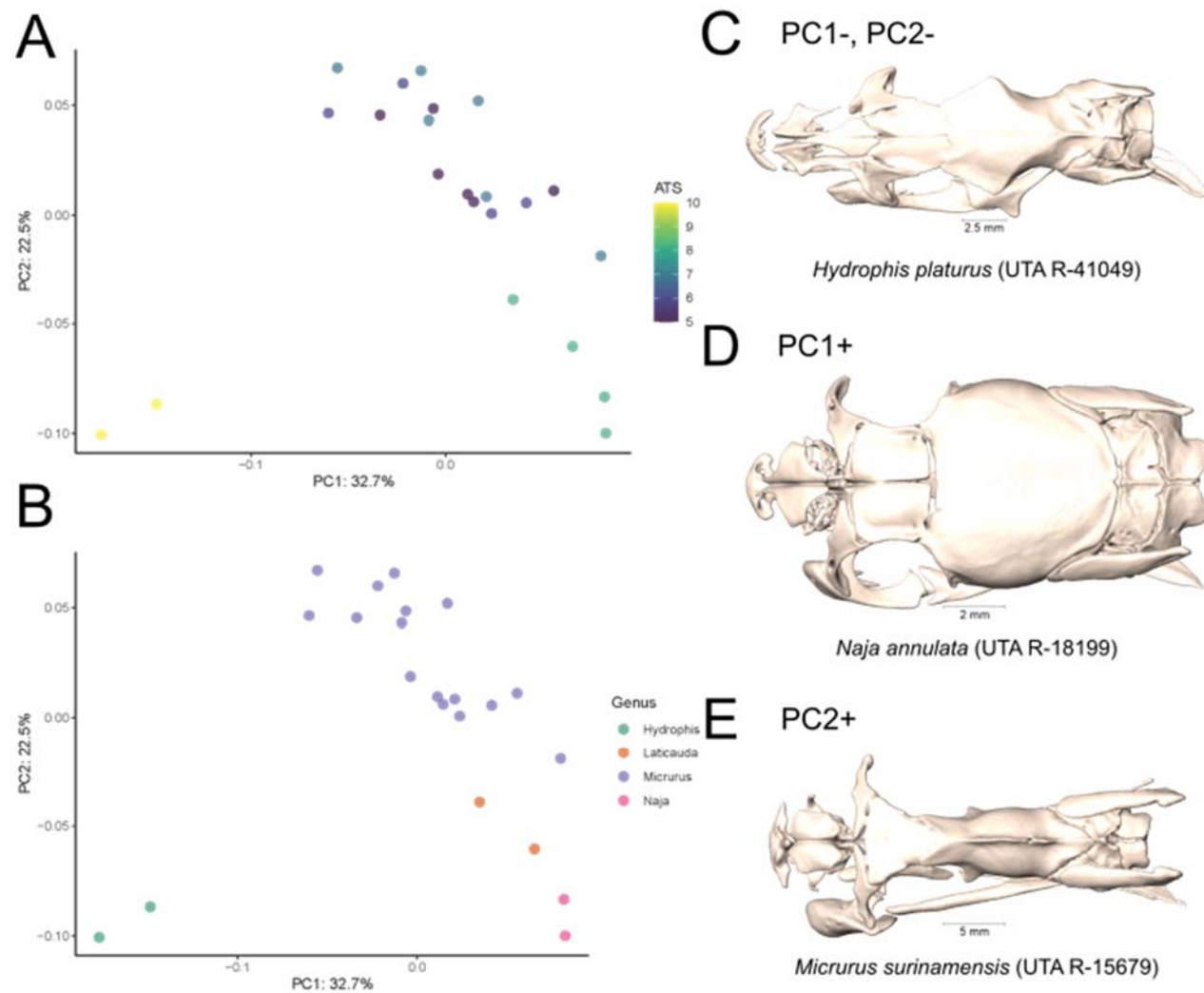


Figure 3.3. PCA of the skull of the semi-aquatic and aquatic subset (>5 ATS), colored by ATS (A) and genus (B). Images of the skull of specimens at the minimum of PC1 and PC2 (C) and maximum of PC1 (D) and maximum of PC2 (E) in dorsal view.

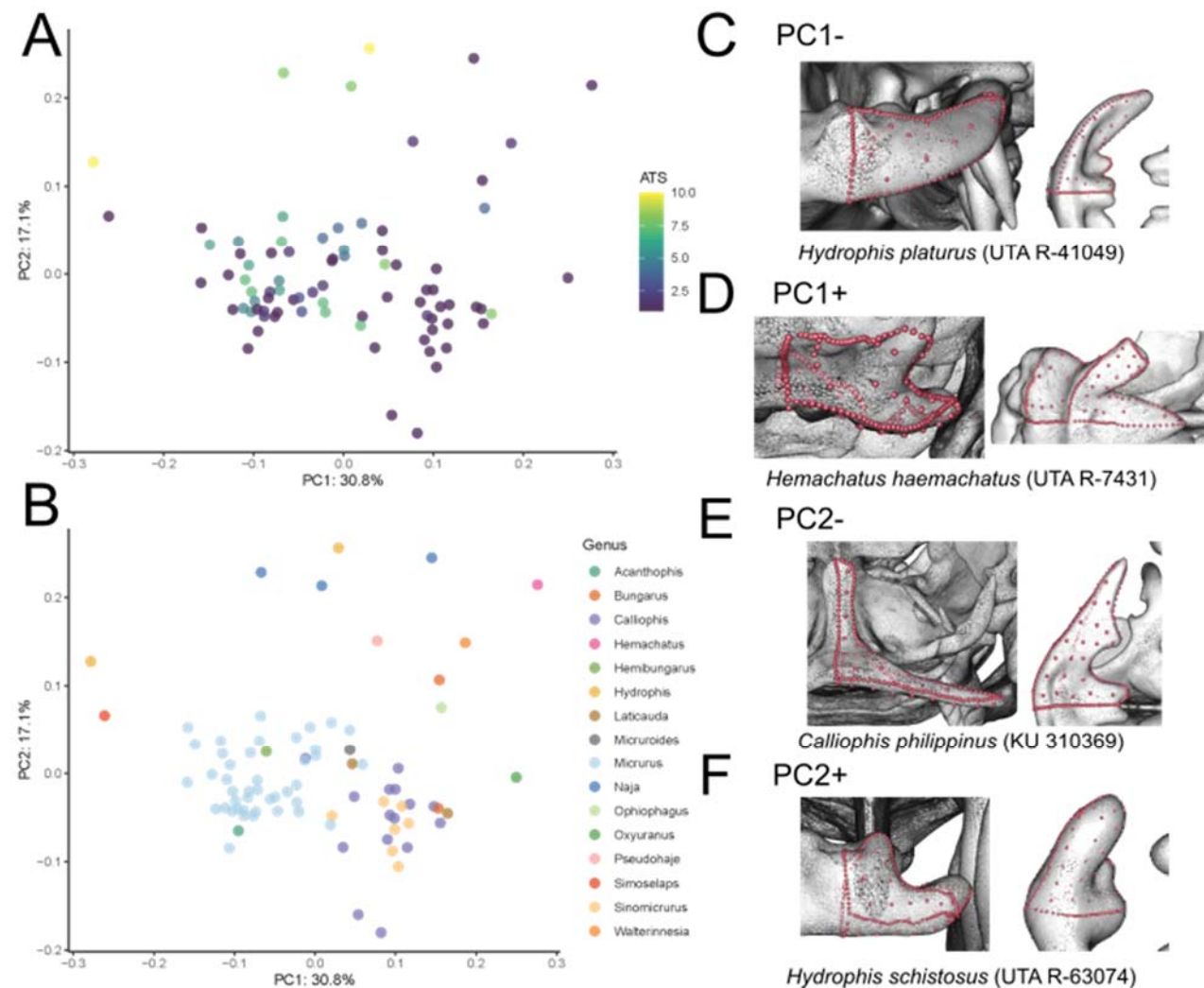


Figure 3.4. PCA of the premaxilla module, utilizing all specimens, colored by ATS (A) and genus (B). Images of the premaxilla of specimens at the extremes of PC1 (C-D) and PC2 (E-F) in frontal (left) and ventral (right) view.

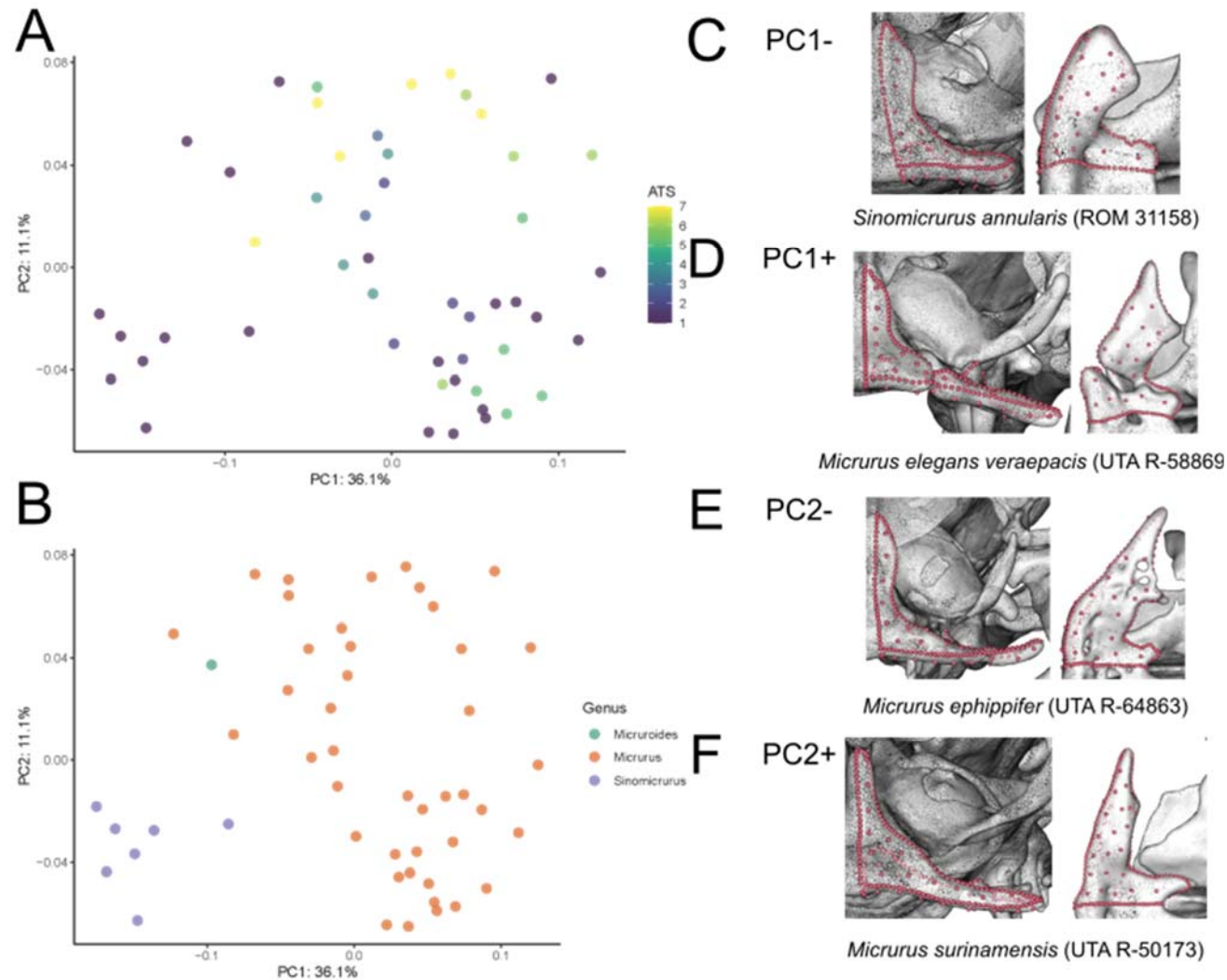


Figure 3.5. PCA of the premaxilla module conducted on the coralsnake subset, colored by ATS (A) and genus (B). Images of the premaxilla of specimens at the extremes of PC1 (C-D) and PC2 (E-F) in frontal (left) and ventral (right) view.

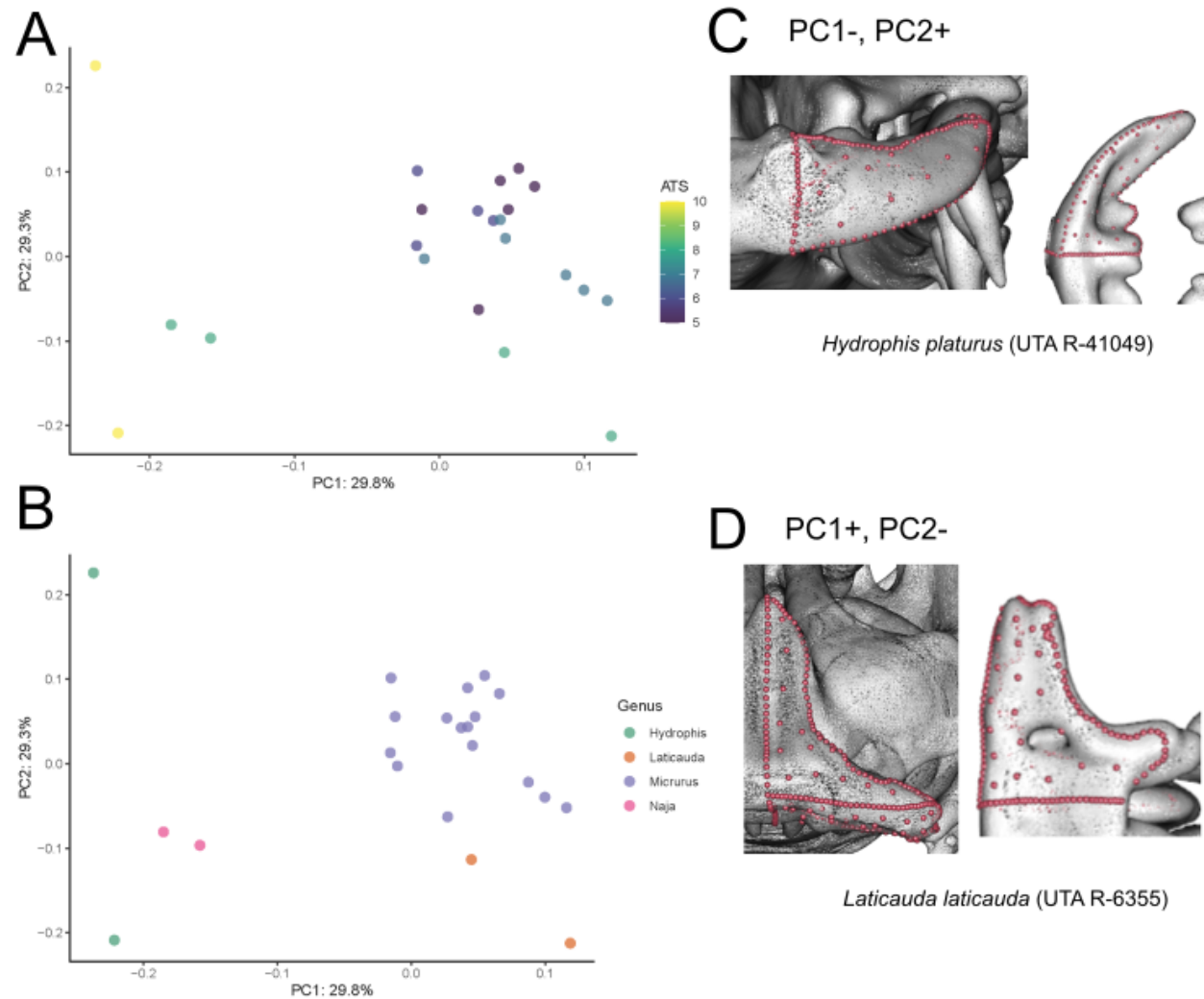


Figure 3.6. PCA of the premaxilla module conducted on the semi-aquatic and aquatic subset (>5 ATS), colored by ATS (A) and genus (B). Images of the premaxilla of specimens at the extremes of PC1 and PC2 (C-D) in frontal (left) and ventral (right) view.

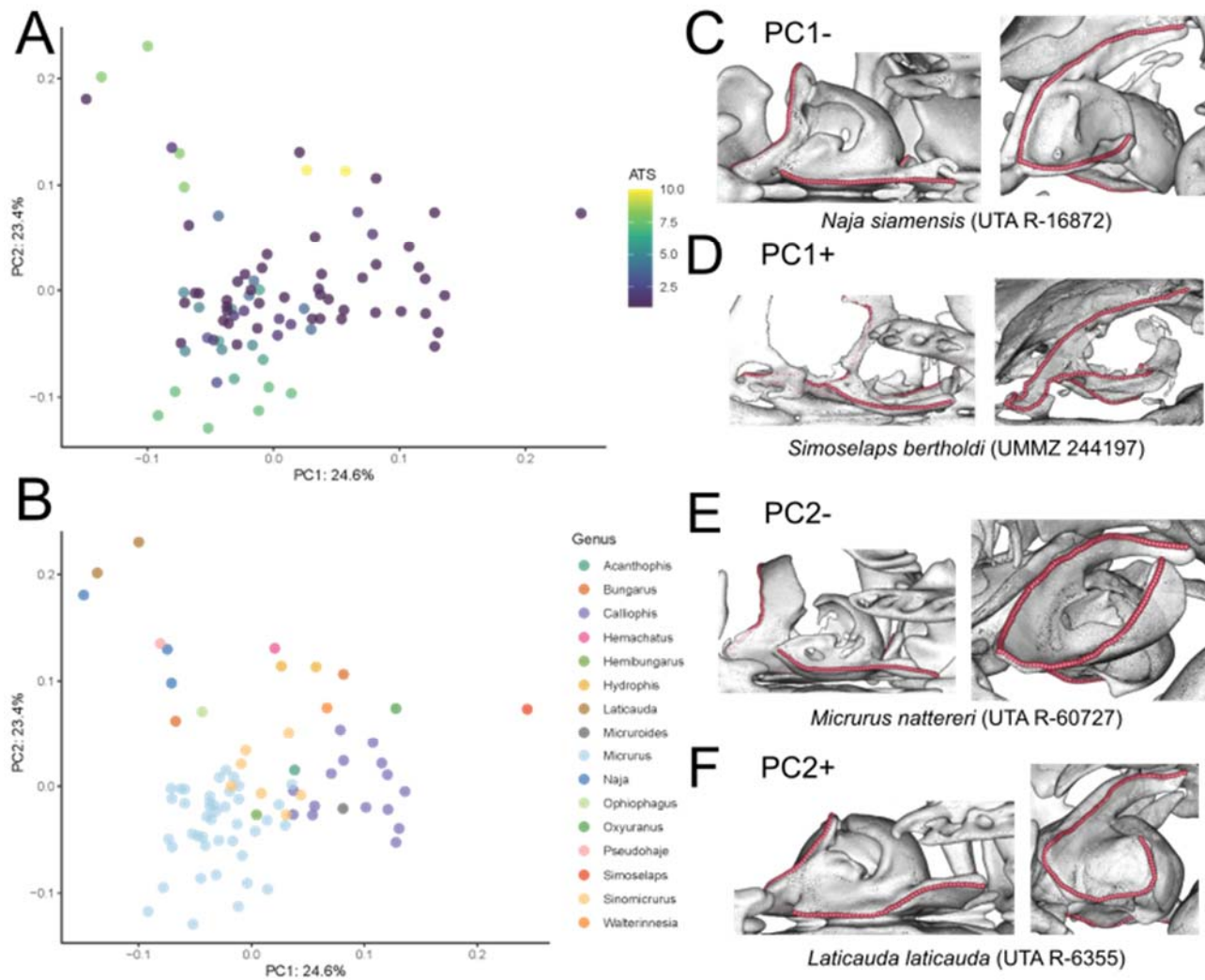


Figure 3.7. PCA of the septomaxilla and vomer module, utilizing all specimens, colored by ATS (A) and genus (B). Images of the septomaxilla and vomer of specimens at the extremes of PC1 (C-D) and PC2 (E-F) in ventral (left) and anterolateral (right) view.

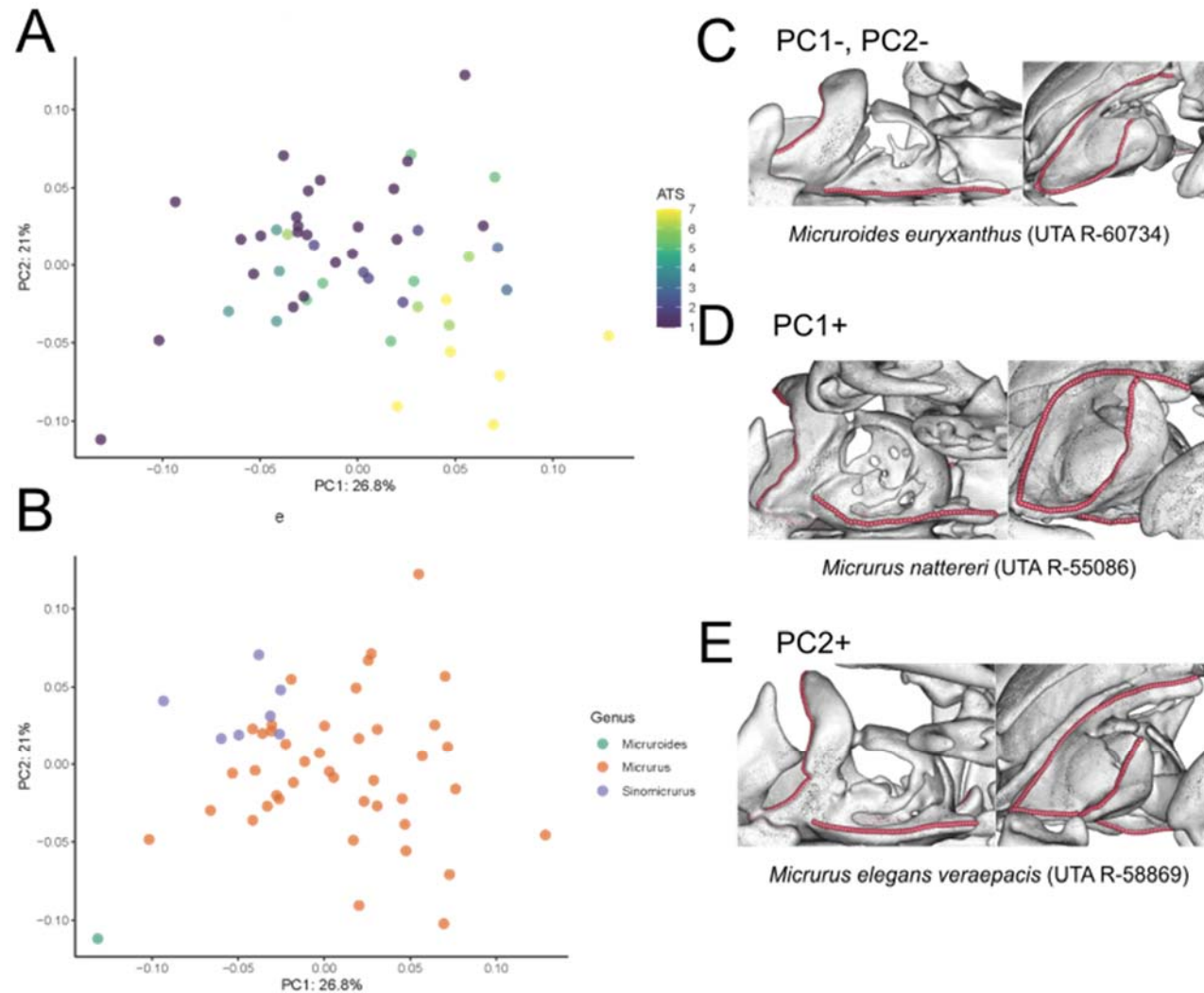


Figure 3.8. PCA of the septomaxilla and vomer module conducted on the coralsnake subset, colored by ATS (A) and genus (B).

Images of this module of specimens at the extremes of PC1 (C-D) and PC2 (E-F) in ventral (left) and anterolateral (right) view.

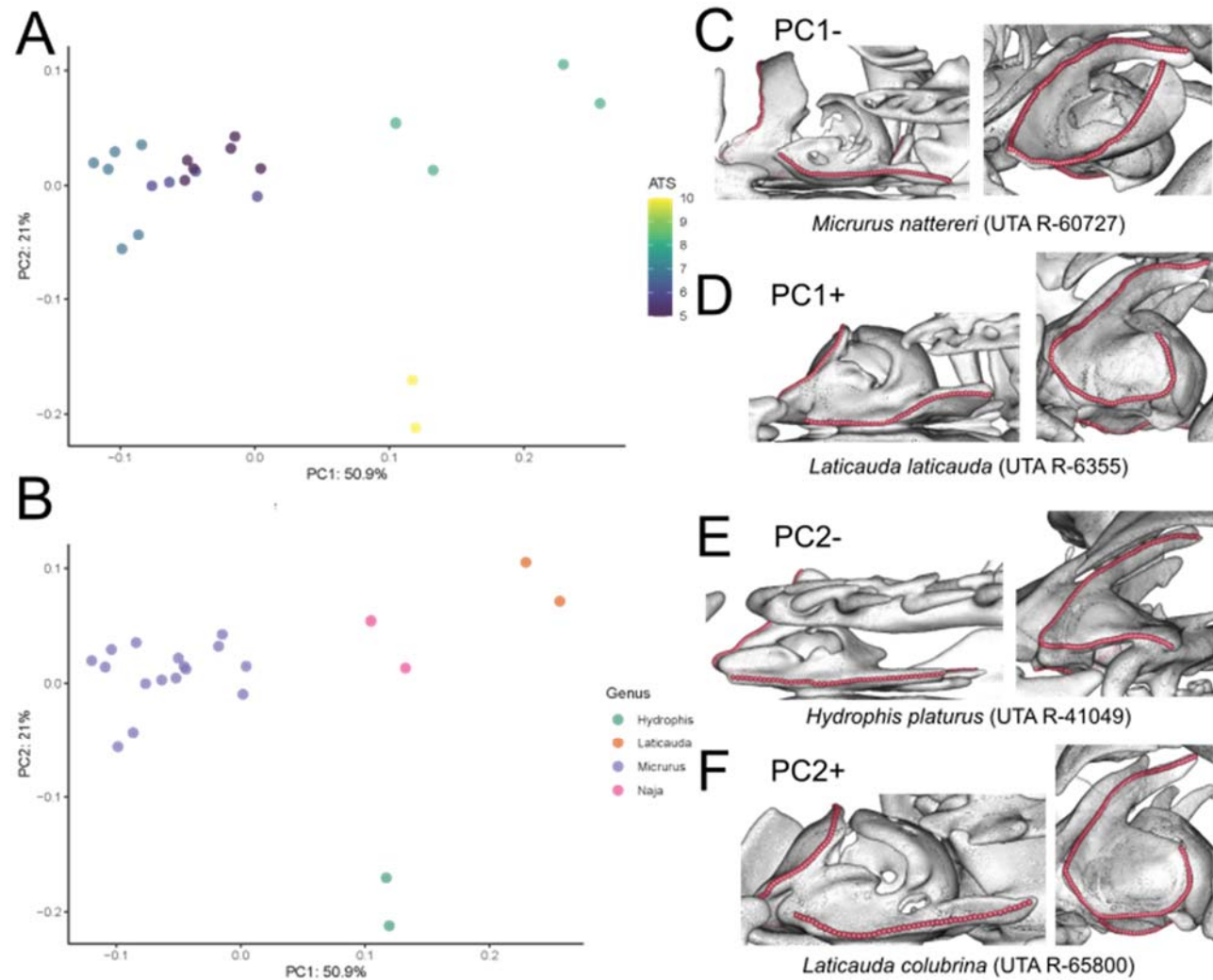


Figure 3.9. PCA of the septomaxilla and vomer module conducted on the semi-aquatic and aquatic subset (>5 ATS), colored by ATS (A) and genus (B). Images of specimens at the extremes of PC1 (C-D) and PC2 (E-F) in ventral (left) and anterolateral (right) view.

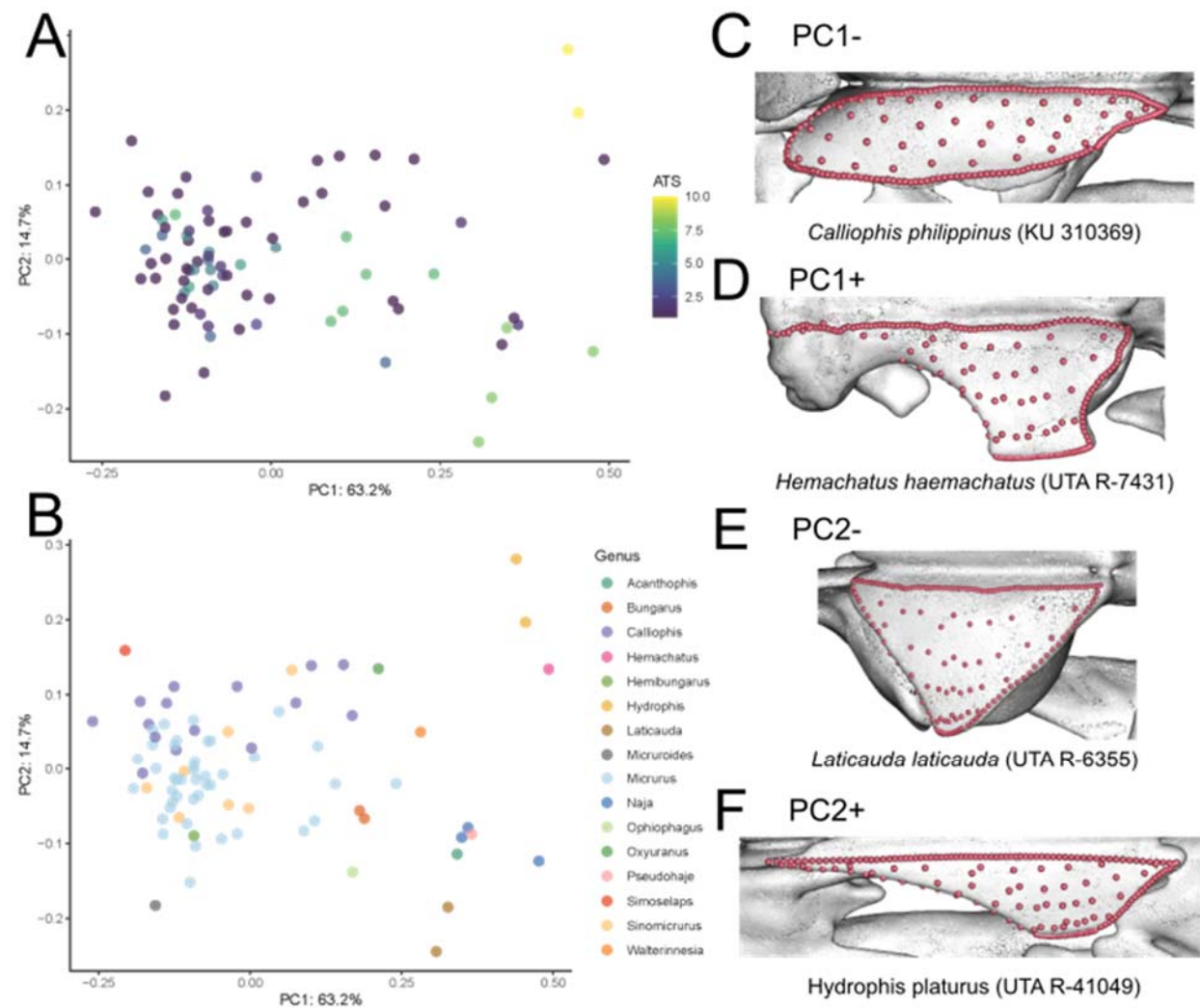


Figure 3.10. PCA of the nasal module, utilizing all specimens, colored by ATS (A) and genus (B). Images of the nasal of specimens at the extremes of PC1 (C-D) and PC2 (E-F) in dorsal view.

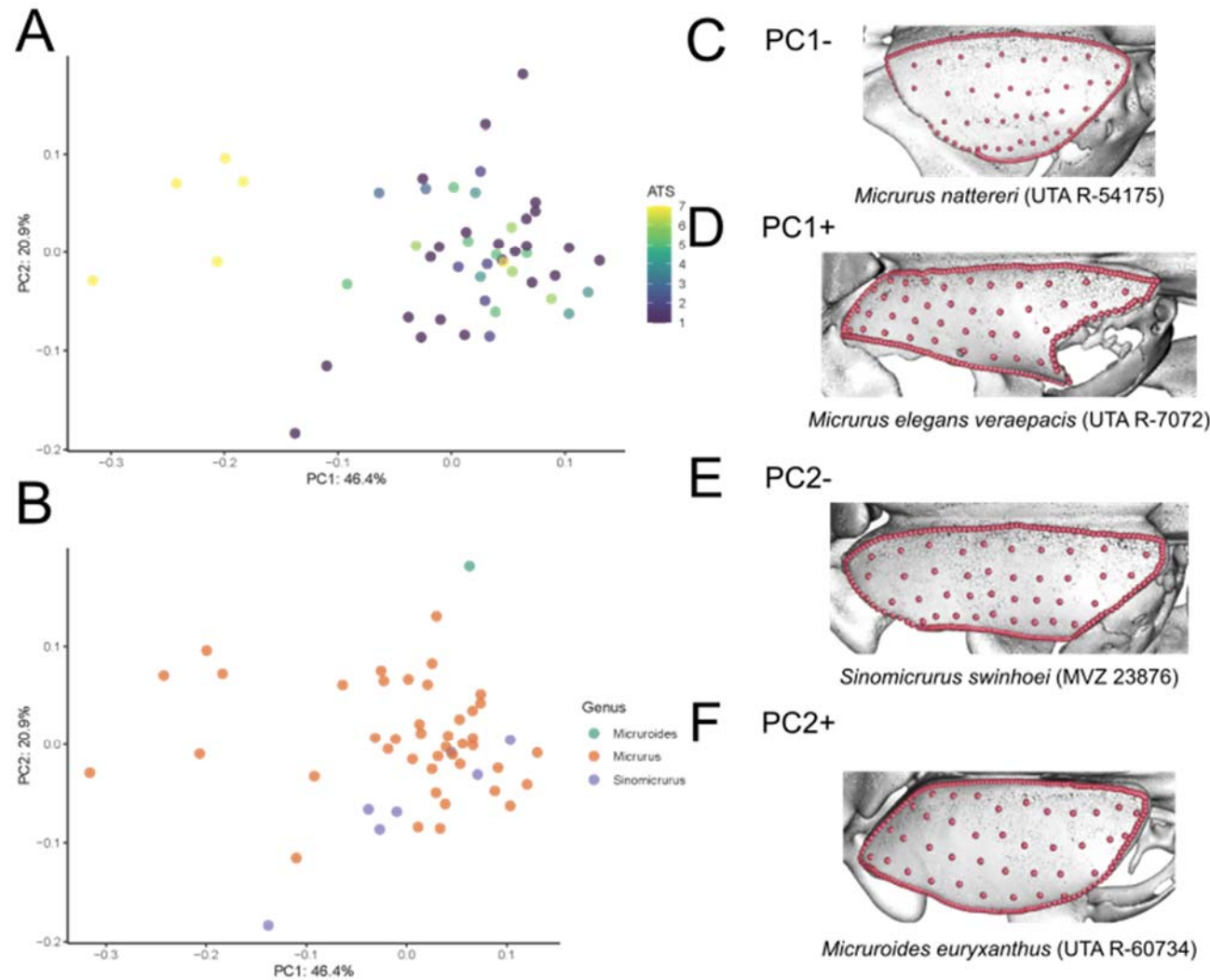


Figure 3.11. PCA of the nasal module conducted on the coralsnake subset, colored by ATS (A) and genus (B). Images of the nasal of specimens at the extremes of PC1 (C-D) and PC2 (E-F) in dorsal view.

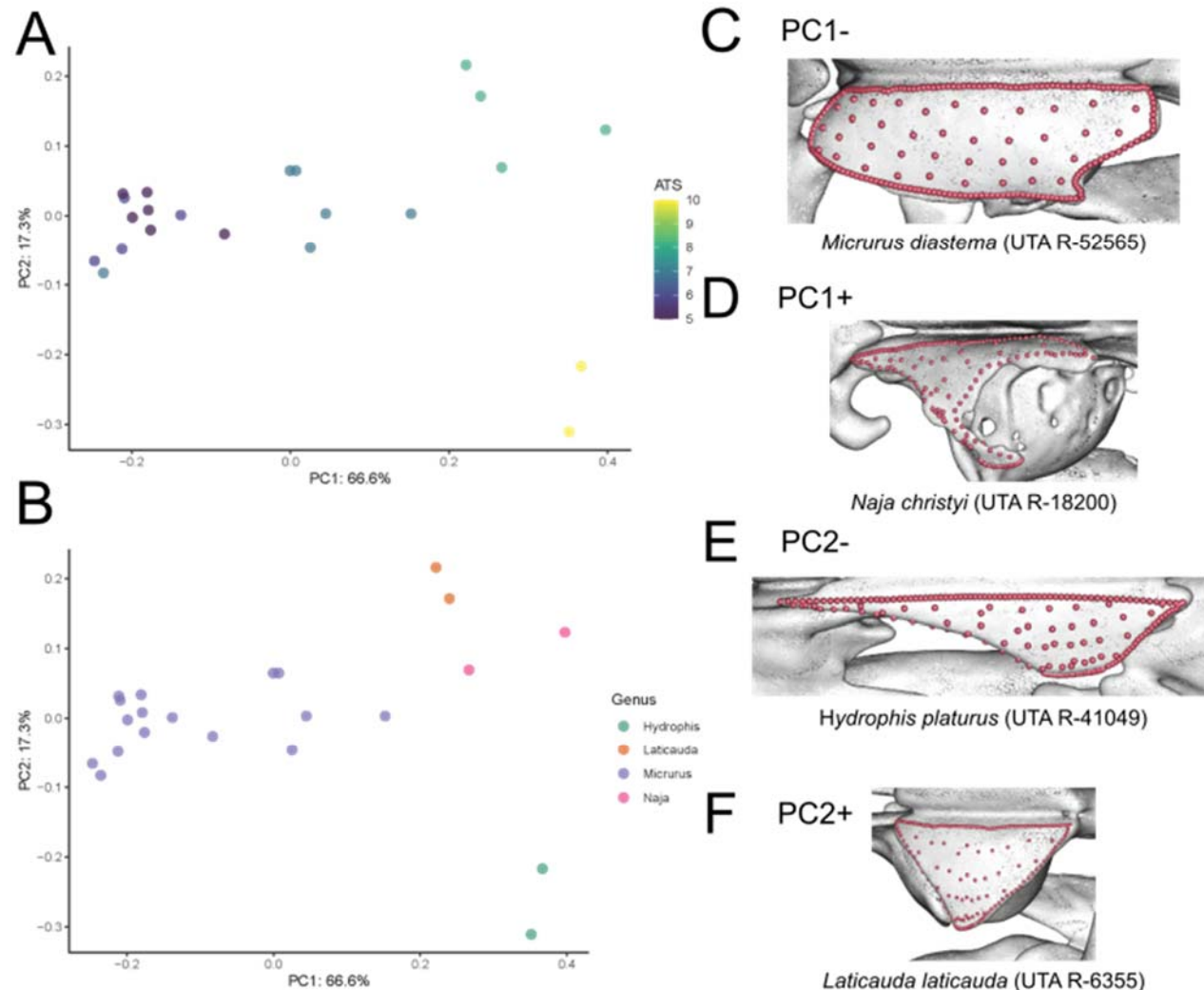


Figure 3.12. PCA of the nasal module conducted on the semi-aquatic and aquatic subset (>5 ATS), colored by ATS (A) and genus (B).

Images of the nasal of specimens at the extremes of PC1 (C-D) and PC2 (E-F) in dorsal view.

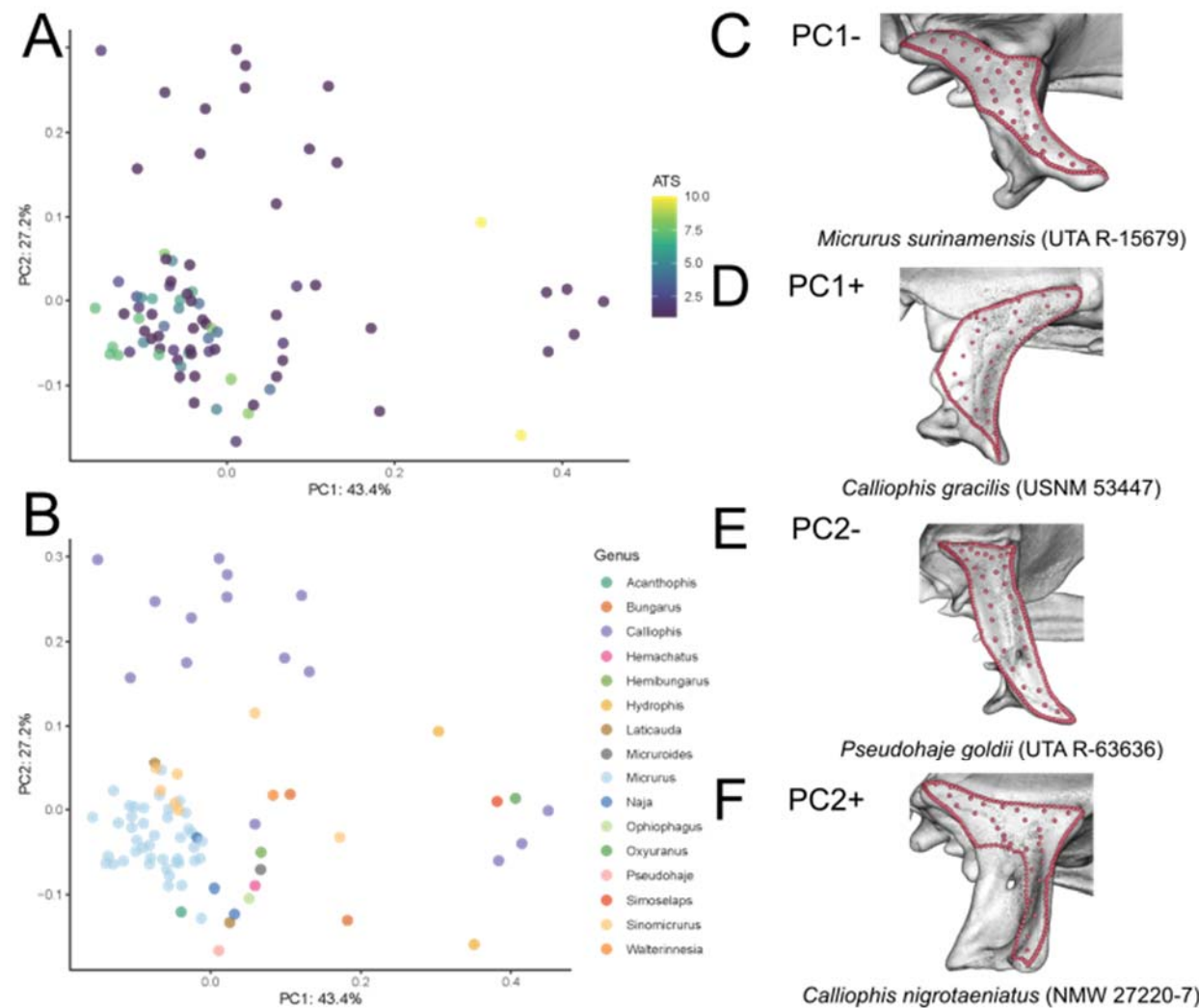


Figure 3.13. PCA of the prefrontal module, utilizing all specimens, colored by ATS (A) and genus (B). Images of the prefrontal of specimens at the extremes of PC1 (C-D) and PC2 (E-F) in dorsolateral view.

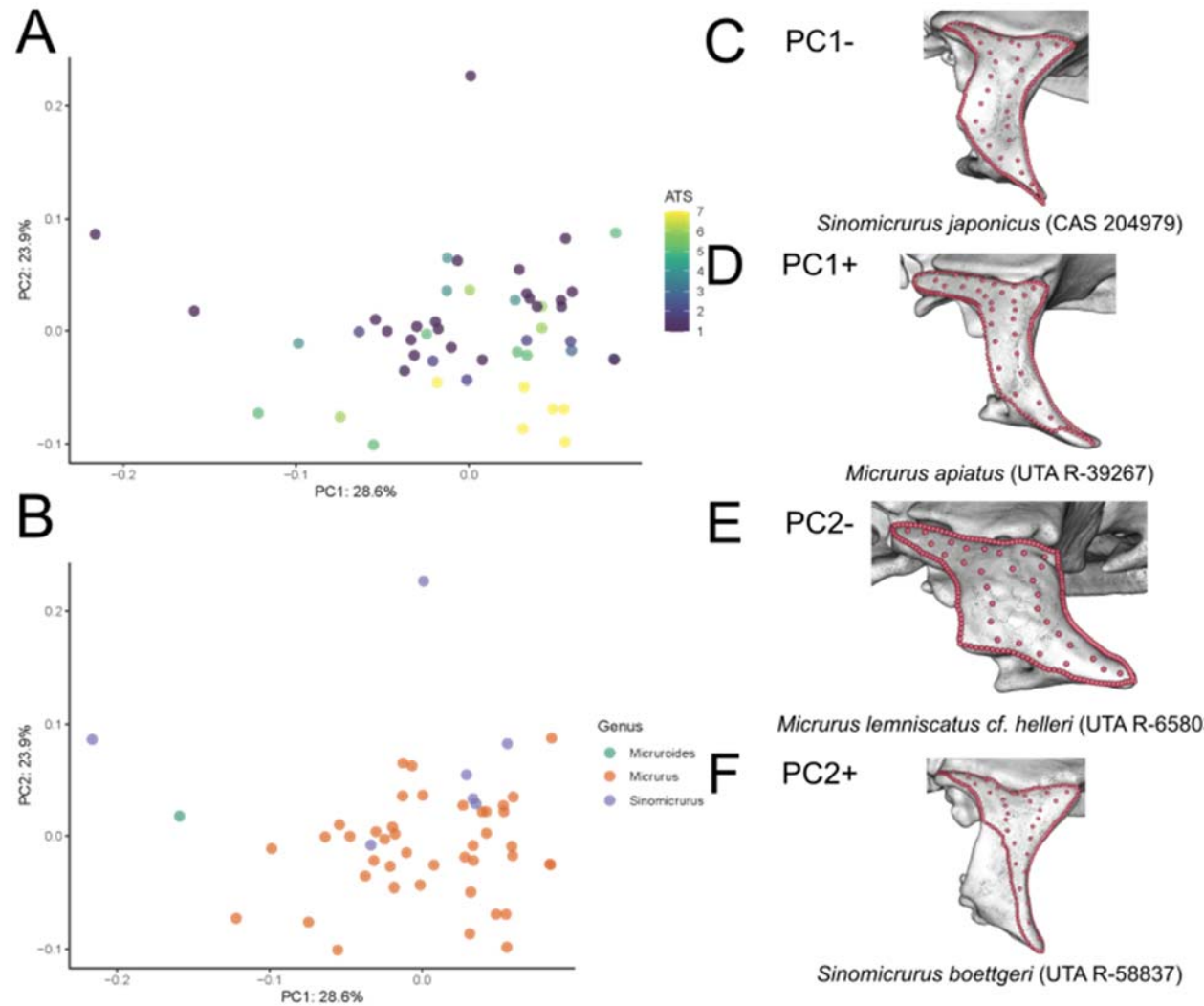


Figure 3.14. PCA of the prefrontal module conducted on the coralsnake subset, colored by ATS (A) and genus (B). Images of the prefrontal of specimens at the extremes of PC1 (C-D) and PC2 (E-F) in dorsolateral view.

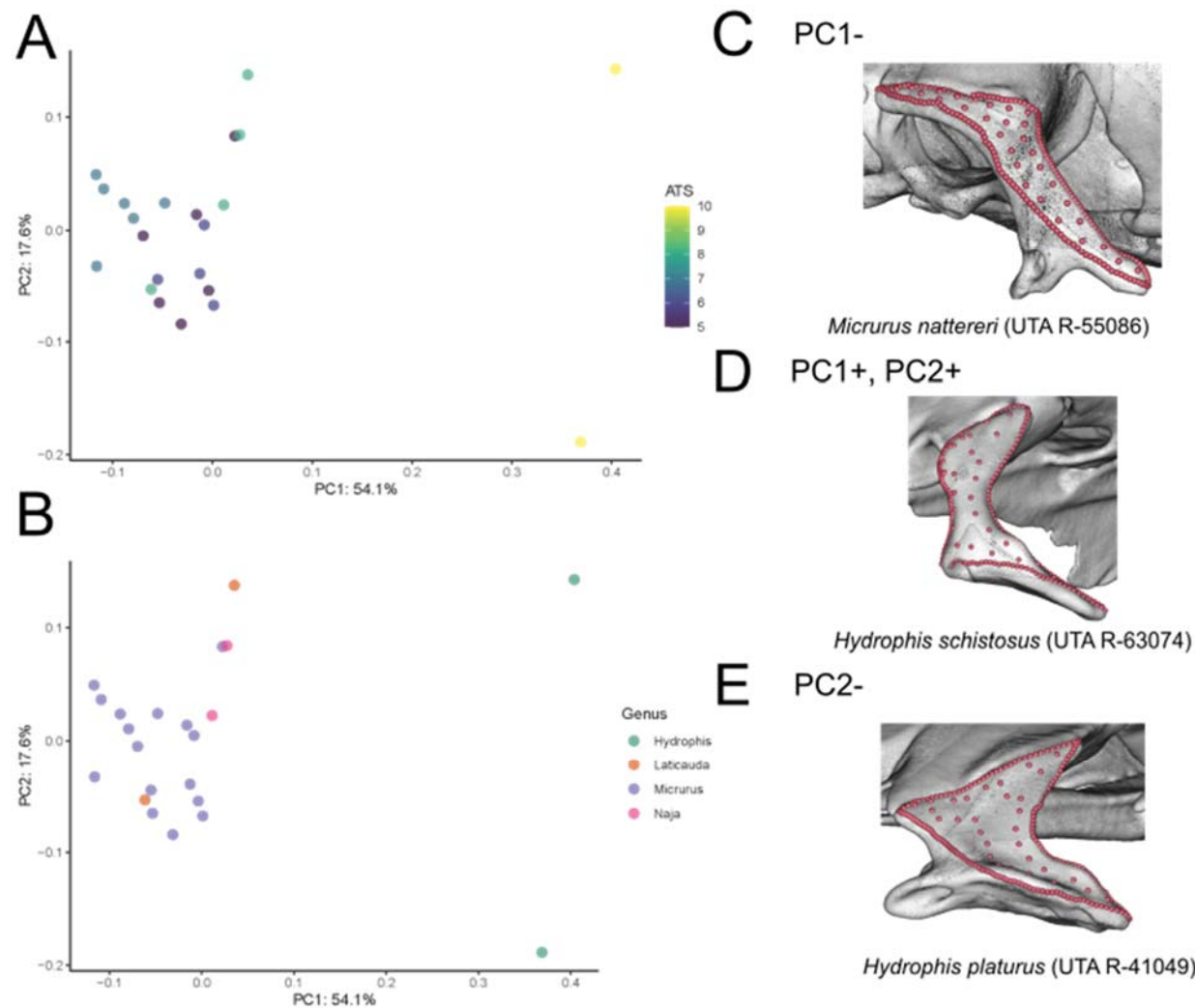


Figure 3.15. PCA of the prefrontal module conducted on the semi-aquatic and aquatic subset (>5 ATS), colored by ATS (A) and genus (B). Images of the prefrontal of specimens at the extremes of PC1 (C-D) and PC2 (D-E) in dorsolateral view.

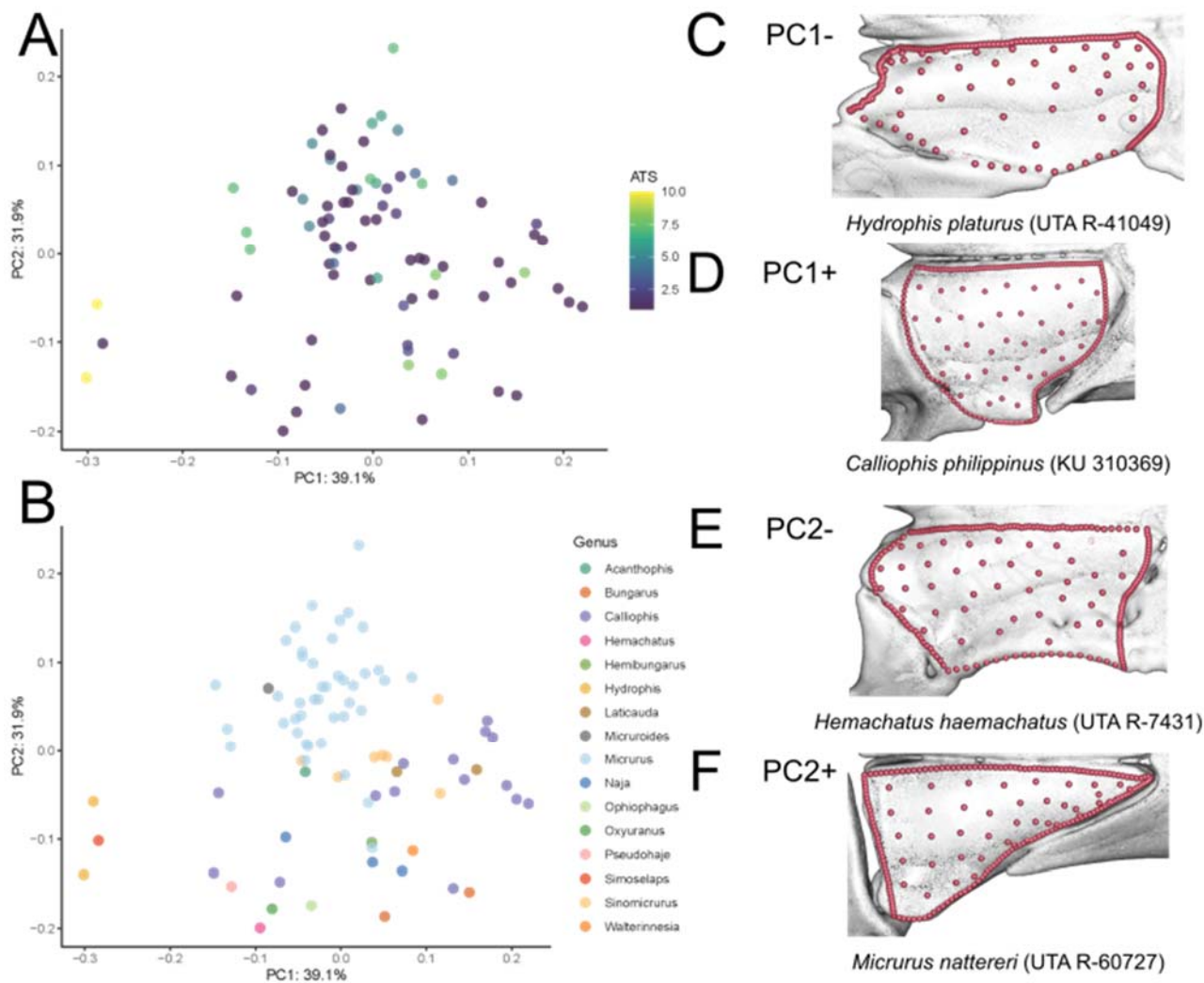


Figure 3.16. PCA of the frontal module, utilizing all specimens, colored by ATS (A) and genus (B). Images of the frontal of specimens at the extremes of PC1 (C-D) and PC2 (E-F) in dorsal view.

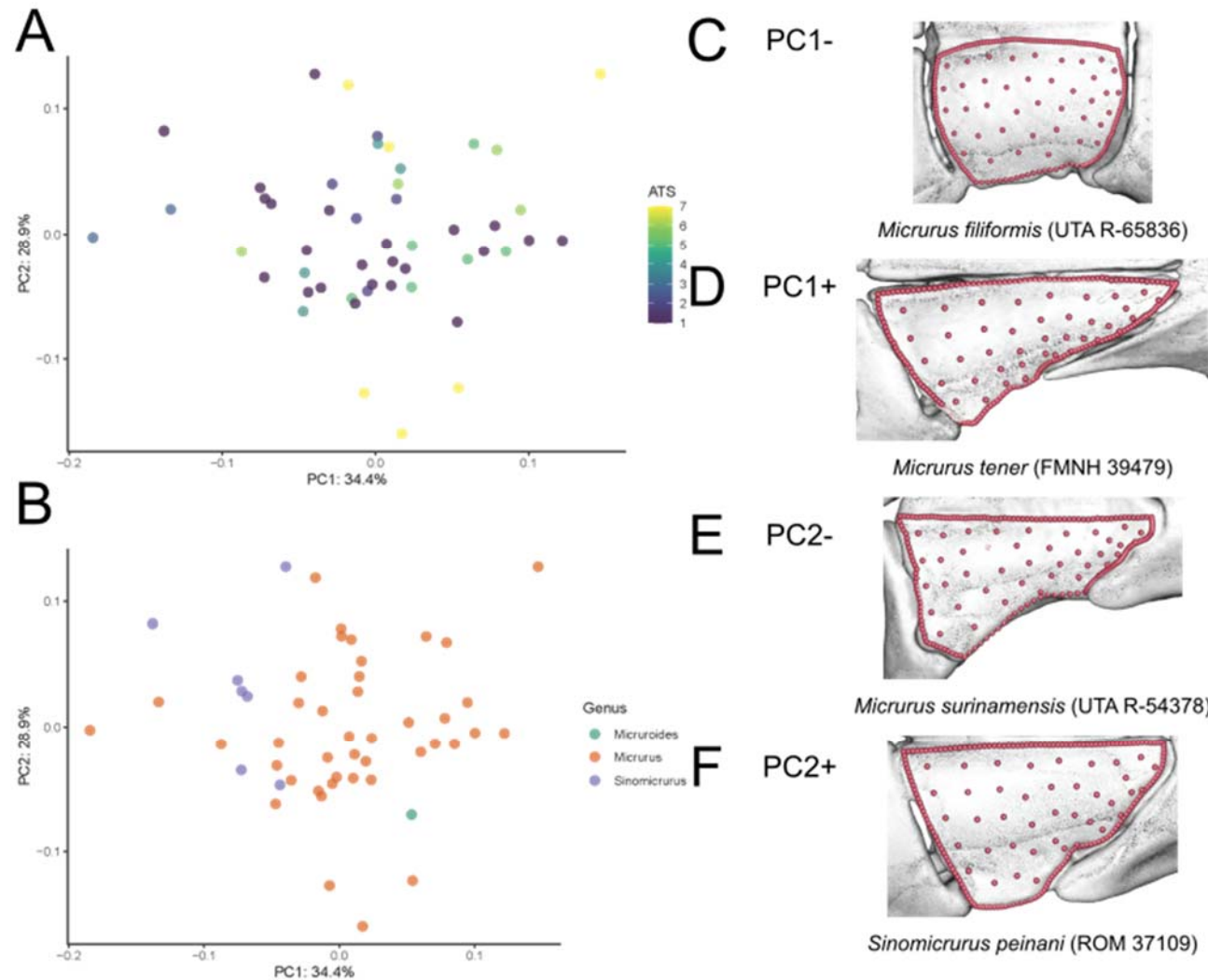


Figure 3.17. PCA of the frontal module conducted on the coralsnake subset, colored by ATS (A) and genus (B). Images of the frontal of specimens at the extremes of PC1 (C-D) and PC2 (E-F) in dorsal view.

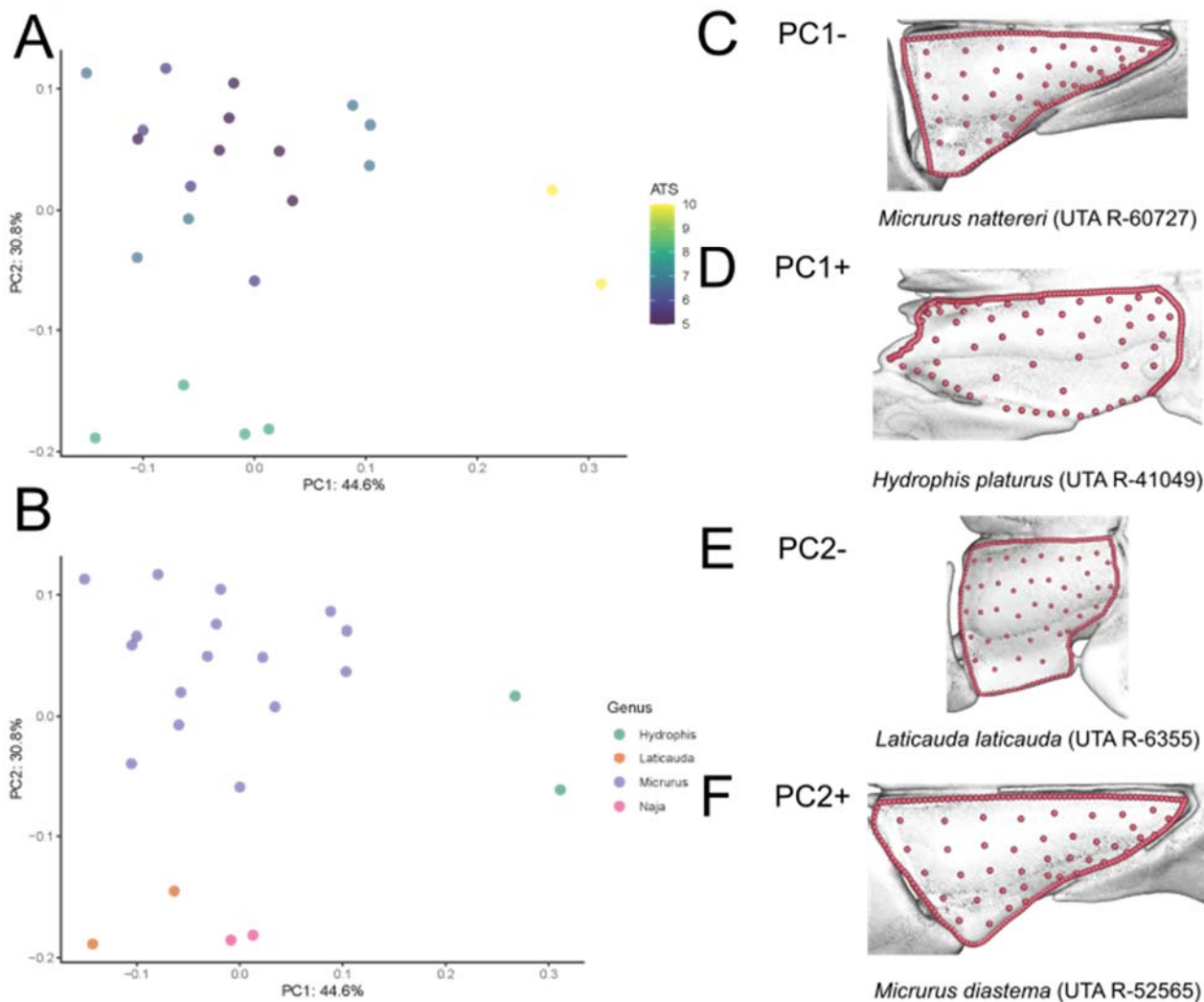


Figure 3.18. PCA of the frontal module conducted on the semi-aquatic and aquatic subset (>5 ATS), colored by ATS (A) and genus (B). Images of the frontal of specimens at the extremes of PC1 (C-D) and PC2 (E-F) in dorsal view.

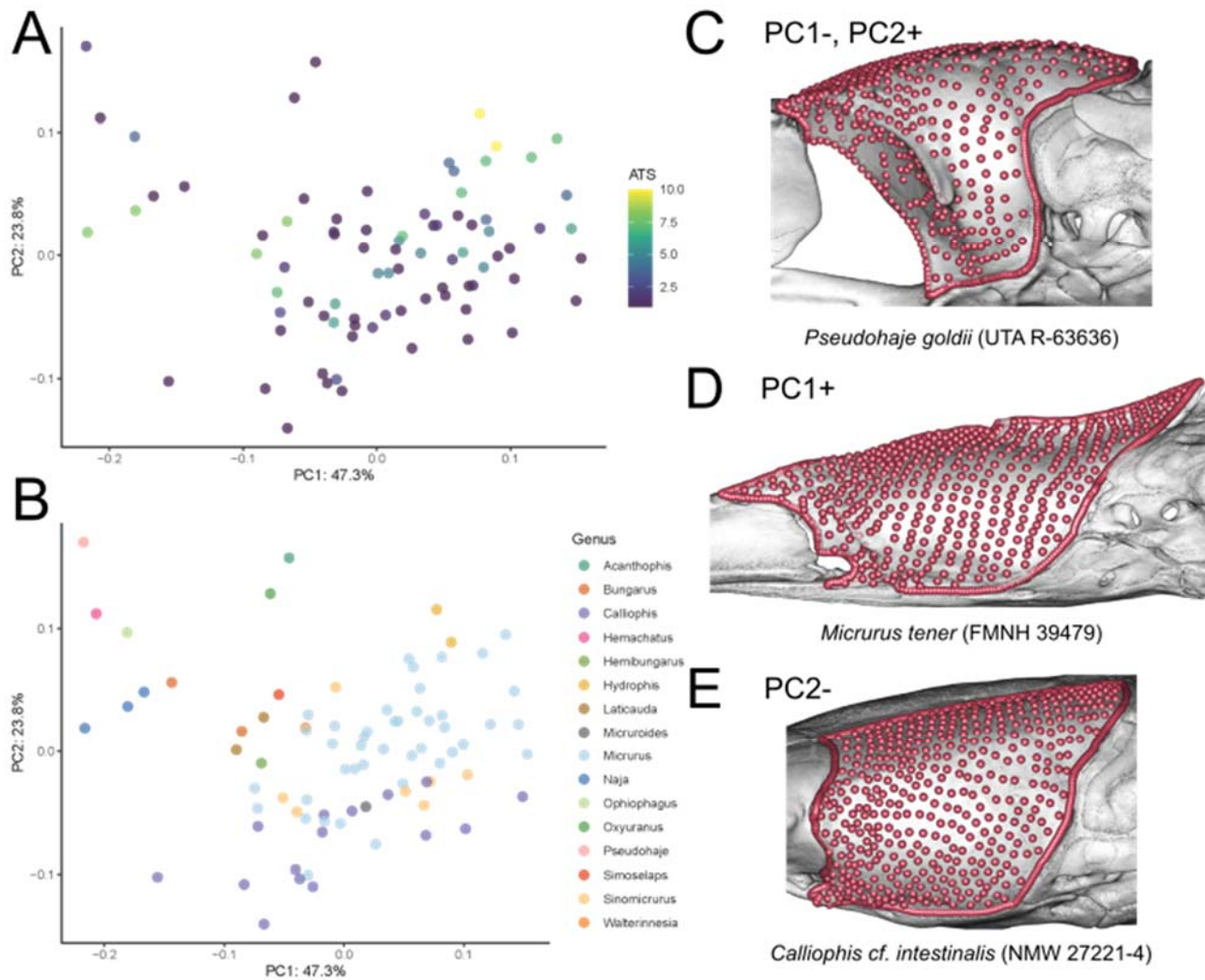


Figure 3.19. PCA of the parietal module, utilizing all specimens, colored by ATS (A) and genus (B). Images of the parietal of specimens at the extremes of PC1 (C-D) and PC2 maximum (C) and minimum (E) in lateral view.

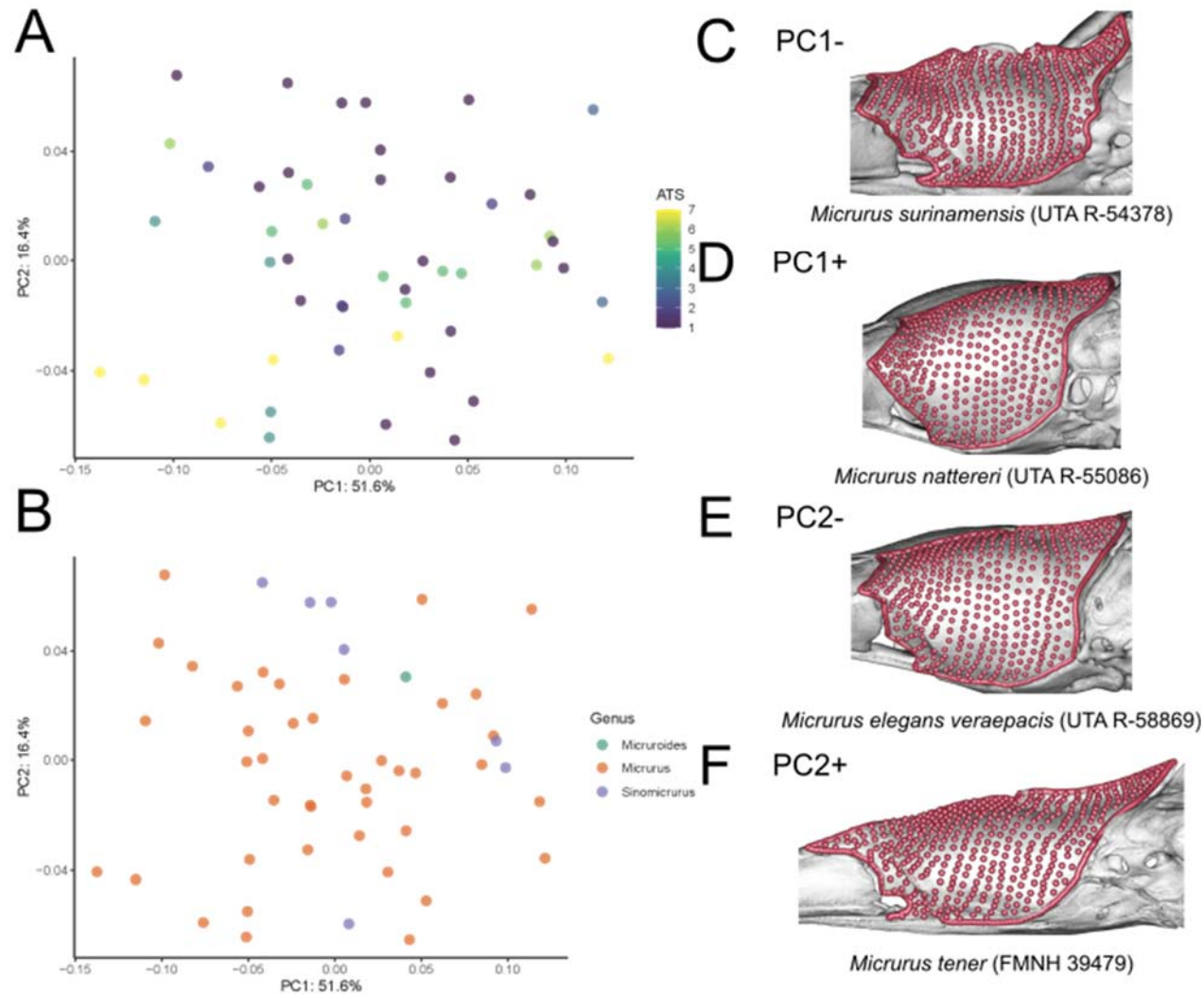


Figure 3.20. PCA of the parietal module conducted on the coralsnake subset, colored by ATS (A) and genus (B). Images of the parietal of specimens at the extremes of PC1 (C-D) and PC2 (E-F) in lateral view.

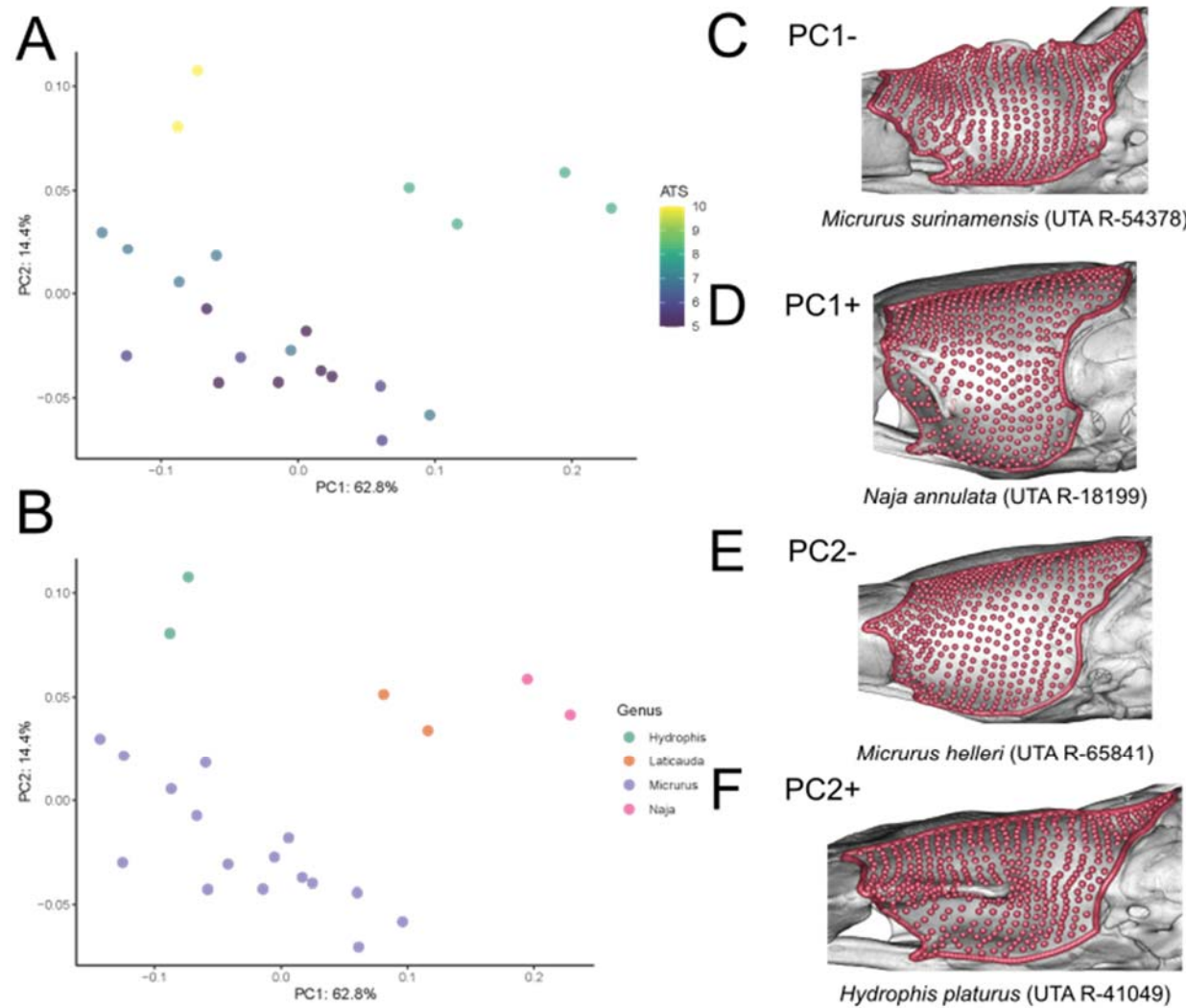


Figure 3.21. PCA of the parietal module conducted on the semi-aquatic and aquatic subset (>5 ATS), colored by ATS (A) and genus (B). Images of the parietal of specimens at the extremes of PC1 (C-D) and PC2 (E-F) in lateral view.

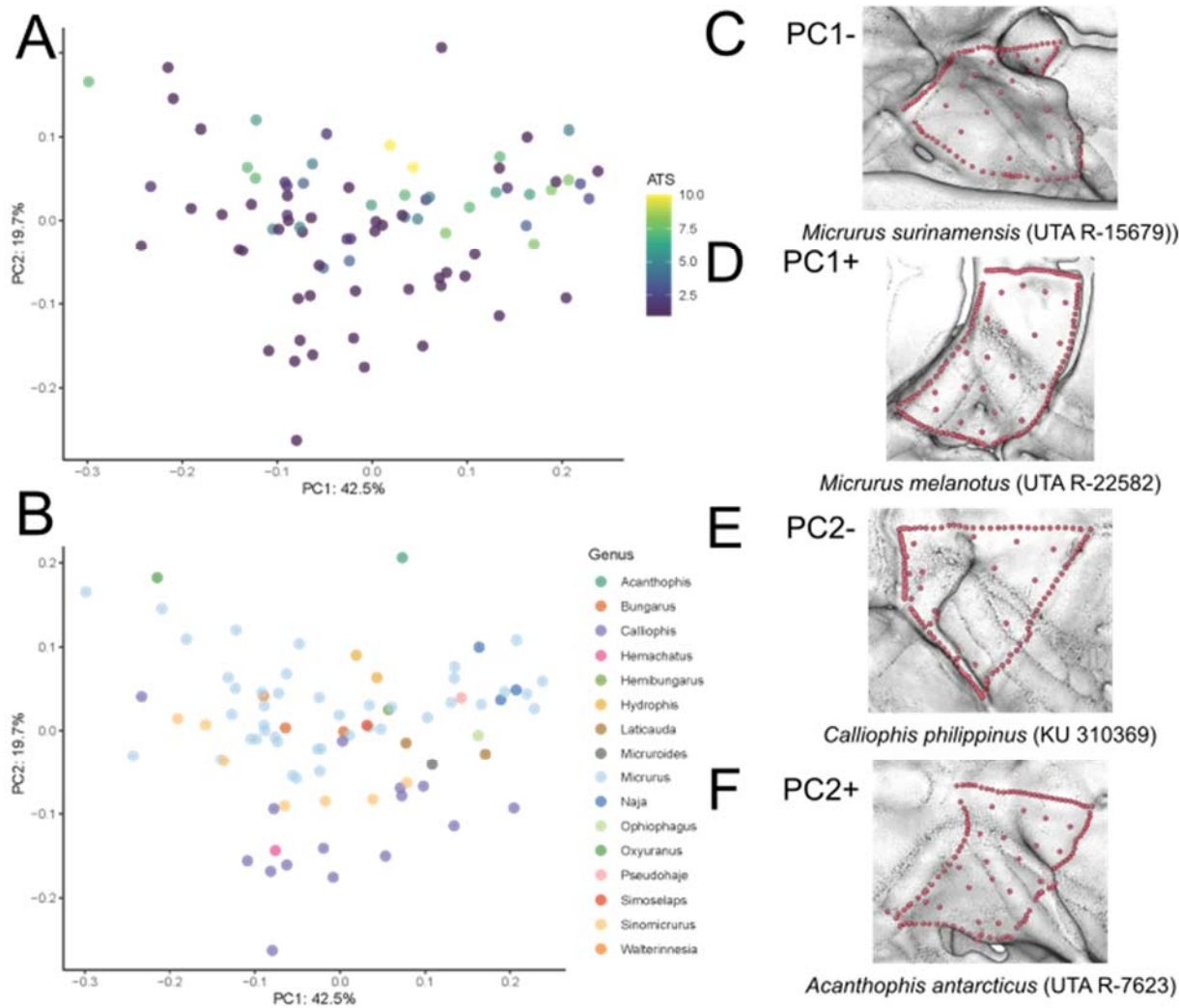


Figure 3.22. PCA of the supraoccipital module, utilizing all specimens, colored by ATS (A) and genus (B). Images of the supraoccipital of specimens at the extremes of PC1 (C-D) and PC2 (E-F) in dorsal view.

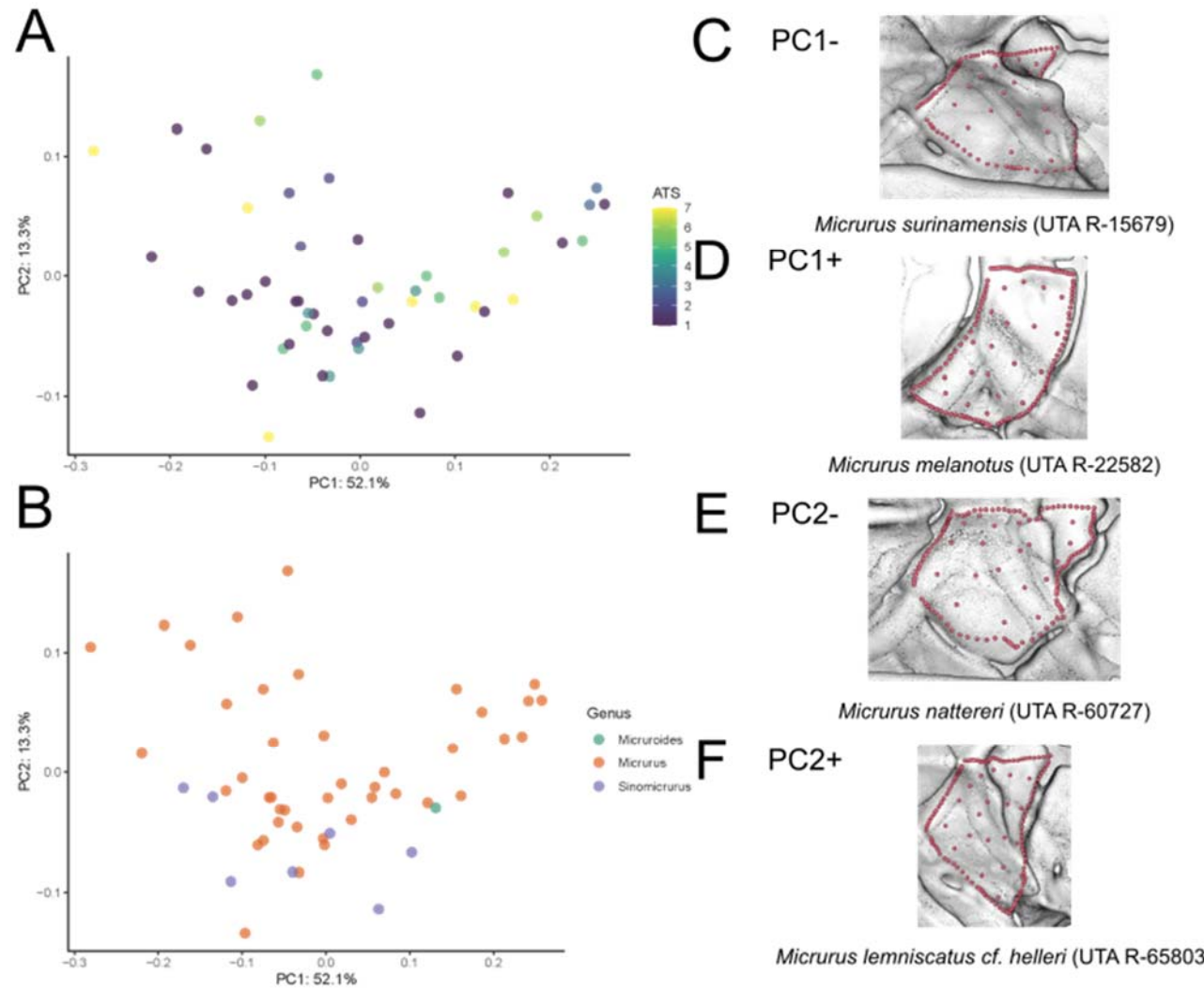


Figure 3.23. PCA of the supraoccipital module conducted on the coralsnake subset, colored by ATS (A) and genus (B). Images of the supraoccipital of specimens at the extremes of PC1 (C-D) and PC2 (E-F) in dorsal view.

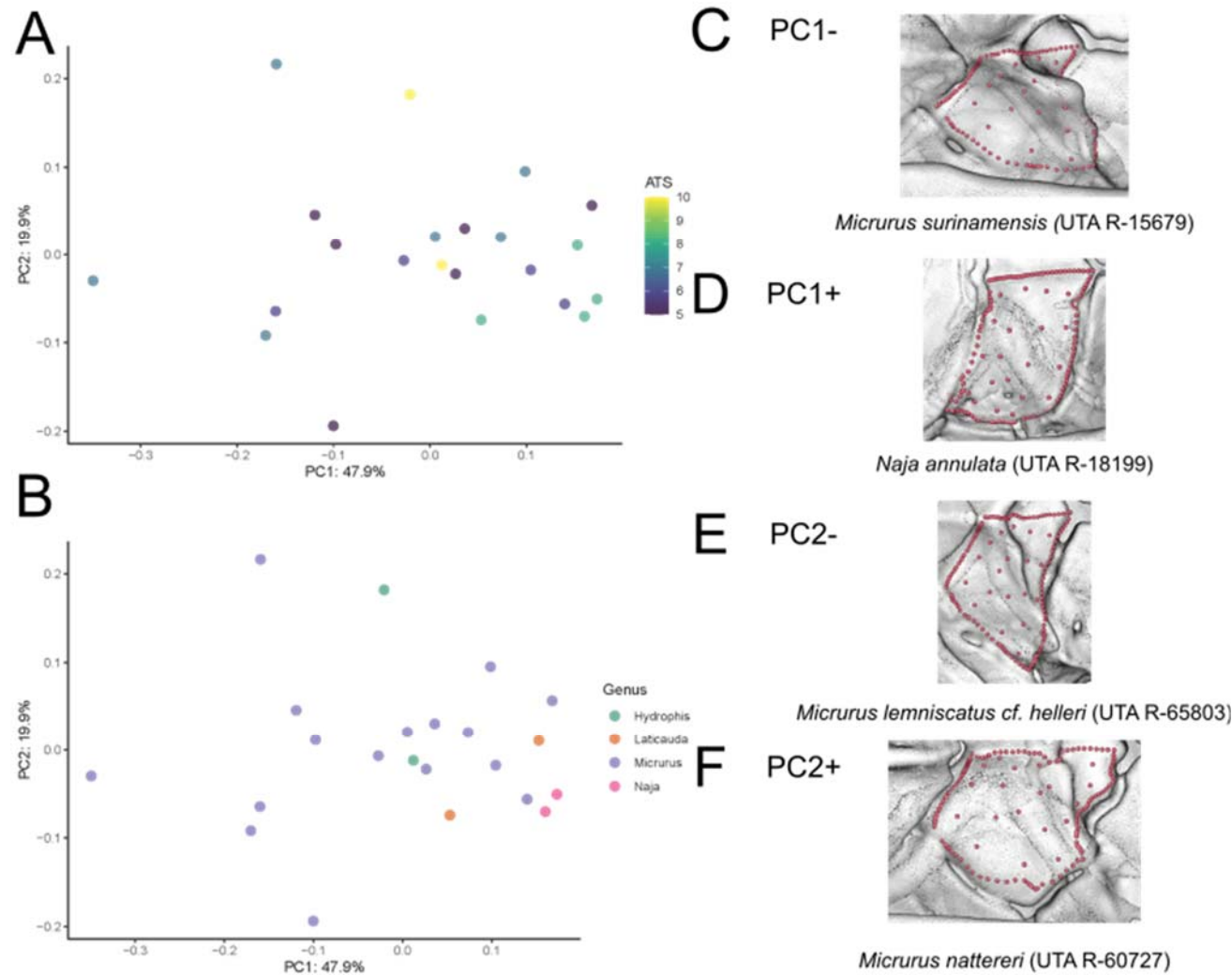


Figure 3.24. PCA of the supraoccipital module conducted on the semi-aquatic and aquatic subset (>5 ATS), colored by ATS (A) and genus (B). Images of the supraoccipital of specimens at the extremes of PC1 (C-D) and PC2 (E-F) in dorsal view.

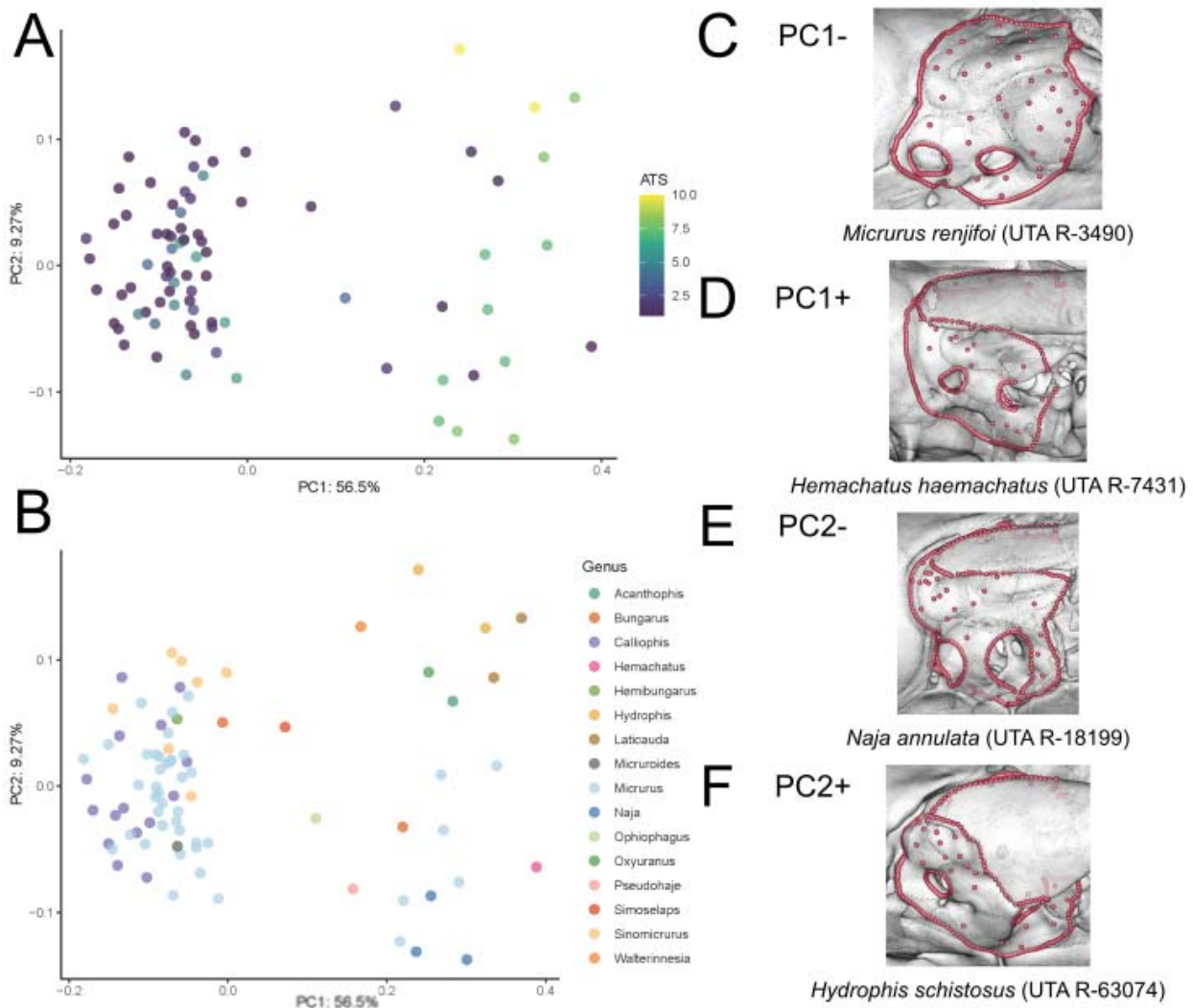


Figure 3.25. PCA of the prootic module utilizing all specimens, colored by ATS (A) and genus (B). Images of the prootic of specimens at the extremes of PC1 (C-D) and PC2 (E-F) in lateral view.

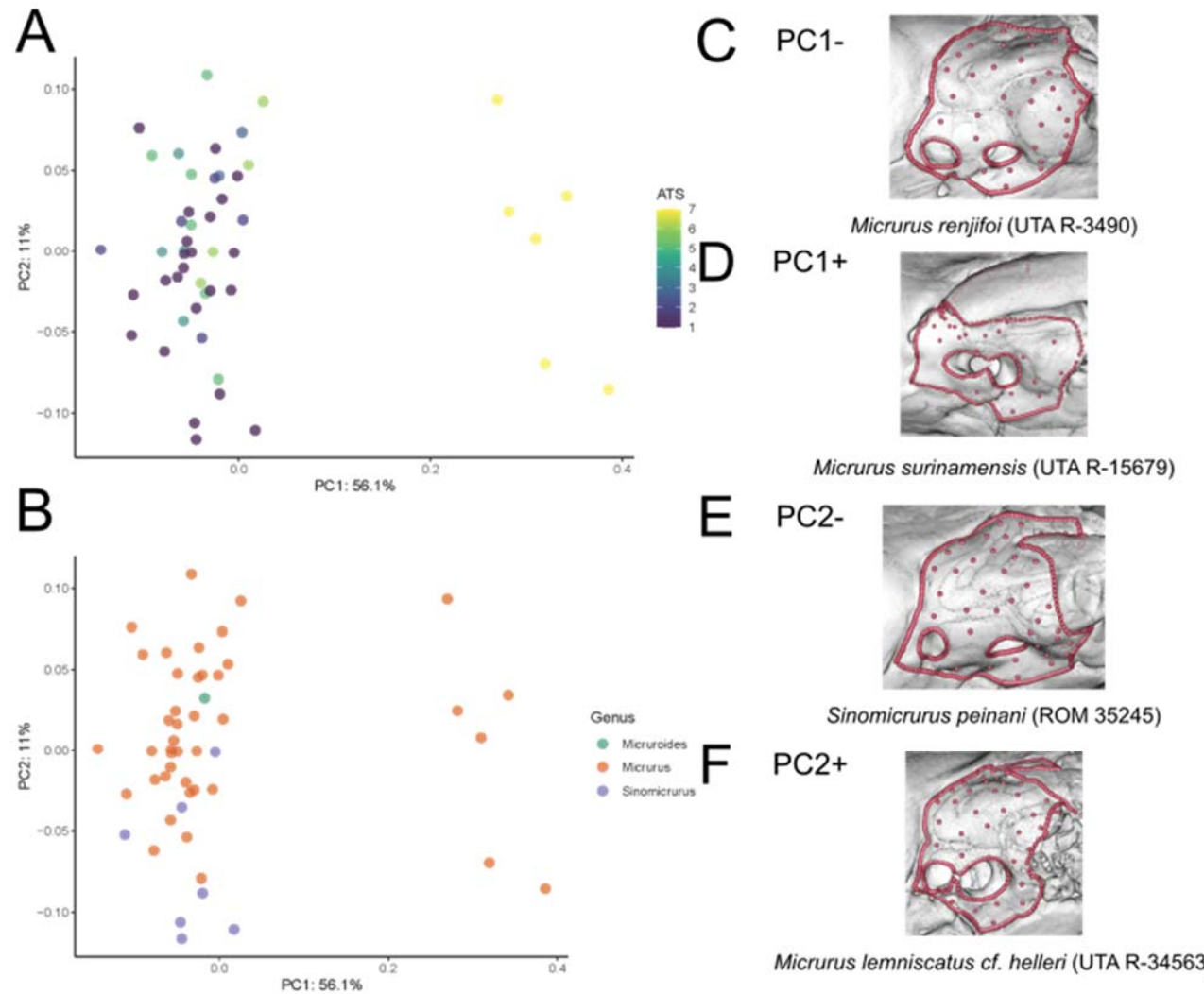


Figure 3.26. PCA of the prootic module conducted on the coralsnake subset, colored by ATS (A) and genus (B). Images of the prootic of specimens at the extremes of PC1 (C-D) and PC2 (E-F) in lateral view.

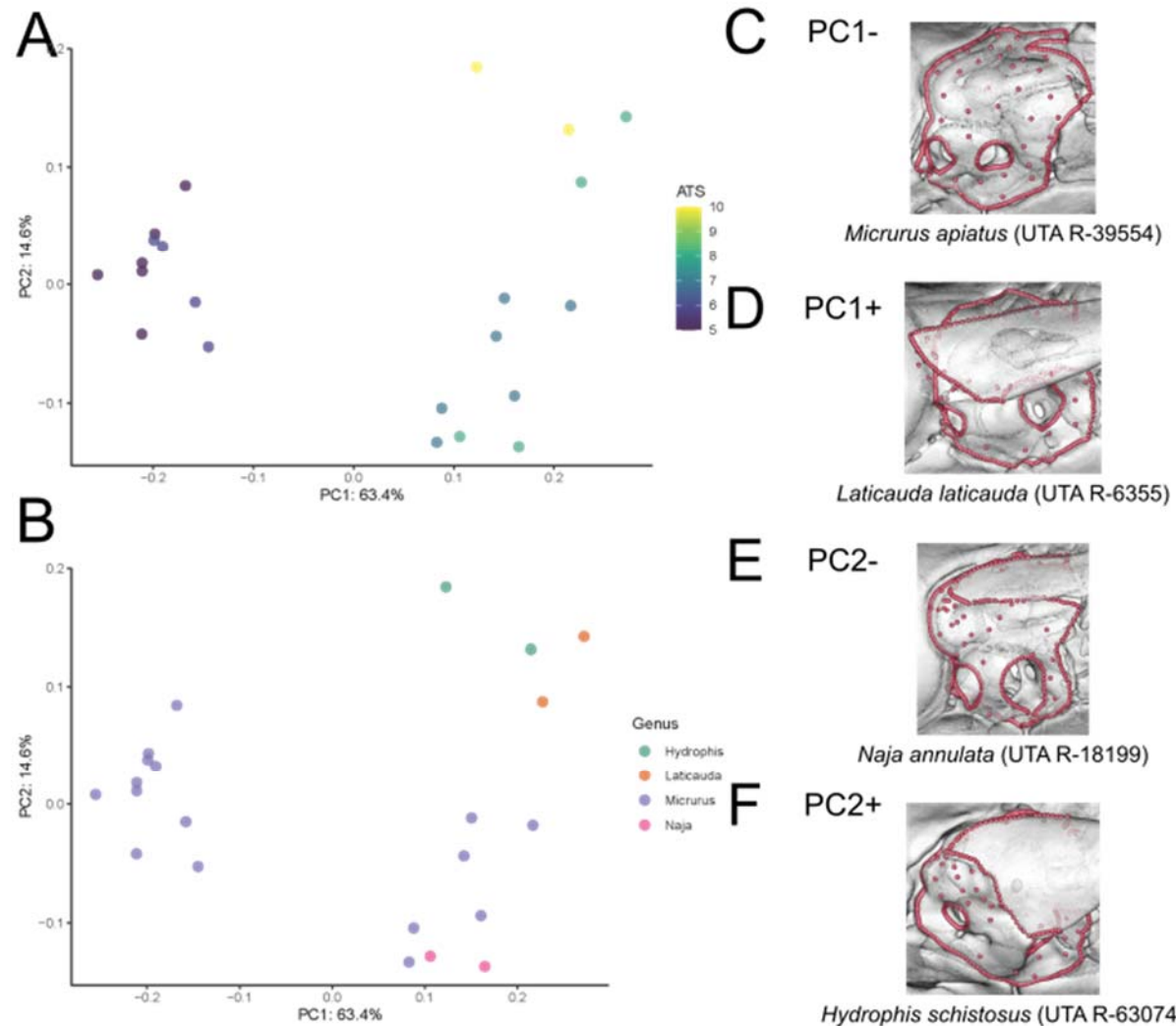


Figure 3.27. PCA of the prootic module conducted on the semi-aquatic and aquatic subset (>5 ATS), colored by ATS (A) and genus (B). Images of the supraoccipital of specimens at the extremes of PC1 (C-D) and PC2 (E-F) in lateral view.

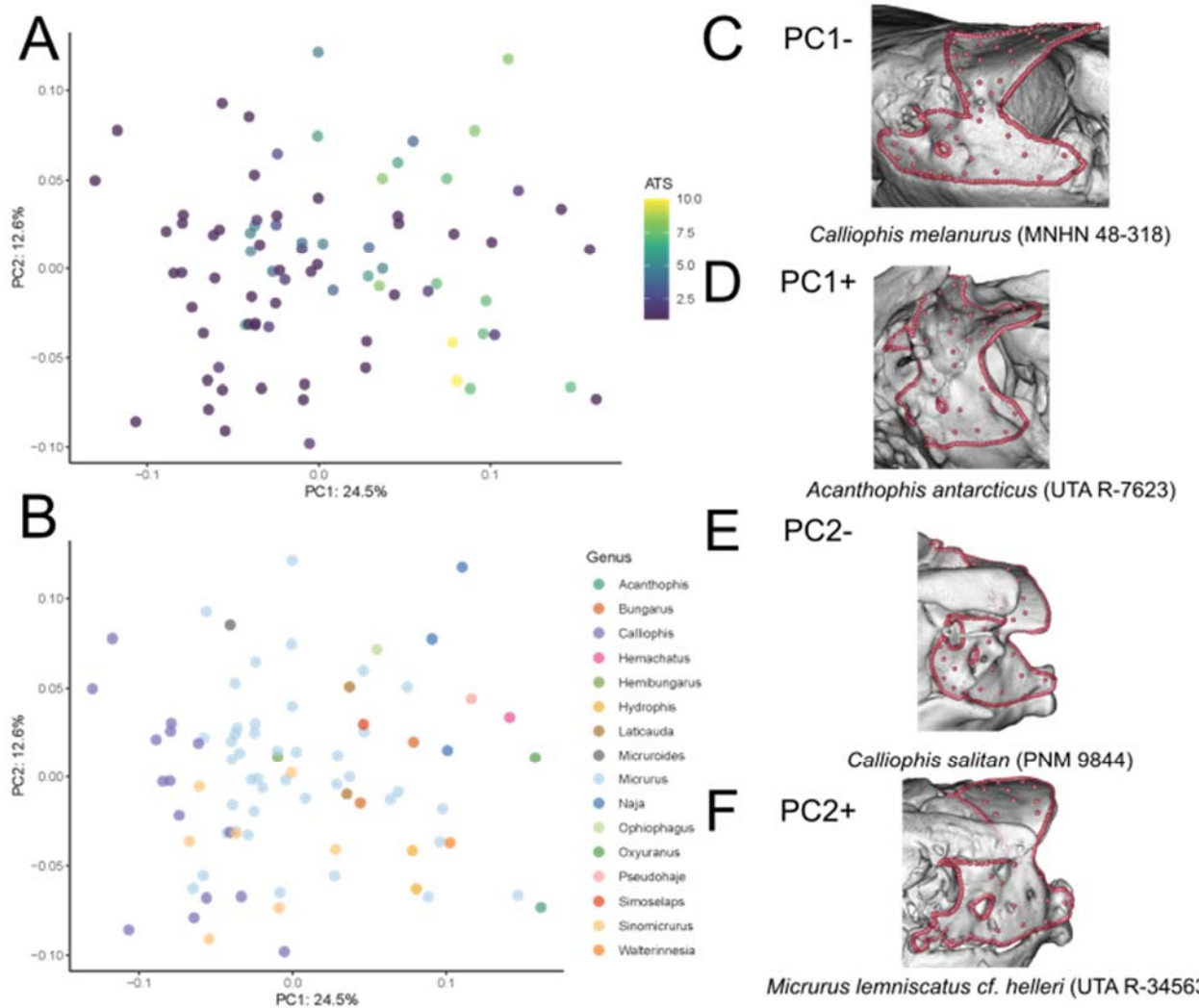


Figure 3.28. PCA of the exoccipital module utilizing all specimens, colored by ATS (A) and genus (B). Images of the exoccipital of specimens at the extremes of PC1 (C-D) and PC2 (E-F) in posterolateral view.

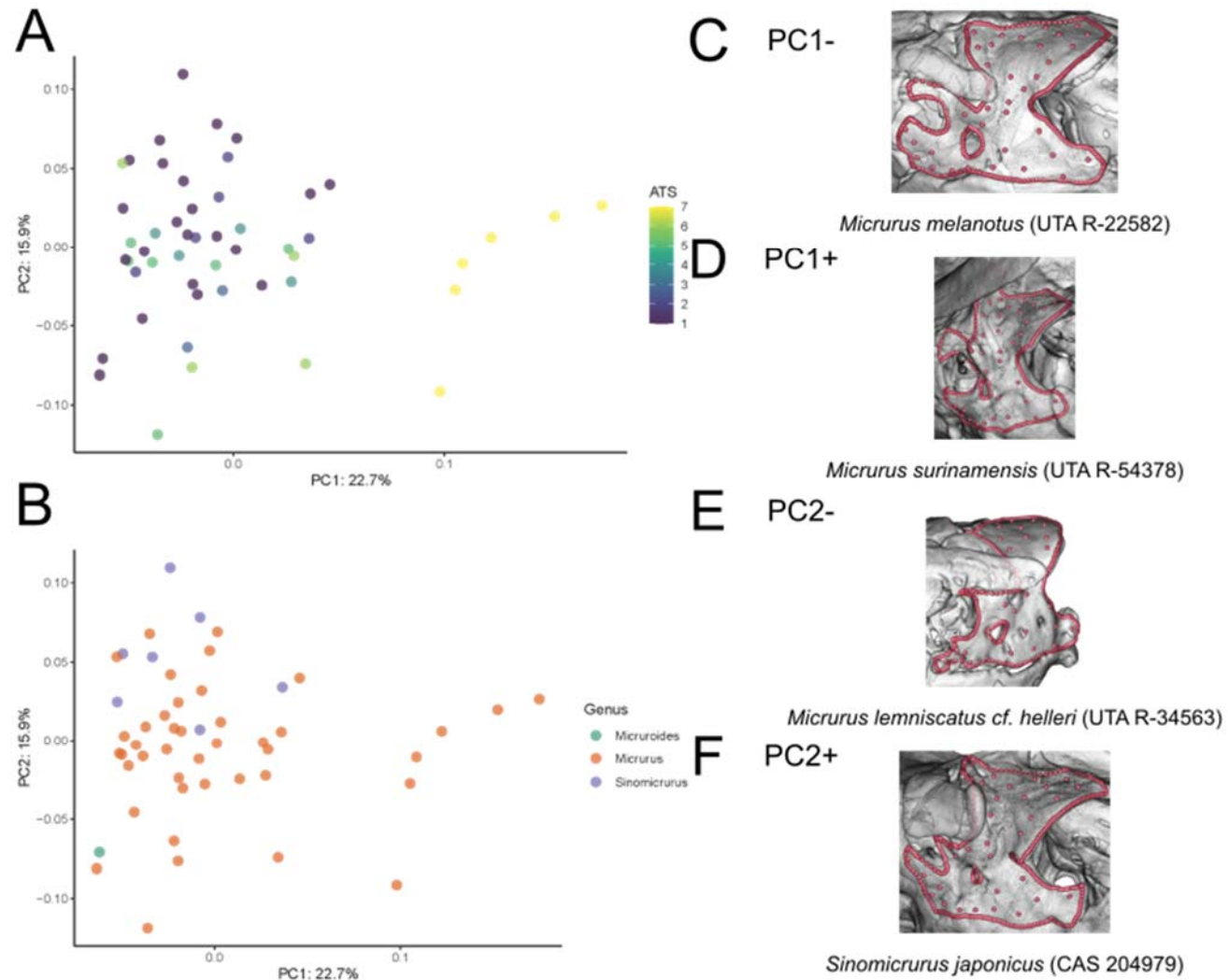


Figure 3.29. PCA of the exoccipital module conducted on the coralsnake subset, colored by ATS (A) and genus (B). Images of the exoccipital of specimens at the extremes of PC1 (C-D) and PC2 (E-F) in posterolateral view.

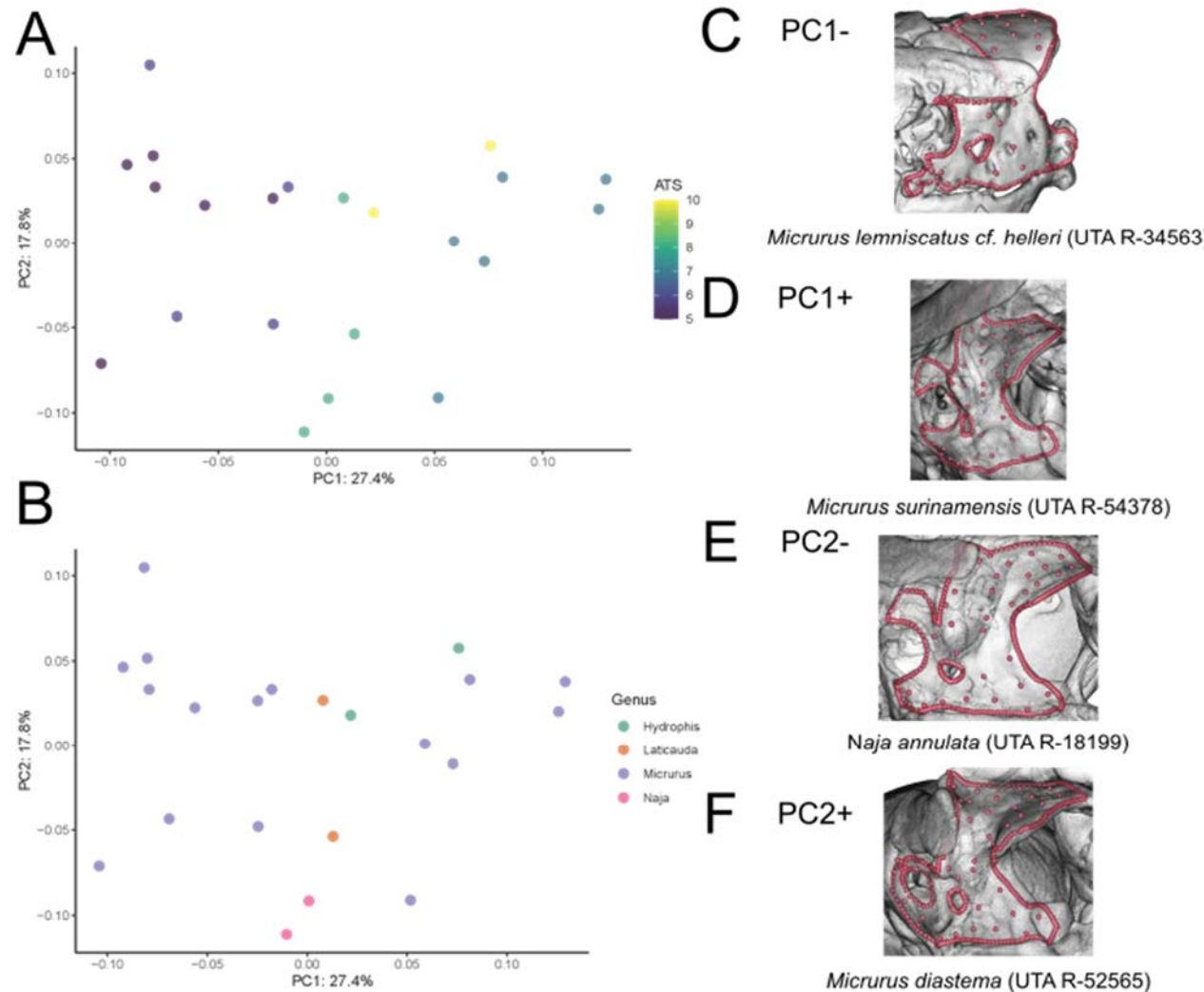


Figure 3.30. PCA of the exoccipital module conducted on the semi-aquatic and aquatic subset (>5 ATS), colored by ATS (A) and genus (B). Images of the exoccipital of specimens at the extremes of PC1 (C-D) and PC2 (E-F) in posterolateral view.

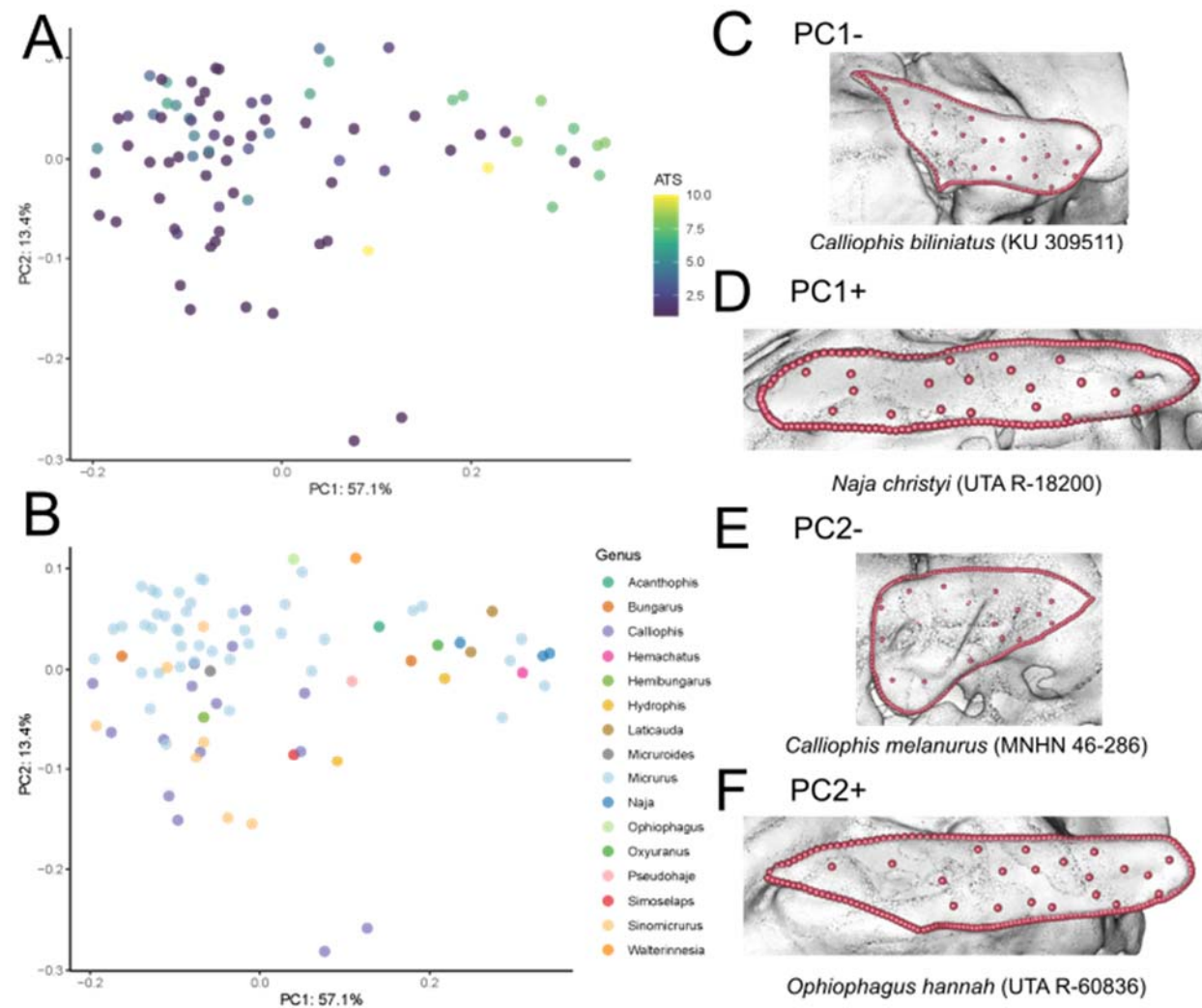


Figure 3.31. PCA of the supratemporal module utilizing all specimens, colored by ATS (A) and genus (B). Images of the supratemporal of specimens at the extremes of PC1 (C-D) and PC2 (E-F) in dorsolateral view.

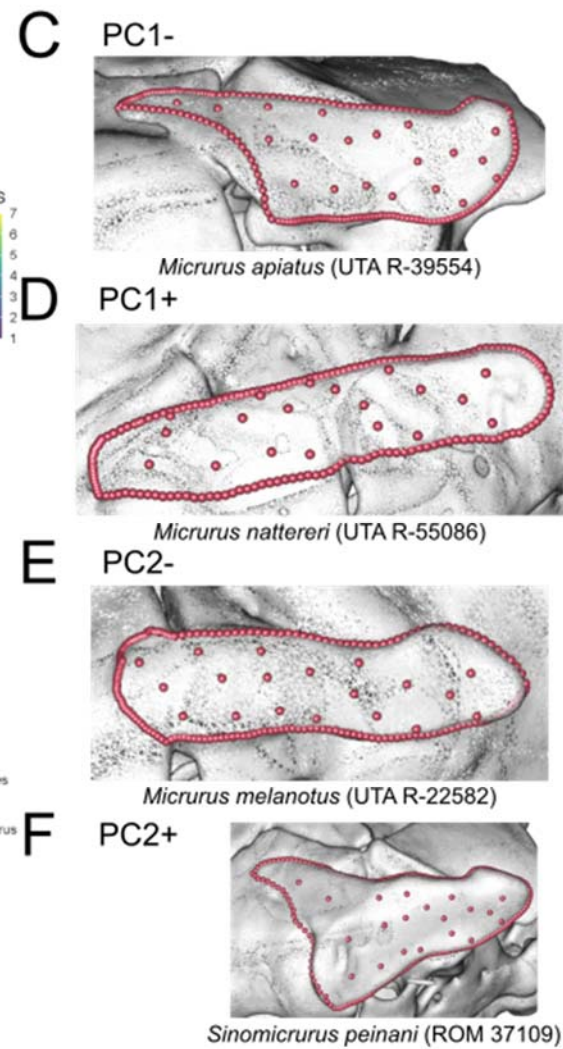
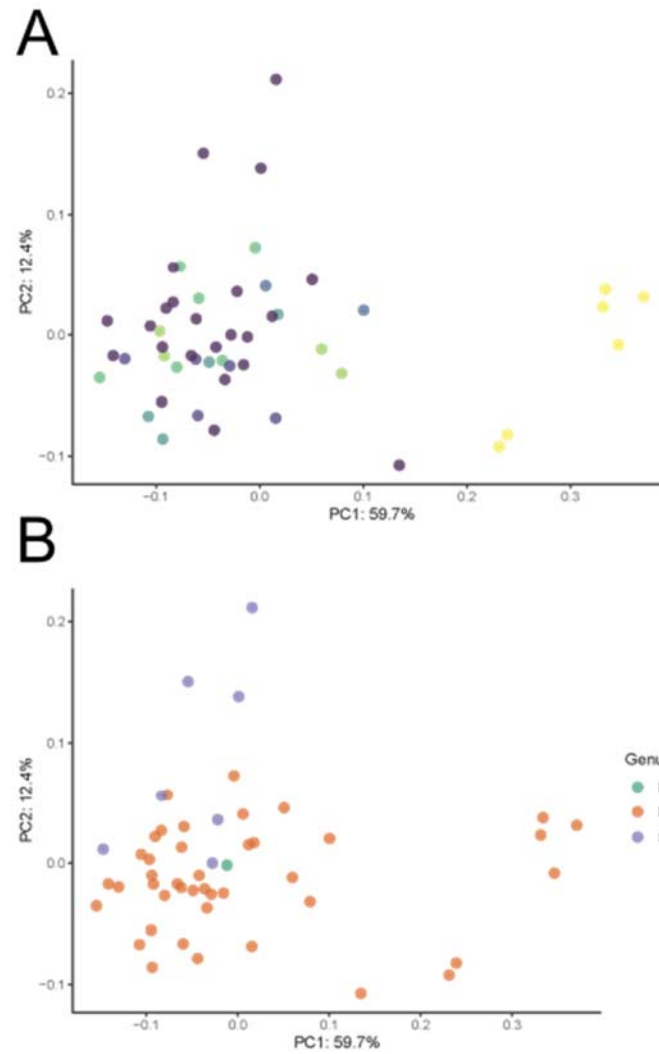


Figure 3.32. PCA of the supratemporal module conducted on the coralsnake subset, colored by ATS (A) and genus (B). Images of the supratemporal of specimens at the extremes of PC1 (C-D) and PC2 (E-F) in dorsolateral view.

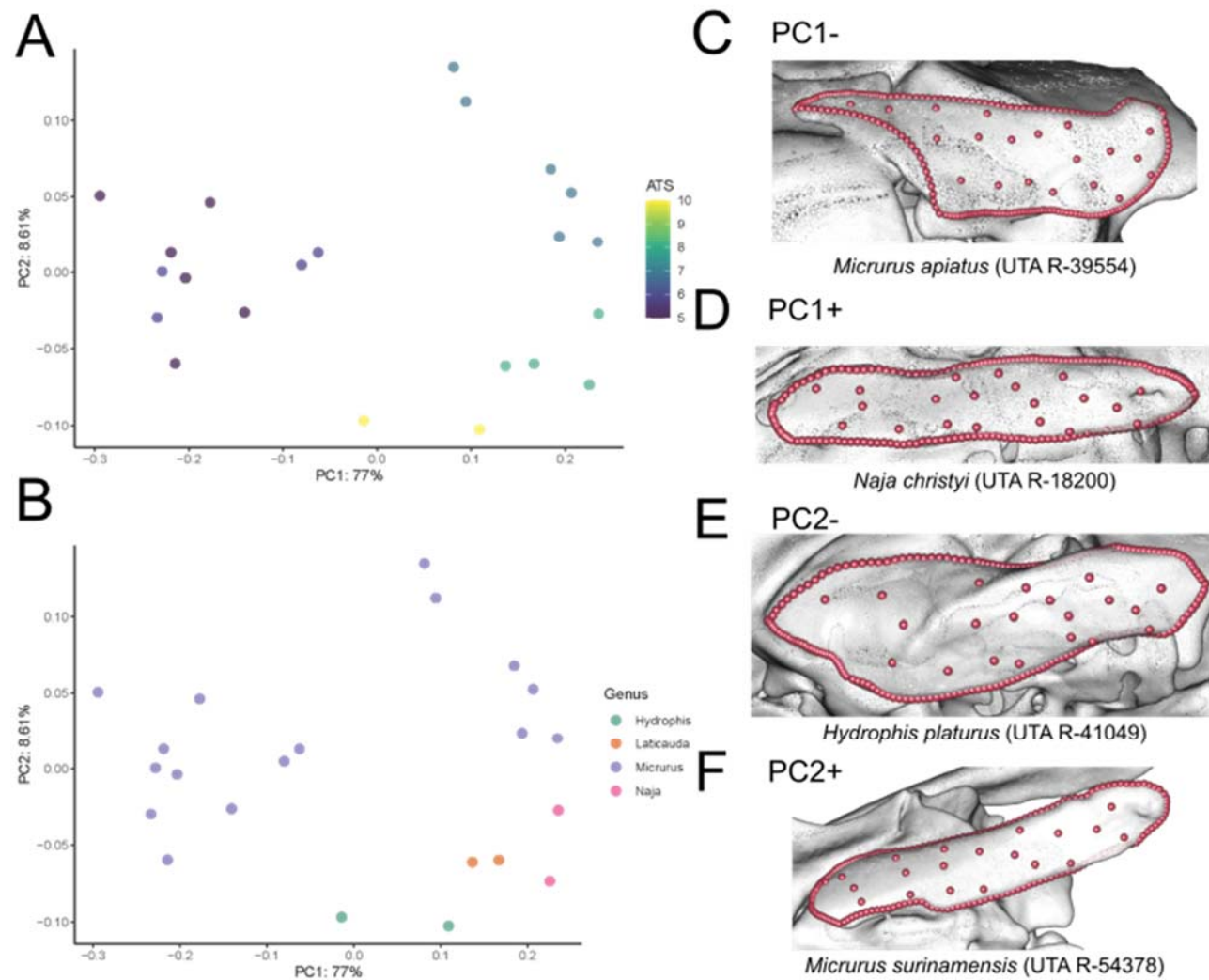


Figure 3.33. PCA of the supratemporal module conducted on the semi-aquatic and aquatic subset (>5 ATS), colored by ATS (A) and genus (B). Images of the supratemporal of specimens at the extremes of PC1 (C-D) and PC2 (E-F) in dorsolateral view.

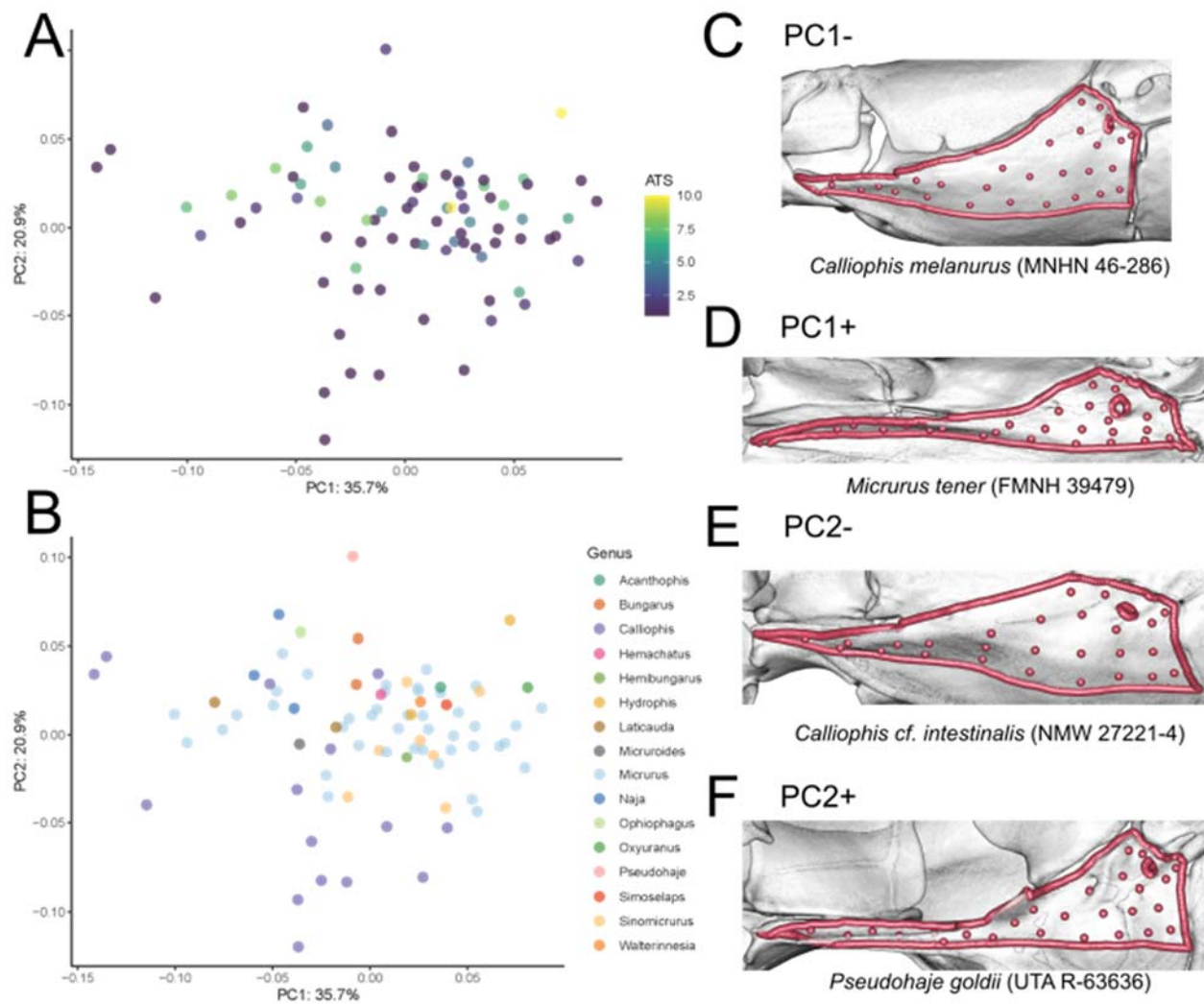


Figure 3.34. PCA of the basisphenoid module utilizing all specimens, colored by ATS (A) and genus (B). Images of the basisphenoid of specimens at the extremes of PC1 (C-D) and PC2 (E-F) in lateral view.

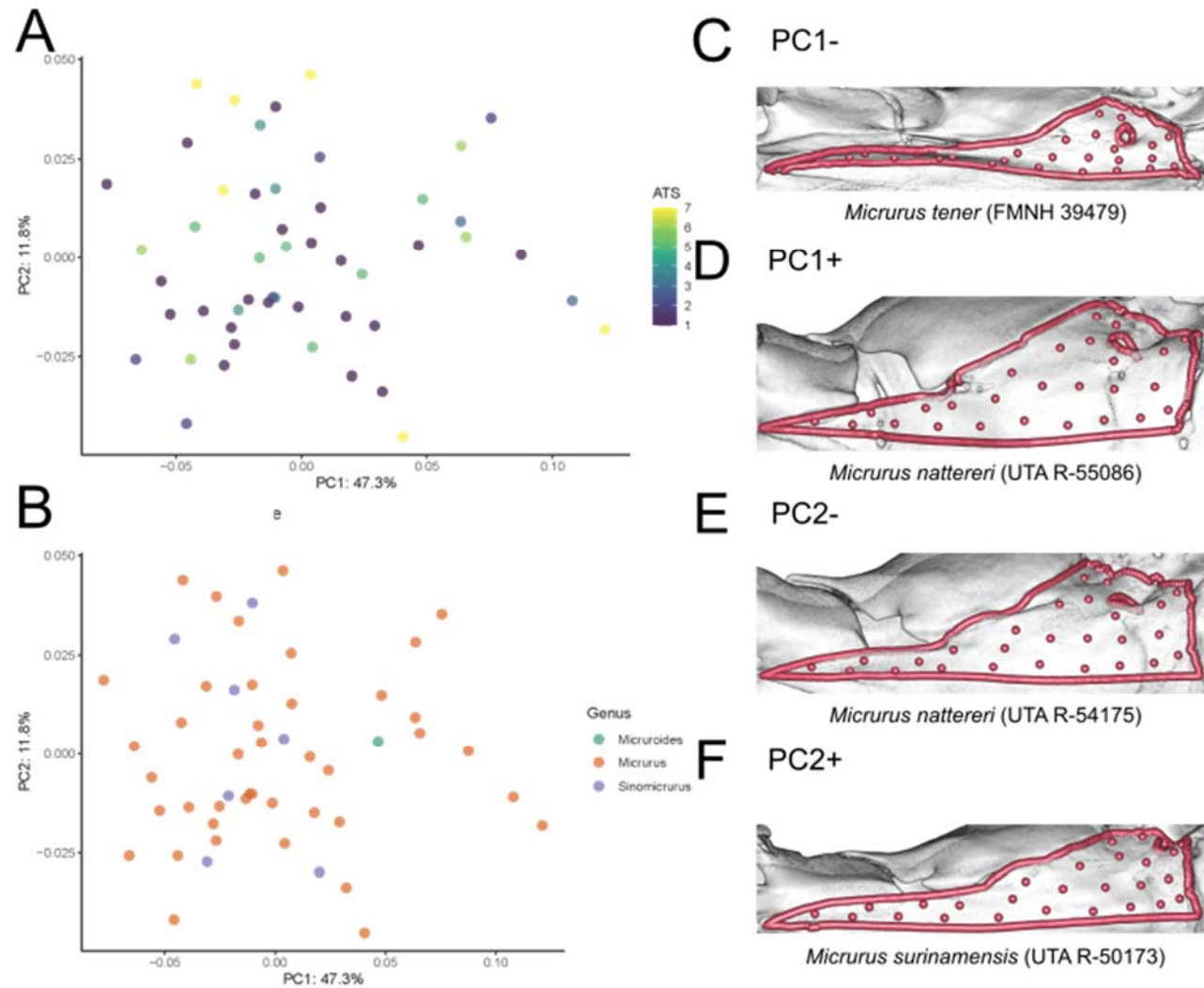


Figure 3.35. PCA of the basisphenoid module conducted on the coralsnake subset, colored by ATS (A) and genus (B). Images of the basisphenoid of specimens at the extremes of PC1 (C-D) and PC2 (E-F) in lateral view.

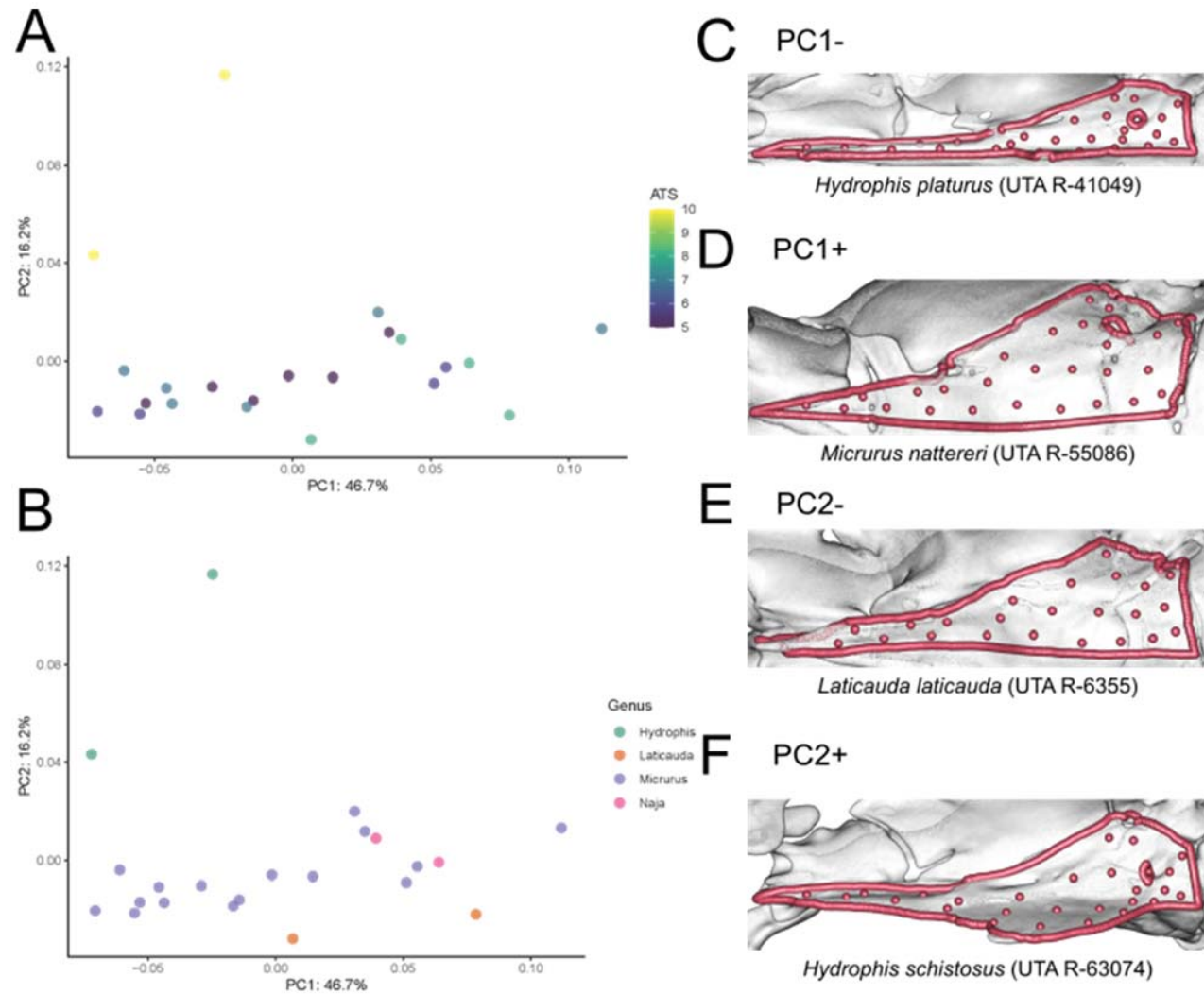


Figure 3.36. PCA of the basisphenoid module conducted on the semi-aquatic and aquatic subset (>5 ATS), colored by ATS (A) and genus (B). Images of the basisphenoid of specimens at the extremes of PC1 (C-D) and PC2 (E-F) in lateral view.

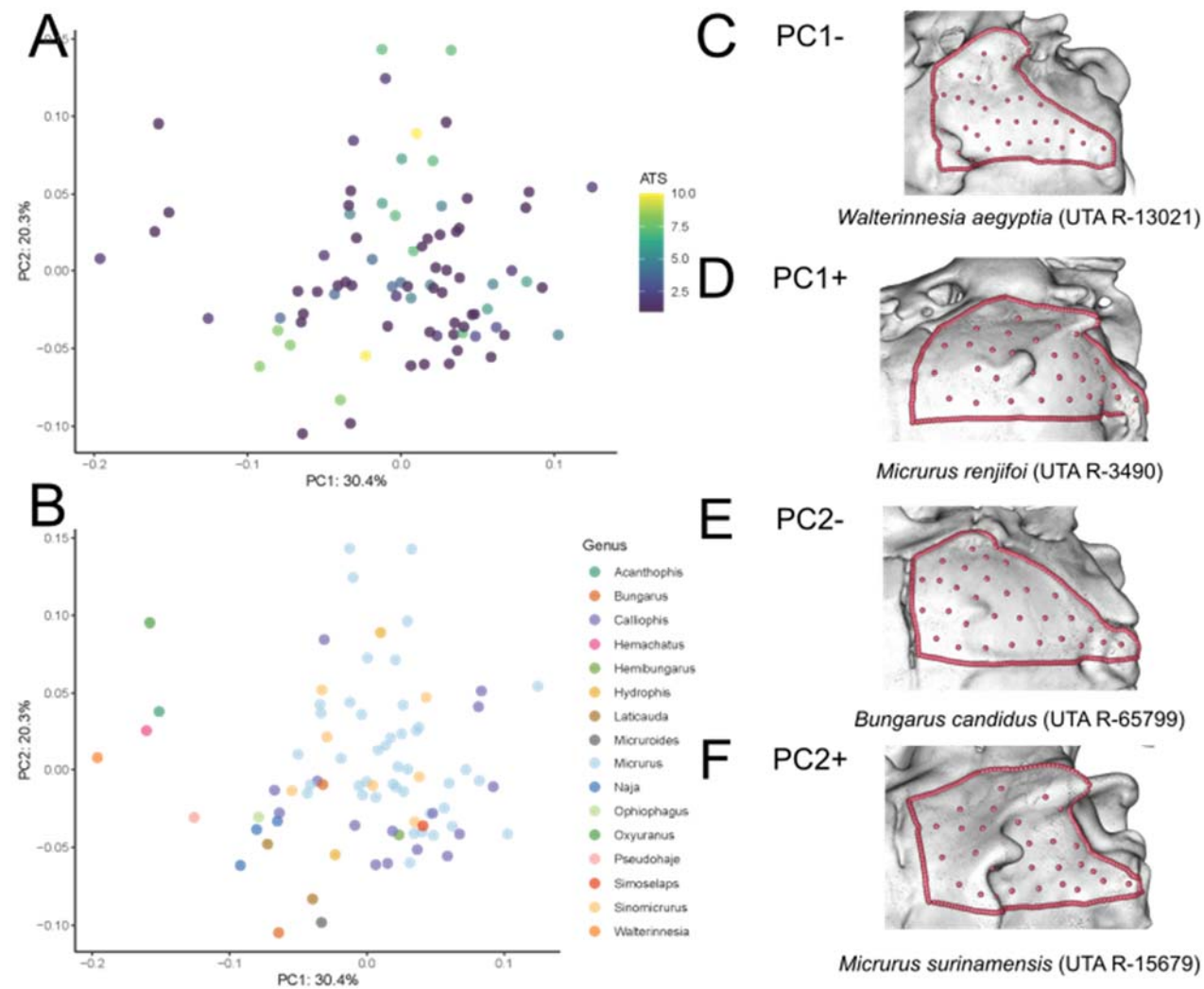


Figure 3.37. PCA of the basioccipital module utilizing all specimens, colored by ATS (A) and genus (B). Images of the basioccipital of specimens at the extremes of PC1 (C-D) and PC2 (E-F) in ventral view.

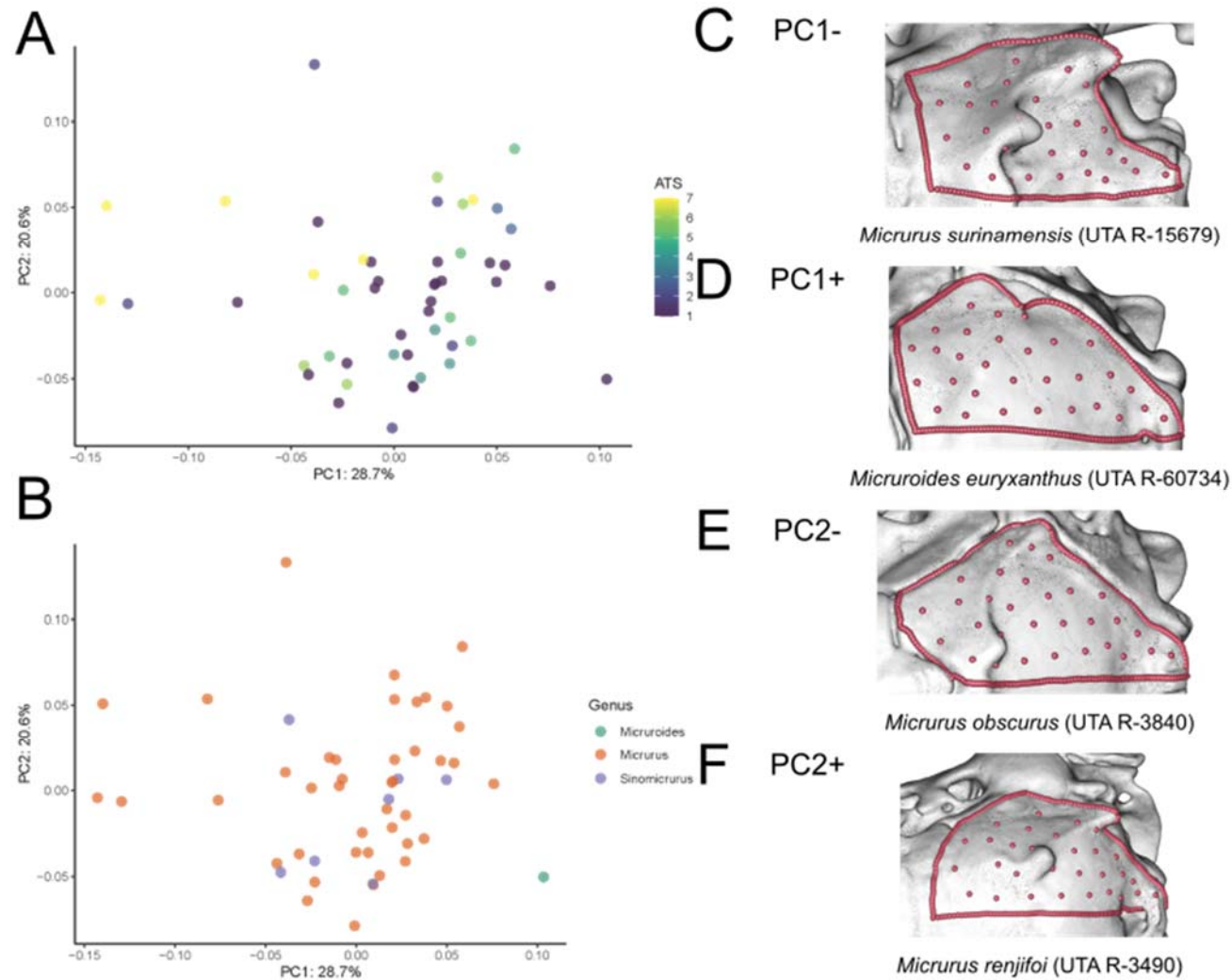


Figure 3.38. PCA of the basioccipital module conducted on the coralsnake subset, colored by ATS (A) and genus (B). Images of the basioccipital of specimens at the extremes of PC1 (C-D) and PC2 (E-F) in ventral view.

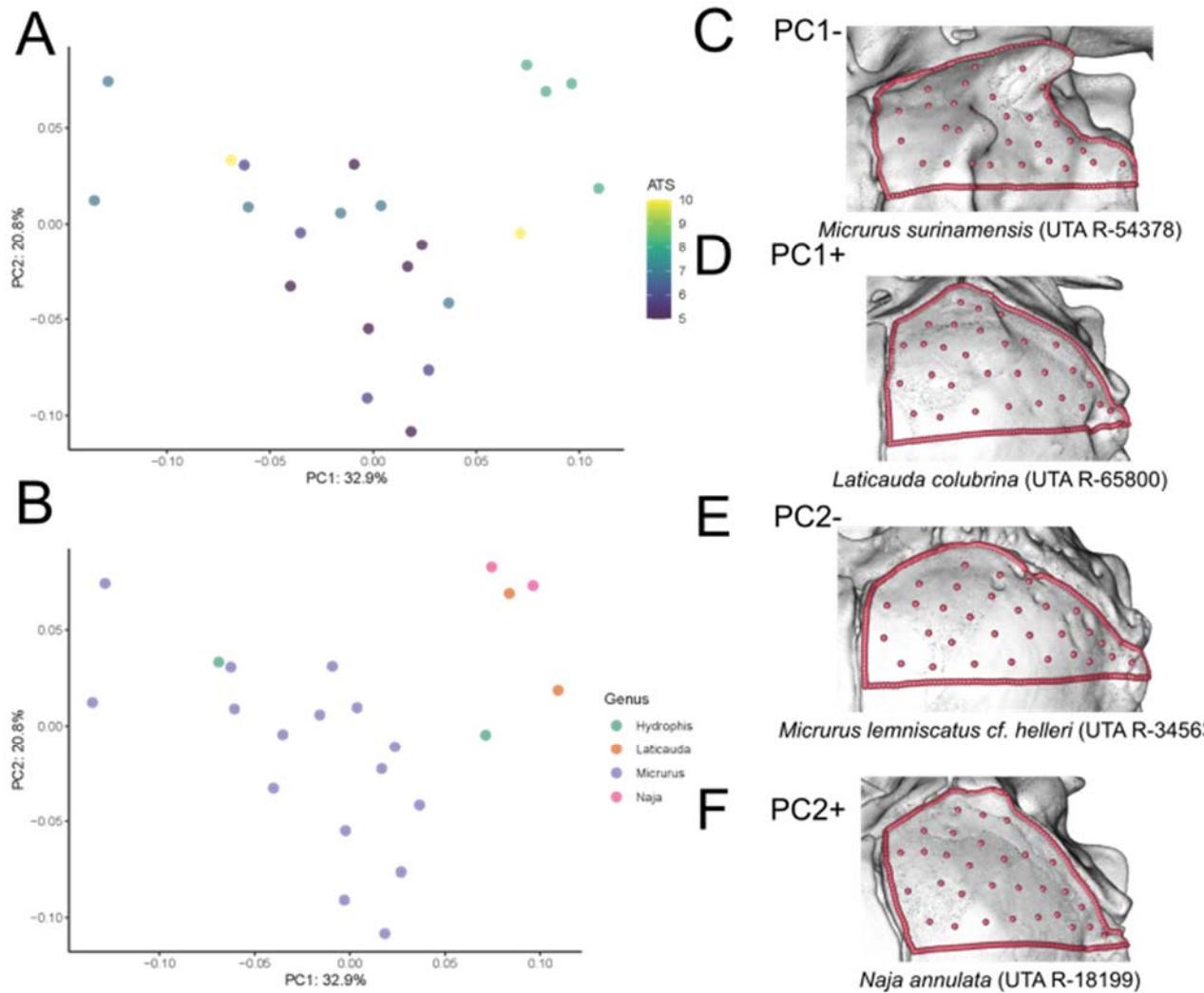


Figure 3.39. PCA of the basioccipital module conducted on the semi-aquatic and aquatic subset (>5 ATS), colored by ATS (A) and genus (B). Images of the basioccipital of specimens at the extremes of PC1 (C-D) and PC2 (E-F) in ventral view.

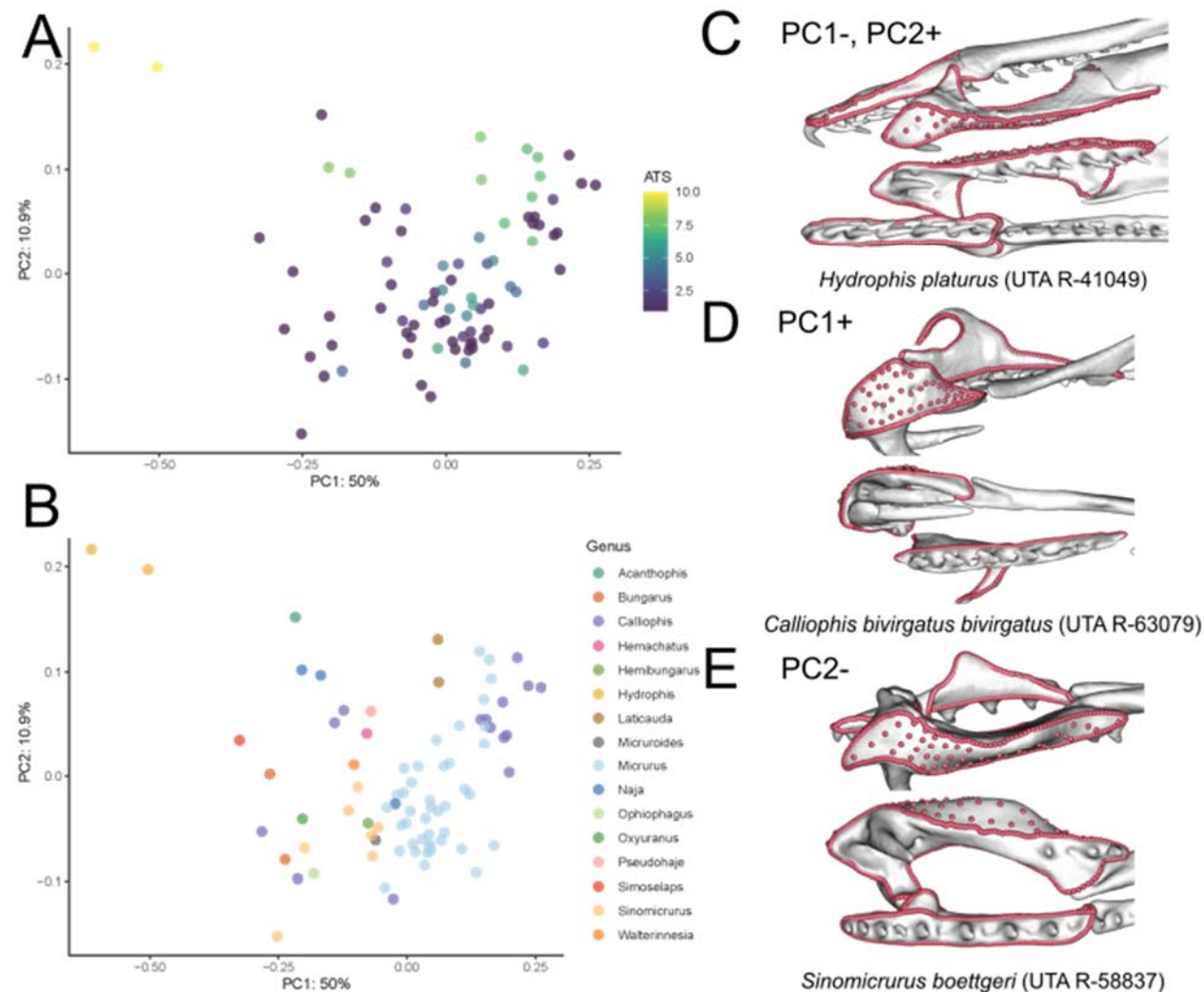


Figure 3.40. PCA of the maxilla and palatine module utilizing all specimens, colored by ATS (A) and genus (B). Images of specimens at the extremes of PC1 (C-D) and the PC2 maximum (C) and minimum (E) in lateral (top) and ventral (bottom) views.

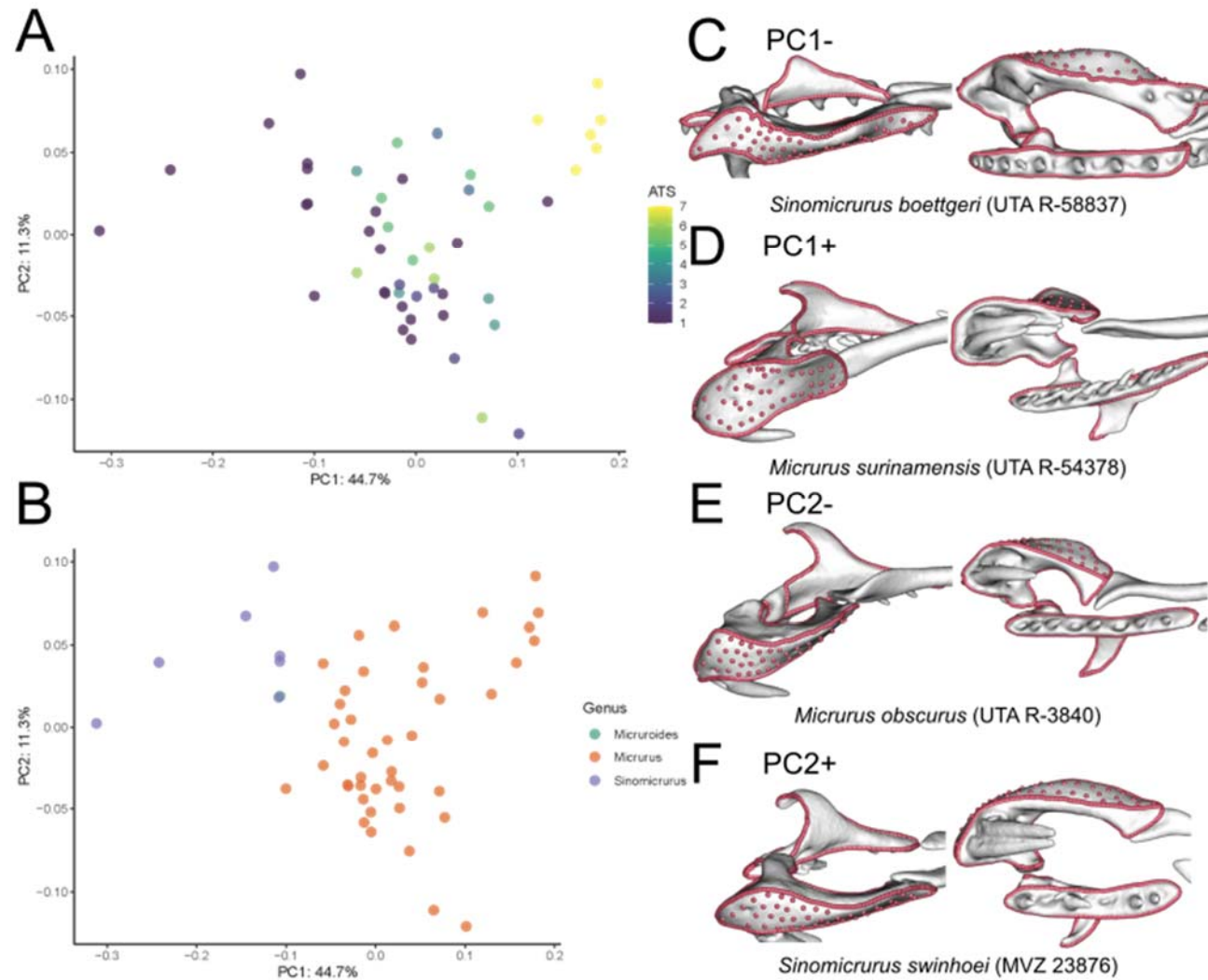


Figure 3.41. PCA of the maxilla and palatine module conducted on the coralsnake subset, colored by ATS (A) and genus (B). Images of the maxilla and palatine of specimens at the extremes of PC1 (C-D) and PC2 (E-F) in anterolateral (left) and ventral (right) views.

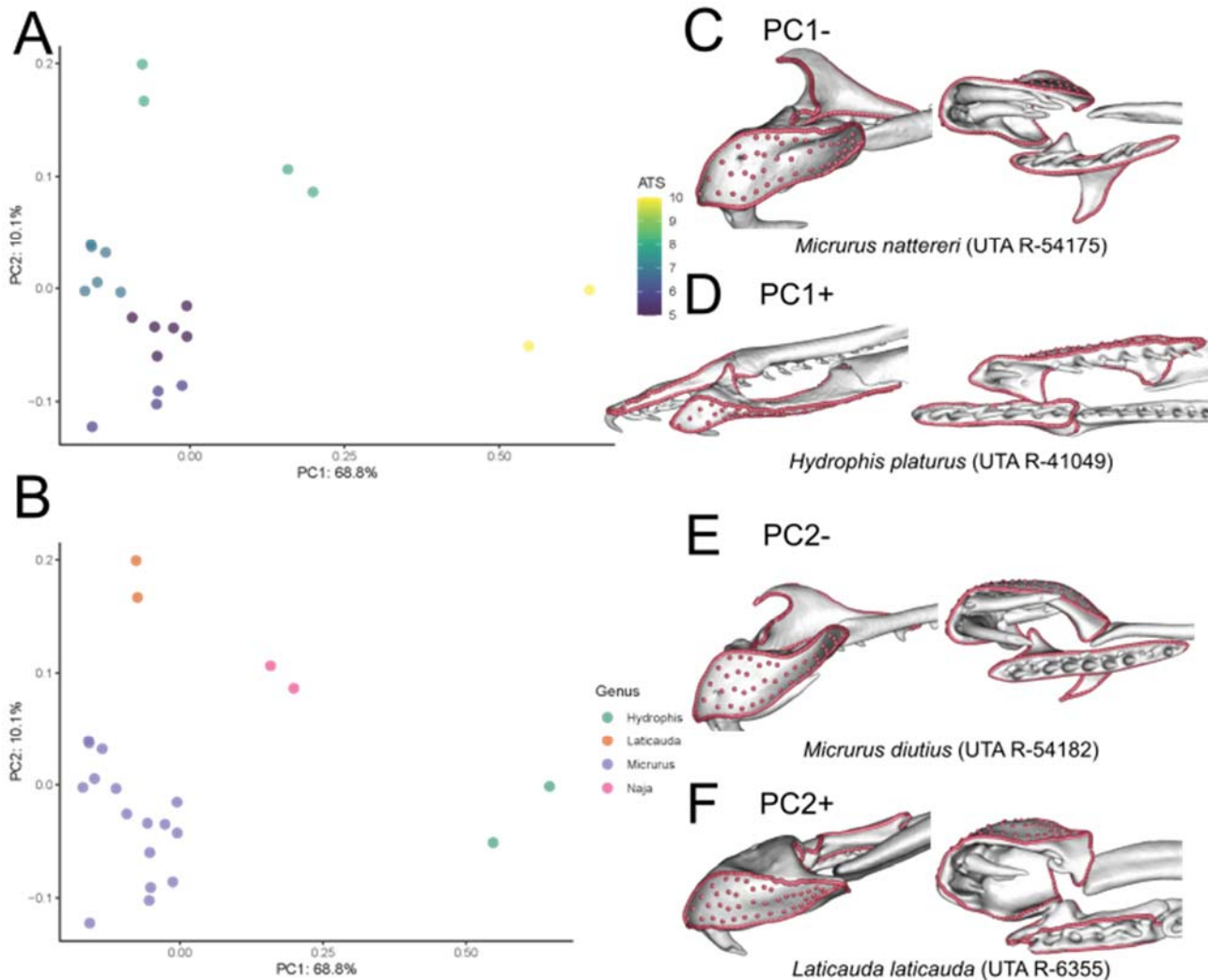


Figure 3.42. PCA of the maxilla and palatine module conducted on the semi-aquatic and aquatic subset (>5 ATS), colored by ATS (A) and genus (B). Images of specimens at the extremes of PC1 (C-D) and PC2 (E-F) in anterolateral (left) and ventral (right) views.

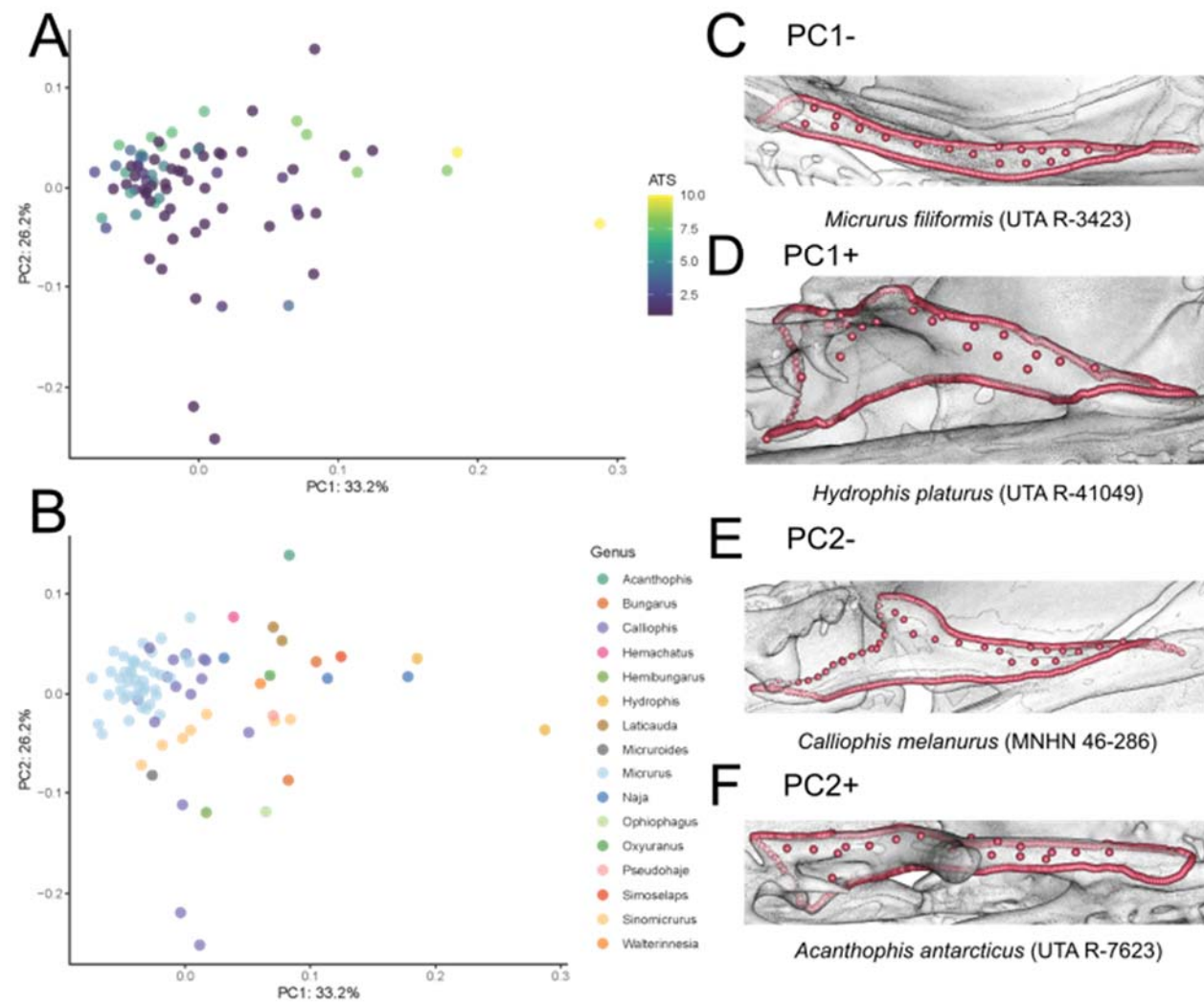


Figure 3.43. PCA of the ectopterygoid module, utilizing all specimens, colored by ATS (A) and genus (B). Images of the ectopterygoid of specimens at the extremes of PC1 (C-D) and PC2 (E-F) in ventral view.

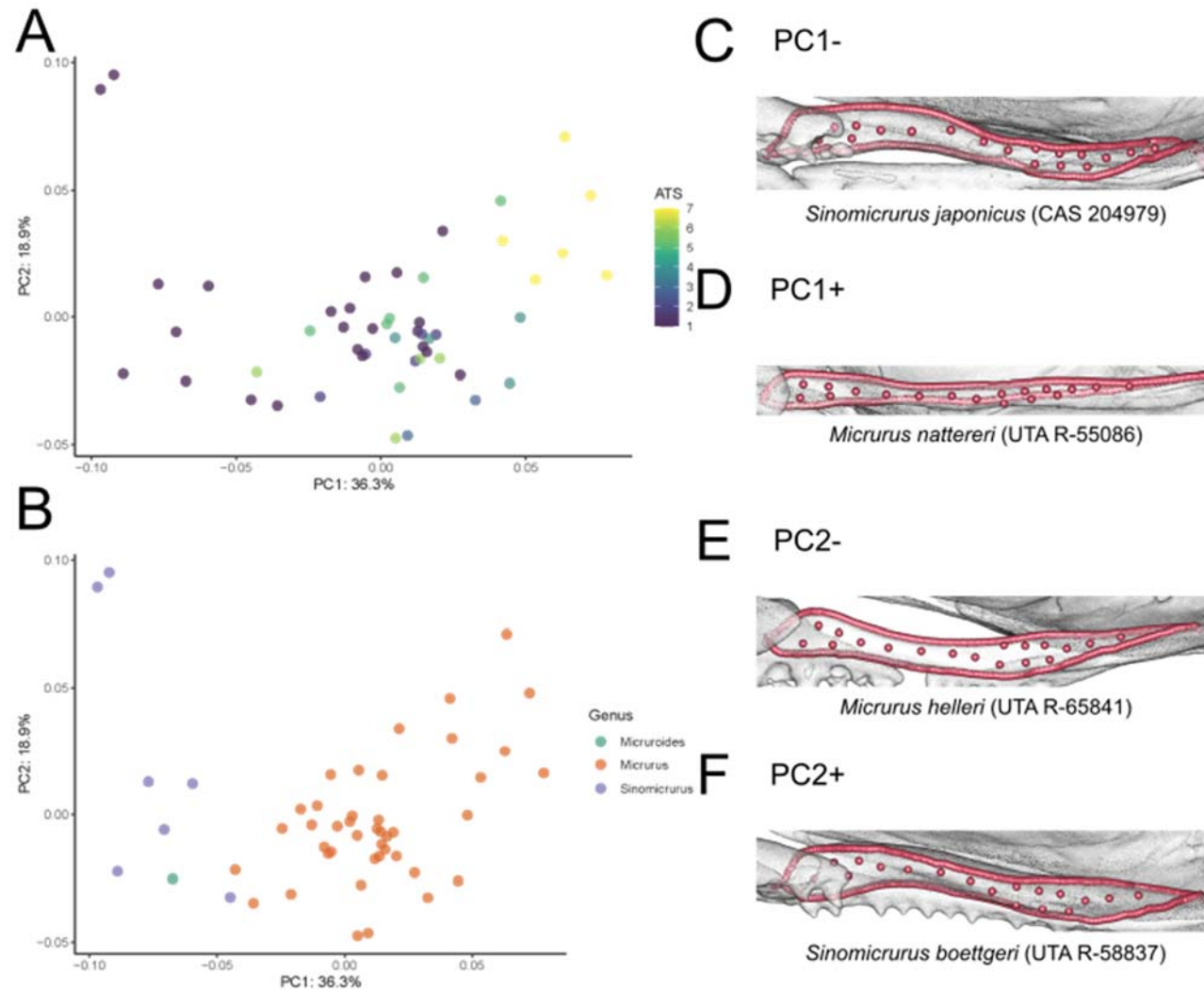


Figure 3.44. PCA of the ectopterygoid module conducted on the coralsnake subset, colored by ATS (A) and genus (B). Images of the ectopterygoid of specimens at the extremes of PC1 (C-D) and PC2 (E-F) in ventral view.

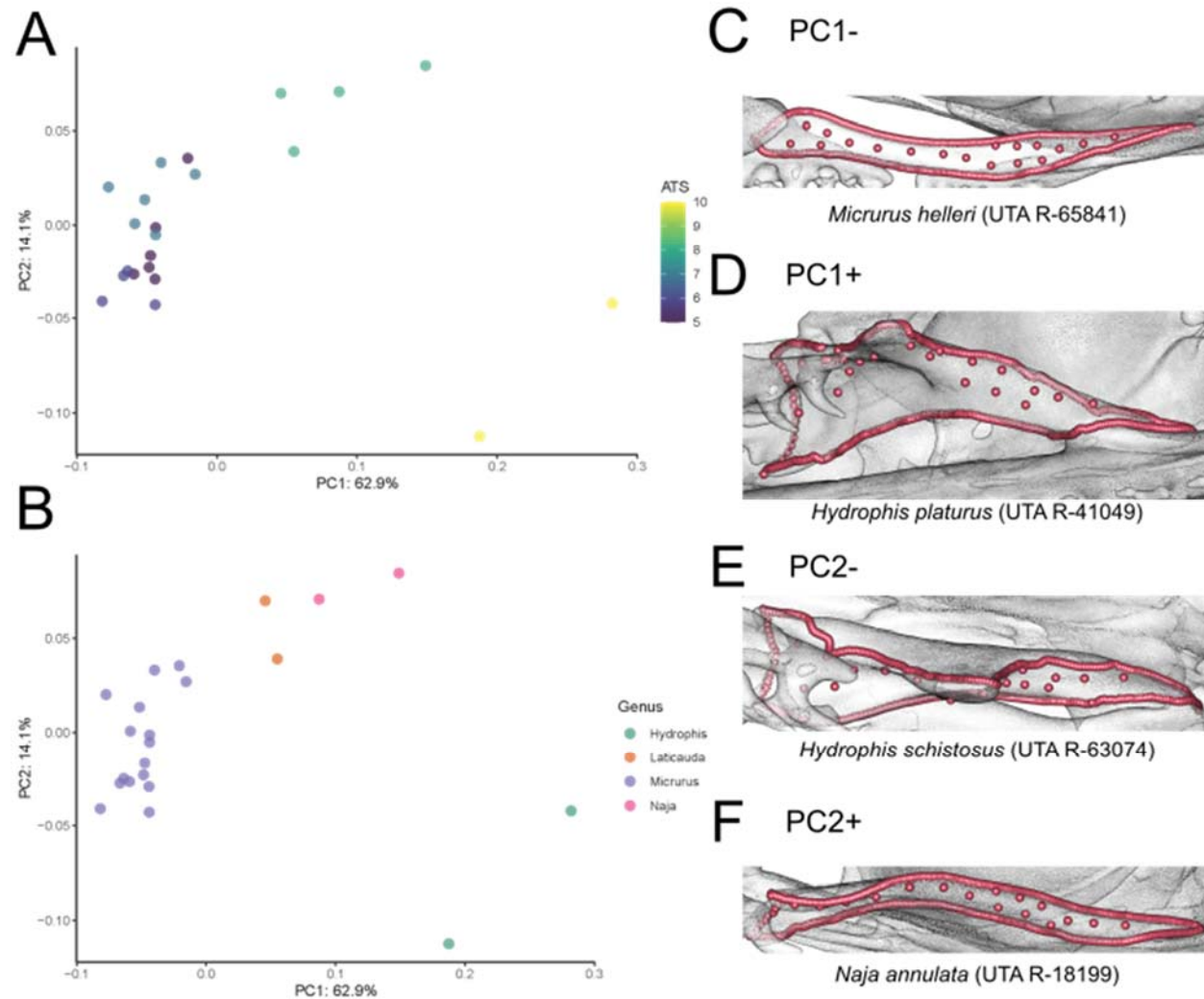


Figure 3.45. PCA of the ectopterygoid module conducted on the semi-aquatic and aquatic subset (>5 ATS), colored by ATS (A) and genus (B). Images of the ectopterygoid of specimens at the extremes of PC1 (C-D) and PC2 (E-F) in ventrolateral view.

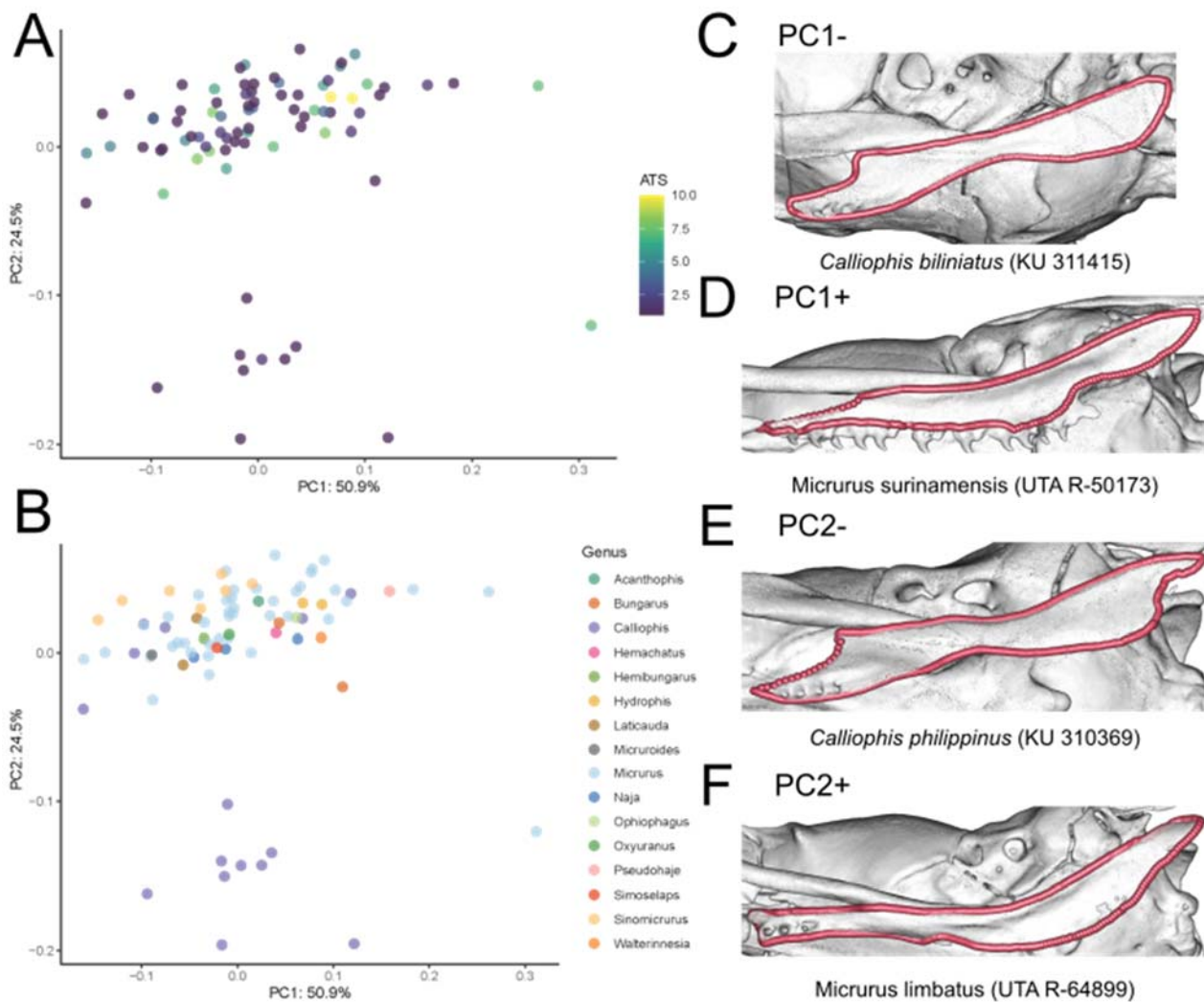


Figure 3.46. PCA of the pterygoid module utilizing all specimens, colored by ATS (A) and genus (B). Images of the pterygoid of specimens at the extremes of PC1 (C-D) and PC2 (E-F) in ventral view.

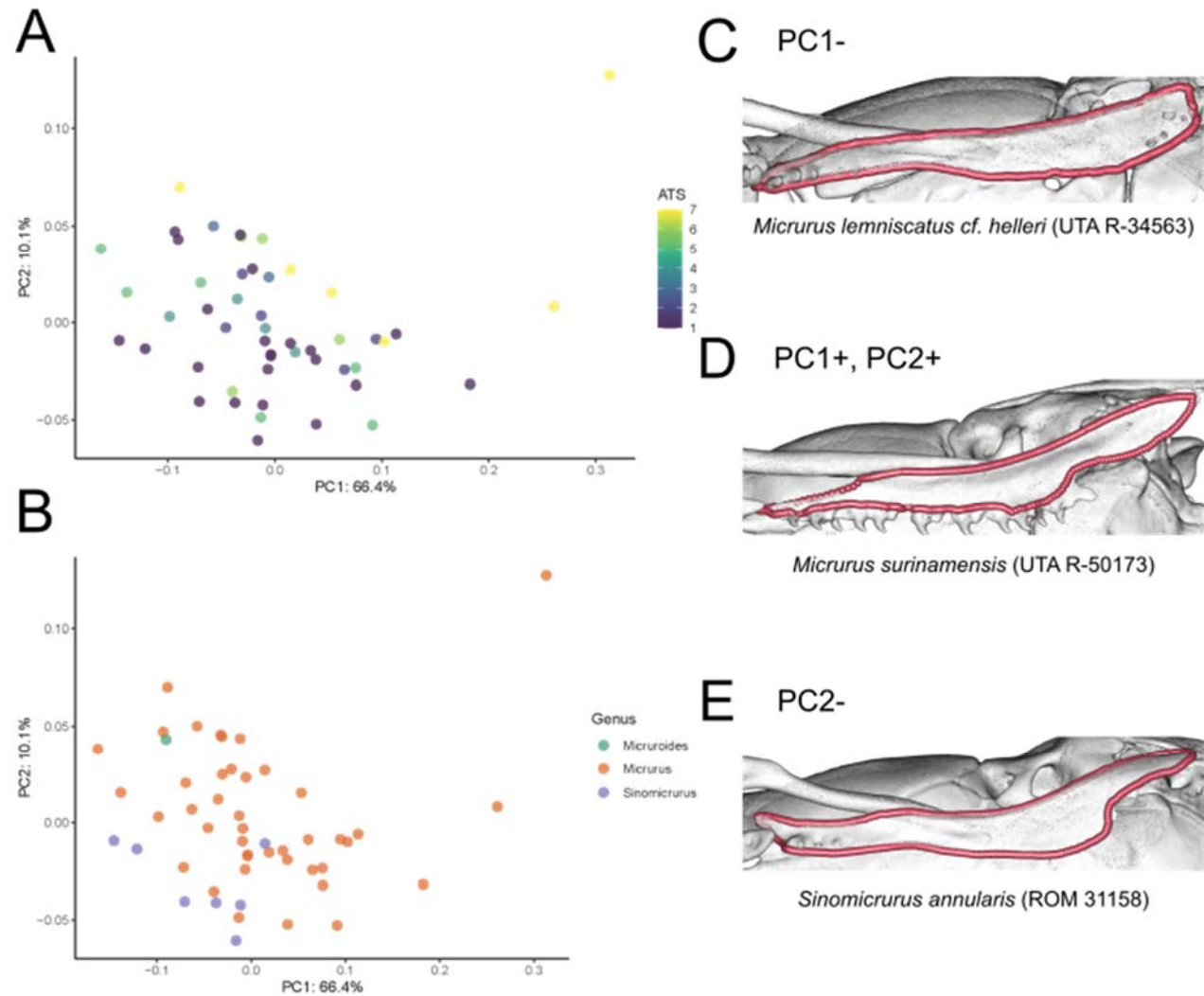


Figure 3.47. PCA of the pterygoid module conducted on the coralsnake subset, colored by ATS (A) and genus (B). Images of the pterygoid of specimens at the PC1 minimum (C) and PC2 minimum (E) and PC1 and PC2 maxima (D).

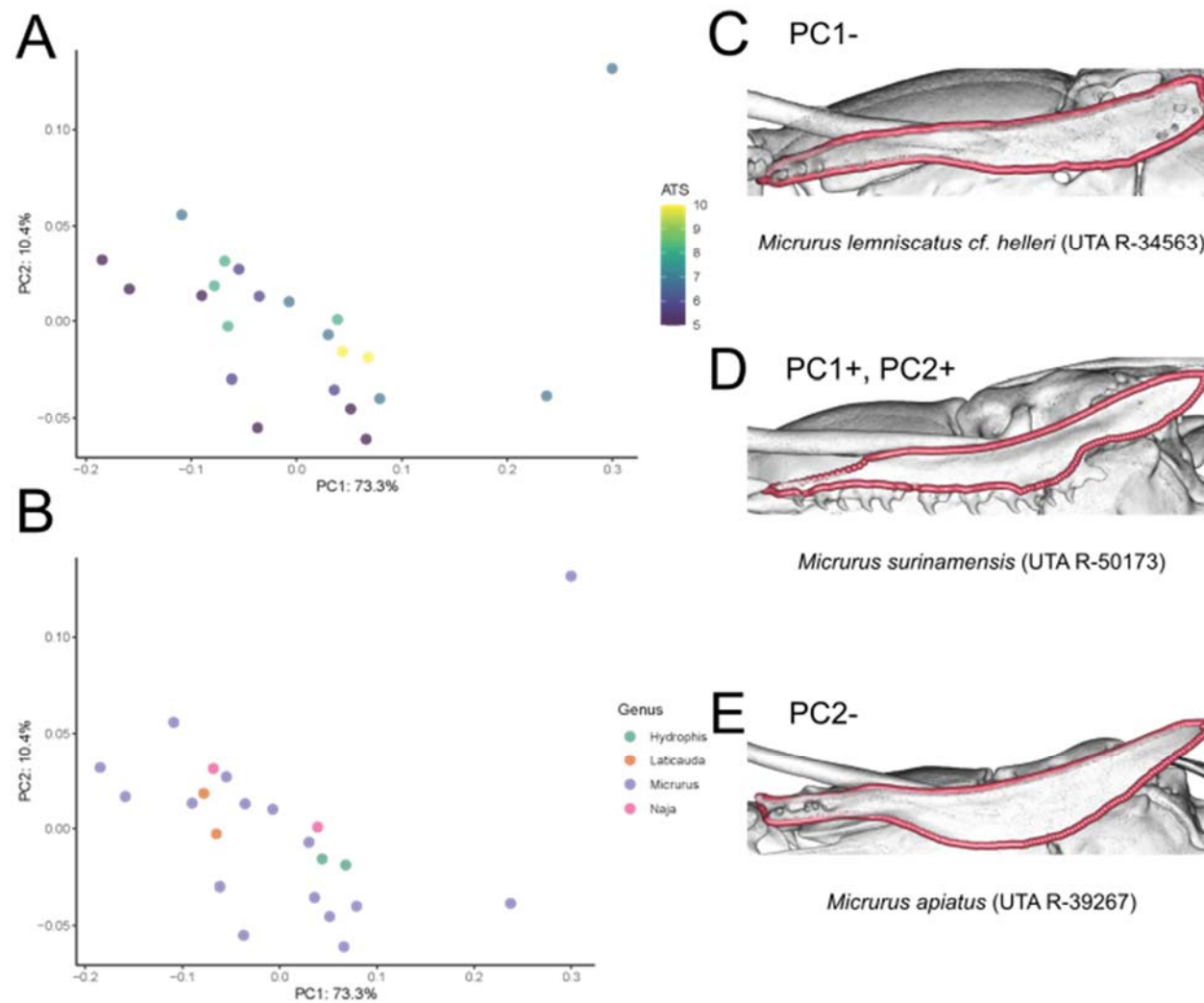


Figure 3.48. PCA of the pterygoid module conducted on the semi-aquatic and aquatic subset (>5 ATS), colored by ATS (A) and genus (B). Images of the pterygoid of specimens at the PC1 minimum (C) and PC2 minimum (E) and PC1 and PC2 maxima (D).

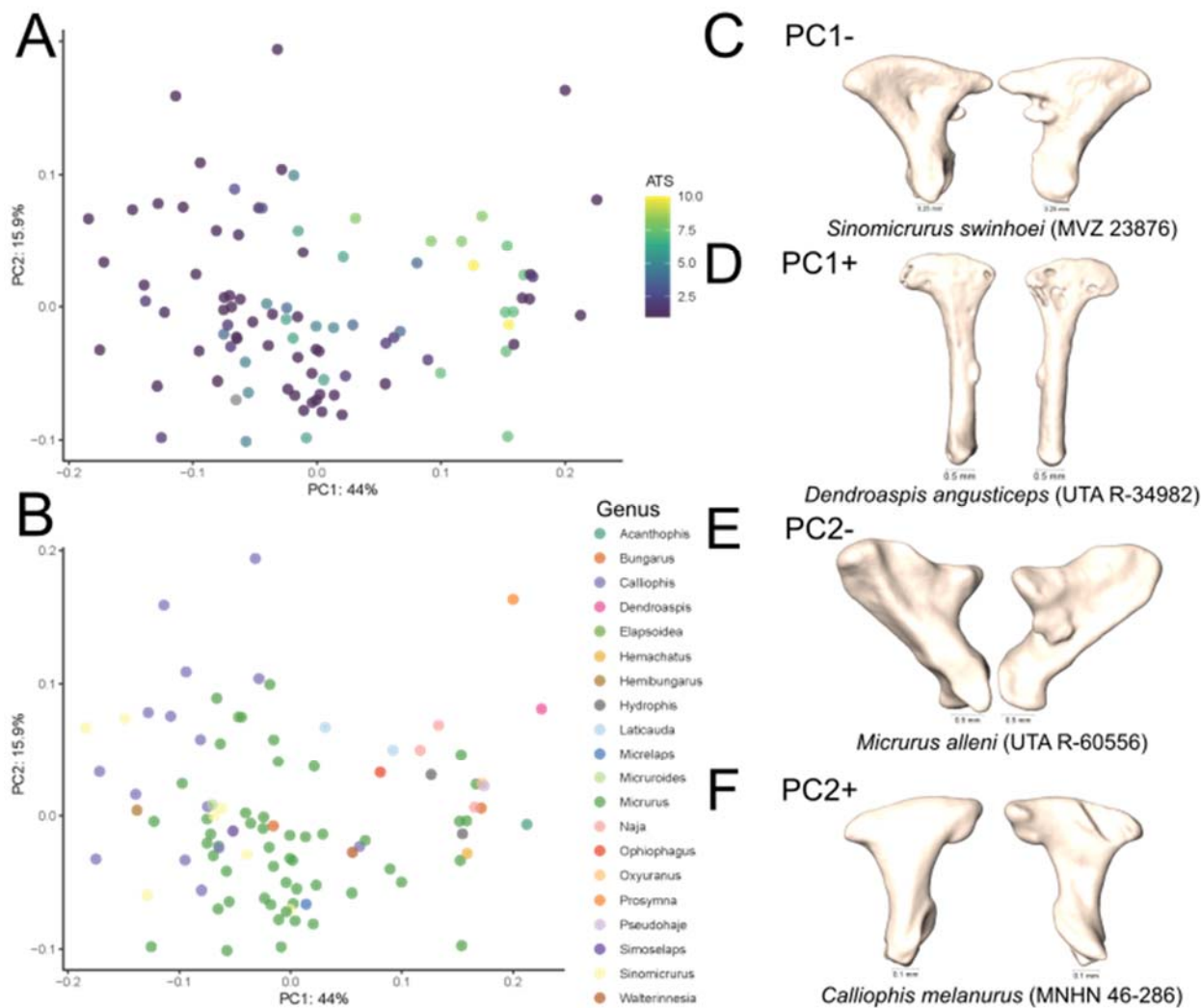


Figure 3.49. PCA of the quadrate dataset utilizing all specimens, colored by ATS (A) and genus (B). Images of the quadrate of specimens at the extremes of PC1 (C-D) and PC2 (E-F) in lateral (left) and medial (right) view.

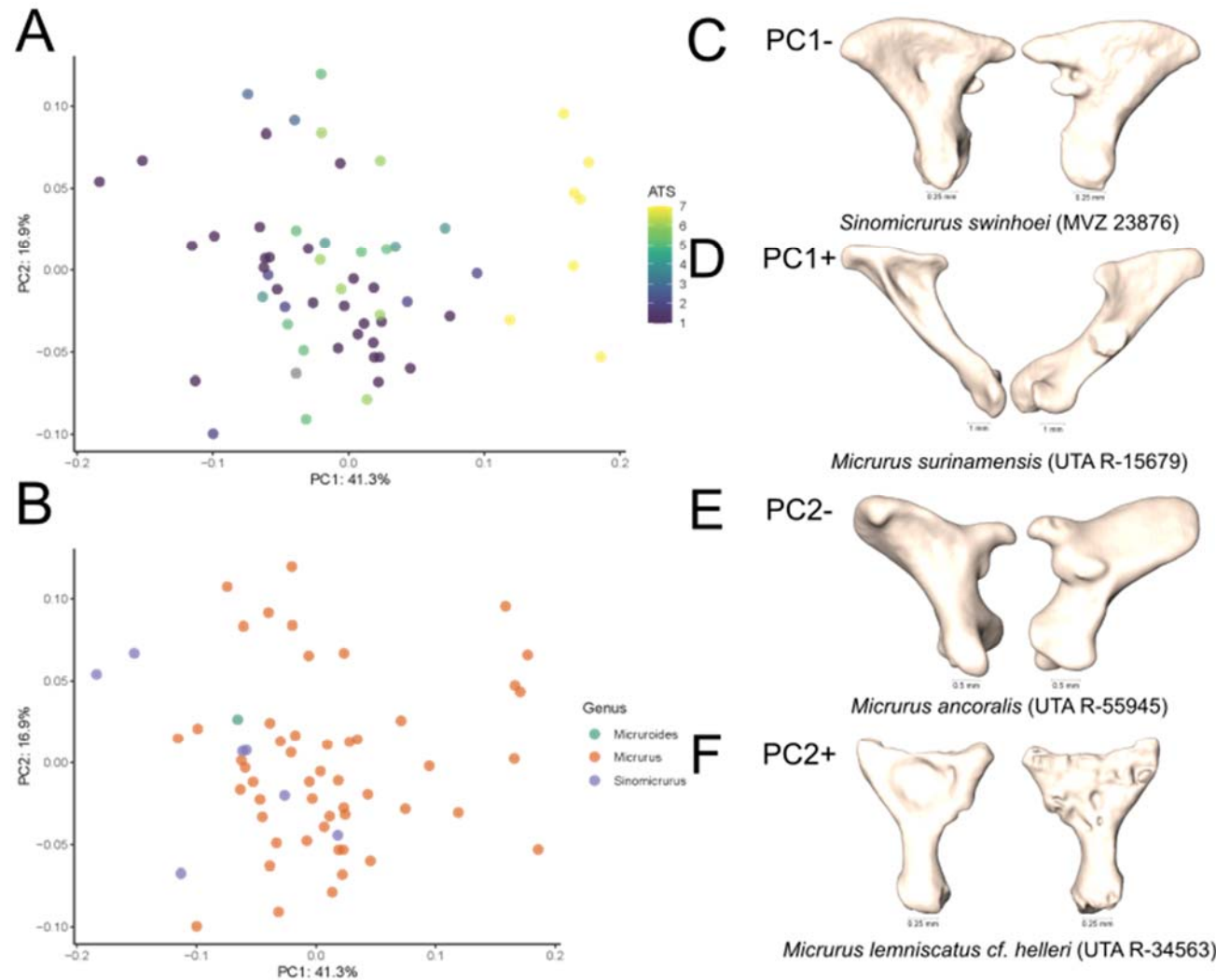


Figure 3.50. PCA of the quadrate dataset conducted on the coralsnake subset, colored by ATS (A) and genus (B). Images of the quadrate of specimens at the extremes of PC1 (C-D) and PC2 (E-F) in lateral (left) and medial (right) view.

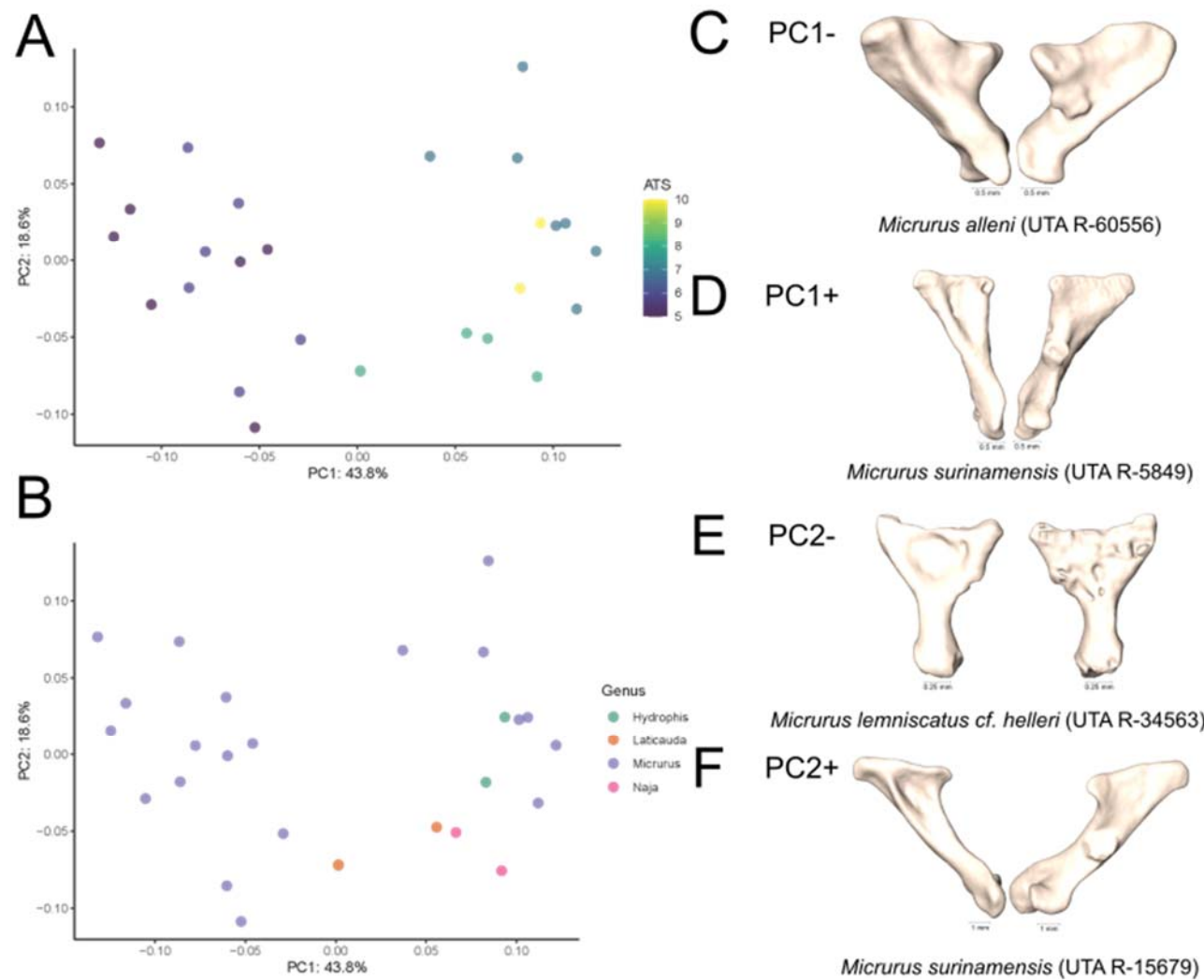


Figure 3.51. PCA of the quadrate dataset conducted on the semi-aquatic and aquatic subset (>5 ATS), colored by ATS (A) and genus (B). Images of the quadrate of specimens at the extremes of PC1 (C-D) and PC2 (E-F) in lateral (left) and medial (right) view.

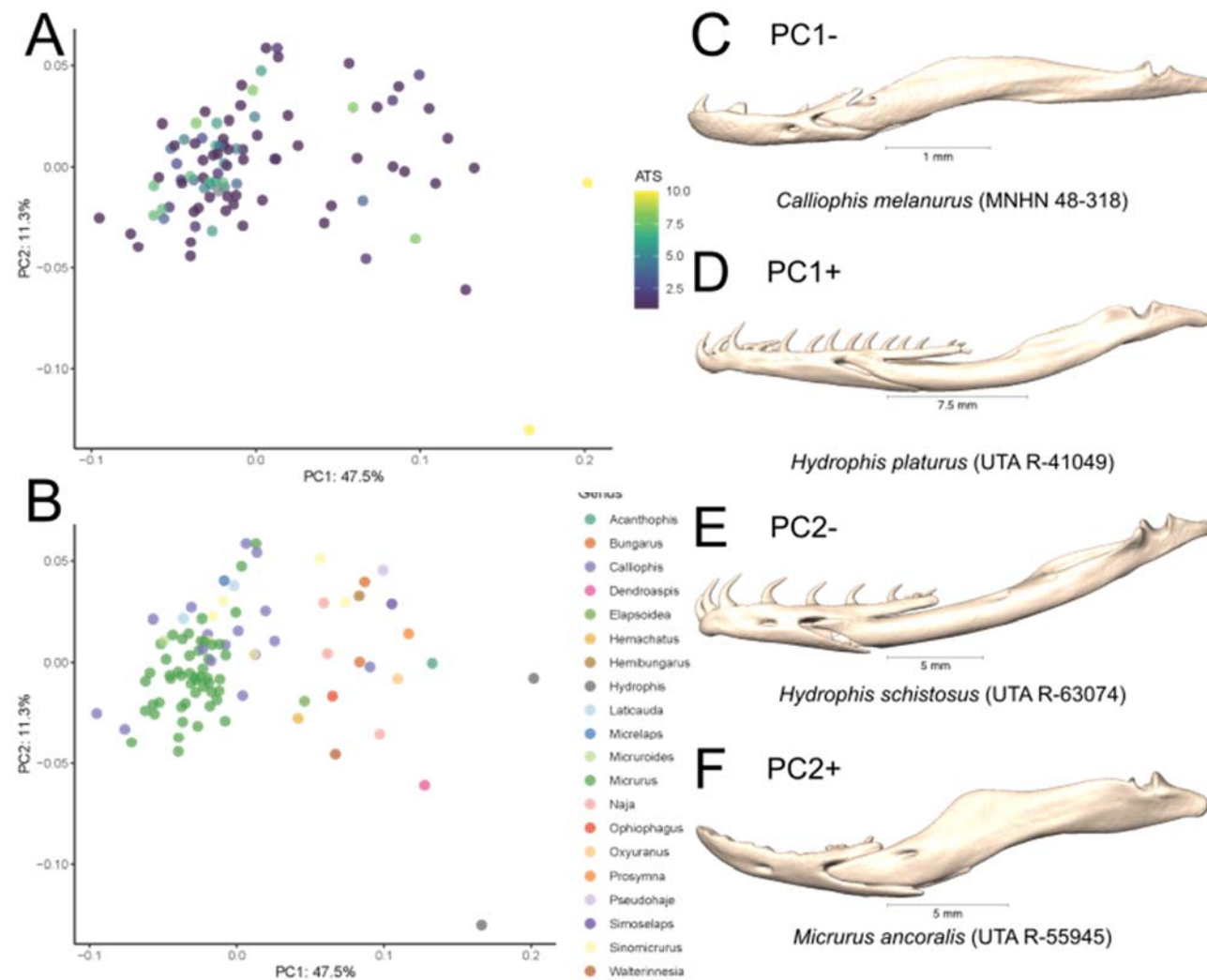


Figure 3.52. PCA of the jaw utilizing all specimens, colored by ATS (A) and genus (B). Images of the jaw of specimens at the extremes of PC1 (C-D) and PC2 (E-F) in lateral view.

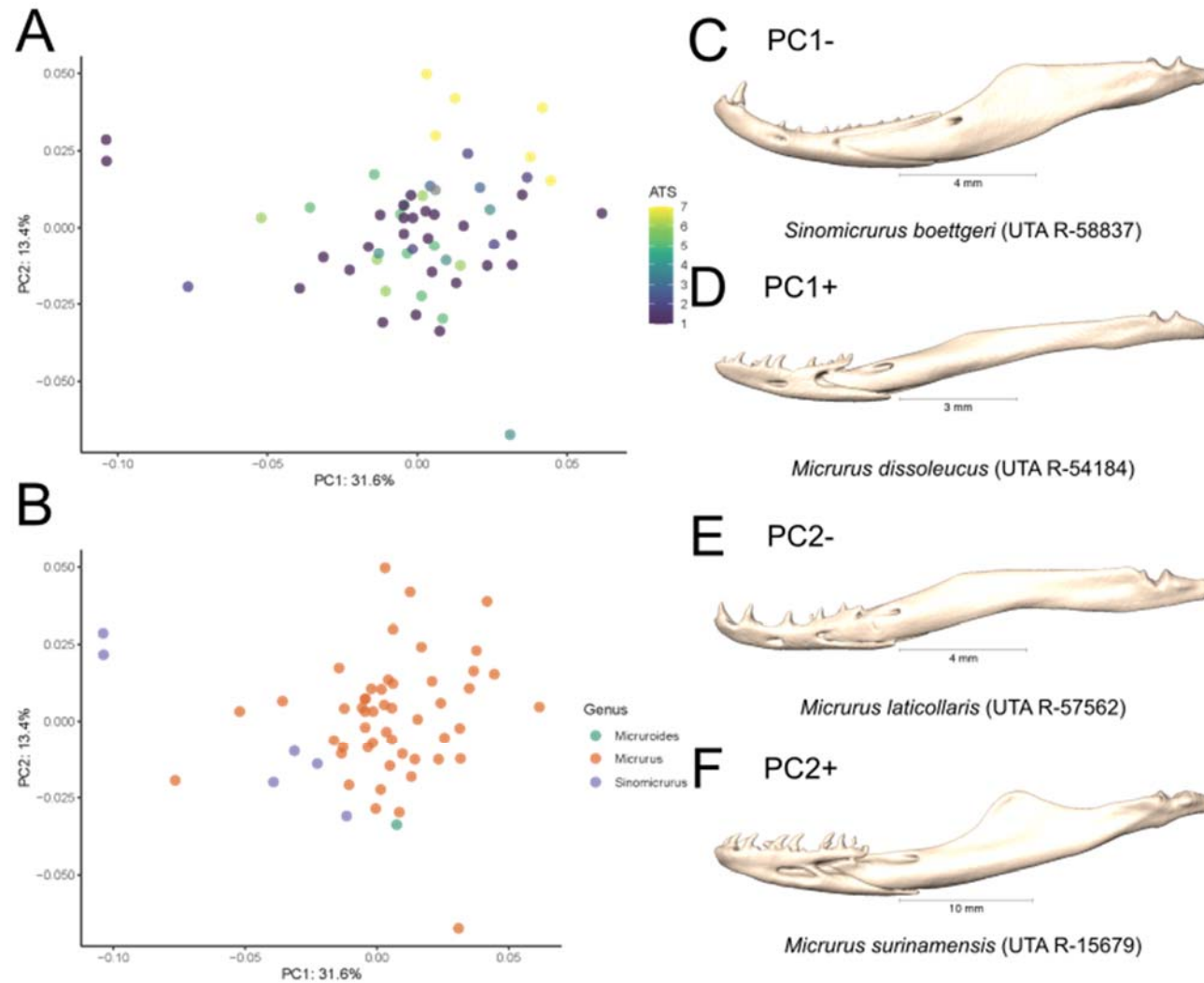


Figure 3.53. PCA of the jaw conducted on the coralsnake subset, colored by ATS (A) and genus (B). Images of the jaw of specimens at the extremes of PC1 (C-D) and PC2 (E-F) in lateral view.

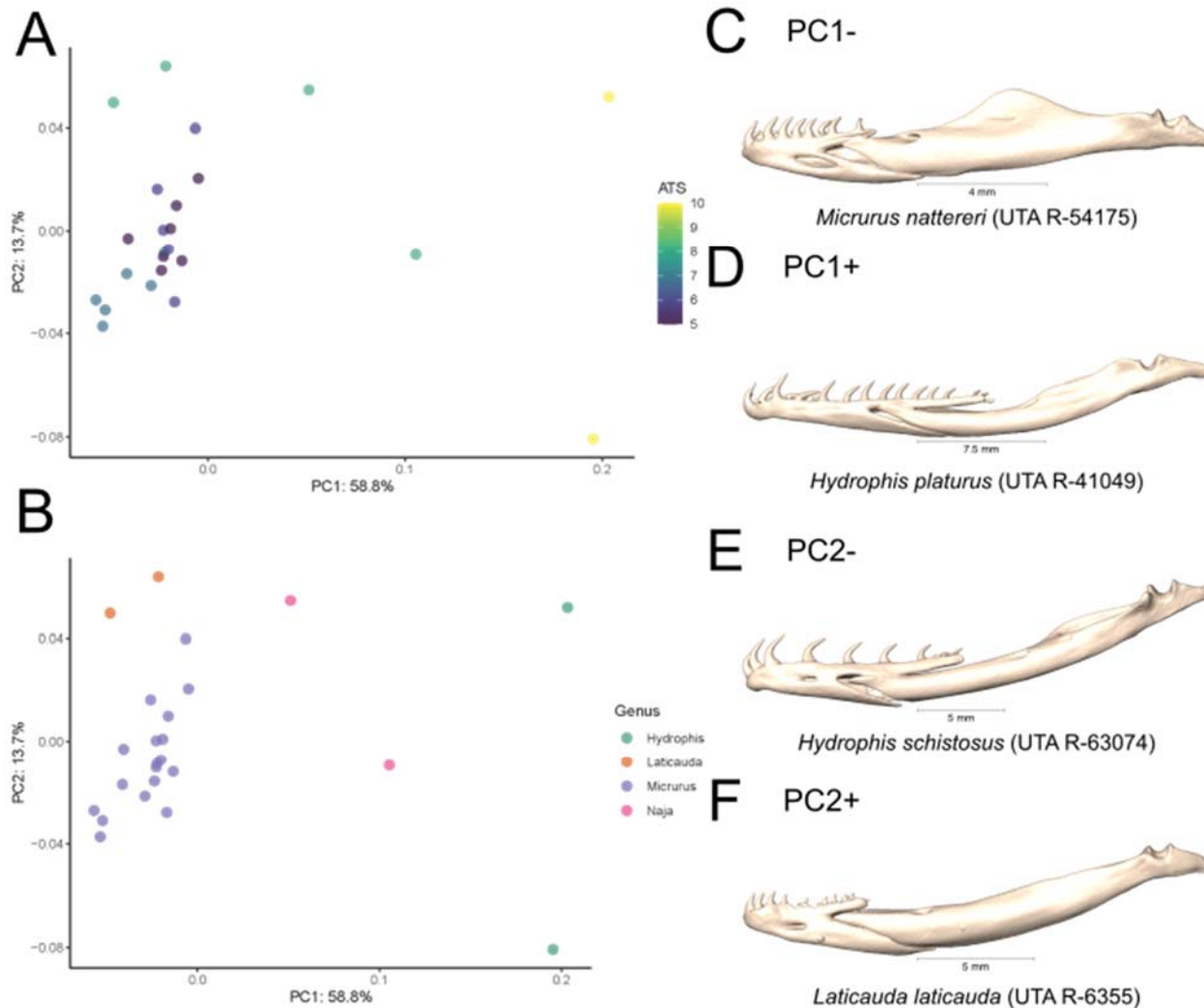


Figure 3.54. PCA of the jaw conducted on the semi-aquatic and aquatic subset (>5 ATS), colored by ATS (A) and genus (B). Images of the jaw of specimens at the extremes of PC1 (C-D) and PC2 (E-F) in lateral view.

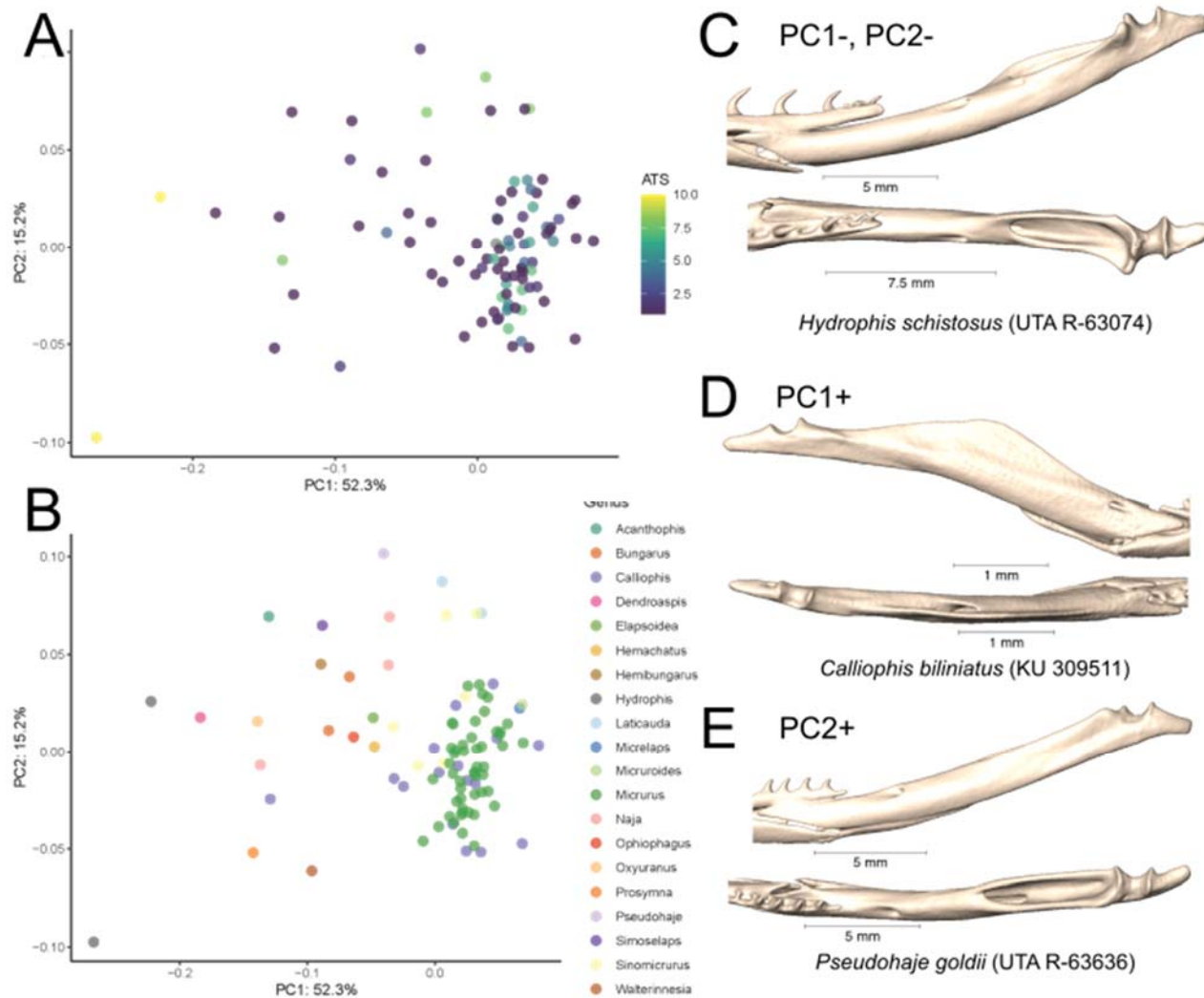


Figure 3.55. PCA of the compound module utilizing all specimens, colored by ATS (A) and genus (B). Images of the compound of specimens at the extremes of PC1 (C-D) and PC2 minimum (C) and maximum (E) in lateral (top) and dorsal (bottom) views.

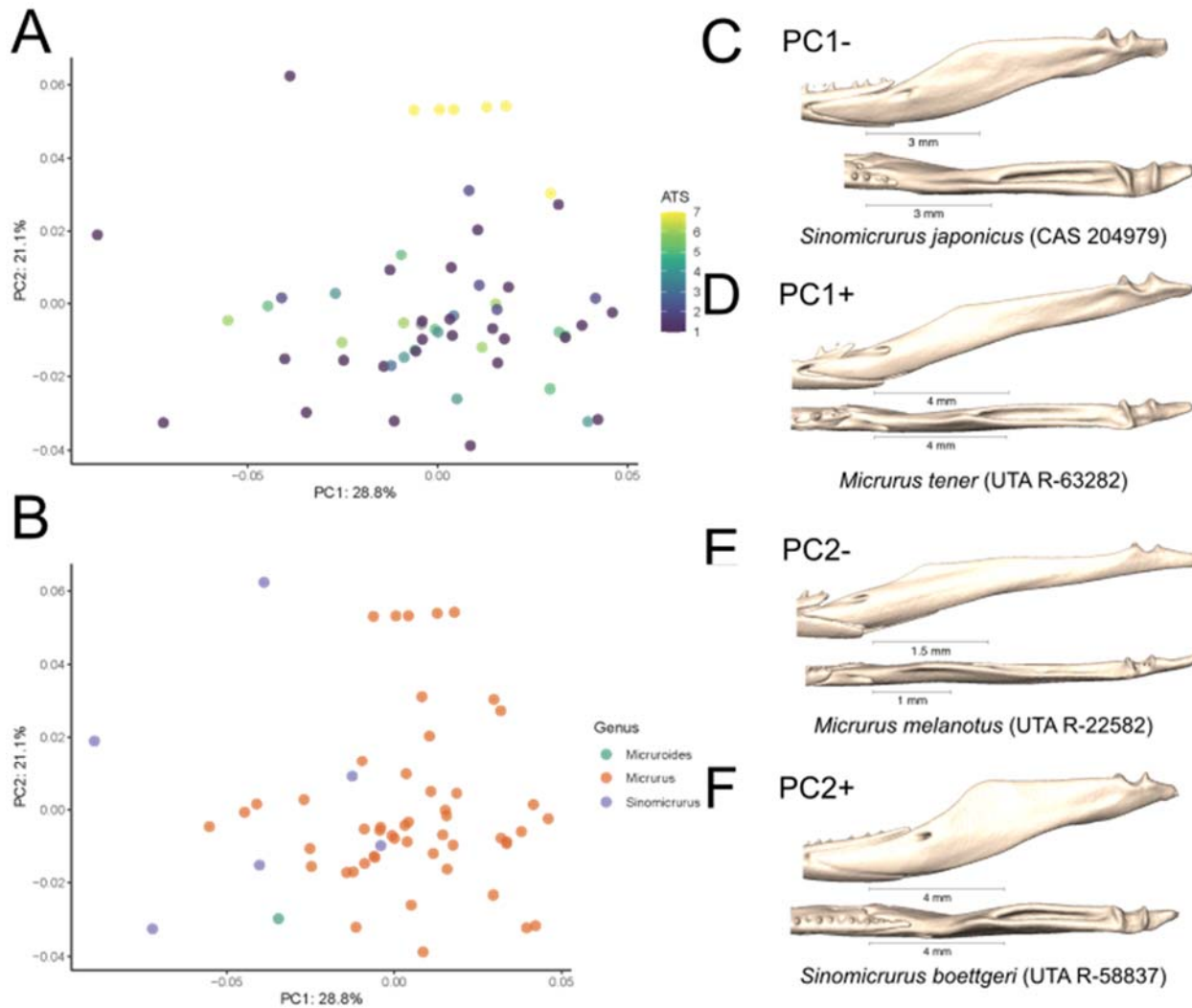


Figure 3.56. PCA of the compound module conducted on the coralsnake subset, colored by ATS (A) and genus (B). Images of the compound of specimens at the extremes of PC1 (C-D) and PC2 (E-F) in lateral (top) and dorsal (bottom) views.

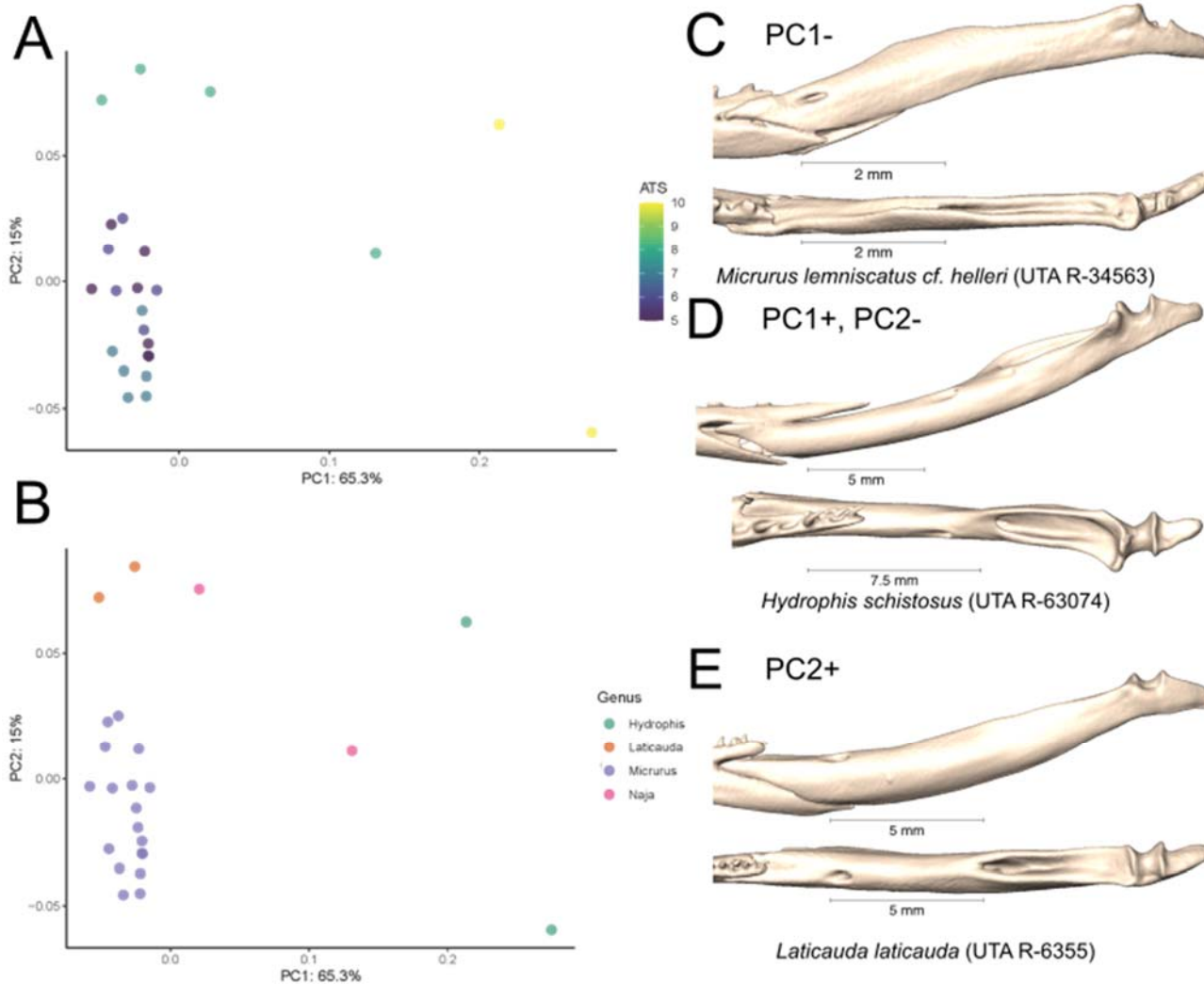


Figure 3.57. PCA of the compound module conducted on the semi-aquatic and aquatic subset (>5 ATS), colored by ATS (A) and genus (B). Images 5 of specimens at the extremes of PC1 (C-D) and PC2 (D-E) in lateral (top) and dorsal (bottom) views.

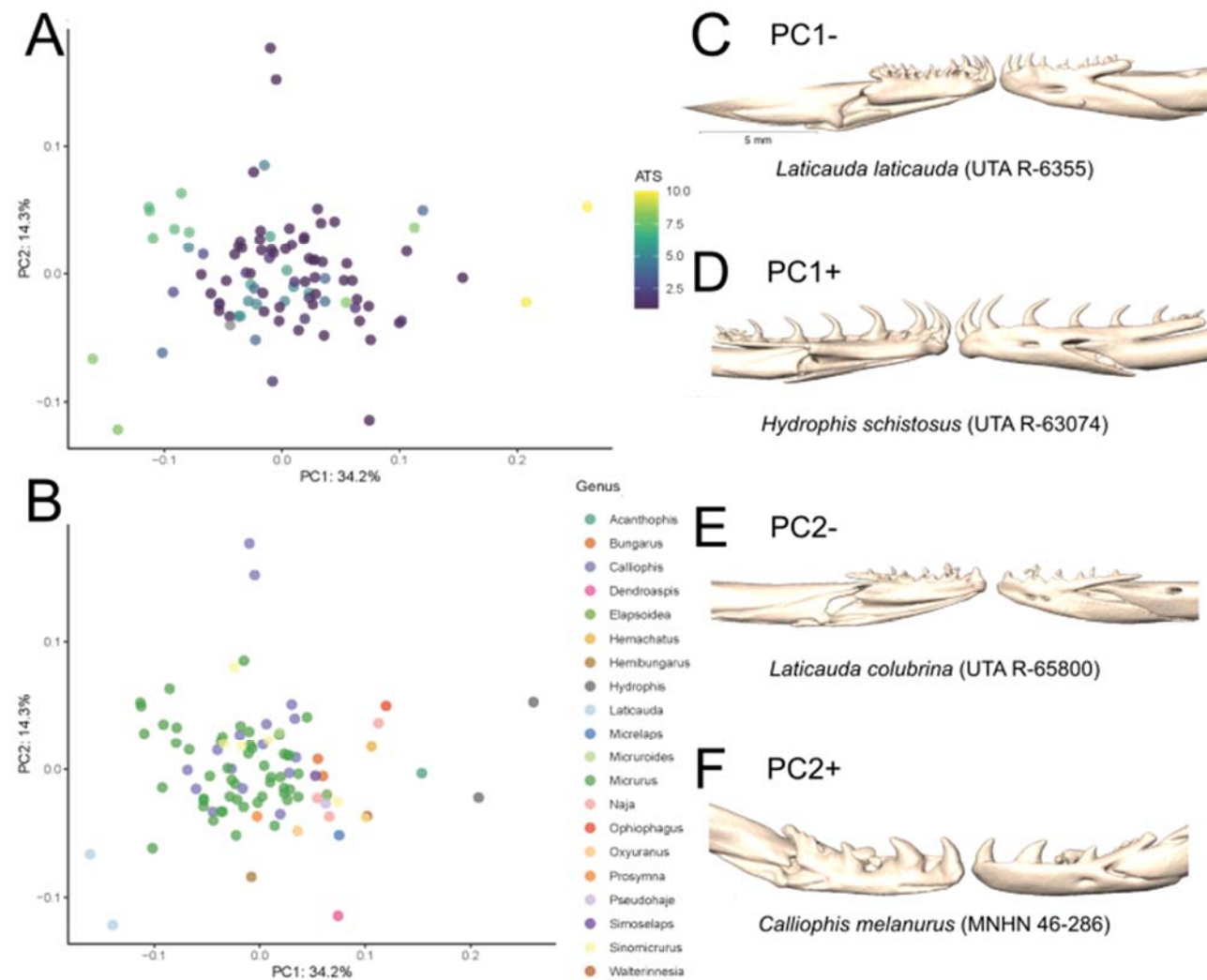


Figure 3.58. PCA of the dentary, angular, and splenial module utilizing all specimens, colored by ATS (A) and genus (B). Images of the dentary, angular, and splenial of specimens at the extremes of PC1 (C-D) and PC2 (E-F) in medial (left) and lateral (right) views.

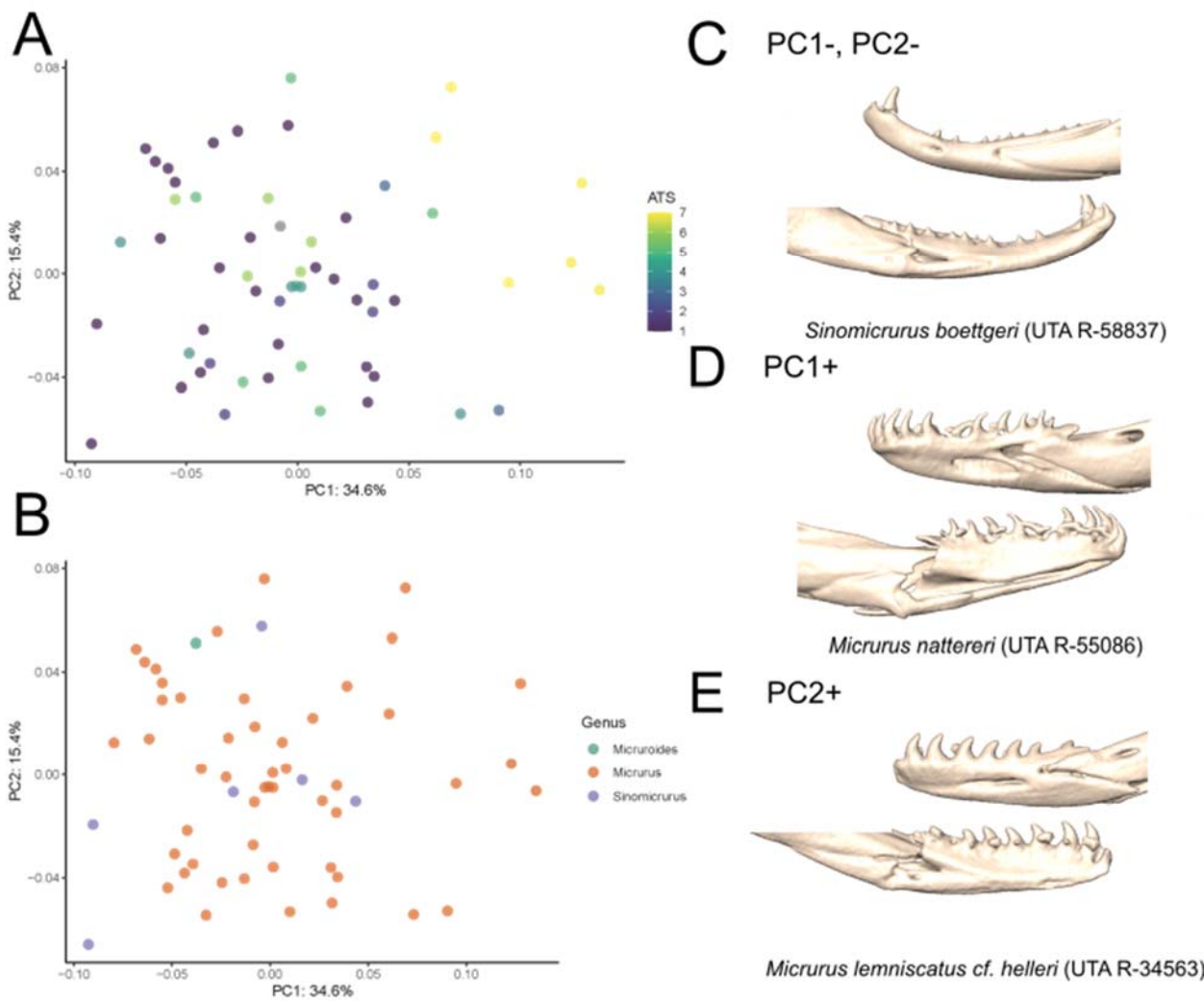


Figure 3.59. PCA of the dentary, angular, and splenial module conducted on the coralsnake subset, colored by ATS (A) and genus (B).

Images of specimens at the extremes of PC1 (C-D) and PC2 (C, E) in medial (left) and lateral (right) views.

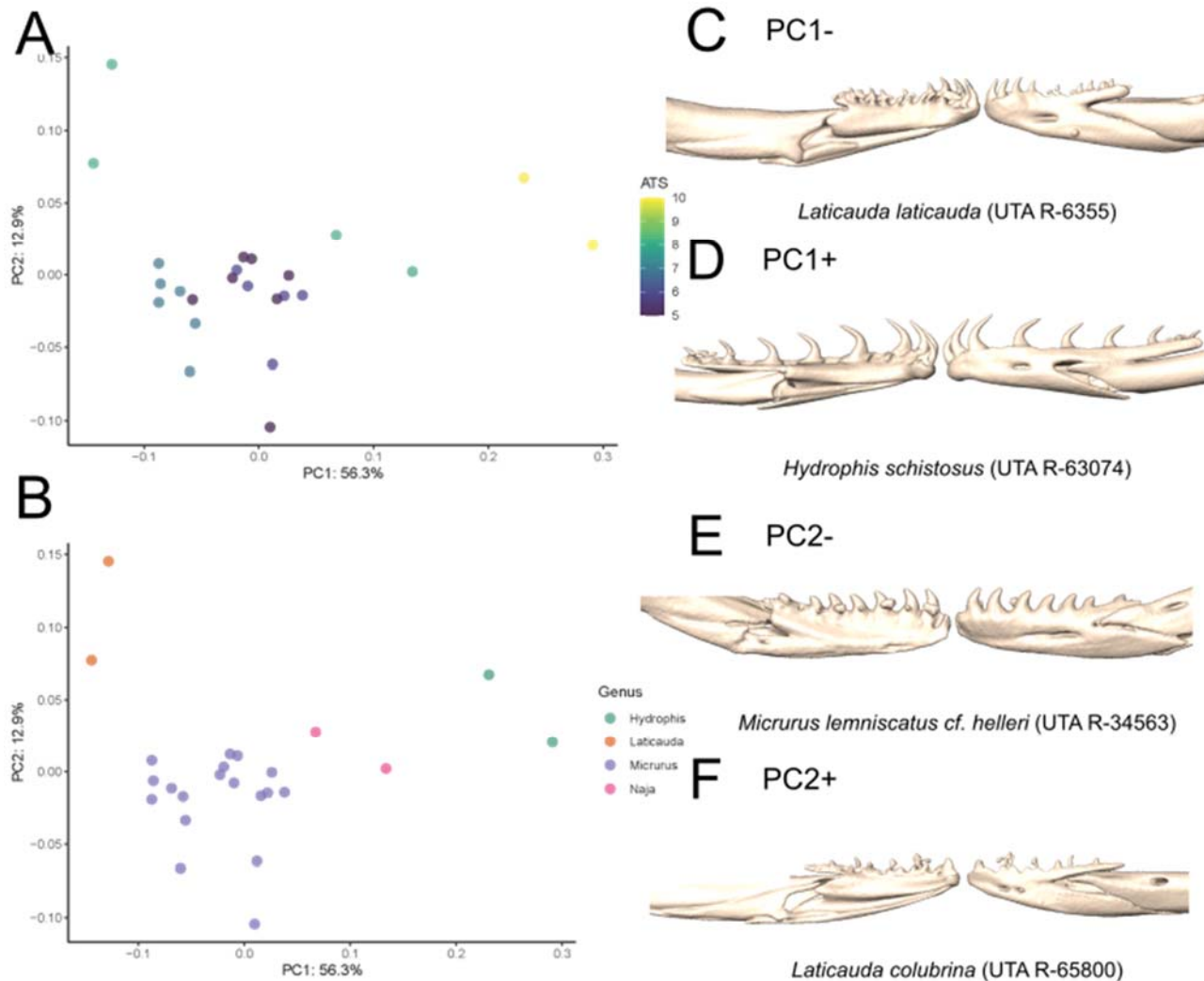


Figure 3.60. PCA of the dentary, angular, and splenial module conducted on the semi-aquatic and aquatic subset (>5 ATS), colored by ATS (A) and genus (B). Images of specimens at the extremes of PC1 (C-D) and PC2 (E-F) in medial (left) and lateral (right) views.

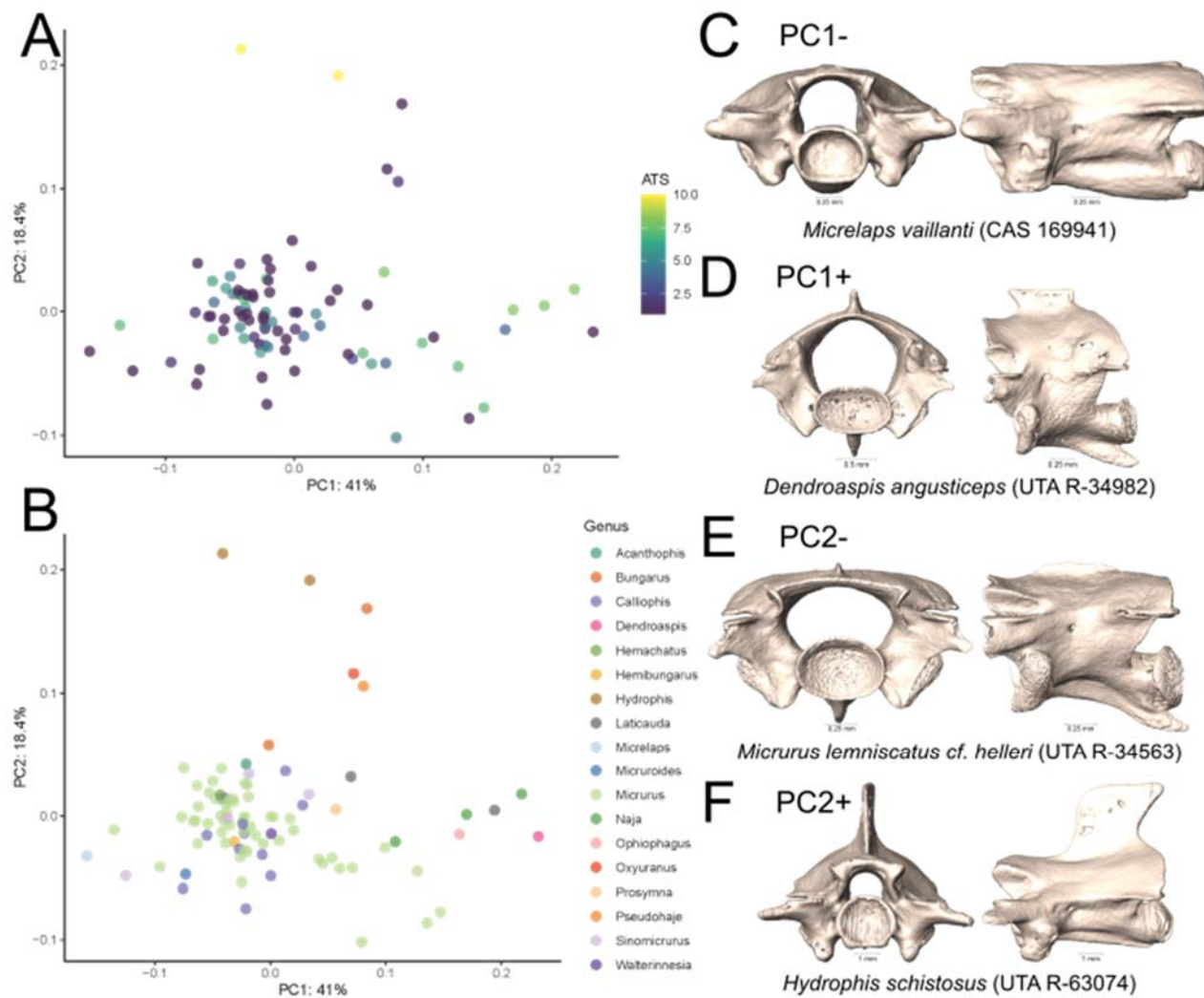


Figure 3.61. PCA of the midbody vertebra dataset, utilizing all specimens, colored by ATS (A) and genus (B). Images of the midbody vertebra of specimens at the extremes of PC1 (C-D) and PC2 (E-F) in the anterior (left) and lateral (right) views.

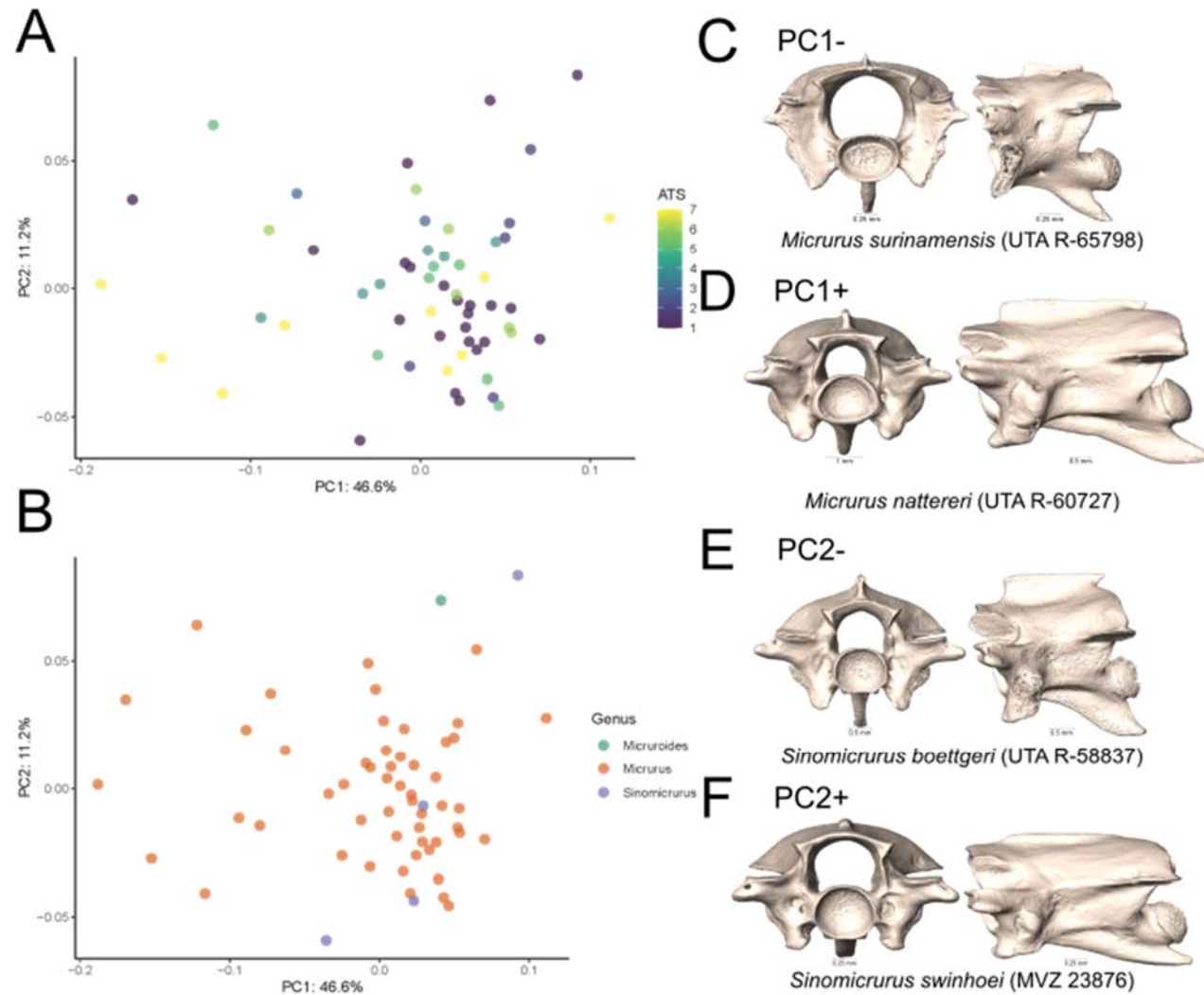


Figure 3.62. PCA of the midbody vertebra dataset conducted on the coralsnake subset, colored by ATS (A) and genus (B). Images of the midbody vertebra of specimens at the extremes of PC1 (C-D) and PC2 (E-F) in the anterior (left) and lateral (right) views.

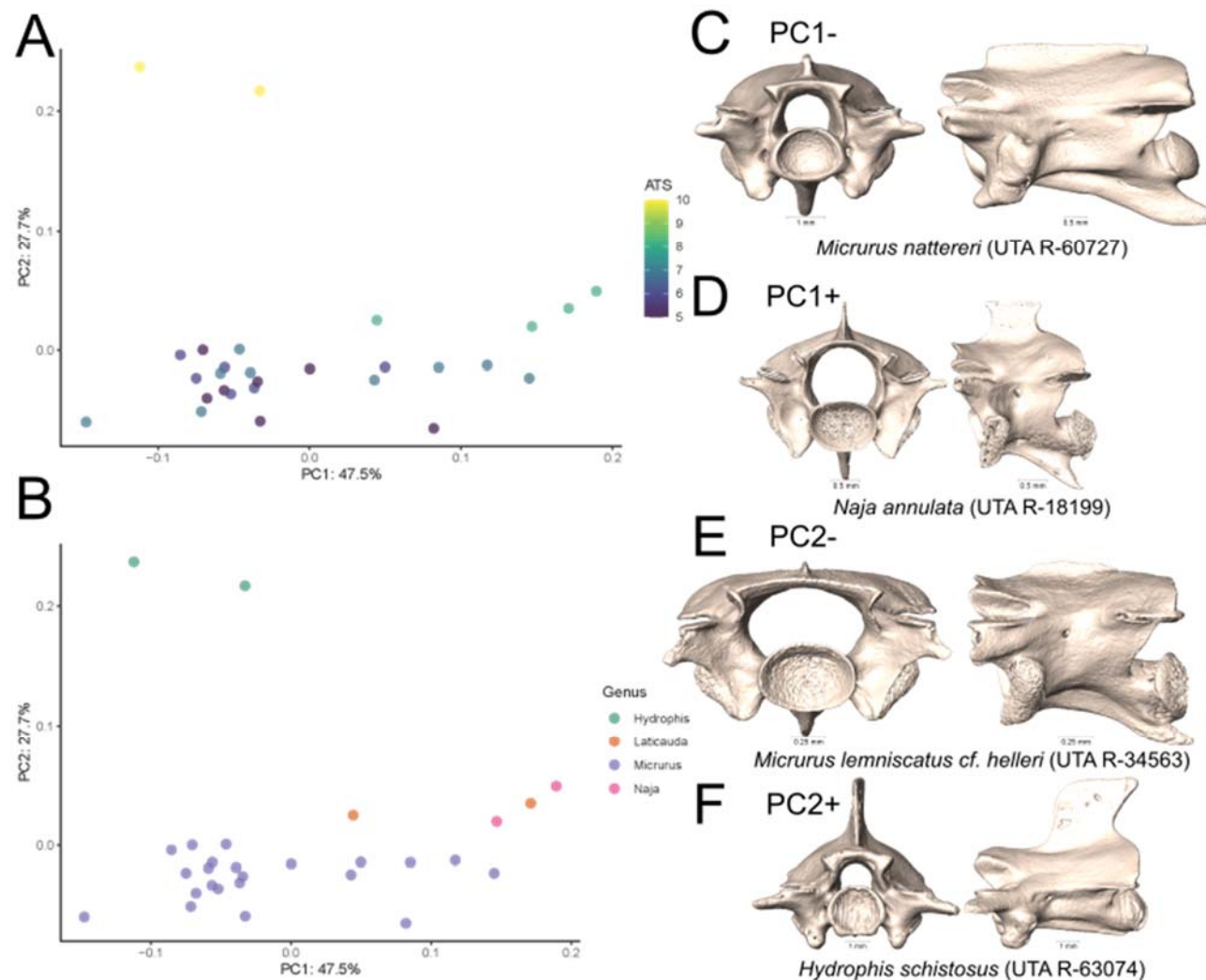


Figure 3.63. PCA of the midbody vertebra dataset conducted on the semi-aquatic and aquatic subset (>5 ATS), colored by ATS (A) and genus (B). Images at the extremes of PC1 (C-D) and PC2 (E-F) in the anterior (left) and lateral (right) views.

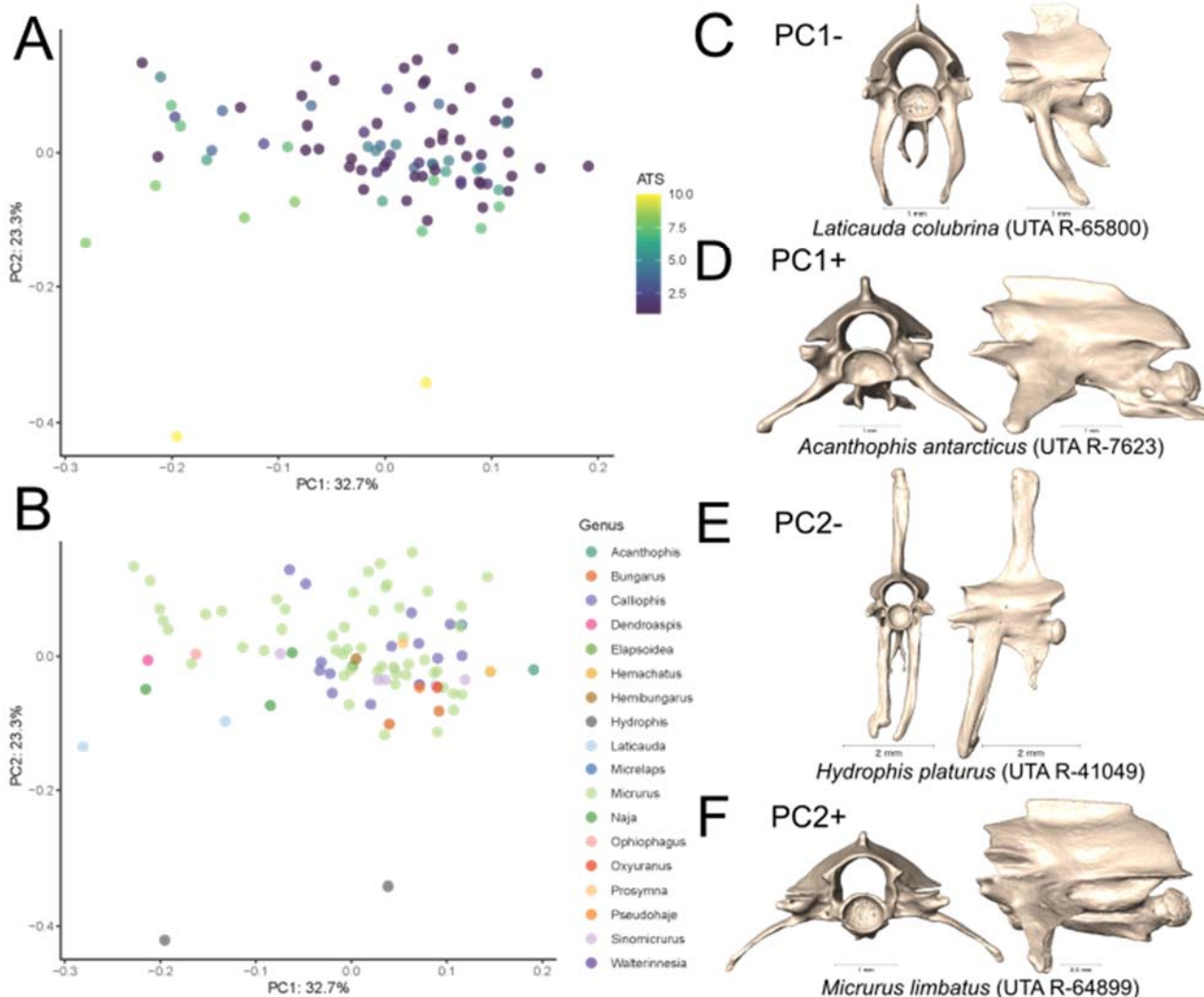


Figure 3.64. PCA of the caudal vertebra dataset, utilizing all specimens, colored by ATS (A) and genus (B). Images of the midbody vertebra of specimens at the extremes of PC1 (C-D) and PC2 (E-F) in the anterior (left) and lateral (right) views.

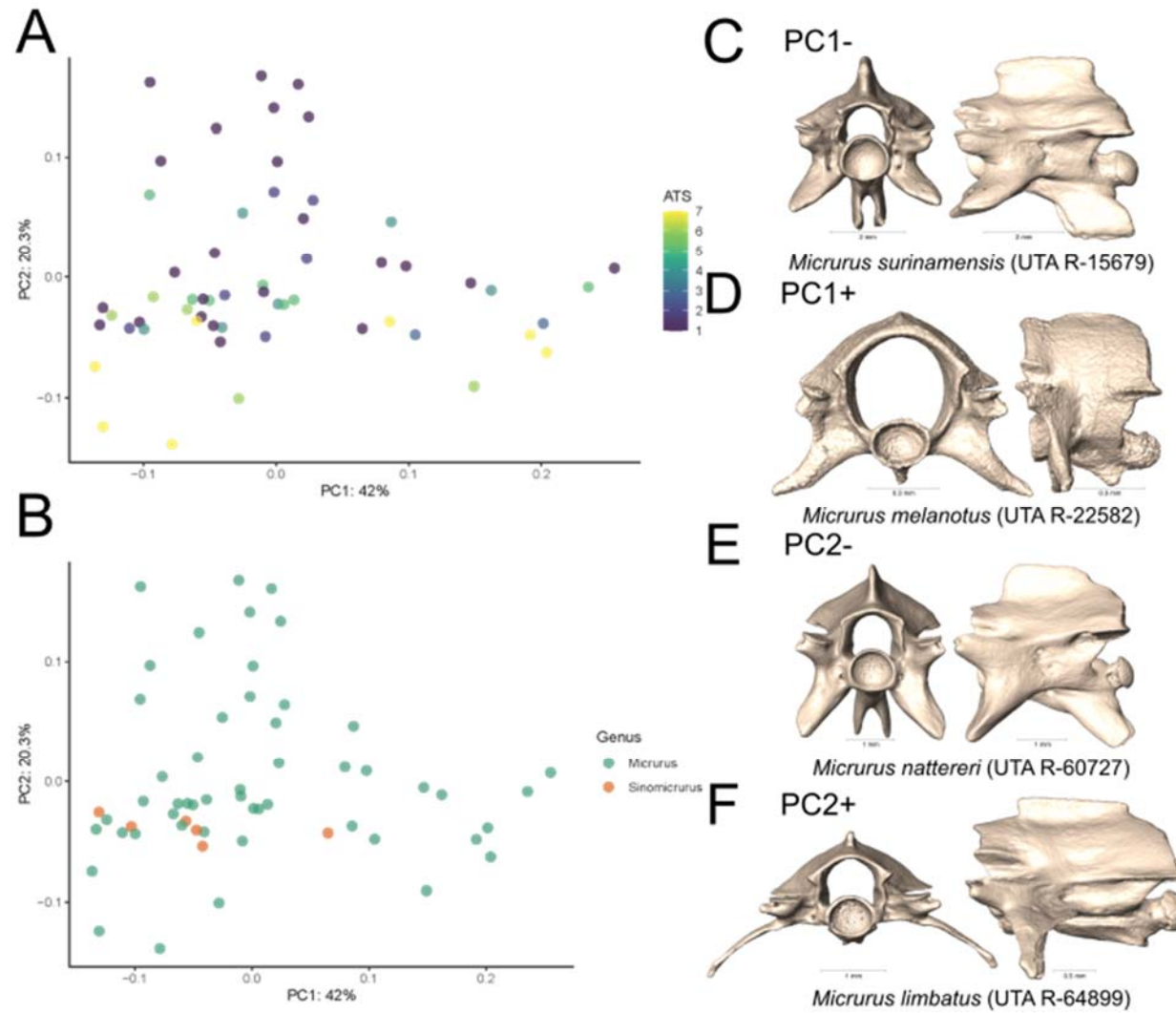


Figure 3.65. PCA of the caudal vertebra dataset conducted on the coralsnake subset, colored by ATS (A) and genus (B). Images of the midbody vertebra of specimens at the extremes of PC1 (C-D) and PC2 (E-F) in the anterior (left) and lateral (right) views.

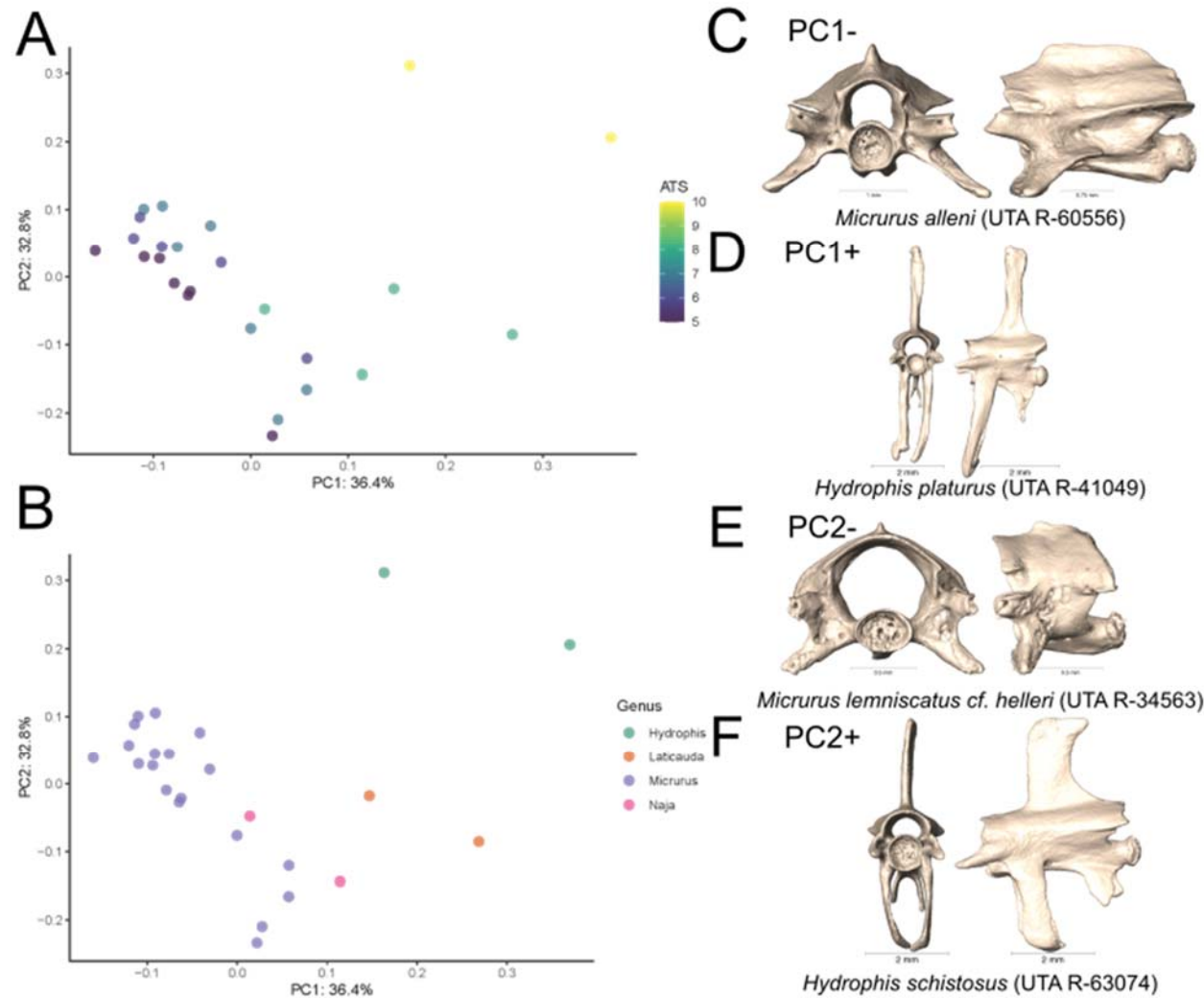


Figure 3.66. PCA of the caudal vertebra dataset conducted on the semi-aquatic and aquatic subset (>5 ATS), colored by ATS (A) and genus (B). Images of specimens at the extremes of PC1 (C-D) and PC2 (E-F) in the anterior (left) and lateral (right) views.

CHAPTER FOUR

Discussion

MODULARITY

In this study morphological variation of 24 bones was quantified and analyzed to elucidate the evolutionary trends of aquatic elapids in largely terrestrial genera. The results suggest that the skull of elapids is highly modular, with the highest supported hypothesis splitting the 17 bones of the skull data set into 15 separate modules. This study found that the maxilla and palatine form a module, this contradicts recent studies that found the palatine and pterygoid to form a module (Watanabe et al. 2019; Rhoda et al. 2021). This difference in result from Watababe *et al.*(2019) is likely due to their inclusion of many less kinetic taxa including lizards. The present study also found modularity within the mandible where Rhoda *et al.* (2021) found it be a single module. This difference in result could be due to the variable bones present in each study and the structure of the dataset. Rhoda *et al.* (2021) focused on the feeding system, did not include the skull itself and investigated the modularity of the upper jaw and mandible within a single dataset. Whereas here we included the upper jaw with the skull dataset and analyzed the jaw separately due to the condition of specimens used. This study found that the septomaxilla and vomer form a single module. This makes sense as they are defined simply in our landmark scheme and consistently fused together across the dataset.

As for the lower jaw, of the 14 model structures tested, model 2C had the greatest support. The two modules were the compound as a separate bone and the angular, dentary and splenial together as the 2nd module. These two modules act during feeding but perform different tasks. The compound is the site of jaw muscle attachment while the dentary is integral in piercing prey.

GENERALIZED PROCRUSTES ANALYSIS

The results of the Generalized Procrustes Analysis (GPA) contain clear trends associated with aquatic tendency. The results can be broken into three categories: morphological trends within *Micrurus*, possible diversity within *Calliophis* and modules with relatedness associated clustering.

Trends within *Micrurus*

Sister taxa, *Micrurus surinamensis* and *M. nattereri*, are the main drivers of the trends observed in the PCAs. Both species are 7 ATS, the highest ATS assigned to a coralsnake taxon. As such there are marked morphological differences that are not seen in other coral snakes, even species that within closely related *M. lemniscatus* species complex. This complex is represented by nine samples in our dataset; two *M. diutius*, three *M. helleri*, two *M. filiformis*, and two *M. lemniscatus cf. helleri*, all of which have aquatic tendencies to a lesser extent in comparison to *M. surinamensis* and *M. nattereri* (Table 2.1). The differences are first apparent in the whole skull PCAs where elongated supratemporals and diminutive supratemporal and exoccipital can be seen. Looking at the modules individually, *M. surinamensis* and *M. nattereri* have more extreme variation in 17 of the 20 modules investigated than the majority of their congeners, the most dramatic of which are discussed here.

Despite the septomaxilla and vomer module consisting of three curves, the complex geometry makes it difficult to discern what variation is being described by the principal component extremes. It appears the choanal process of the septomaxilla is more extensive in *M. surinamensis* and *M. nattereri* than in other *Micrurus*. This character is consistent with

Laticauda but not *Hydrophis*, in which it is nearly absent. This leads to the conclusion that it is not an inherently aquatic trait but could be used as a diagnostic character within the genus.

Most coralsnakes have nasals with a blunt anterior edge, in comparison with the swept back morphology of nasals in *Hydrophis*. *Micrurus surinamensis* and *M. nattereri* have similarly swept back nasals. This could aid in developing the hydrodynamic snake head discussed by Young (1990).

The length of the supratemporal was an identifying feature of *M. surinamensis* and *M. nattereri* that was identified in preliminary work and again seen in the results here. The length of the supratemporal, in conjunction with the length of the quadrate, is likely associated with gape size (Rhoda et al. 2021). This could facilitate aquatic feeding habits. Due to the anterior portion of the supratemporal overlapping the prootic, the prootic module defined in this study is better at describing the variation in of the anterior portion of the supratemporal than the prootic itself. *Micrurus surinamensis* and *M. nattereri* have supratemporals that not only overlap with the prootic but nearly touch the parietal. In this way these two taxa cleanly associate with *Laticauda* and *Hydrophis* more than their congeners.

Another part of the gape size equation, the quadrate, was substantially longer in *M. surinamensis* and *M. nattereri* than their congeners and more closely associated with *Laticauda* and *Hydrophis*.

The exoccipital is a bone of complex geometry that forms the dorsoposterior and lateral surfaces of the braincase. The ventral suture connects it with the basioccipital. Variation along this suture is where *M. surinamensis* and *M. nattereri* diverge from their congeners. Consistent with the whole skull observations of a smaller posterior braincase, the exoccipital-basioccipital suture is shorter in length. This character was associated with PC1 and compared to other

principal components, 27.4% is not the strongest descriptor of variation. That being said, *M. surinamensis* and *M. nattereri* were more extreme along this axis than *Laticauda* and *Hydrophis*. The reduction in size of the exoccipital is involved in the larger trend of the reduction in size of the posterior braincase, again this possibly enables the aquatic snakes to more easily cut through the water.

Moving on to the jaw, we see a drastic difference between aquatic *Micrurus* and other aquatic clades. *Hydrophis* has a much more slender and delicate jaw in comparison with the robust jaw of *M. nattereri*. The large coronoid processes in *M. surinamensis* and *M. nattereri* was not as visible in non-aquatic *Micrurus*.

The jaws of both aquatic *Micrurus* and *Hydrophis* show adaptation toward aquatic life by different means. The dentary of *Hydrophis* is long with many teeth while the compound is more slender. The dentary of *M. nattereri* is shorter but the more robust compound and large coronoid processes increases surface area available for muscle attachment. This yields possibility for a stronger bite force, or at least a sustained bite.

This could be due to the difference of their diet. *Hydrophis* is piscivorous or fish eating while *Micrurus nattereri* eats lizards, fish and eels. A need for a sustained bite could be more important in terrestrial feeding in comparison to feeding just on fish. Also, while eels are technically fish, they are elongate with a body plan that differs from what comes to mind when most think of the word fish. *Hydrophis* likely swallows an entire fish of a typical body plan fairly quickly in comparison to *M. nattereri* feeding upon a swamp eel.

The teeth of aquatic *Micrurus* and *Hydrophis* differ. The teeth of *M. surinamensis* and *M. nattereri* are wider and less numerous than the needle-like teeth in *Hydrophis*. It is possible that

these needle-like teeth give more opportunity to slip between the hard scales of fish while aquatic *Micrurus* are able to clamp down on an eel more easily.

Micrurus surinamensis and *M. nattereri* are two aquatic species that distinguish themselves morphologically from their terrestrial and semi-fossorial congeners. These changes are predominantly reducing braincase size and increasing gape size, both of which are found also in the aquatic genera *Laticauda* and *Hydrophis*.

The midbody and caudal vertebrae of *M. surinamensis* and *M. nattereri* are morphologically more similar to other *Micrurus* than those of *Laticauda* and *Hydrophis*. A more developed neural spine than most *Micrurus* is present in the midbody vertebrae but is not developed to the extent of *Laticauda* and *Hydrophis*. The same can be seen in the caudal vertebrae where the neural spine and pleurapophyses are developed but not to the extreme extent as seen in *Laticauda* and *Hydrophis*. The dramatic length of the neural spine and pleurapophyses of these two mostly marine genera are aquatic adaptations that were necessary for the development of their laterally compressed tails, a trait not seen in *Micrurus*.

Specimens of the *Micrurus lemniscatus* species complex associate with other semi-aquatic *Micrurus* specifically and all other *Micrurus* generally over clustering with *M. surinamensis* and *M. nattereri*, despite being more related to the aquatic pair than other terrestrial *Micrurus*. We did not see any evidence that this species complex had an intermediary trend between *M. surinamensis* and *M. nattereri* and terrestrial *Micrurus*. More so to the opposite effect, *M. lemniscatus* species complex specimens were clustered with semi-aquatic *Micrurus* and away from *M. surinamensis* and *M. nattereri* on the semiaquatic and aquatic subset PCAs of the nasal; prefrontal; prootic; exoccipital; supratemporal; maxilla and palatine; quadrate; and dentary, angular and splenial modules (Figures 3.12, 3.15, 3.30, 3.33, 3.42, 3.51, 3.60). Few

exceptions are worth noting but do not change this interpretation of the results. For the prefrontal module, one sample of *M. cf. helleri* (UTA R-34563) was close to samples of *M. surinamensis* and *M. nattereri* but was still well associated with semi-aquatic *Micrurus*. For the maxilla and palatine module, both samples of *M. cf. helleri* are the closest to aquatic *Micrurus* but are still well within the semi-aquatic *Micrurus* cluster. For the dentary, angular and splenial module of the lower jaw, one sample of *M. helleri* (UTA R-65803) is found with aquatic *Micrurus* but still not that distant from the remaining *Micrurus*.

Calliophis Diversity

Small and fossorial to semi-fossorial snakes, *Calliophis*, were consistently rated low ATS. This genus is the most basal in Elapidae and as such is thought to have a morphology that is most consistent with the familial most recent common ancestor. Though not a primary goal of this study, variation was found amongst the *Calliophis* in our dataset.

The prefrontals of *C. melanurus* (MNHN 48-318 and MNHN 46-286) and *gracilis* (USNM 53447) are connected by their dorsal edge to the dorsolateral edge of the frontals. This is similar to the positioning seen in *Hydrophis* but unlike the remainder of their congeners which are connected to the anterodorsal surface of the frontals. The supratemporals of *C. melanurus* are diminutive in comparison to their congeners and are fused to the exoccipital to the degree that their outline is difficult to discern.

The upper jaw of *C. melanurus* also differs from its congeners. The palatines are less than the length of their maxillae in ventral view and the maxillary process of the ectopterygoid is exceptionally wide. This taxon also has a divergent dentary, angular and splenial module, the morphological difference of which could not be easily ascertained.

There is genetic evidence for further undescribed diversity within *Calliophis* (E.N Smith, Pers. Com. 2021). It is possible that the shape of the prefrontal and that other diversity uncovered by these analyses could be used as a morphologically diagnosable characters within the genus.

Ecological Signal in Vertebrae

Significant trends could not be discovered in the analysis of the midbody or caudal vertebrae in terms of aquatic tendency. While vertebral form can be a fantastic source of diagnostic characters (Hoffsetter 1939; Holman 1977; Rage 1984; Slowinski 1994; Ikeda 2007), it is a poor predictor of ecology. Vertebral form reflects taxonomic status to a higher degree than ecology (Johnson 1955). Osteosclerosis of extinct and extant snake vertebrae is not a reliable predictor of snake ecology (Hampton 2019).

CHAPTER FIVE

General Conclusion

Elapidae is an extremely diverse family of snakes, as illustrated by its expansive geographic distribution and in the variety of life histories. In this project I attempt to classify the disparate habits of the family using a classification scheme dubbed the Aquatic Tendency Score to understand the evolutionary history and adaptations the group has utilized to become so speciose and phenotypically diverse. This project aims to have other studies replicate and modify this scheme for use in subsequent explorations of morphology.

Through the large-scale CT data collection completed for this project, a data set has been created that will serve future researchers after it is uploaded to an online repository (Morphosource). This data set contains scans of 108 specimens of 76 species from 20 genera with sampling focused primarily on new world coralsnakes. Three scans were taken of each specimen, the skull, midbody vertebra and caudal vertebra. The skull scans were split into three datasets, the lower jaw, quadrate, and the rest of the skull, thus creating five datasets.

Through a high-density 3D geometric morphometric methodology, it has been shown that the elapid skull is highly modular, and that the mandible consists of at least two modules. Of the 17 regions of the skull, defined *a priori*, 13 were found to be independent with the remaining four forming two modules, one of septomaxilla and vomer and the other of maxilla and palatine. The two modules of the jaw were found to be the compound bone, in a single module, and the dentary, angular and splenial as the second.

Further, principal component analyses of the five datasets revealed that aquatic coralsnakes, *Micrurus surinamensis* and *M. nattereri*, have morphological characters that are divergent from their semi-aquatic and terrestrial congeners, and that are consistent with the

morphology of aquatic *Hydrophis* and *Laticauda*. The characters revolve around reducing the size of the braincase, possibly for more efficient aquatic locomotion, and increased gape size. Specifically, the exoccipital plays a key role in the trend of the reduction in braincase size and, the anteroposterior lengthening of the supratemporal and dorsoventral lengthening of the quadrate relate to an increased gape size.

Morphological diversity has been uncovered in *Calliophis* which, with further study, can be used to reorganize its taxonomy to provide a more accurate picture of the biodiversity within. The two morphological differences that are apparent from these analyses are the angle of attachment of the prefrontal to the frontal (either anteriorly as in *C. salitan* or laterally as in *C. gracilis*) and the comparison of the length of the maxilla to the palatine. In *C. salitan* the maxilla is stunted anteroposteriorly, which contrasts with an extended palatine, while in *C. melanurus*, the maxilla and palatine are of roughly the same length.

Much like the skull, elapid vertebrae are morphologically diverse. This diversity has shown to be more associated with taxonomic relationships and vertebrae were confirmed to not be an accurate predictor of aquatic habitat. It is possible that ecological based trends can be uncovered through the use of a vertebrae dataset, but for now, that was out of the scope of this project.

REFERENCES

- Adams, D.C., Collyer, M.L., Kaliontzopoulou, A. and Balken, E.K., 2021. ‘Geomorph: Software for geometric morphometric analyses.’ R package version 4.0.
- Ahmed, M.F., Das, A. and Dutta, S.K., 2009. *Amphibians and reptiles of Northeast India: A photographic guide*. Aaranyak, Guwahati.
- Aitchison, J.C., Ali, J.R. and Davis, A.M., 2007. ‘When and where did India and Asia collide?’ *Journal of Geophysical Research: Solid Earth*, 112(B5).
- Ali, J.R. and Aitchison, J.C., 2008. ‘Gondwana to Asia: plate tectonics, paleogeography and the biological connectivity of the Indian sub-continent from the Middle Jurassic through latest Eocene (166-35 Ma).’ *Earth-Science Reviews*, 88(3-4), 145-166.
- Altekar, G., Dwarkadas, S., Huelsenbeck, J.P. and Ronquist, F., 2004. ‘Parallel Metropolis-coupled Markov chain Monte Carlo for Bayesian phylogenetic inference.’ *Bioinformatics* 20, 407-415.
- Álvarez del Toro, M. and Smith, H.M., 1956. ‘Notulae herpetologicae chiapasiae I.’ *Herpetologica*, 12(1), 3-17.
- Amaral, A.D., 1933. ‘Mecanismo e gênero de alimentação das serpentes do Brasil.’ *Boletim Biologia, São Paulo*, 1(1), 2-4.
- Amaral, A.D., 1978. *Serpentes do Brasil: iconografia colorida: a colour iconography*. Melhoramentos, São Paulo.
- Archis, J.N., Akcali, C., Stuart, B.L., Kikuchi, D. and Chunco, A.J., 2018. ‘Is the future already here? The impact of climate change on the distribution of the eastern coral snake (*Micrurus fulvius*).’ *PeerJ*, 6.
- Arévalo-Páez, M.A., Montes-Correa, A.C., Rada, E., Saboyá-Acosta, L.P. and Renjifo, J.M., 2015. ‘Notes on the diet of pigmy coral snake (*Micrurus dissolitus*) (Cope, 1860) (Elapidae) in northern Colombia.’ *Herpetology Notes*, 8, 39-41.
- Arteaga, A., Bustamante-Enríquez, L.M. and Guayasamin, J.M., 2013. *The amphibians and reptiles of Mindo*. Universidad Tecnológica Indoamérica, Quito.
- Aubret, F., 2004. ‘Aquatic locomotion and behaviour in two disjunct populations of Western Australian tiger snakes, *Notechis ater occidentalis*.’ *Australian Journal of Zoology*, 52(4), 357-368.
- Ávila, R.W., Kawashita-Ribeiro, R.A., Ferreira, V.L. and Strüssmann, C., 2010. ‘Natural history of the coral snake *Micrurus pyrrhocryptus* Cope 1862 (Elapidae) from semideciduous forests of western Brazil.’ *South American Journal of Herpetology* 5(2), 97-101.
- Ávila, R.W., Morais, D.H., Anjos, L., Almeida, W.O. and Silva, R.J., 2013. ‘Endoparasites infecting the semiaquatic coral snake *Micrurus surinamensis* (Squamata: Elapidae) in the southern amazonian region, Mato Grosso state, Brazil.’ *Brazilian Journal of Biology*, 73, 645-647.

- Azevedo, A.C.P., 1961. 'Notas sobre cobra corais (Serpentes-Elapidae) III a VII.' *Inheringia, Zoologia*, 18:1-23.
- Babb, R.D. and Brennan, T.C., 2018., 'Micruroides euryxanthus (Sonoran Coralsnake).' *Herpetological Review*, 49(3), 550.
- Baken, E.K., Collyer, M.L., Kaliontzopoulou A. and Adams D.C., 2021. 'gmShiny and geomorph v4.0: new graphical interface and enhanced analytics for a comprehensive morphometric experience.' *Methods in Ecology and Evolution*. Submitted.
- Bardua, C., Felice, R.N., Watanabe, A., Fabre, A.C. and Goswami, A., 2019. 'A practical guide to sliding and surface semilandmarks in morphometric analyses.' *Integrative Organismal Biology*, 1(1), p.obz016.
- Bardua, C., Wilkinson, M., Gower, D.J., Sherratt, E. and Goswami, A., 2019. 'Morphological Evolution And Modularity Of The Caecilian Skull.' *BMC Evolutionary Biology*, 19(1).
- Bean, B.A., 1924. 'A curious fish trap.' *Copeia*, 131, 57-58.
- Beebe, W., 1946. 'Field notes on the snakes of Kartabo, British Guiana, and Caripito, Venezuela.' *Zoologica* (New York), 31(1-4), 11-52.
- Benítez Gálvez, J.E., 1997. *Los ofidios de Puebla*. Ecologistas, Puebla, Mexico.
- Bernarde, P.S. and Turci, L.C.B., Abegg, A.D. and Franco, F.L., 2018. 'A remarkable new species of coralsnake of the *Micrurus hemprichii* species group from the Brazilian Amazon.' *Salamandra*, 54(4), 249-258.
- Blaney, R. M. and Blaney, P.K., 1978. 'Notes on three species of *Micrurus* (Serpentes: Elapidae) from Mexico.' *Herpetological Review*. 9(3), 92.
- Bogert, C.M., 1943. 'Dentitional phenomena in cobras and other elapids, with notes on adaptive modifications of fangs.' *Bulletin of the American Museum of Natural History*, 81, 285-360.
- von Boie, F., 1827. 'Bemerkungen über Merrem 's Versuch eines Systems der Amphibien, 1. Lieferung: Ophidier.' *Isis van Oken* 20, 508-566.
- Boos, H.E.A., 1984. 'A consideration of the terrestrial reptile fauna on some offshore islands north west of Trinidad.' *Living World, Journal of the Trinidad and Tobago Field Naturalists' Club*, 19-26.
- Boucot, A.J., Xu, C., Scotese, C.R. and Morley, R.J., 2013. 'Phanerozoic paleoclimate: an atlas of lithologic indicators of climate.' *SEPM Concepts in Sedimentology and Paleontology*, 11. Map Folio.
- Boulenger, G.A., 1896. *Catalogue of the Snakes in the British Museum (Natural History)*. Vol. 3. London: Printed by order of the Trustees of the British museum.
- Boulenger, G.A., 1913. 'On a collection of batrachians and reptiles made by Dr. H.G.F. Spurrell, F.Z.S., in the Choco, Colombia.' *Proc. of the Zool. Soc. London*, 1019-1038.

- Brecko J, Vervust B, Herrel A, Van Damme R., 2011. ‘Head Morphology and Diet in the Dice Snake (*Natrix tessellata*).’ *Mertensiella*, 18: 20-29
- Brischoux, F., Shine, R., 2006. ‘Morphological Adaptations to Marine Life in Snakes.’ *Journal of Morphology*, 272(5), 566-572.
- Britt, E.J., Clark, A.J., Bennett, A.F., 2009, ‘Dental morphologies in gartersnakes (*Thamnophis*) and their connection to dietary preferences.’ *Journal of Herpetology*, 43(2), 252-259.
- Brown, R.M., Smart, U., Leviton, A.E. and Smith, E.N., 2018. ‘A new species of long-glanded coralsnake of the genus *Calliophis* (Squamata: Elapidae) from Dinagat Island, with notes on the biogeography and species diversity of Philippine *Calliophis* and *Hemibungarus*.’ *Herpetologica*, 74(1), 89-104.
- Burger, R.M., 1997. ‘Predation by two species of coral snakes in Limón Province, Costa Rica.’ *Bull. Chicago Herpetol. Soc.*, 32(7), 145.
- Cacciali, P., Wüest, U., Espínola, D., Viñales, S.C., Cabral, H., 2011. ‘Squamata, Serpentes, *Micrurus silviae* Di-Bernardo, Borges-Martins and Silva, 2007: Presence confirmation in Paraguay.’ *Check List*, 7, 809.
- Cadle, J.E. and Sarich, V.M., 1981. ‘An immunological assessment of the phylogenetic position of New World coral snakes.’ *Journal of Zoology*, 195(2), 157-167.
- Cadle, J.E., 1987. ‘Geographic distribution: Problems in phylogeny and zoogeography,’ in Siegel, R.A., Collins, J.T. and Novak, S.S. (eds.) *Snakes: Ecology and Evolutionary Biology*, 3, 77-105.
- Cadle, J.E., 1988. ‘Phylogenetic relationships among advanced snakes.’ *University of California Publications in Zoology*, 119: 1-77.
- Campbell, J.A., 1998. *Amphibians and reptiles of northern Guatemala, the Yucatán, and Belize*. University of Oklahoma Press, Norman.
- Campbell, J.A. and Lamar, W.W., 1989. *The venomous reptiles of Latin America*. Cornell University Press, Ithaca.
- Campbell, J.A. and Lamar, W.W., 2004. *The venomous reptiles of the western hemisphere*, Vol. 1. Comstock Pub. Associates, Ithaca.
- Canseco-Márquez, L. and Campbell, J.A., 2003. ‘Variation in Zapotitlan coralsnake, *Micrurus pachecogili* (Serpentes: Elapidae).’ *The Southwestern Naturalist*, 48(4), 705-707.
- Canseco-Márquez, L. and Gutiérrez-Mayen, M.G., 2010. *Anfibios y reptiles del Valle de Tehuacán-Cuicatlán*. Conabio, Cuicatlán A.C. and BUA Puebla
- Carrillo de Espinosa, N., 1983. ‘Contribución al conocimiento de las serpientes venenosas del Perú de las familias Viperidae, Elapidae, e Hydrophiidae (Ophidia:Reptilia).’ *Public. Mus. Hist. Nat. (UNMSM)*, Serie A, Zoología, 30, 1-55

- Casas-Andreu, G., López-Forment, W.C., 1978. 'Notas sobre *Micrurus browni taylori* Schmidt y Smith, en Guerrero, México.' *An. Inst. Biol. Univ. Nacional Autónoma de México*, 49(1), 291- 294.
- Castoe, T.A., Smith, E.N., Brown, R.M., Parkinson, C.L., 2007. 'Higher-level phylogeny of Asian and American coralsnakes, their placement within the Elapidae (Squamata), and the systematic affinities of the enigmatic Asian coralsnake *Hemibungarus calligaster* (Wiegmann, 1834).' *Zoological Journal of the Linnean Society*, 151(4), 809-831.
- Caívalcanti, L., Santos-Protázio, A., Albuquerque, R., Pedro, C.K.B. and Mesquita, D.O., 2012. 'Death of a coral snake *Micrurus ibiboboca* (Merrem, 1820)(Elapidae) due to failed predation on bigger prey: a cat-eyed night snake *Leptodeira annulata* (Linnaeus, 1758)(Dipsadidae).' *Herpetology notes*, 5, 129-131.
- Champion, H.G., 1936. 'A preliminary survey of the forest types of India and Burma.' *Indian Forest Record (New Series)*, 1, 1-286.
- Champion, H.G. and Seth, S.K., 1968. *A Revised Survey of the Forest Types of India*. Government of India Press, New Delhi.
- Chan-Ard, T., Nabhitabhata, J. and Parr, J.W.K., 2015. *A field guide to the reptiles of Thailand*. Oxford University Press.
- Chance, B., 1970. 'A note on the feeding habits of *Micrurus fulvius fulvius*.' *Bull. Maryland Herpetol. Soc.*, 6, 56.
- Chanhome, L., Cox, M.J., Vasaruchapong, T., Chaiyabutr, N. and Sitprija, V., 2011. 'Characterization of venomous snakes of Thailand.' *Asian Biomedicine*, 5(3), 311-328.
- Chippaux, J.-P. and Jackson, K., 2019. *Snakes of Central and Western Africa*. JHU Press.
- Cisneros-Heredia, D.F., 2005. 'Predation upon *Amphisbaena fuliginosa* LINNAEUS, 1758 by *Micrurus anchoralis* (JAN, 1872).' *Herpetozoa*, 18(1/2), 93-94.
- Cope, E.D., 1882. 'Third contribution to the history of the Vertebrata of the Permian formation of Texas.' *Proceedings of the American Philosophical Society*, 20(112), 447-461.
- Cogger, H.G., 1975. 'Sea Snakes of Australia and New Guinea,' in Dunson, W.A. (ed.) *The Biology of Sea Snakes*. Baltimore London & Tokyo: University Park Press, 59–139.
- Cogger, H.G., 2018. *Reptiles and amphibians of Australia*. CSIRO Publishing, Melbourne.
- Cogger, H.G. and Heatwole, H., 1981. 'The Australian reptiles: Origins, biogeography, distribution patterns and island evolution,' in Keast, A. (ed.) *Monographiae Biologicae Vol 41. Ecological Biogeography of Australia Vol 2*. The Hague: Junk, 1331-1374.
- Collyer, M.L. and Adams, D.C., 2018. 'RRPP: An R package for fitting linear models to high-dimensional data using residual randomization.' *Methods in Ecology and Evolution*, 9(2), 1772-1779.
- Collyer, M.L. and Adams, D.C., 2021. *RRPP: Linear Model Evaluation with Randomized Residuals in a Permutation Procedure*.

- Corkill, N.L. and Cochrane, J.A., 1966. 'The snakes of the Arabian Peninsula and Socotra.' *J. Bombay nat. Hist. Soc.*, 62(3), 475-506.
- Crowley, C.W., 2012. *An atlas of cenozoic climate zones*. MS thesis, University of Texas at Arlington.
- Cundall, D. and Irish, F., 2008. 'The Snake Skull,' in Gans, C., Gaunt, A.S. and Adler, K. (eds.), *Biology of the Reptilia. Volume 20. Morphology H. The Skull of Lepidosauria*. Ithaca: Society for the Study of Amphibians and Reptiles, 349-692.
- Cunha, O.R. and Nascimento, F.P., 1978. 'Ofídios da Amazônia X - As cobras da região leste do Pará.' *Publicações Avulsas*, n.31.
- Cunha, O.R. and Nascimento, F.P., 1982. 'Ofídios da Amazonia XIV - As especies de *Micrurus*, *Bothrops*, *Lachesis* e *Crotalus* do sul do Para e oeste do Maranhão, incluindo areas de cerrado deste estado. (Ophidia: Elapidae e Viperidae).' *Bol. Mus. Par. Emilio Goeldi*, 112, 1-58.
- Cunha, O.R. and Nascimento, F.P., 1993. 'Ofídios da Amazônia. As cobras da região Leste do Pará.' *Papéis Avulsos Museu Paraense Emílio Goeldi, n. ser. Zool., Belém*, 9(1), 1-191.
- Curtis, L., 1952. 'Cannibalism in the Texas coral snake.' *Herpetologica*, 8(2), 27.
- Darlington, P.J., 1957. *Zoogeography: The Geographical Distribution of Animals*. John Wiley and Sons.
- Das, I., 2007. *Amphibians and reptiles of Brunei*. Natural History Publications, Borneo.
- Das, I., 2010. *A field guide to the reptiles of South-East Asia*. Bloomsbury Publishing, London.
- Das, I., 2012. *A Naturalist's Guide to the Snakes of South-east Asia: Including Malaysia, Singapore, Thailand, Myanmar, Borneo, Sumatra, Java and Bali*. JB/John Beaufoy Publishing, Singapore.
- Davidson, T.M. and Eisner, J., 1996. 'United States coral snakes.' *Wilderness and Environmental Medicine* 7(1), 38-45.
- van Denburgh, J. and Thompson, J.C., 1908. 'Description of a new species of sea snake from the Philippine Islands, with a note on the palatine teeth in the Proteroglypha.' *Proc. Calif Acad. Sci.*, 3, 41-48.
- Dessauer, H.C., Cadle, J.E. and Lawson, R., 1987. 'Patterns of snake evolution suggested by their proteins.' *Fieldiana, Zoology, New Series*, 34, 1-34.
- Deufel, A., Cundall, D., 2009. 'Functional morphology of the palato-maxillary apparatus in 'Palatine dragging' snakes (Serpentes: Elapidae: *Acanthophis*, *Oxyuranus*).'*Journal of Morphology*, 271(1) 73-85.
- Di-Bernardo, M., Borges-Martins, M. and Silva Jr., N.J., 2007. 'A new species of coralsnake (*Micrurus*: Elapidae) from southern Brazil.' *Zootaxa* 1447(1), 1-26.

- Dixon, J.R. and Soini, P., 1986. *The reptiles of the Upper Amazon Basin, Iquitos Region, Peru*, 2nd ed., Milwaukee Public Museum, Milwaukee.
- Dowling, H.G., 1959. ‘Classification of the Serpentes: a critical review.’ *Copeia*, 1, 38-52.
- Duellman, W.E., 1978. ‘The biology of an equatorial herpetofauna in Amazonian Ecuador.’ *Miscellaneous Publications of the Museum of Natural History, University of Kansas*, 165, 1-352.
- Duellman, W.E. and Mendelson, J.R. III., 1995. ‘Amphibians and reptiles from northern Departamento Loreto, Peru: taxonomy and biogeography.’ *Univ. Kansas Sci. Bull.*, 55, 329-376.
- Duellman, W.E. and Salas, A.W., 1991. ‘Annotated checklist of the amphibians and reptiles of Cuzco Amazonico, Peru.’ *Occ. Pap. Mus. Nat. Hist. Univ. Kansas*, 143, 1-13.
- Edgar, R.C., 2004. ‘MUSCLE: multiple sequence alignment with high accuracy and high throughput.’ *Nucleic Acids Research*, 32(5), 1792–1797
- Emsley, M., 1977. ‘Snakes, and Trinidad and Tobago.’ *Bull. Maryland Herpetol. Soc.*, 13(4), 201-304.
- Evans, S.E., 2008. ‘The Skull of Lizards and Tuatara.’ in C. Gans, A. S. Gaunt, and K. Adler (eds.), *Biology of the Reptilia. Volume 20. Morphology H. The Skull of Lepidosauria*. Ithaca: Society for the Study of Amphibians and Reptiles, 1-348.
- Feitosa, D.T., Passos, P. and Prudente, A.L.C., 2007. ‘Taxonomic status and geographic variation of the slender coralsnake, *Micruurus filiformis* (Günther, 1859) (Serpentes, Elapidae).’ *South American Journal of Herpetology*, 2: 149-156.
- Figueroa, A., McKelvy, A.D., Grismer, L.L., Bell, C.D. and Lailvaux, S.P., 2016. ‘A Species-Level Phylogeny of Extant Snakes with Description of a New Colubrid Subfamily and Genus.’ *PLOS One*, 11(9).
- Floriano, R.S., Schezaro-Ramos, R., Silva, N.J., Bucaretti, F., Rowan, E.G. and Hyslop, S., 2019. ‘Neurotoxicity of *Micrurus lemniscatus lemniscatus* (South American coralsnake) venom in vertebrate neuromuscular preparations in vitro and neutralization by antivenom.’ *Archives of Toxicology*, 93: 2065-2086.
- de Freitas, M.A., 1999. *Serpentes da Bahia e do Brasil*. Editora Dall, Bahia.
- de Freitas, M.A., 2003. *Serpentes brasileiras*. Feira de Santana, Bahia.
- Fuchs, J., Weiler, S. and Meier, J., 2019. Envenomation by a western green mamba (*Dendroaspis viridis*)-A report of three episodes in Switzerland. *Toxicon*, 168, 76-82.
- Fukuyama, I., Vogel, G., Matsui, M., Eto, K., Munir, M., Hossman, M.Y., Hamidy, A. and Nishikawa, K., 2020. ‘Systematics of *Calliophis intestinalis* with the Resurrection of *Calliophis nigrotaeniatus* (Elapidae, Serpentes).’ *Zoological Science*, 37(6).
- Gaige, H.T., Hartweg, N. and Stuart, L.C., 1937. ‘Notes on a collection of amphibians and reptiles from eastern Nicaragua.’ *Occas. Pap. Mus. Zool. Univ. Michigan*, 357, 1-8.

- Galvis-Rizo, C., Carvajal-Cogollo, J.E., Arredondo, J.C., Passos, P., López-Victoria, M., Velasco, J.A., Bock, B.C., Toro, F.A., Daza, J.M., Páez, V.P. and Rojas-Rivera, M.A., 2016. *Libro Rojo de Reptiles de Colombia* (2015).
- Gasperetti, J., 1988. ‘Snakes of Arabia,’ in Buttiker, W. and Krupp, F. (eds), *Fauna of Saudi Arabia* Vol. 9, National Commission for Wildlife Conservation and Development, Riyadh, 164-450.
- Gauthier, J.A., Kluge, A.G. and Rowe, T., 1988. ‘The early evolution of the Amniota.’ *The phylogeny and classification of the tetrapods*, 1, 103-155.
- Goris, R.C. and Maeda, N., 2004. *Guide to the Amphibians and Reptiles of Japan*. Krieger Publishing Company, Malabar.
- Gower, J.C., 1975. ‘Generalized procrustes analysis.’ *Psychometrika*, 40(1), 33-51.
- Greene, H.W., 1973. *The food habits and feeding behavior of New World coral snakes*. University of Texas at Arlington, master ‘s thesis.
- Greene, H.W., 1984. ‘Feeding behavior and diet of the eastern coral snake, *Micruurus fulvius*.’ *Museum of Natural History, University of Kansas, Special Publication*, 10, 147-162.
- Greene, H.W., 1997. *Snakes: The Evolution of Mystery in Nature*. University of California Press, Berkeley
- Hall, R. 2011., ‘Australia-SE Asia collision: plate tectonics and crustal flow.’ *Geological Society, London, Special Publications*, 355(1), 75-109.
- Hall, R., 2012. ‘Sundaland and Wallacea: geology, plate tectonics and palaeogeographyn’ in Gower, D., Johnson, K., Richardson, J., Rosen, B., Rüber, L. and Williams S. (eds.) *Biotic Evolution and Environmental Change in Southeast Asia*, Cambridge University Press, 32-78.
- Hamanaka, K., Mori, A., and Moriguchi, H. 2014. ‘Literature survey on food habit of snakes in Japan: Revisited.’ *Hachū-ryōseirui Gakkai hō*, 2014(2), 167-181
- Hampton P.M., 2011. ‘Comparison of cranial form and function in association with diet in natricine snakes.’ *Journal of Morphology*, 272, 1435-1443.
- Hampton, P.M., Moon, B.R., 2012. ‘Gape size, its morphological basis, and the validity of gape indices in western diamond-backed rattlesnakes (*crotalus atrox*).’ *Journal of Morphology*, 274(2), 194-202.
- Hampton, P.M., 2019. ‘Foraging ecology influences the number of vertebrae in hydrophiine sea snakes.’ *Biological Journal of the Linnean Society*, 128(3), 645-650
- Harvey, M.B., Aparicio, J.E. and Gonzalez, L.A., 2003. ‘Revision of the venomous snakes of Bolivia. Part 1. The coralsnakes (Elapidae: *Micrurus*).’ *Annals of Carnegie Museum*, 72, 1-52.

- Harzhauser, M., Kroh, A., Mandic, O., Piller, W.E., Göhlich, U., Reuter, M. and Berning, B., 2007. ‘Biogeographic responses to geodynamics: A key study all around the Oligo-Miocene Tethyan Seaway.’ *Zoologischer Anzeiger-A Journal of Comparative Zoology*, 246(4), 241-256.
- Hedges, S.B., 2012. ‘Amniote phylogeny and the position of turtles.’ *BMC biology*, 10(1), 64.
- Heimes, P., 2016. *Herpetofauna Mexicana Vol. I. Snakes of Mexico*. Frankfurt am Main, Germany, Edition Chimaira.
- Heinrich, G., 1996. ‘Natural history notes: *Micrurus fulvius fulvius* (eastern coral snake).’ *Diet. Herpetol. Rev.* 27(1), 25.
- Herrel, A., Schaeirlaeken, V., Meyers, J.J., Metzger, K.A. and Ross, C.F., 2007. ‘The evolution of cranial design and performance in squamates: Consequences of skull-bone reduction on feeding behavior.’ *Integrative and Comparative Biology*, 47(1), 107-117.
- Herrera-Lopera, J.M., Ramírez-Castaño, V.A. and García-Oviedo, F.A., 2018. ‘*Micruroides euryxanthus* (Sonoran Coralsnake).’ *Herpetological Review* 49(3), 550.
- Hirasawa, T. and Kuratani, S., 2015. ‘Evolution of the vertebrate skeleton: morphology, embryology, and development.’ *Zoological Letters*, 1(1), 2.
- Hoffstetter, R., 1939. ‘Contribution à l’étude des Elapidae actuels et fossiles et de l’ostéologie des ophidiens.’ *Publications du musée des Confluences*, 15(1), 1-78.
- Hoge, A.R., Federsoni, P.A. Jr., 1981. ‘Manutenção e criação de serpentes em cativeiro.’ *Revista Bioterios*, 1, 63-73.
- Holman, J.A., 1977. ‘Upper Miocene snakes (Reptilia, Serpentes) from southeastern Nebraska.’ *Journal of Herpetology*, 323-335.
- Hu, Y., Ajay, L. and Jing, L., 2020. ‘Three-dimensional segmentation of computed tomography data using Drishti Paint:new tools and developments.’ *R. Soc. open sci.* 7:201033.
- Huelsenbeck, J. P. and Ronquist, F., 2001. ‘MRBAYES: Bayesian inference of phylogeny.’ *Bioinformatics* 17, 754-755.
- Hurtado Gómez, J.P., Vargas Ramírez, M., Ruiz Gómez, F.J., Fouquet, A. and Fritz, U., 2021. ‘Multilocus phylogeny clarifies relationships and diversity within the *Micrurus lemniscatus* complex (Serpentes: Elapidae).’ *Salamandra*, 57(2), 229-239.
- Ikeda, T., 2007. ‘A comparative morphological study of the vertebrae of snakes occurring in Japan and adjacent regions.’ *Current Herpetology*, 26(1), 13-34.
- Irwin, K.J., 2004. *Arkansas Snake Guide*. Arkansas Game and Fish Commission Pocket Guide.
- Ivanov, M., 2000. ‘Snakes of the lower/middle Miocene transition at Vieux Collonges (Rhône, France), with comments on the colonisation of western Europe by colubroids.’ *Geodiversitas*, 22(4), 559-588.

- Jackson, D.R. and Franz, R., 1981. ‘Ecology of the eastern coral snake (*Micrurus fulvius*) in northern peninsular Florida.’ *Herpetologica*, 37(4), 213-228.
- Jayne, B. C. 1982., ‘Comparative morphology of the semispinalis-spinalis muscle of snakes and correlations with locomotion and constriction.’ *Journal of Morphology*, 172(1), 83-96.
- Johnson, R.G. 1955., ‘The adaptive and phylogenetic significance of vertebral form in snakes.’ *Evolution*, 367-388.
- Jowers, M.J., Mudarra, J.L.G., Charles, S.P. and Murphy, J.C., 2019. ‘Phylogeography of West Indies Coral snakes (*Micrurus*): Island colonisation and banding patterns.’ *Zoologica Scripta*, 48(3), 263-276.
- Jurestovsky, D.J., Jayne, B.C. and Astley, H.C., 2020 ‘Experimental modification of morphology reveals the effects of the zygosphene-zygantrum joint on the range of motion of snake vertebrae.’ *Journal of Experimental Biology*, 223(7).
- Kannan, P., 2006. ‘Occurance of the striped coral snake (*Calliophis nigrescens* Gunther) in Mudumalai wildlife sanctuary, southern India.’ *Cobra*, 63, 11-13
- Kardong, K.V., 2009. *Vertebrates: Comparative anatomy, function, evolution*. New York, NY: McGraw-Hill Education.
- Kaucka, M. and Adameyko, I., 2017. ‘Evolution and development of the cartilaginous skull: from a lancelet towards a human face.’ *Seminars in cell and developmental biology*, 91, 2-12.
- Kelly, C.M.R., Barker, N.P., Villet, M.H. and Broadley, D.G., 2009. ‘Phylogeny, biogeography and classification of the snake superfamily Elapoidea: a rapid radiation in the late Eocene.’ *Cladistics*, 25(1), 38-63.
- Keogh, J.S., 1998. ‘Molecular phylogeny of elapid snakes and a consideration of their biogeographic history.’ *Biological journal of the Linnean Society*, 63(2), 177-203.
- Klaczko, J., Sherratt, E., Setz, E.Z.F., 2016. ‘Are Diet Preferences Associated to Skulls Shape Diversification in Xenodontine Snakes?’ *PLOS One*, 11(2).
- Klawe, W.L., 1964. ‘Food of the black-and-yellow sea snake, *Pelamis platurus*, from Ecuadorian coastal waters.’ *Copeia*, 4, 712-713.
- Köhler, G., Cedeño-Vázquez, J.R. and Beutelspacher-García, P.M., 2016. ‘The Chetumal Snake Census: generating biological data from road-killed snakes.’ *Mesoamerican Herpetology*, 3(3), 640-660.
- Krysko, K.L. and Abdelfattah, K.R., 2002. ‘Natural history notes: *Micrurus Fulvius* (eastern coral snake).’ *Prey. Herpetol. Rev.* 33(1), 57-58.
- Lamar, W. 2003., ‘A new species of slender coralsnake from Colombia, and its clinal an ontogenetic variation (Serpentes, Elapidae : *Leptomicrurus*).’ *Revista de biología tropical*, 51, 805-10.

- Landy, M.J., Langebartel, D.A., Moll, E.O. and Smith, H.M., 1966. ‘A collection of snakes from Volcán Tacaná, Chiapas, Mexico.’ *Journal of the Ohio Herpetological Society*, 5(3), 93-101.
- Lee, J.C., 1996. *The Amphibians and Reptiles of the Yucatán Peninsula*. Cornell University Press, Ithaca, New York.
- Lee, M.S.Y., Sanders, K.L., King, B. and Palci, A., 2016. ‘Diversification rates and phenotypic evolution in venomous snakes (Elapidae).’ *Royal Society open science*, 3(1), 150277.
- de Lema, T., de Araujo, M.L. and de Azevedo, A.C.P., 1983. ‘Contribuição ao conhecimento da alimentação e do modo alimentar de serpentes do Brasil.’ *Comunicaciones Museo Ciências Pontifícia Universidade Católica do Rio Grande do Sul*, 26, 41-121.
- Leynaud, G.C., Reati, G.J. and Bucher, E.H., 2008. ‘Annual activity patterns of snakes from central Argentina (Córdoba province).’ *Studies on Neotropical Fauna and Environment*, 43(1), 19-24.
- Limaye, A.A., 2012. ‘Drishti: a volume exploration and presentation tool.’ *Proc. SPIE, Developments in X-Ray Tomography VIII*, 85060.
- Liu, Q., Yan, J.W., Hou, S.B., Wang, P., Nguyen, S.N., Murphy, R.W., Che, J. and Guo, P., 2020. ‘A new species of the genus *Sinomicrurus* (Serpentes: Elapidae) from China and Vietnam.’ *Zoological research*, 41(2), 194.
- Lobo, A.S., 2006. ‘Uropeltis macrolepis in the diet of *Calliophis nigrescens*.’ *Hamadryad*, 30(1), 203-204.
- Loveridge, A., 1938. ‘Food of *Micrurus fulvius fulvius*.’ *Copeia*, 4, 201-202.
- Loveridge, A., 1944. ‘Cannibalism in the common coral snake.’ *Copeia*, 4, 254.
- Lowe, C.H., Schwalbe, C.R. and Johnson, T.B., 1986. *The venomous reptiles of Arizona*. Arizona Game and Fish Department, Phoenix.
- Lukoschek, V.i, Keogh, J.S. and Avise, J.C., 2012. ‘Evaluating fossil calibrations for dating phylogenies in light of rates of molecular evolution: a comparison of three approaches.’ *Systematic Biology*, 61, 1(22).
- Marais, J., 2004. *A complete guide to the snakes of southern Africa*. Penguin Random House South Africa.
- Marques, O.A., 2002. ‘Natural history of the coral snake *Micrurus decoratus* (Elapidae) from the Atlantic Forest in southeast Brazil, with comments on possible mimicry.’ *Amphibia-Reptilia*, 23, 228-232.
- Marques, O.A. and Sazima, I., 1997. ‘Diet and feeding behavior of the coral snake, *Micrurus corallinus*, from the Atlantic forest of Brazil.’ *Herpetological Natural History*, 5(1), 88-91.
- Martins, M., Oliveira and M.E., 1998. ‘Natural history of snakes in forests of the Manaus region, Central Amazonia, Bril.’ *Herpetological Natural History*, 6(2), 78-150.

- Matsuhashi, T. and Kyōichi, T. 2007. ‘Nihon no kame tokage hebi.’ *Yamakei handi zukan*, 10, 1-256.
- McCarthy, C.J., 1985. ‘Monophyly of elapid snakes (Serpentes: Elapidae). An assessment of the evidence.’ *Zoological Journal of the Linnean Society*, 83(1), 79-93.
- McDowell, S.B., 1968. ‘Affinities of the snakes usually called *Elaps lacteus* and *E. dorsalis*.’ *Zoological Journal of the Linnean Society*, 47(313), 561-578.
- McLeod, D.S., Siler, C.D., Diesmos, A.C., Diesmos, M.L., Garcia, V.S., Arkonceo, A.O., Balaquit, K.L., Uy, C.C., Villaseran, M.M., Yarra, E.C. and Brown, R.M., 2011. ‘Amphibians and Reptiles of Luzon Island, V: The Herpetofauna of Angat Dam Watershed, Bulacan Province, Luzon Island, Philippines.’ *Asian Herpetological Research*, 2.4, 177-198.
- Melo-Sampaio, P.R., Lima Maciel, J.M., de Oliveira, C.M.B., da Silva Moura, R. and de Lima, L.C.B., 2013. ‘*Micrurus Obscurus* (Black-necked Amazonian Coralsnake). Maximum Size.’ *Herpetological Review*, 44(1), 155
- Meseguer, A.S., Lobo, J.M., Ree, R., Beerling, D.J. and Sanmartín, I., 2015. ‘Integrating fossils, phylogenies, and niche models into biogeography to reveal ancient evolutionary history: the case of Hypericum (Hypericaceae).’ *Systematic Biology*, 64(2), 215-232.
- Meyer, H.V., 1857. ‘Beiträge zur näheren Kenntnis fossiler Reptilien.’ *Neues Jahrbuch für Mineralogie, Geologie, Paläontologie*, 103-104.
- Minton, S.A., 1966. ‘A contribution to the herpetology of West Pakistan.’ *Bull. Amer. Mus. Nat. Hist.*, 134(2), 143-152.
- Mole, R.R., 1924. ‘The Trinidad Snakes.’ *Proc. Zool. Soc. London*, 1, 235-278.
- Mole, R.R. and Urich, F.W., 1894. ‘Biological notes upon some of the Ophidia of Trinidad, B.W.I., with a preliminary list of the species recorded from the island.’ *Proc. Zool. Soc. London*, 499-518.
- Moon, B.R., Penning, D.A., Segall, M., Herrel, A., 2019. ‘Feeding in Snakes: Form, Function, and Evolution of the Feeding System.’ *Die Anästhesiologie*, 527-574.
- Mori, A. and Moriguchi, H., 1988. ‘Food habits of the snakes in Japan: a critical review.’ *The Snake*, 20(2), 98-113.
- Morley, R.J., 2011. ‘Cretaceous and Tertiary climate change and the past distribution of megathermal rainforests.’ in Bush, M.B. and Flenley, J.R. (eds.) *Tropical rainforest responses to climatic change*. Berlin, Heidelberg: Springer, 1-34.
- Müller, J. and Tsuji, L.A., 2007. ‘Impedance-matching hearing in Paleozoic reptiles: evidence of advanced sensory perception at an early stage of amniote evolution.’ *PLOS One*, 2(9), e889.
- Muñoz-Saravia, A., Rivas-Torrico, L.R., Gonzales, L. and Quispe, J., 2009. ‘Reptilia, Serpentes, Elapidae, *Micrurus serranus*: distribution extension.’ *Check List*, 5(3), 510-512.

- Murphy, J.C., 1997. *Amphibians and reptiles of Trinidad and Tobago*. Krieger, Malabar.
- Murphy, J.C., 2012. ‘Marine Invasions by Non-Sea Snakes, with Thoughts on Terrestrial-Aquatic-Marine Transitions.’ *Integrative and Comparative Biology*, 52(2), 217-226
- Myers, C.W., 1965. ‘Biology of the ringneck snake, *Diadophis punctatus*, in Florida.’ *Bulletin of the Florida State Museum*, 10(2), 43-90.
- Nagy, Z.T., Joger, U., Wink, M., Glaw, F. and Vences, M., 2003. ‘Multiple colonization of Madagascar and Socotra by colubrid snakes: evidence from nuclear and mitochondrial gene phylogenies.’ *Proceedings of the Royal Society of London. Series B: Biological Sciences*, 270(1533), 2613-2621.
- Nilson, Göran and Rastegar-Pouyani, N., 2007. ‘*Walterinnesia aegyptia* Lataste, 1887 (Ophidia: Elapidae) and the status of *Naja morgani* Mocquard 1905.’ *Russian Journal of Herpetology*, 14(1), 7-14.
- Nock, C.J., 2001. *Molecular Phylogenetics of the Australian Elapid Snakes:(Serpentes: Elapidae, Hydrophiinae)*. Master’s Thesis, Southern Cross University.
- Obrecht, C.B., 1946. ‘Notes on South Carolina reptiles and amphibians.’ *Copeia*, 2, 71-74.
- Ohara, Y. 2013. ‘Ha i ni yo ru a ma mi ta ka chihohébi no hoshoku kōdō no kansatsu.’ *Akamata*, 24, 1-2.
- Olson, E.C., 1947. ‘The family Diadectidae and its bearing on the classification of reptiles.’ *Fieldiana: Geology*, 11(1), 1-53.
- Osborn, H.F., 1903. ‘On the primary division of the Reptilia into two sub-classes, Synapsida and Diapsida.’ *Science*, 17(424), 275-276.
- Ōta, H. 2014. ‘Kaitei zōho-ban Nihon no zetsumetsu kigu seibutsu,’ in Kankyōshō (ed.) *Reddodētabukku. Ryōseirui hachūrui*. Tokyo.
- Papenfuss, T.J., 1982. ‘The ecology and systematics of the amphisbaenian genus *Bipes*.’ *Occas. Pap. California Acad. Sci.*, 136: 1-42.
- Passos, P. and Fernandes, D.S., 2005. ‘Variation and taxonomic status of the aquatic coral snake *Micruurus surinamensis* (Cuvier, 1817)(Serpentes: Elapidae).’ *Zootaxa*, 953(1), 1-8.
- Peng, L., Wang, L., Ding, L., Zhu, Y., Luo, J., Yang, D., Huang, R., Lu, S. and Huang, S., 2018. ‘A new species of the genus *Sinomicrurus* Slowinski, Boundy and Lawson, 2001 (Squamata: Elapidae) from Hainan Province, China.’ *Asian Herpetological Research*, 9(2), 65-73.
- Palci, A., Lee, M.S. and Hutchinson, M.N., 2016. ‘Patterns of postnatal ontogeny of the skull and lower jaw of snakes as revealed by micro-CT scan data and three-dimensional geometric morphometrics.’ *Journal of Anatomy*, 229(6), 723-754.

- Palci, A., Caldwell, M.W., Hutchinson, M.N., Konishi, T., Lee, M.S.Y., 2020. 'The morphological diversity of the quadrate bone in squamate reptiles as revealed by high-resolution computed tomography and geometric morphometrics.' *Journal of Anatomy*, 236(2), 210-227.
- Popov, S.V., Rozanov, A.Y., Rögl, F., Steininger, F.F., Shcherba, I.G. and Kovac, M., 2004. 'Lithological-paleogeographic maps of paratethys: 10 maps Late Eocene to Pliocene.' *Courier Forschungsinstitut Senckenberg*, 1-46.
- Pyron, R., Burbrink, F.T. and Wiens, J.J., 2013. 'A Phylogeny and Revised Classification of Squamata, Including 4161 Species of Lizards and Snakes.' *BMC Evolutionary Biology* 13(1), 93.
- R Core Team, 2021. *R: A language and environment for statistical computing*. R Foundation for Statistical Computing, Vienna, Austria.
- Rage, J.C., 1984. *Serpentes*. Handbuch der Paläoherpetologie Teil 11. Gustav Fischer Verlag, Stuttgart.
- Rage, J.C. and Holman, J.A., 1984. 'Des serpents (Reptilia, Squamata) de type nord-américain dans le Miocène Français. Évolution parallèle ou dispersion?' *Geobios*, 17(1), 89-104.
- Rahman, M.M., Ahsan, M.F., Al Haidar, I.K. and Islam, M.A., 2017. 'First Confirmed Record of the MacClelland 's Coral Snake *Sinomicrurus maclellandi* (Reinhardt, 1844) from Bangladesh.' *Russian Journal of Herpetology* 24(3), 241-244.
- Rambaut, A., Drummond, A.J., Xie, D., Baele, G. and Suchard, M.A., 2018. 'Posterior summarisation in Bayesian phylogenetics using Tracer 1.7.' *Systematic Biology* syy032. doi:10.1093/sysbio/syy032
- Ramírez-Bautista, A., 1994. 'Manual y claves ilustradas de los anfibios y reptiles de la región de Chamela, Jalisco, México.' *Instituto de Biología, UNAM, Mexico, Cuadernos*, 23.
- Ray, J.M., 2017. *Snakes of Panama: A Field Guide to All Species*. Team Snake Panama.
- Reams, R.D., Franklin, C.J. and Davis, J.M., 1999. 'Natural history notes: *Micruurus fulvius tener* (Texas coral snake).' *Diet. Herpetol. Rev.*, 30(4), 228-229.
- Reisz, R.R., Müller, J., Tsuji, L. and Scott, D., 2007. 'The cranial osteology of *Belebey vegrandis* (Parareptilia: Bolosauridae), from the Middle Permian of Russia, and its bearing on reptilian evolution.' *Zoological Journal of the Linnean Society*, 151(1), 191-214.
- Reza, Ali M., 2004. 'Realization of the contrast limited adaptive histogram equalization (CLAHE) for real-time image enhancement.' *Journal of VLSI signal processing systems for signal, image and video technology*, 38(1), 35-44.
- Rhoda, D., Polly, P.D., Raxworthy, C. and Segall, M., 2021. 'Morphological integration and modularity in the hyperkinetic feeding system of aquatic-foraging snakes.' *Evolution*, 75(1), 56-72.

- Rodríguez, M.E., Arzamendia, V., Bellini, G.P. and Giraudo, A.R., 2018. ‘Natural history of the threatened coral snake *Micrurus altirostris* (Serpentes: Elapidae) in Argentina.’ *Revista mexicana de biodiversidad*, 89(4), 1255-1262.
- Rodríguez-García, J., Pérez-Higareda, G., Smith, H.M. and Chiszar, D., 1998. ‘Natural history notes: *Micrurus diastema* and *M. limbatus* (diastema coral snake and Tuxtlan coral snake, respectively).’ *Diet. Herpetol. Rev.*, 29(1), 45.
- Rögl, F., 1998. ‘Palaeogeographic considerations for Mediterranean and Paratethys seaways (Oligocene to Miocene).’ *Annalen des Naturhistorischen Museums in Wien. Serie A für Mineralogie und Petrographie, Geologie und Paläontologie, Anthropologie und Prähistorie*, 279-310.
- Rögl, F. 1999., ‘Mediterranean and Paratethys. Facts and hypotheses of an Oligocene to Miocene paleogeography (short overview).’ *Geologica carpathica*, 50(4), 339-349.
- Rojas-Morales, J.A., Cabrera-Vargas, F.A. and Ruiz-Valderrama, D.H., 2018. ‘*Ninia hudsoni* (Serpentes: Dipsadidae) as prey of the coral snake *Micrurus hemprichii ortonii* (Serpentes: Elapidae) in northwestern Amazonia.’ *Boletín Científico. Centro de Museos. Museo de Historia Natural*, 22(1), 102-105.
- Romer, A.S., 1956. *Osteology of the Reptiles*. University of Chicago Press, Chicago.
- Ronquist, F. and Huelsenbeck, J.P., 2003. ‘MRBAYES 3: Bayesian phylogenetic inference under mixed models.’ *Bioinformatics* 19, 1572-1574.
- Roze, J.A., 1982. ‘New World coral snakes (Elapidae): a taxonomic and biological summary.’ *Mem. Inst. Butantan*, 46, 305-338.
- Roze, J.A., 1996. *Coral snakes of the Americas: biology, identification, and venoms*. Krieger, Malabar.
- Roze, J.A., Trebbau, P. 1958. ‘Un nuevo género de corales venenosas (*Leptomicrurus*) para Venezuela.’ *Acta Biológica Venezolana*, 9, 128-130.
- Ruick, J.D., 1948. ‘Collecting coral snakes, *Micrurus fulvius tenere* in Texas.’ *Herpetologica*, 4(6), 215-216.
- Sanders, K.L. and Lee, M.S., 2007. ‘Molecular evidence for a rapid late-Miocene radiation of Australasian venomous snakes (Elapidae, Colubroidea).’ *Molecular Phylogenetics and Evolution* 46(3), 1165-1173.
- Sanders, K.L., Lee, M.S.Y., Leys, R., Foster, R. and Keogh, J.S., 2008. ‘Molecular phylogeny and divergence dates for Australasian elapids and sea snakes (Hydrophiinae): evidence from seven genes for rapid evolutionary radiations.’ *Journal of Evolutionary Biology*, 21(3), 682-695.
- Sazima, I. and Abe, A.S., 1991. ‘Habits of five Brazilian snakes with coral-snake pattern, including a summary of defensive tactics.’ *Studies on Neotropical Fauna and Environment*, 26(3), 159-164.

- Scanlon, J.D., Lee, M.S.Y., Archer, M., 2003. ‘Mid-Tertiary elapid snakes (Squamata, Colubroidea) from Riversleigh, northern Australia: early steps in a continent-wide adaptive radiation.’ *Geobios*, 36(5), 573-601.
- Schlager, S., 2017. ‘Morpho and Rvcg - Shape Analysis in R,’ in Zheng, G., Li, S., Szekely, G. (eds.) *Statistical Shape and Deformation Analysis*. Academic Press, 217-256.
- Schmidt, K.P., 1932. ‘Stomach contents of some American coral snakes, with the description of a new species of *Geophis*.’ *Copeia*, 1, 6-9.
- Schmidt, K.P., 1952. ‘The Surinam Coral Snake: *Micrurus Surinamensis*.’ *Fieldiana Zoology*, 34(4), 25-34.
- Schmidt, K.P., 1953. ‘Hemprich ‘s coral snake *Micrurus hemprichii*.’ *Fieldiana Zoology*, 34, 165-170.
- Schmidt, K.P., 1953b. ‘The Amazonian Coral Snake: *Micrurus Spixi*.’ *Fieldiana Zoology*, 34(14), 171-180.
- Schmidt, K.P., 1954. ‘The Annellated Coral Snake: *Micrurus Annellatus* Peters.’ *Fieldiana Zoology*, 34(30), 319-325.
- Schmidt, K.P. and Smith, H.M., 1943. ‘Notes on coral snakes from Mexico.’ *Publication. Field Museum of Natural History. Zoological series*. 29(2): 25-31.
- Schneider, C.A., Rasband, W.S. and Eliceiri, K., 2012. ‘NIH Image to ImageJ: 25 years of image analysis.’ *Nature methods*, 9(7), 671-675.
- Schoch, R.R., 2014. ‘Amphibian skull evolution: the developmental and functional context of simplification, bone loss and heterotopy.’ *Journal of Experimental Zoology Part B: Molecular and Developmental Evolution*, 322(8), 619-630.
- Schwaner, T.D., Baverstock, P.R., Dessauer, H.C. and Mengden, G.A., 1985. ‘Immunological evidence for the phylogenetic relationships of Australian elapid snakes,’ in Grigg, G., Shine, R., Ehmann, H. (eds.) *Biology of Australasian Frogs and Reptiles*. Sydney: Surrey Beatty and Sons, 177-184.
- Segall, M., Cornette, R., Fabre, A.C., Godoy-Diana, R., Herrel, A., 2016. ‘Does aquatic foraging impact head shape evolution in snakes?’ *Proceedings of the Royal Society B-Biological Sciences*, 283(1837).
- Segall, M., Cornette, R., Godoy-Diana, R. and Herrel, A., 2020. ‘Exploring the functional meaning of head shape disparity in aquatic snakes.’ *Ecology and Evolution*, 10(14), 6993-7005.
- Seib, R.L., 1985. *Feeding ecology and organization of Neotropical snake faunas*. University of California at Berkeley, PhD dissertation.
- Shankar, P.G. and Ganesh, S.R., 2009. ‘Sighting record and range extension of *Calliophis*.’ *Herpetological bulletin*, 108, 10-13.

- Sherratt, E., Coutts, F.J., Rasmussen, A.R. and Sanders, K.L., 2019. ‘Vertebral evolution and ontogenetic allometry: The developmental basis of extreme body shape divergence in microcephalic sea snakes.’ *Evolution and Development*, 21(3), 135-144.
- Sherratt, E., Rasmussen, A.R. and Sanders, K.L., 2018. ‘Trophic specialization drives morphological evolution in sea snakes.’ *Royal Society Open Science*, 5(3).
- Shu, D.G., Luo, H.L., Morris, S.C., Zhang, X.L., Hu, S.X., Chen, L., Han, J.I., Zhu, M., Li, Y. and Chen, L.Z., 1999. ‘Lower Cambrian vertebrates from south China.’ *Nature*, 402(6757), 42.
- Silva, A., Jayakody, S., Ranasinghe, N., Manawaduge, A. and Perera, K., 2020. ‘First Authenticated Case of a Bite by Rare and Elusive Blood-Bellied Coral Snake (*Calliophis haematoetron*).’ *Wilderness and Environmental Medicine*, 31(4), 466-469.
- Silva, F.M., Prudente, A.L.U.D., Machado, F.A., Santos, M.M., Zaher, H., Hingst-Zaher, E., 2018. ‘Aquatic adaptations in a Neotropical coral snake: A study of morphological convergence.’ *Journal of Zoological Systematics and Evolutionary Research*, 56(3), 382-394.
- da Silva, F. O., Fabre, A.-C., Savriama, Y., Ollonen, J., Mahlow, K., Herrel, A., Müller, J., Di-Poï, N., 2018. ‘The ecological origins of snakes as revealed by skull evolution.’ *Nature Communications*, 9(1).
- da Silva, N.J. Jr., 1993. ‘The snakes from Samuel hydroelectric power plant and vicinity, Rondonia, Brazil.’ *Herpetol. Nat. Hist.*, 1, 37-86.
- Smart, U., 2016. *Tracing The Dawn of The Elapidae Through the Molecular Systematics and Historical Biogeography of Old World Coralsnakes*. University of Texas at Arlington, PhD dissertation.
- Smart, U., Ingrasci, M.J., Sarker, G.C., Lalremsanga, H., Murphy, R.W., Ota, H., Tu, M.C., Shouche, Y., Orlov, N.L. and Smith, E.N., 2021. ‘A comprehensive appraisal of evolutionary diversity in venomous Asian coralsnakes of the genus *Sinomicrurus* (Serpentes: Elapidae) using Bayesian coalescent inference and supervised machine learning.’ *Journal of Zoological Systematics and Evolutionary Research*. 00, 1-66.
- Smith, E.N., 1994. *Biology of the snake fauna of the Caribbean rainforest of Guatemala*. University of Texas at Arlington, Master’s thesis.
- Smith, E.N., Manamendra-Arachchi, K. and Somaweera, R., 2008. ‘A new species of coralsnake of the genus *Calliophis* (Squamata: Elapidae) from the Central Province of Sri Lanka.’ *Zootaxa*, 1847(1), 19-33.
- Smith, H.M., Rozella B.S. and Sawin, H.L., 1977. ‘A summary of snake classification (Reptilia, Serpentes).’ *Journal of Herpetology*, 115-121.
- Smith, H.M. and Grant, C., 1958. ‘New and noteworthy snakes from Panama.’ *Herpetologica*, 14(4), 207-215.

- Smith, M.A., 1926. *Monograph of the sea-snakes (Hydrophiidae)*. London: Printed by order of the Trustees of the British museum.
- Smith, M.A., 1935. ‘The sea snakes (Hydrophiidae).’ *Dana Report*, 8(6).
- Slowinski, J.B., 1994. ‘A phylogenetic analysis of *Bungarus* (Elapidae) based on morphological characters.’ *Journal of Herpetology*, 440-446.
- Slowinski, J.B., 1995. ‘A phylogenetic analysis of the New World coral snakes (Elapidae: *Leptomicrurus*, *Micruroides*, and *Micrurus*) based on allozymic and morphological characters.’ *Journal of Herpetology*, pp.325-338.
- Slowinski, J.B., Knight, A. and Rooney, A.P., 1997. ‘Inferring species trees from gene trees: a phylogenetic analysis of the Elapidae (Serpentes) based on the amino acid sequences of venom proteins.’ *Molecular phylogenetics and evolution*, 8(3), 349-362.
- Slowinski, J.B., Boundy, J. and Lawson, R., 2001. ‘The phylogenetic relationships of Asian coral snakes (Elapidae: *Calliophis* and *Maticora*) based on morphological and molecular characters.’ *Herpetologica*, 233-245.
- Soini, P., 1974a. ‘Polychromatism in a population of *Micrurus langsdorffi*.’ *J. Herpetol.* 8(3), 267-269.
- Soini, P., 1974b. Ofidios venenosos del nor-oriente peruano. Unpublished ms. 93
- Solórzano, A. 2004. *Serpientes de Costa Rica*. Universidad de Costa Rica, San José.
- Solórzano, A. 2005. ‘A fish prey found in the coral snake *Micrurus alleni* (Serpentes: Elapidae) in Costa Rica.’ *Revista de biología tropical*, 53(1-2), 227-228.
- Sosa, R., Braga, L., Schalk, C.M. and Pinto Ledezma, J.N., 2013. ‘*Micrurus Serranus* (Coral Verdadera). Diet.’ *Herpetological Review*, 44(1), 15.
- de Sousa, B.M., Gomides, S.C., Hudson, A.D.A., Ribeiro, L.B. and Novelli, I.A., 2012. ‘Reptiles of the municipality of Juiz de Fora, Minas Gerais state, Brazil.’ *Biota Neotropica*, 12, 35-49.
- Souza, S.M., Junqueira, A.B., Jakovac, A.C.C., Assunção, P.A. and Correia, J.A., 2011. ‘Feeding behavior and ophiophagous habits of two poorly known Amazonian coral snakes, *Micrurus albicinctus* Amaral 1926 and *Micrurus paraensis* Cunha and Nascimento 1973 (Squamata, Elapidae).’ *Herpetology notes*, 4, 369-372.
- Spakman, W. and Hall, R., 2010. ‘Surface deformation and slab-mantle interaction during Banda arc subduction rollback.’ *Nature Geoscience*, 3(8), 562-566.
- Spawls, S., Howell K.H. and Drewes, R.C., 2006. *Reptiles and Amphibians of East Africa*. Princeton Pocket Guides.
- Spawls, S., Howell, K.H., Drewes, R.C. and Ashe, J., 2004. *Reptiles and Amphibians of East Africa: Kenya, Tanzania, Uganda, Rwanda and Burundi*. London.

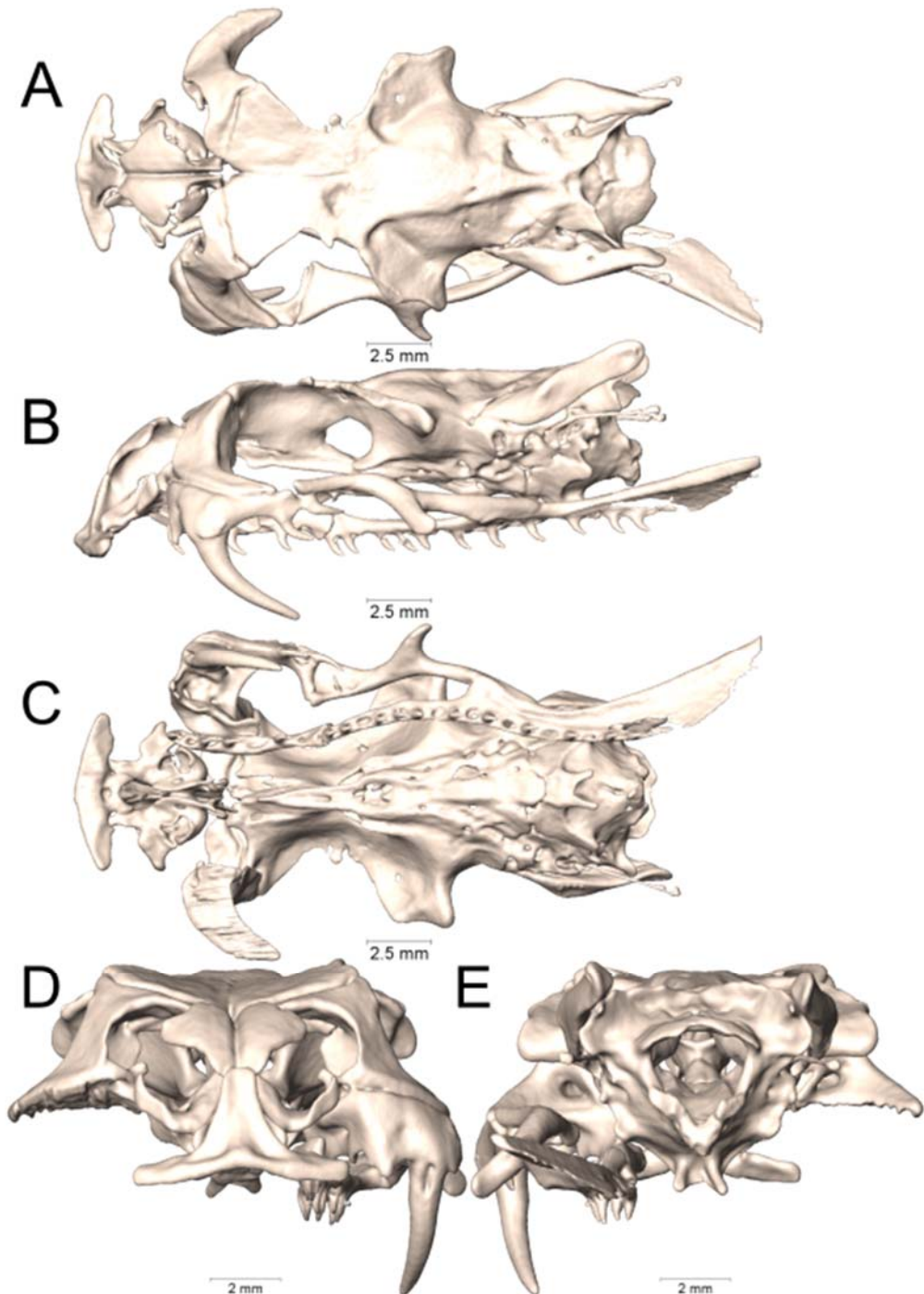
- Spencer, C.L., Koo, M.S. and Slowinski, J.B., 1999. 'Natural history notes: *Micrurus browni browni* (Brown 's coral snake).' *Diet. Herpetol. Rev.* 30(3), 169.
- Stechert, R. 1980., 'Observations on northeastern snake dens.' *Bulletin of the New York Herpetological Society*, 15, 7-14.
- Stuebing, R.B., Inger, R.F. and Tan, F.L. 2014., *Field guide to the snakes of Borneo*, 2nd ed. Natural History Publications, Borneo.
- Suazo-Ortuño, I., Flores-Villela, O. and García-Parra, D., 2004. 'Micrurus distans (West Mexican Coral Snake). Tree climbing.' *Herpetological Review*, 35(3), 276.
- Takahashi, K. and Ota, H. 1995. 'Ryūkyūdaigaku hakubutsukan no hebi-rui hyōhon yori e rareta hanshoku shokusei bunpu ni kansuru chiken.' *Hachū ryō serrui-gaku zasshi*, 16(2), 74.
- Tassy, P., 1990. 'The 'Proboscidean Datum Event:' How many proboscideans and how many events?' *European Neogene mammal chronology*, 237-252. Springer, Boston.
- Terribile, L.C., Feitosa, D.T., Pires, M.G., de Almeida, P.C.R., de Oliveira, G., Diniz-Filho, J.A.F. and Silva, N.J., 2018. 'Reducing Wallacean shortfalls for the coralsnakes of the *Micrurus lemniscatus* species complex: Present and future distributions under a changing climate.' *PloS One*, 13: e0205164.
- Tsuji, L.A. and Müller, J., 2009. 'Assembling the history of the Parareptilia: phylogeny, diversification, and a new definition of the clade.' *Fossil Record*, 12(1), 71-81.
- Tweedie, M.W.F., 1983. *The Snakes of Malaya*. Singapore National Printers, Singapore.
- Tyler, M.J., 1979. 'Herpetofaunal relationships of South America with Australia,' in Duellman, W.E. (ed.) *The South American Herpetofauna: Its Origins, Evolution and Dispersal*. University of Kansas, 73-106.
- Uğurtaş, I.H., Papenfuss, T.J. and Orlov, N.L., 2001. 'New record of *Walterinnesia aegyptia* Lataste, 1887 (Ophidia: Elapidae: Bungarinae) in Turkey.' *Russian Journal of Herpetology*, 8(3), 239-245.
- Uetz, P. and Etzold, T., (1996) 'The EMBL/EBI Reptile Database.' *Herpetological Review*, 27(4), 174-175.
- Underwood, G., 1967. *A Contribution to the Classification of Snakes*. Trustees British Museum (Natural History), London.
- Underwood, G. and Kochva, E., 1993. 'On the affinities of the burrowing asps *Atractaspis* (Serpentes: Atractaspididae).' *Zoological Journal of the Linnean Society*, 107(1), 3-64.
- Urdaneta, A.H., Bolaños, F. and Gutiérrez, J.M., 2004. 'Feeding behavior and venom toxicity of coral snake *Micrurus nigrocinctus* (Serpentes: Elapidae) on its natural prey in captivity.' *Comparative Biochemistry and Physiology Part C: Toxicology and Pharmacology*, 138(4), 485-492.

- van Hinsbergen, D.J., Lippert, P.C., Dupont-Nivet, G., McQuarrie, N., Doubrovine, P.V., Spakman, W. and Torsvik, T.H., 2012. 'Greater India Basin hypothesis and a two-stage Cenozoic collision between India and Asia.' *Proceedings of the National Academy of Sciences*, 109(20), 7659-7664.
- van Hinsbergen, D.J., Lippert, P.C., Li, S., Huang, W., Advokaat, E.L. and Spakman, W., 2019. 'Reconstructing Greater India: Paleogeographic, kinematic, and geodynamic perspectives.' *Tectonophysics*, 760, 69-94.
- Valencia, J.H., Garzón-Tello, K., Barragán-Paladines, M.E. and Oxford, P., 2016. *Serpientes venenosas del Ecuador: sistemática, taxonomía, historia natural, conservación, envenenamiento y aspectos antropológicos*. Fundación Herpetológica Gustavo Orcés and Fondo Ambiental Nacional, Quito, Ecuador; Texas University, Arlington, Texas.
- Vanzolini, P.E., 1986. 'Levantamento herpetológico da área do estado de Rondônia sob a influência da Rondonia BR 363.' *Progr. Polonoroeste Relat. de Pesq.*, 1, 1-50.
- Viana, P.F., de Mello Mendes, D.M., 2015. 'Feeding behavior and first record of *Rhinatremabivittatum* (Guérin-Méneville, 1829) as part of the diet of the ribbon coral snake, *Micrurus lemniscatus* (Linnaeus, 1758) in the Central Amazon region (Serpentes: Elapidae).' *Herpetology Notes*, 8, 45-447.
- Vidal, N., Branch, W.R., Pauwels, O.S., Hedges, S.B., Broadley, D.G., Wink, M., Cruaud, C., Joger, U. and Nagy, Z.T., 2008. 'Dissecting the major African snake radiation: a molecular phylogeny of the Lamprophiidae Fitzinger (Serpentes, Caenophidia).' *Zootaxa* 1945, 51-66.
- Vincent, S.E., Brändle, M.C., Herrel, A. and Alfaro, M.E., 2009. 'Convergence in trophic morphology and feeding performance among piscivorous natricine snakes.' *Journal of Evolutionary Biology*, 22, 1203-1211.
- Visser, J., 1967. 'Color varieties, brood size, and food of South African *Pelamis platurus* (Ophidia: Hydrophiidae).' *Copeia*, 1, 219.
- Vitt, L.J. and Hulse, A.C., 1973. 'Observations on feeding habits and tail display of the Sonoran coral snake, *Micruroides euryxanthus*.' *Herpetologica*, 302-304.
- Volsøe, H., 1939. 'The sea-snakes of the Iranian Gulf and the Gulf of Oman with a Summary of the Biology of the Sea Snakes,' in Jensen, K. and Sparck, R. (eds) *Danish Scientific Investigation in Iran*, Part 1, Copenhagen, 9-45.
- Voris, H.K., 1972. 'The role of sea snakes (Hydrophiidae) in the trophic structure of coastal ocean communities.' *J Mar Biol Assoc India*, 14, 429-442.
- Wall, F., 1921. *Ophidia Taprobanica; Or, the Snakes of Ceylon*. Colombo.
- Wang, T. and Abe, A.S., 1994. 'Oxygen uptake in snakes: is there a reduction in fossorial species?' *Comparative Biochemistry and Physiology Part A: Physiology*, 107(3), 483-485.

- Watanabe, A., Fabre, A.C., Felice, R.N., Maisano, J.A., Müller, J., Herrel, A. and Goswami, A., 2019. ‘Ecomorphological diversification in squamates from conserved pattern of cranial integration.’ *Proceedings of the National Academy of Sciences*, 116(29), 14688-14697.
- Wehekind, L., 1955. ‘Notes on the foods of the Trinidad snakes.’ *British Journal of Herpetology*, 2, 9-13.
- West, T.R., Schramer, T.D., Kalki, Y. and Wylye, D.B., 2019. ‘Dietary Notes on the Variable Coral Snake, *Micruurus diastema* (Duméril, Bibron and Duméril, 1854).’ *Bulletin of the Chicago Herpetological Society*, 54(1), 4-8.
- Westoll, T. S., 1938. ‘Ancestry of the tetrapods.’ *Nature*, 141(3559), 127.
- White, H.P., 1996. ‘Snakes,’ in Descotes, J. (ed.) *Human toxicology*. Elsevier Science B.V., 757-802.
- Whitaker, R. and Captain, A., 2004. *Snakes of India: The Field Guide*. Draco Books.
- Williston, S.W., 1917. ‘The phylogeny and classification of reptiles.’ *The Journal of Geology*, 25(5), 411-421.
- Wüster, W., Crookes, S., Ineich, I., Mané, Y., Pook, C.E., Trape, J.-F. and Broadley, D.G., 2007. ‘The phylogeny of cobras inferred from mitochondrial DNA sequences: evolution of venom spitting and the phylogeography of the African spitting cobras (Serpentes: Elapidae: *Naja nigricollis* complex).’ *Molecular phylogenetics and evolution*, 45(2), 437-453.
- Zaher, H., Murphy, R.W., Arredondo, J.C., Graboski, R., Machado-Filho, P.R., Mahlow, K., Montingelli G.G., Quadros, A.B., Orlov, N.L., Wilkinson, M., Zhang, Y.-P. and Grazziotin, F.G., 2019. ‘Large-Scale Molecular Phylogeny, Morphology, Divergence-Time Estimation, and the Fossil Record of Advanced Caenophidian Snakes (Squamata: Serpentes).’ *PLOS One* 14(5).
- Zheng, Y. and Wiens, J.J., 2016. ‘Combining phylogenomic and supermatrix approaches, and a time-calibrated phylogeny for squamate reptiles (lizards and snakes) based on 52 genes and 4162 Species’. *Molecular Phylogenetics and Evolution* 94, 537-547.

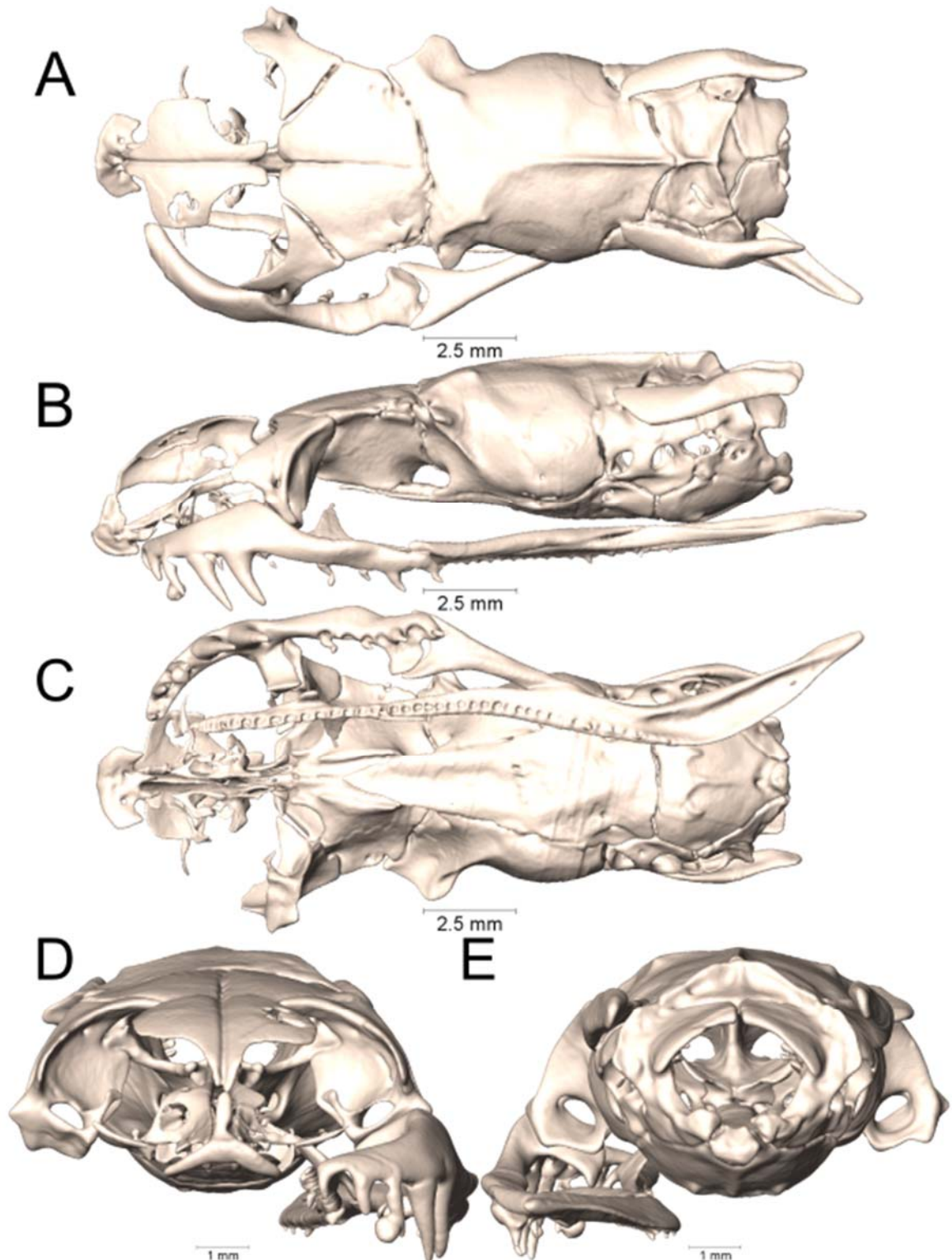
APPENDIX

Supplemental Figures

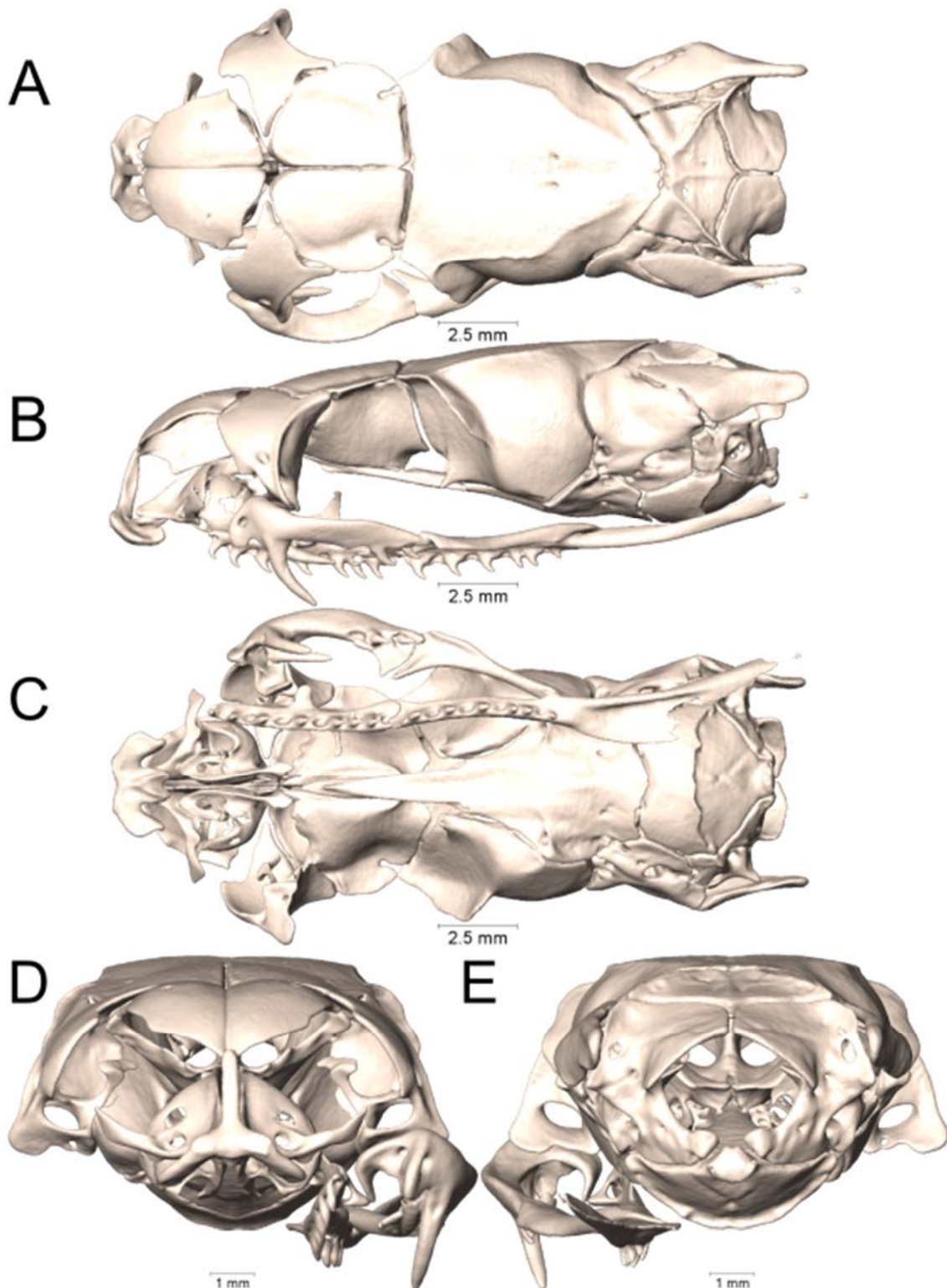


Supplemental Figure 1.1. Dorsal, lateral, ventral, anterior, and posterior views (A-E, respectively)

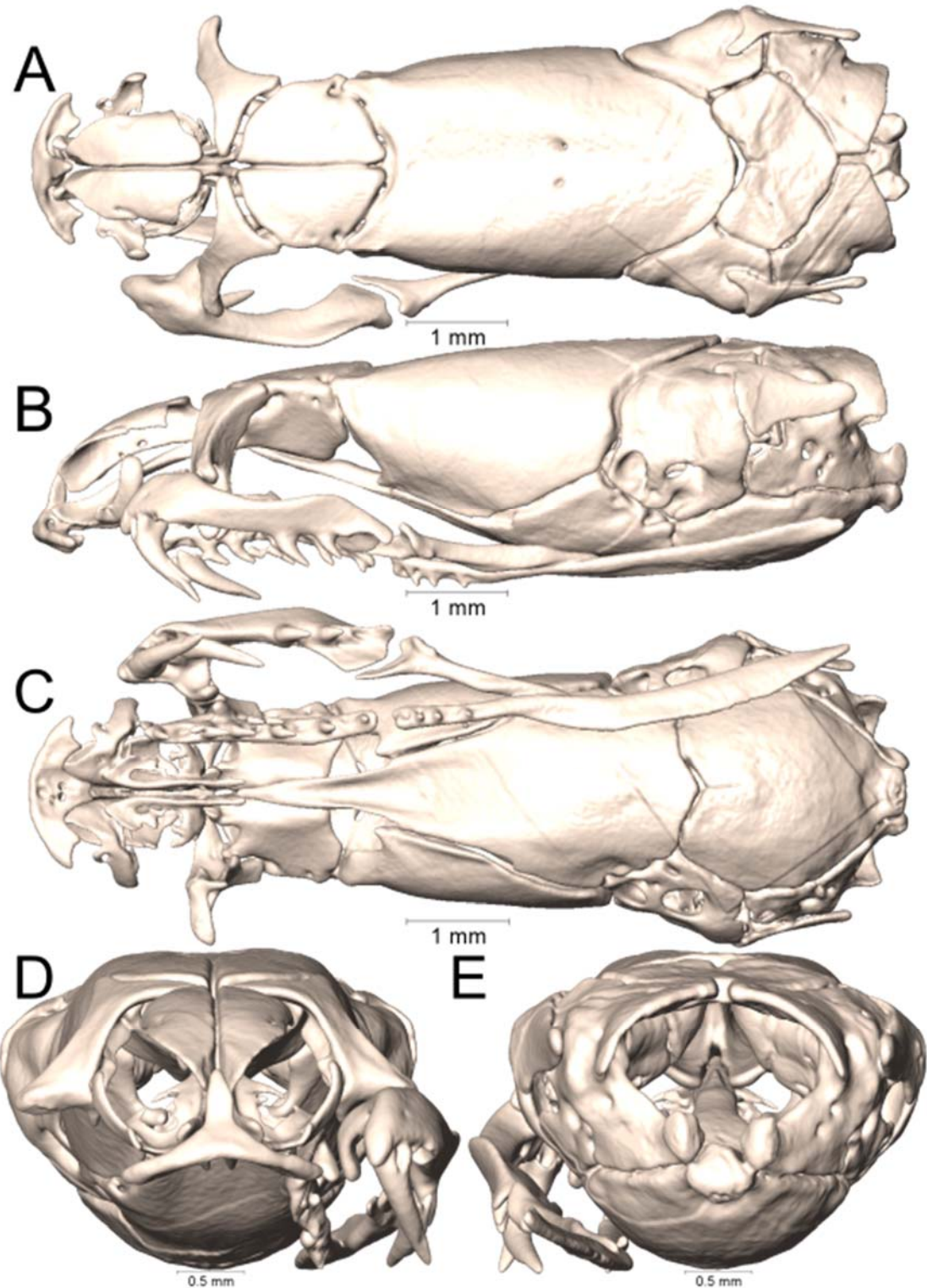
of the skull of *Acanthophis antarcticus* (UTA R-7623). Right suspensorium excluded.



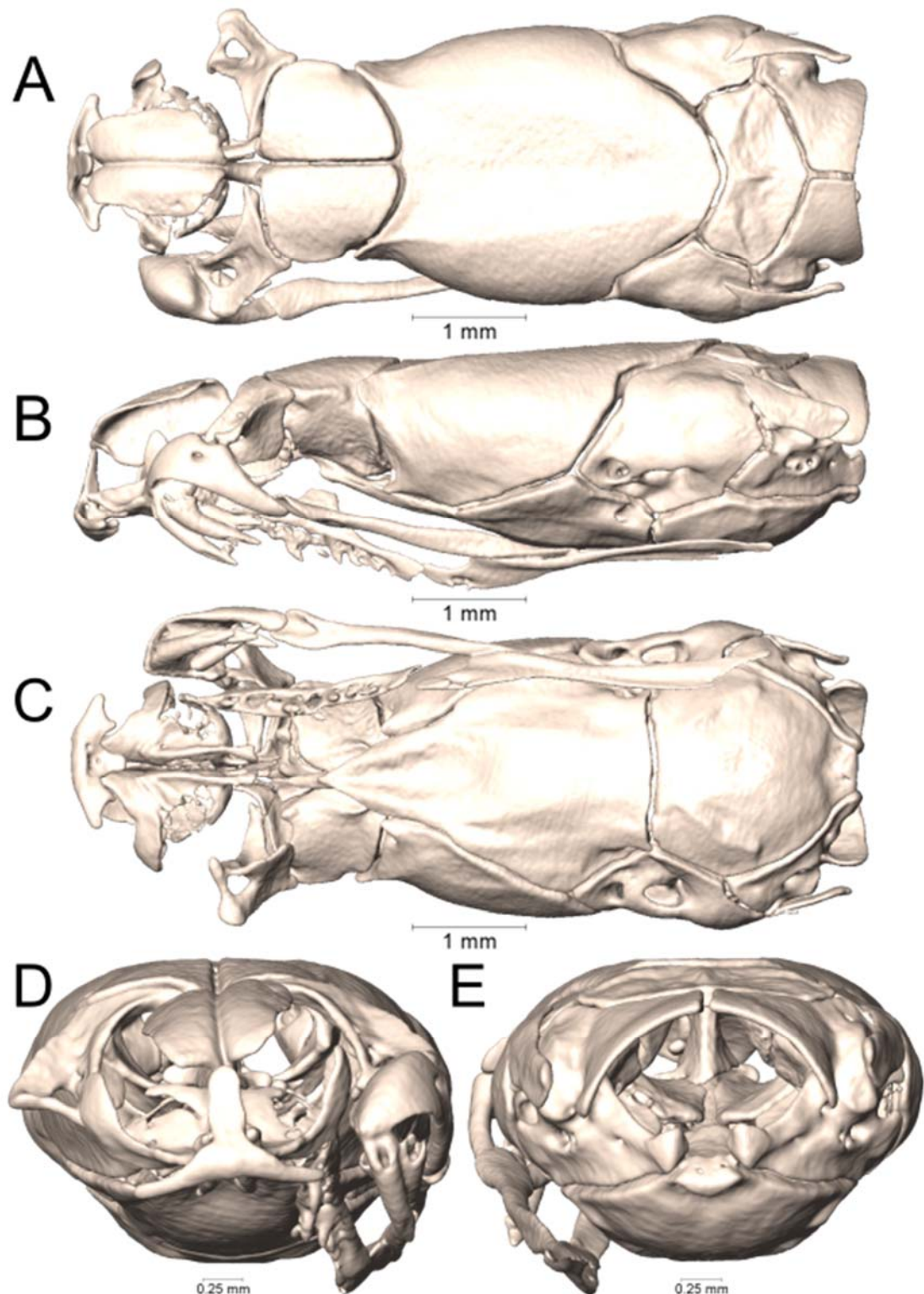
Supplemental Figure 1.2. Dorsal, lateral, ventral, anterior, and posterior views (A-E, respectively) of the skull of *Bungarus candidus* (UTA R-65799). Right suspensorium excluded.



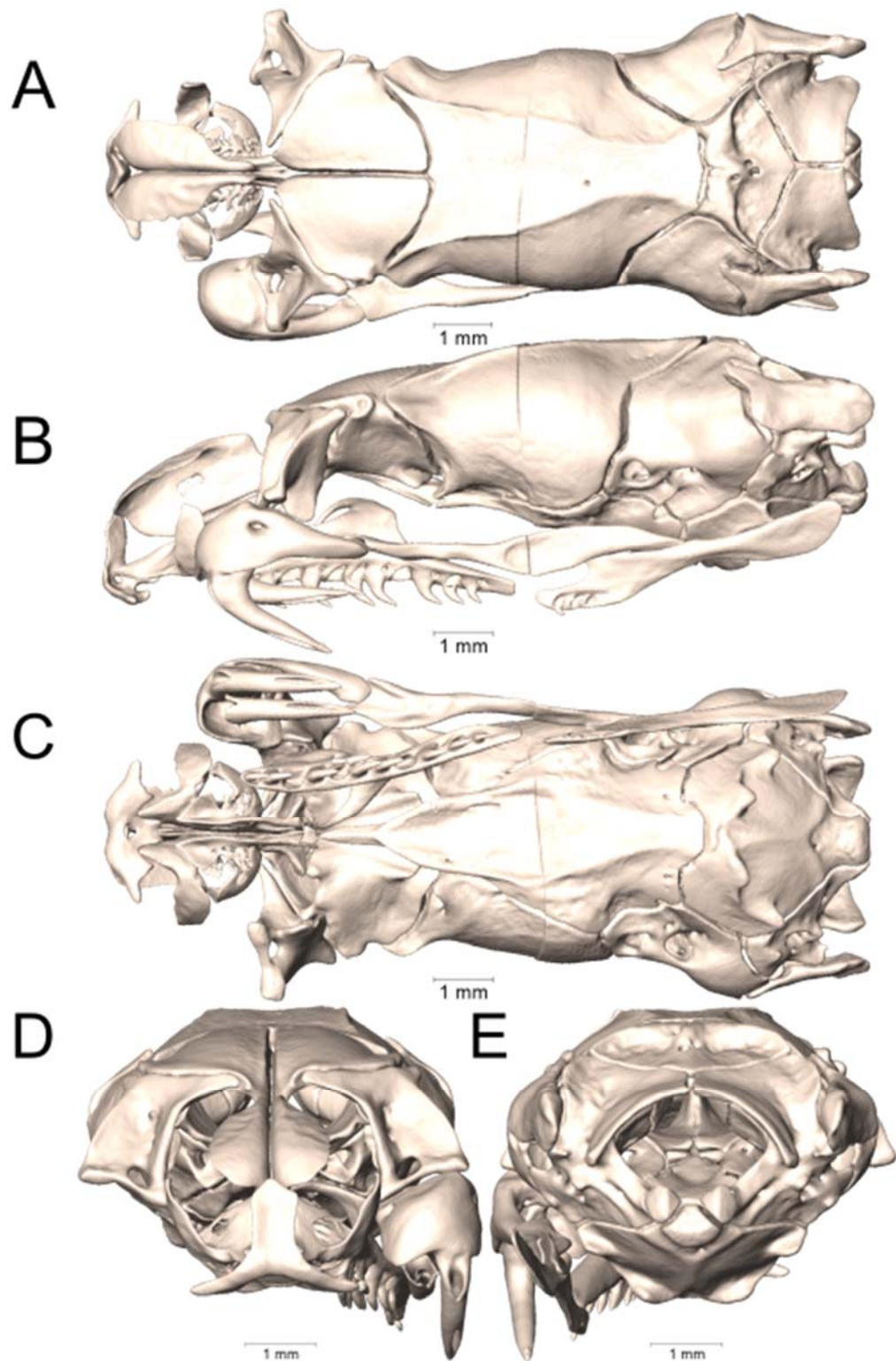
Supplemental Figure 1.3. Dorsal, lateral, ventral, anterior, and posterior views (A-E, respectively) of the skull of *Bungarus flaviceps* (UTA R-62257). Right suspensorium excluded.



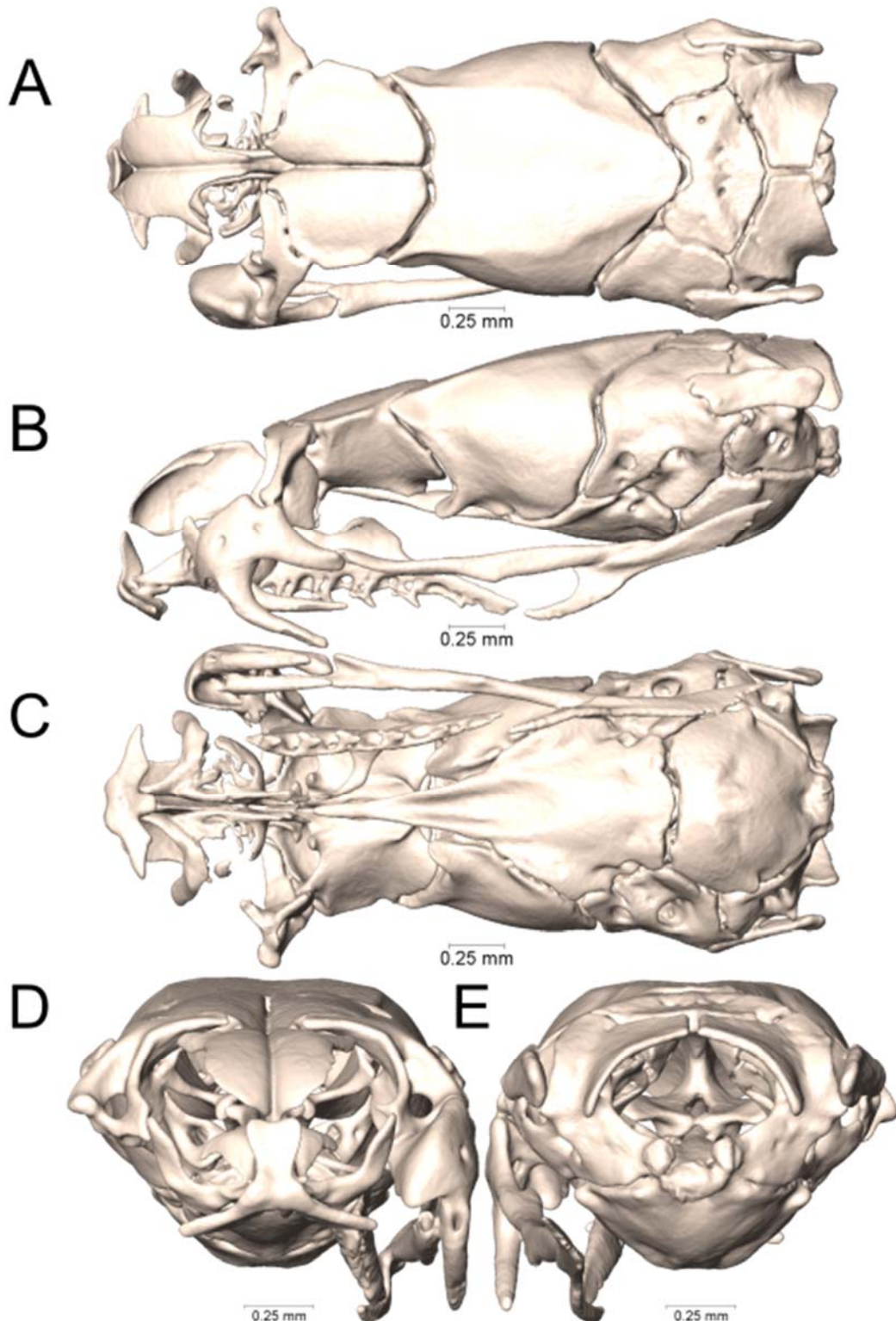
Supplemental Figure 1.4. Dorsal, lateral, ventral, anterior, and posterior views (A-E, respectively) of the skull of *Calliophis beddomei* (MNHN 46-81). Right suspensorium excluded.



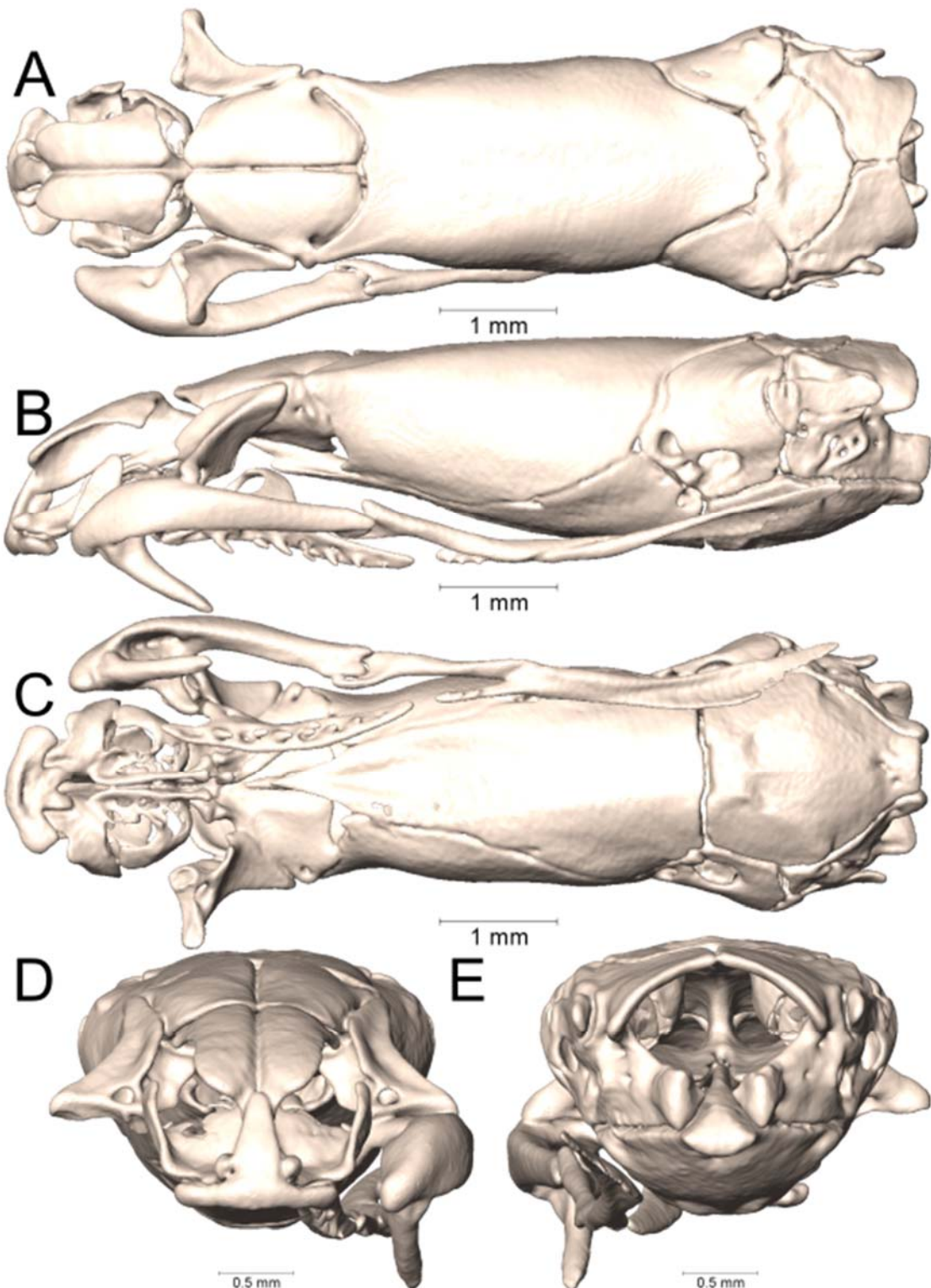
Supplemental Figure 1.5. Dorsal, lateral, ventral, anterior, and posterior views (A-E, respectively) of the skull of *Calliophis biliniatus* (KU 309511). Right suspensorium excluded.



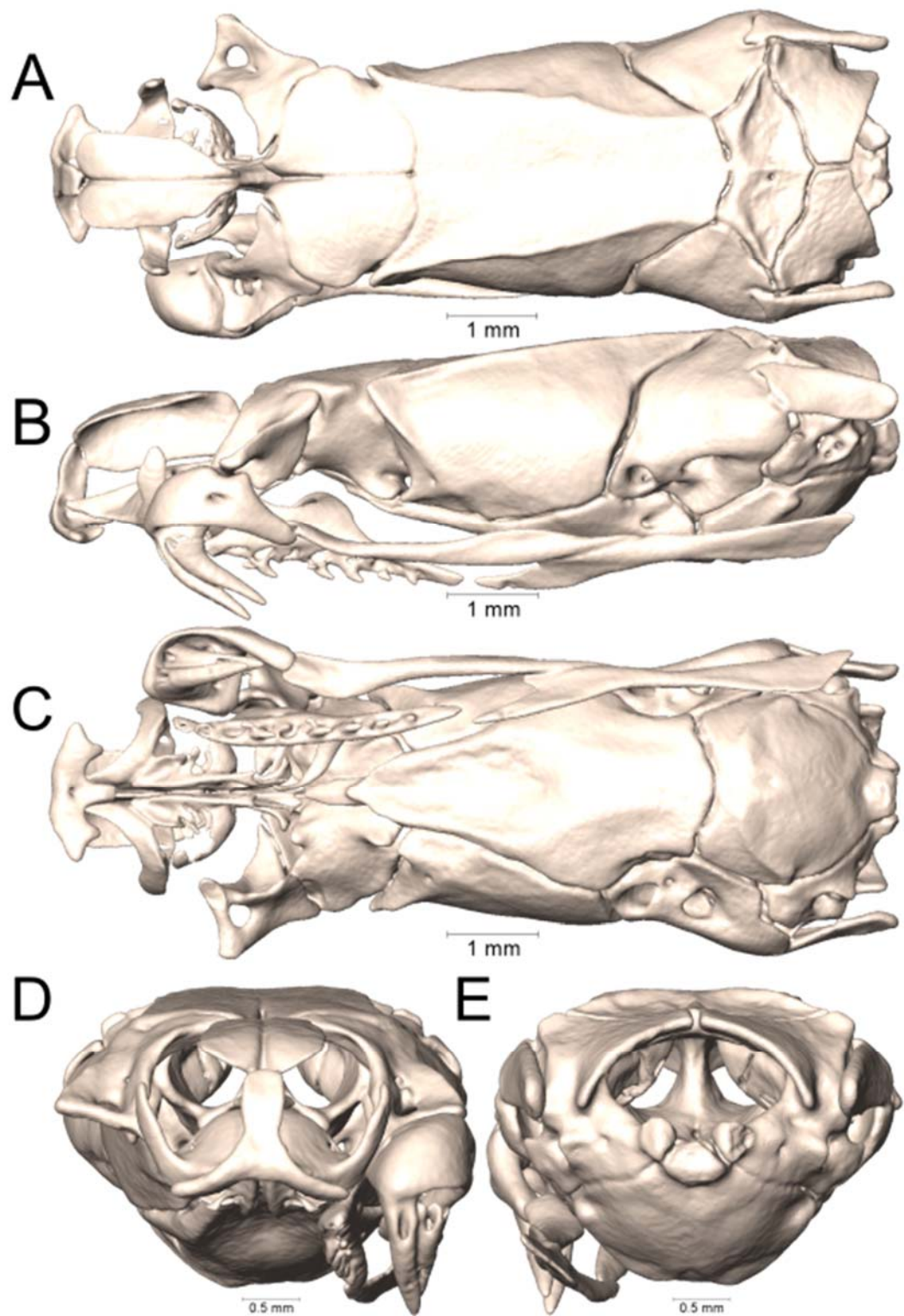
Supplemental Figure 1.6. Dorsal, lateral, ventral, anterior, and posterior views (A-E, respectively) of the skull of *Calliophis biliniatus* (KU 311415). Right suspensorium excluded.



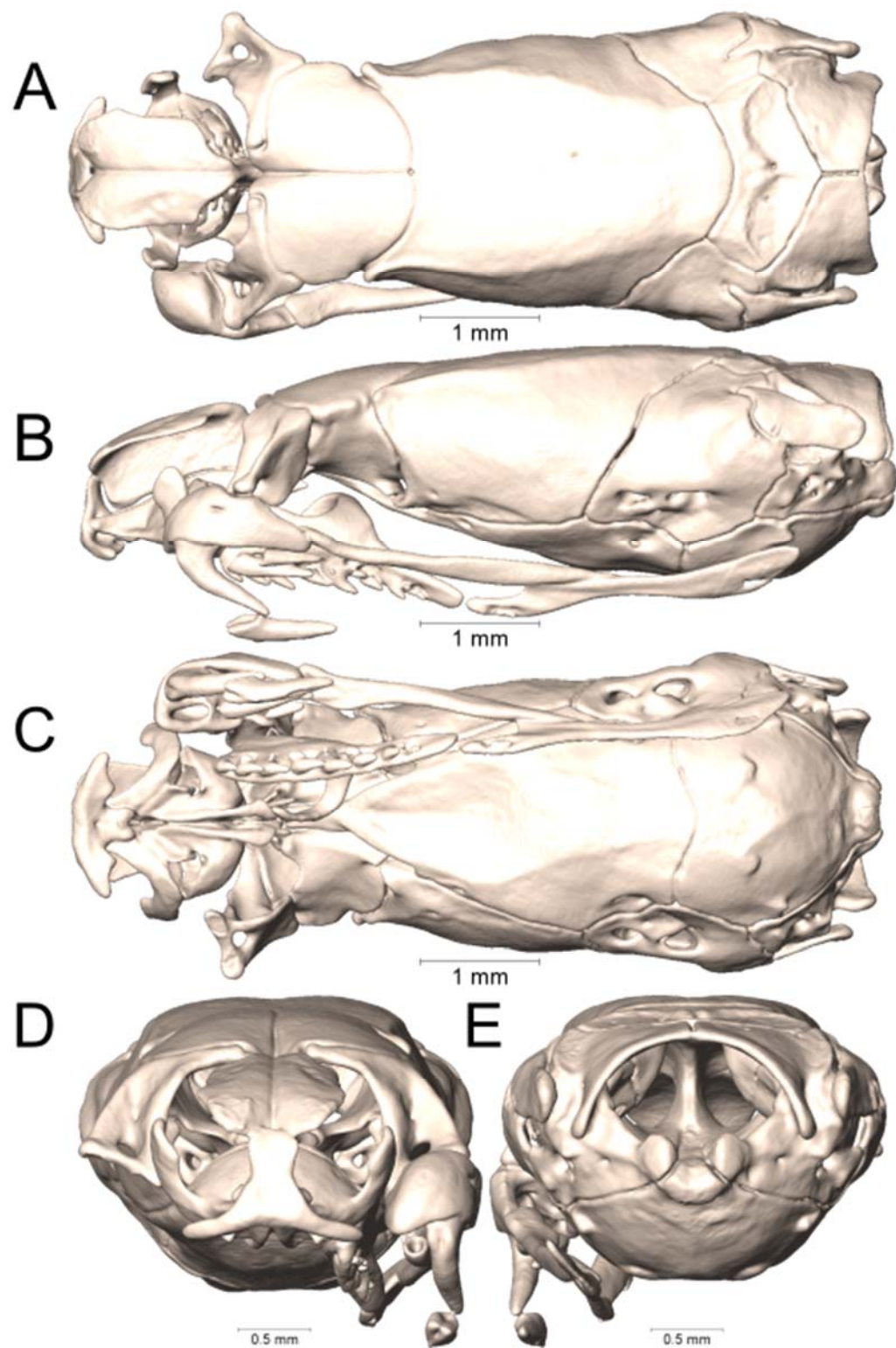
Supplemental Figure 1.7. Dorsal, lateral, ventral, anterior, and posterior views (A-E, respectively) of the skull of *Calliophis bivirgatus bivirgatus* (UTA R-63079). Right suspensorium excluded.



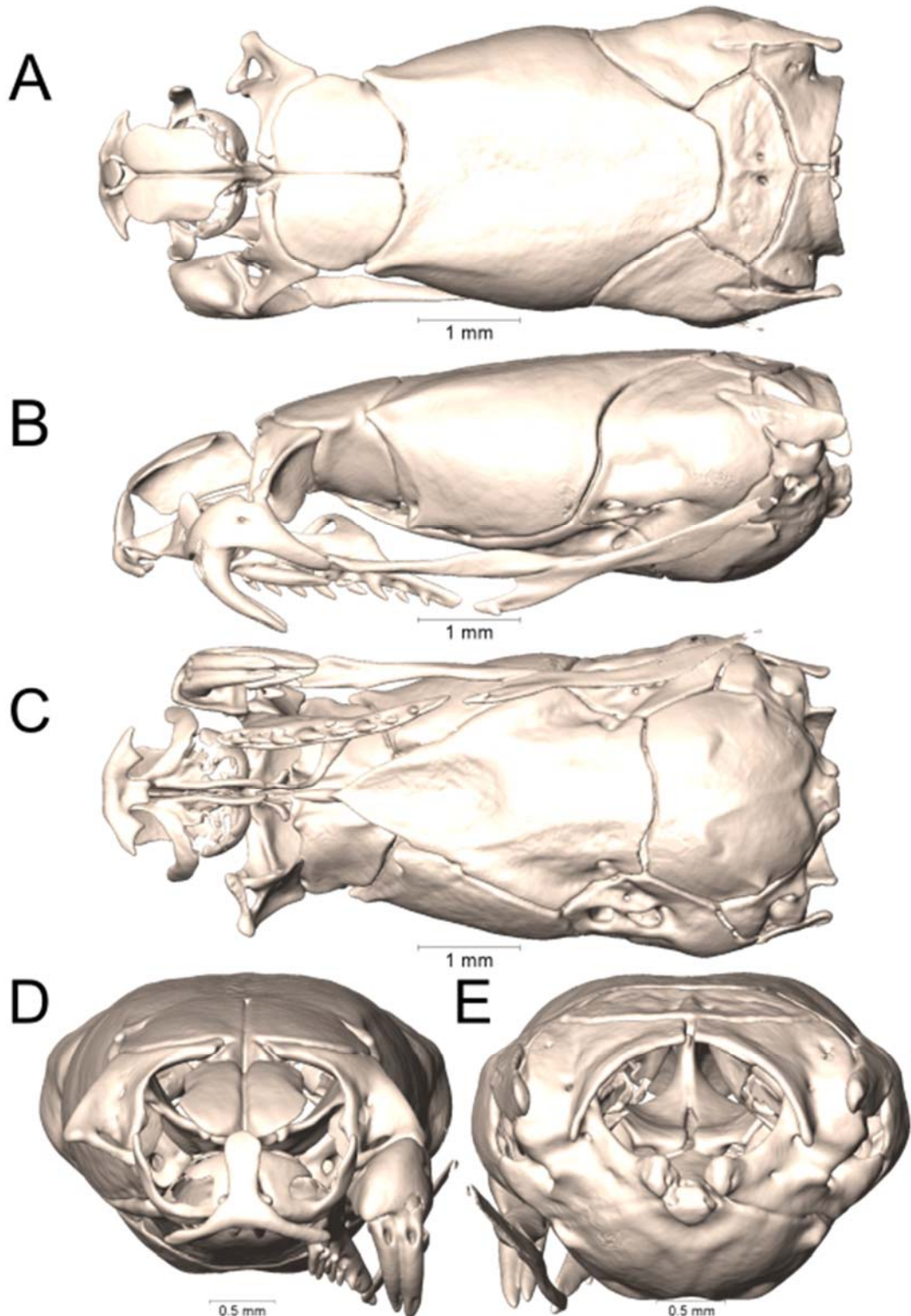
Supplemental Figure 1.8. Dorsal, lateral, ventral, anterior, and posterior views (A-E, respectively) of the skull of *Calliophis gracilis* (USNM 53447). Right suspensorium excluded.



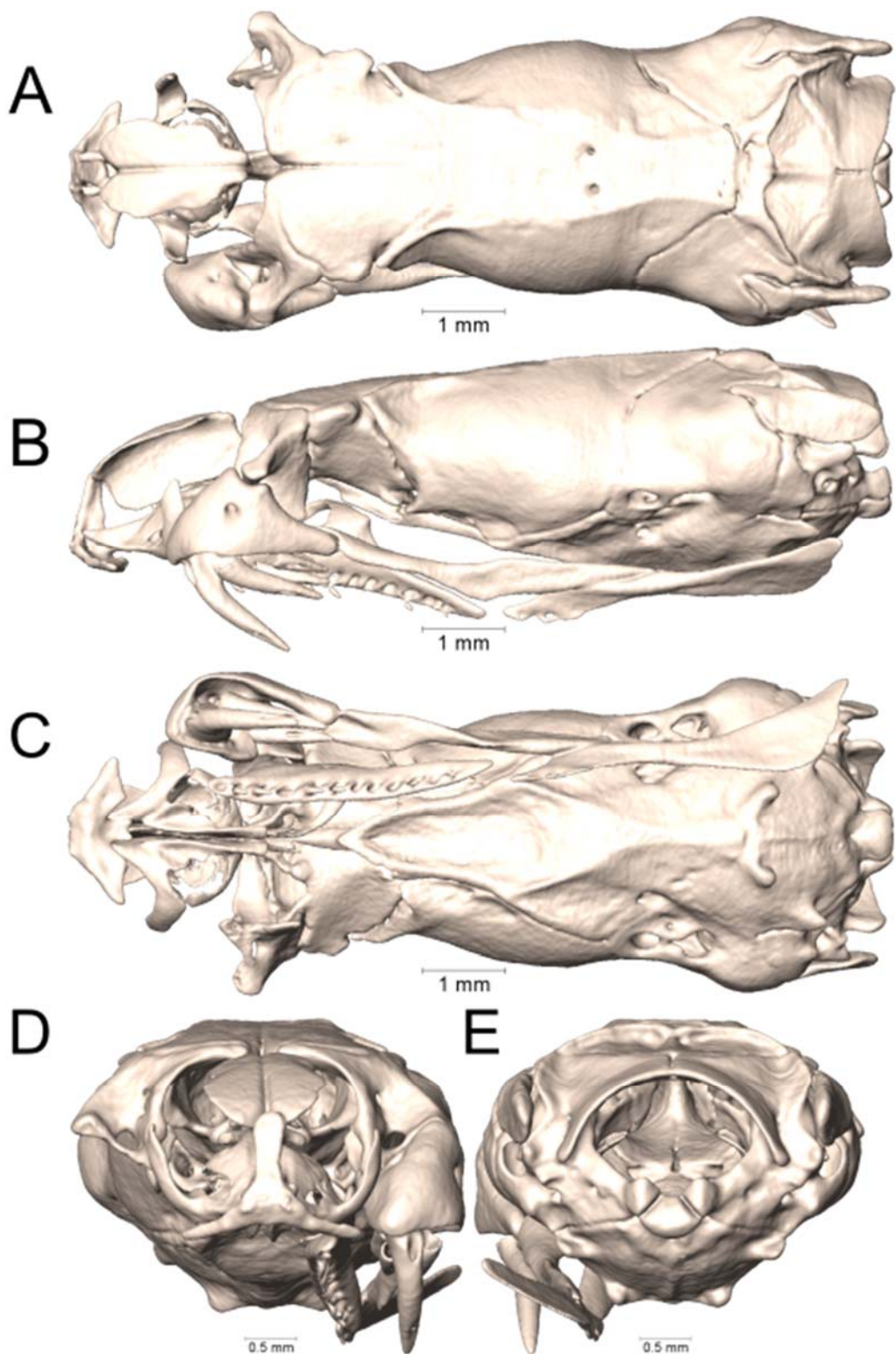
Supplemental Figure 1.9. Dorsal, lateral, ventral, anterior, and posterior views (A-E, respectively) of the skull of *Calliophis intestinalis* (UTA R-60738). Right suspensorium excluded.



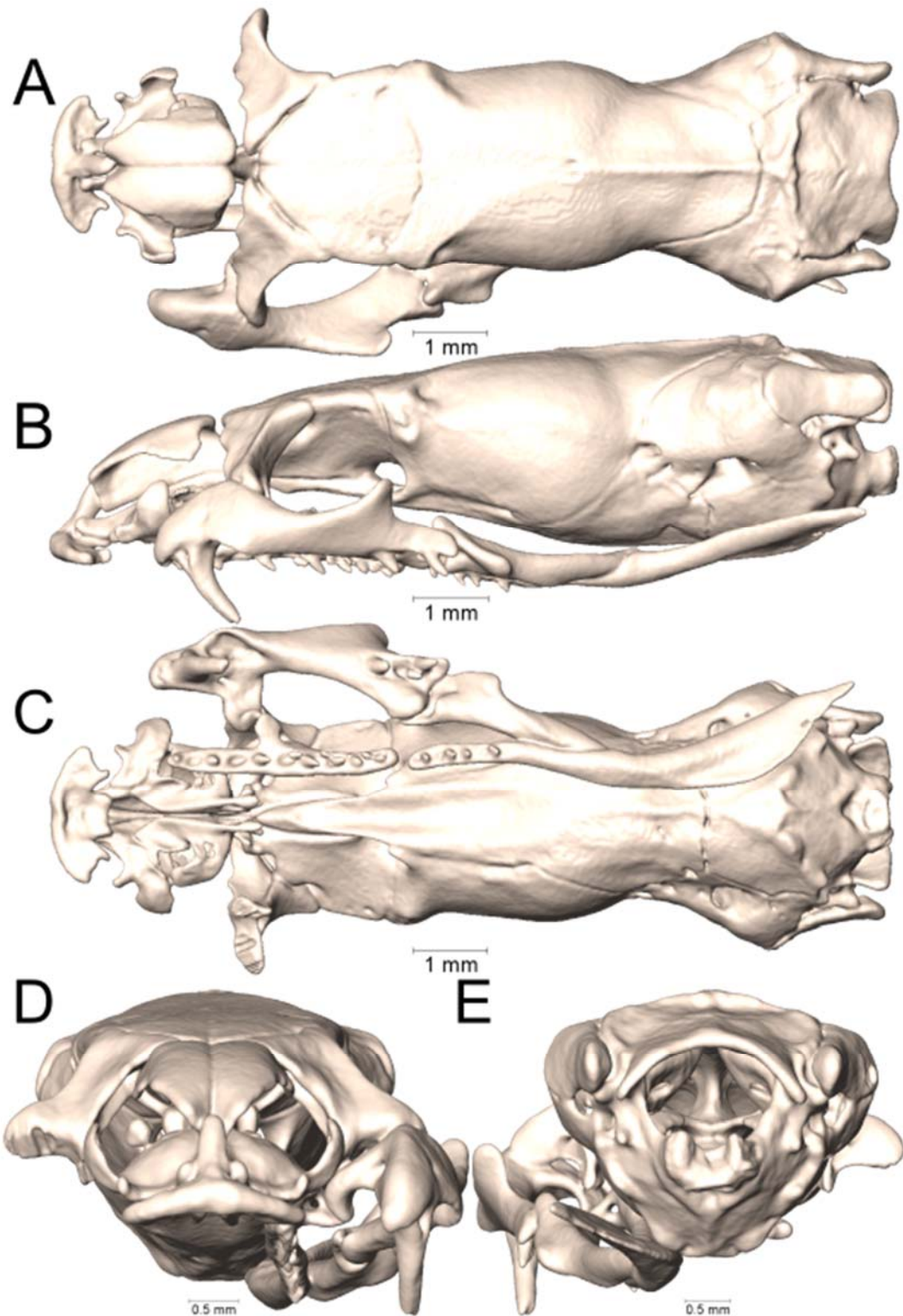
Supplemental Figure 1.10. Dorsal, lateral, ventral, anterior, and posterior views (A-E, respectively) of the skull of *Calliophis cf. intestinalis* (NMW 27221-4). Right suspensorium excluded.



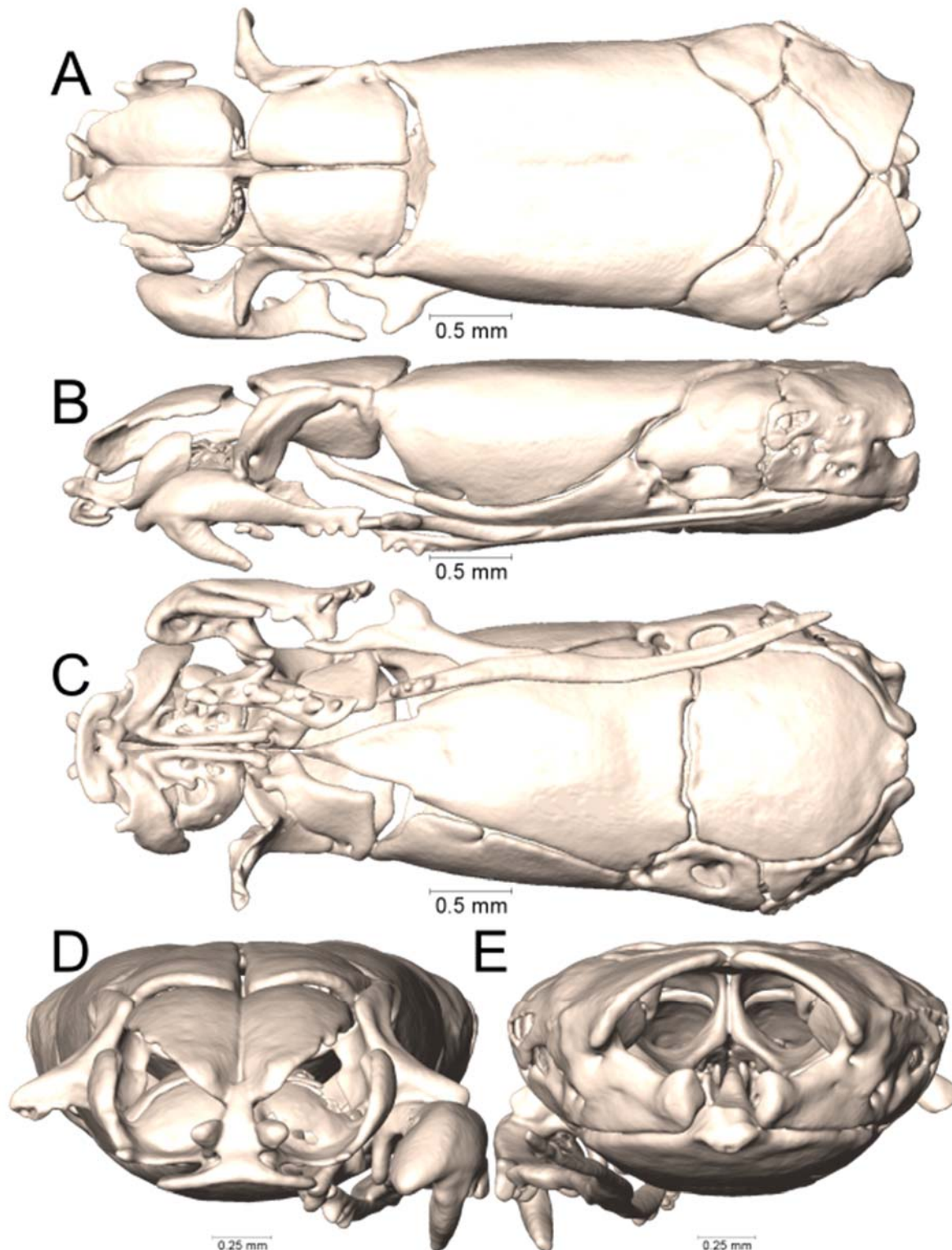
Supplemental Figure 1.11. Dorsal, lateral, ventral, anterior, and posterior views (A-E, respectively) of the skull of *Calliophis intestinalis immaculata* (UTA R-65802). Right suspensorium excluded.



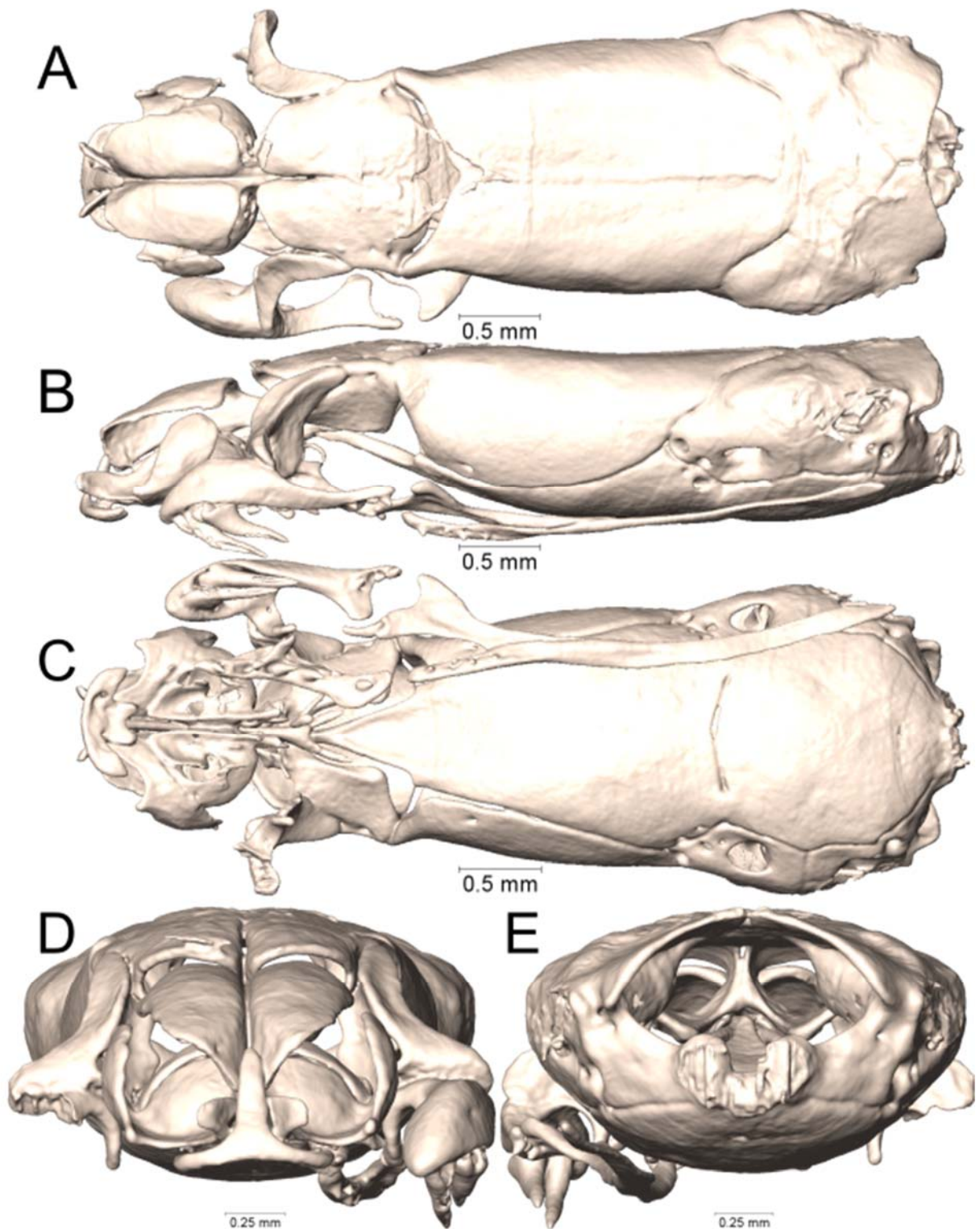
Supplemental Figure 1.12. Dorsal, lateral, ventral, anterior, and posterior views (A-E, respectively) of the skull of *Calliophis intestinalis lineata* (UTA R-65801). Right suspensorium excluded.



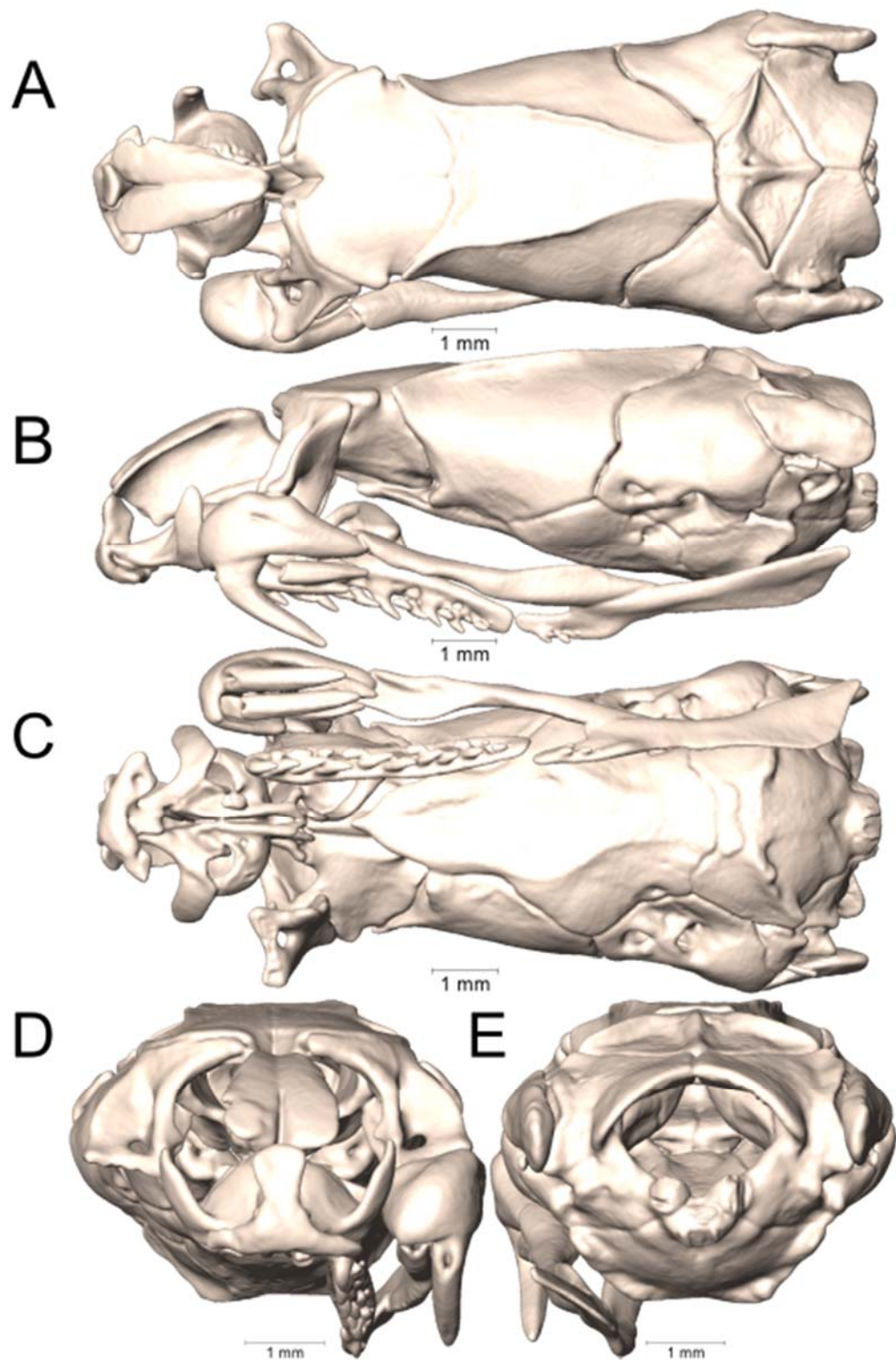
Supplemental Figure 1.13. Dorsal, lateral, ventral, anterior, and posterior views (A-E, respectively) of the skull of *Calliophis maculiceps* (MNHN 5459). Right suspensorium excluded.



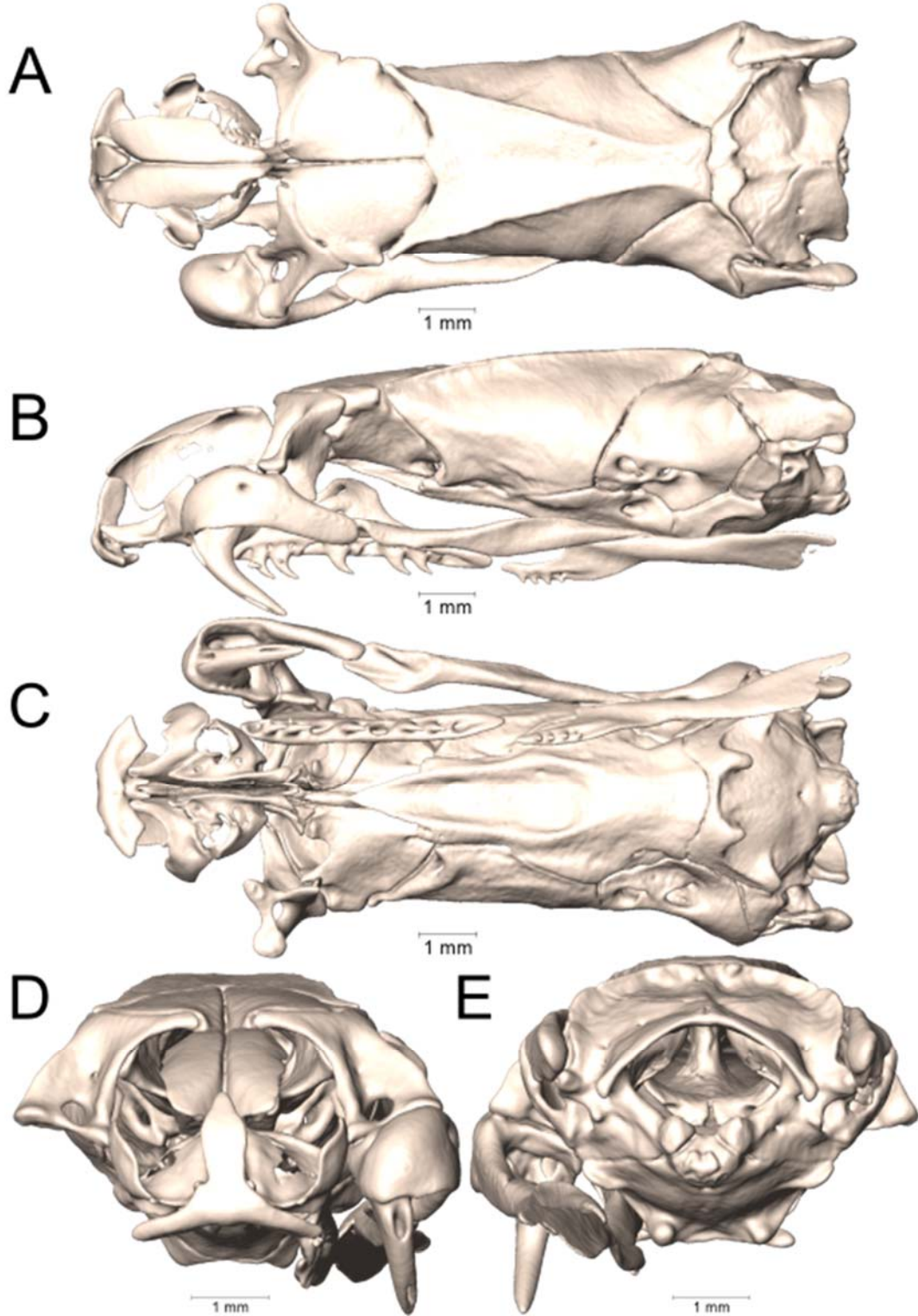
Supplemental Figure 1.14. Dorsal, lateral, ventral, anterior, and posterior views (A-E, respectively) of the skull of *Calliophis melanurus* (MNHN 46-286). Right suspensorium excluded.



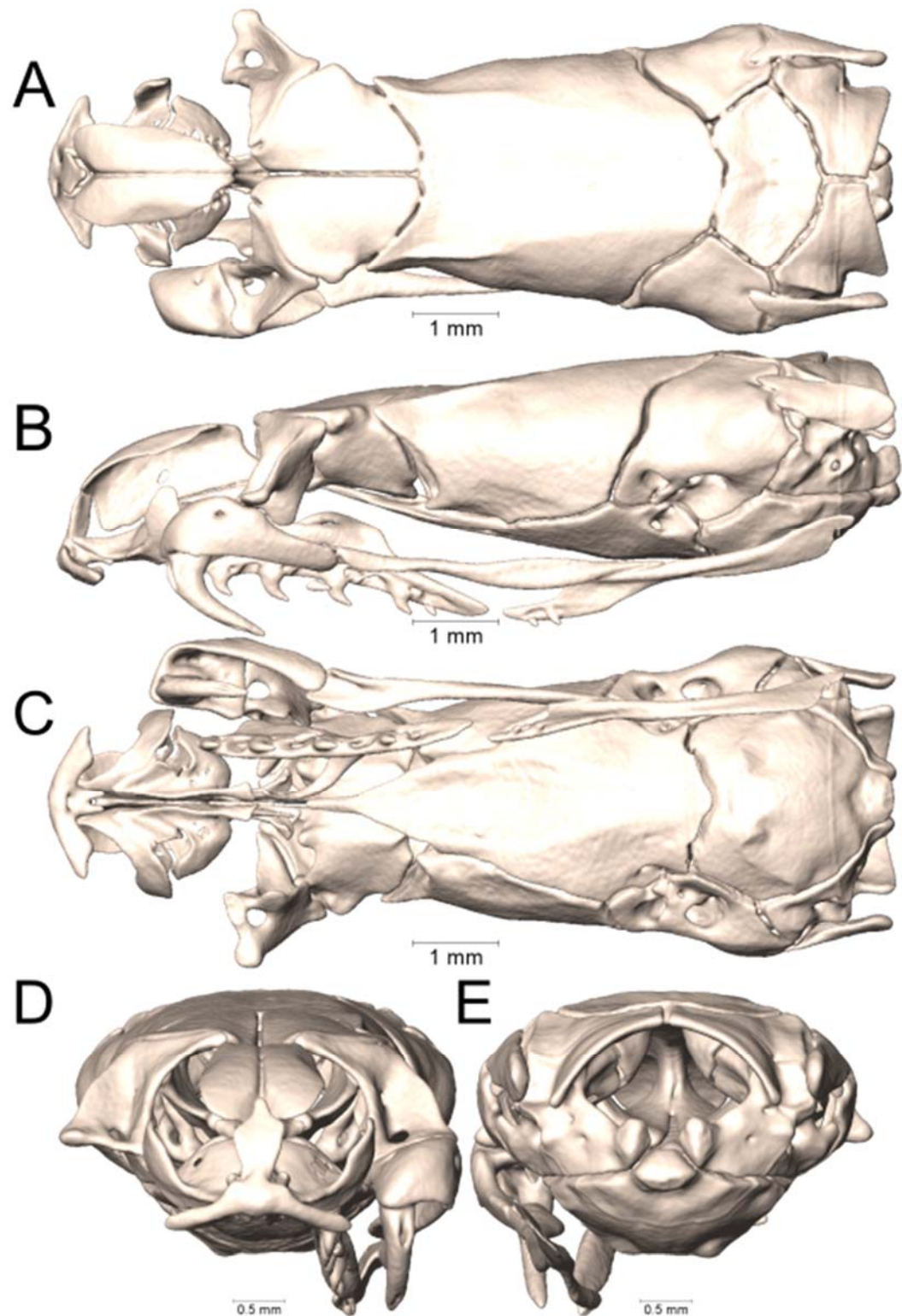
Supplemental Figure 1.15. Dorsal, lateral, ventral, anterior, and posterior views (A-E, respectively) of the skull of *Calliophis melanurus* (MNHN 48-318). Right suspensorium excluded.



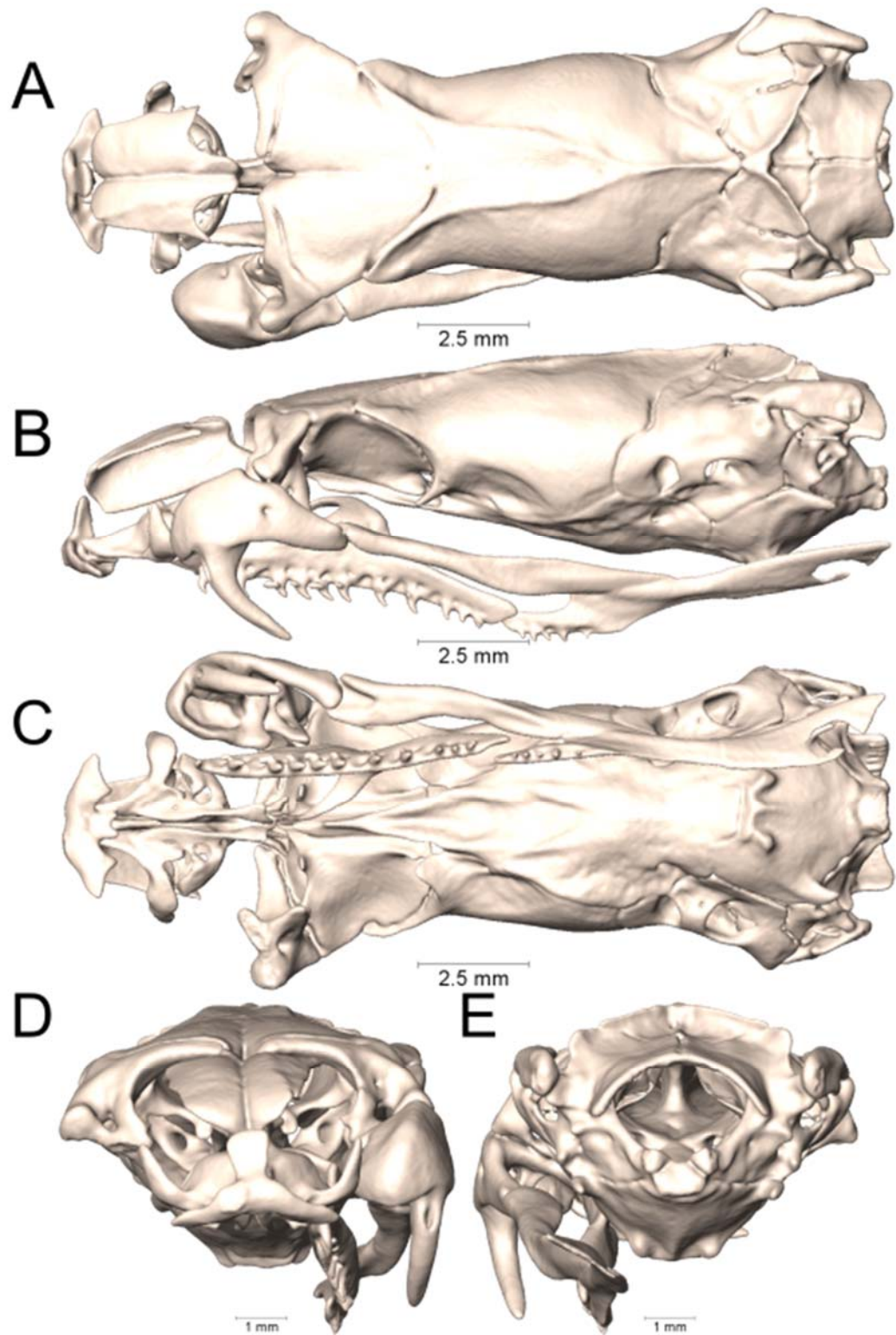
Supplemental Figure 1.16. Dorsal, lateral, ventral, anterior, and posterior views (A-E, respectively) of the skull of *Calliophis nigrotaeniatus* (NMW 27220-7). Right suspensorium excluded.



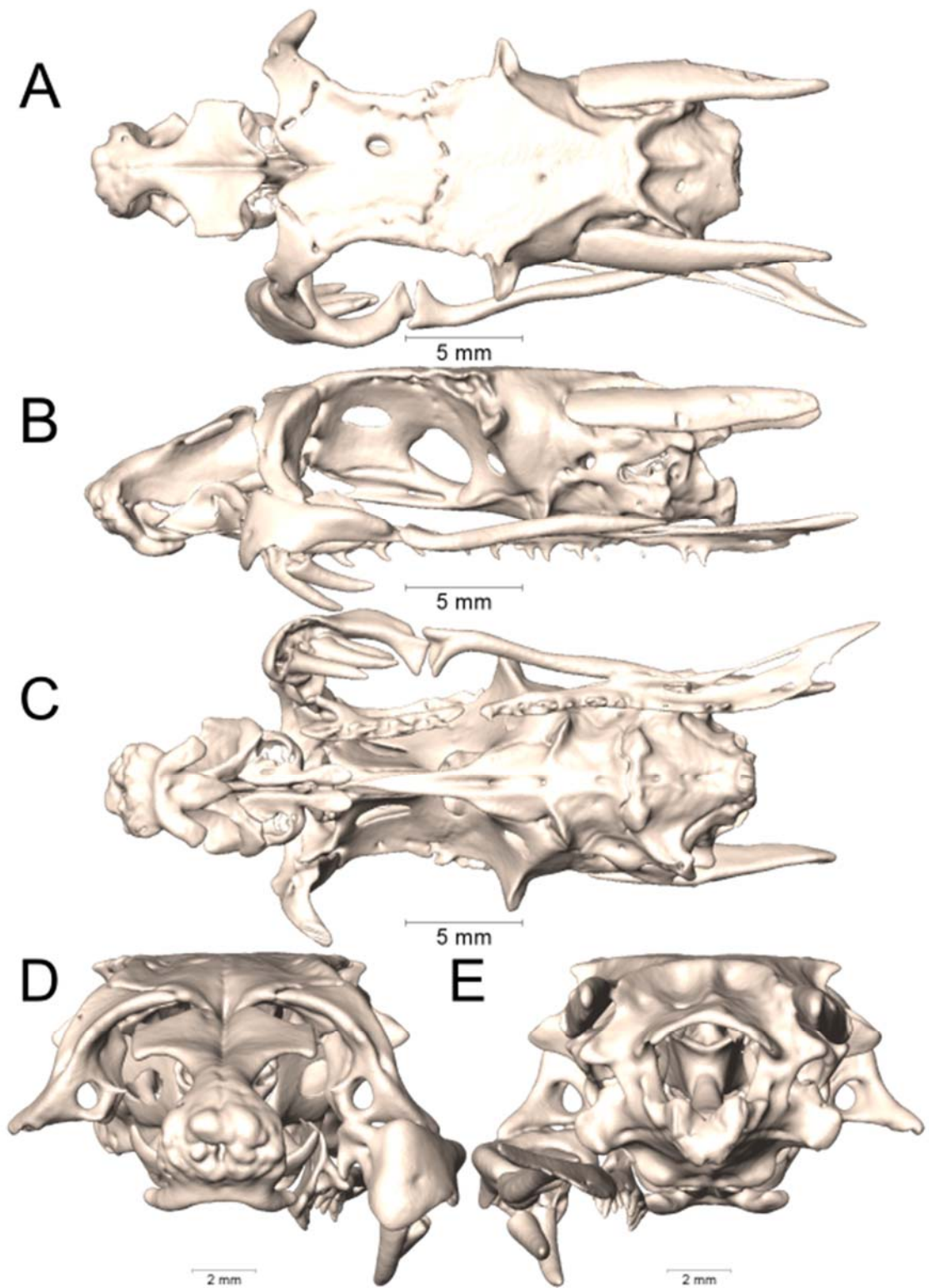
Supplemental Figure 1.17. Dorsal, lateral, ventral, anterior, and posterior views (A-E, respectively) of the skull of *Calliophis philippinus* (KU 310369). Right suspensorium excluded.



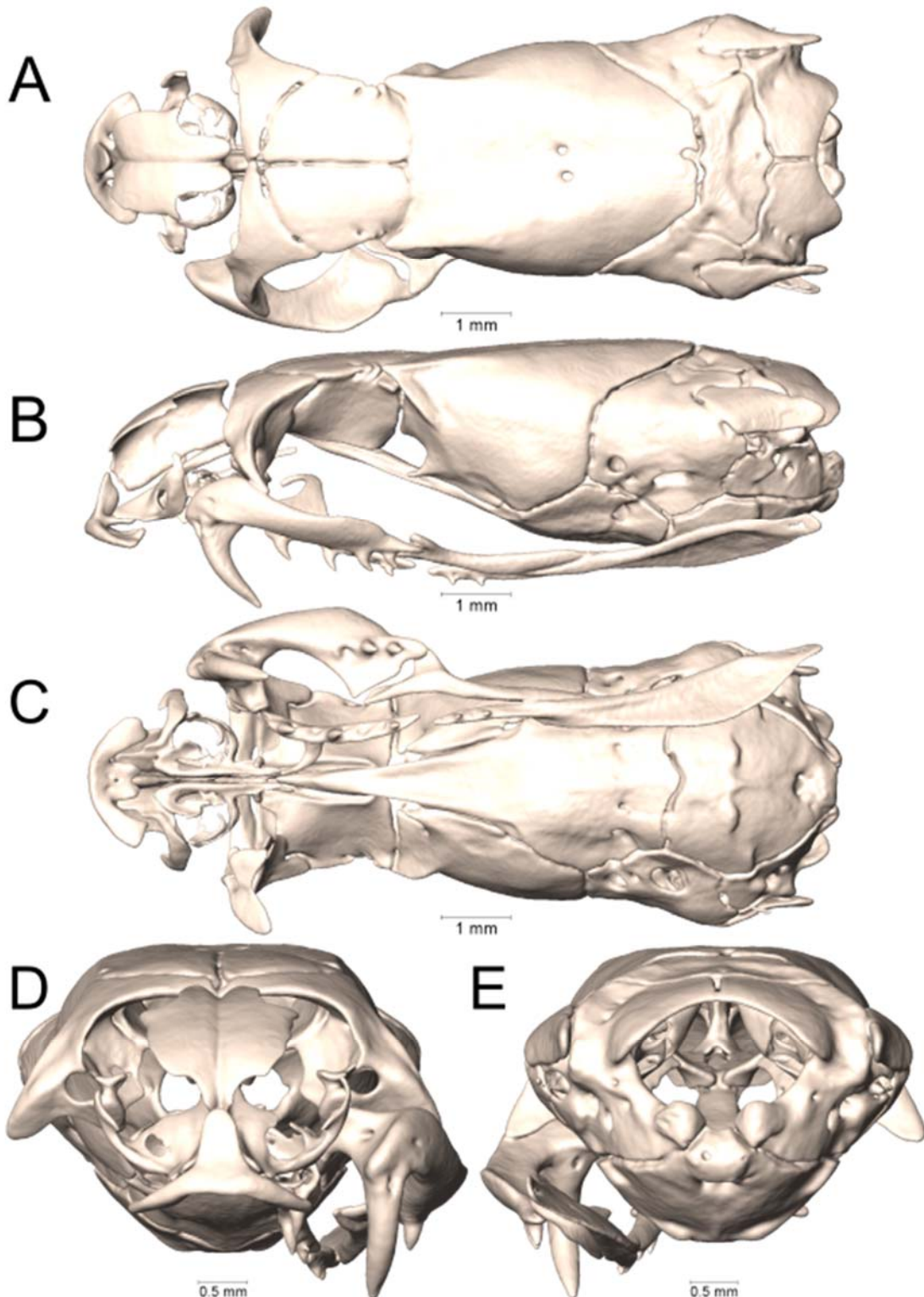
Supplemental Figure 1.18. Dorsal, lateral, ventral, anterior, and posterior views (A-E, respectively) of the skull of *Calliophis philippinus* (KU 314913). Right suspensorium excluded.



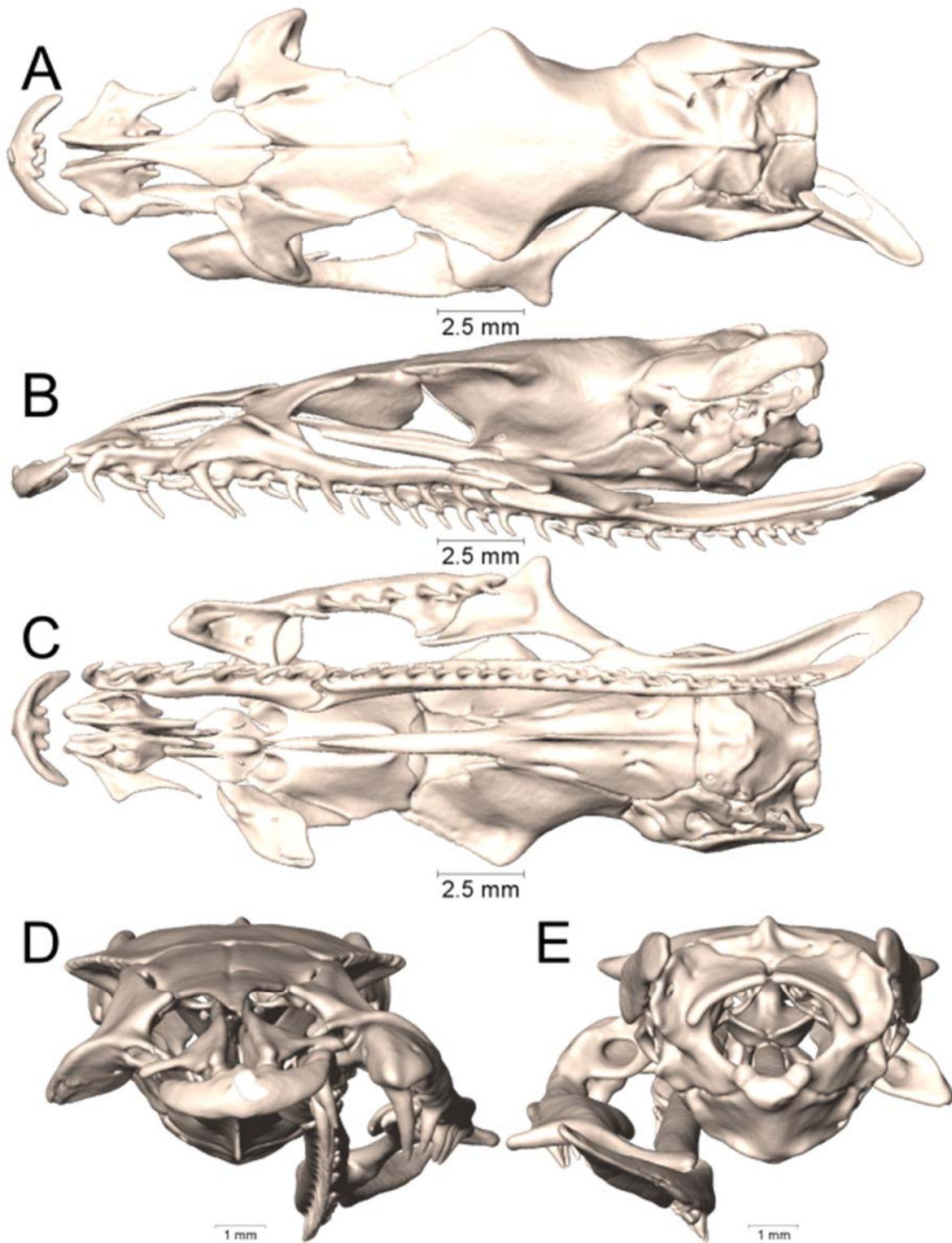
Supplemental Figure 1.19. Dorsal, lateral, ventral, anterior, and posterior views (A-E, respectively) of the skull of *Calliophis salitan* (PNM 9844). Right suspensorium excluded.



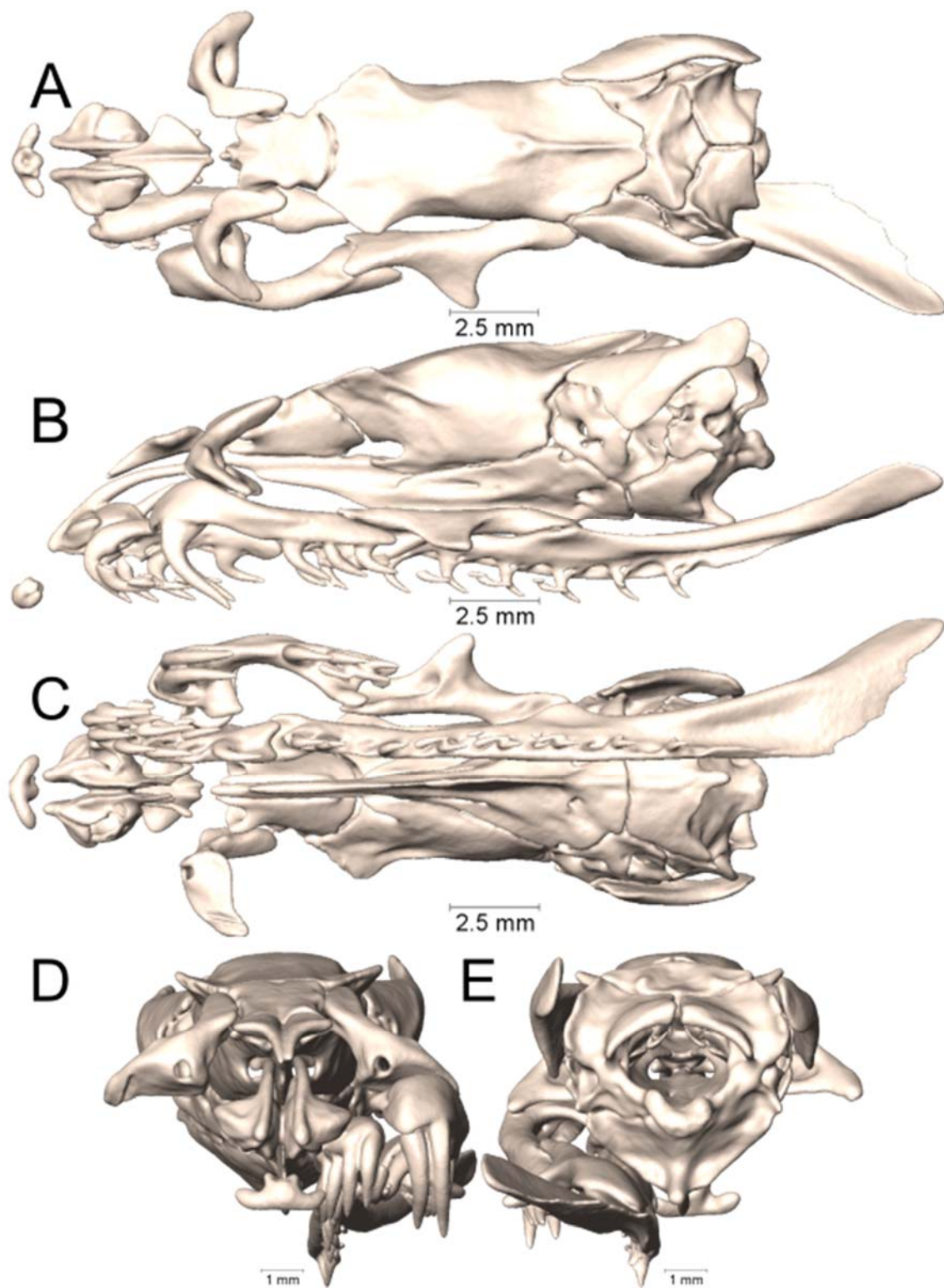
Supplemental Figure 1.20. Dorsal, lateral, ventral, anterior, and posterior views (A-E, respectively) of the skull of *Hemachatus haemachatus* (UTA R-7431). Right suspensorium excluded.



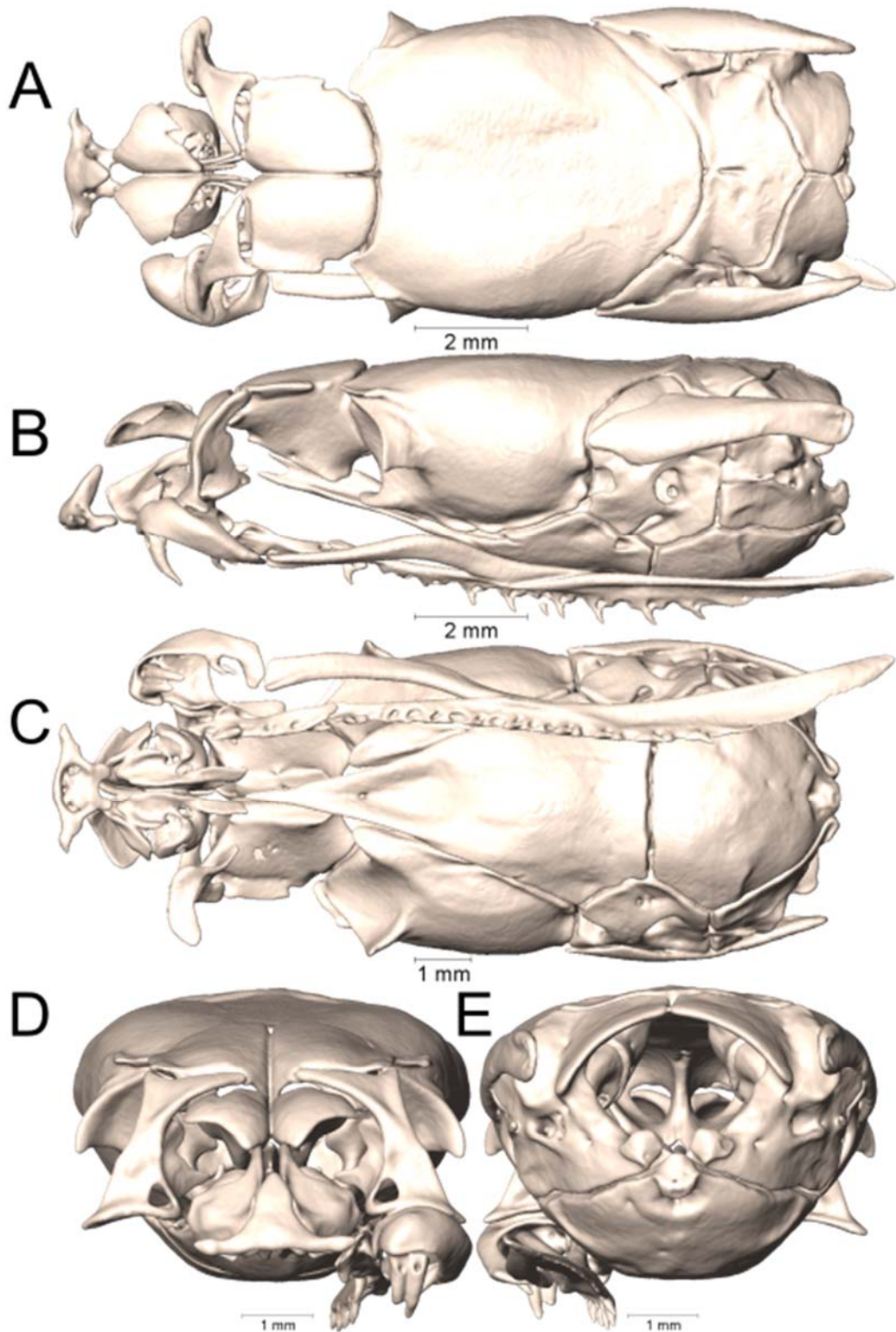
Supplemental Figure 1.21. Dorsal, lateral, ventral, anterior, and posterior views (A-E, respectively) of the skull of *Hemibungarus calligaster* (KU 307474). Right suspensorium excluded.



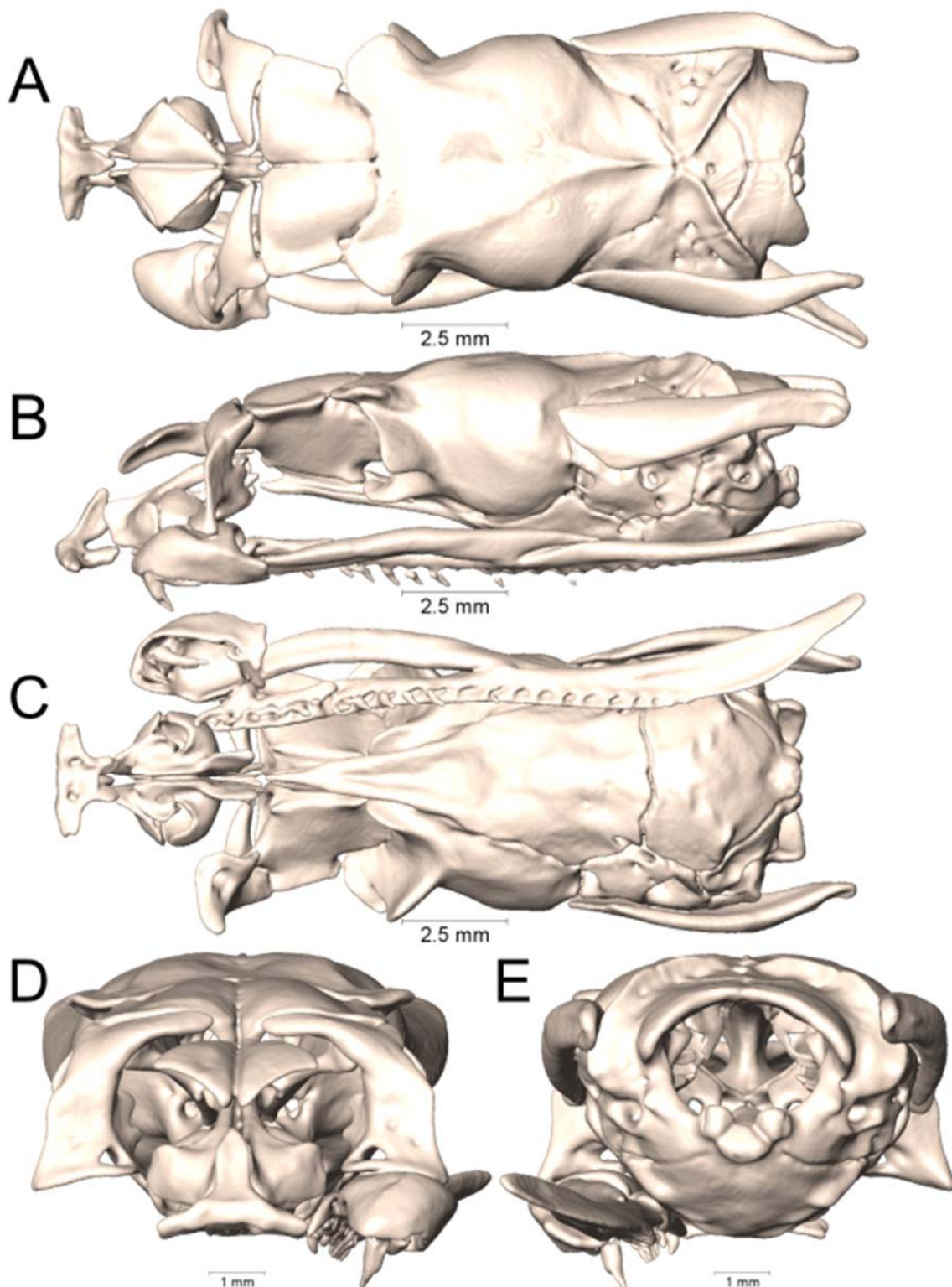
Supplemental Figure 1.22. Dorsal, lateral, ventral, anterior, and posterior views (A-E, respectively) of the skull of *Hydrophis platurus* (UTA R-41049). Right suspensorium excluded.



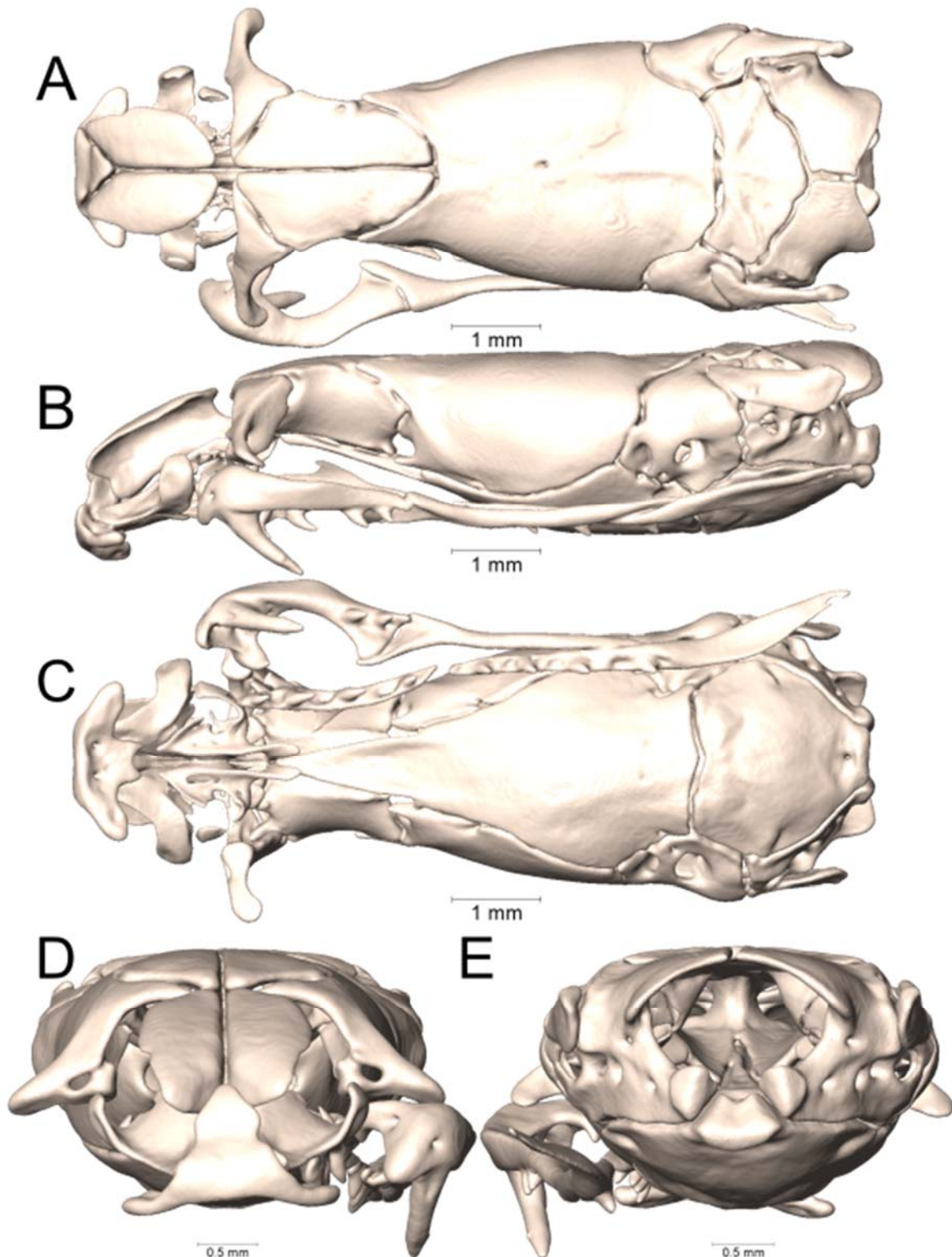
Supplemental Figure 1.23. Dorsal, lateral, ventral, anterior, and posterior views (A-E, respectively) of the skull of *Hydrophis schistosus* (UTA R-63074). Right suspensorium excluded.



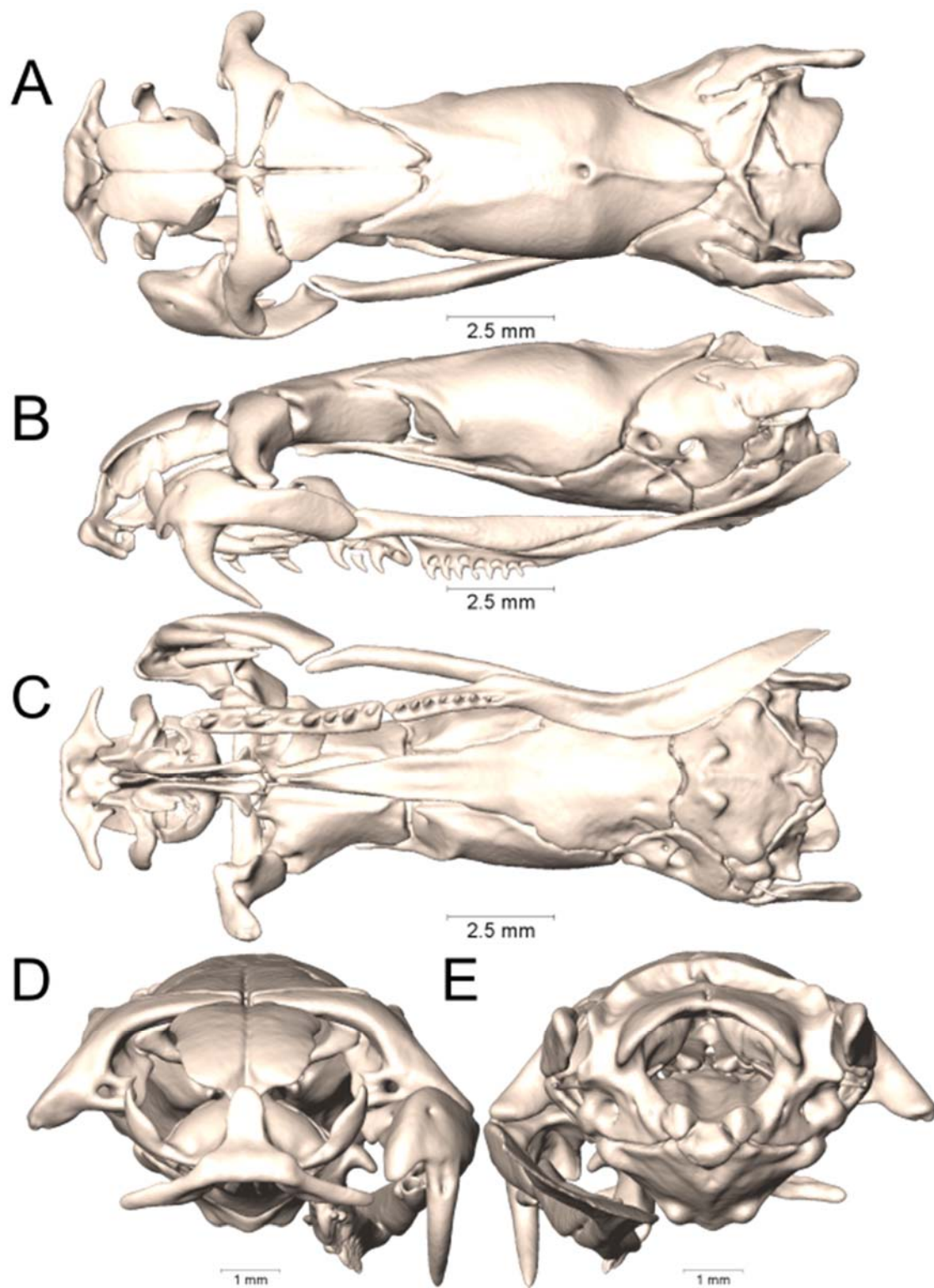
Supplemental Figure 1.24. Dorsal, lateral, ventral, anterior, and posterior views (A-E, respectively) of the skull of *Laticauda colubrina* (UTA R-65800). Right suspensorium excluded.



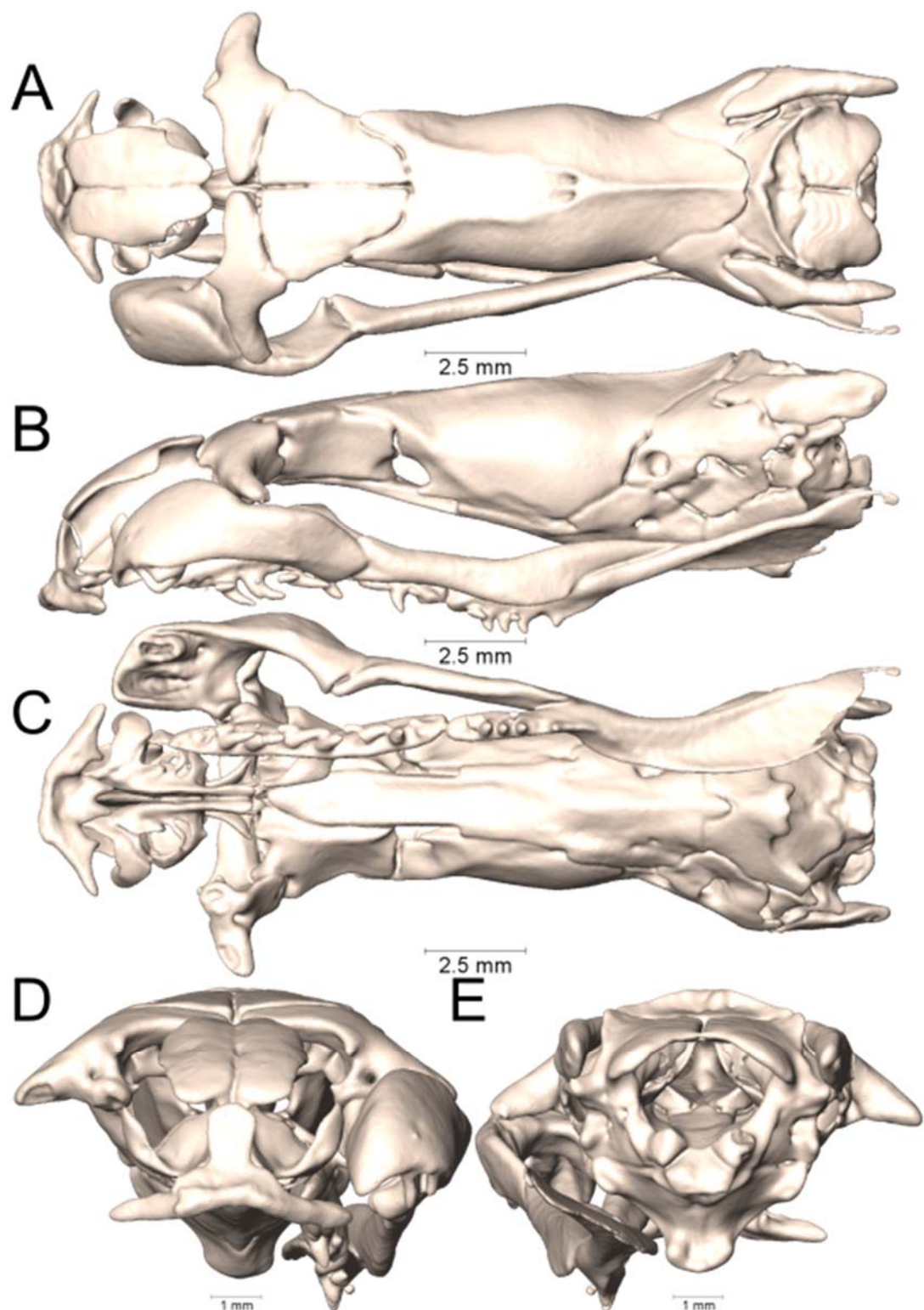
Supplemental Figure 1.25. Dorsal, lateral, ventral, anterior, and posterior views (A-E, respectively) of the skull of *Laticauda laticauda* (UTA R-6355). Right suspensorium excluded.



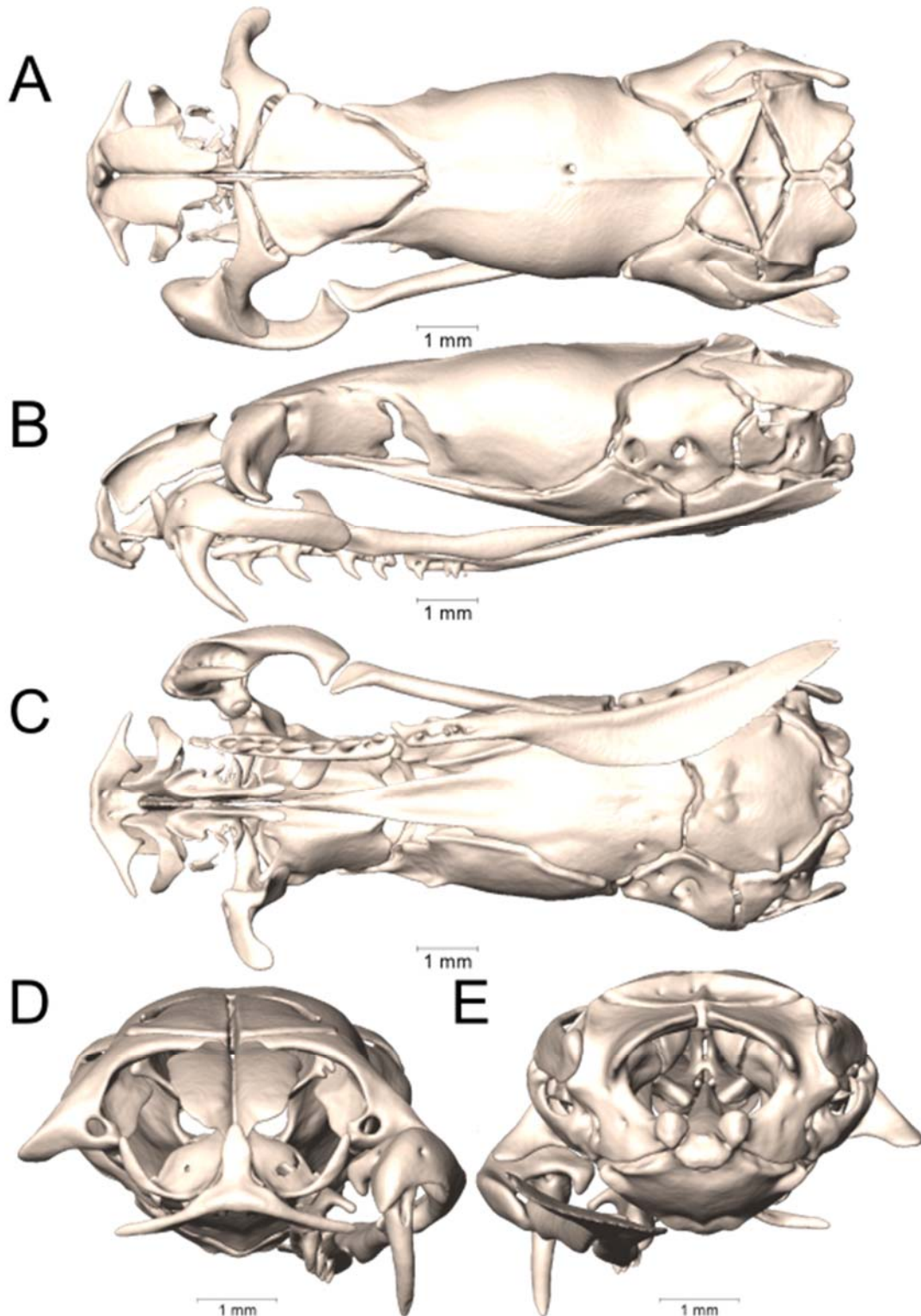
Supplemental Figure 1.26. Dorsal, lateral, ventral, anterior, and posterior views (A-E, respectively) of the skull of *Micruroides euryxanthus* (UTA R-60734). Right suspensorium excluded.



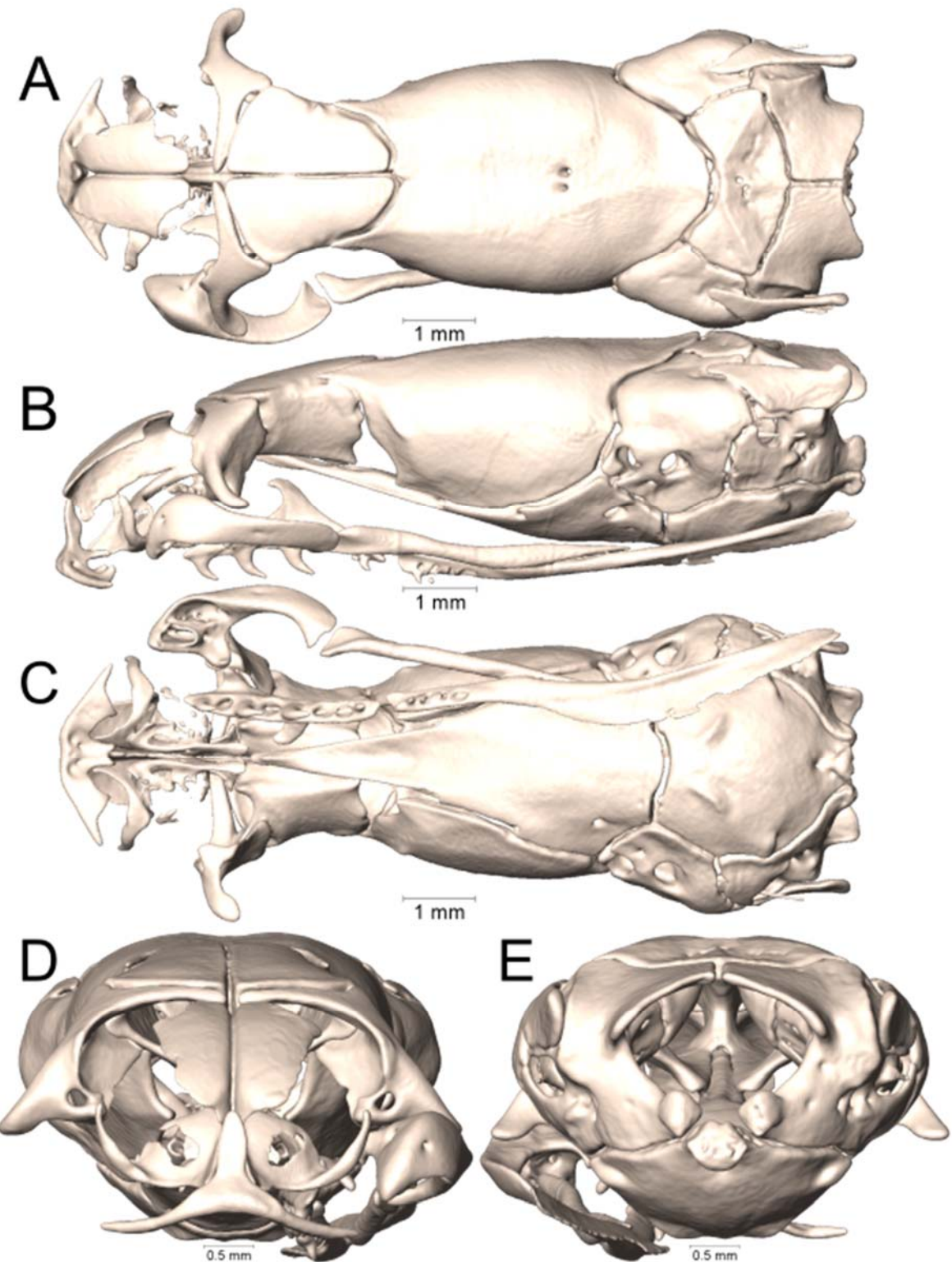
Supplemental Figure 1.27. Dorsal, lateral, ventral, anterior, and posterior views (A-E, respectively) of the skull of *Micrurus alleni* (UTA R-60556). Right suspensorium excluded.



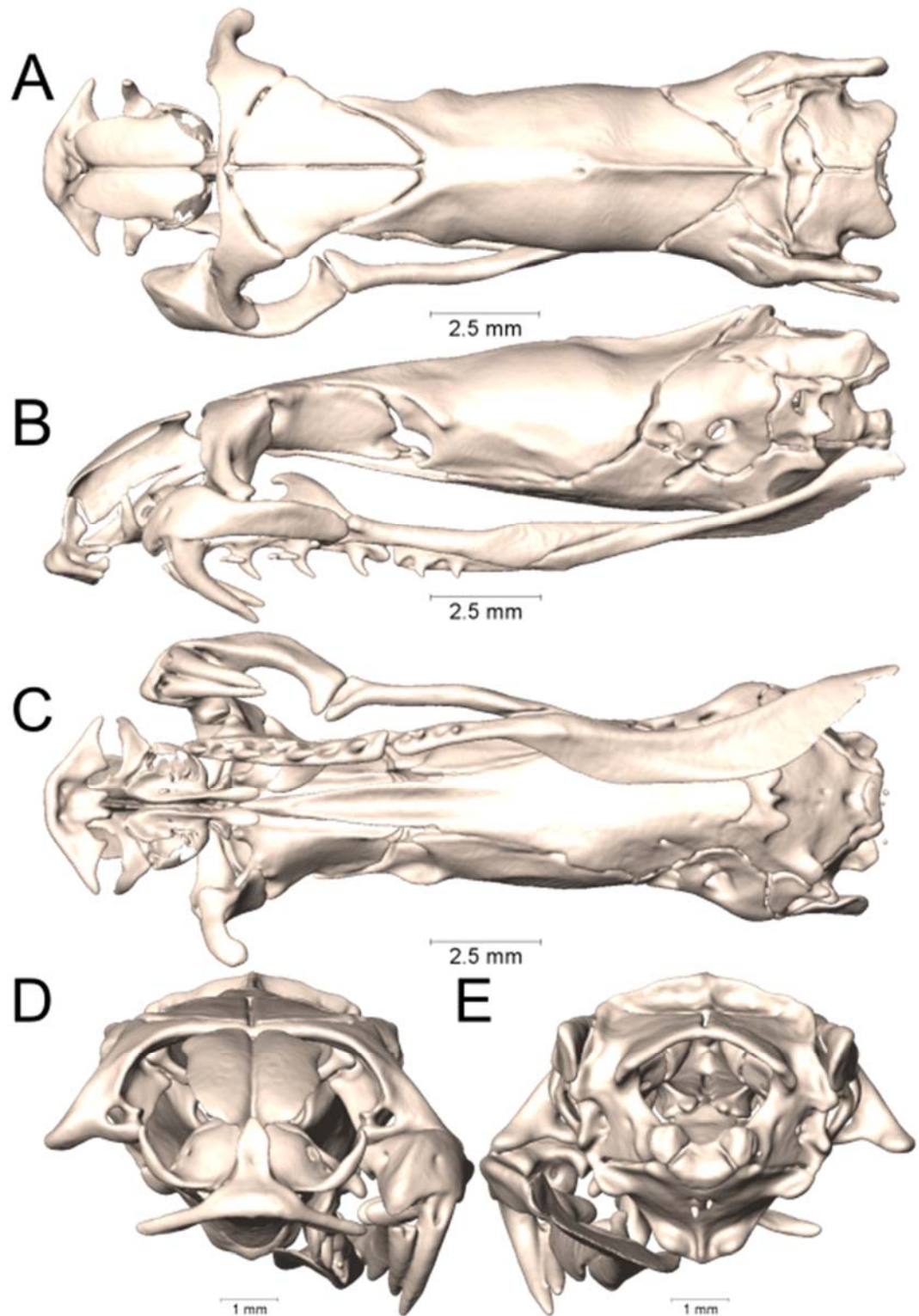
Supplemental Figure 1.28. Dorsal, lateral, ventral, anterior, and posterior views (A-E, respectively) of the skull of *Micrurus anchoralis* (UTA R-55945). Right suspensorium excluded.



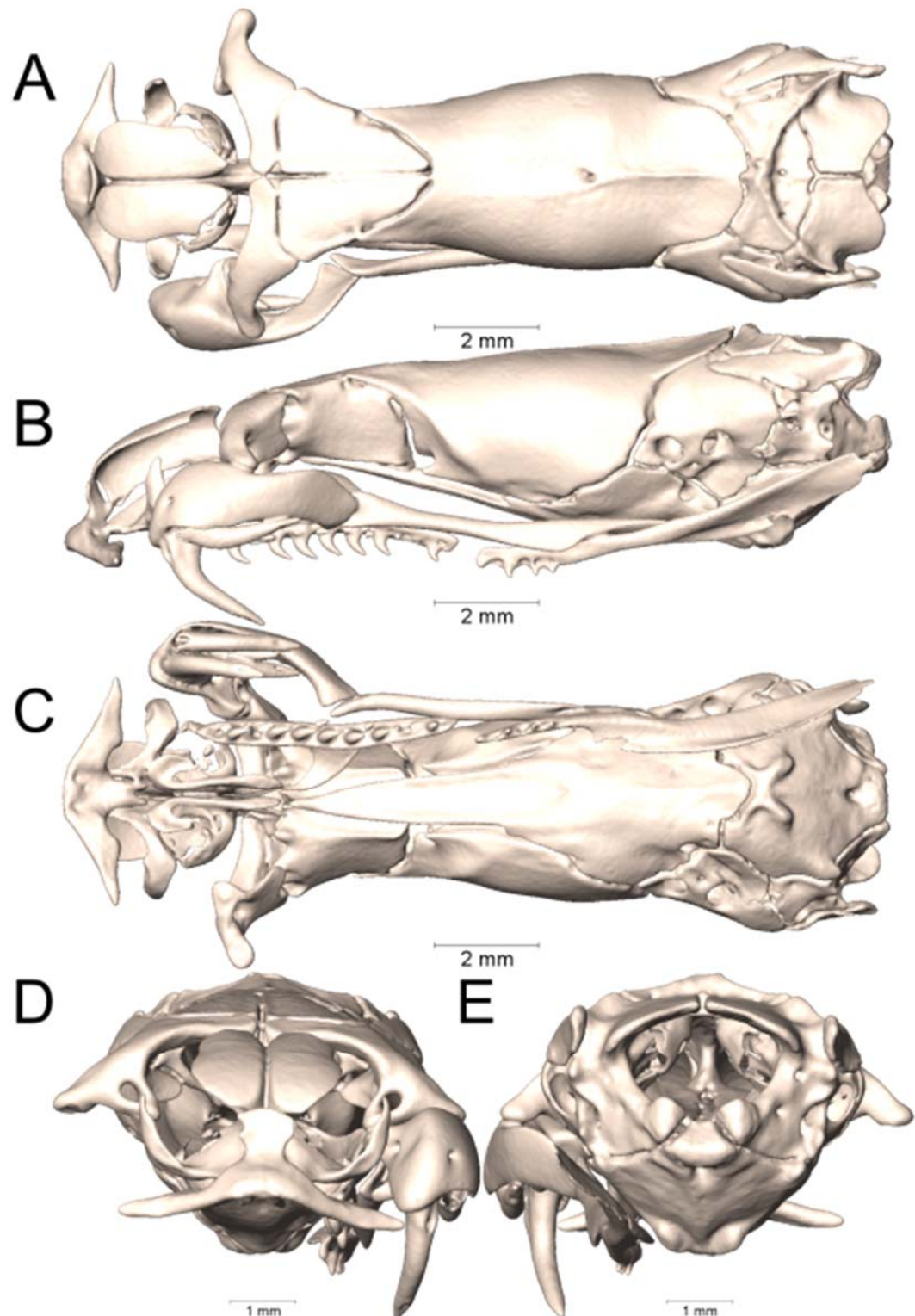
Supplemental Figure 1.29. Dorsal, lateral, ventral, anterior, and posterior views (A-E, respectively) of the skull of *Micrurus apiatus* (UTA R-39267). Right suspensorium excluded.



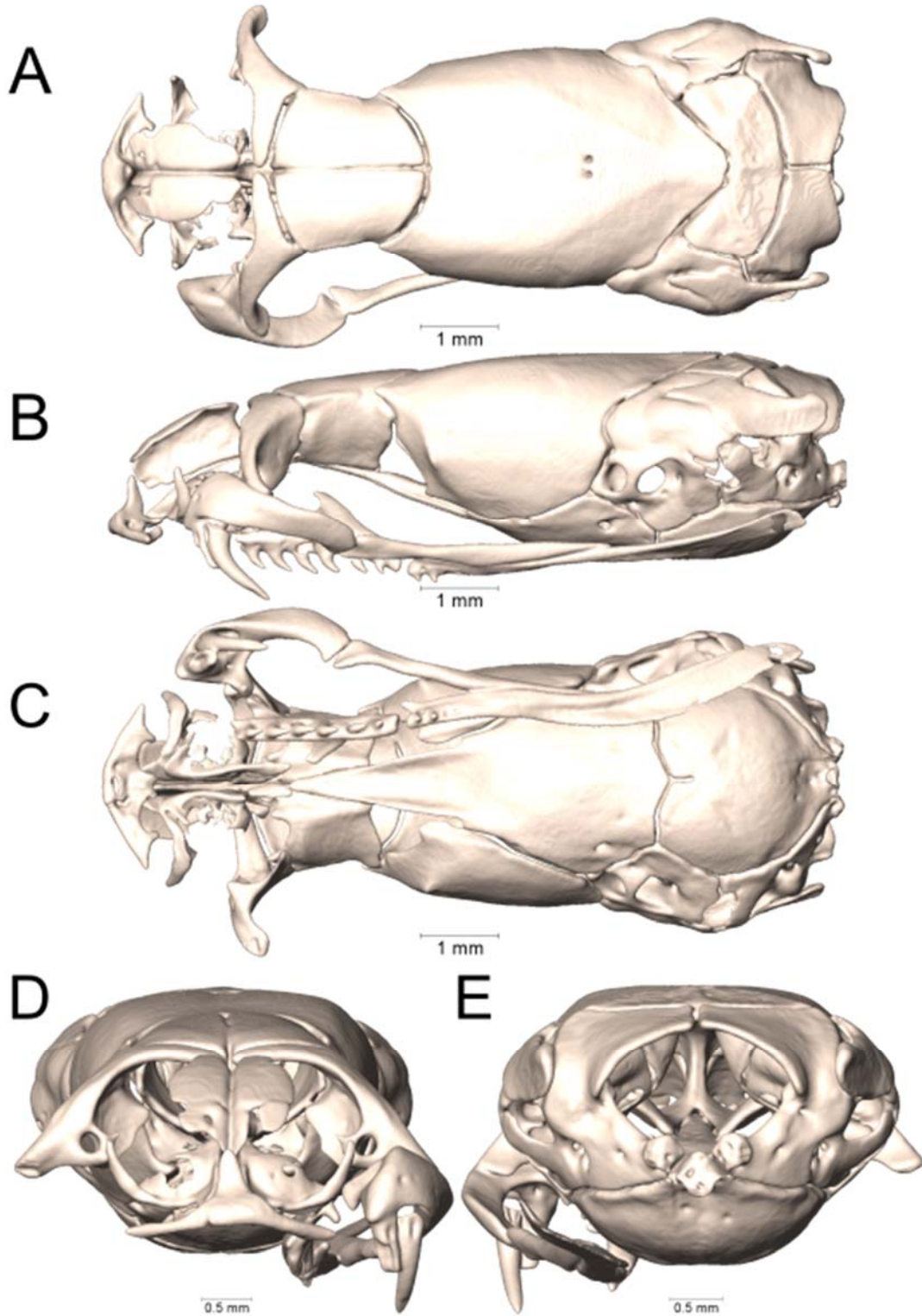
Supplemental Figure 1.30. Dorsal, lateral, ventral, anterior, and posterior views (A-E, respectively) of the skull of *Micrurus apiatus* (UTA R-39554). Right suspensorium excluded.



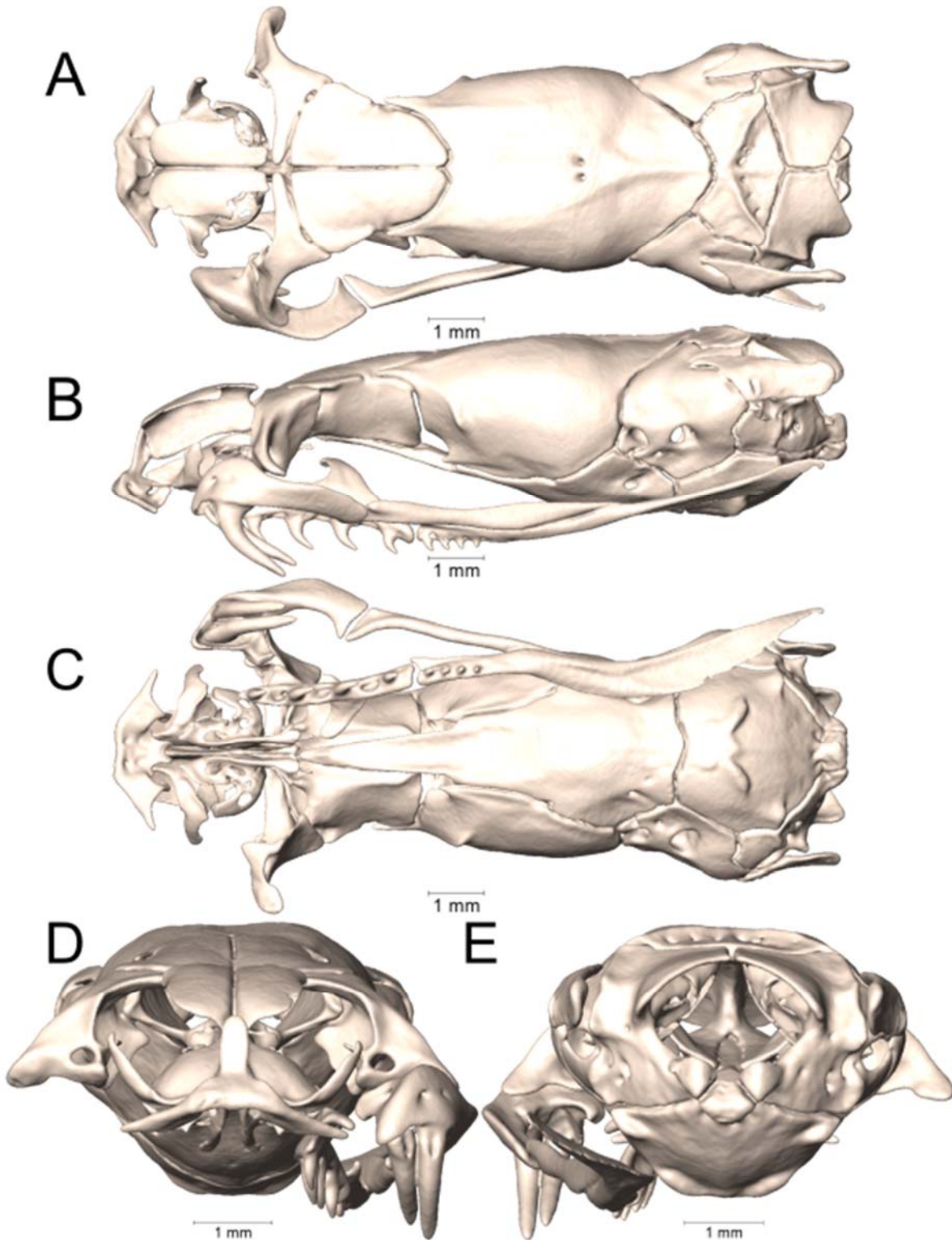
Supplemental Figure 1.31. Dorsal, lateral, ventral, anterior, and posterior views (A-E, respectively) of the skull of *Micrurus diastema* (UTA R-52565). Right suspensorium excluded.



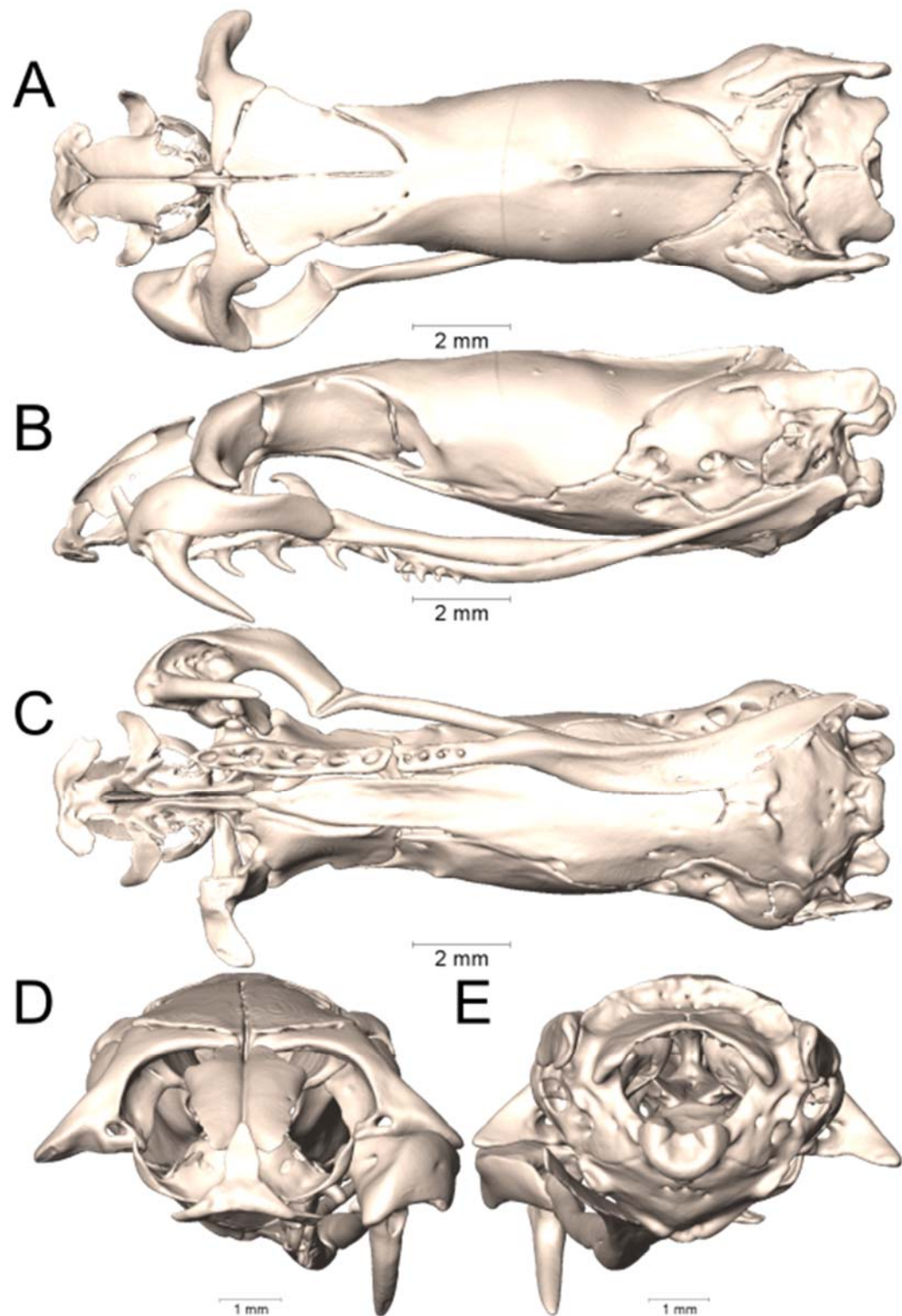
Supplemental Figure 1.32. Dorsal, lateral, ventral, anterior, and posterior views (A-E, respectively) of the skull of *Micrurus diutius* (UTA R-54182). Right suspensorium excluded.



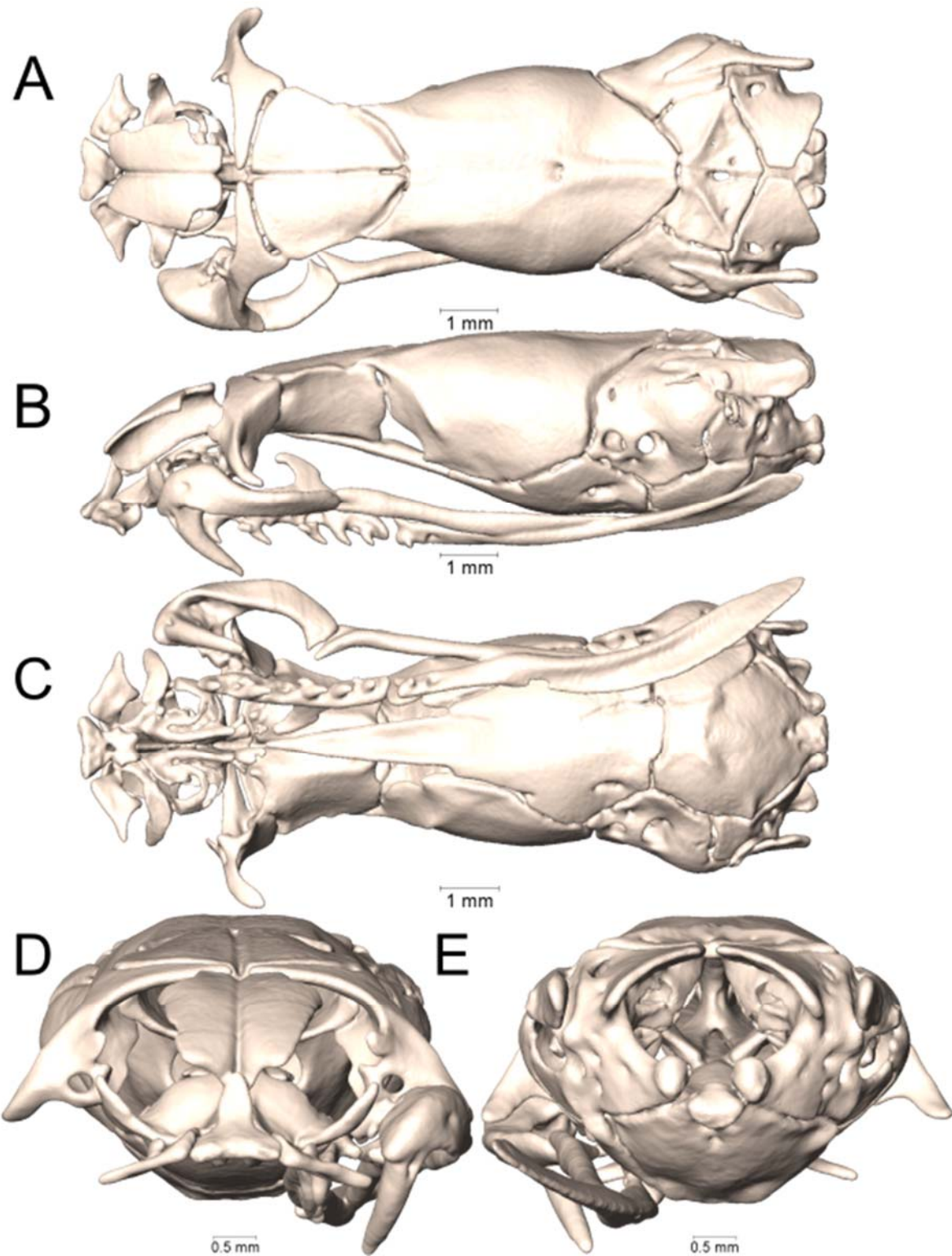
Supplemental Figure 1.33. Dorsal, lateral, ventral, anterior, and posterior views (A-E, respectively) of the skull of *Micrurus dumerilii* (AMNH 35951). Right suspensorium excluded.



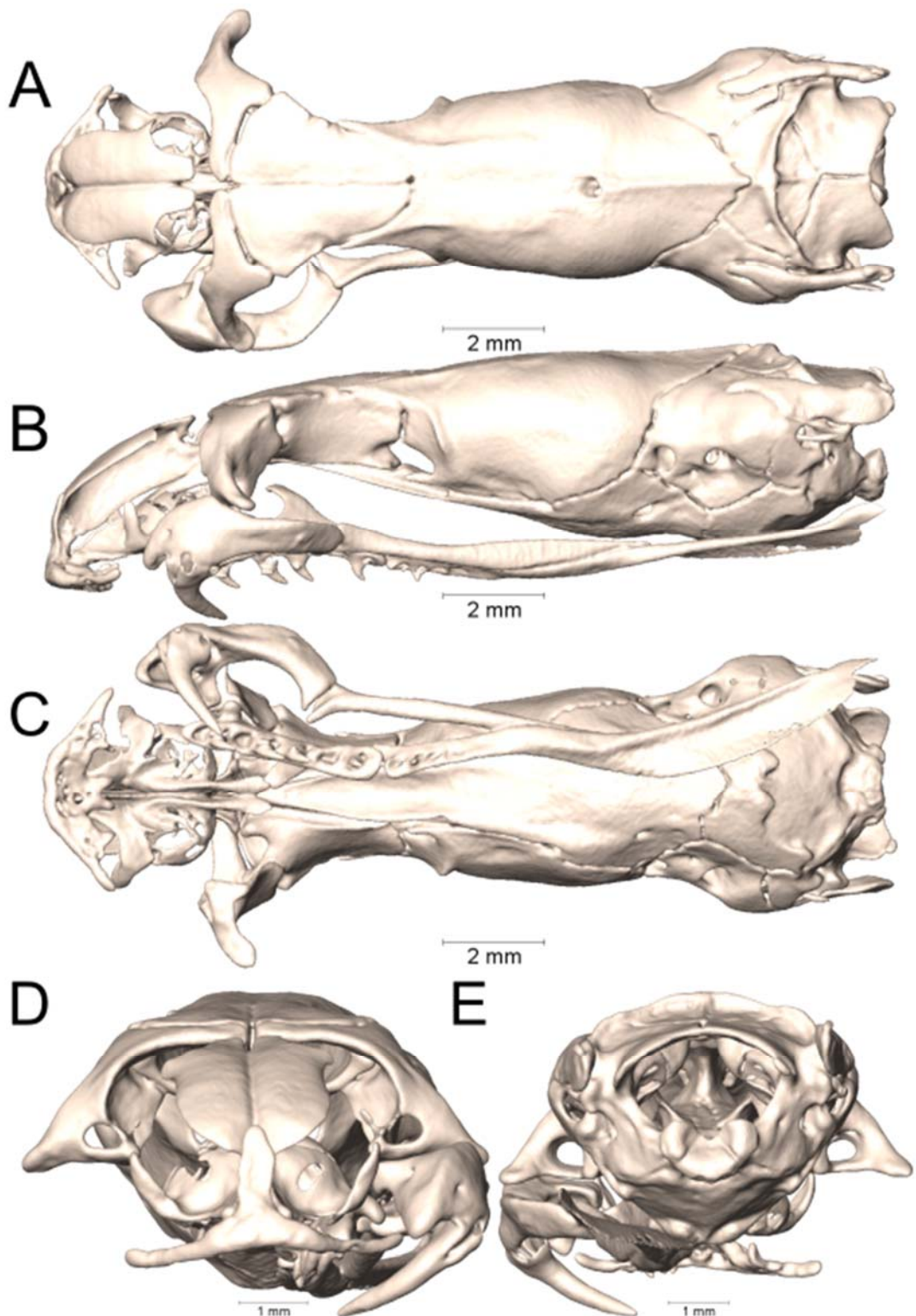
Supplemental Figure 1.34. Dorsal, lateral, ventral, anterior, and posterior views (A-E, respectively) of the skull of *Micrurus elegans elegans* (MZFC 18819). Right suspensorium excluded.



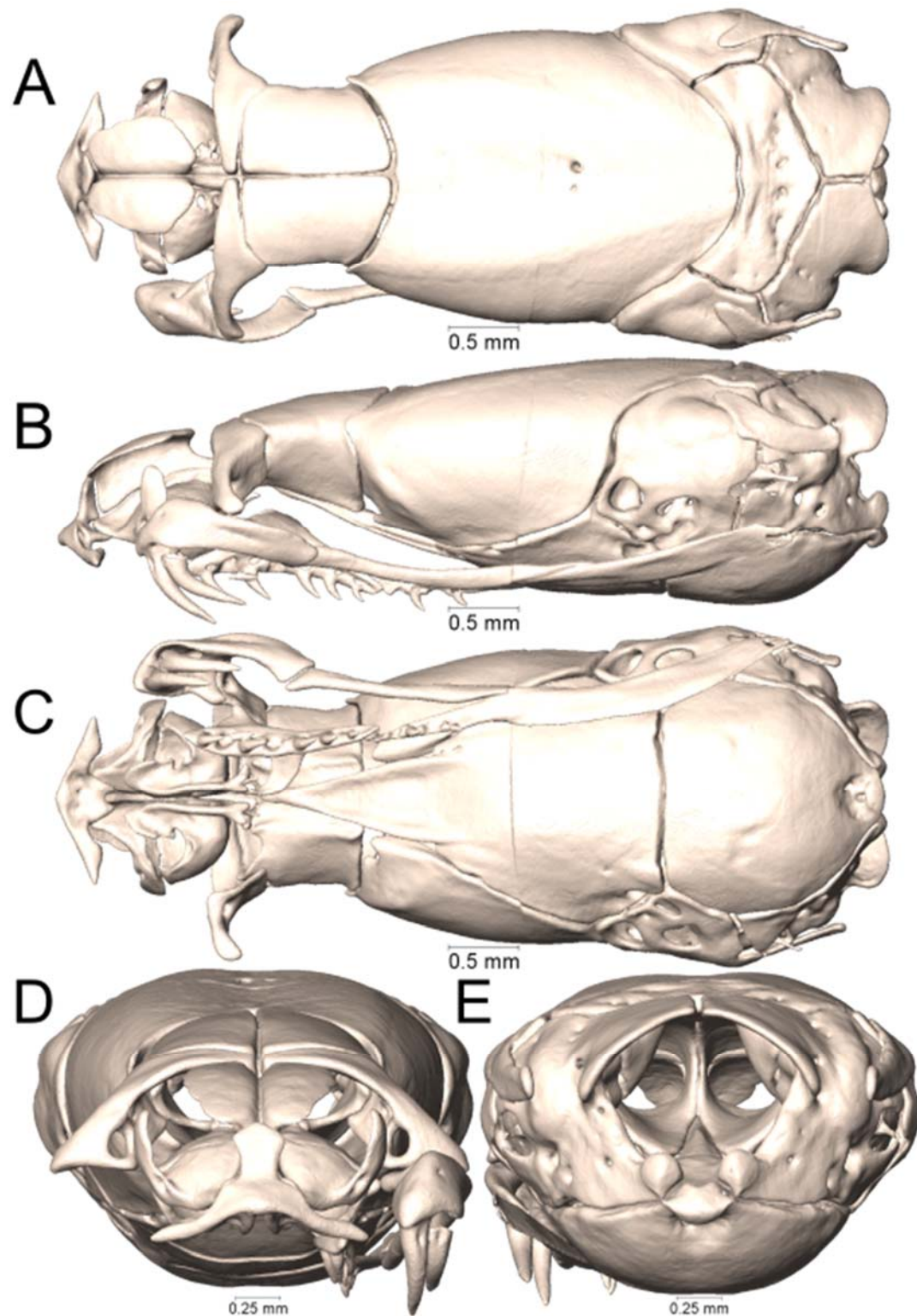
Supplemental Figure 1.45. Dorsal, lateral, ventral, anterior, and posterior views (A-E, respectively) of the skull of *Micrurus elegans veraepacis* (UTA R-7072). Right suspensorium excluded.



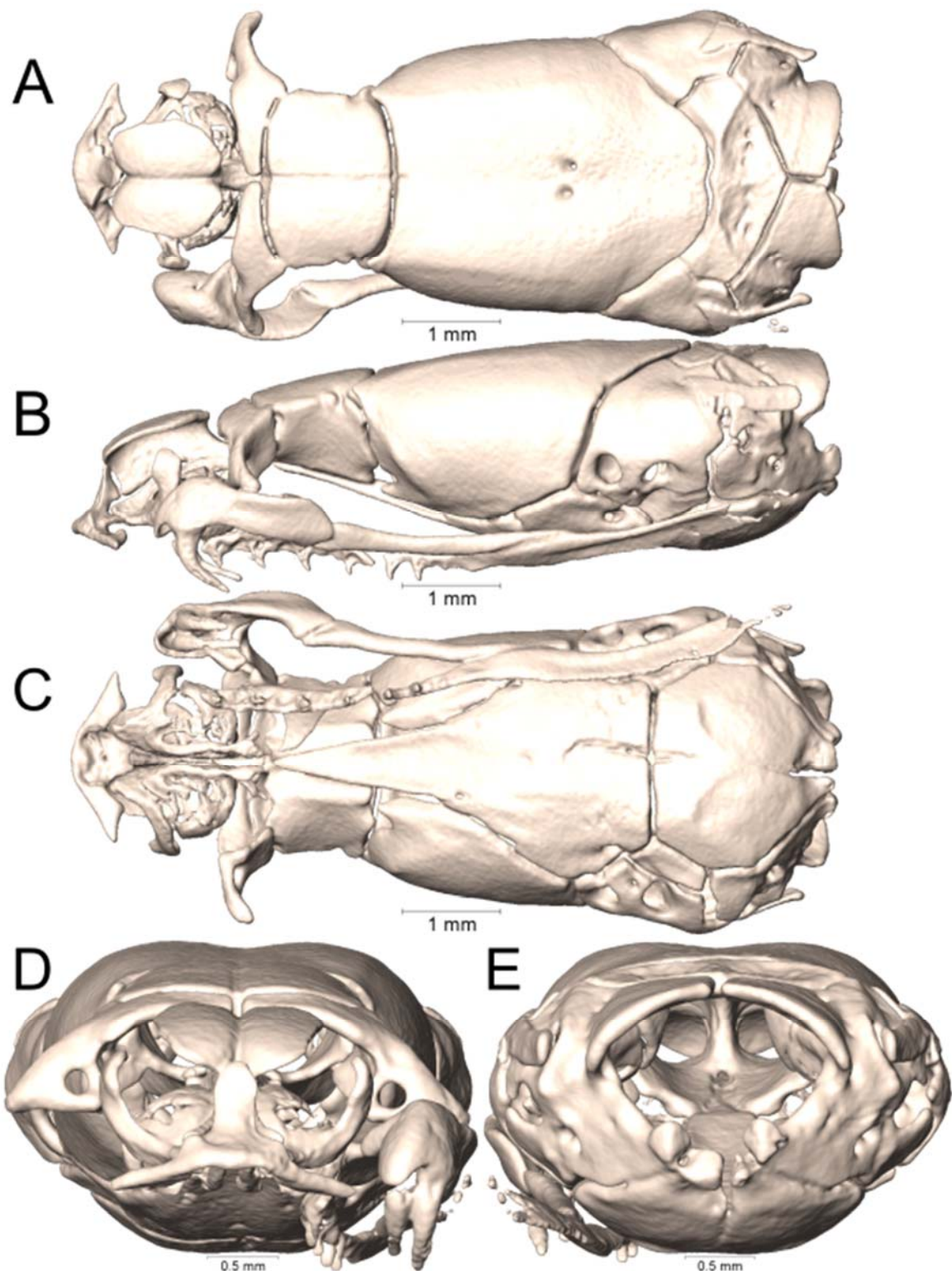
Supplemental Figure 1.36. Dorsal, lateral, ventral, anterior, and posterior views (A-E, respectively) of the skull of *Micrurus elegans veraepacis* (UTA R-58869). Right suspensorium excluded.



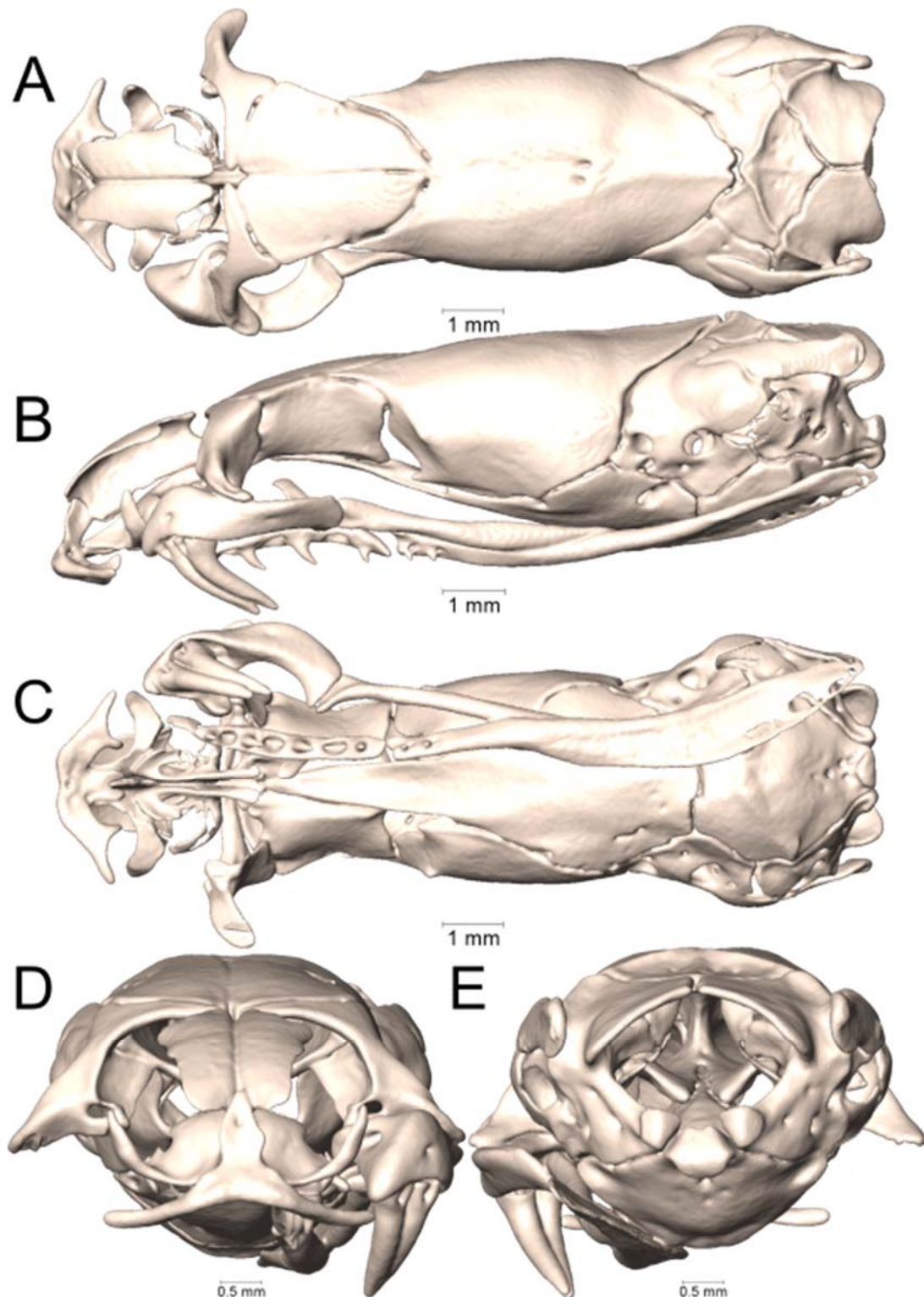
Supplemental Figure 1.37. Dorsal, lateral, ventral, anterior, and posterior views (A-E, respectively) of the skull of *Micrurus ephippifer* (UTA R-64863). Right suspensorium excluded.



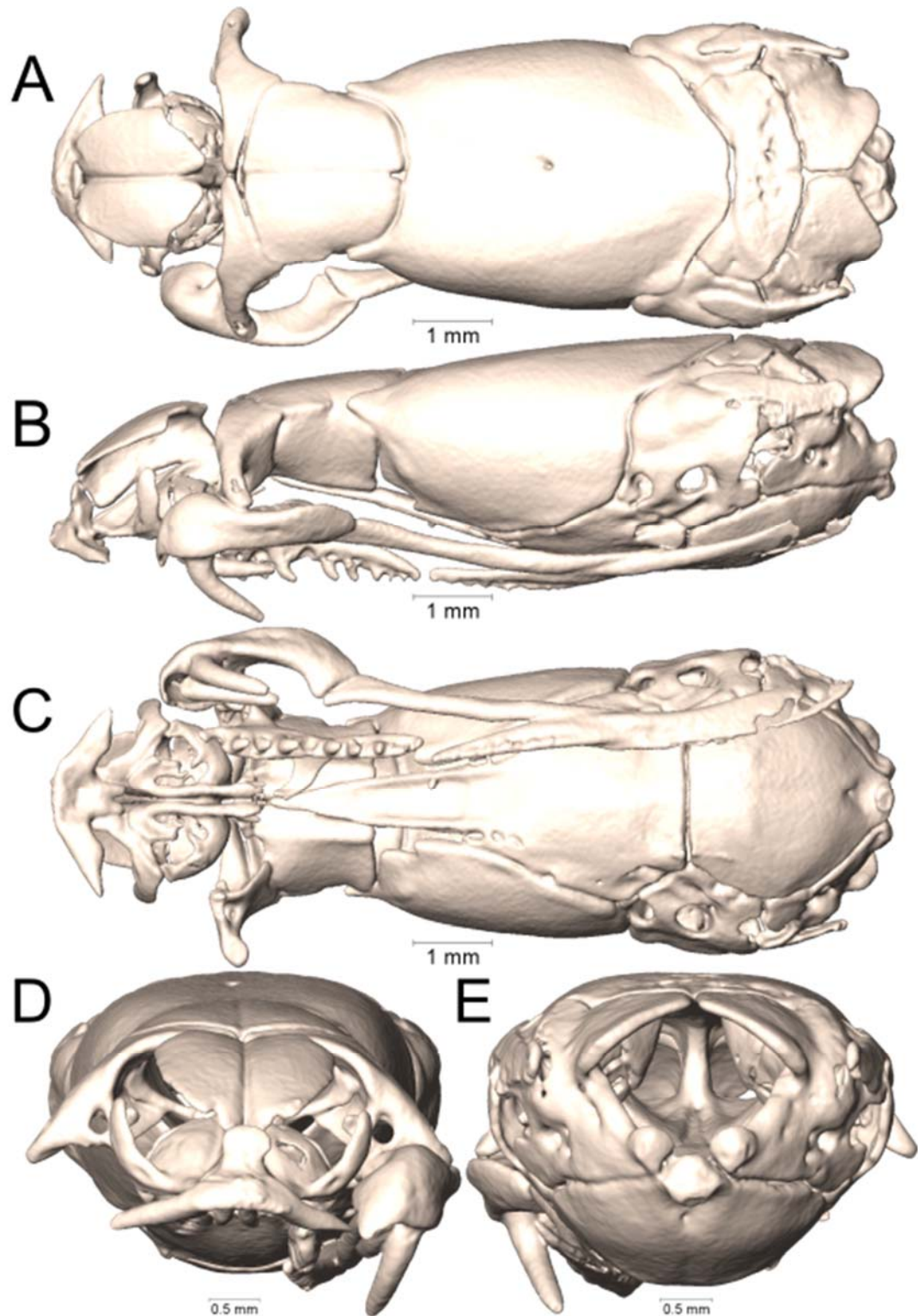
Supplemental Figure 1.38. Dorsal, lateral, ventral, anterior, and posterior views (A-E, respectively) of the skull of *Micrurus filiformis* (UTA R-3423). Right suspensorium excluded.



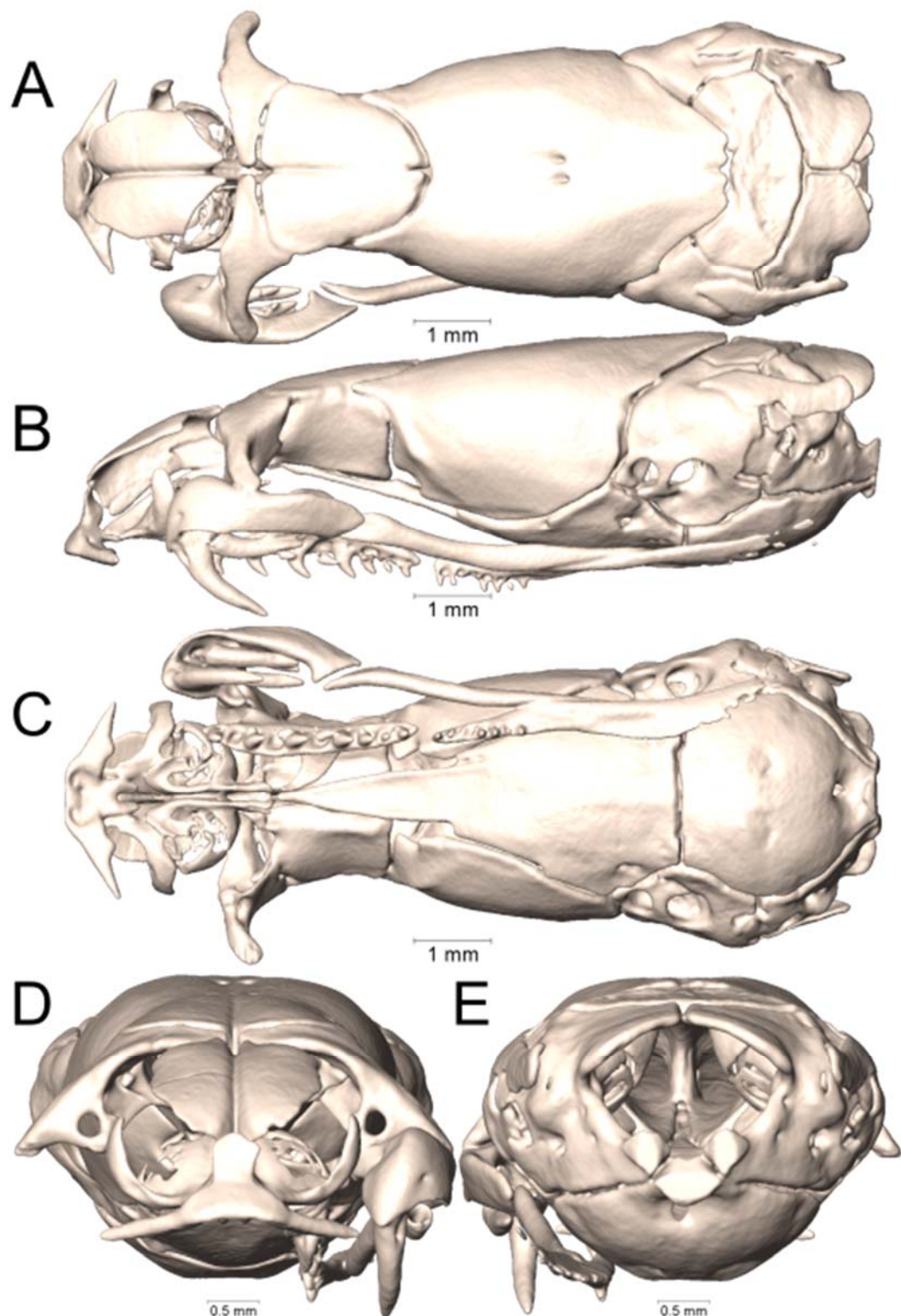
Supplemental Figure 1.39. Dorsal, lateral, ventral, anterior, and posterior views (A-E, respectively) of the skull of *Micrurus filiformis* (UTA R-65836). Right suspensorium excluded.



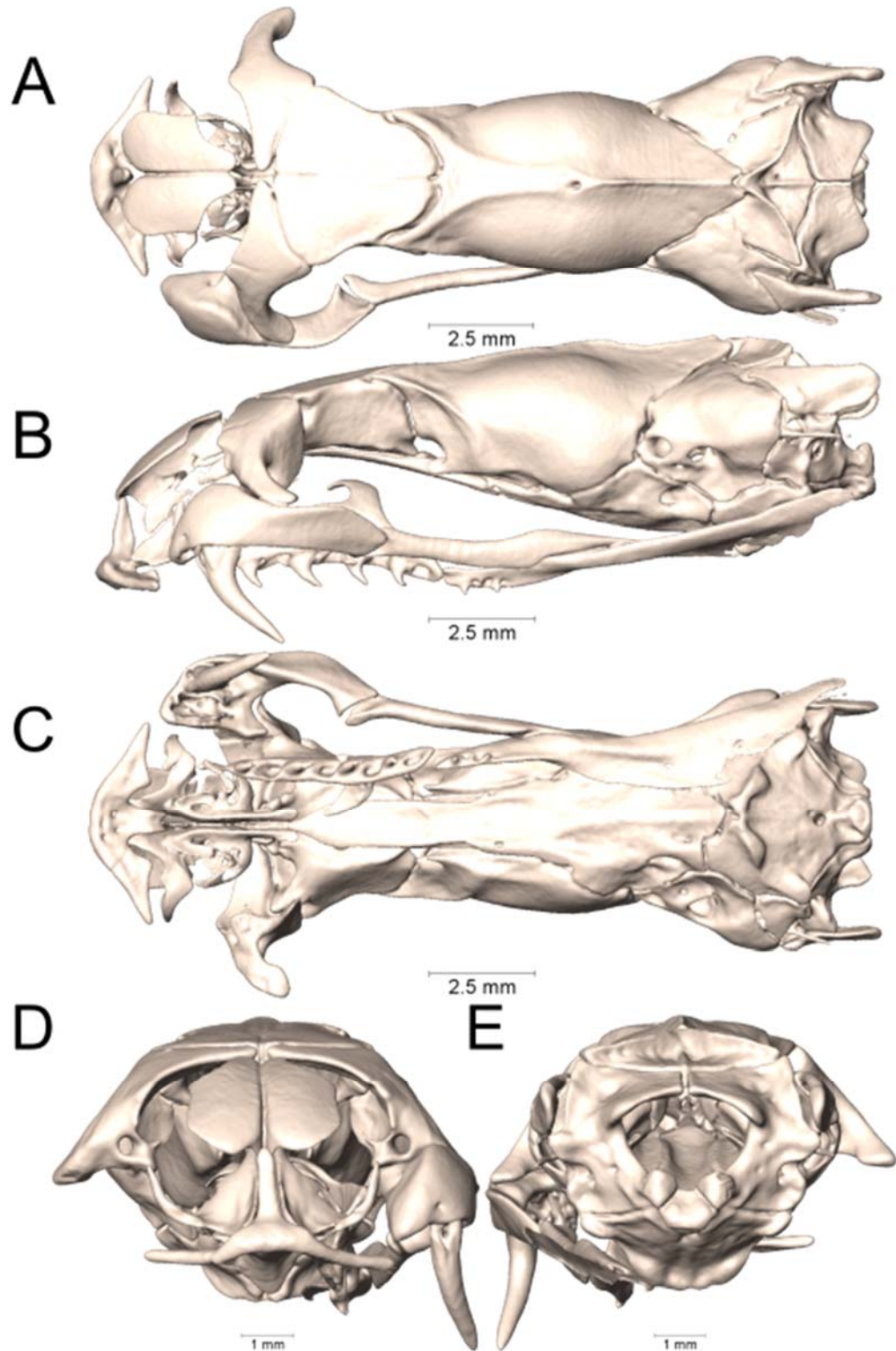
Supplemental Figure 1.40. Dorsal, lateral, ventral, anterior, and posterior views (A-E, respectively) of the skull of *Micrurus fulvius* (UTA R-61632). Right suspensorium excluded.



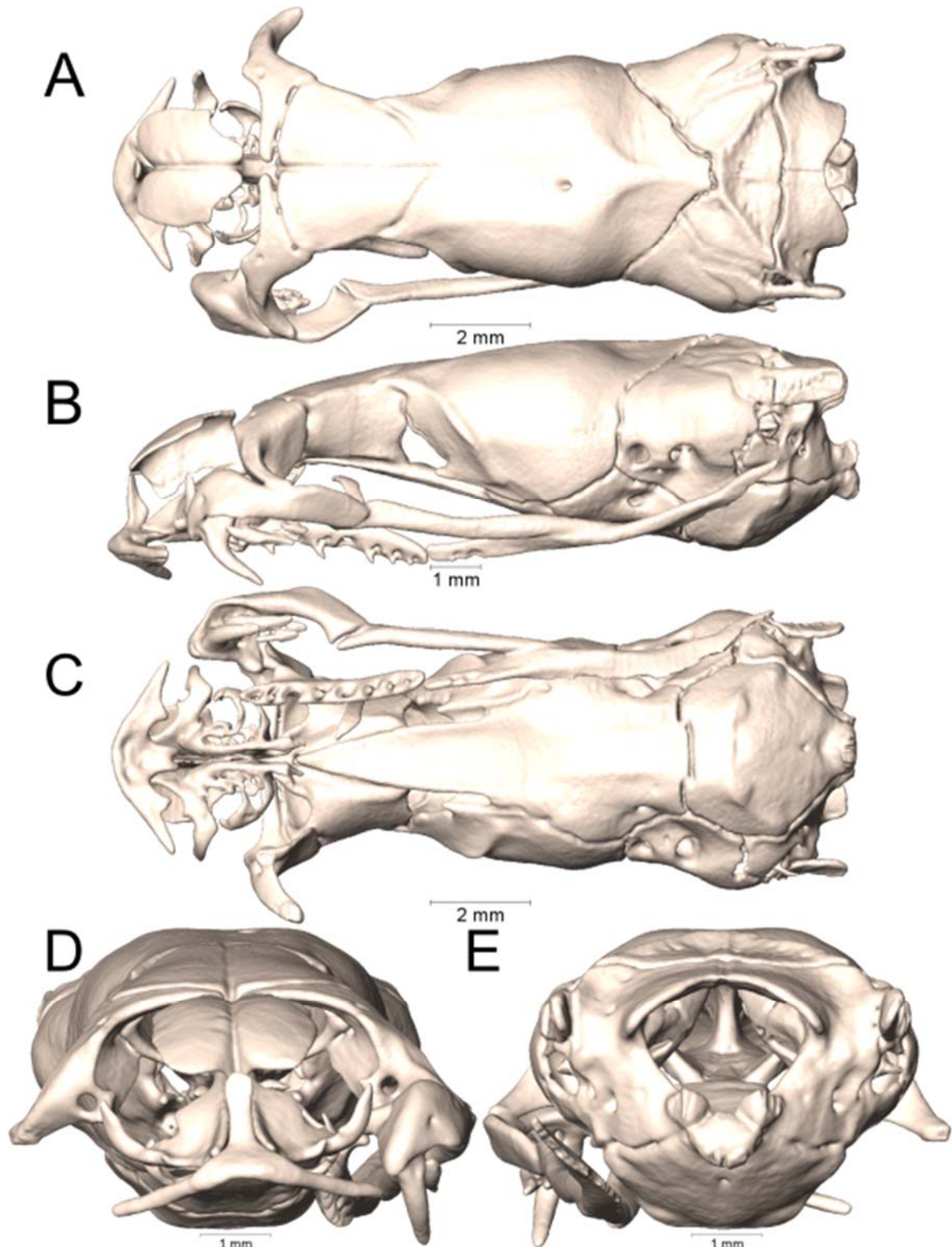
Supplemental Figure 1.41. Dorsal, lateral, ventral, anterior, and posterior views (A-E, respectively) of the skull of *Micrurus helleri* (UTA R-38005). Right suspensorium excluded.



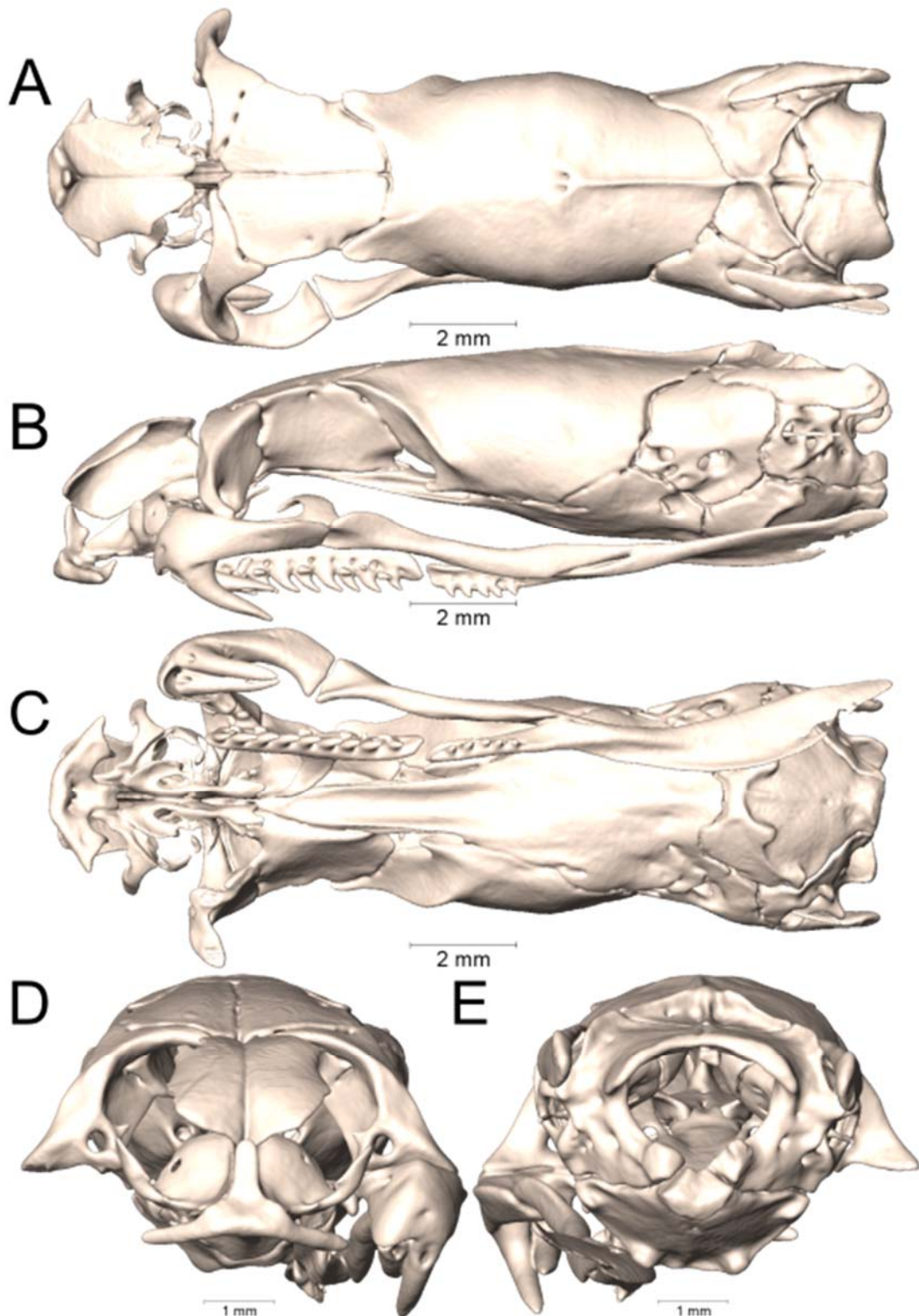
Supplemental Figure 1.42. Dorsal, lateral, ventral, anterior, and posterior views (A-E, respectively) of the skull of *Micrurus helleri* (UTA R-65841). Right suspensorium excluded.



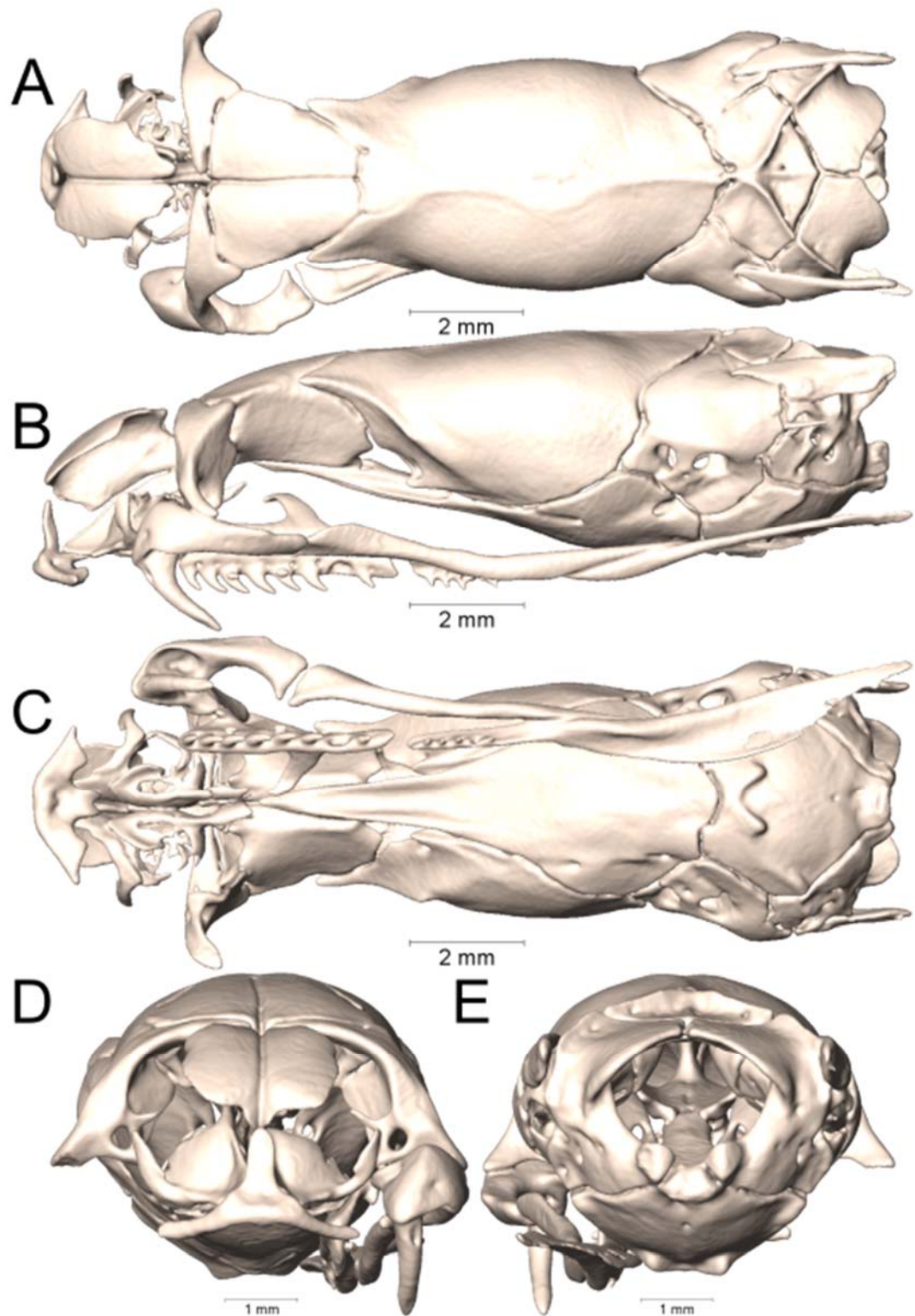
Supplemental Figure 1.43. Dorsal, lateral, ventral, anterior, and posterior views (A-E, respectively) of the skull of *Micrurus hemprichii* (UTA R-9683). Right suspensorium excluded.



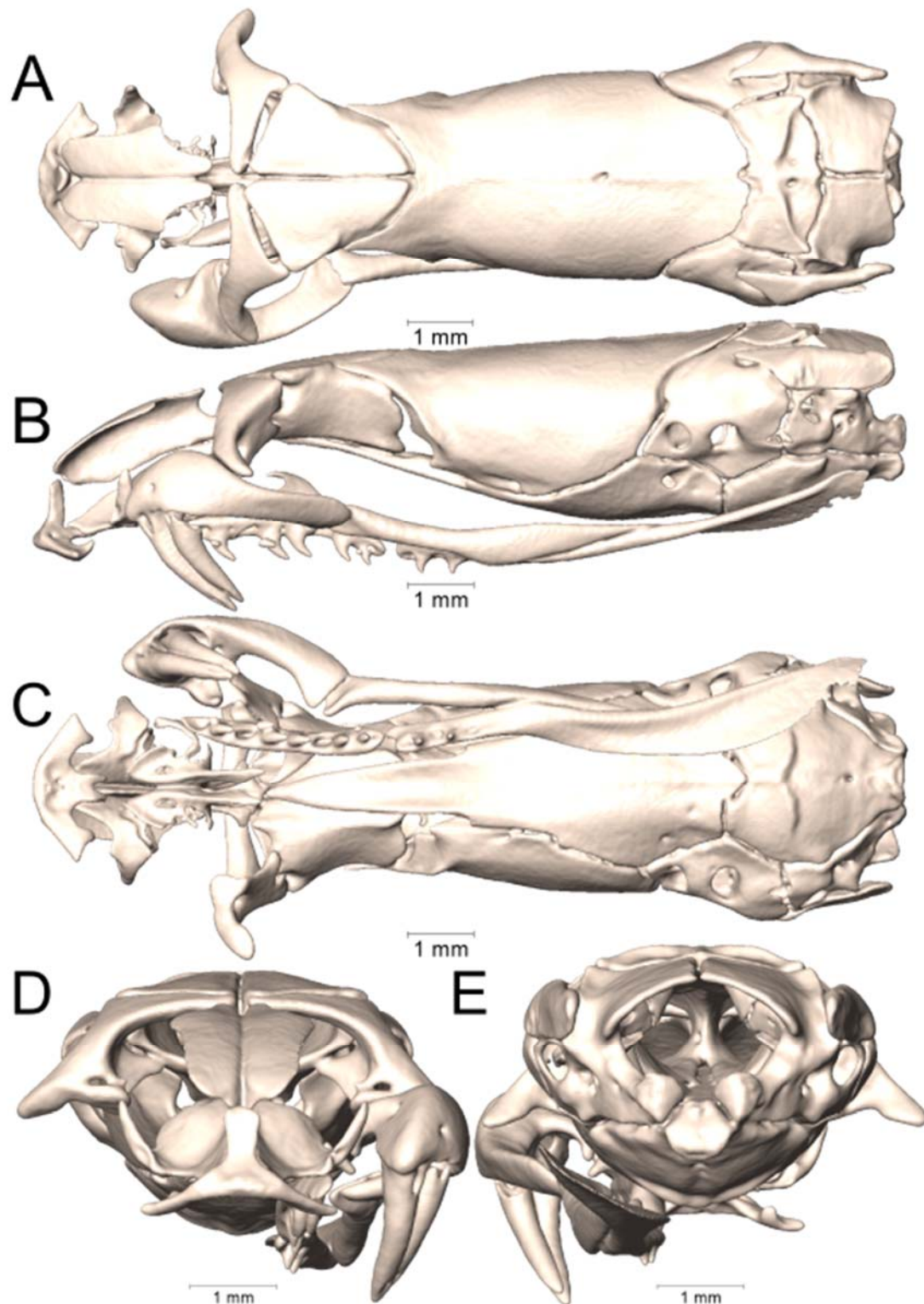
Supplemental Figure 1.44. Dorsal, lateral, ventral, anterior, and posterior views (A-E, respectively) of the skull of *Micrurus hemprichii* (UTA R-29997). Right suspensorium excluded.



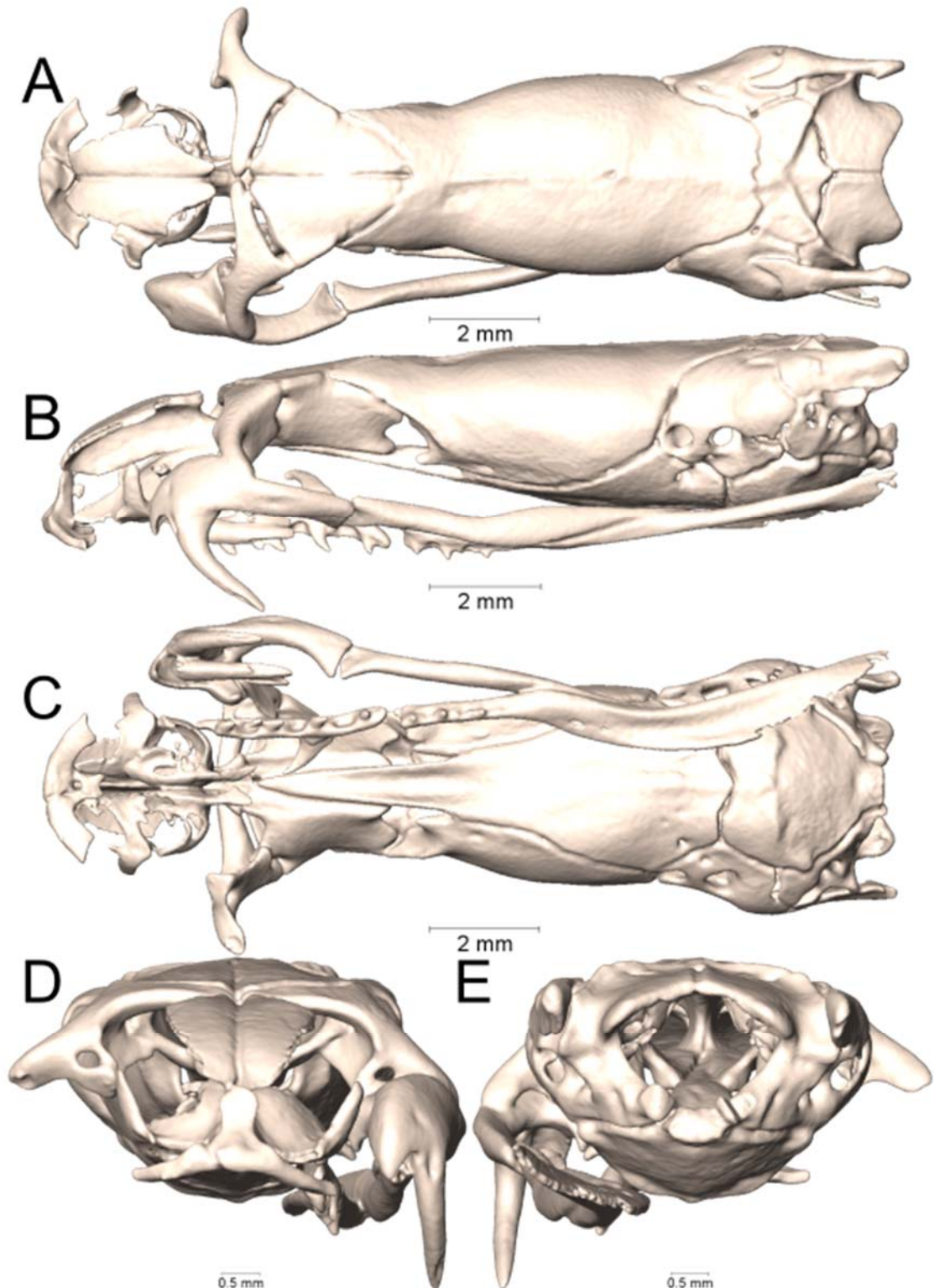
Supplemental Figure 1.45. Dorsal, lateral, ventral, anterior, and posterior views (A-E, respectively) of the skull of *Micrurus isozonus* (UTA R-3951). Right suspensorium excluded.



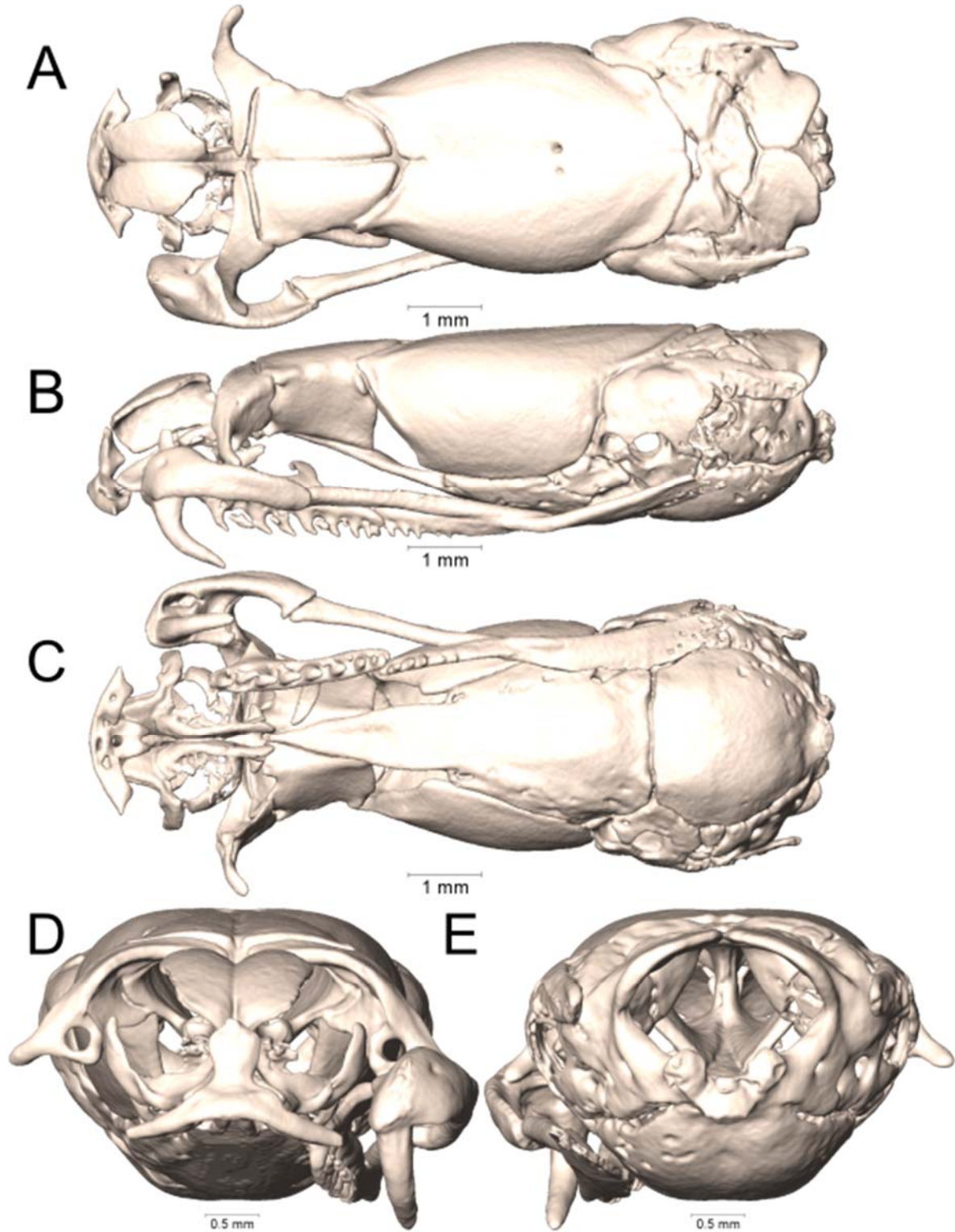
Supplemental Figure 1.46. Dorsal, lateral, ventral, anterior, and posterior views (A-E, respectively) of the skull of *Micrurus isozonus* (UTA R-22589). Right suspensorium excluded.



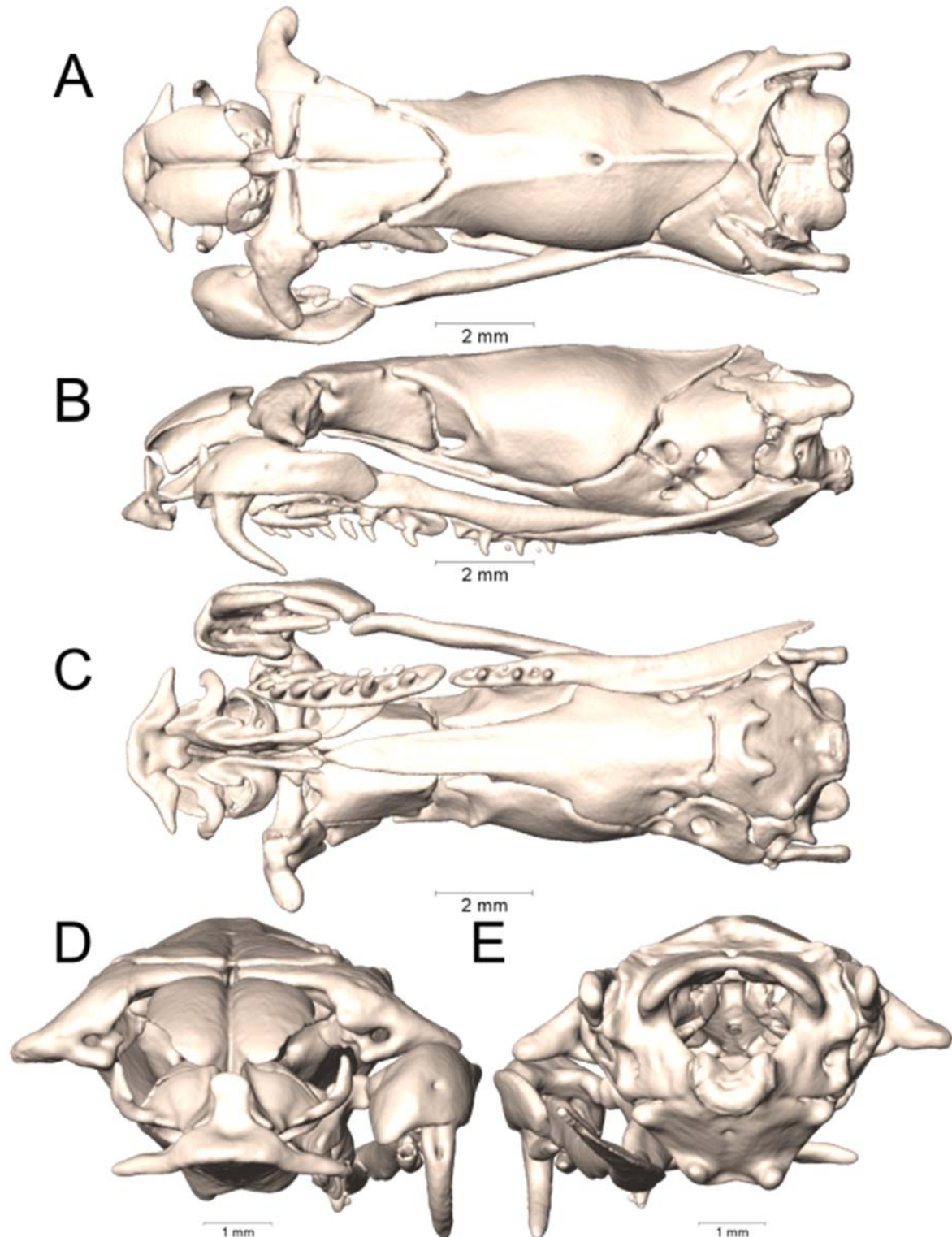
Supplemental Figure 1.47. Dorsal, lateral, ventral, anterior, and posterior views (A-E, respectively) of the skull of *Micrurus laticollaris* (UTA R-52559). Right suspensorium excluded.



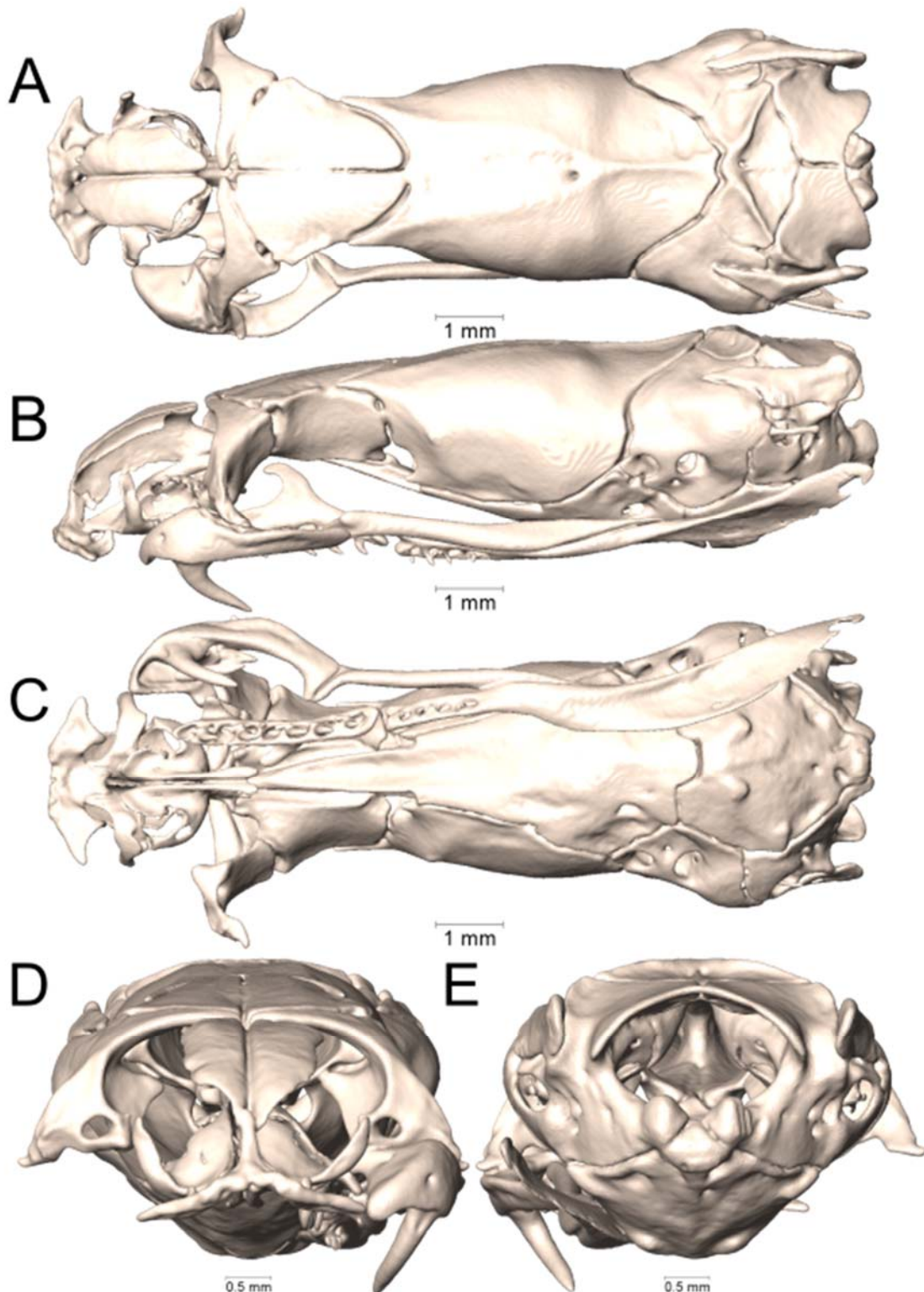
Supplemental Figure 1.48. Dorsal, lateral, ventral, anterior, and posterior views (A-E, respectively) of the skull of *Micrurus laticollaris* (UTA R-57562). Right suspensorium excluded.



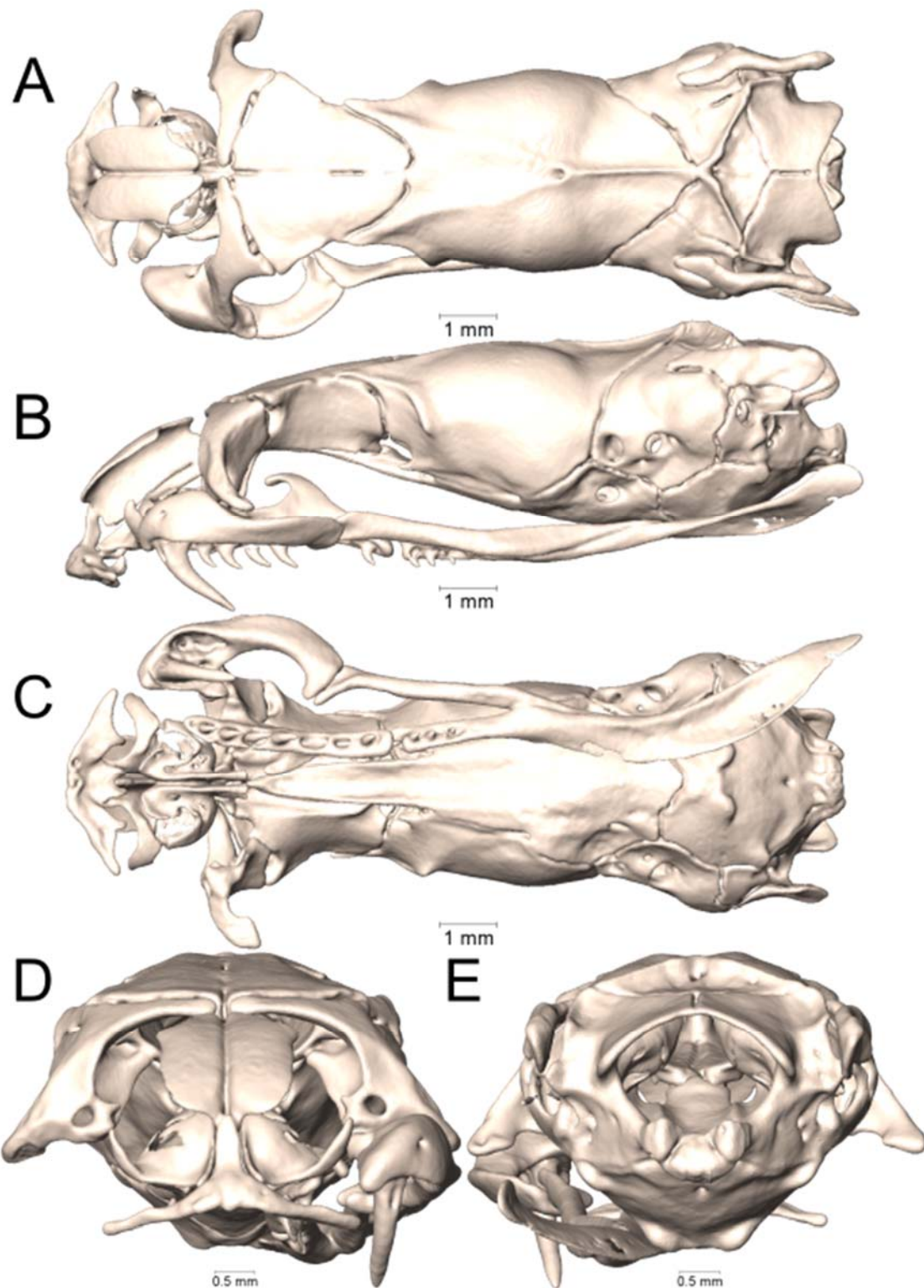
Supplemental Figure 1.49. Dorsal, lateral, ventral, anterior, and posterior views (A-E, respectively) of the skull of *Micrurus lemniscatus* cf. *helleri* (UTA R-34563). Right suspensorium excluded.



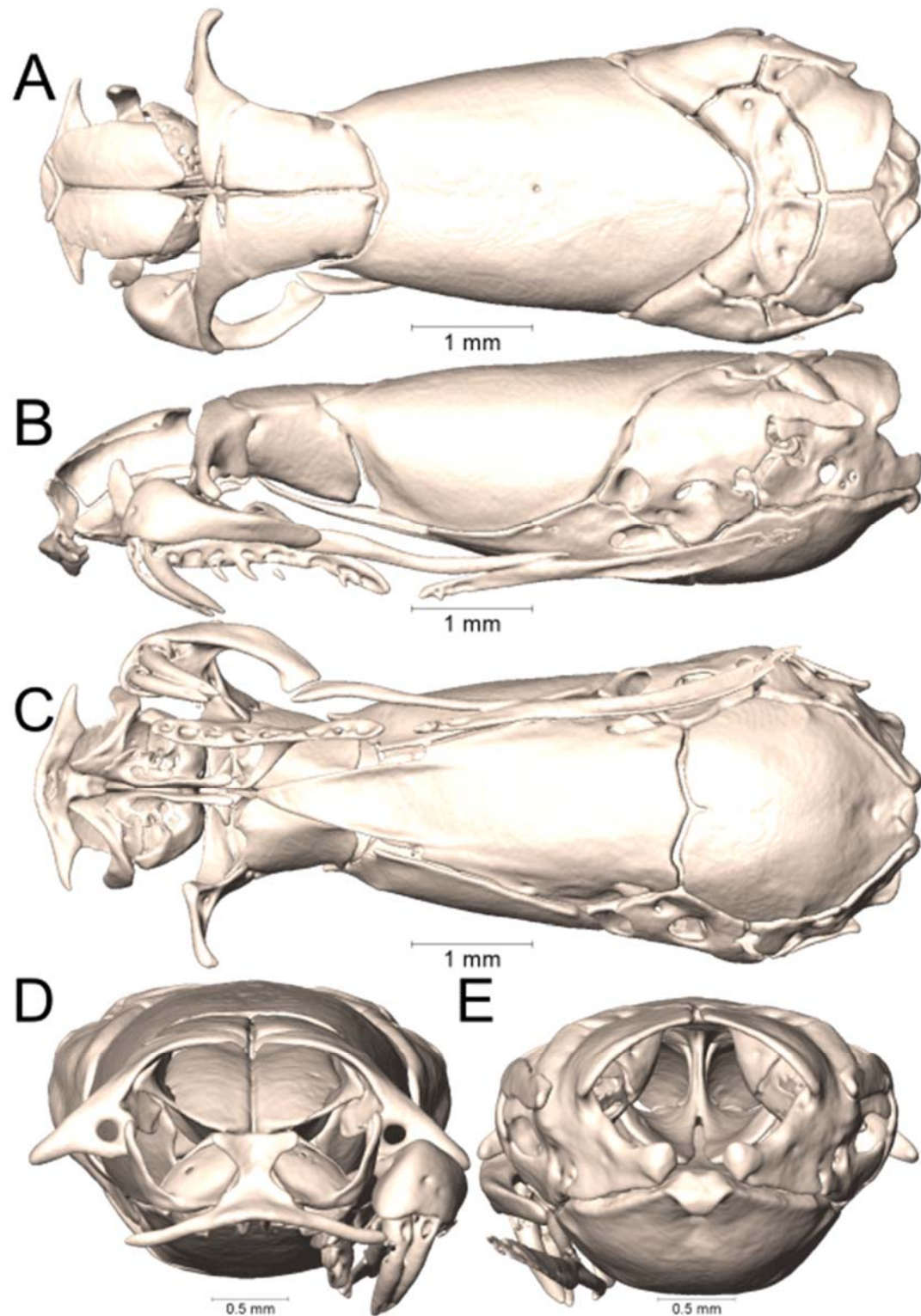
Supplemental Figure 1.50. Dorsal, lateral, ventral, anterior, and posterior views (A-E, respectively) of the skull of *Micrurus lemniscatus* cf. *helleri* (UTA R-65803). Right suspensorium excluded.



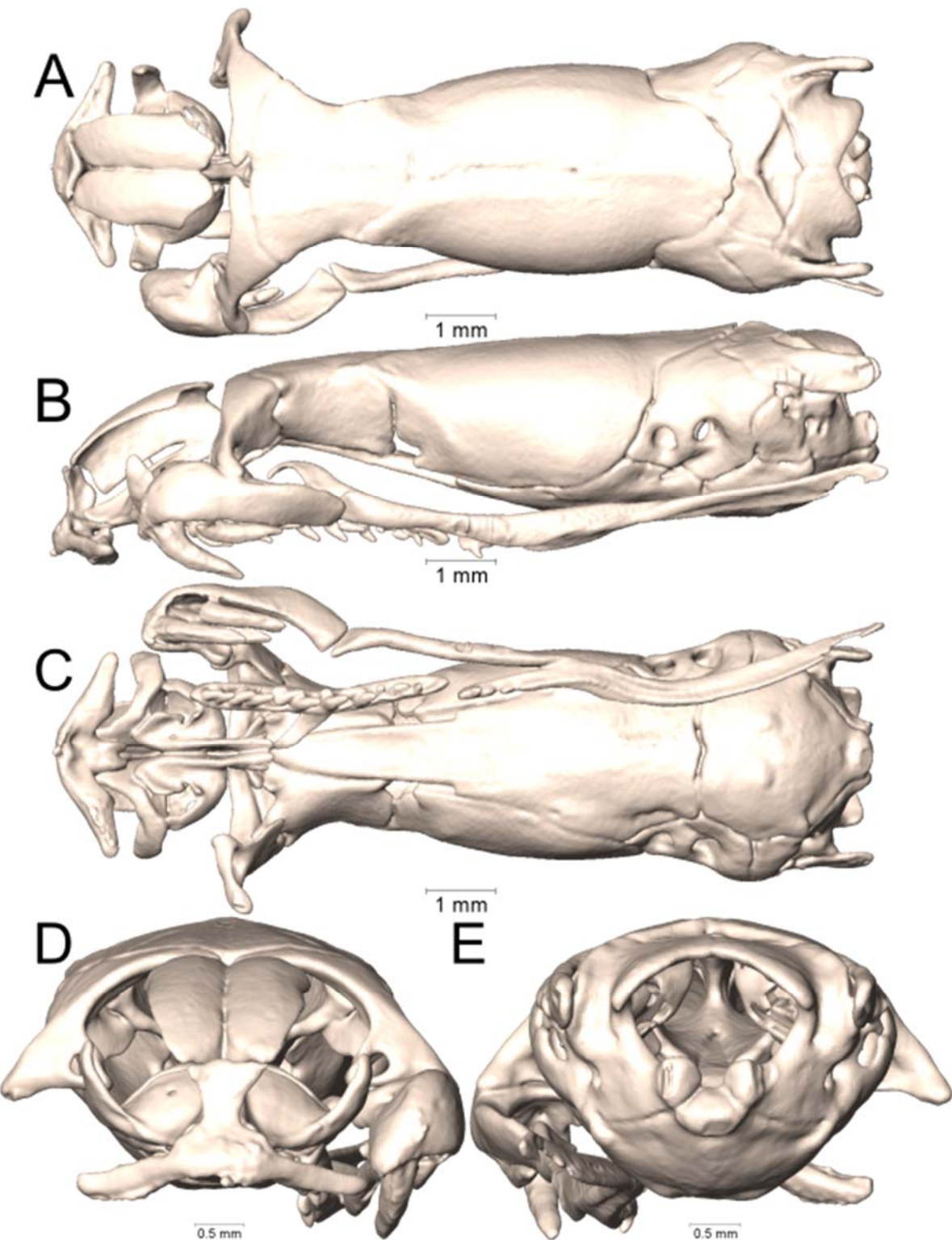
Supplemental Figure 1.51. Dorsal, lateral, ventral, anterior, and posterior views (A-E, respectively) of the skull of *Micrurus limbatus* (UTA R-64852). Right suspensorium excluded.



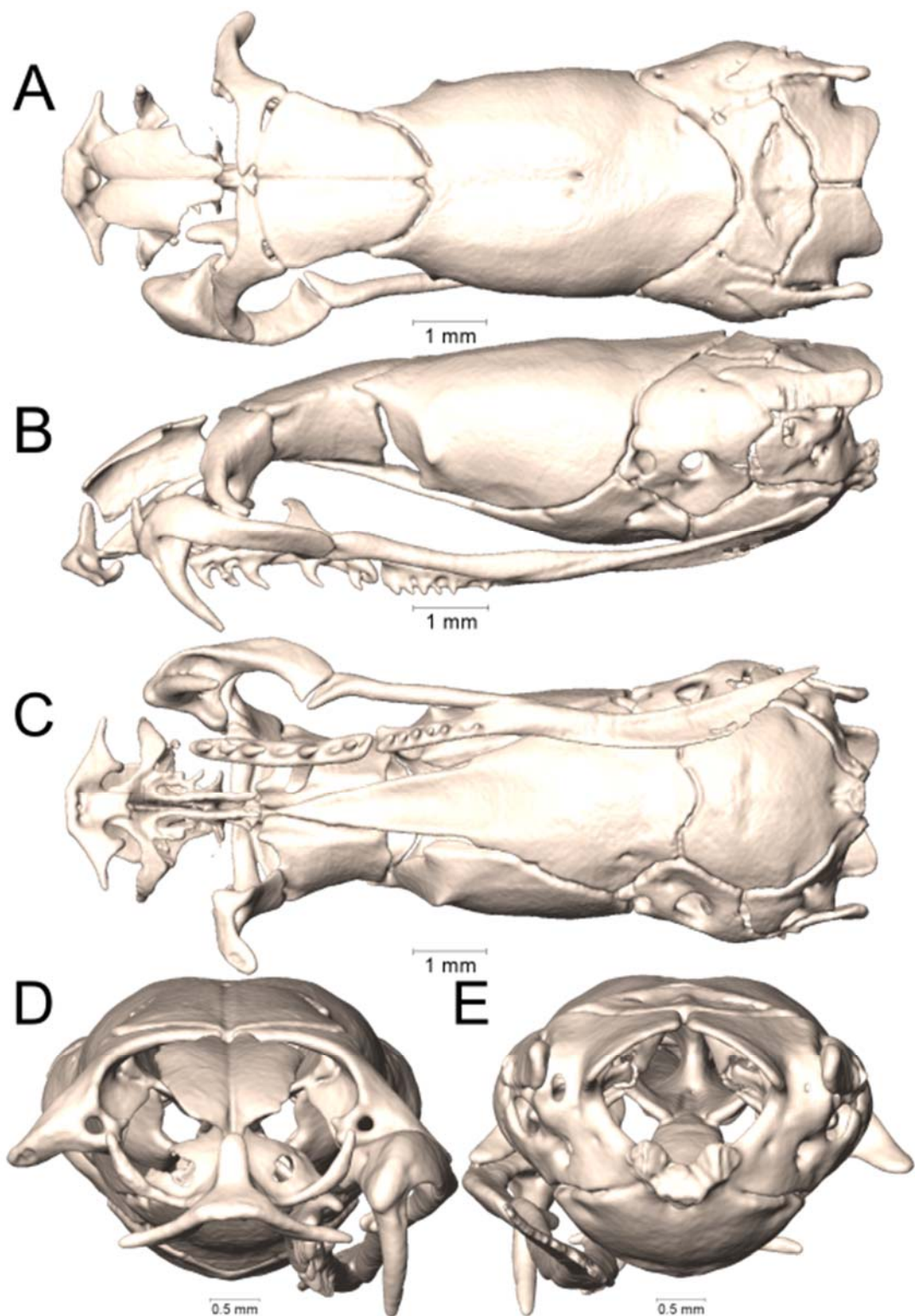
Supplemental Figure 1.52. Dorsal, lateral, ventral, anterior, and posterior views (A-E, respectively) of the skull of *Micrurus limbatus* (UTA R-64899). Right suspensorium excluded.



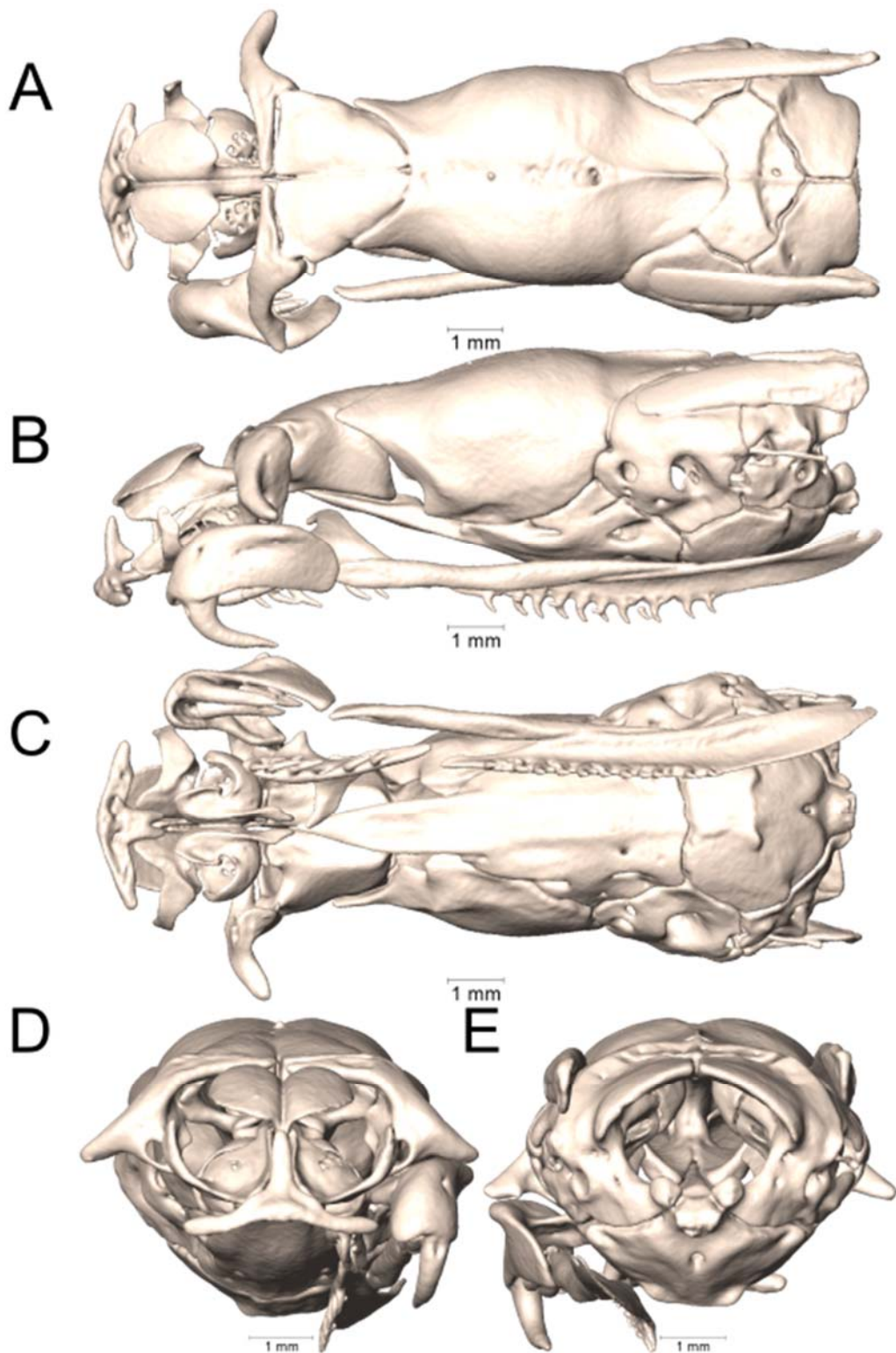
Supplemental Figure 1.53. Dorsal, lateral, ventral, anterior, and posterior views (A-E, respectively) of the skull of *Micrurus melanotus* (UTA R-22582). Right suspensorium excluded.



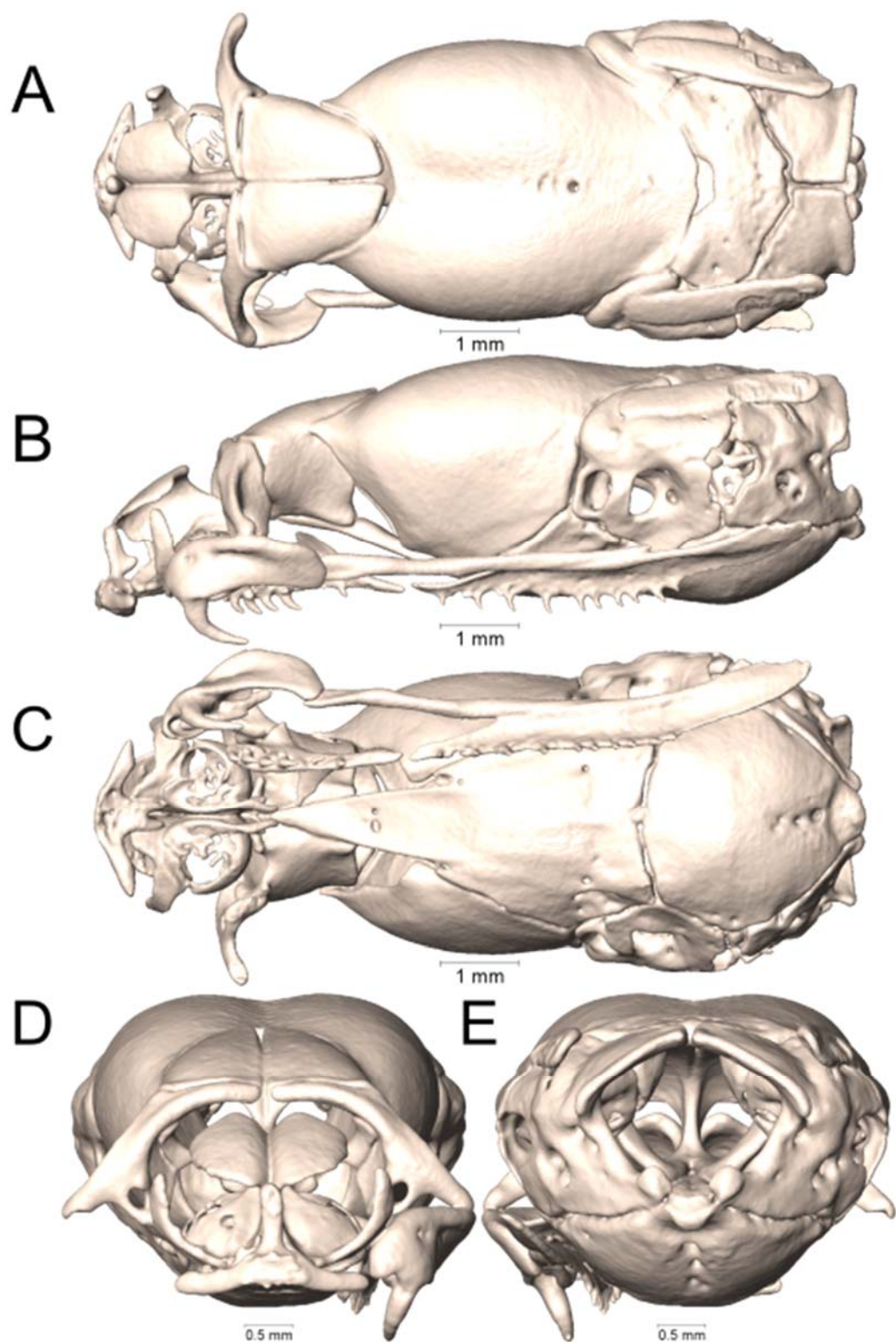
Supplemental Figure 1.54. Dorsal, lateral, ventral, anterior, and posterior views (A-E, respectively) of the skull of *Micrurus mipartitus* (UTA R-54187). Right suspensorium excluded.



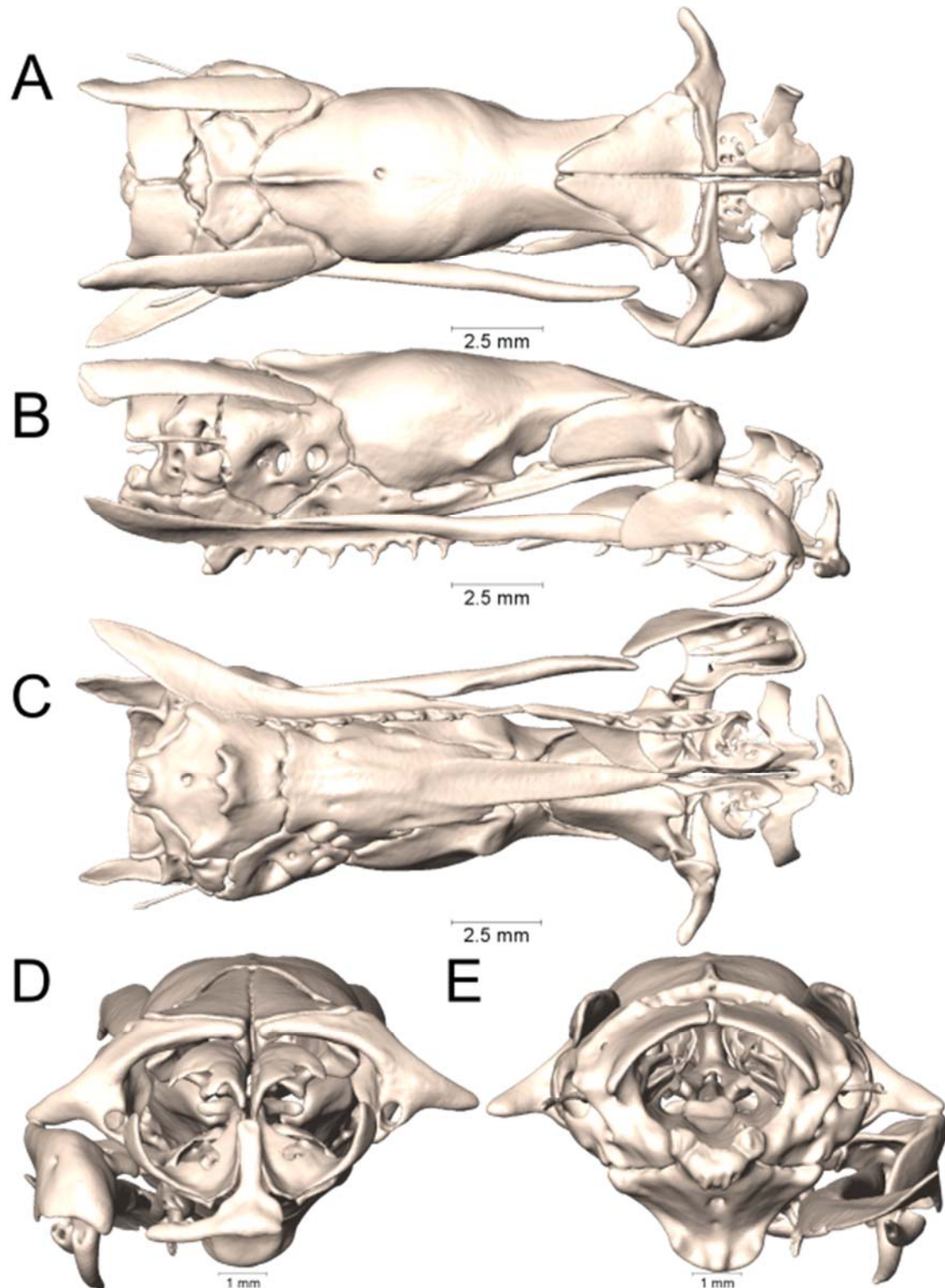
Supplemental Figure 1.55. Dorsal, lateral, ventral, anterior, and posterior views (A-E, respectively) of the skull of *Micrurus mosquitensis* (UTA R-12919). Right suspensorium excluded.



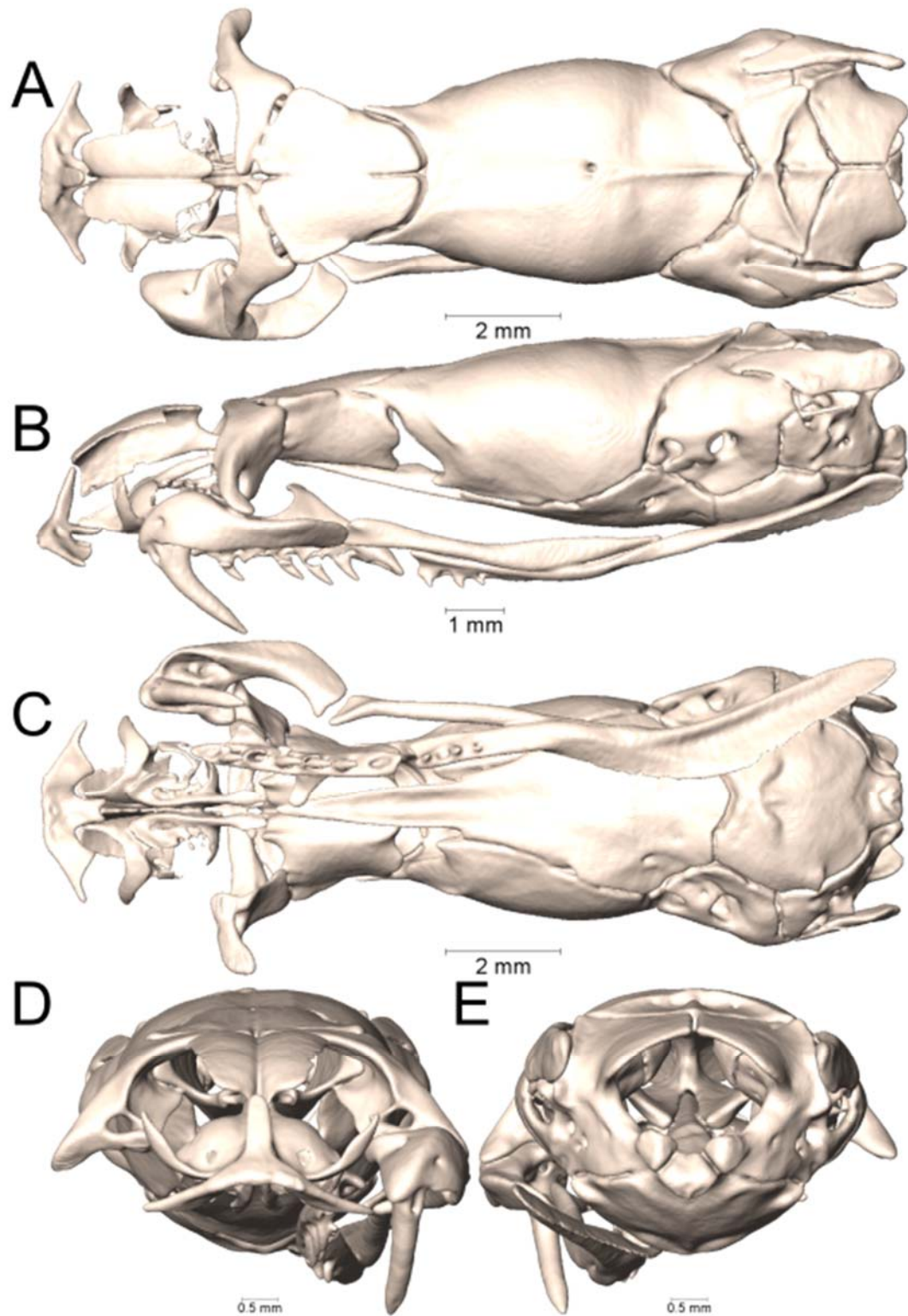
Supplemental Figure 1.56. Dorsal, lateral, ventral, anterior, and posterior views (A-E, respectively) of the skull of *Micrurus nattereri* (UTA R-54175). Right suspensorium excluded.



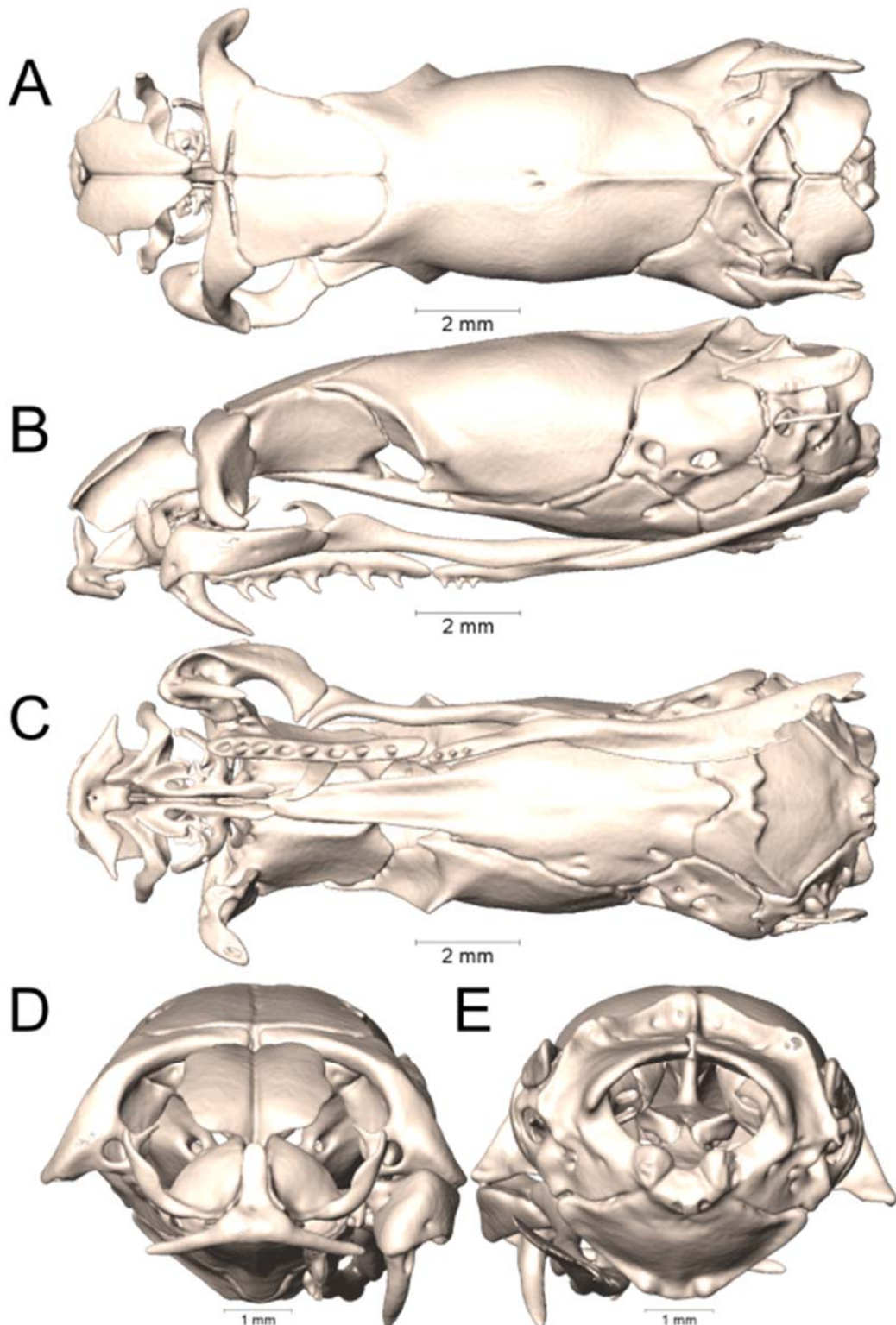
Supplemental Figure 1.57. Dorsal, lateral, ventral, anterior, and posterior views (A-E, respectively) of the skull of *Micrurus nattereri* (UTA R-55086). Right suspensorium excluded.



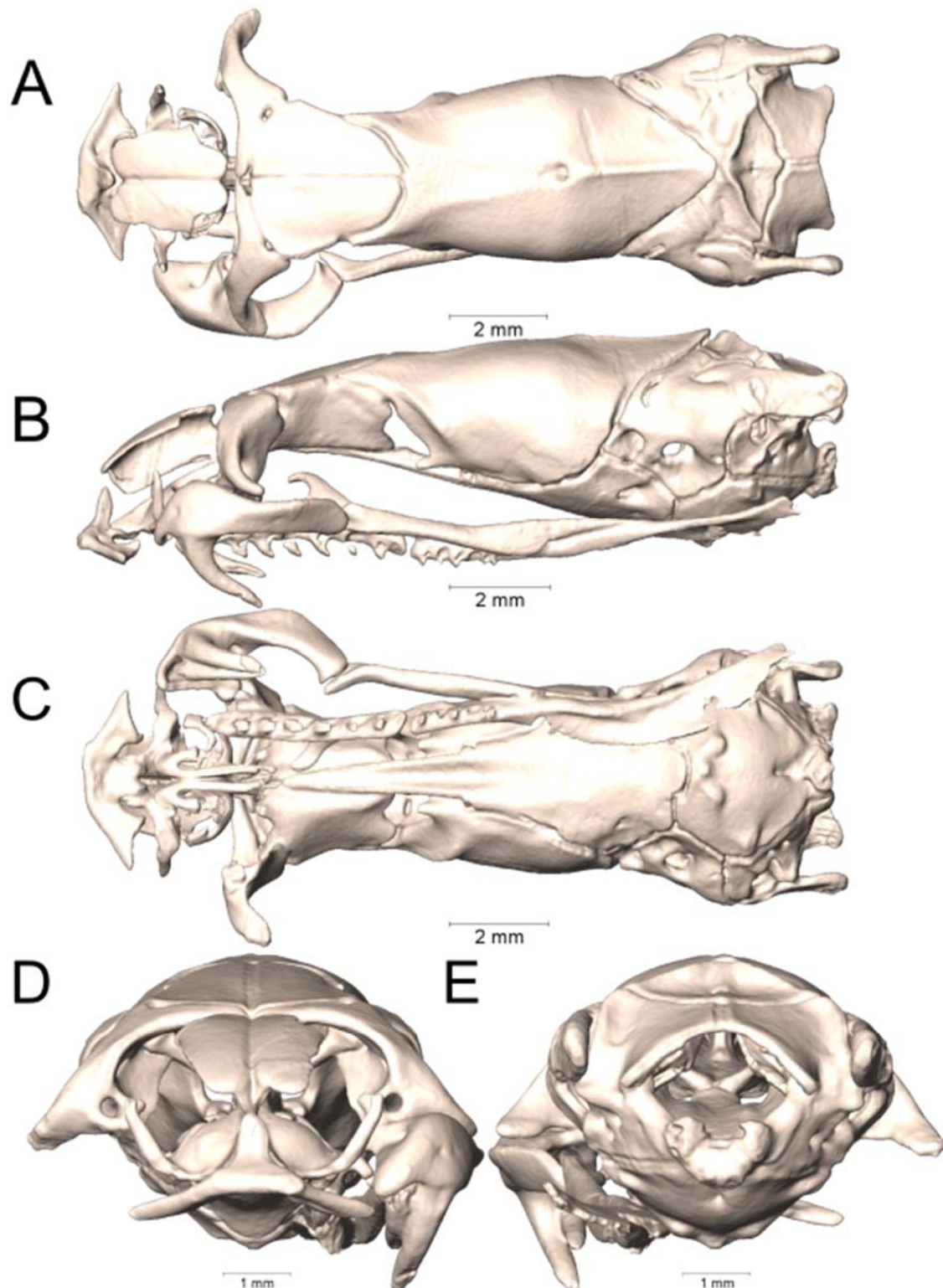
Supplemental Figure 1.58. Dorsal, lateral, ventral, anterior, and posterior views (A-E, respectively) of the skull of *Micrurus nattereri* (UTA R-60727). Left suspensorium excluded.



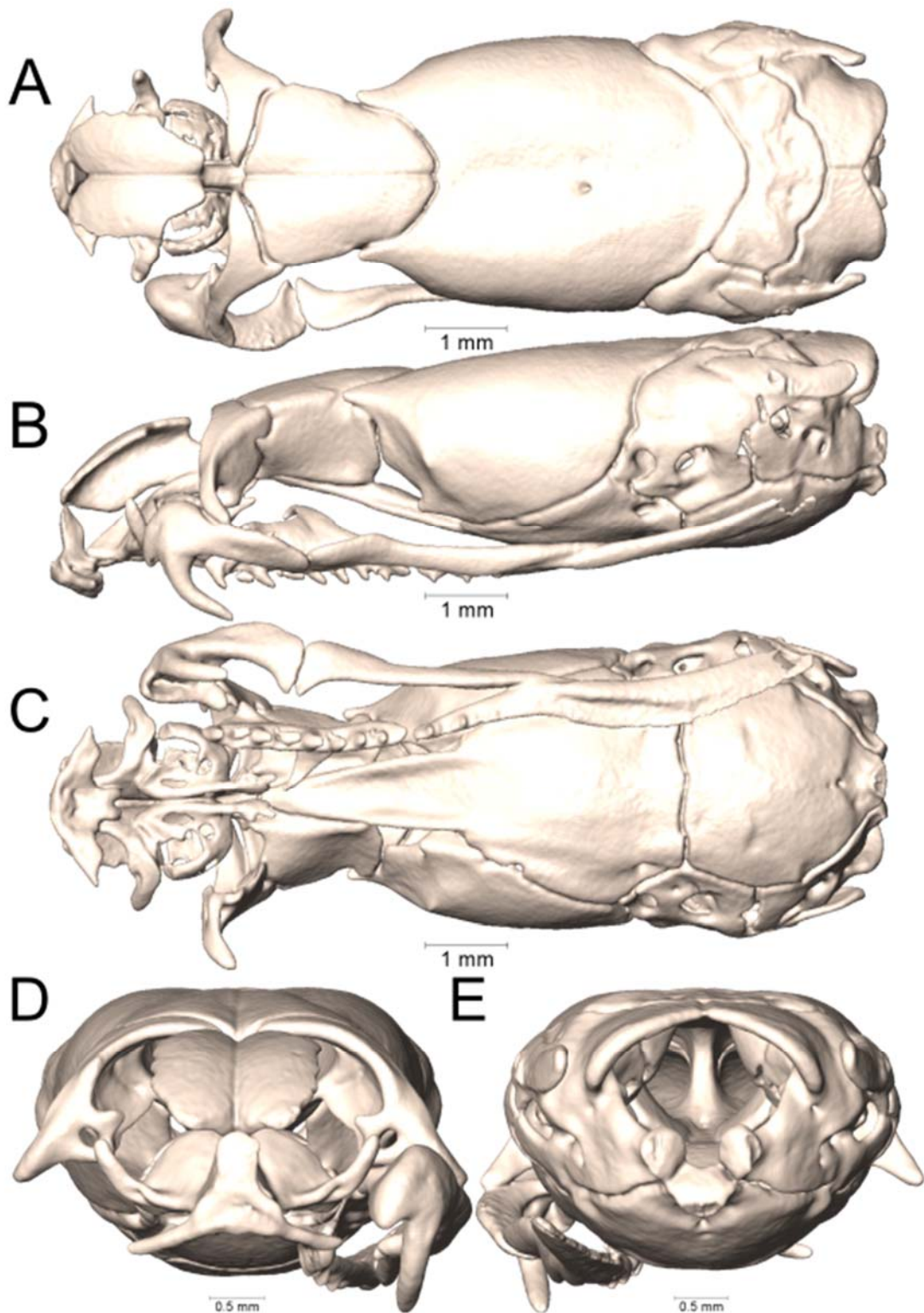
Supplemental Figure 1.59. Dorsal, lateral, ventral, anterior, and posterior views (A-E, respectively) of the skull of *Micrurus nigrocinctus zunilensis* (UTA R-64858). Right suspensorium excluded.



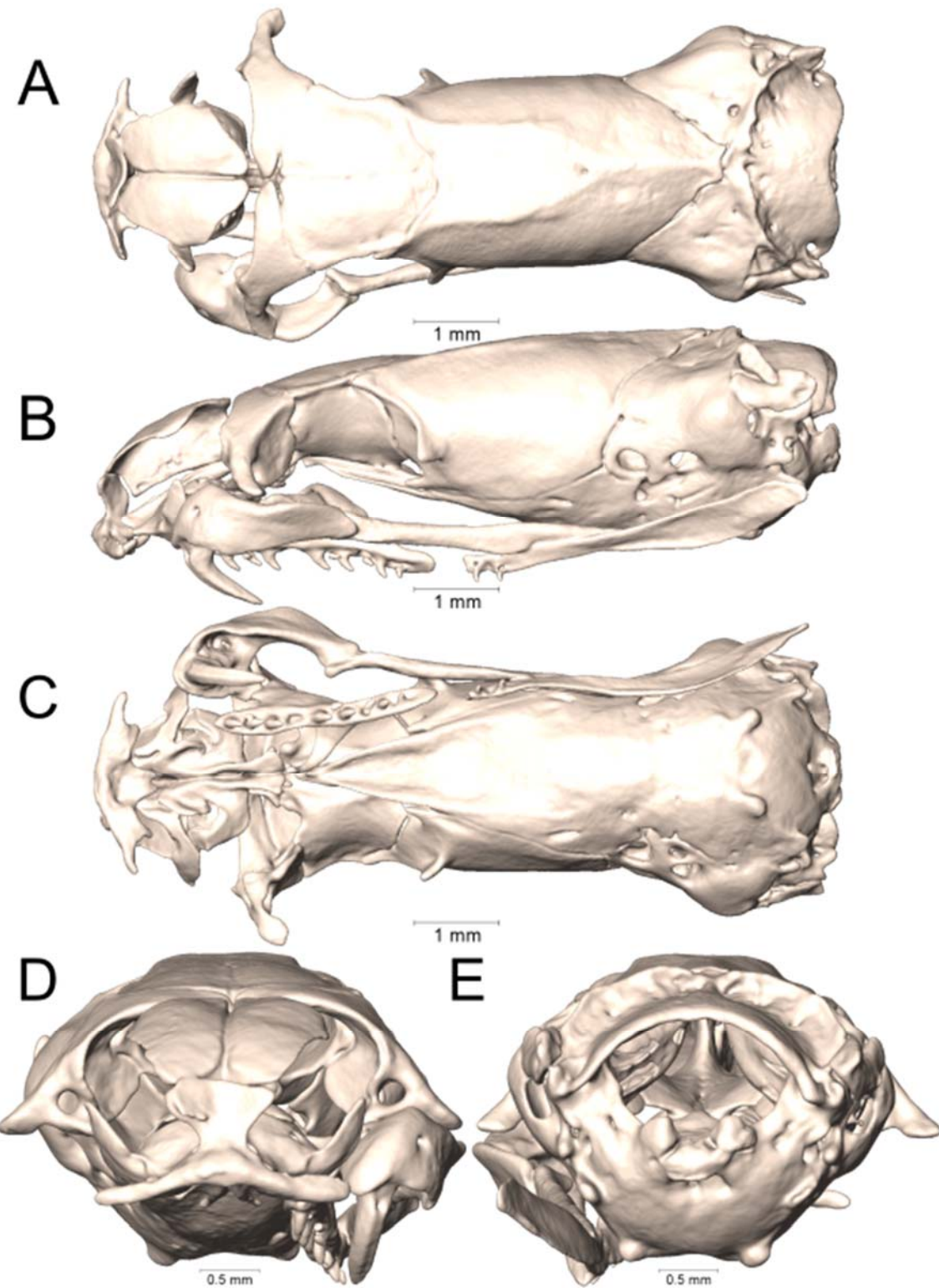
Supplemental Figure 1.60. Dorsal, lateral, ventral, anterior, and posterior views (A-E, respectively) of the skull of *Micrurus obscurus* (UTA R-3840). Right suspensorium excluded.



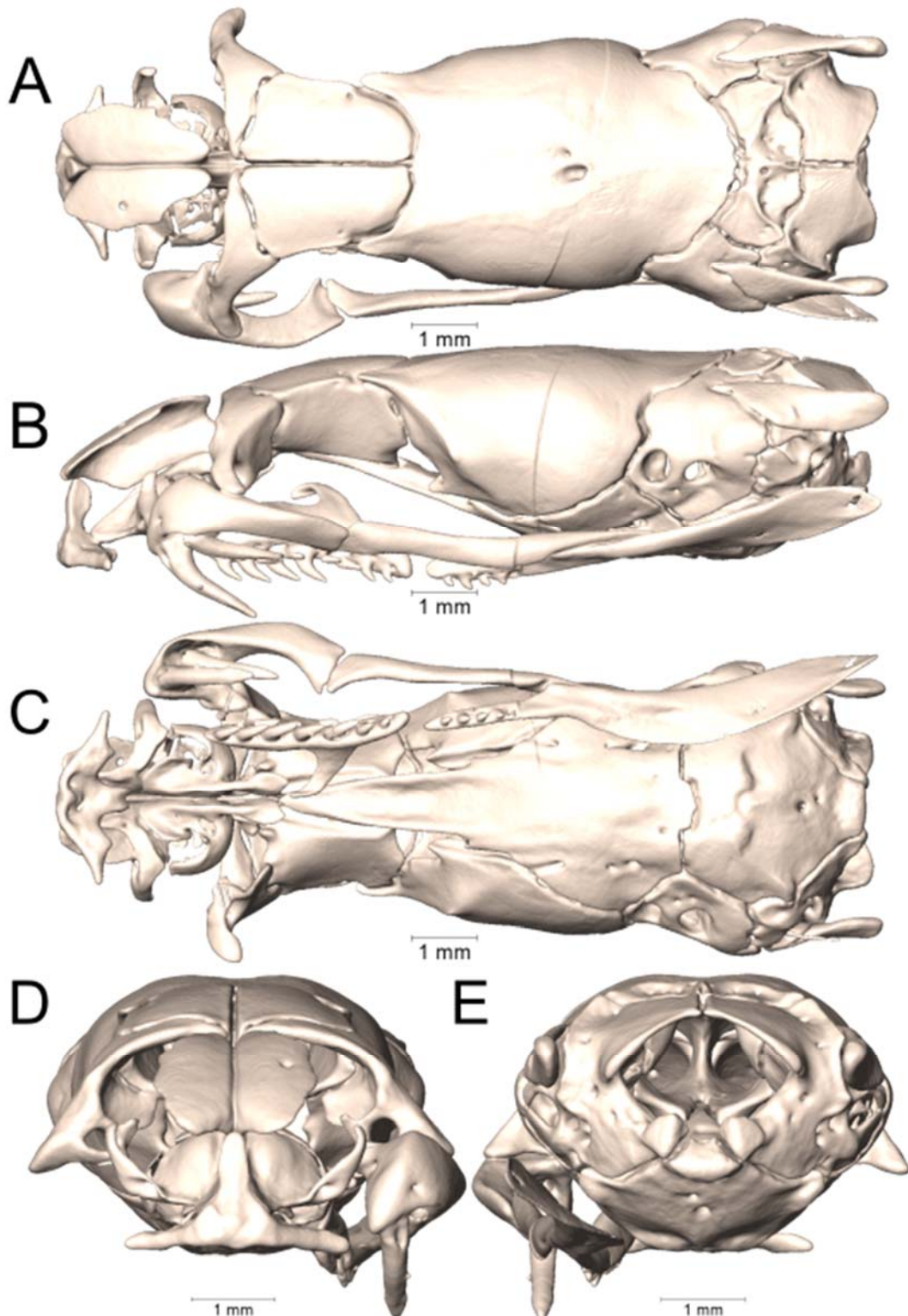
Supplemental Figure 1.61. Dorsal, lateral, ventral, anterior, and posterior views (A-E, respectively) of the skull of *Micrurus ornatissimus* (UTA R-60724). Right suspensorium excluded.



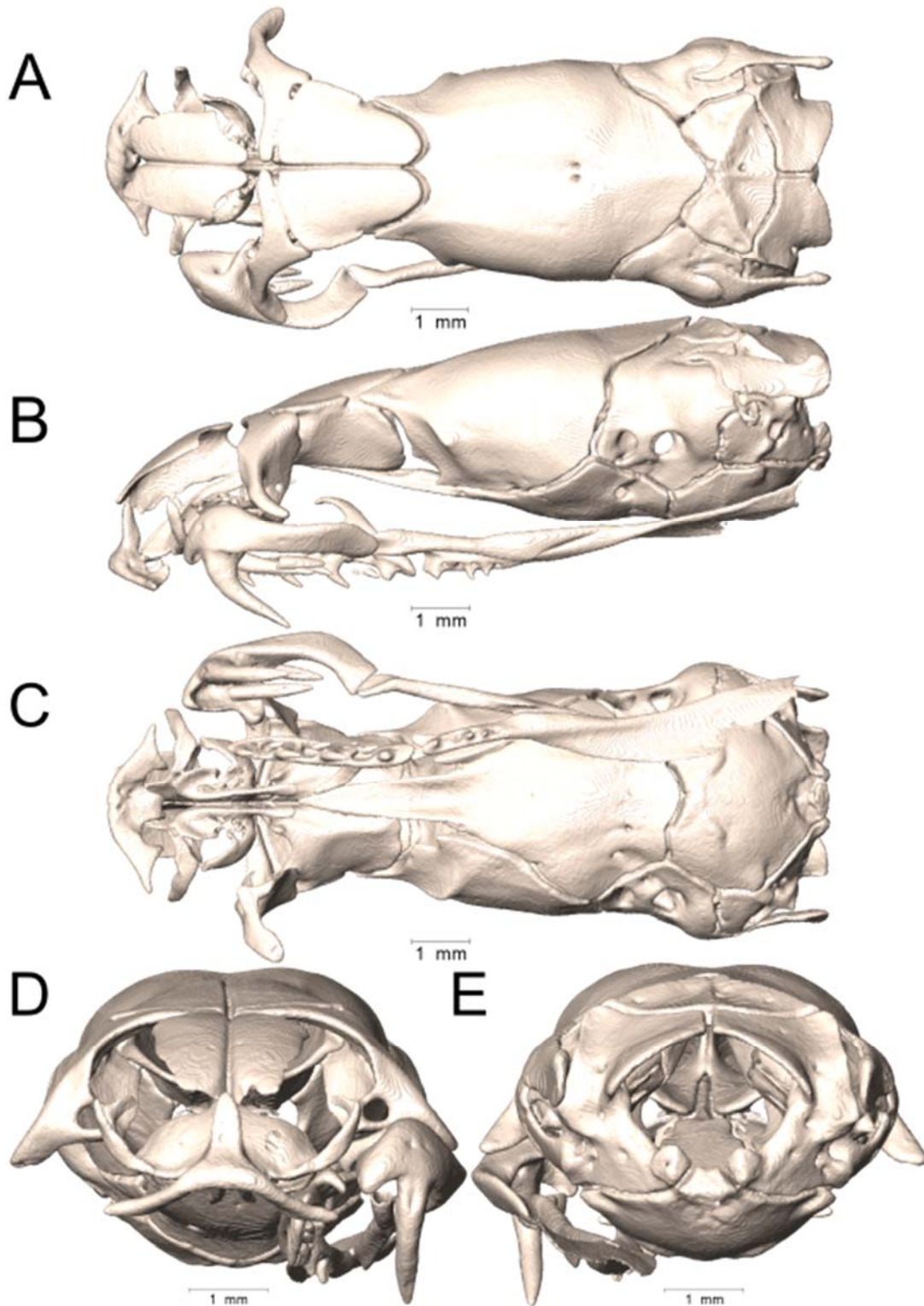
Supplemental Figure 1.62. Dorsal, lateral, ventral, anterior, and posterior views (A-E, respectively) of the skull of *Micrurus pyrrhocryptus* (UTA R-51404). Right suspensorium excluded.



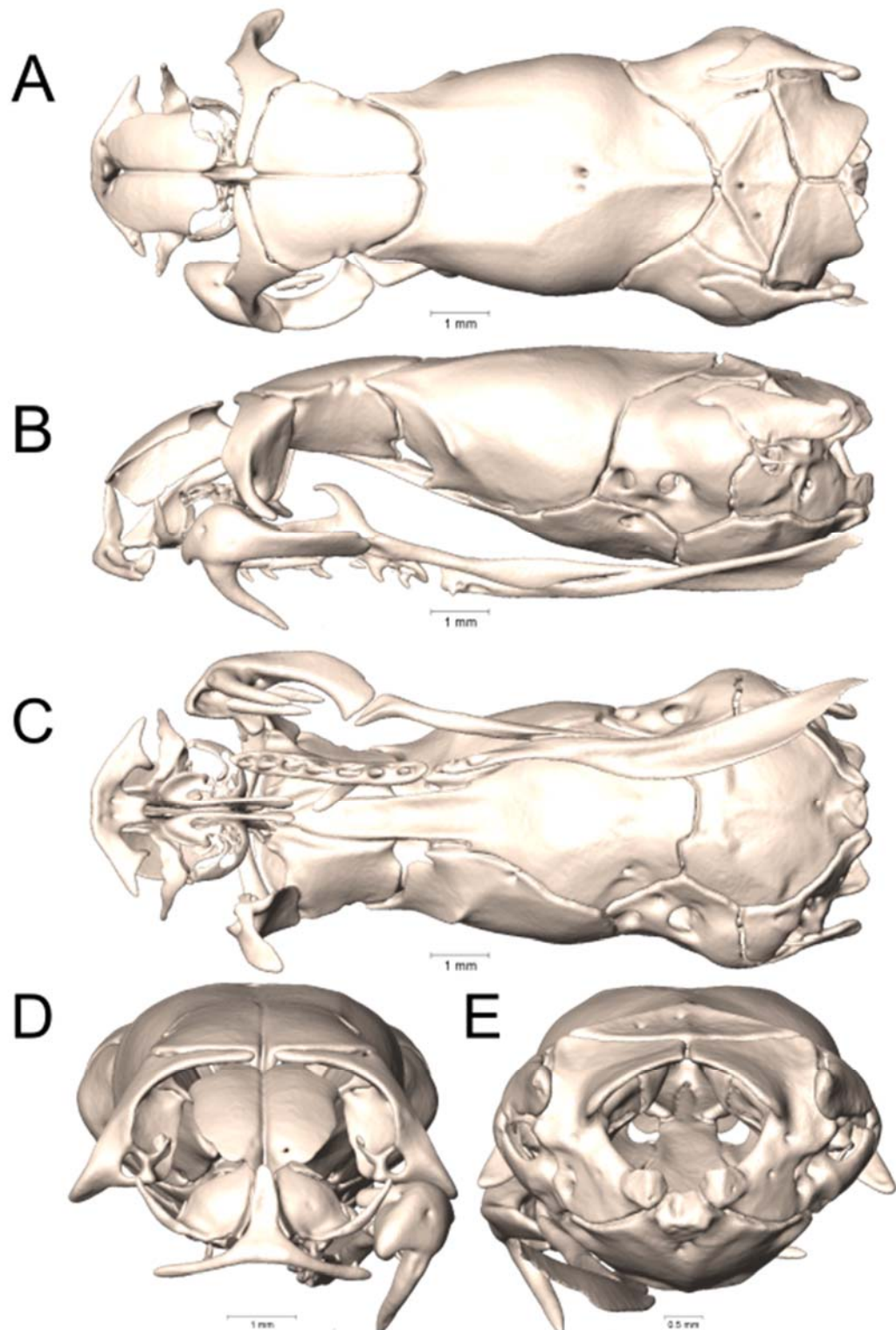
Supplemental Figure 1.63. Dorsal, lateral, ventral, anterior, and posterior views (A-E, respectively) of the skull of *Micrurus renjifoi* (UTA R-3490). Right suspensorium excluded.



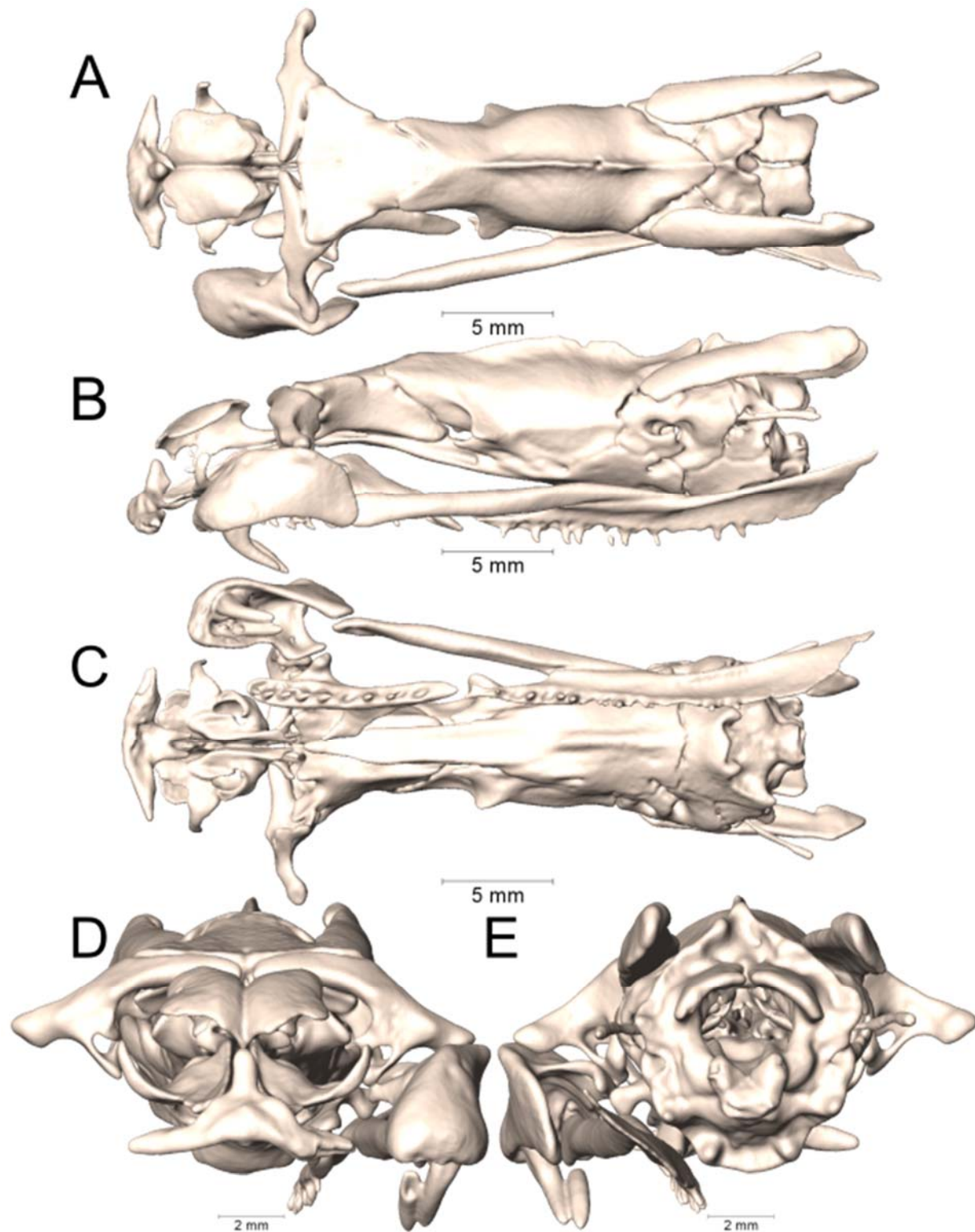
Supplemental Figure 1.64. Dorsal, lateral, ventral, anterior, and posterior views (A-E, respectively) of the skull of *Micrurus serranus* (UTA R-34561). Right suspensorium excluded.



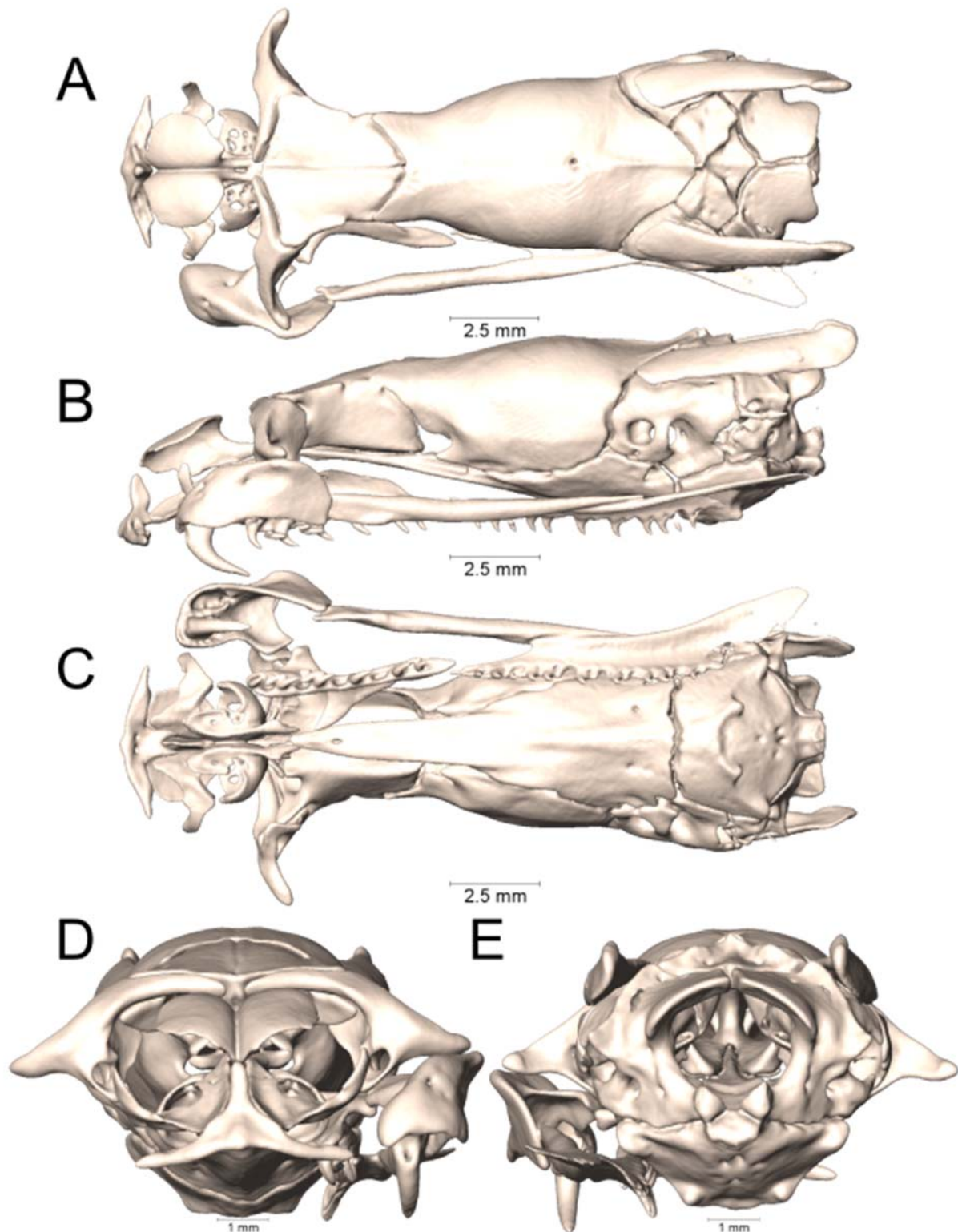
Supplemental Figure 1.65. Dorsal, lateral, ventral, anterior, and posterior views (A-E, respectively) of the skull of *Micrurus steindachneri* (AMNH 28846). Right suspensorium excluded.



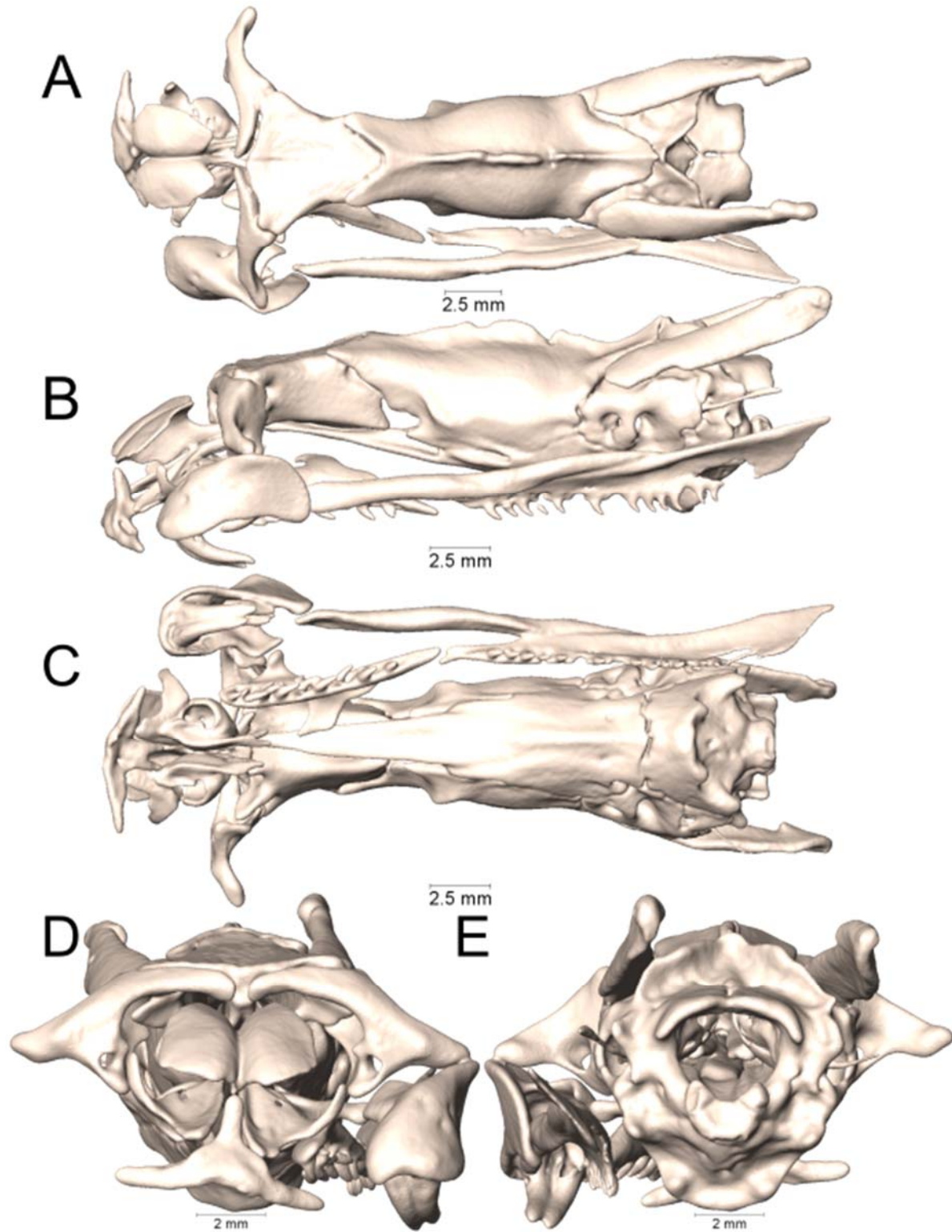
Supplemental Figure 1.66. Dorsal, lateral, ventral, anterior, and posterior views (A-E, respectively) of the skull of *Micrurus steindachneri* (AMNH 35819). Right suspensorium excluded.



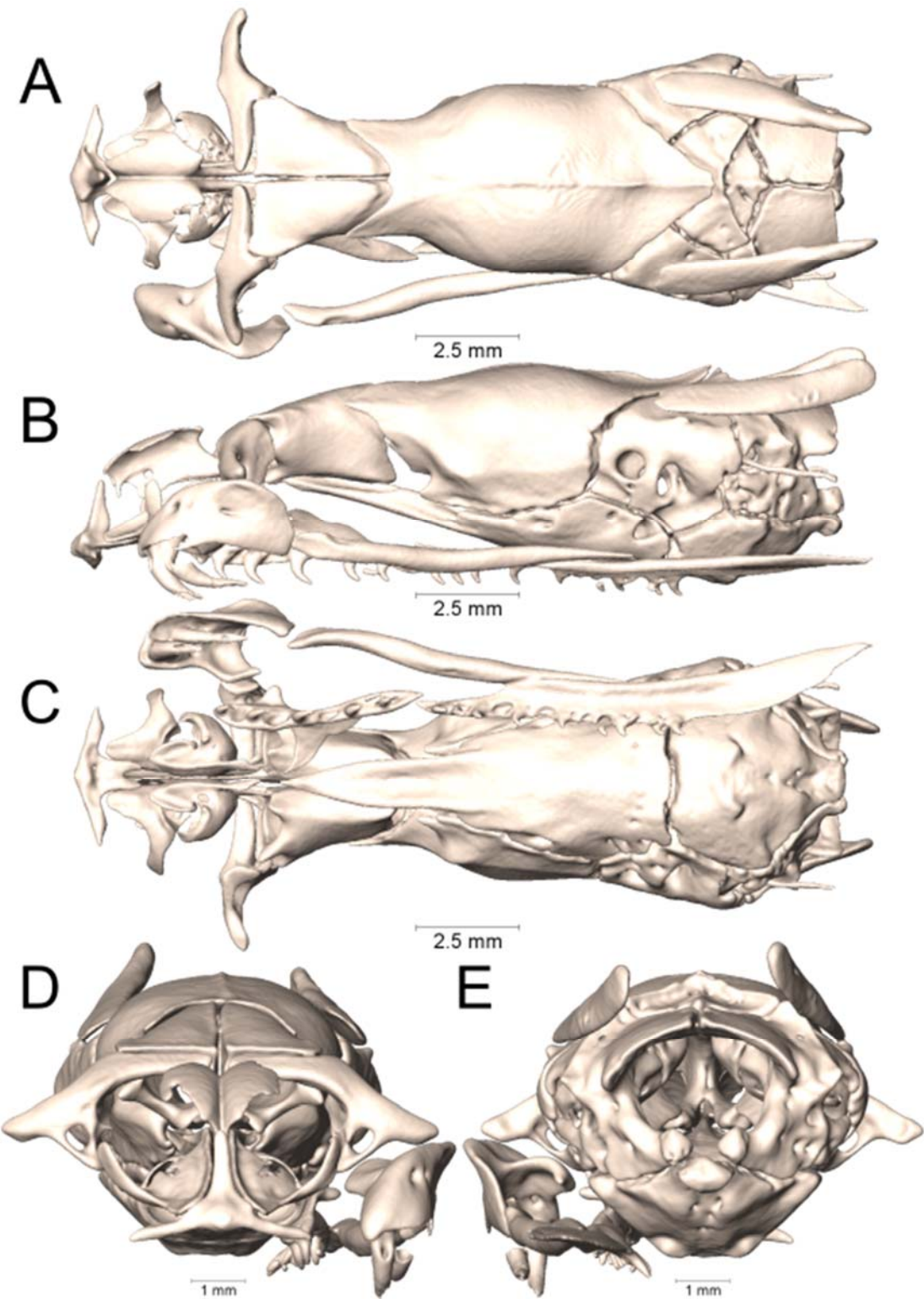
Supplemental Figure 1.67. Dorsal, lateral, ventral, anterior, and posterior views (A-E, respectively) of the skull of *Micrurus surinamensis* (UTA R-15679). Right suspensorium excluded.



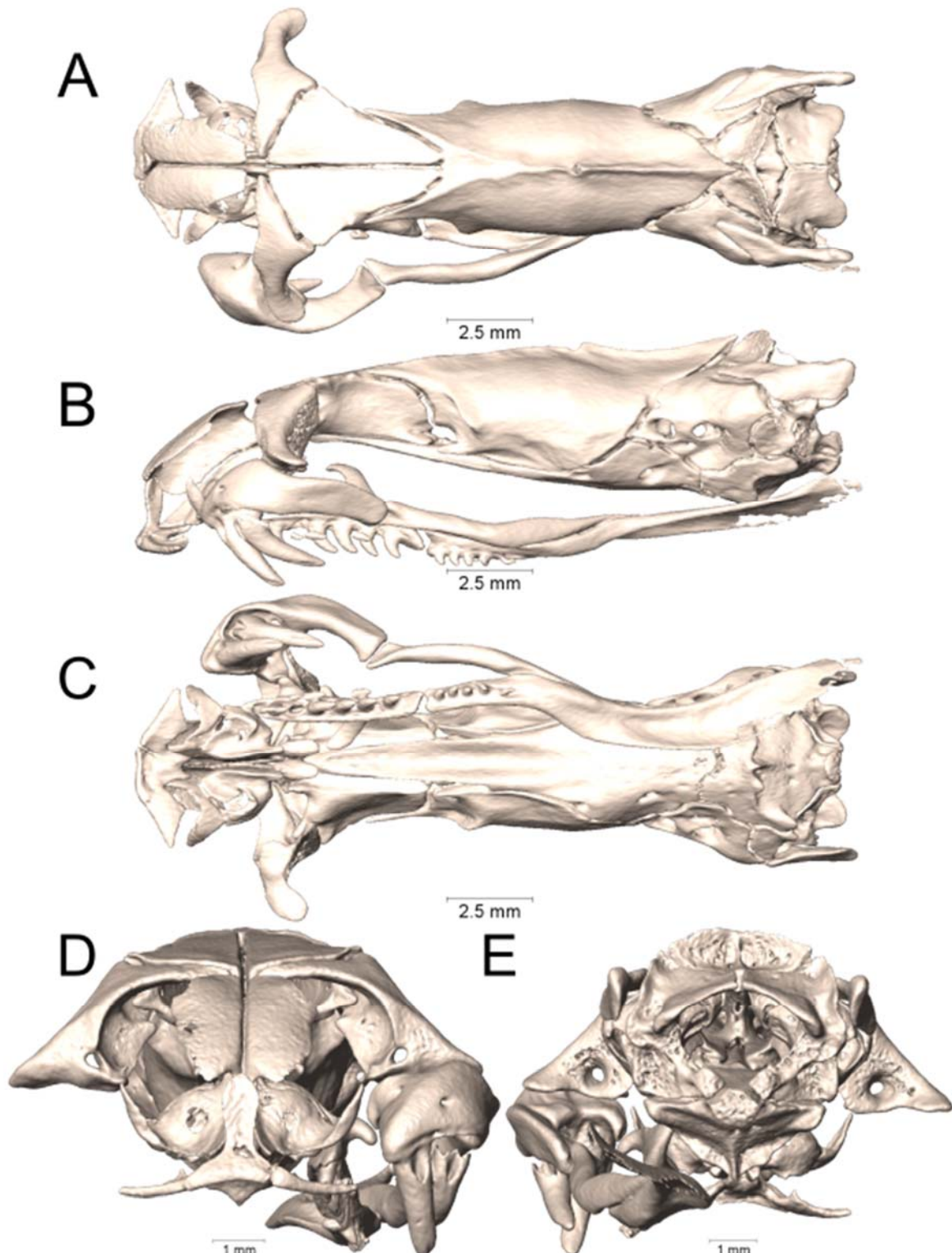
Supplemental Figure 1.68. Dorsal, lateral, ventral, anterior, and posterior views (A-E, respectively) of the skull of *Micrurus surinamensis* (UTA R-50173). Right suspensorium excluded.



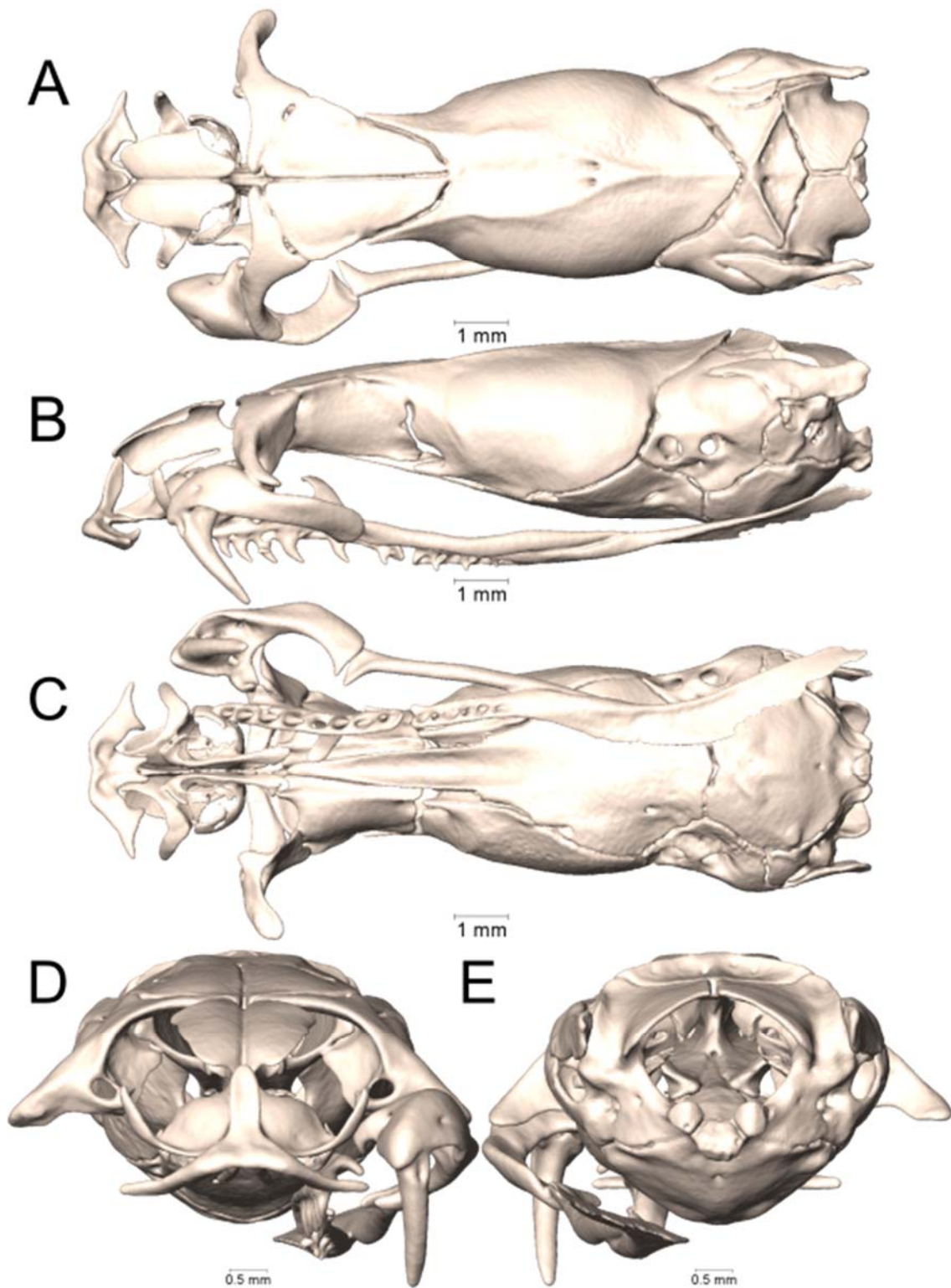
Supplemental Figure 1.69. Dorsal, lateral, ventral, anterior, and posterior views (A-E, respectively) of the skull of *Micrurus surinamensis* (UTA R-54378). Right suspensorium excluded.



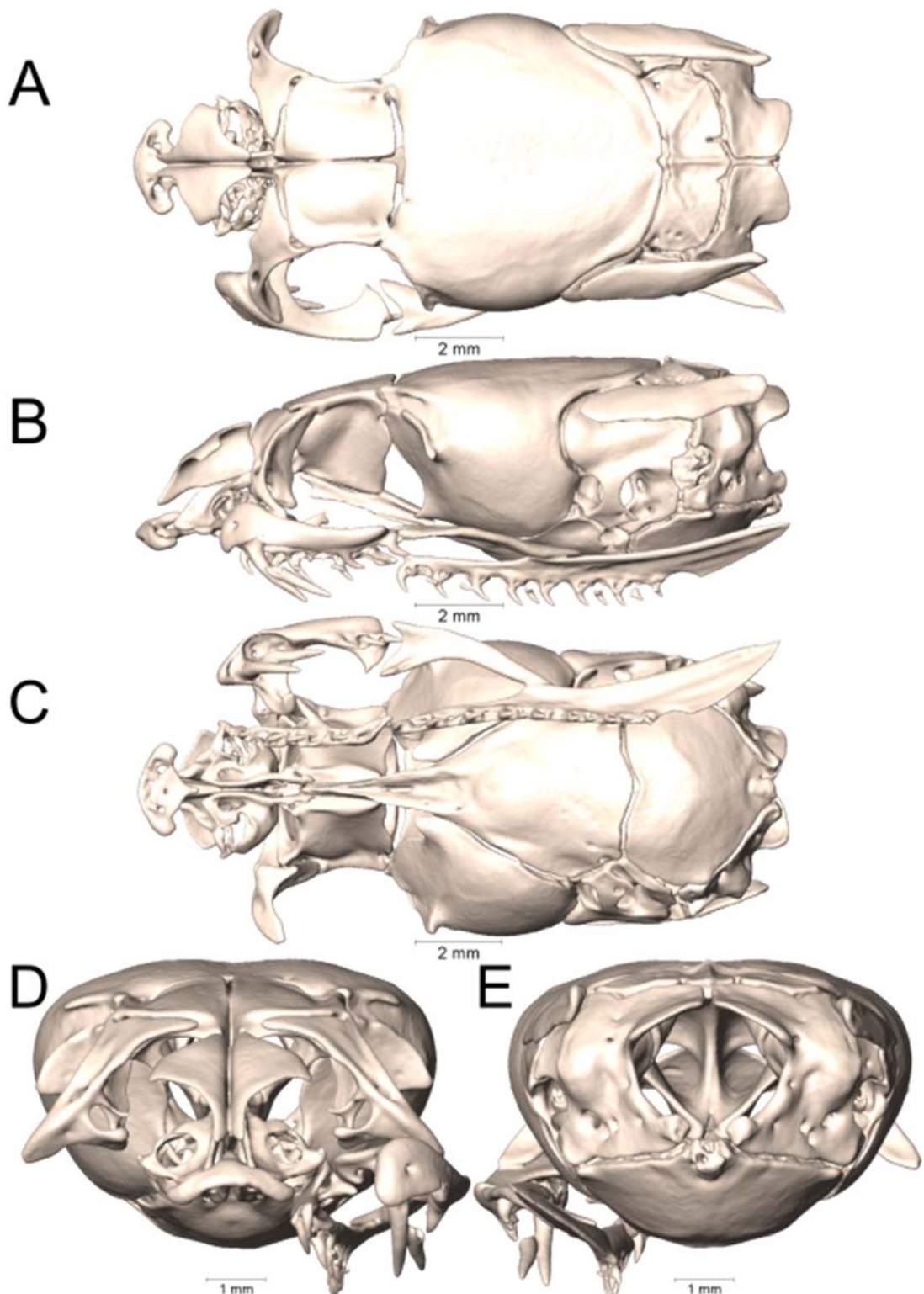
Supplemental Figure 1.70. Dorsal, lateral, ventral, anterior, and posterior views (A-E, respectively) of the skull of *Micrurus surinamensis* (UTA R-65844). Right suspensorium excluded.



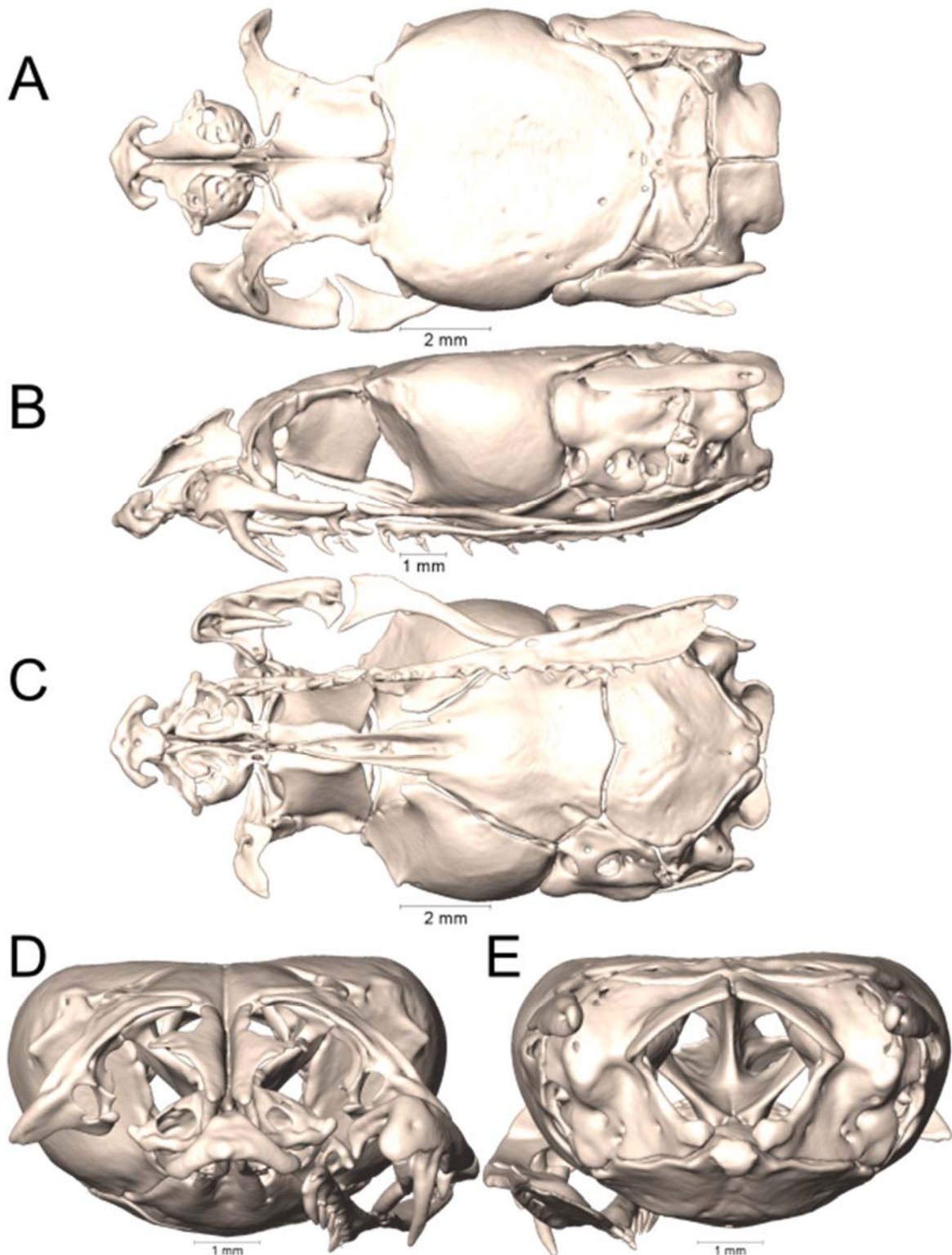
Supplemental Figure 1.71. Dorsal, lateral, ventral, anterior, and posterior views (A-E, respectively) of the skull of *Micrurus tener* (FMNH 39479). Right suspensorium excluded.



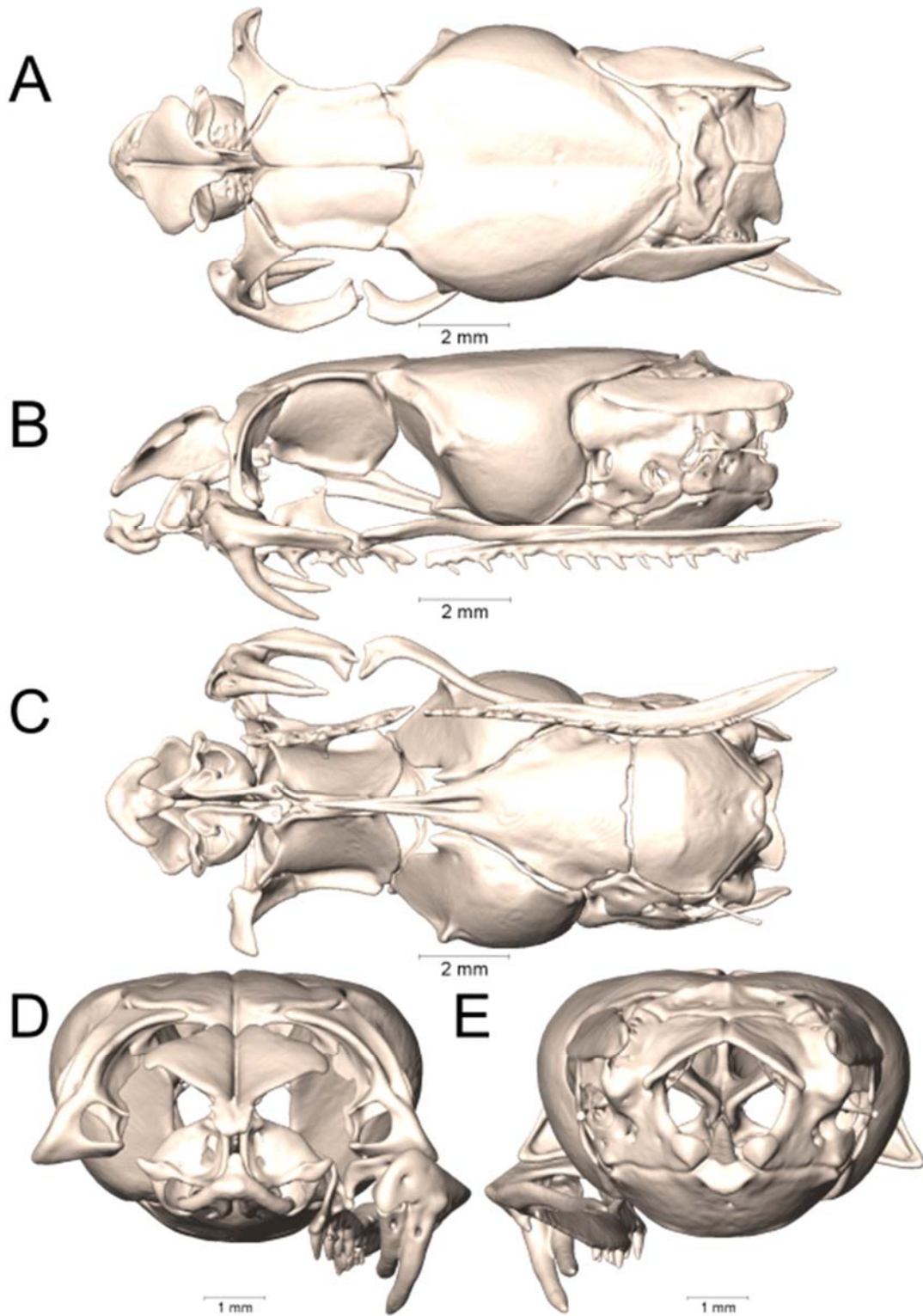
Supplemental Figure 1.72. Dorsal, lateral, ventral, anterior, and posterior views (A-E, respectively) of the skull of *Micrurus tener* (UTA R-63282). Right suspensorium excluded.



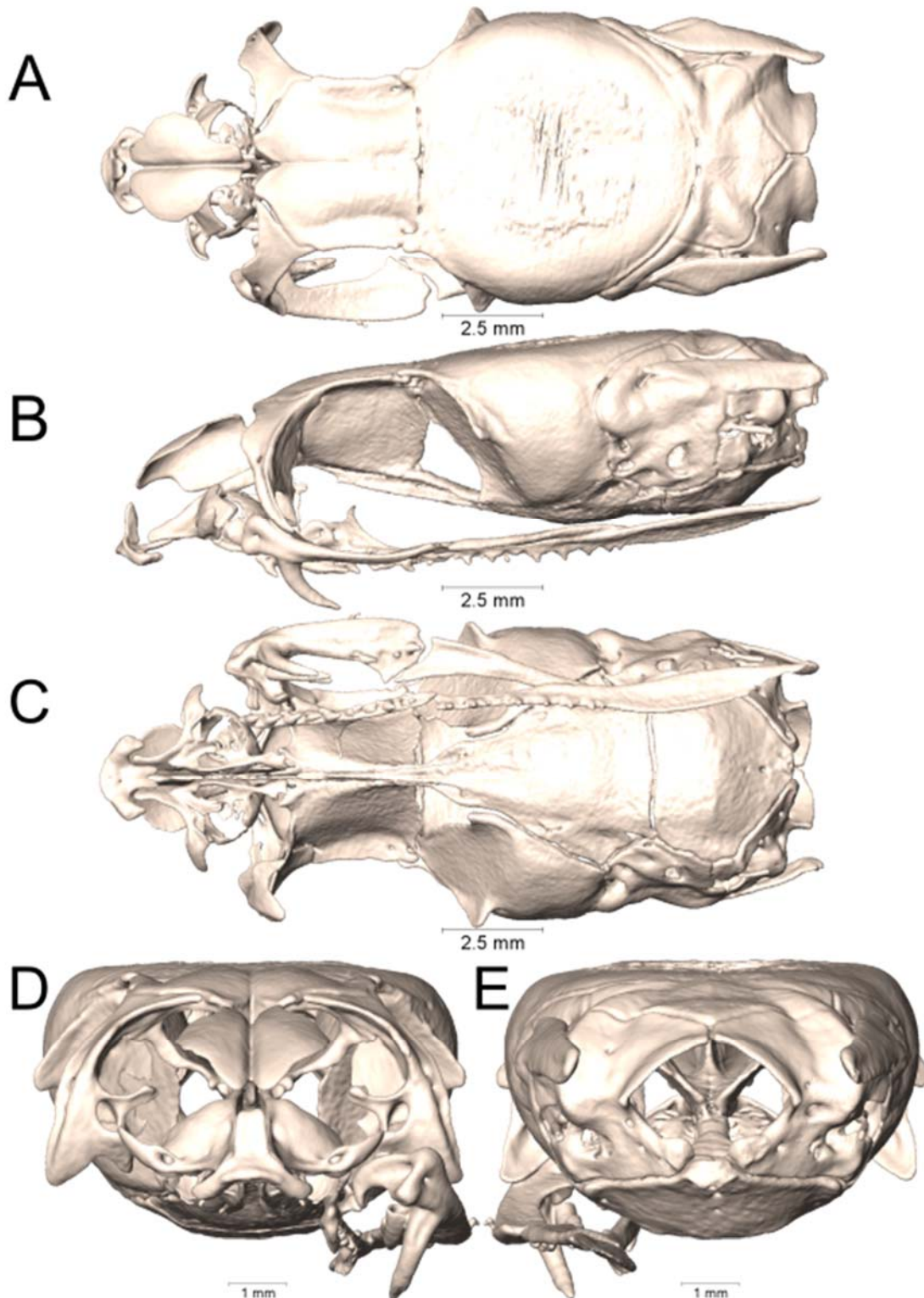
Supplemental Figure 1.73. Dorsal, lateral, ventral, anterior, and posterior views (A-E, respectively) of the skull of *Naja annulata* (UTA R-18199). Right suspensorium excluded.



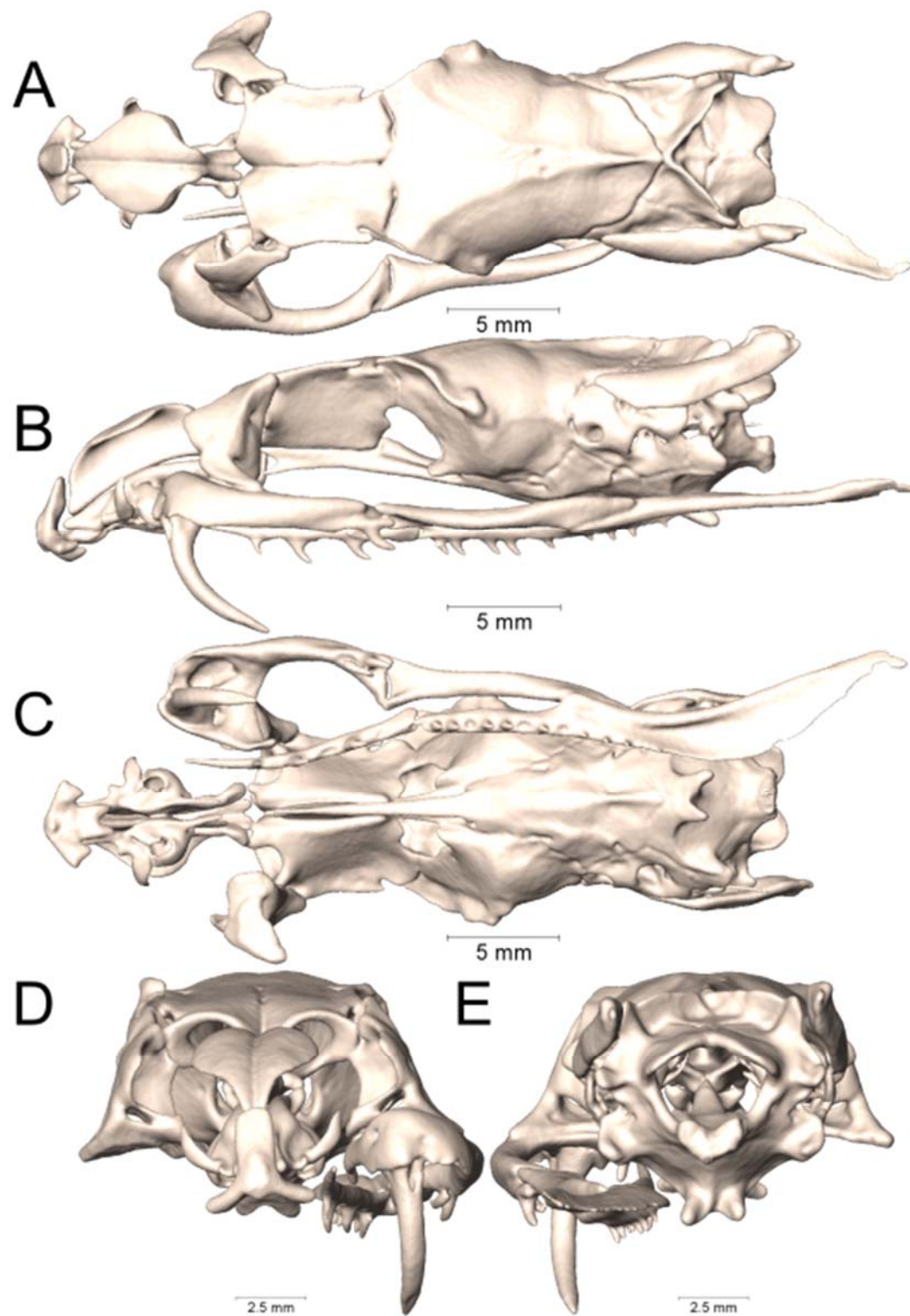
Supplemental Figure 1.74. Dorsal, lateral, ventral, anterior, and posterior views (A-E, respectively) of the skull of *Naja christyi* (UTA R-18200). Right suspensorium excluded.



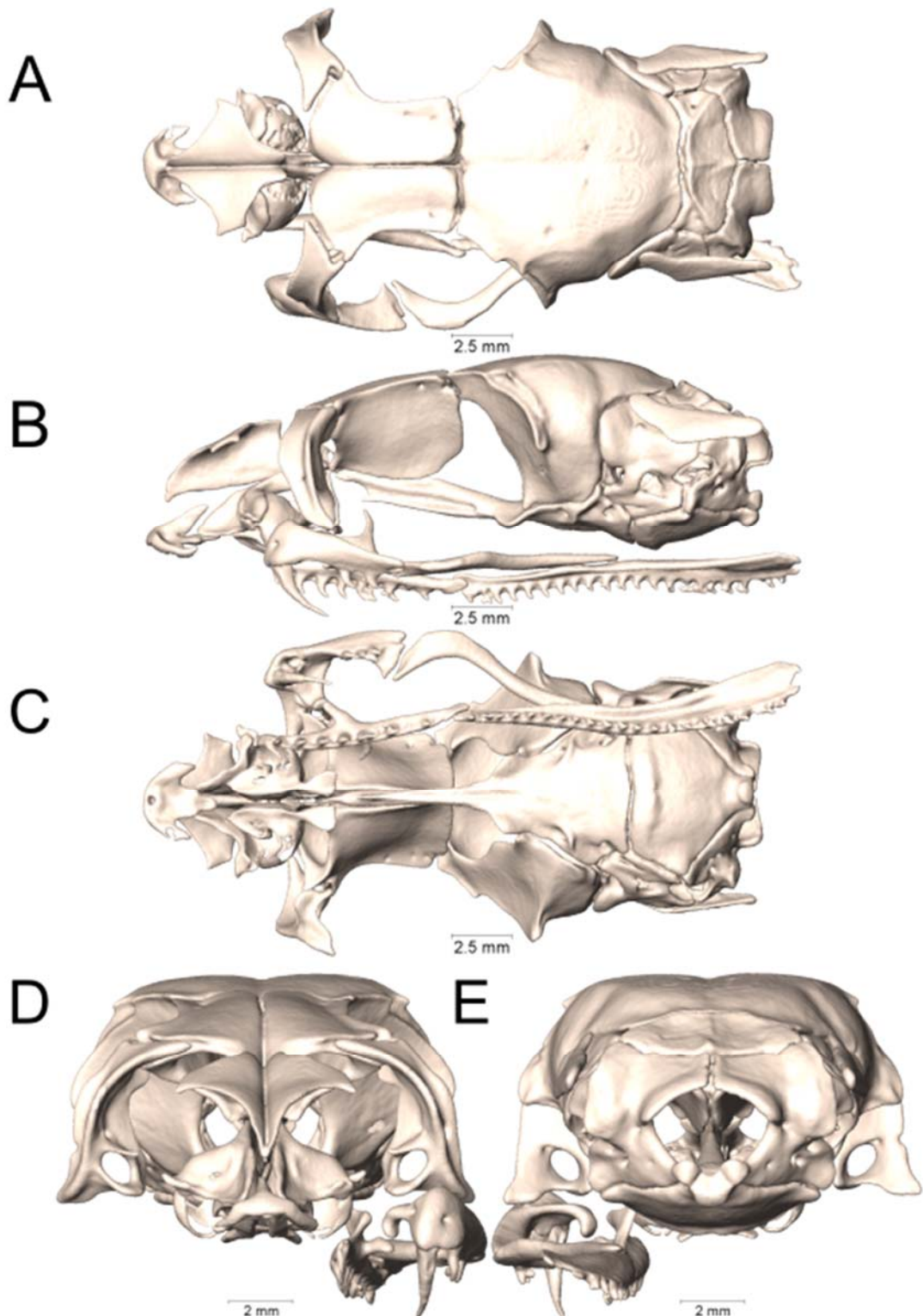
Supplemental Figure 1.75. Dorsal, lateral, ventral, anterior, and posterior views (A-E, respectively) of the skull of *Naja siamensis* (UTA R-16872). Right suspensorium excluded.



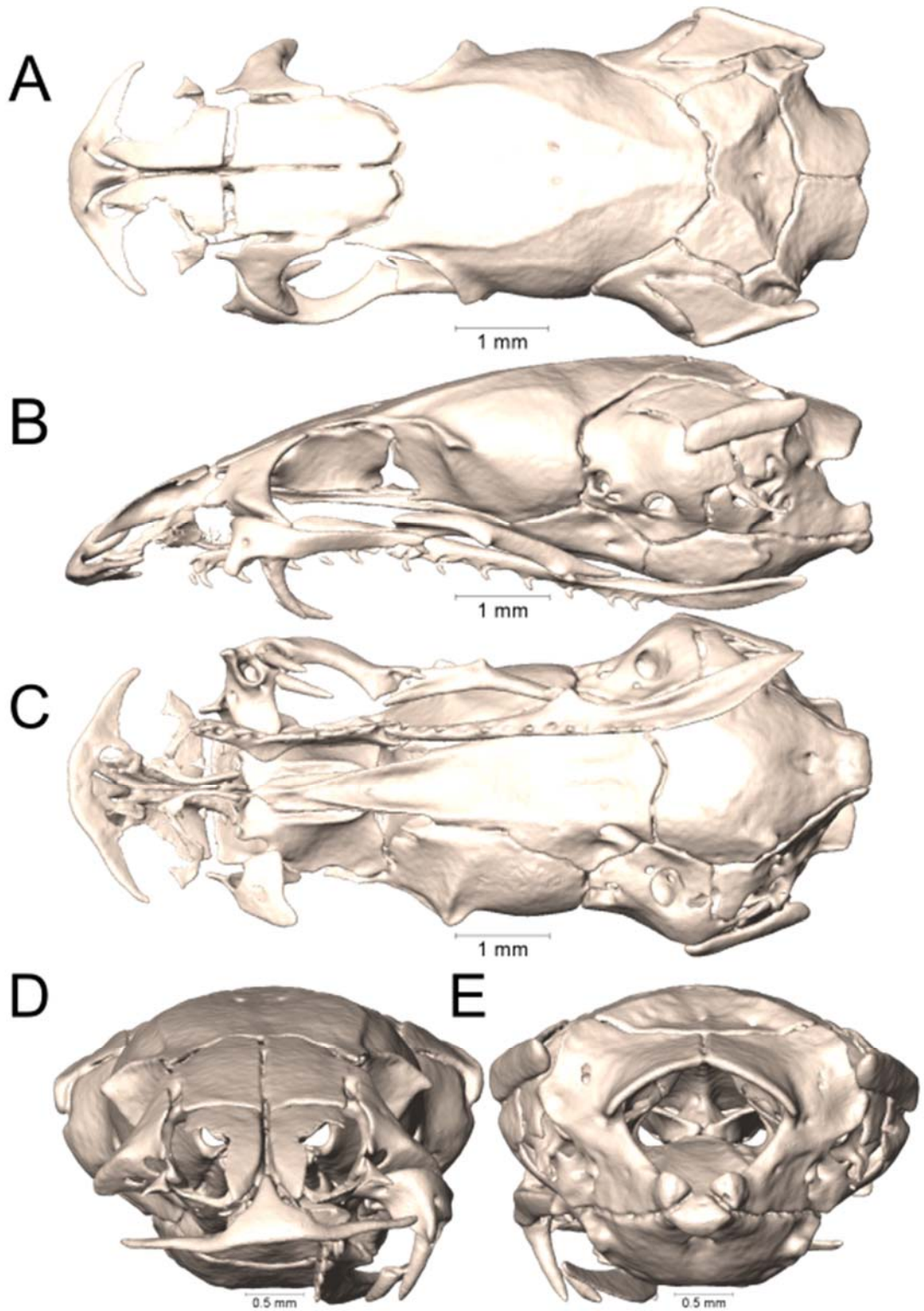
Supplemental Figure 1.76. Dorsal, lateral, ventral, anterior, and posterior views (A-E, respectively) of the skull of *Ophiophagus hannah* (UTA R-60836). Right suspensorium excluded.



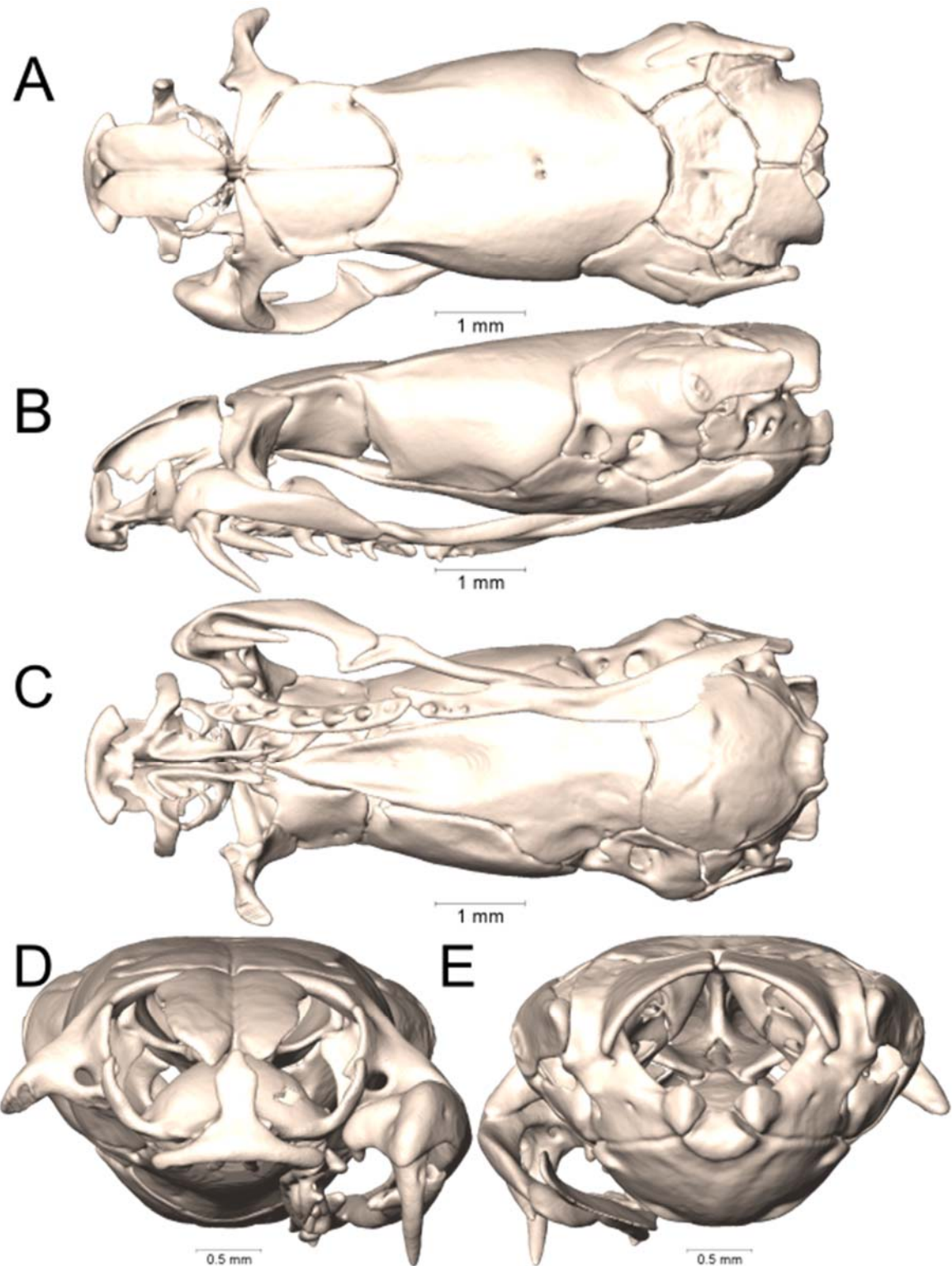
Supplemental Figure 1.77. Dorsal, lateral, ventral, anterior, and posterior views (A-E, respectively) of the skull of *Oxyuranus scutellatus* (UTA R-60839). Right suspensorium excluded.



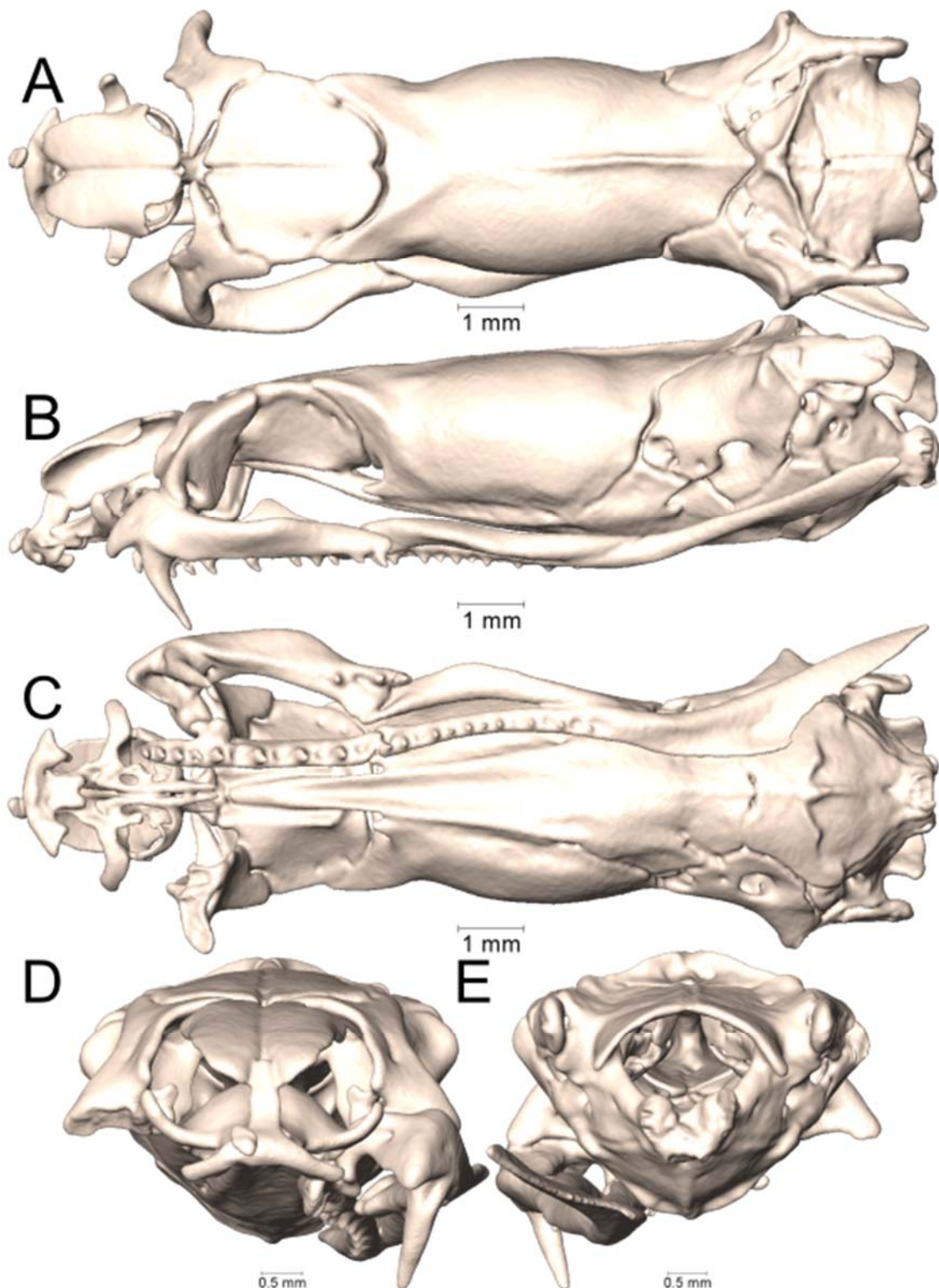
Supplemental Figure 1.78. Dorsal, lateral, ventral, anterior, and posterior views (A-E, respectively) of the skull of *Pseudohaje goldii* (UTA R-63636). Right suspensorium excluded.



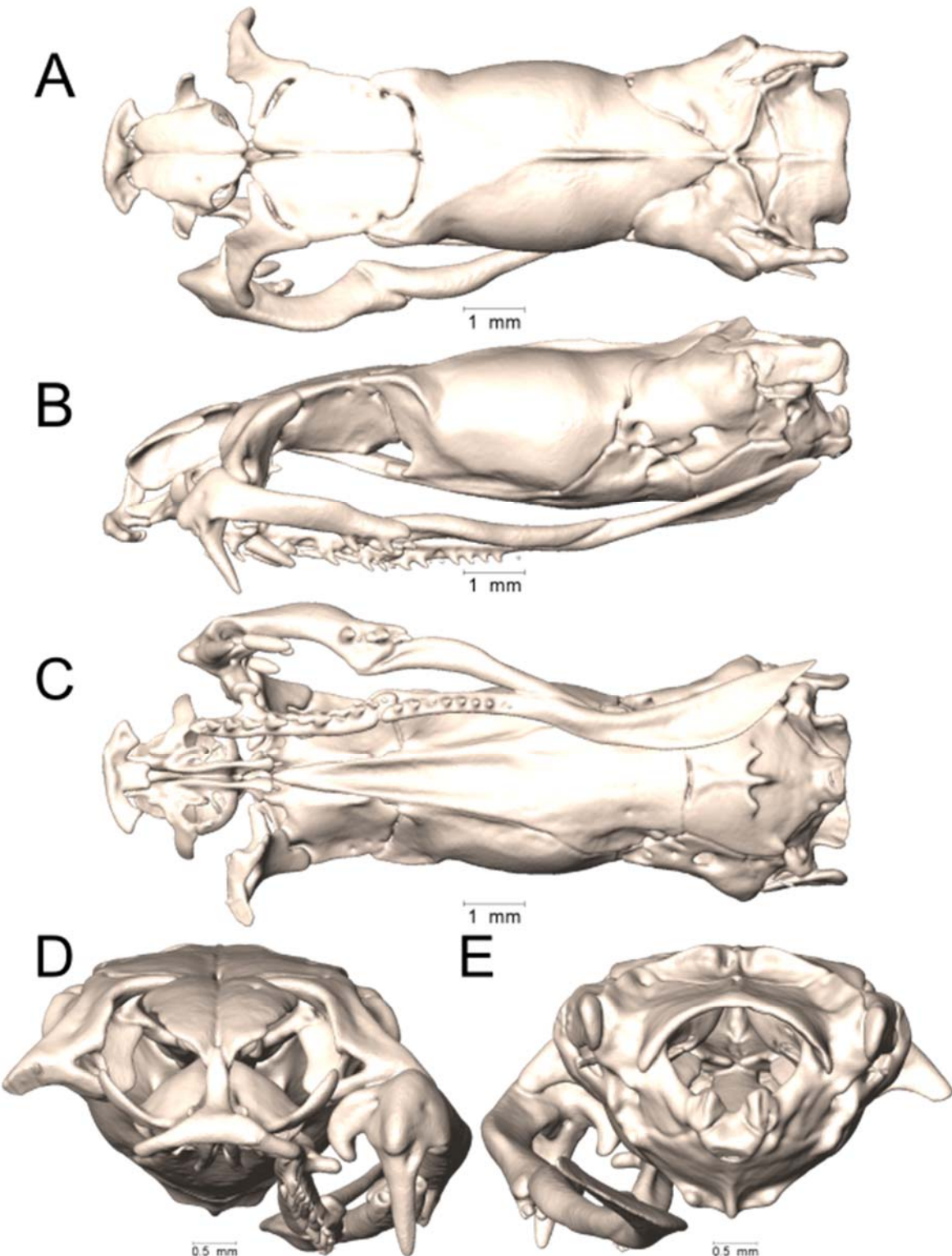
Supplemental Figure 1.79. Dorsal, lateral, ventral, anterior, and posterior views (A-E, respectively) of the skull of *Simoselaps bertholdi* (UMMZ 244197). Right suspensorium excluded.



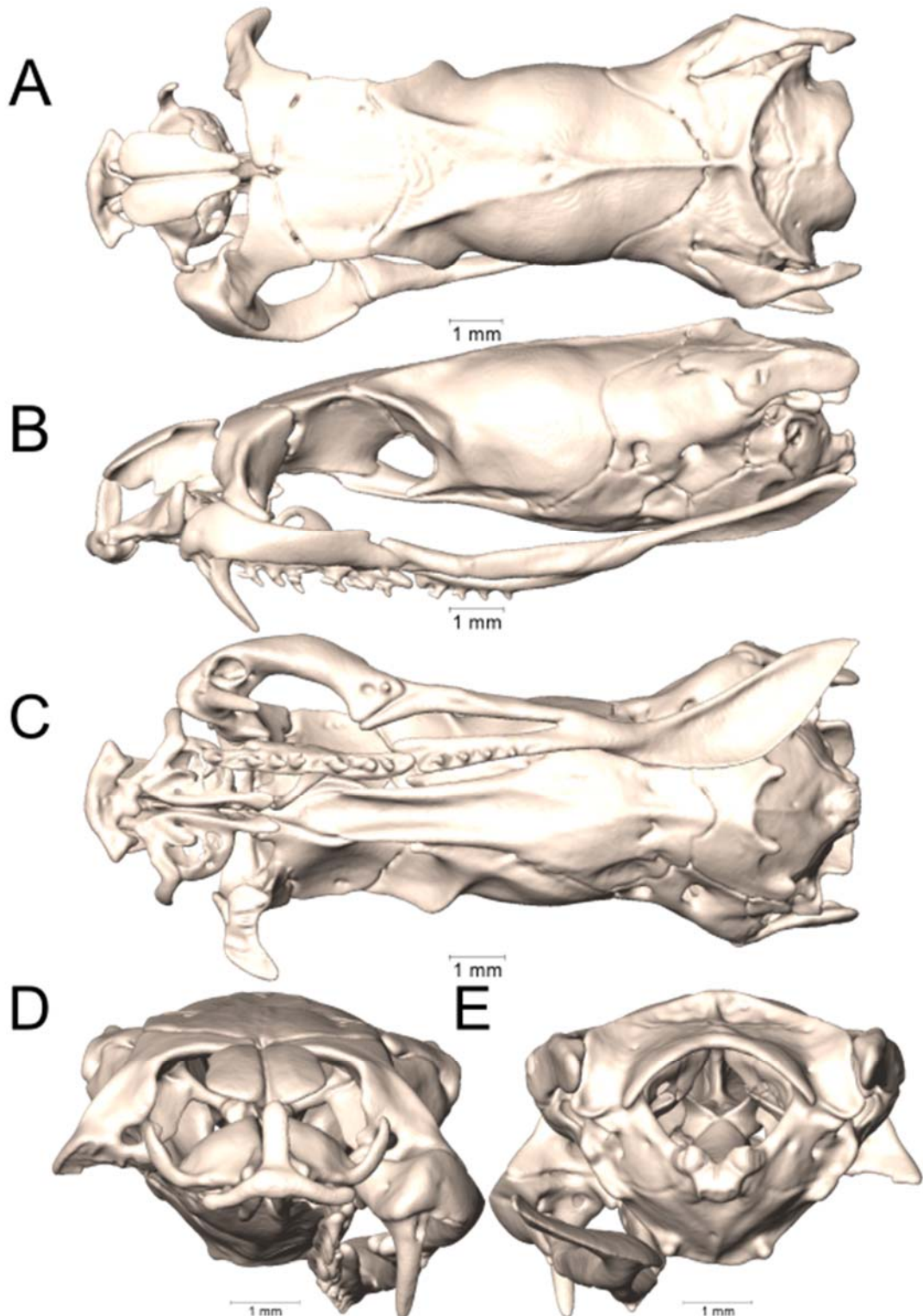
Supplemental Figure 1.80. Dorsal, lateral, ventral, anterior, and posterior views (A-E, respectively) of the skull of *Sinomicrurus annularis* (ROM 31158). Right suspensorium excluded.



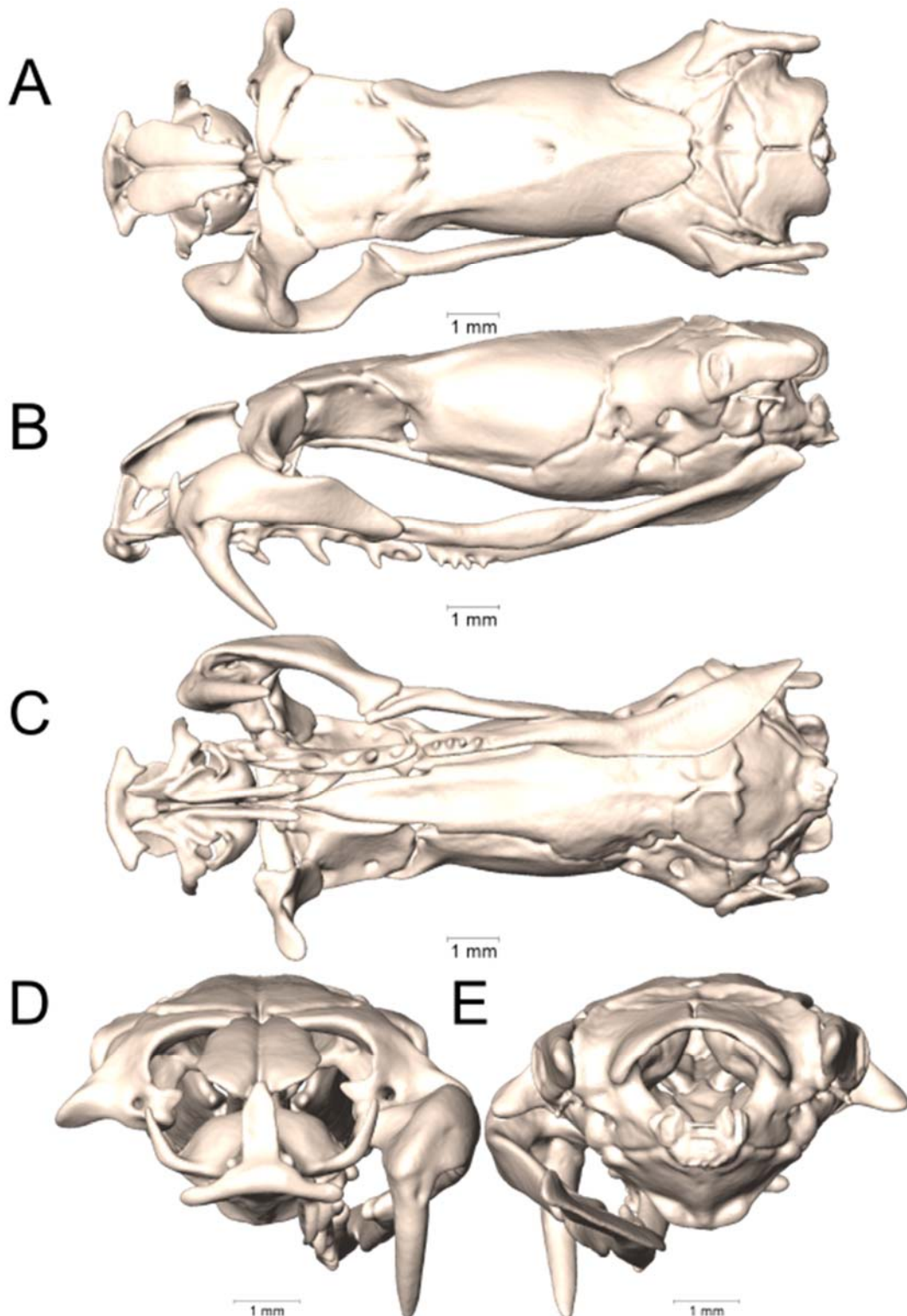
Supplemental Figure 1.81. Dorsal, lateral, ventral, anterior, and posterior views (A-E, respectively) of the skull of *Sinomicrurus boettgeri* (UTA R-58837). Right suspensorium excluded.



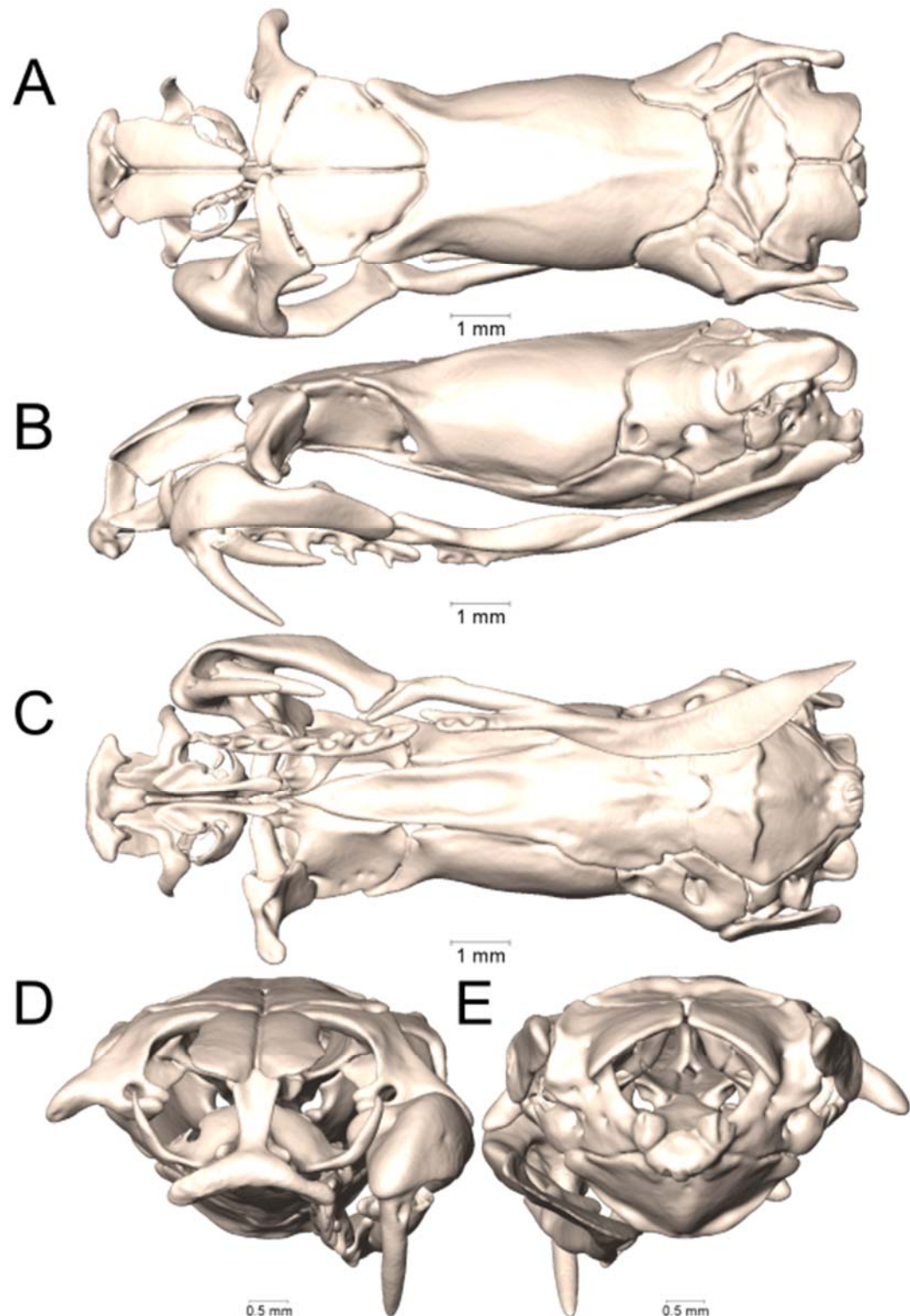
Supplemental Figure 1.82. Dorsal, lateral, ventral, anterior, and posterior views (A-E, respectively) of the skull of *Sinomicrurus japonicus* (CAS 204979). Right suspensorium excluded.



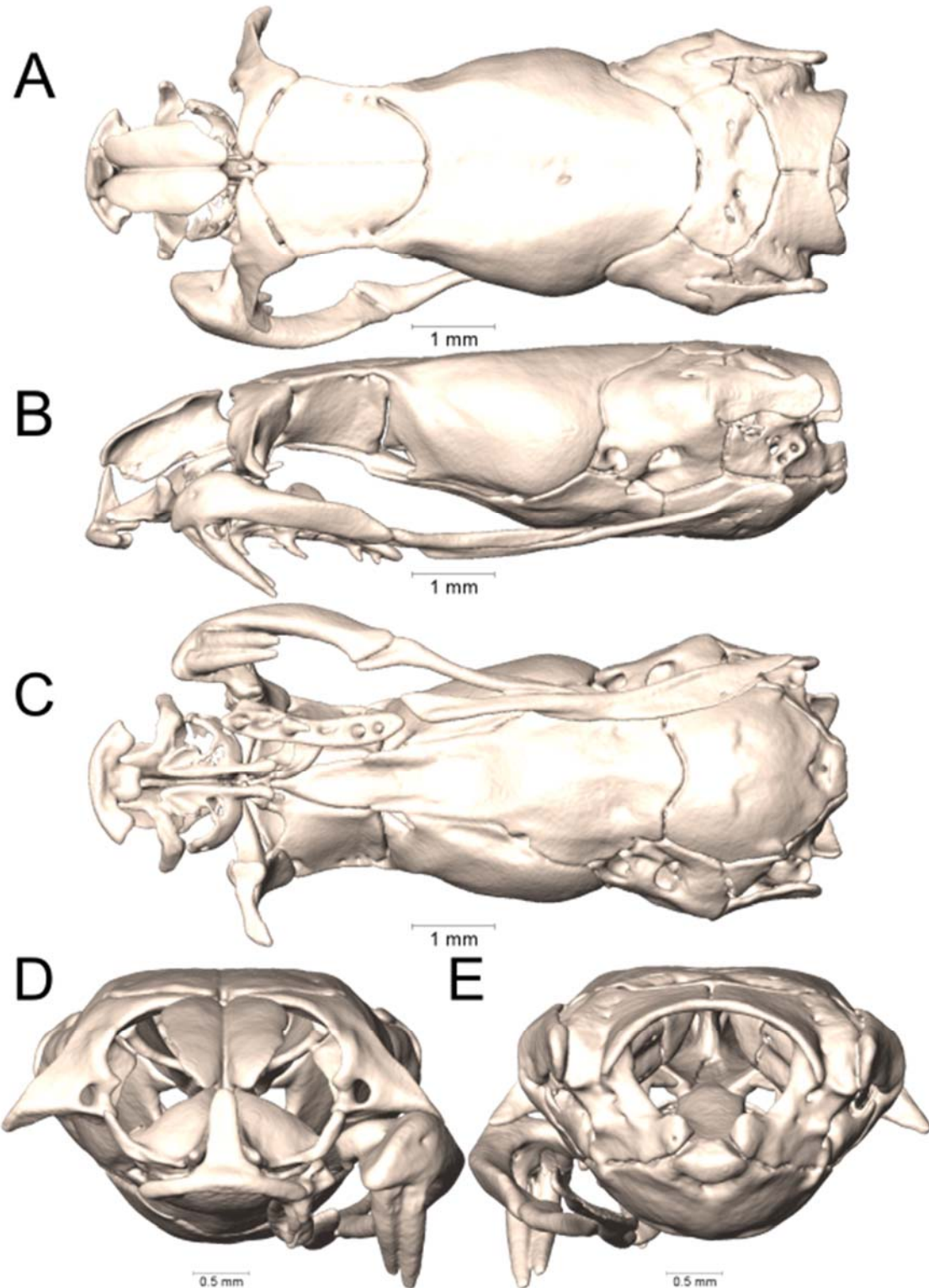
Supplemental Figure 1.83. Dorsal, lateral, ventral, anterior, and posterior views (A-E, respectively) of the skull of *Sinomicrurus kelloggi* (ROM 37079). Right suspensorium excluded.



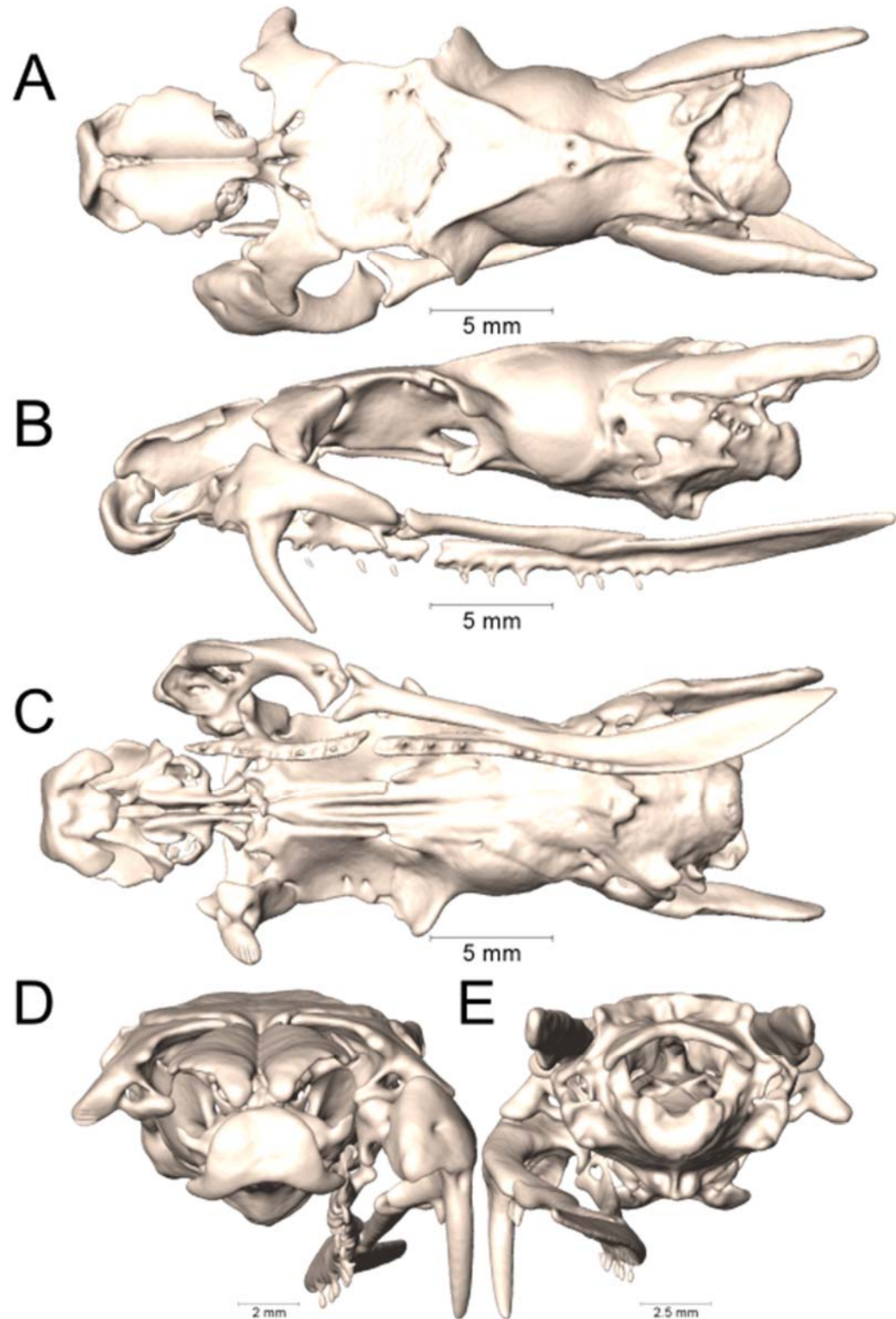
Supplemental Figure 1.84. Dorsal, lateral, ventral, anterior, and posterior views (A-E, respectively) of the skull of *Sinomicrurus peinani* (ROM 35245). Right suspensorium excluded.



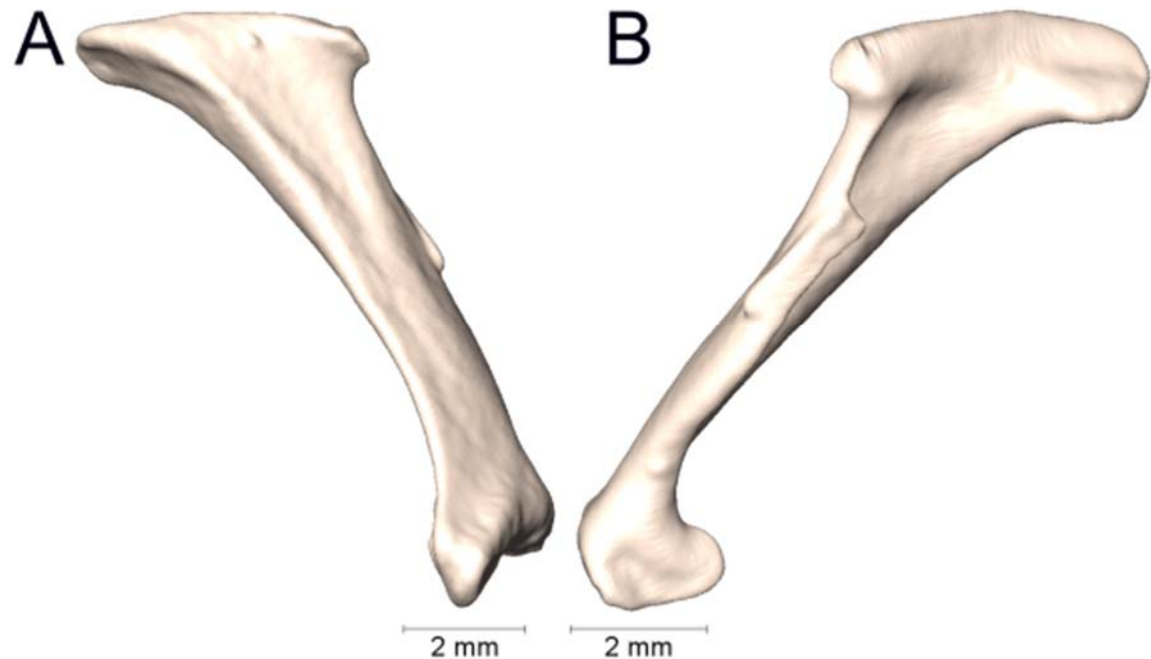
Supplemental Figure 1.85. Dorsal, lateral, ventral, anterior, and posterior views (A-E, respectively) of the skull of *Sinomicrurus peinani* (ROM 37109). Right suspensorium excluded.



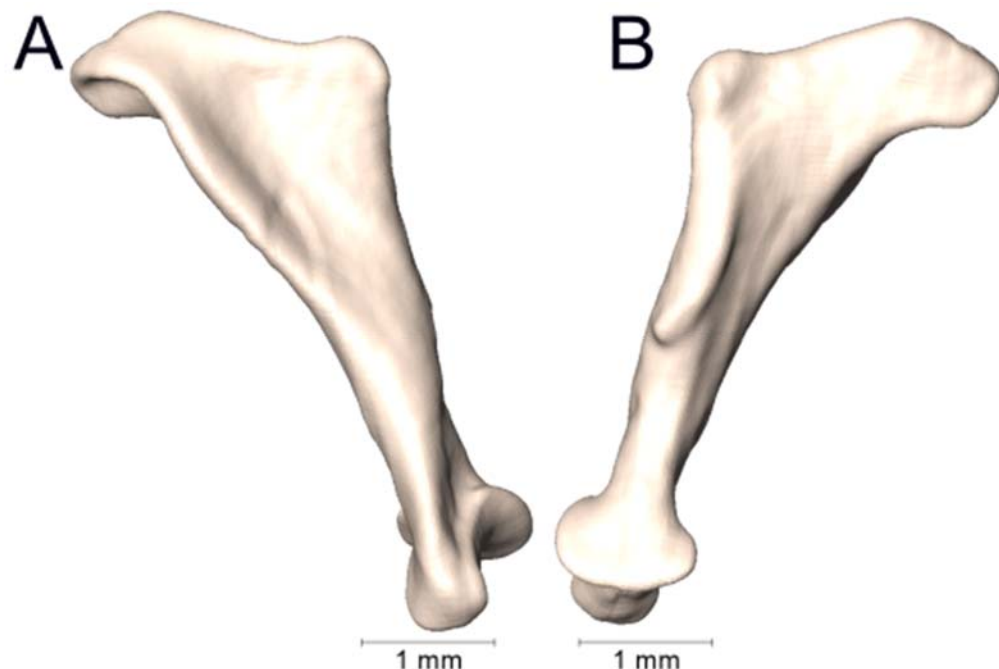
Supplemental Figure 1.86. Dorsal, lateral, ventral, anterior, and posterior views (A-E, respectively) of the skull of *Sinomicrurus swinhoei* (MVZ 23876). Right suspensorium excluded.



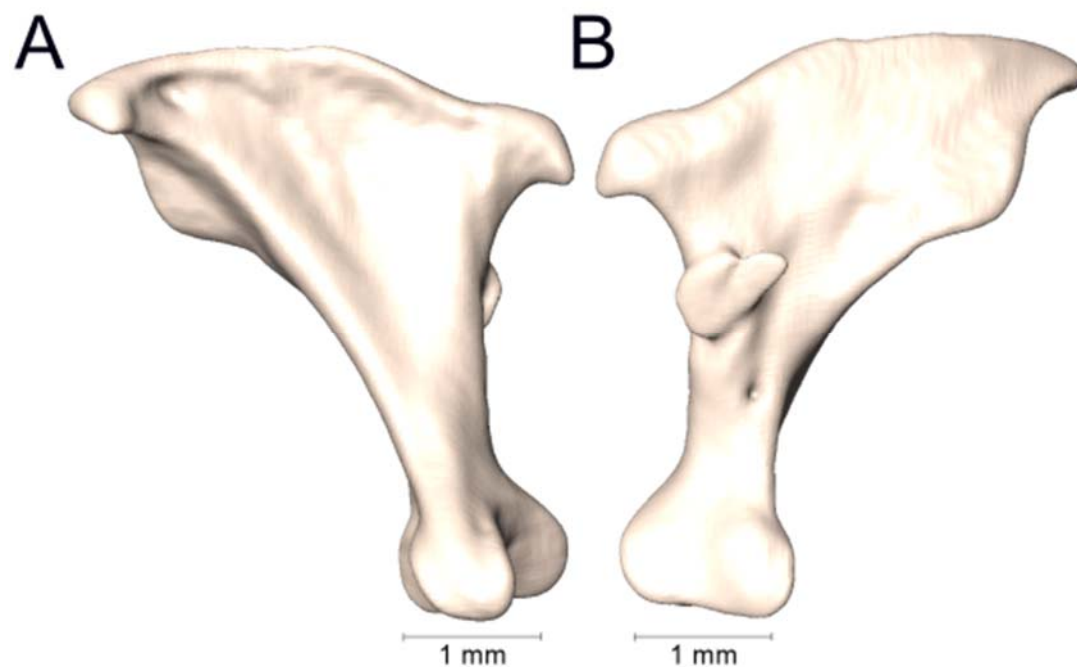
Supplemental Figure 1.87. Dorsal, lateral, ventral, anterior, and posterior views (A-E, respectively) of the skull of *Walterinnesia aegyptia* (UTA R-13021). Right suspensorium excluded.



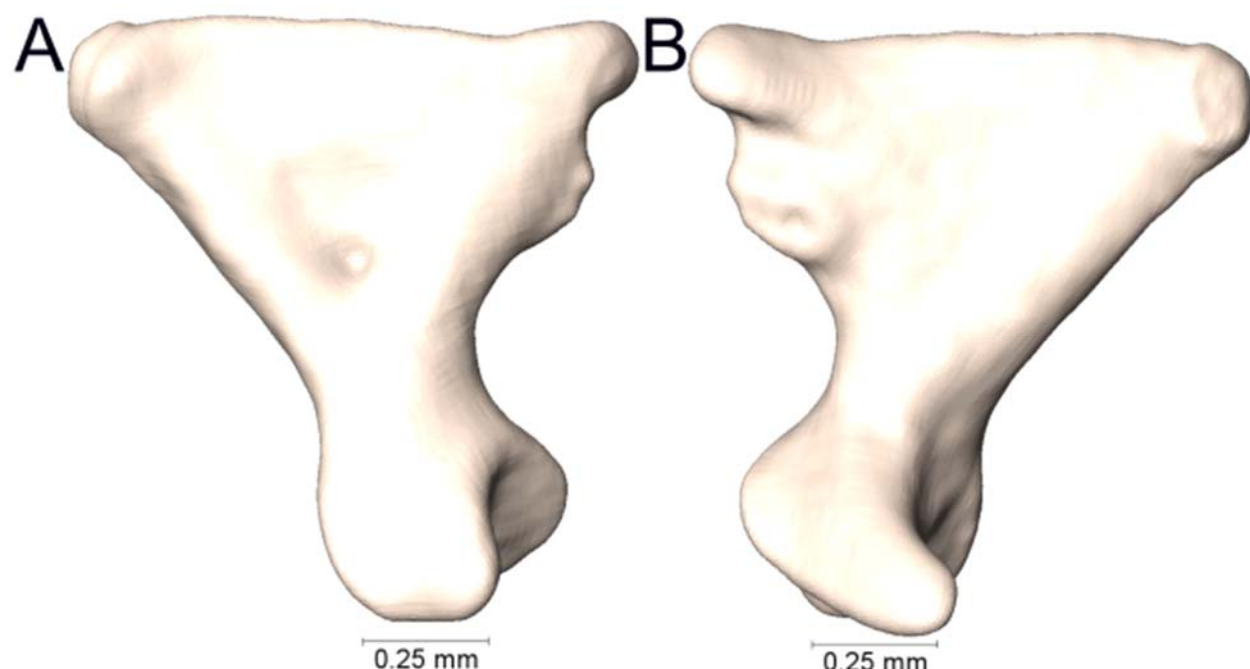
Supplemental Figure 2.1. Lateral and medial views (A-B, respectively) of the left quadrate of *Acanthophis antarcticus* (UTA R-7623).



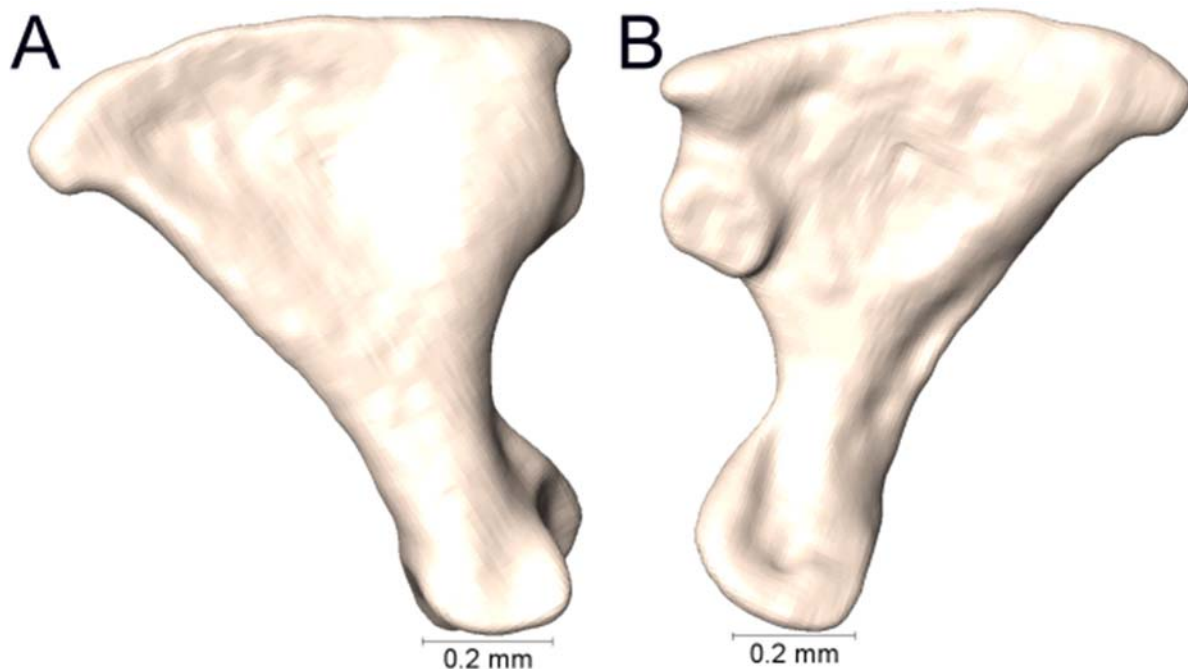
Supplemental Figure 2.2. Lateral and medial views (A-B, respectively) of the left quadrate of *Bungarus candidus* (UTA R-65799).



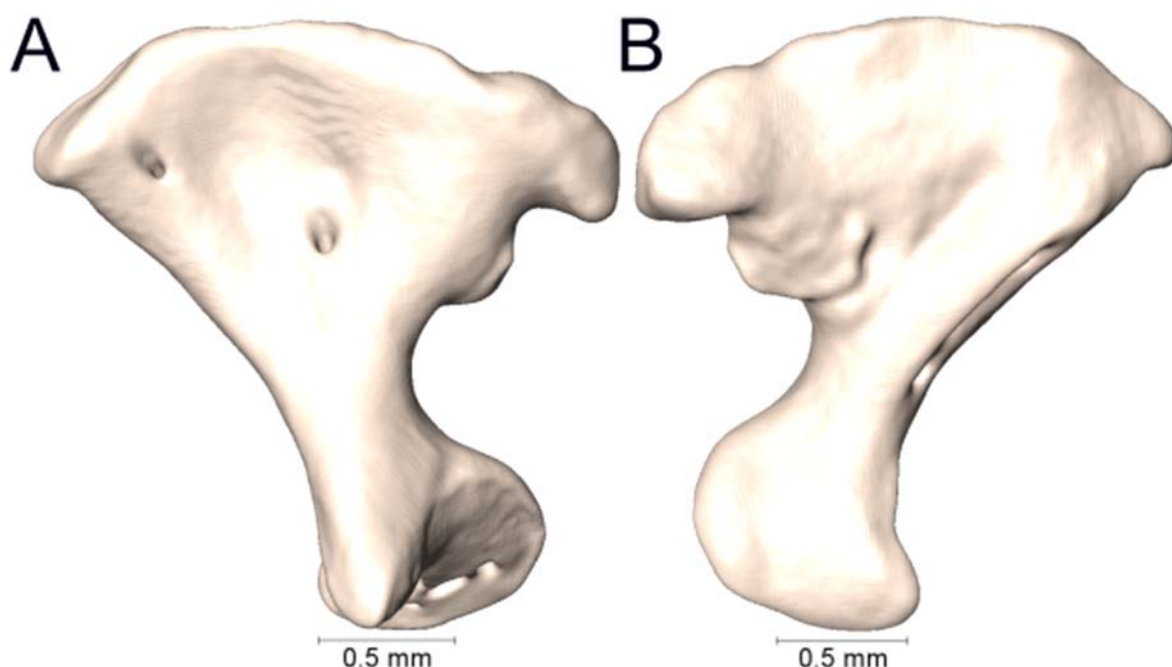
Supplemental Figure 2.3. Lateral and medial views (A-B, respectively) of the left quadrate of *Bungarus flaviceps* (UTA R-62257).



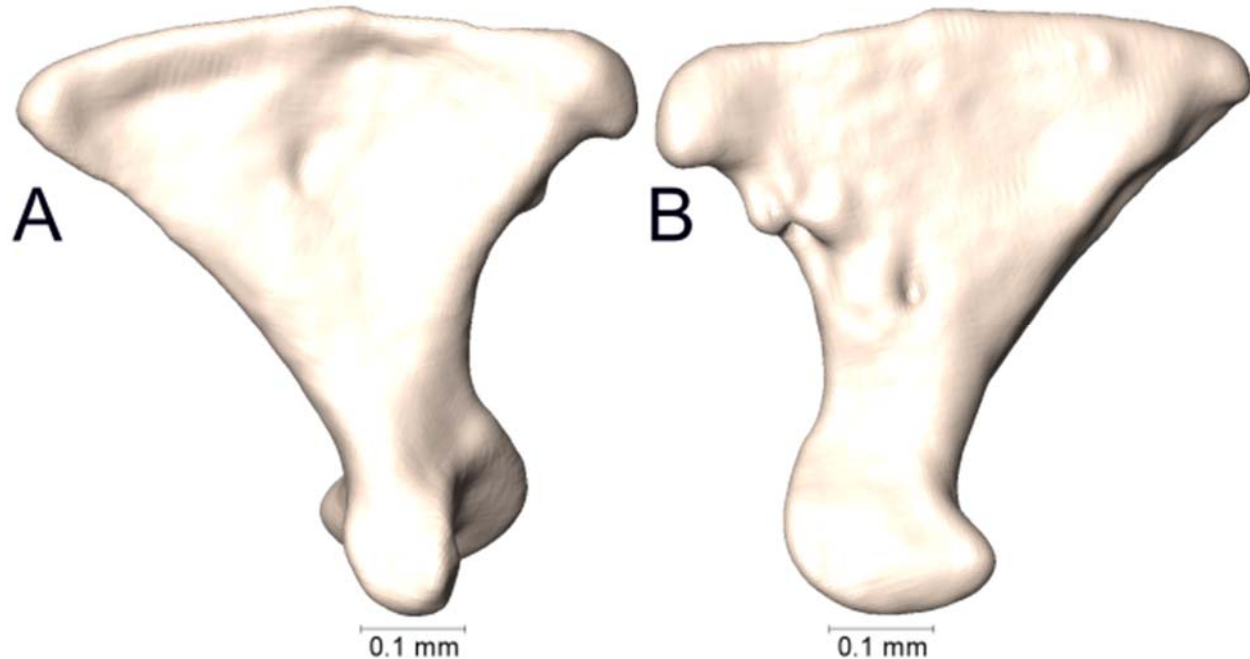
Supplemental Figure 2.4. Lateral and medial views (A-B, respectively) of the left quadrate of *Calliophis beddomei* (MNHN 46-81).



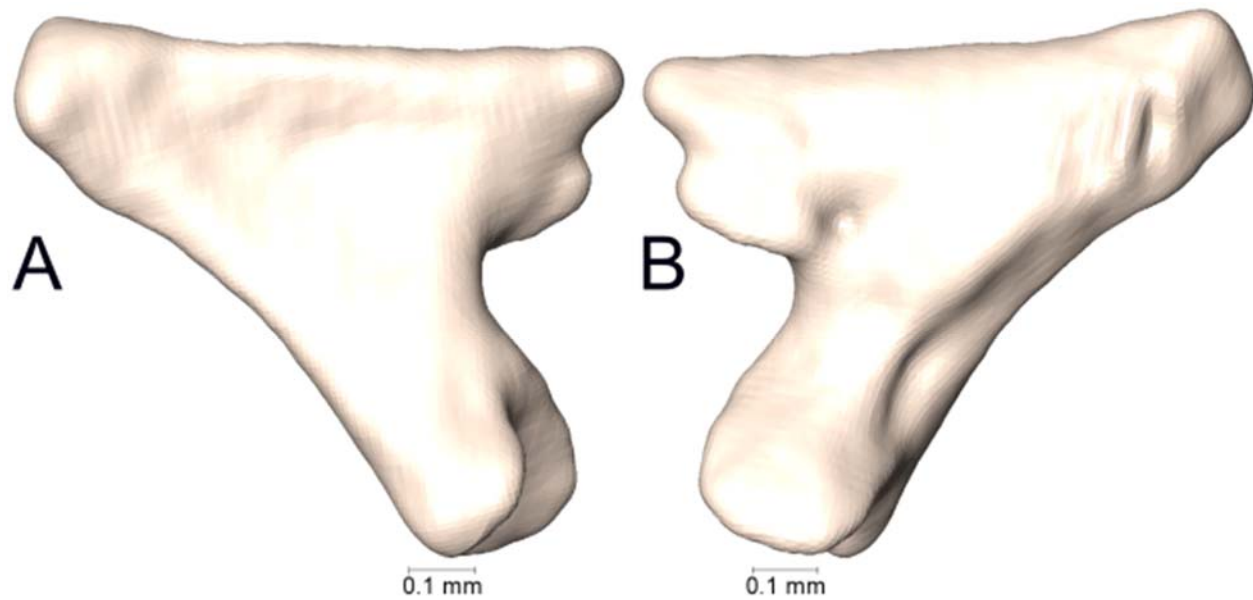
Supplemental Figure 2.5. Lateral and medial views (A-B, respectively) of the left quadrate of *Calliophis biliniatus* (KU 309511).



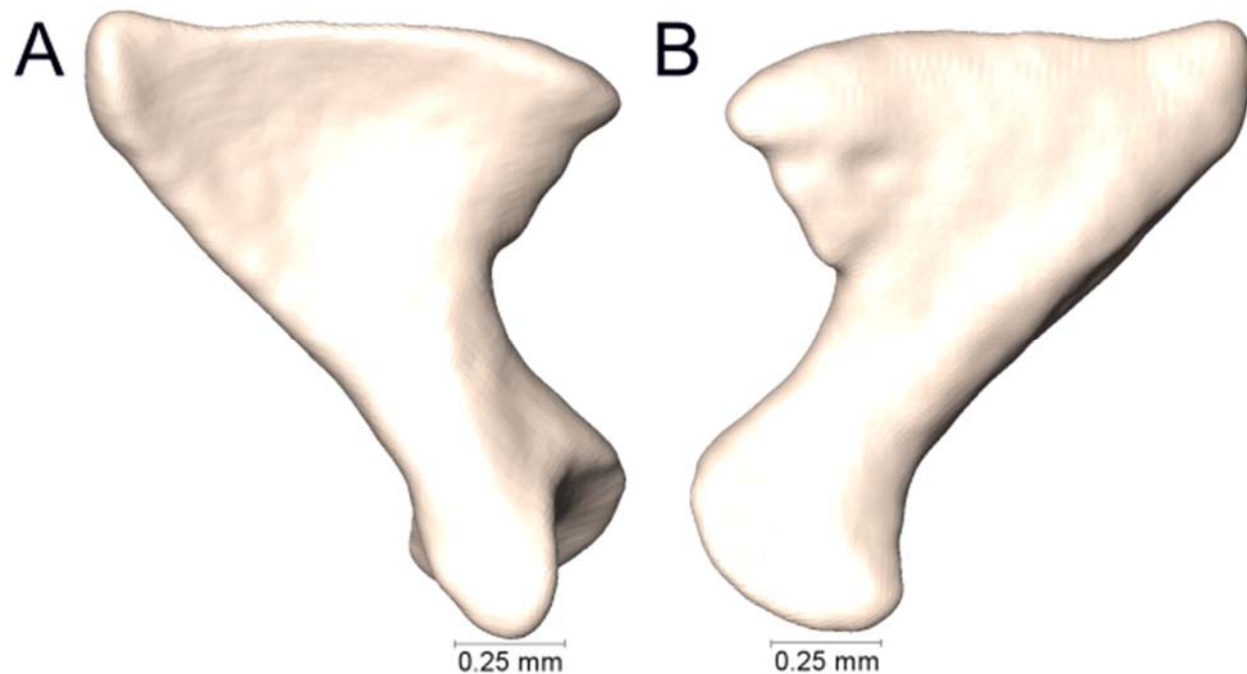
Supplemental Figure 2.6. Lateral and medial views (A-B, respectively) of the left quadrate of *Calliophis biliniatus* (KU 311415).



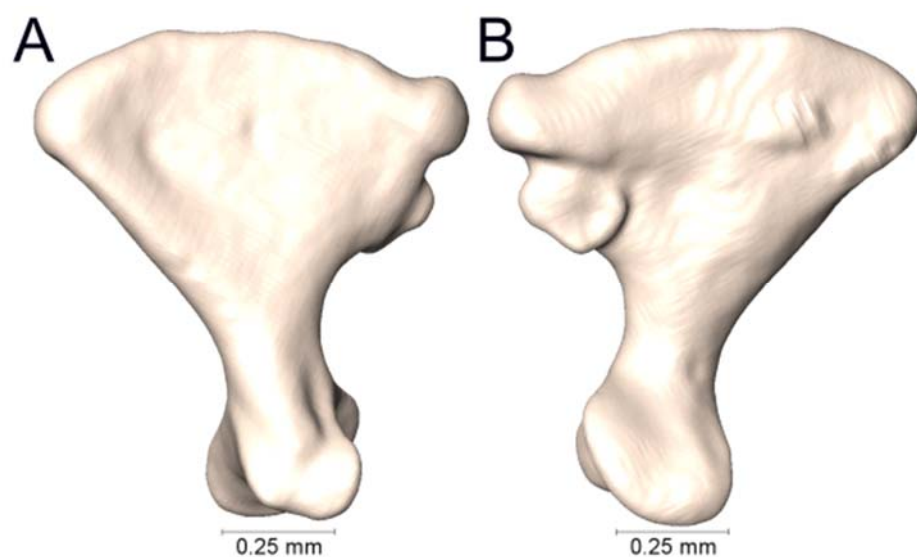
Supplemental Figure 2.7. Lateral and medial views (A-B, respectively) of the left quadrate of *Calliophis bivirgatus bivirgatus* (UTA R-63079).



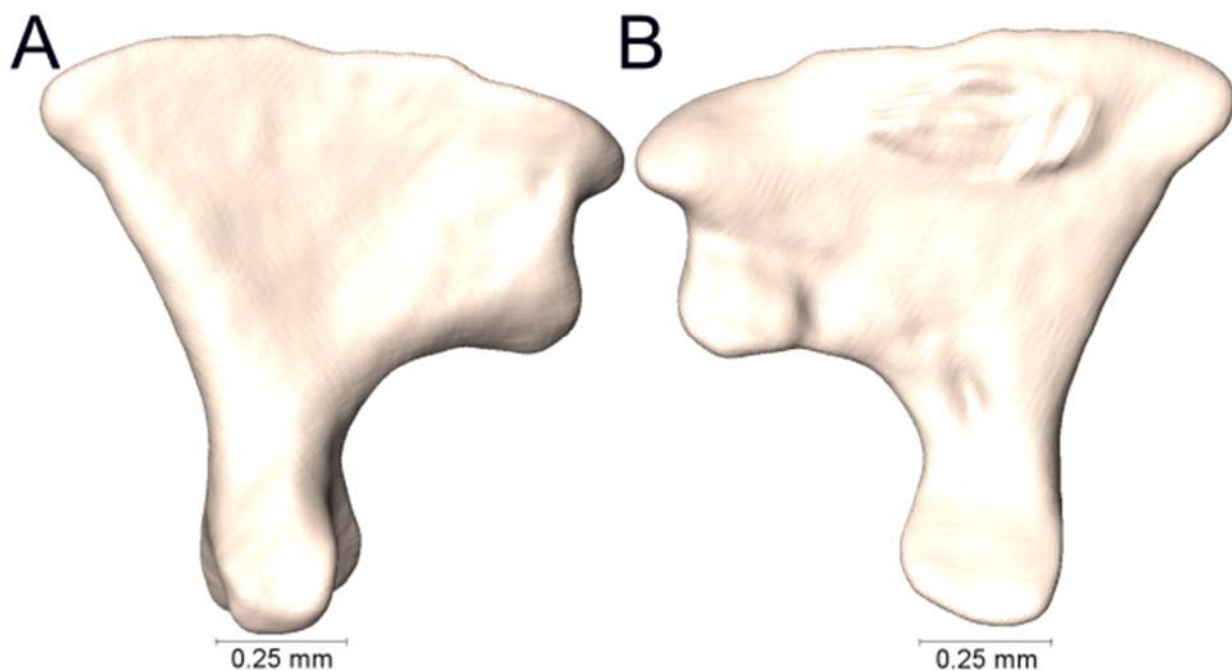
Supplemental Figure 2.8. Lateral and medial views (A-B, respectively) of the left quadrate of *Calliophis gracilis* (USNM 53447).



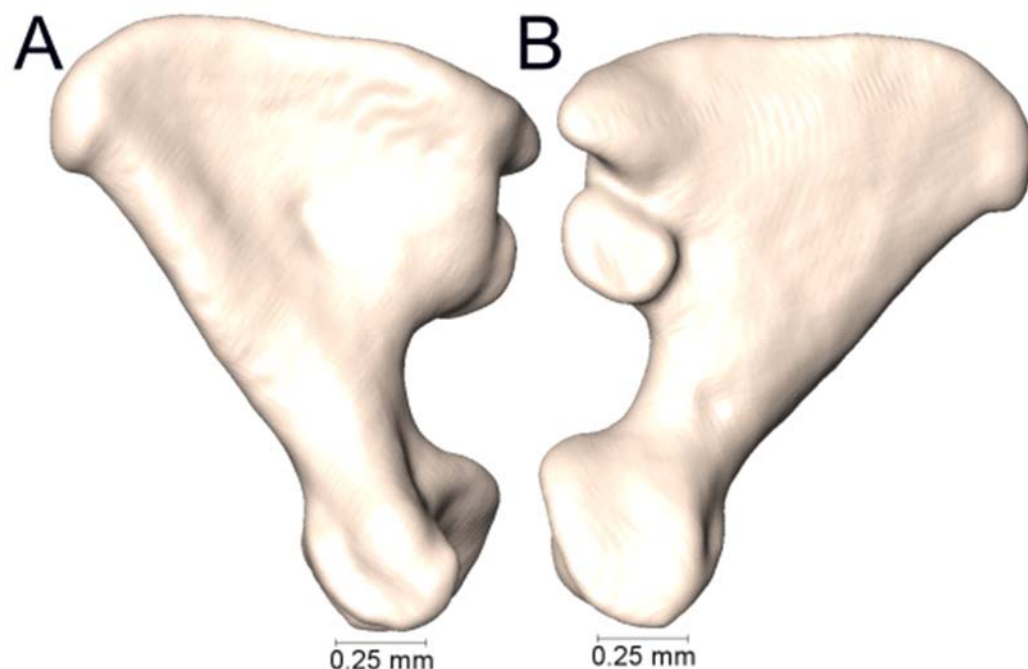
Supplemental Figure 2.9. Lateral and medial views (A-B, respectively) of the left quadrate of *Calliophis intestinalis* (UTA R-60738).



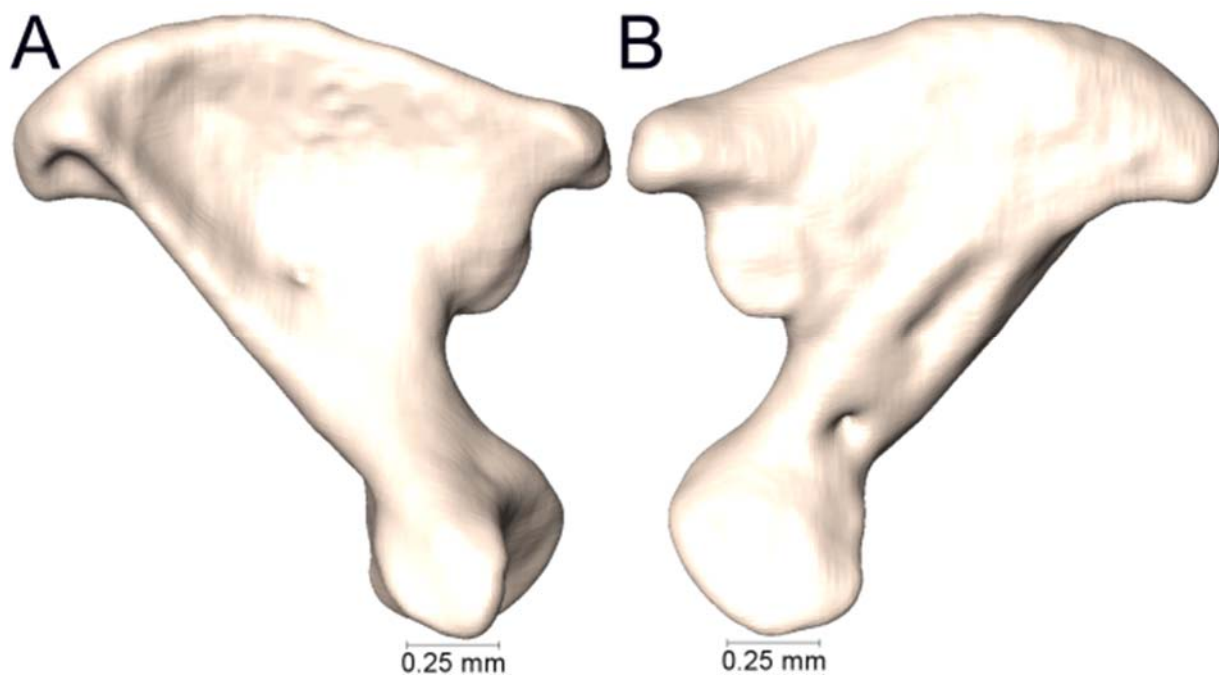
Supplemental Figure 2.10. Lateral and medial views (A-B, respectively) of the left quadrate of *Calliophis cf. intestinalis* (NMW 27221-4).



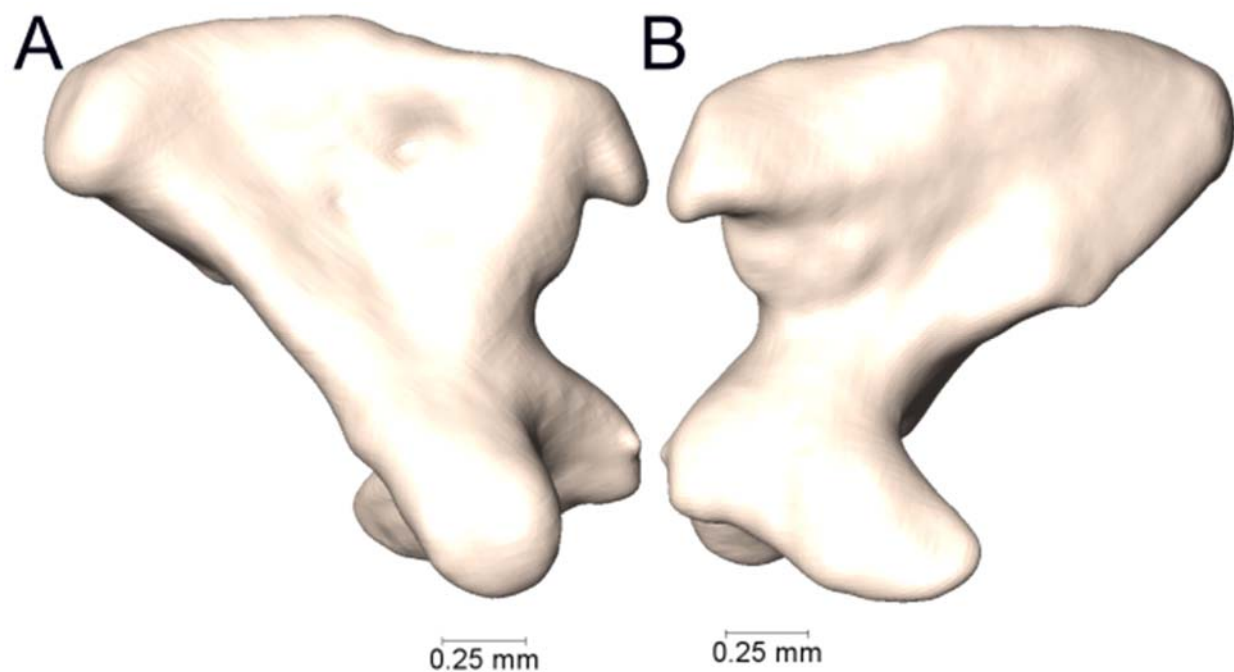
Supplemental Figure 2.11. Lateral and medial views (A-B, respectively) of the left quadrate of *Calliophis intestinalis* *immaculata* (UTA R-65802).



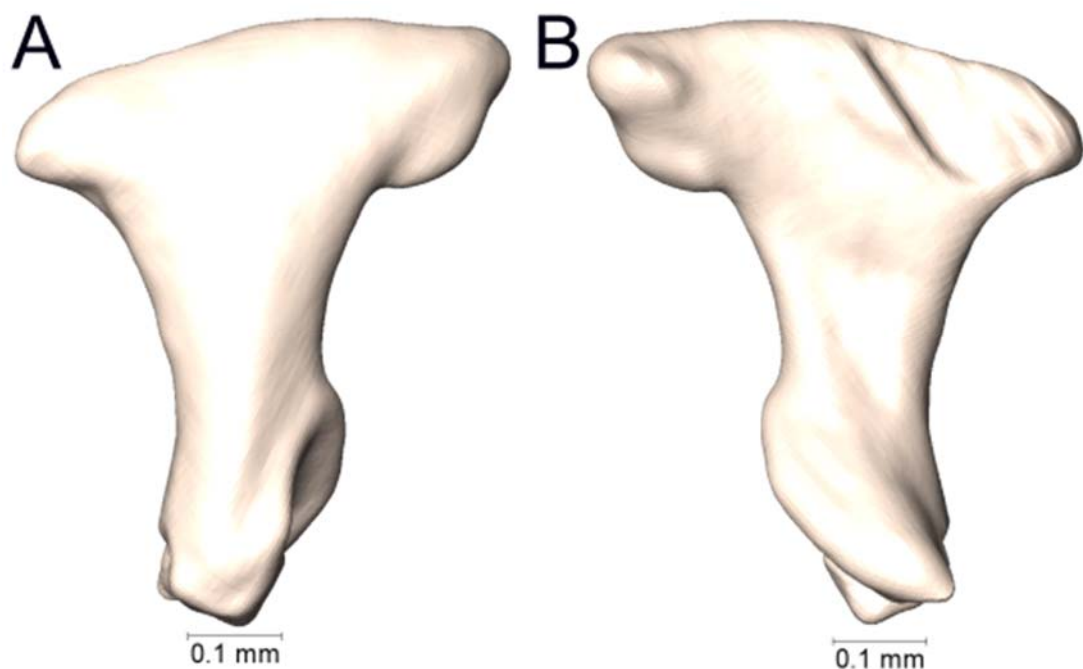
Supplemental Figure 2.12. Lateral and medial views (A-B, respectively) of the left quadrate of *Calliophis intestinalis* *cf. immaculata* (NMW 27192-1).



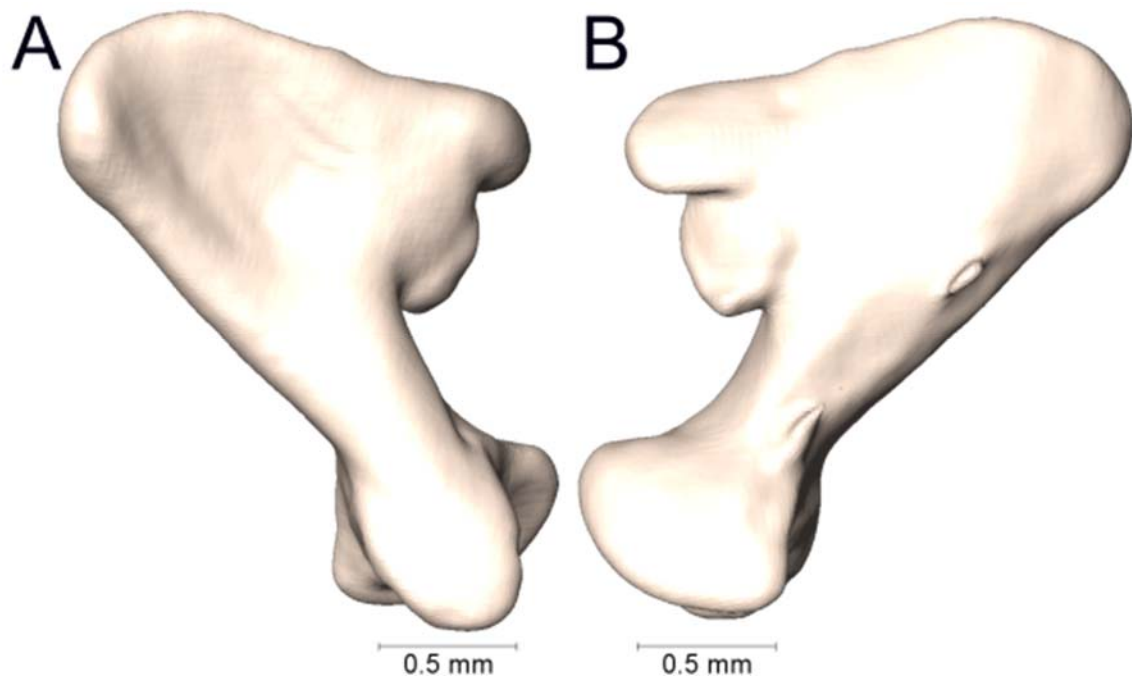
Supplemental Figure 2.13. Lateral and medial views (A-B, respectively) of the left quadrate of *Calliophis intestinalis lineata* (UTA R-65801).



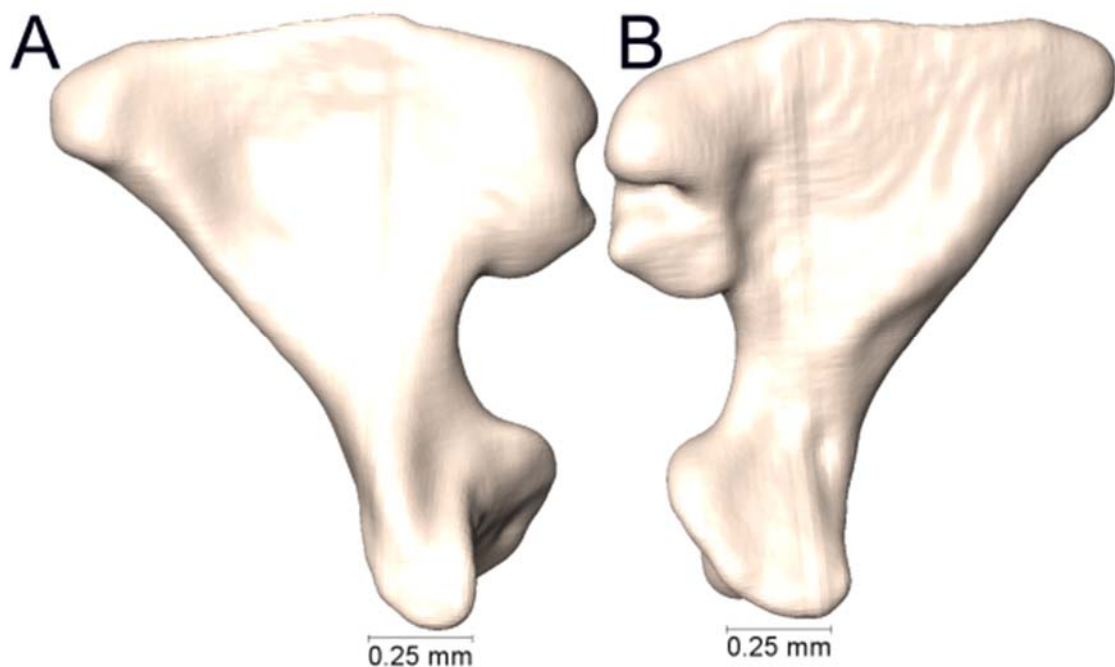
Supplemental Figure 2.14. Lateral and medial views (A-B, respectively) of the left quadrate of *Calliophis maculiceps* (MNHN 5459).



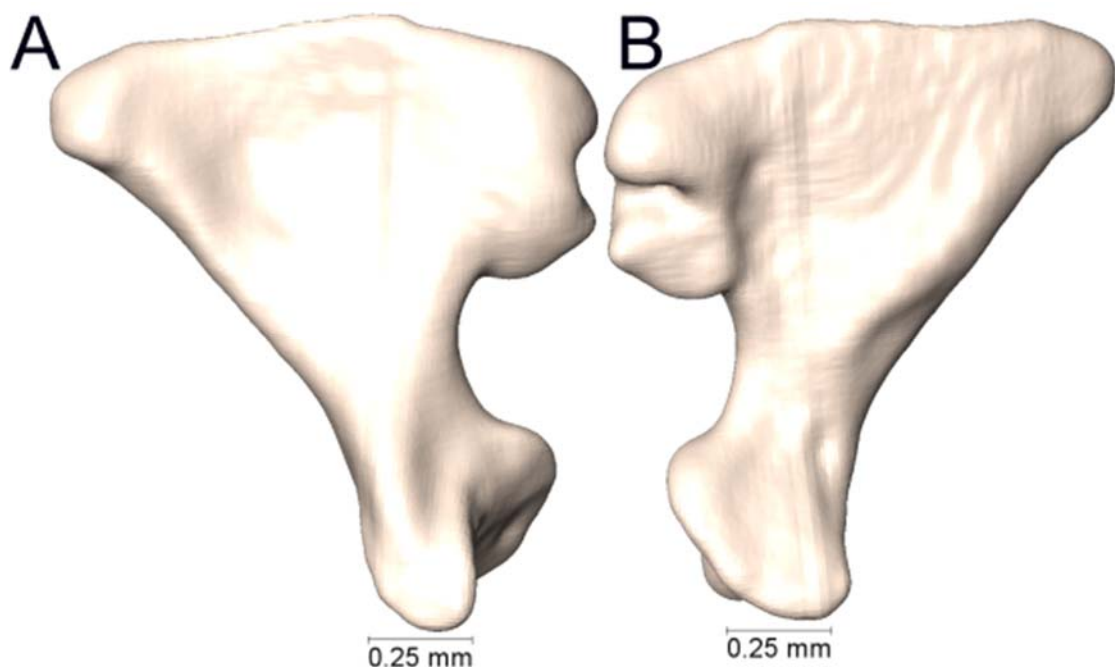
Supplemental Figure 2.15. Lateral and medial views (A-B, respectively) of the left quadrate of *Calliophis melanurus* (MNHN 46-286).



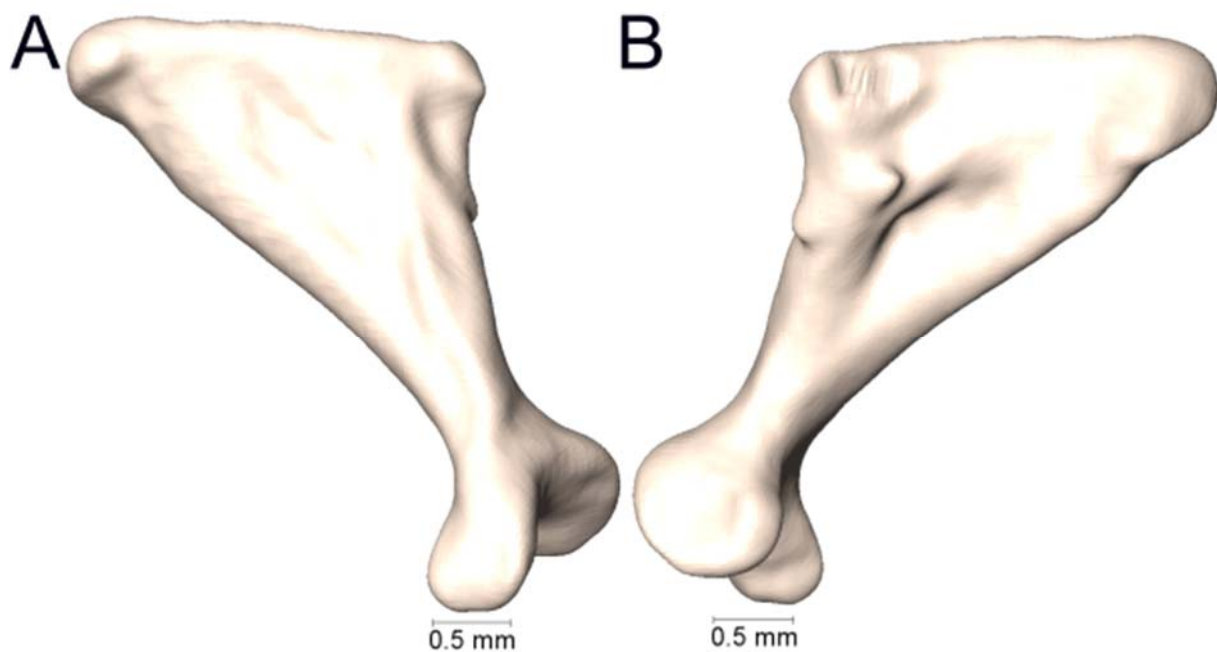
Supplemental Figure 2.16. Lateral and medial views (A-B, respectively) of the left quadrate of *Calliophis nigrotaeniatus* (NMW 27220-7).



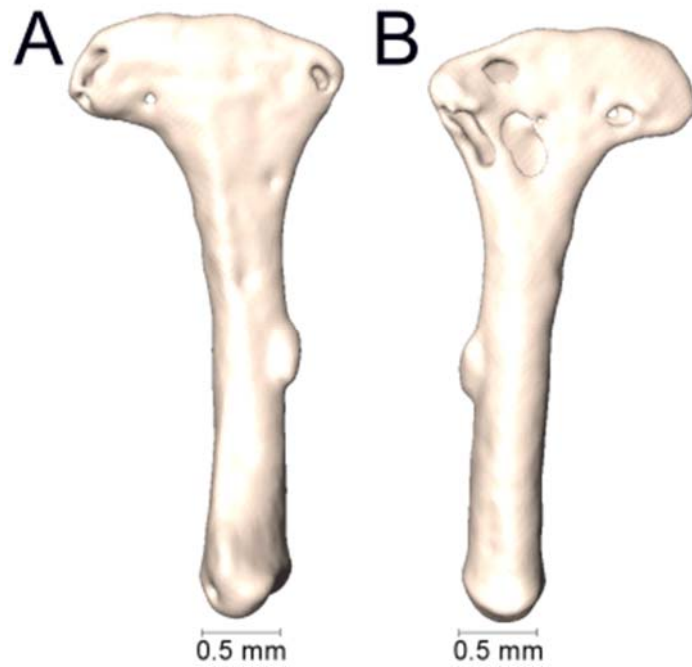
Supplemental Figure 2.17. Lateral and medial views (A-B, respectively) of the left quadrate of *Calliophis philippinus* (KU 310369).



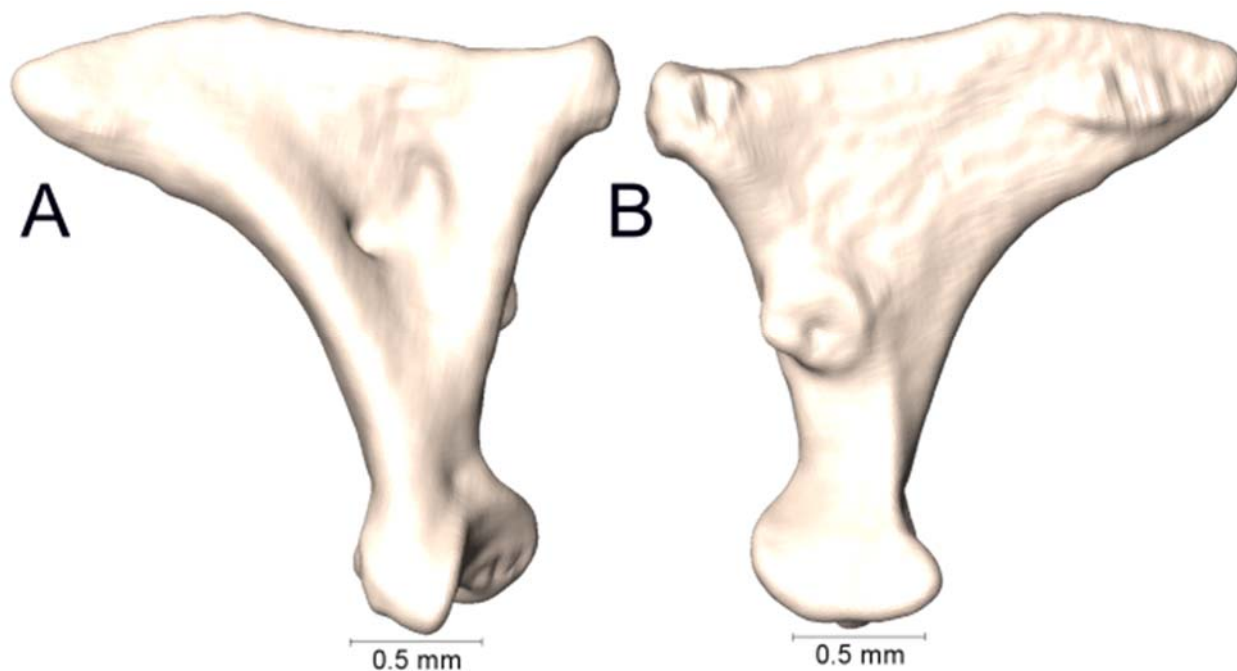
Supplemental Figure 2.18. Lateral and medial views (A-B, respectively) of the left quadrate of *Calliophis philippinus* (KU 314913).



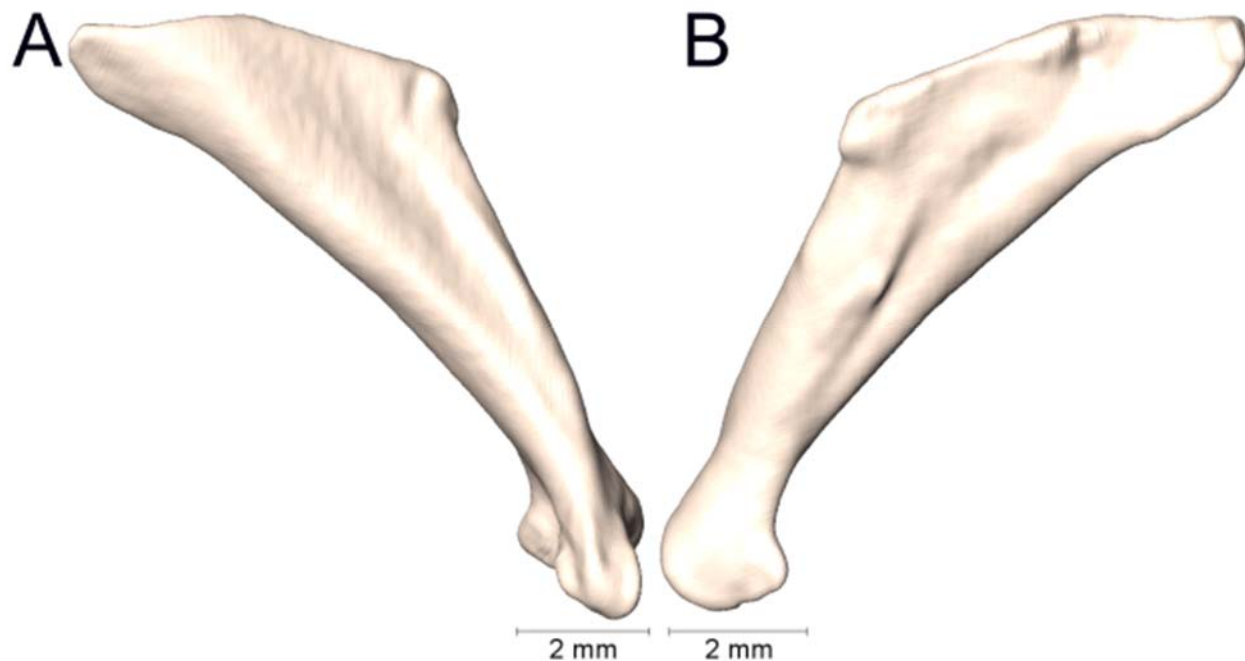
Supplemental Figure 2.19. Lateral and medial views (A-B, respectively) of the left quadrate of *Calliophis salitan* (PNM 9844).



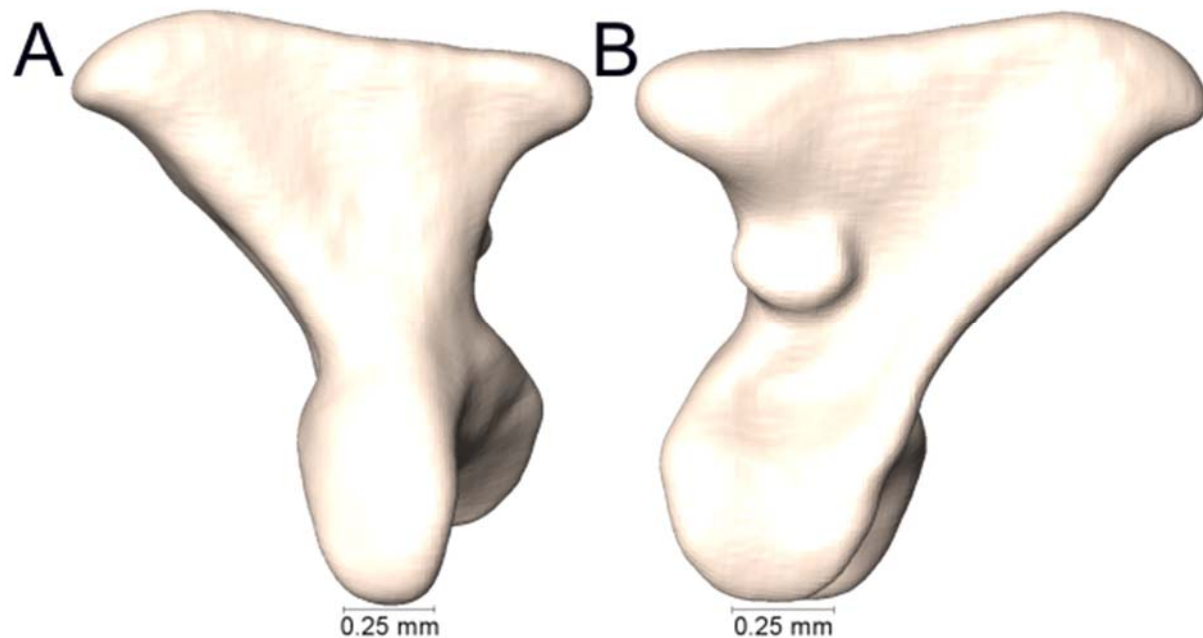
Supplemental Figure 2.20. Lateral and medial views (A-B, respectively) of the left quadrate of *Dendroaspis angusticeps* (UTA R-34982).



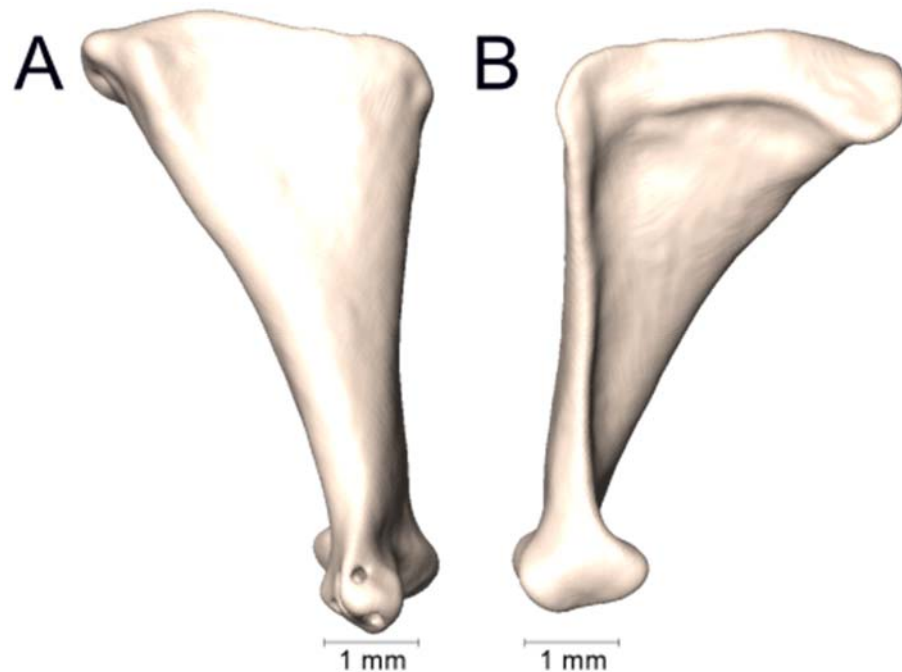
Supplemental Figure 2.21. Lateral and medial views (A-B, respectively) of the left quadrate of *Elapsoidea nigra* (CAS 168978).



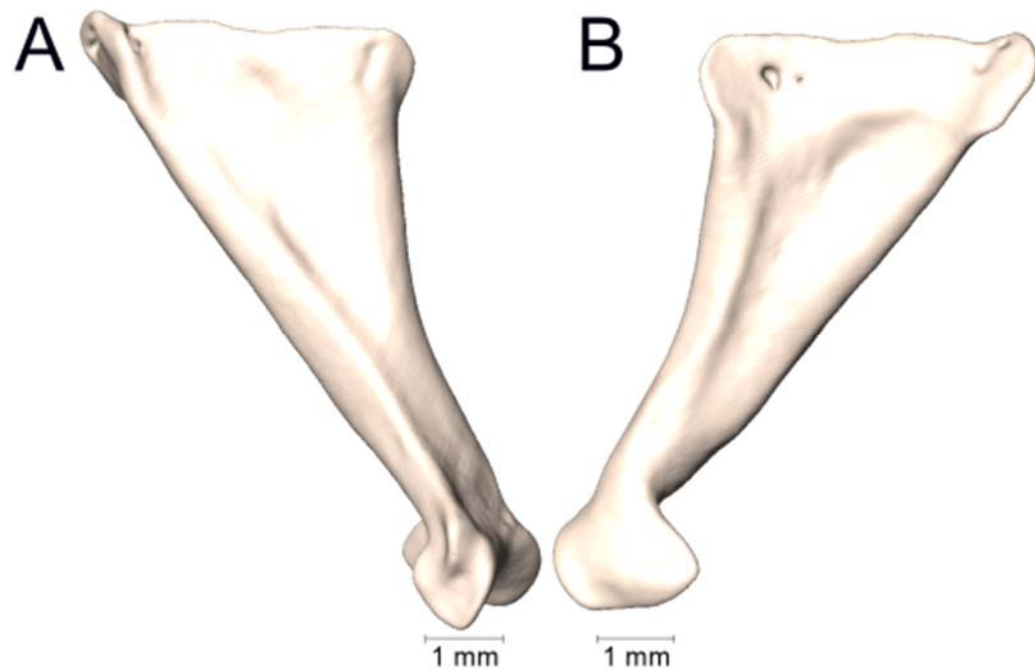
Supplemental Figure 2.22. Lateral and medial views (A-B, respectively) of the left quadrate of *Hemachatus haemachatus* (UTA R-7431).



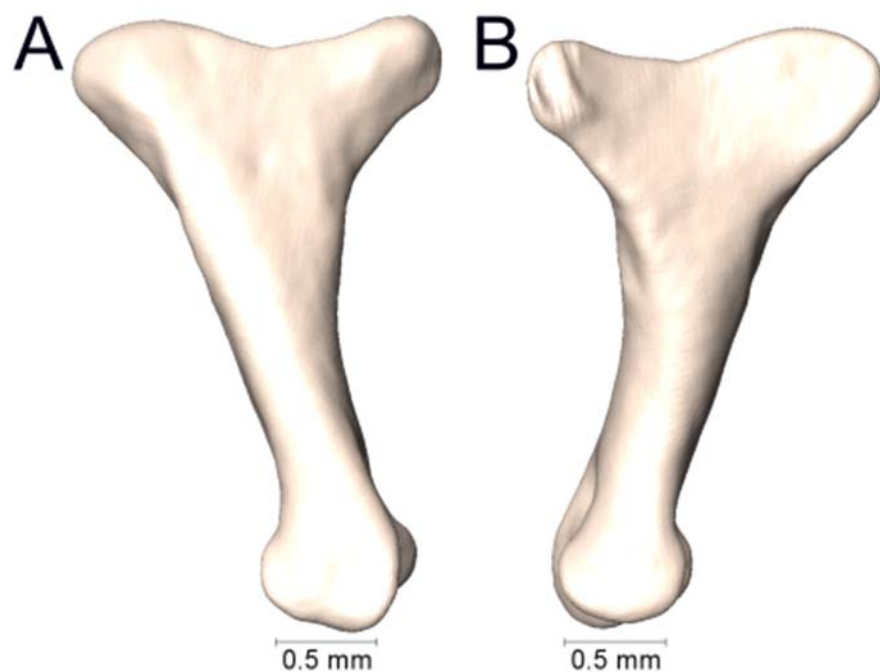
Supplemental Figure 2.23. Lateral and medial views (A-B, respectively) of the left quadrate of *Hemibungarus calligaster* (KU 307474).



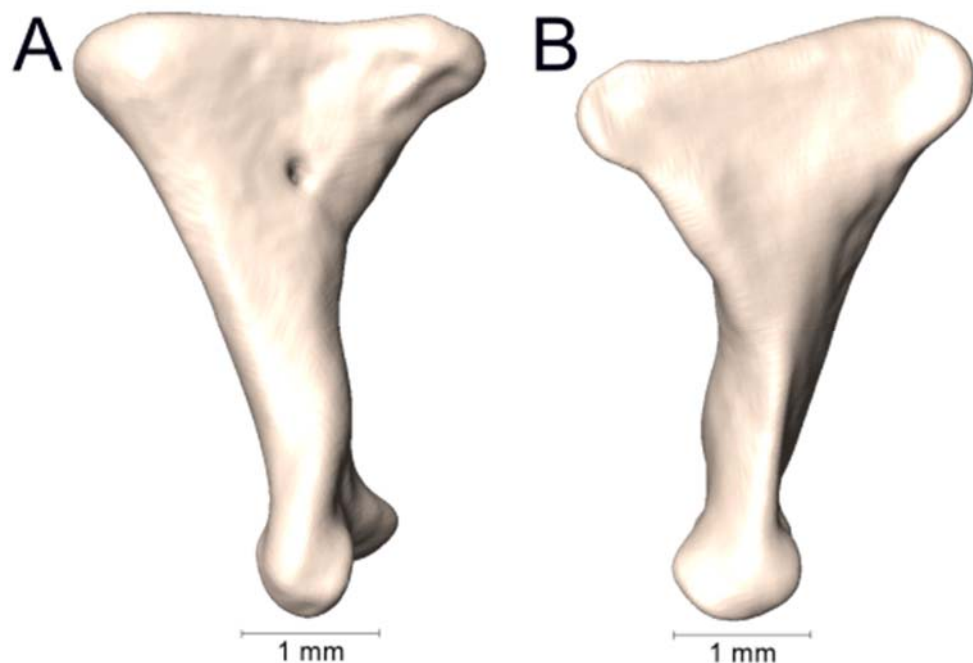
Supplemental Figure 2.24. Lateral and medial views (A-B, respectively) of the left quadrate of *Hydrophis platurus* (UTA R-41049).



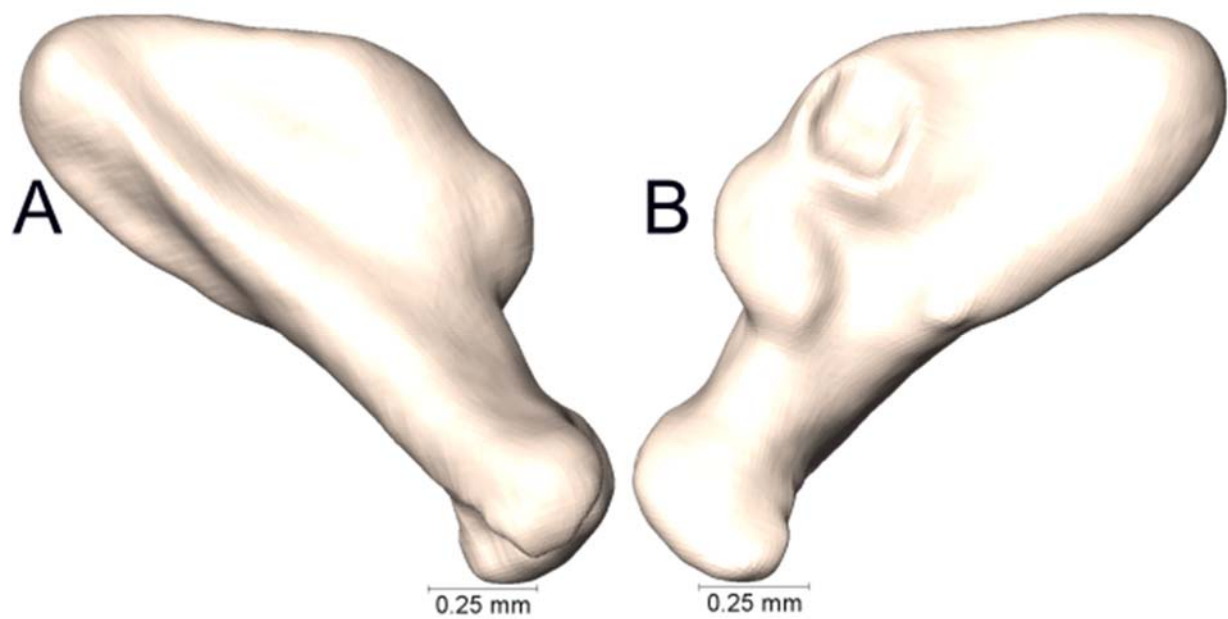
Supplemental Figure 2.25. Lateral and medial views (A-B, respectively) of the left quadrate of *Hydrophis schistosus* (UTA R-63074).



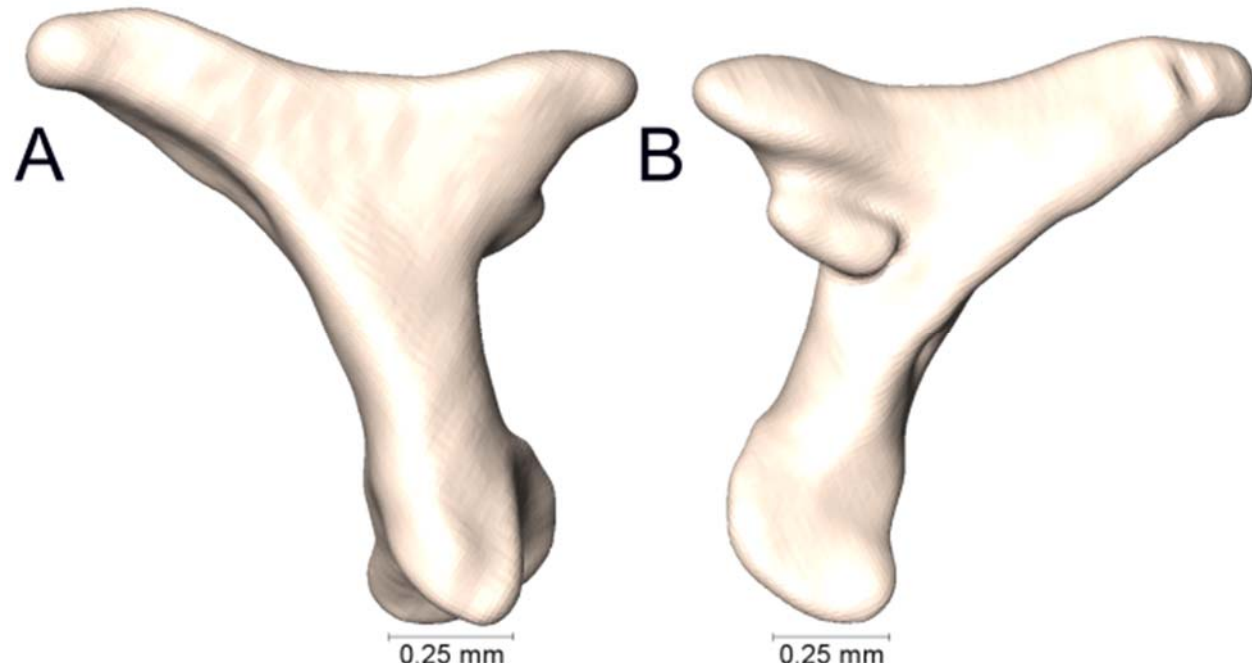
Supplemental Figure 2.26. Lateral and medial views (A-B, respectively) of the left quadrate of *Laticauda colubrina* (UTA R-65800).



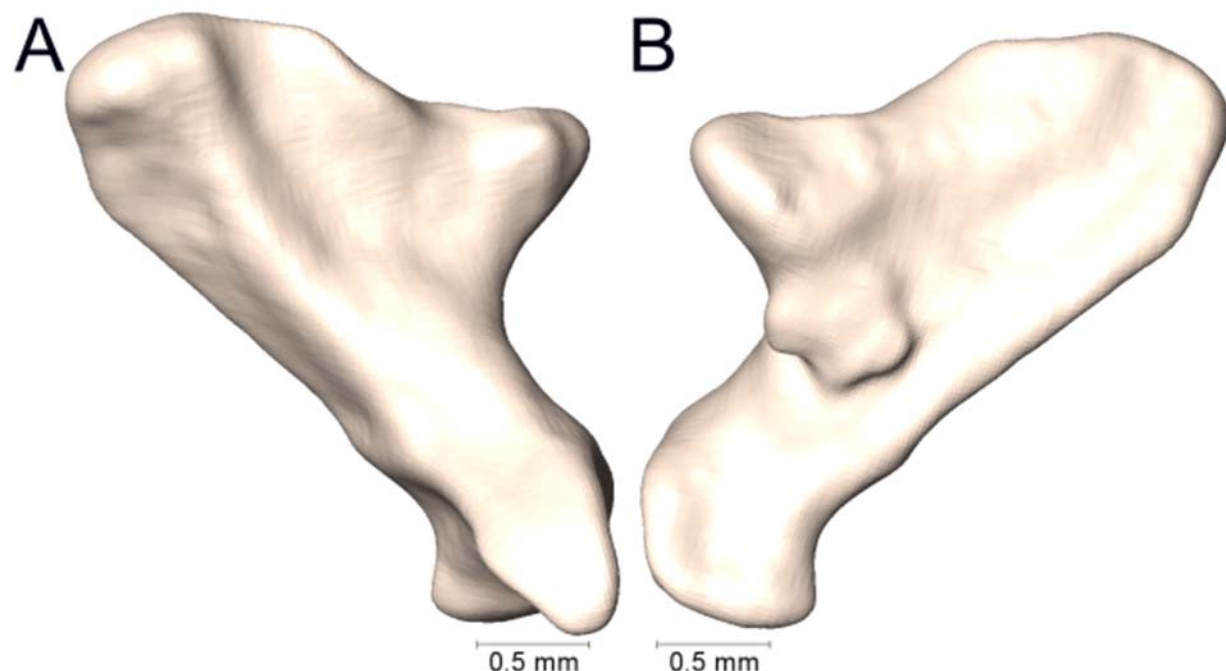
Supplemental Figure 2.27. Lateral and medial views (A-B, respectively) of the left quadrate of *Laticauda laticauda* (UTA R-6355).



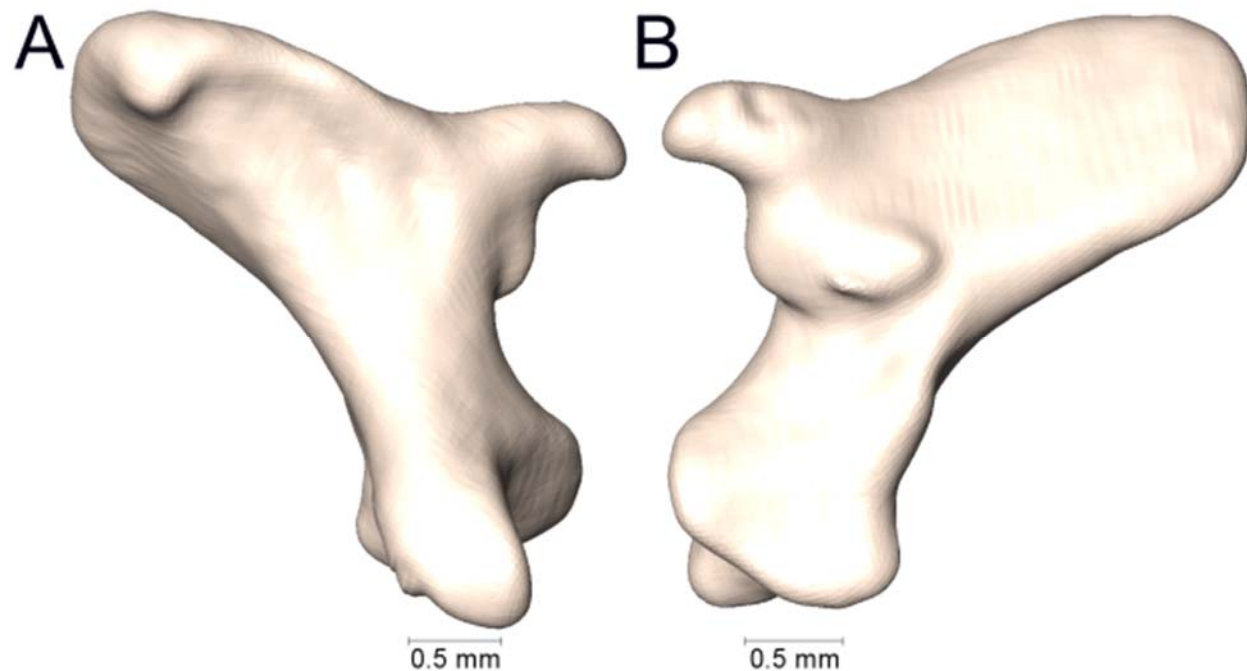
Supplemental Figure 2.28. Lateral and medial views (A-B, respectively) of the left quadrate of *Micrelaps vaillanti* (CAS 169941).



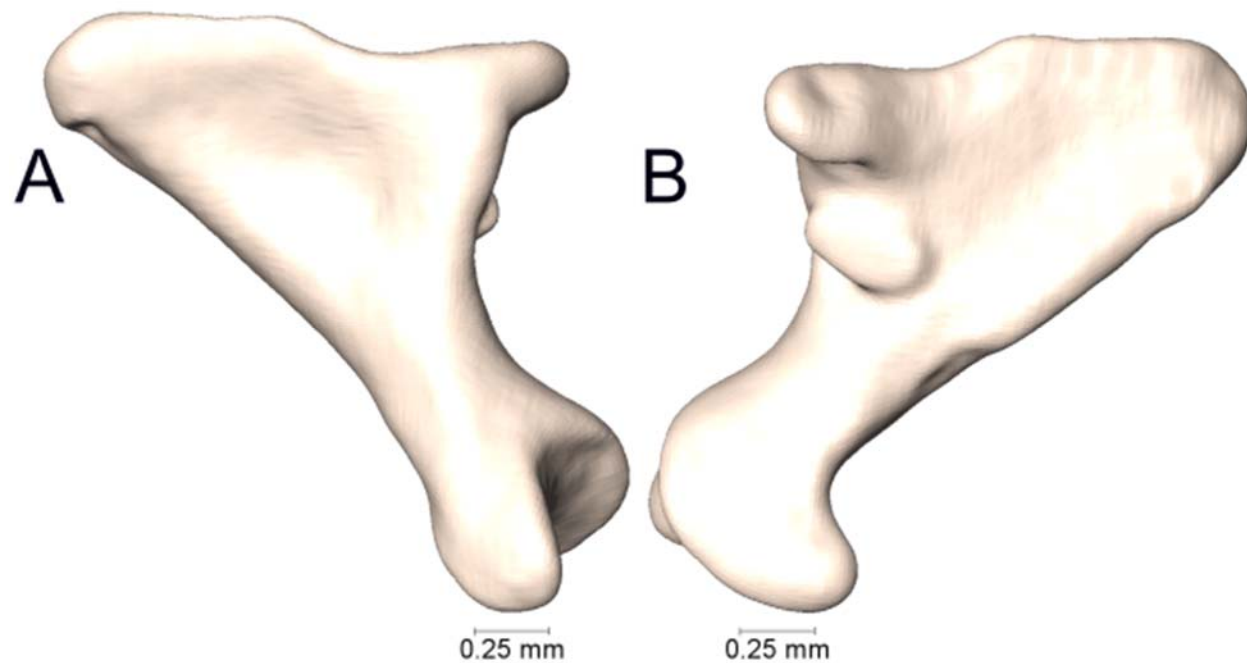
Supplemental Figure 2.29. Lateral and medial views (A-B, respectively) of the left quadrate of *Micruroides euryxanthus* (UTA R-60734).



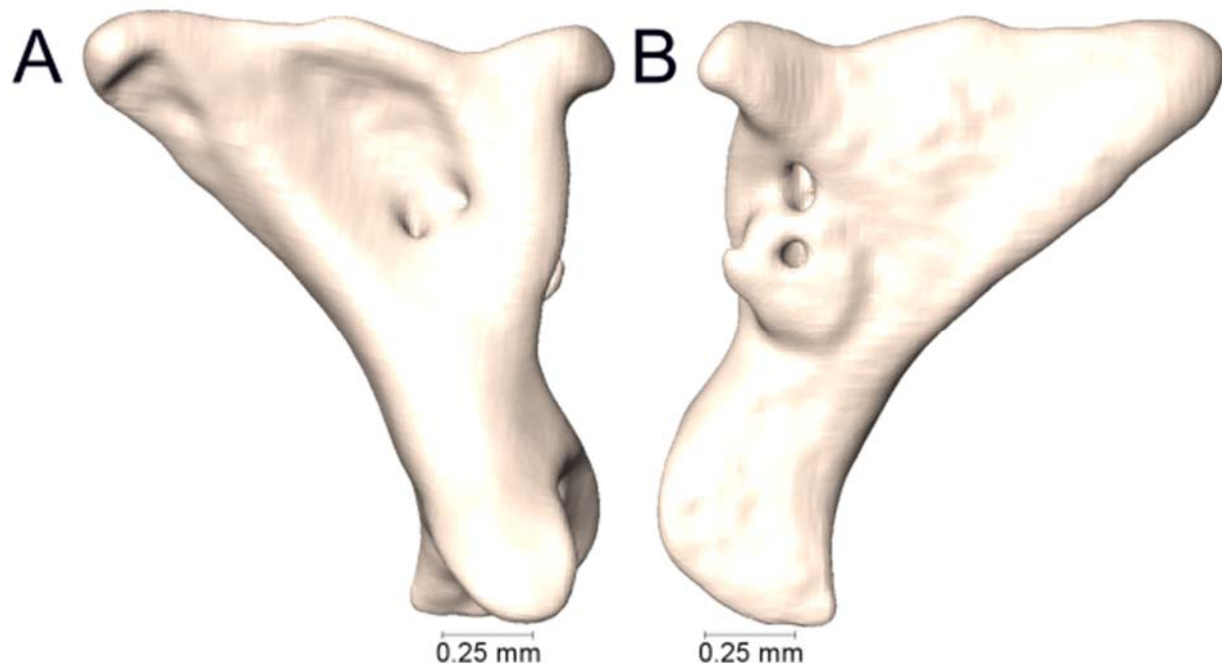
Supplemental Figure 2.30. Lateral and medial views (A-B, respectively) of the left quadrate of *Micrurus alleni* (UTA R-60556).



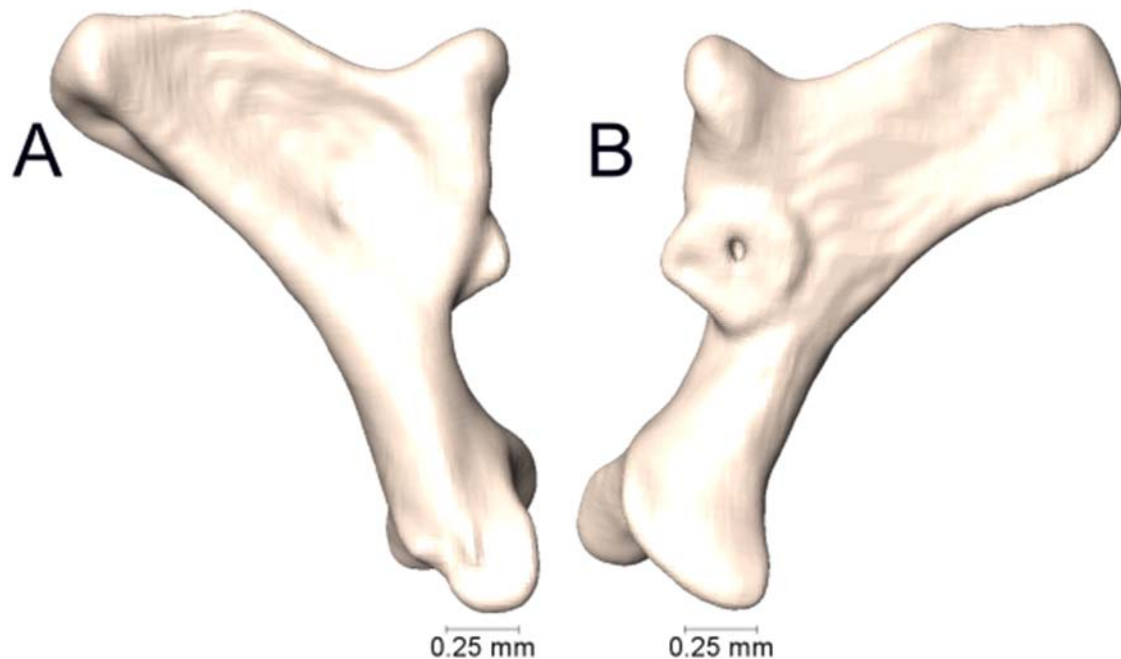
Supplemental Figure 2.31. Lateral and medial views (A-B, respectively) of the left quadrate of *Micrurus anchoralis* (UTA R-55945).



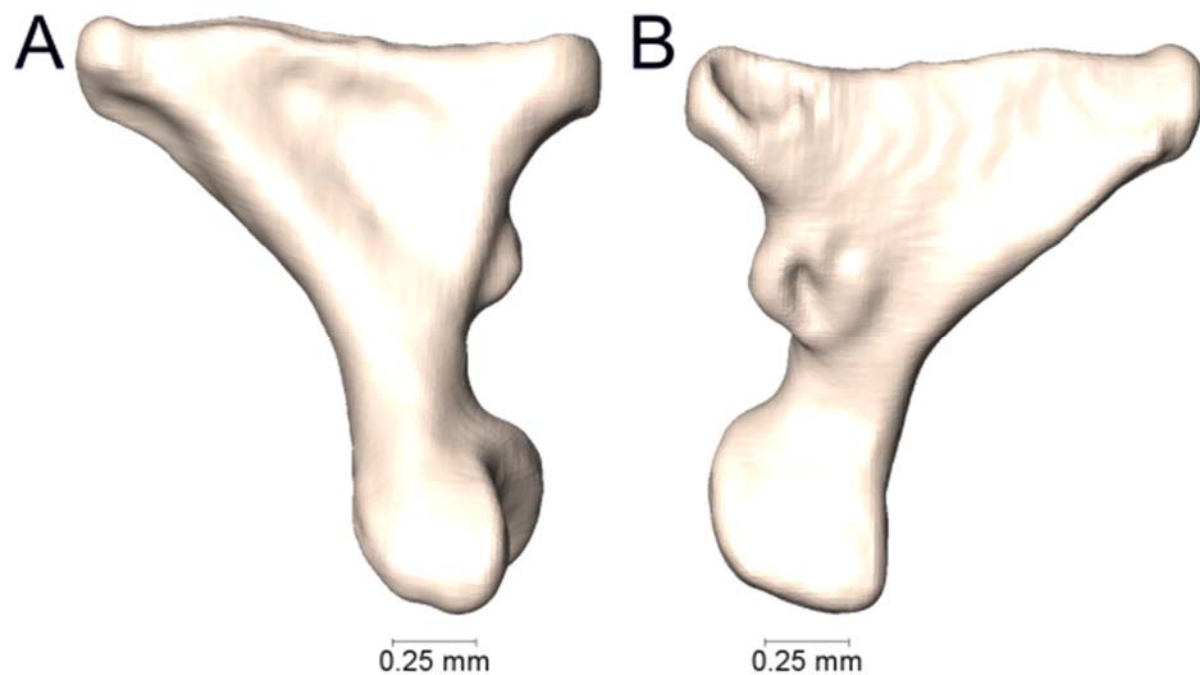
Supplemental Figure 2.32. Lateral and medial views (A-B, respectively) of the left quadrate of *Micrurus apiatus* (UTA R-39267).



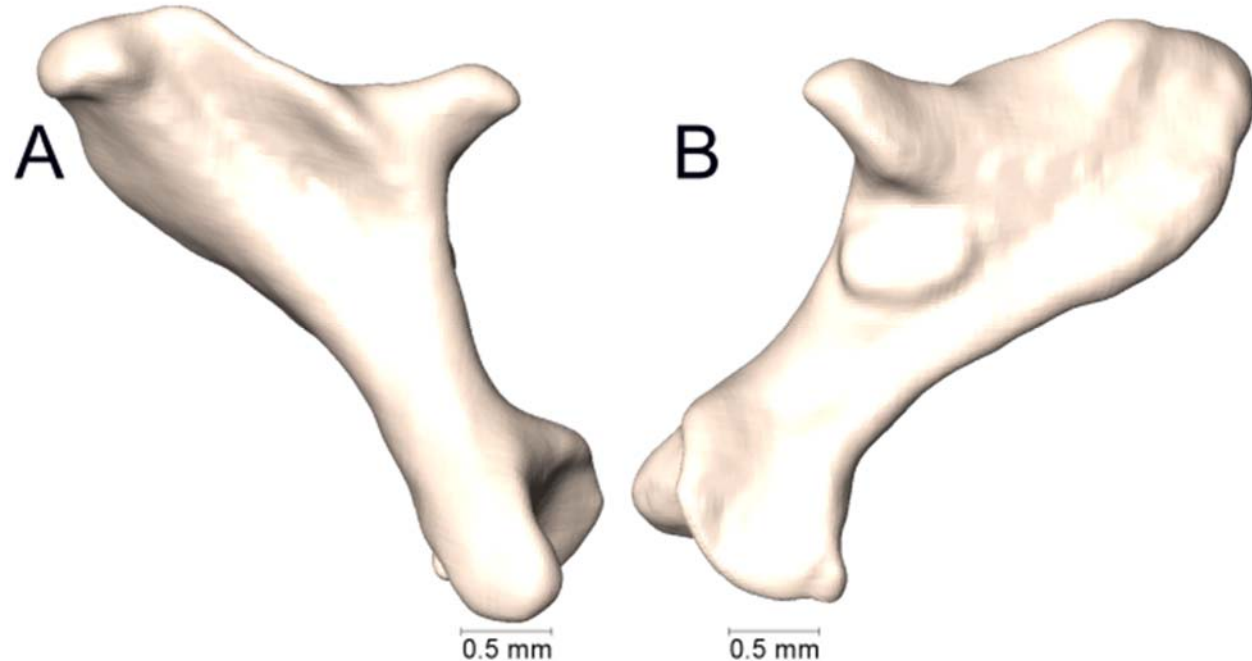
Supplemental Figure 2.33. Lateral and medial views (A-B, respectively) of the left quadrate of *Micrurus apiatus* (UTA R-39554).



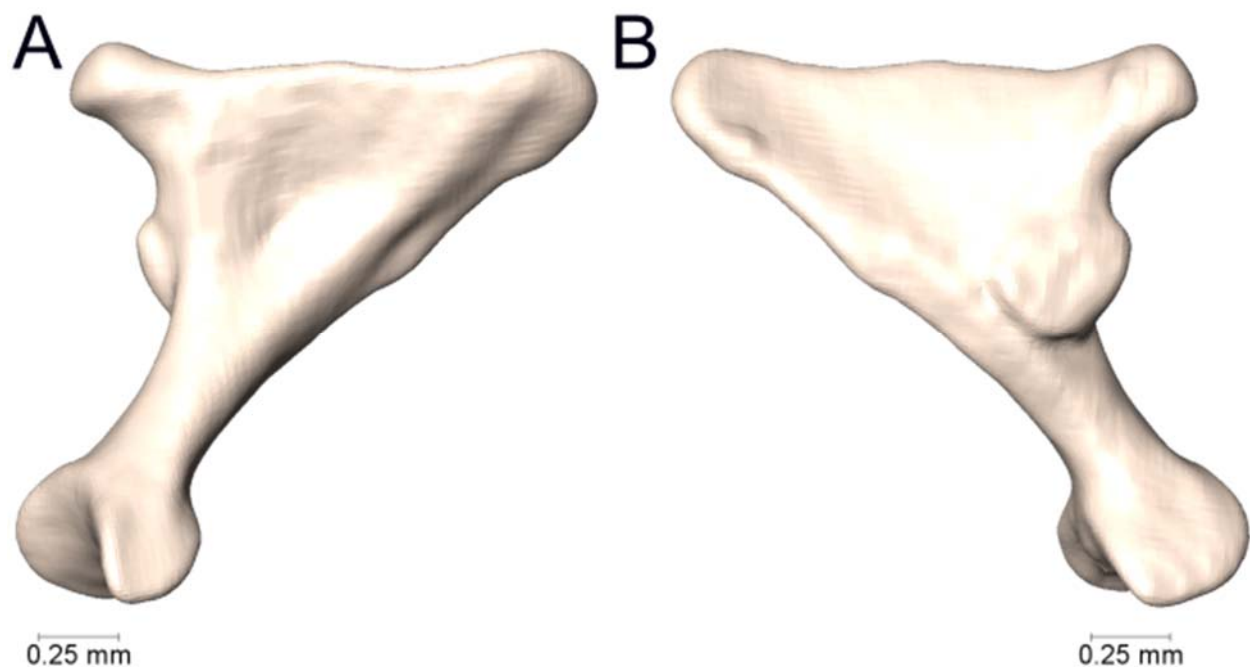
Supplemental Figure 2.34. Lateral and medial views (A-B, respectively) of the left quadrate of *Micrurus apiatus* (UTA R-53450).



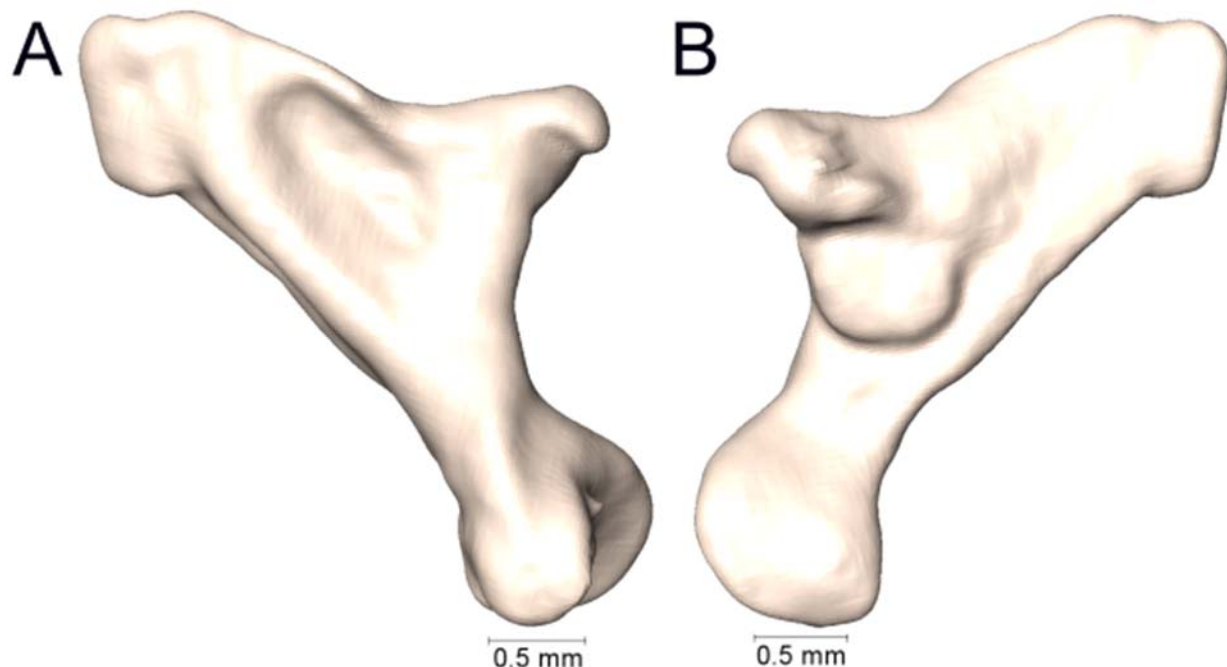
Supplemental Figure 2.35. Lateral and medial views (A-B, respectively) of the left quadrate of *Micrurus bocourti* (UTA R-58145).



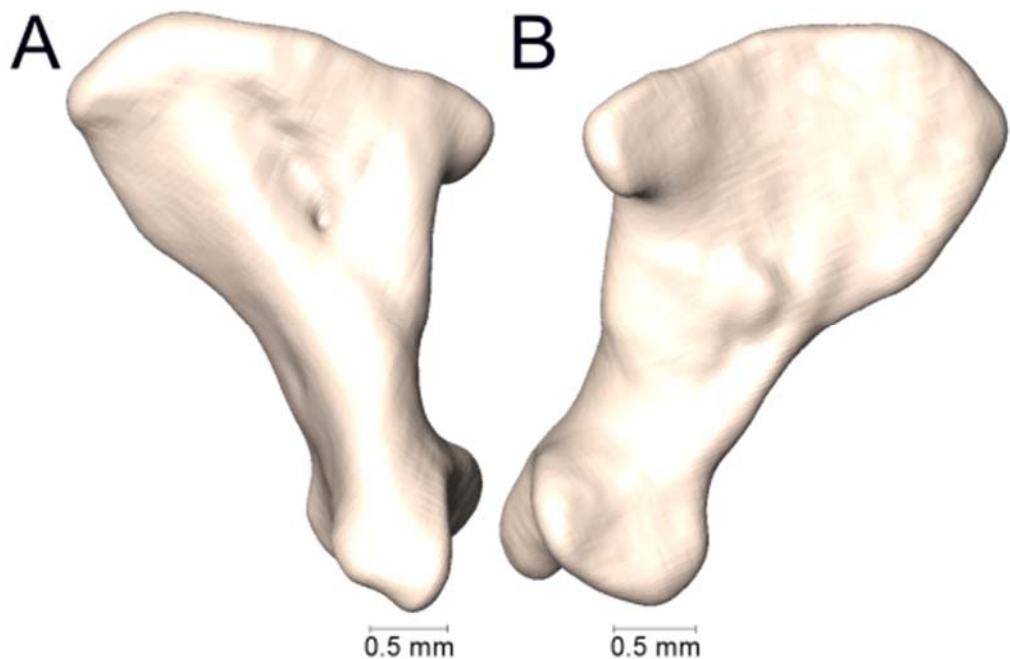
Supplemental Figure 2.36. Lateral and medial views (A-B, respectively) of the left quadrate of *Micrurus diastema* (UTA R-52565).



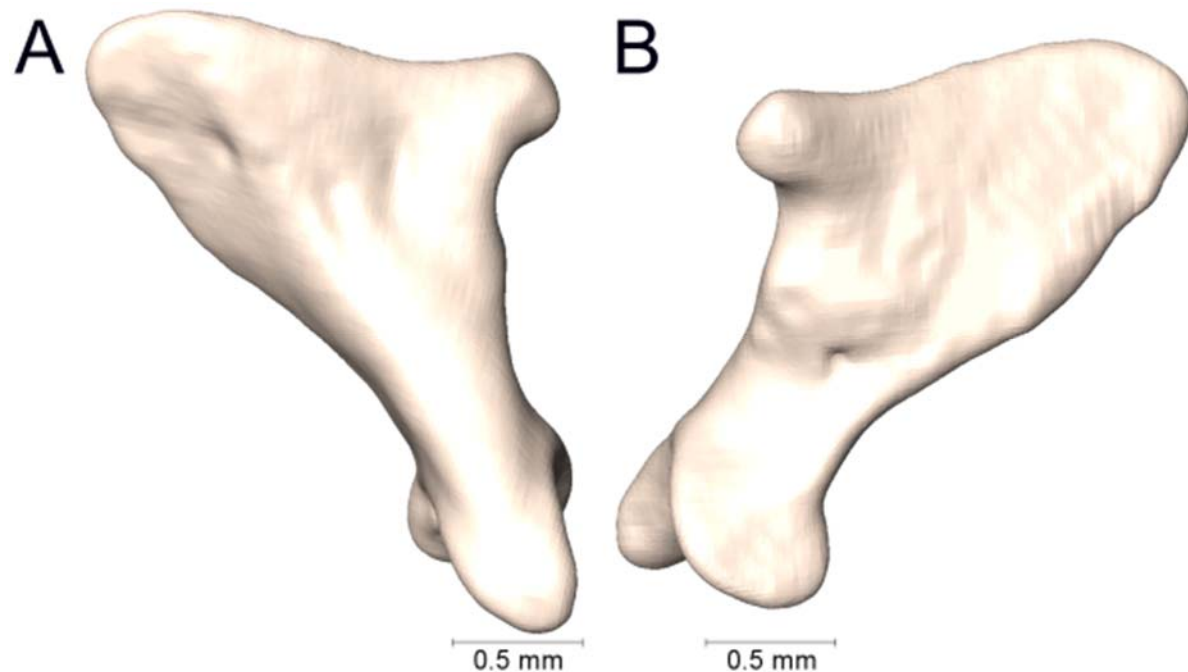
Supplemental Figure 2.37. Lateral and medial views (A-B, respectively) of the right quadrate of *Micrurus disssoleucus* (UTA R-54184).



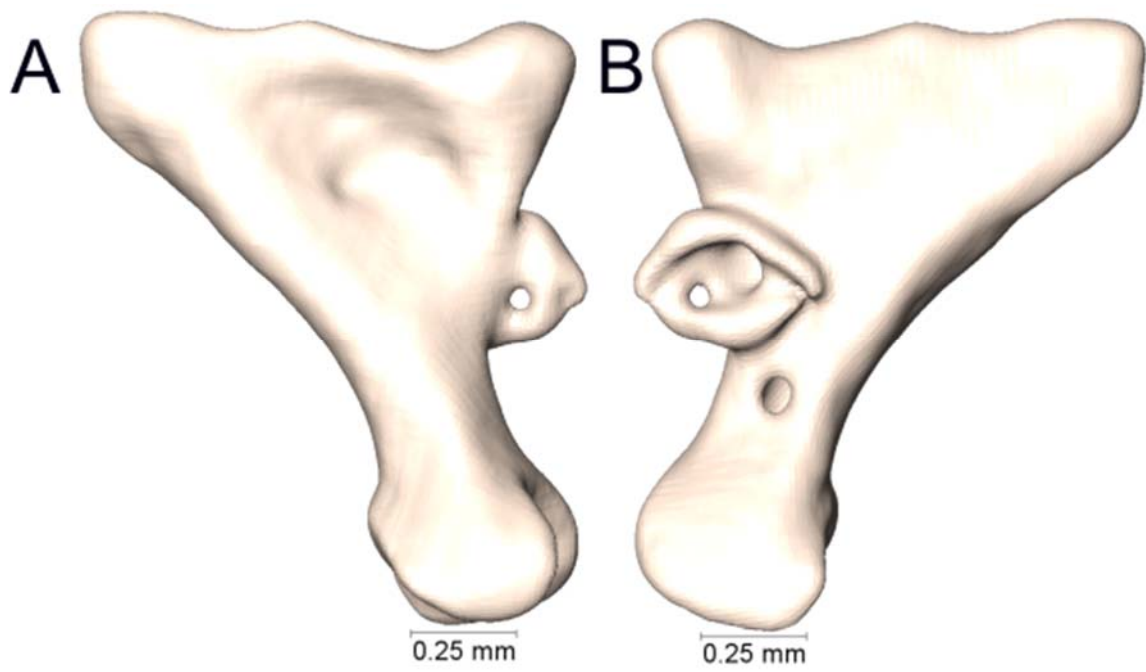
Supplemental Figure 2.38. Lateral and medial views (A-B, respectively) of the left quadrate of *Micrurus distans* (UTA R-14471).



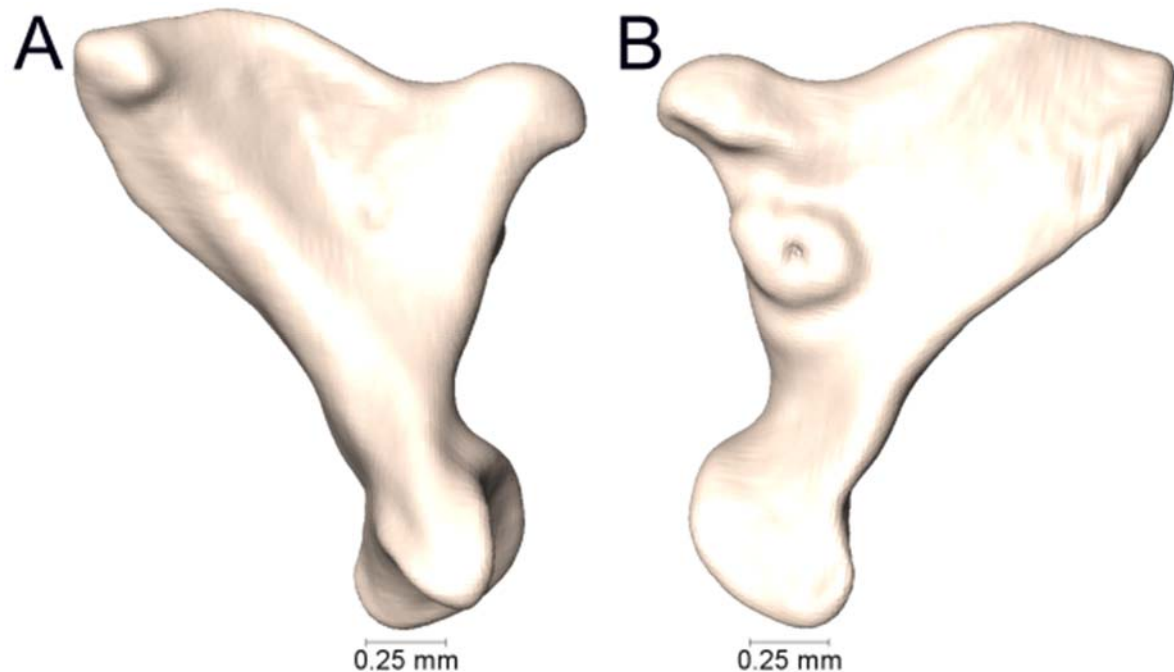
Supplemental Figure 2.39. Lateral and medial views (A-B, respectively) of the left quadrate of *Micrurus lemniscatus diutius* (UTA R-20756).



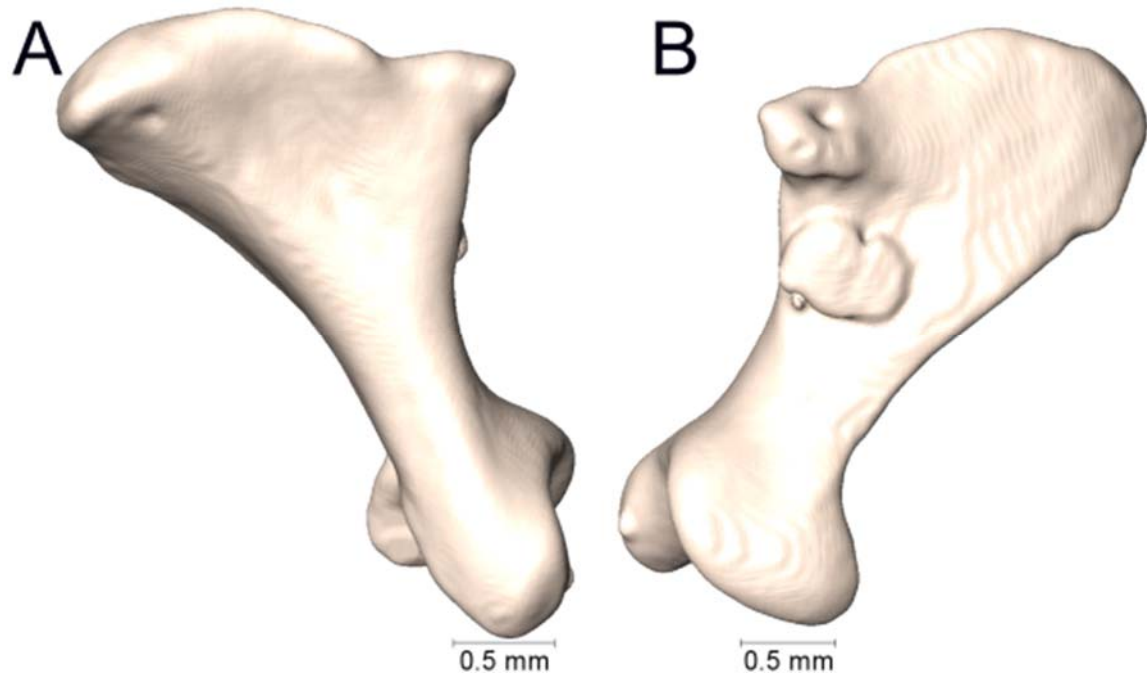
Supplemental Figure 2.40. Lateral and medial views (A-B, respectively) of the left quadrate of *Micrurus diutius* (UTA R-54182).



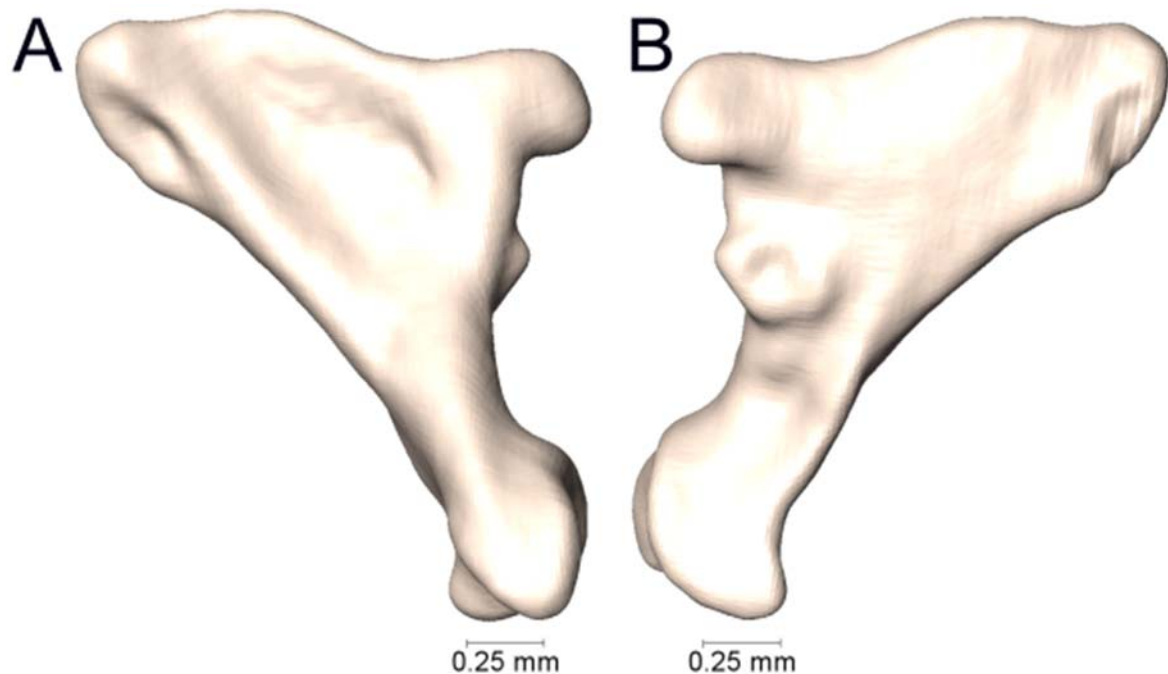
Supplemental Figure 2.41. Lateral and medial views (A-B, respectively) of the left quadrate of *Micrurus dumerilii* (AMNH 35951).



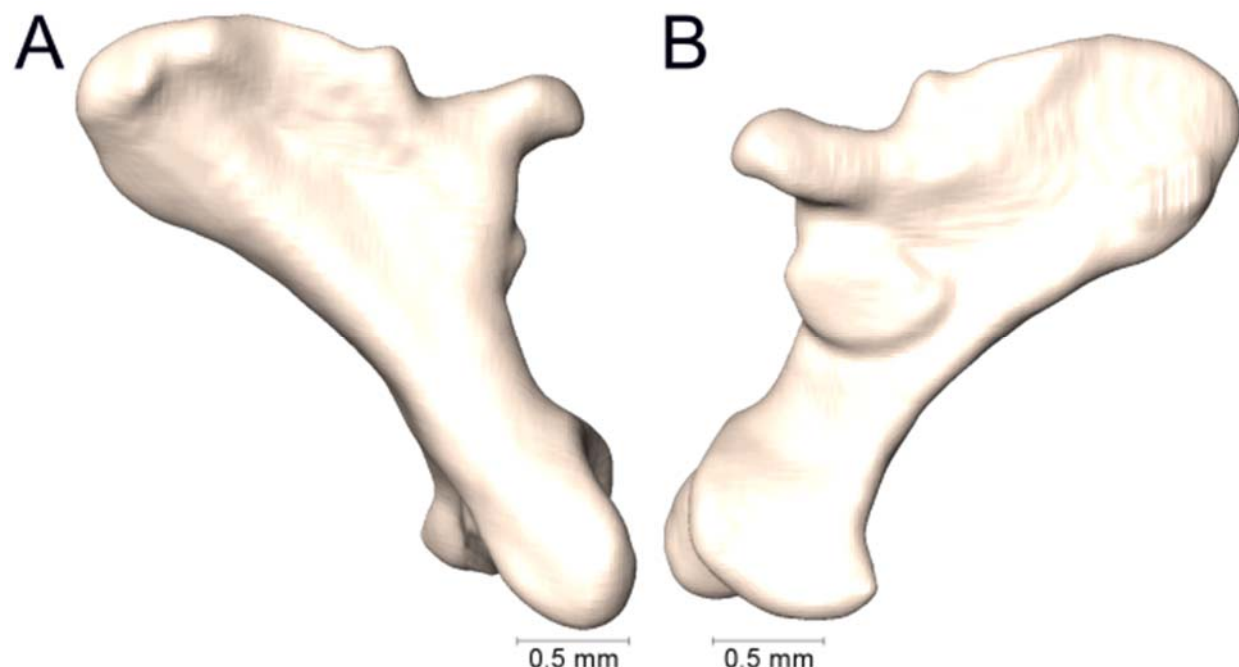
Supplemental Figure 2.42. Lateral and medial views (A-B, respectively) of the left quadrate of *Micrurus elegans elegans* (MZFC 18819).



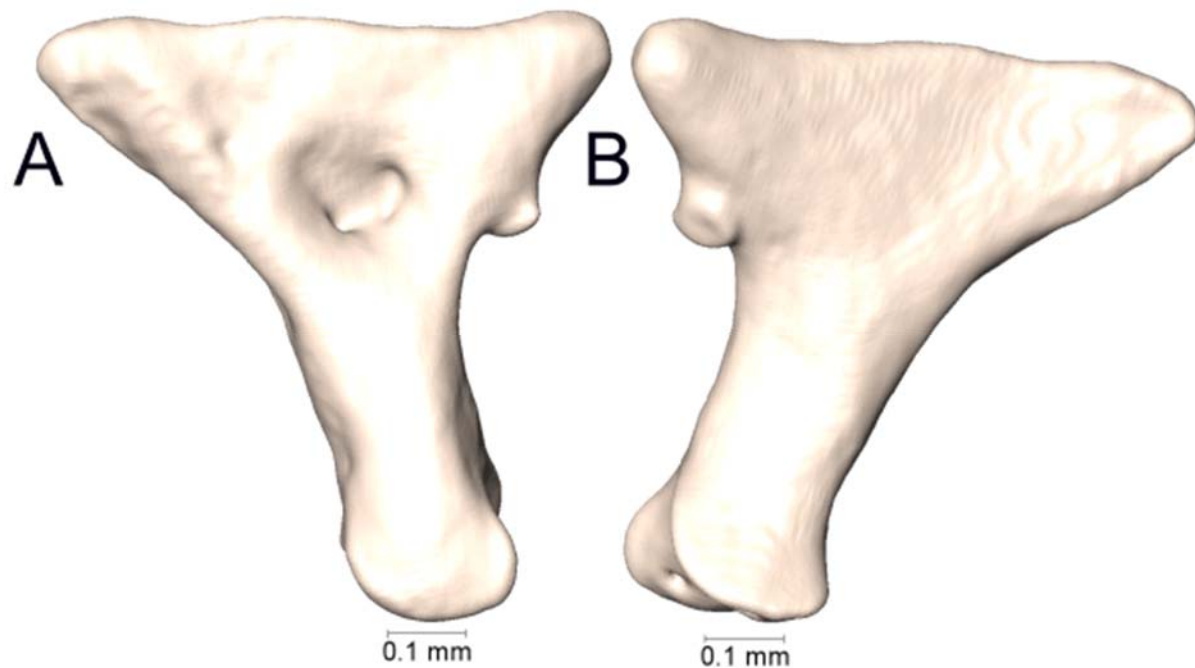
Supplemental Figure 2.43. Lateral and medial views (A-B, respectively) of the left quadrate of *Micrurus elegans veraepacis* (UTA R-7072).



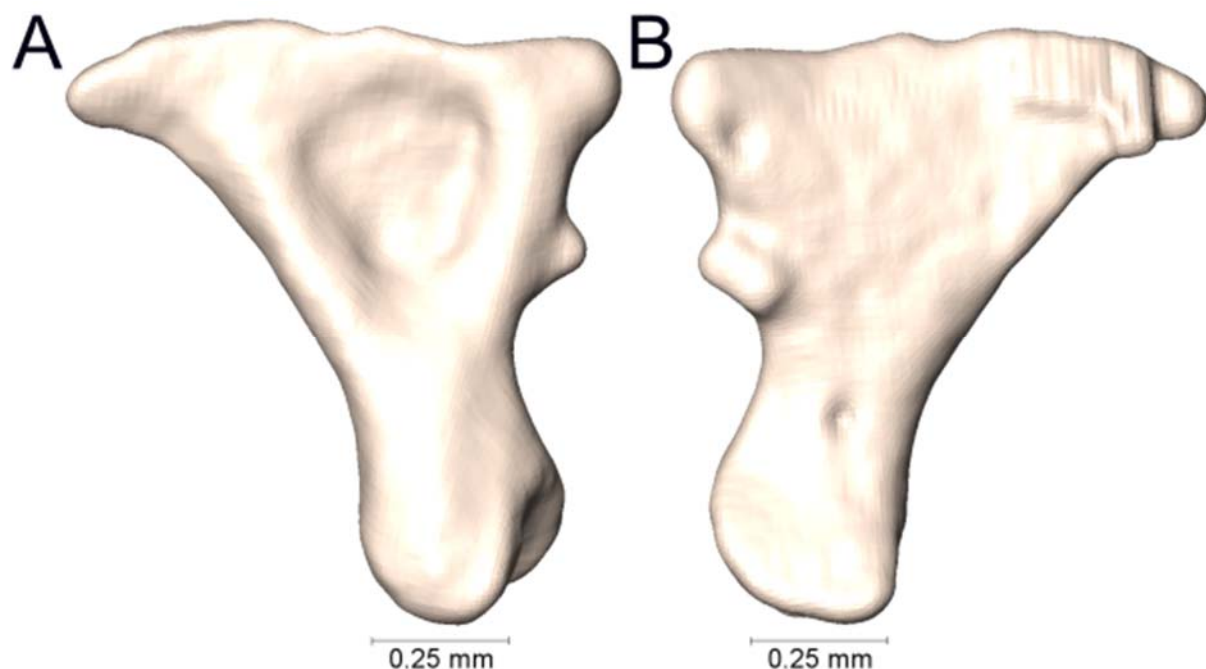
Supplemental Figure 2.44. Lateral and medial views (A-B, respectively) of the left quadrate of *Micrurus elegans veraepacis* (UTA R-58869).



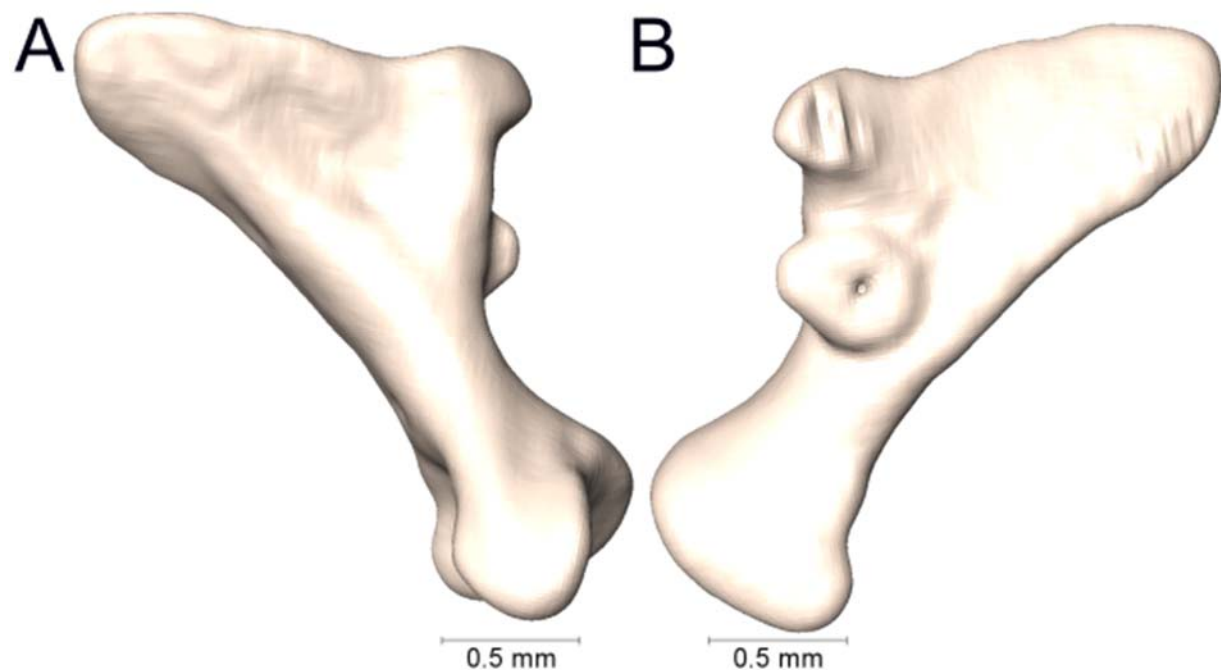
Supplemental Figure 2.45. Lateral and medial views (A-B, respectively) of the left quadrate of *Micrurus ephippifer* (UTA R-64863).



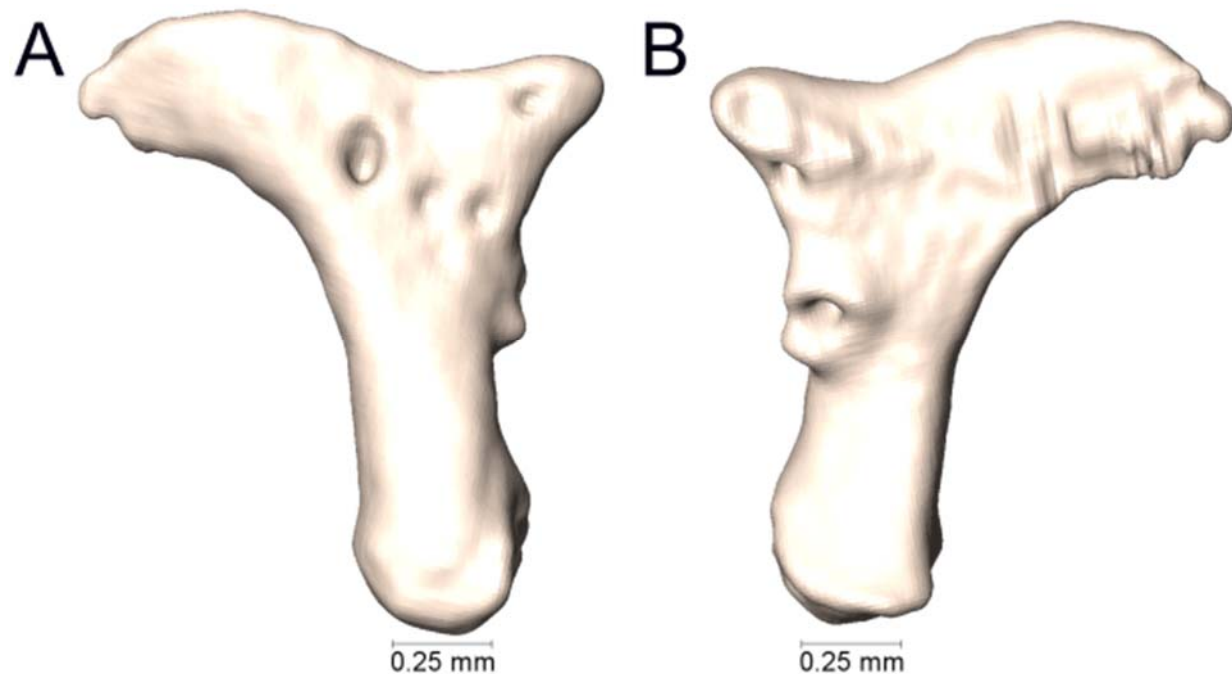
Supplemental Figure 2.46. Lateral and medial views (A-B, respectively) of the left quadrate of *Micrurus filiformis* (UTA R-3423).



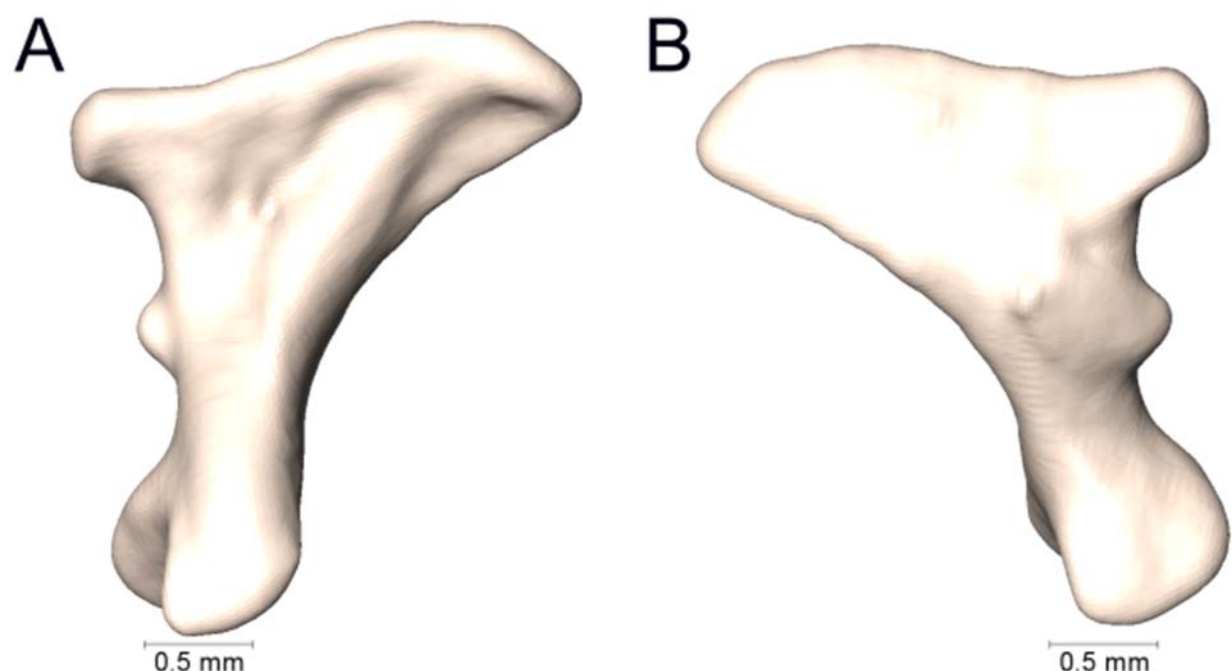
Supplemental Figure 2.47. Lateral and medial views (A-B, respectively) of the left quadrate of *Micrurus filiformis* (UTA R-65836).



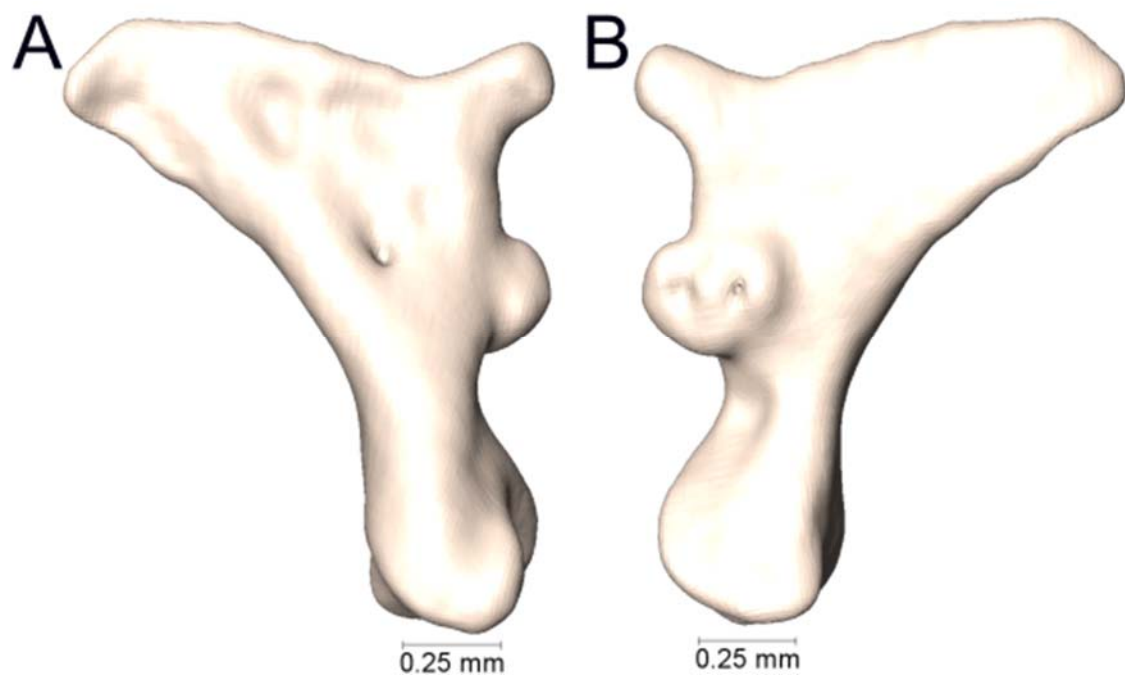
Supplemental Figure 2.48. Lateral and medial views (A-B, respectively) of the left quadrate of *Micrurus fulvius* (UTA R-61632).



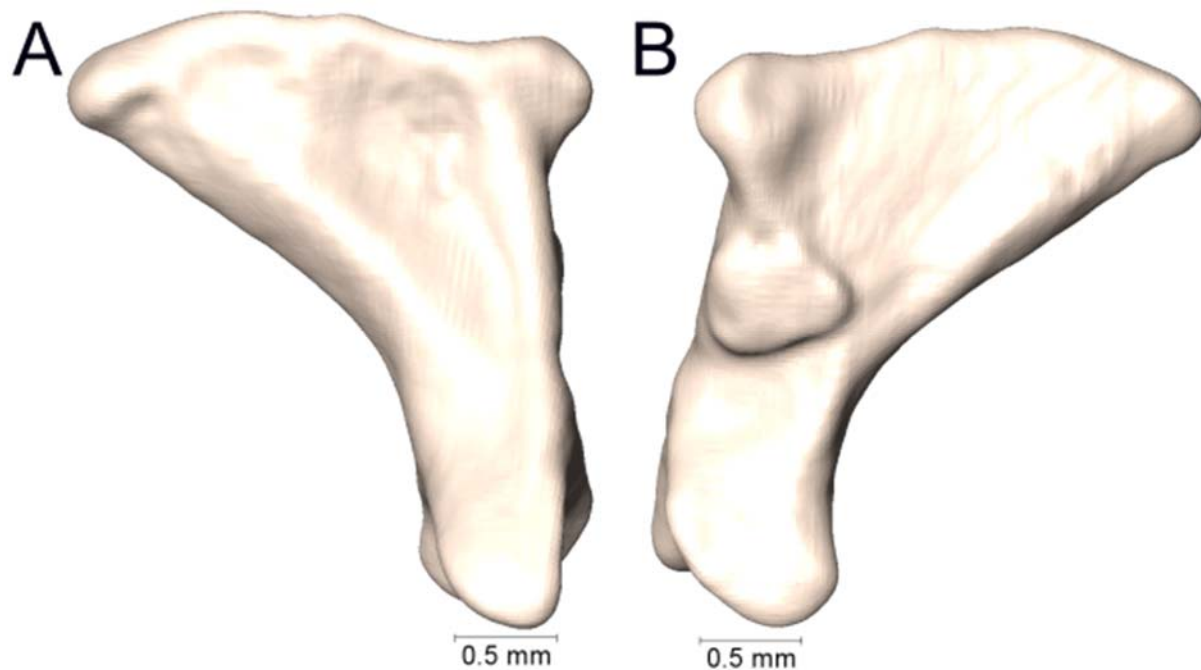
Supplemental Figure 2.49. Lateral and medial views (A-B, respectively) of the left quadrate of *Micrurus helleri* (UTA R-38005).



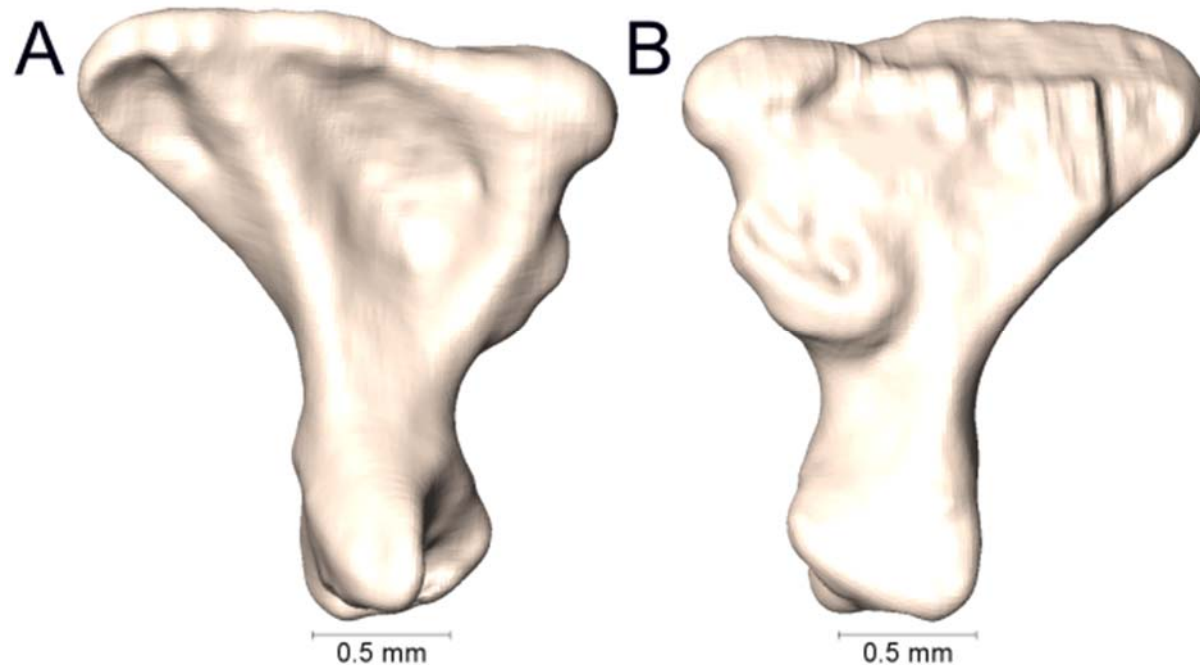
Supplemental Figure 2.50. Lateral and medial views (A-B, respectively) of the right quadrate of *Micrurus helleri* (UTA R-55977).



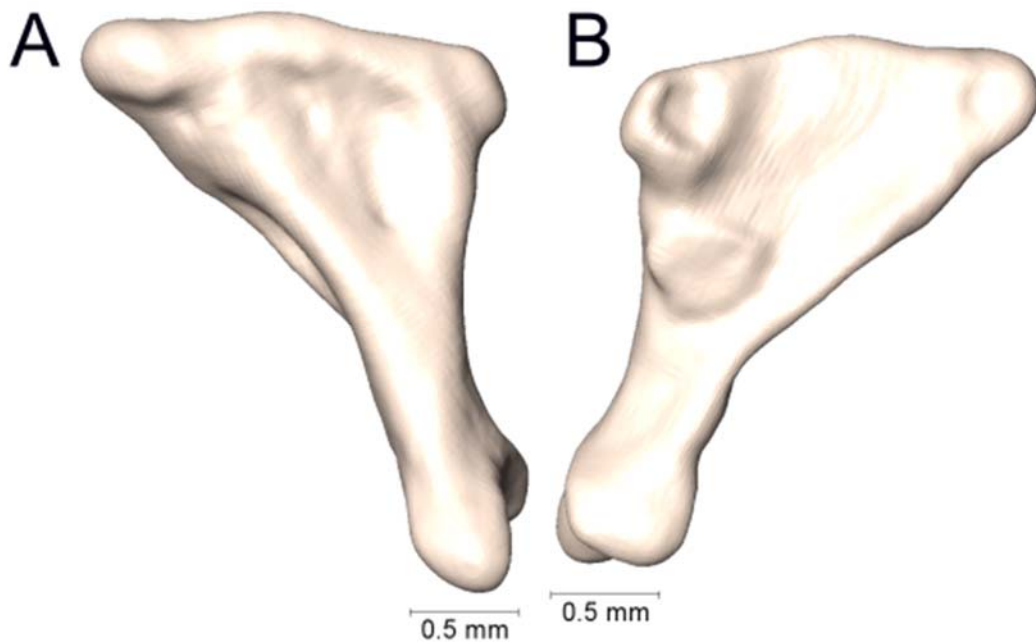
Supplemental Figure 2.51. Lateral and medial views (A-B, respectively) of the left quadrate of *Micrurus helleri* (UTA R-65841).



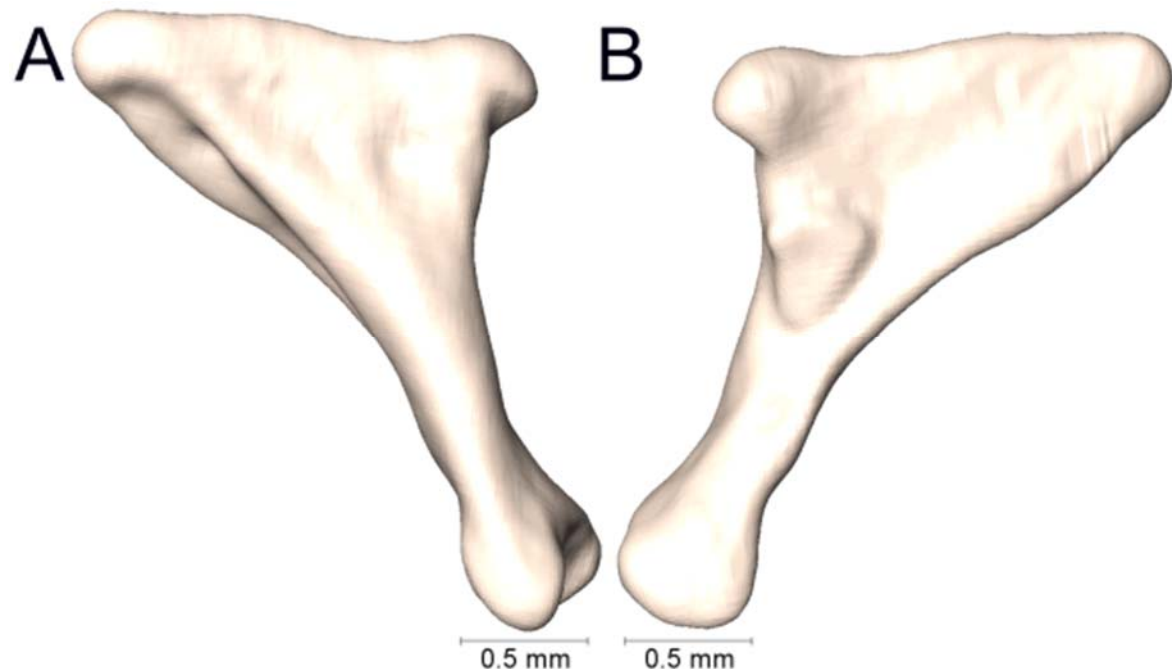
Supplemental Figure 2.52. Lateral and medial views (A-B, respectively) of the left quadrate of *Micrurus hemprichii* (UTA R-9683).



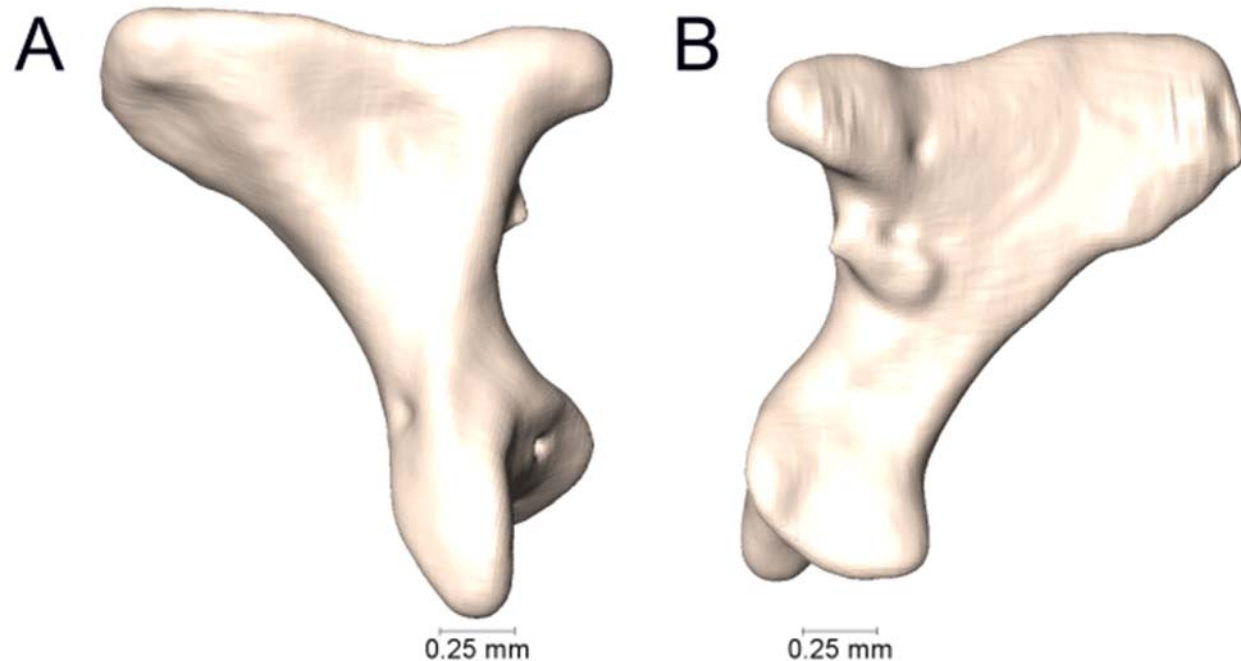
Supplemental Figure 2.53. Lateral and medial views (A-B, respectively) of the left quadrate of *Micrurus hemprichii* (UTA R-29997).



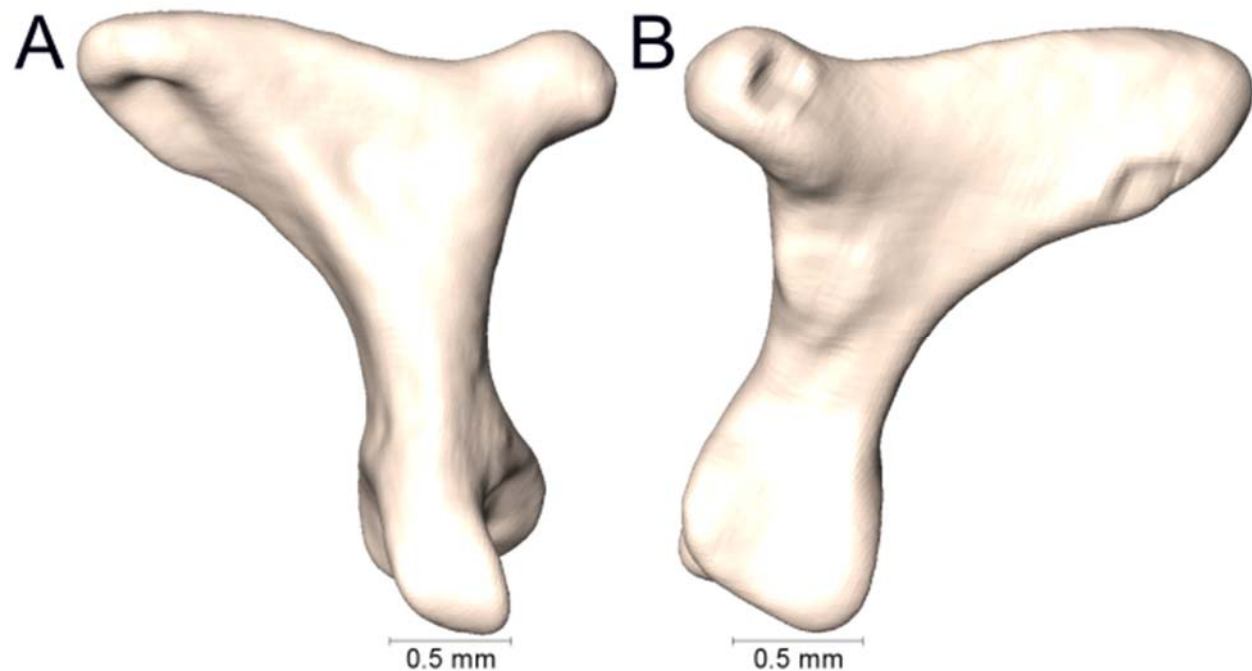
Supplemental Figure 2.54. Lateral and medial views (A-B, respectively) of the left quadrate of *Micrurus isozonus* (UTA R-3951).



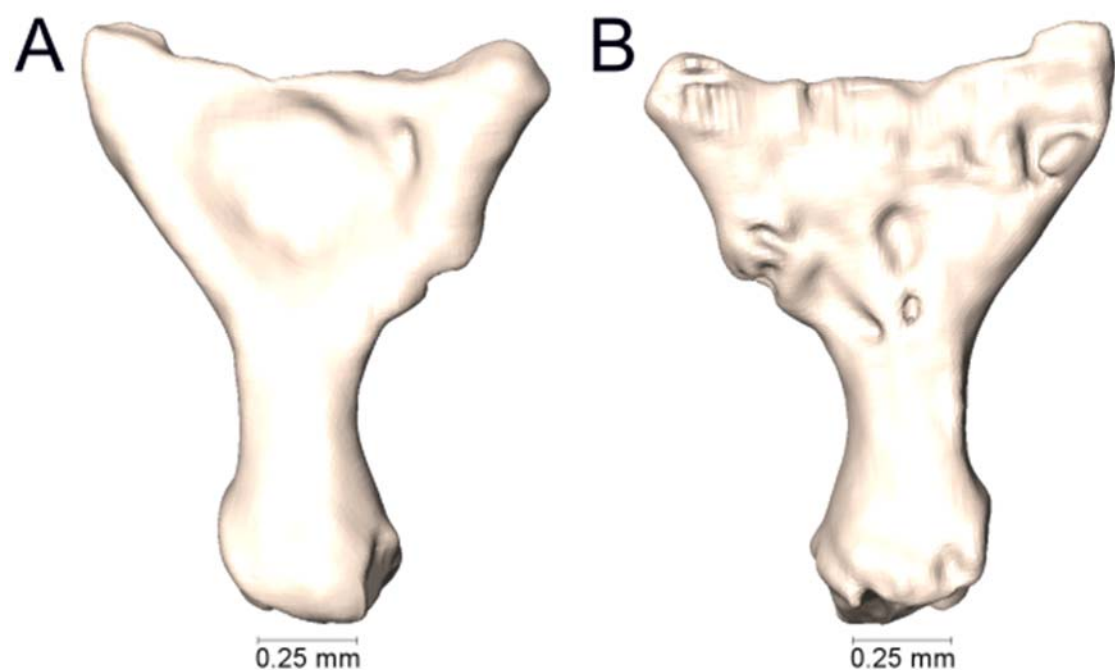
Supplemental Figure 2.55. Lateral and medial views (A-B, respectively) of the left quadrate of *Micrurus isozonus* (UTA R-22589).



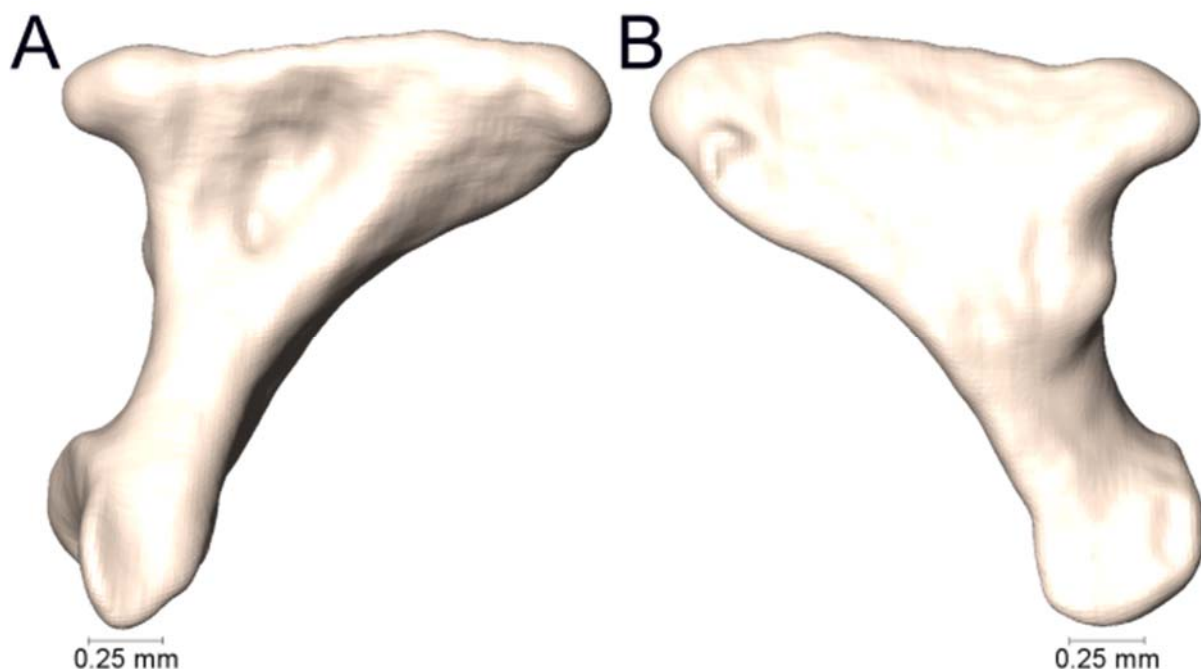
Supplemental Figure 2.56. Lateral and medial views (A-B, respectively) of the left quadrate of *Micrurus laticollaris* (UTA R-52559).



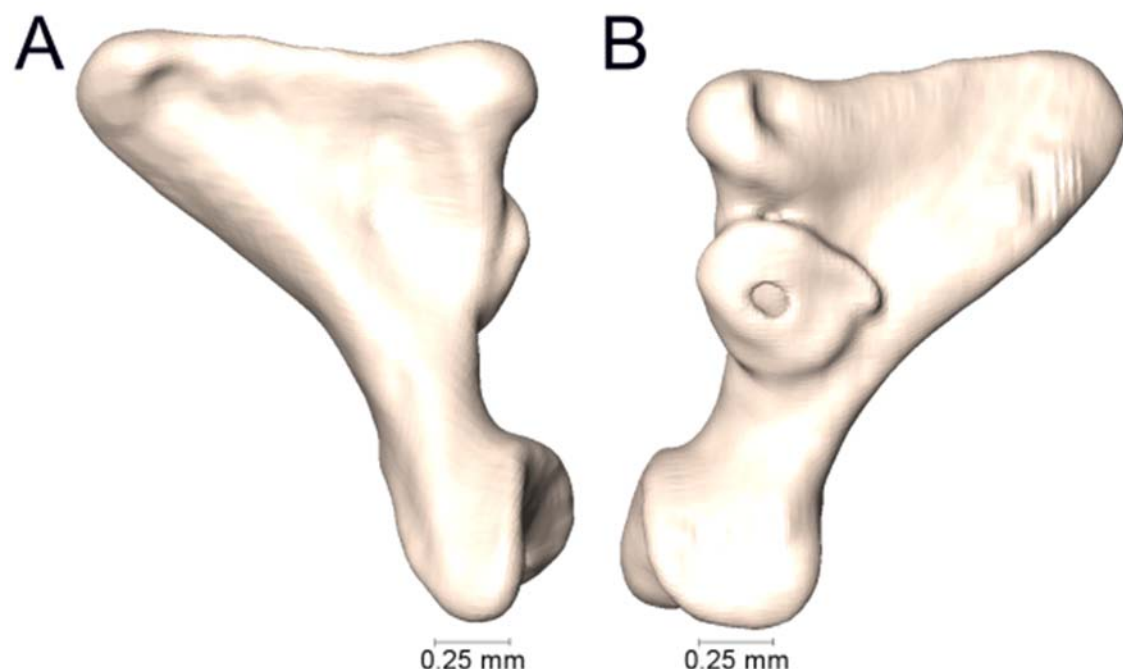
Supplemental Figure 2.57. Lateral and medial views (A-B, respectively) of the left quadrate of *Micrurus laticollaris* (UTA R-57562).



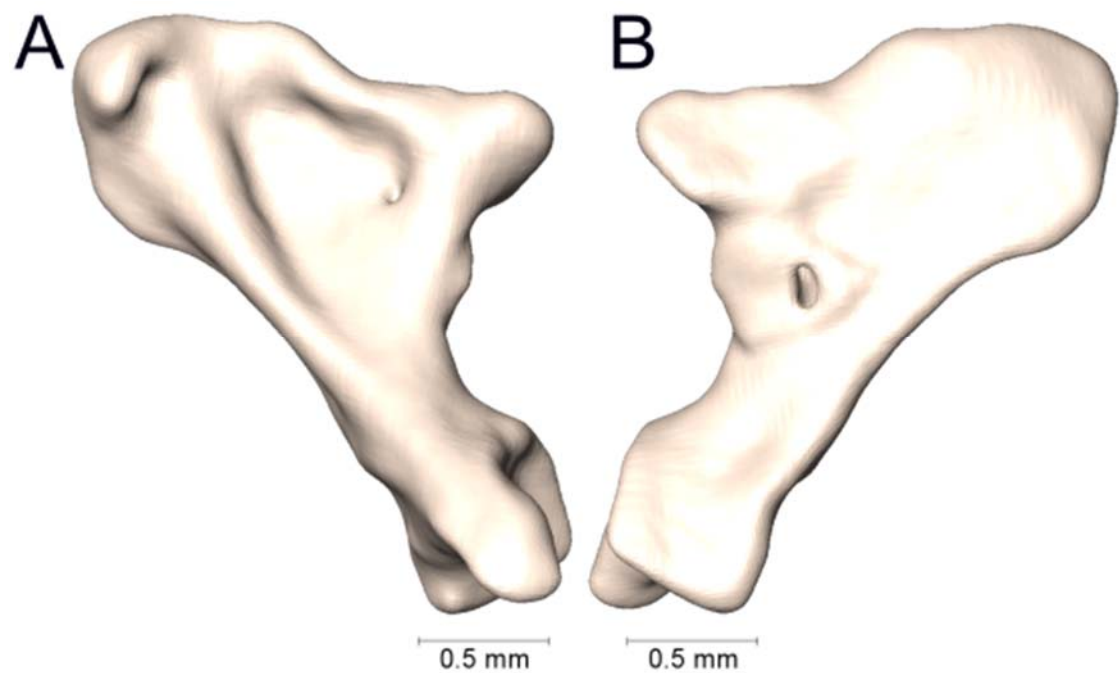
Supplemental Figure 2.58. Lateral and medial views (A-B, respectively) of the left quadrate of *Micrurus lemniscatus cf. helleri* (UTA R-34563).



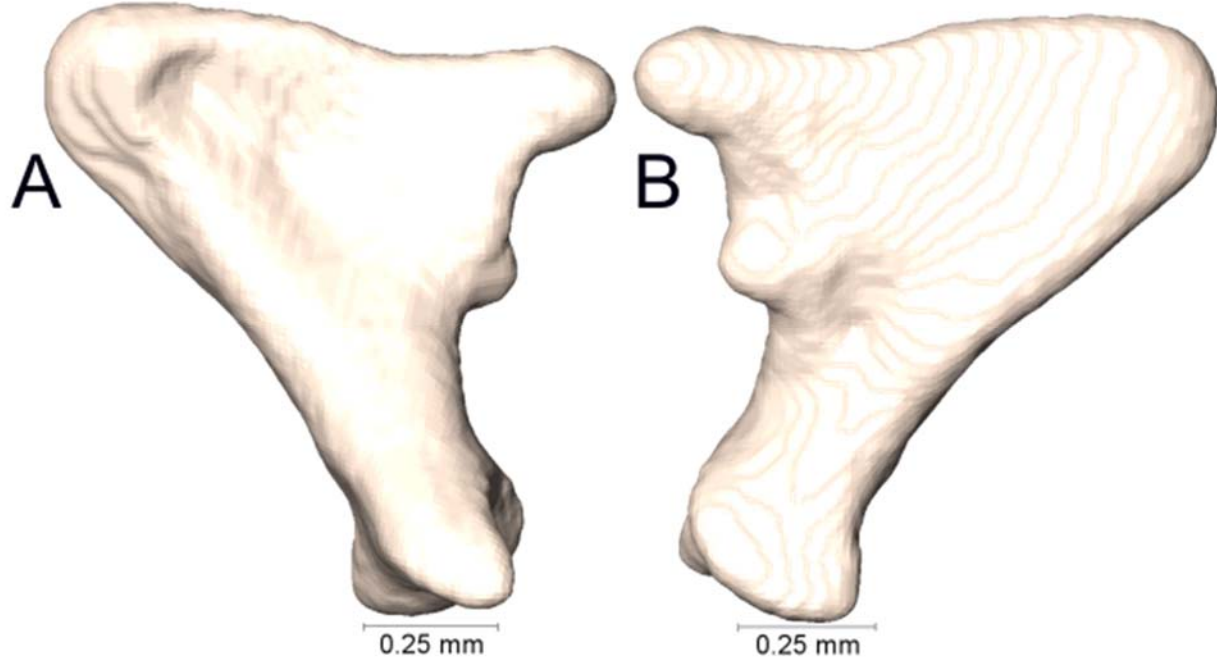
Supplemental Figure 2.59. Lateral and medial views (A-B, respectively) of the right quadrate of *Micrurus lemniscatus* cf. *helleri* (UTA R-65803).



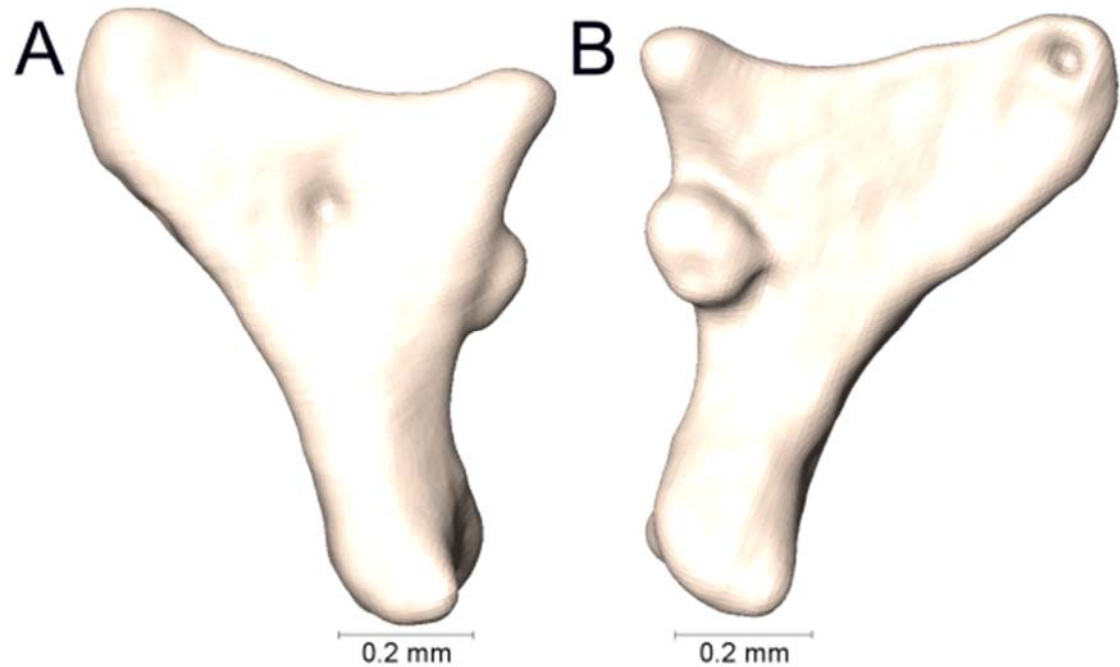
Supplemental Figure 2.60. Lateral and medial views (A-B, respectively) of the left quadrate of *Micrurus limbatus* (UTA R-64852).



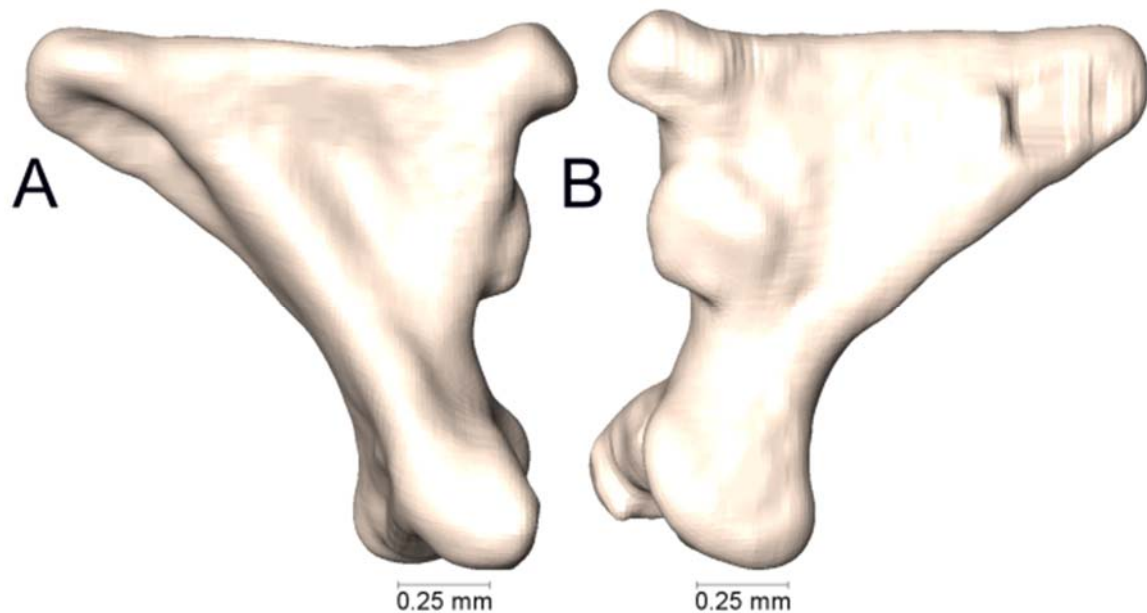
Supplemental Figure 2.61. Lateral and medial views (A-B, respectively) of the left quadrate of *Micrurus limbatus* (UTA R-64899).



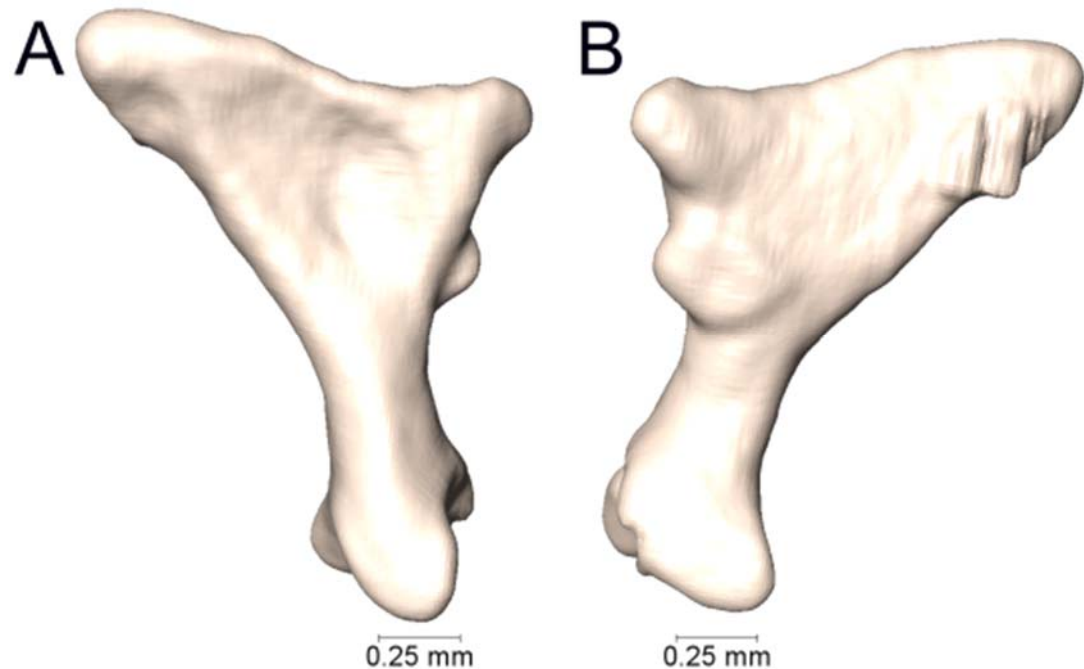
Supplemental Figure 2.62. Lateral and medial views (A-B, respectively) of the left quadrate of *Micrurus melanotus* (AMNH 35934).



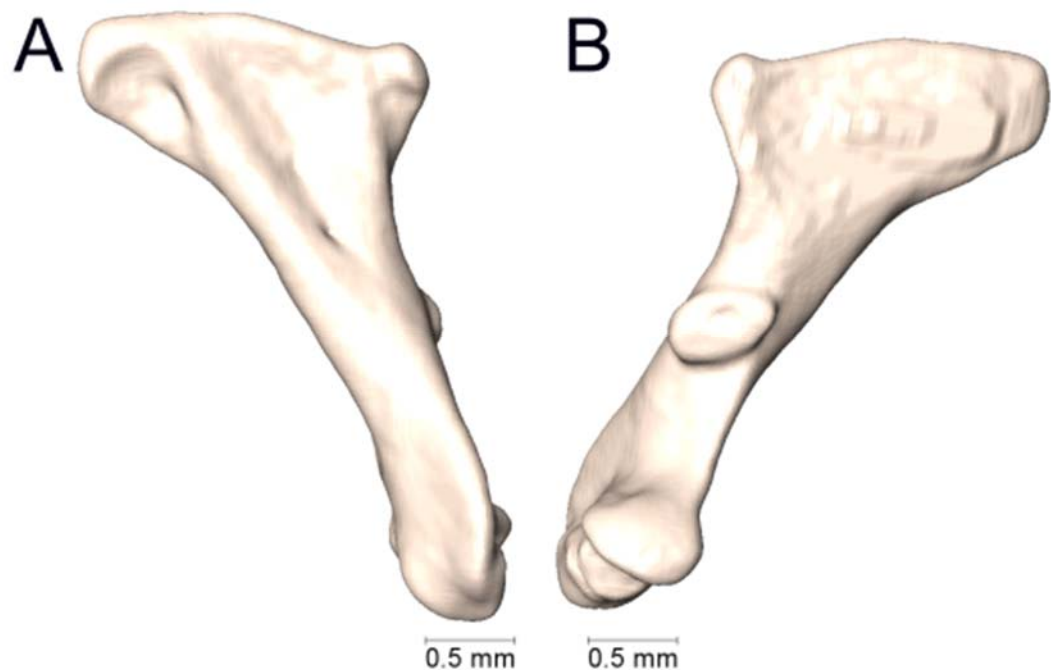
Supplemental Figure 2.63. Lateral and medial views (A-B, respectively) of the left quadrate of *Micrurus melanotus* (UTA R-22582).



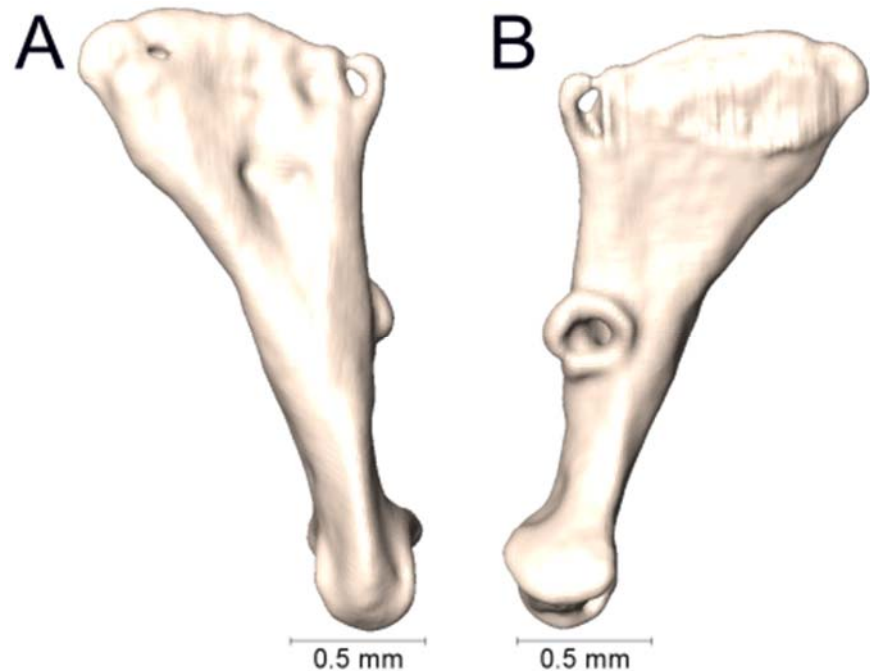
Supplemental Figure 2.64. Lateral and medial views (A-B, respectively) of the left quadrate of *Micrurus mipartitus* (UTA R-54187).



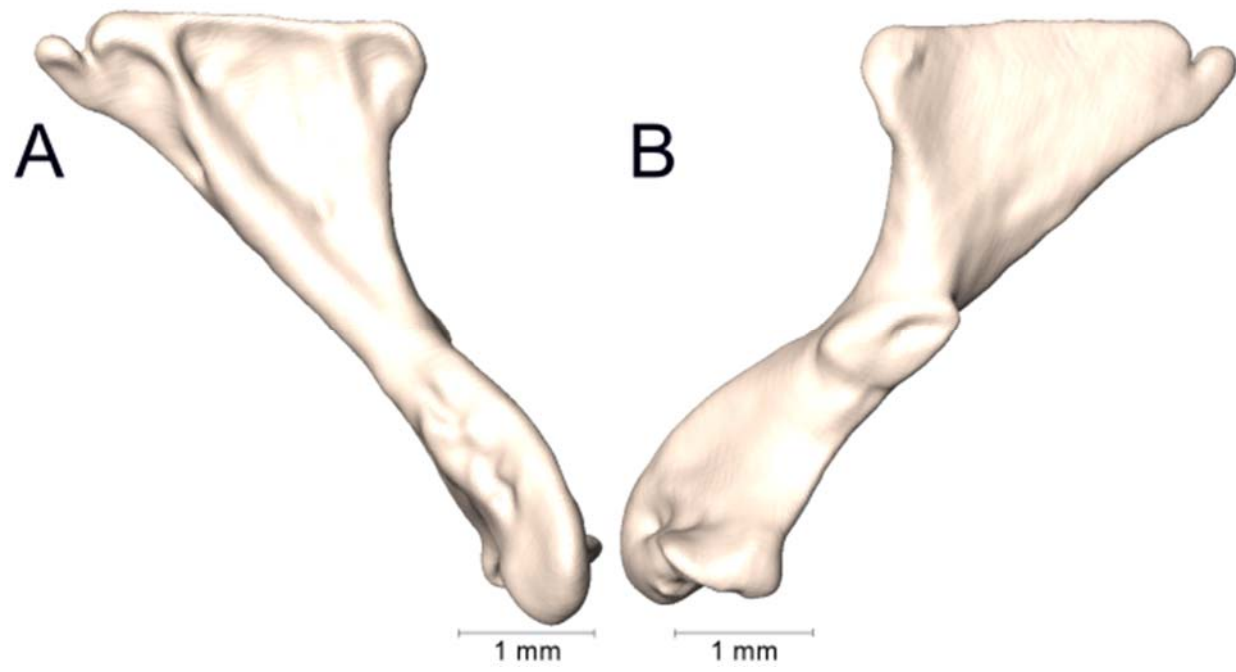
Supplemental Figure 2.65. Lateral and medial views (A-B, respectively) of the left quadrate of *Micrurus mosquitensis* (UTA R-12919).



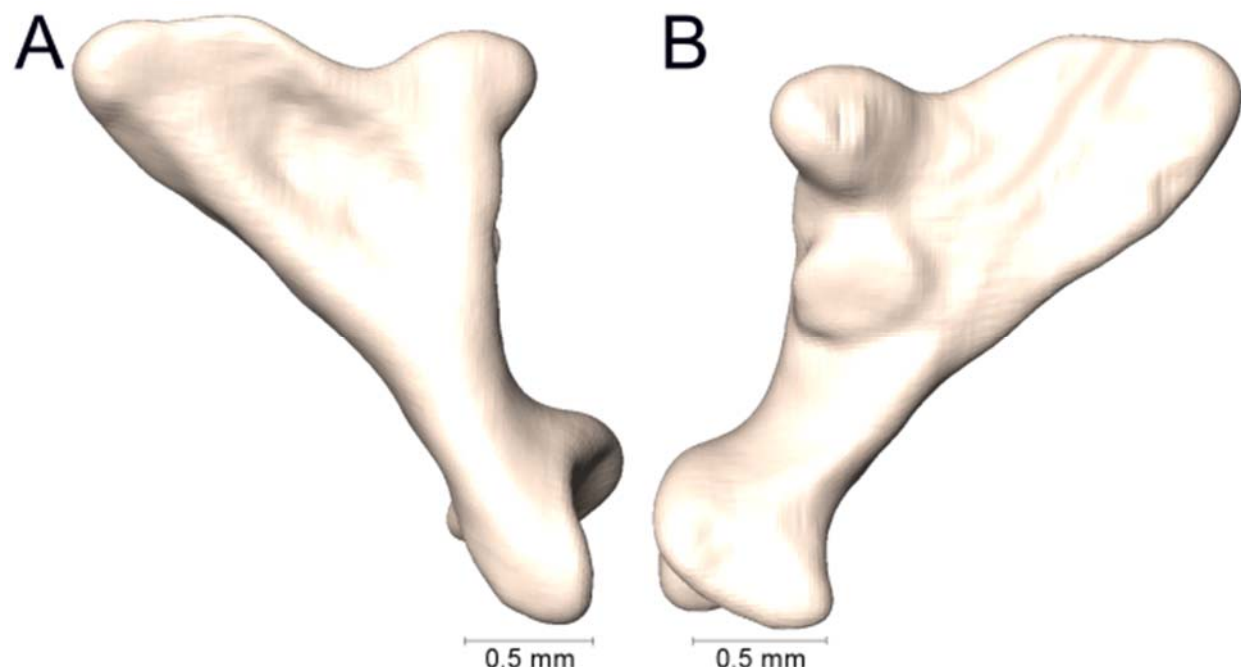
Supplemental Figure 2.66. Lateral and medial views (A-B, respectively) of the left quadrate of *Micrurus nattereri* (UTA R-54175).



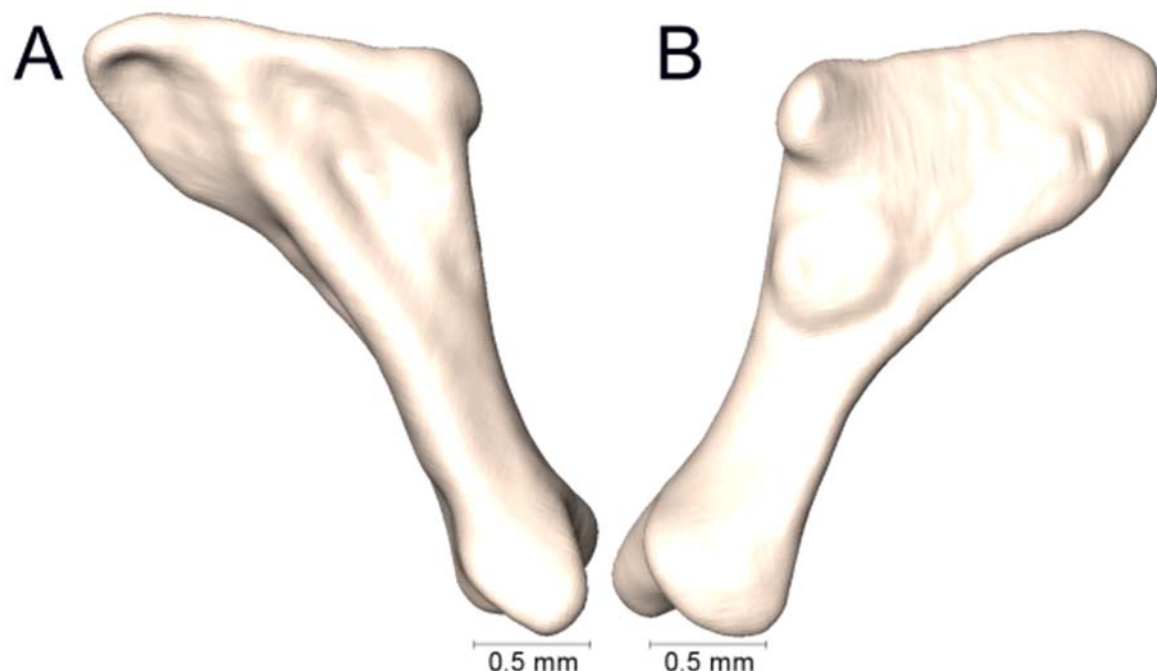
Supplemental Figure 2.67. Lateral and medial views (A-B, respectively) of the left quadrate of *Micrurus nattereri* (UTA R-55086).



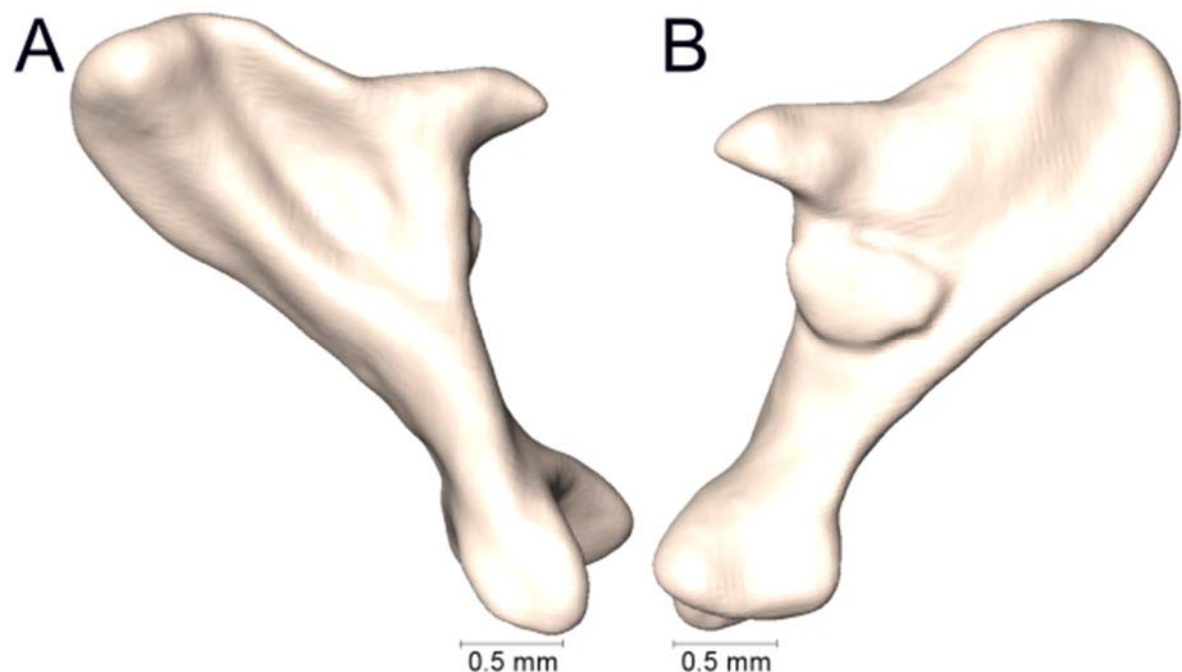
Supplemental Figure 2.68. Lateral and medial views (A-B, respectively) of the left quadrate of *Micrurus nattereri* (UTA R-60727).



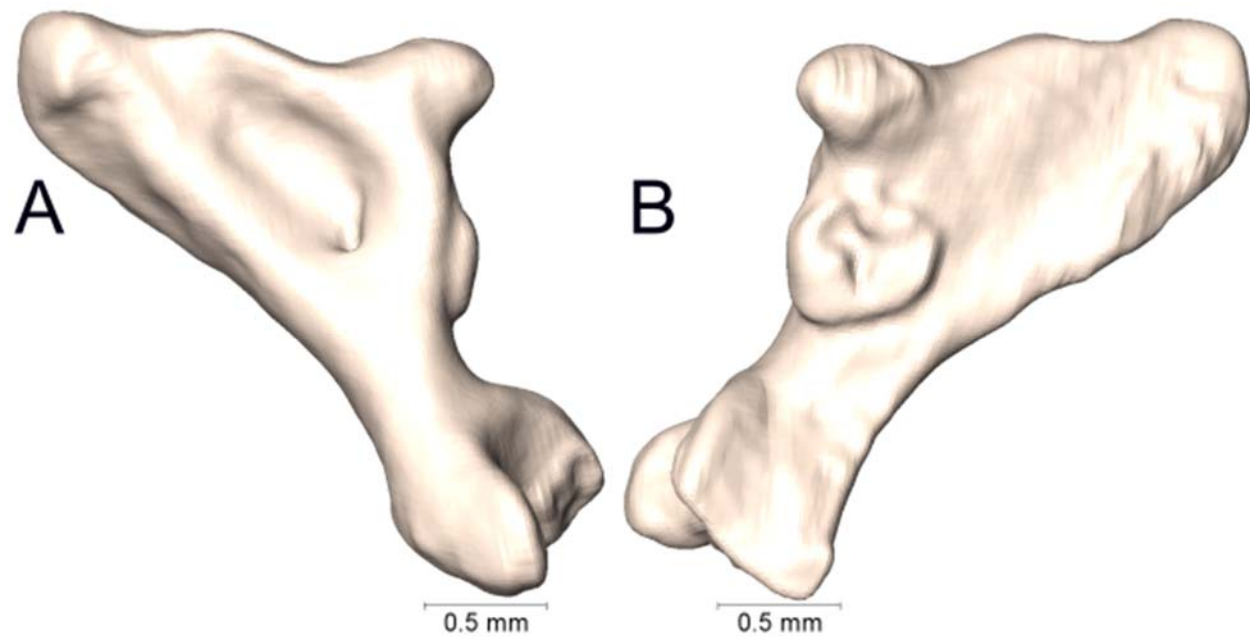
Supplemental Figure 2.69. Lateral and medial views (A-B, respectively) of the left quadrate of *Micrurus nigrocinctus zunilensis* (UTA R-64858).



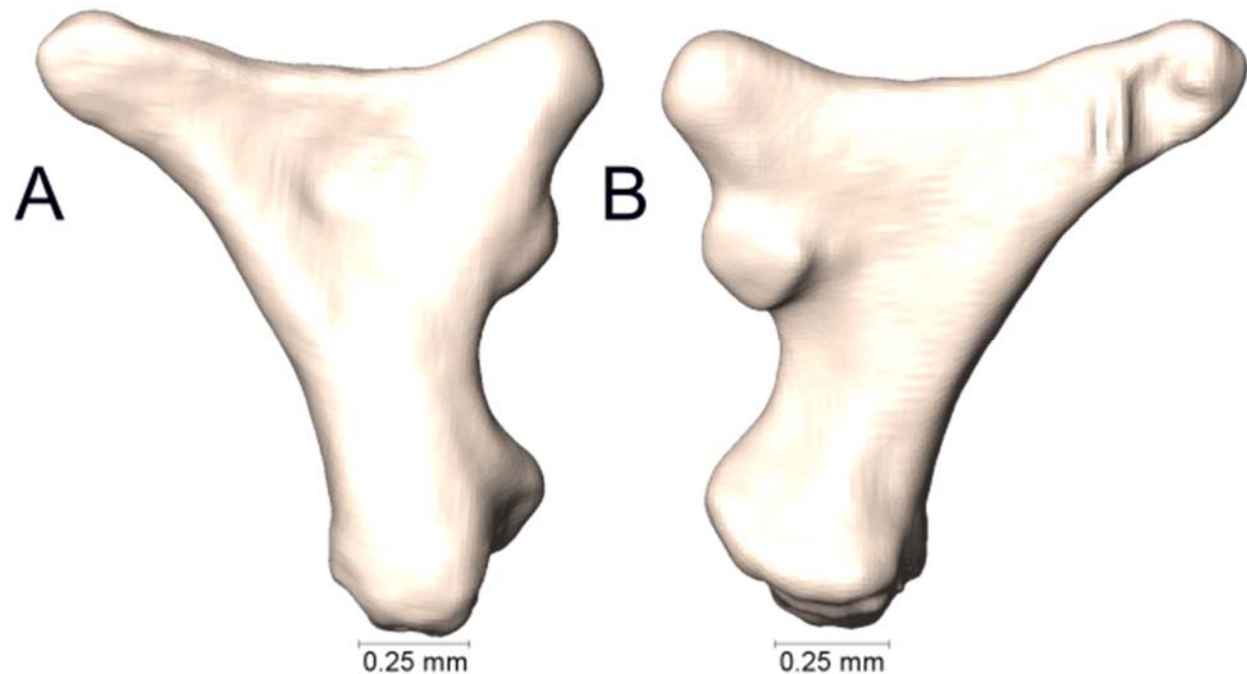
Supplemental Figure 2.70. Lateral and medial views (A-B, respectively) of the left quadrate of *Micrurus obscurus* (UTA R-3840).



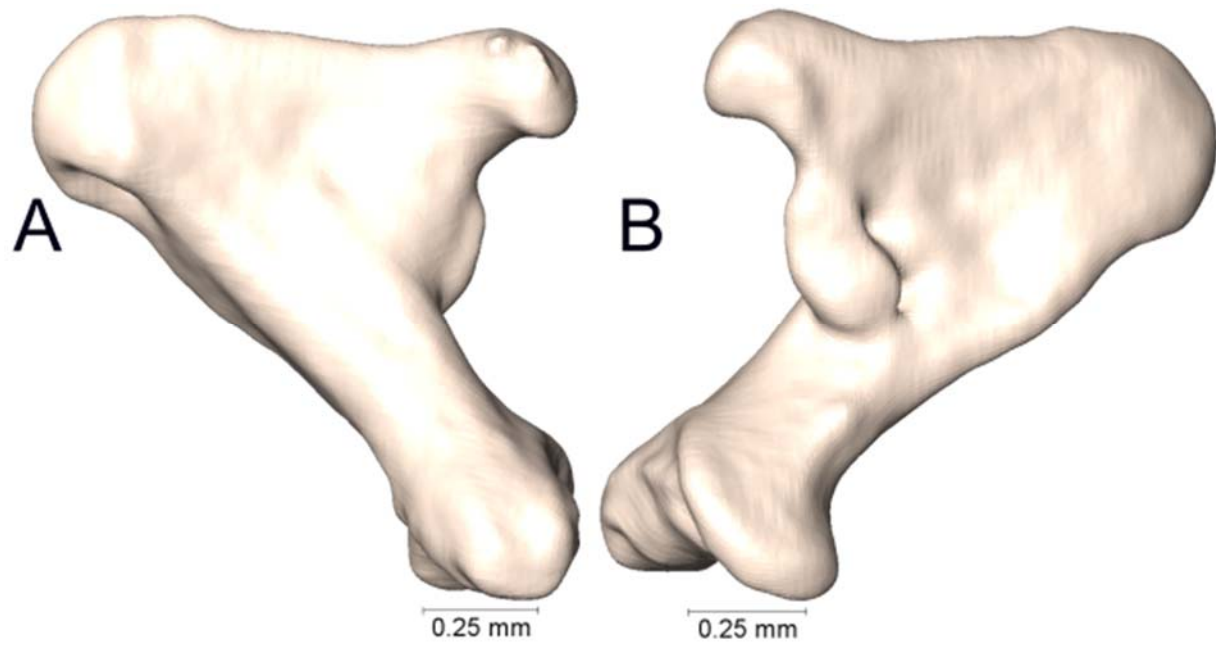
Supplemental Figure 2.71. Lateral and medial views (A-B, respectively) of the left quadrate of *Micrurus oliveri* (UTA R-64893).



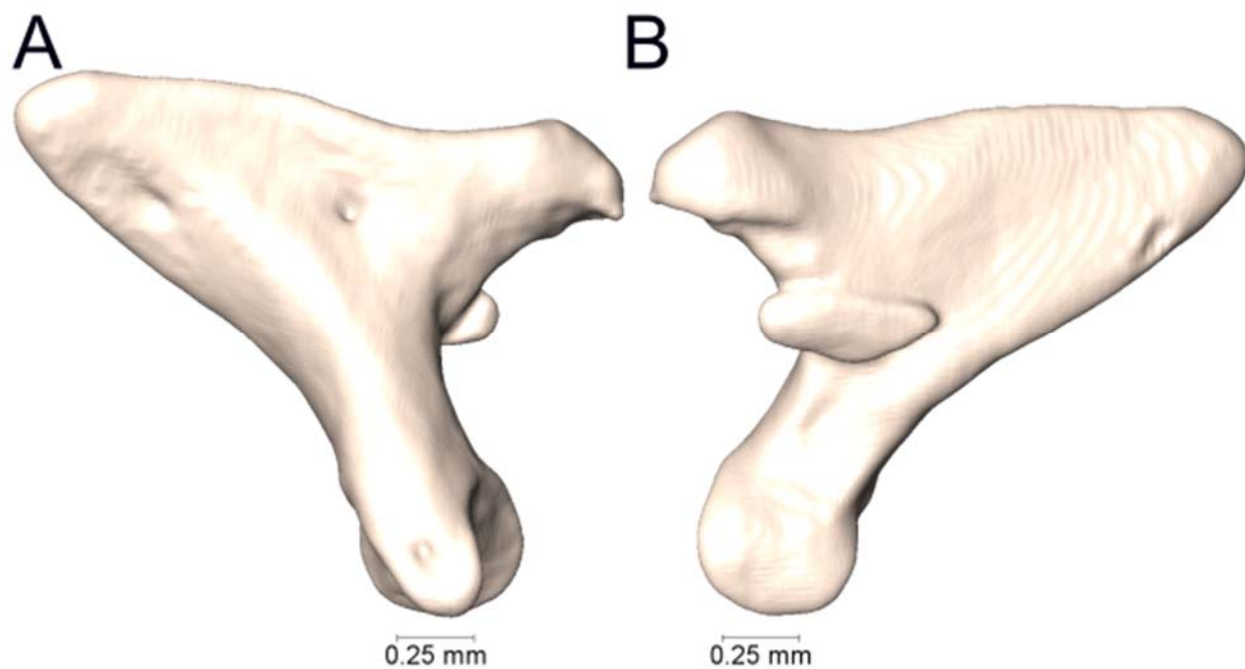
Supplemental Figure 2.72. Lateral and medial views (A-B, respectively) of the left quadrate of *Micrurus ornatissimus* (UTA R-60724).



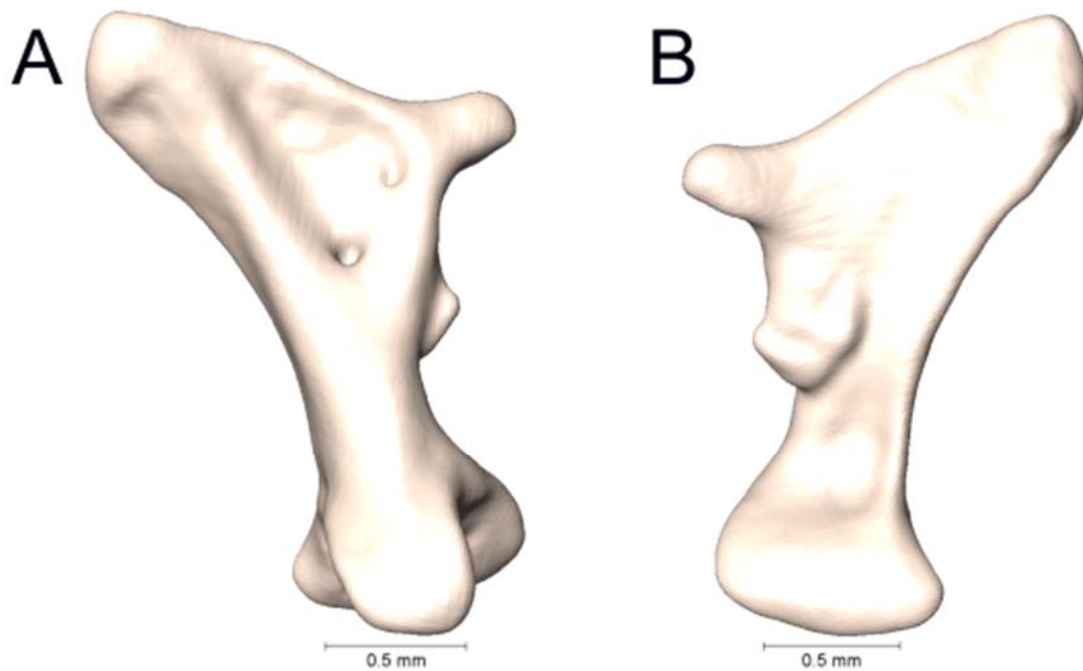
Supplemental Figure 2.73. Lateral and medial views (A-B, respectively) of the left quadrate of *Micrurus pyrrhocryptus* (UTA R-51404).



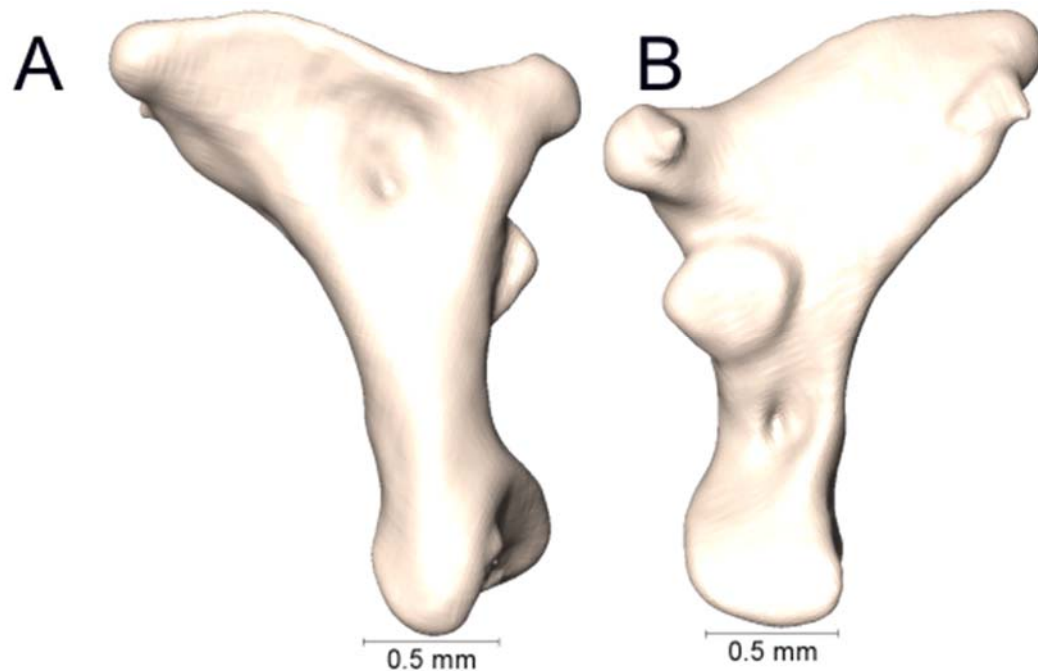
Supplemental Figure 2.74. Lateral and medial views (A-B, respectively) of the left quadrate of *Micrurus renjifoi* (UTA R-3490).



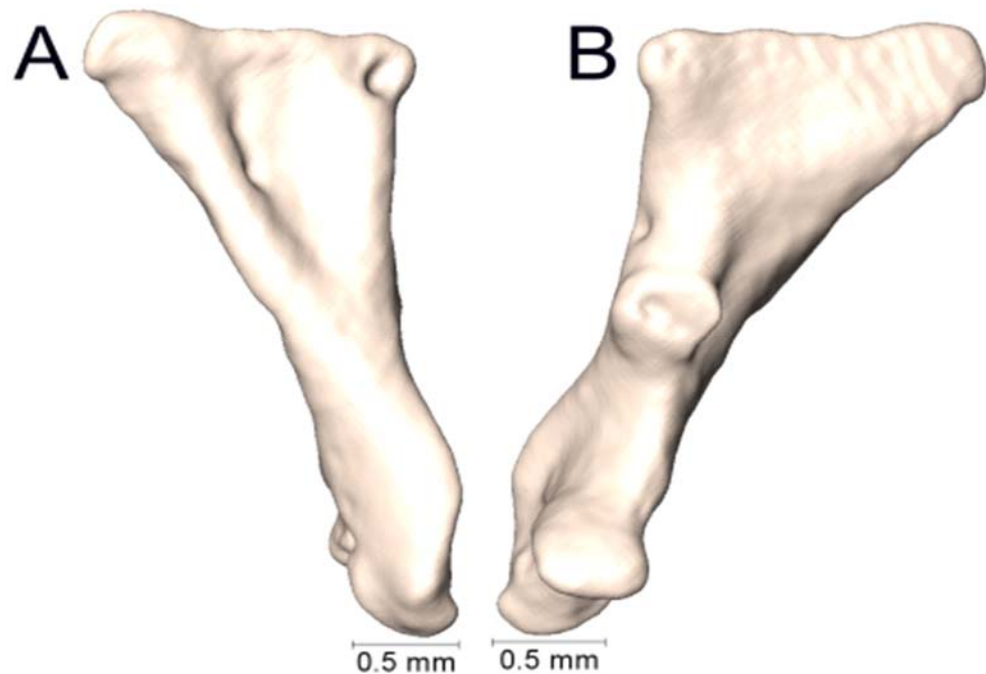
Supplemental Figure 2.75. Lateral and medial views (A-B, respectively) of the left quadrate of *Micrurus serranus* (UTA R-34561).



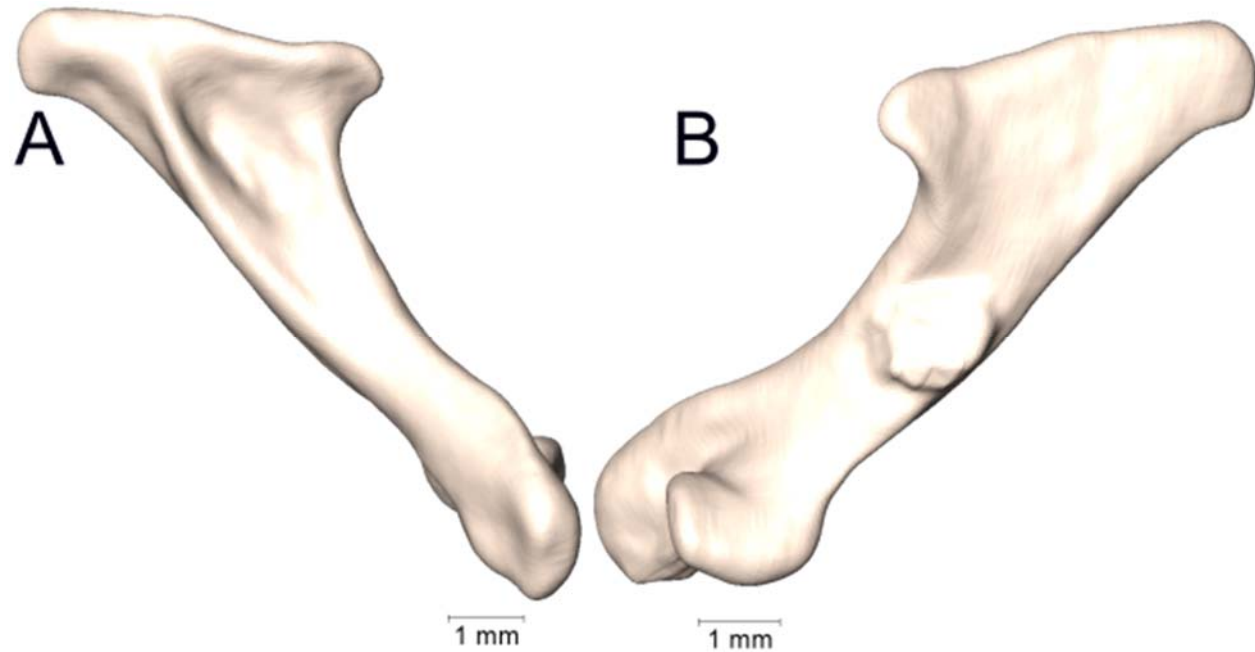
Supplemental Figure 2.76. Lateral and medial views (A-B, respectively) of the left quadrate of *Micrurus steindachneri* (AMNH 28846).



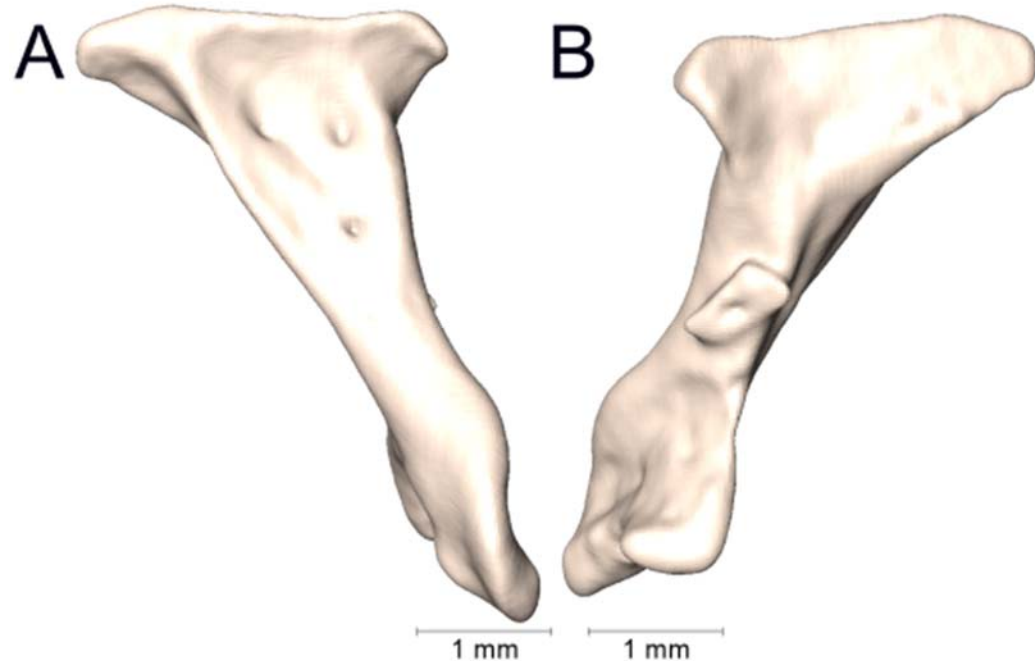
Supplemental Figure 2.77. Lateral and medial views (A-B, respectively) of the left quadrate of *Micrurus steindachneri* (AMNH 35819).



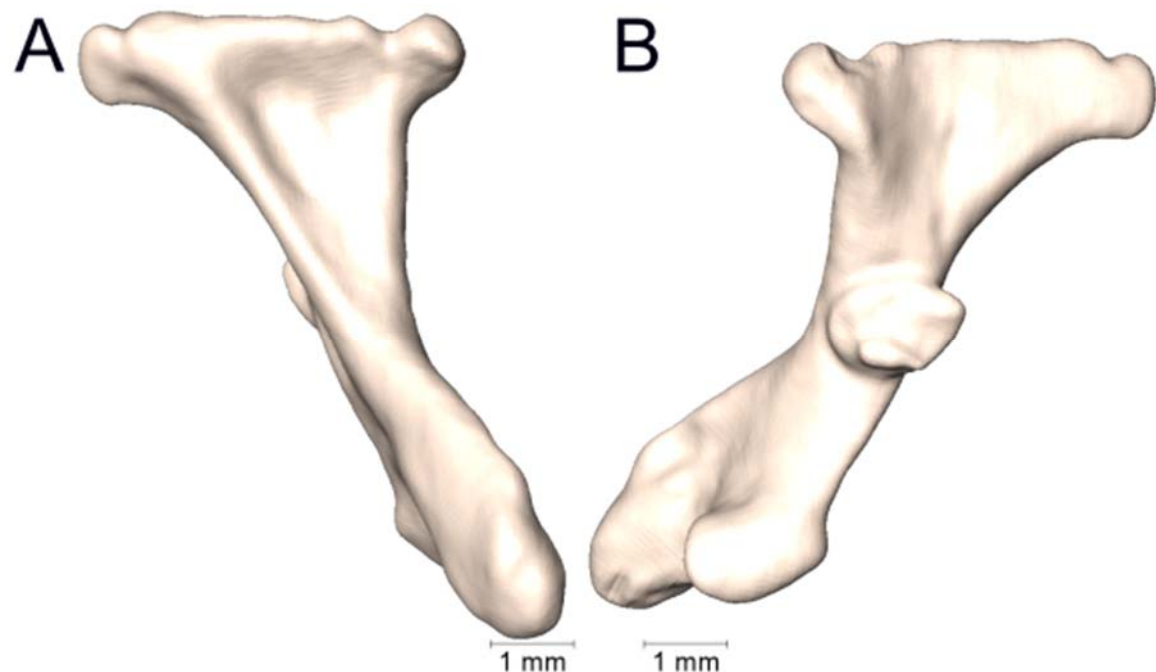
Supplemental Figure 2.78. Lateral and medial views (A-B, respectively) of the left quadrate of *Micrurus surinamensis* (UTA R-5849).



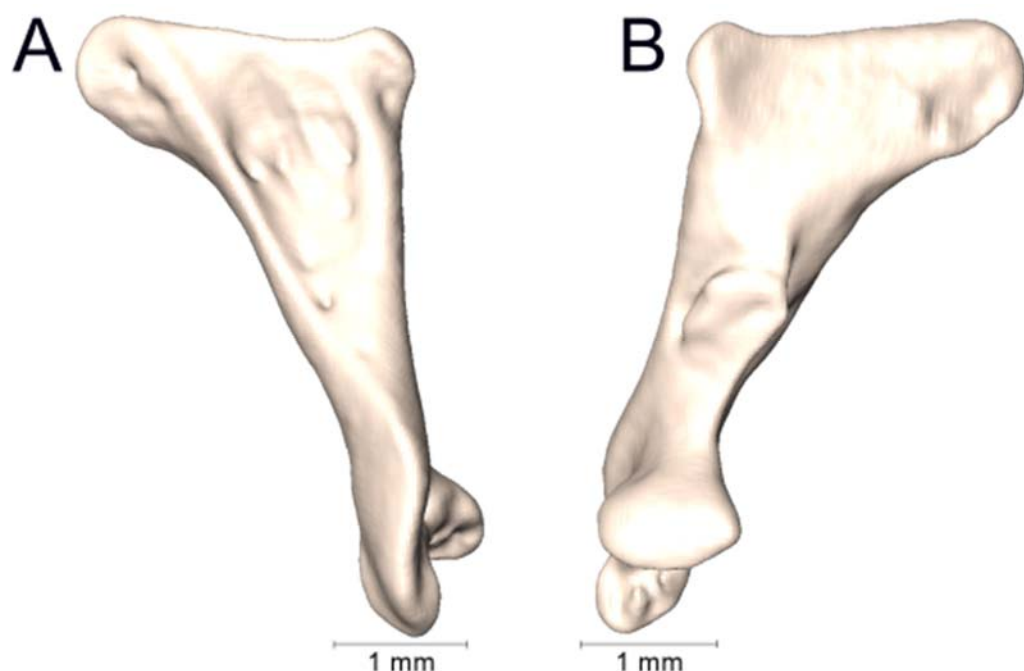
Supplemental Figure 2.79. Lateral and medial views (A-B, respectively) of the left quadrate of *Micrurus surinamensis* (UTA R-15679).



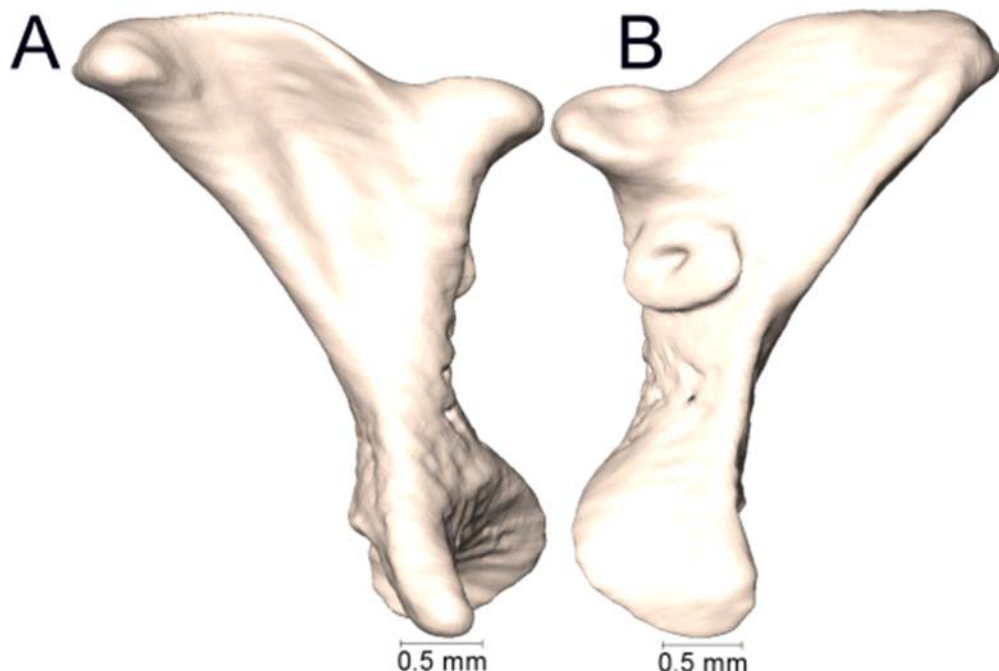
Supplemental Figure 2.80. Lateral and medial views (A-B, respectively) of the left quadrate of *Micrurus surinamensis* (UTA R-50173).



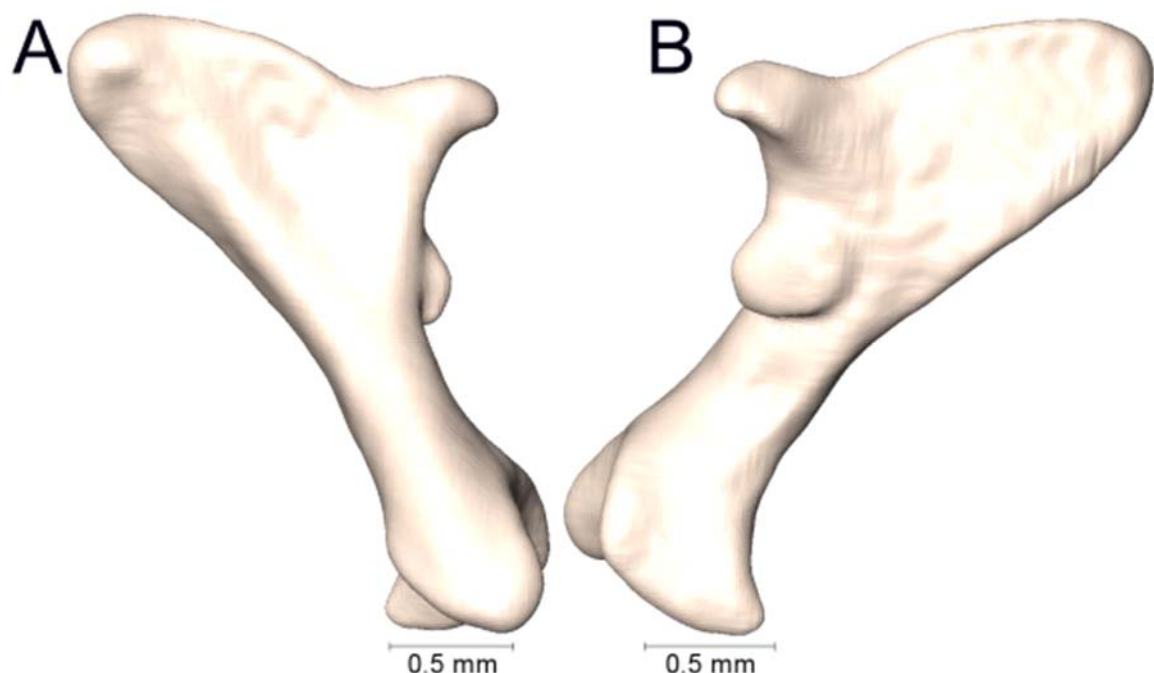
Supplemental Figure 2.81. Lateral and medial views (A-B, respectively) of the left quadrate of *Micrurus surinamensis* (UTA R-54378).



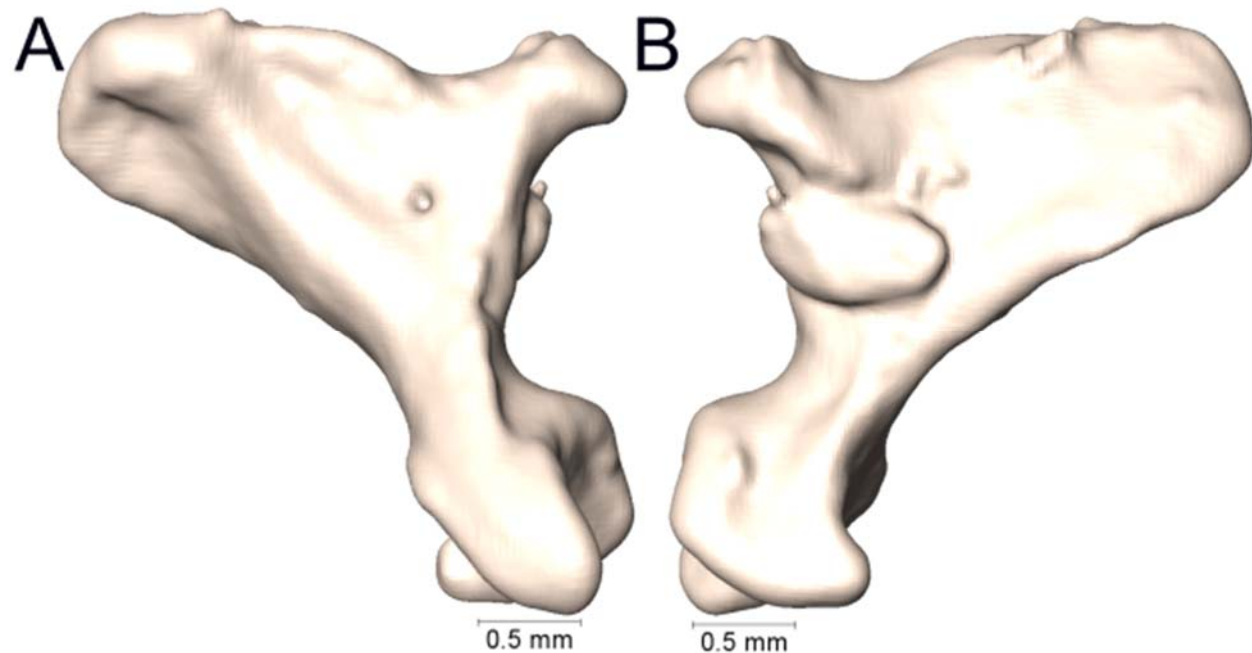
Supplemental Figure 2.82. Lateral and medial views (A-B, respectively) of the left quadrate of *Micrurus surinamensis* (UTA R-65844).



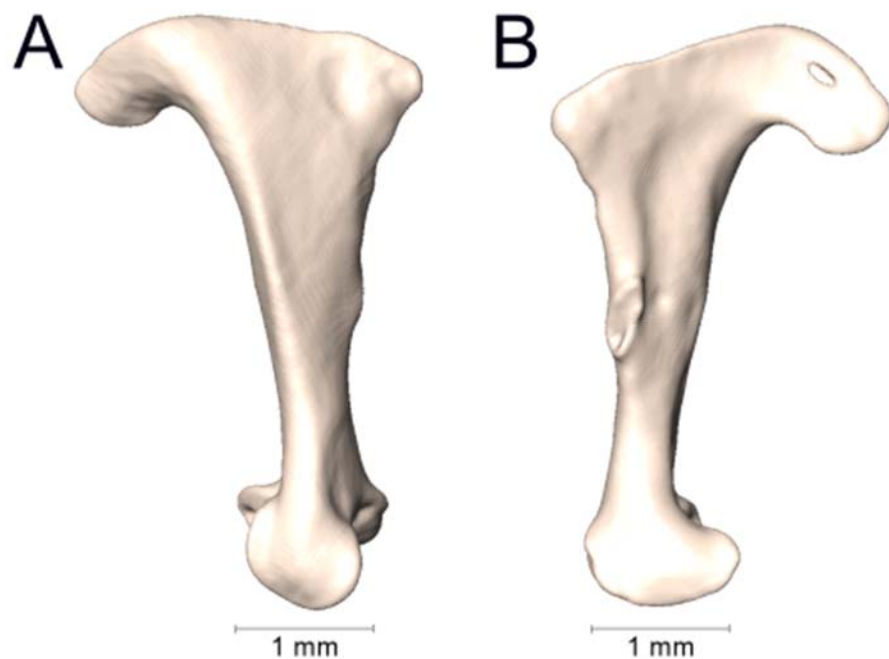
Supplemental Figure 2.83. Lateral and medial views (A-B, respectively) of the left quadrate of *Micrurus tener* (FMNH 39479).



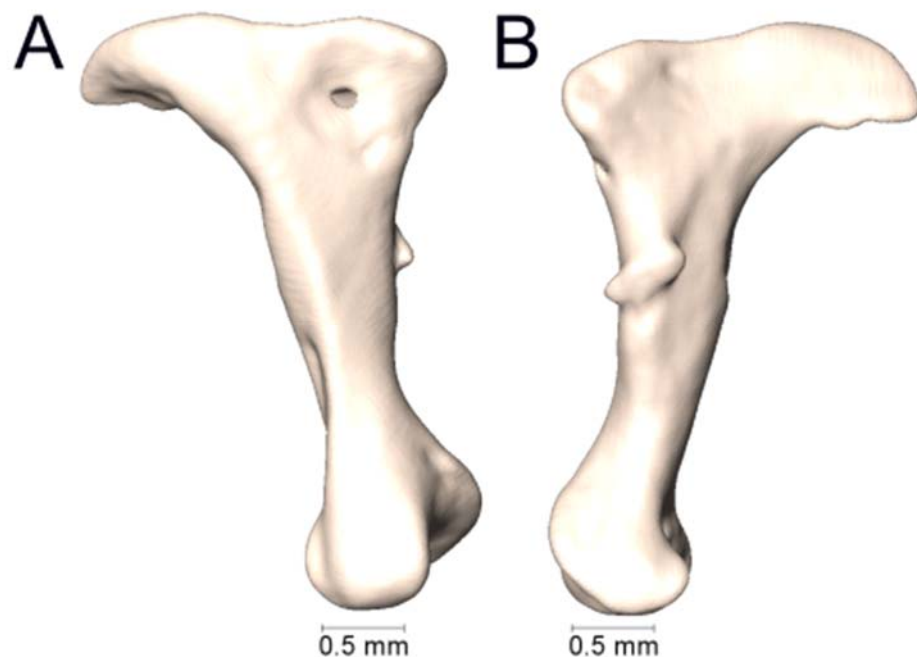
Supplemental Figure 2.84. Lateral and medial views (A-B, respectively) of the left quadrate of *Micrurus tener* (UTA R-63282).



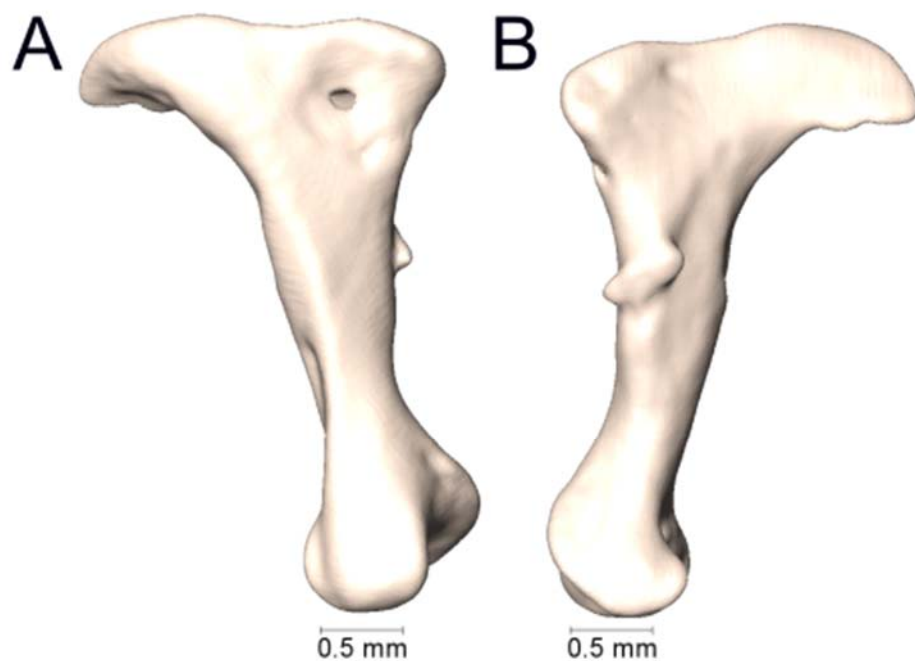
Supplemental Figure 2.85. Lateral and medial views (A-B, respectively) of the left quadrate of *Micrurus* sp. (UTA R-6086).



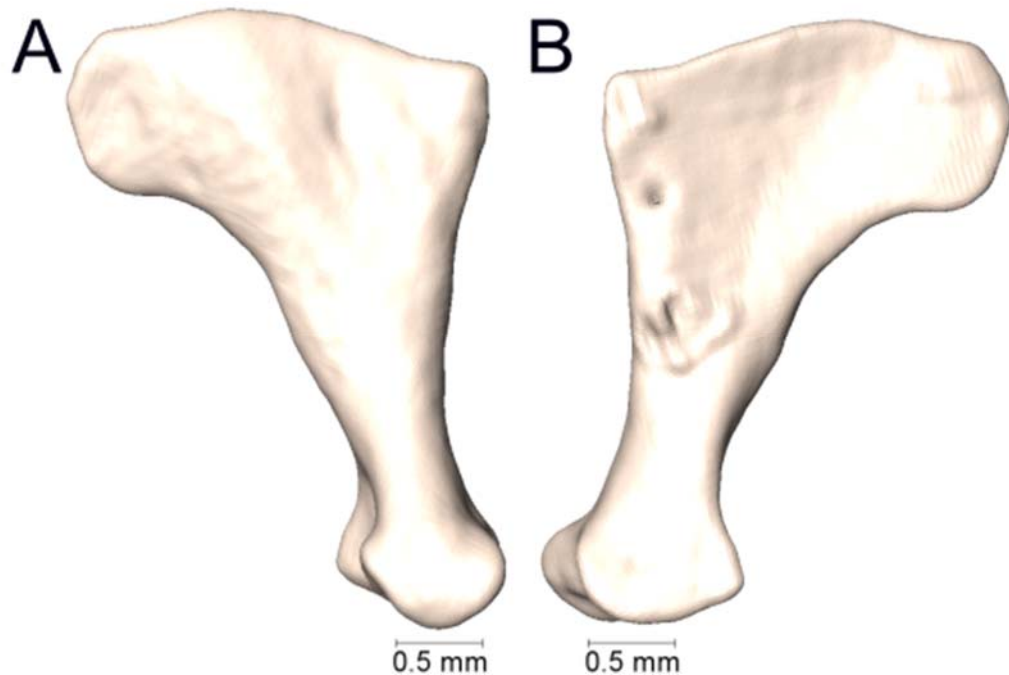
Supplemental Figure 2.86. Lateral and medial views (A-B, respectively) of the left quadrate of *Naja annulata* (UTA R-18199).



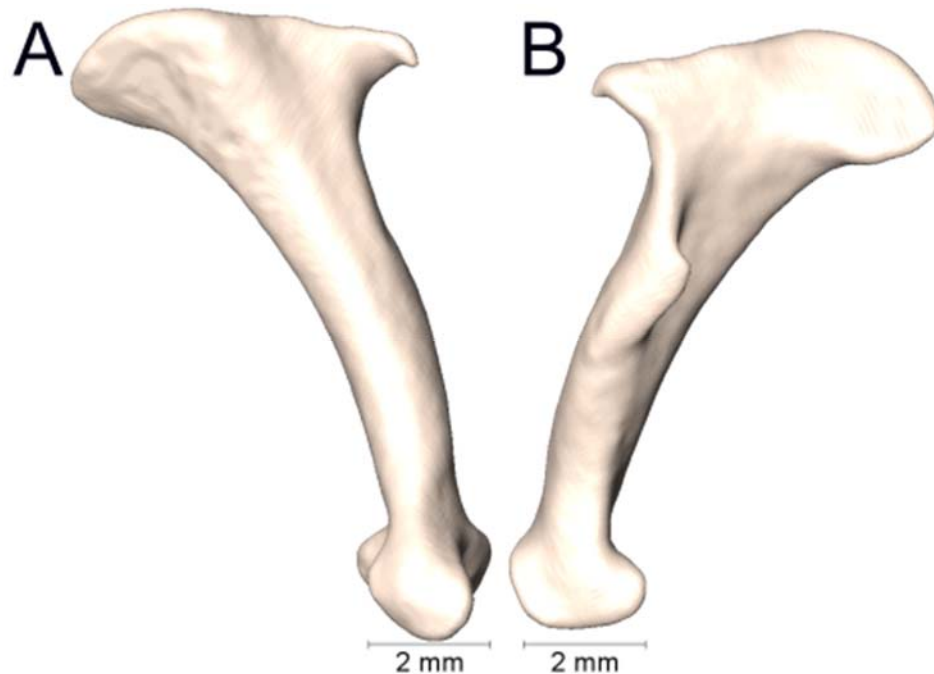
Supplemental Figure 2.87. Lateral and medial views (A-B, respectively) of the left quadrate of *Naja christyi* (UTA R-18200).



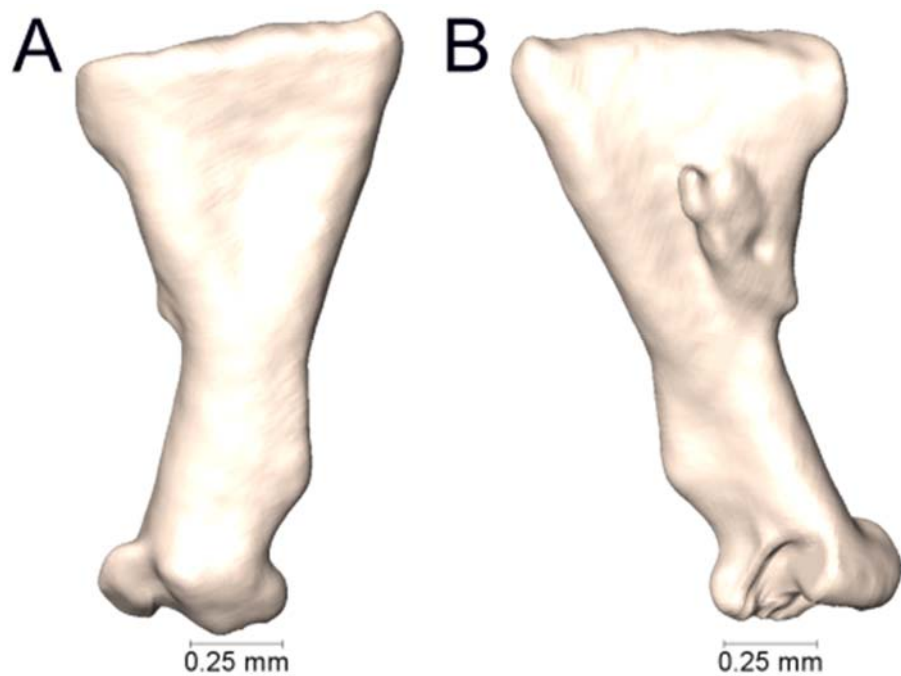
Supplemental Figure 2.88. Lateral and medial views (A-B, respectively) of the left quadrate of *Naja siamensis* (UTA R-16872).



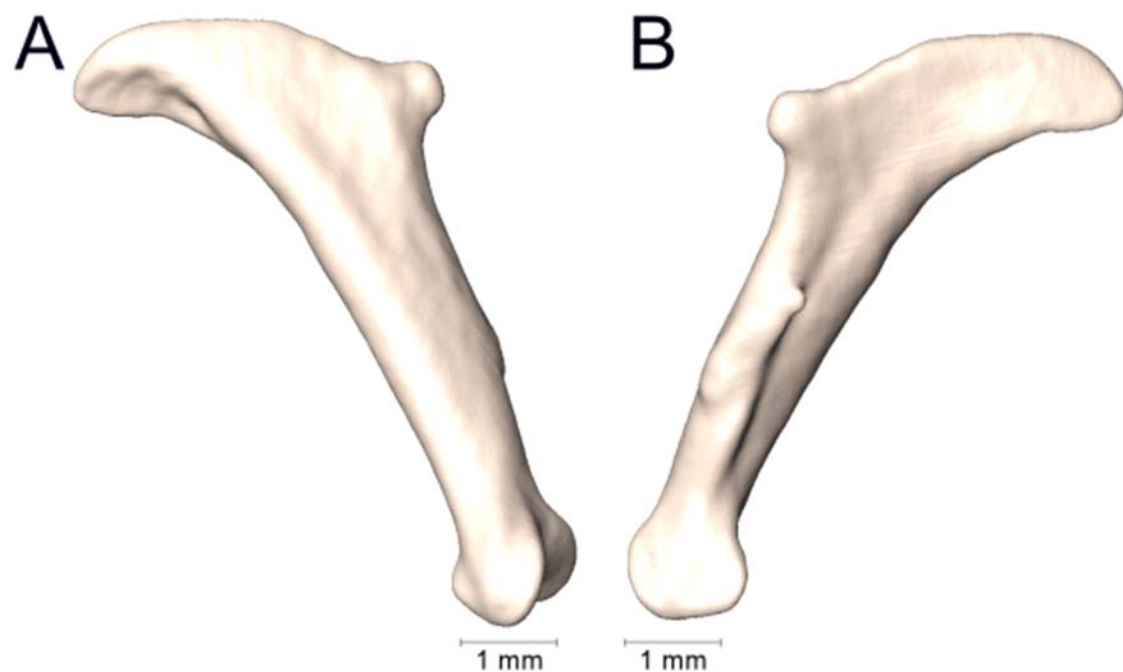
Supplemental Figure 2.89. Lateral and medial views (A-B, respectively) of the left quadrate of *Ophiophagus hannah* (UTA R-60836).



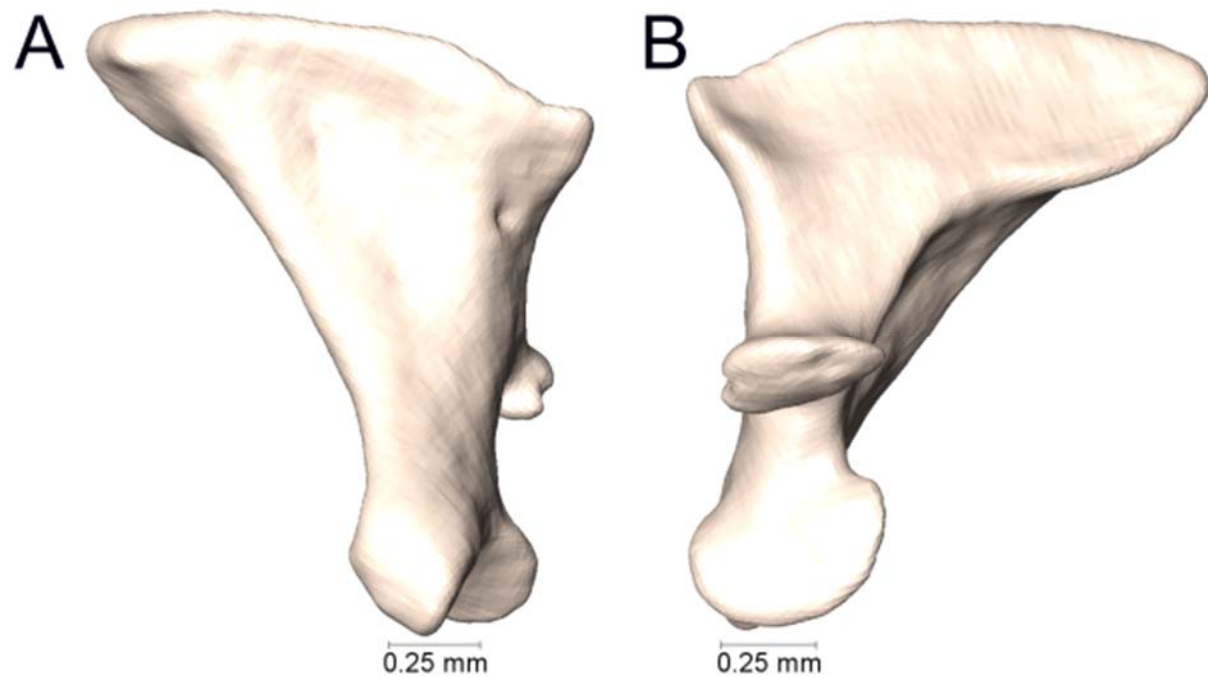
Supplemental Figure 2.90. Lateral and medial views (A-B, respectively) of the left quadrate of *Oxyuranus scutellatus* (UTA R-60839).



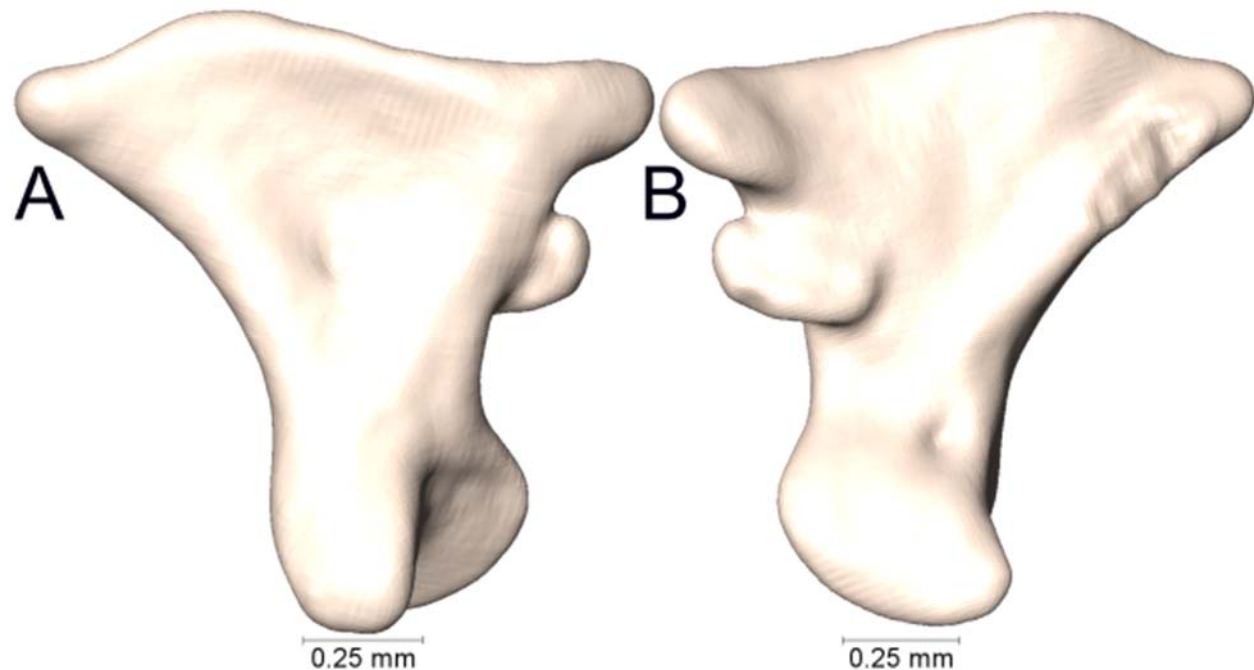
Supplemental Figure 2.91. Lateral and medial views (A-B, respectively) of the left quadrate of *Prosymna stuhlmanni* (UTA R-64493).



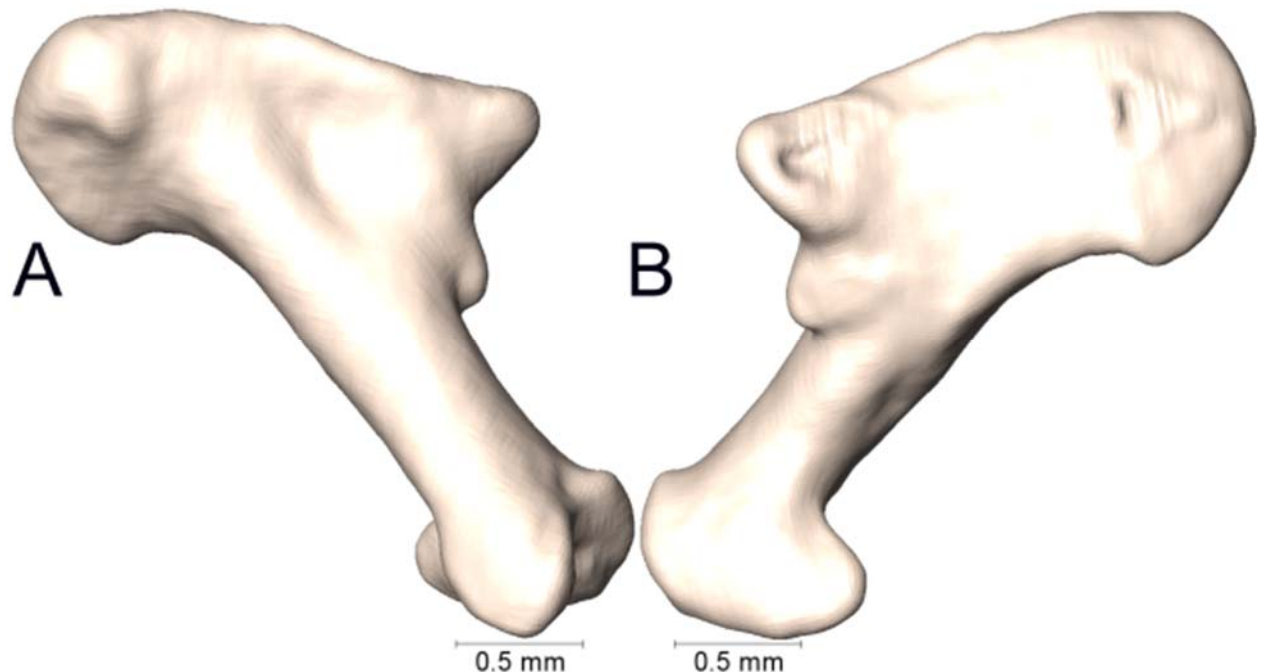
Supplemental Figure 2.92. Lateral and medial views (A-B, respectively) of the left quadrate of *Pseudohaje goldii* (UTA R-63636).



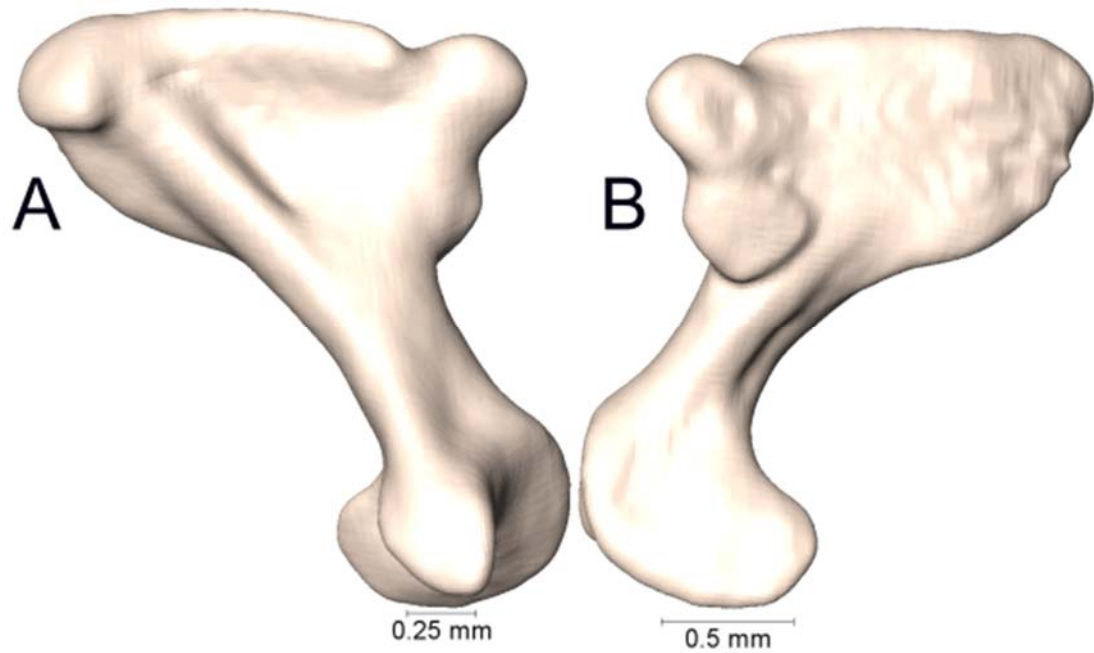
Supplemental Figure 2.93. Lateral and medial views (A-B, respectively) of the left quadrate of *Simoselaps bertholdi* (UMMZ 244197).



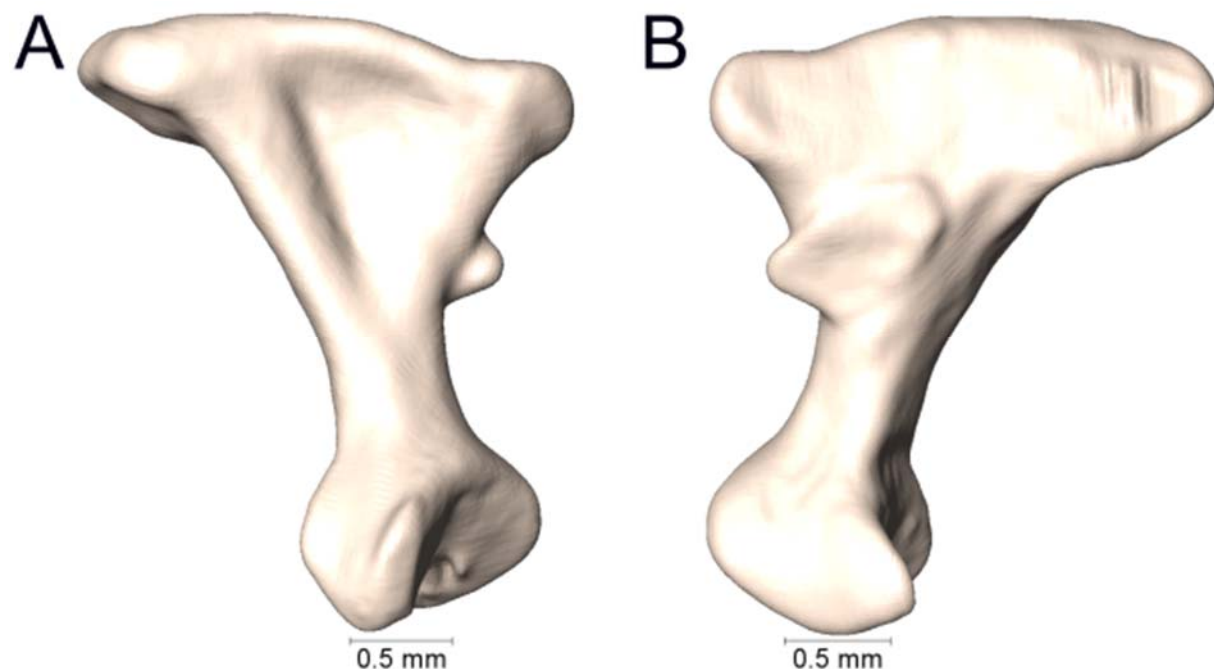
Supplemental Figure 2.94. Lateral and medial views (A-B, respectively) of the left quadrate of *Sinomicrurus annularis* (ROM 31158).



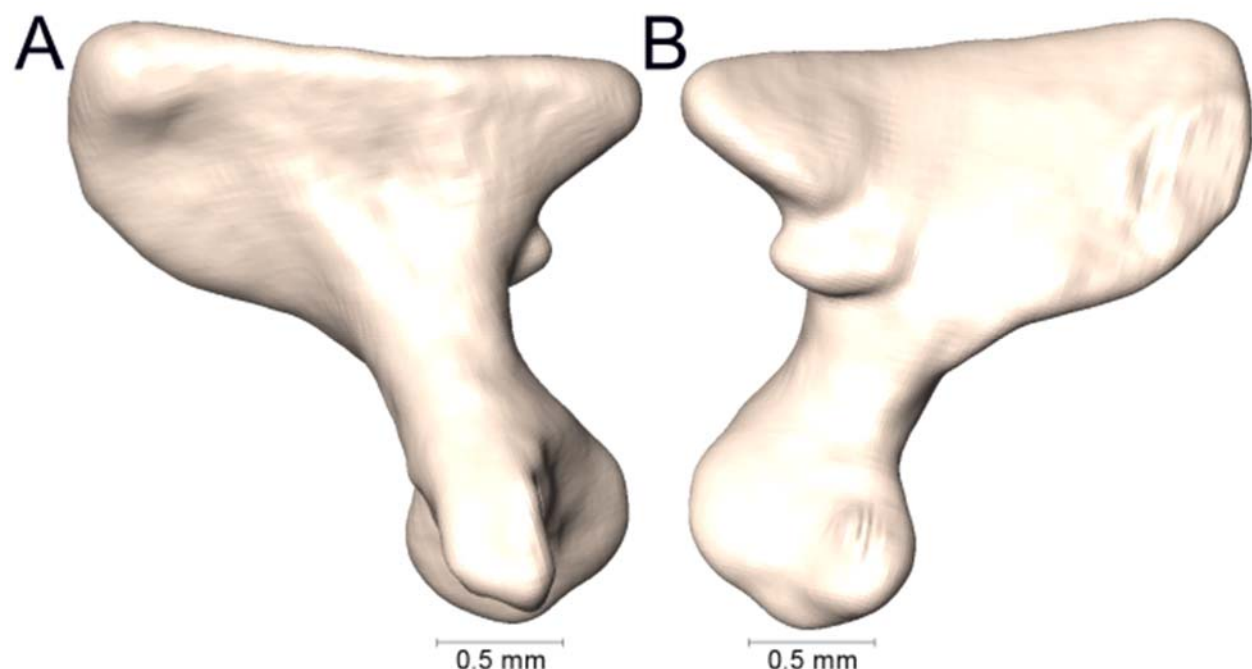
Supplemental Figure 2.95. Lateral and medial views (A-B, respectively) of the left quadrate of *Sinomicrurus boettgeri* (UTA R-58837).



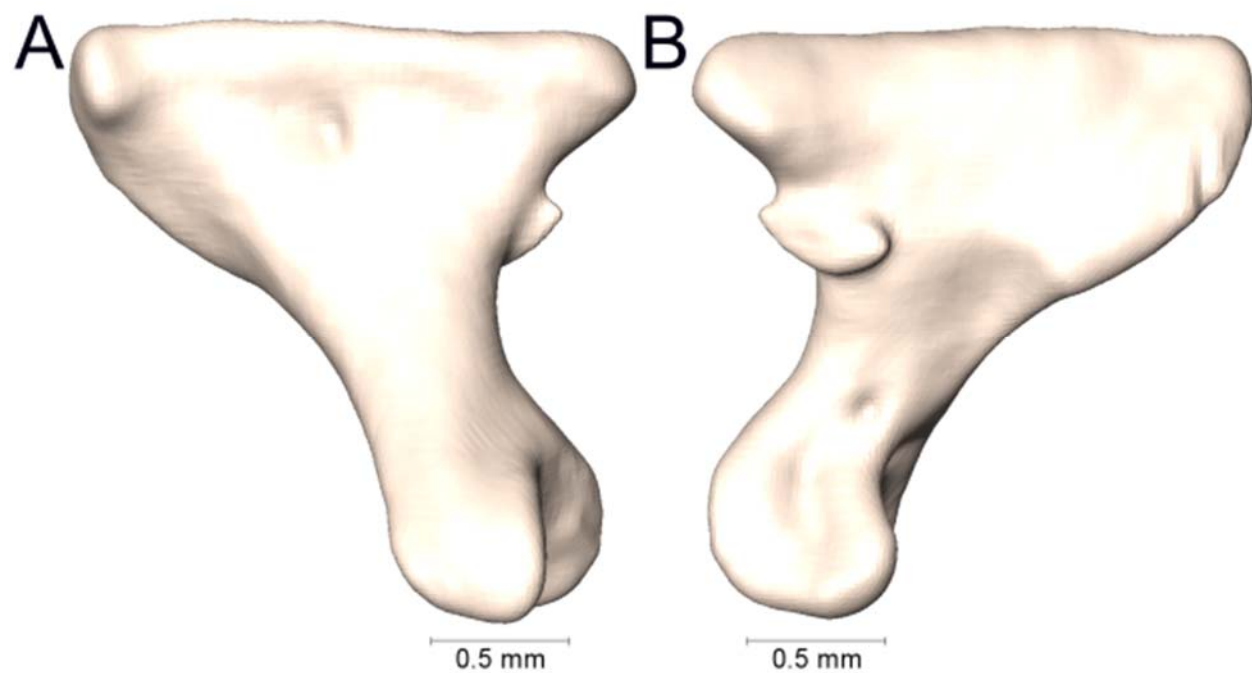
Supplemental Figure 2.96. Lateral and medial views (A-B, respectively) of the left quadrate of *Sinomicrurus japonicus* (CAS 204979).



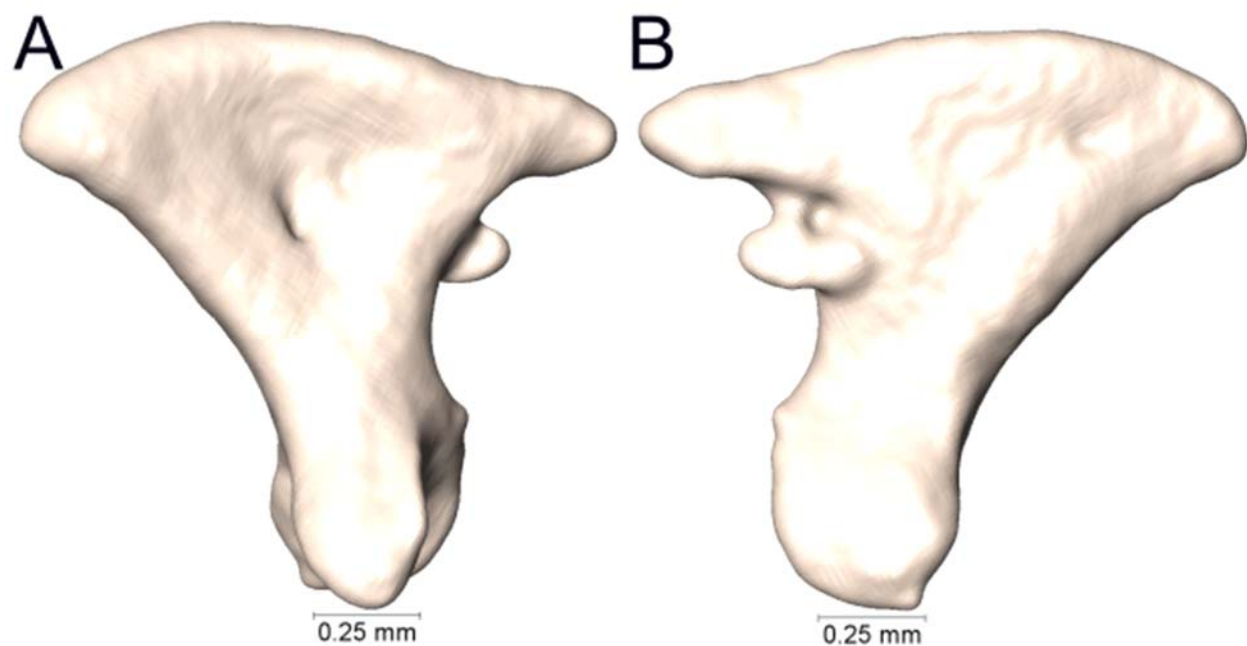
Supplemental Figure 2.97. Lateral and medial views (A-B, respectively) of the left quadrate of *Sinomicrurus kelloggi* (ROM 37079).



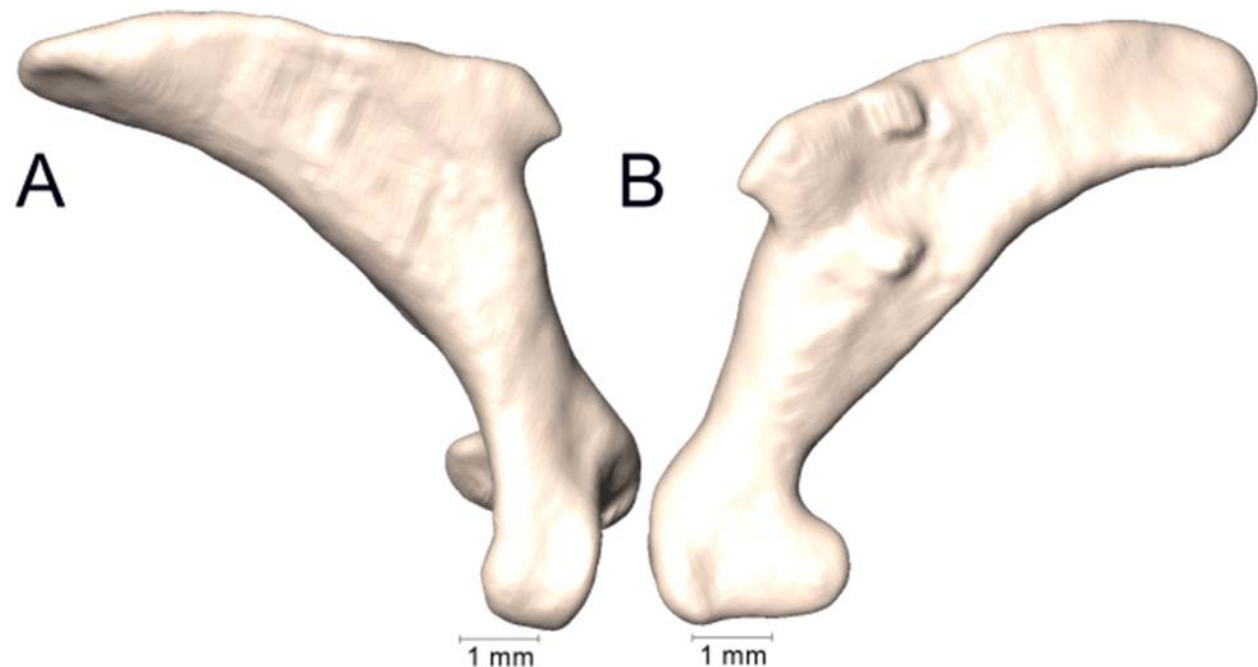
Supplemental Figure 2.98. Lateral and medial views (A-B, respectively) of the left quadrate of *Sinomicrurus peinani* (ROM 35245).



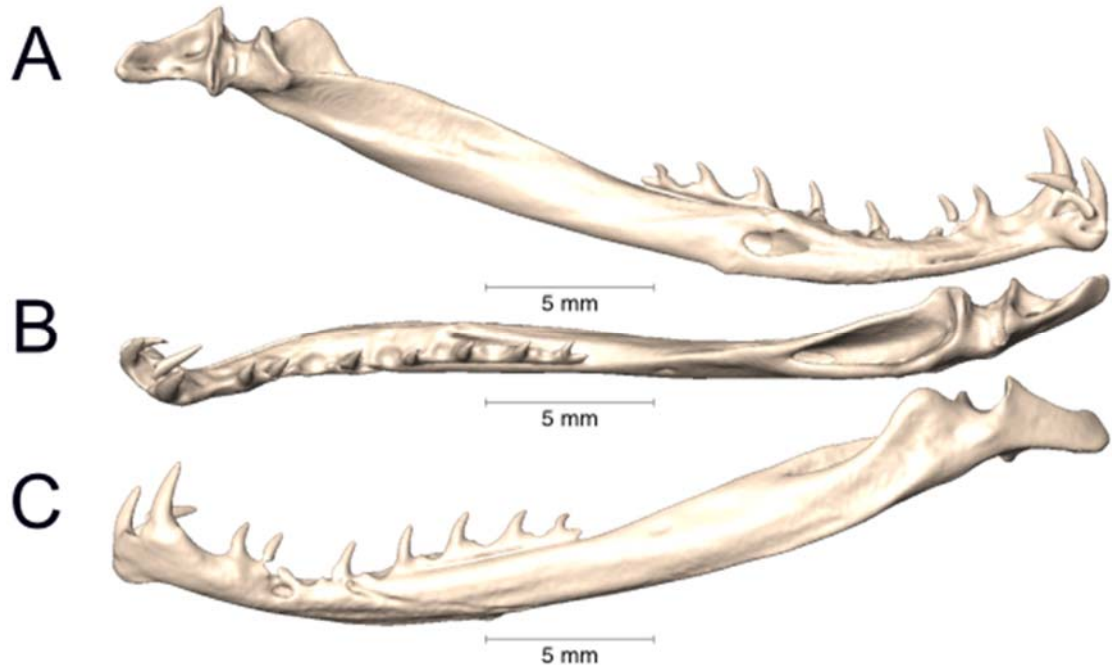
Supplemental Figure 2.99. Lateral and medial views (A-B, respectively) of the left quadrate of *Sinomicrurus peinani* (ROM 37109).



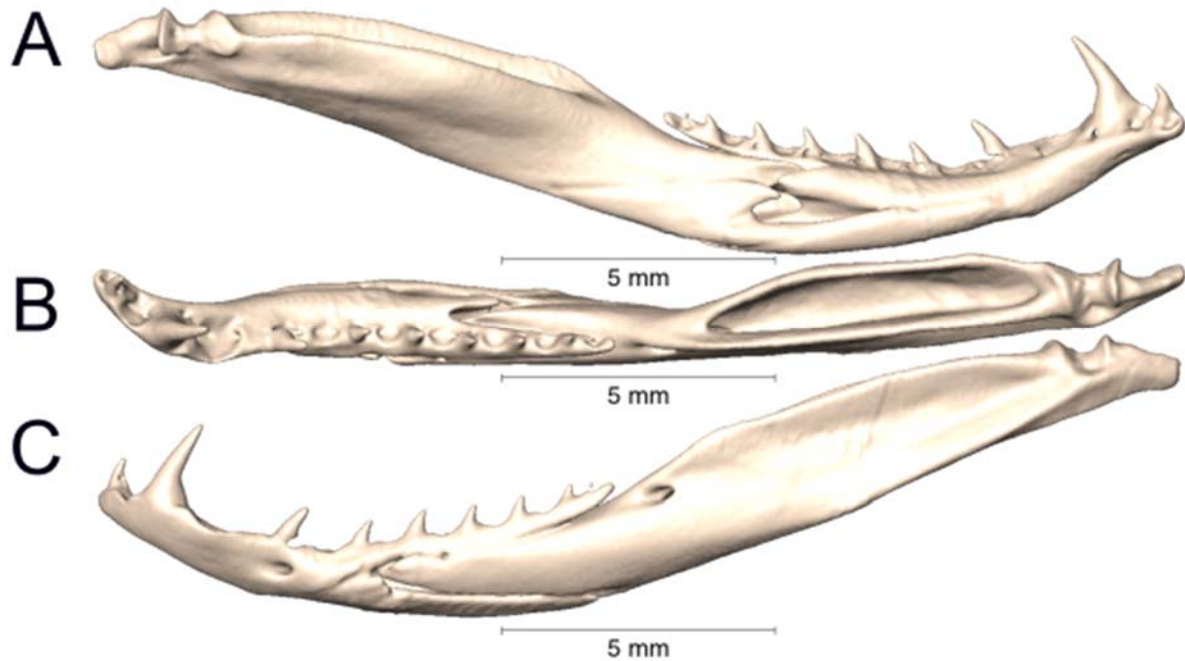
Supplemental Figure 2.100. Lateral and medial views (A-B, respectively) of the left quadrate of *Sinomicrurus swinhoei* (MVZ 23876).



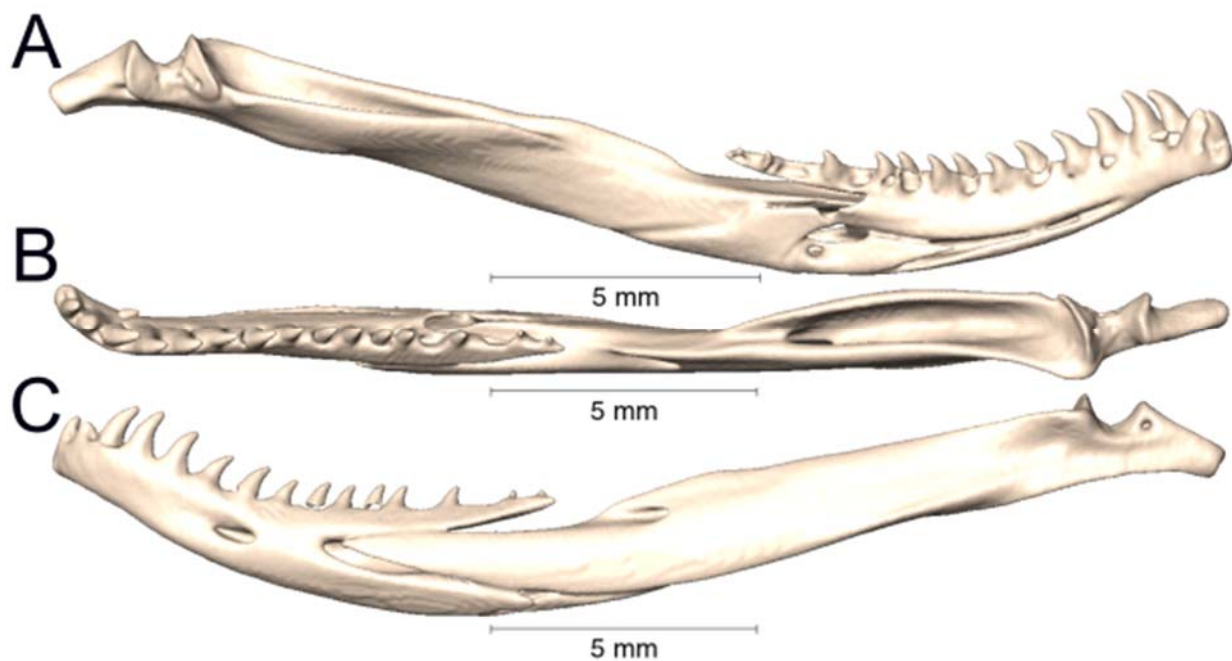
Supplemental Figure 2.101. Lateral and medial views (A-B, respectively) of the left quadrate of *Walterinnesia aegyptia* (UTA R-13021).



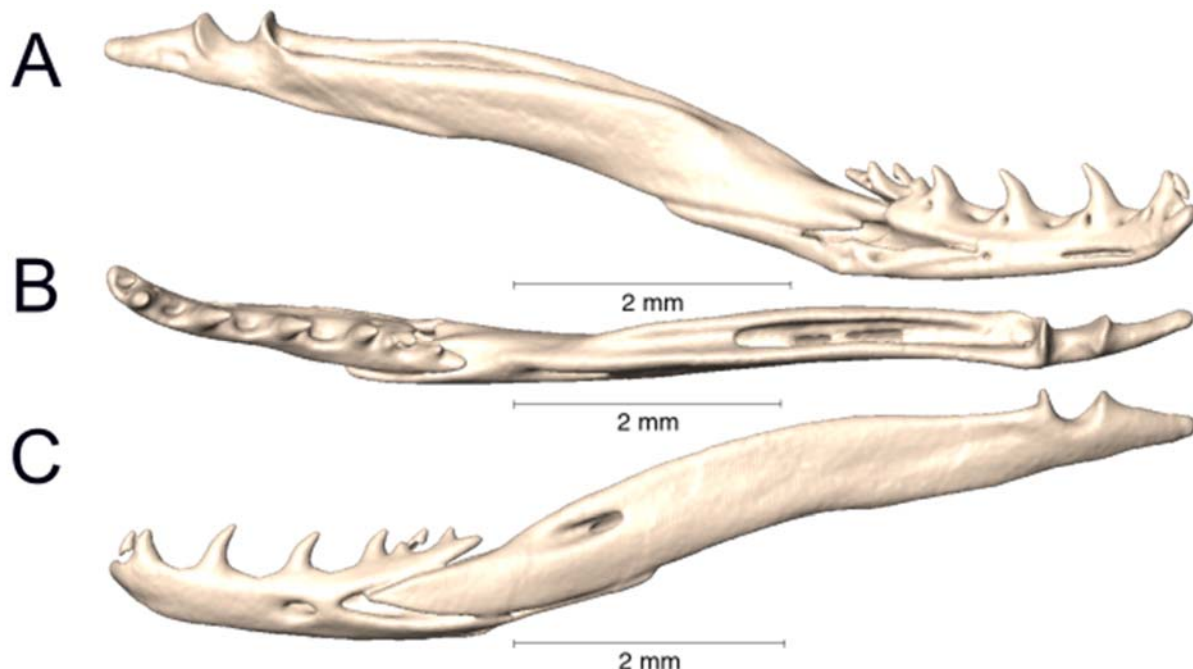
Supplemental Figure 3.1. Medial, dorsal, and lateral views (A-C, respectively) of the left lower jaw of *Acanthophis antarcticus* (UTA R-7623).



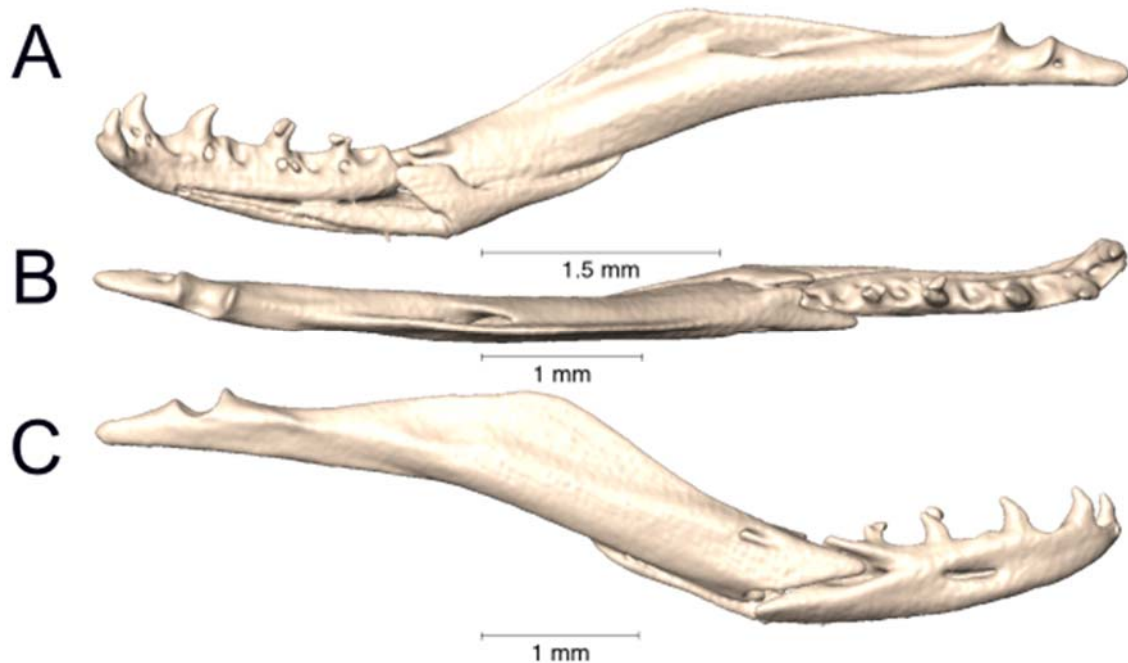
Supplemental Figure 3.2. Medial, dorsal, and lateral views (A-C, respectively) of the left lower jaw of *Bungarus candidus* (UTA R-65799).



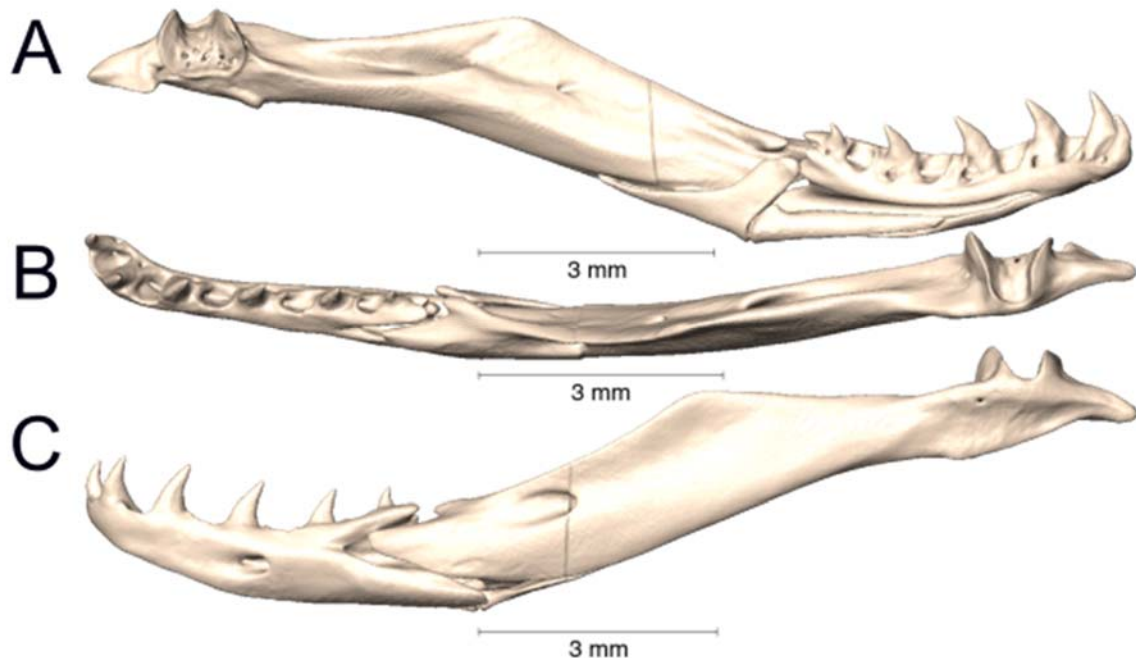
Supplemental Figure 3.3. Medial, dorsal, and lateral views (A-C, respectively) of the left lower jaw of *Bungarus flaviceps* (UTA R-62257).



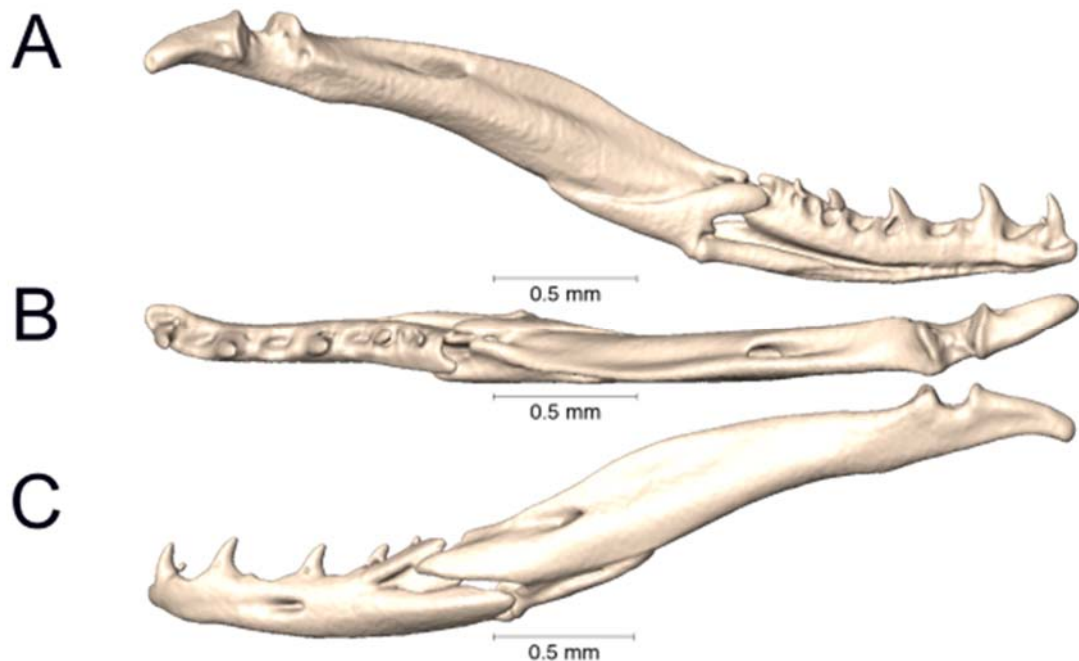
Supplemental Figure 3.4. Medial, dorsal, and lateral views (A-C, respectively) of the left lower jaw of *Calliophis beddomei* (MNHN 46-81).



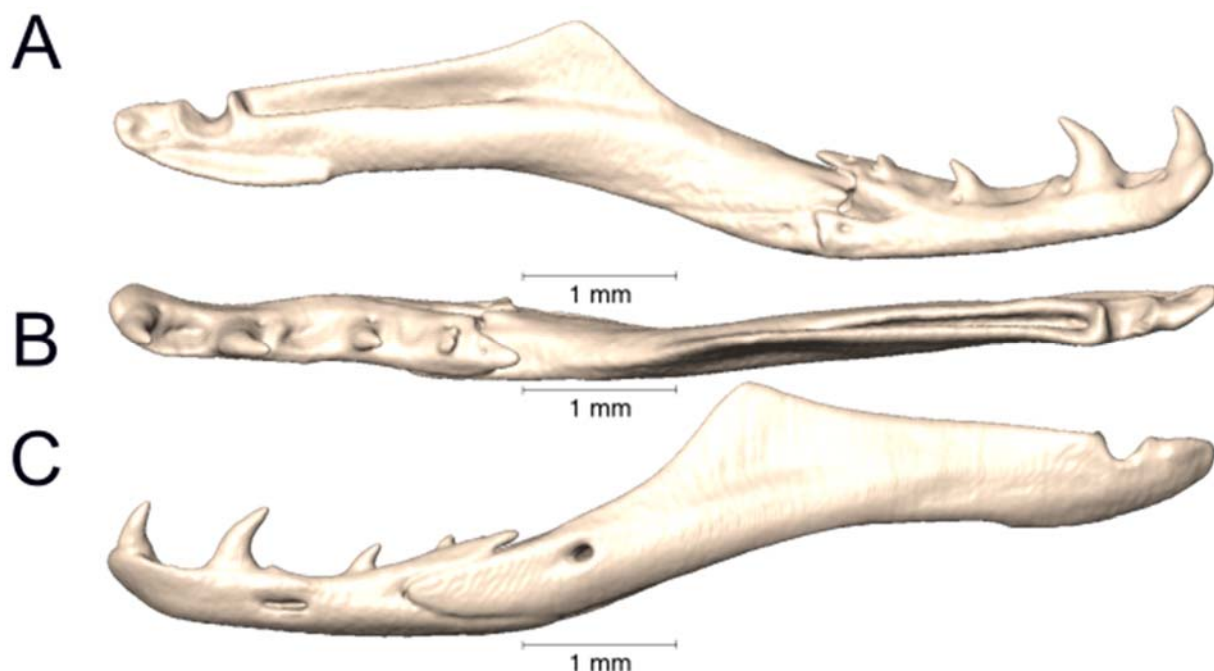
Supplemental Figure 3.5. Medial, dorsal, and lateral views (A-C, respectively) of the right lower jaw of *Calliophis biliniatus* (KU 309511).



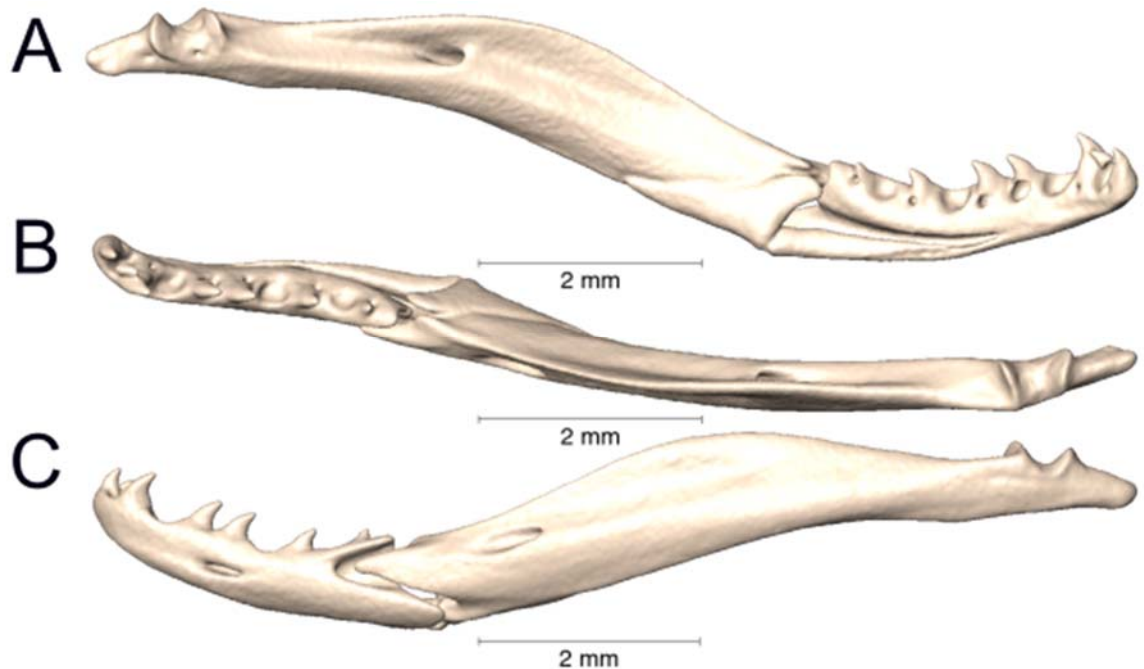
Supplemental Figure 3.6. Medial, dorsal, and lateral views (A-C, respectively) of the left lower jaw of *Calliophis biliniatus* (KU 311415).



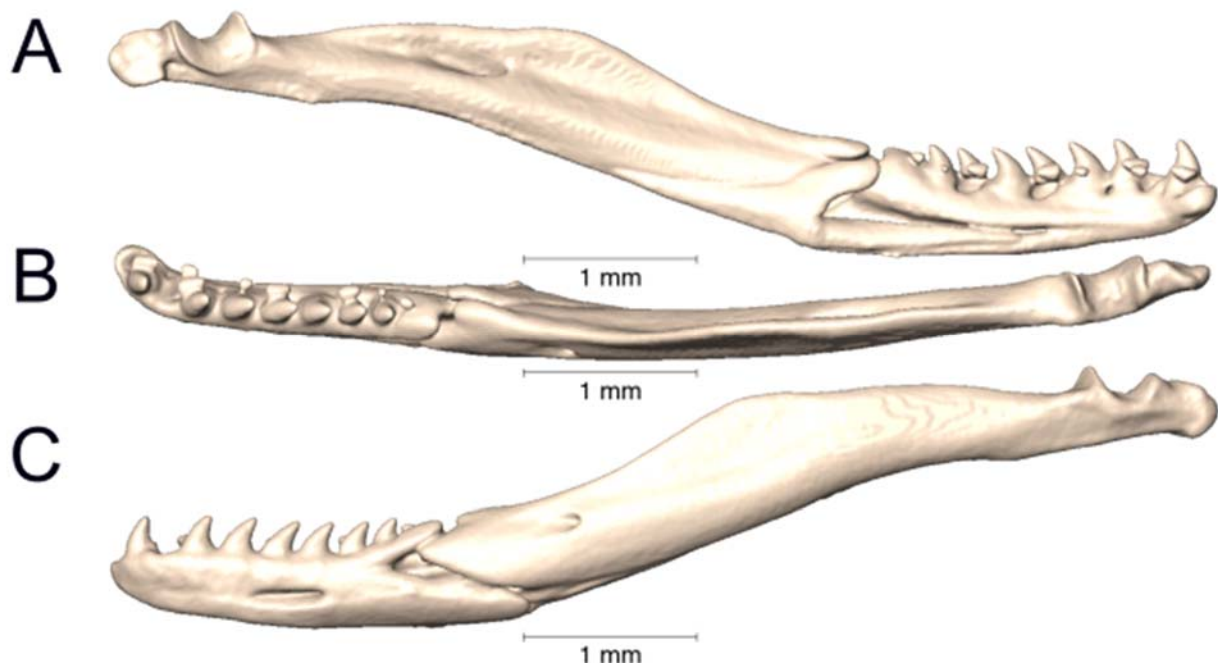
Supplemental Figure 3.7. Medial, dorsal, and lateral views (A-C, respectively) of the left lower jaw of *Calliophis bivirgatus bivirgatus* (UTA R-63079).



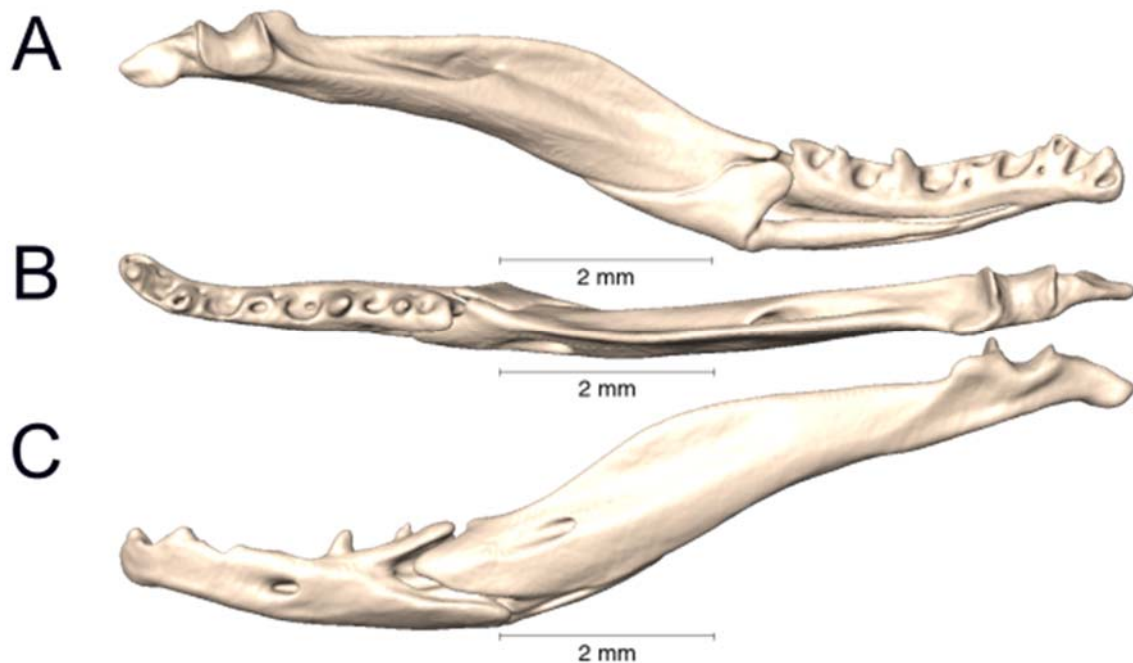
Supplemental Figure 3.8. Medial, dorsal, and lateral views (A-C, respectively) of the left lower jaw of *Calliophis gracilis* (USNM 53447).



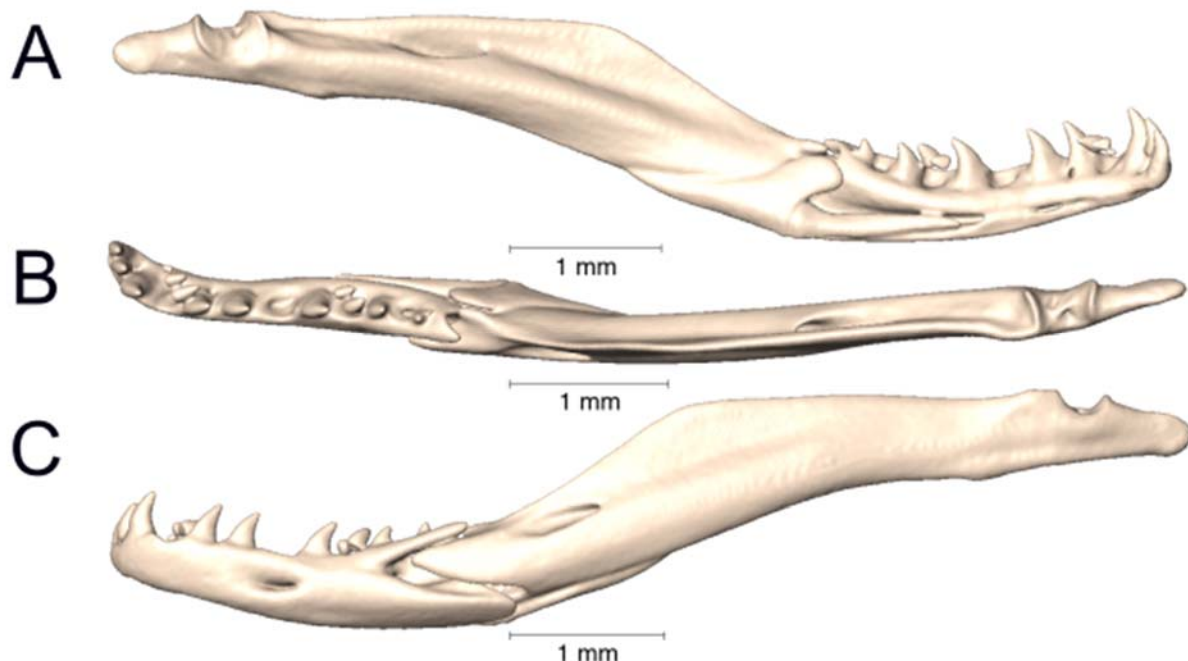
Supplemental Figure 3.9. Medial, dorsal, and lateral views (A-C, respectively) of the left lower jaw of *Calliophis intestinalis* (UTA R-60738).



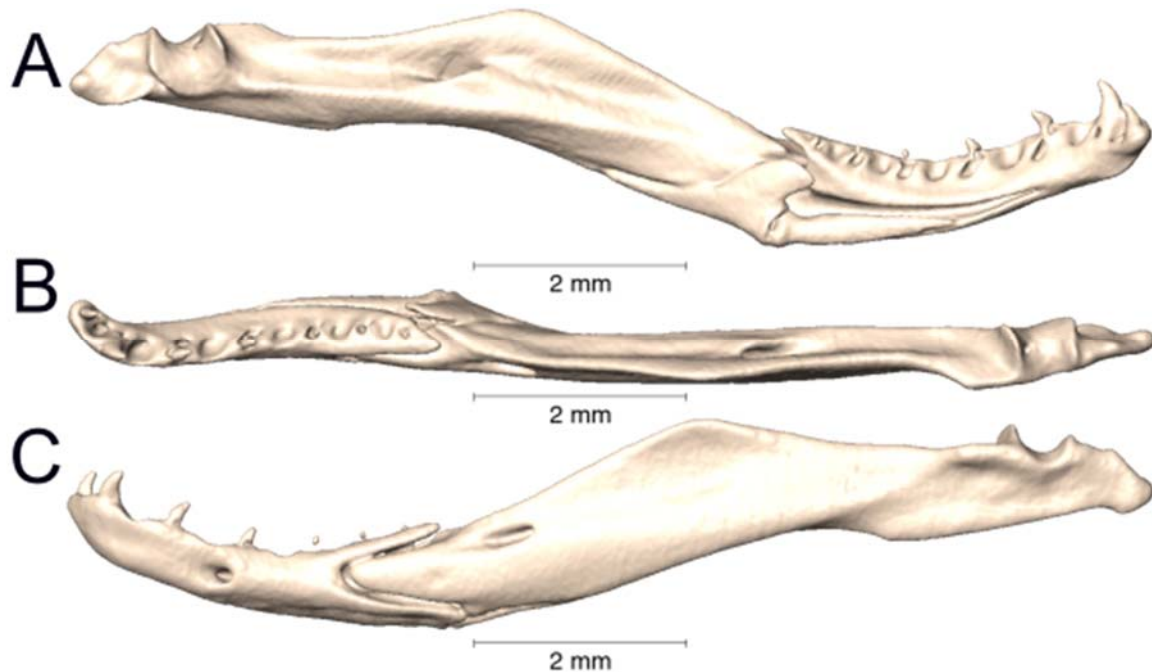
Supplemental Figure 3.10. Medial, dorsal, and lateral views (A-C, respectively) of the left lower jaw of *Calliophis cf. intestinalis* (NMW 27221-4).



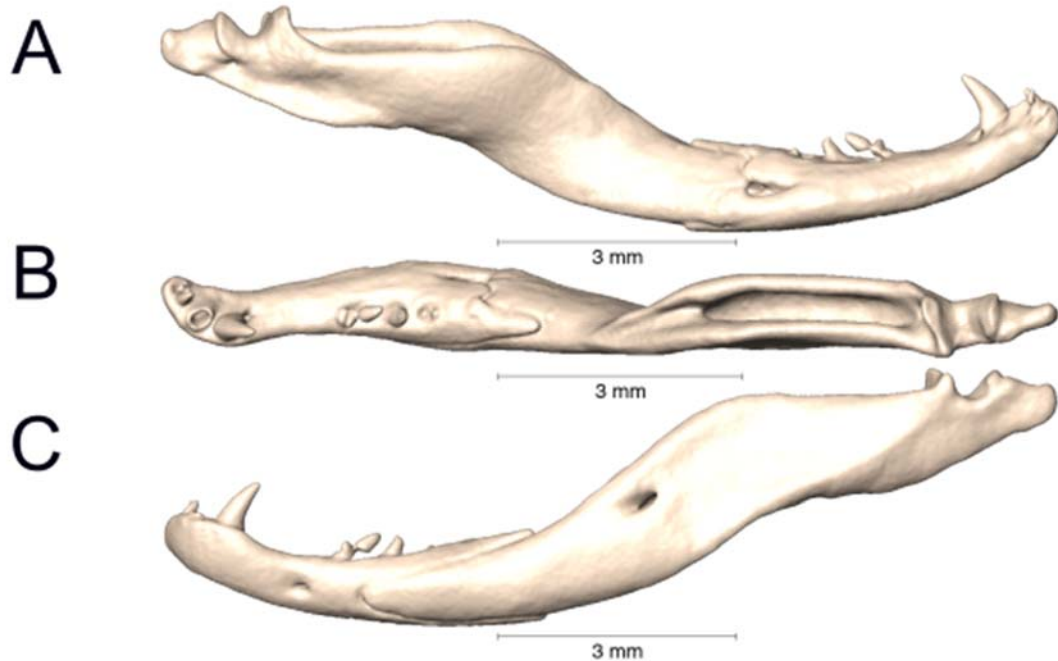
Supplemental Figure 3.11. Medial, dorsal, and lateral views (A-C, respectively) of the left lower jaw of *Calliophis intestinalis* cf. *immaculata* (NMW 27192-1).



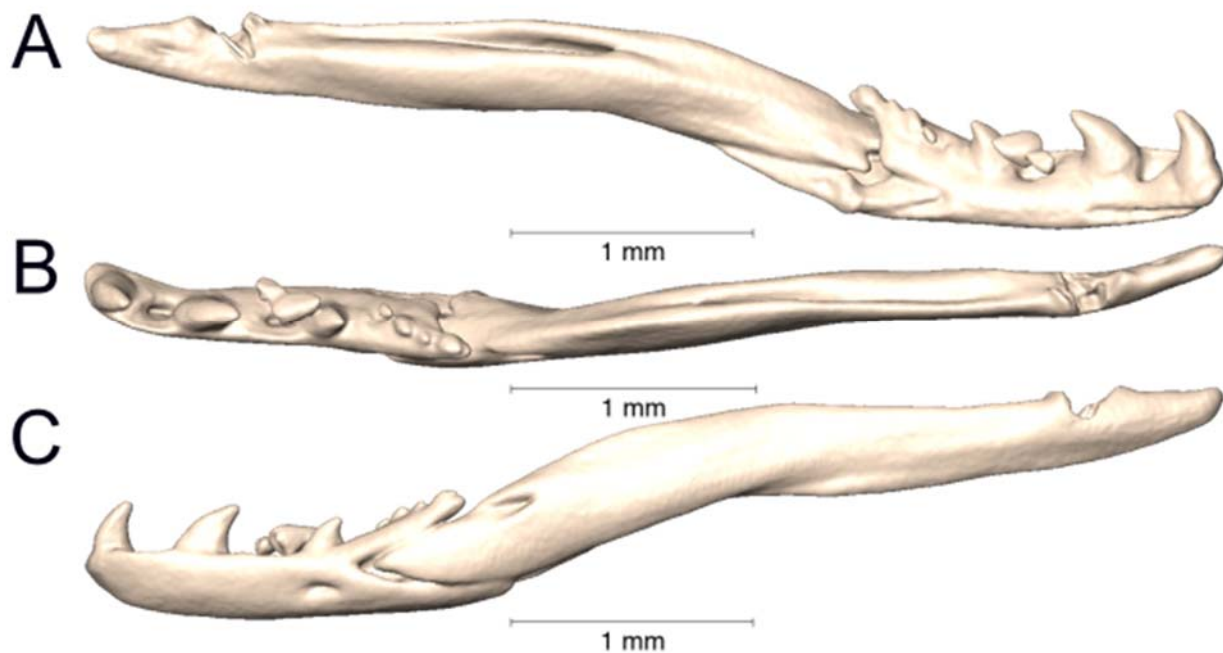
Supplemental Figure 3.12. Medial, dorsal, and lateral views (A-C, respectively) of the left lower jaw of *Calliophis intestinalis* *immaculata* (UTA R-65802).



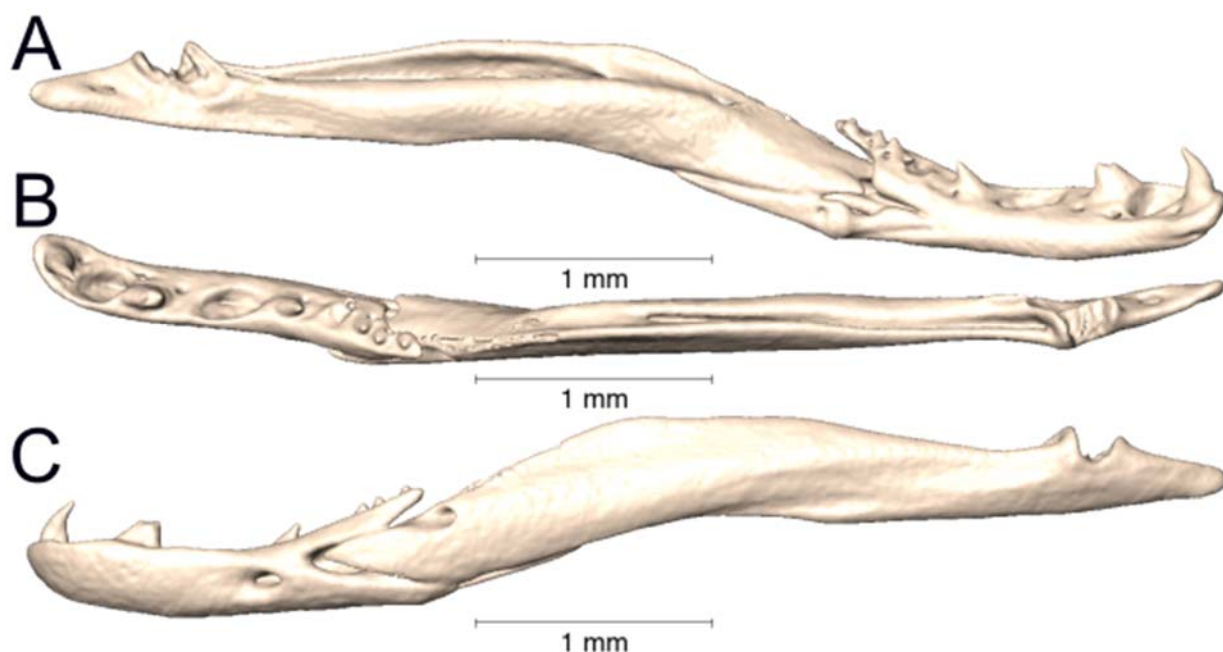
Supplemental Figure 3.13. Medial, dorsal, and lateral views (A-C, respectively) of the left lower jaw of *Calliophis intestinalis lineata* (UTA R-65801).



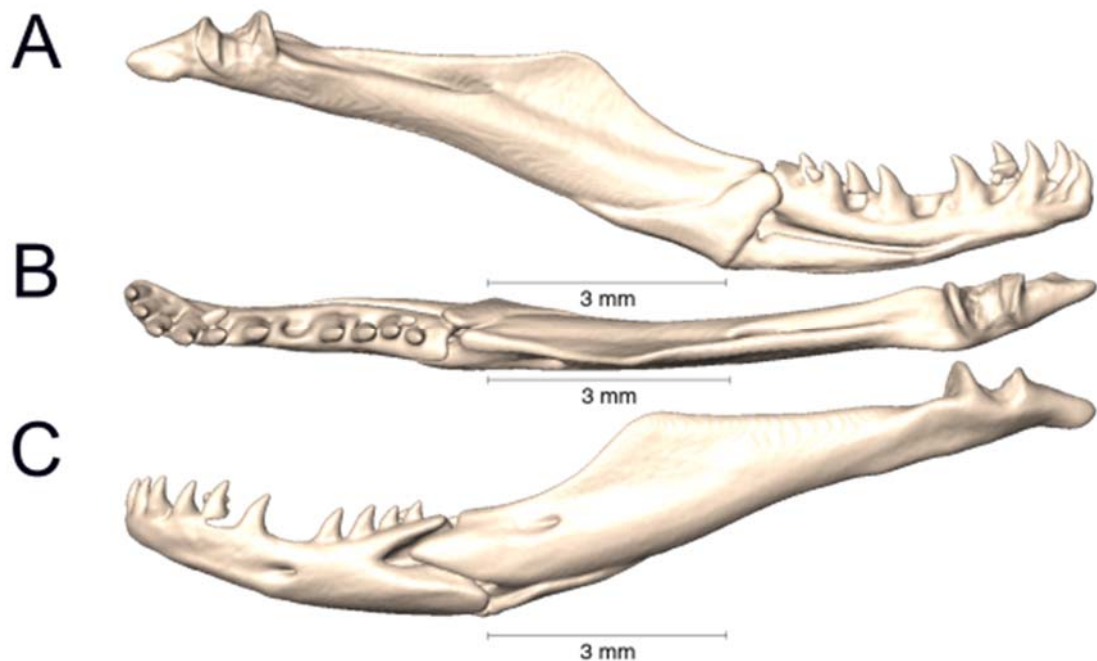
Supplemental Figure 3.14. Medial, dorsal, and lateral views (A-C, respectively) of the left lower jaw of *Calliophis maculiceps* (MNHN 5459).



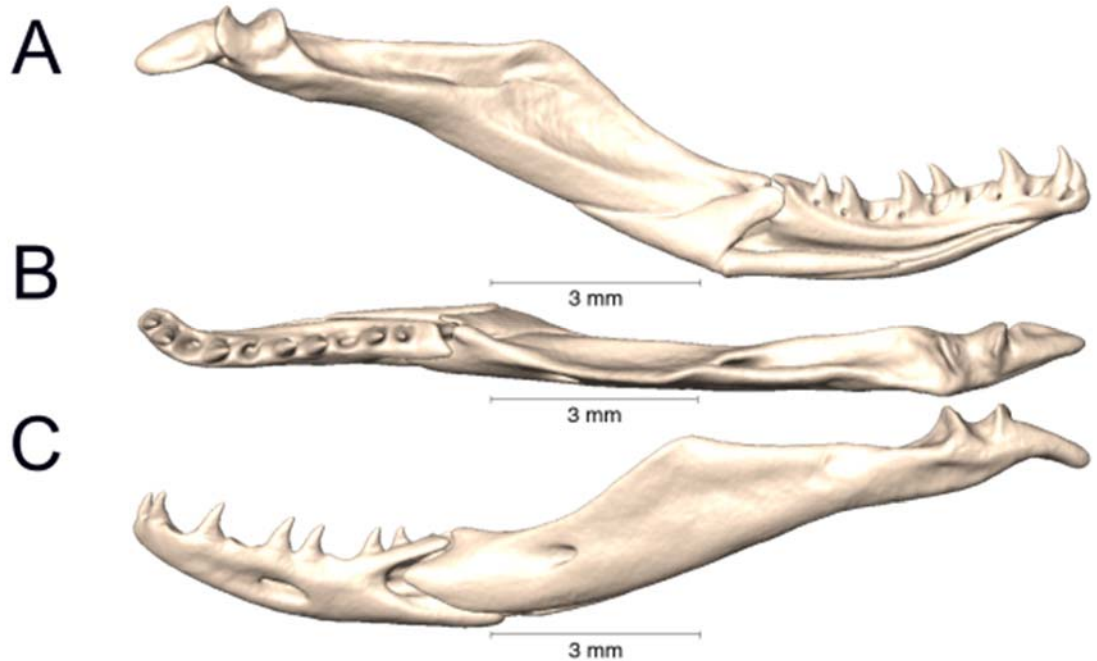
Supplemental Figure 3.15. Medial, dorsal, and lateral views (A-C, respectively) of the left lower jaw of *Calliophis melanurus* (MNHN 46-286).



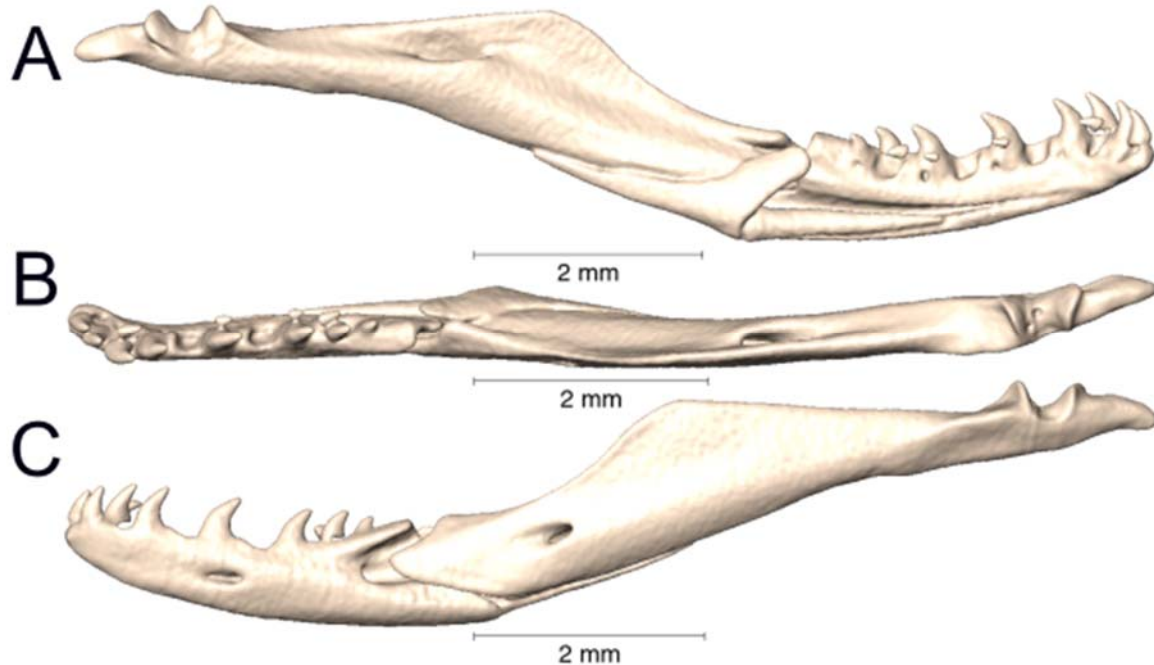
Supplemental Figure 3.16. Medial, dorsal, and lateral views (A-C, respectively) of the left lower jaw of *Calliophis melanurus* (MNHN 48-318).



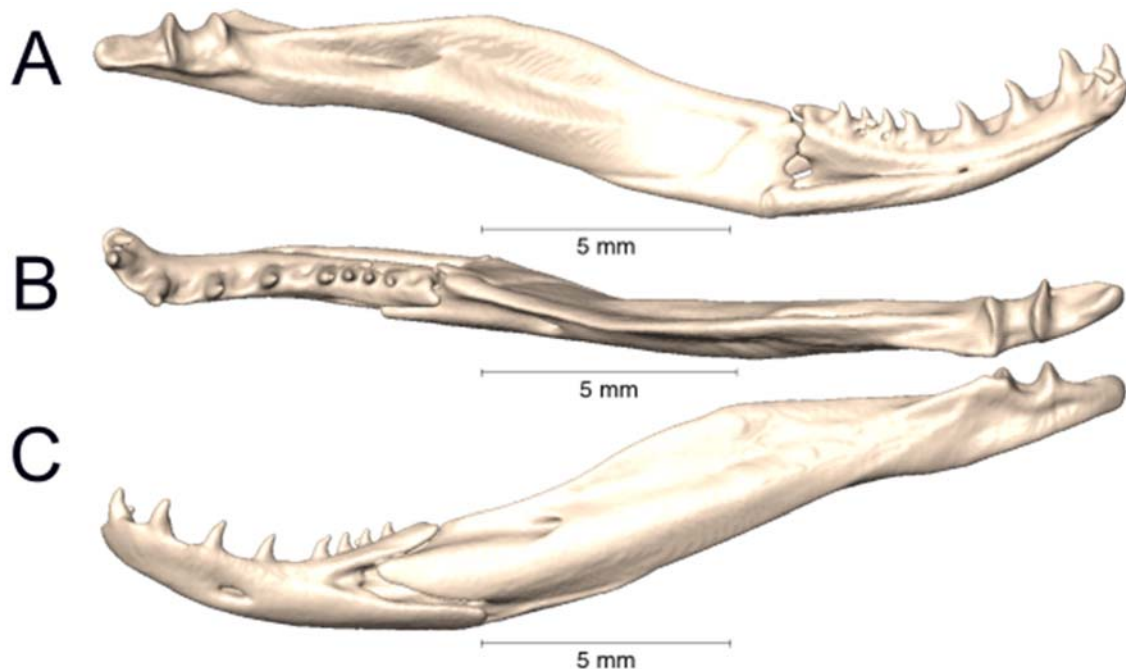
Supplemental Figure 3.17. Medial, dorsal, and lateral views (A-C, respectively) of the left lower jaw of *Calliophis nigrotaeniatus* (NMW 27220-7).



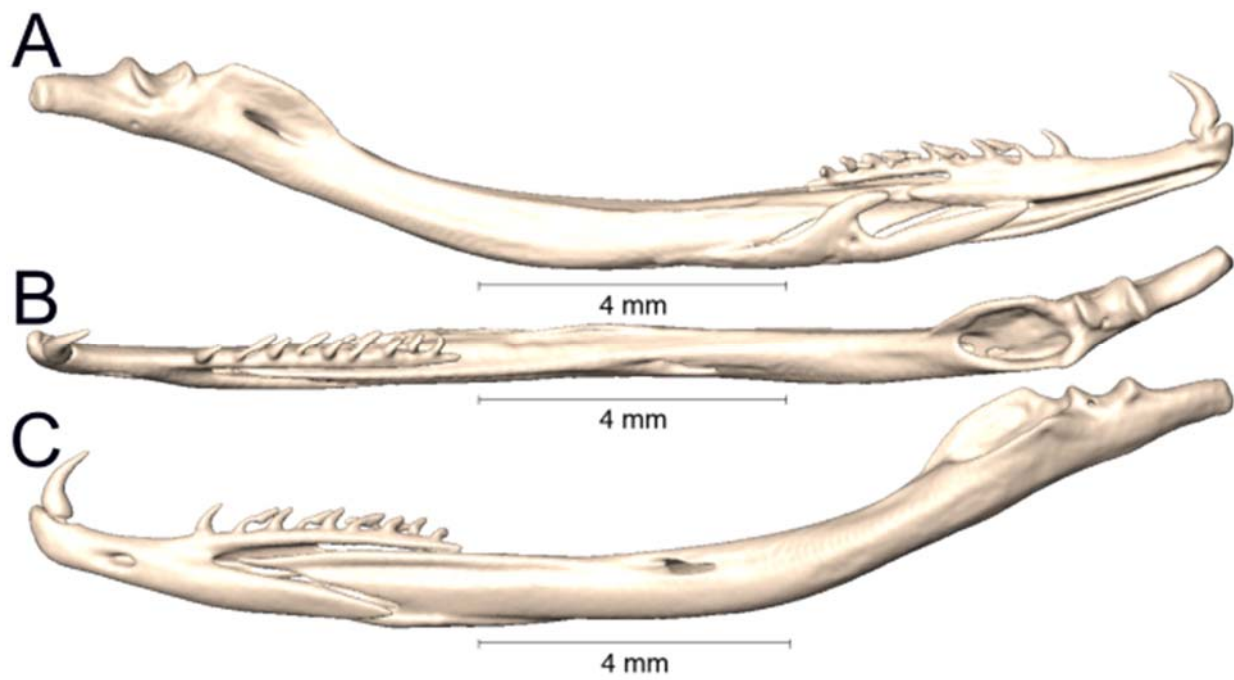
Supplemental Figure 3.18. Medial, dorsal, and lateral views (A-C, respectively) of the left lower jaw of *Calliophis philippinus* (KU 310369).



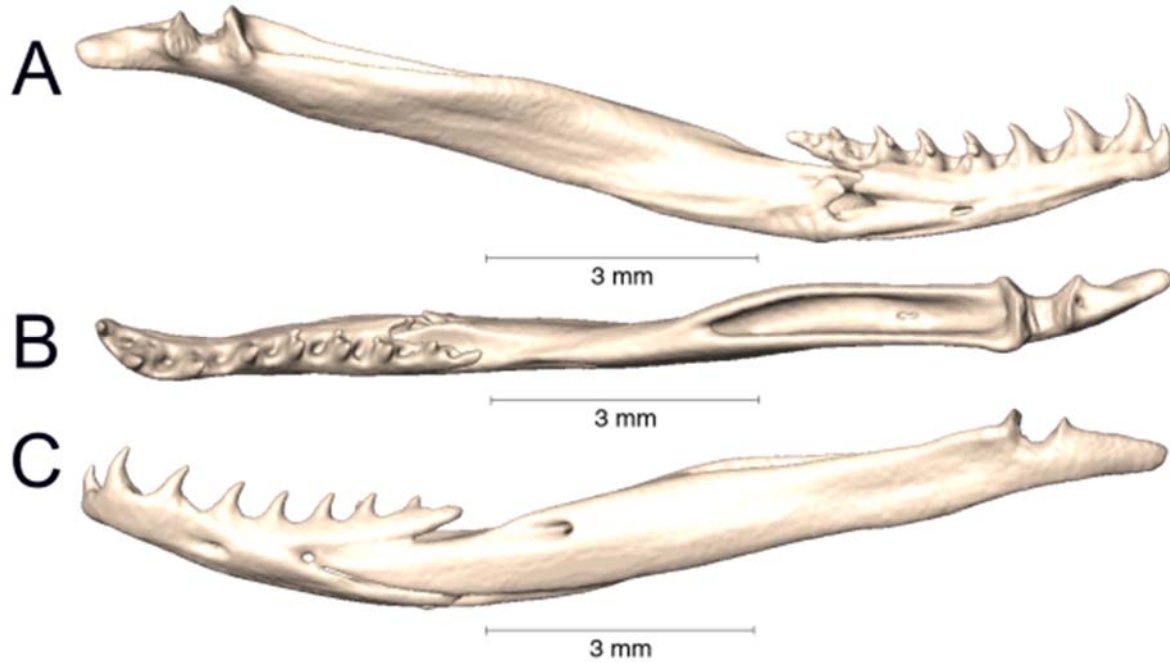
Supplemental Figure 3.19. Medial, dorsal, and lateral views (A-C, respectively) of the left lower jaw of *Calliophis philippinus* (KU 314913).



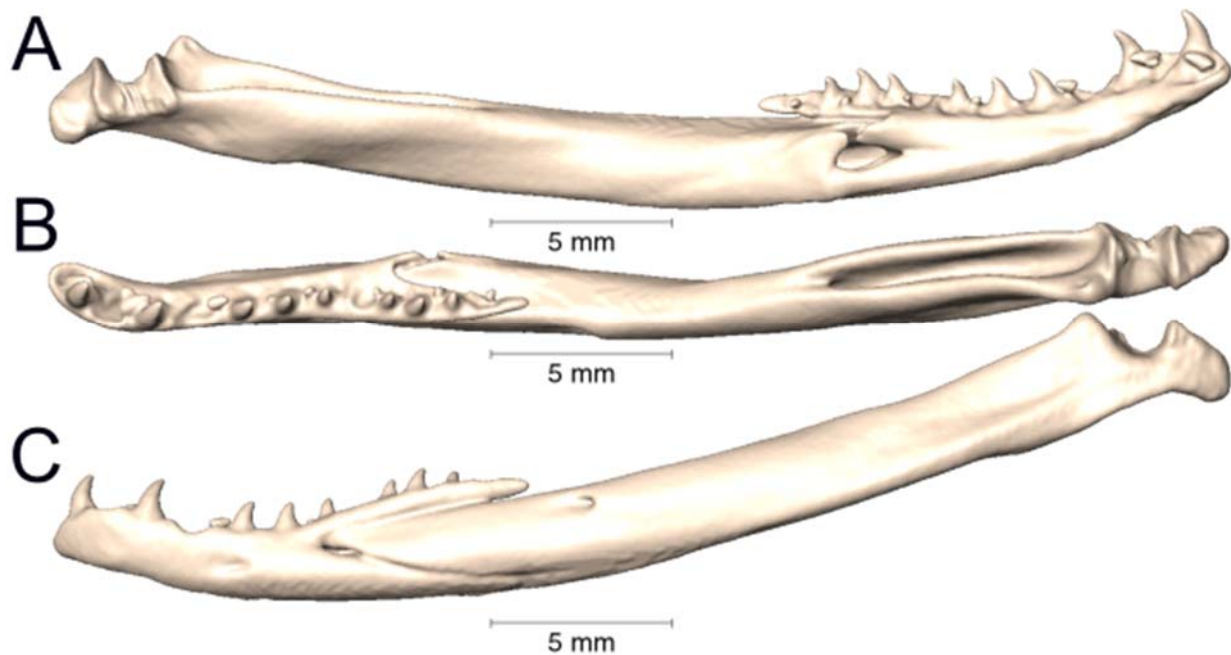
Supplemental Figure 3.20. Medial, dorsal, and lateral views (A-C, respectively) of the left lower jaw of *Calliophis salitan* (PNM 9844).



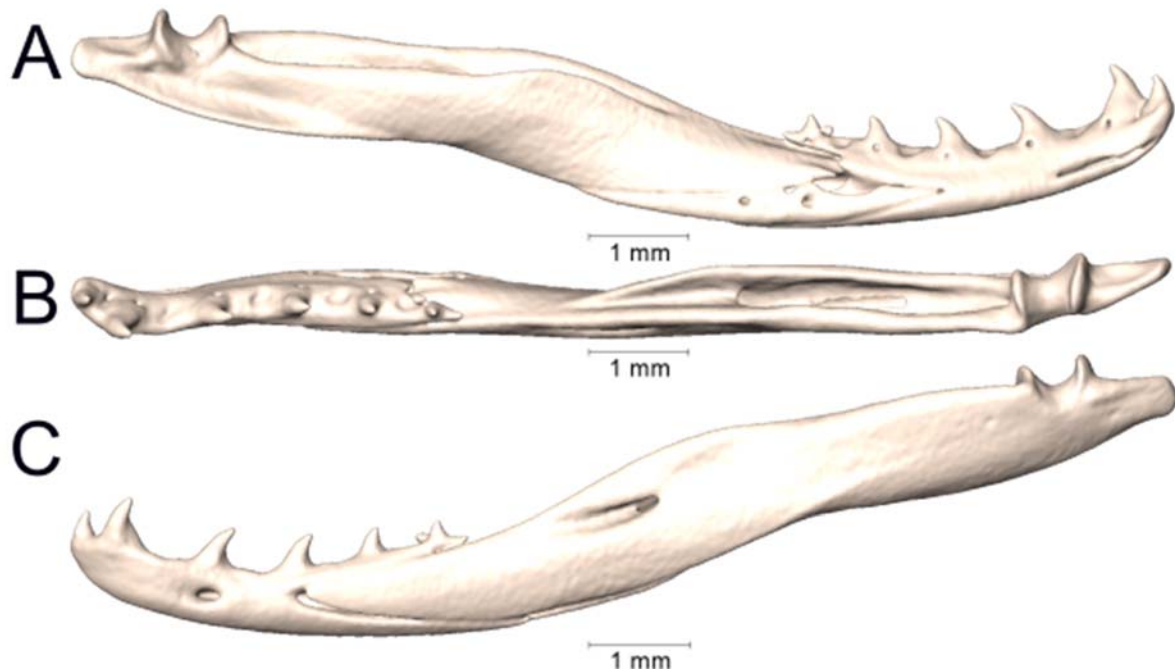
Supplemental Figure 3.21. Medial, dorsal, and lateral views (A-C, respectively) of the left lower jaw of *Dendroaspis angusticeps* (UTA R-34982).



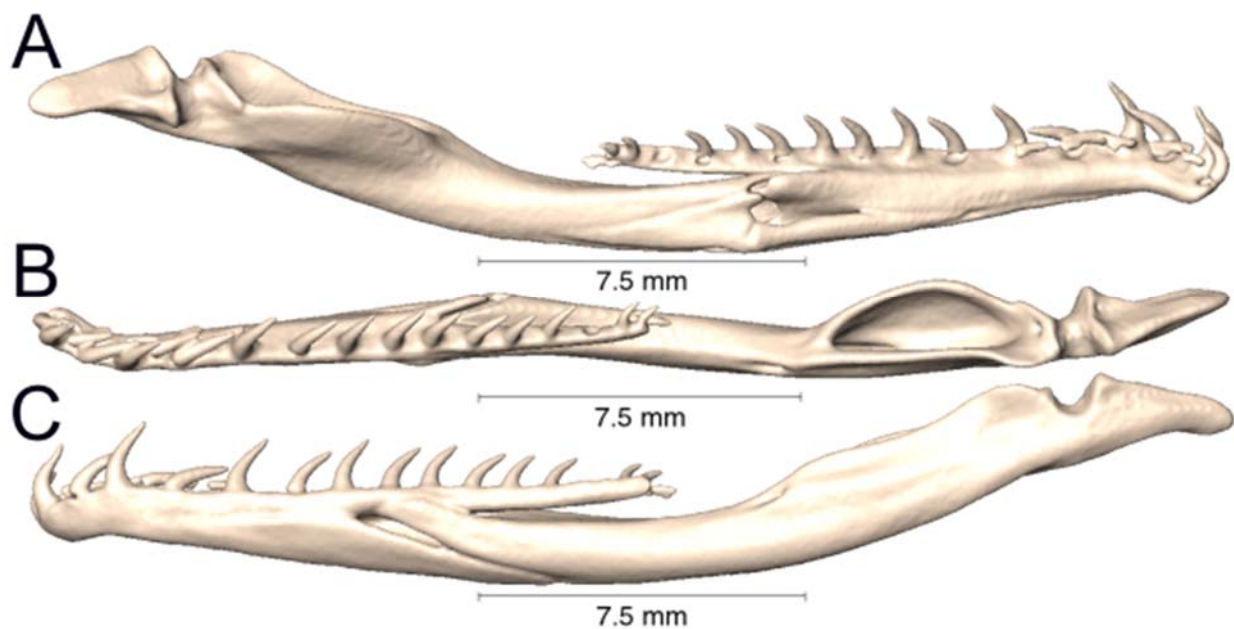
Supplemental Figure 3.22. Medial, dorsal, and lateral views (A-C, respectively) of the left lower jaw of *Elapsoidea nigra* (CAS 168978).



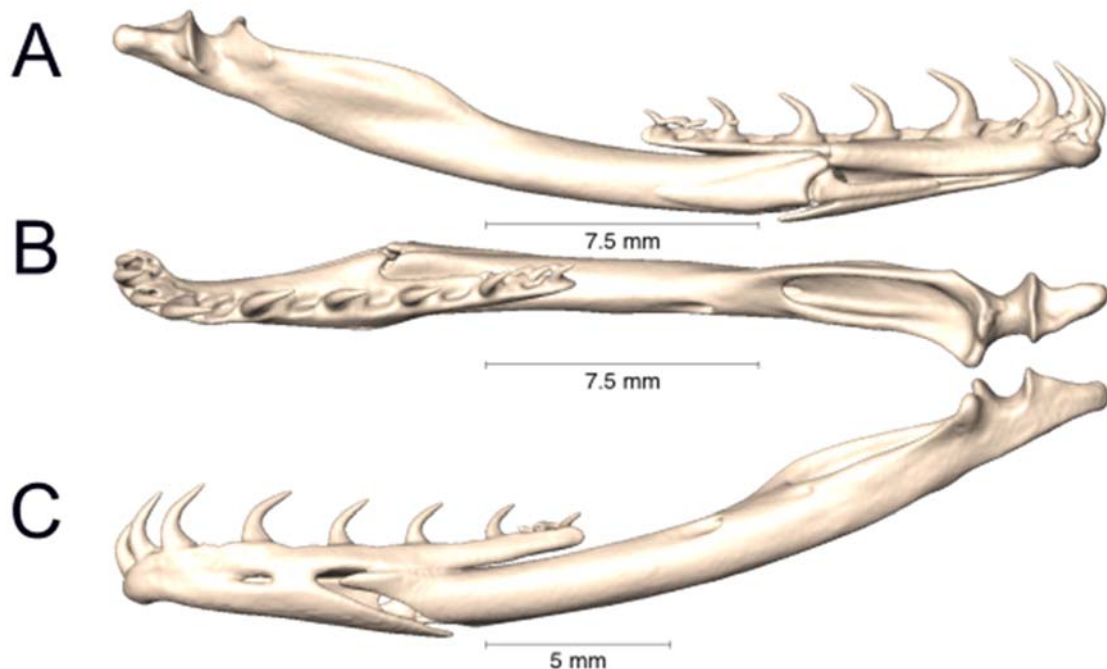
Supplemental Figure 3.23. Medial, dorsal, and lateral views (A-C, respectively) of the left lower jaw of *Hemachatus haemachatus* (UTA R-7431).



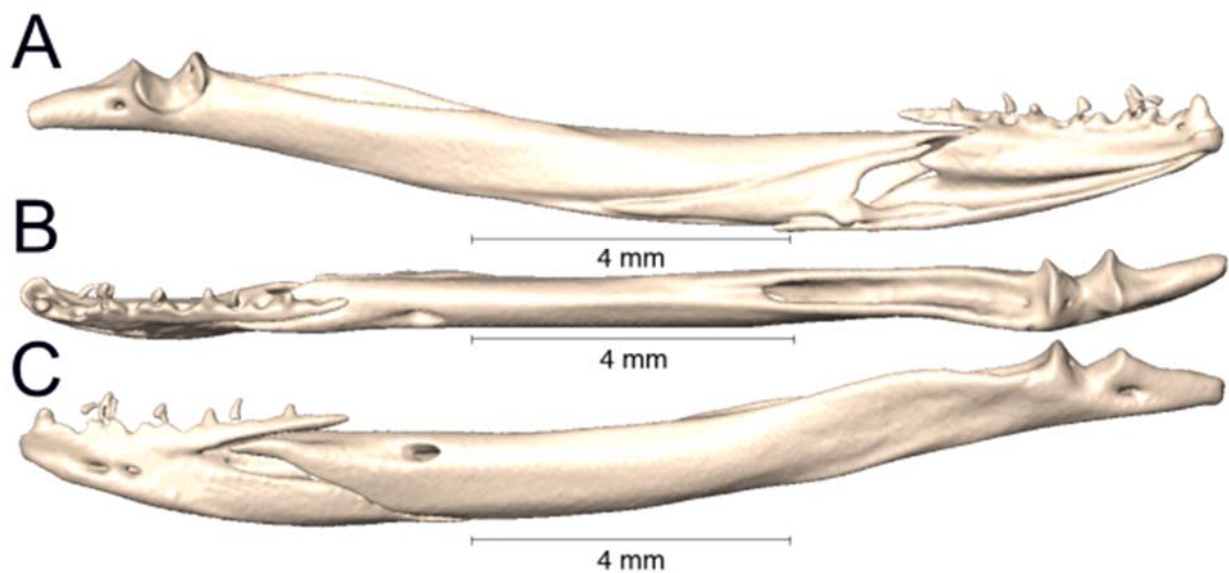
Supplemental Figure 3.24. Medial, dorsal, and lateral views (A-C, respectively) of the left lower jaw of *Hemibungarus calligaster* (KU 307474).



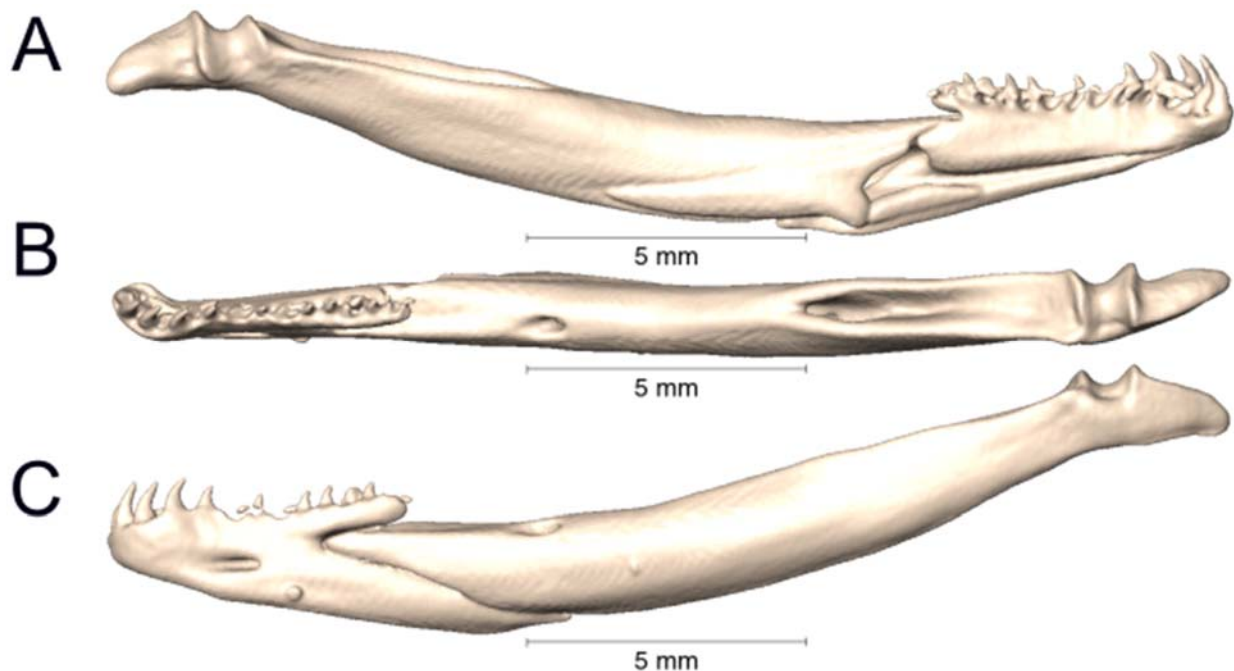
Supplemental Figure 3.25. Medial, dorsal, and lateral views (A-C, respectively) of the left lower jaw of *Hydrophis platurus* (UTA R-41049).



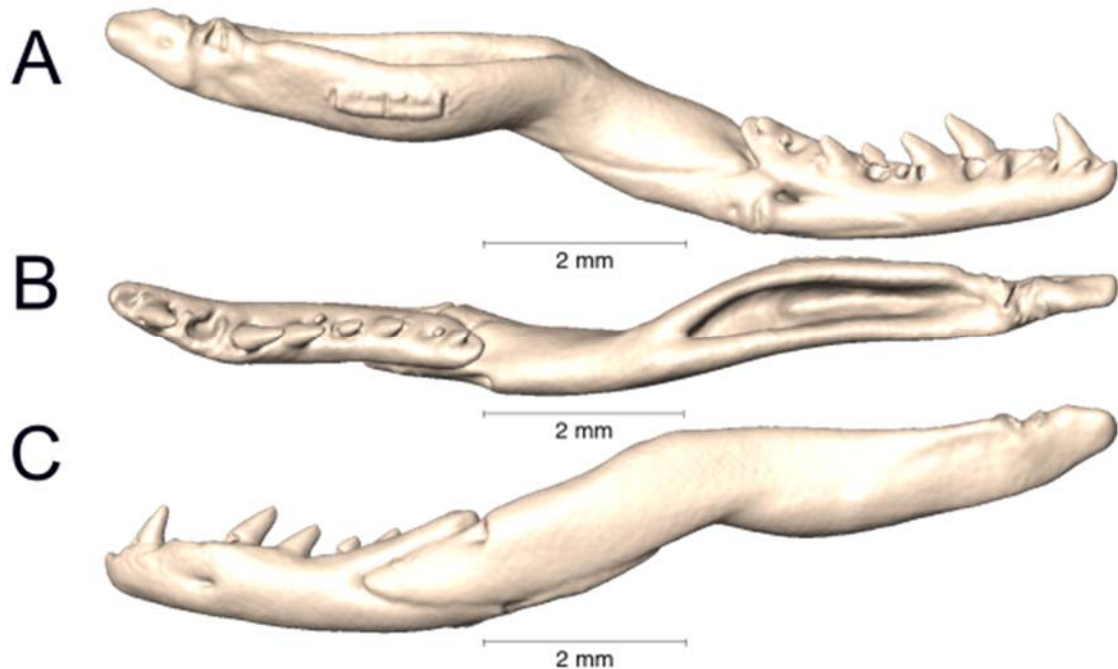
Supplemental Figure 3.26. Medial, dorsal, and lateral views (A-C, respectively) of the left lower jaw of *Hydrophis schistosus* (UTA R-63074).



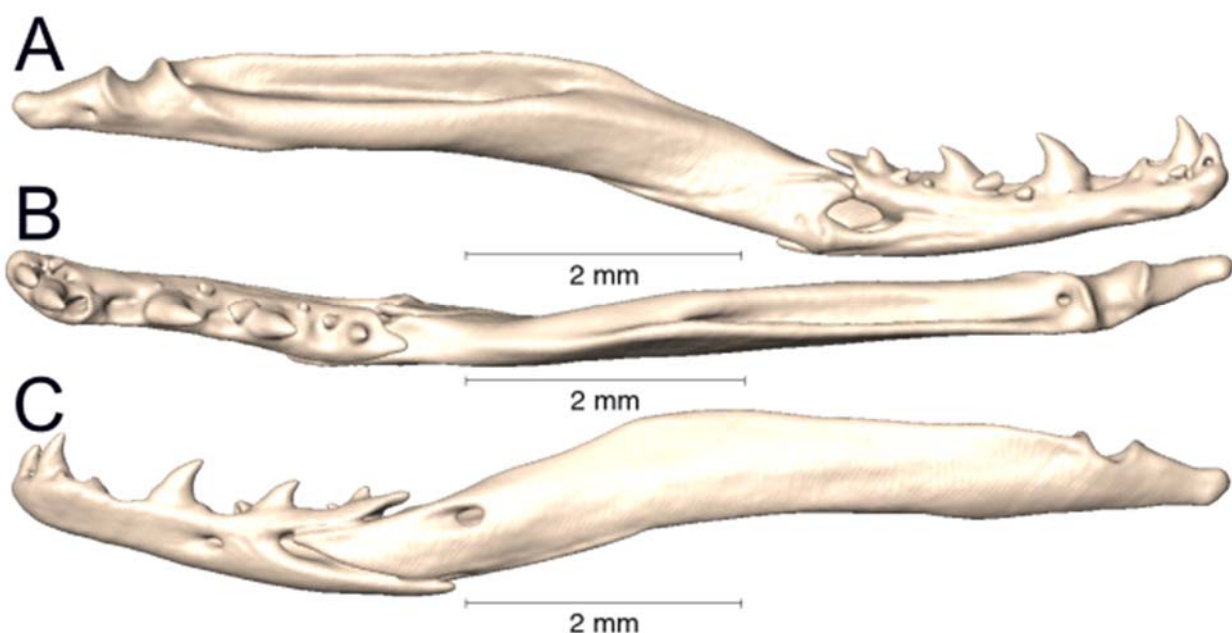
Supplemental Figure 3.27. Medial, dorsal, and lateral views (A-C, respectively) of the left lower jaw of *Laticauda colubrina* (UTA R-65800).



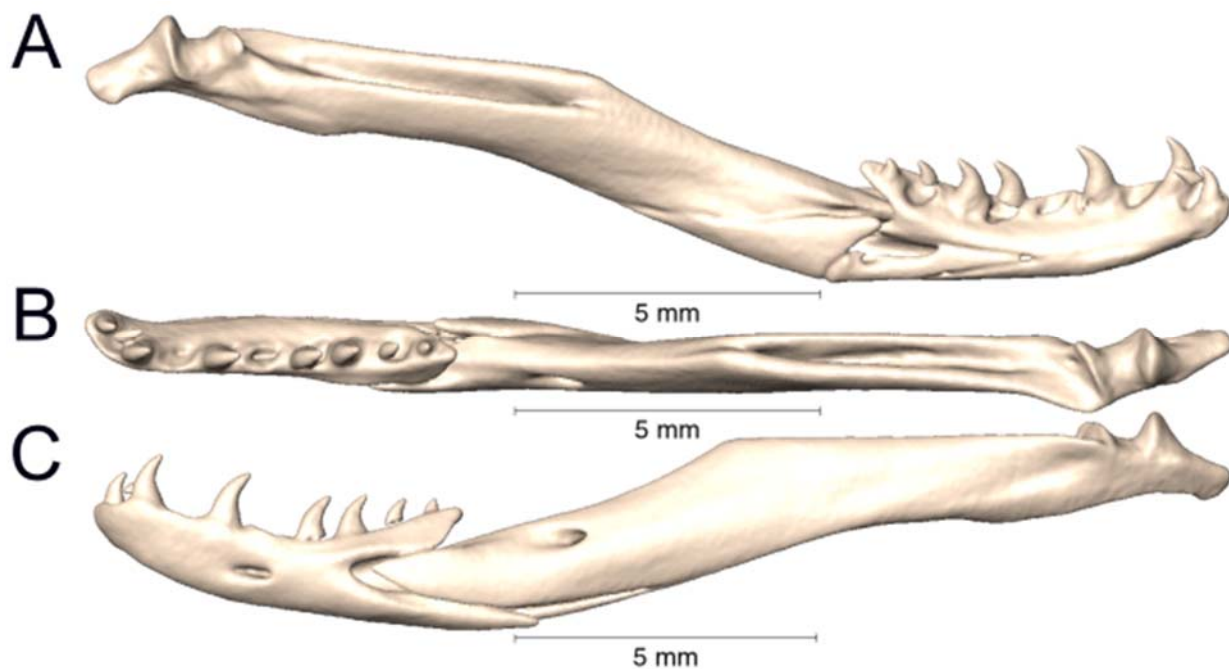
Supplemental Figure 3.28. Medial, dorsal, and lateral views (A-C, respectively) of the left lower jaw of *Laticauda laticauda* (UTA R-6355).



Supplemental Figure 3.29. Medial, dorsal, and lateral views (A-C, respectively) of the left lower jaw of *Micrelaps vaillanti* (CAS 169941).



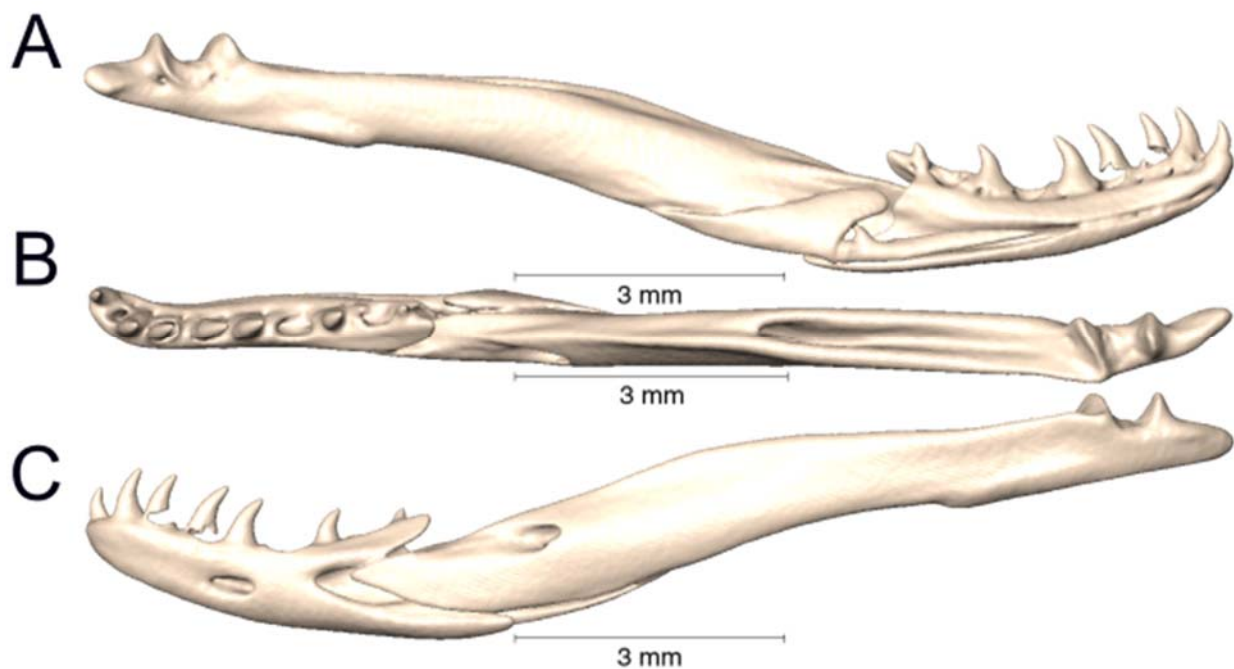
Supplemental Figure 3.30. Medial, dorsal, and lateral views (A-C, respectively) of the left lower jaw of *Micruroides euryxanthus* (UTA R-60734).



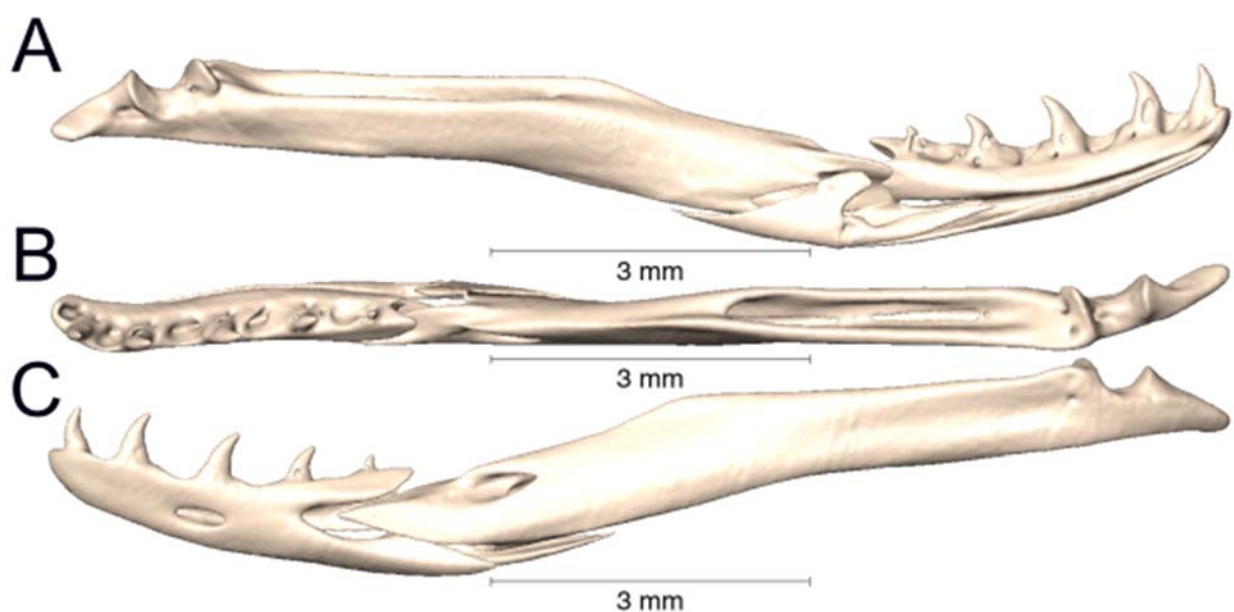
Supplemental Figure 3.31. Medial, dorsal, and lateral views (A-C, respectively) of the left lower jaw of *Micrurus alleni* (UTA R-60556).



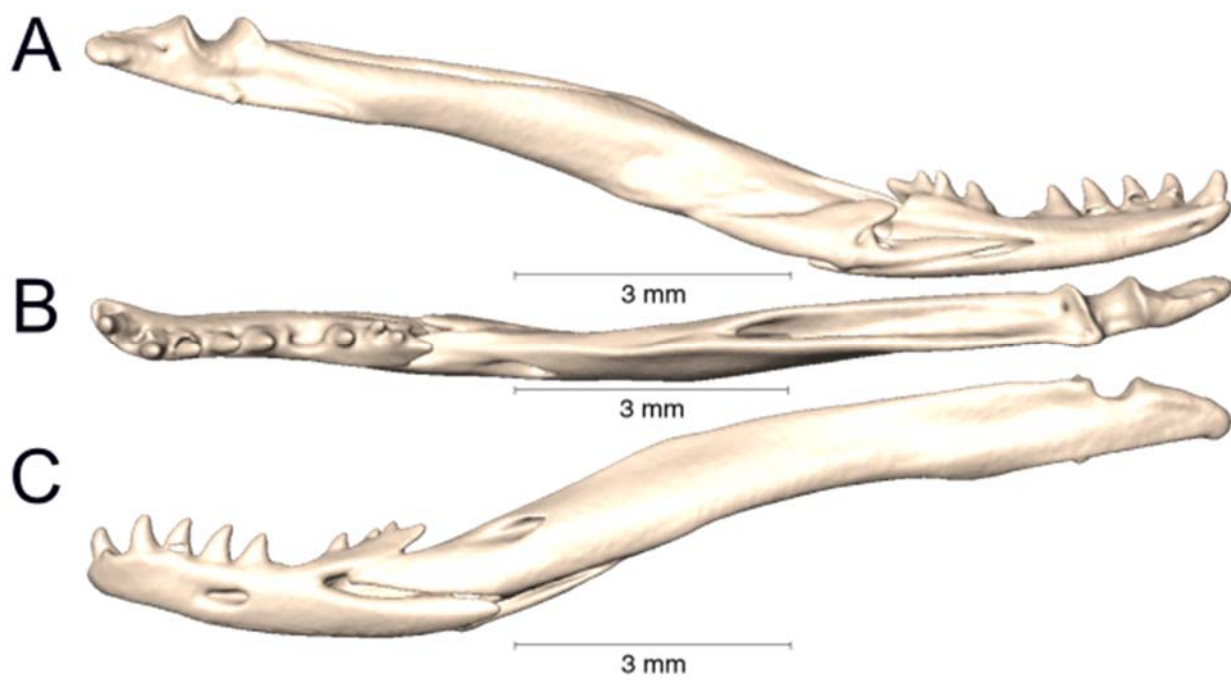
Supplemental Figure 3.32. Medial, dorsal, and lateral views (A-C, respectively) of the left lower jaw of *Micrurus anchoralis* (UTA R-55945).



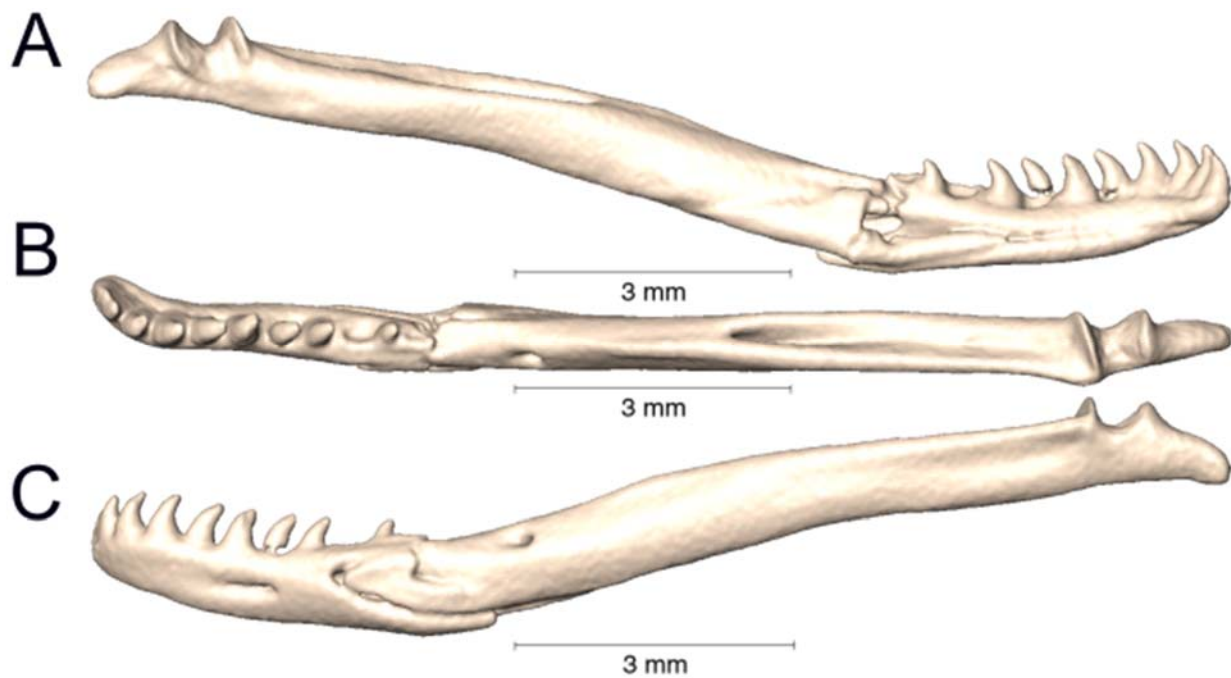
Supplemental Figure 3.33. Medial, dorsal, and lateral views (A-C, respectively) of the left lower jaw of *Micrurus apiatus* (UTA R-39267).



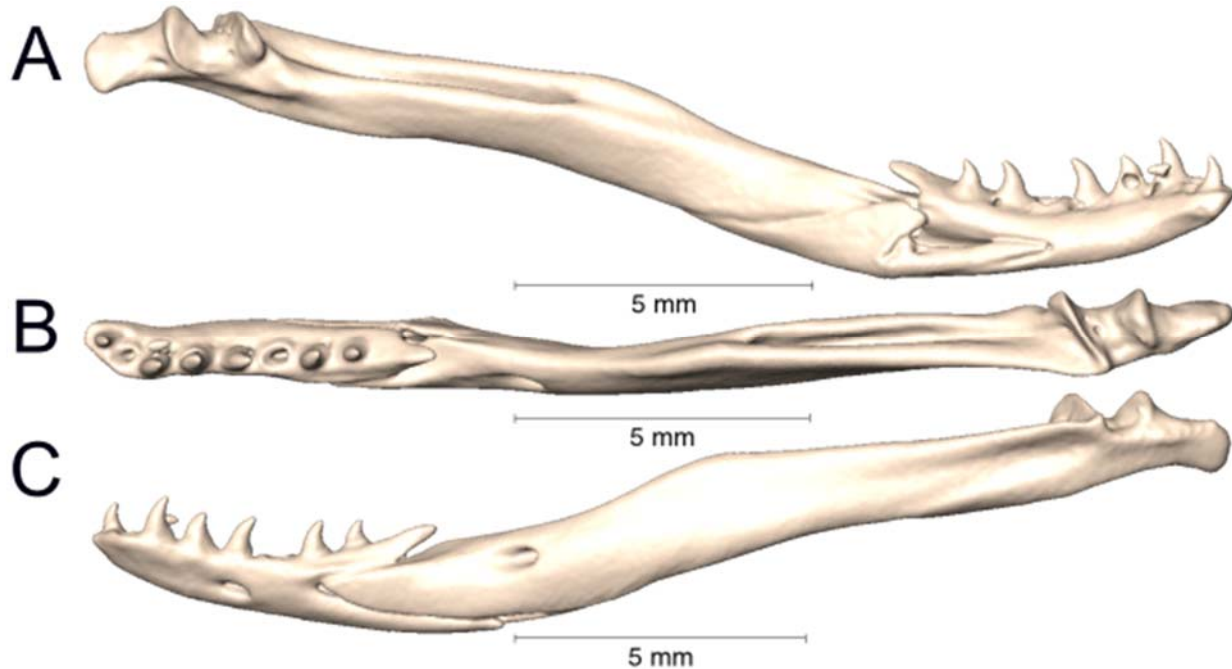
Supplemental Figure 3.34. Medial, dorsal, and lateral views (A-C, respectively) of the left lower jaw of *Micrurus apiatus* (UTA R-39554).



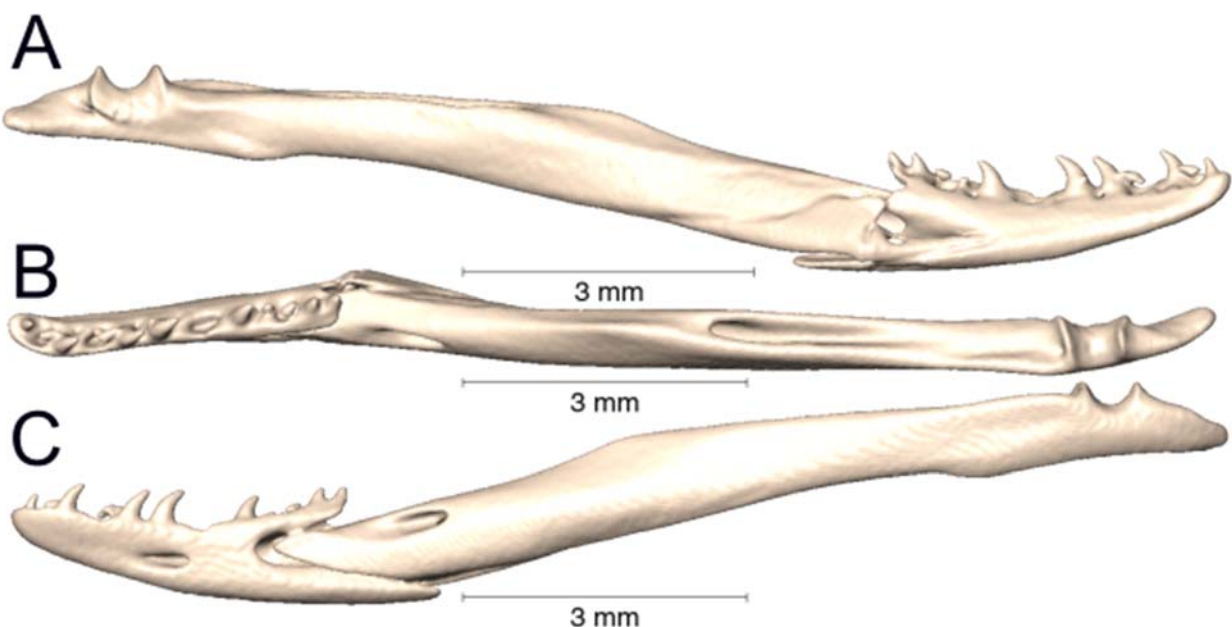
Supplemental Figure 3.35. Medial, dorsal, and lateral views (A-C, respectively) of the left lower jaw of *Micrurus apiatus* (UTA R-53450).



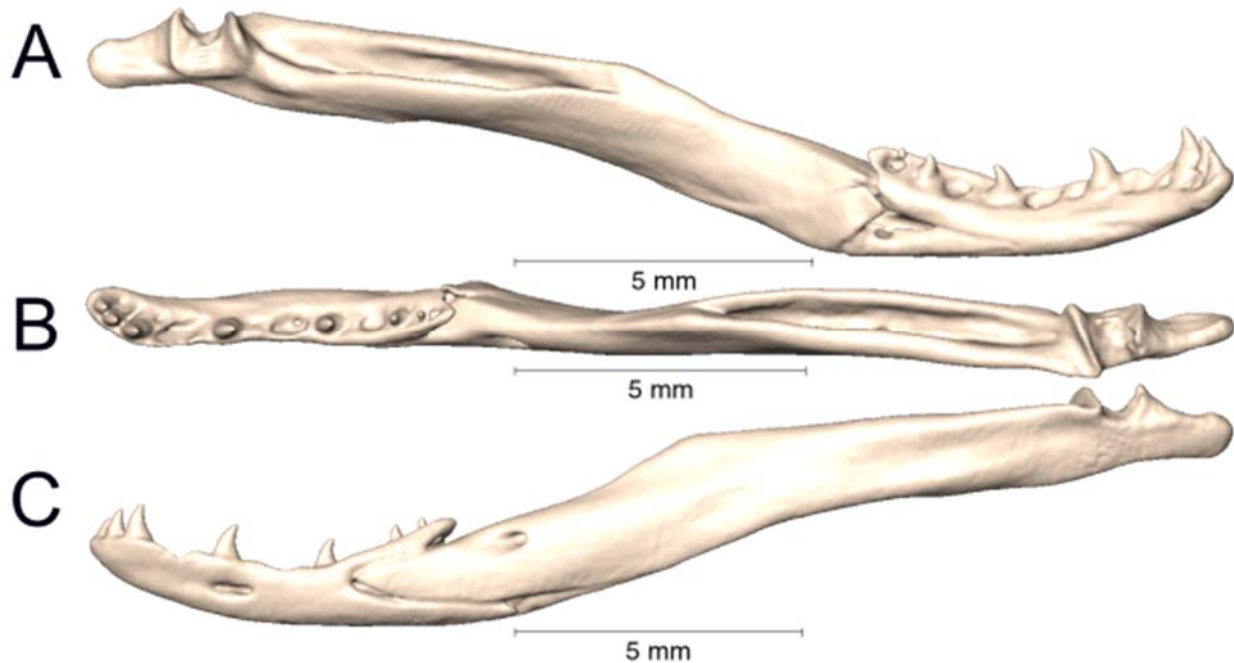
Supplemental Figure 3.36. Medial, dorsal, and lateral views (A-C, respectively) of the left lower jaw of *Micrurus bocourti* (UTA R-58145).



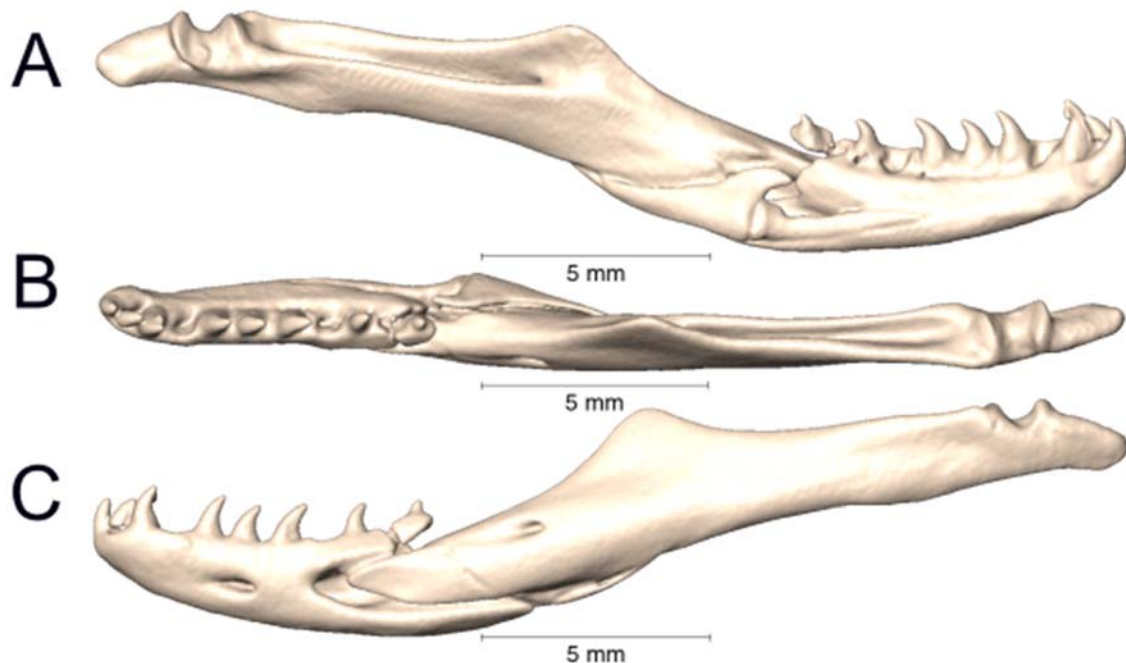
Supplemental Figure 3.37. Medial, dorsal, and lateral views (A-C, respectively) of the left lower jaw of *Micrurus diastema* (UTA R-52565).



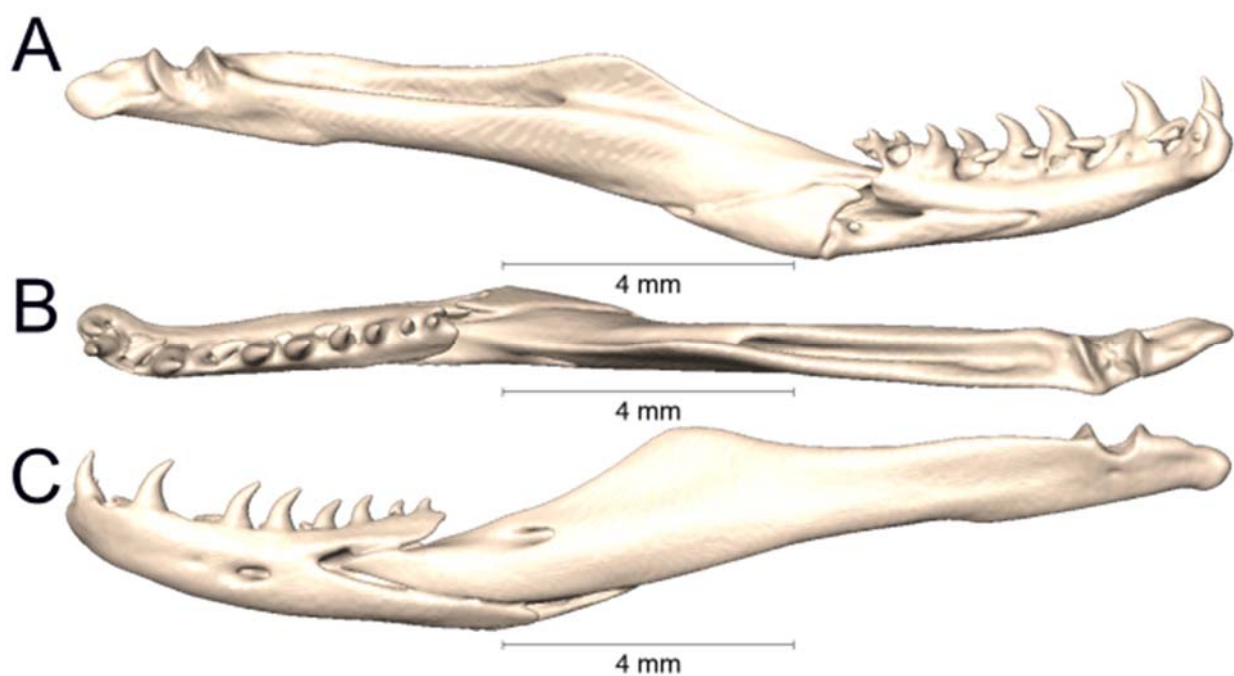
Supplemental Figure 3.38. Medial, dorsal, and lateral views (A-C, respectively) of the left lower jaw of *Micrurus disssoleucus* (UTA R-54184).



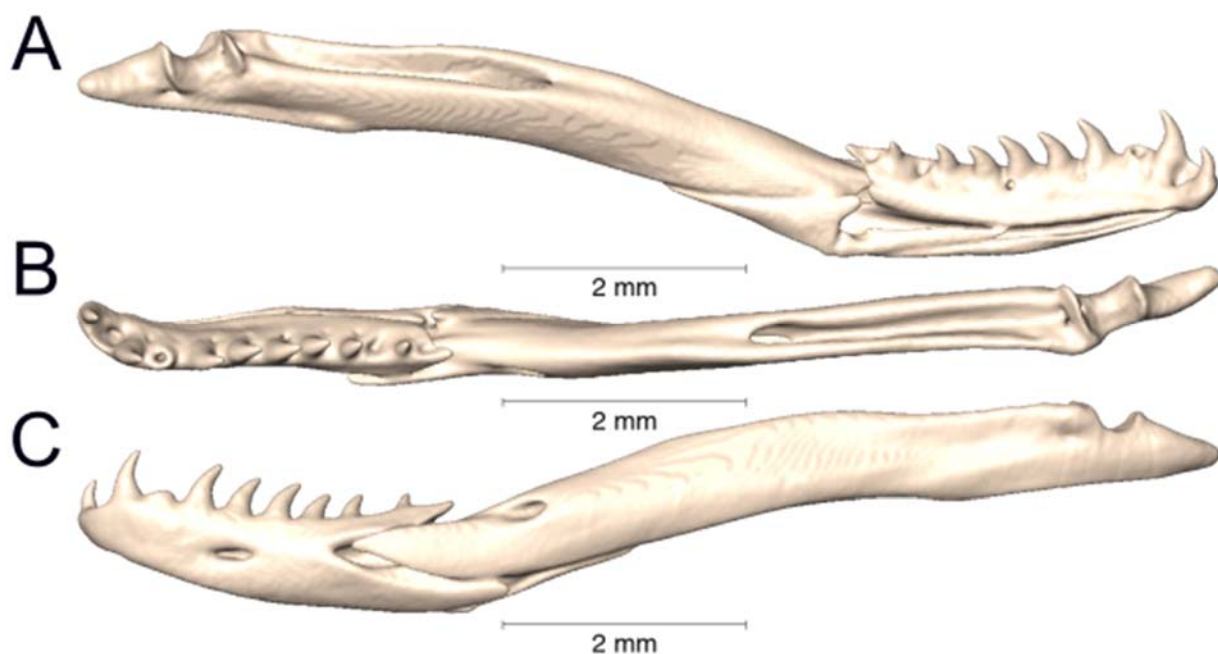
Supplemental Figure 3.39. Medial, dorsal, and lateral views (A-C, respectively) of the left lower jaw of *Micrurus distans* (UTA R-14471).



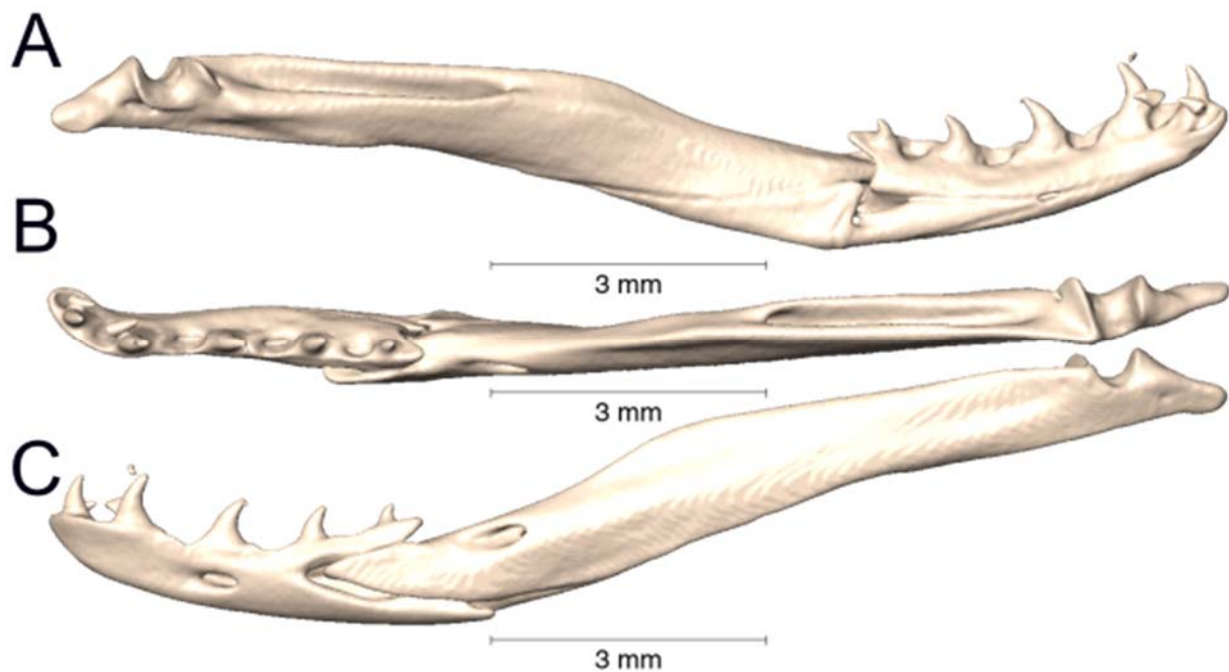
Supplemental Figure 3.40. Medial, dorsal, and lateral views (A-C, respectively) of the left lower jaw of *Micrurus diutius* (UTA R-20756).



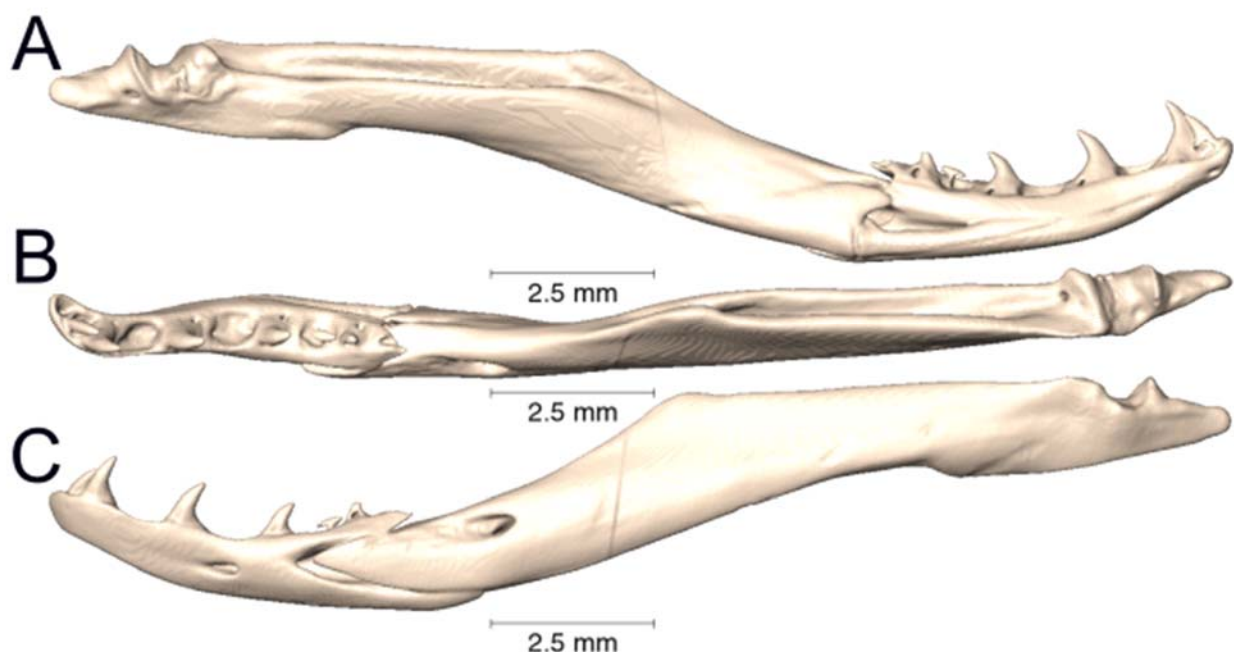
Supplemental Figure 3.41. Medial, dorsal, and lateral views (A-C, respectively) of the left lower jaw of *Micrurus diutius* (UTA R-54182).



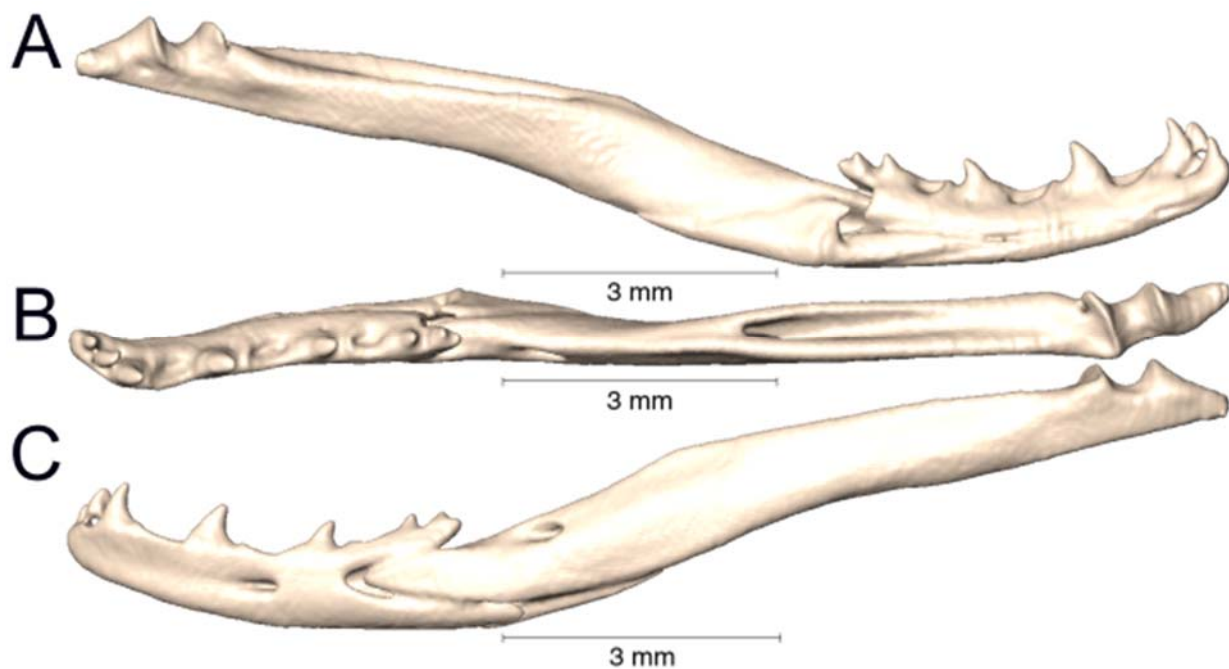
Supplemental Figure 3.42. Medial, dorsal, and lateral views (A-C, respectively) of the left lower jaw of *Micrurus dumerilii* (AMNH 35951).



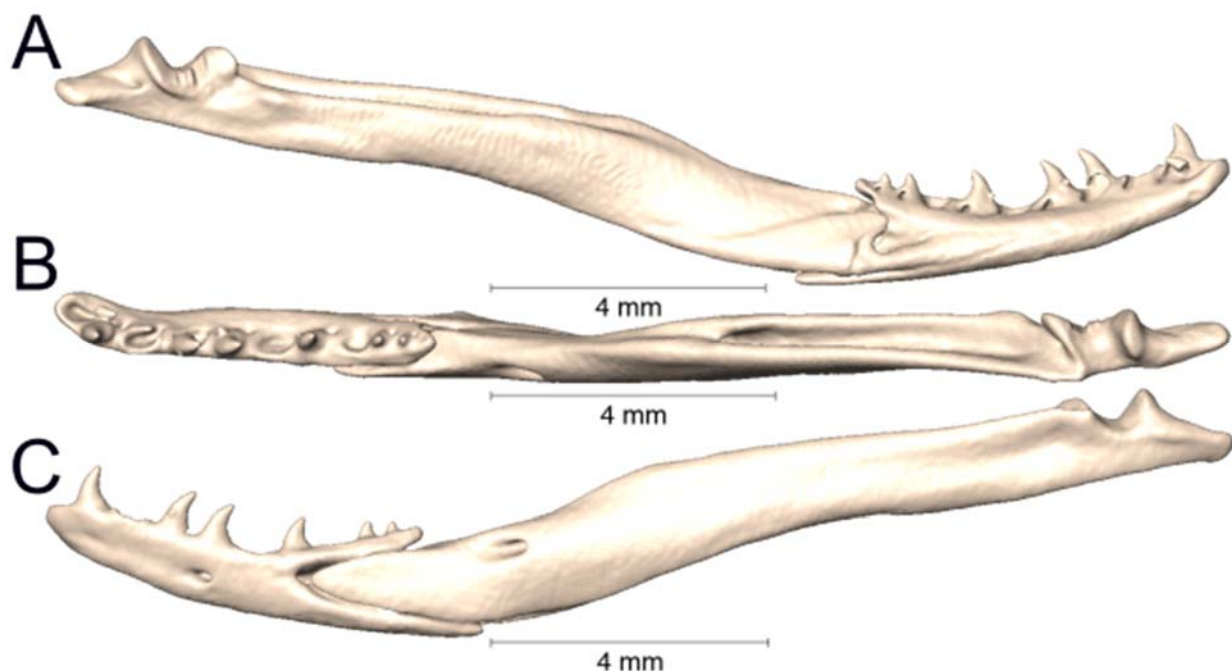
Supplemental Figure 3.43. Medial, dorsal, and lateral views (A-C, respectively) of the left lower jaw of *Micrurus elegans* (MZFC 18819).



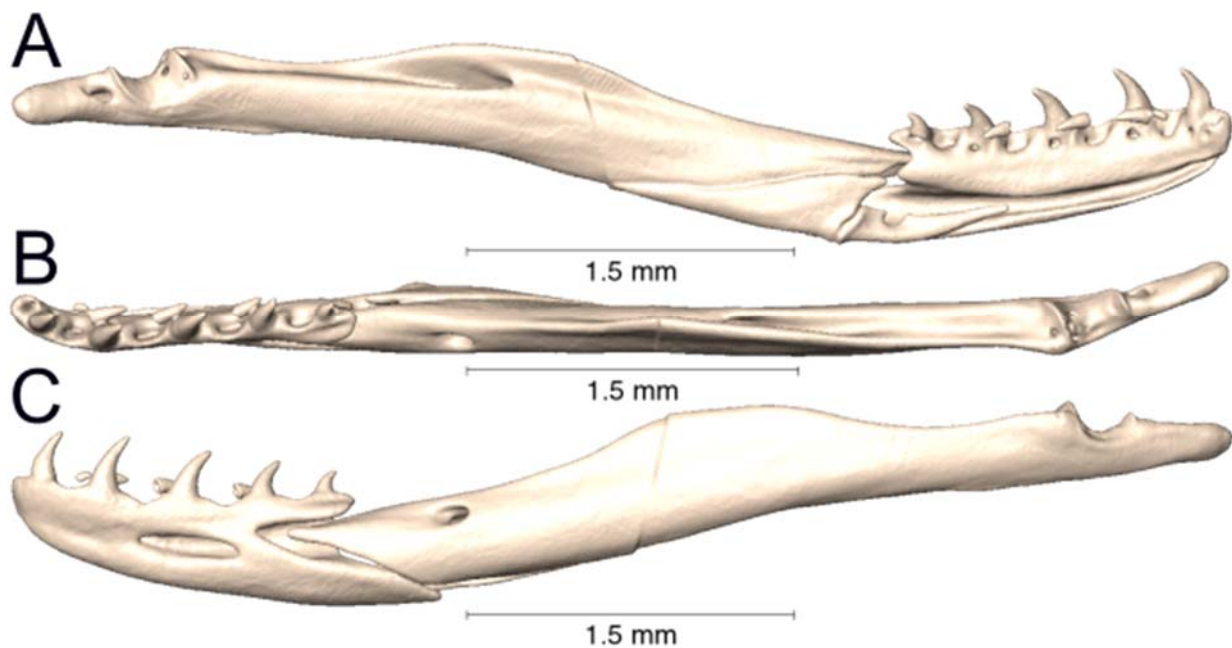
Supplemental Figure 3.44. Medial, dorsal, and lateral views (A-C, respectively) of the left lower jaw of *Micrurus elegans veraepacis* (UTA R-7072).



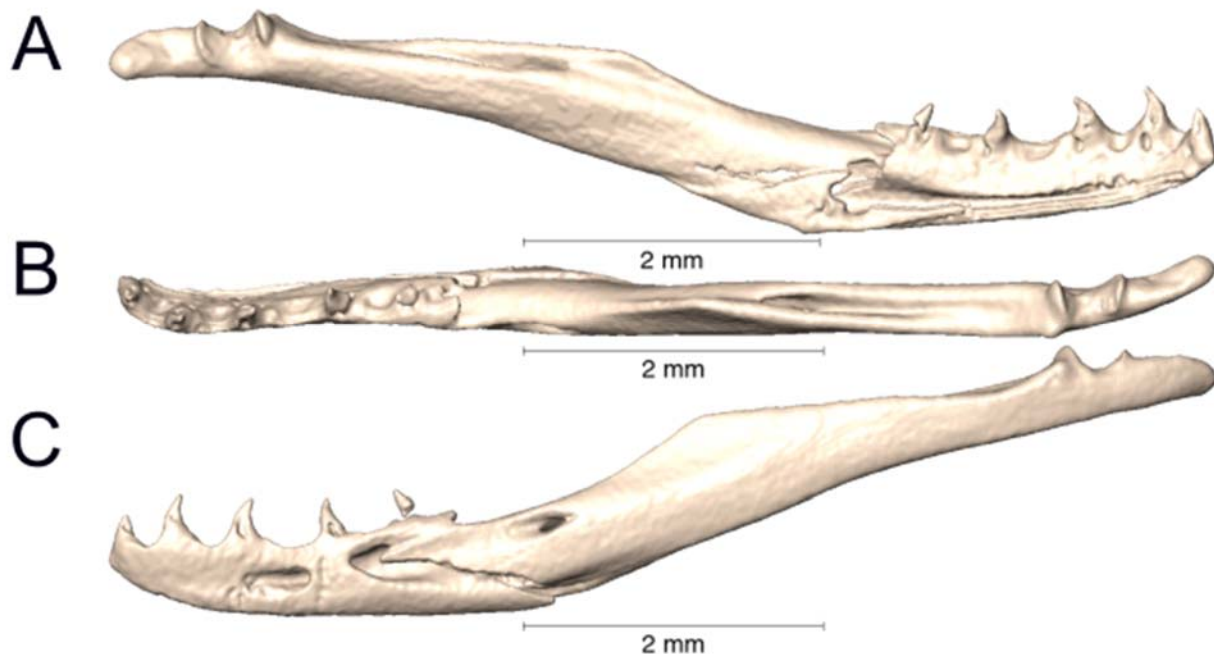
Supplemental Figure 3.45. Medial, dorsal, and lateral views (A-C, respectively) of the left lower jaw of *Micrurus elegans veraepacis* (UTA R-58869).



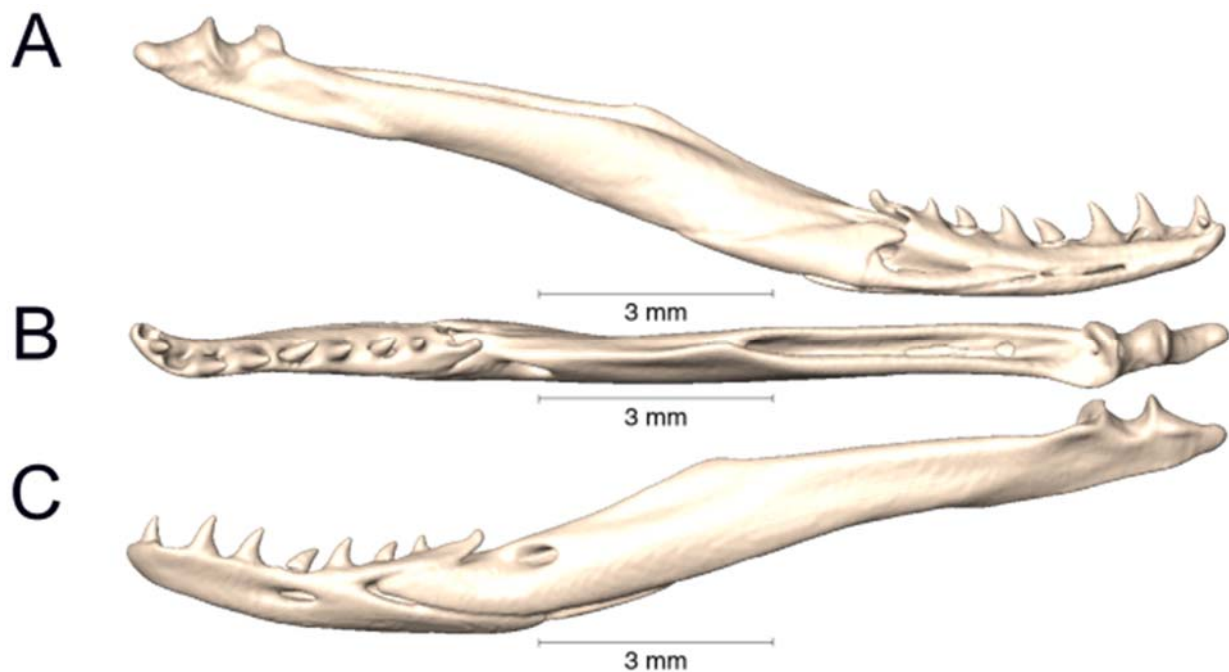
Supplemental Figure 3.46. Medial, dorsal, and lateral views (A-C, respectively) of the left lower jaw of *Micrurus ephippifer* (UTA R-64863).



Supplemental Figure 3.47. Medial, dorsal, and lateral views (A-C, respectively) of the left lower jaw of *Micrurus filiformis* (UTA R-3423).



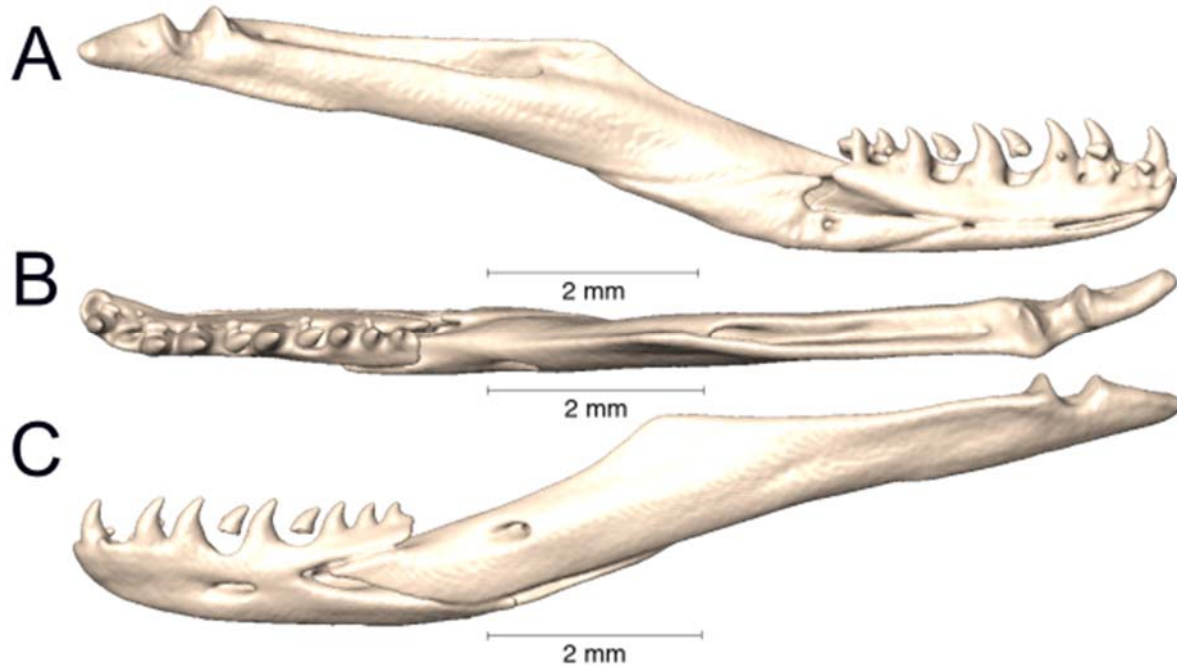
Supplemental Figure 3.48. Medial, dorsal, and lateral views (A-C, respectively) of the left lower jaw of *Micrurus filiformis* (UTA R-65836).



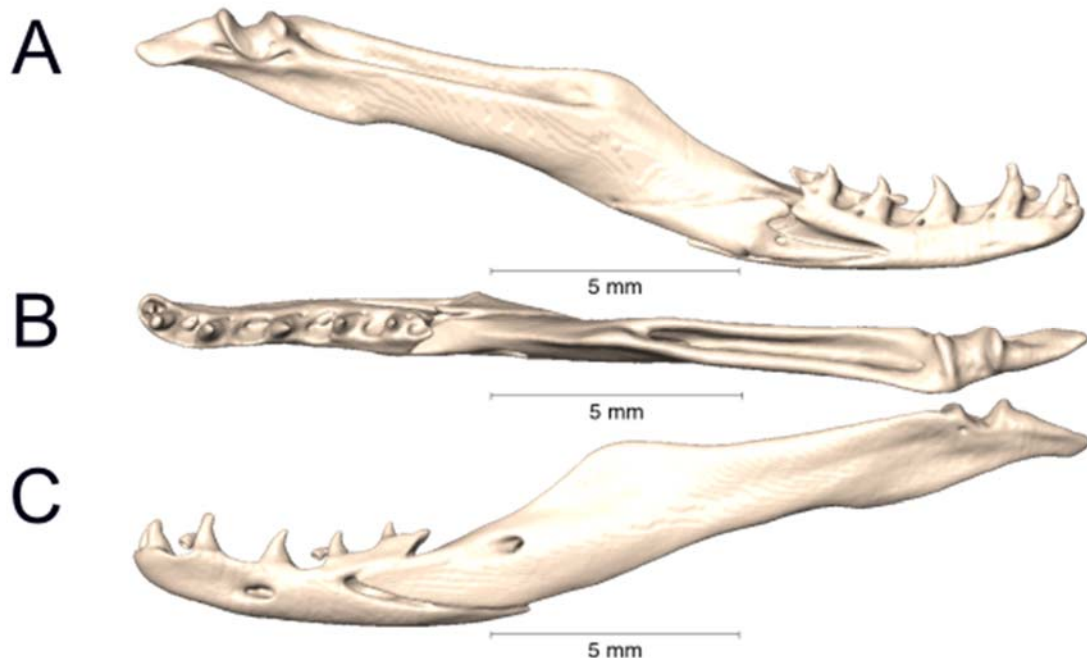
Supplemental Figure 3.49. Medial, dorsal, and lateral views (A-C, respectively) of the left lower jaw of *Micrurus fulvius* (UTA R-61632).



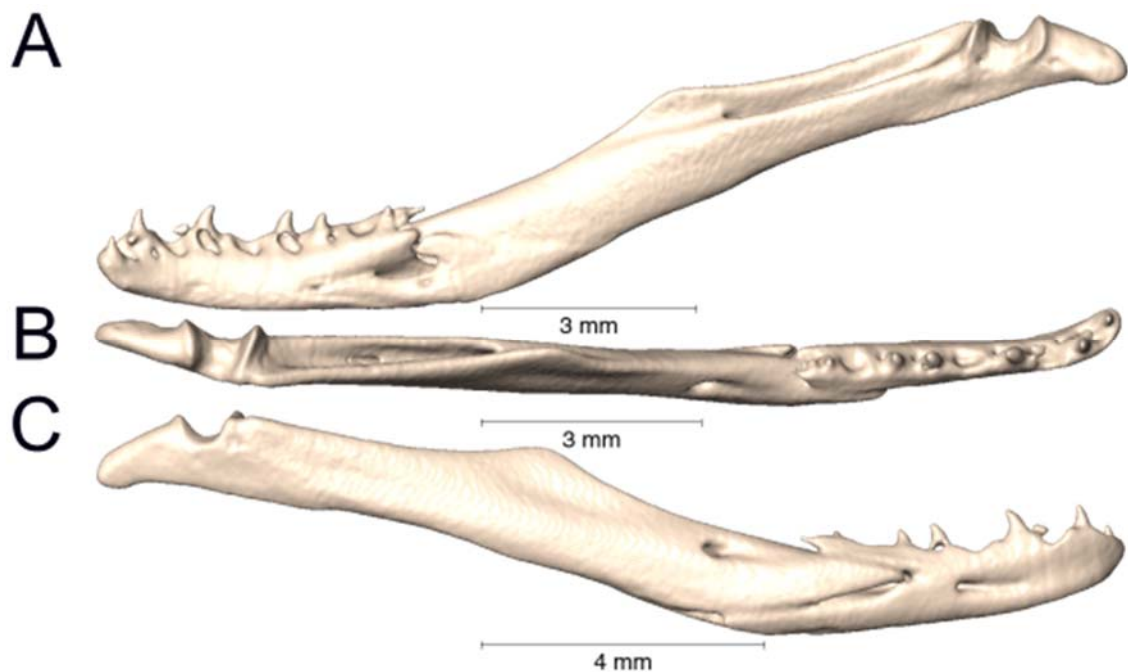
Supplemental Figure 3.50. Medial, dorsal, and lateral views (A-C, respectively) of the left lower jaw of *Micrurus helleri* (UTA R-38005).



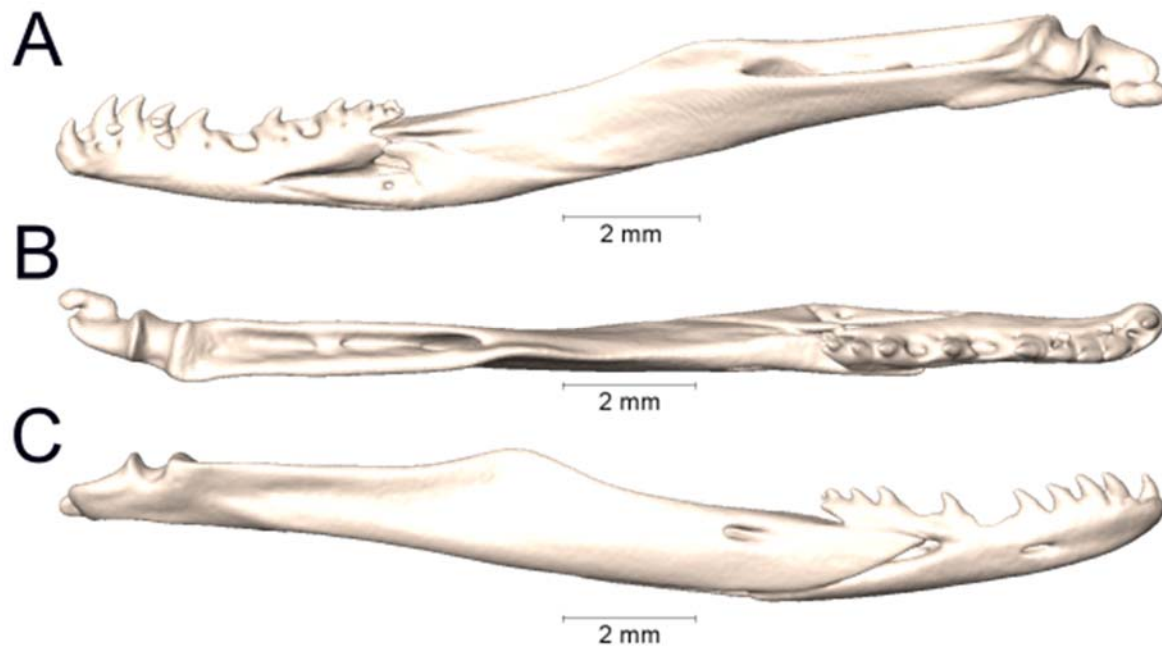
Supplemental Figure 3.51. Medial, dorsal, and lateral views (A-C, respectively) of the left lower jaw of *Micrurus helleri* (UTA R-65841).



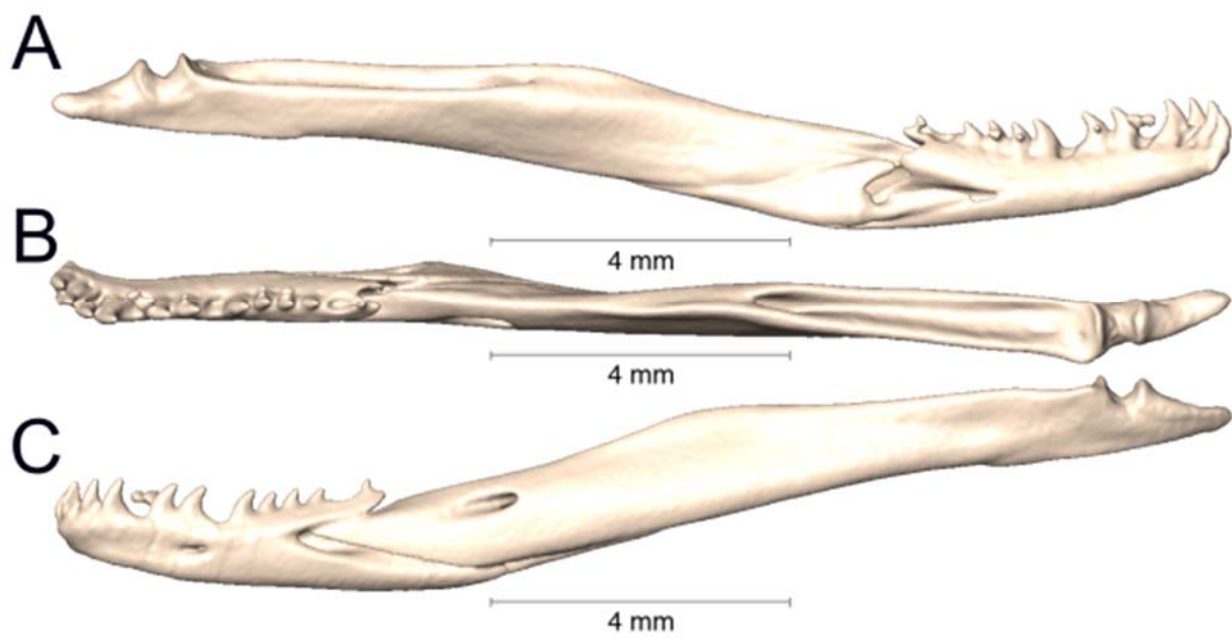
Supplemental Figure 3.52. Medial, dorsal, and lateral views (A-C, respectively) of the left lower jaw of *Micrurus hemprichii* (UTA R-9683).



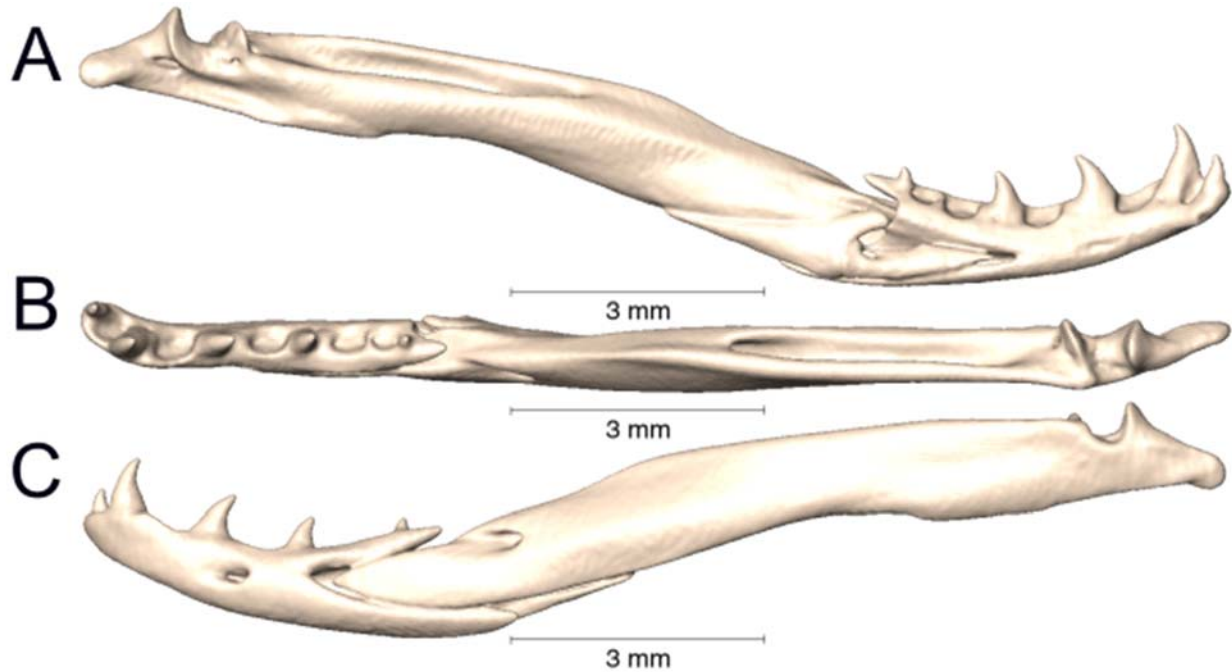
Supplemental Figure 3.53. Medial, dorsal, and lateral views (A-C, respectively) of the right lower jaw of *Micrurus hemprichii* (UTA R-29997).



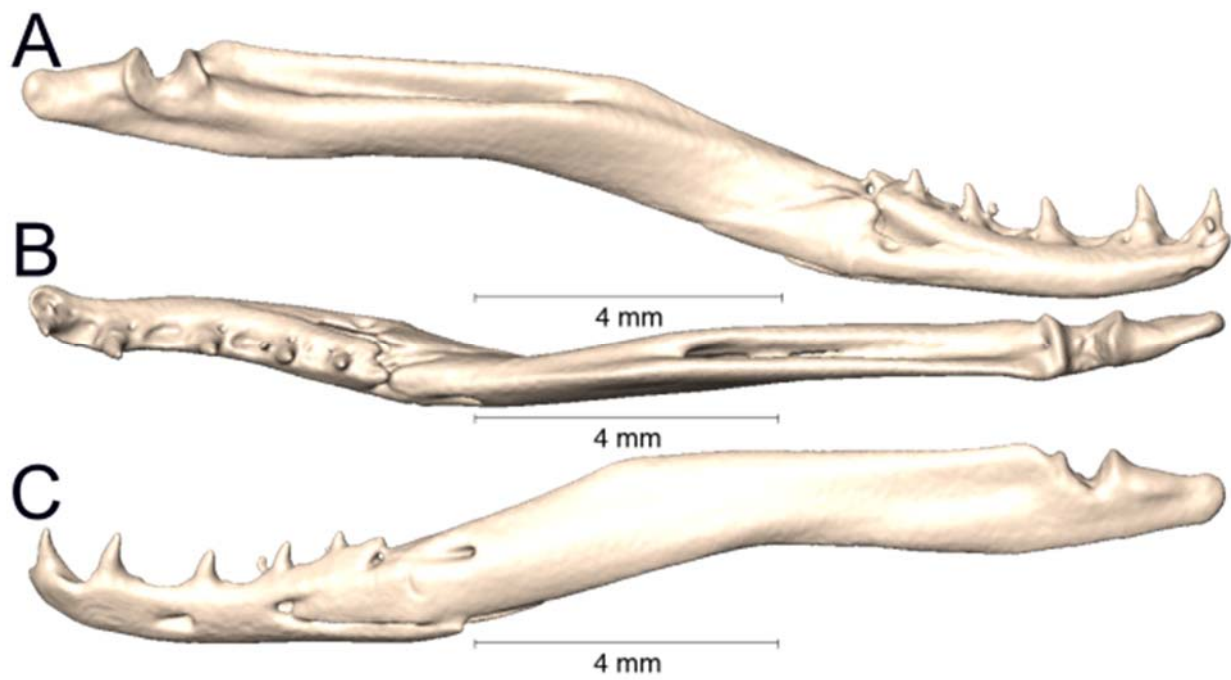
Supplemental Figure 3.54. Medial, dorsal, and lateral views (A-C, respectively) of the right lower jaw of *Micrurus isozonus* (UTA R-3951).



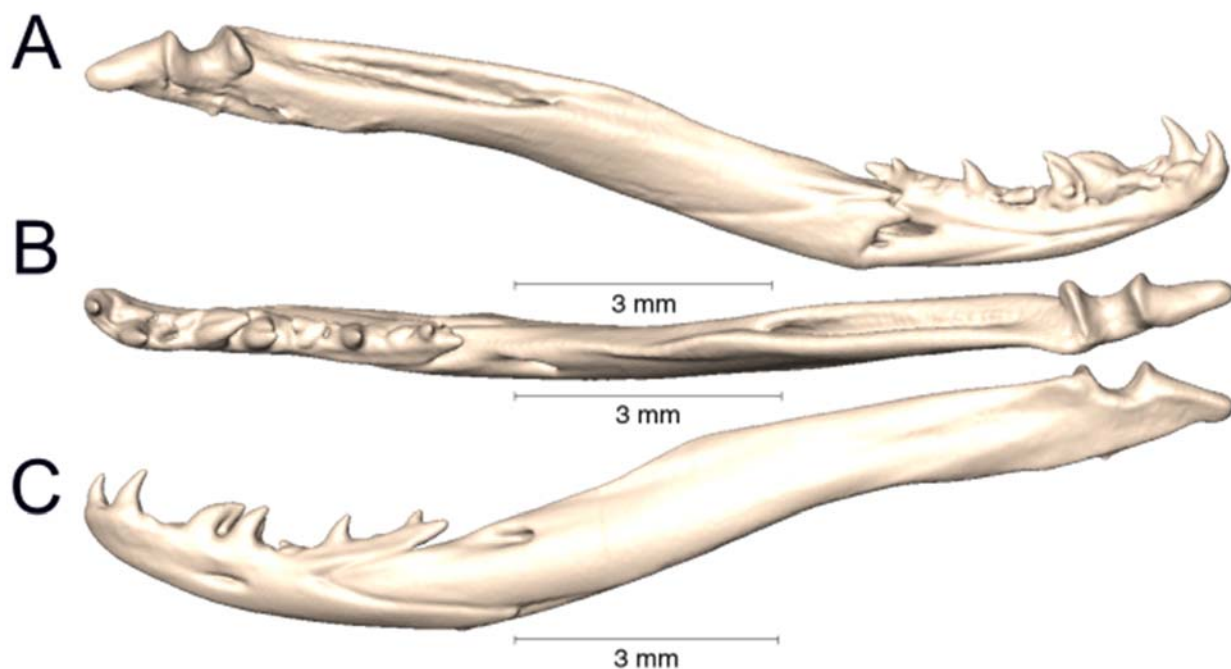
Supplemental Figure 3.55. Medial, dorsal, and lateral views (A-C, respectively) of the left lower jaw of *Micrurus isozonus* (UTA R-22589).



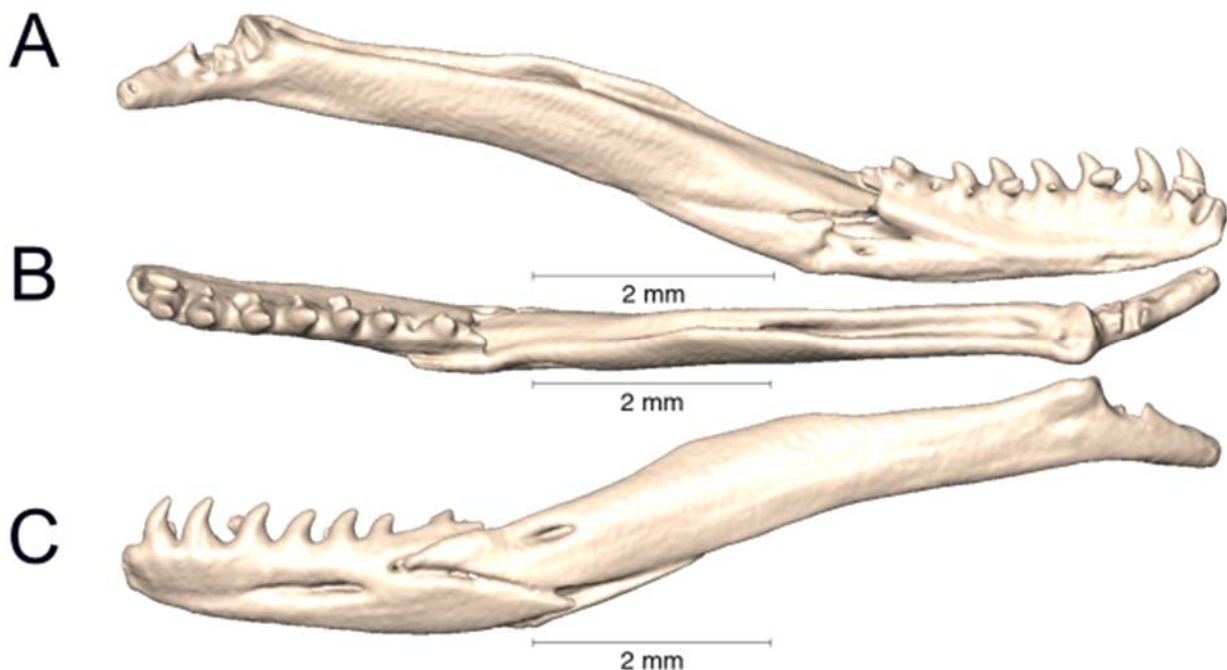
Supplemental Figure 3.56. Medial, dorsal, and lateral views (A-C, respectively) of the left lower jaw of *Micrurus laticollaris* (UTA R-52559).



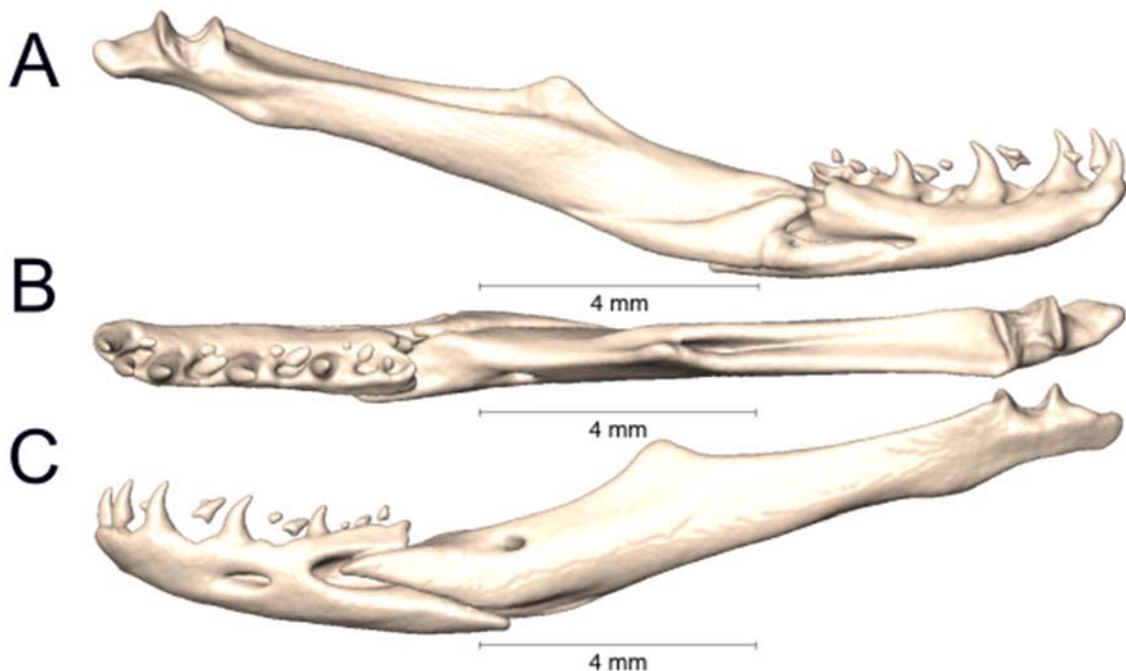
Supplemental Figure 3.57. Medial, dorsal, and lateral views (A-C, respectively) of the left lower jaw of *Micrurus laticollaris* (UTA R-57562).



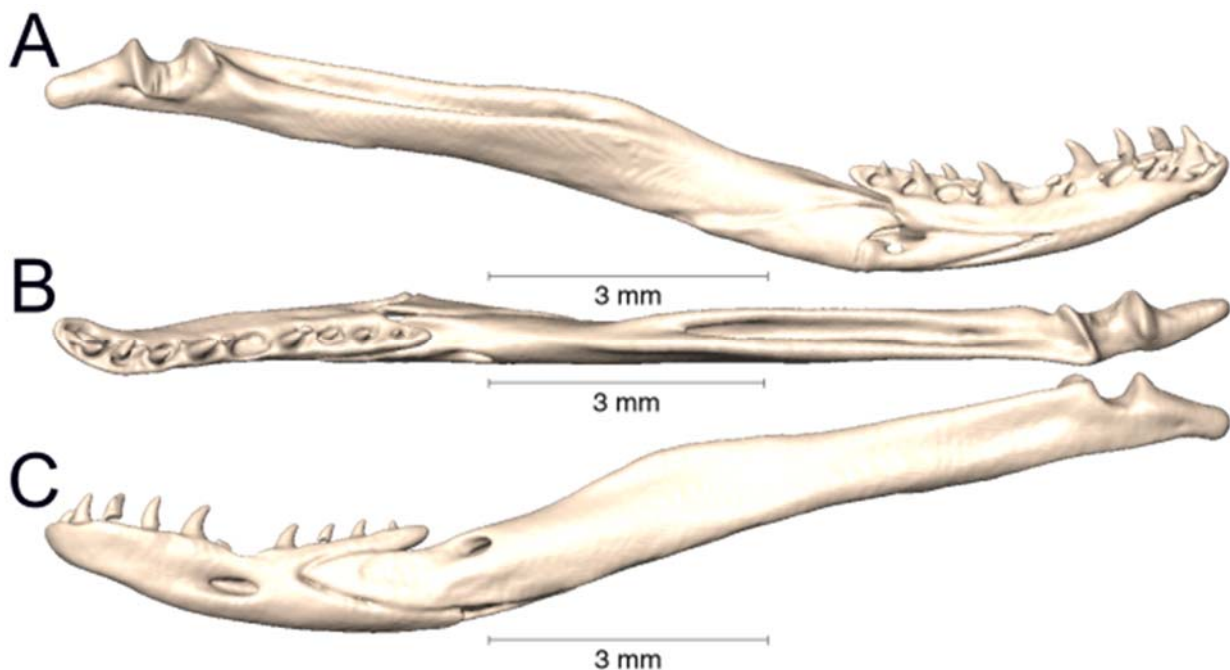
Supplemental Figure 3.58. Medial, dorsal, and lateral views (A-C, respectively) of the left lower jaw of *Micrurus latifasciatus* (UTA R-4606).



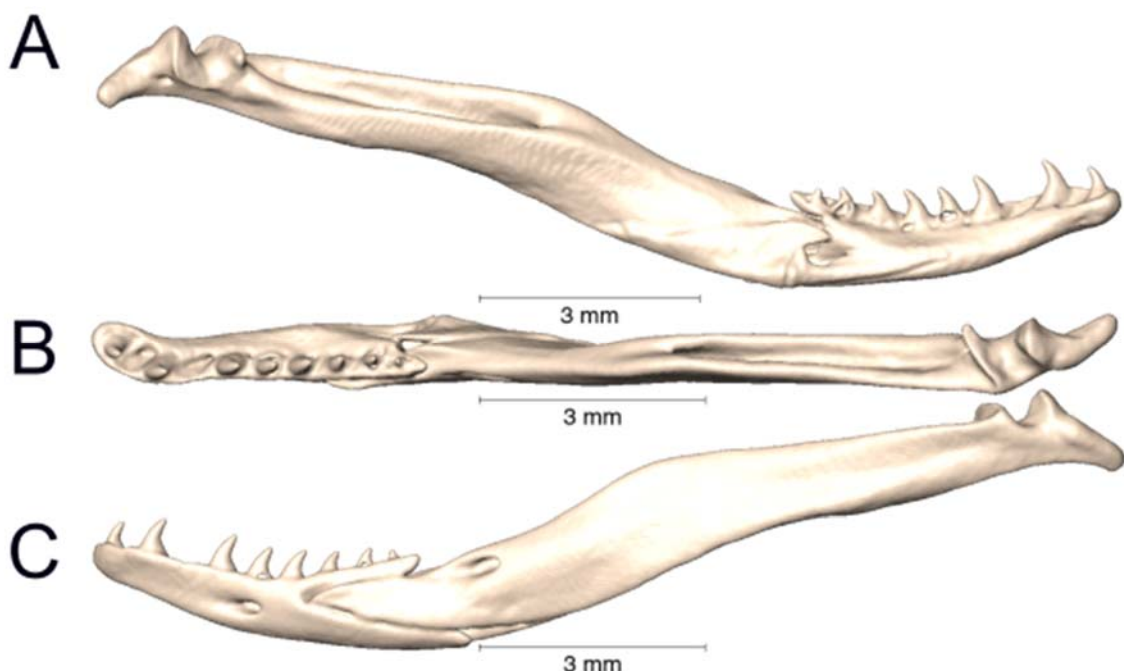
Supplemental Figure 3.59. Medial, dorsal, and lateral views (A-C, respectively) of the left lower jaw of *Micrurus lemniscatus* cf. *helleri* (UTA R-34563).



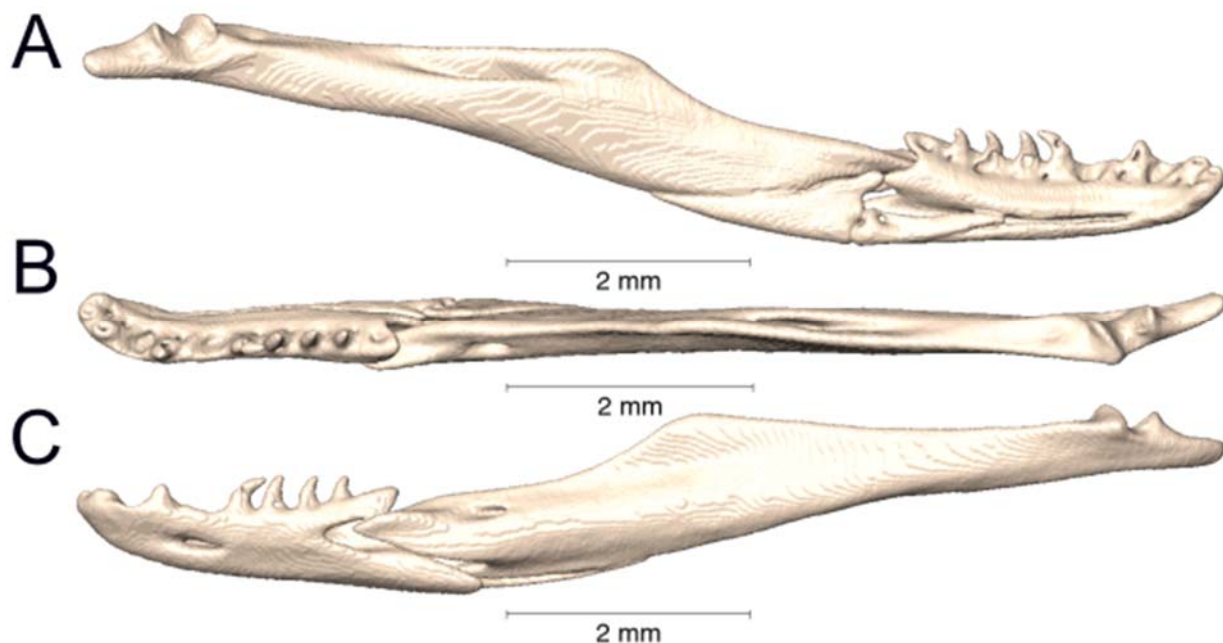
Supplemental Figure 3.60. Medial, dorsal, and lateral views (A-C, respectively) of the left lower jaw of *Micrurus lemniscatus* cf. *helleri* (UTA R-65803).



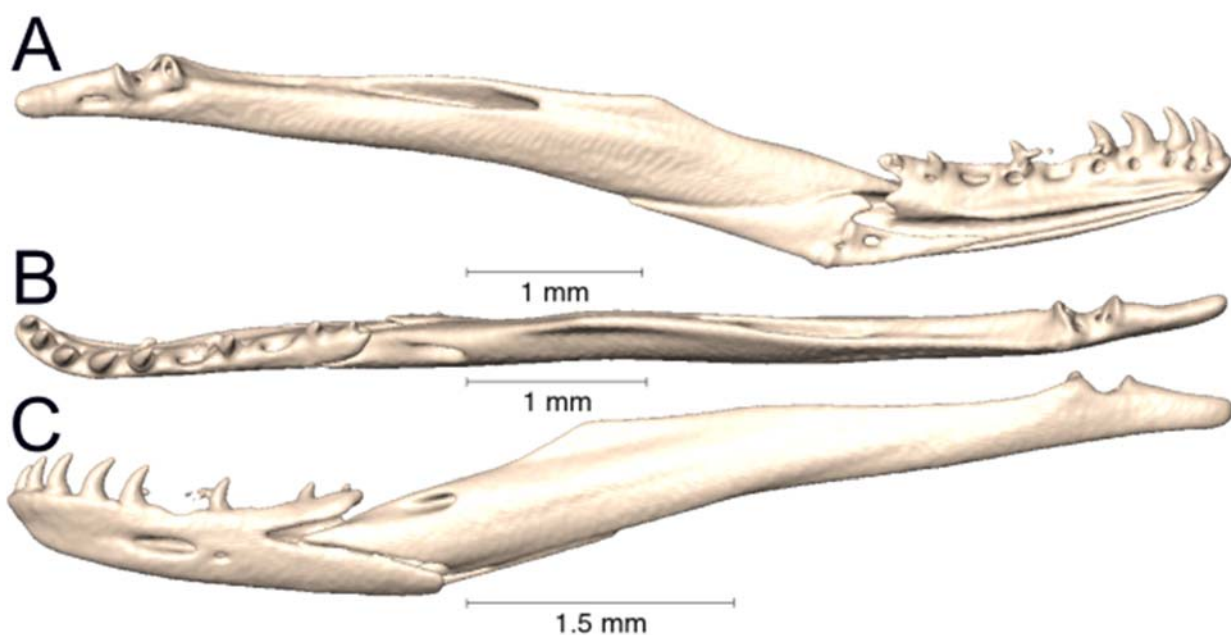
Supplemental Figure 3.61. Medial, dorsal, and lateral views (A-C, respectively) of the left lower jaw of *Micrurus limbatus* (UTA R-64852).



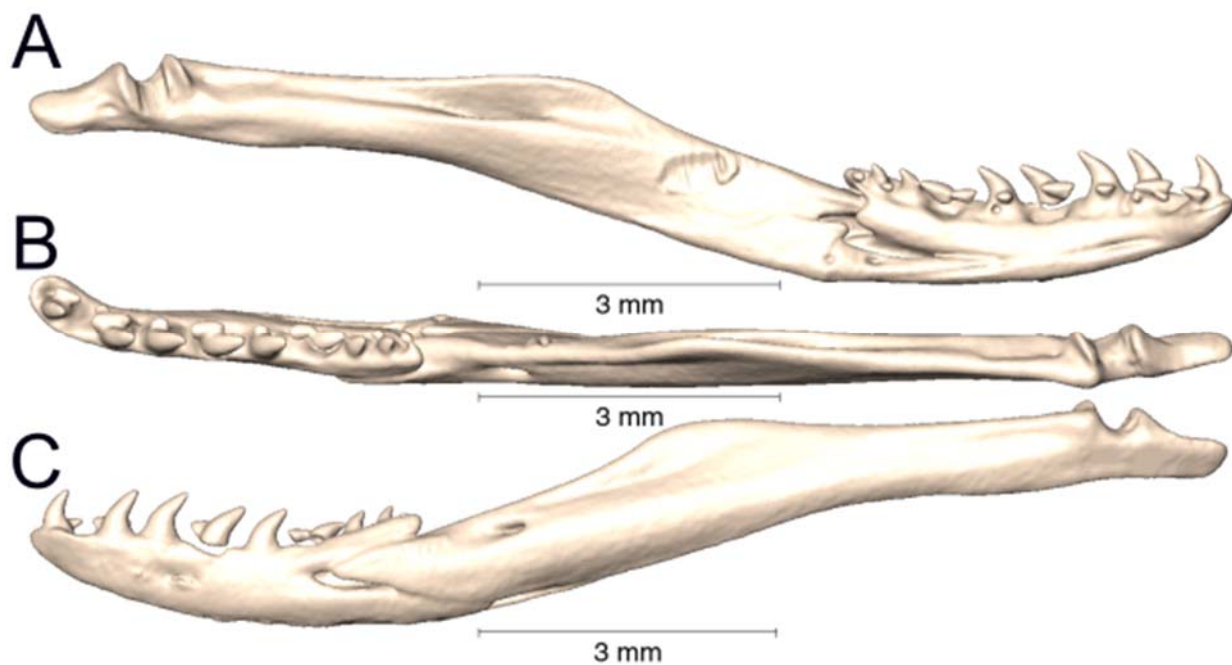
Supplemental Figure 3.62. Medial, dorsal, and lateral views (A-C, respectively) of the left lower jaw of *Micrurus limbatus* (UTA R-64899).



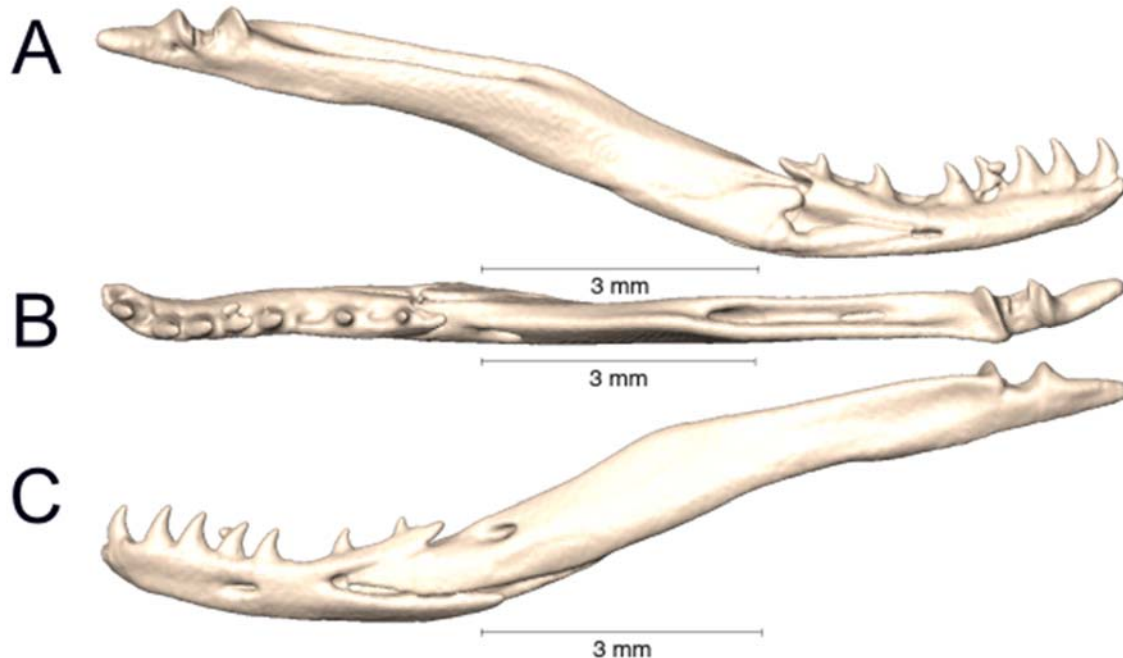
Supplemental Figure 3.63. Medial, dorsal, and lateral views (A-C, respectively) of the left lower jaw of *Micrurus melanotus* (AMNH 35934).



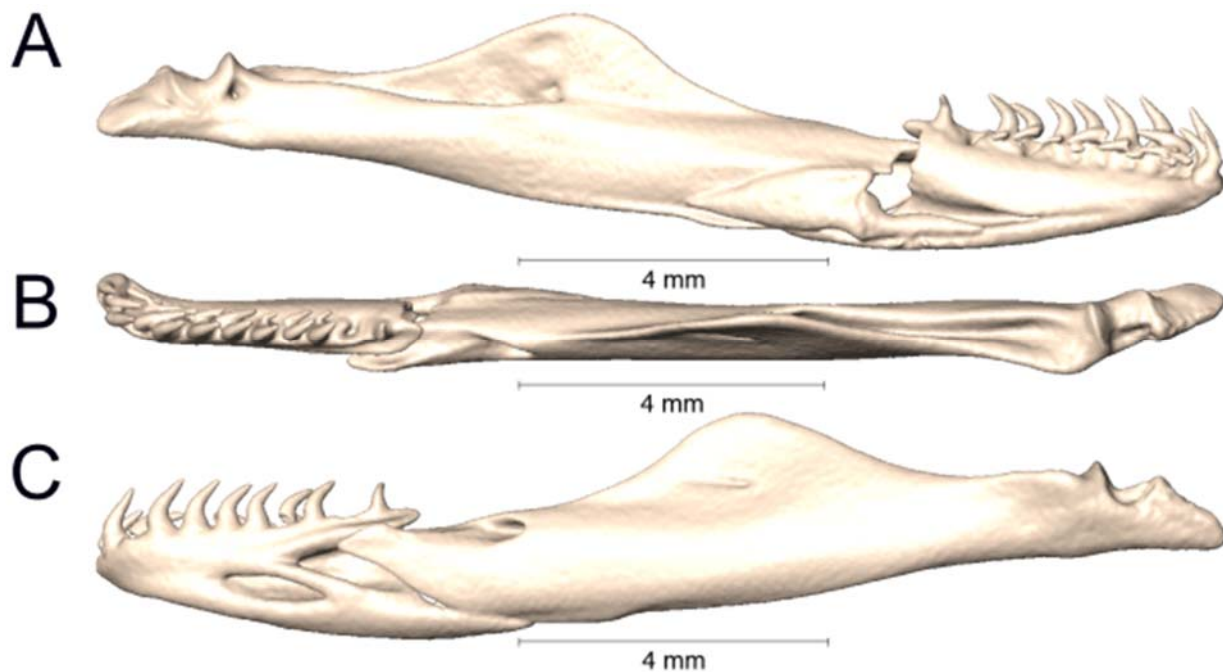
Supplemental Figure 3.64. Medial, dorsal, and lateral views (A-C, respectively) of the left lower jaw of *Micrurus melanotus* (UTA R-22582).



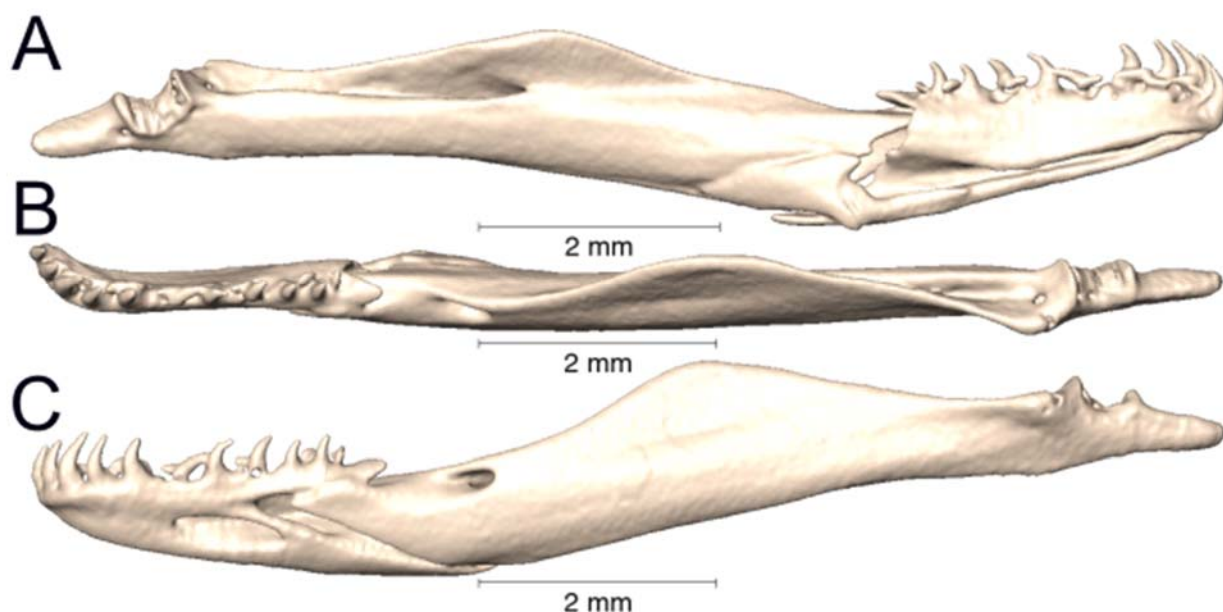
Supplemental Figure 3.65. Medial, dorsal, and lateral views (A-C, respectively) of the left lower jaw of *Micrurus mipartitus* (UTA R-54187).



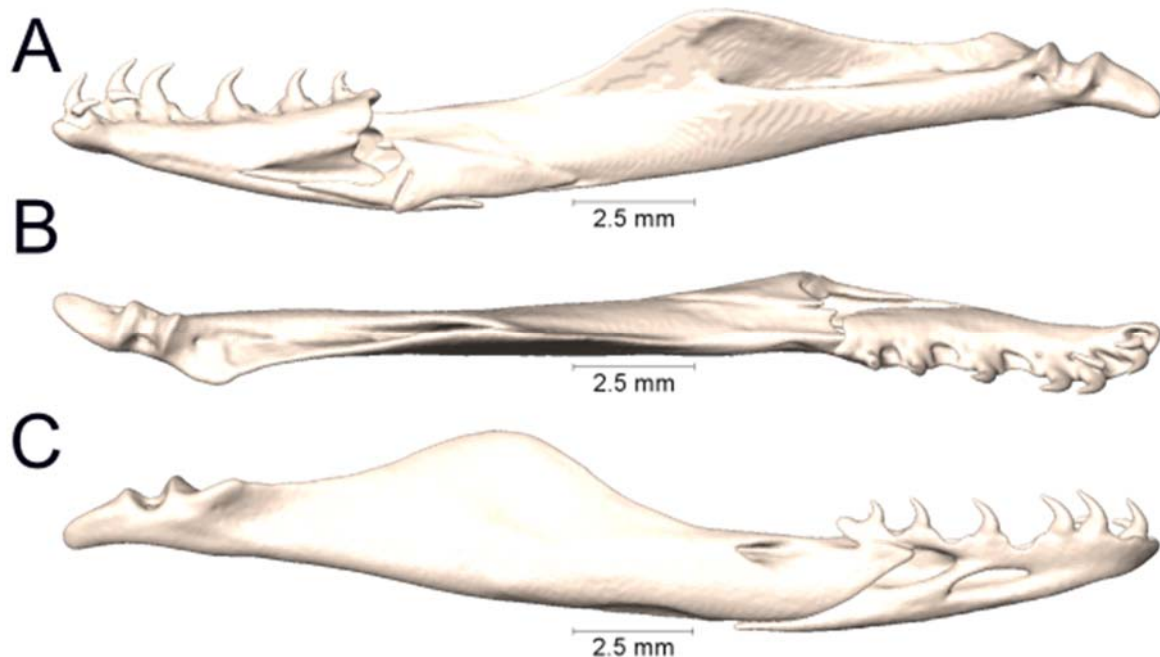
Supplemental Figure 3.66. Medial, dorsal, and lateral views (A-C, respectively) of the left lower jaw of *Micrurus mosquitensis* (UTA R-12919).



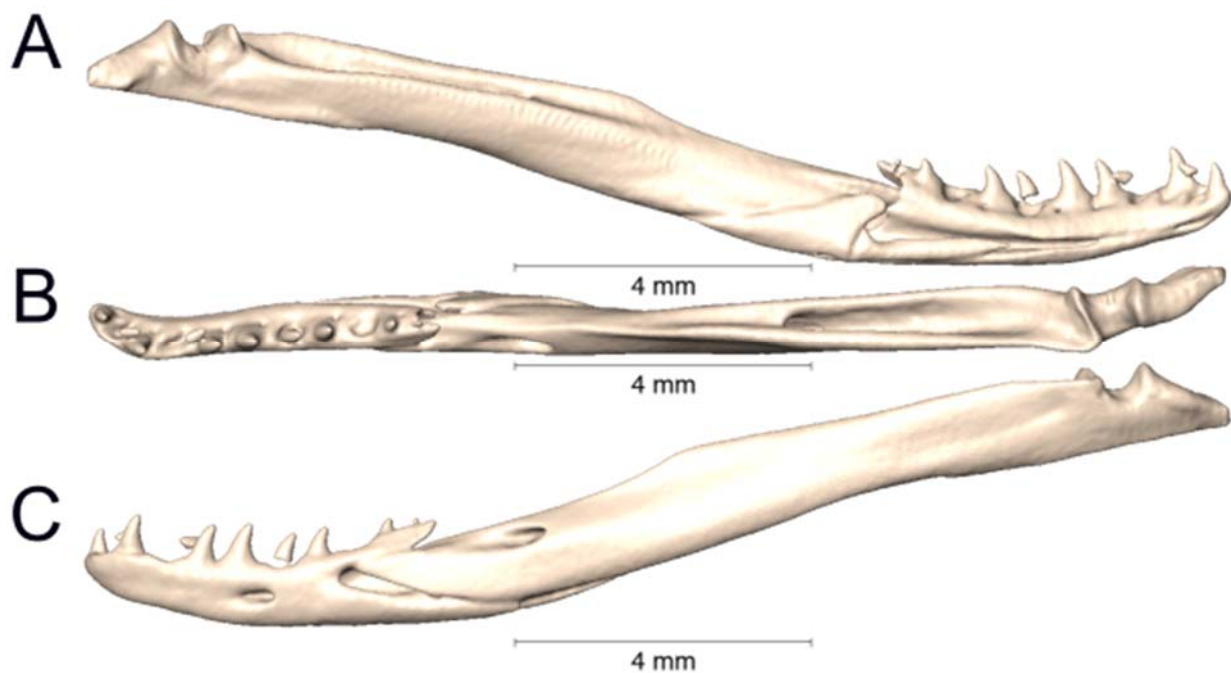
Supplemental Figure 3.67. Medial, dorsal, and lateral views (A-C, respectively) of the left lower jaw of *Micrurus nattereri* (UTA R-54175).



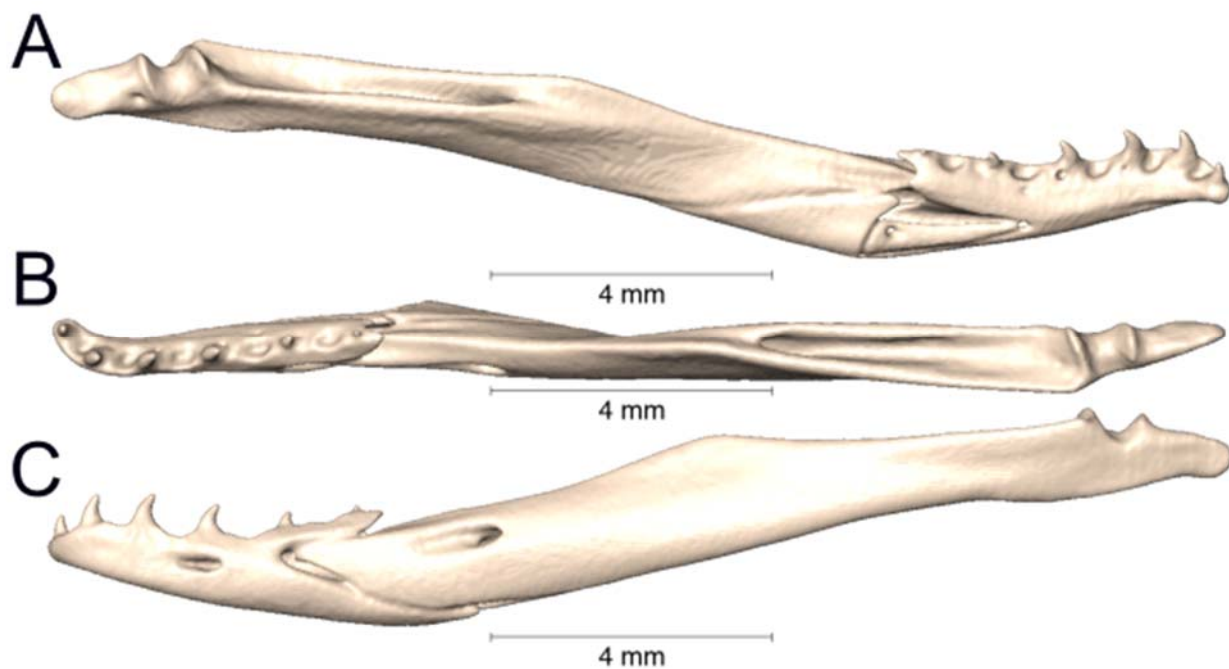
Supplemental Figure 3.68. Medial, dorsal, and lateral views (A-C, respectively) of the left lower jaw of *Micrurus nattereri* (UTA R-55086).



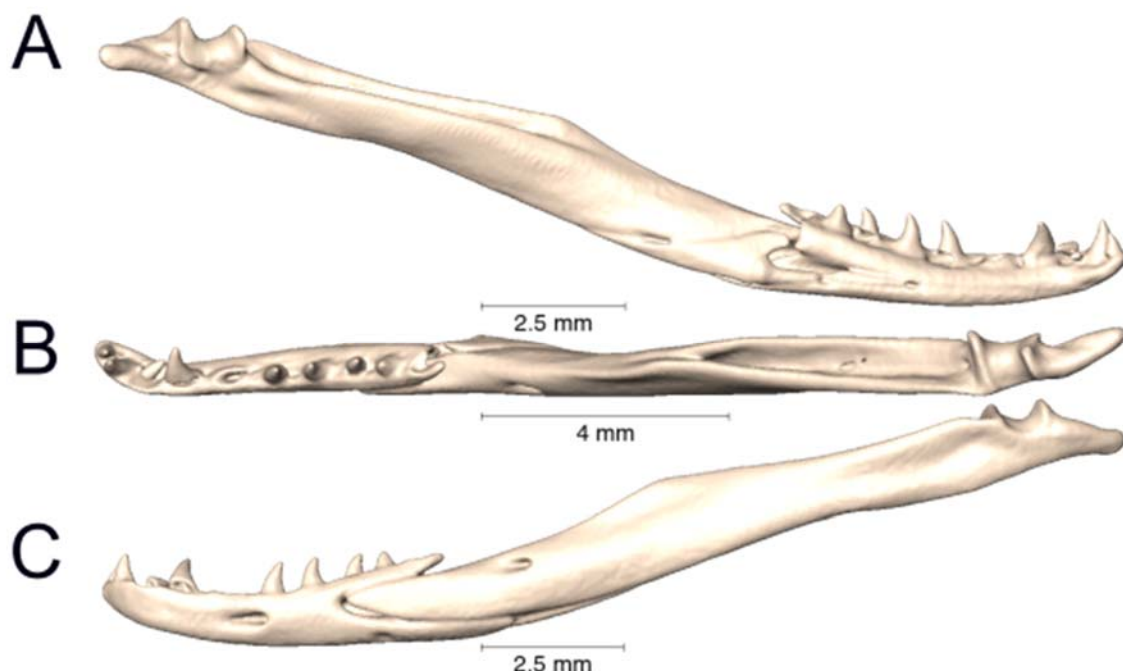
Supplemental Figure 3.69. Medial, dorsal, and lateral views (A-C, respectively) of the right lower jaw of *Micrurus nattereri* (UTA R-60727).



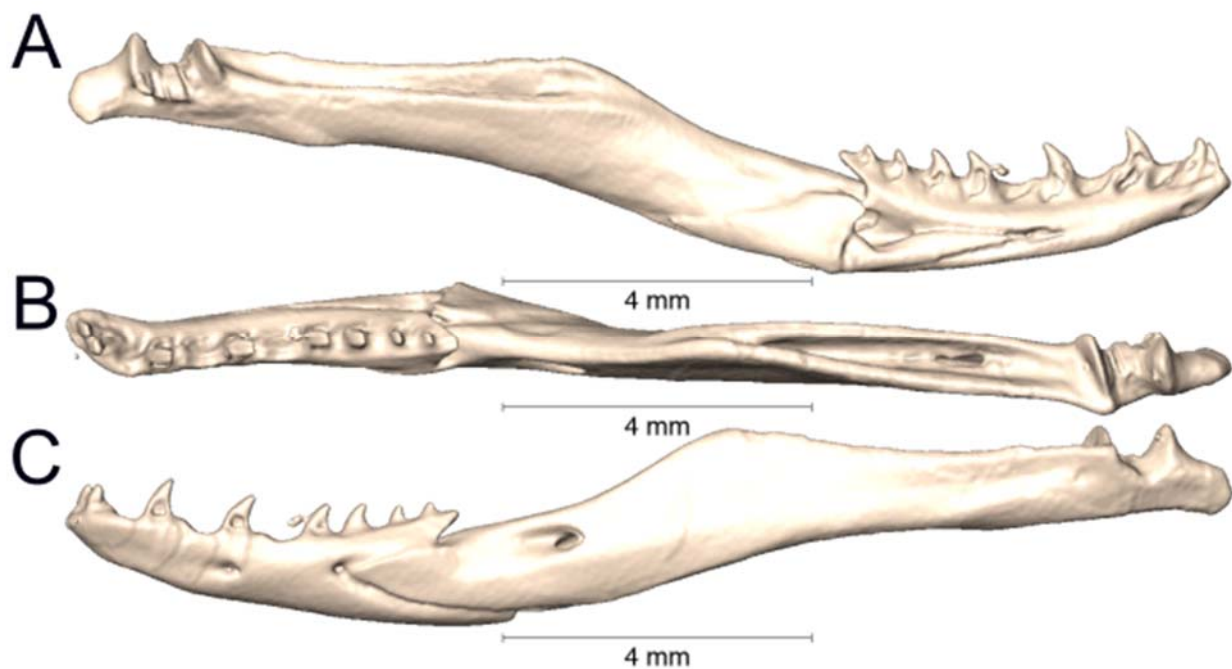
Supplemental Figure 3.70. Medial, dorsal, and lateral views (A-C, respectively) of the left lower jaw of *Micrurus nigrocinctus zunilensis* (UTA R-64858).



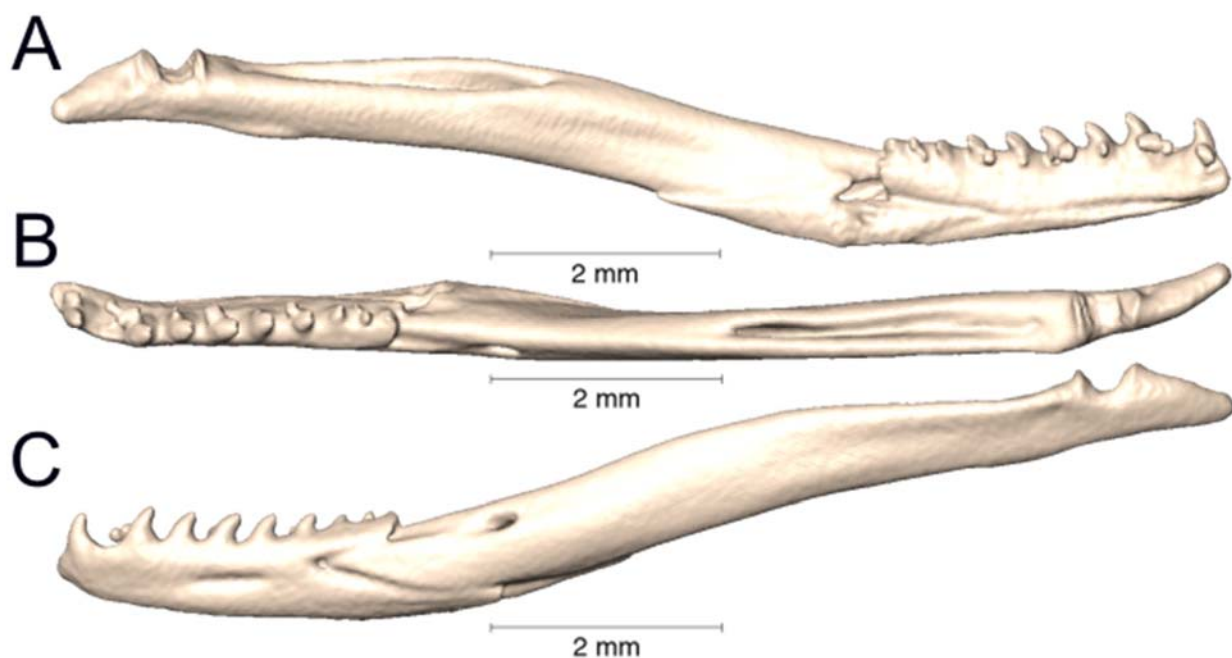
Supplemental Figure 3.71. Medial, dorsal, and lateral views (A-C, respectively) of the left lower jaw of *Micrurus obscurus* (UTA R-3840).



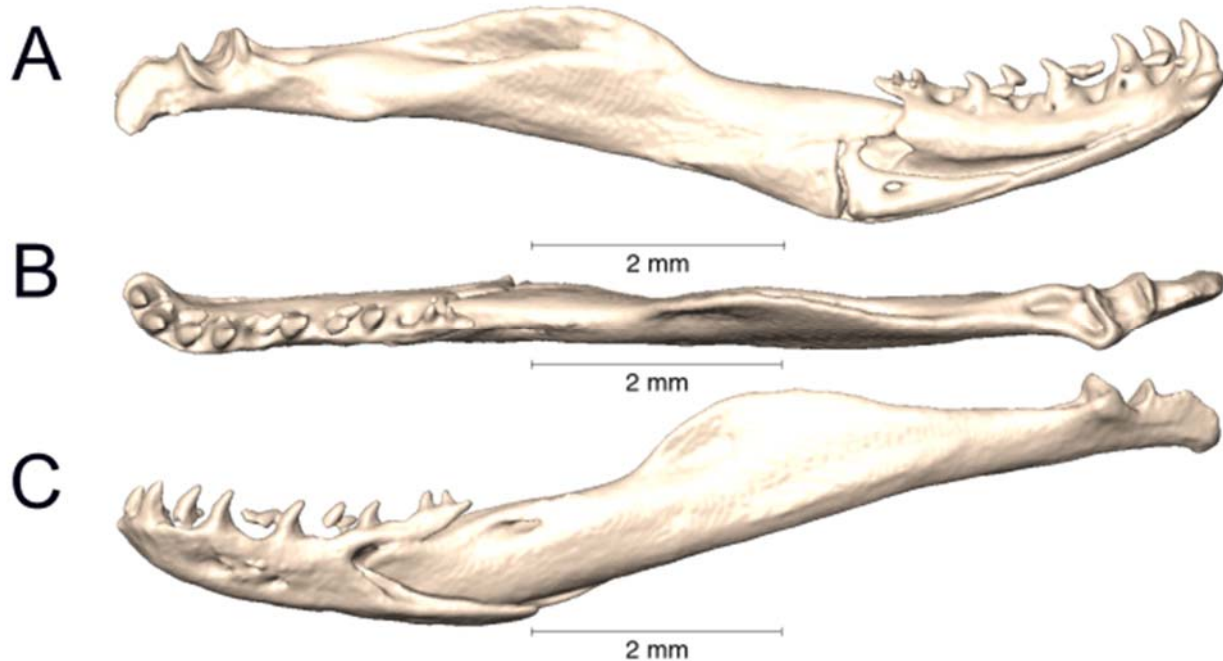
Supplemental Figure 3.72. Medial, dorsal, and lateral views (A-C, respectively) of the left lower jaw of *Micrurus oliveri* (UTA R-64893).



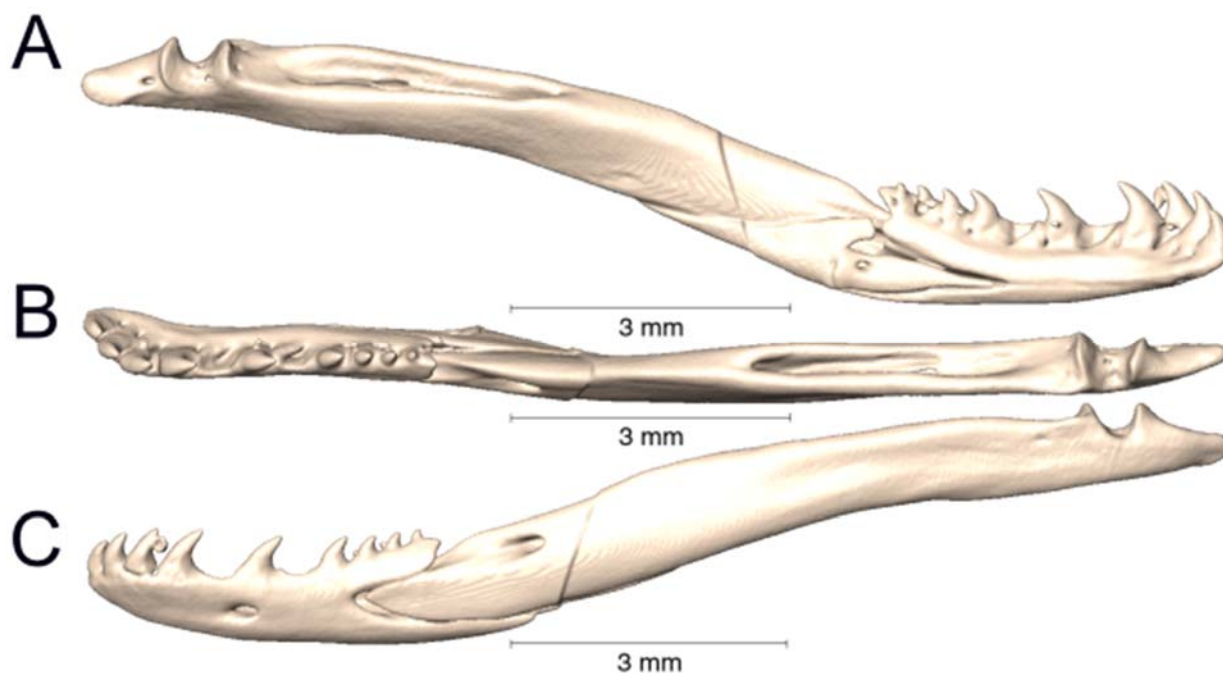
Supplemental Figure 3.73. Medial, dorsal, and lateral views (A-C, respectively) of the left lower jaw of *Micrurus ornatissimus* (UTA R-60724).



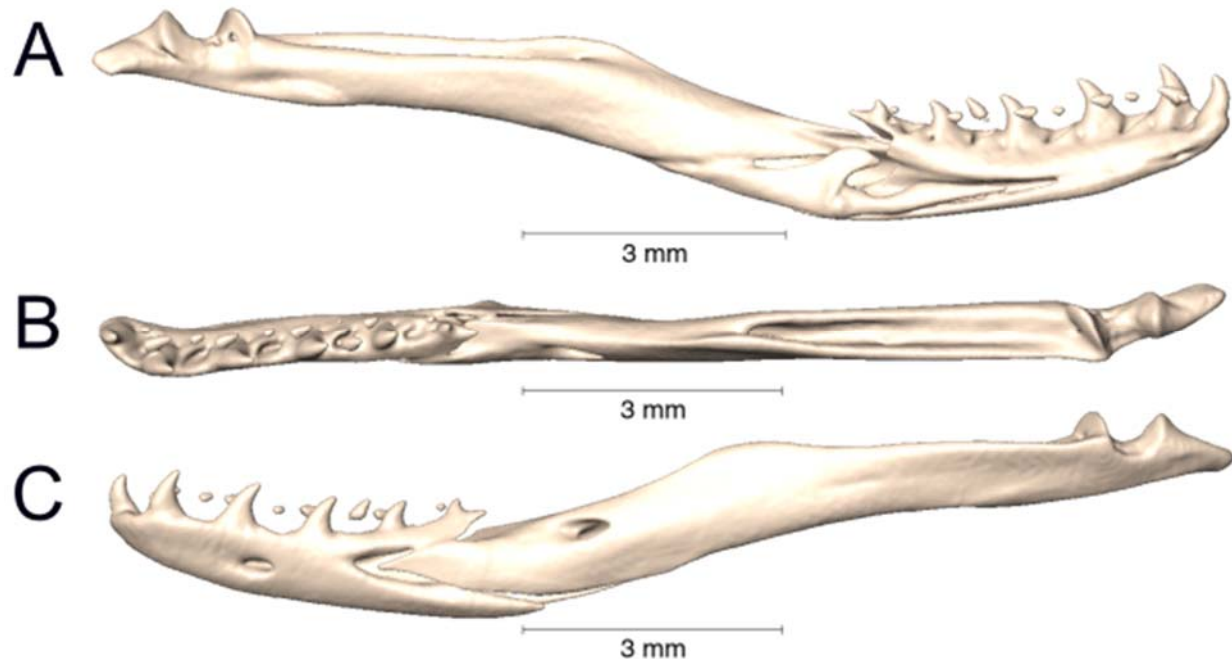
Supplemental Figure 3.74. Medial, dorsal, and lateral views (A-C, respectively) of the left lower jaw of *Micrurus pyrrhocryptus* (UTA R-51404).



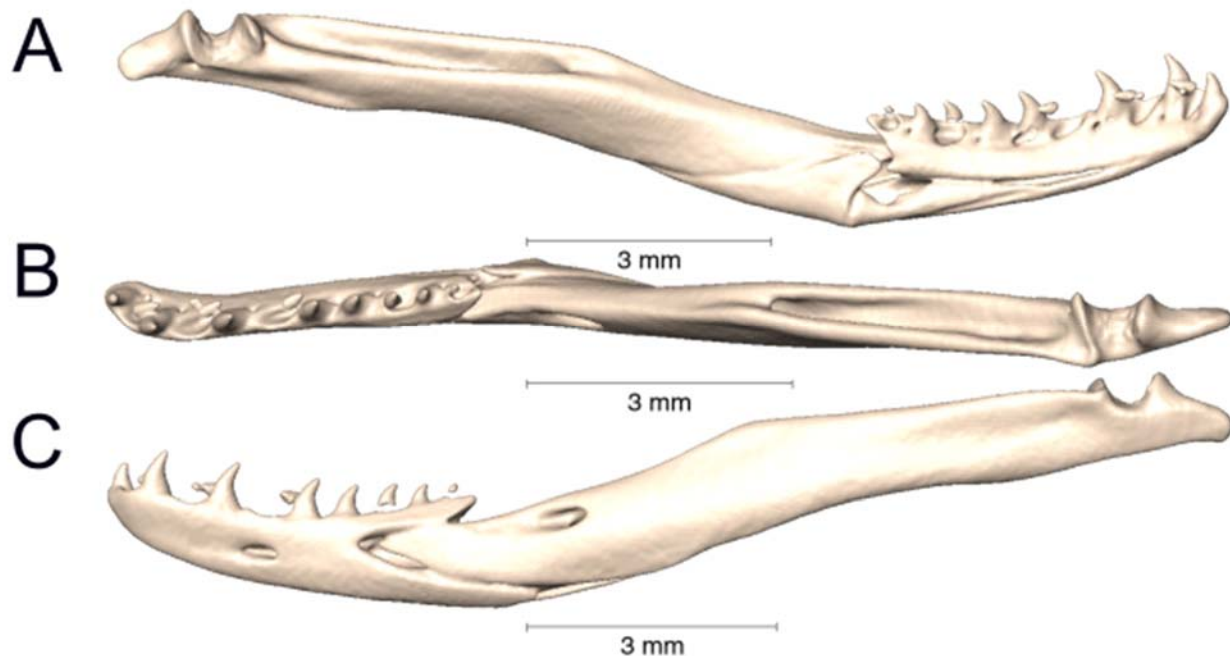
Supplemental Figure 3.75. Medial, dorsal, and lateral views (A-C, respectively) of the left lower jaw of *Micrurus renjifoii* (UTA R-3490).



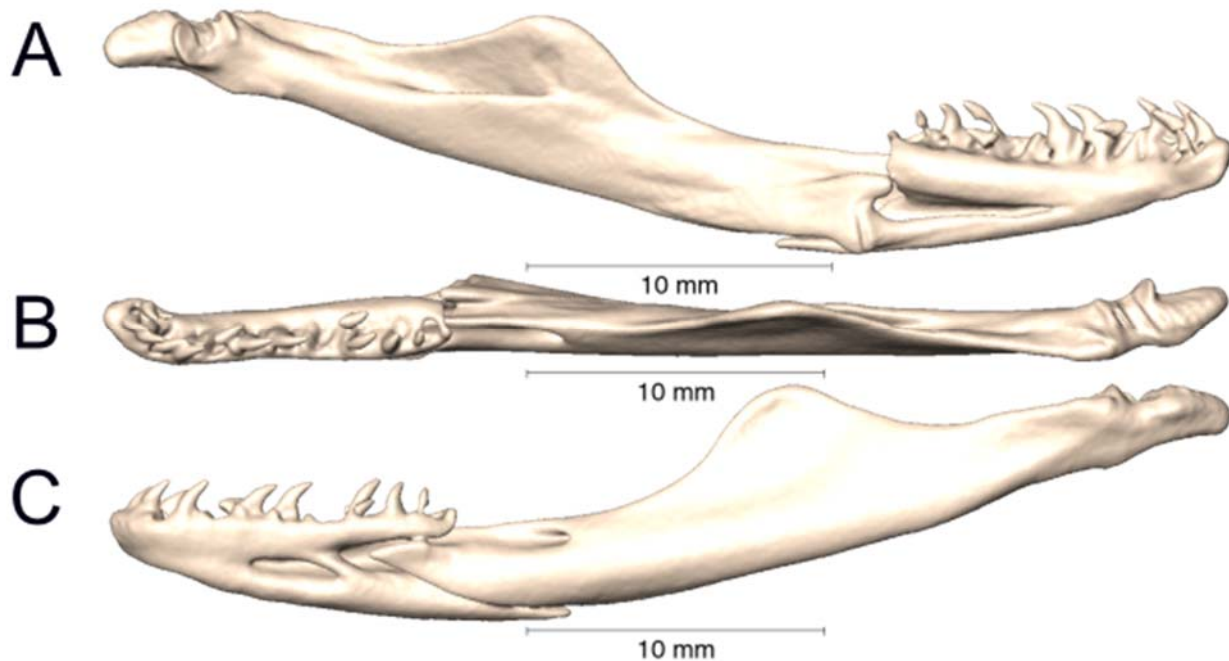
Supplemental Figure 3.76. Medial, dorsal, and lateral views (A-C, respectively) of the left lower jaw of *Micrurus serranus* (UTA R-34561).



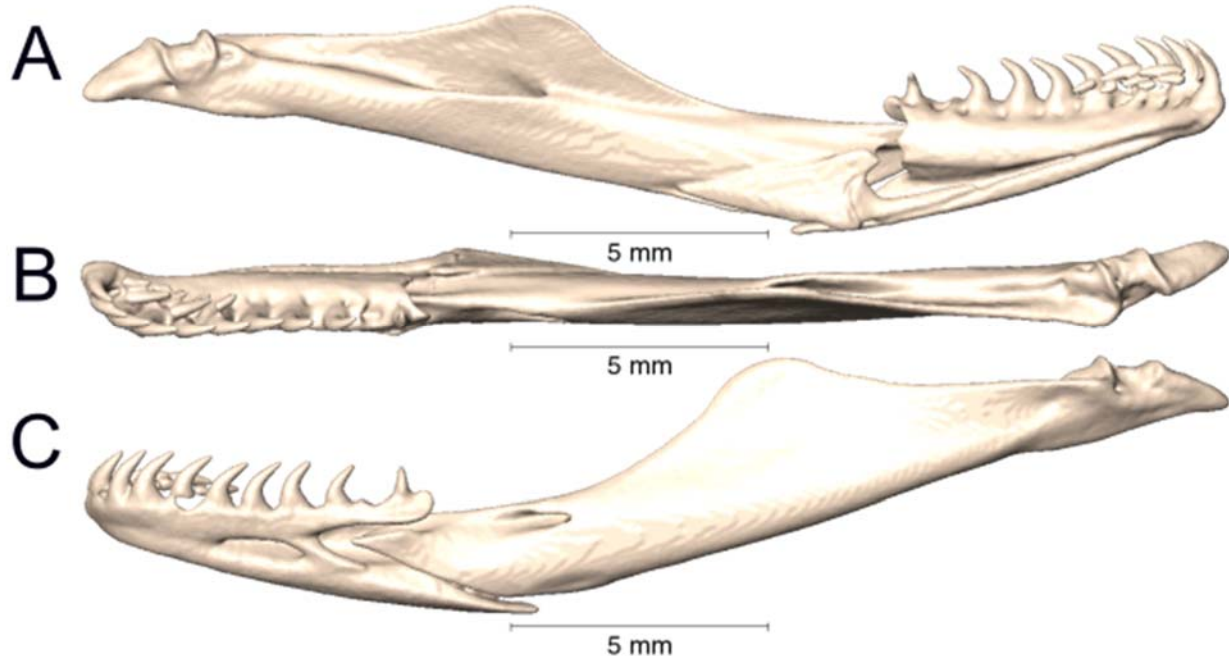
Supplemental Figure 3.77. Medial, dorsal, and lateral views (A-C, respectively) of the left lower jaw of *Micrurus steindachneri* (AMNH 28846).



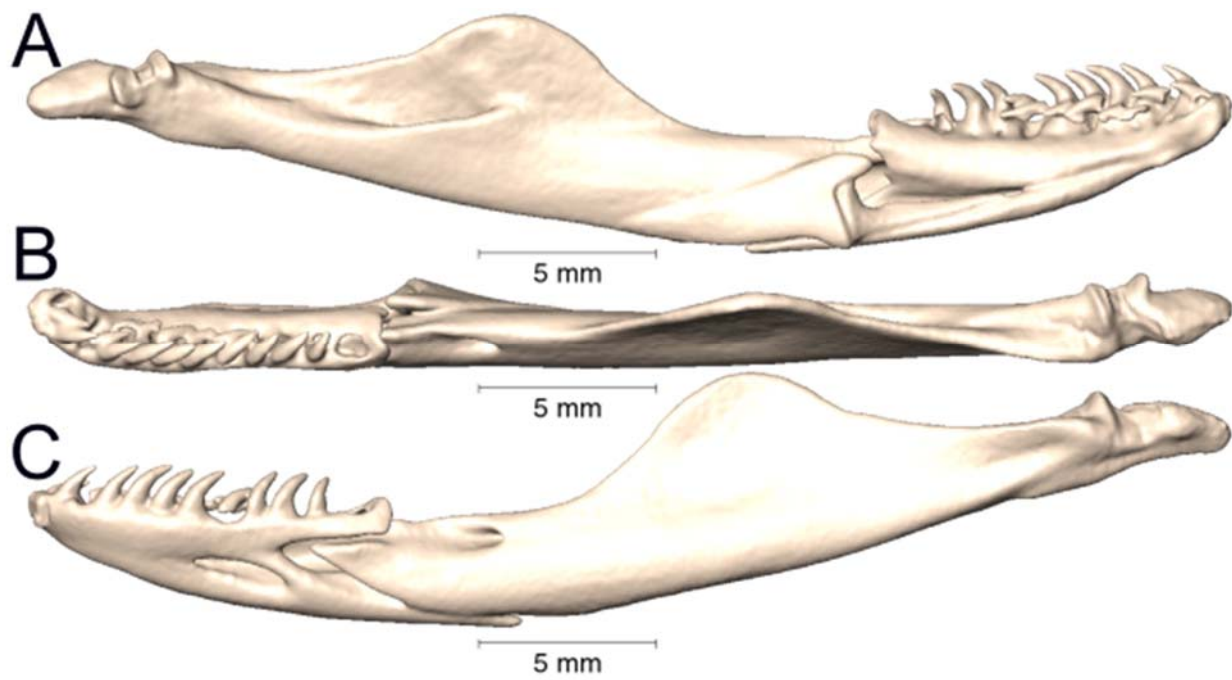
Supplemental Figure 3.78. Medial, dorsal, and lateral views (A-C, respectively) of the left lower jaw of *Micrurus steindachneri* (AMNH 35819).



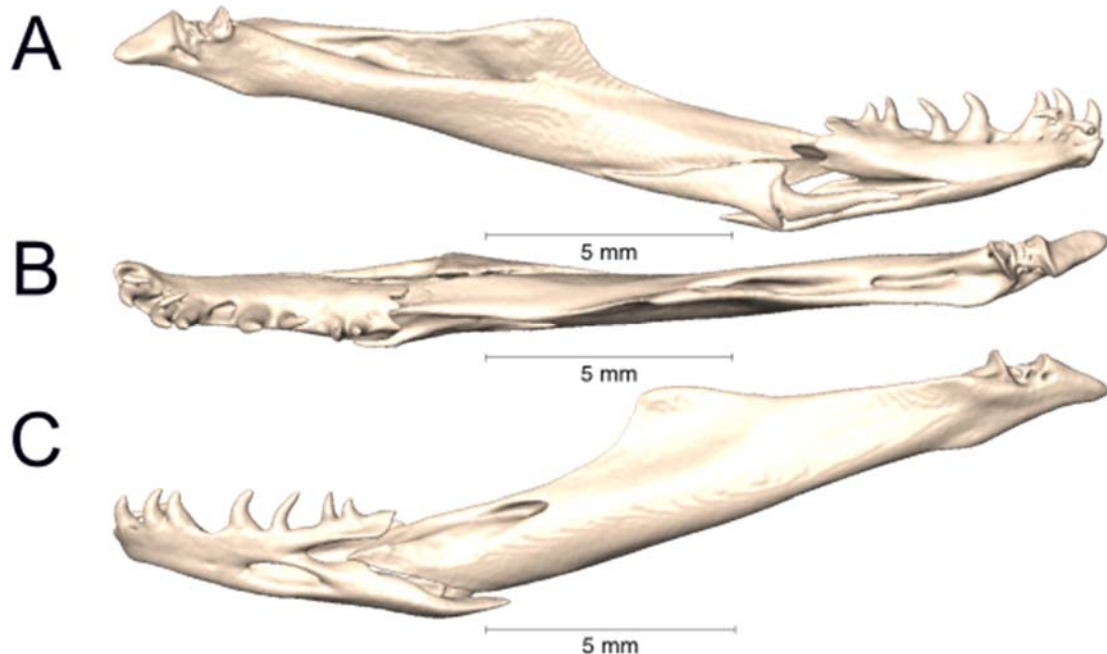
Supplemental Figure 3.79. Medial, dorsal, and lateral views (A-C, respectively) of the left lower jaw of *Micrurus surinamensis* (UTA R-15679).



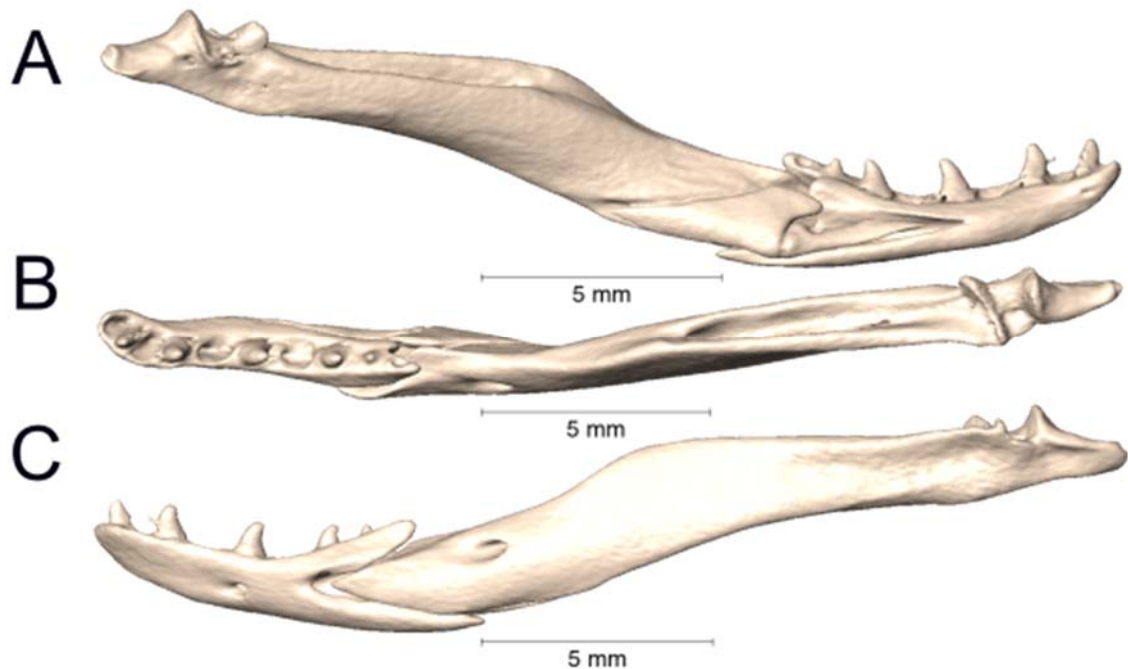
Supplemental Figure 3.80. Medial, dorsal, and lateral views (A-C, respectively) of the left lower jaw of *Micrurus surinamensis* (UTA R-50173).



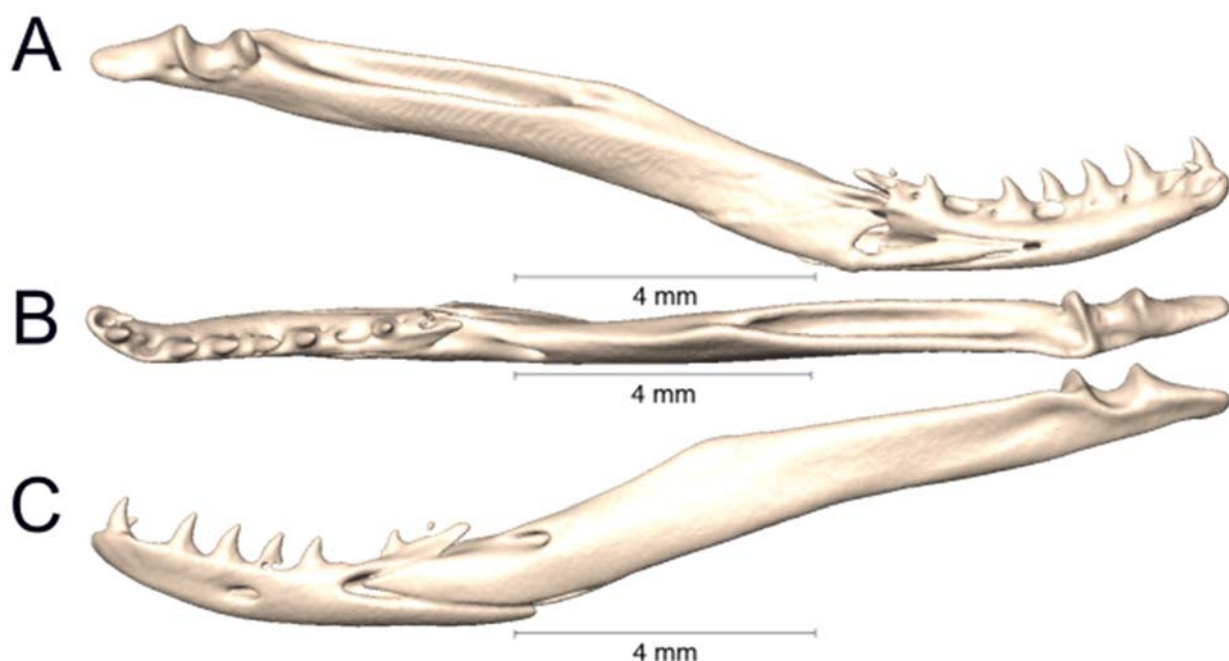
Supplemental Figure 3.81. Medial, dorsal, and lateral views (A-C, respectively) of the left lower jaw of *Micrurus surinamensis* (UTA R-54378).



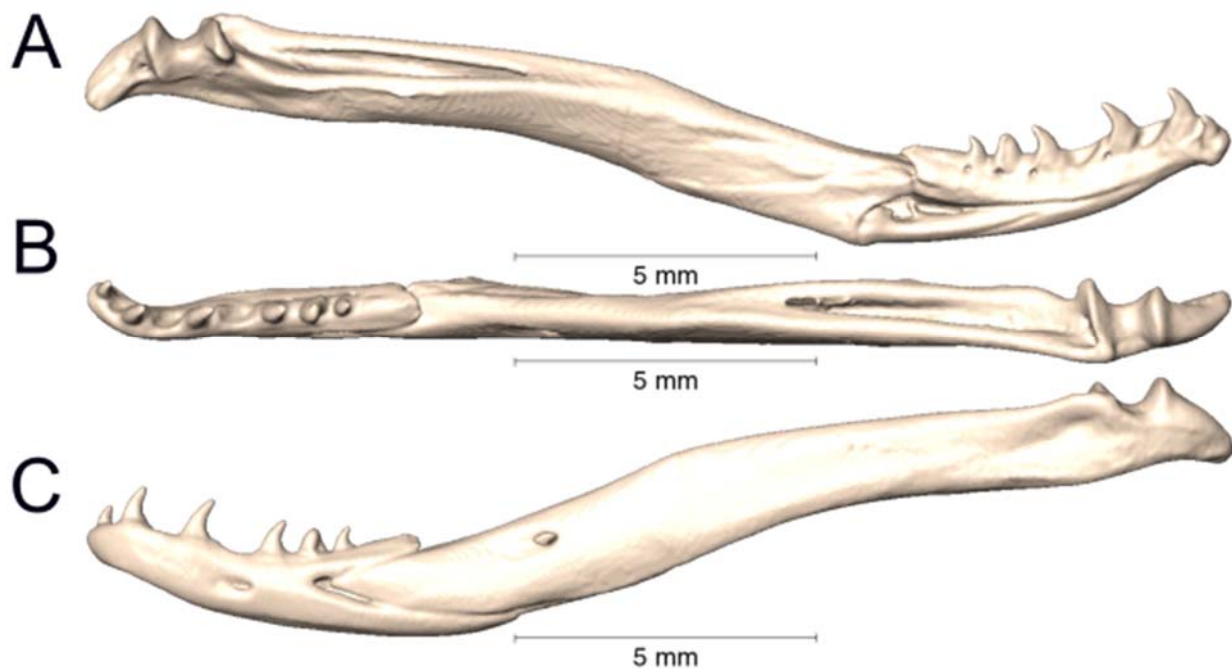
Supplemental Figure 3.82. Medial, dorsal, and lateral views (A-C, respectively) of the left lower jaw of *Micrurus surinamensis* (UTA R-65844).



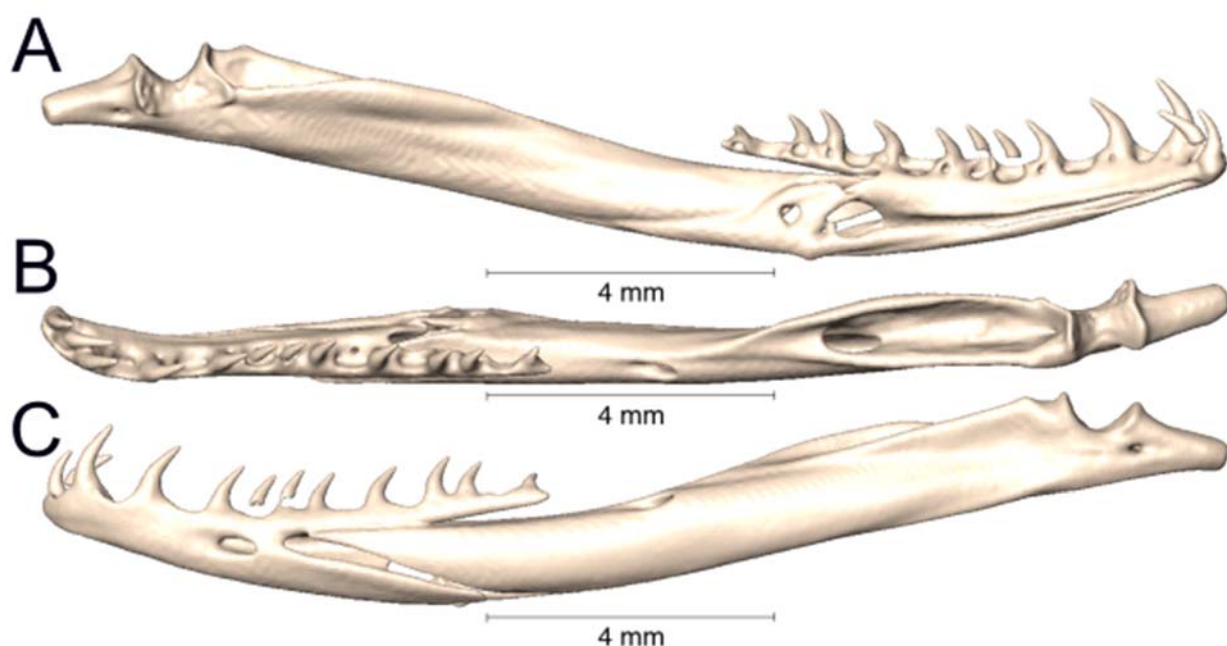
Supplemental Figure 3.83. Medial, dorsal, and lateral views (A-C, respectively) of the left lower jaw of *Micrurus tener* (FMNH 39479).



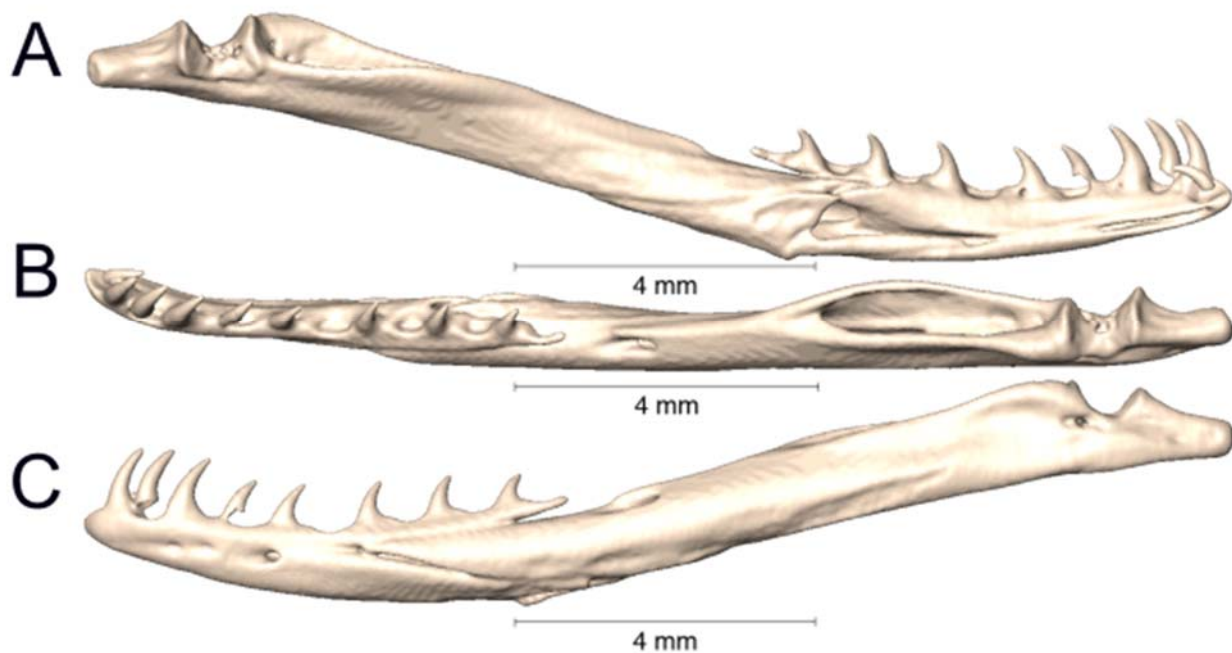
Supplemental Figure 3.84. Medial, dorsal, and lateral views (A-C, respectively) of the left lower jaw of *Micrurus tener* (UTA R-63282).



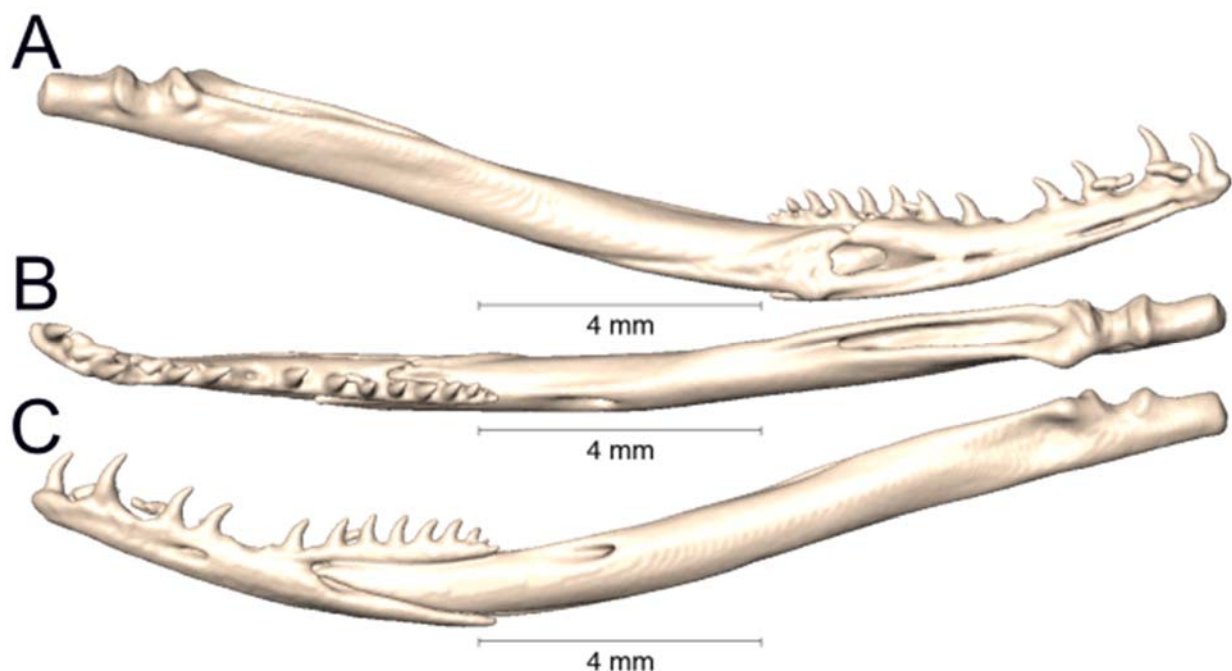
Supplemental Figure 3.85. Medial, dorsal, and lateral views (A-C, respectively) of the left lower jaw of *Micrurus* sp. (UTA R-6086).



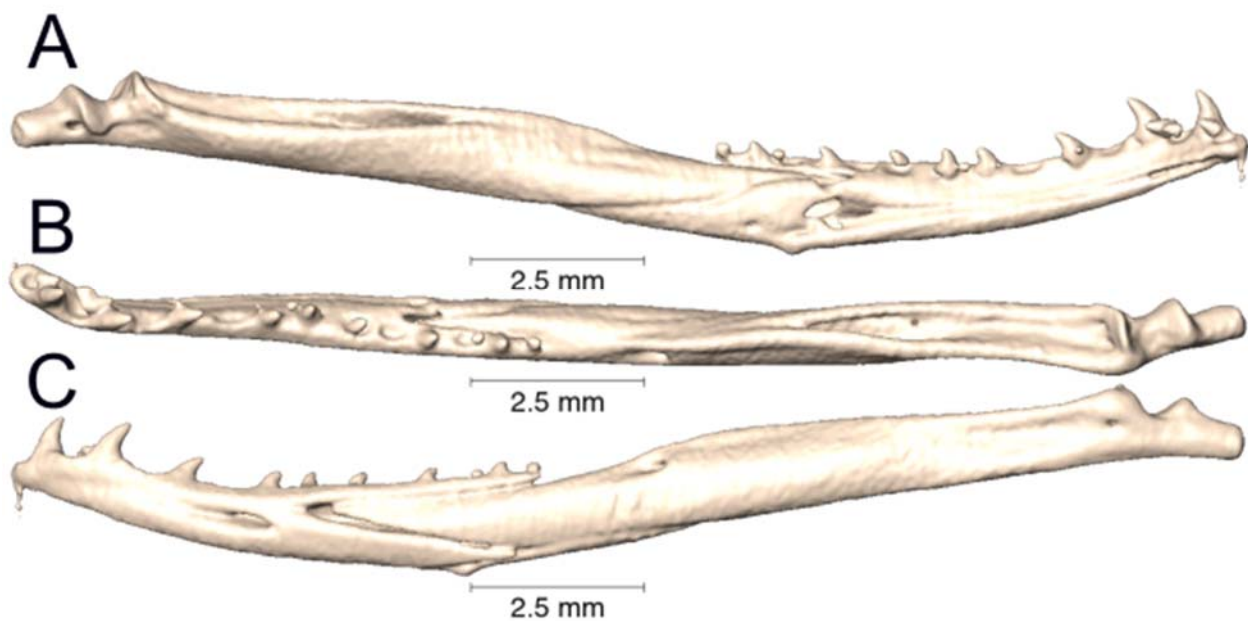
Supplemental Figure 3.86. Medial, dorsal, and lateral views (A-C, respectively) of the left lower jaw of *Naja annulata* (UTA R-18199).



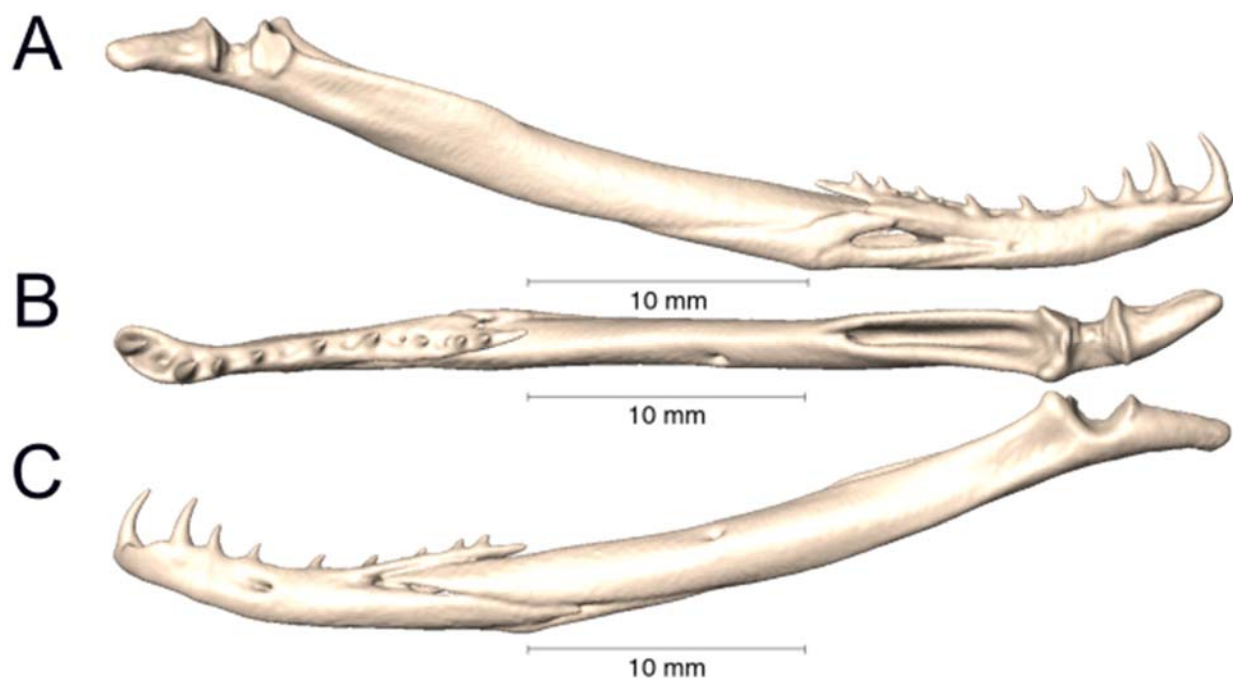
Supplemental Figure 3.87. Medial, dorsal, and lateral views (A-C, respectively) of the left lower jaw of *Naja christyi* (UTA R-18200).



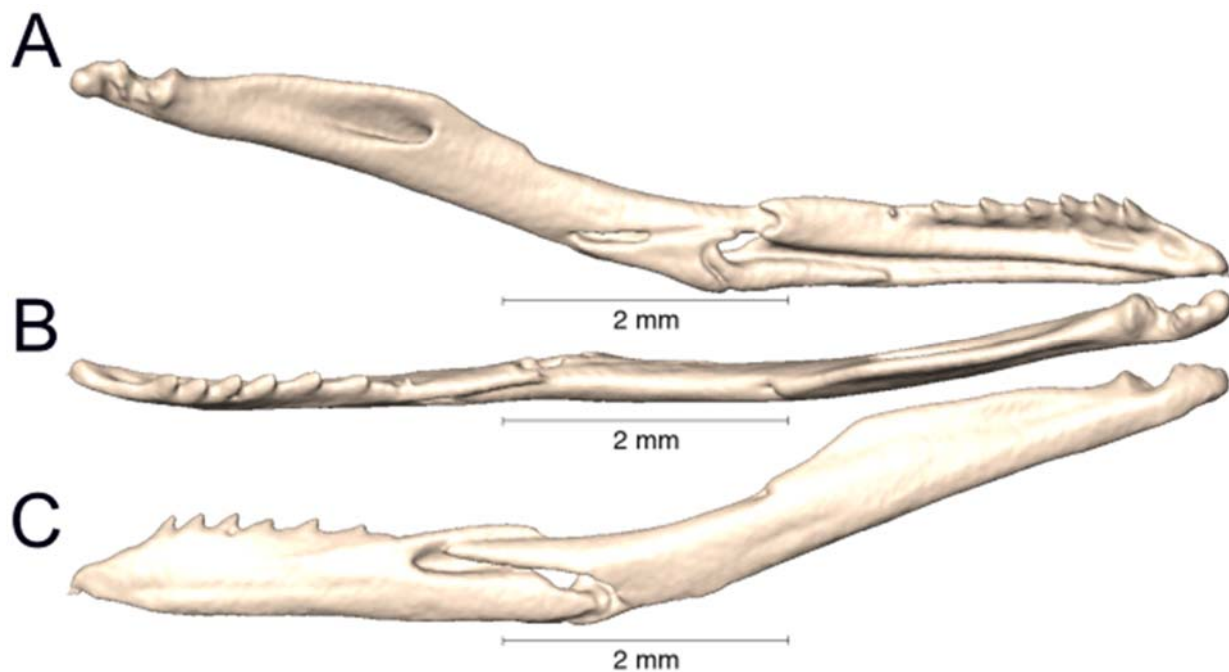
Supplemental Figure 3.88. Medial, dorsal, and lateral views (A-C, respectively) of the left lower jaw of *Naja siamensis* (UTA R-16872).



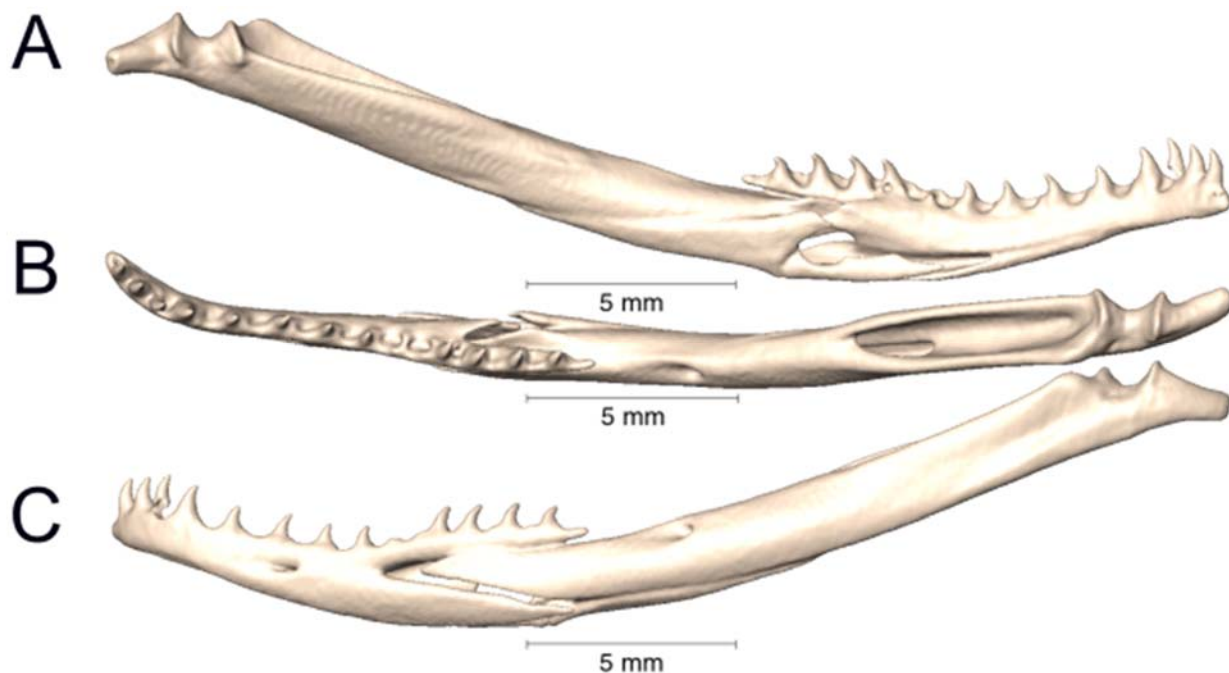
Supplemental Figure 3.89. Medial, dorsal, and lateral views (A-C, respectively) of the left lower jaw of *Ophiophagus hannah* (UTA R-60836).



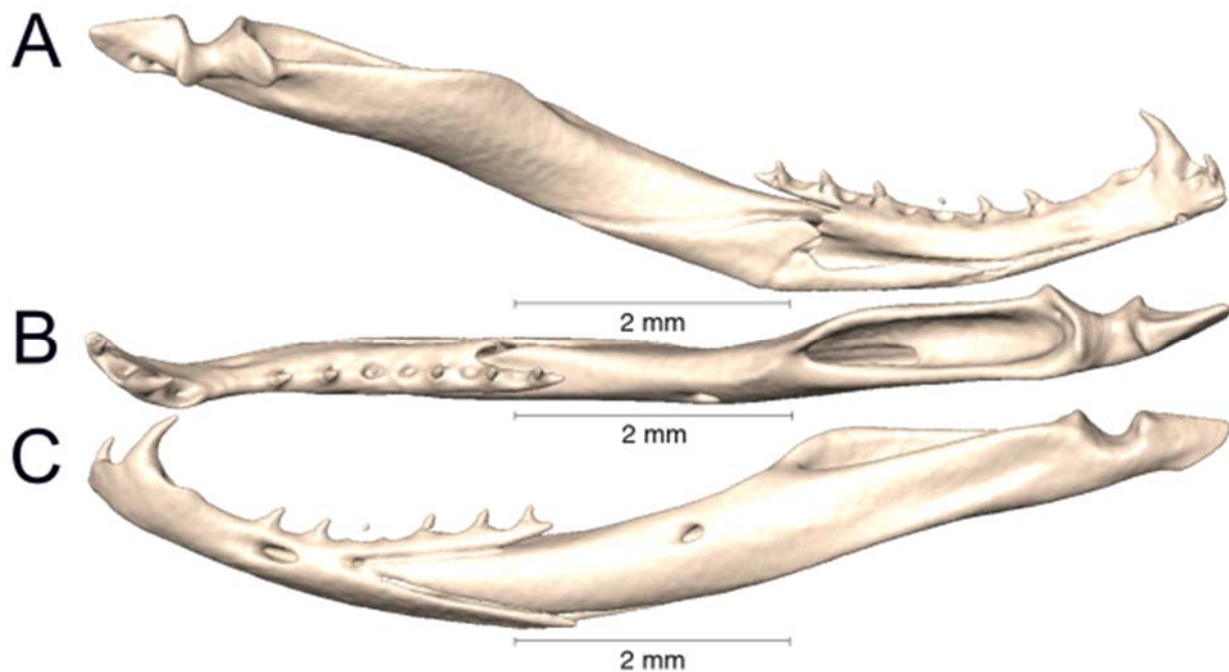
Supplemental Figure 3.90. Medial, dorsal, and lateral views (A-C, respectively) of the left lower jaw of *Oxyuranus scutellatus* (UTA R-60839).



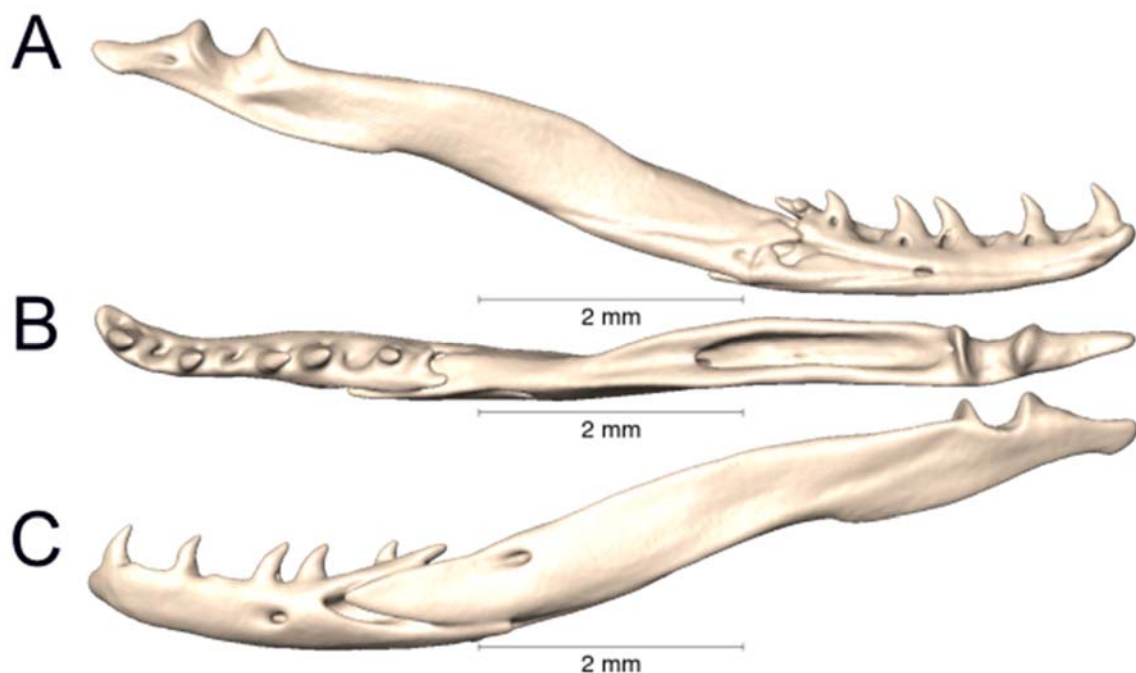
Supplemental Figure 3.91. Medial, dorsal, and lateral views (A-C, respectively) of the left lower jaw of *Prosymna stuhlmanni* (UTA R-64493).



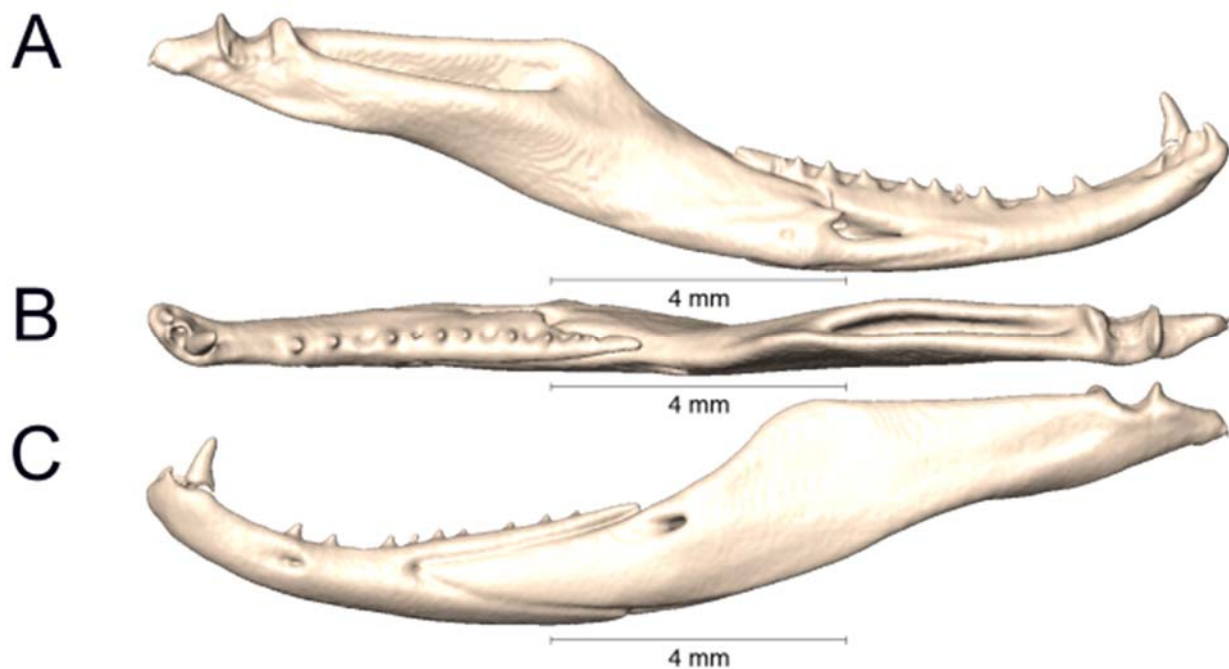
Supplemental Figure 3.92. Medial, dorsal, and lateral views (A-C, respectively) of the left lower jaw of *Pseudohaje goldii* (UTA R-63636).



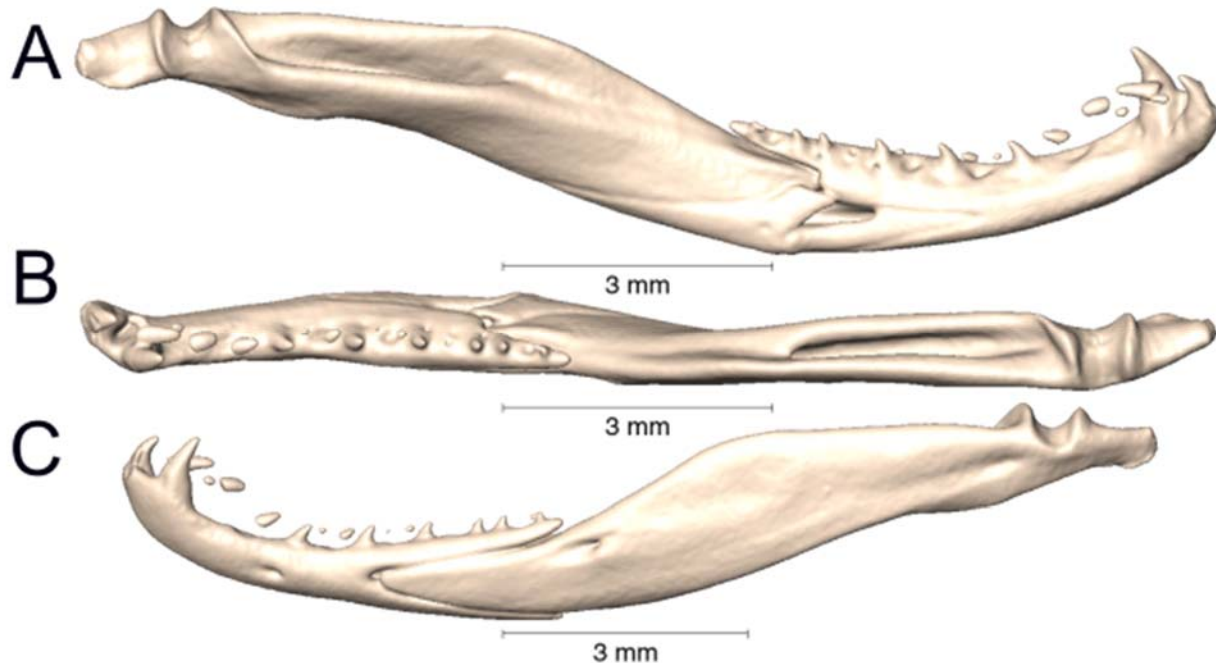
Supplemental Figure 3.93. Medial, dorsal, and lateral views (A-C, respectively) of the left lower jaw of *Simoselaps bertholdi* (UMMZ 244197).



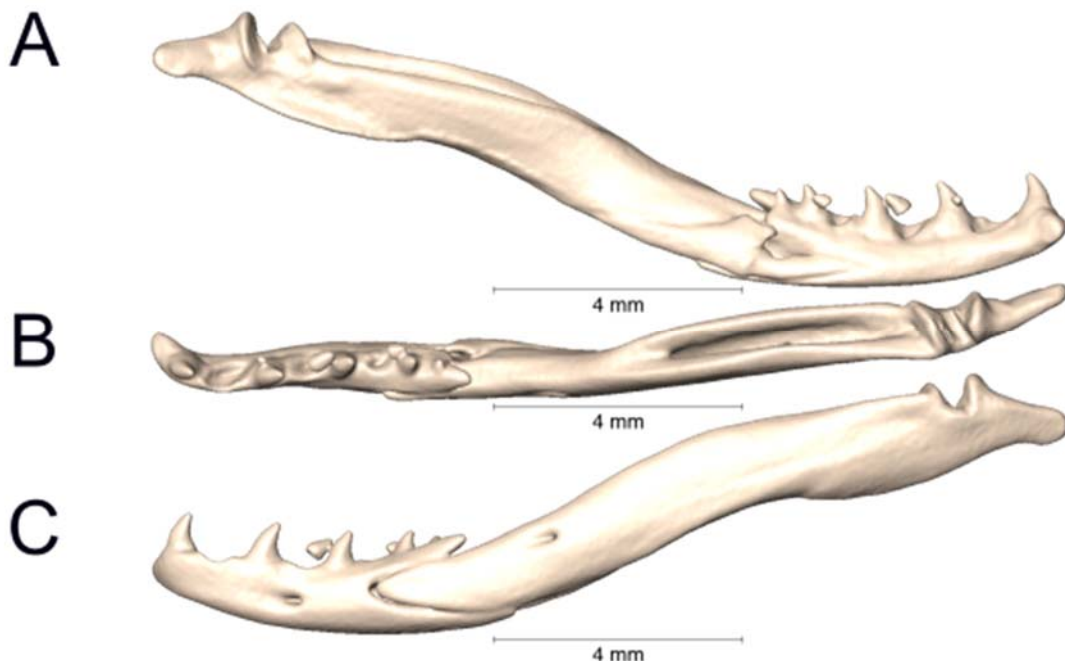
Supplemental Figure 3.94. Medial, dorsal, and lateral views (A-C, respectively) of the left lower jaw of *Sinomicrurus annularis* (ROM 31158).



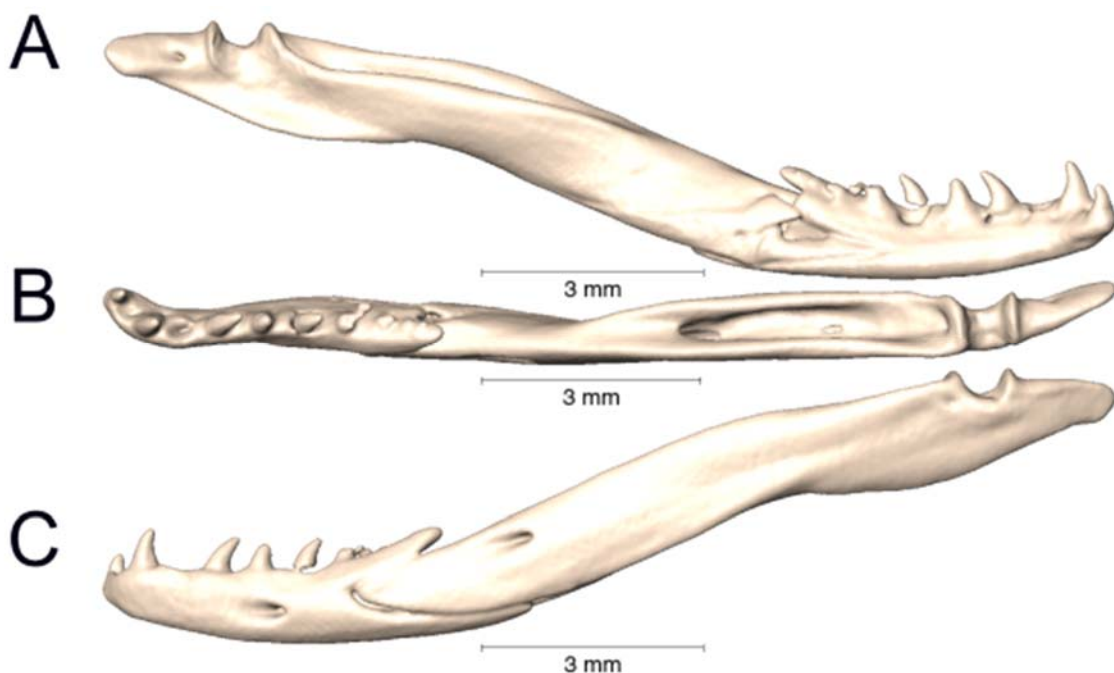
Supplemental Figure 3.95. Medial, dorsal, and lateral views (A-C, respectively) of the left lower jaw of *Sinomicrurus boettgeri* (UTA R-58837).



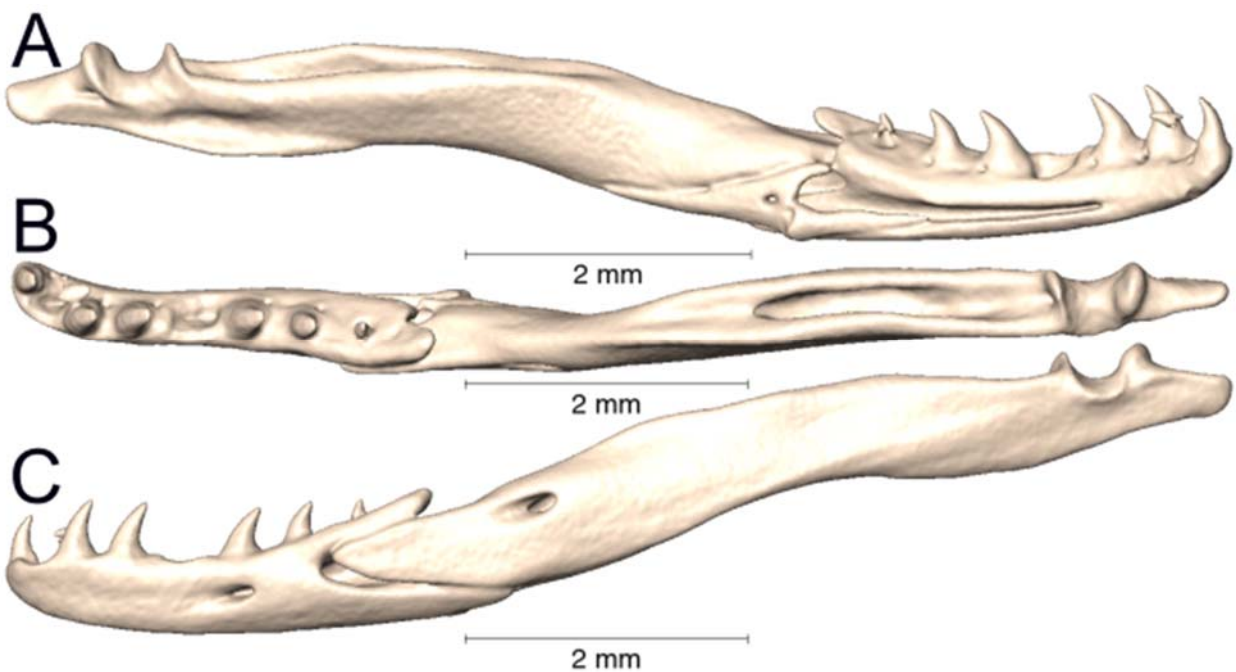
Supplemental Figure 3.96. Medial, dorsal, and lateral views (A-C, respectively) of the left lower jaw of *Sinomicrurus japonicus* (CAS 204979).



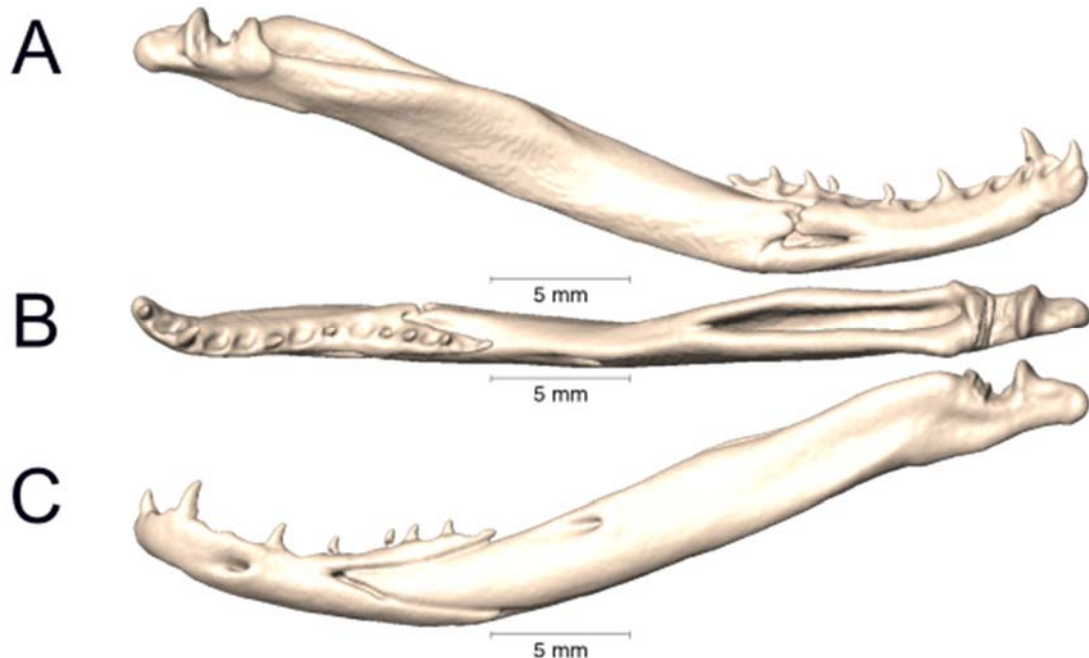
Supplemental Figure 3.97. Medial, dorsal, and lateral views (A-C, respectively) of the left lower jaw of *Sinomicrurus peinani* (ROM 35245).



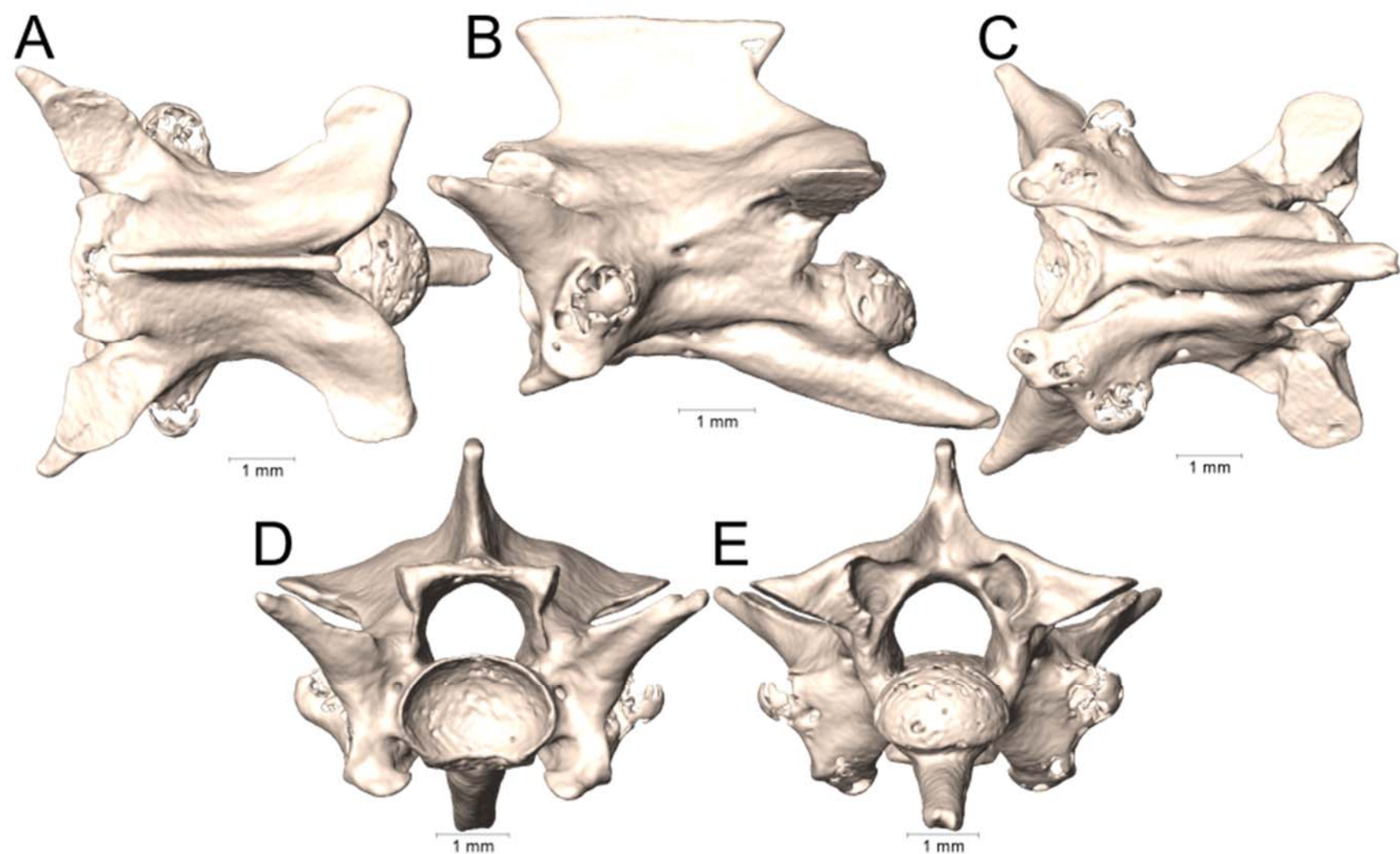
Supplemental Figure 3.98. Medial, dorsal, and lateral views (A-C, respectively) of the left lower jaw of *Sinomicrurus peinani* (ROM 37109).



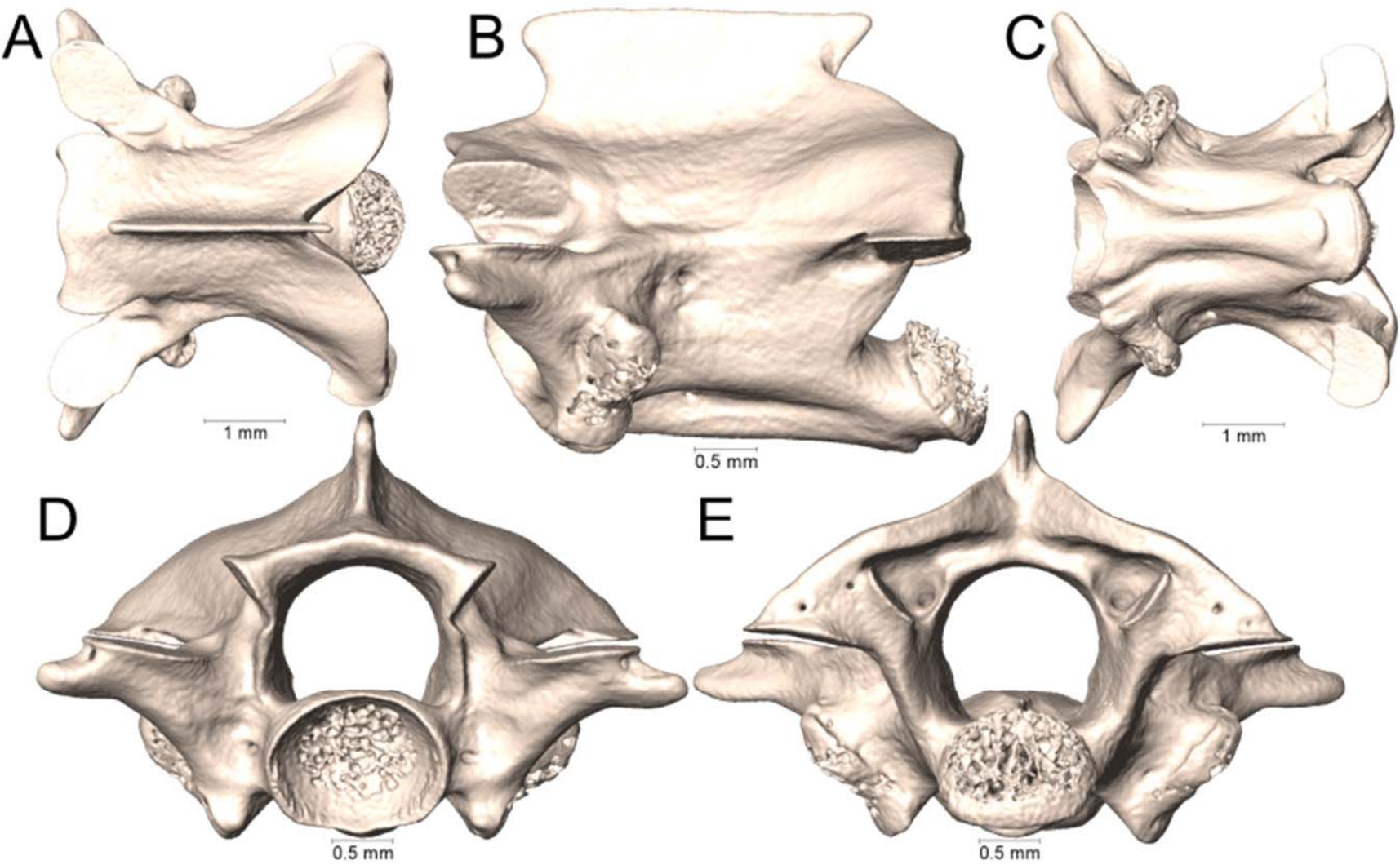
Supplemental Figure 3.99. Medial, dorsal, and lateral views (A-C, respectively) of the left lower jaw of *Sinomicrurus swinhoei* (MVZ 23876).



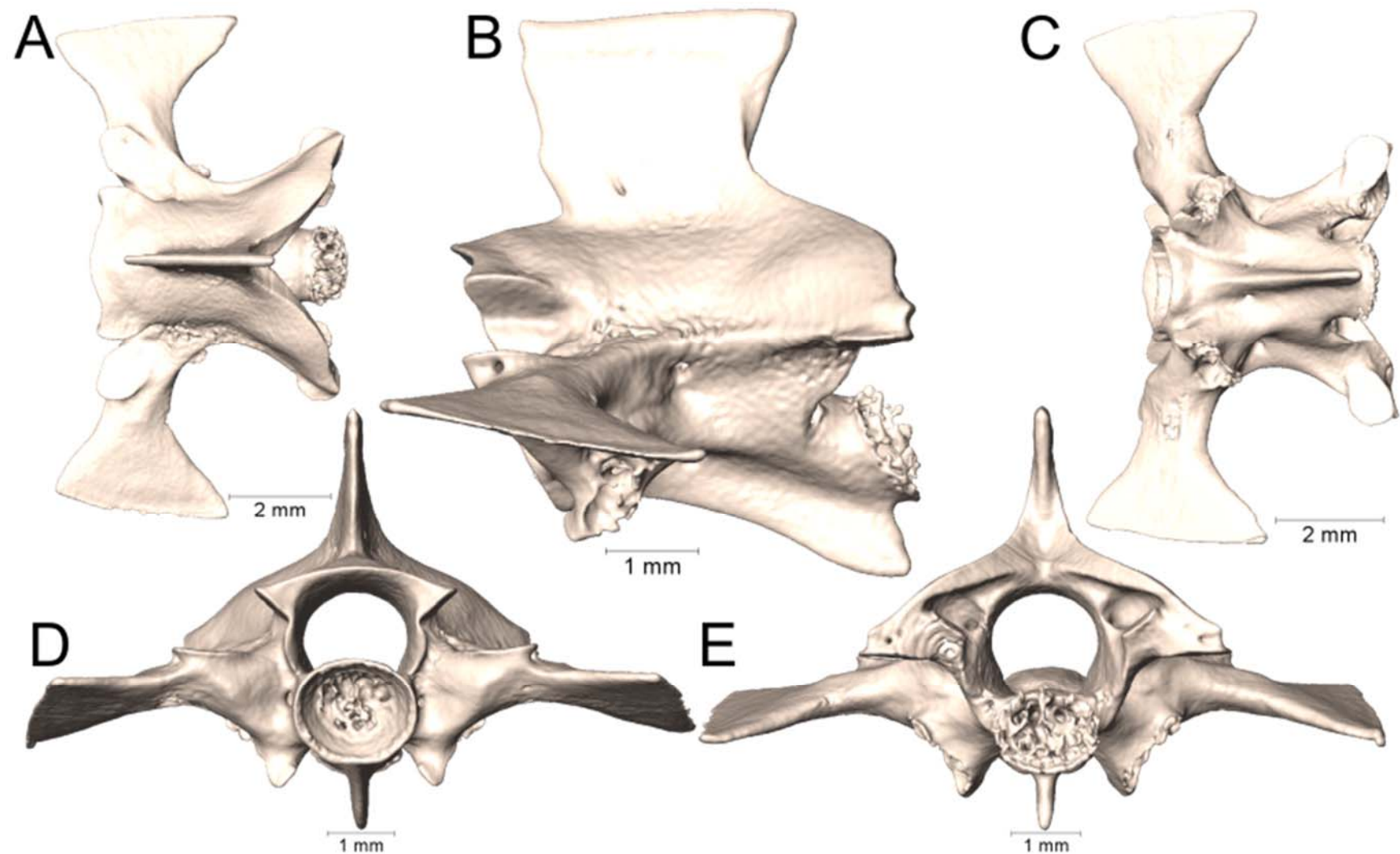
Supplemental Figure 3.100. Medial, dorsal, and lateral views (A-C, respectively) of the left lower jaw of *Walterinnesia aegyptia* (UTA R-13021).



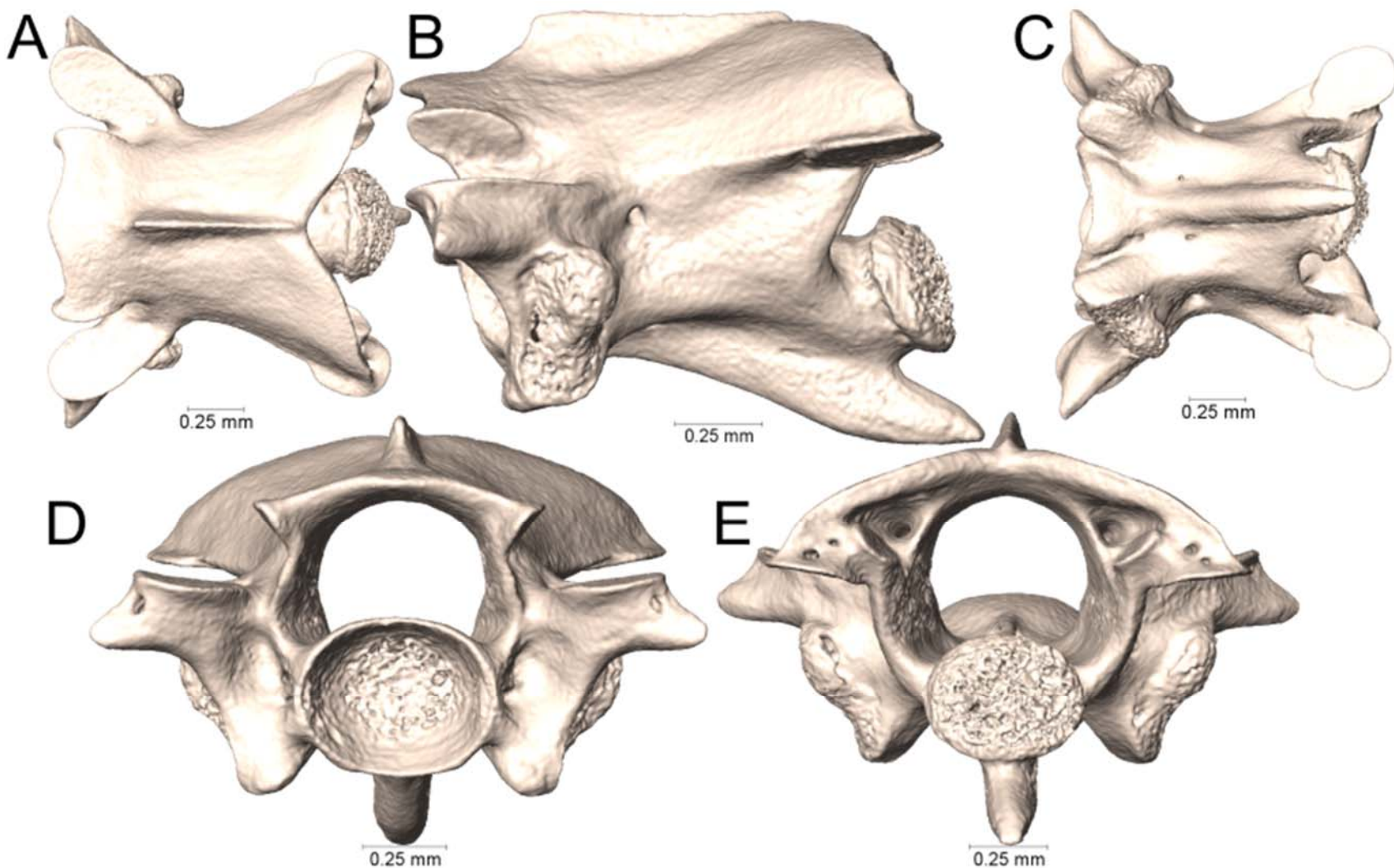
Supplemental Figure 4.1. Dorsal, lateral, ventral, anterior, and posterior views (A-E, respectively) of the midbody vertebra of *Acanthophis antarcticus* (UTA R-7623).



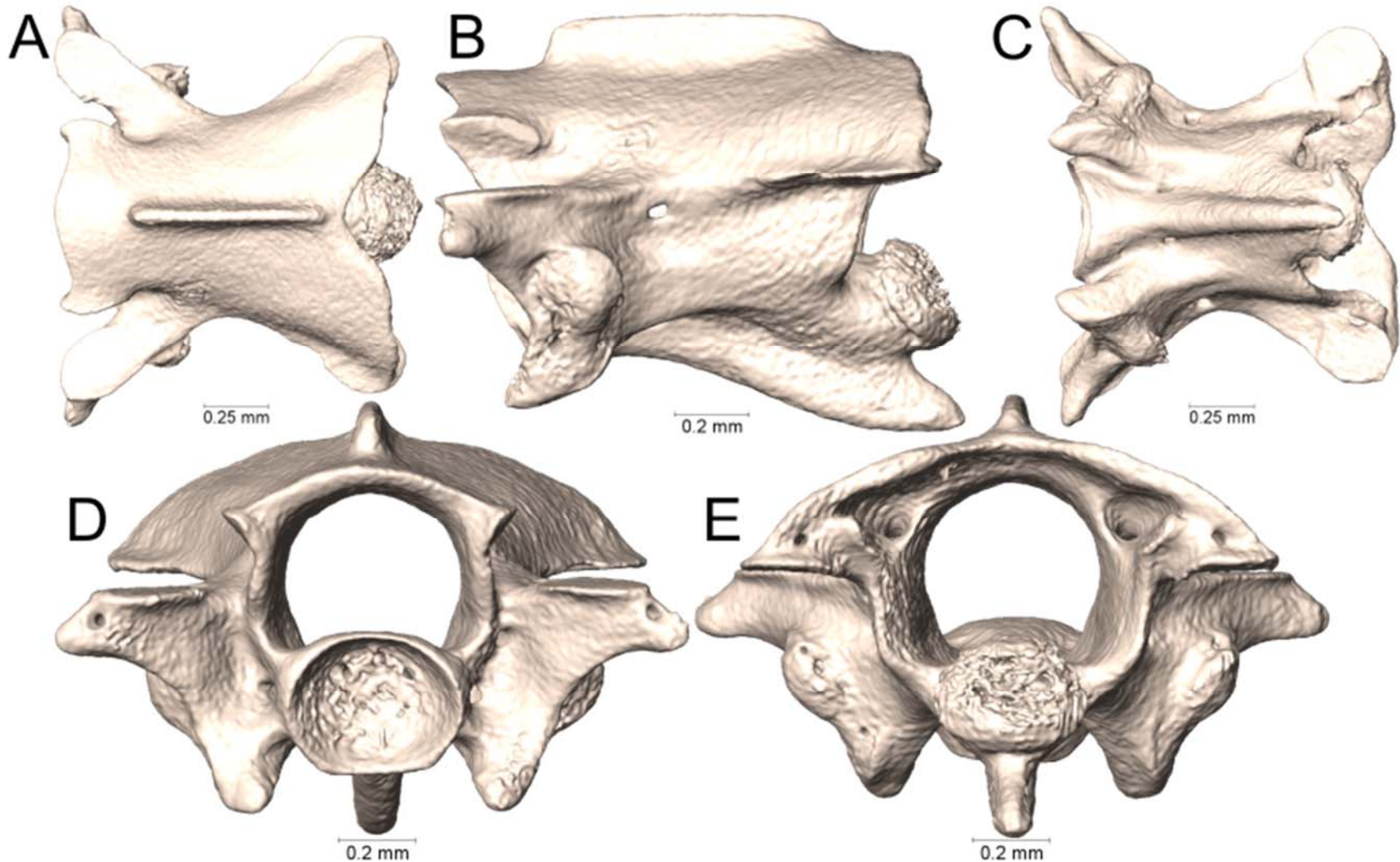
Supplemental Figure 4.2. Dorsal, lateral, ventral, anterior, and posterior views (A-E, respectively) of the midbody vertebra of *Bungarus candidus* (UTA R-65799).



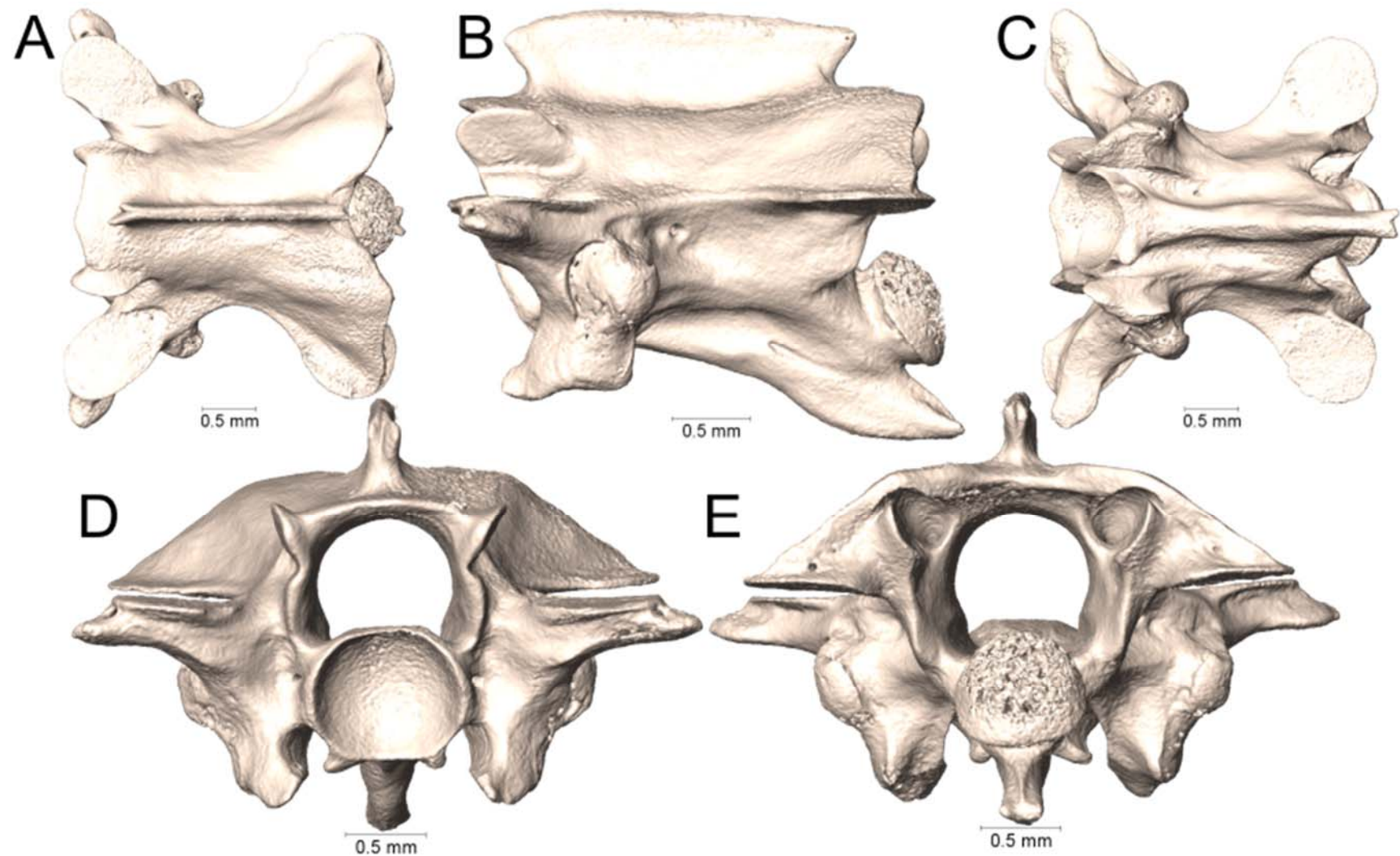
Supplemental Figure 4.3. Dorsal, lateral, ventral, anterior, and posterior views (A-E, respectively) of the midbody vertebra of *Bungarus flaviceps* (UTA R-62257).



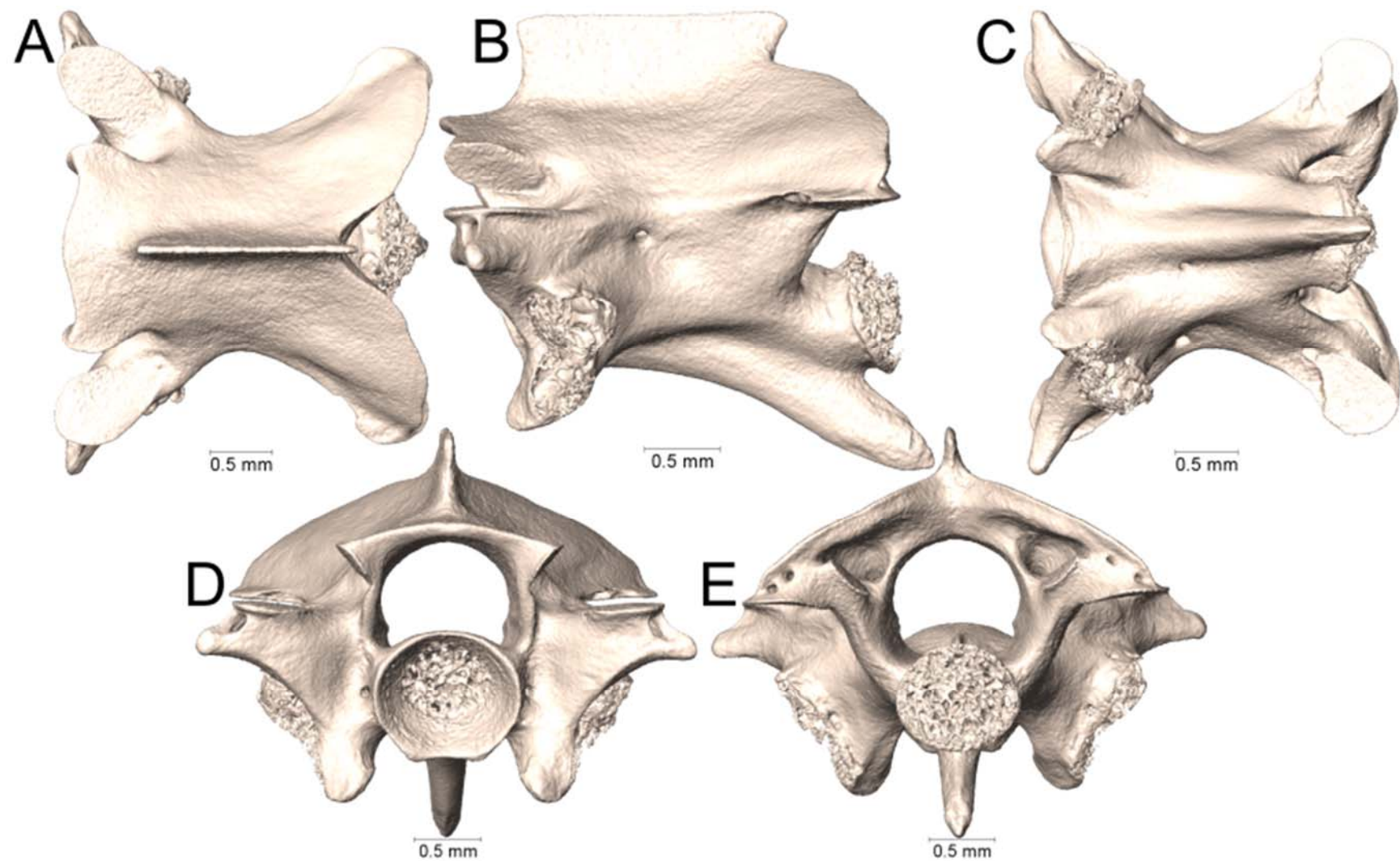
Supplemental Figure 4.4. Dorsal, lateral, ventral, anterior, and posterior views (A-E, respectively) of the midbody vertebra of *Calliophis beddomei* (MNHN 46-81).



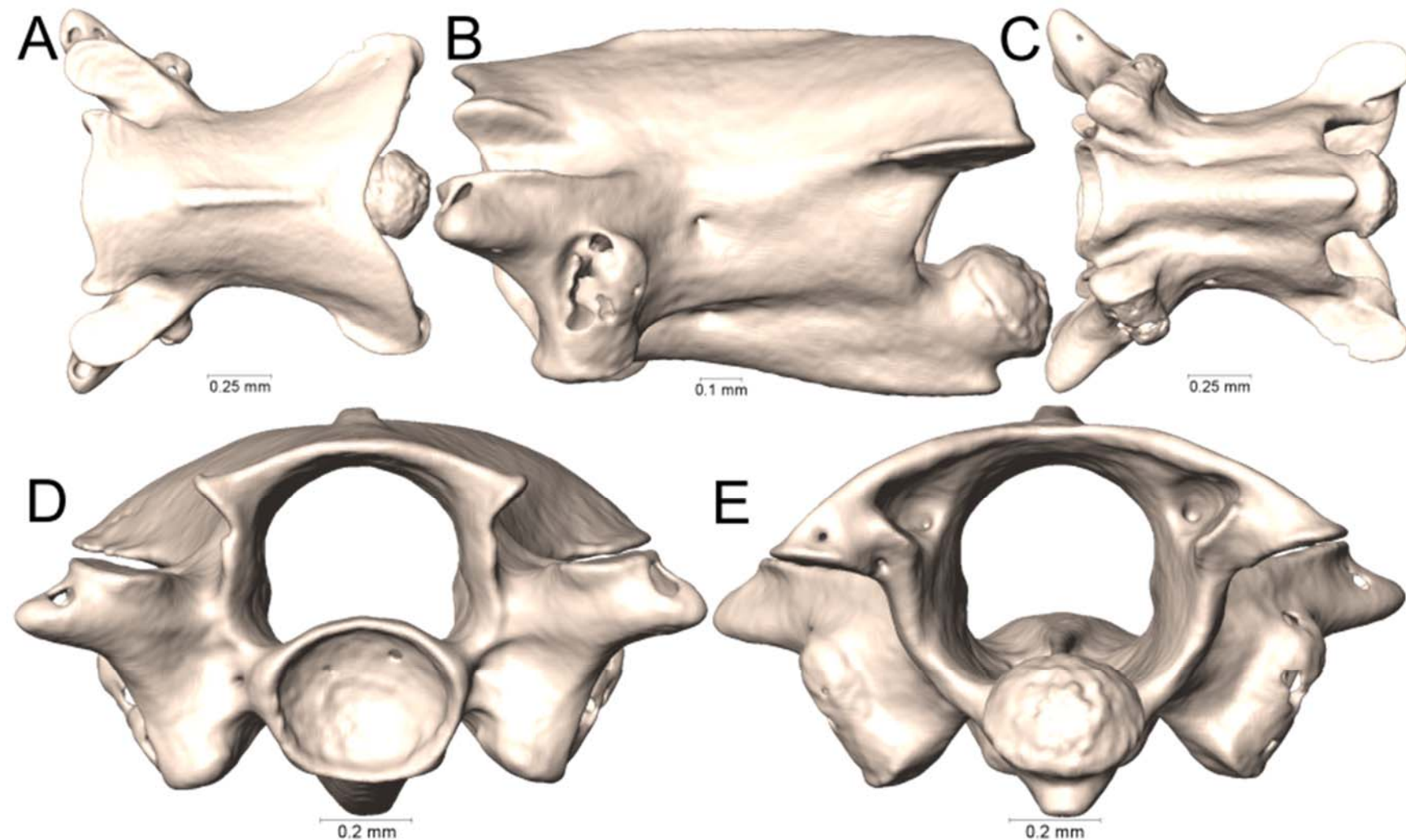
Supplemental Figure 4.5. Dorsal, lateral, ventral, anterior, and posterior views (A-E, respectively) of the midbody vertebra of *Calliophis biliniatus* (KU 309511).



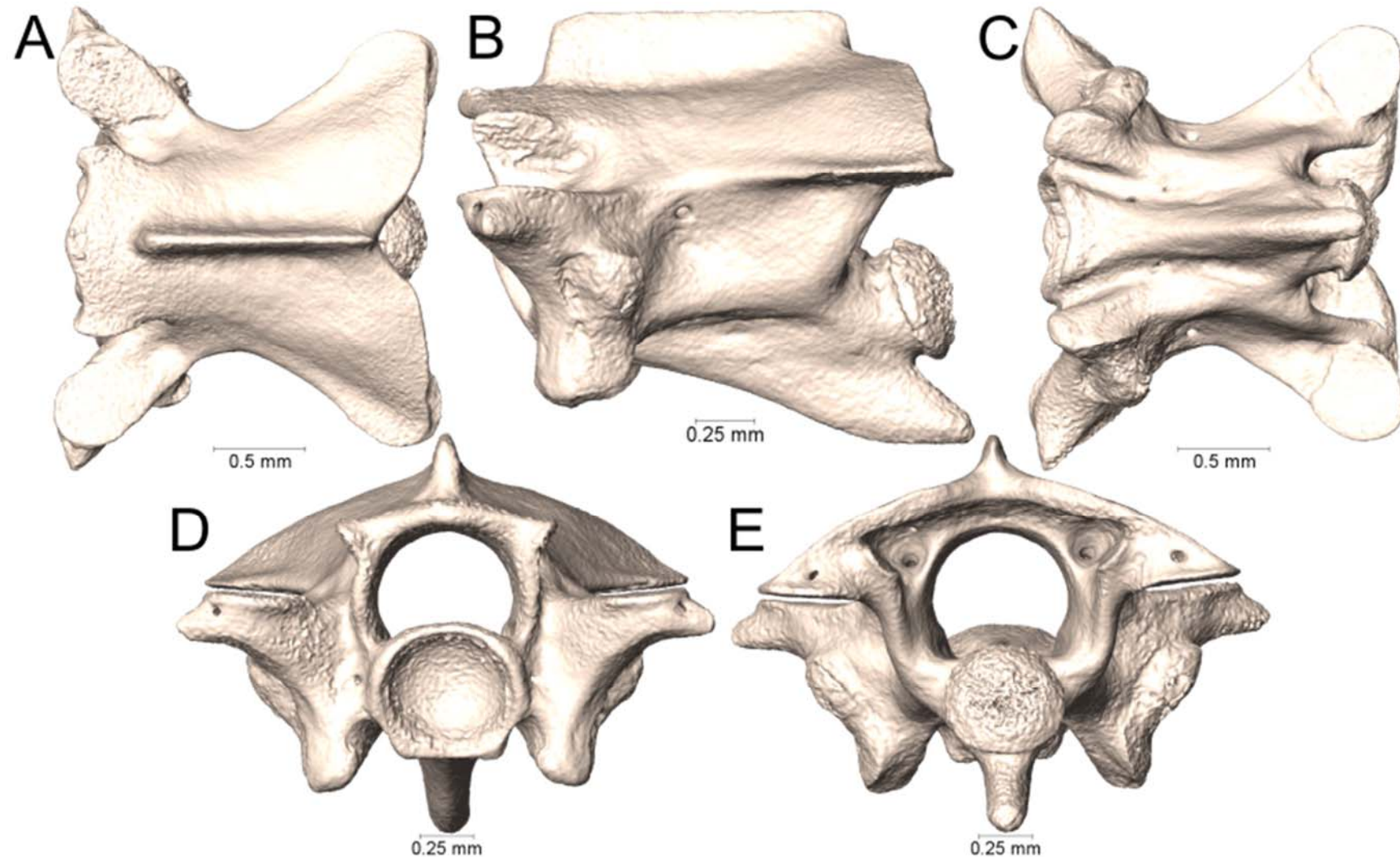
Supplemental Figure 4.6. Dorsal, lateral, ventral, anterior, and posterior views (A-E, respectively) of the midbody vertebra of *Calliophis biliniatus* (KU 311415).



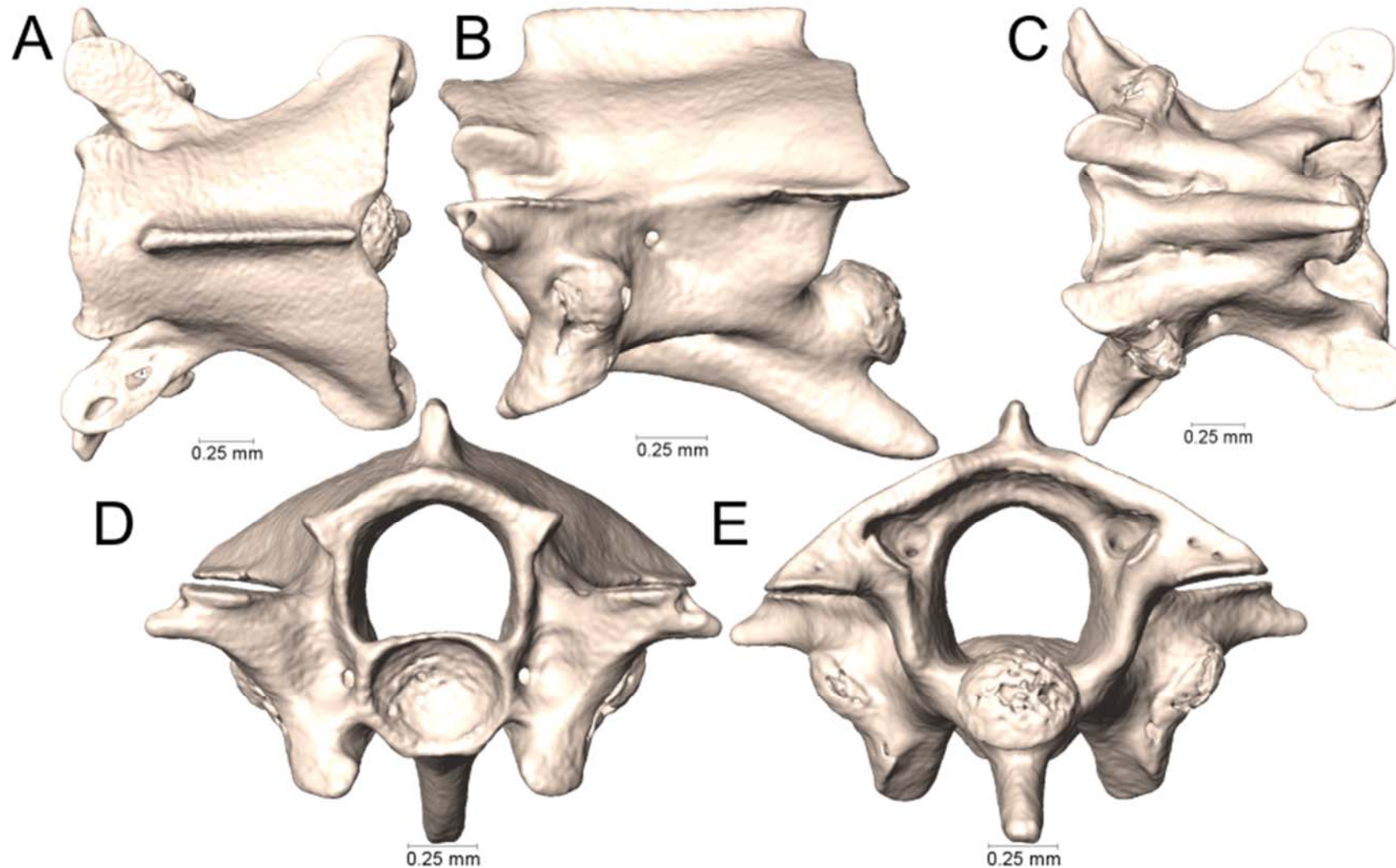
Supplemental Figure 4.7. Dorsal, lateral, ventral, anterior, and posterior views (A-E, respectively) of the midbody vertebra of *Calliophis bivirgatus bivirgatus* (UTA R-63079).



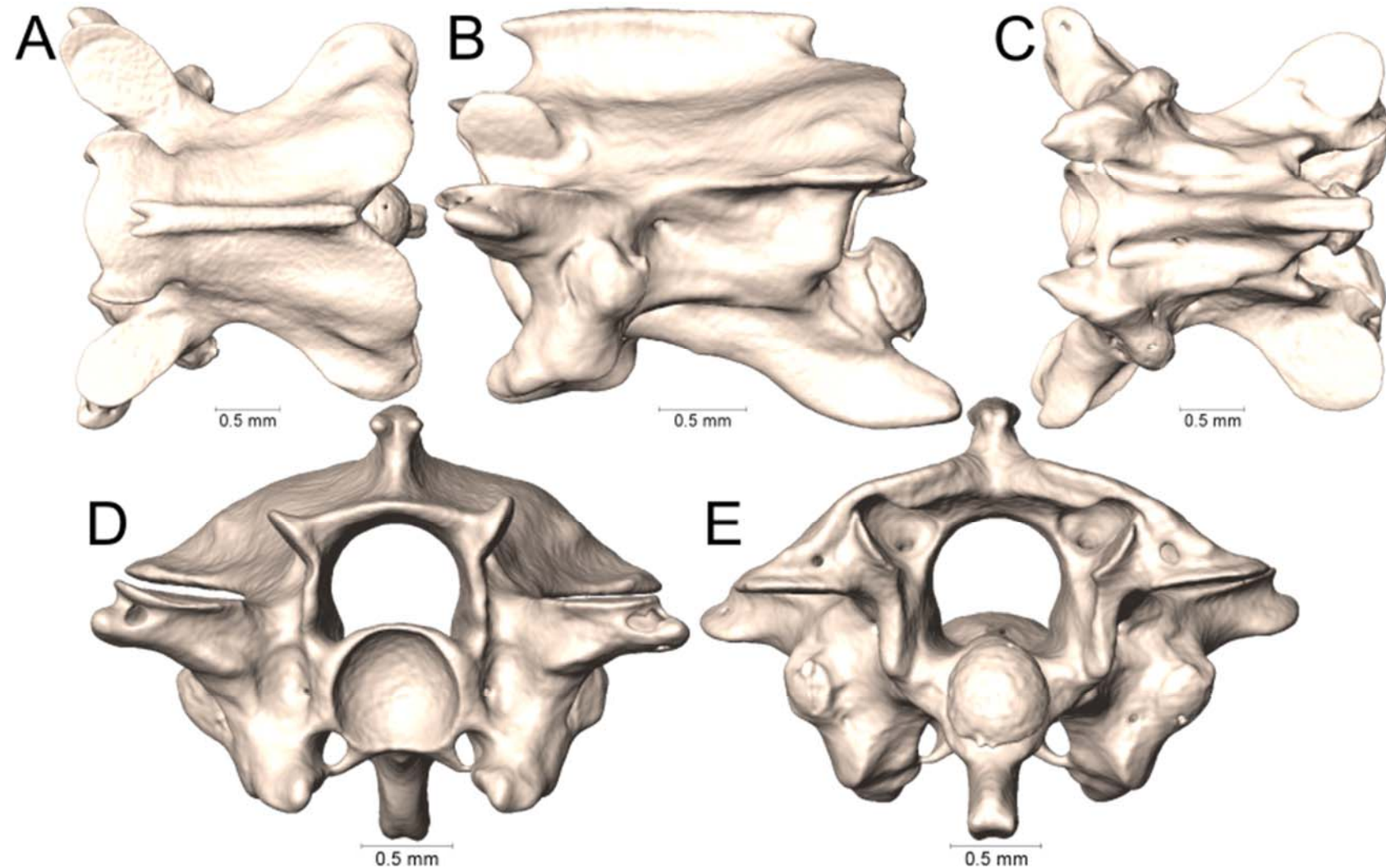
Supplemental Figure 4.8. Dorsal, lateral, ventral, anterior, and posterior views (A-E, respectively) of the midbody vertebra of *Calliophis gracilis* (USNM 53447).



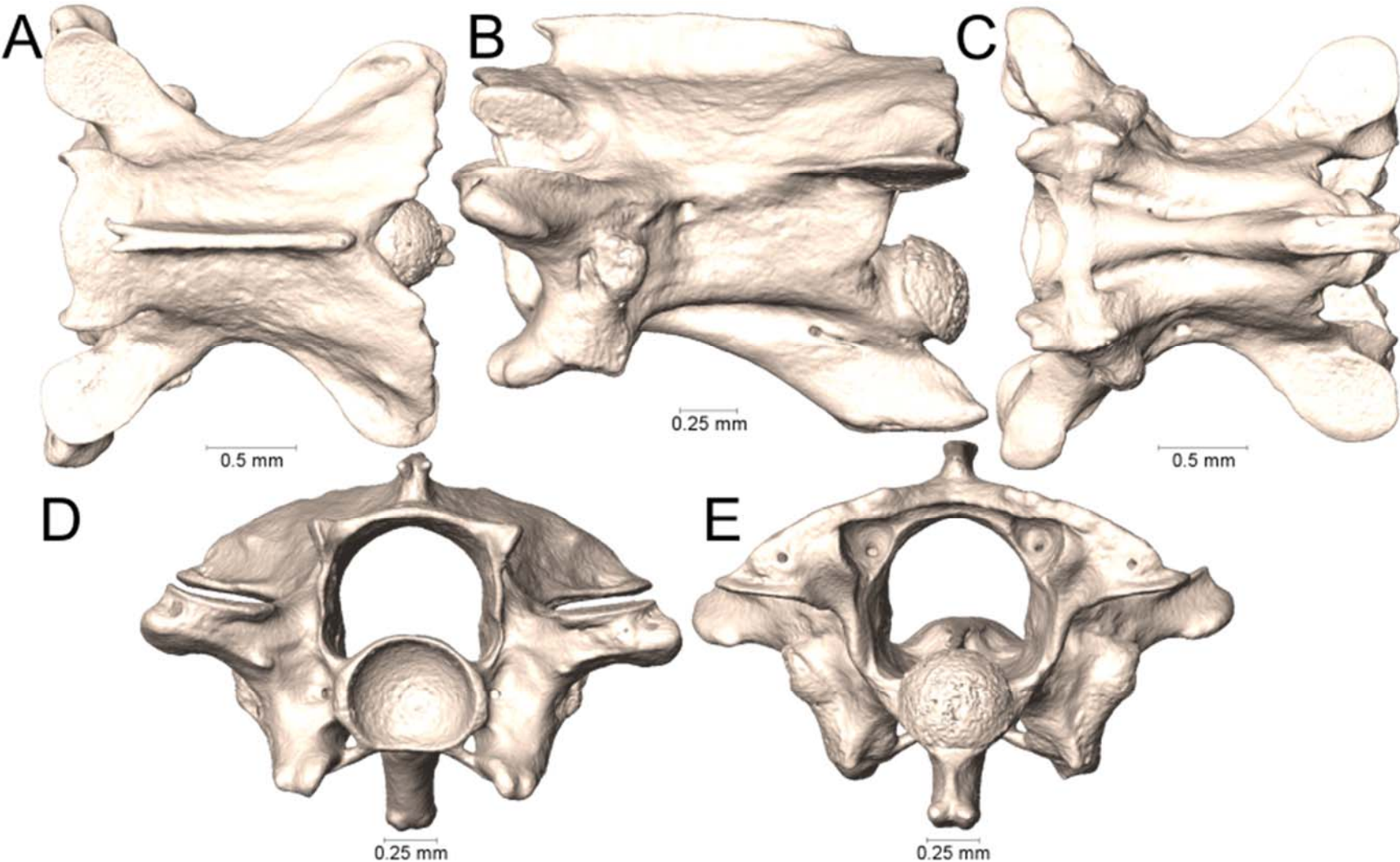
Supplemental Figure 4.9. Dorsal, lateral, ventral, anterior, and posterior views (A-E, respectively) of the midbody vertebra of *Calliophis intestinalis* (UTA R-60738).



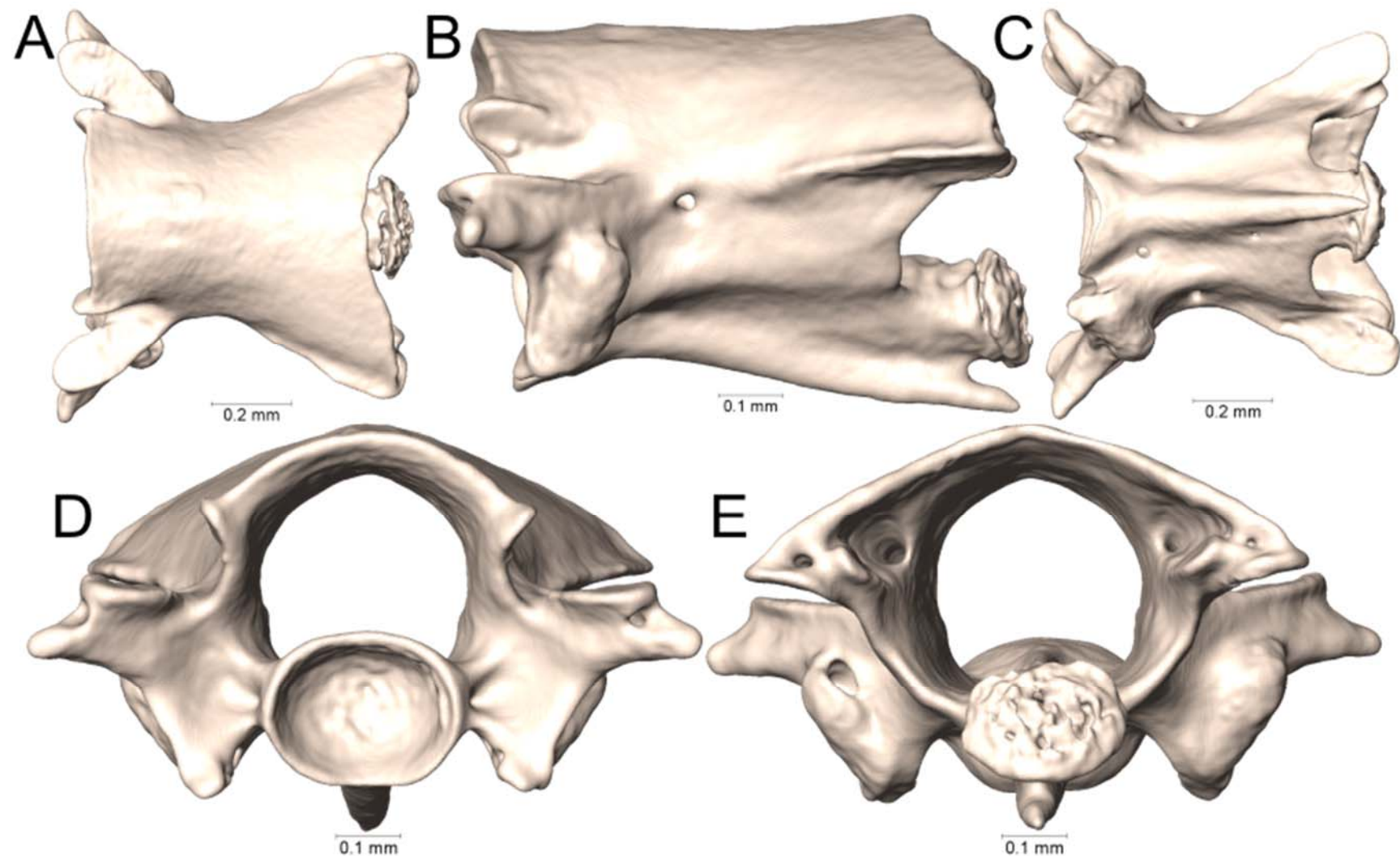
Supplemental Figure 4.10. Dorsal, lateral, ventral, anterior, and posterior views (A-E, respectively) of the midbody vertebra of *Calliophis intestinalis immaculata* (UTA R-65802).



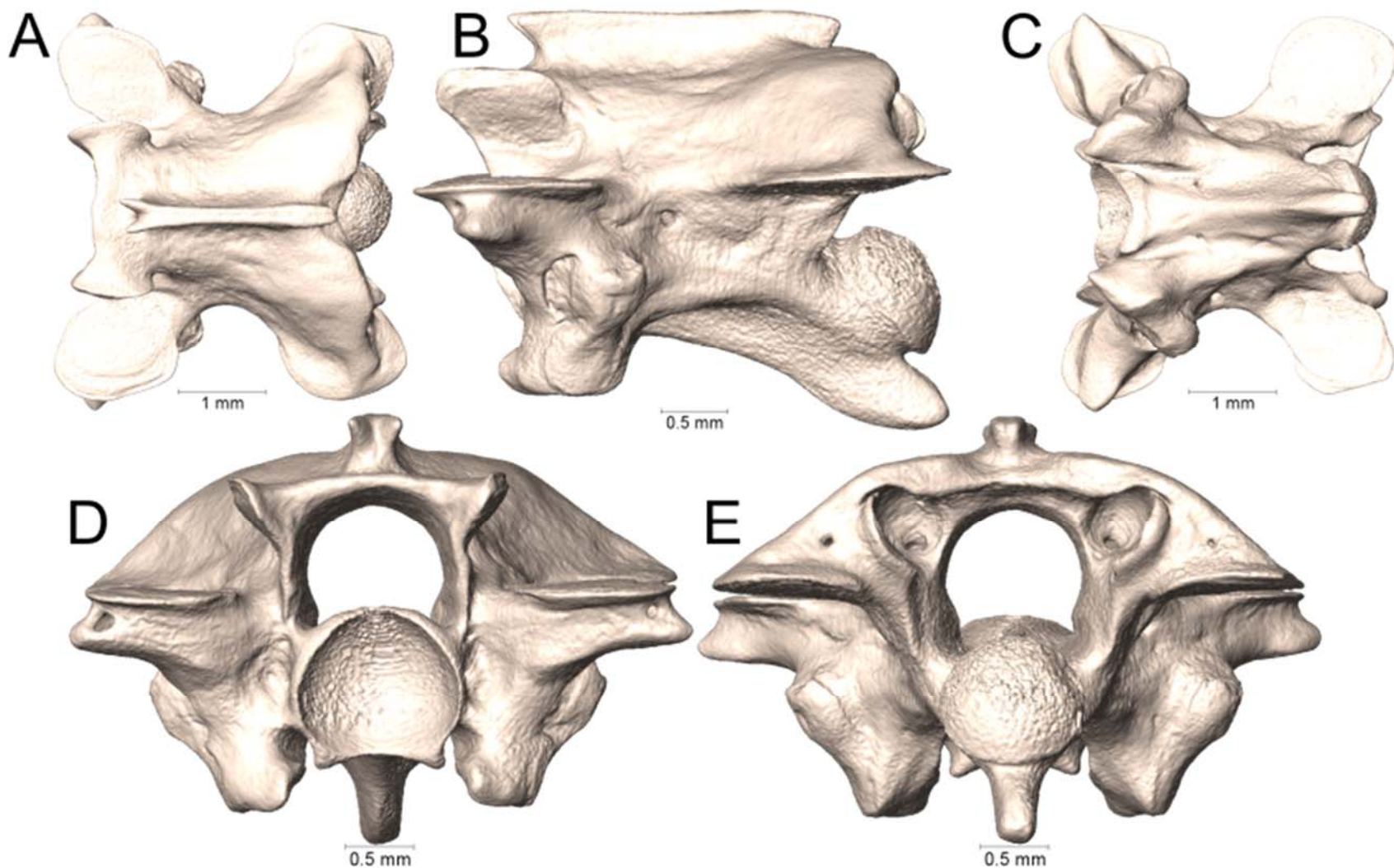
Supplemental Figure 4.11. Dorsal, lateral, ventral, anterior, and posterior views (A-E, respectively) of the midbody vertebra of *Calliophis intestinalis lineata* (UTA R-65801).



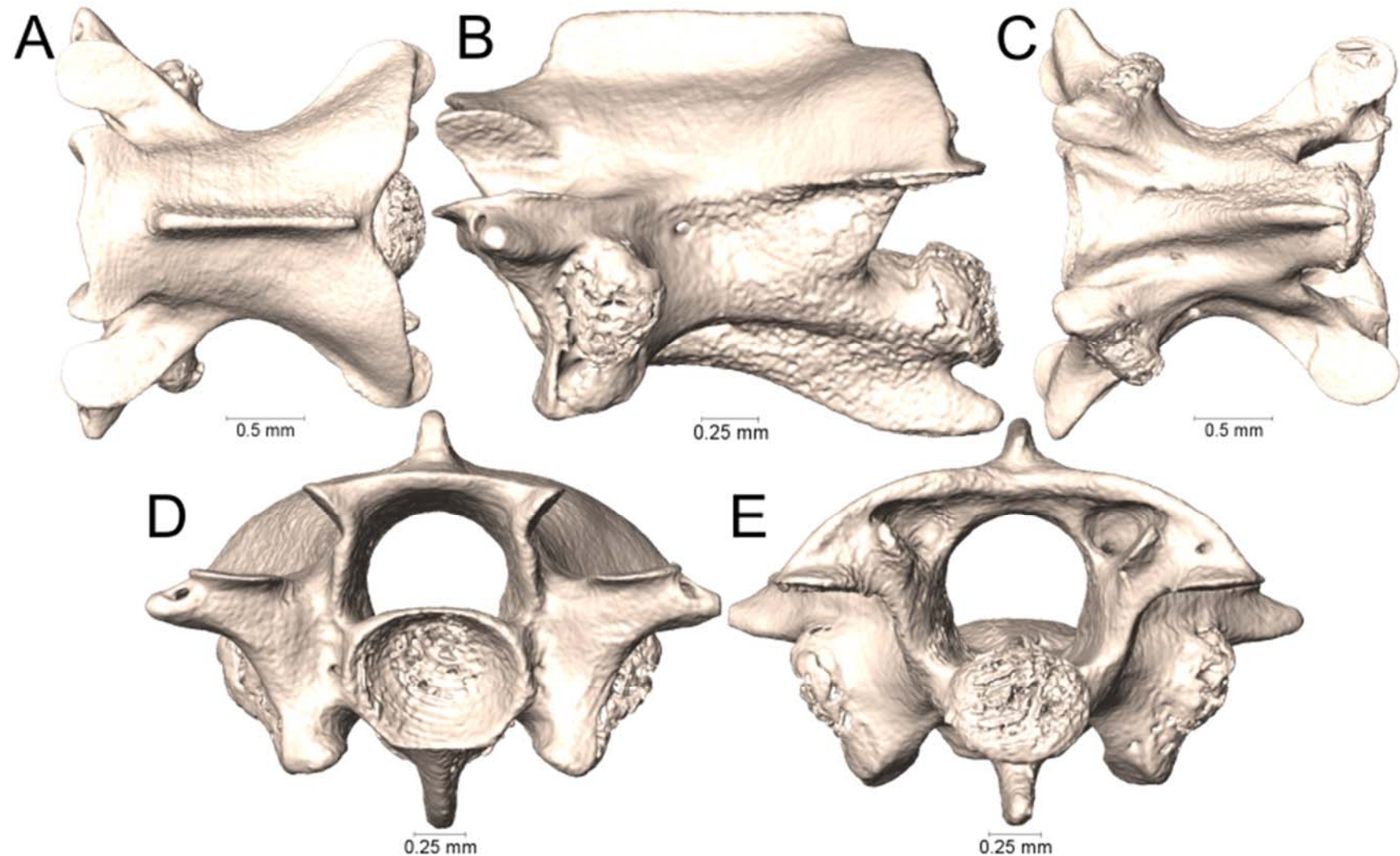
Supplemental Figure 4.12. Dorsal, lateral, ventral, anterior, and posterior views (A-E, respectively) of the midbody vertebra of *Calliophis maculiceps* (MNHN 5459).



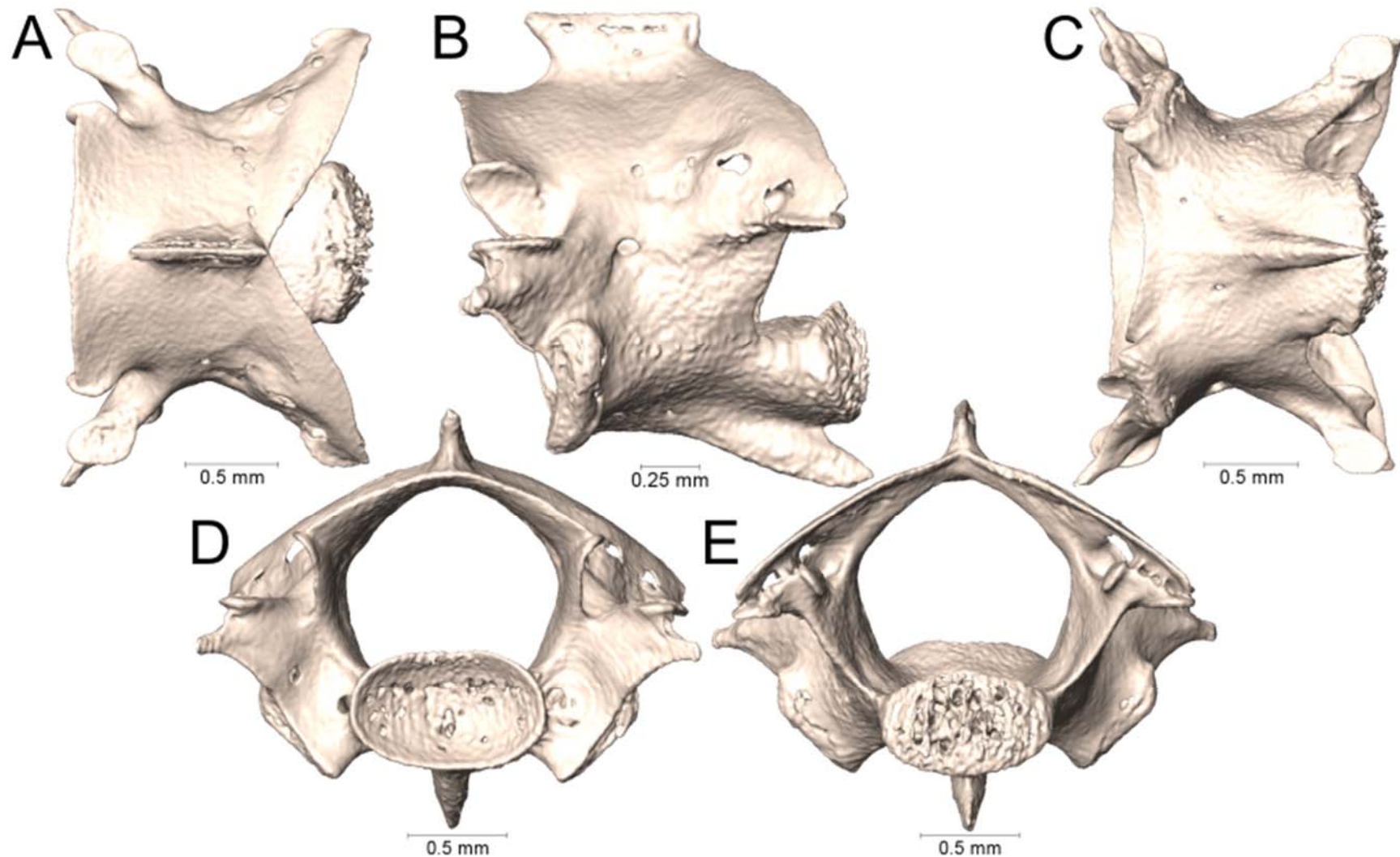
Supplemental Figure 4.13. Dorsal, lateral, ventral, anterior, and posterior views (A-E, respectively) of the midbody vertebra of *Calliophis melanurus* (MNHN 46-286).



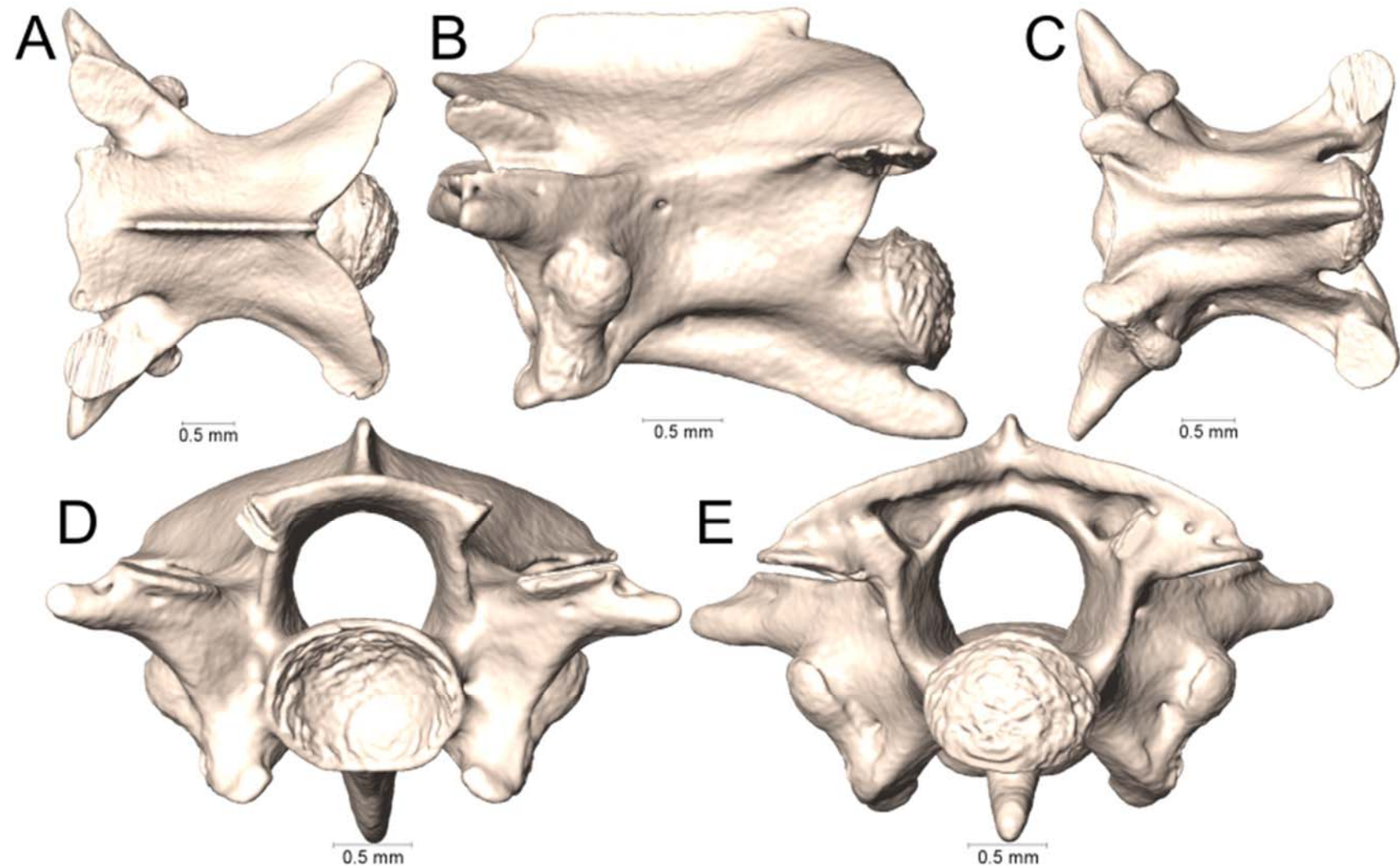
Supplemental Figure 4.14. Dorsal, lateral, ventral, anterior, and posterior views (A-E, respectively) of the midbody vertebra of *Calliophis philippinus* (KU 310369).



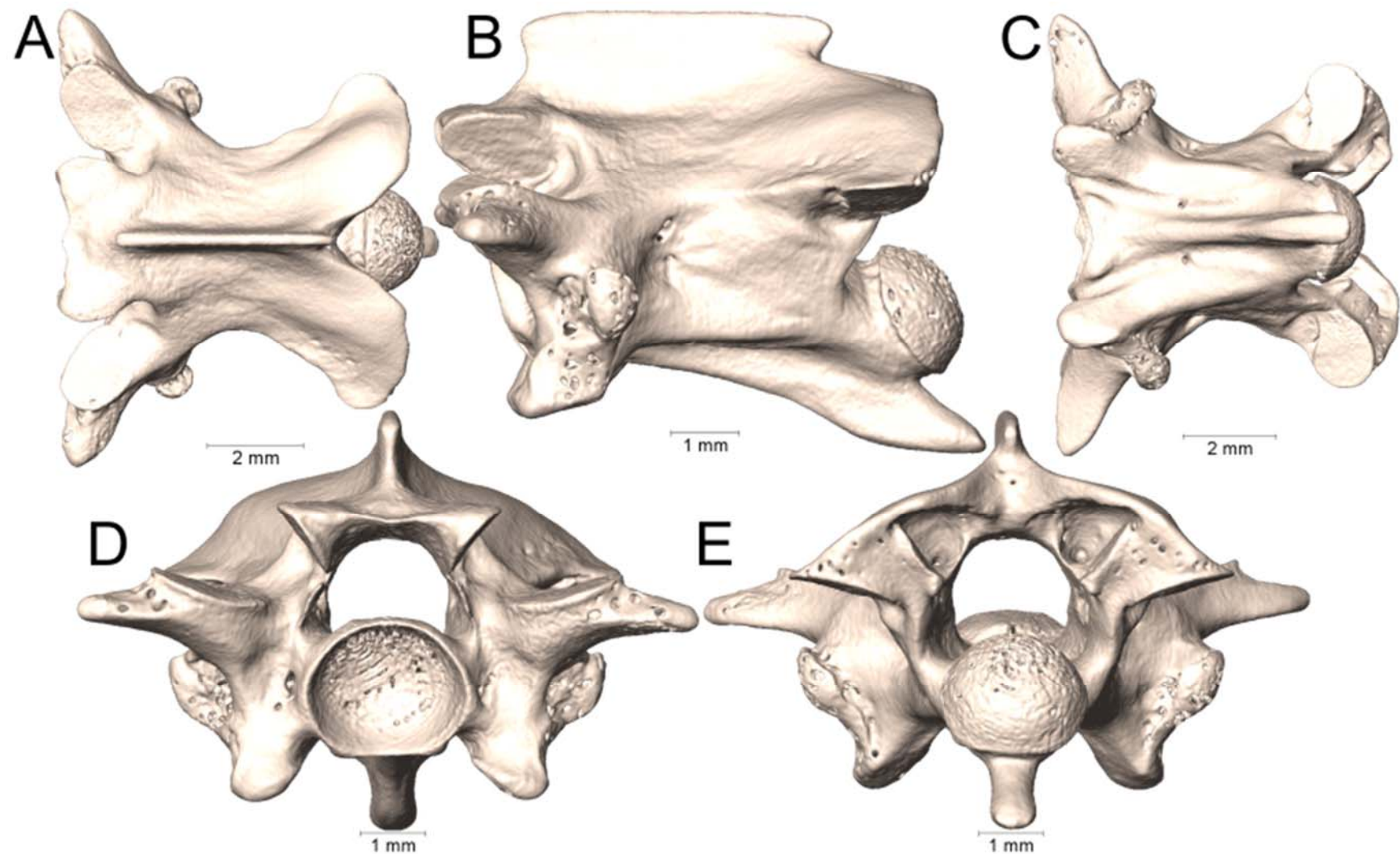
Supplemental Figure 4.15. Dorsal, lateral, ventral, anterior, and posterior views (A-E, respectively) of the midbody vertebra of *Calliophis philippinus* (KU 314913).



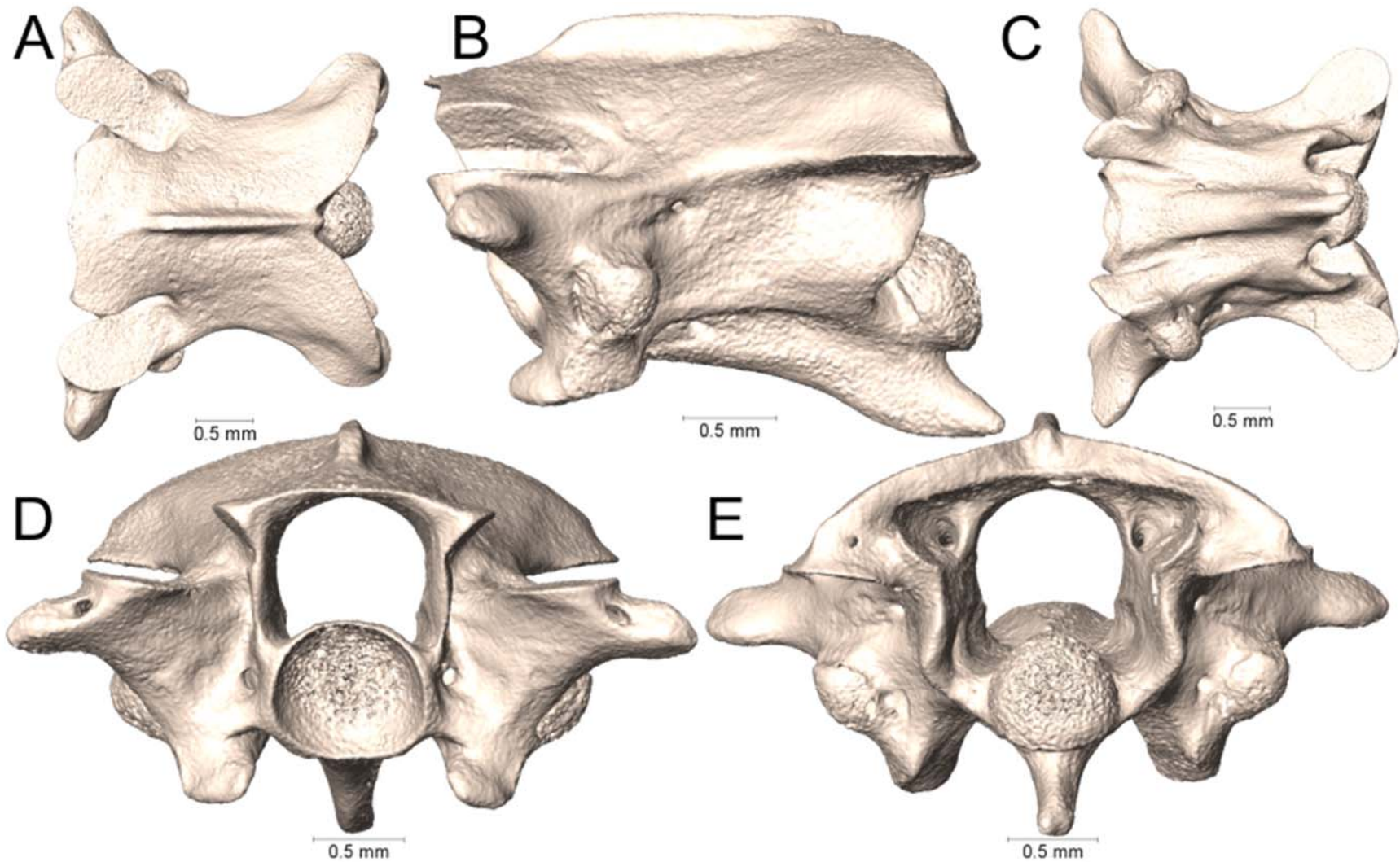
Supplemental Figure 4.16. Dorsal, lateral, ventral, anterior, and posterior views (A-E, respectively) of the midbody vertebra of *Dendroaspis angusticeps* (UTA R-34982).



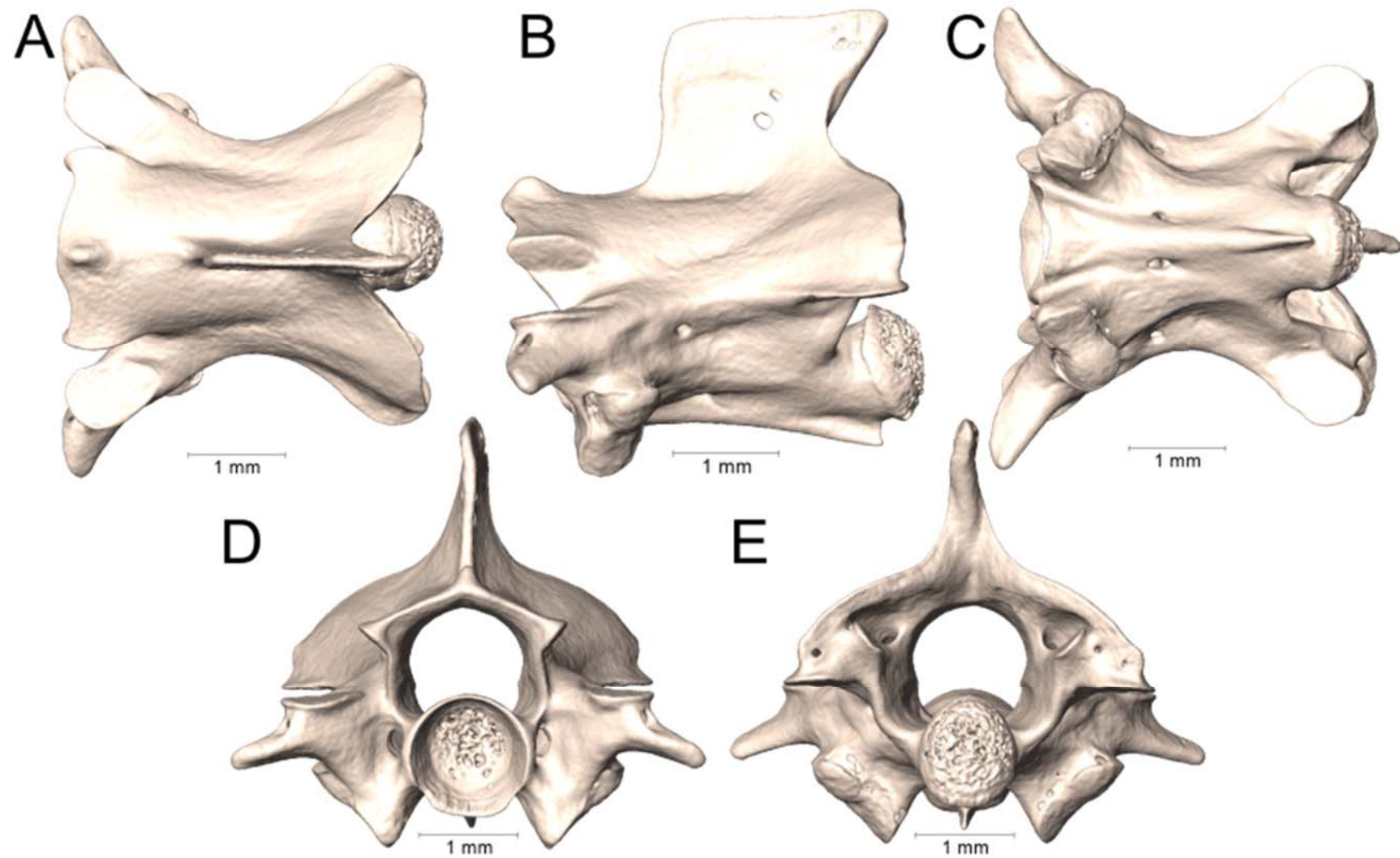
Supplemental Figure 4.17. Dorsal, lateral, ventral, anterior, and posterior views (A-E, respectively) of the midbody vertebra of *Elapsoidea nigra* (CAS 168978).



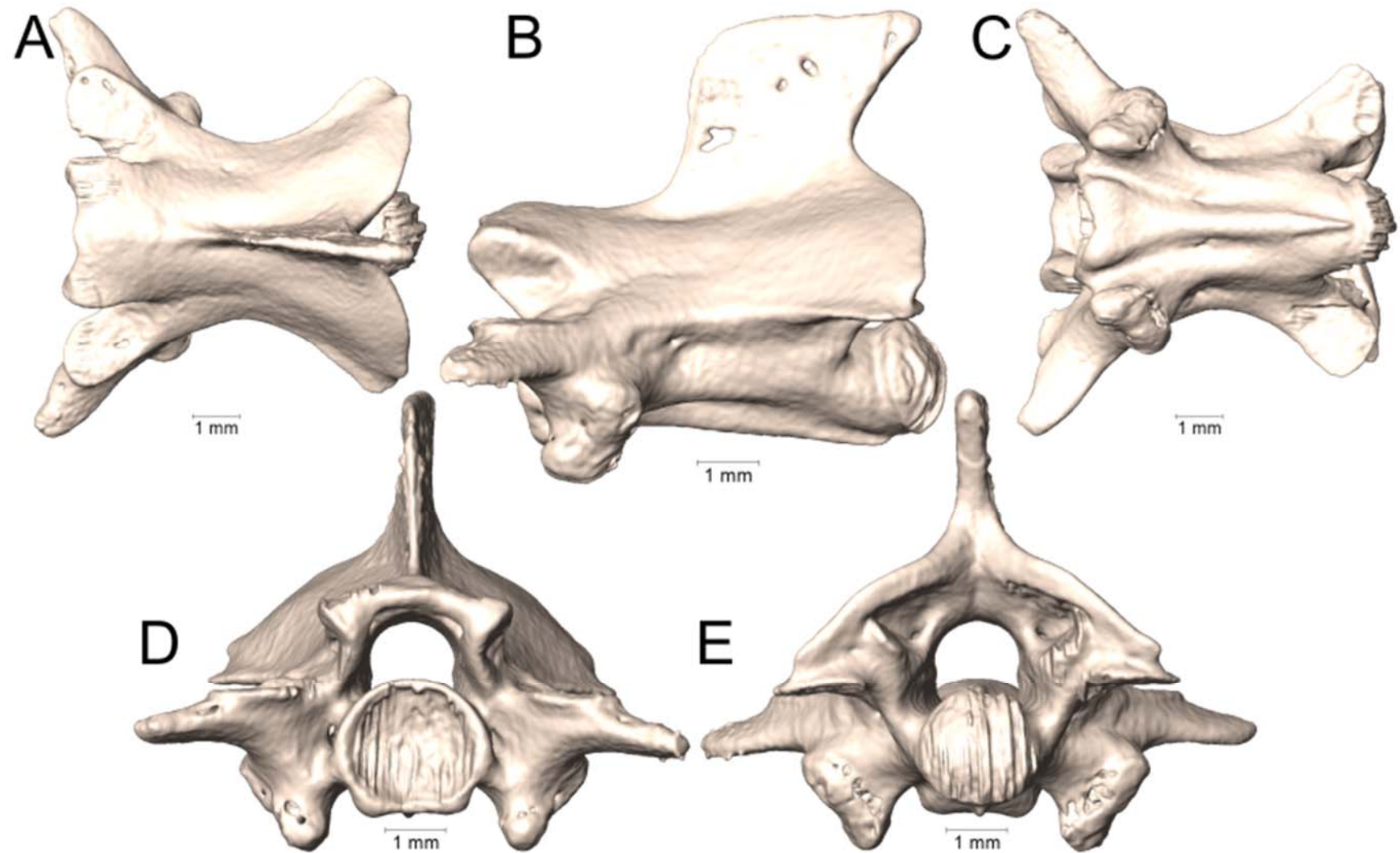
Supplemental Figure 4.18. Dorsal, lateral, ventral, anterior, and posterior views (A-E, respectively) of the midbody vertebra of *Hemachatus haemachatus* (UTA R-7431).



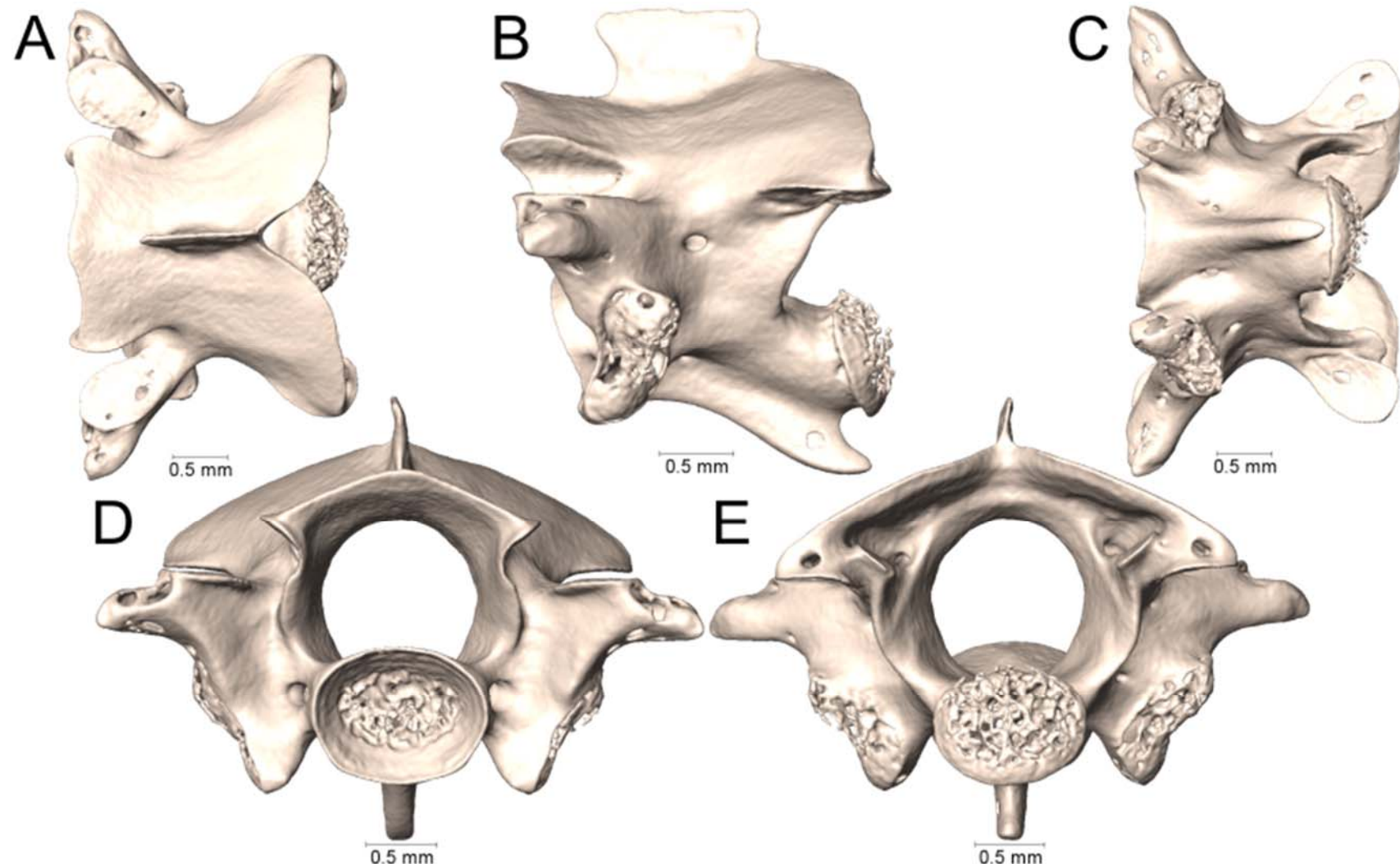
Supplemental Figure 4.19. Dorsal, lateral, ventral, anterior, and posterior views (A-E, respectively) of the midbody vertebra of *Hemibungarus calligaster* (KU 307474).



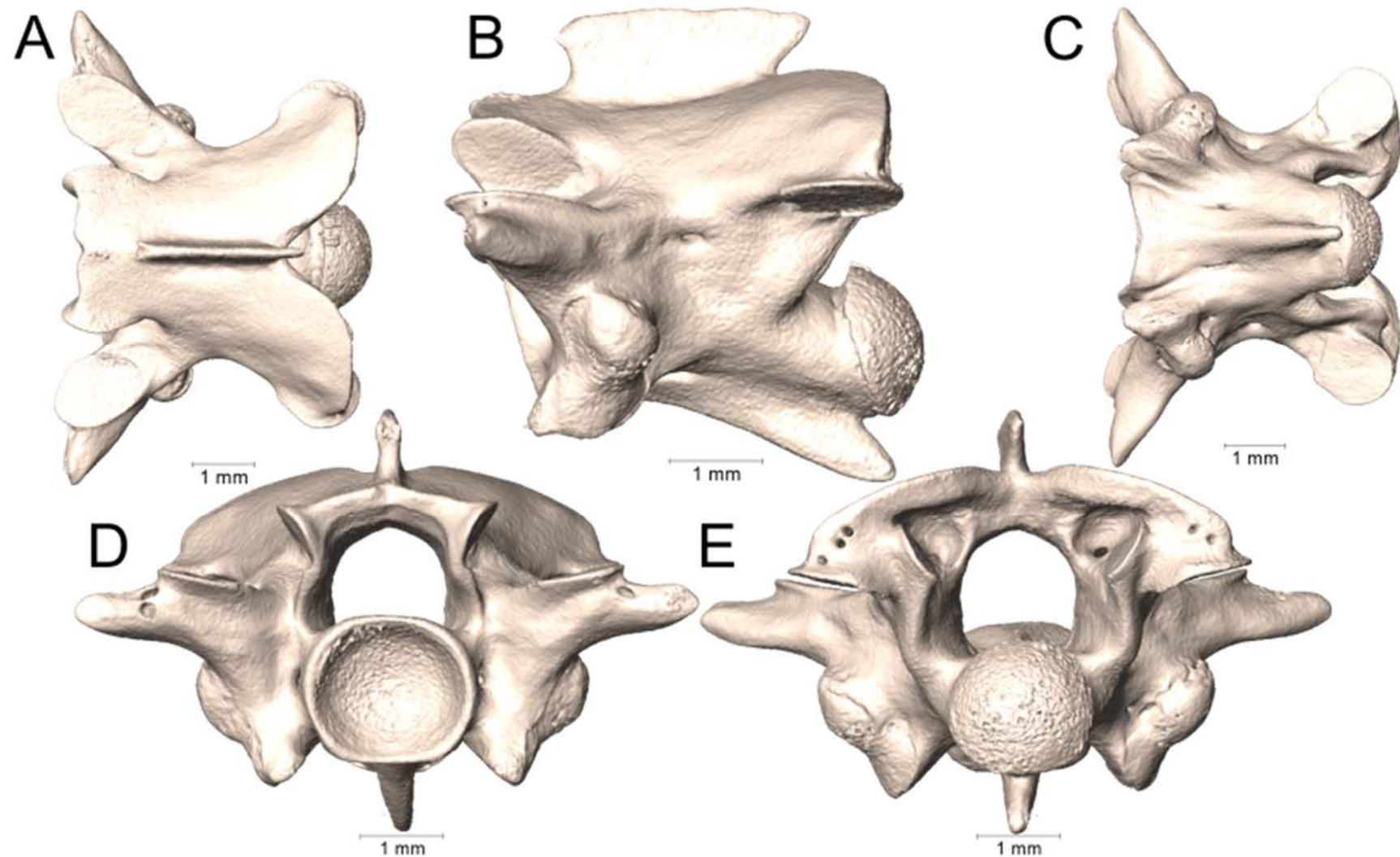
Supplemental Figure 4.20. Dorsal, lateral, ventral, anterior, and posterior views (A-E, respectively) of the midbody vertebra of *Hydrophis platurus* (UTA R-41049).



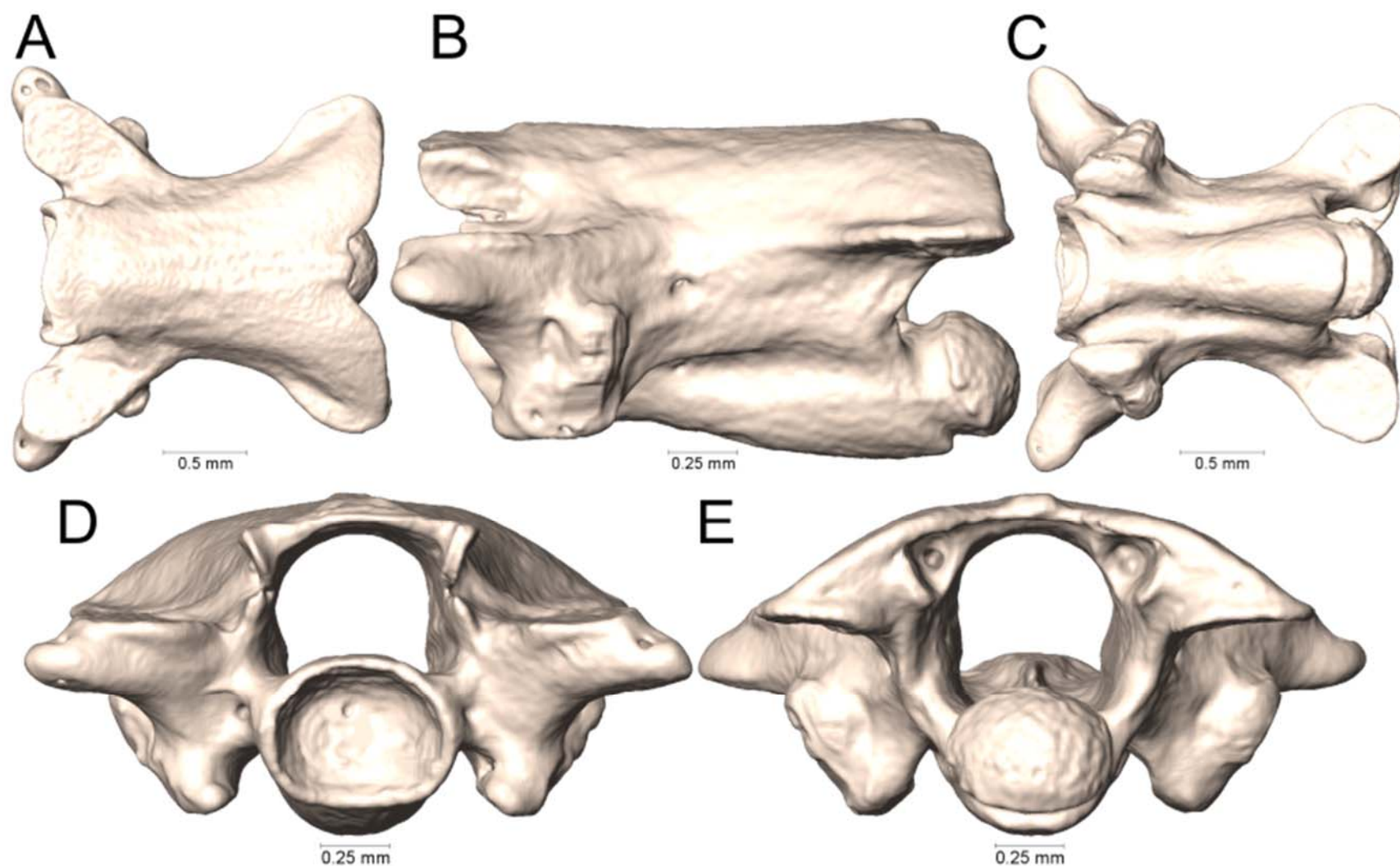
Supplemental Figure 4.21. Dorsal, lateral, ventral, anterior, and posterior views (A-E, respectively) of the midbody vertebra of *Hydrophis schistosus* (UTA R-63074).



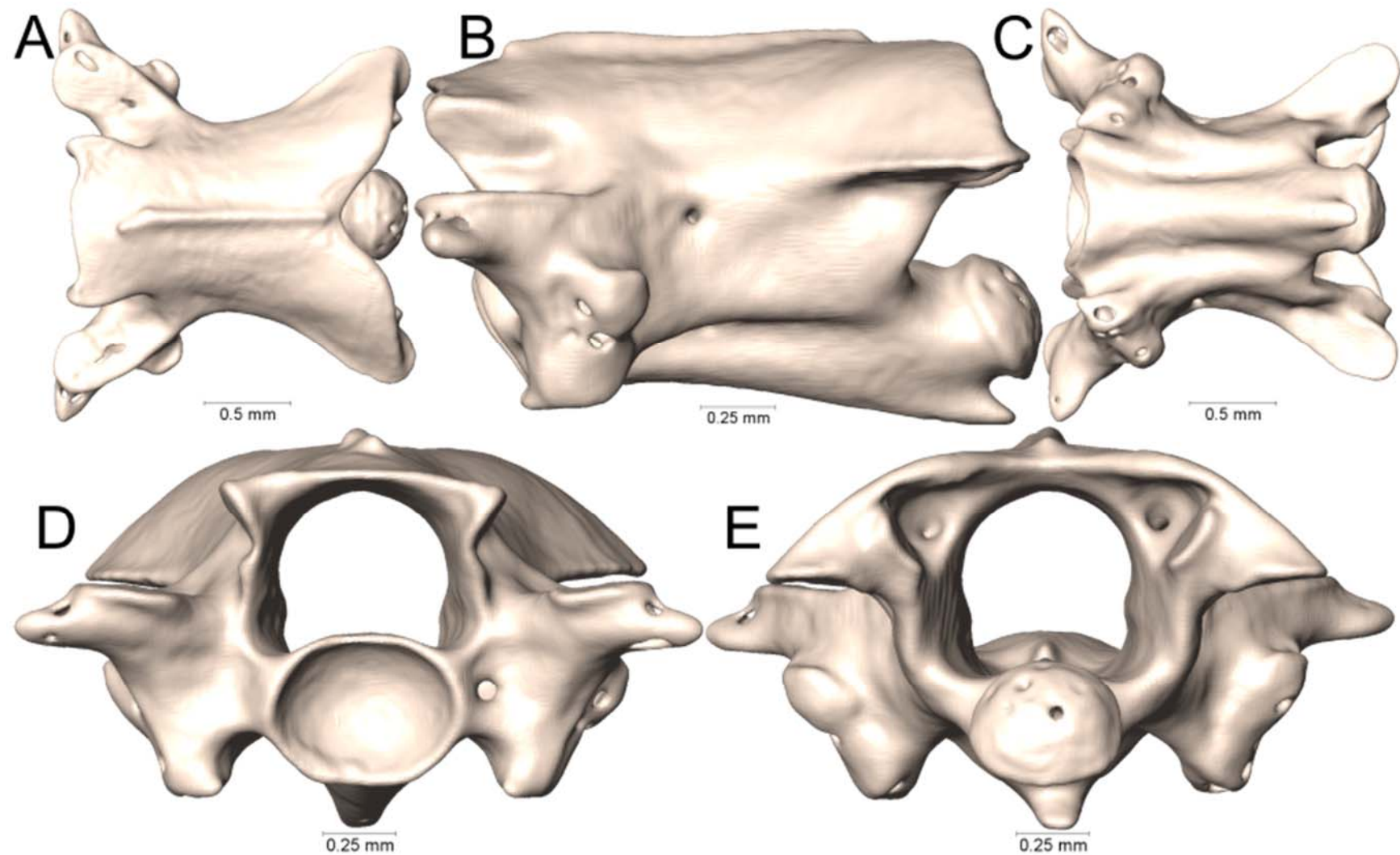
Supplemental Figure 4.22. Dorsal, lateral, ventral, anterior, and posterior views (A-E, respectively) of the midbody vertebra of *Laticauda colubrina* (UTA R-65800).



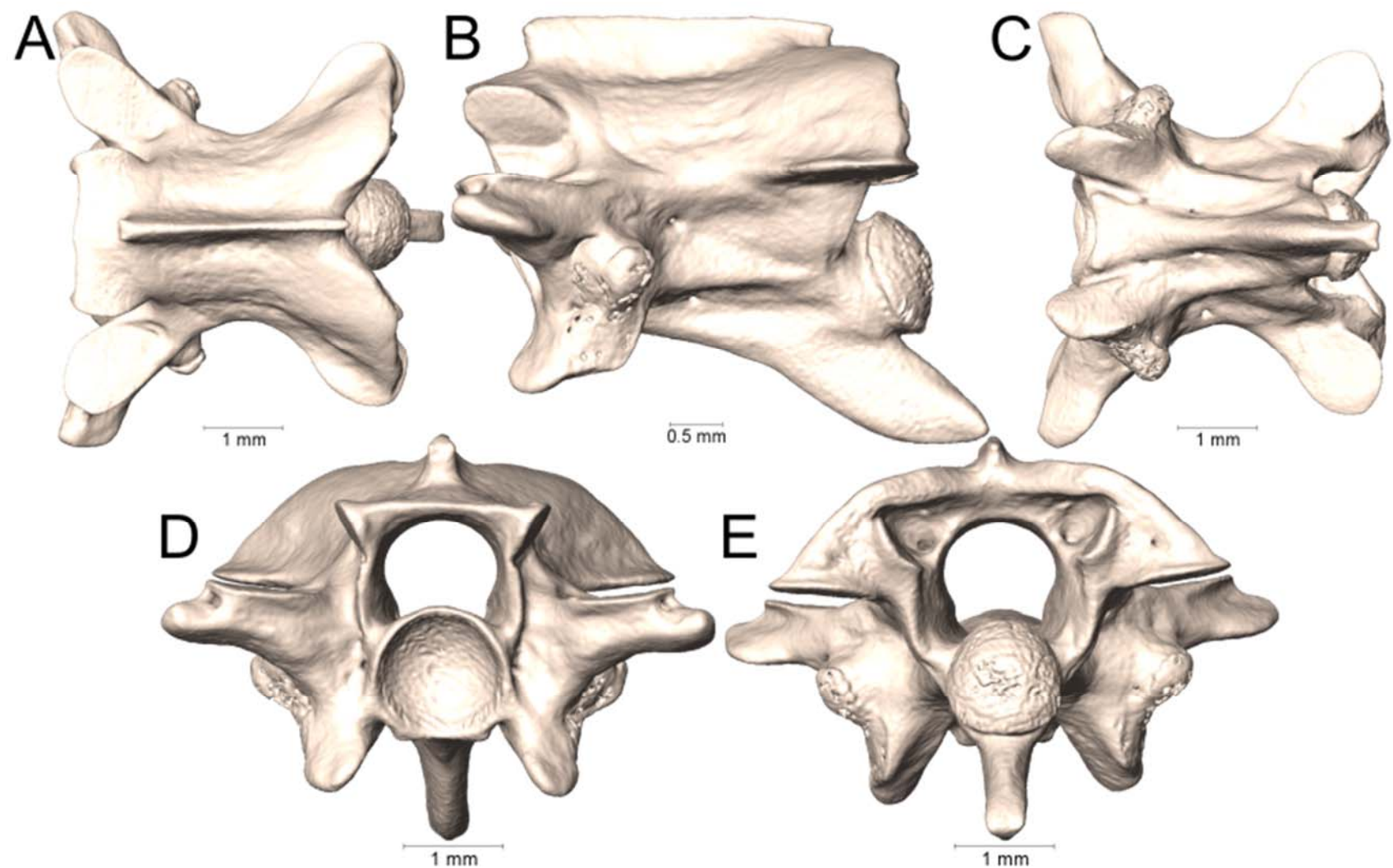
Supplemental Figure 4.23. Dorsal, lateral, ventral, anterior, and posterior views (A-E, respectively) of the midbody vertebra of *Laticauda laticauda* (UTA R-6355).



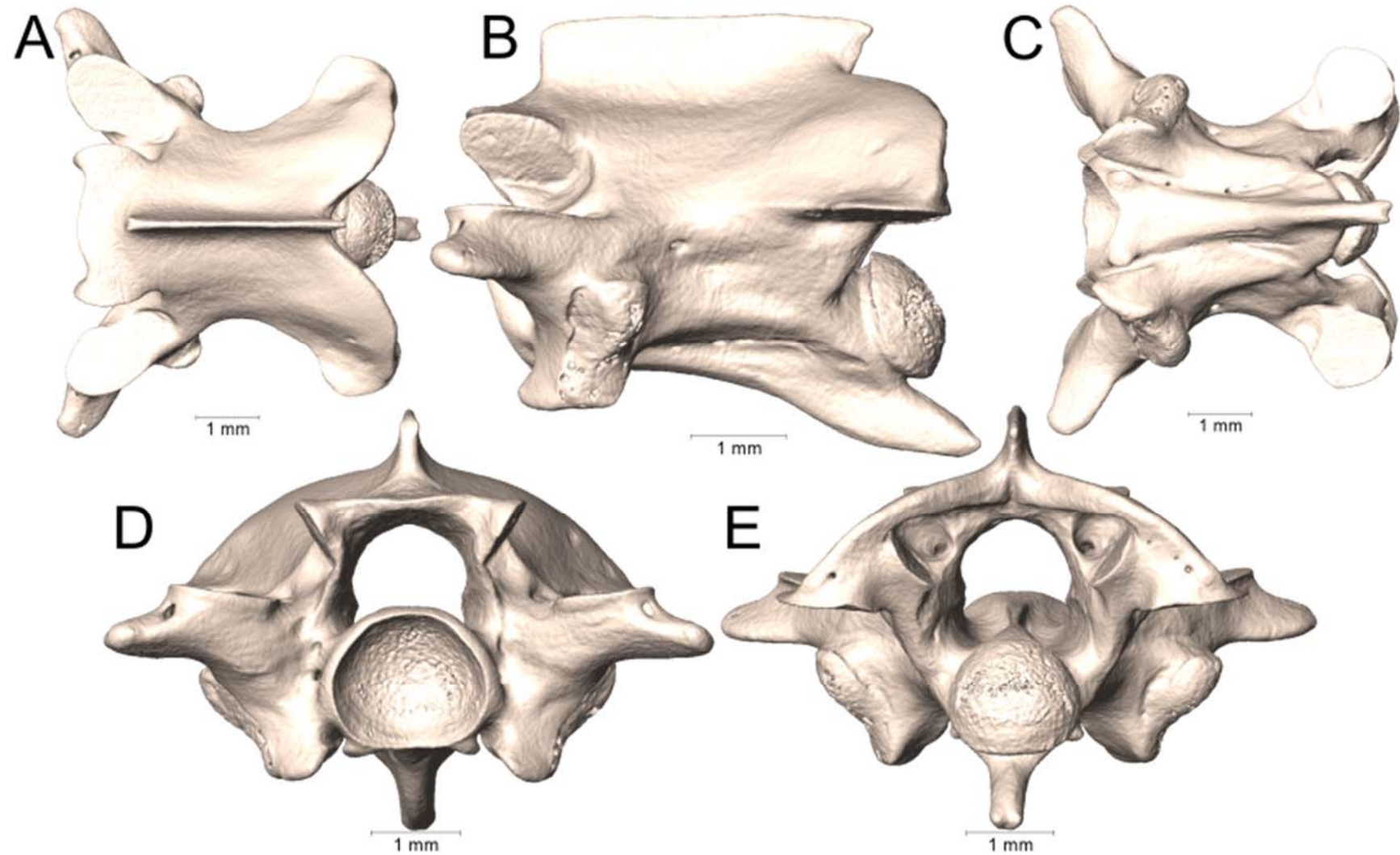
Supplemental Figure 4.24. Dorsal, lateral, ventral, anterior, and posterior views (A-E, respectively) of the midbody vertebra of *Micrelaps vaillanti* (CAS 169941).



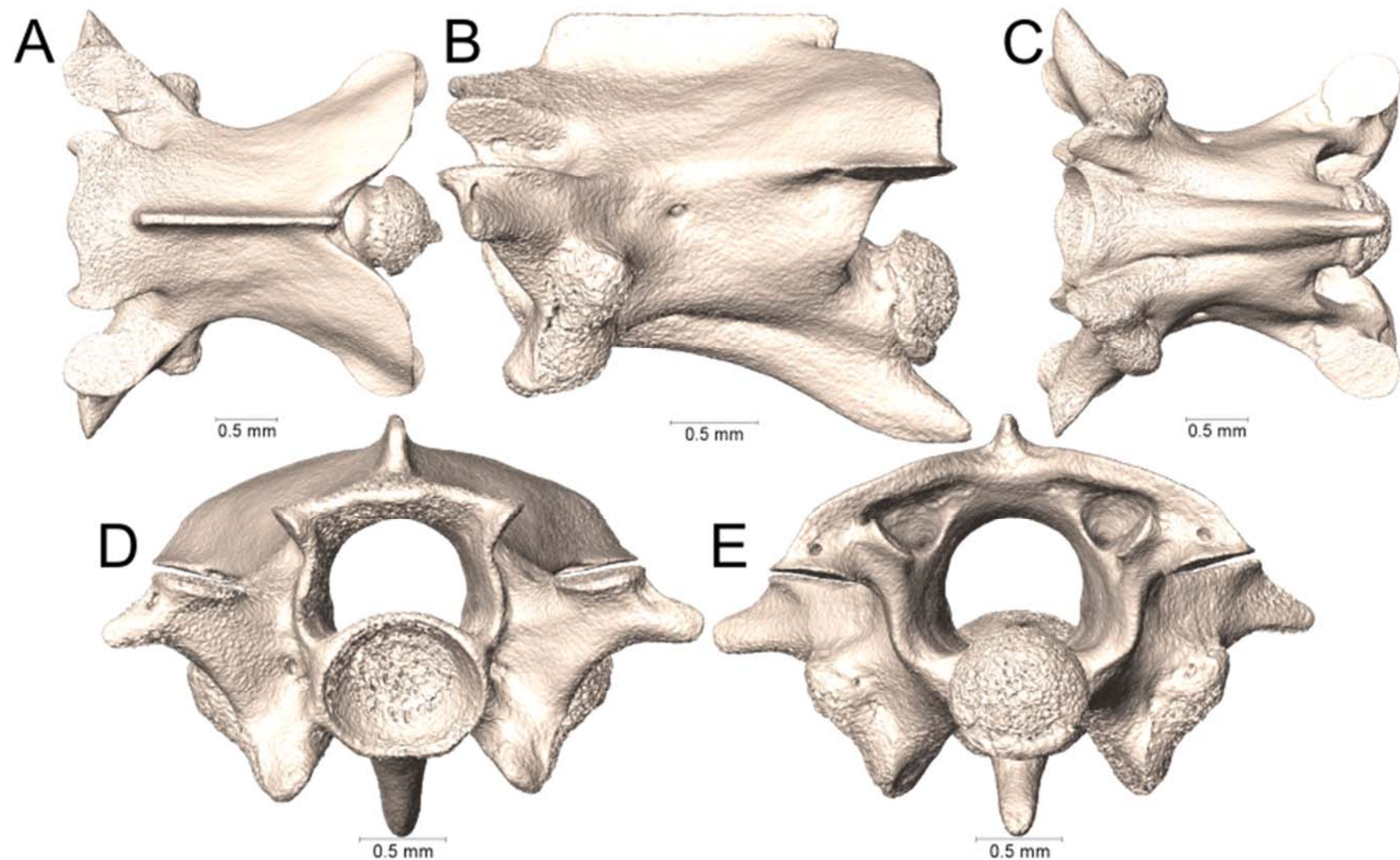
Supplemental Figure 4.25. Dorsal, lateral, ventral, anterior, and posterior views (A-E, respectively) of the midbody vertebra of *Micruroides euryxanthus* (UTA R-60734).



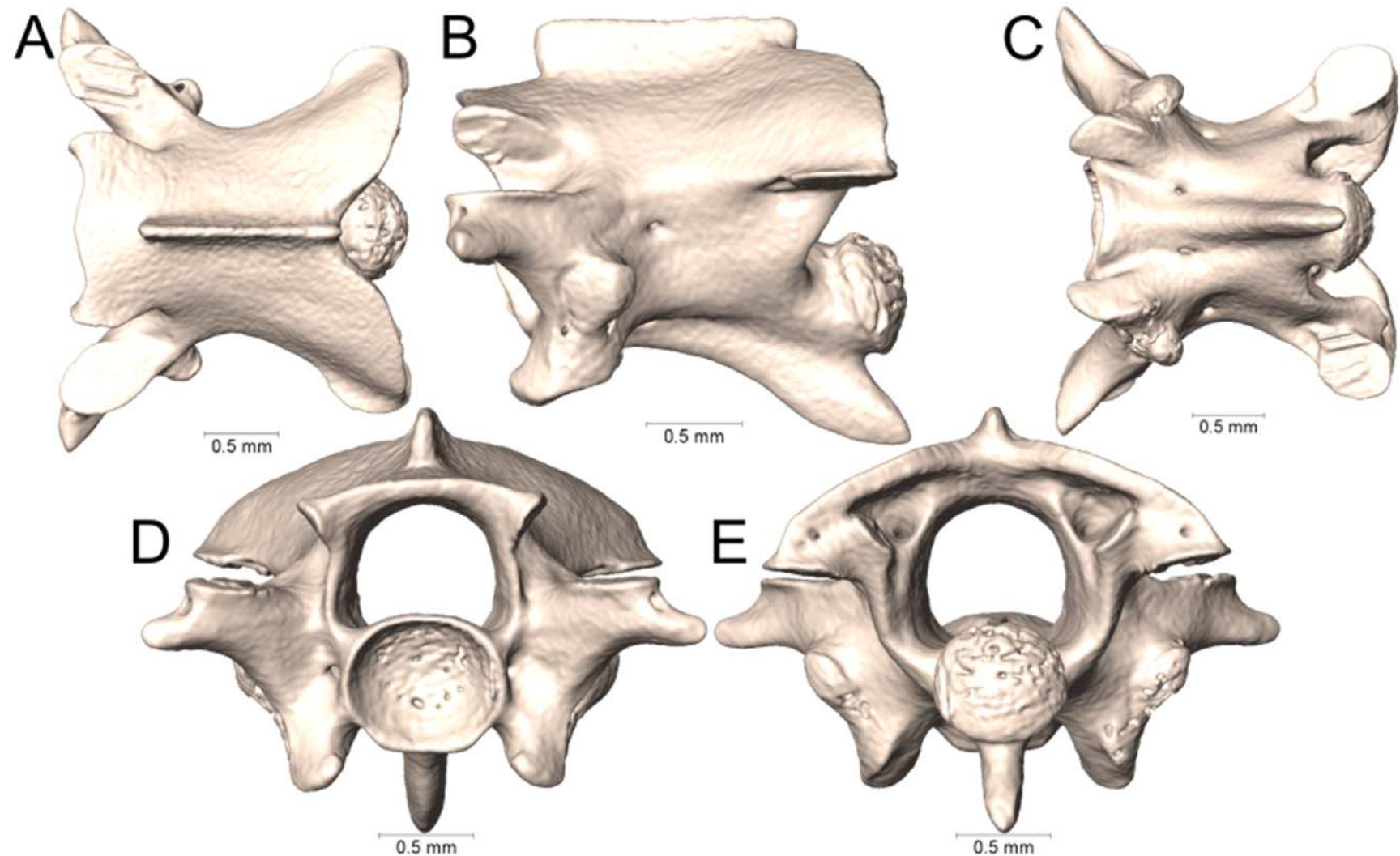
Supplemental Figure 4.26. Dorsal, lateral, ventral, anterior, and posterior views (A-E, respectively) of the midbody vertebra of *Micrurus alleni* (UTA R-60556).



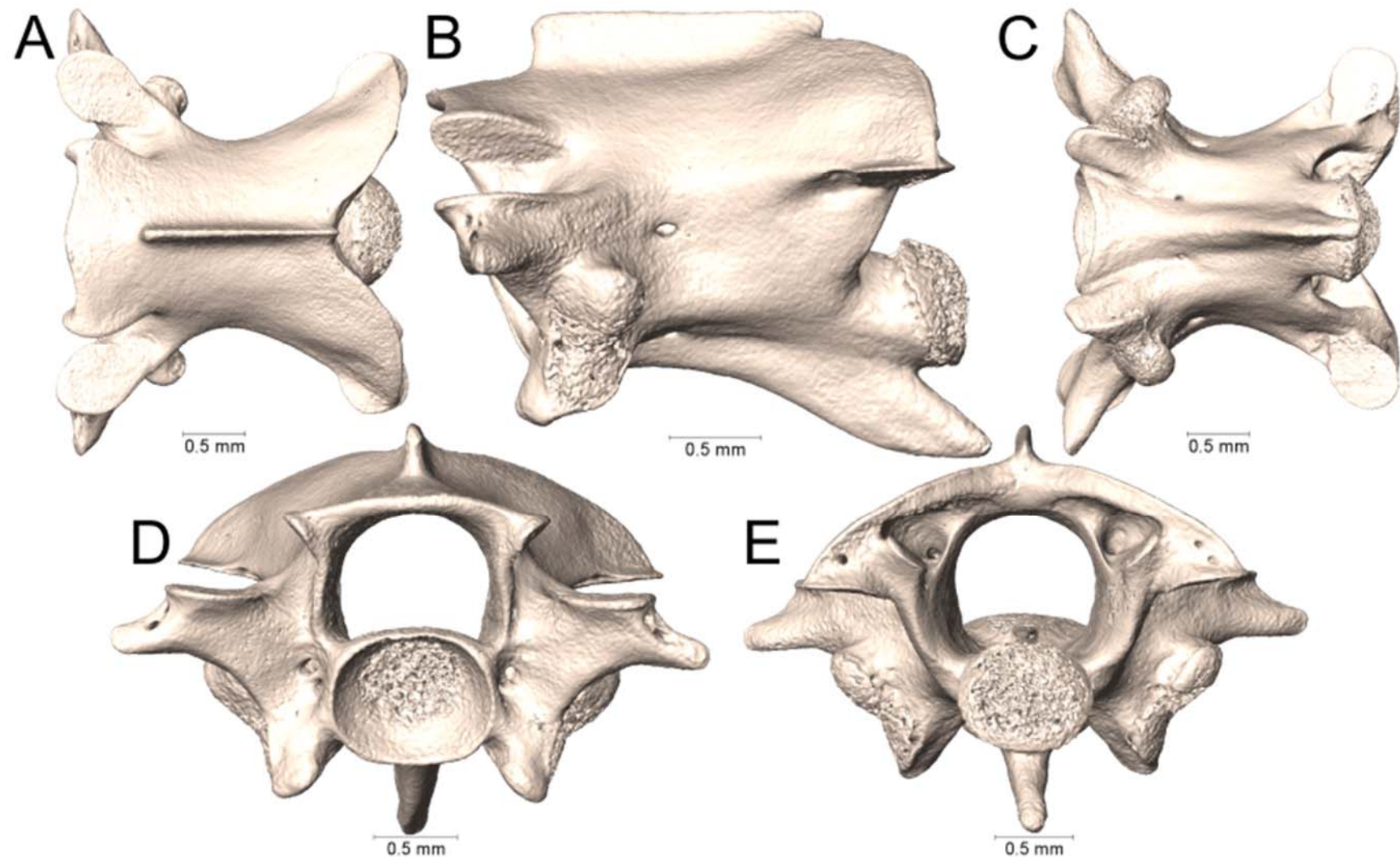
Supplemental Figure 4.27. Dorsal, lateral, ventral, anterior, and posterior views (A-E, respectively) of the midbody vertebra of *Micrurus anchoralis* (UTA R-55945).



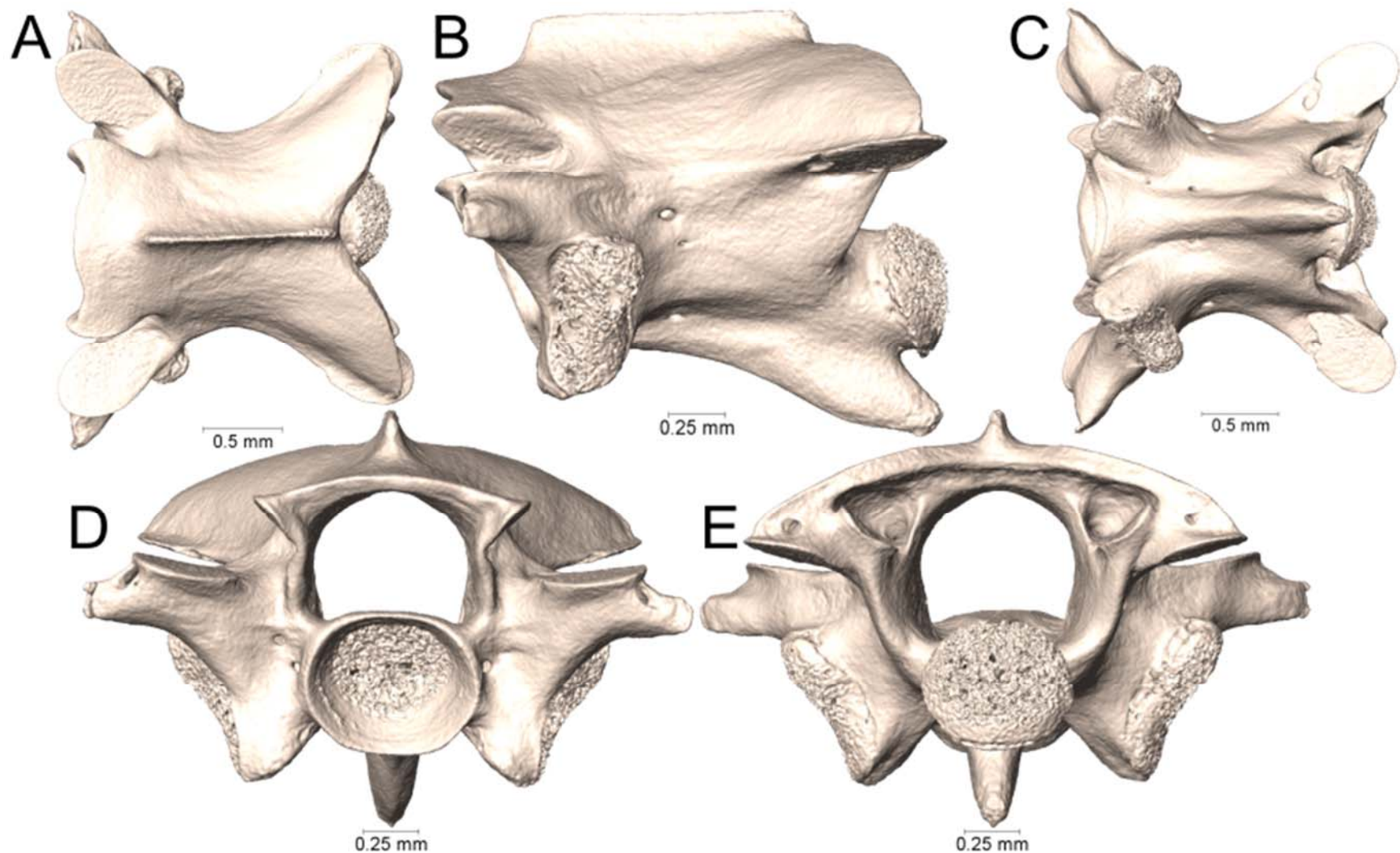
Supplemental Figure 4.28. Dorsal, lateral, ventral, anterior, and posterior views (A-E, respectively) of the midbody vertebra of *Micrurus apiatus* (UTA R-39267).



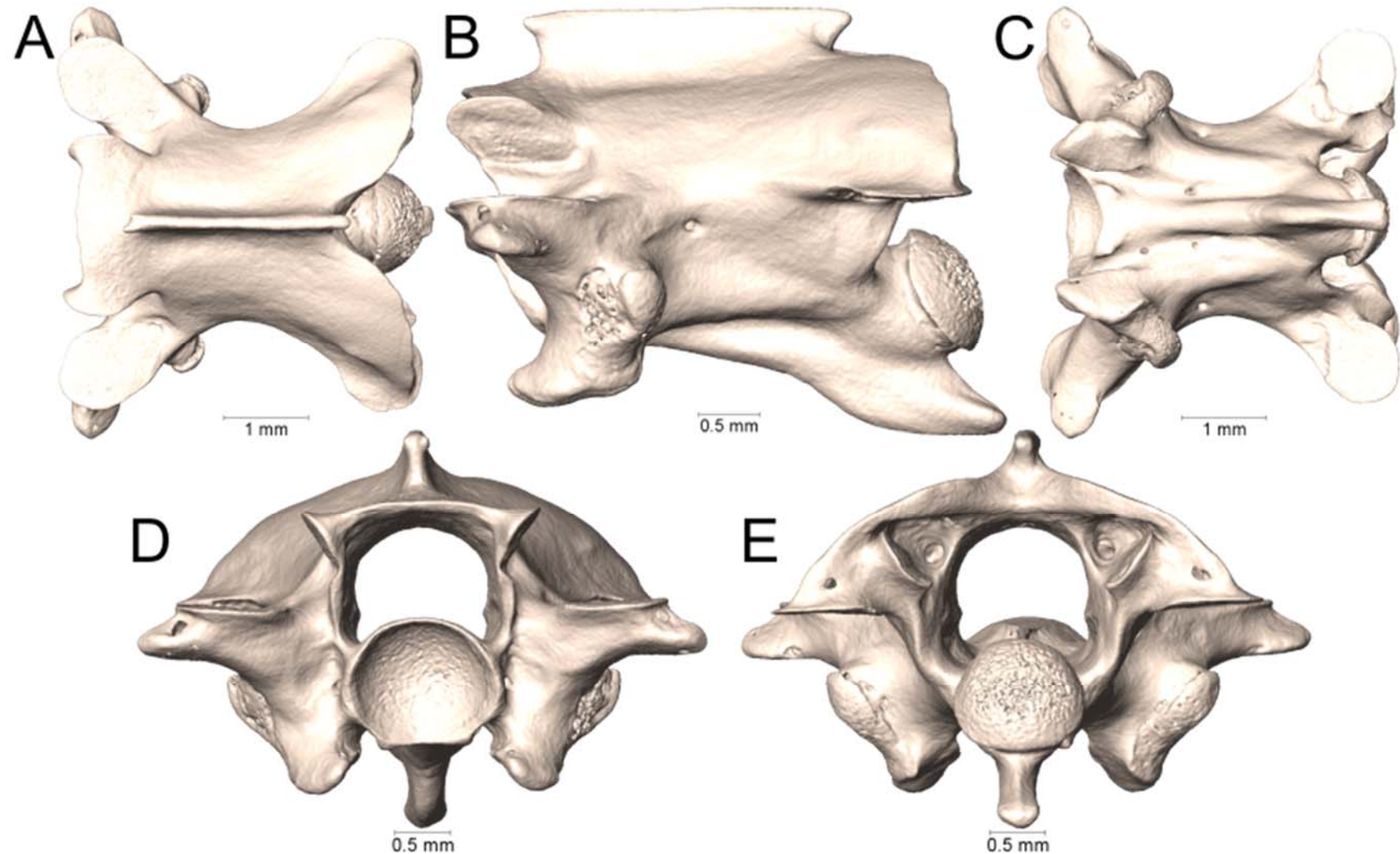
Supplemental Figure 4.29. Dorsal, lateral, ventral, anterior, and posterior views (A-E, respectively) of the midbody vertebra of *Micrurus apiatus* (UTA R-39554).



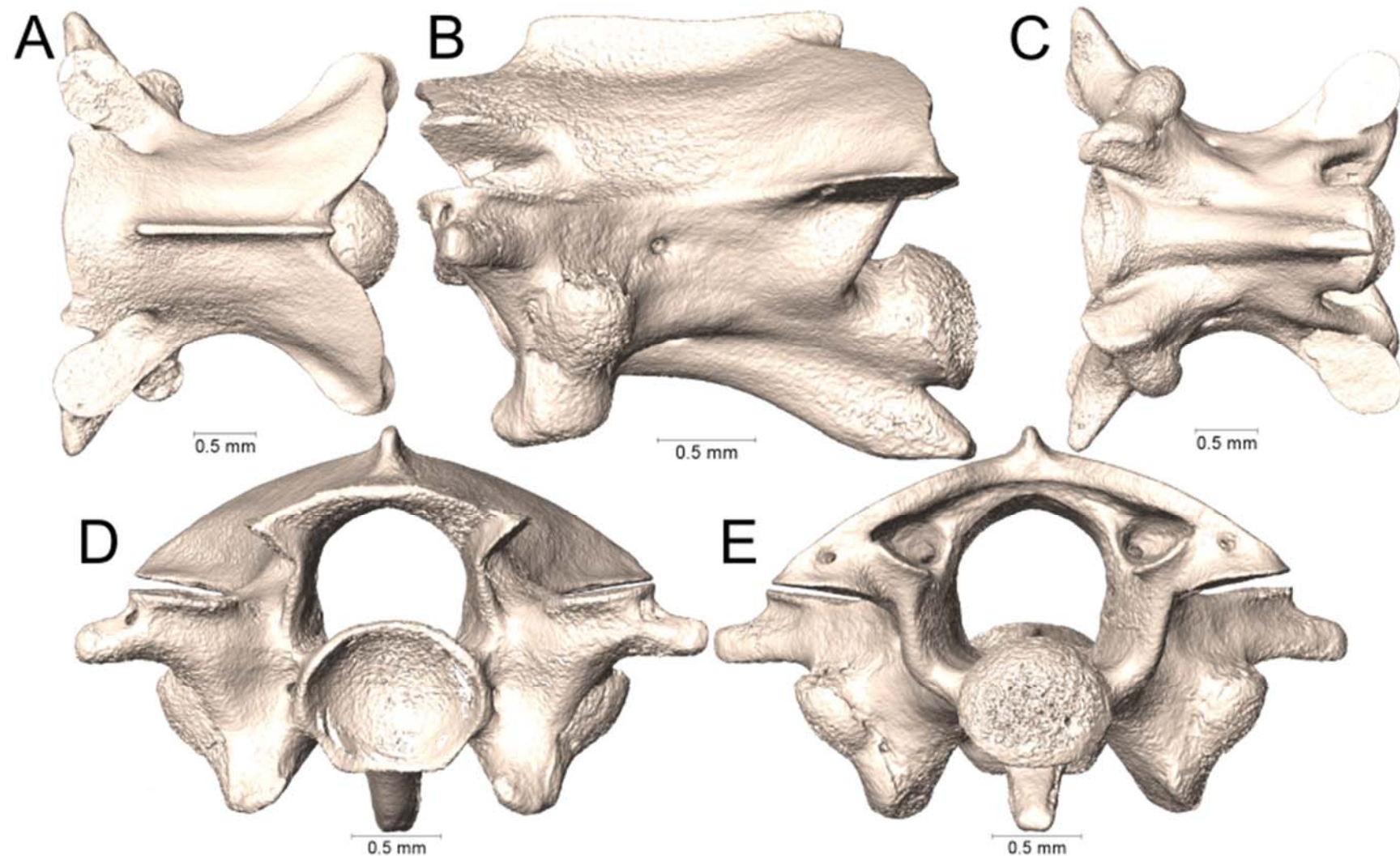
Supplemental Figure 4.30. Dorsal, lateral, ventral, anterior, and posterior views (A-E, respectively) of the midbody vertebra of *Micrurus apiatus* (UTA R-53450).



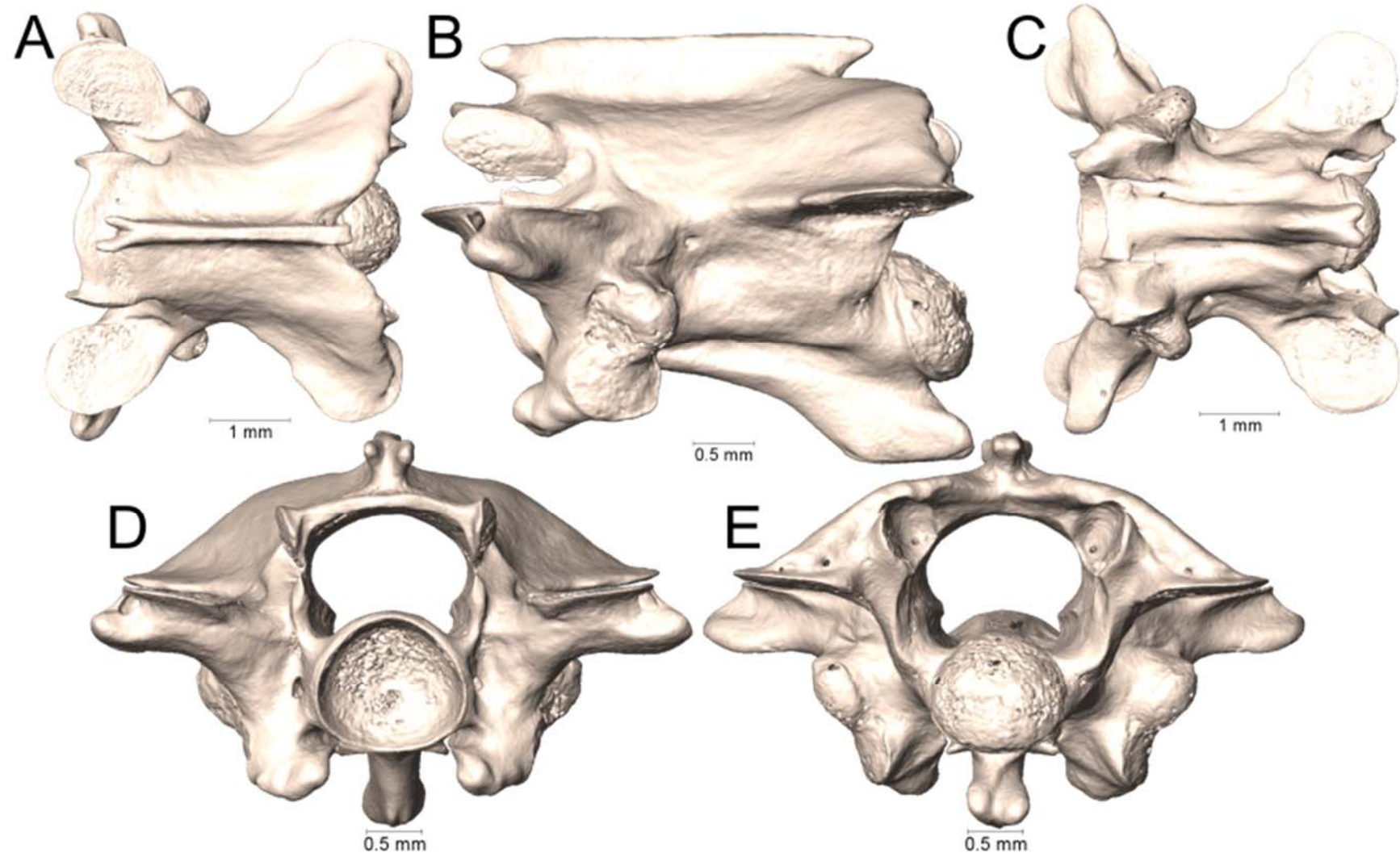
Supplemental Figure 4.31. Dorsal, lateral, ventral, anterior, and posterior views (A-E, respectively) of the midbody vertebra of *Micrurus bocourti* (UTA R-58145).



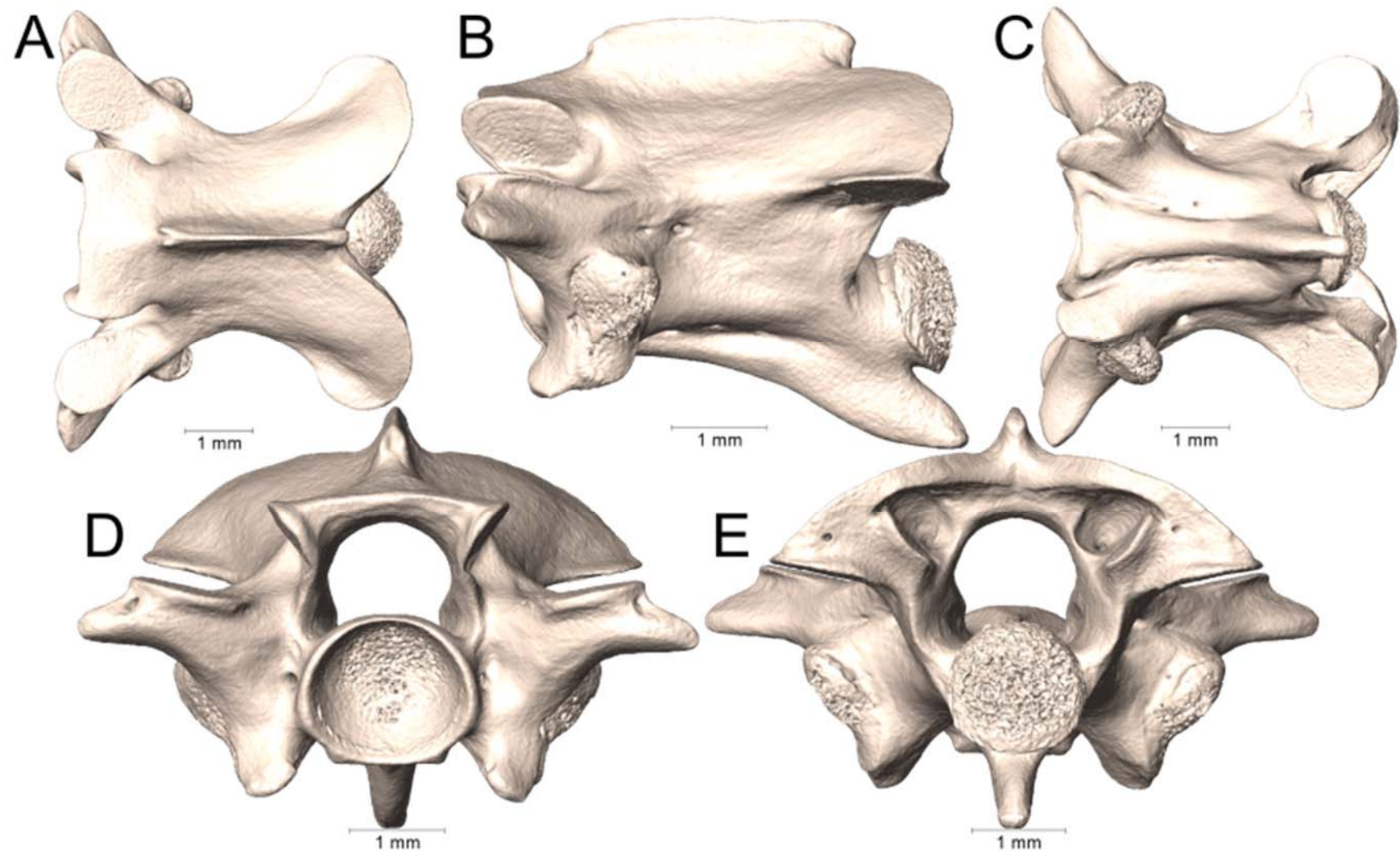
Supplemental Figure 4.32. Dorsal, lateral, ventral, anterior, and posterior views (A-E, respectively) of the midbody vertebra of *Micrurus diastema* (UTA R-52565).



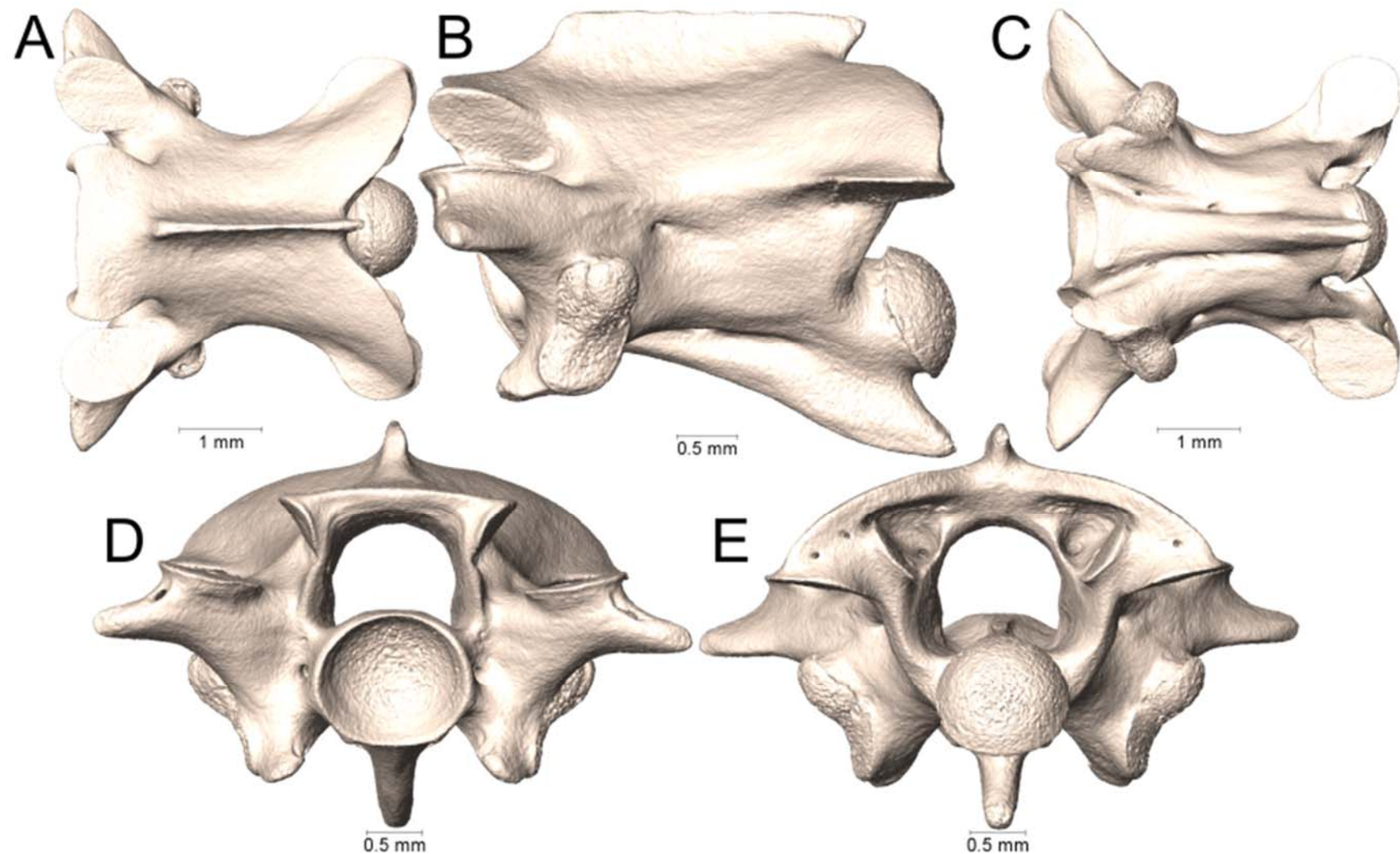
Supplemental Figure 4.33. Dorsal, lateral, ventral, anterior, and posterior views (A-E, respectively) of the midbody vertebra of *Micrurus dissolucus* (UTA R-54184).



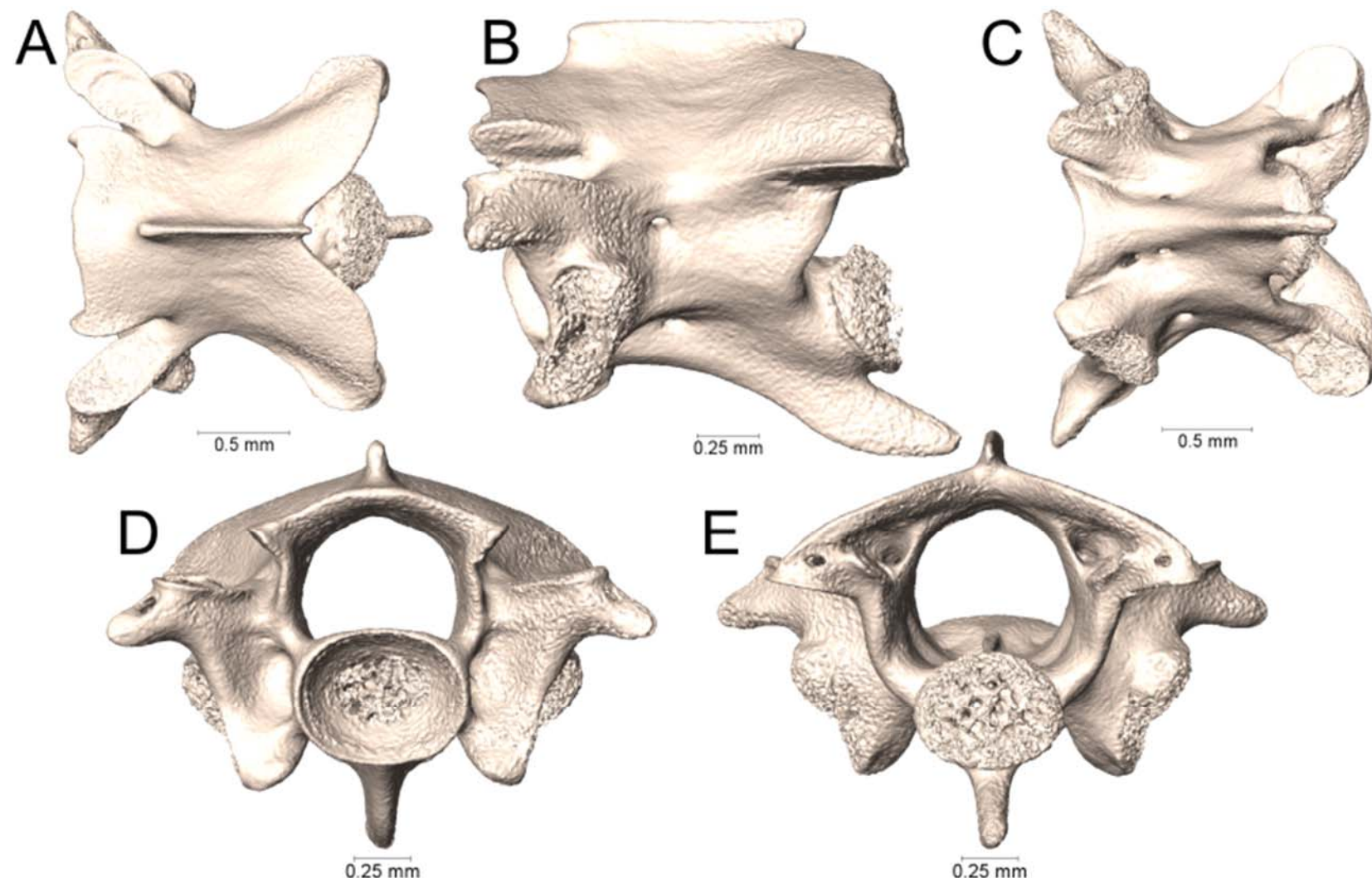
Supplemental Figure 4.34. Dorsal, lateral, ventral, anterior, and posterior views (A-E, respectively) of the midbody vertebra of *Micrurus distans* (UTA R-14471).



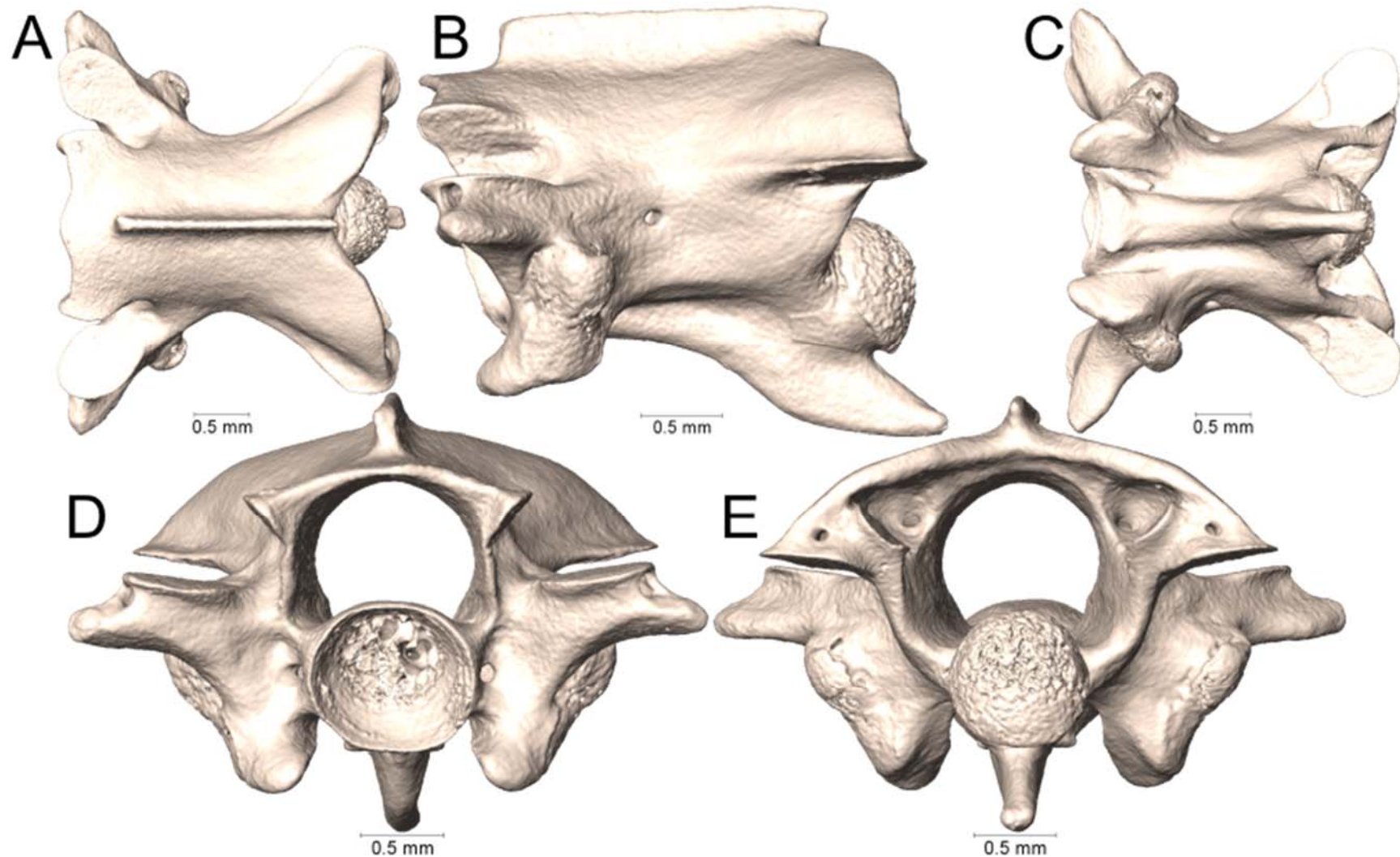
Supplemental Figure 4.35. Dorsal, lateral, ventral, anterior, and posterior views (A-E, respectively) of the midbody vertebra of *Micrurus diutius* (UTA R-20756).



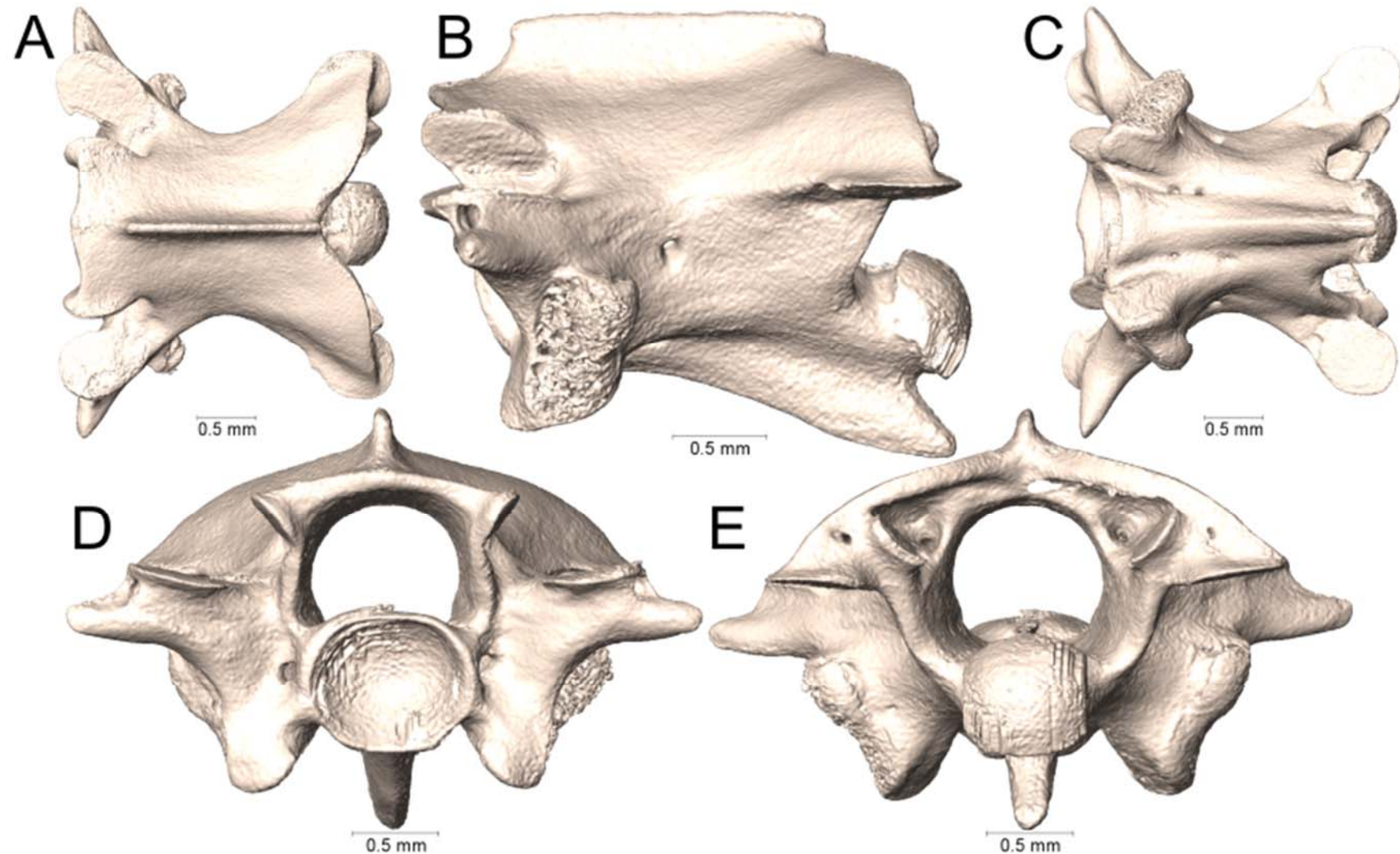
Supplemental Figure 4.36. Dorsal, lateral, ventral, anterior, and posterior views (A-E, respectively) of the midbody vertebra of *Micrurus diutius* (UTA R-54182).



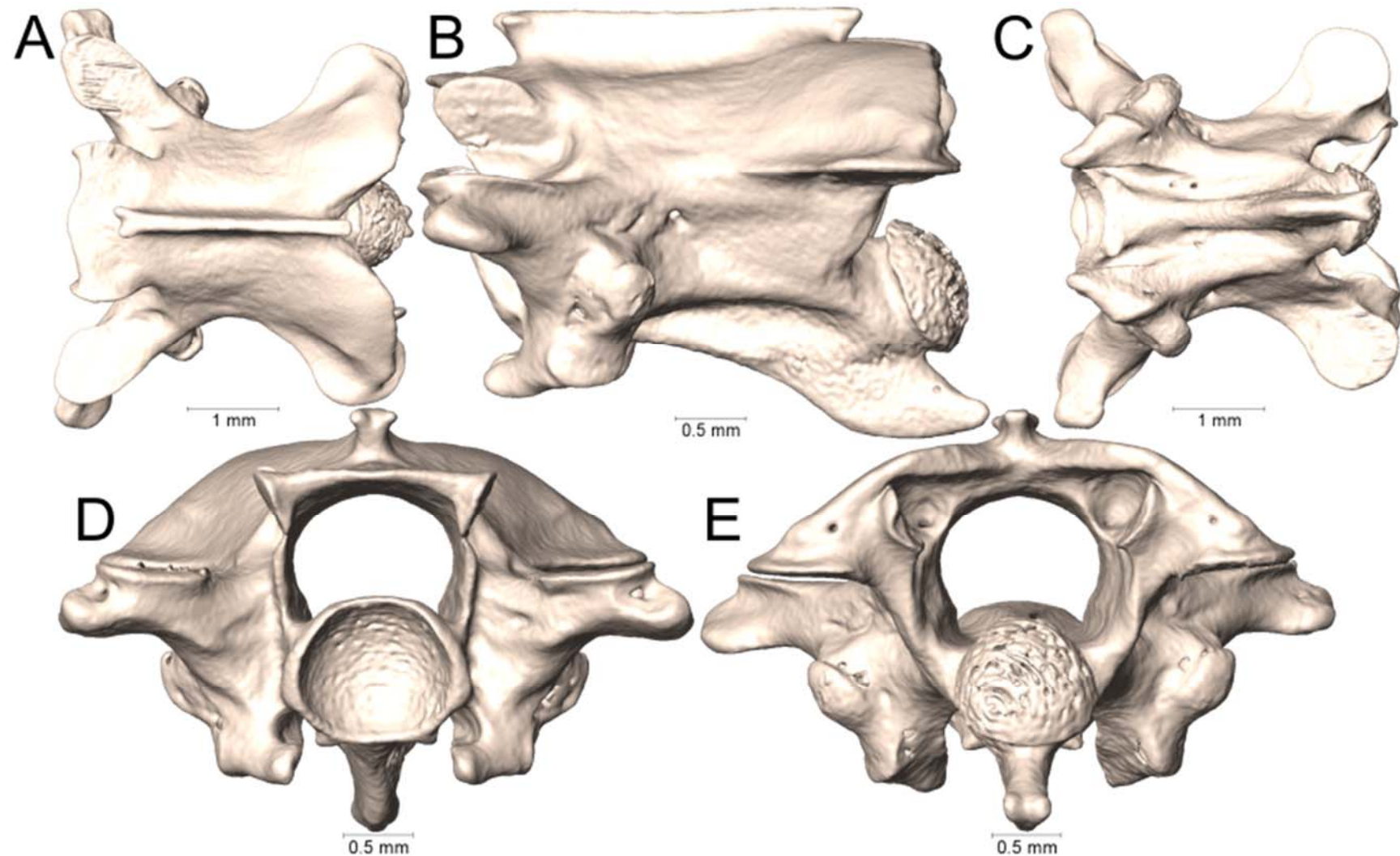
Supplemental Figure 4.37. Dorsal, lateral, ventral, anterior, and posterior views (A-E, respectively) of the midbody vertebra of *Micrurus dumerilii* (AMNH 35951).



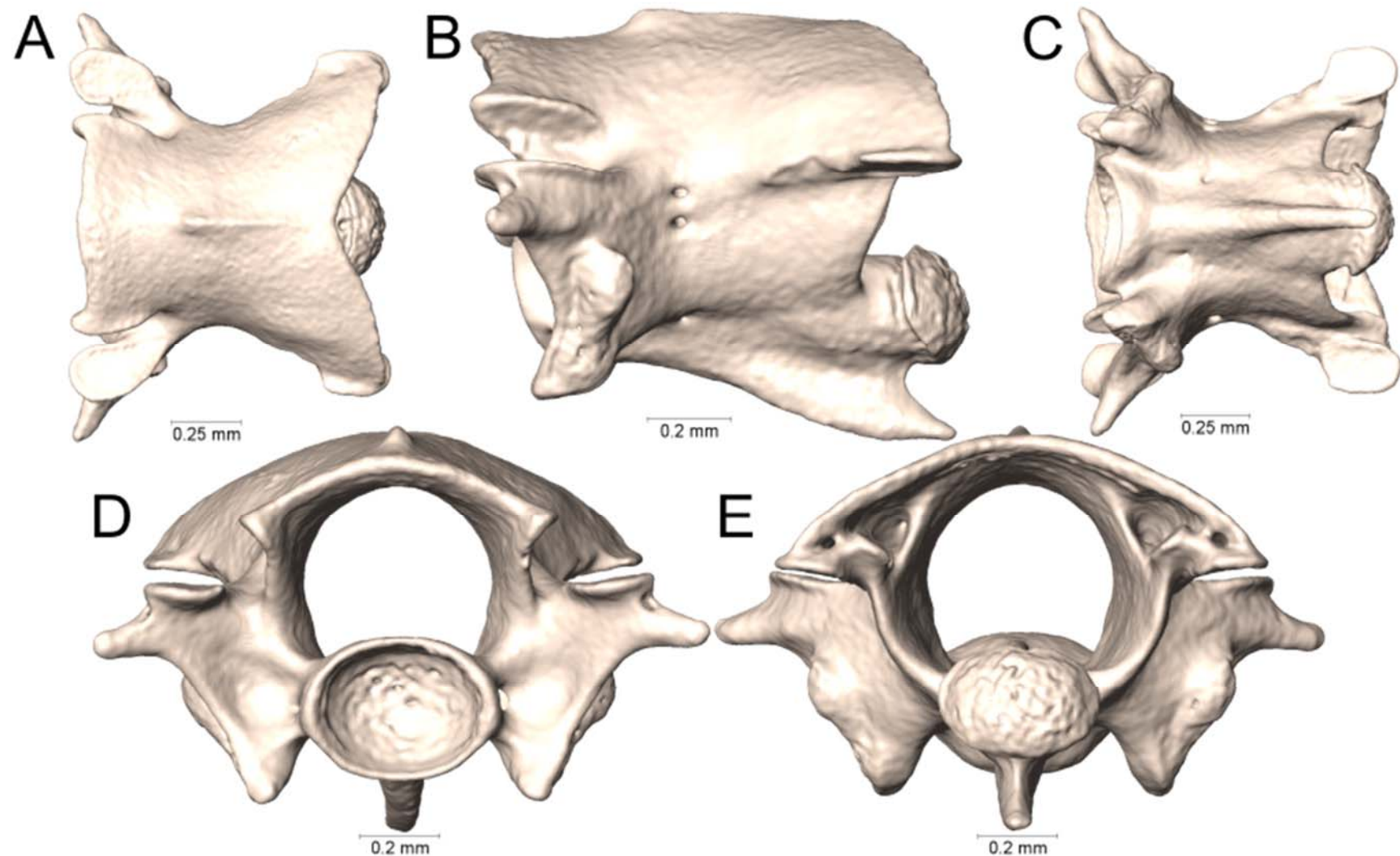
Supplemental Figure 4.38. Dorsal, lateral, ventral, anterior, and posterior views (A-E, respectively) of the midbody vertebra of *Micrurus elegans elegans* (MZFC 18819).



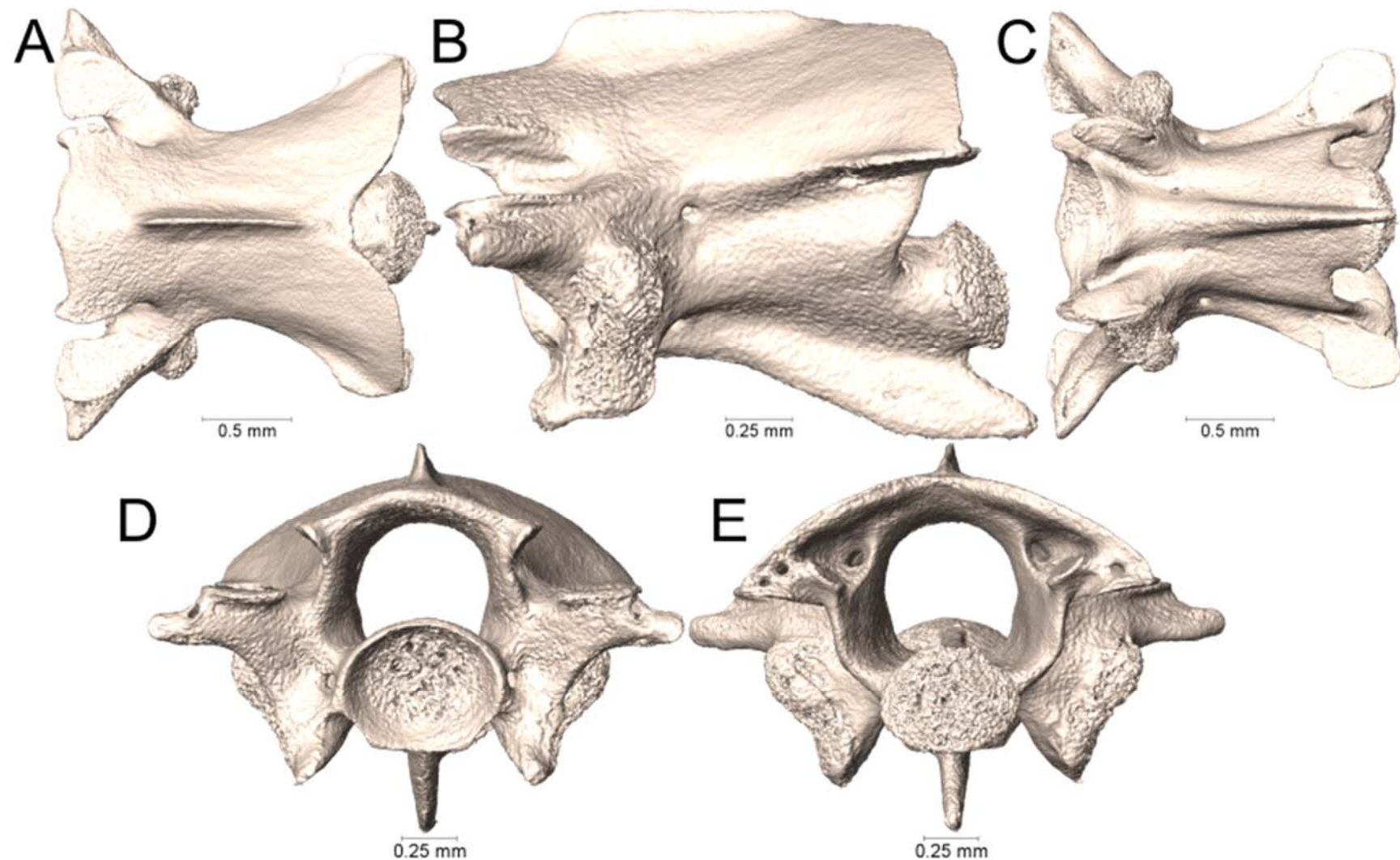
Supplemental Figure 4.39. Dorsal, lateral, ventral, anterior, and posterior views (A-E, respectively) of the midbody vertebra of *Micrurus elegans veraepacis* (UTA R-58869).



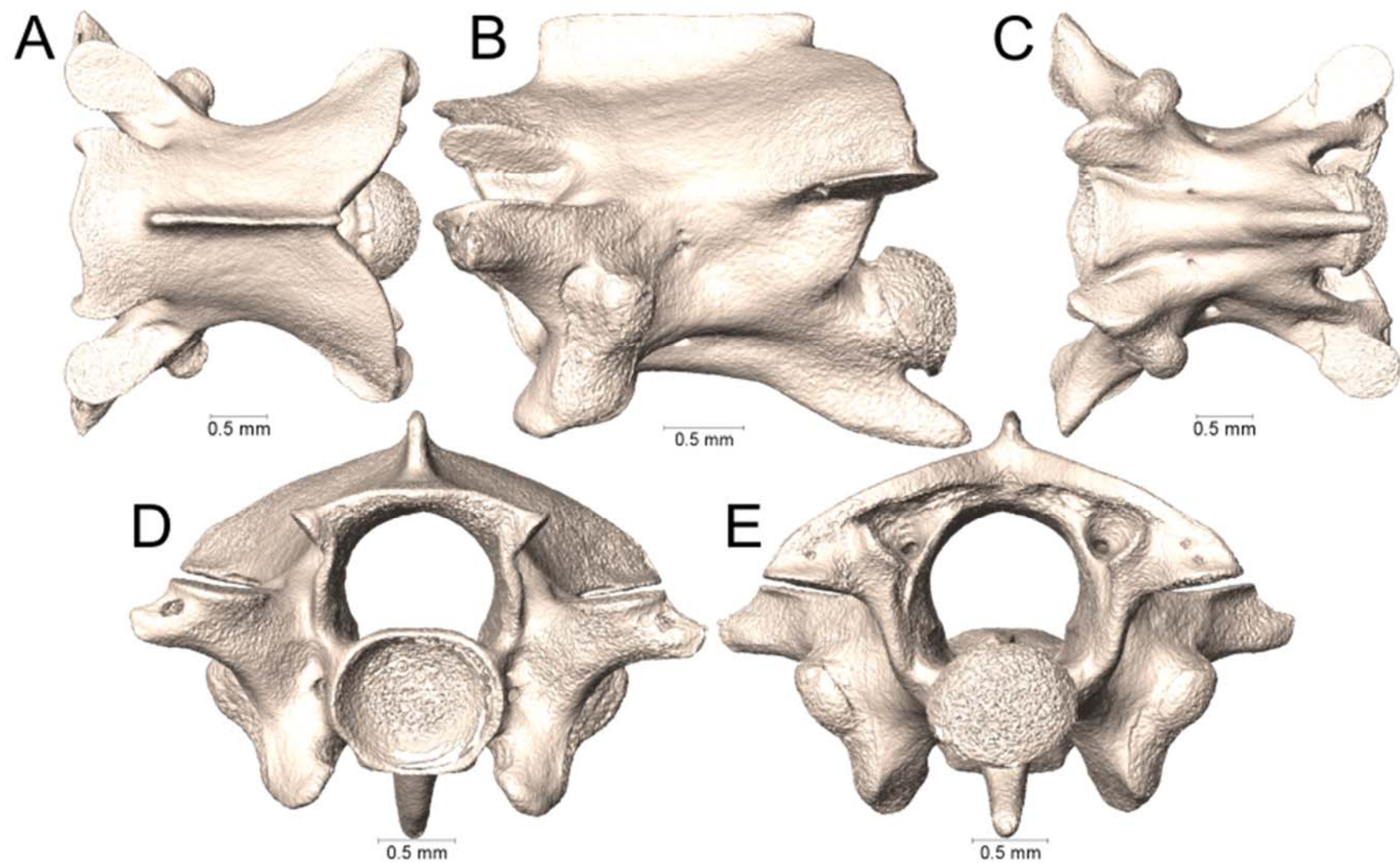
Supplemental Figure 4.40. Dorsal, lateral, ventral, anterior, and posterior views (A-E, respectively) of the midbody vertebra of *Micrurus ephippifer* (UTA R-64863).



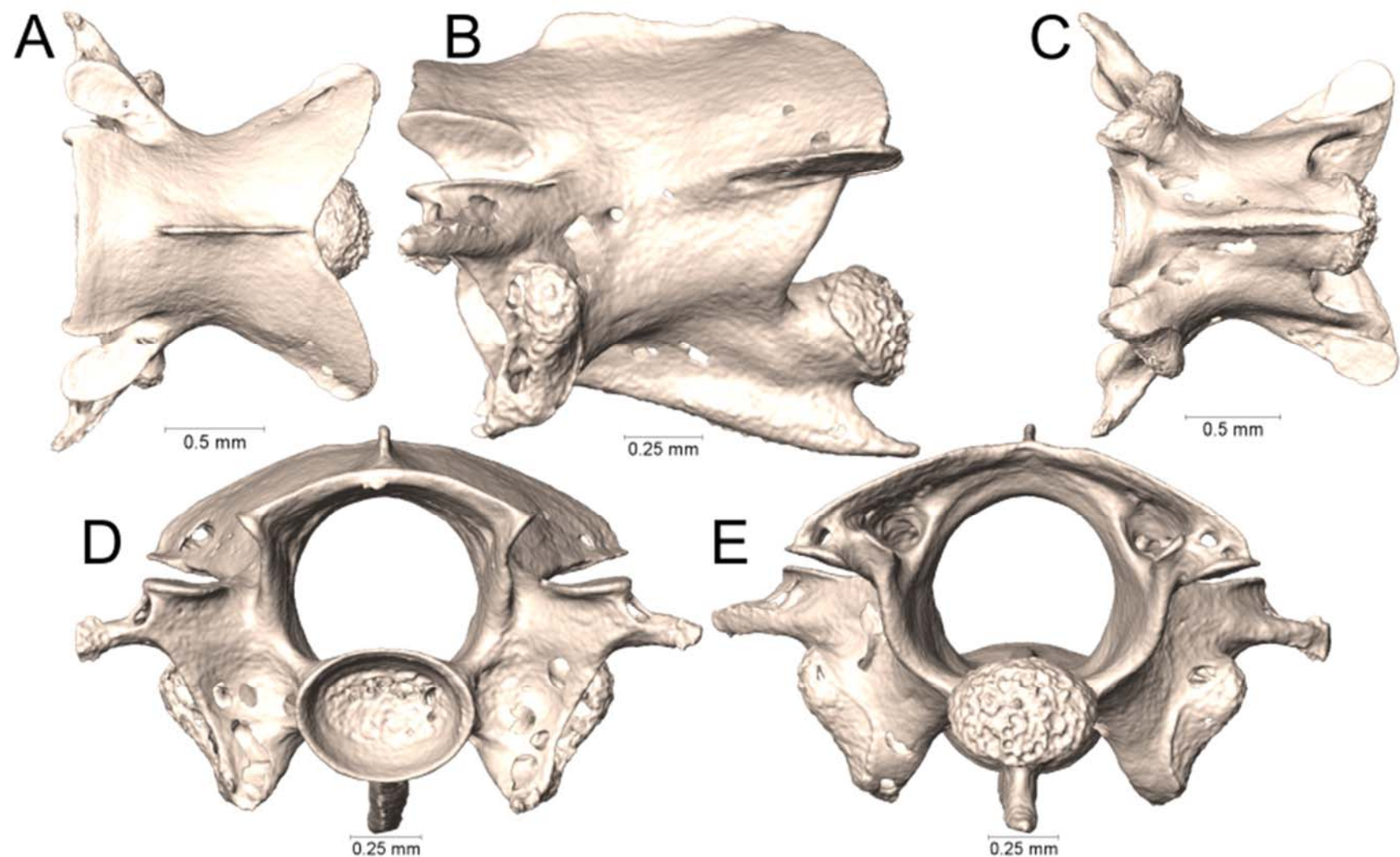
Supplemental Figure 4.41. Dorsal, lateral, ventral, anterior, and posterior views (A-E, respectively) of the midbody vertebra of *Micrurus filiformis* (UTA R-3423).



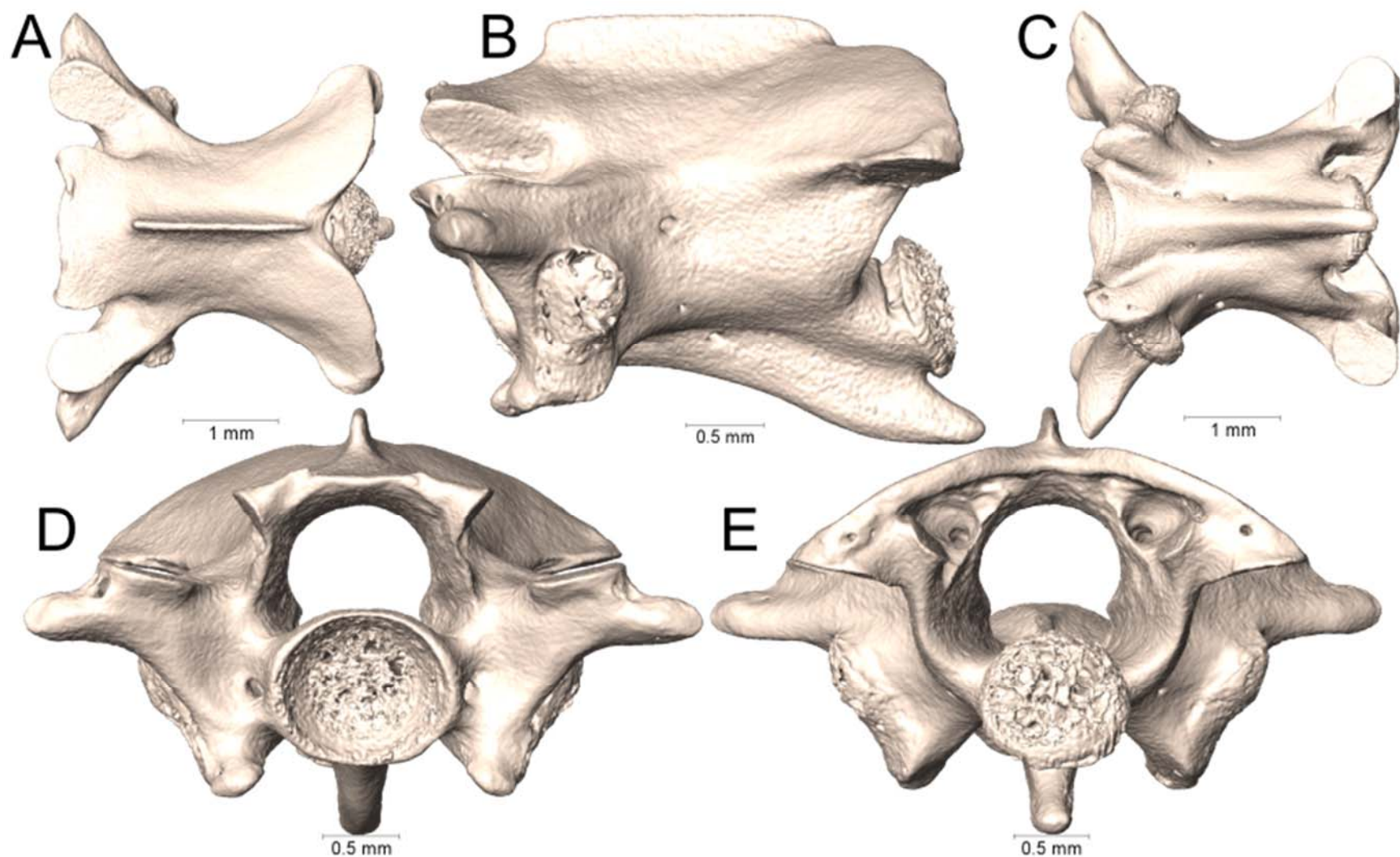
Supplemental Figure 4.42. Dorsal, lateral, ventral, anterior, and posterior views (A-E, respectively) of the midbody vertebra of *Micrurus filiformis* (UTA R-65836).



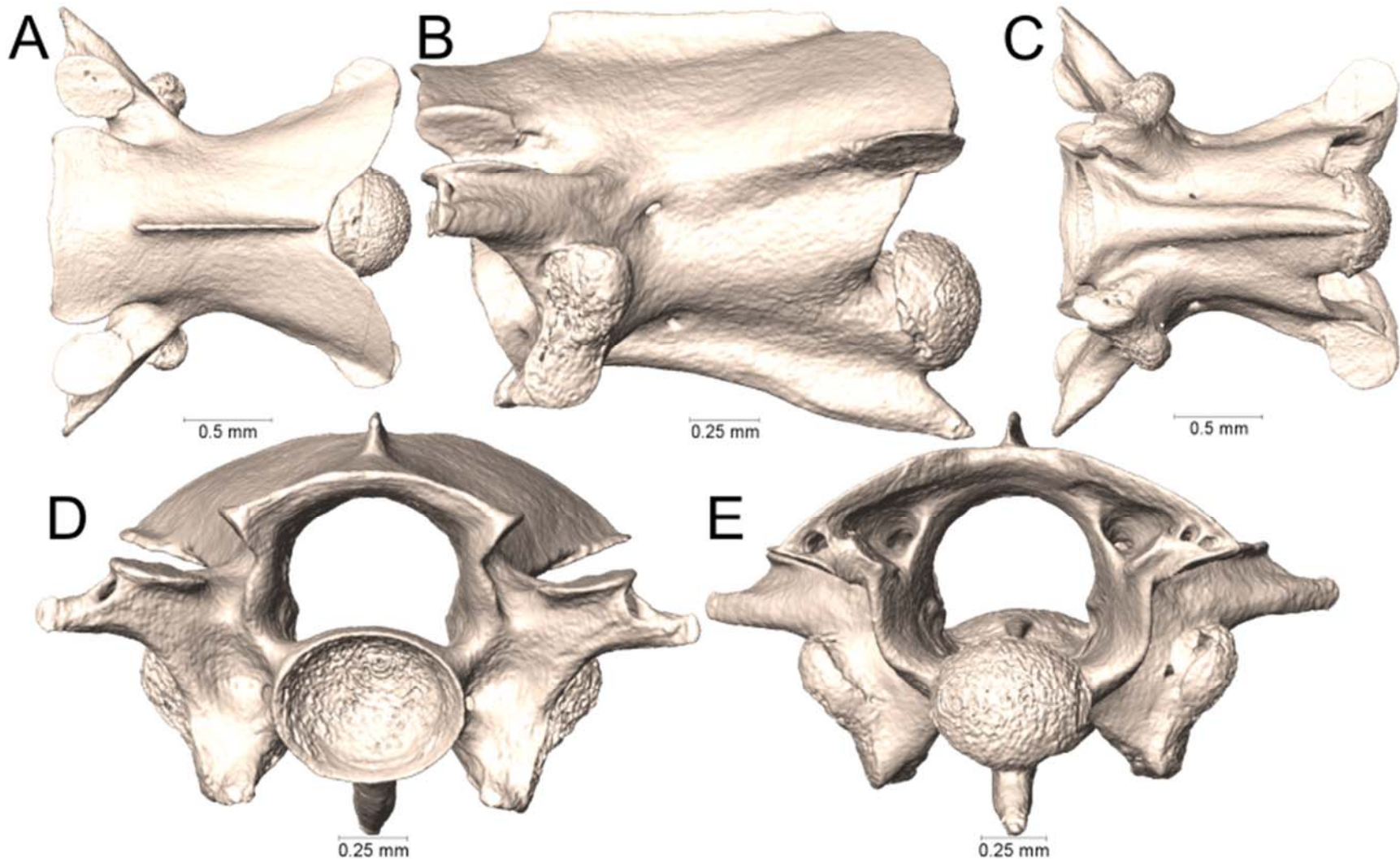
Supplemental Figure 4.43. Dorsal, lateral, ventral, anterior, and posterior views (A-E, respectively) of the midbody vertebra of *Micrurus fulvius* (UTA R-61632).



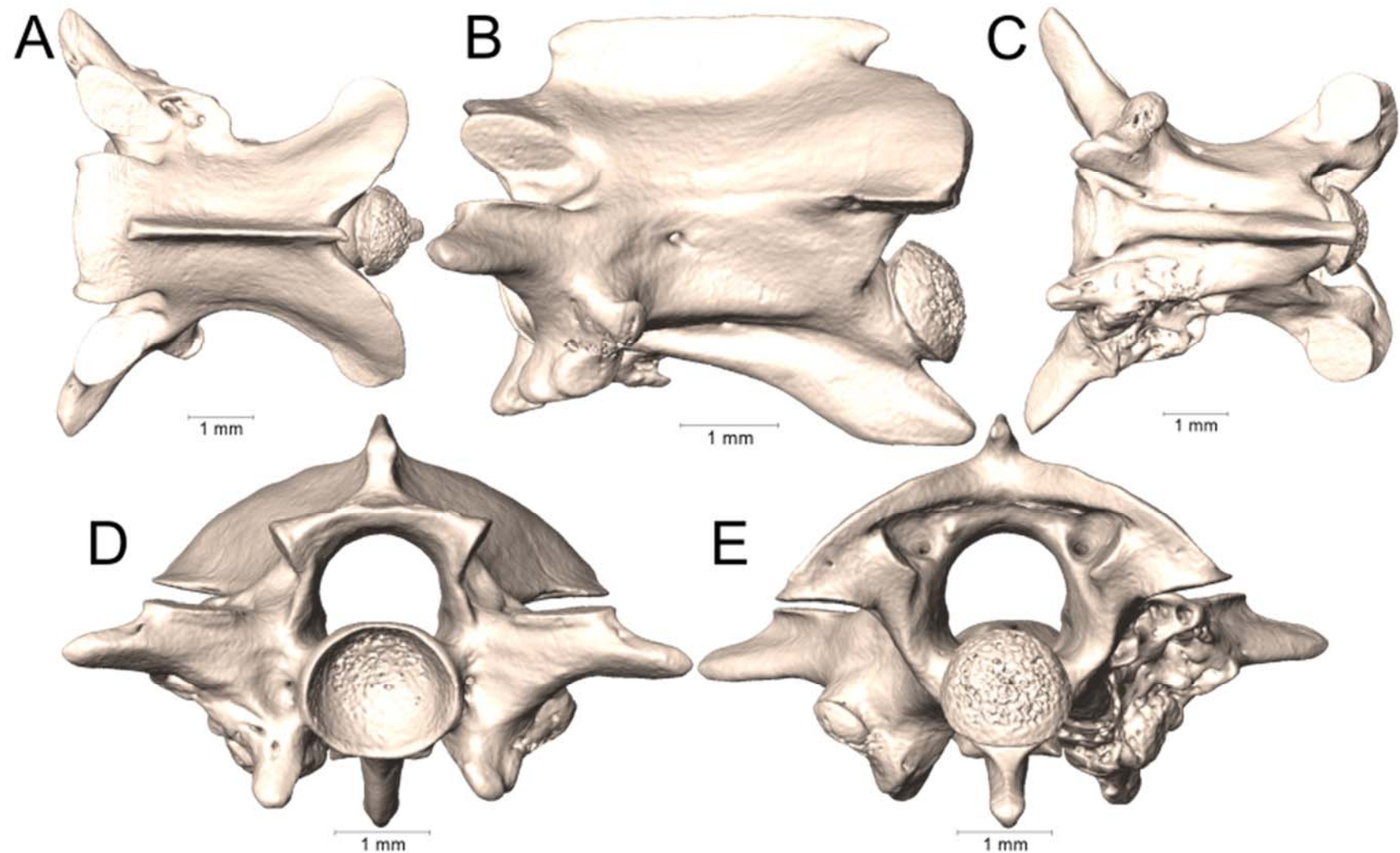
Supplemental Figure 4.44. Dorsal, lateral, ventral, anterior, and posterior views (A-E, respectively) of the midbody vertebra of *Micrurus helleri* (UTA R-38005).



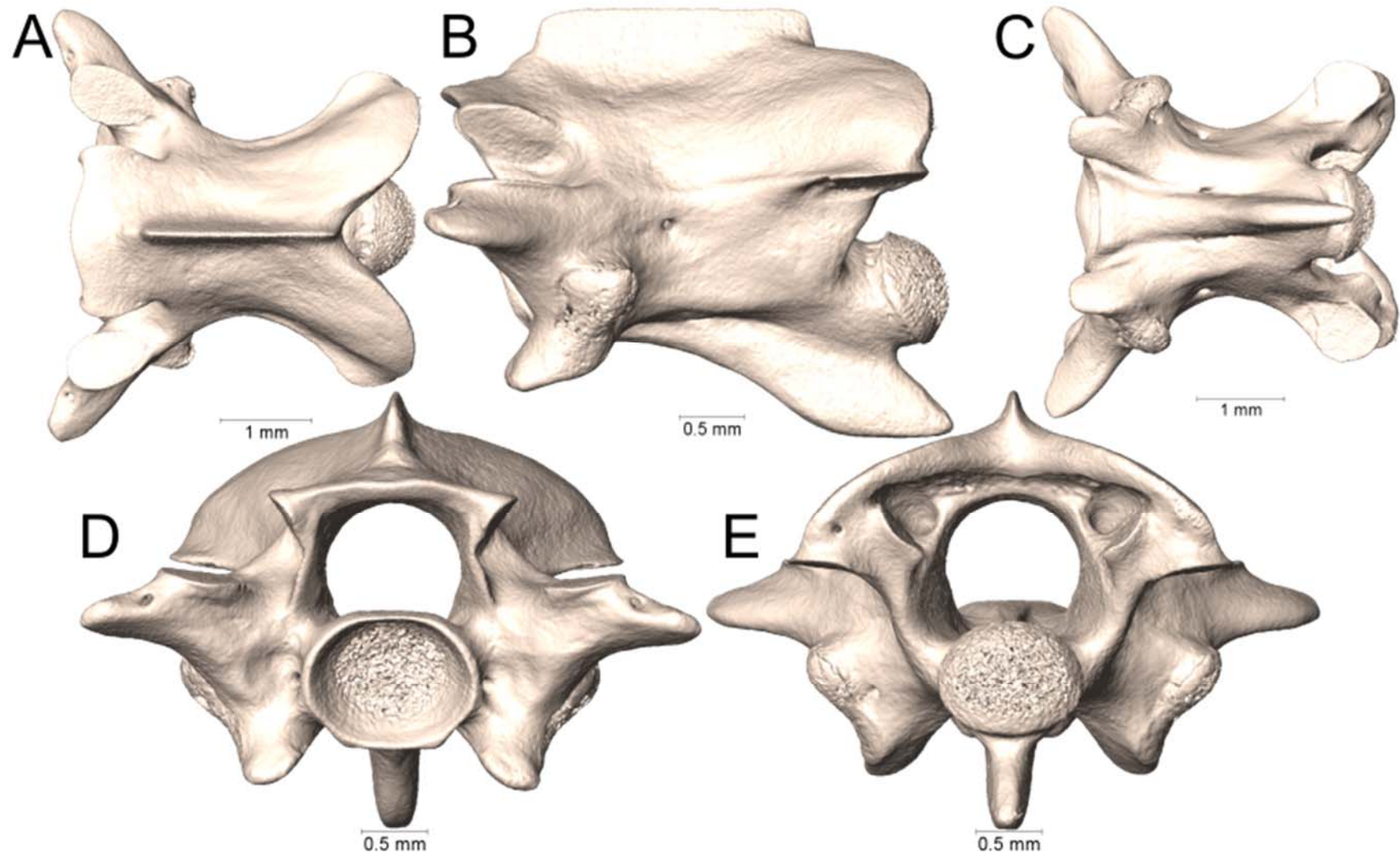
Supplemental Figure 4.45. Dorsal, lateral, ventral, anterior, and posterior views (A-E, respectively) of the midbody vertebra of *Micrurus helleri* (UTA R-55977).



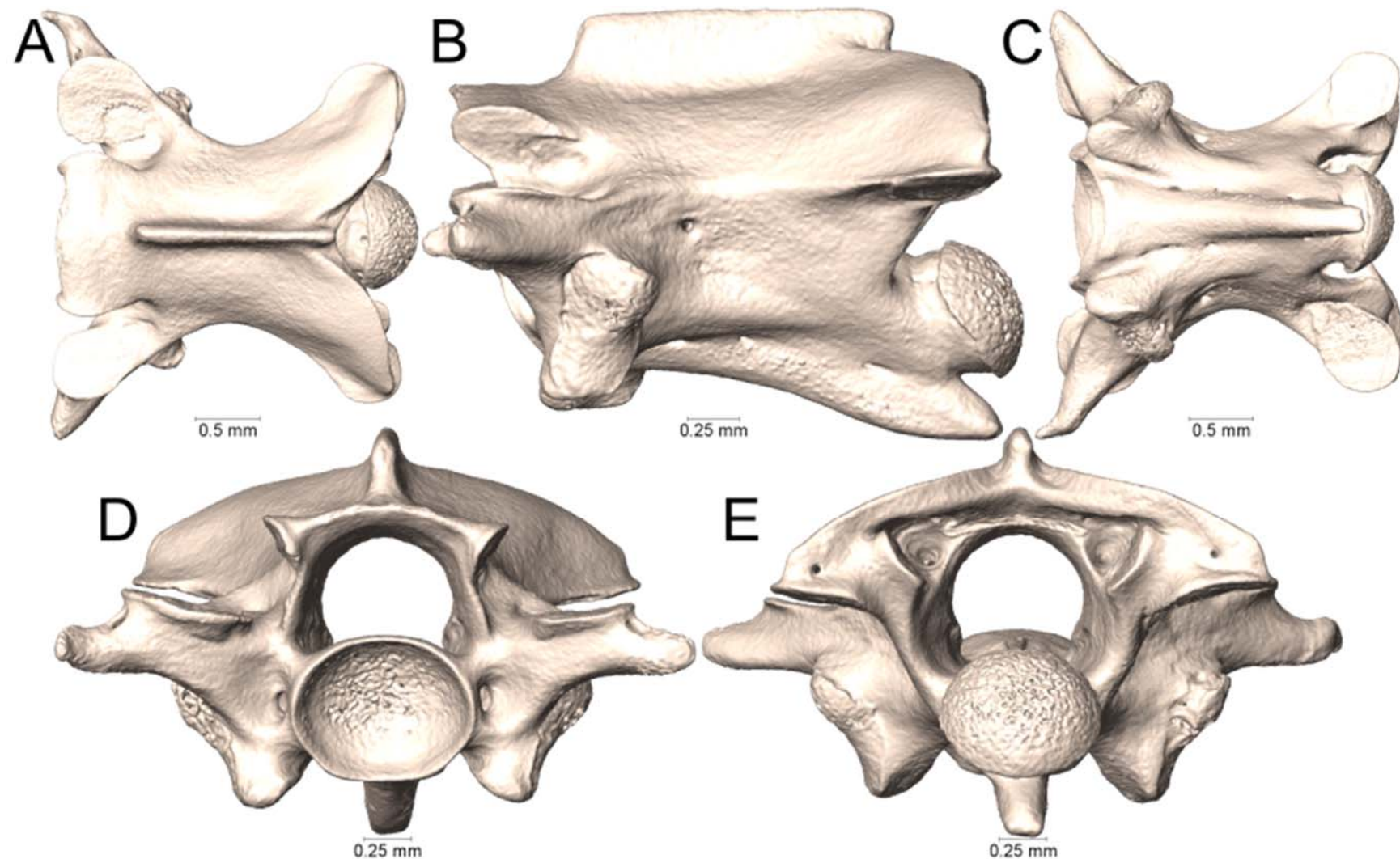
Supplemental Figure 4.46. Dorsal, lateral, ventral, anterior, and posterior views (A-E, respectively) of the midbody vertebra of *Micrurus helleri* (UTA R-65841).



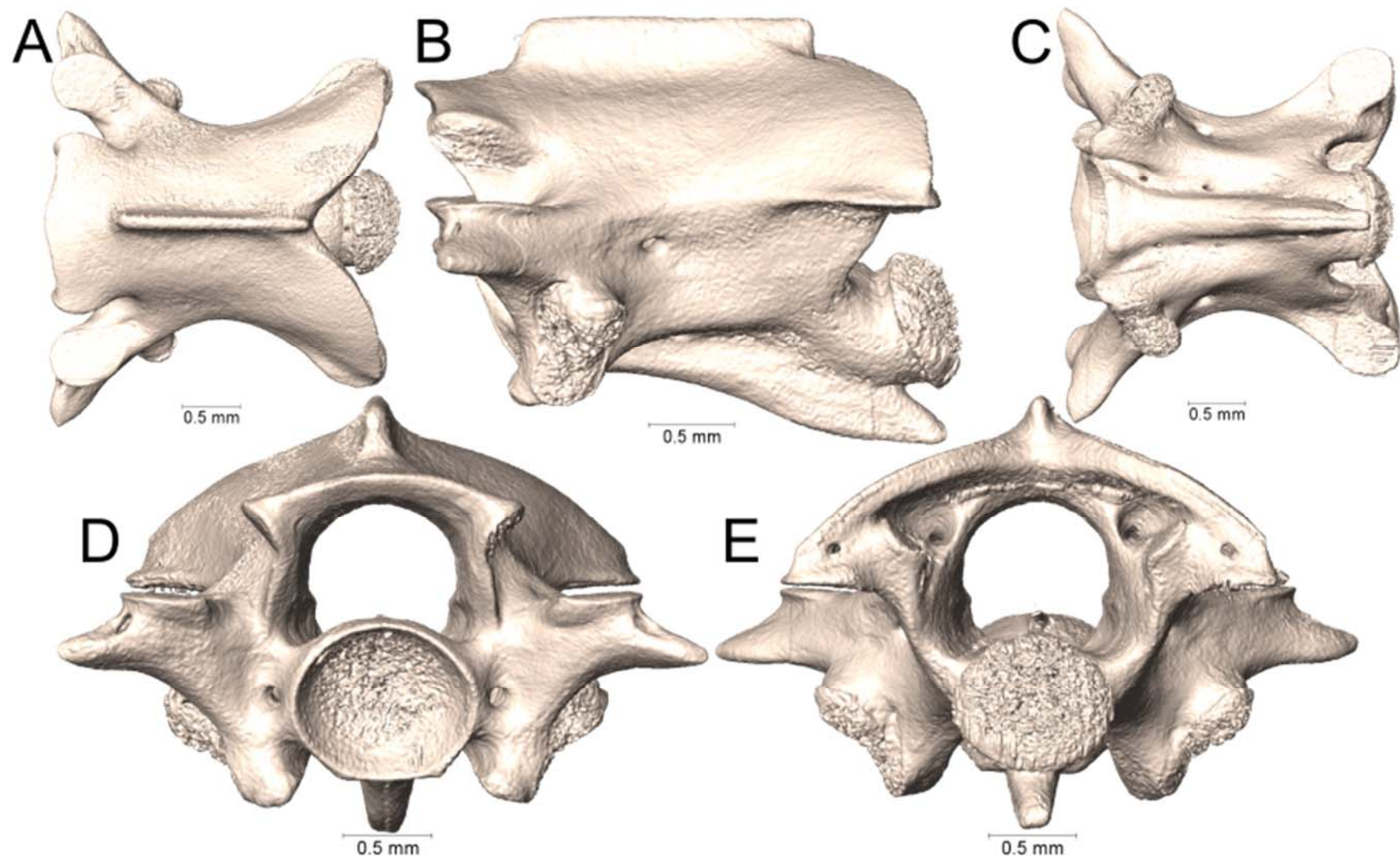
Supplemental Figure 4.47. Dorsal, lateral, ventral, anterior, and posterior views (A-E, respectively) of the midbody vertebra of *Micrurus hemprichii* (UTA R-9683).



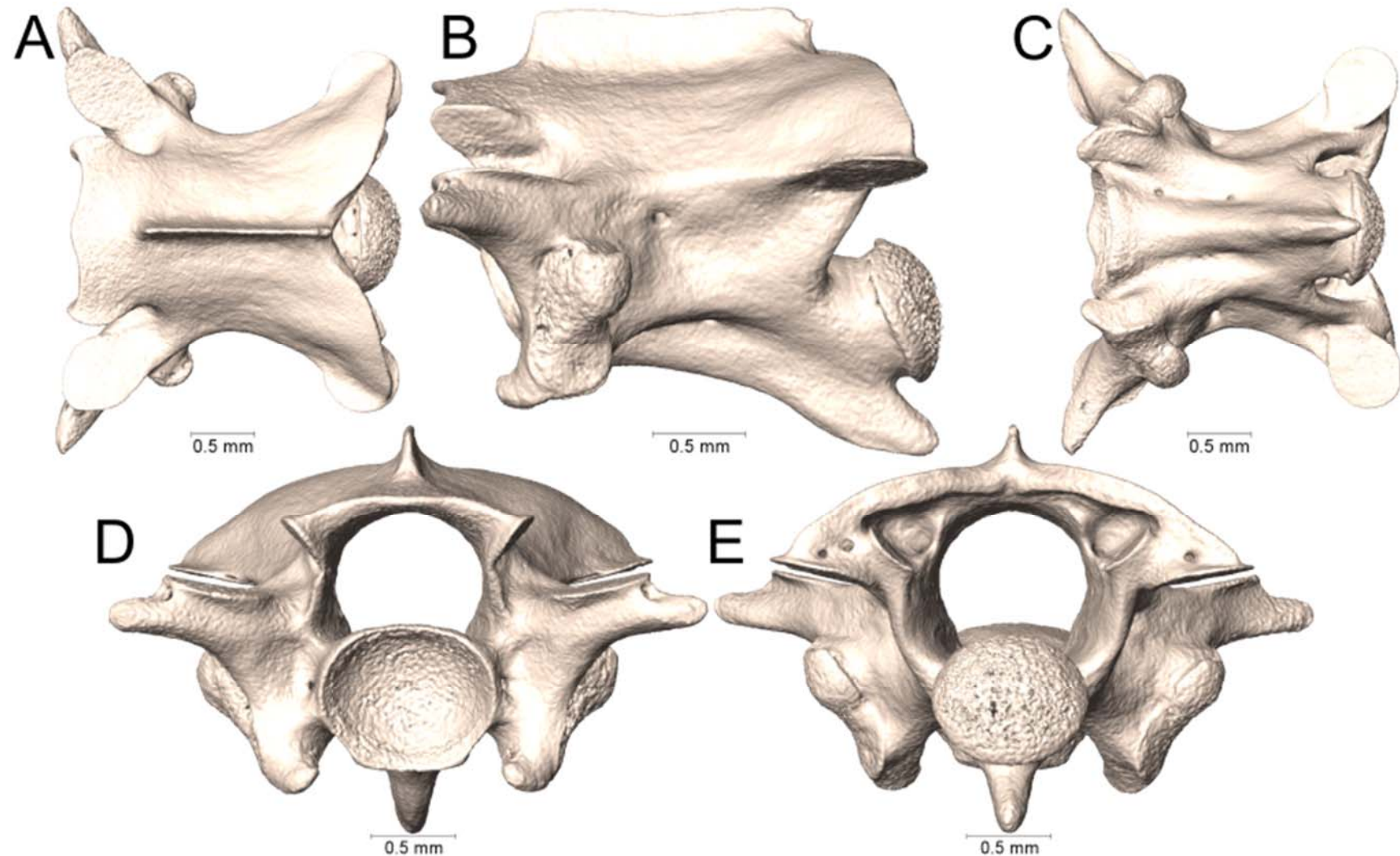
Supplemental Figure 4.48. Dorsal, lateral, ventral, anterior, and posterior views (A-E, respectively) of the midbody vertebra of *Micrurus hemprichii* (UTA R-29997).



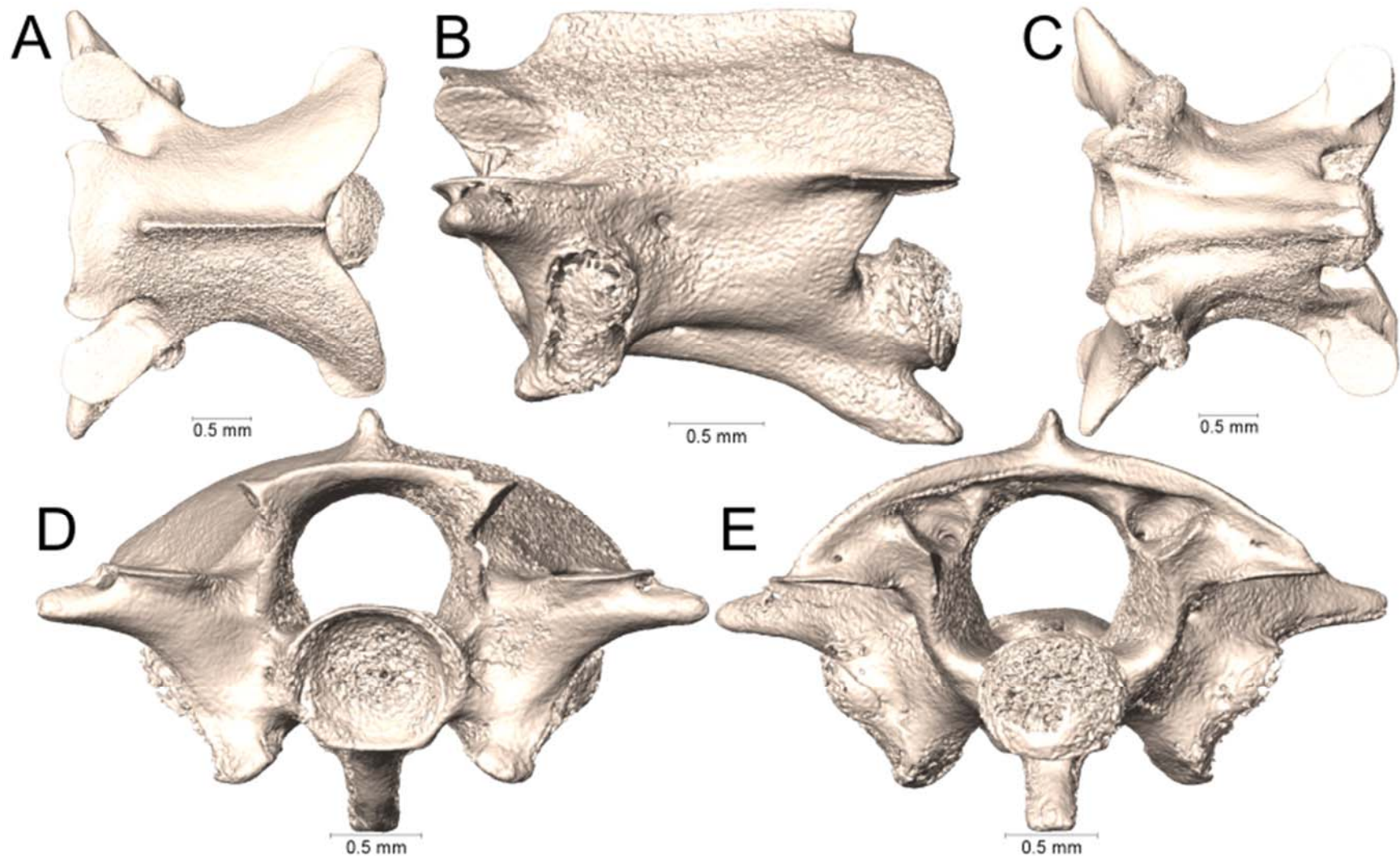
Supplemental Figure 4.49. Dorsal, lateral, ventral, anterior, and posterior views (A-E, respectively) of the midbody vertebra of *Micrurus isozonus* (UTA R-3951).



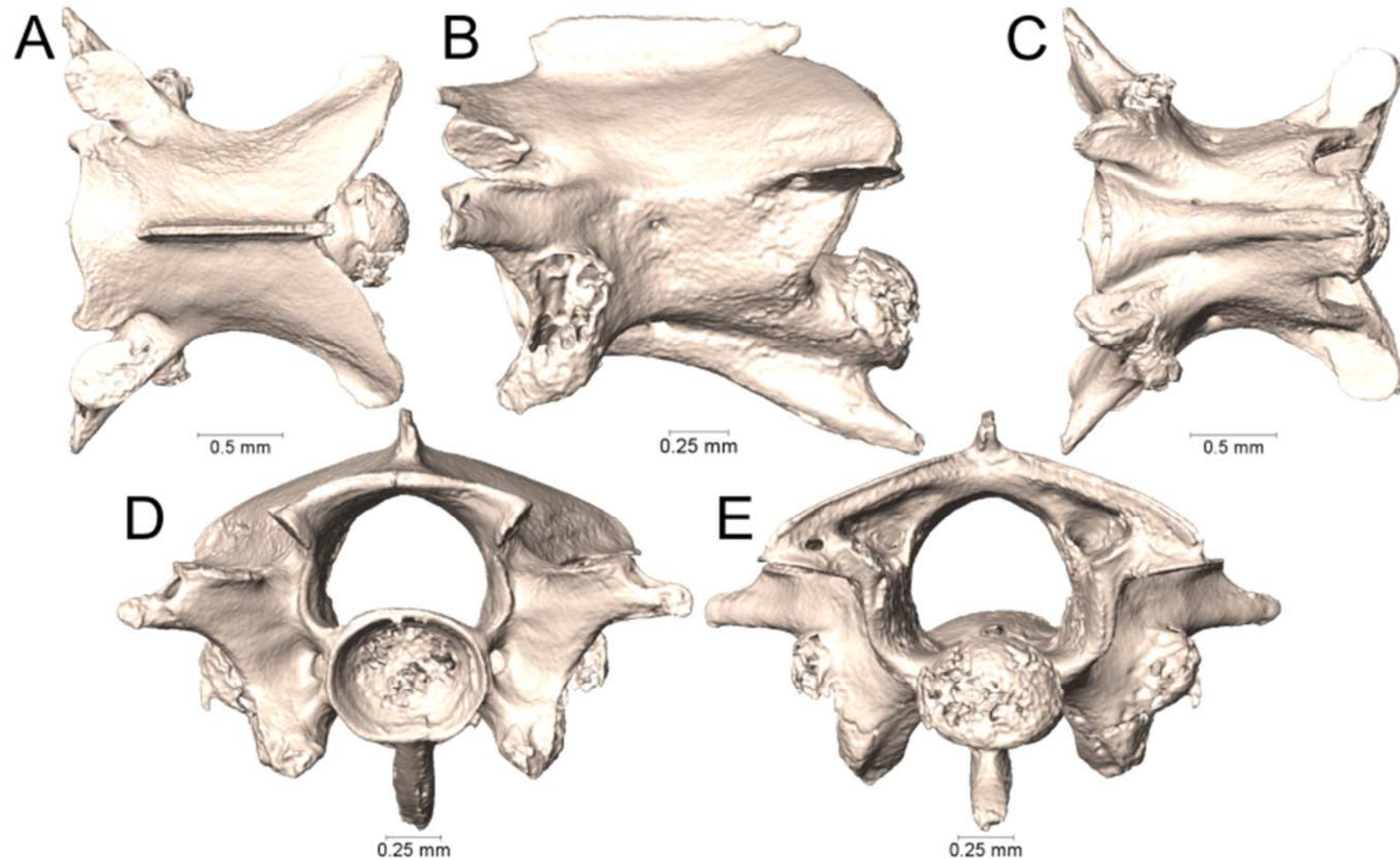
Supplemental Figure 4.50. Dorsal, lateral, ventral, anterior, and posterior views (A-E, respectively) of the midbody vertebra of *Micrurus isozonus* (UTA R-22589).



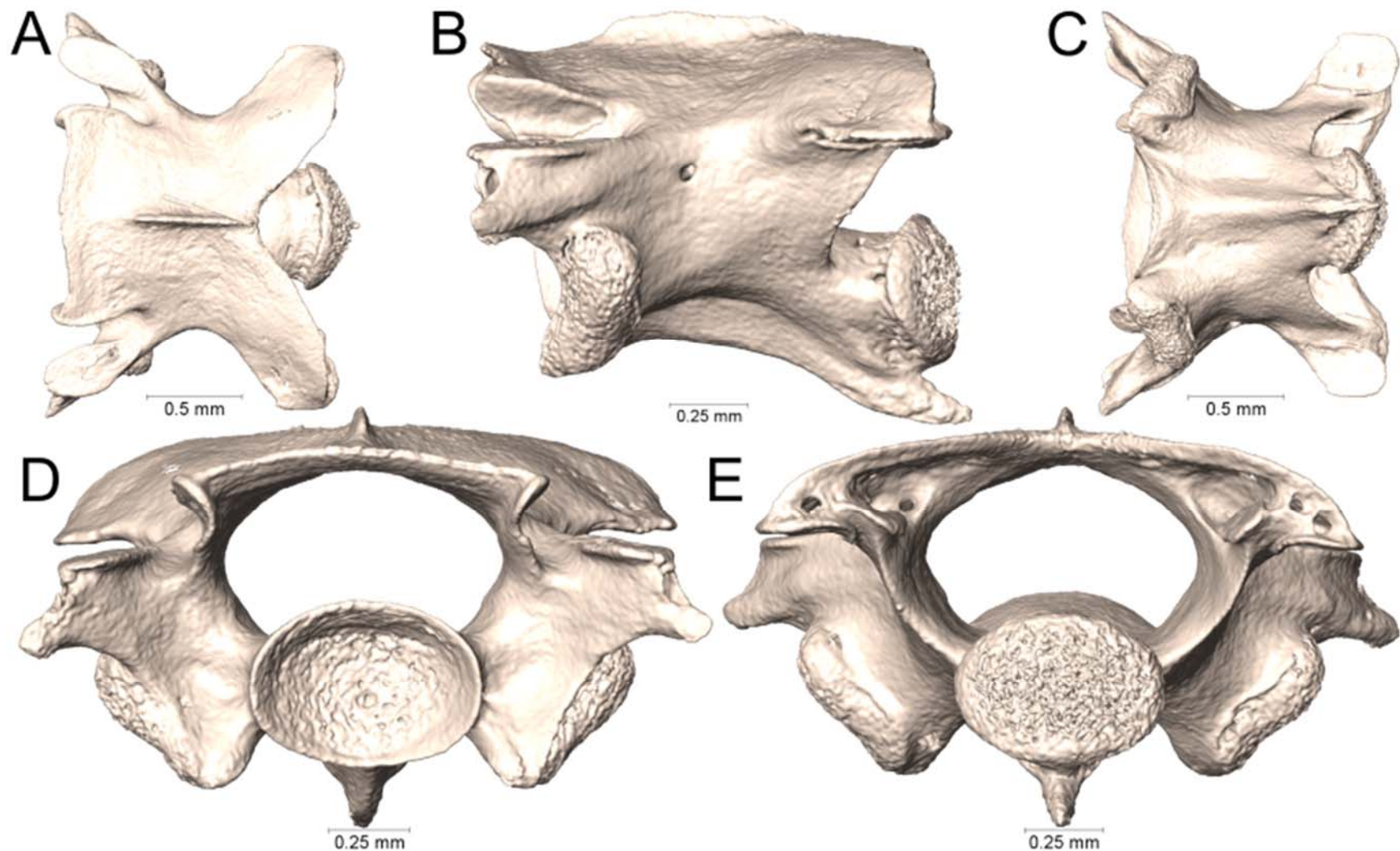
Supplemental Figure 4.51. Dorsal, lateral, ventral, anterior, and posterior views (A-E, respectively) of the midbody vertebra of *Micrurus laticollaris* (UTA R-52559).



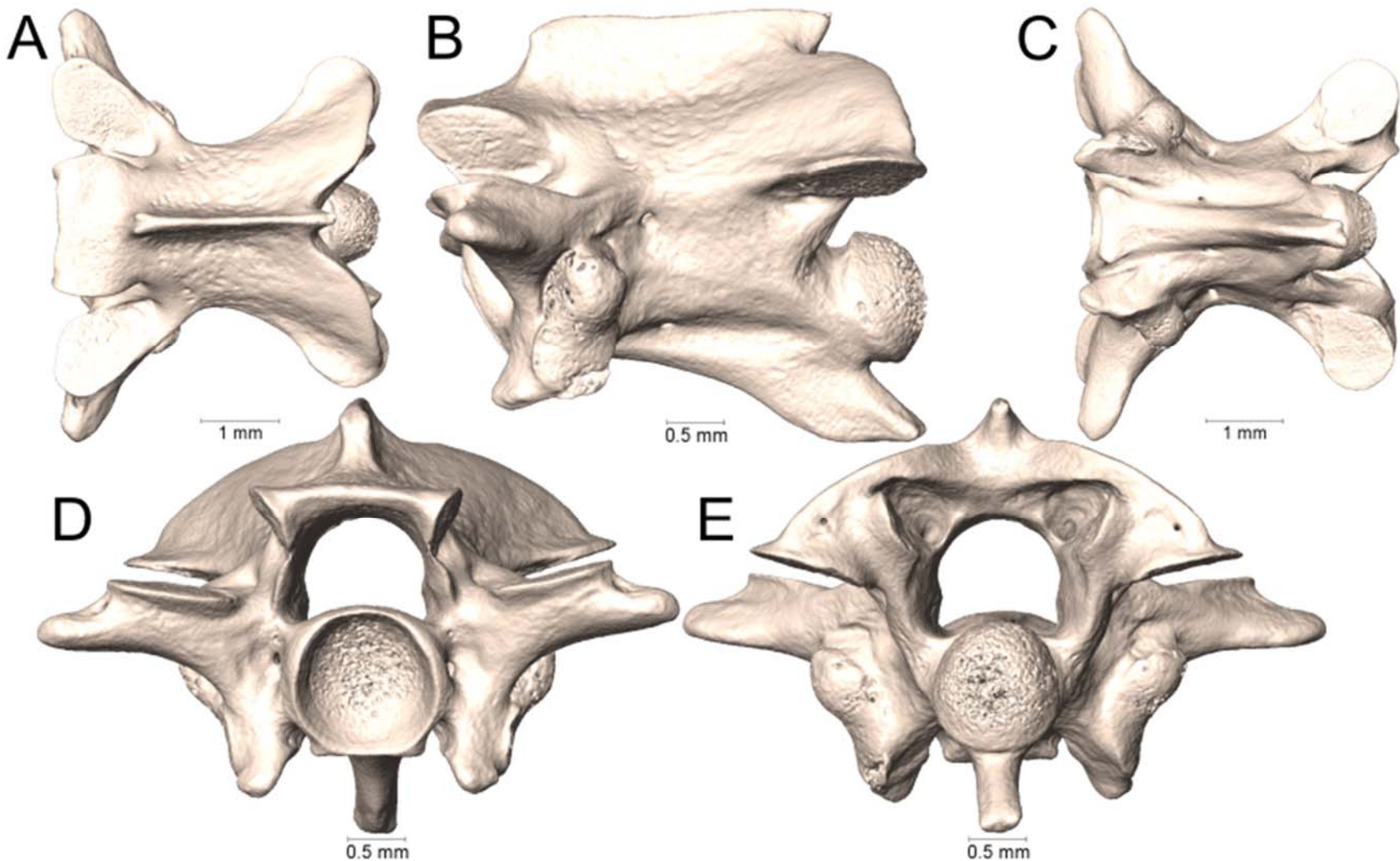
Supplemental Figure 4.52. Dorsal, lateral, ventral, anterior, and posterior views (A-E, respectively) of the midbody vertebra of *Micrurus laticollaris* (UTA R-57562).



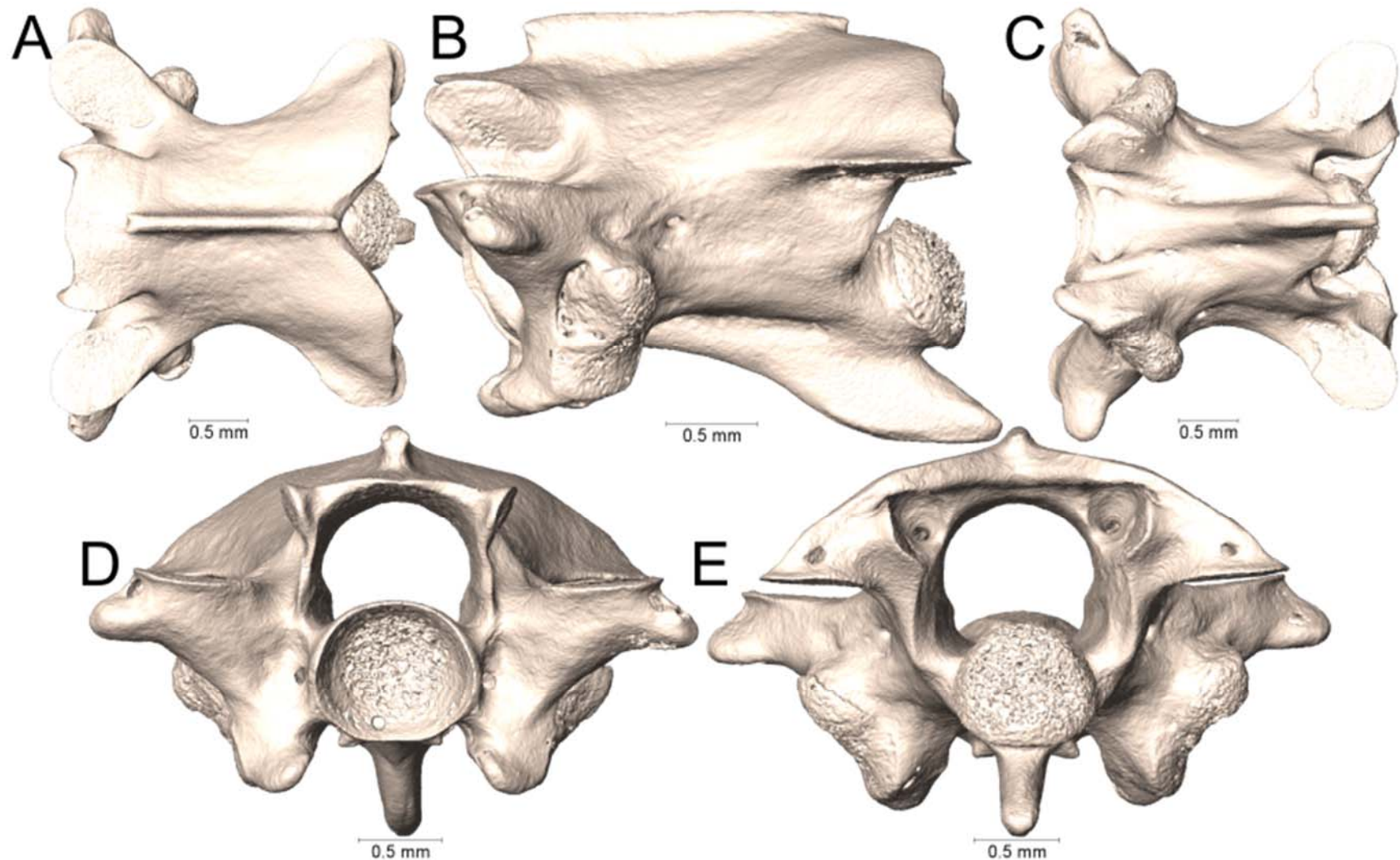
Supplemental Figure 4.53. Dorsal, lateral, ventral, anterior, and posterior views (A-E, respectively) of the midbody vertebra of *Micrurus latifasciatus* (UTA R-4606).



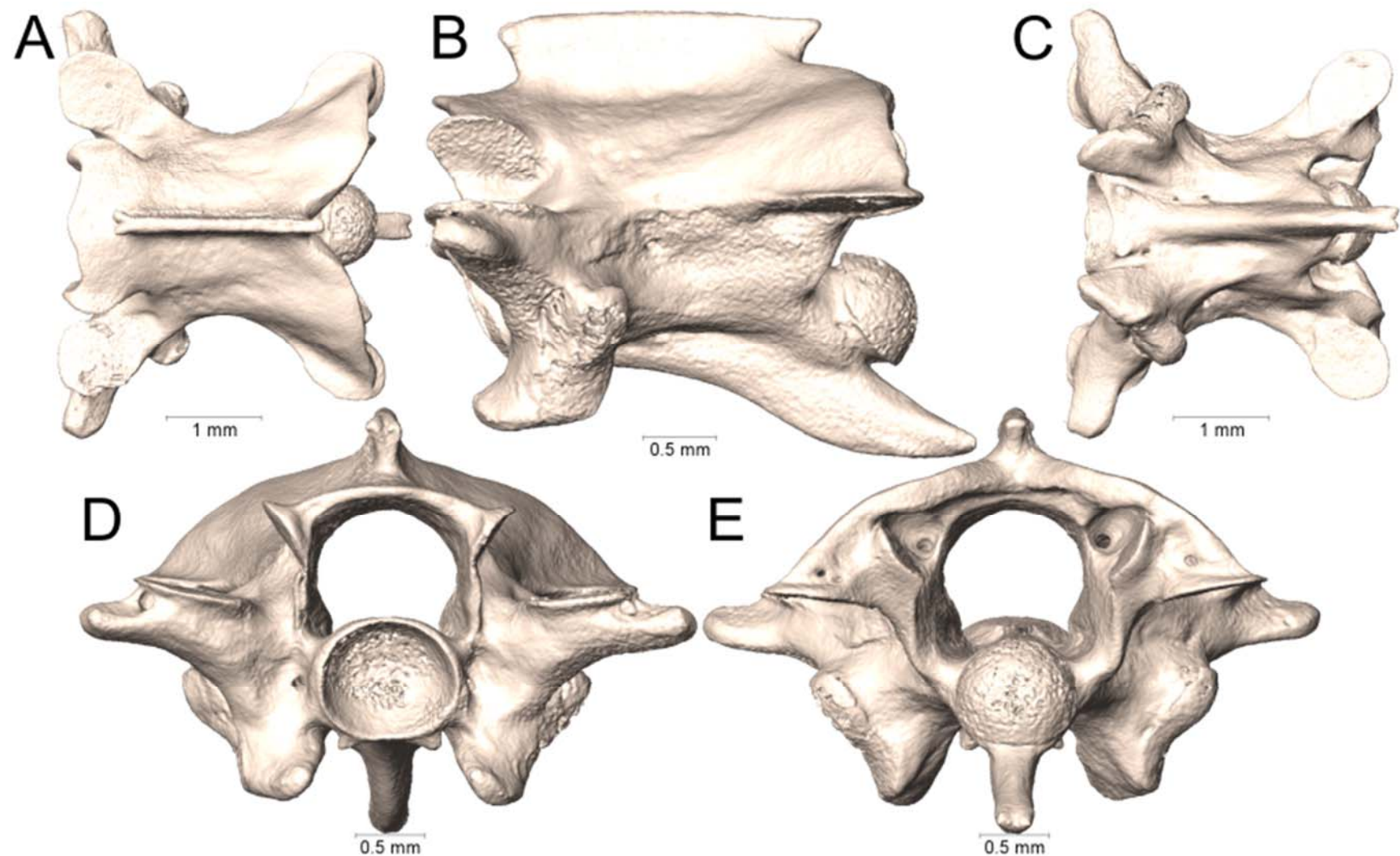
Supplemental Figure 4.54. Dorsal, lateral, ventral, anterior, and posterior views (A-E, respectively) of the midbody vertebra of *Micrurus lemniscatus* cf. *helleri* (UTA R-34563).



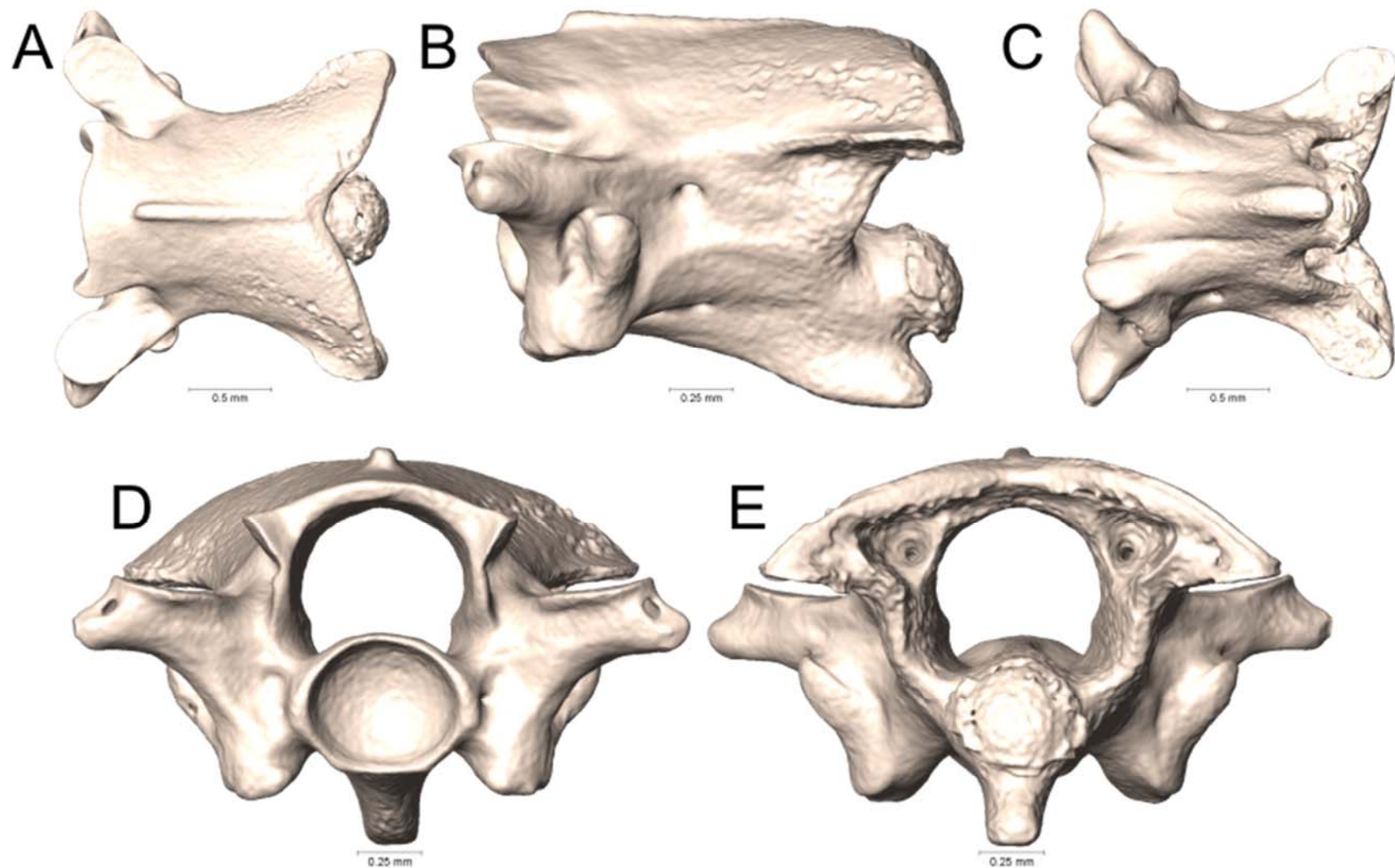
Supplemental Figure 4.55. Dorsal, lateral, ventral, anterior, and posterior views (A-E, respectively) of the midbody vertebra of *Micrurus lemniscatus* cf. *helleri* (UTA R-65803).



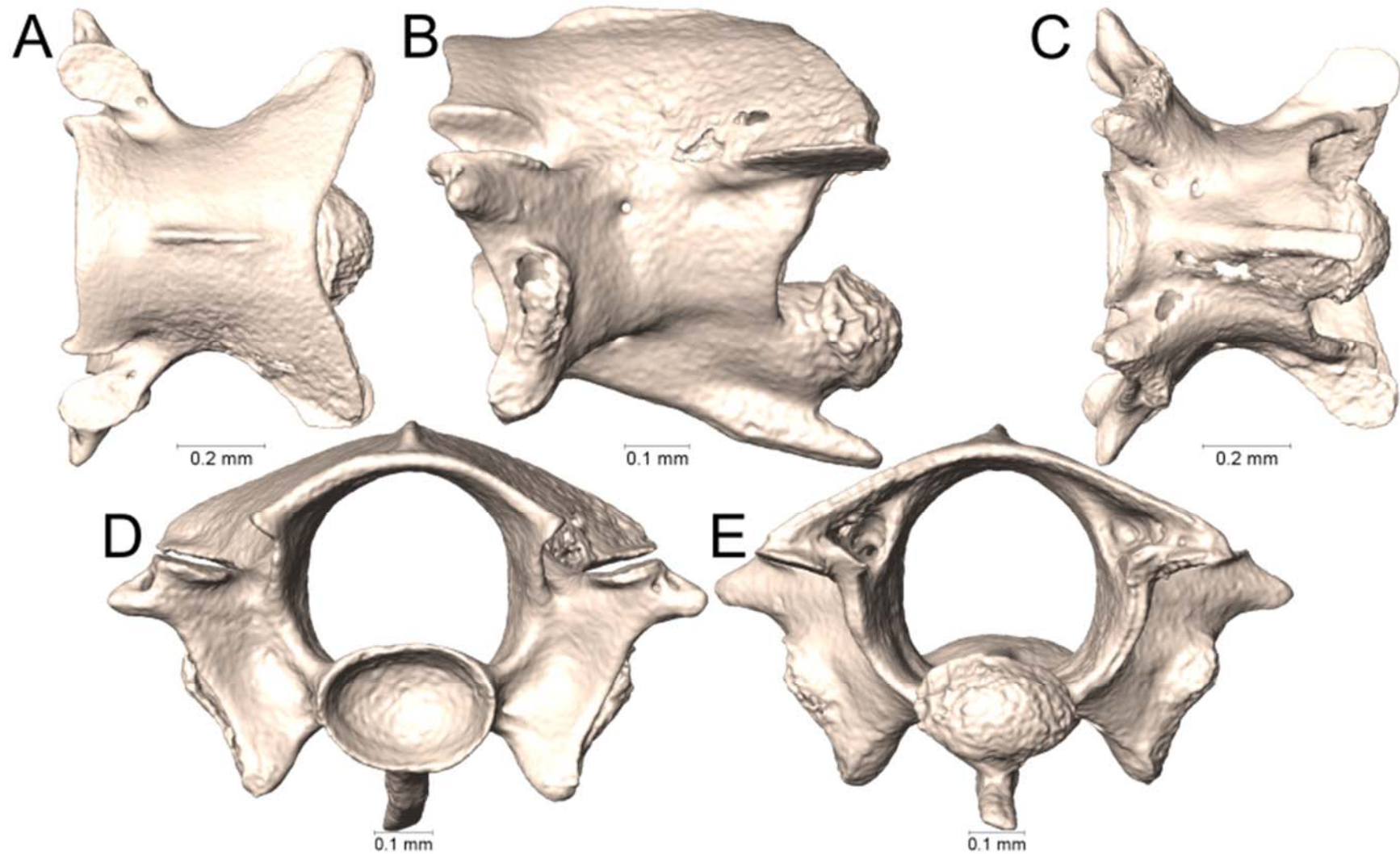
Supplemental Figure 4.56. Dorsal, lateral, ventral, anterior, and posterior views (A-E, respectively) of the midbody vertebra of *Micrurus limbatus* (UTA R-64852).



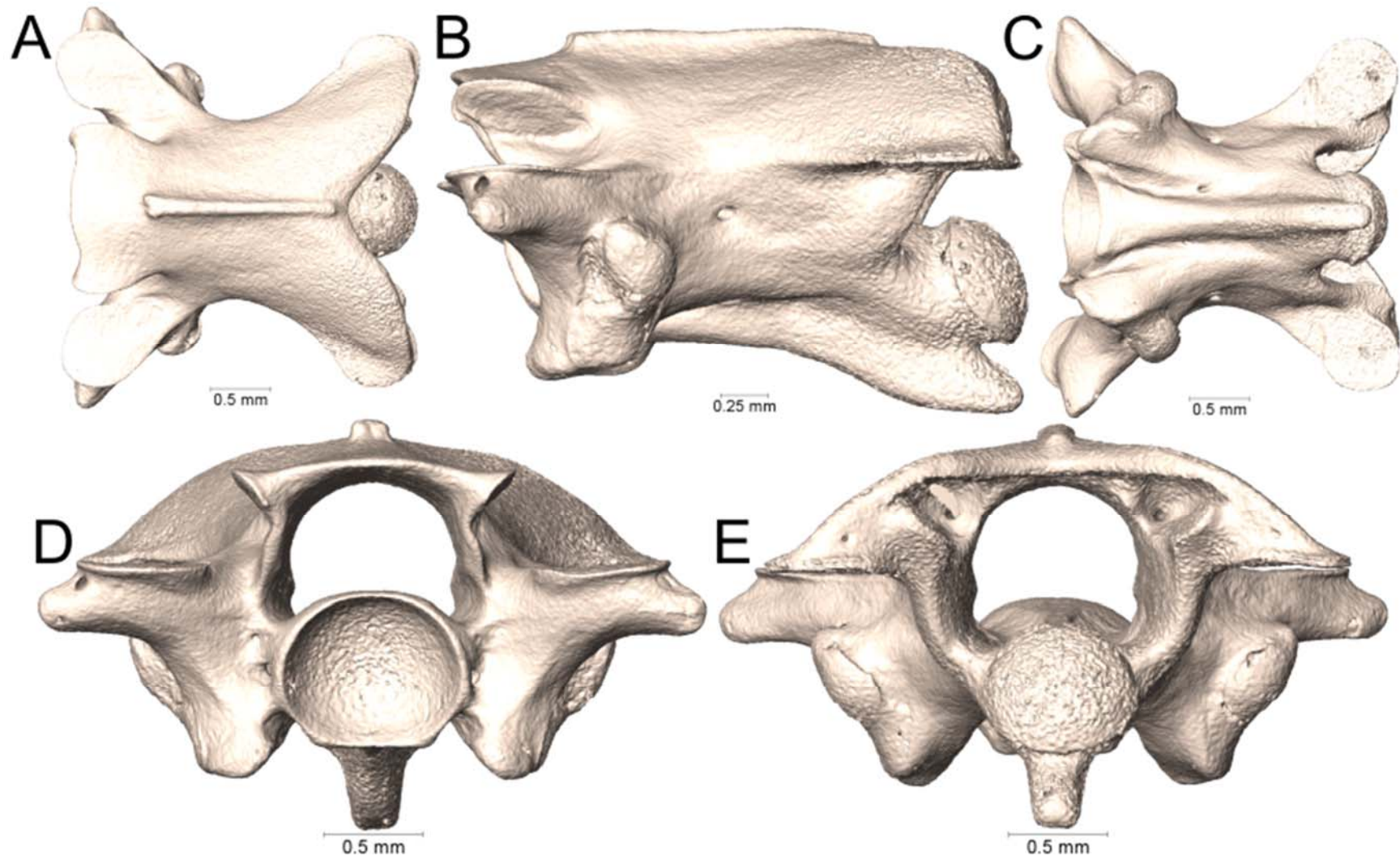
Supplemental Figure 4.57. Dorsal, lateral, ventral, anterior, and posterior views (A-E, respectively) of the midbody vertebra of *Micrurus limbatus* (UTA R-64899).



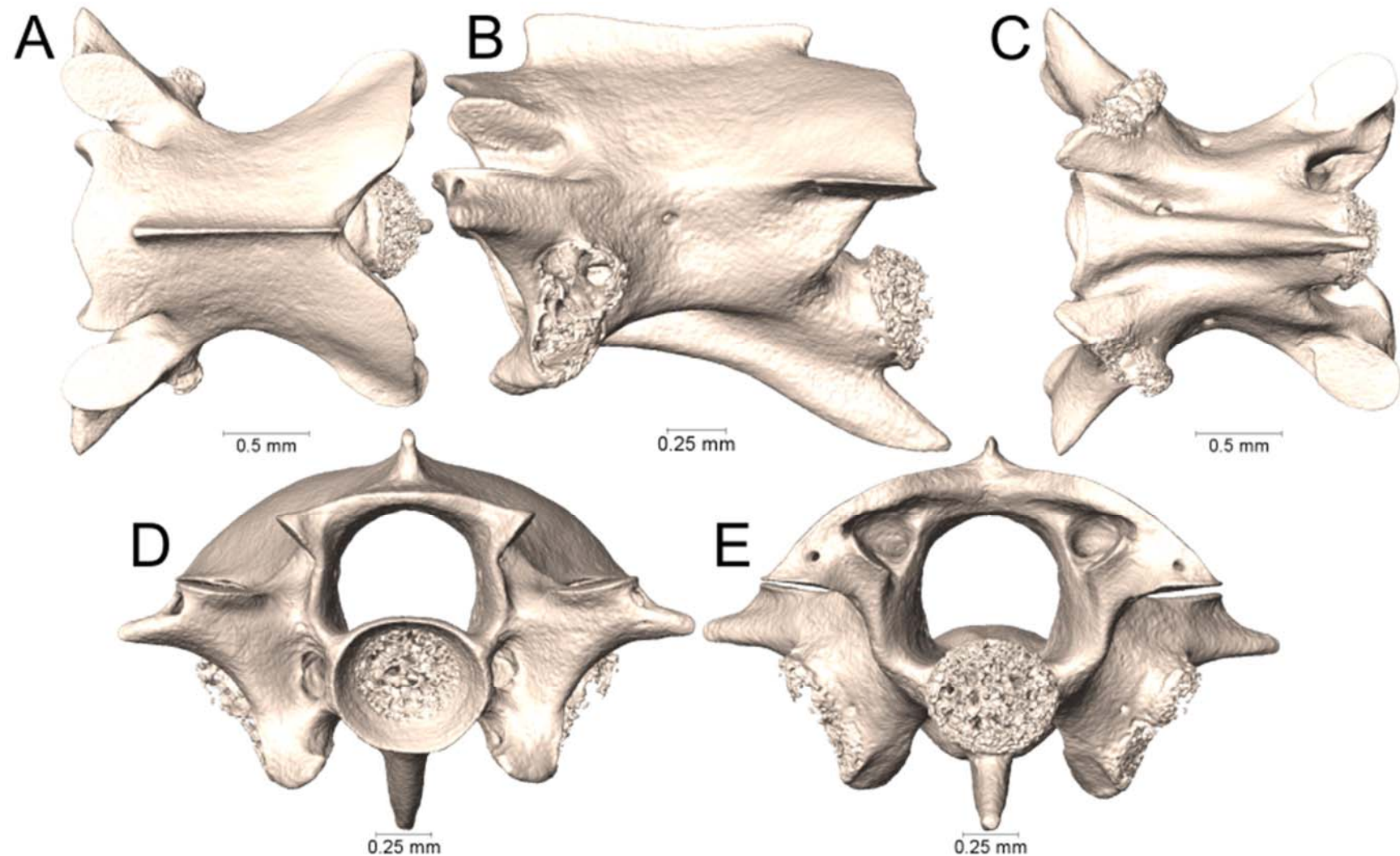
Supplemental Figure 4.58. Dorsal, lateral, ventral, anterior, and posterior views (A-E, respectively) of the midbody vertebra of *Micrurus melanotus* (AMNH 35934).



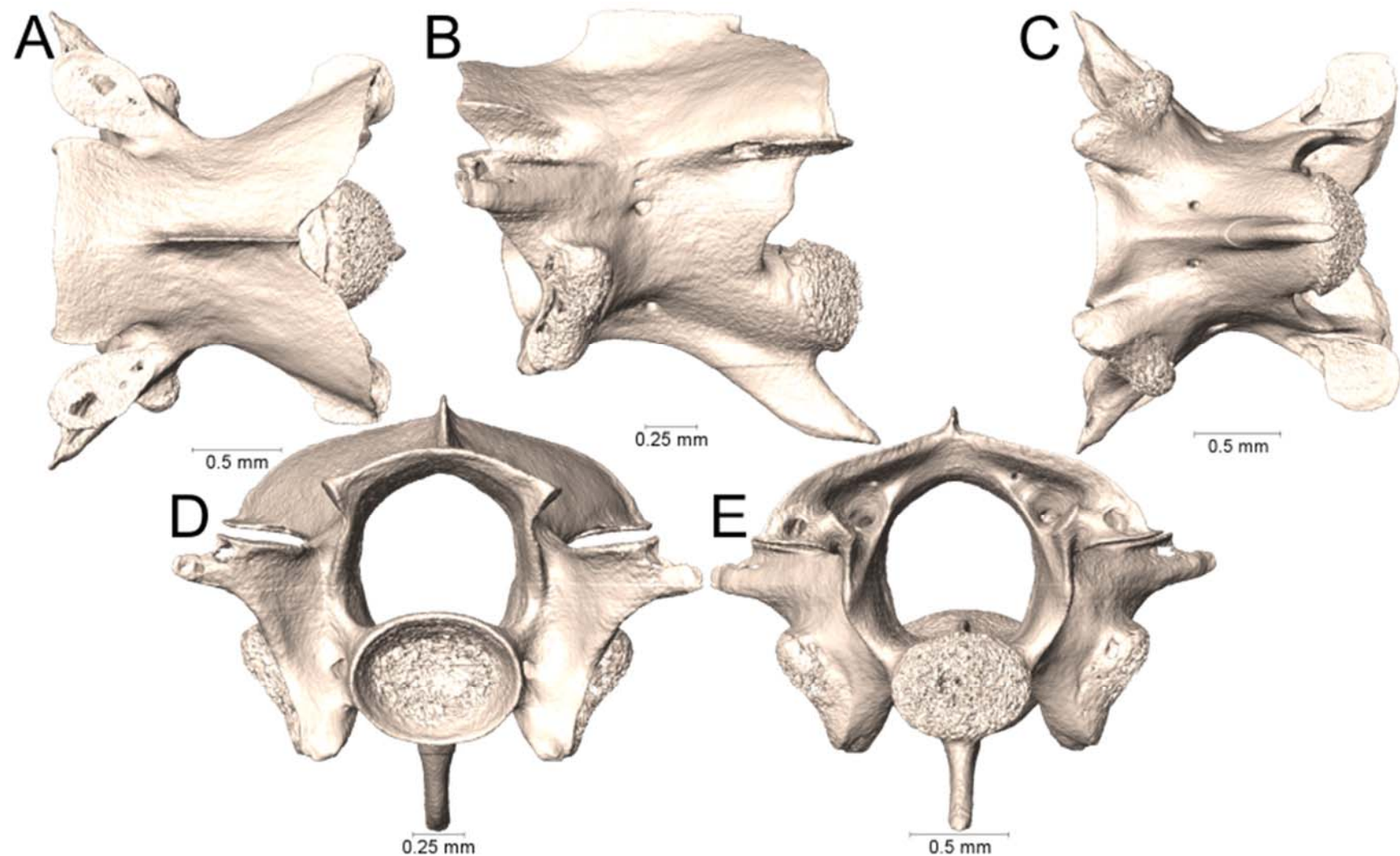
Supplemental Figure 4.59. Dorsal, lateral, ventral, anterior, and posterior views (A-E, respectively) of the midbody vertebra of *Micrurus melanotus* (UTA R-22582).



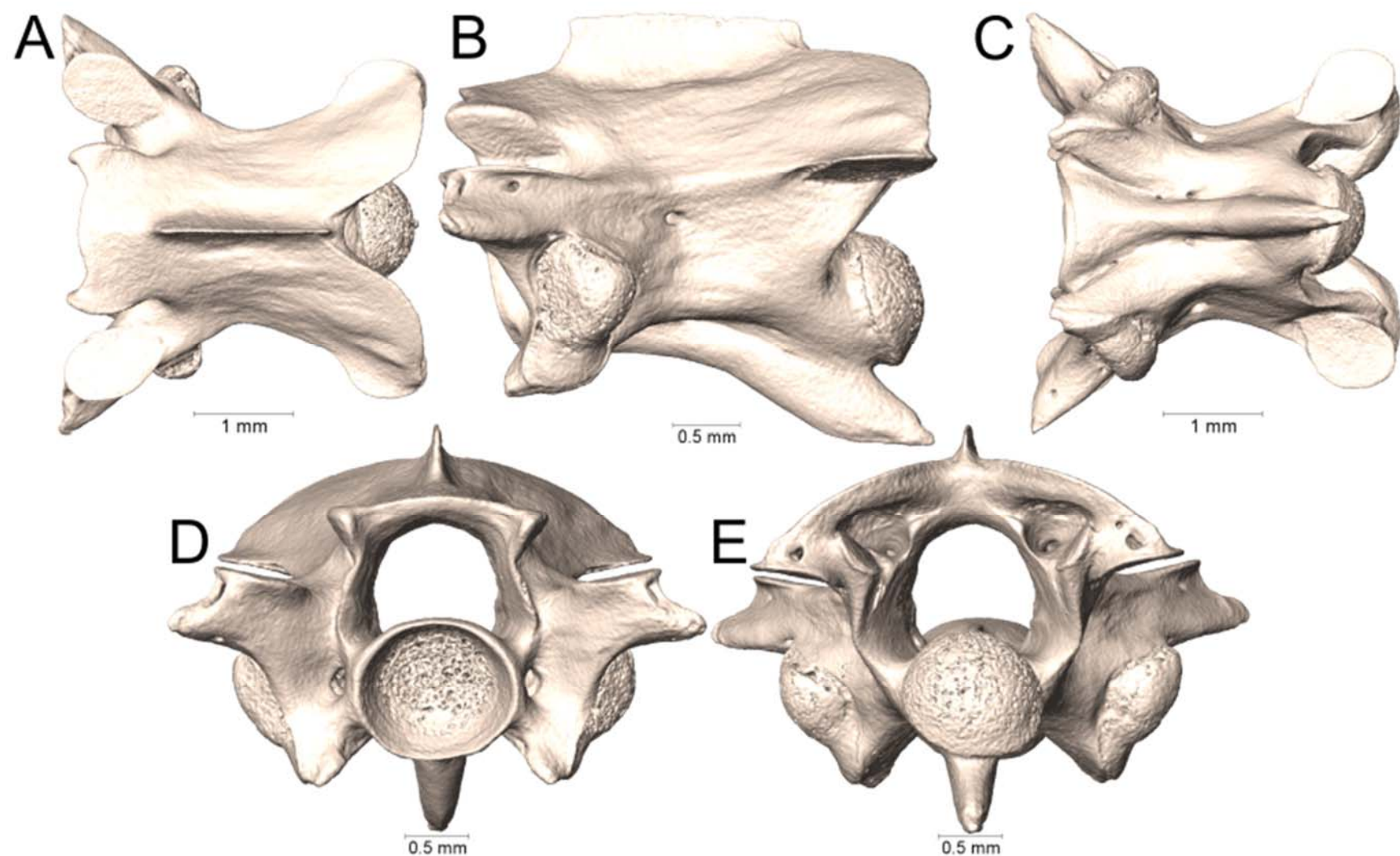
Supplemental Figure 4.60. Dorsal, lateral, ventral, anterior, and posterior views (A-E, respectively) of the midbody vertebra of *Micrurus mipartitus* (UTA R-54187).



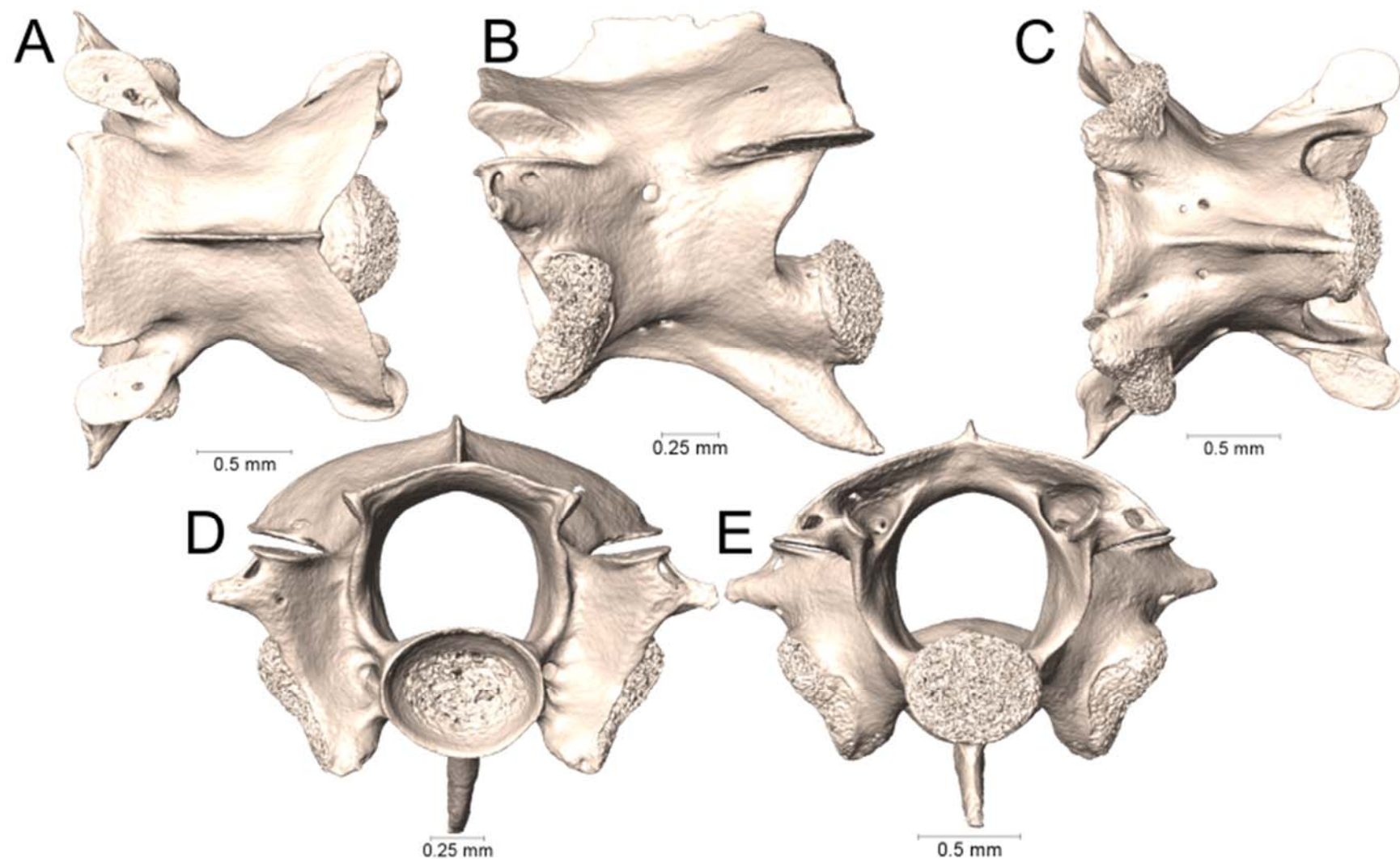
Supplemental Figure 4.61. Dorsal, lateral, ventral, anterior, and posterior views (A-E, respectively) of the midbody vertebra of *Micrurus mosquitensis* (UTA R-12919).



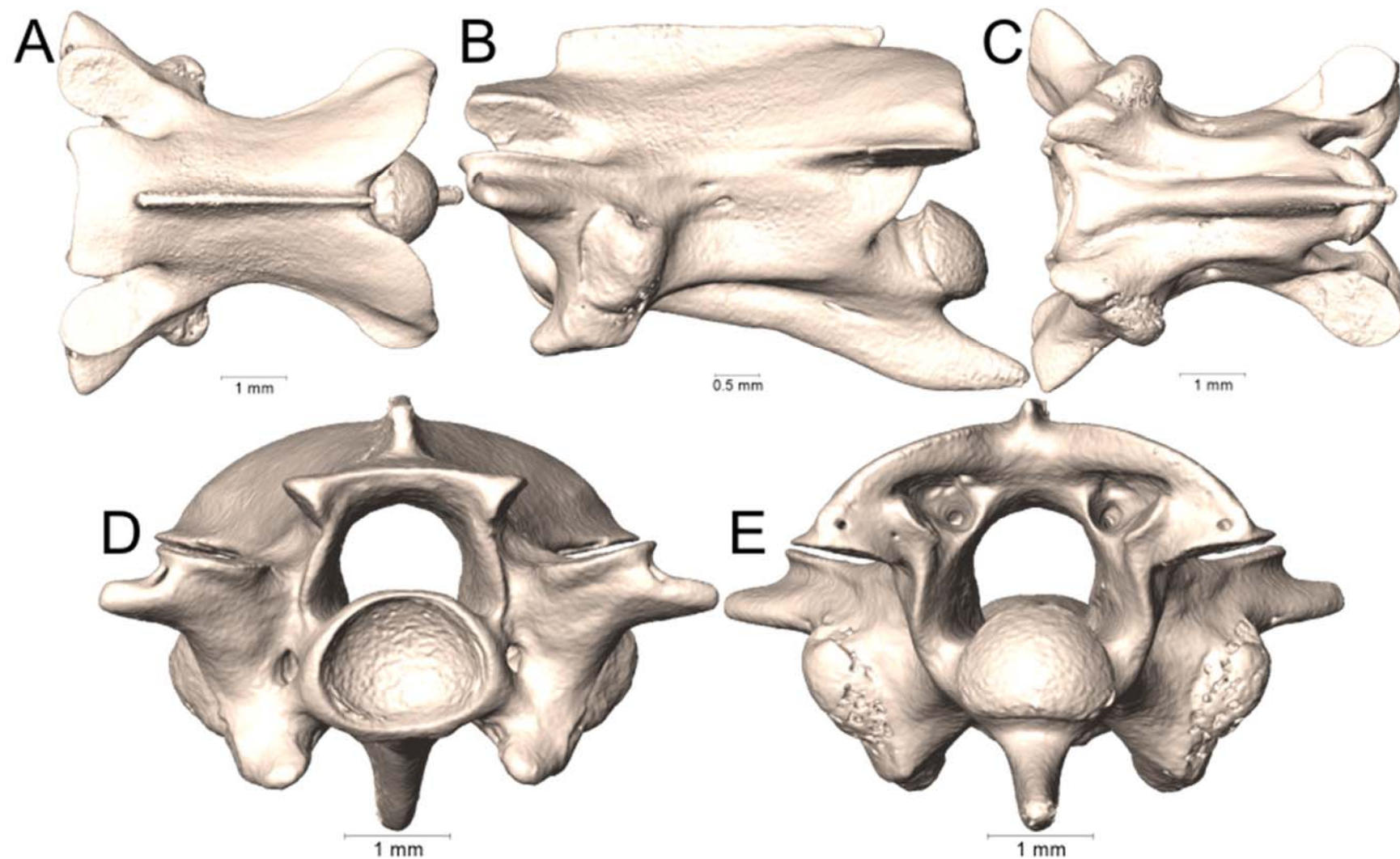
Supplemental Figure 4.62. Dorsal, lateral, ventral, anterior, and posterior views (A-E, respectively) of the midbody vertebra of *Micrurus nattereri* (UTA R-3594).



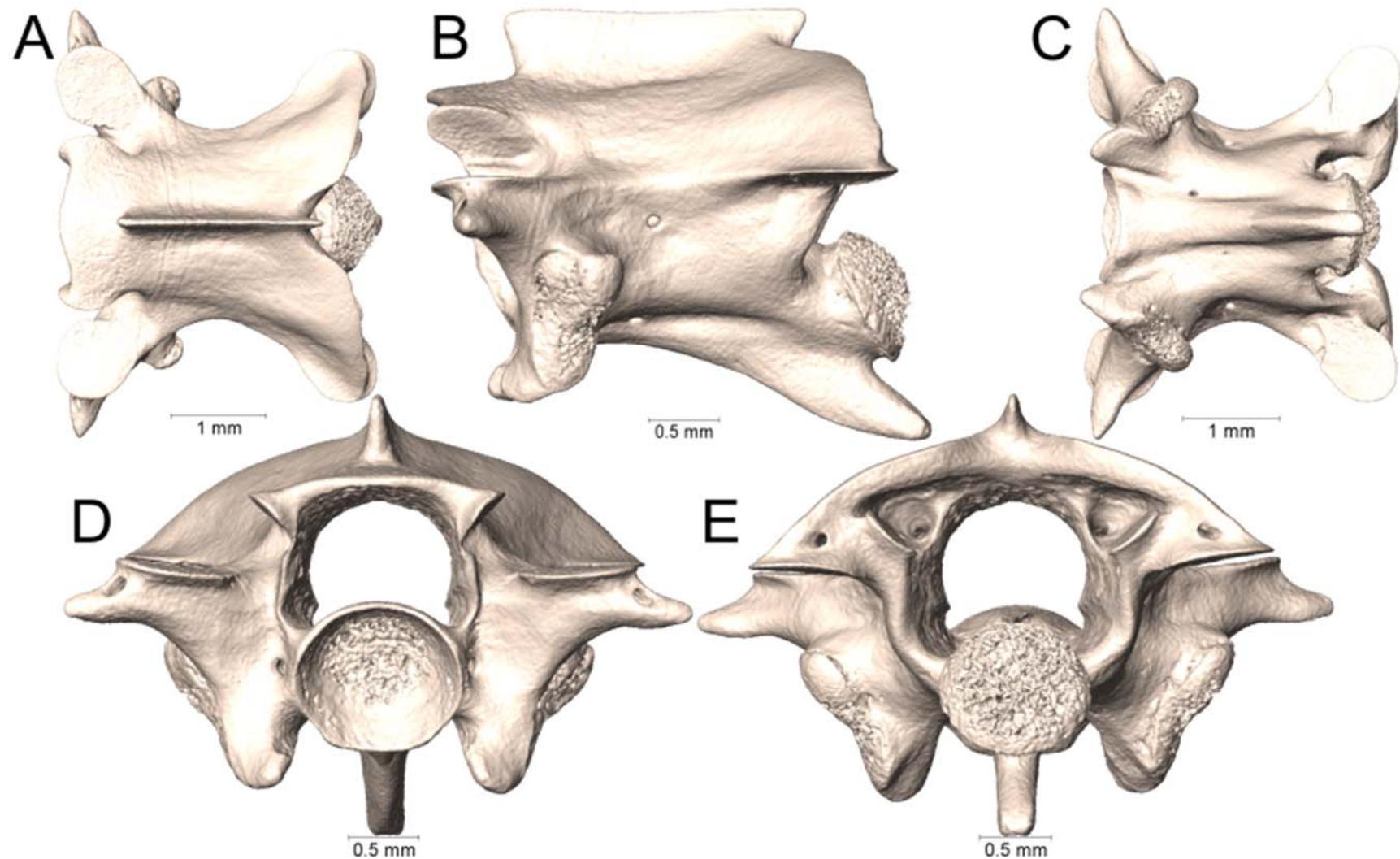
Supplemental Figure 4.63. Dorsal, lateral, ventral, anterior, and posterior views (A-E, respectively) of the midbody vertebra of *Micrurus nattereri* (UTA R-54175).



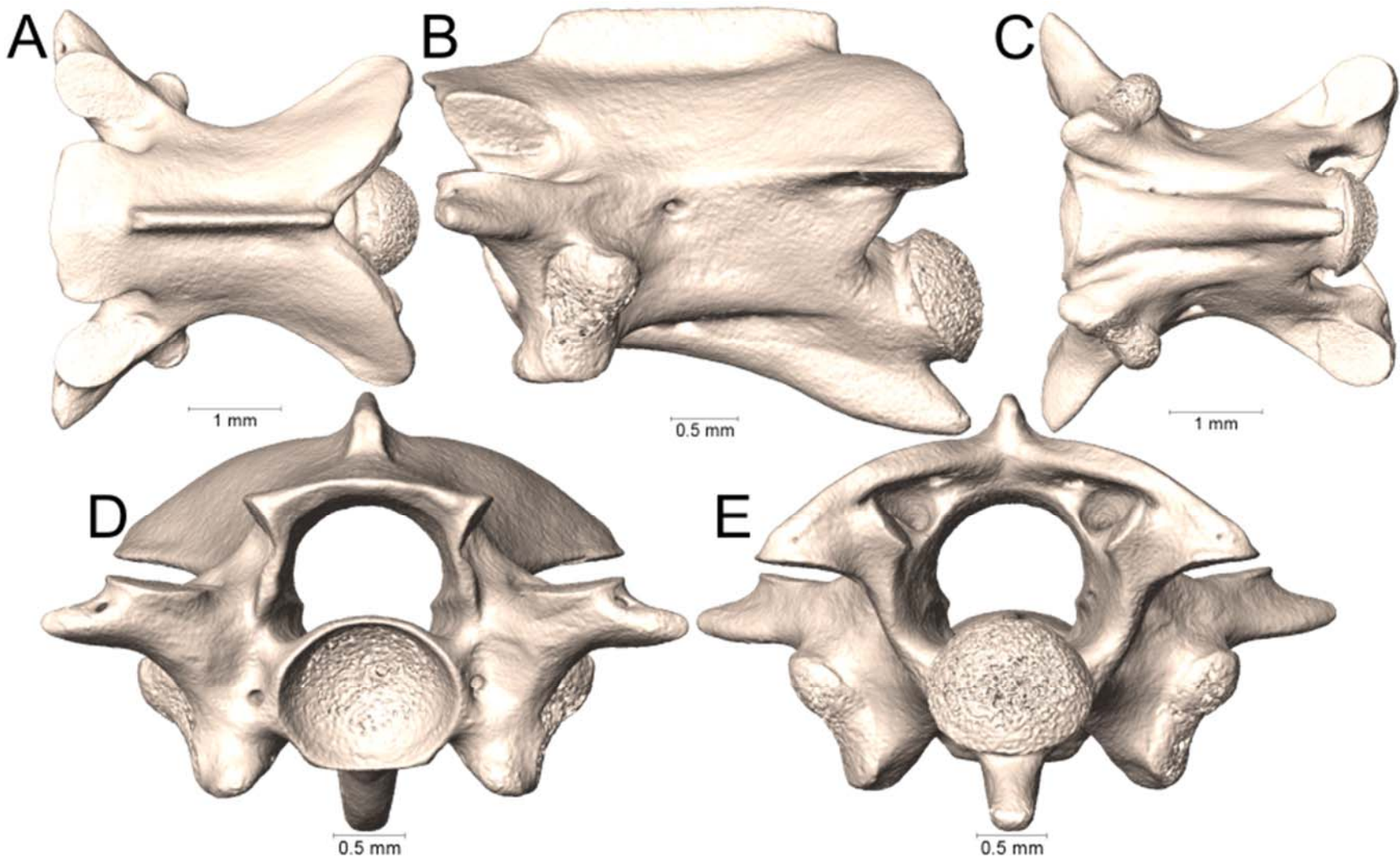
Supplemental Figure 4.64. Dorsal, lateral, ventral, anterior, and posterior views (A-E, respectively) of the midbody vertebra of *Micrurus nattereri* (UTA R-55086).



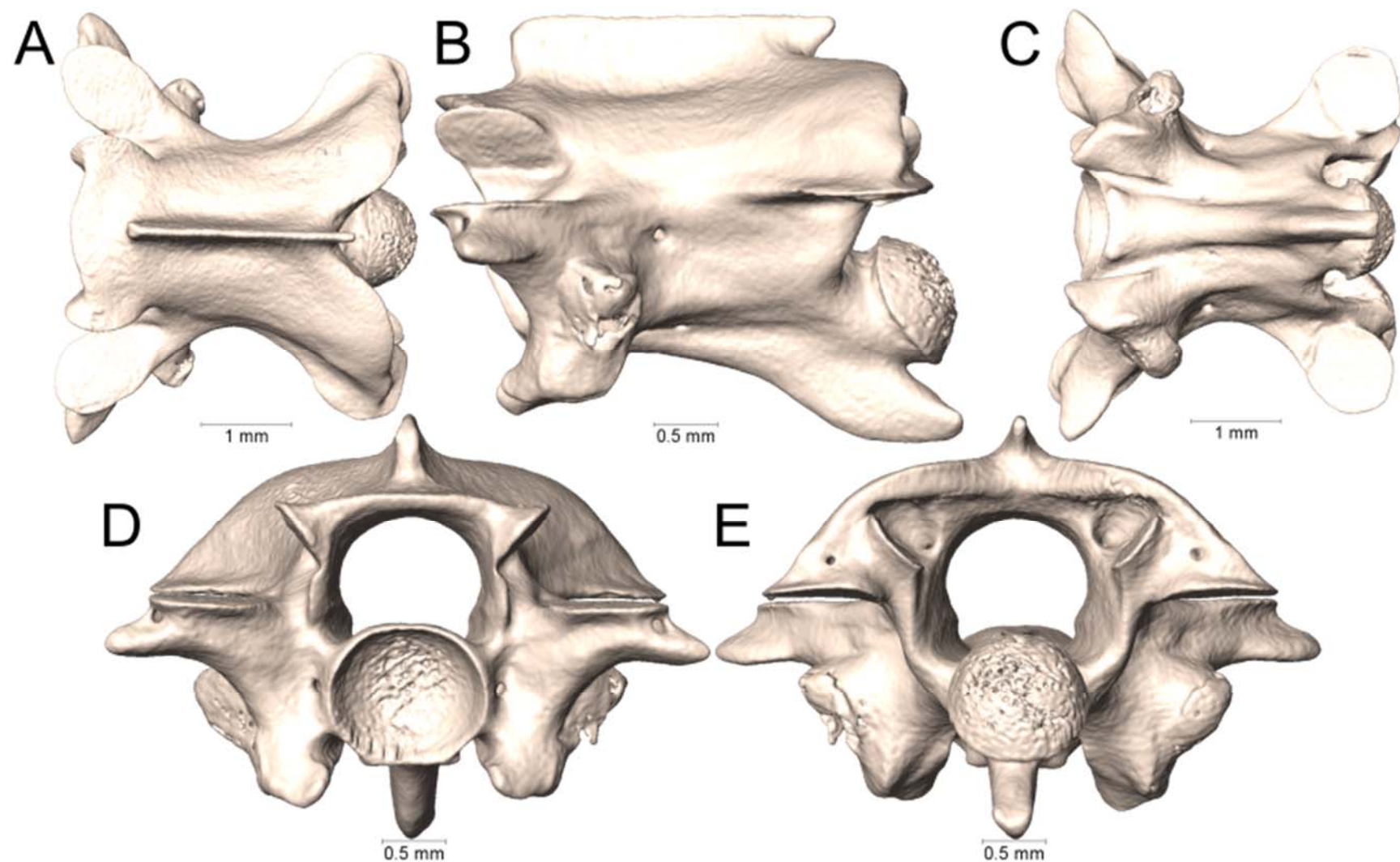
Supplemental Figure 4.65. Dorsal, lateral, ventral, anterior, and posterior views (A-E, respectively) of the midbody vertebra of *Micrurus nattereri* (UTA R-60727).



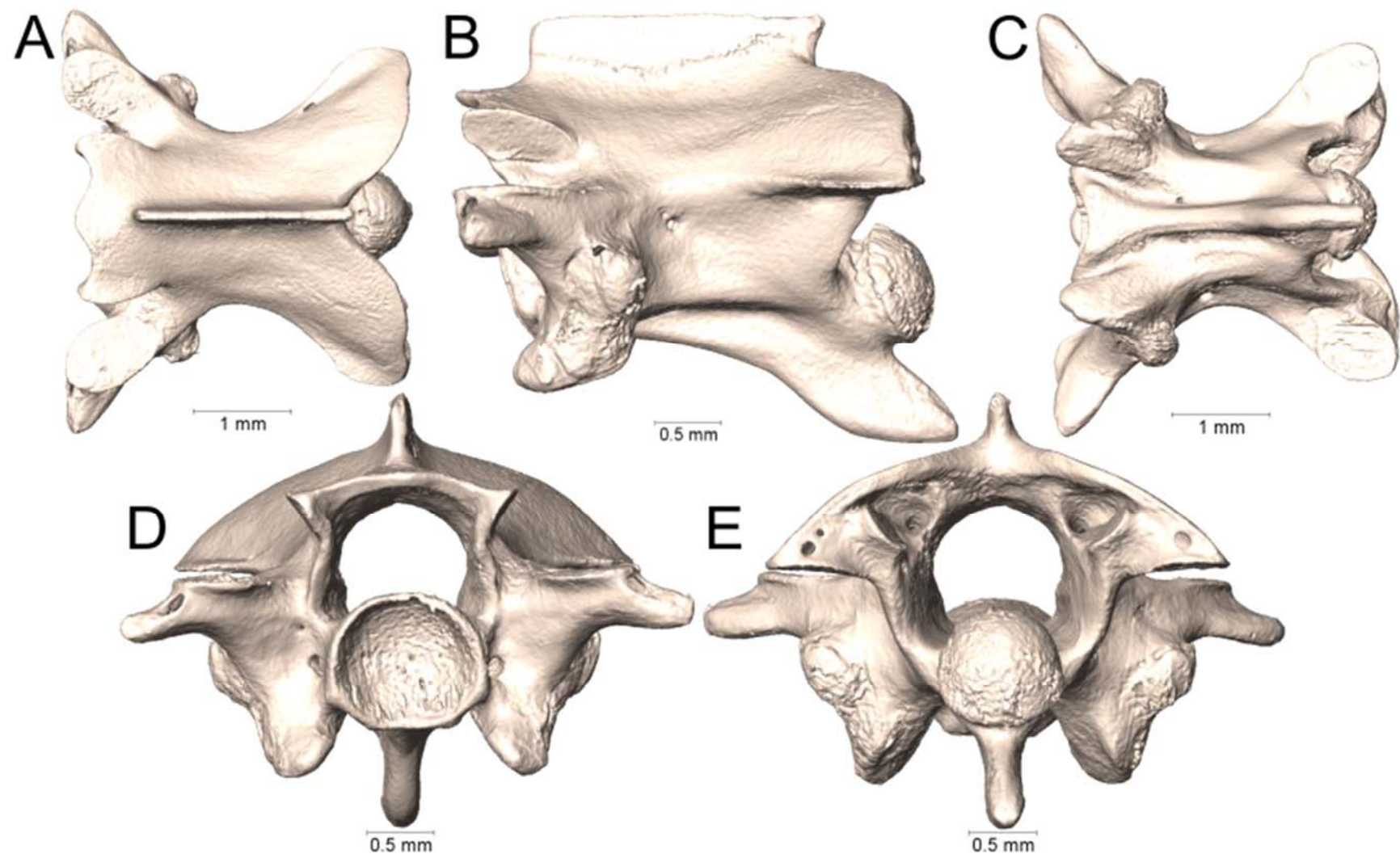
Supplemental Figure 4.66. Dorsal, lateral, ventral, anterior, and posterior views (A-E, respectively) of the midbody vertebra of *Micrurus nigrocinctus zunilensis* (UTA R-64858).



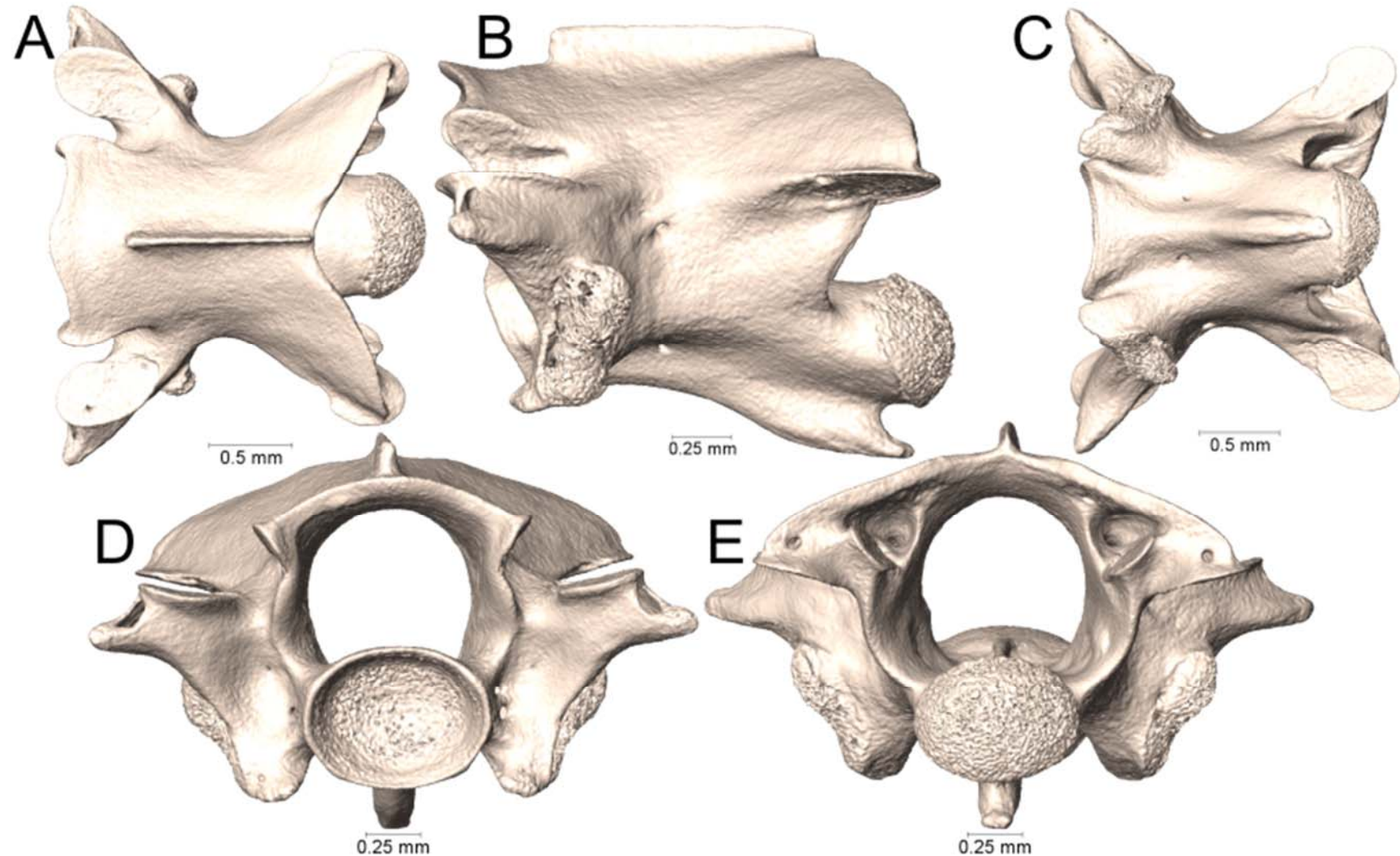
Supplemental Figure 4.67. Dorsal, lateral, ventral, anterior, and posterior views (A-E, respectively) of the midbody vertebra of *Micrurus obscurus* (UTA R-3840).



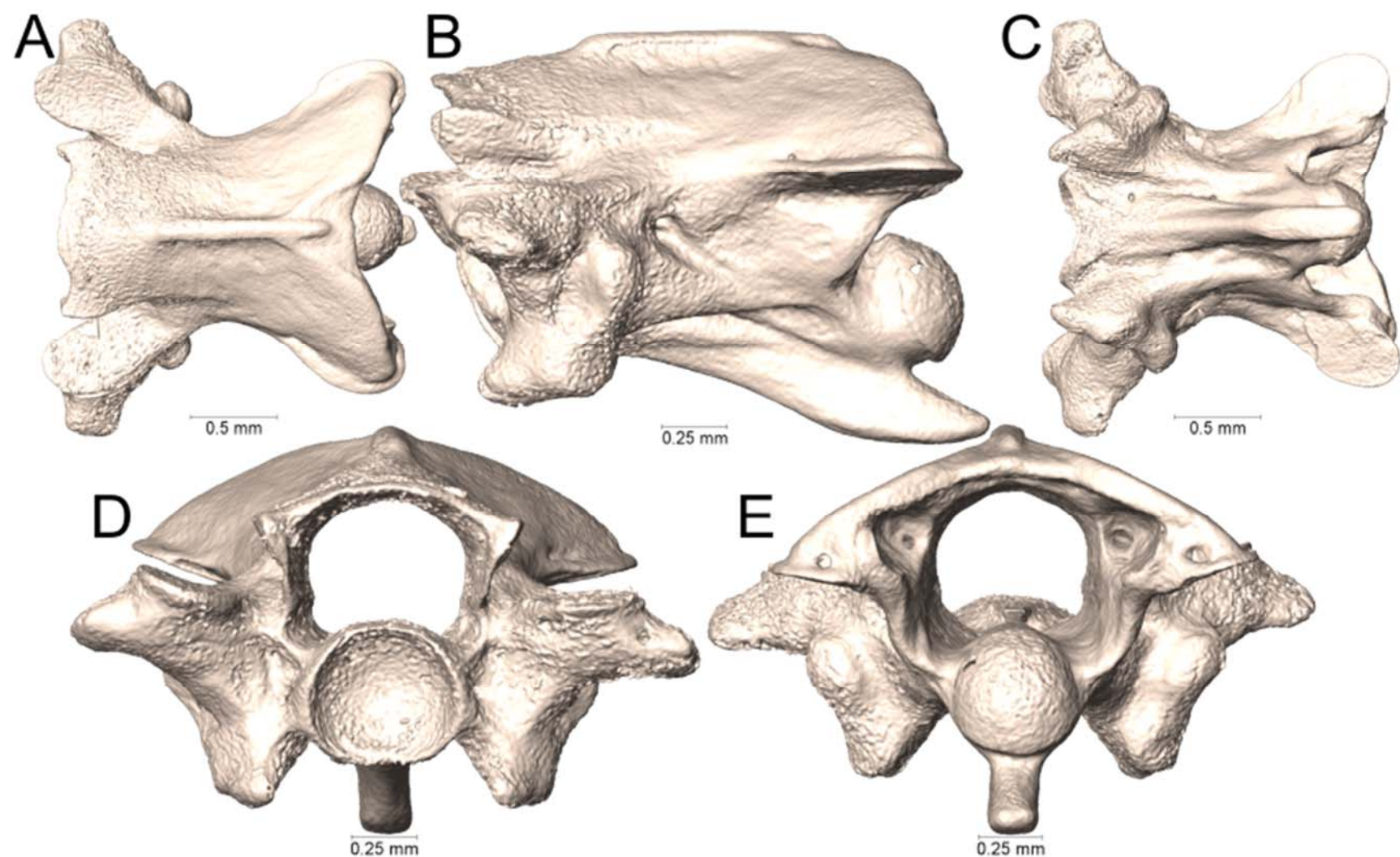
Supplemental Figure 4.68. Dorsal, lateral, ventral, anterior, and posterior views (A-E, respectively) of the midbody vertebra of *Micrurus oliveri* (UTA R-64893).



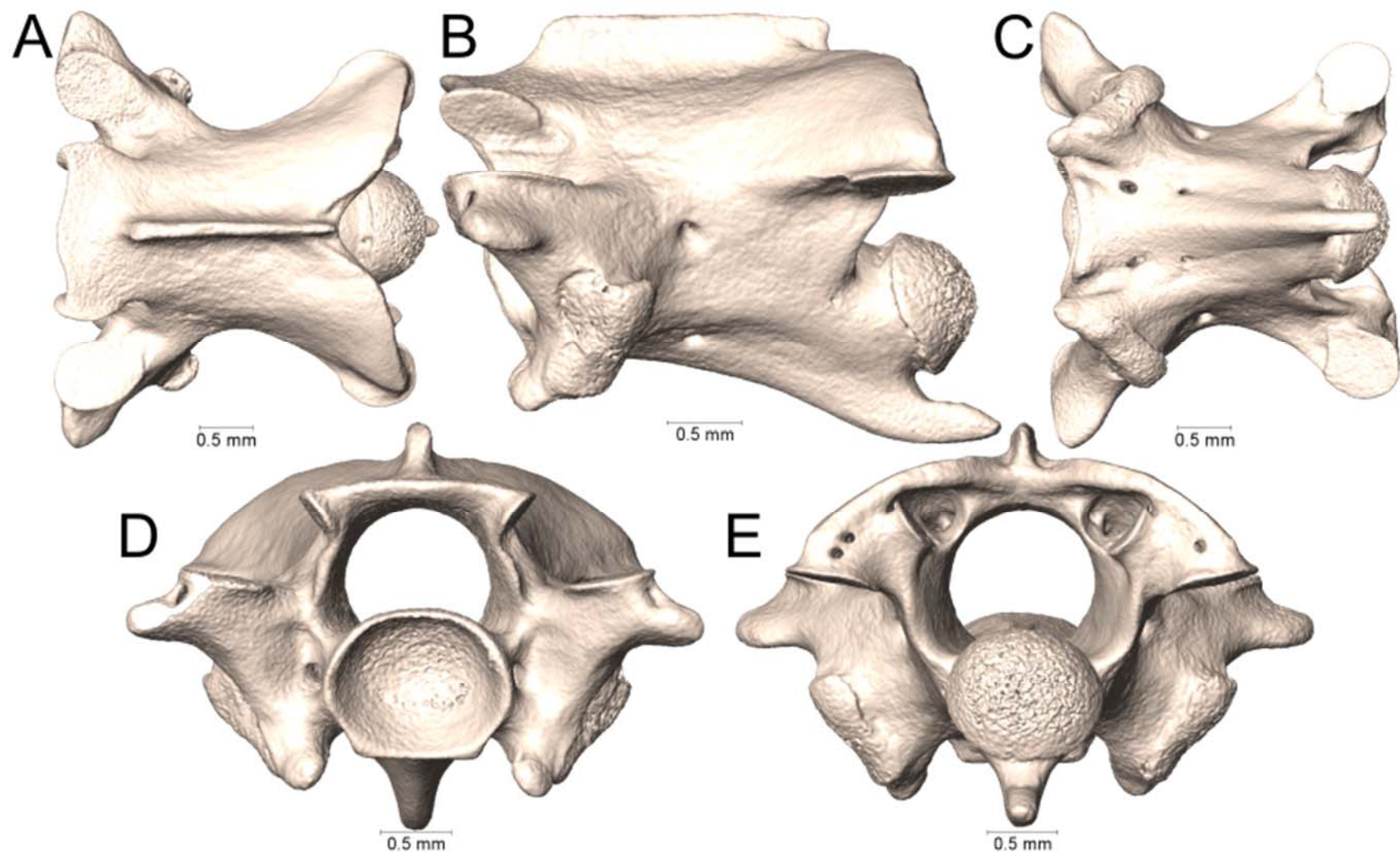
Supplemental Figure 4.69. Dorsal, lateral, ventral, anterior, and posterior views (A-E, respectively) of the midbody vertebra of *Micrurus ornatissimus* (UTA R-60724).



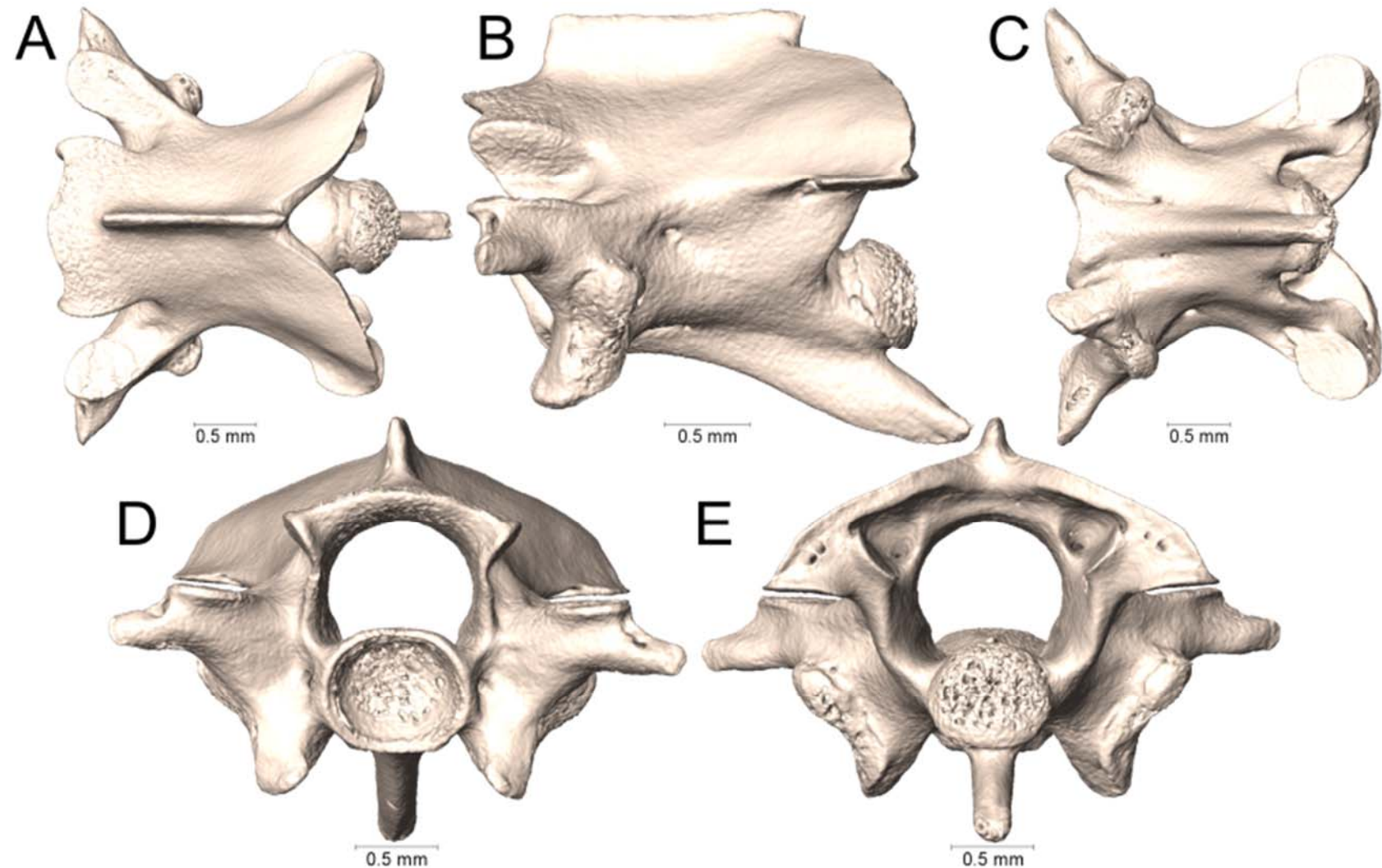
Supplemental Figure 4.70. Dorsal, lateral, ventral, anterior, and posterior views (A-E, respectively) of the midbody vertebra of *Micrurus pyrrhocryptus* (UTA R-51404).



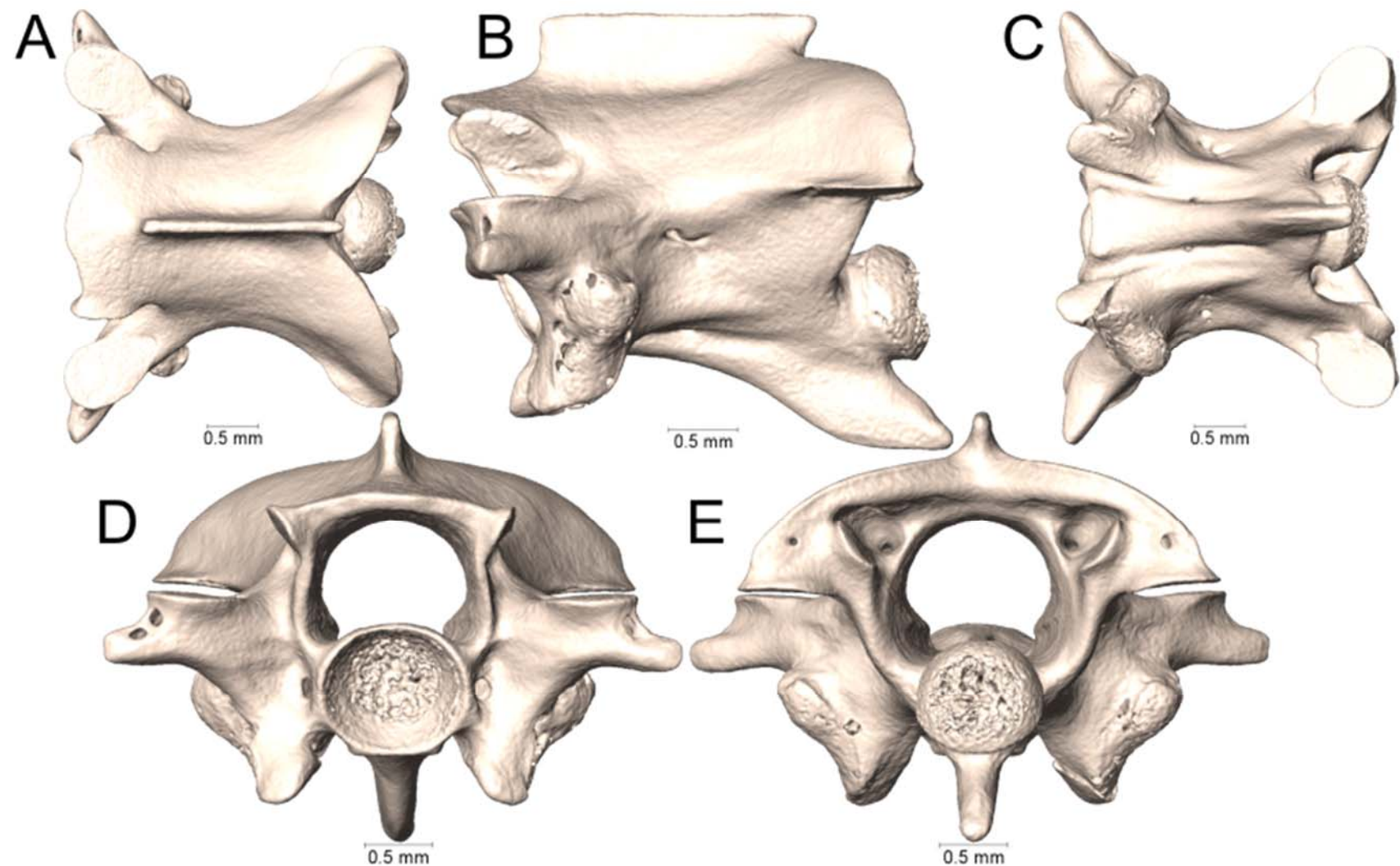
Supplemental Figure 4.71. Dorsal, lateral, ventral, anterior, and posterior views (A-E, respectively) of the midbody vertebra of *Micrurus renjifoi* (UTA R-3490).



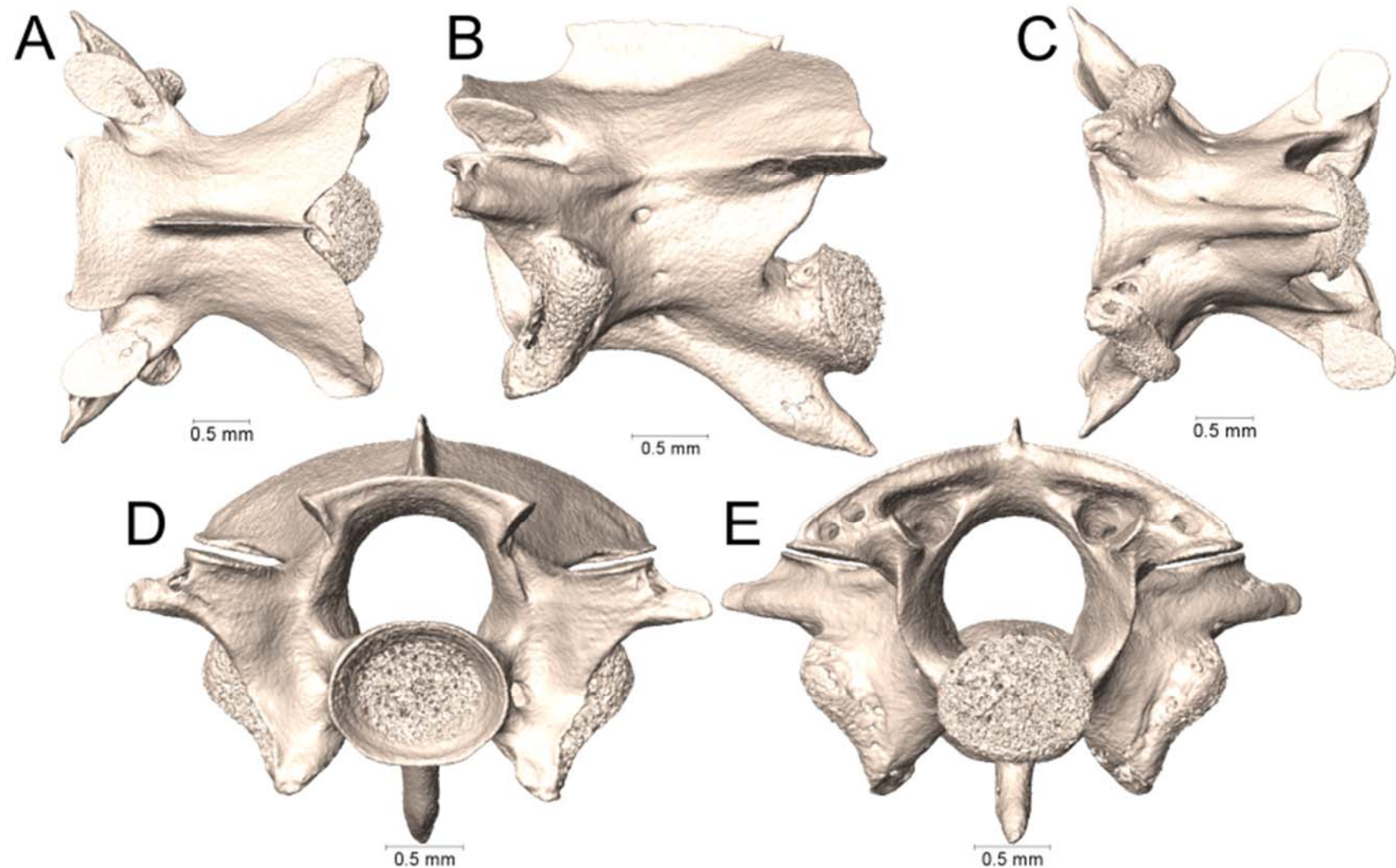
Supplemental Figure 4.72. Dorsal, lateral, ventral, anterior, and posterior views (A-E, respectively) of the midbody vertebra of *Micrurus serranus* (UTA R-34561).



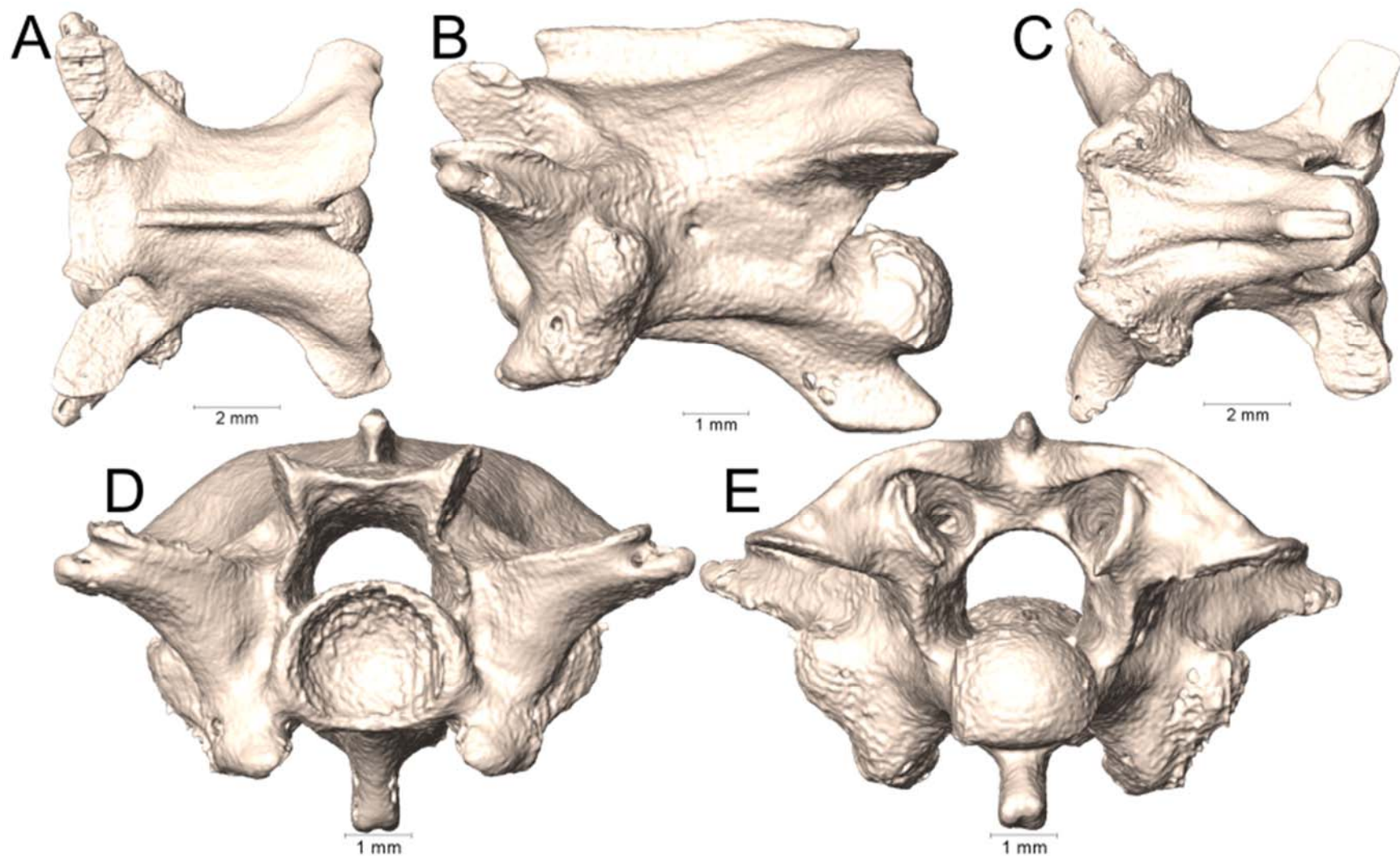
Supplemental Figure 4.73. Dorsal, lateral, ventral, anterior, and posterior views (A-E, respectively) of the midbody vertebra of *Micrurus steindachneri* (AMNH 28846).



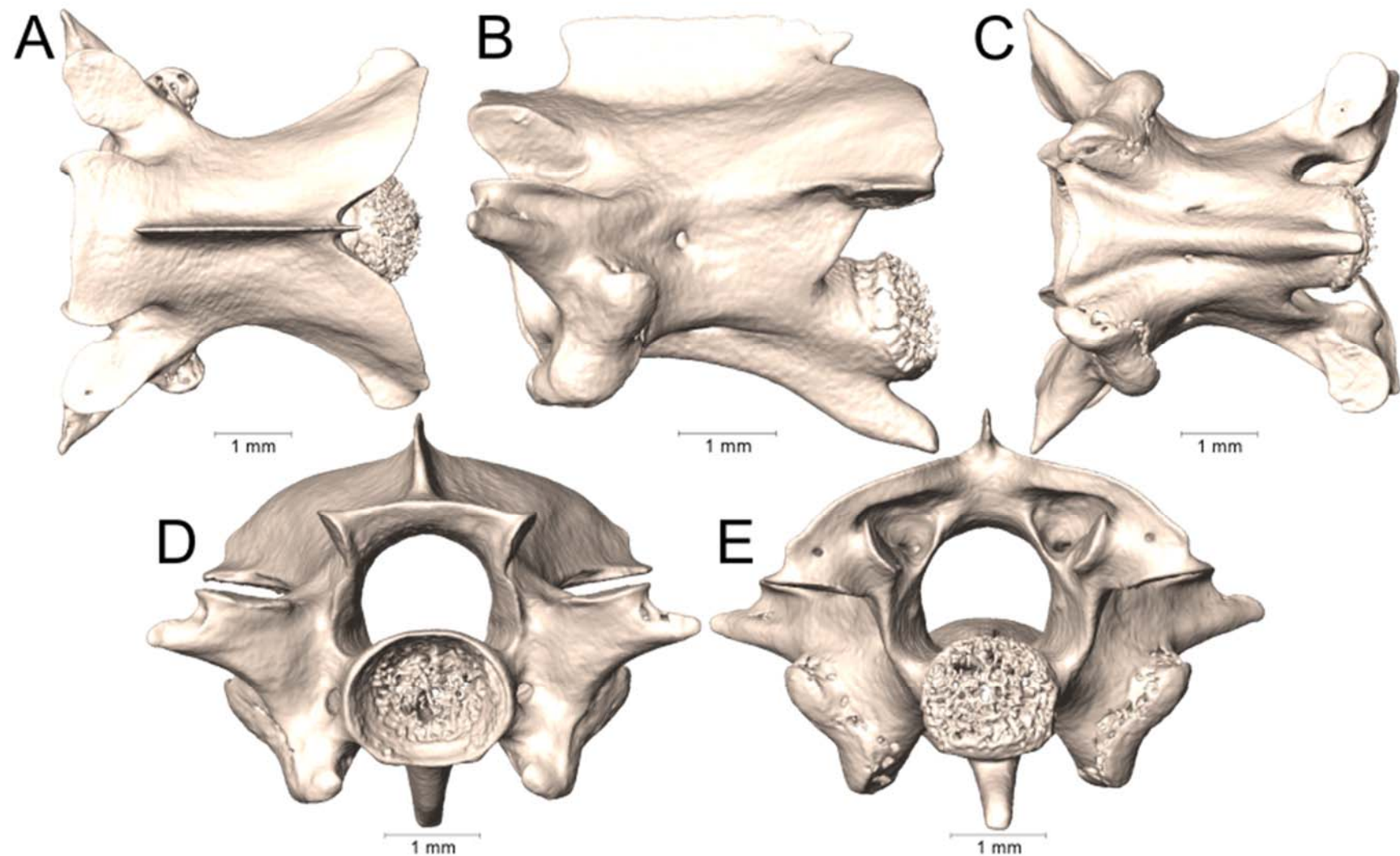
Supplemental Figure 4.74. Dorsal, lateral, ventral, anterior, and posterior views (A-E, respectively) of the midbody vertebra of *Micrurus steindachneri* (AMNH 35819).



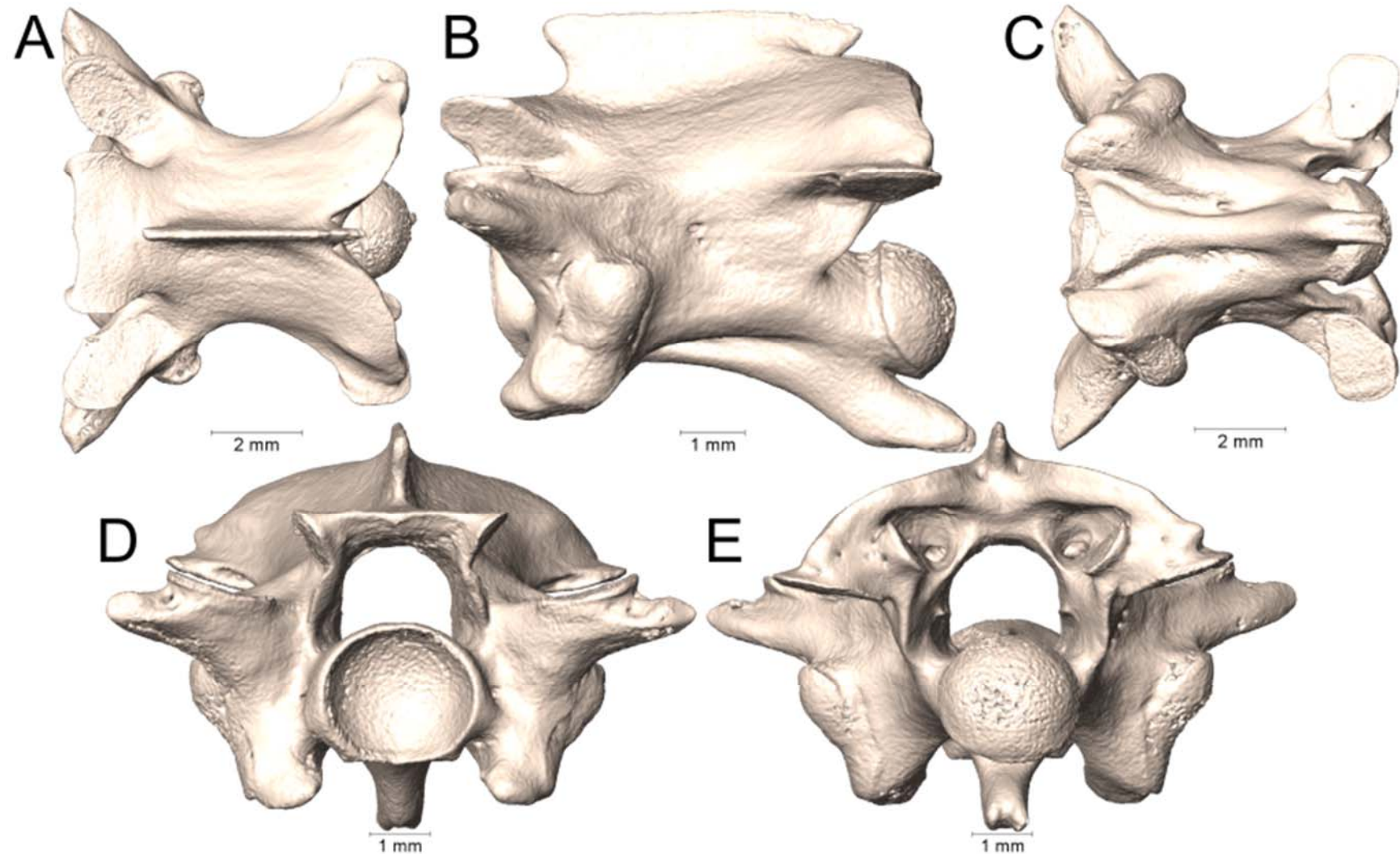
Supplemental Figure 4.75. Dorsal, lateral, ventral, anterior, and posterior views (A-E, respectively) of the midbody vertebra of *Micrurus surinamensis* (UTA R-5849).



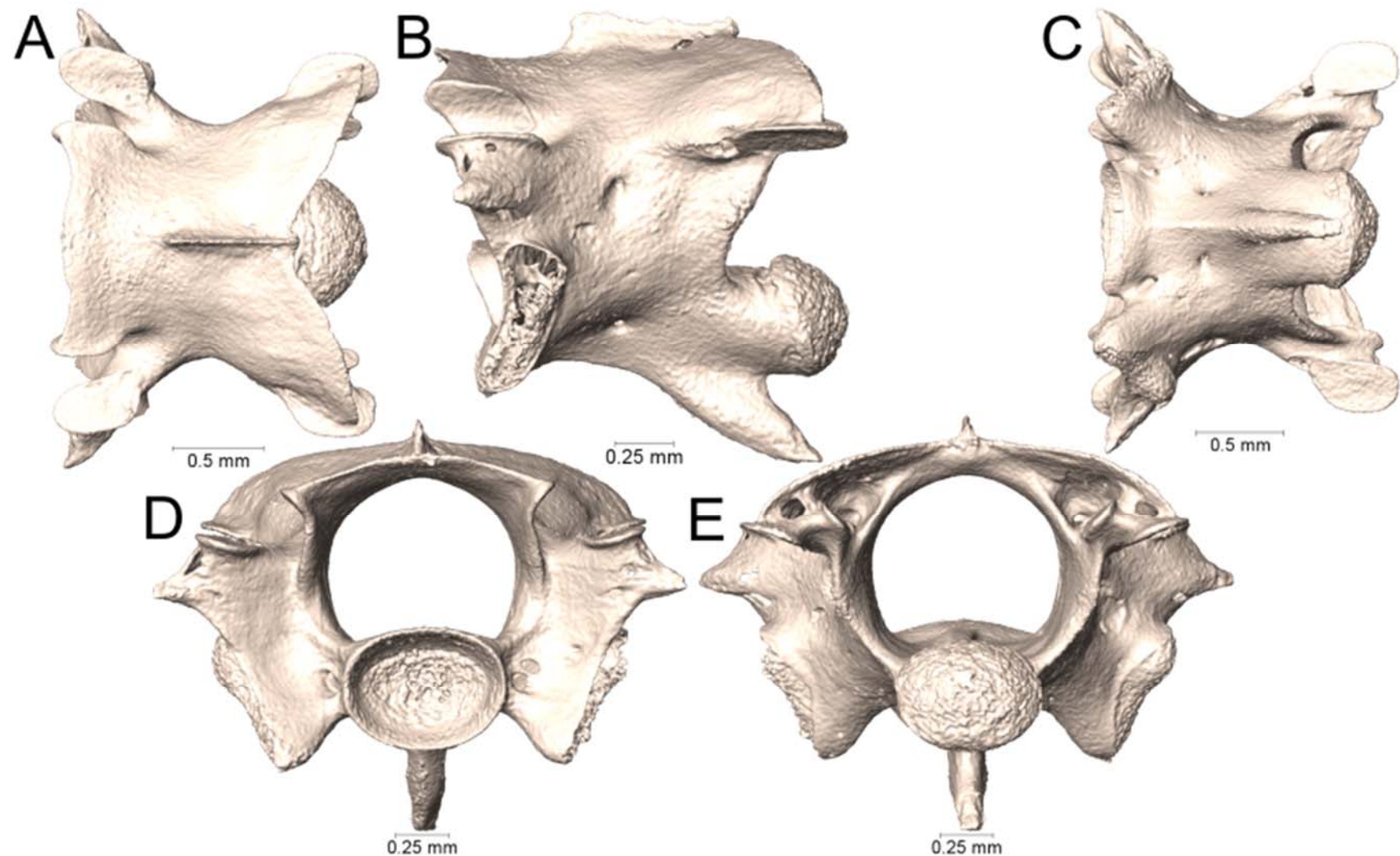
Supplemental Figure 4.76. Dorsal, lateral, ventral, anterior, and posterior views (A-E, respectively) of the midbody vertebra of *Micrurus surinamensis* (UTA R-15679).



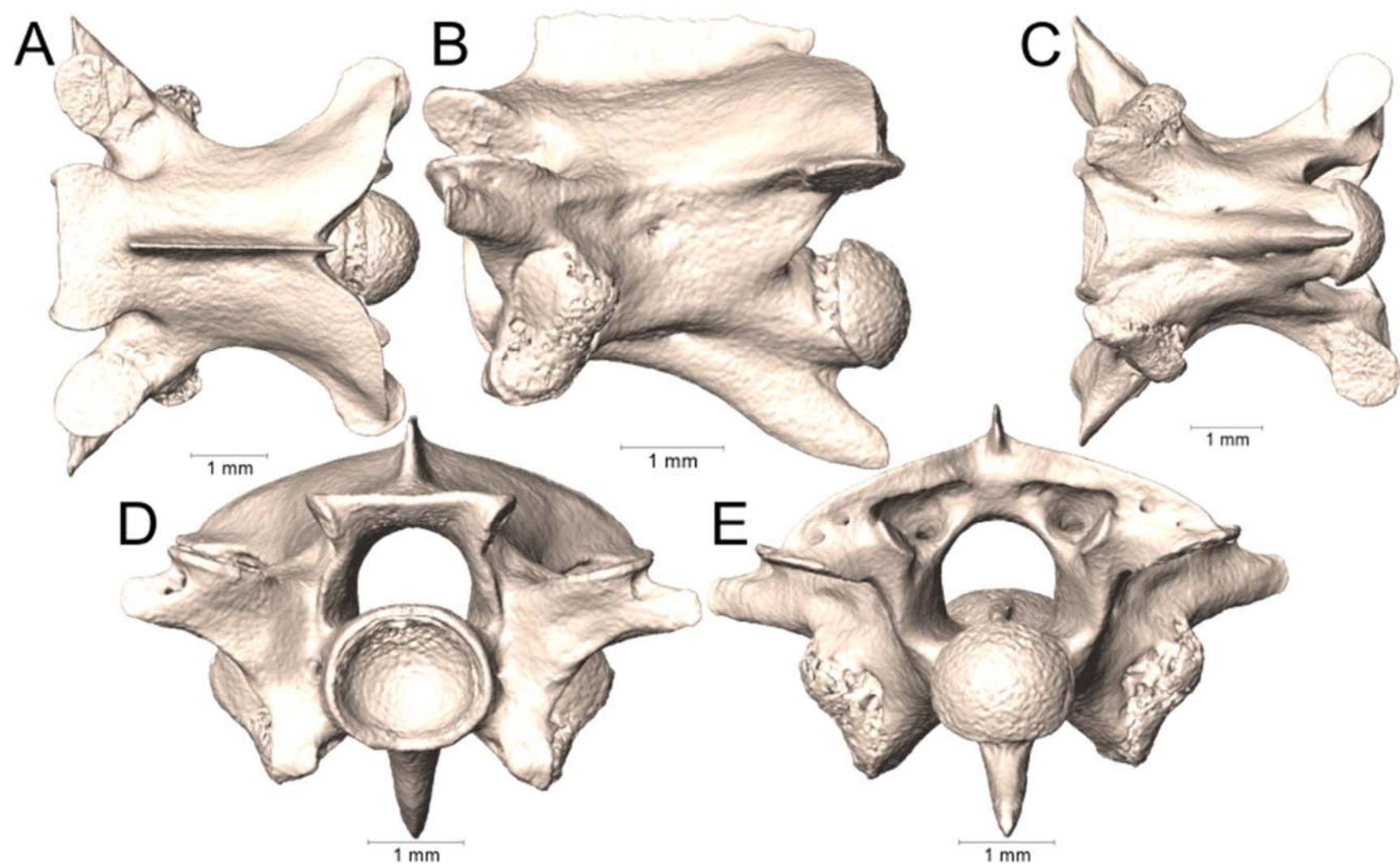
Supplemental Figure 4.77. Dorsal, lateral, ventral, anterior, and posterior views (A-E, respectively) of the midbody vertebra of *Micrurus surinamensis* (UTA R-50173).



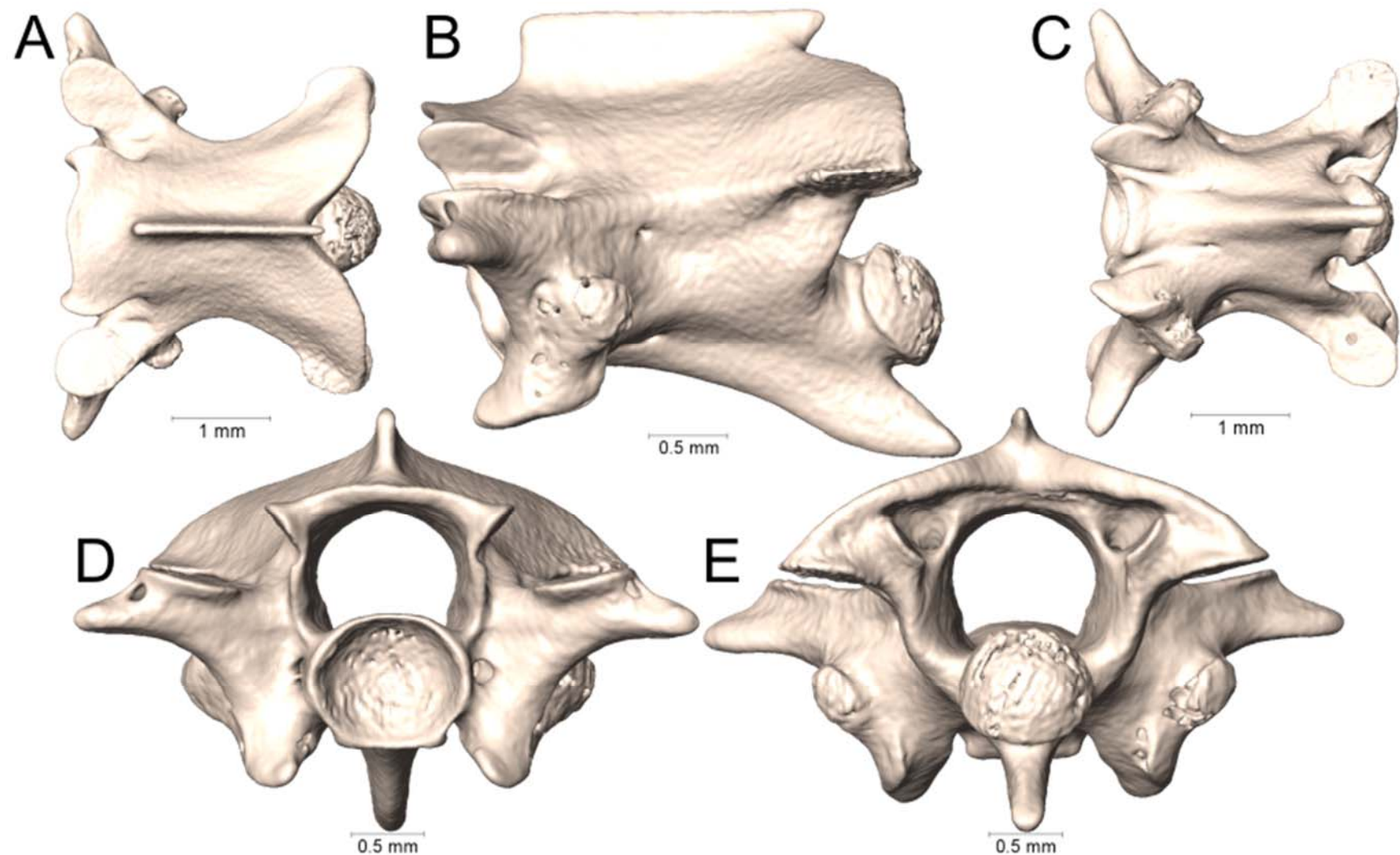
Supplemental Figure 4.78. Dorsal, lateral, ventral, anterior, and posterior views (A-E, respectively) of the midbody vertebra of *Micrurus surinamensis* (UTA R-54378).



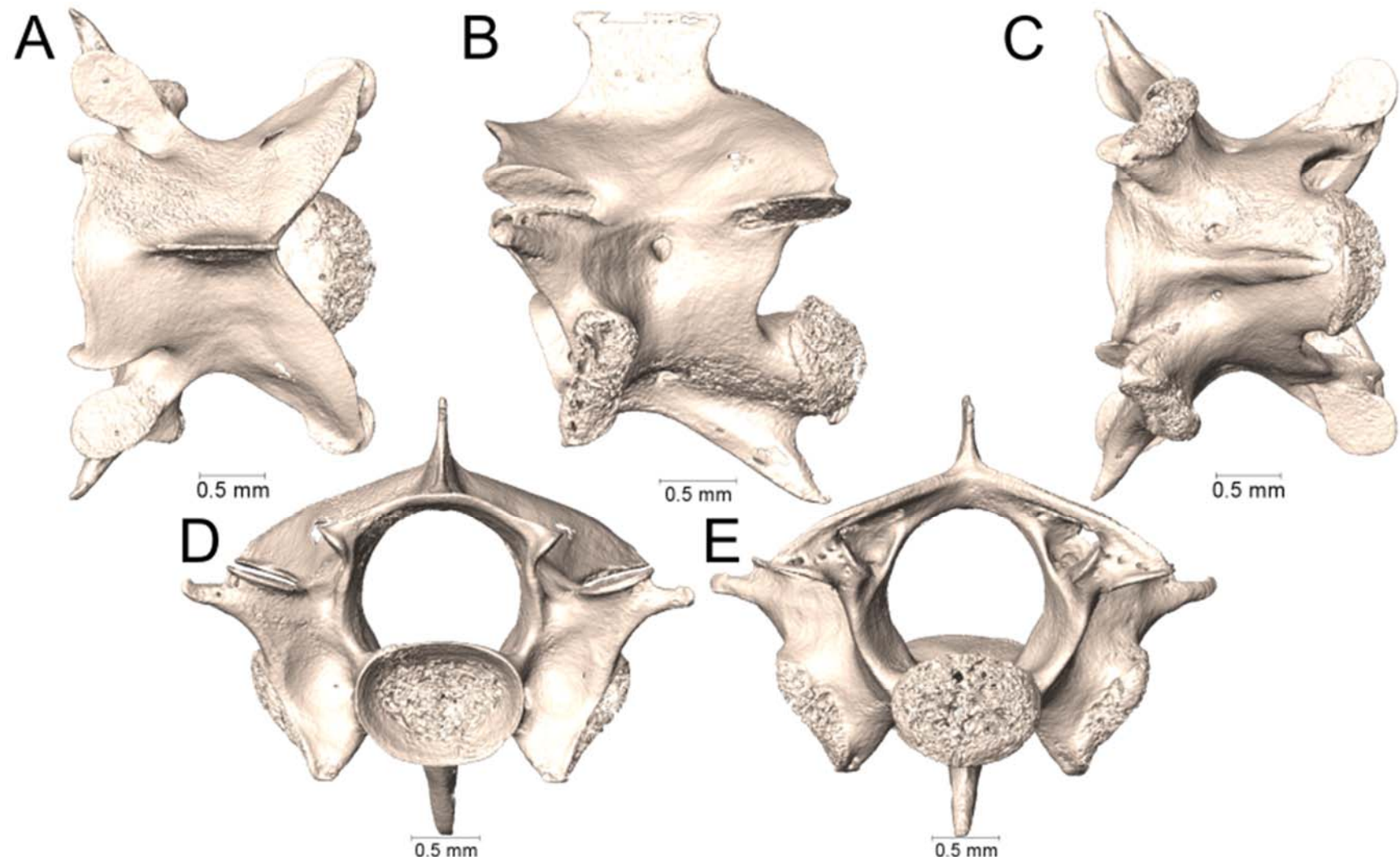
Supplemental Figure 4.79. Dorsal, lateral, ventral, anterior, and posterior views (A-E, respectively) of the midbody vertebra of *Micrurus surinamensis* (UTA R-65798).



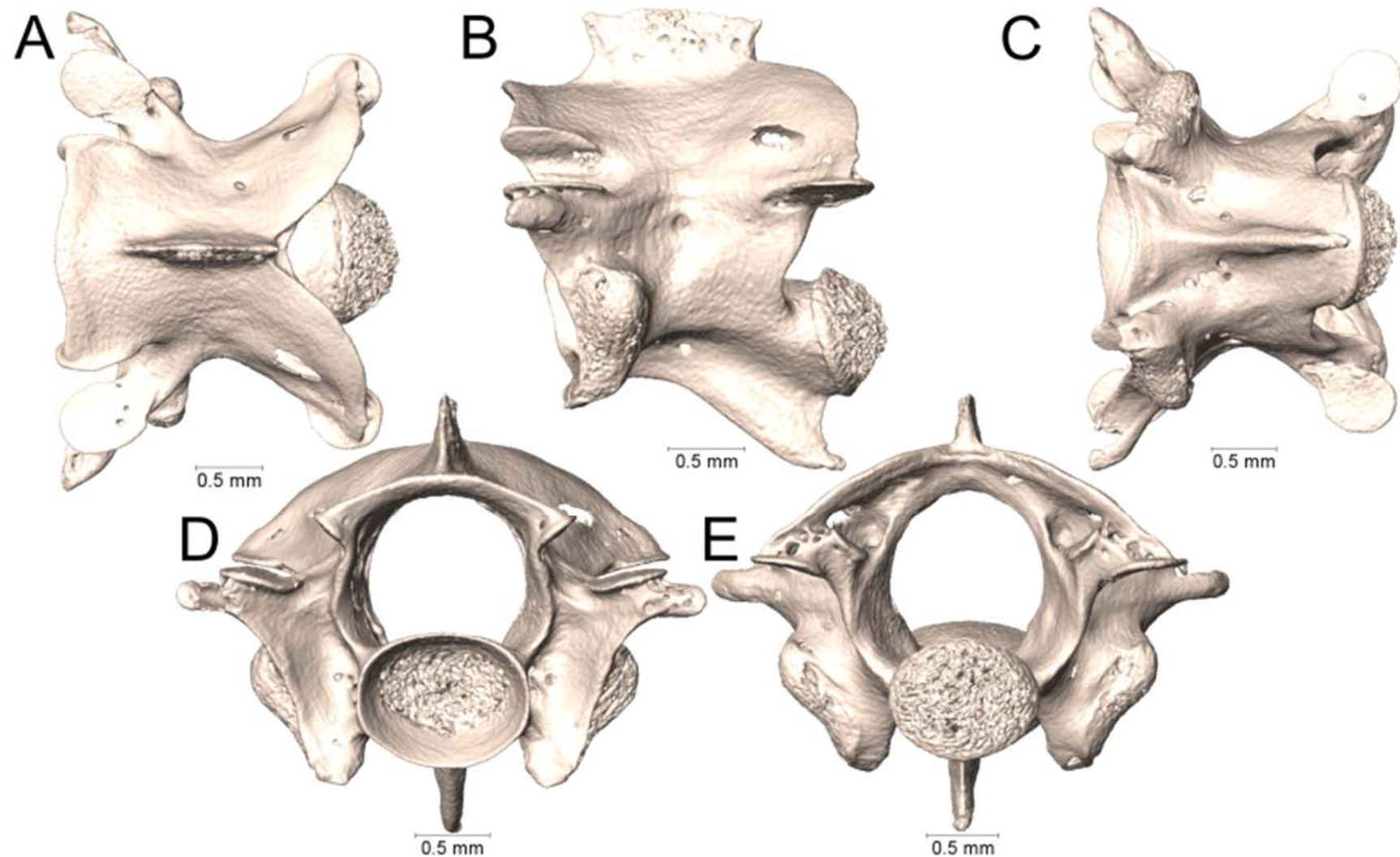
Supplemental Figure 4.80. Dorsal, lateral, ventral, anterior, and posterior views (A-E, respectively) of the midbody vertebra of *Micrurus surinamensis* (UTA R-65844).



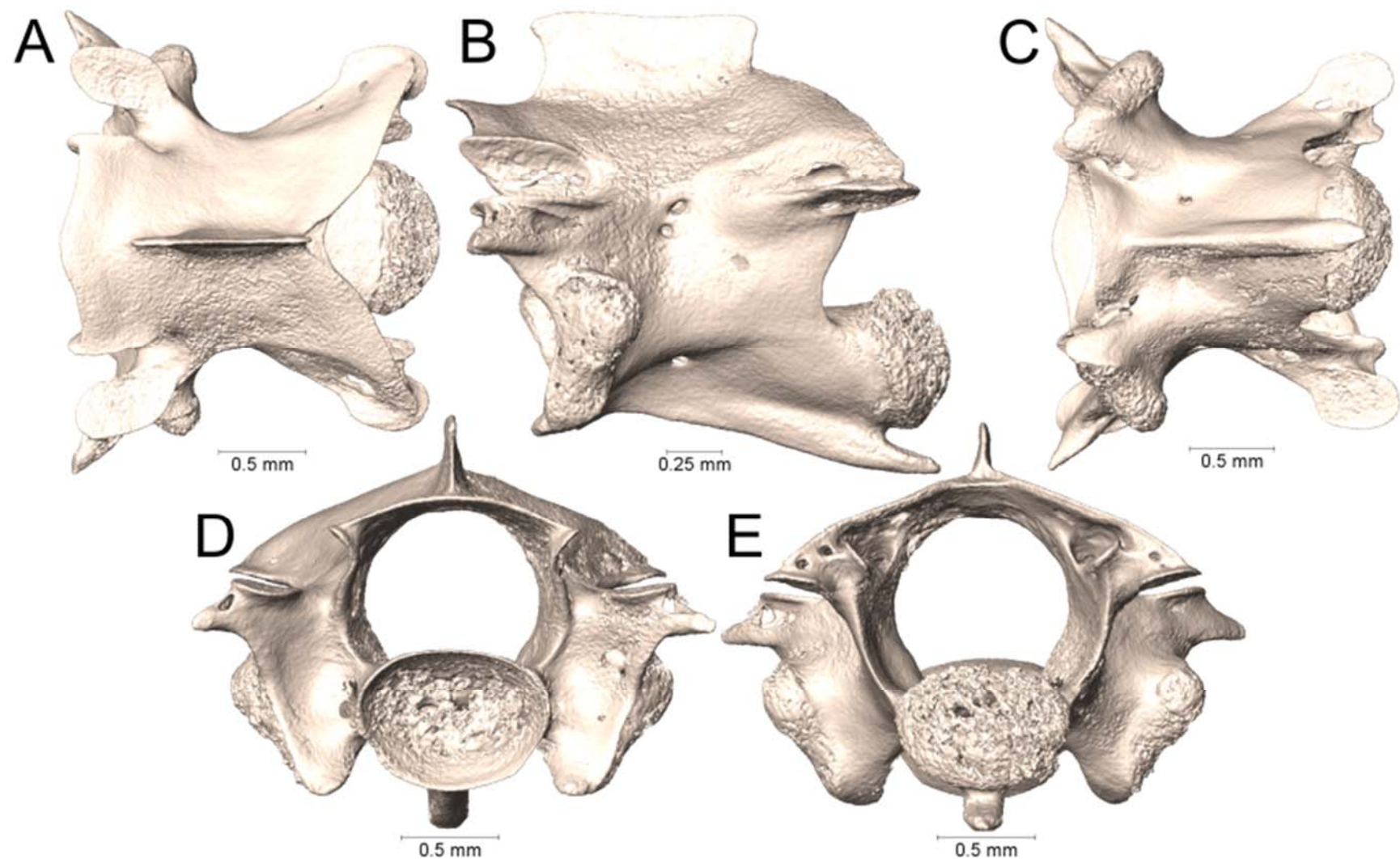
Supplemental Figure 4.81. Dorsal, lateral, ventral, anterior, and posterior views (A-E, respectively) of the midbody vertebra of *Micrurus tener* (UTA R-63282).



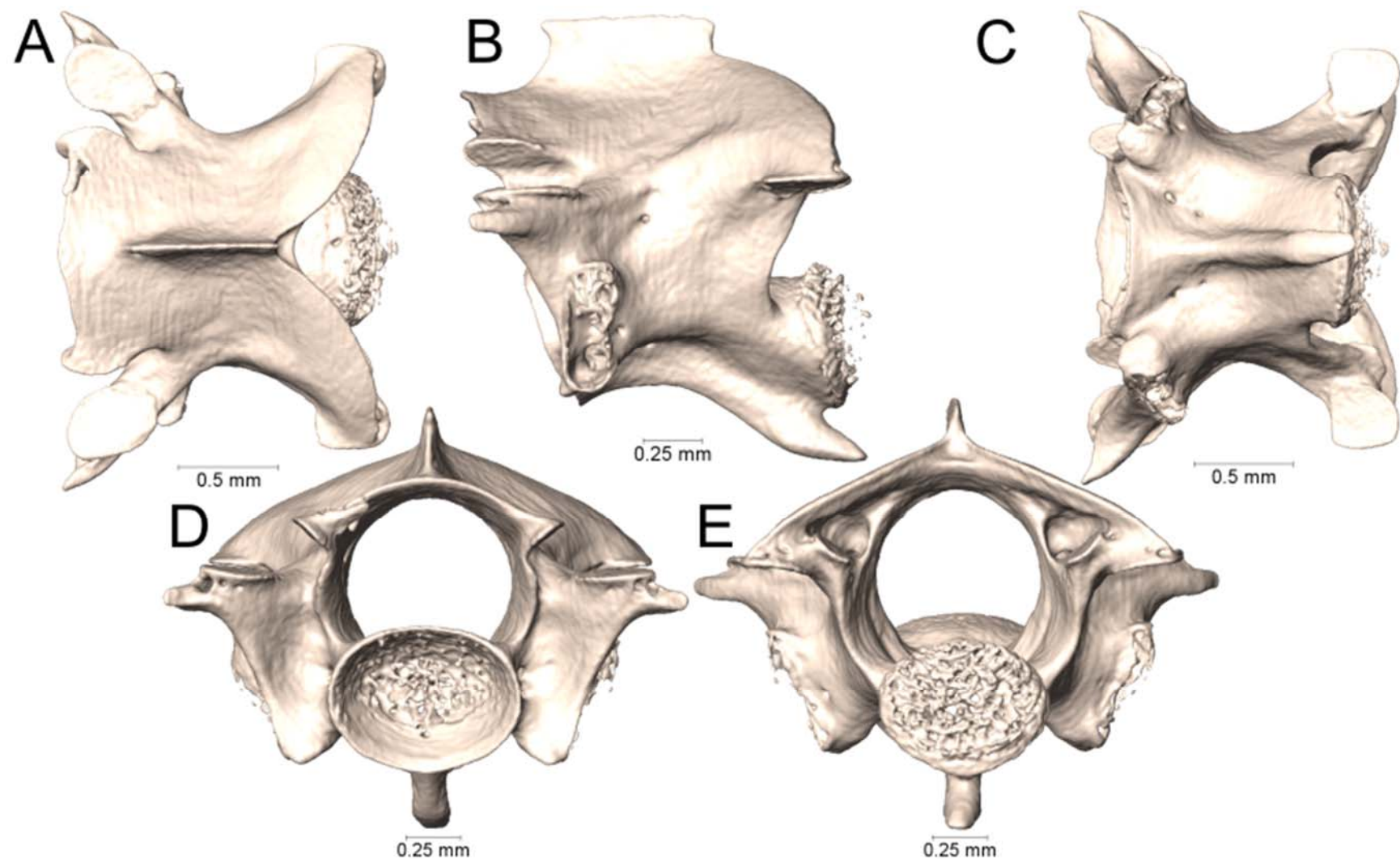
Supplemental Figure 4.82. Dorsal, lateral, ventral, anterior, and posterior views (A-E, respectively) of the midbody vertebra of *Naja annulata* (UTA R-18199).



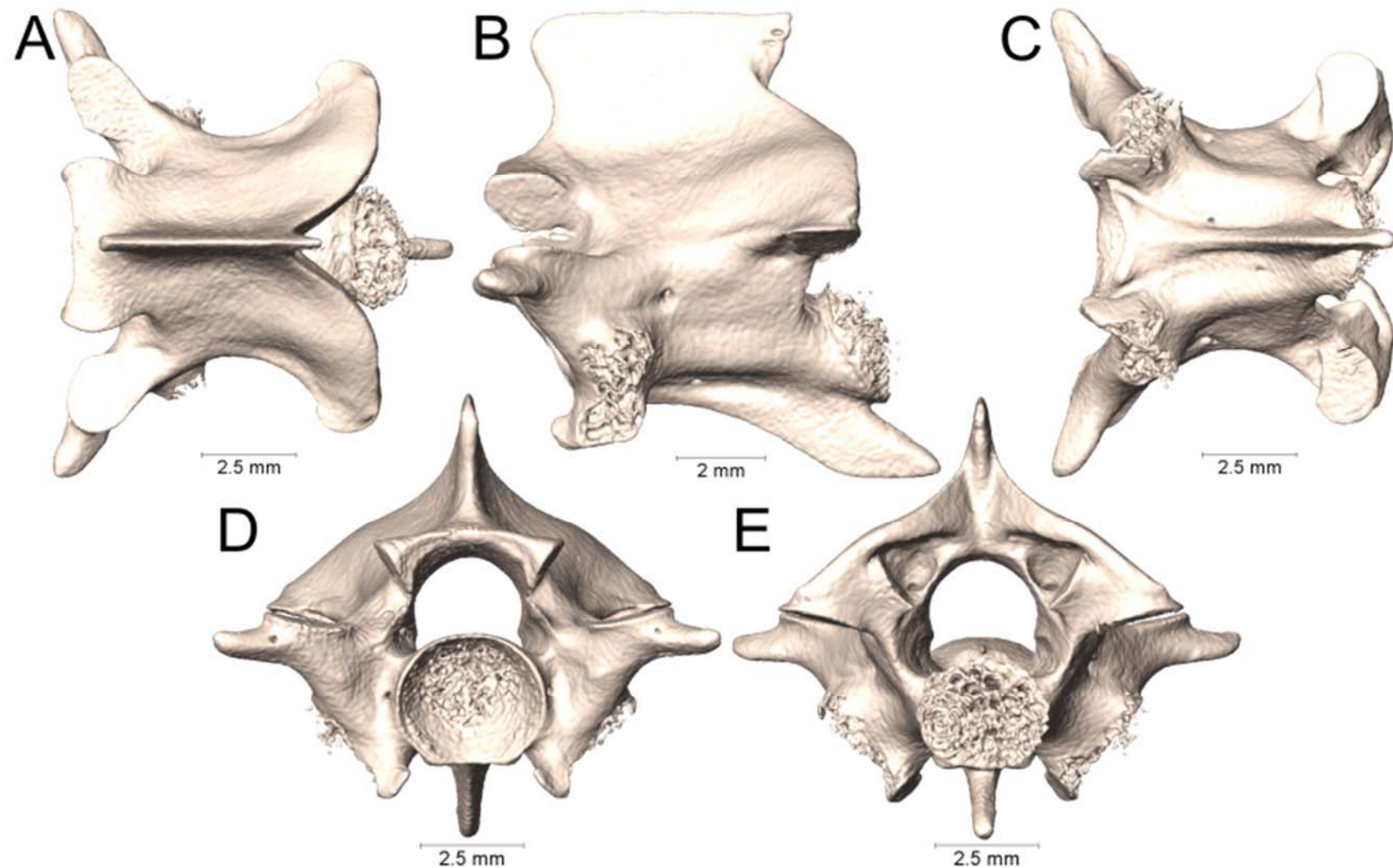
Supplemental Figure 4.83. Dorsal, lateral, ventral, anterior, and posterior views (A-E, respectively) of the midbody vertebra of *Naja christyi* (UTA R-18200).



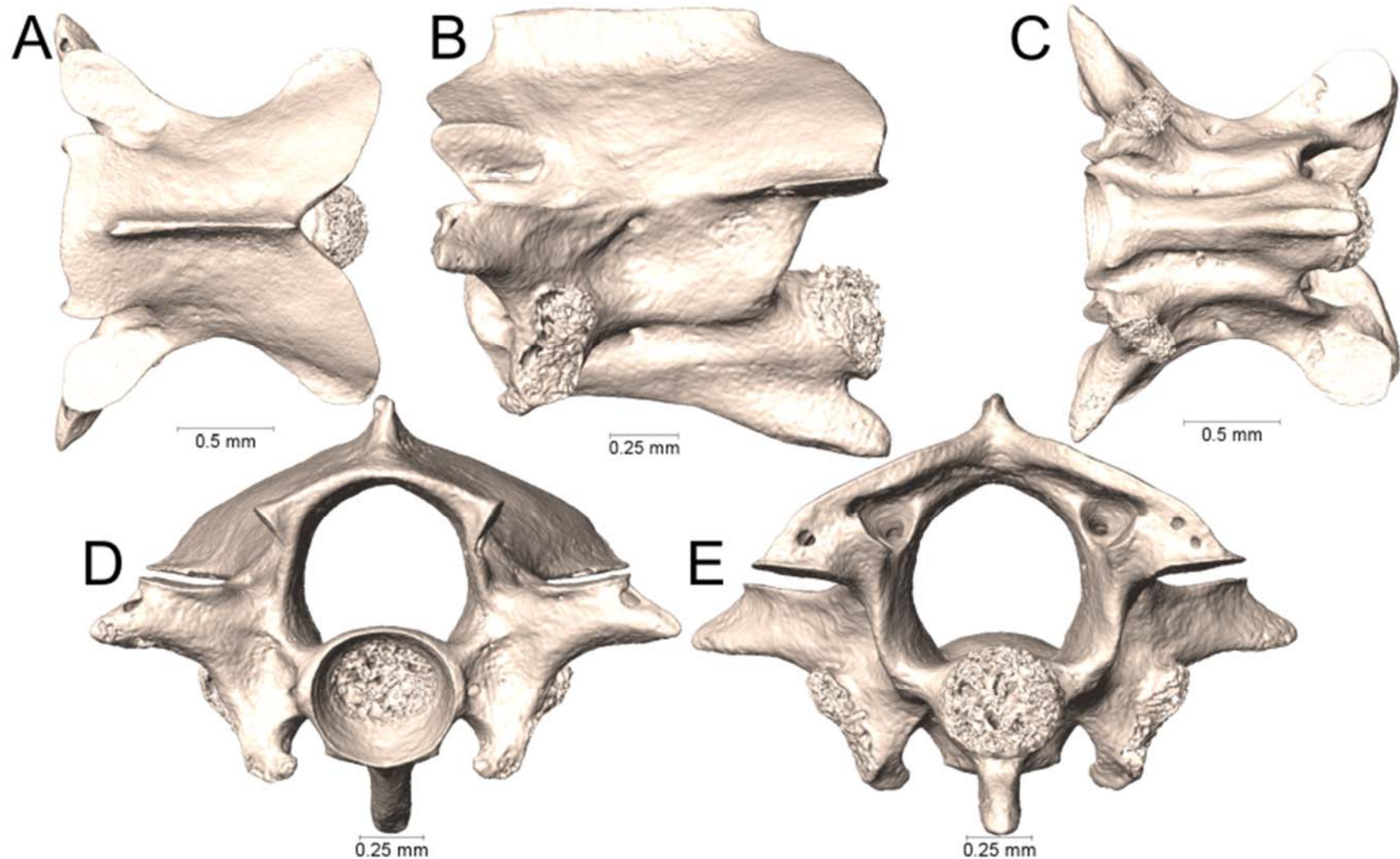
Supplemental Figure 4.84. Dorsal, lateral, ventral, anterior, and posterior views (A-E, respectively) of the midbody vertebra of *Naja siamensis* (UTA R-16872).



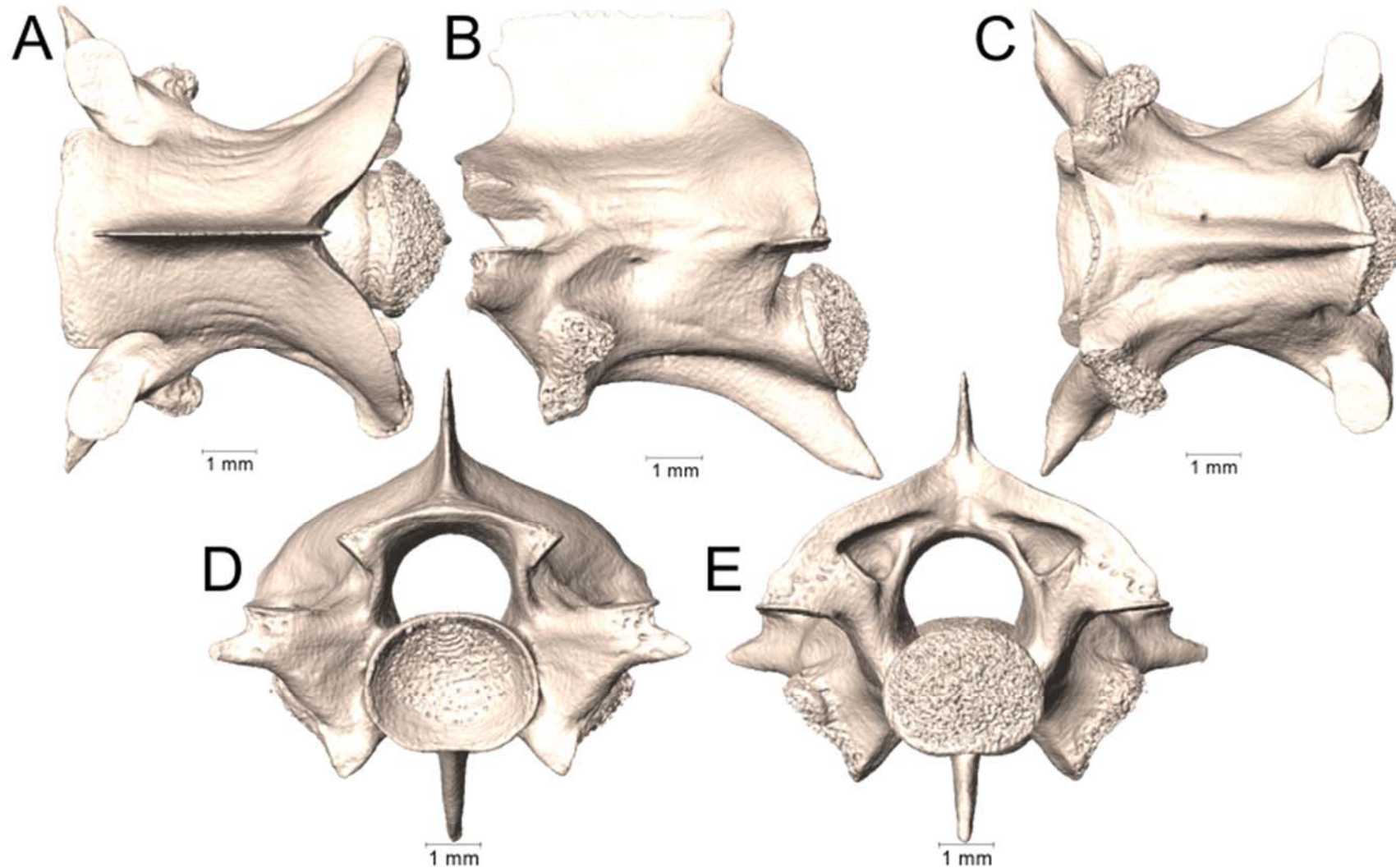
Supplemental Figure 4.85. Dorsal, lateral, ventral, anterior, and posterior views (A-E, respectively) of the midbody vertebra of *Ophiophagus hannah* (UTA R-60836).



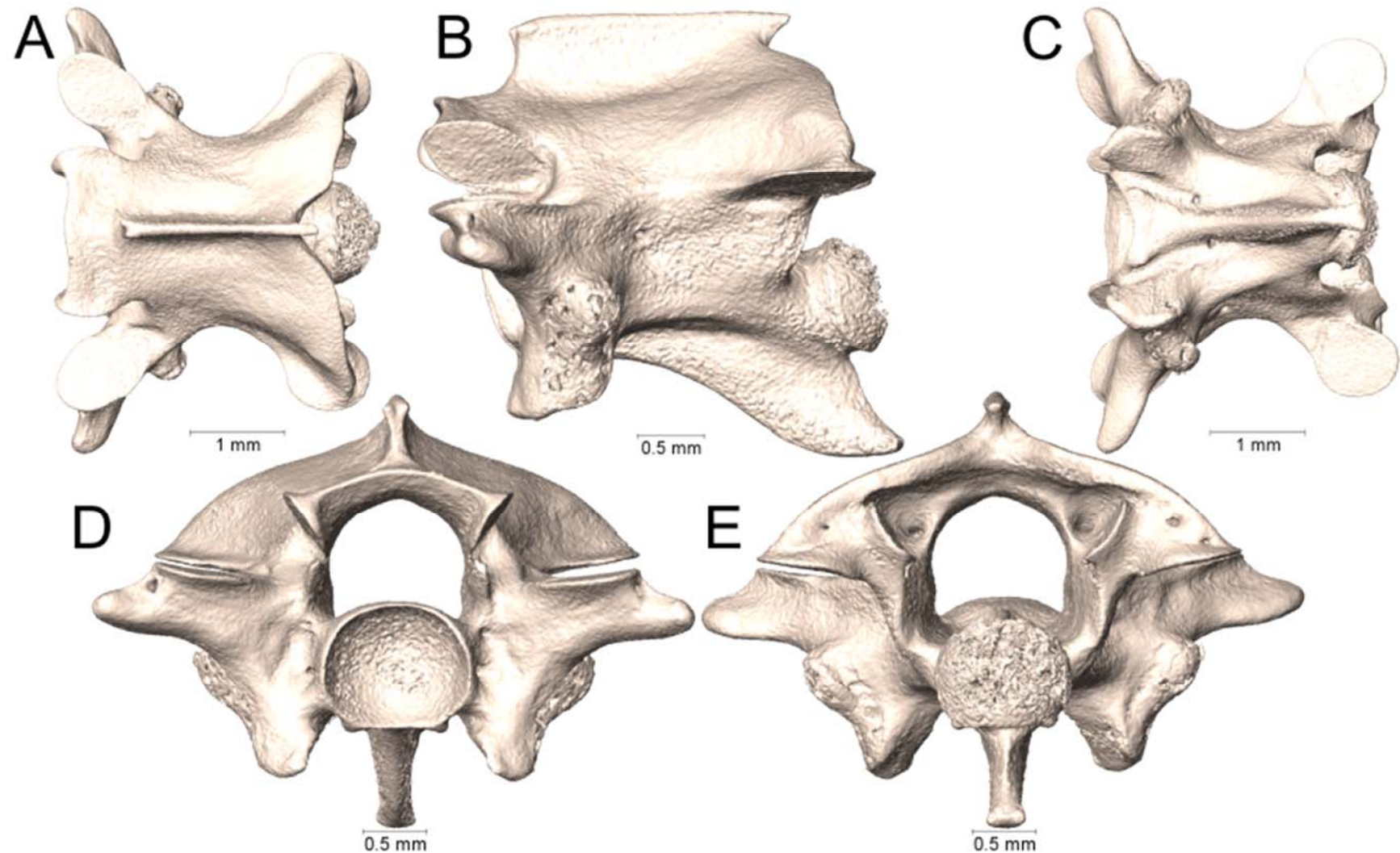
Supplemental Figure 4.86. Dorsal, lateral, ventral, anterior, and posterior views (A-E, respectively) of the midbody vertebra of *Oxyuranus scutellatus* (UTA R-60839).



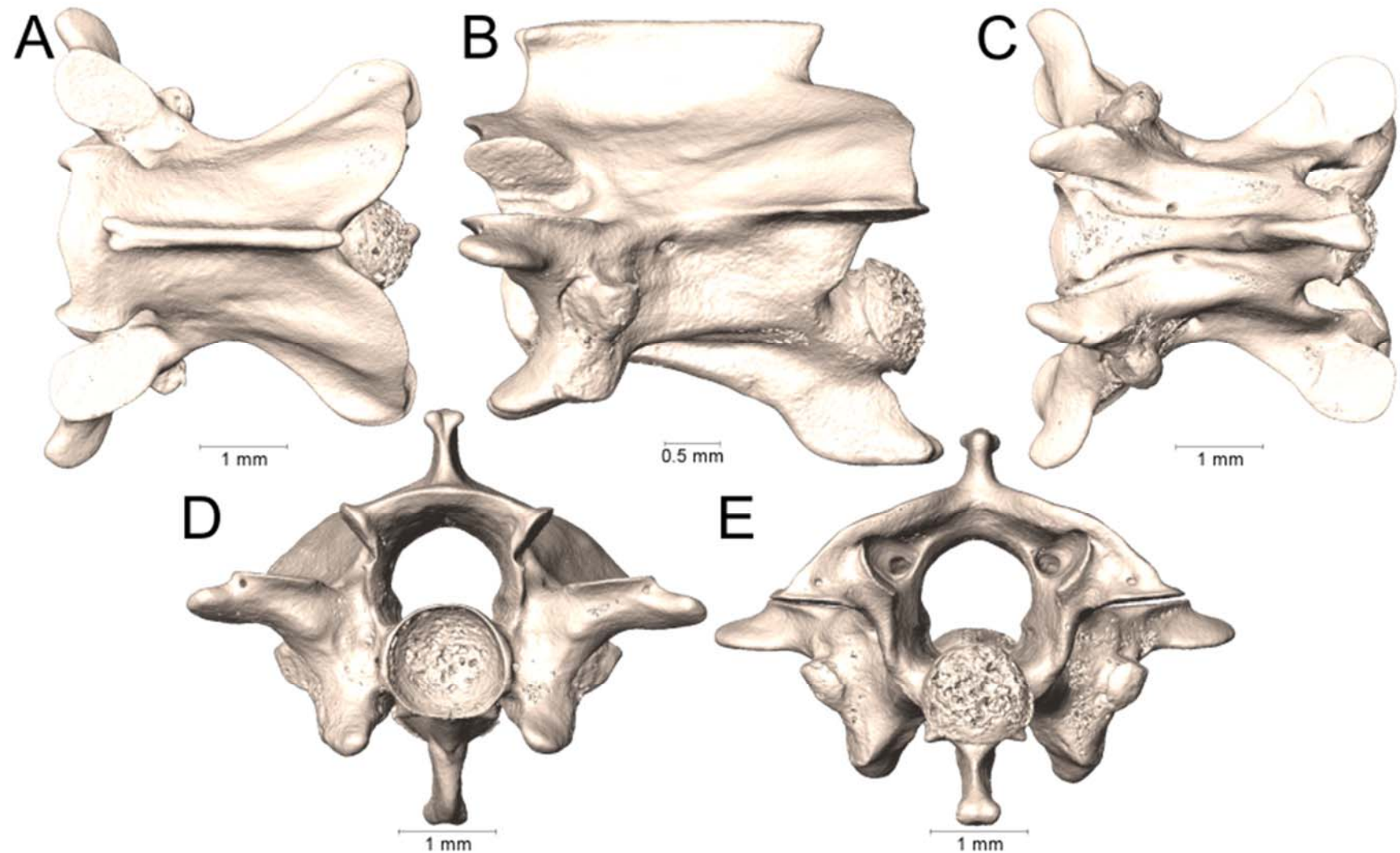
Supplemental Figure 4.87. Dorsal, lateral, ventral, anterior, and posterior views (A-E, respectively) of the midbody vertebra of *Prosymna stuhlmanni* (UTA R-64493).



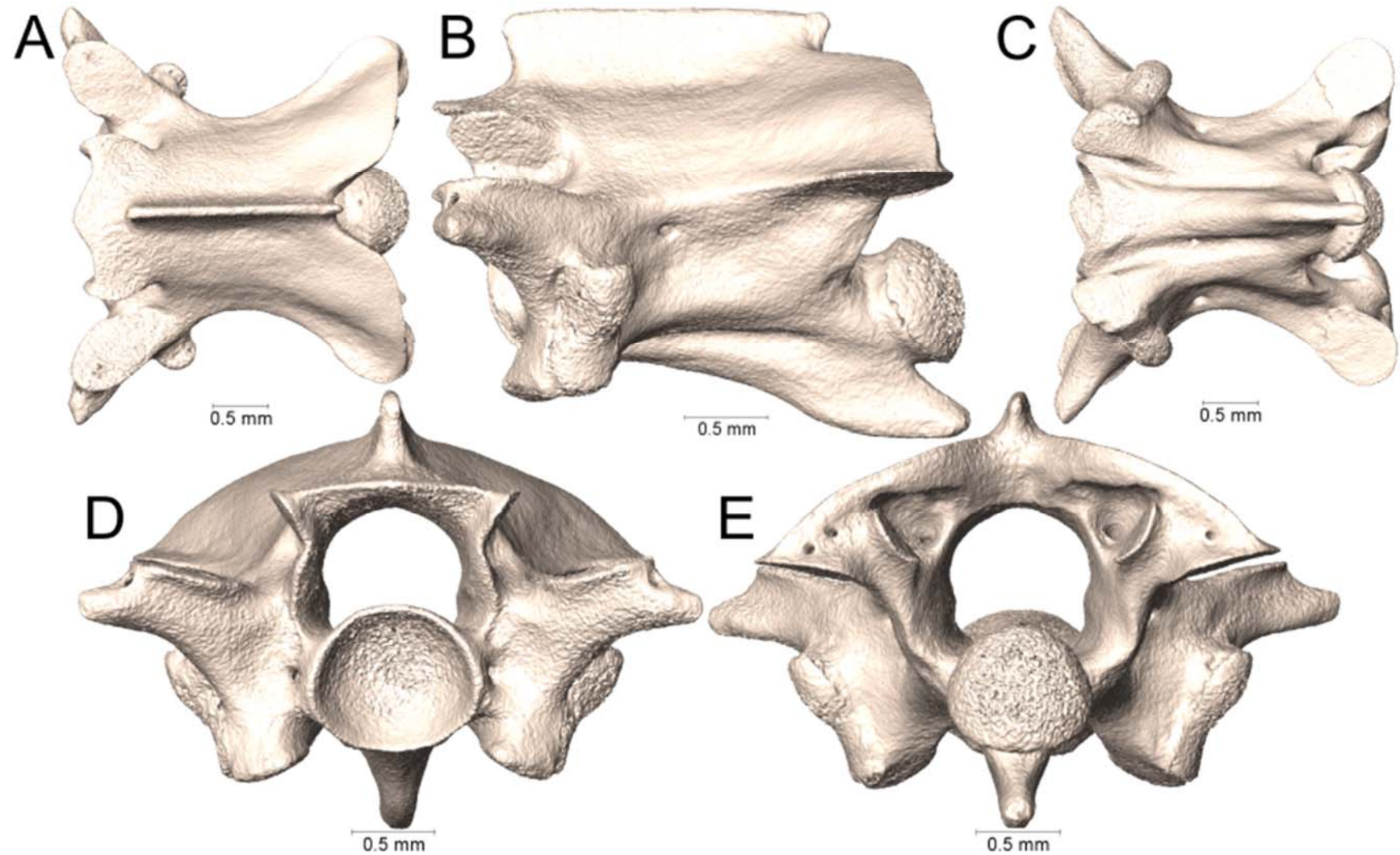
Supplemental Figure 4.88. Dorsal, lateral, ventral, anterior, and posterior views (A-E, respectively) of the midbody vertebra of *Pseudohaje goldii* (UTA R-63636).



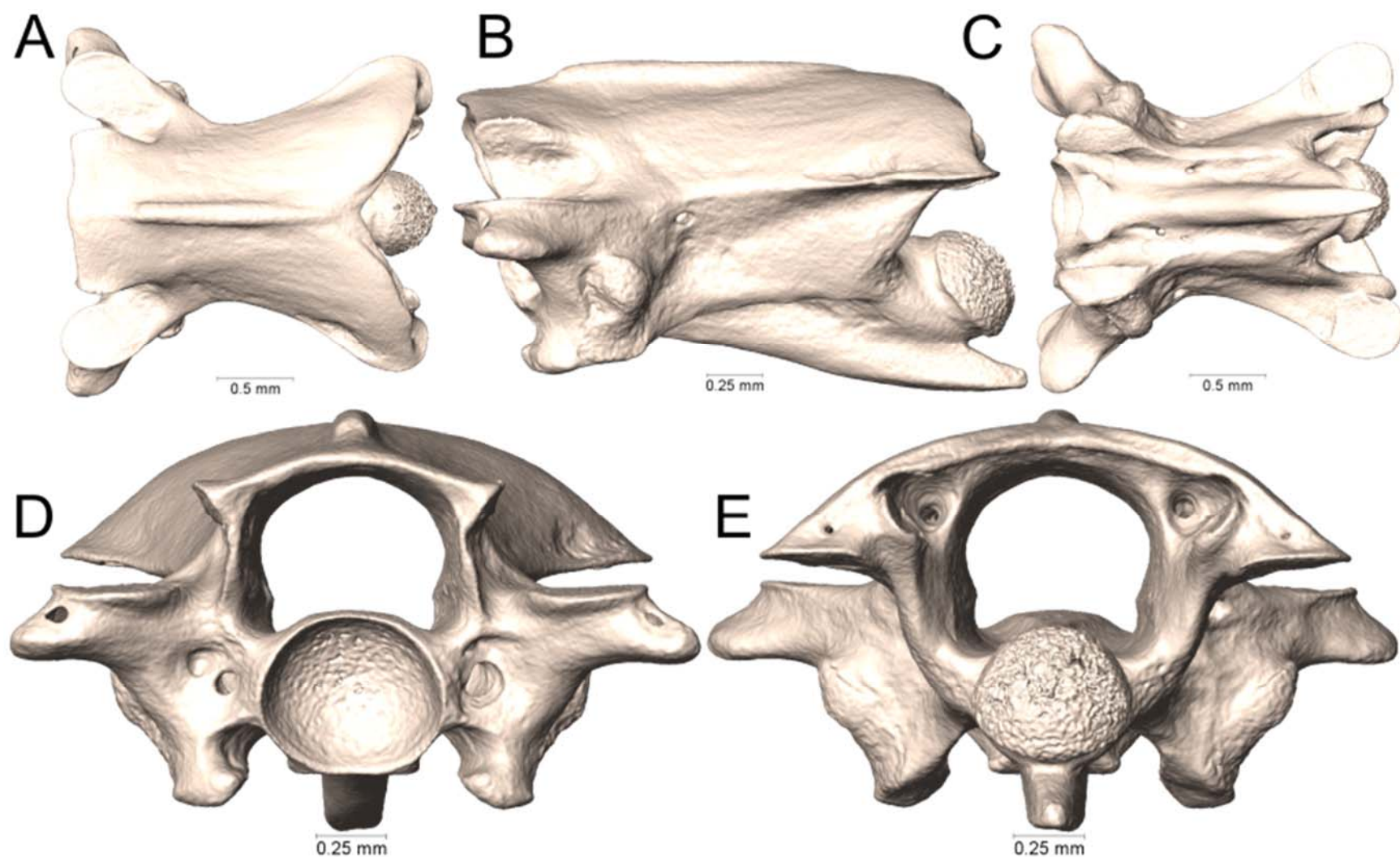
Supplemental Figure 4.89. Dorsal, lateral, ventral, anterior, and posterior views (A-E, respectively) of the midbody vertebra of *Sinomicrurus boettgeri* (UTA R-58837).



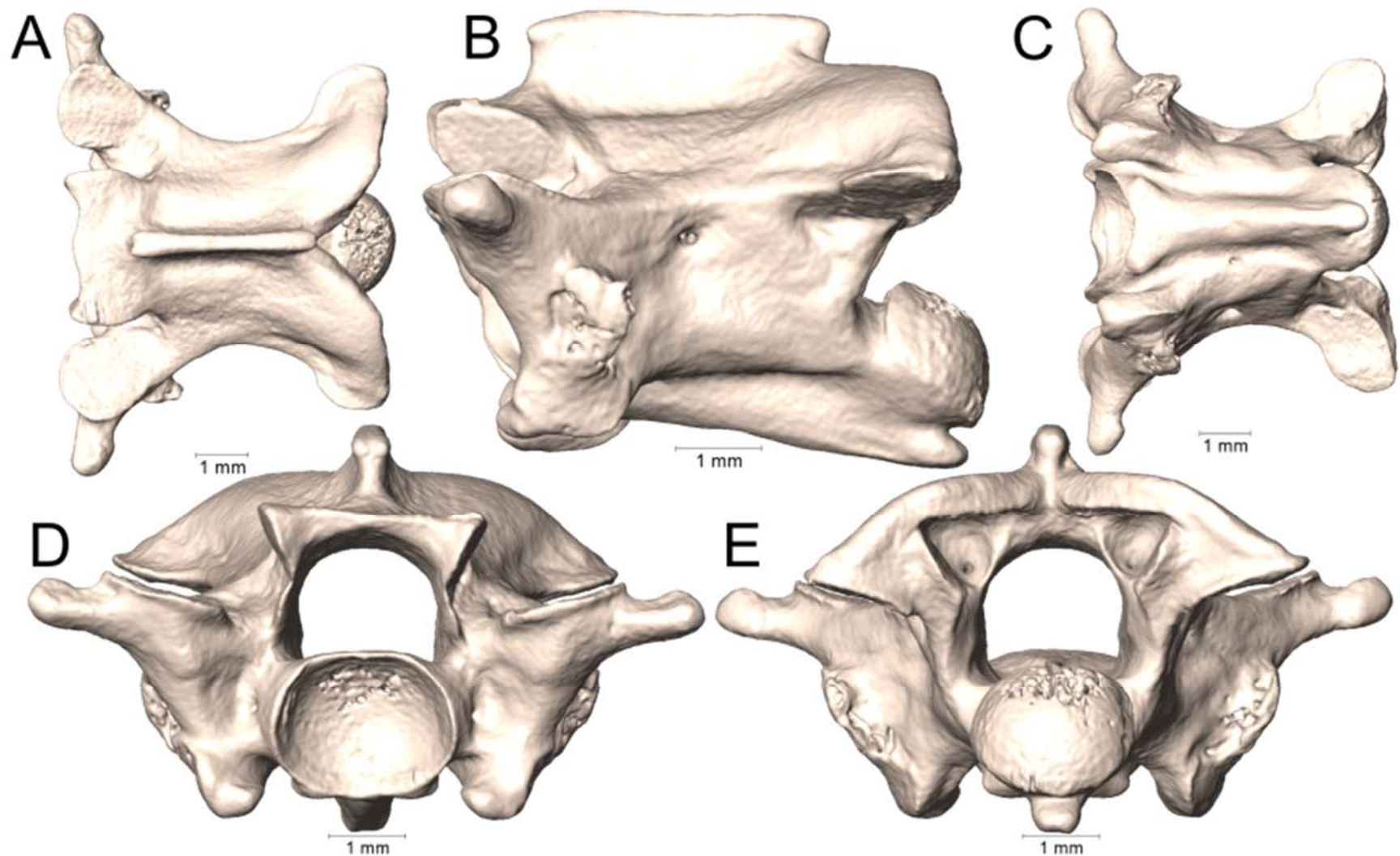
Supplemental Figure 4.90. Dorsal, lateral, ventral, anterior, and posterior views (A-E, respectively) of the midbody vertebra of *Sinomicrurus kelloggi* (ROM 37079).



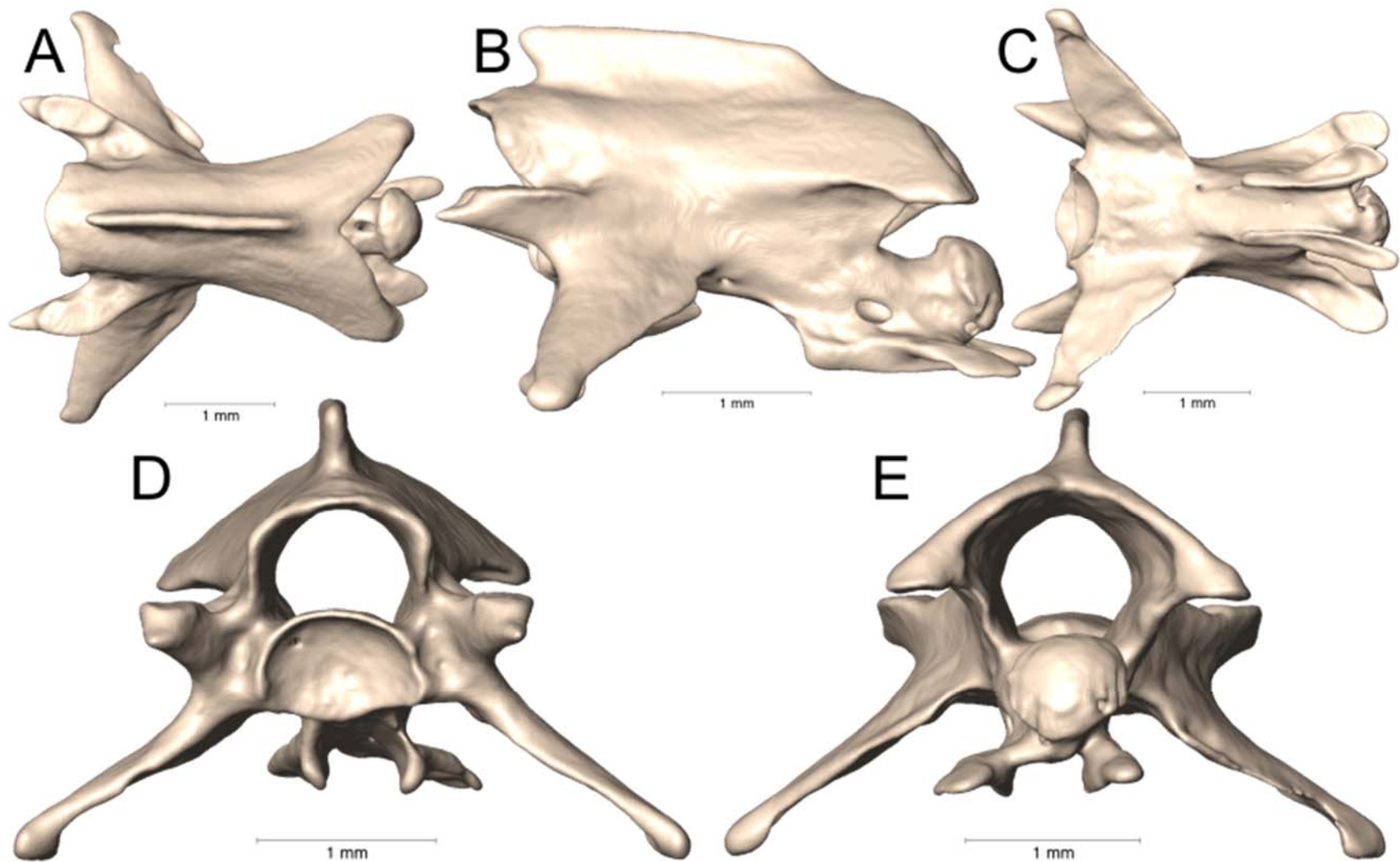
Supplemental Figure 4.91. Dorsal, lateral, ventral, anterior, and posterior views (A-E, respectively) of the midbody vertebra of *Sinomicrurus peinani* (ROM 37109).



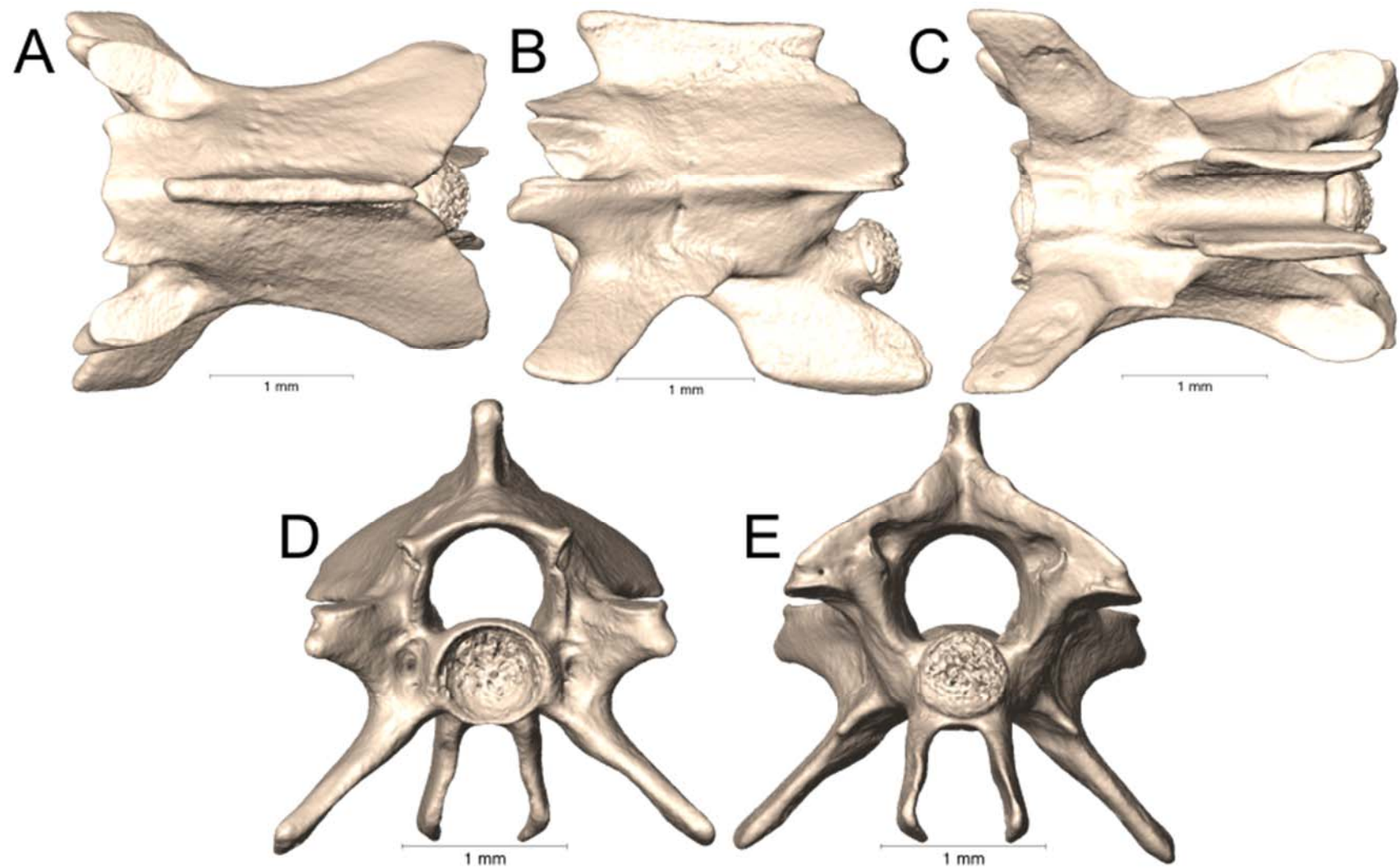
Supplemental Figure 4.92. Dorsal, lateral, ventral, anterior, and posterior views (A-E, respectively) of the midbody vertebra of *Sinomicrurus swinhoei* (MVZ 23876).



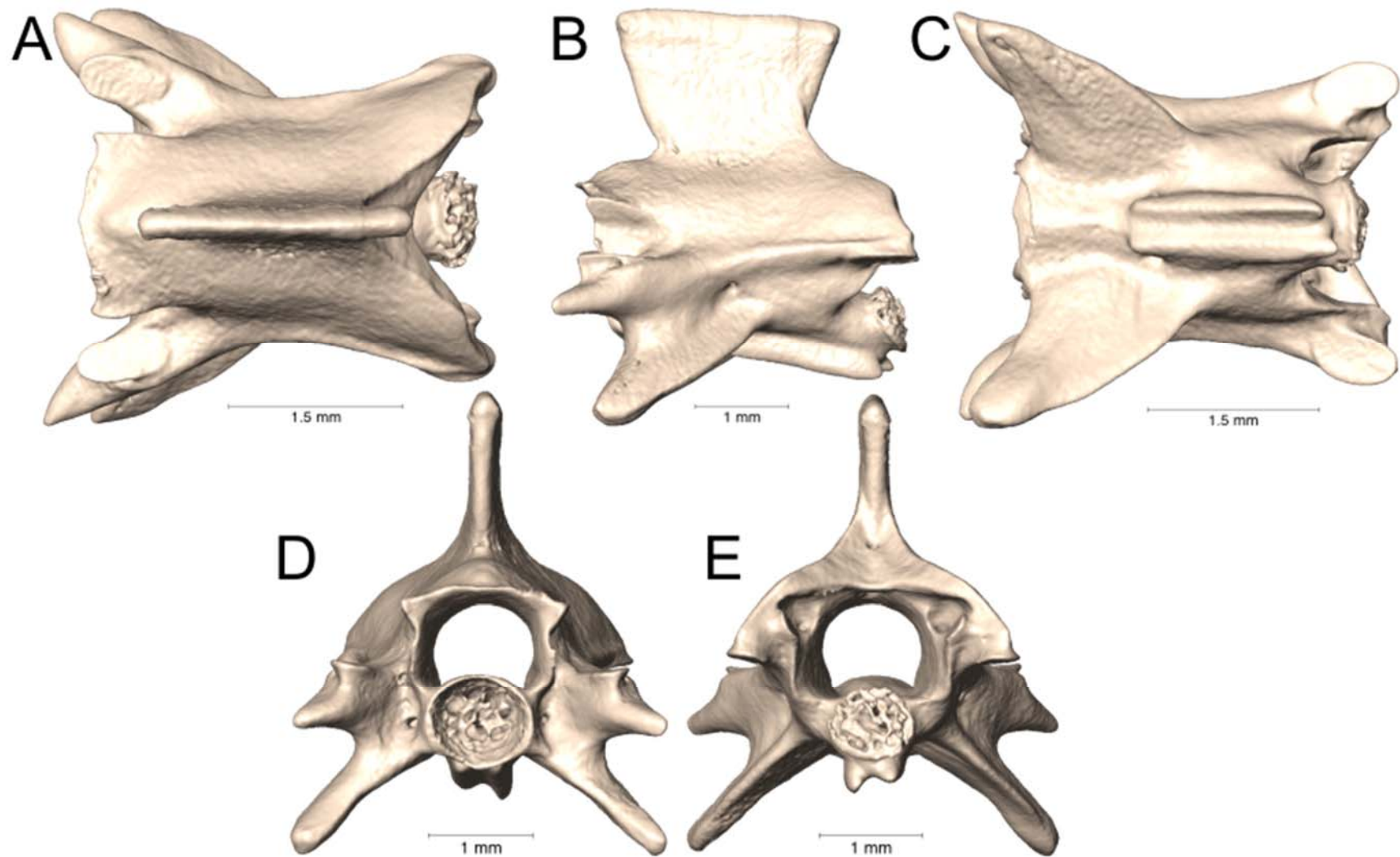
Supplemental Figure 4.93. Dorsal, lateral, ventral, anterior, and posterior views (A-E, respectively) of the midbody vertebra of *Walterinnesia aegyptia* (UTA R-13021).



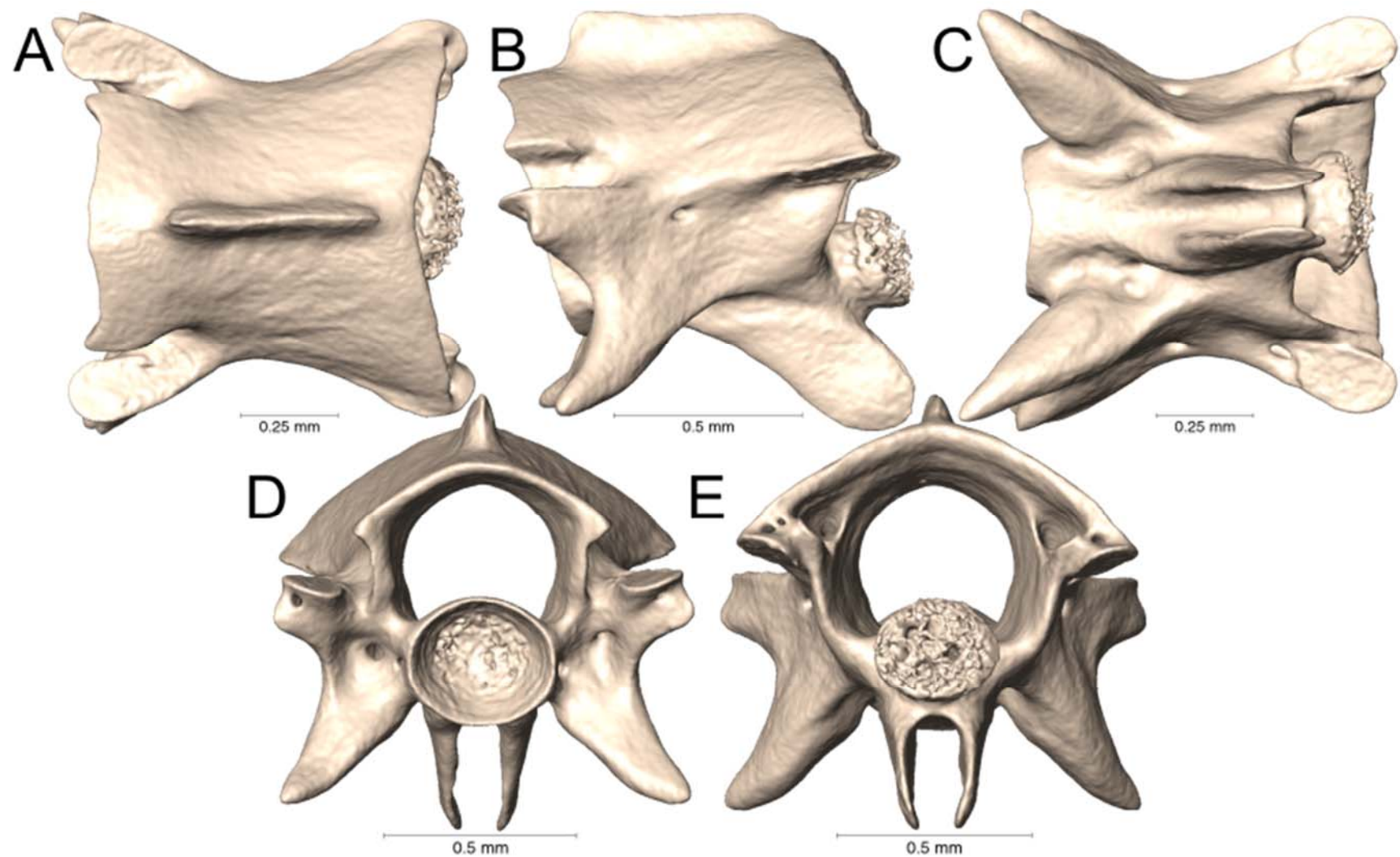
Supplemental Figure 5.1. Dorsal, lateral, ventral, anterior, and posterior views (A-E, respectively) of the caudal vertebra of *Acanthophis antarcticus* (UTA R-7623).



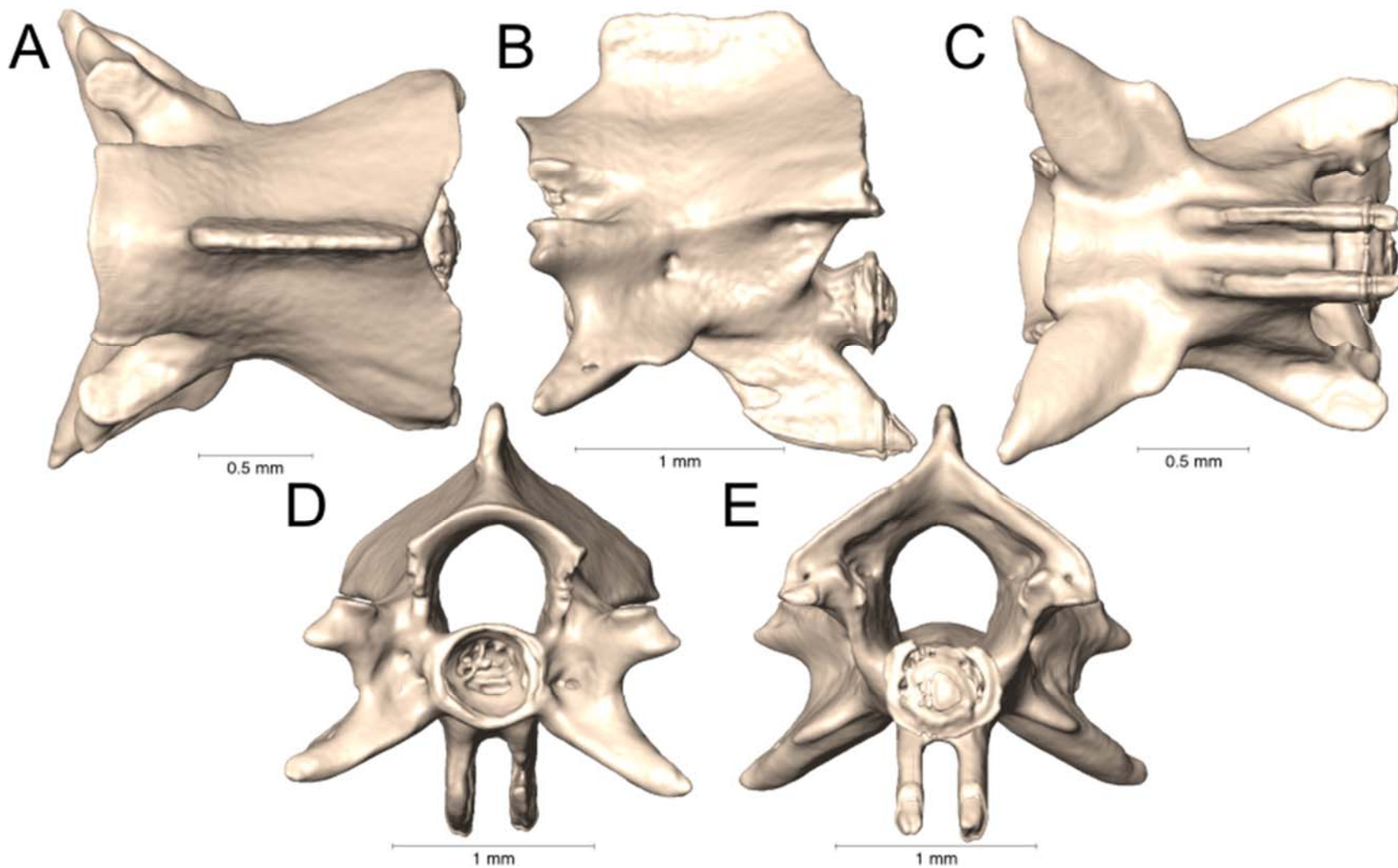
Supplemental Figure 5.2. Dorsal, lateral, ventral, anterior, and posterior views (A-E, respectively) of the caudal vertebra of *Bungarus candidus* (UTA R-65799).



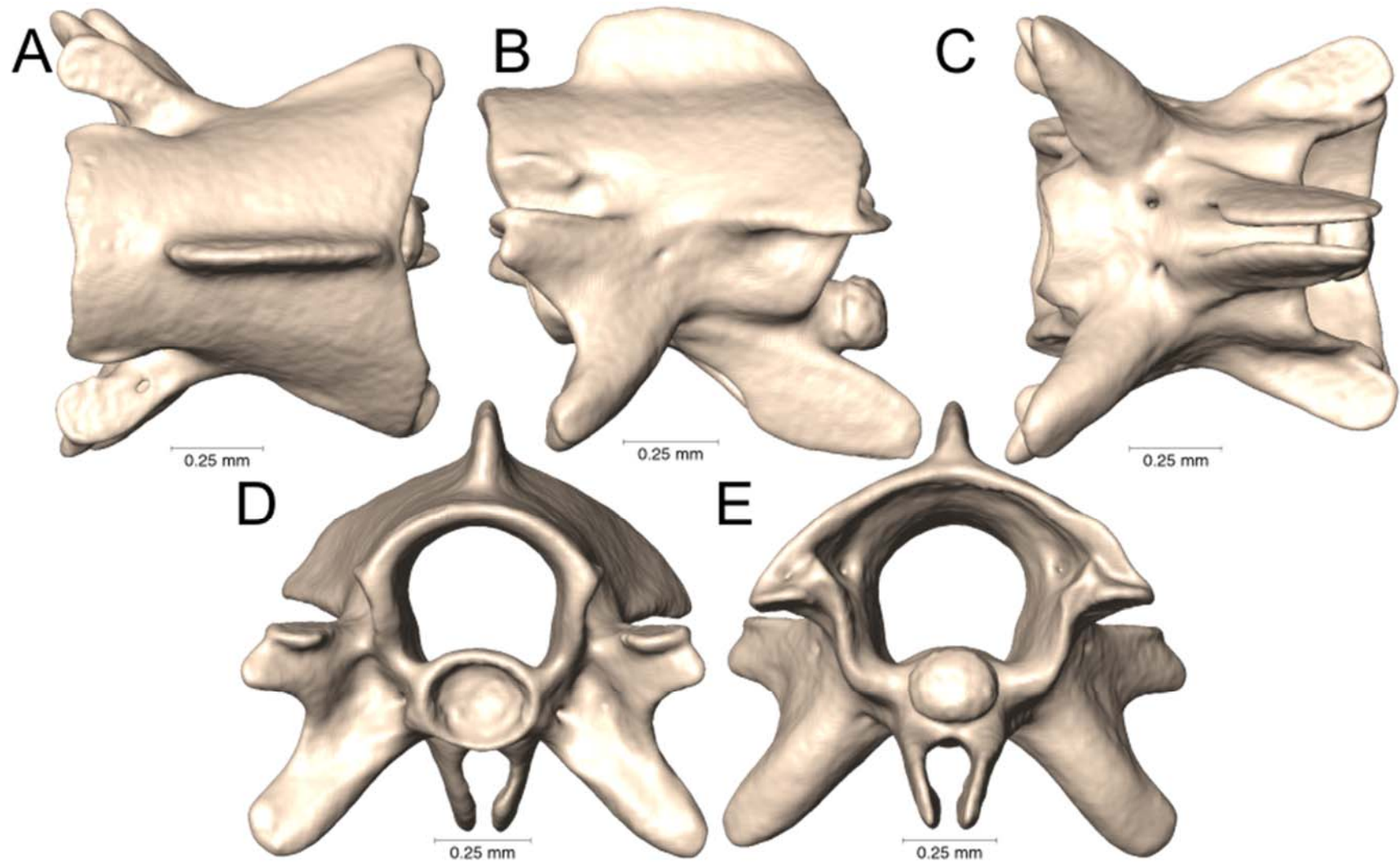
Supplemental Figure 5.3. Dorsal, lateral, ventral, anterior, and posterior views (A-E, respectively) of the caudal vertebra of *Bungarus flaviceps* (UTA R-62257).



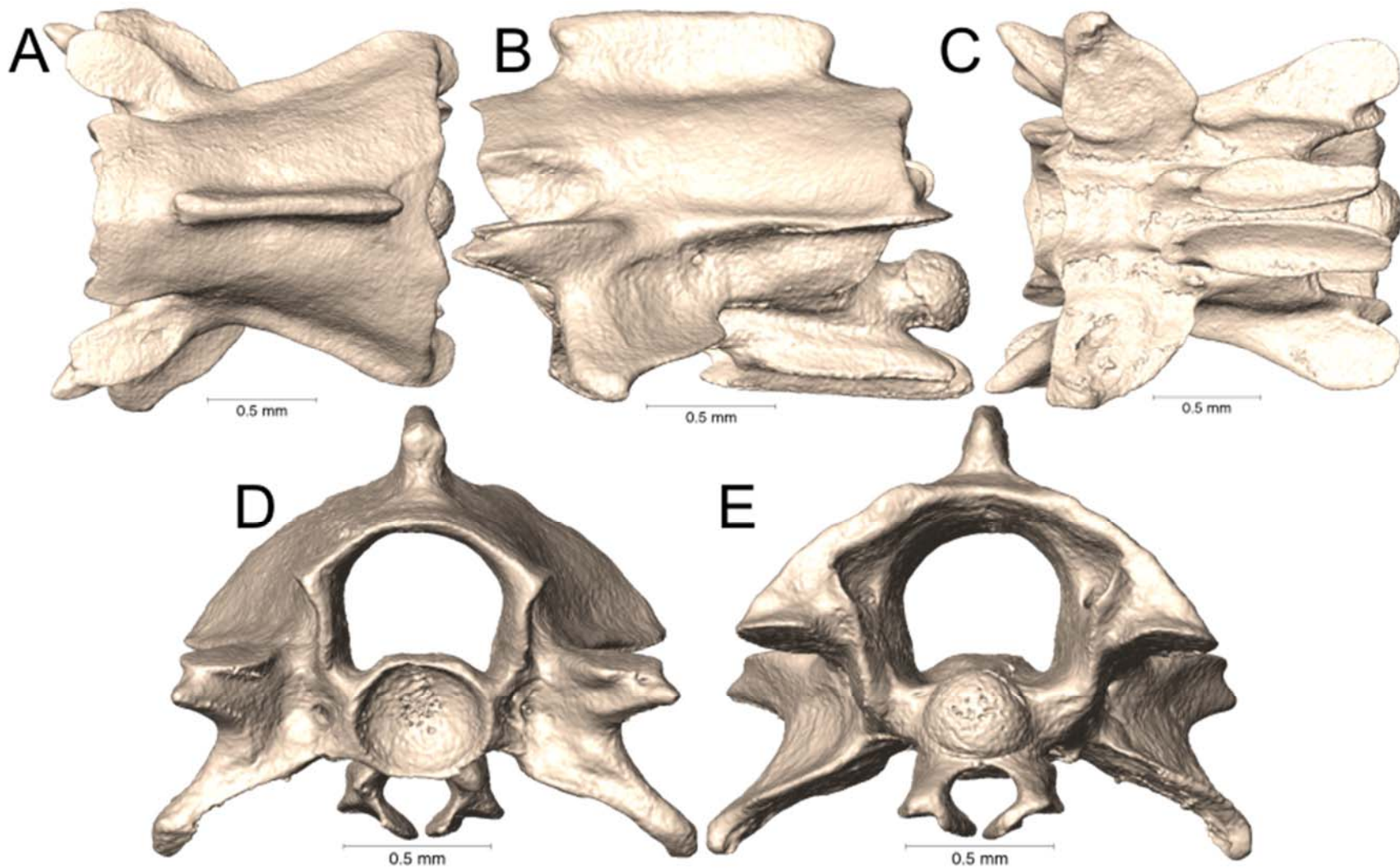
Supplemental Figure 5.4. Dorsal, lateral, ventral, anterior, and posterior views (A-E, respectively) of the caudal vertebra of *Calliophis beddomei* (MNHN 46-81).



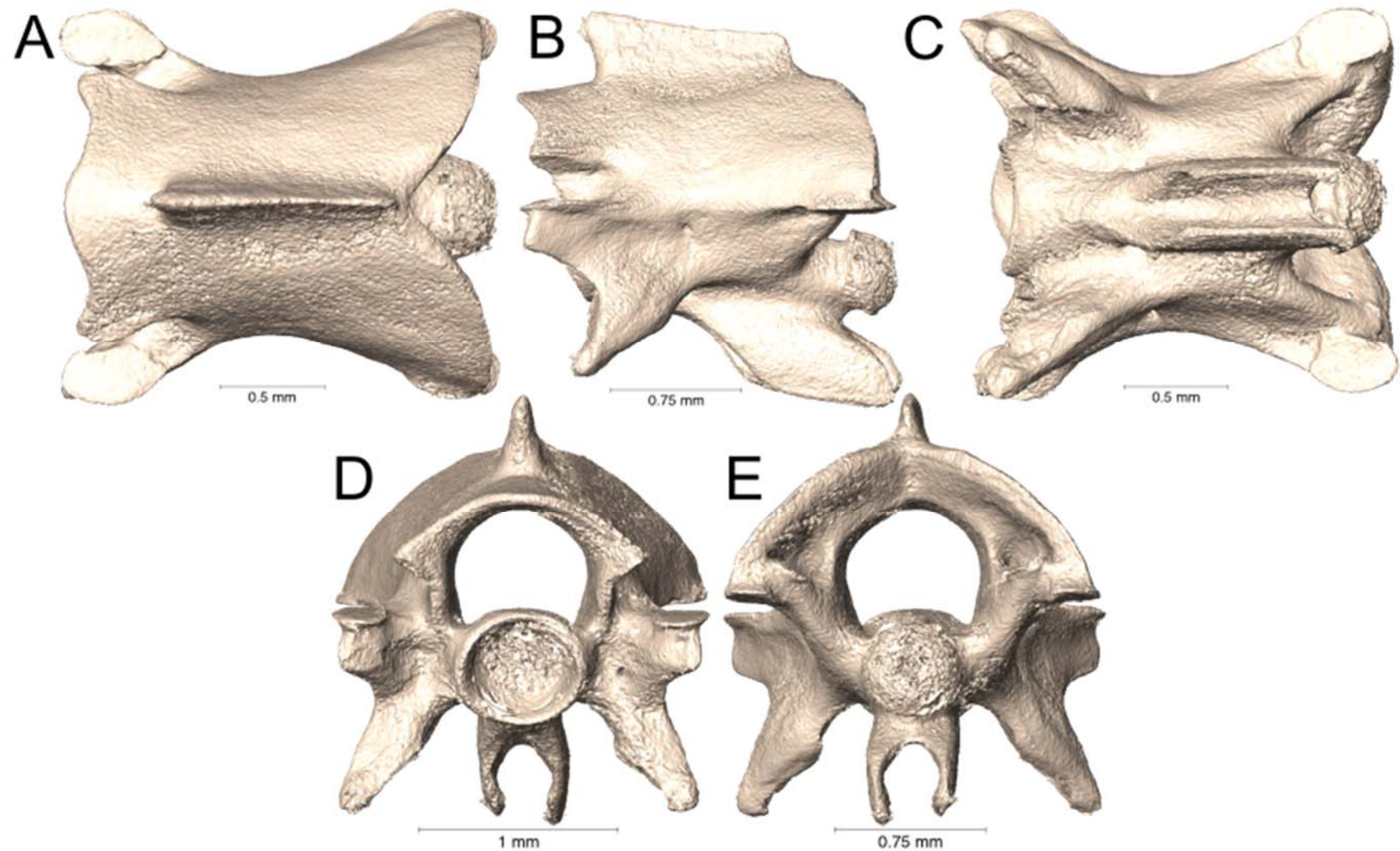
Supplemental Figure 5.5. Dorsal, lateral, ventral, anterior, and posterior views (A-E, respectively) of the caudal vertebra of *Calliophis bibroni* (CAS 17268).



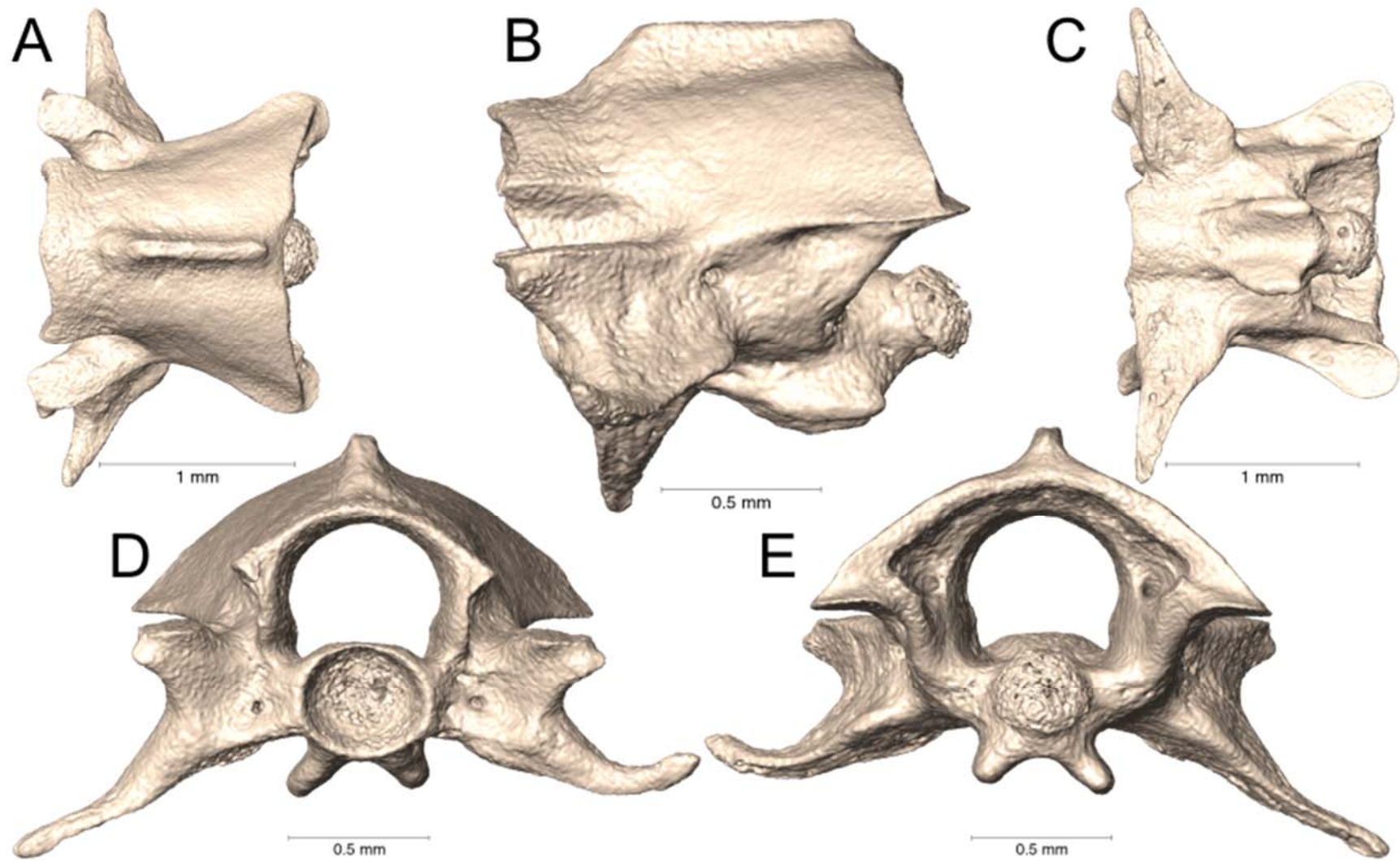
Supplemental Figure 5.6. Dorsal, lateral, ventral, anterior, and posterior views (A-E, respectively) of the caudal vertebra of *Calliophis biliniatus* (KU 309511).



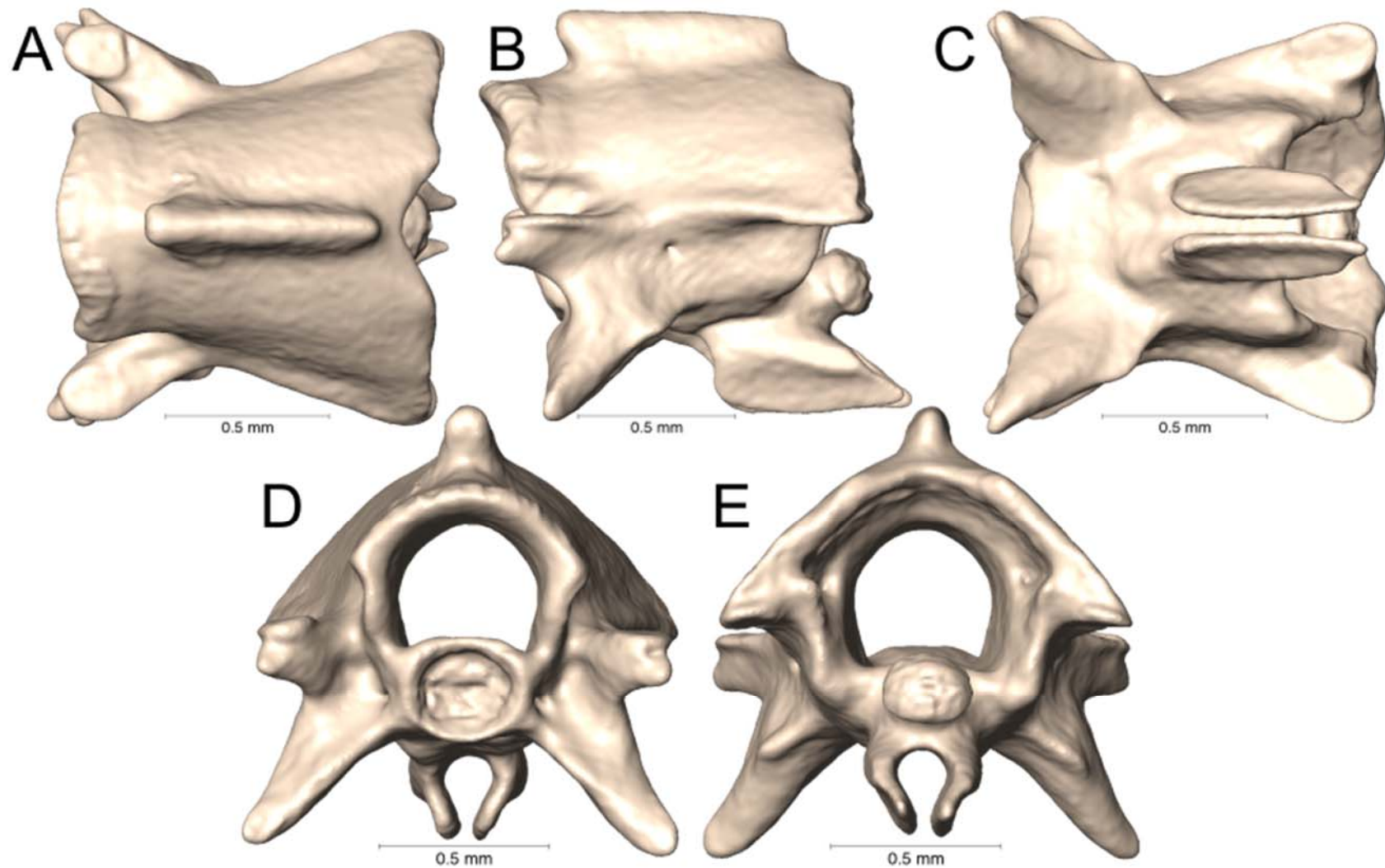
Supplemental Figure 5.7. Dorsal, lateral, ventral, anterior, and posterior views (A-E, respectively) of the caudal vertebra of *Calliophis biliniatus* (KU 311415).



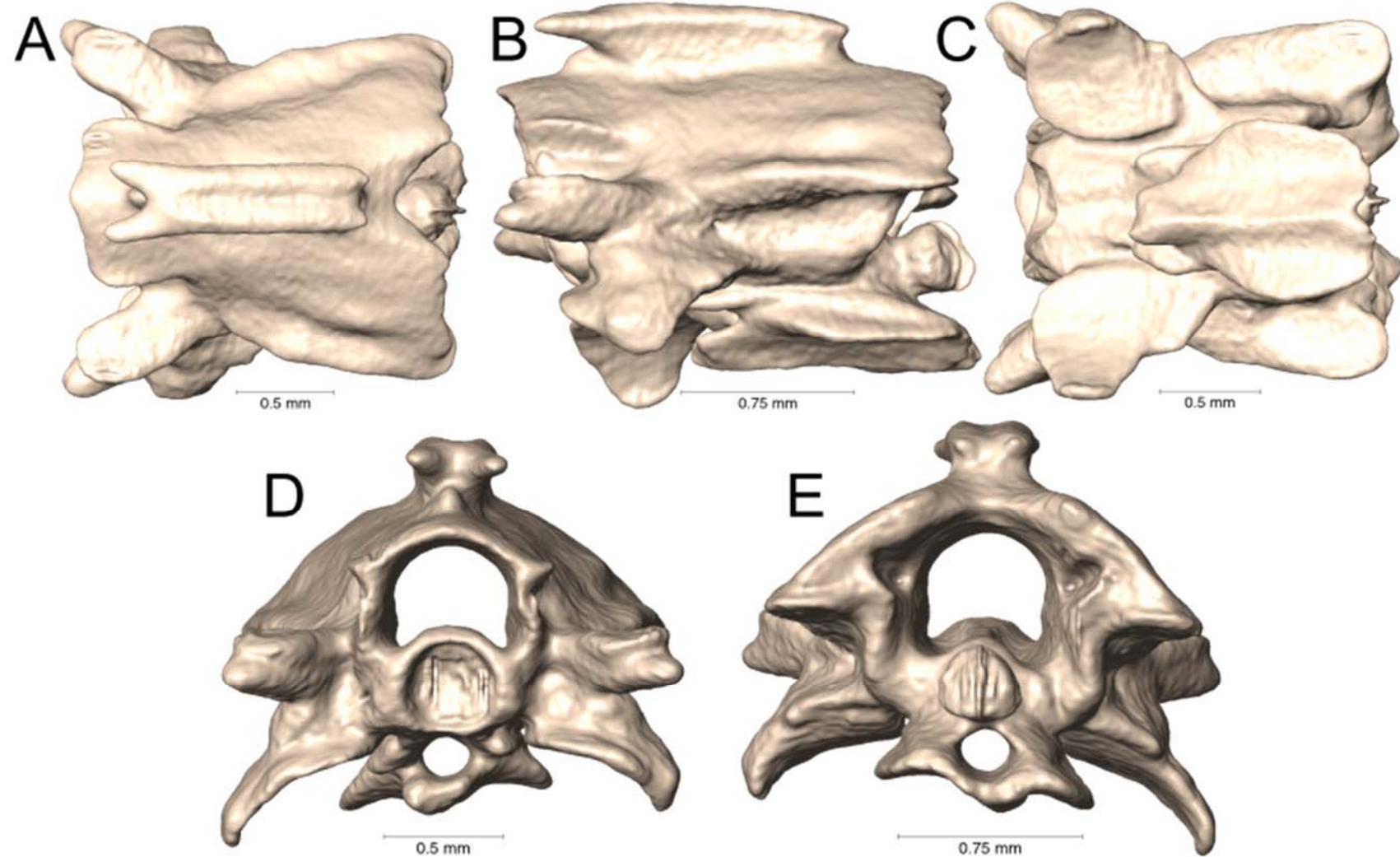
Supplemental Figure 5.8. Dorsal, lateral, ventral, anterior, and posterior views (A-E, respectively) of the caudal vertebra of *Calliophis bivirgatus bivirgatus* (UTA R-63079).



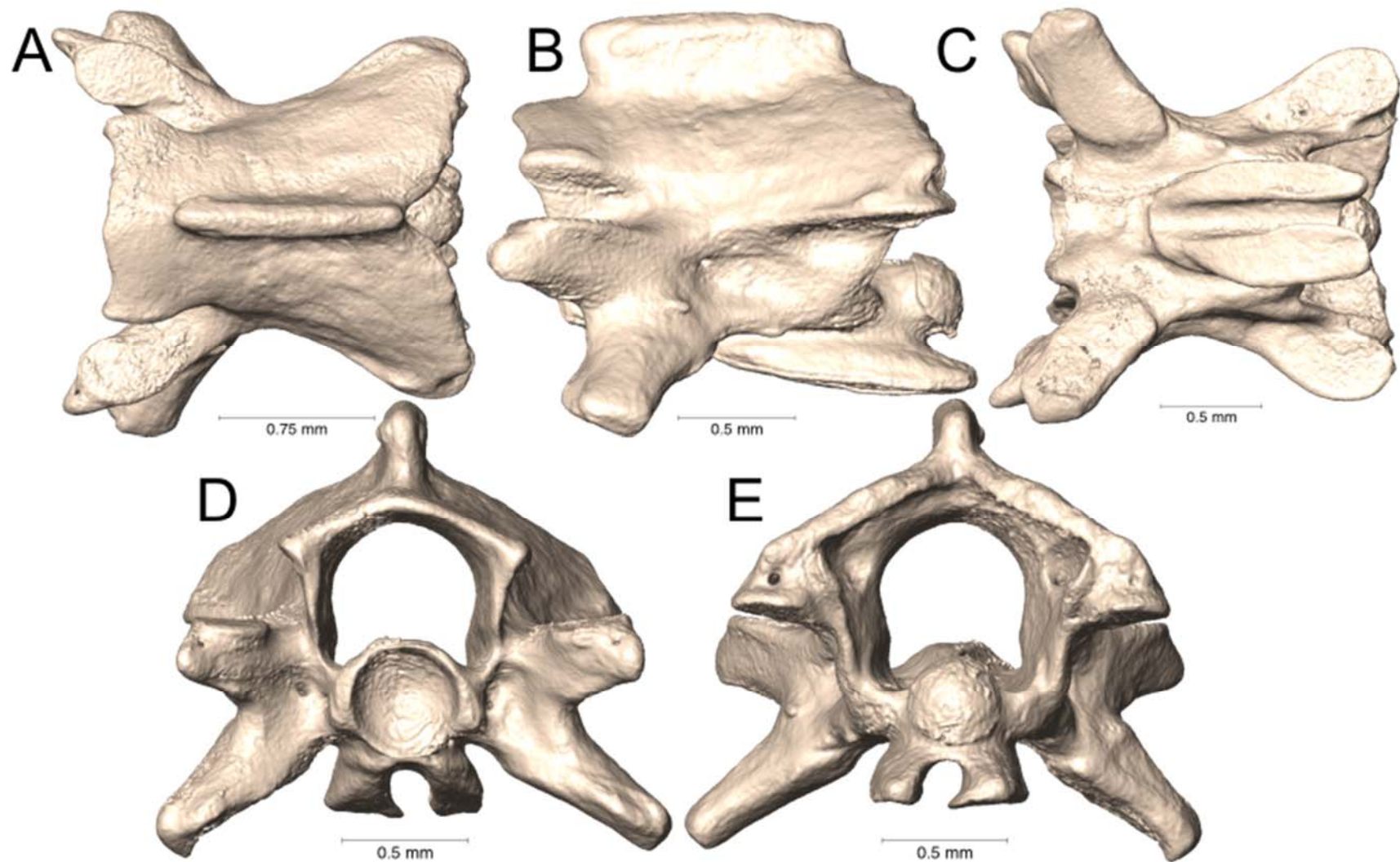
Supplemental Figure 5.9. Dorsal, lateral, ventral, anterior, and posterior views (A-E, respectively) of the caudal vertebra of *Calliophis intestinalis* (UTA R-60738).



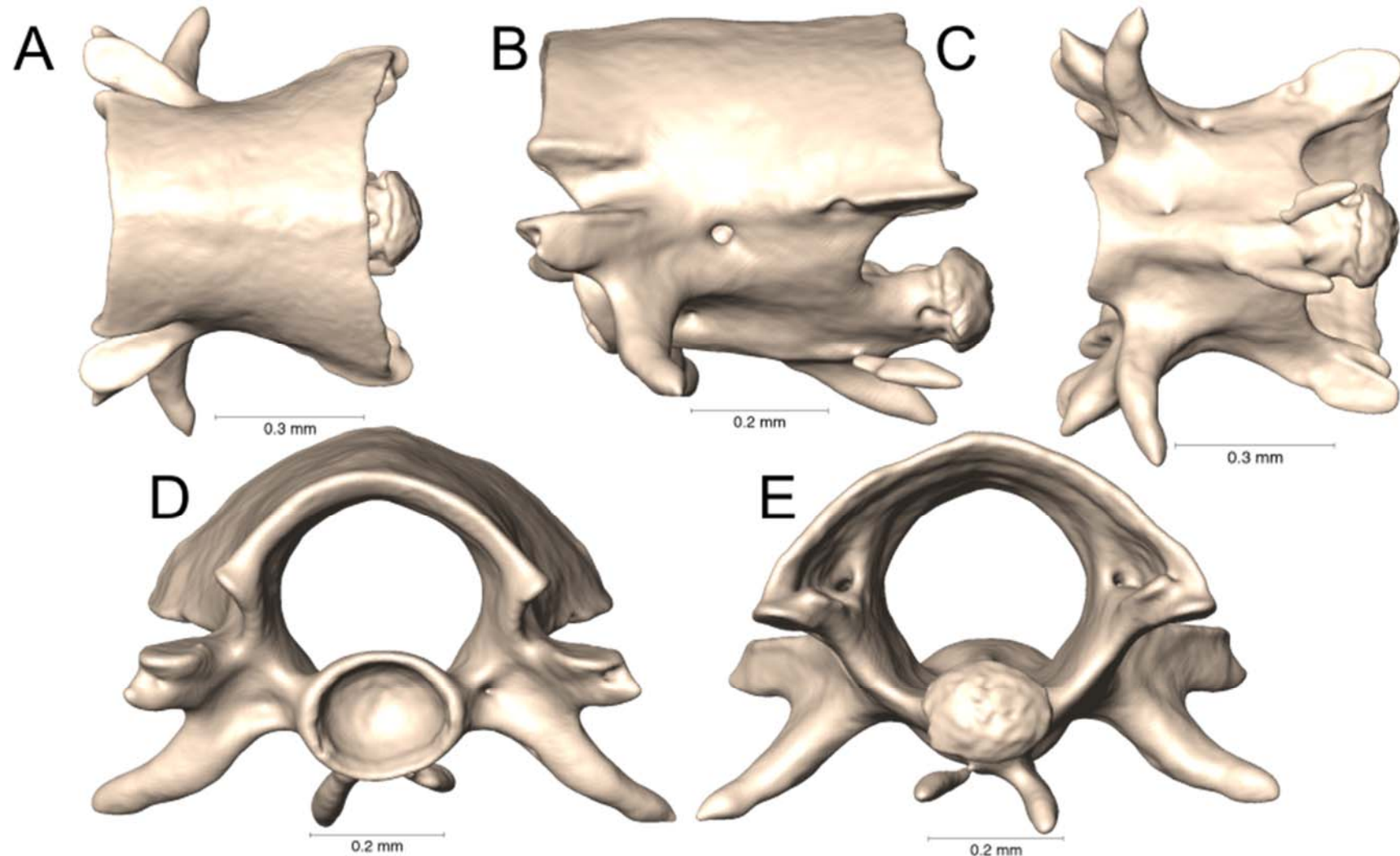
Supplemental Figure 5.10. Dorsal, lateral, ventral, anterior, and posterior views (A-E, respectively) of the caudal vertebra of *Calliophis intestinalis immaculata* (UTA R-65802).



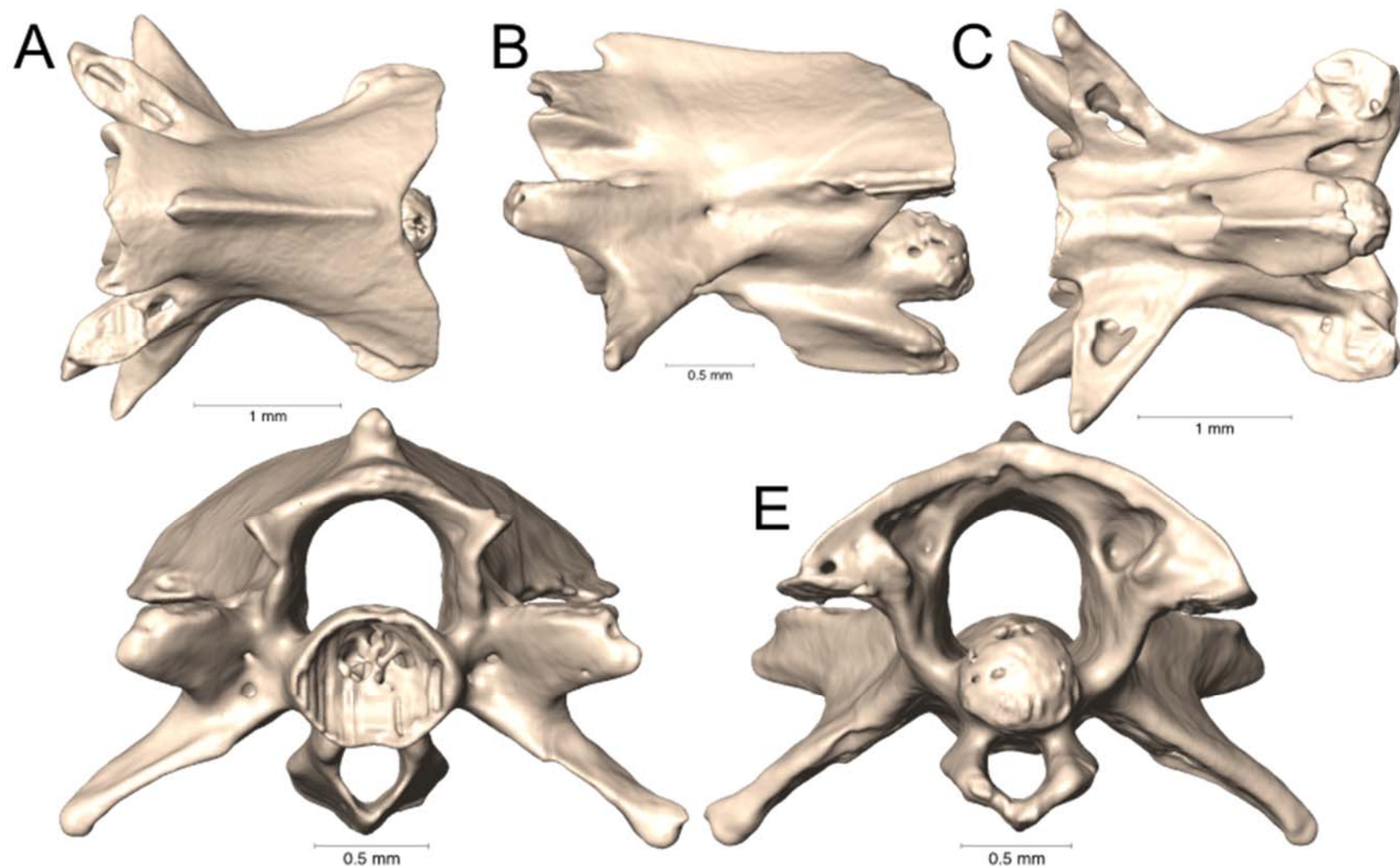
Supplemental Figure 5.11. Dorsal, lateral, ventral, anterior, and posterior views (A-E, respectively) of the caudal vertebra of *Calliophis intestinalis lineata* (UTA R-65801).



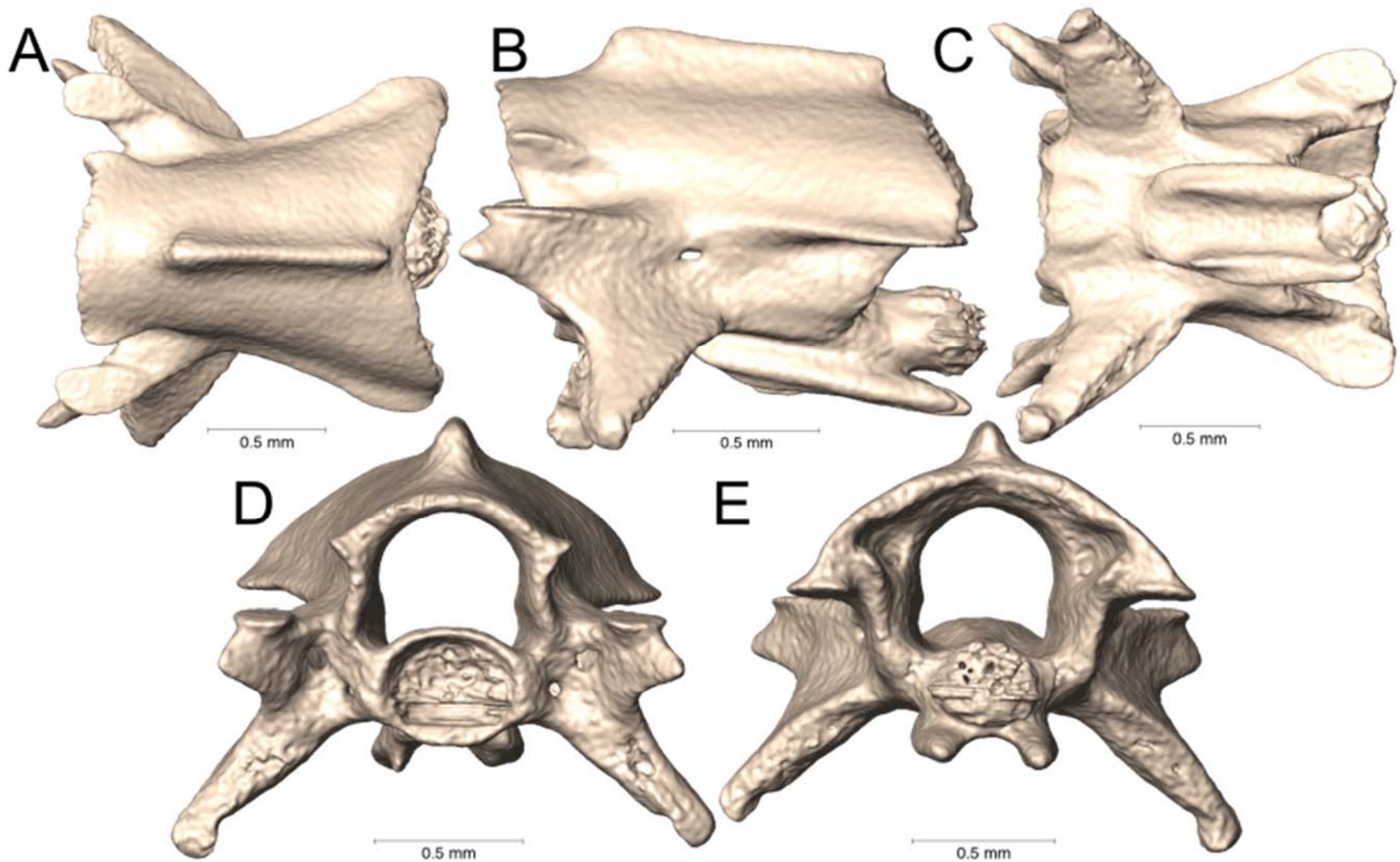
Supplemental Figure 5.12. Dorsal, lateral, ventral, anterior, and posterior views (A-E, respectively) of the caudal vertebra of *Calliophis maculiceps* (MNHN 5459).



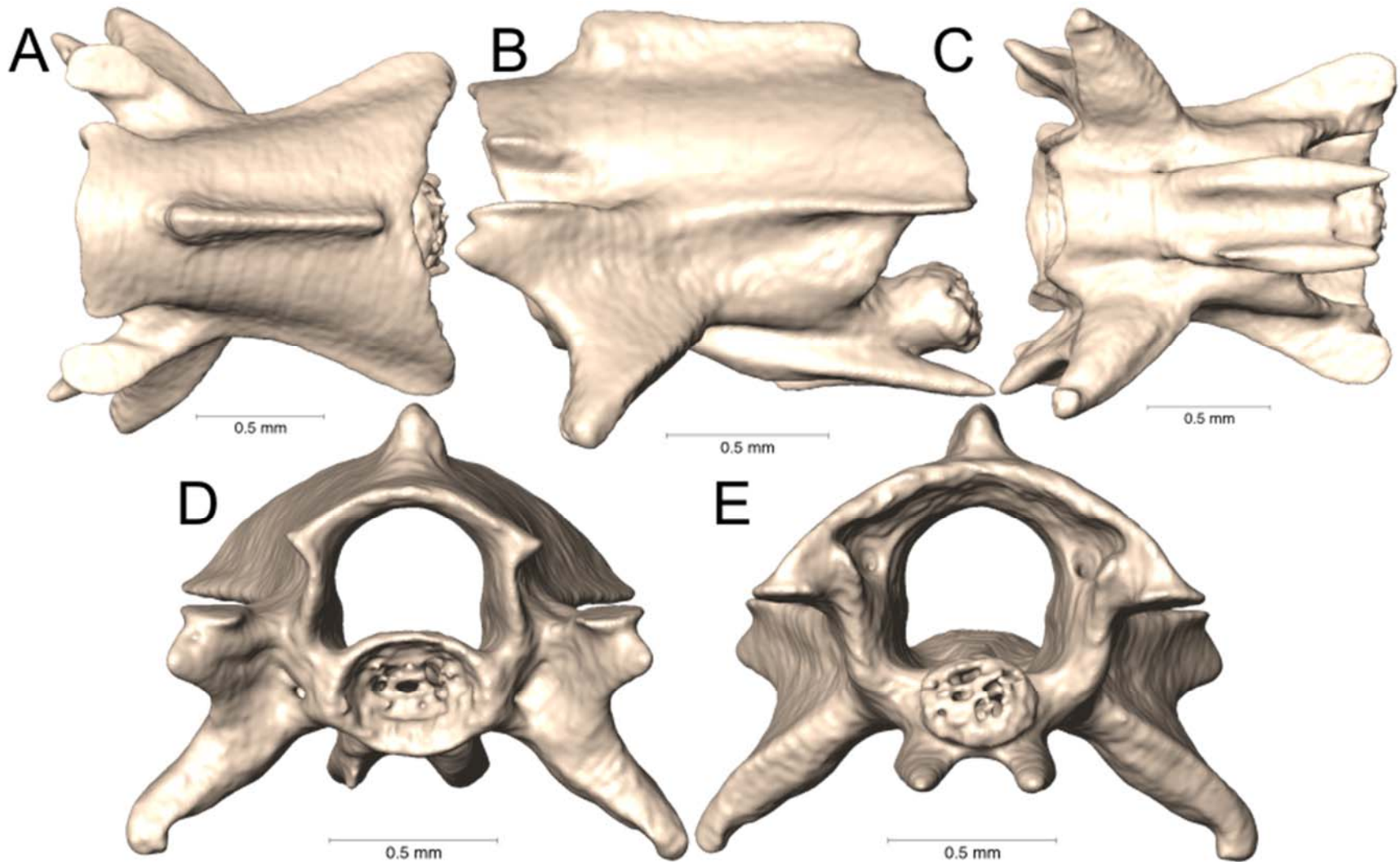
Supplemental Figure 5.13. Dorsal, lateral, ventral, anterior, and posterior views (A-E, respectively) of the caudal vertebra of *Calliophis melanurus* (MNHN 46-286).



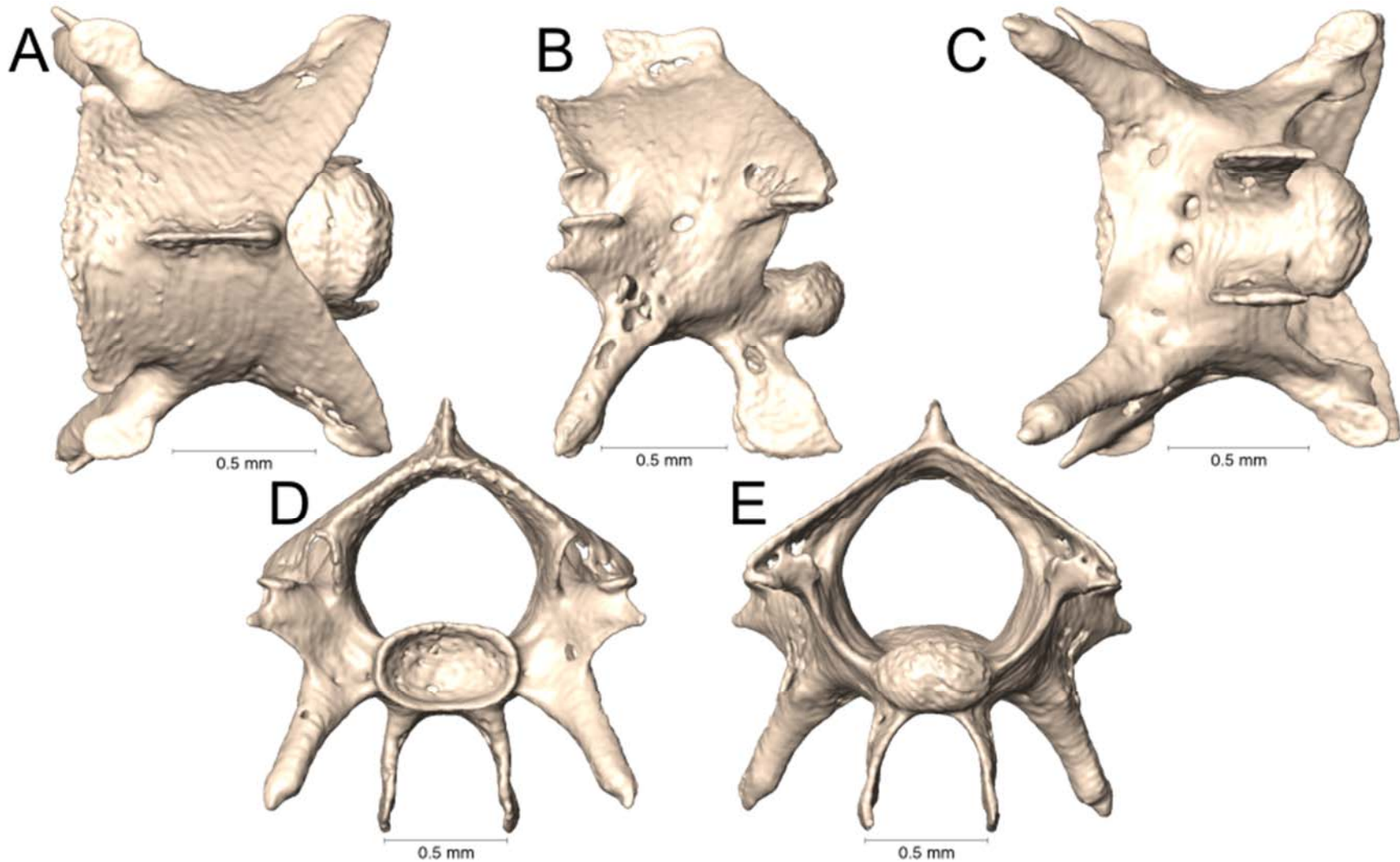
Supplemental Figure 5.14. Dorsal, lateral, ventral, anterior, and posterior views (A-E, respectively) of the caudal vertebra of *Calliophis nigrescens* (CAS 17265).



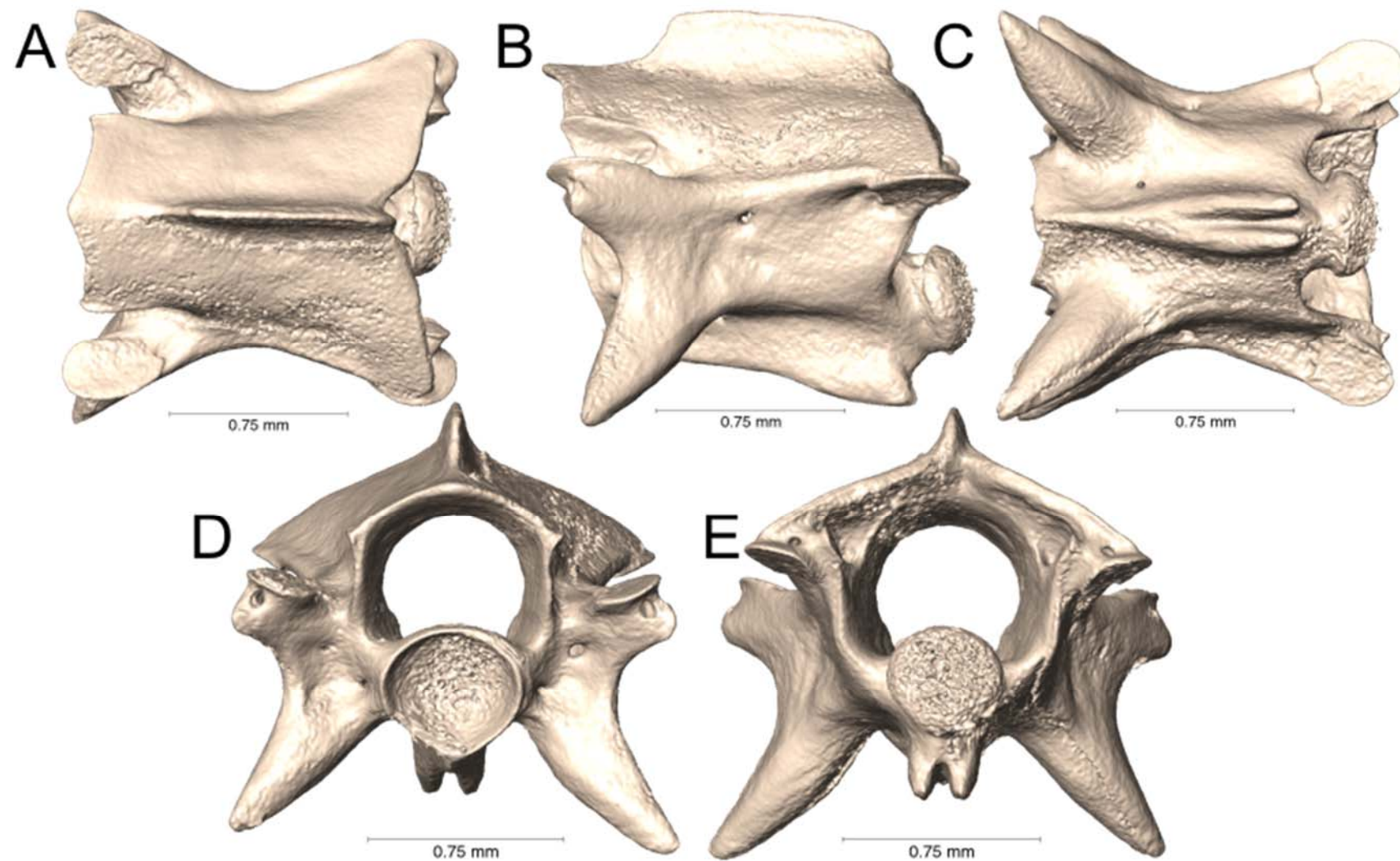
Supplemental Figure 5.15. Dorsal, lateral, ventral, anterior, and posterior views (A-E, respectively) of the caudal vertebra of *Calliophis philippinus* (KU 310369).



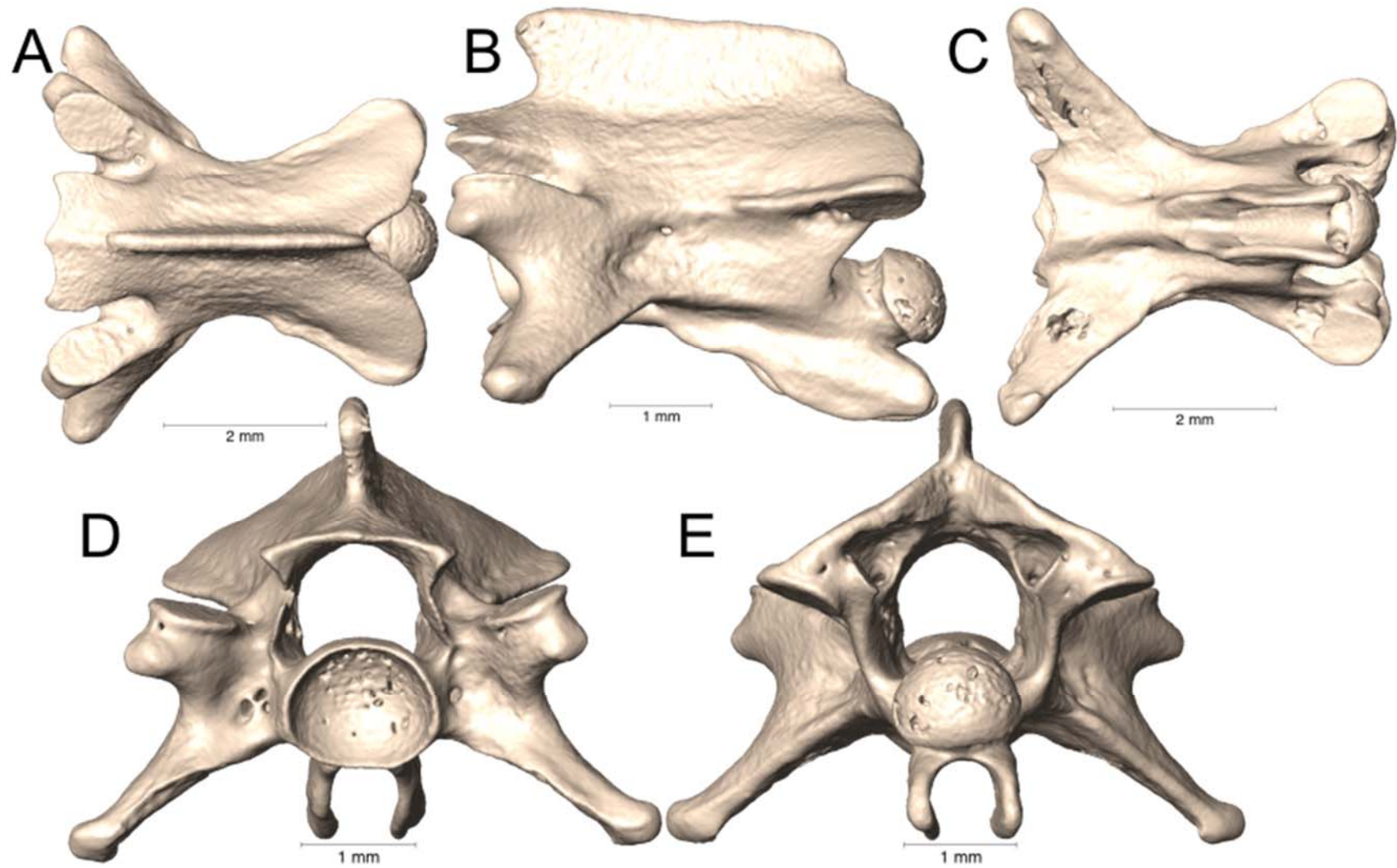
Supplemental Figure 5.16. Dorsal, lateral, ventral, anterior, and posterior views (A-E, respectively) of the caudal vertebra of *Calliophis philippinus* (KU 314913).



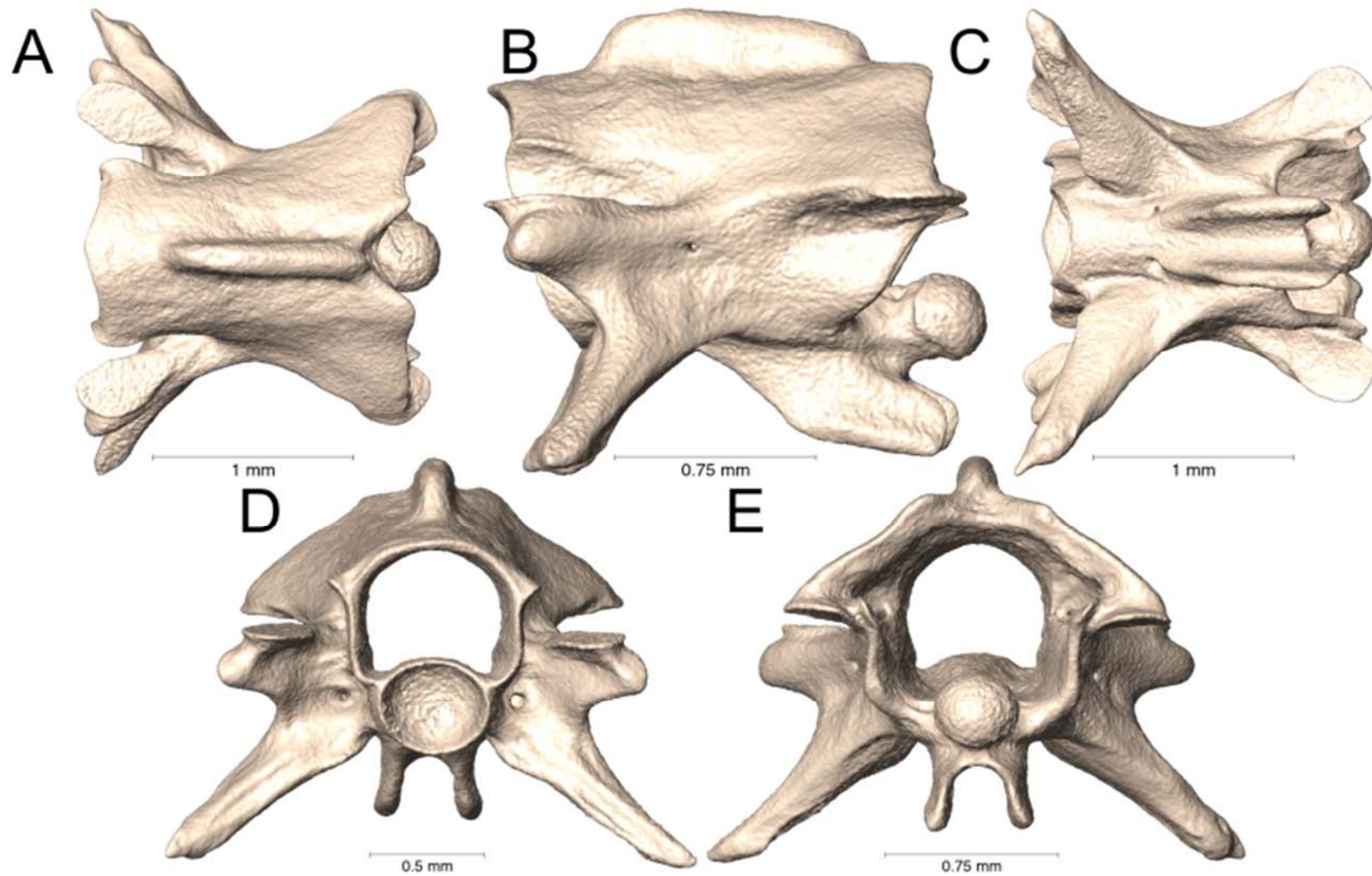
Supplemental Figure 5.17. Dorsal, lateral, ventral, anterior, and posterior views (A-E, respectively) of the caudal vertebra of *Dendroaspis angusticeps* (UTA R-34982).



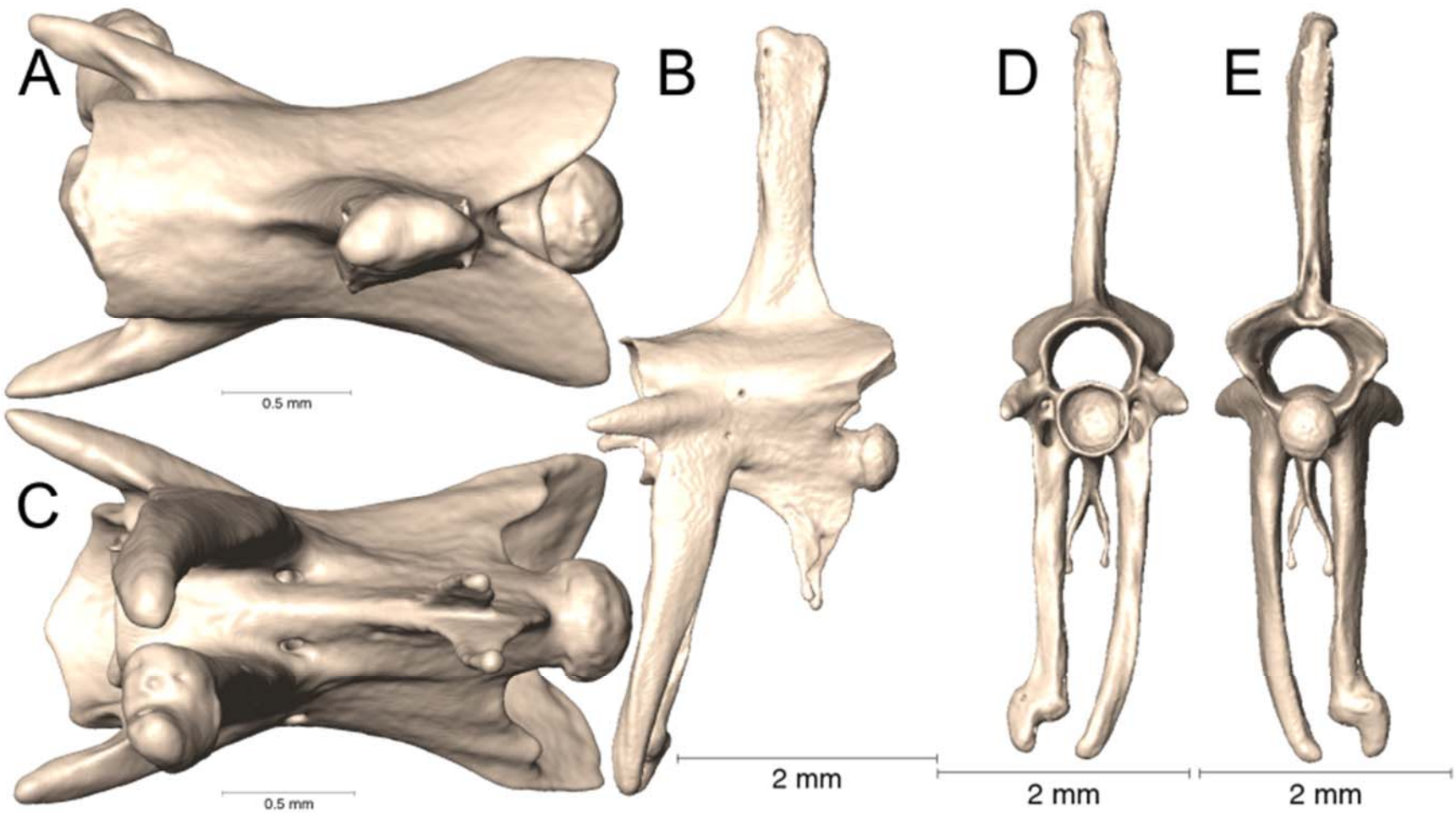
Supplemental Figure 5.18. Dorsal, lateral, ventral, anterior, and posterior views (A-E, respectively) of the caudal vertebra of *Elapsoidea nigra* (CAS 168978).



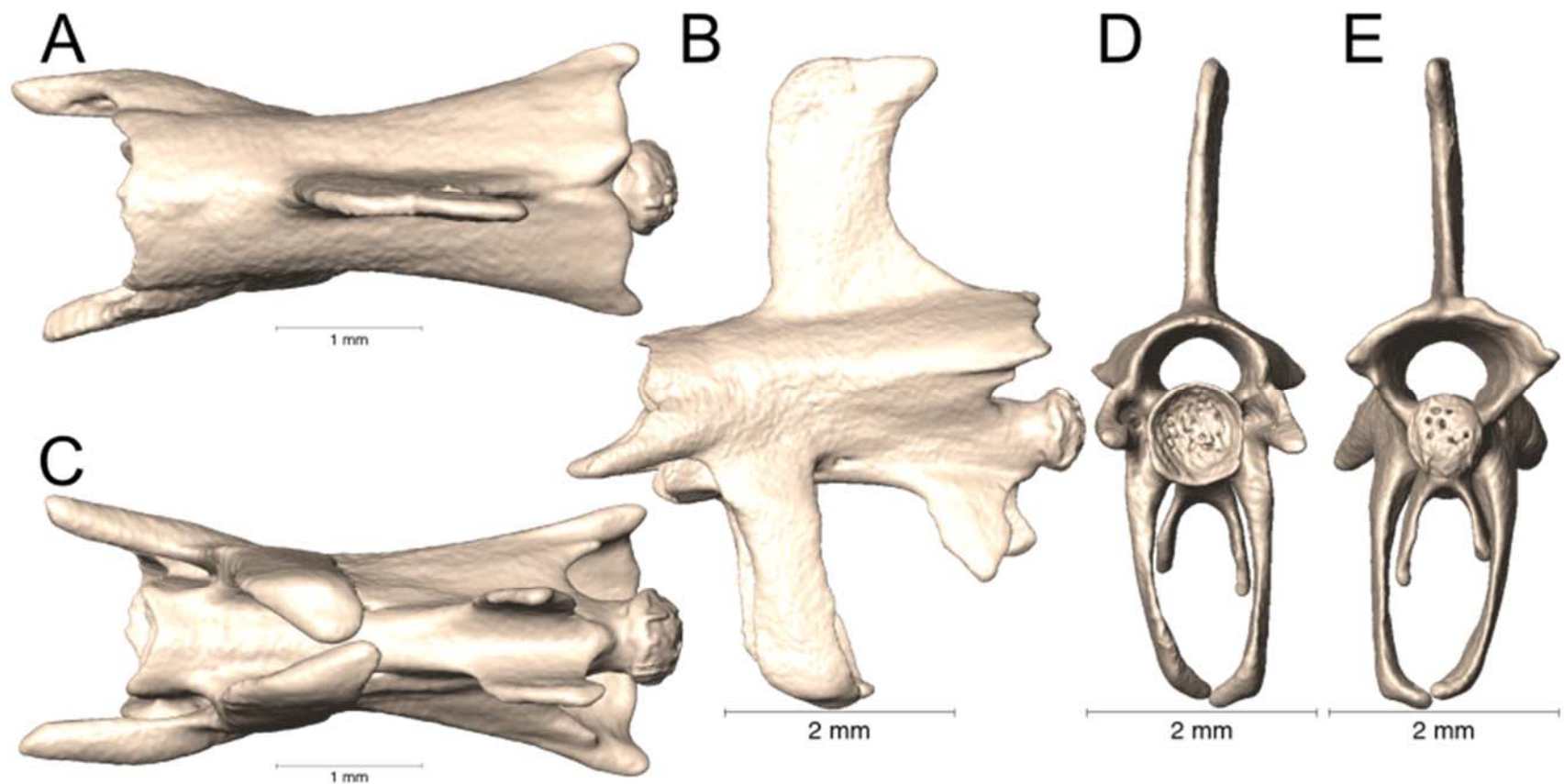
Supplemental Figure 5.19. Dorsal, lateral, ventral, anterior, and posterior views (A-E, respectively) of the caudal vertebra of *Hemachatus haemachatus* (UTA R-7431).



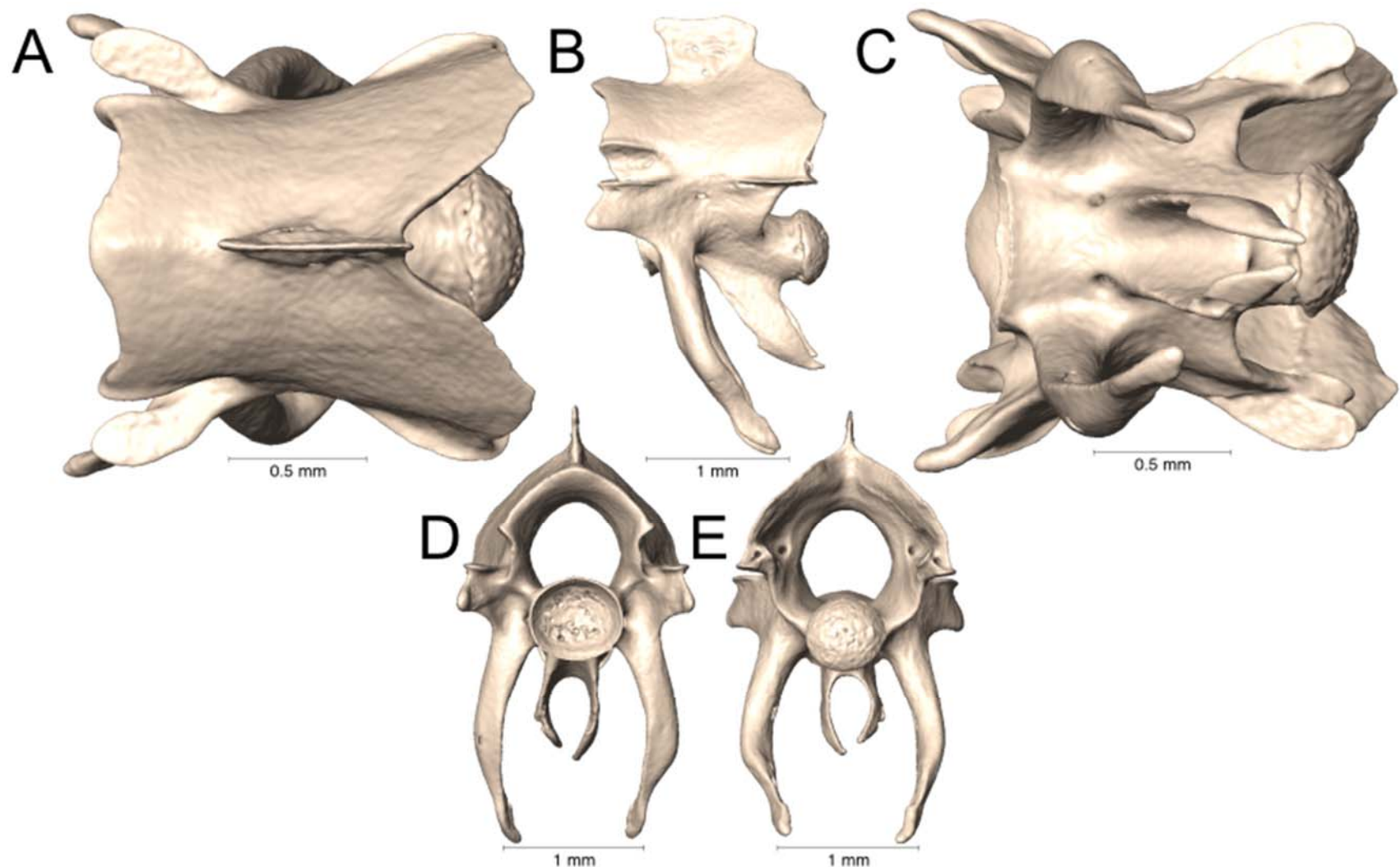
Supplemental Figure 5.20. Dorsal, lateral, ventral, anterior, and posterior views (A-E, respectively) of the caudal vertebra of *Hemibungarus calligaster* (KU 307474).



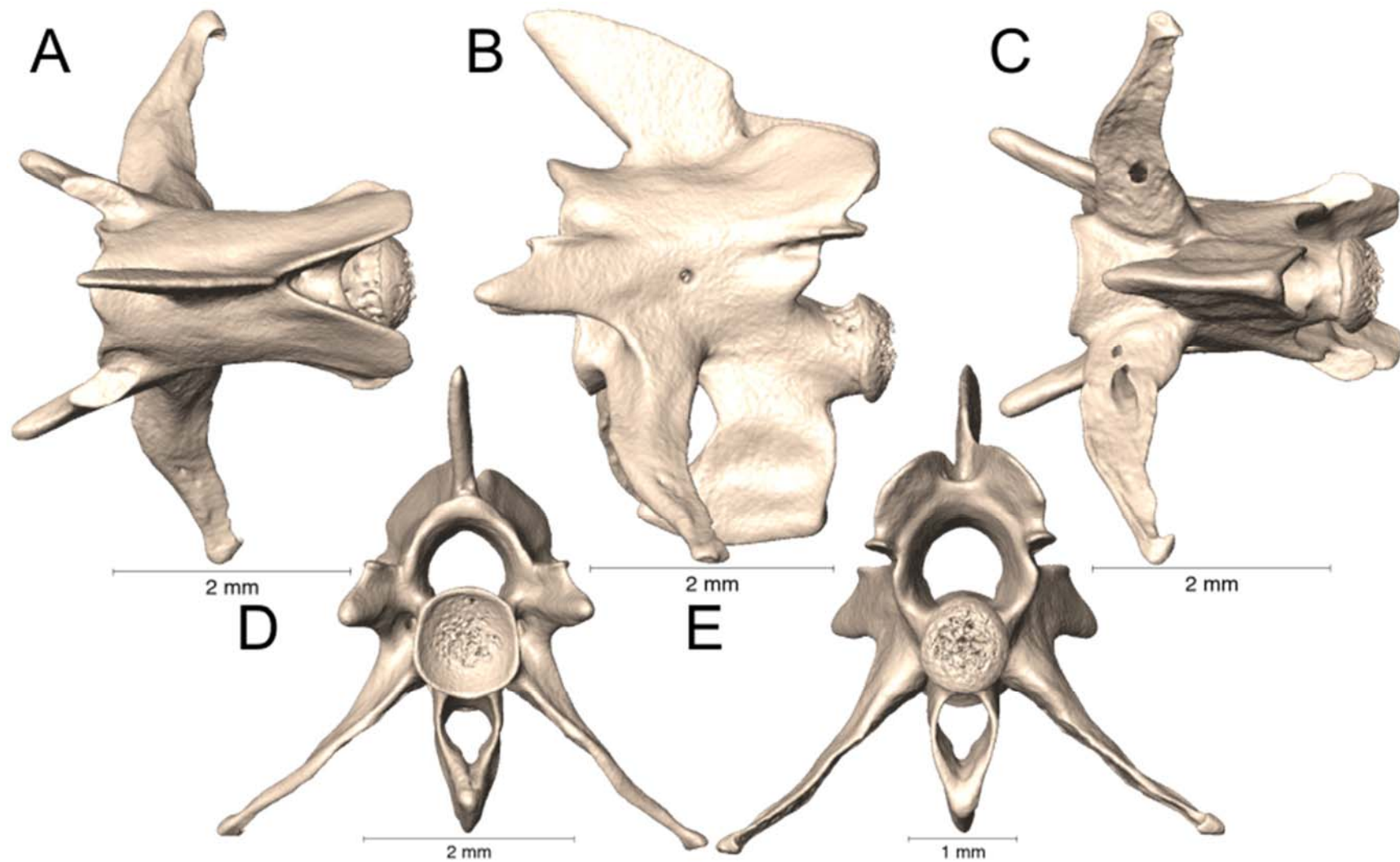
Supplemental Figure 5.21. Dorsal, lateral, ventral, anterior, and posterior views (A-E, respectively) of the caudal vertebra of *Hydrophis platurus* (UTA R-41049).



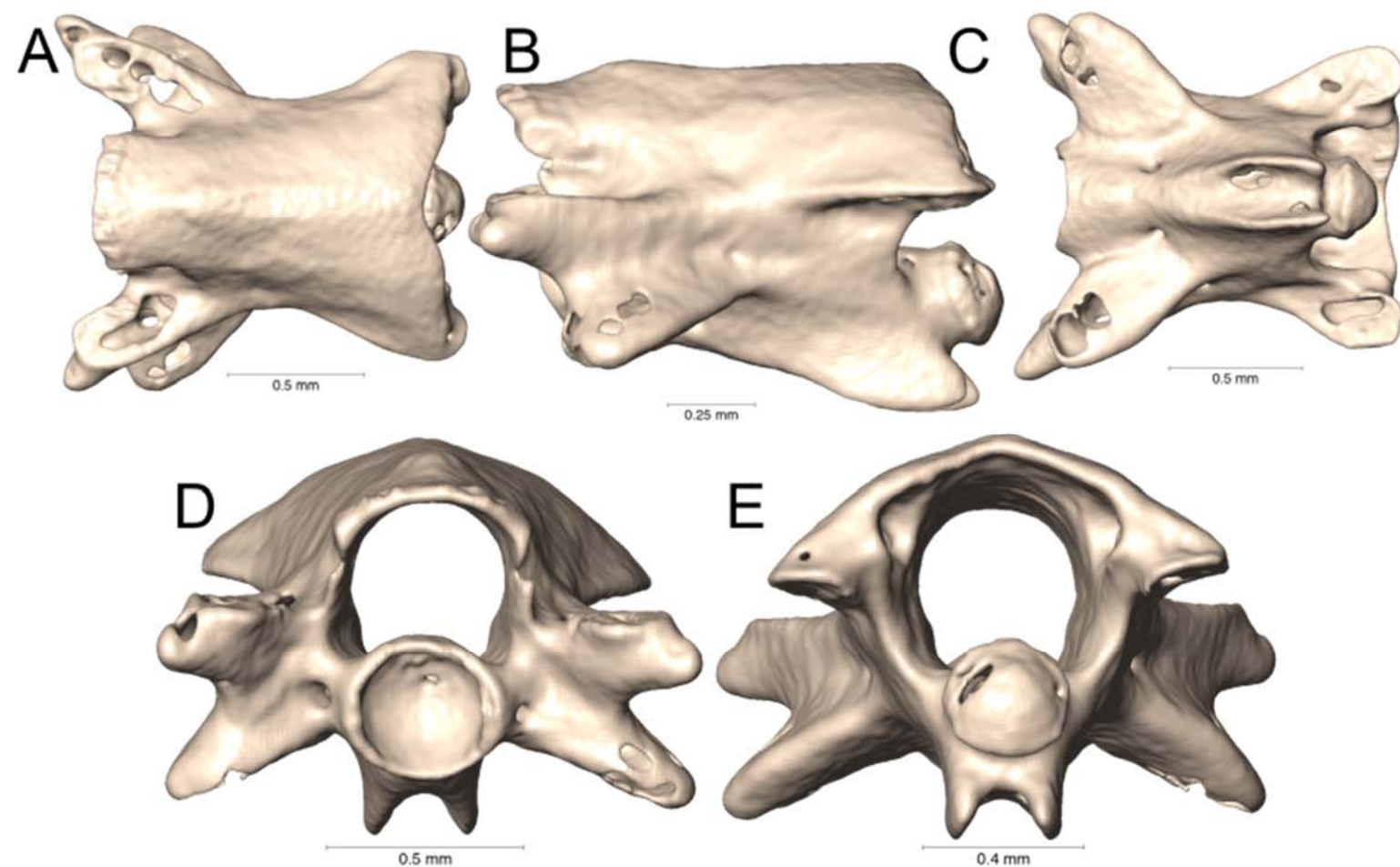
Supplemental Figure 5.22. Dorsal, lateral, ventral, anterior, and posterior views (A-E, respectively) of the caudal vertebra of *Hydrophis schistosus* (UTA R-63074).



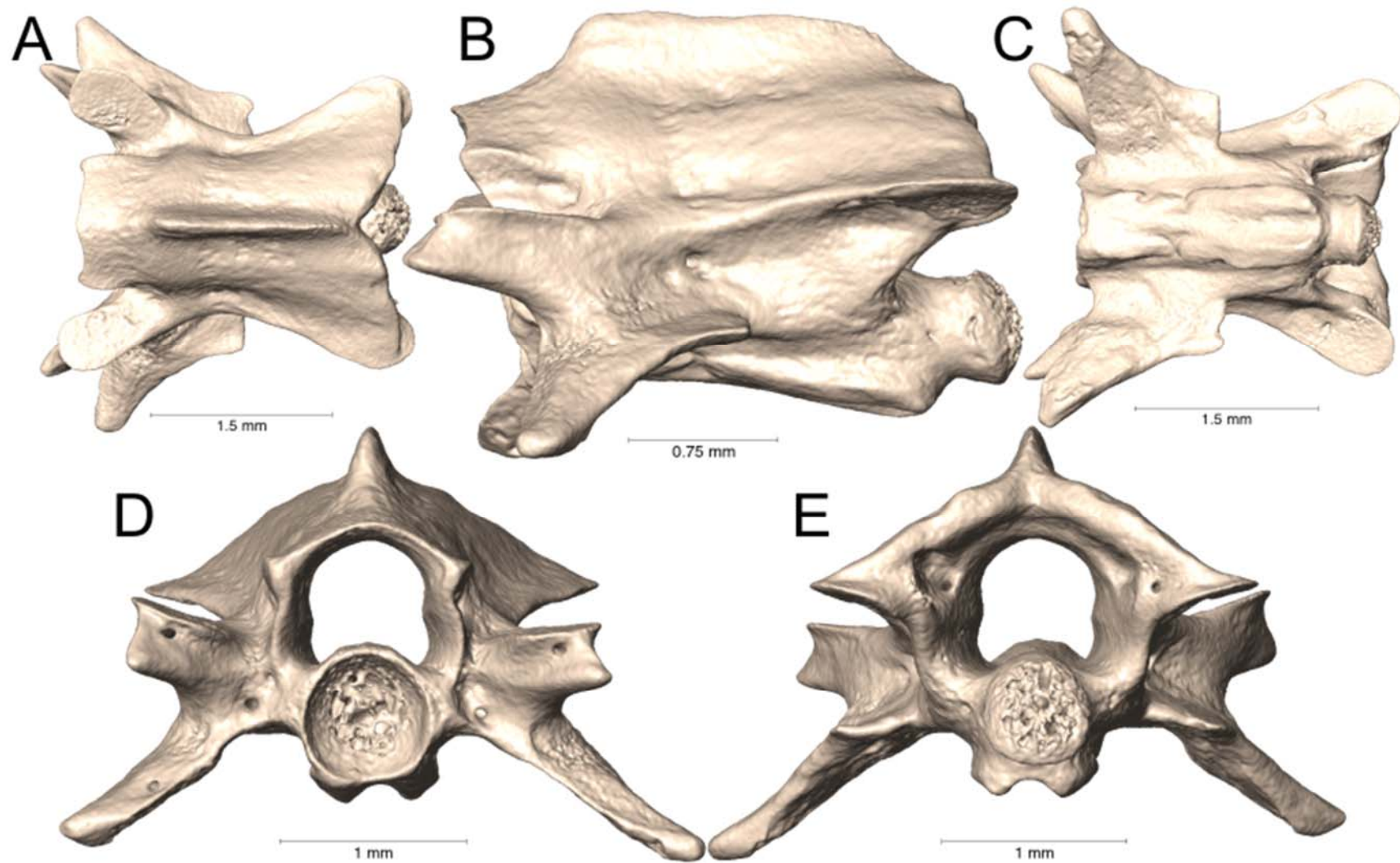
Supplemental Figure 5.23. Dorsal, lateral, ventral, anterior, and posterior views (A-E, respectively) of the caudal vertebra of *Laticauda colubrina* (UTA R-65800).



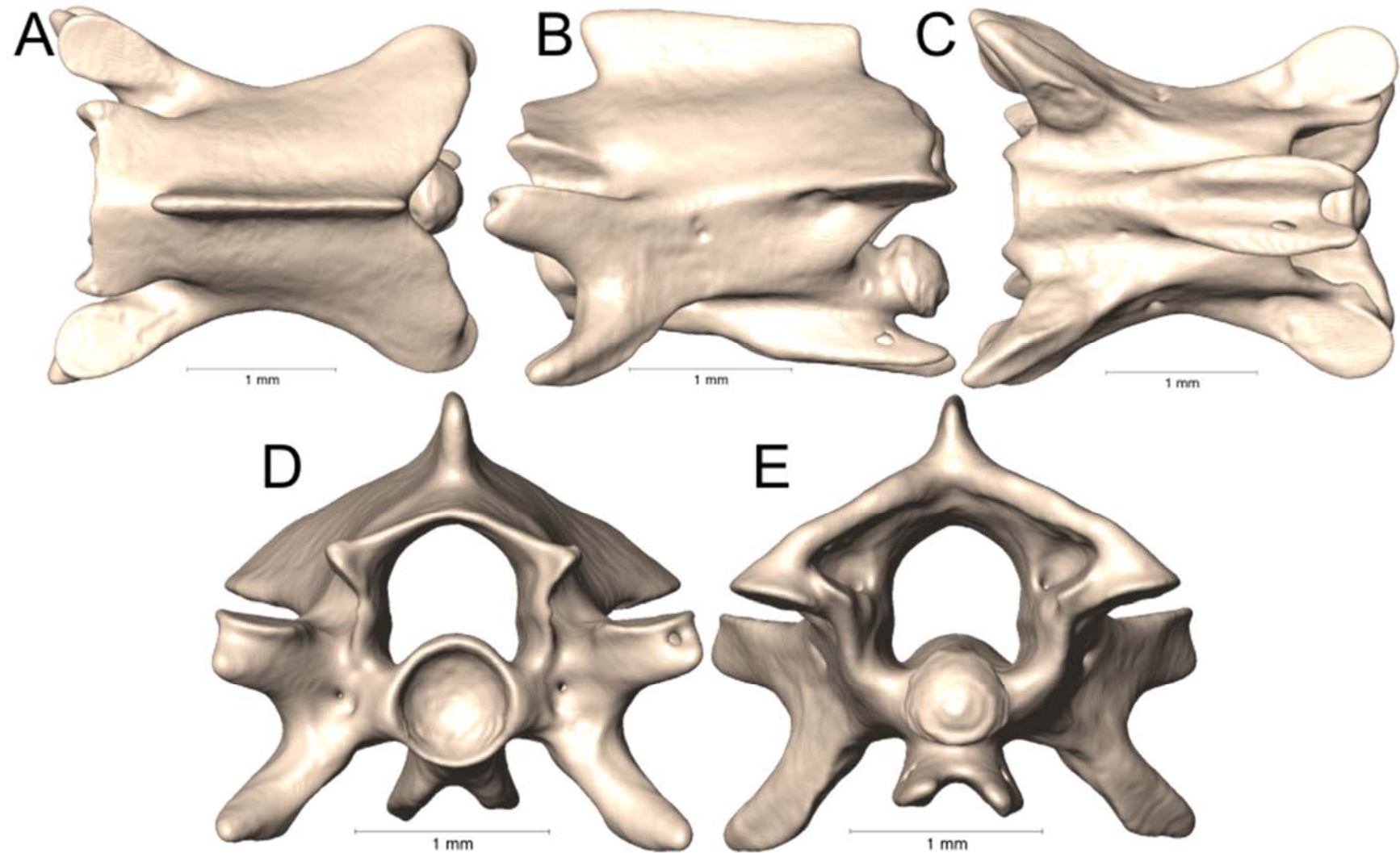
Supplemental Figure 5.24. Dorsal, lateral, ventral, anterior, and posterior views (A-E, respectively) of the caudal vertebra of *Laticauda laticauda* (UTA R-6355).



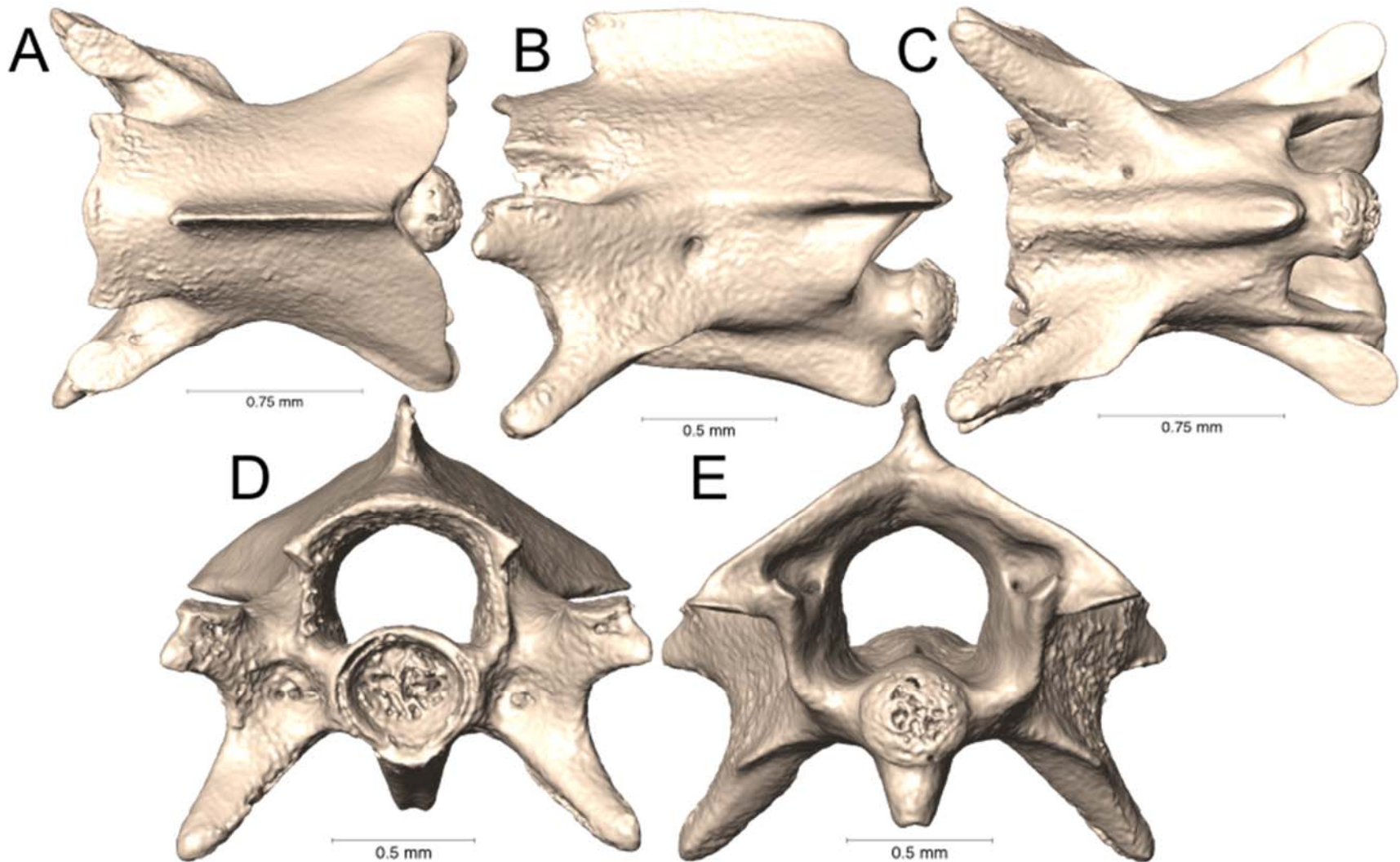
Supplemental Figure 5.25. Dorsal, lateral, ventral, anterior, and posterior views (A-E, respectively) of the caudal vertebra of *Micrelaps vaillanti* (CAS 169941).



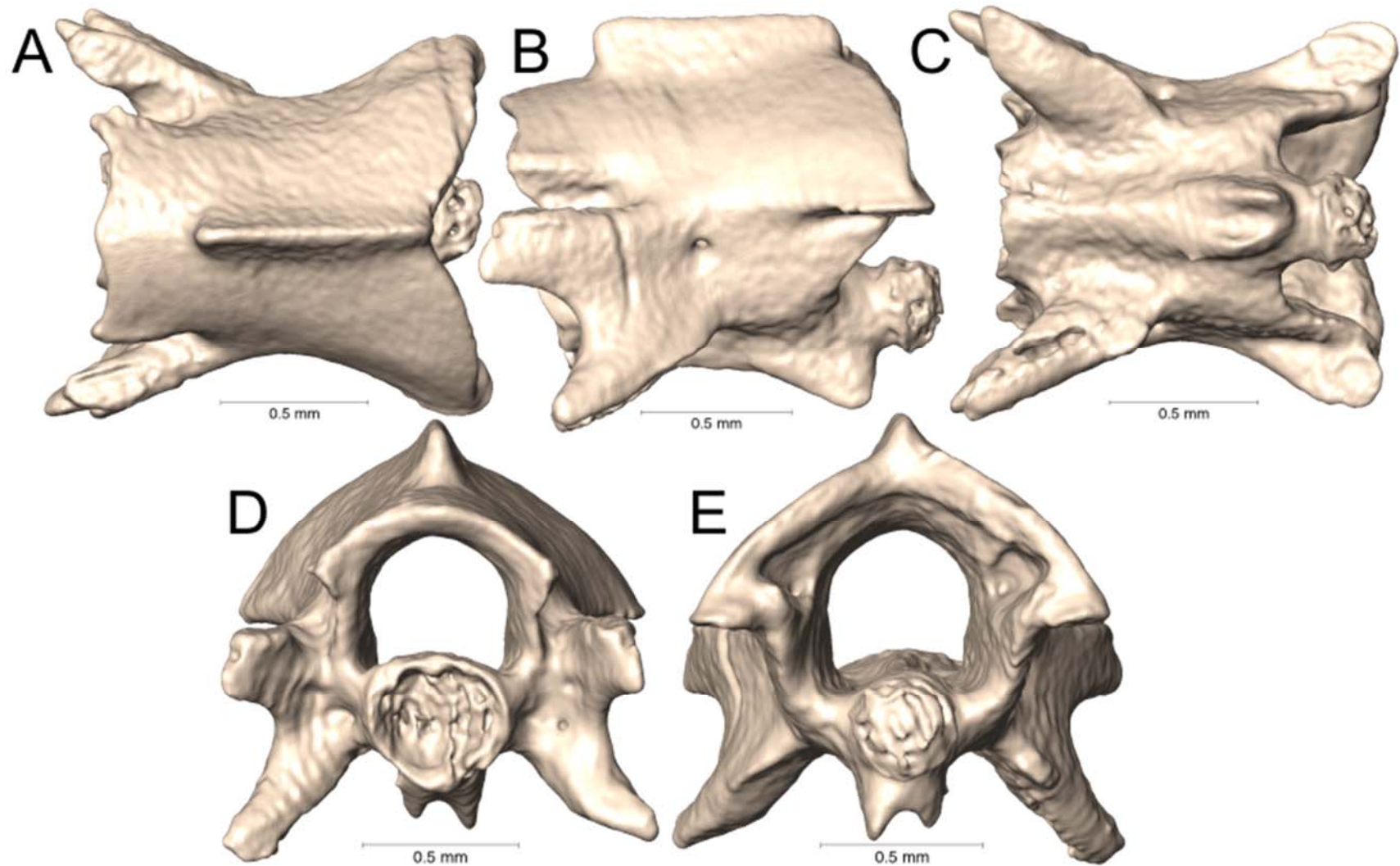
Supplemental Figure 5.26. Dorsal, lateral, ventral, anterior, and posterior views (A-E, respectively) of the caudal vertebra of *Micrurus aleni* (UTA R-60556).



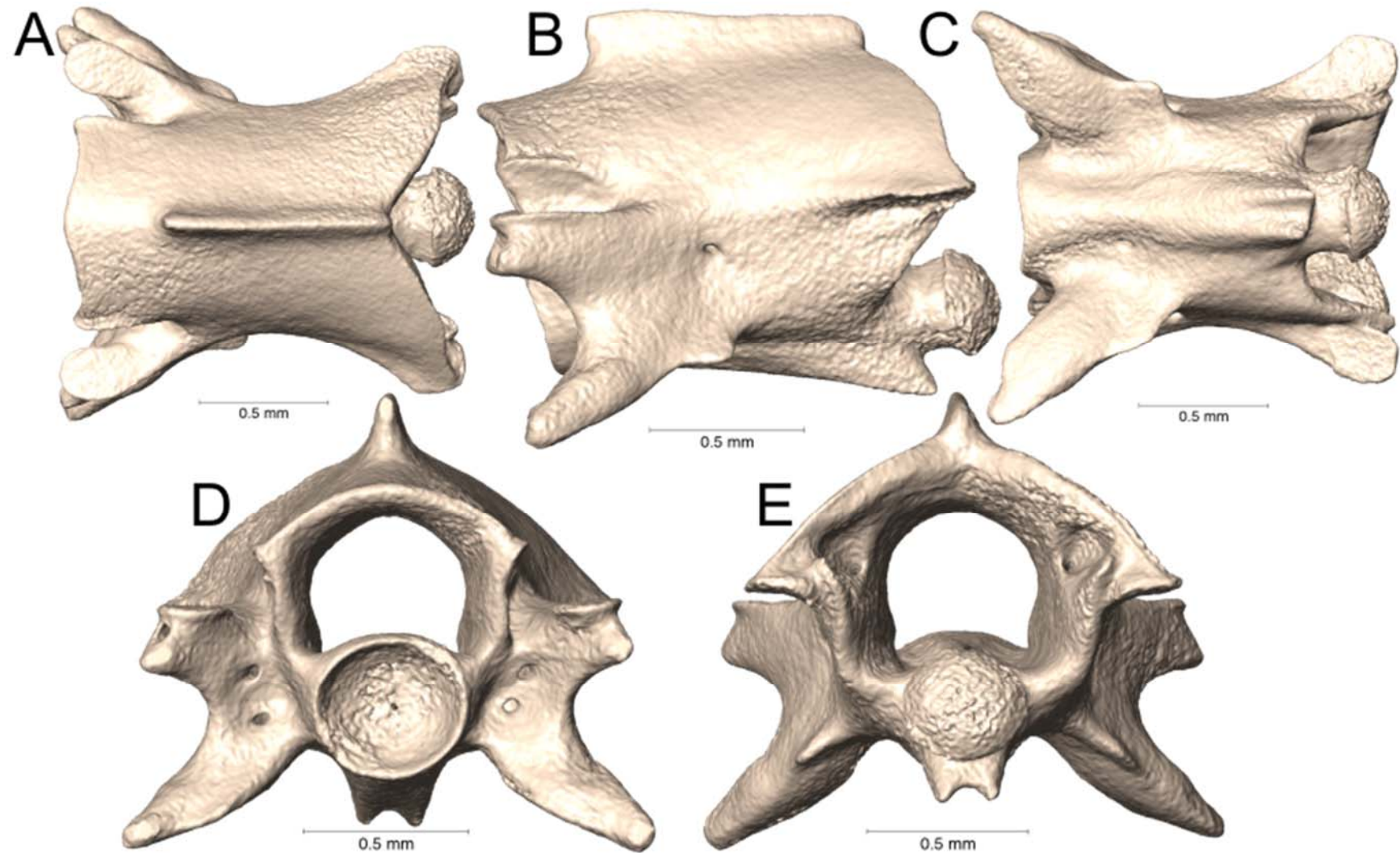
Supplemental Figure 5.27. Dorsal, lateral, ventral, anterior, and posterior views (A-E, respectively) of the caudal vertebra of *Micrurus anchoralis* (UTA R-55945).



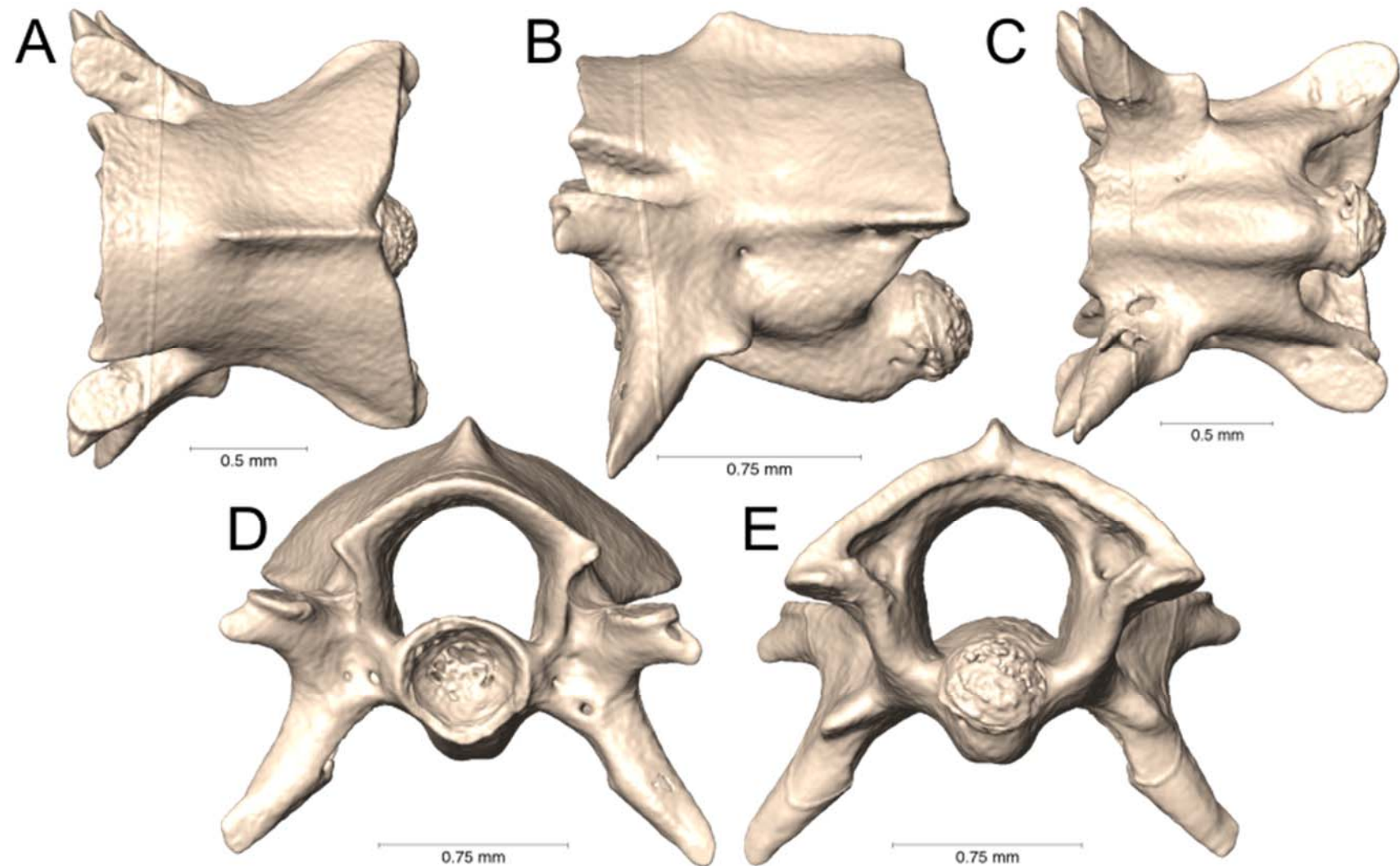
Supplemental Figure 5.28. Dorsal, lateral, ventral, anterior, and posterior views (A-E, respectively) of the caudal vertebra of *Micrurus apiatus* (UTA R-39267).



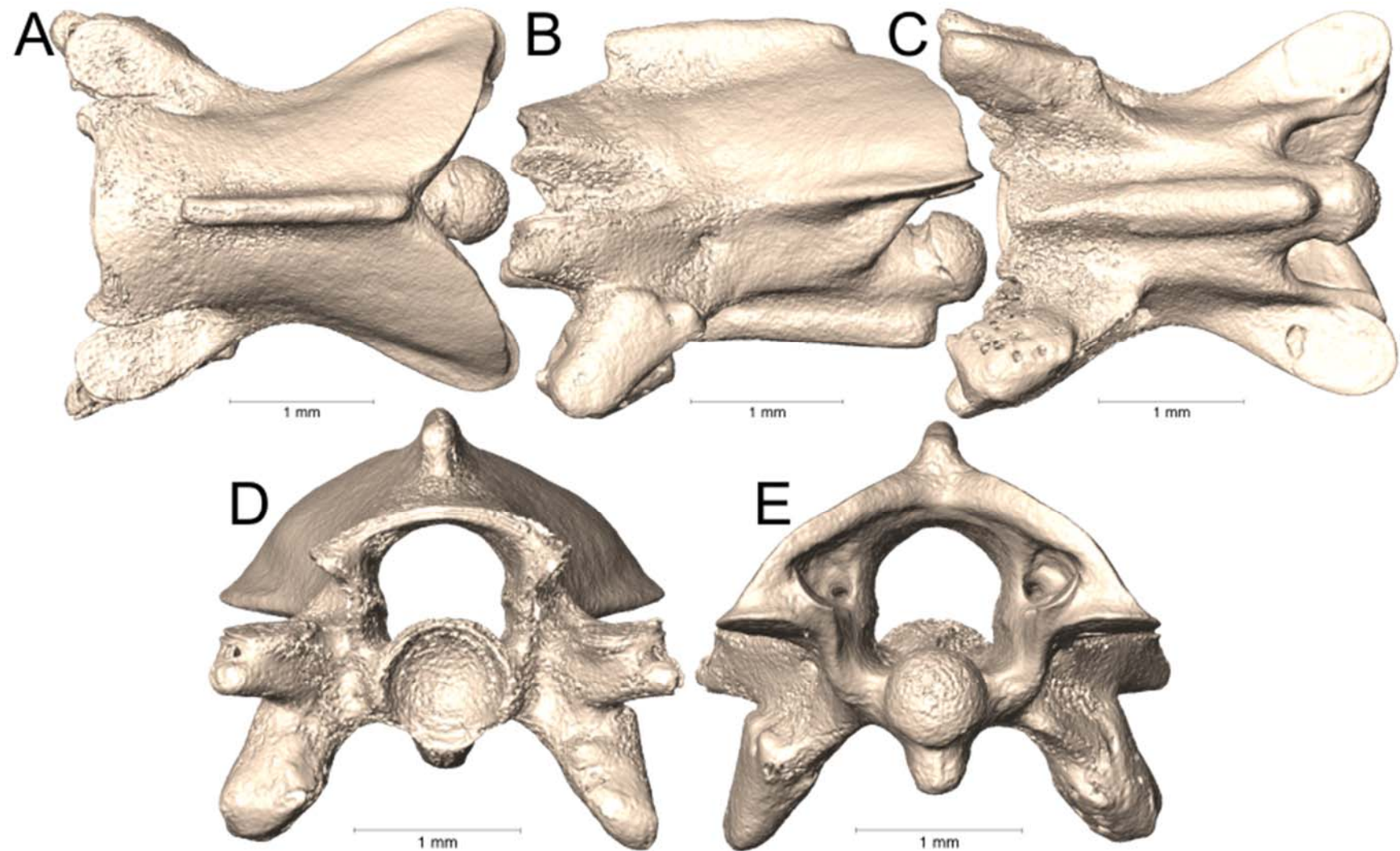
Supplemental Figure 5.29. Dorsal, lateral, ventral, anterior, and posterior views (A-E, respectively) of the caudal vertebra of *Micrurus apiyatus* (UTA R-39554).



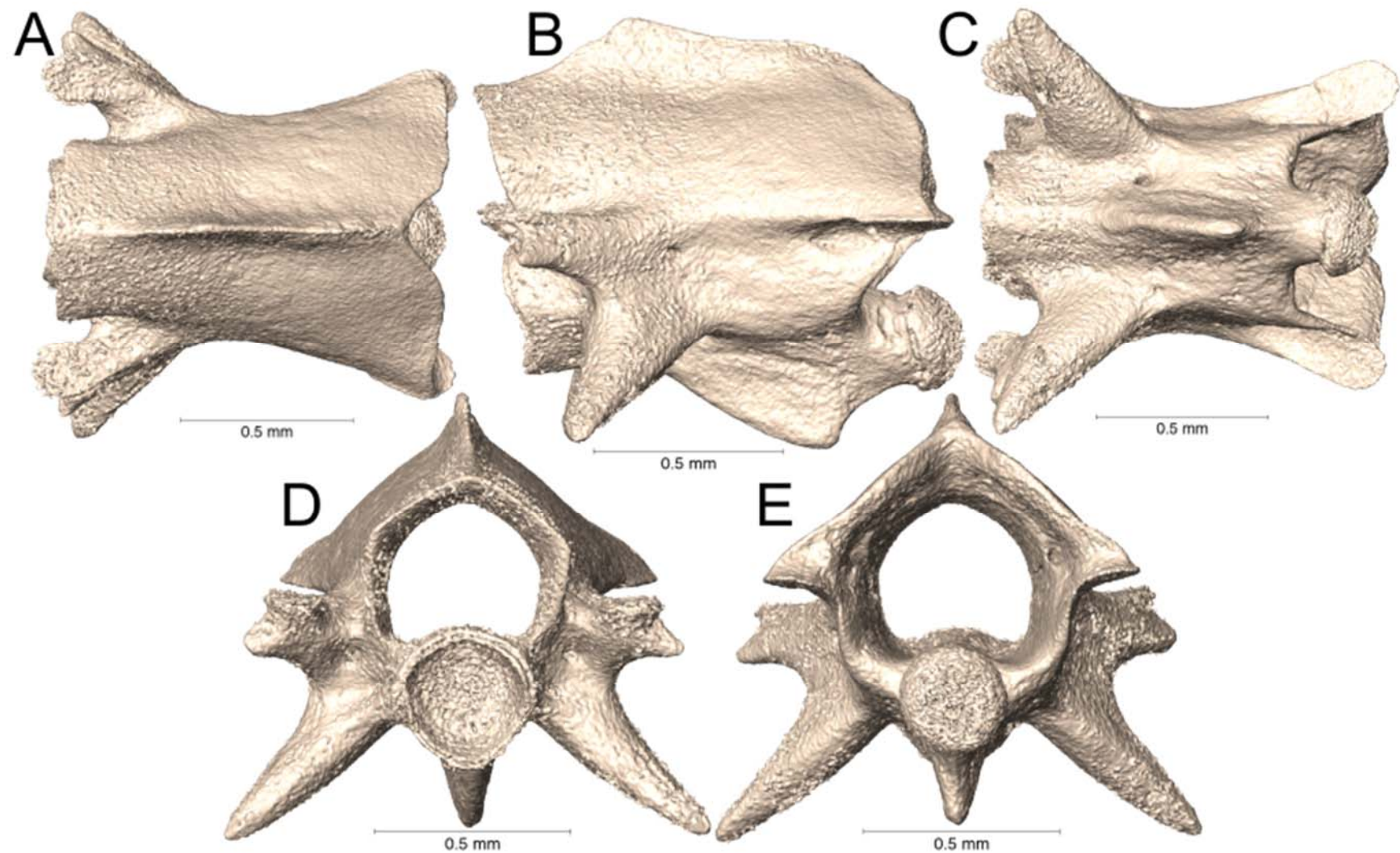
Supplemental Figure 5.30. Dorsal, lateral, ventral, anterior, and posterior views (A-E, respectively) of the caudal vertebra of *Micrurus apiyatus* (UTA R-53450).



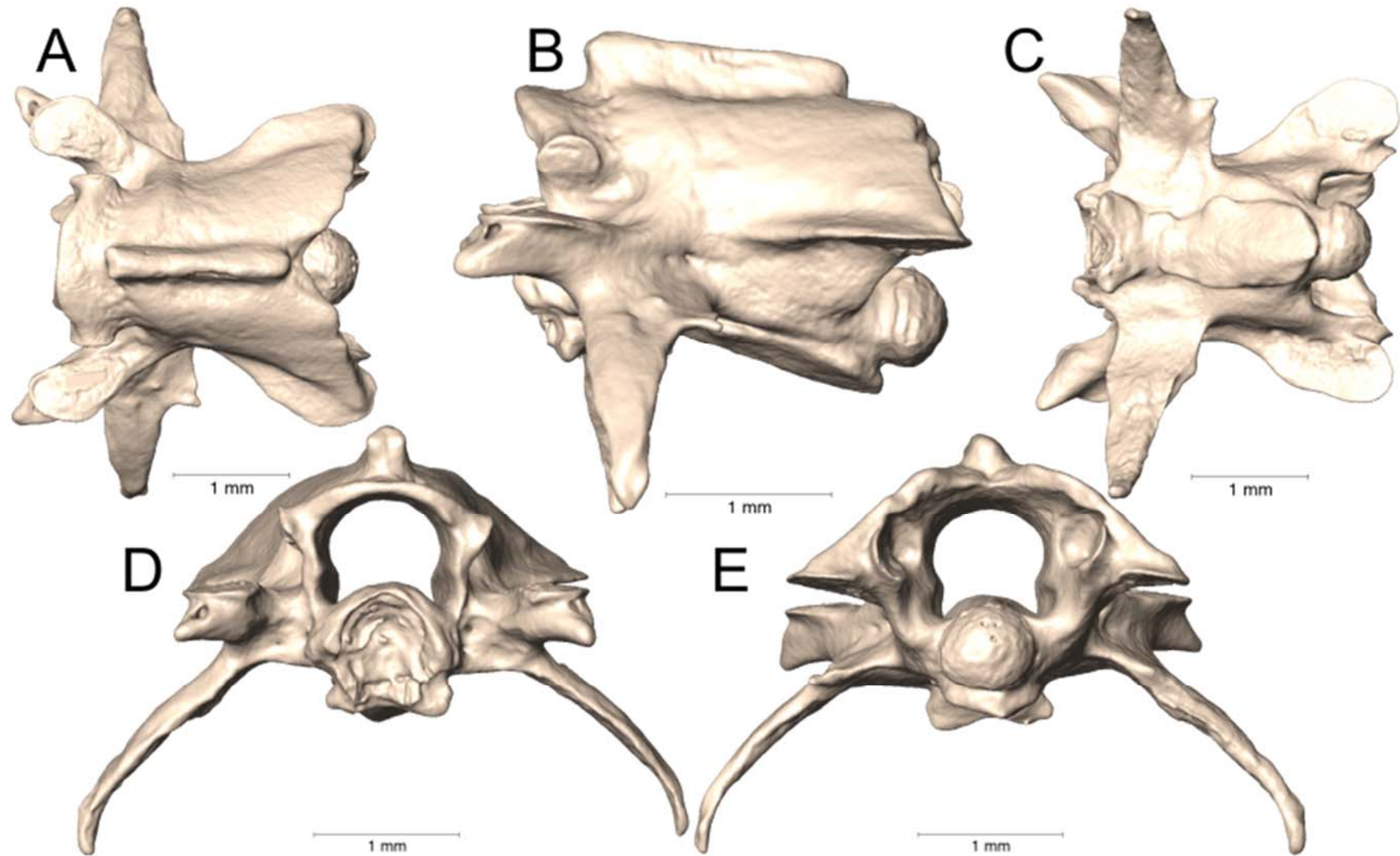
Supplemental Figure 5.31. Dorsal, lateral, ventral, anterior, and posterior views (A-E, respectively) of the caudal vertebra of *Micrurus bocourti* (UTA R-58145).



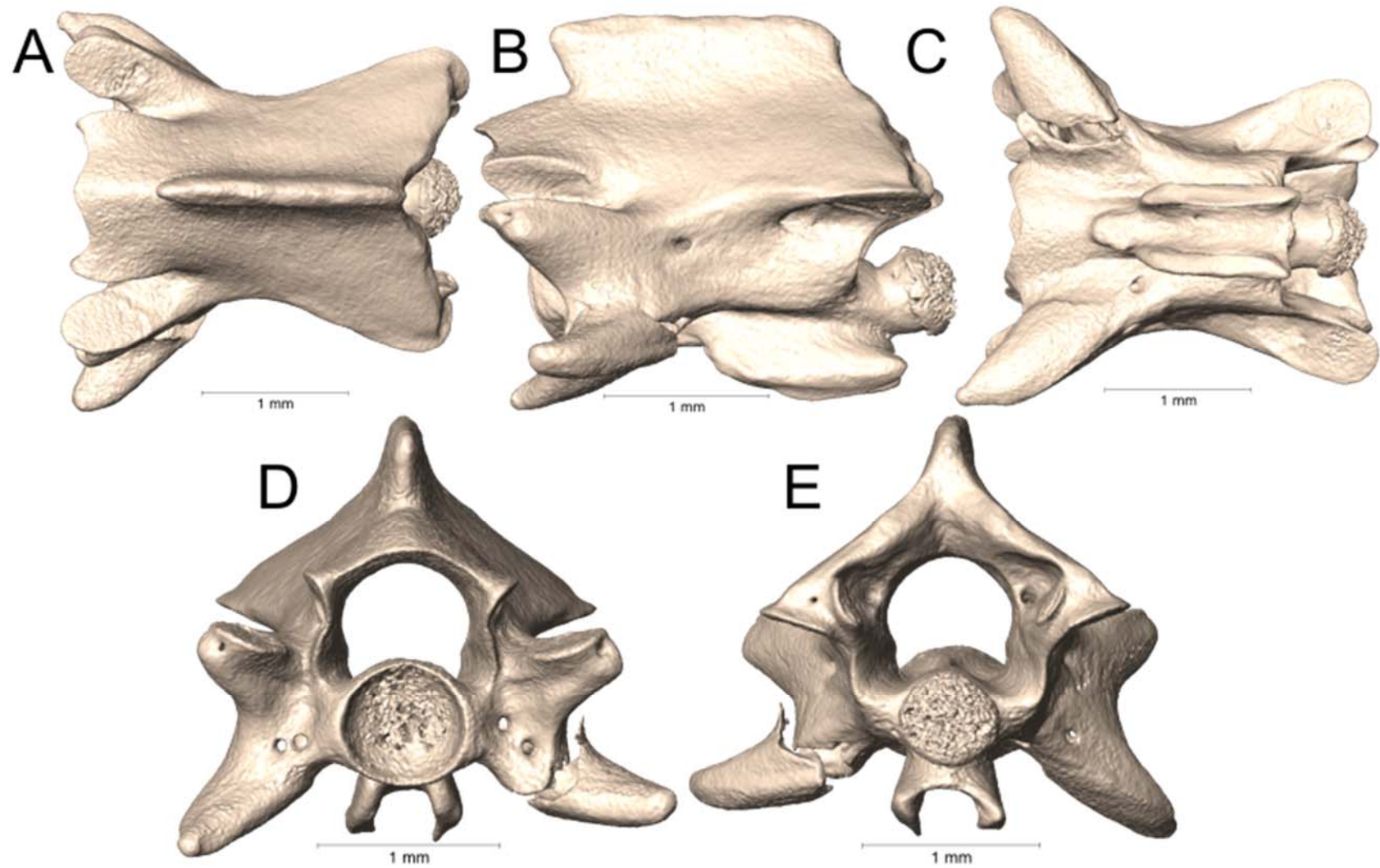
Supplemental Figure 5.32. Dorsal, lateral, ventral, anterior, and posterior views (A-E, respectively) of the caudal vertebra of *Micrurus diastema* (UTA R-52565).



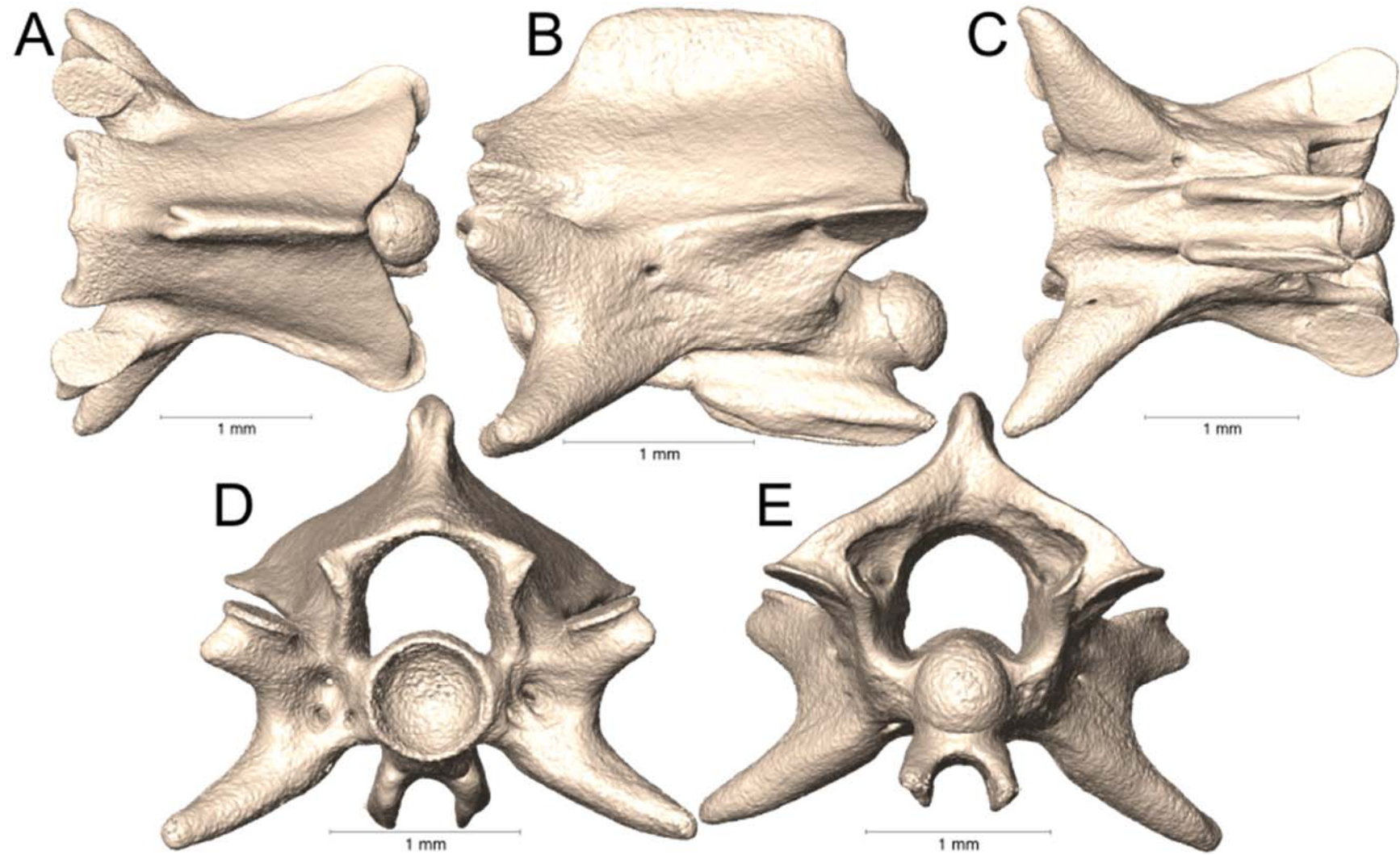
Supplemental Figure 5.33. Dorsal, lateral, ventral, anterior, and posterior views (A-E, respectively) of the caudal vertebra of *Micrurus dissoleucus* (UTA R-54184).



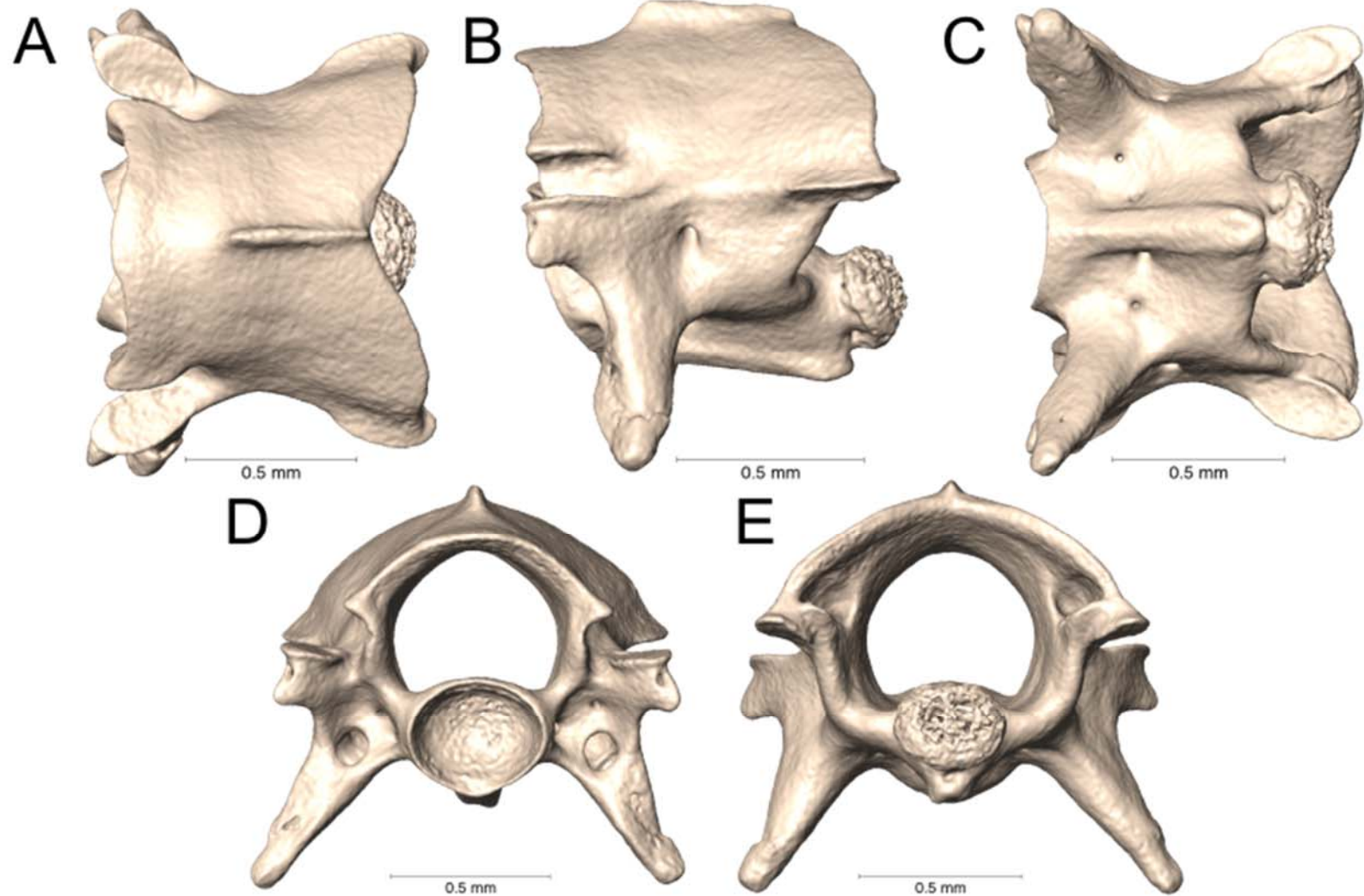
Supplemental Figure 5.34. Dorsal, lateral, ventral, anterior, and posterior views (A-E, respectively) of the caudal vertebra of *Micrurus distans* (UTA R-14471).



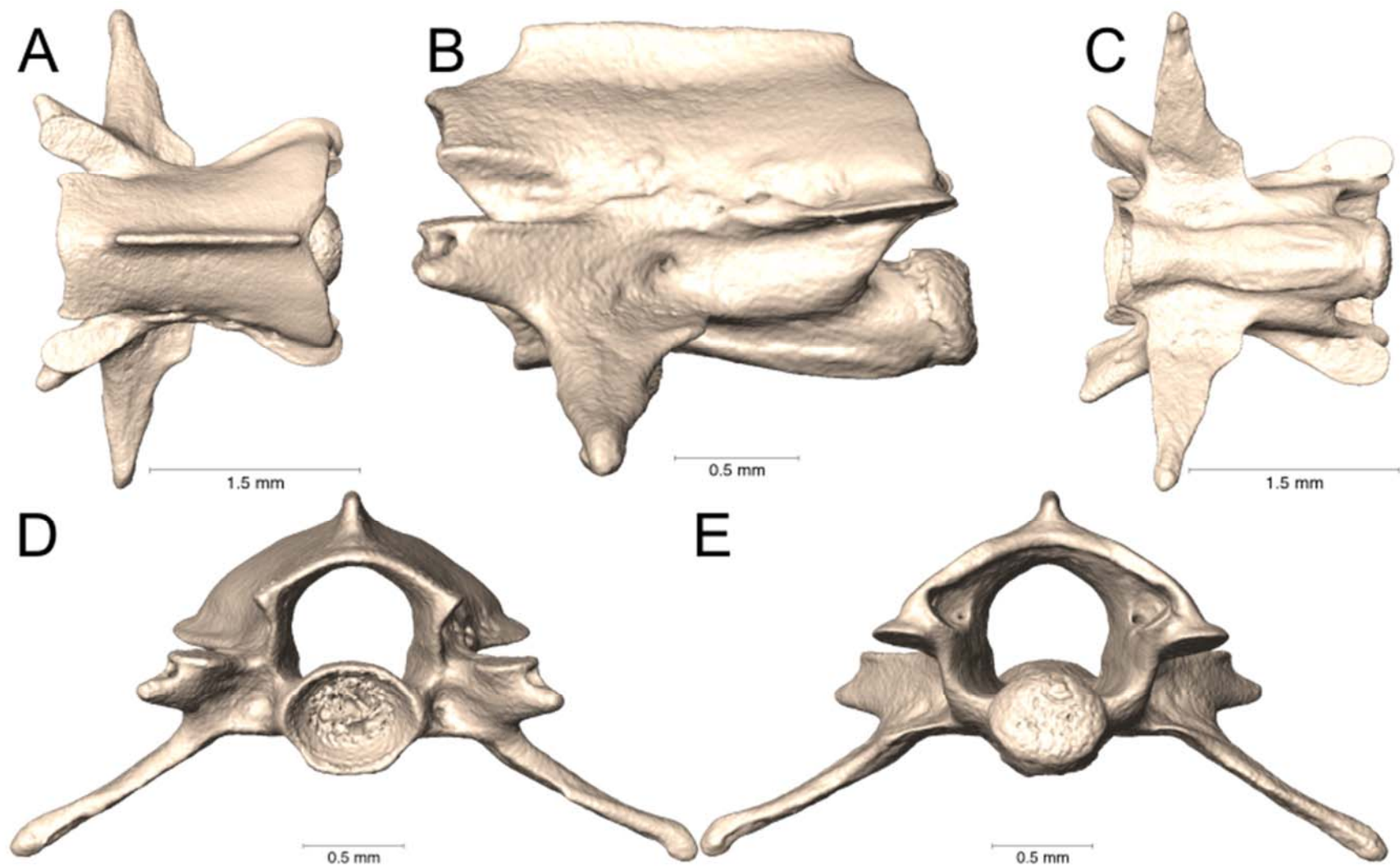
Supplemental Figure 5.35. Dorsal, lateral, ventral, anterior, and posterior views (A-E, respectively) of the caudal vertebra of *Micrurus diutius* (UTA R-20756).



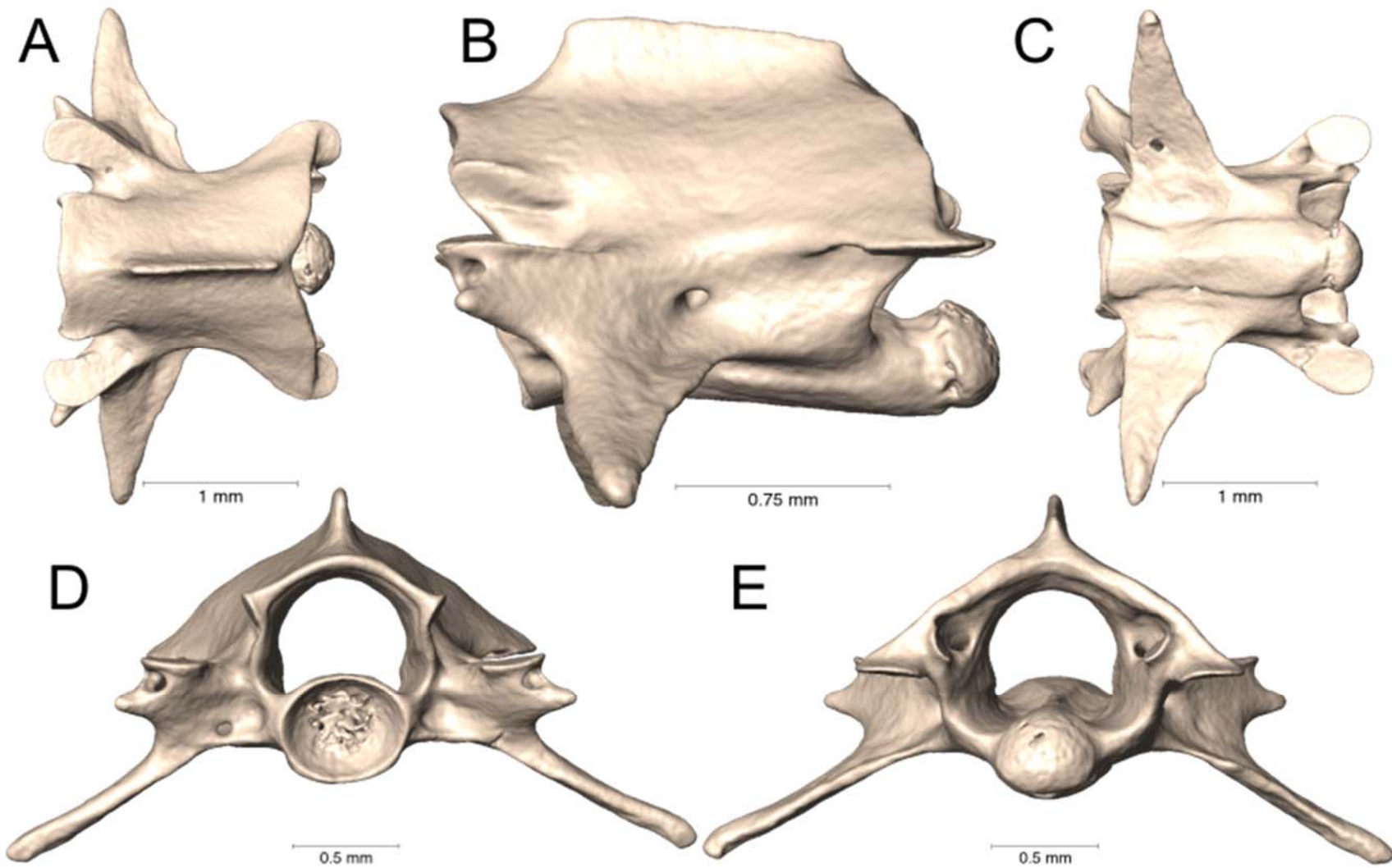
Supplemental Figure 5.36. Dorsal, lateral, ventral, anterior, and posterior views (A-E, respectively) of the caudal vertebra of *Micrurus diutius* (UTA R-54182).



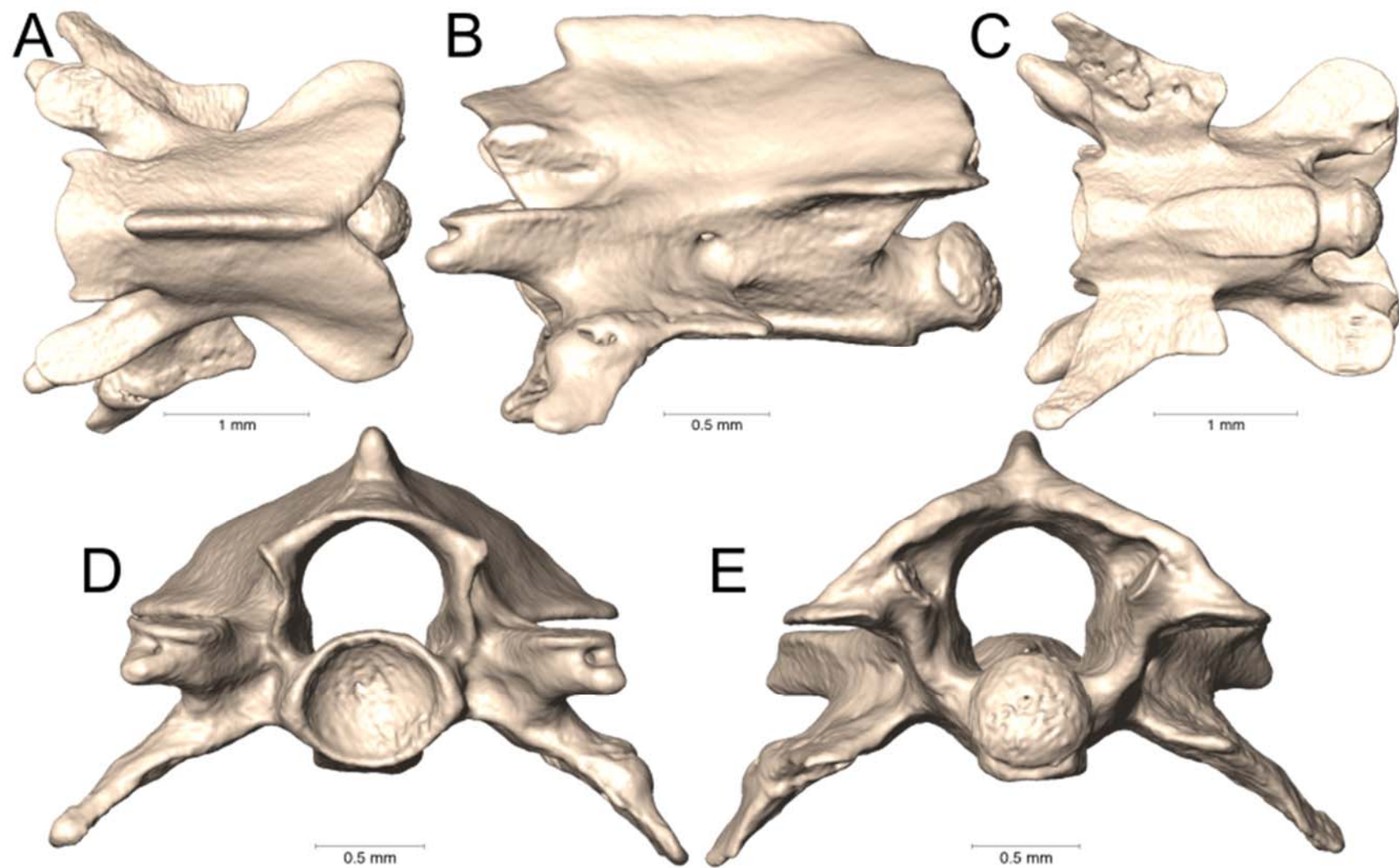
Supplemental Figure 5.37. Dorsal, lateral, ventral, anterior, and posterior views (A-E, respectively) of the caudal vertebra of *Micrurus dumerilii* (AMNH 35951).



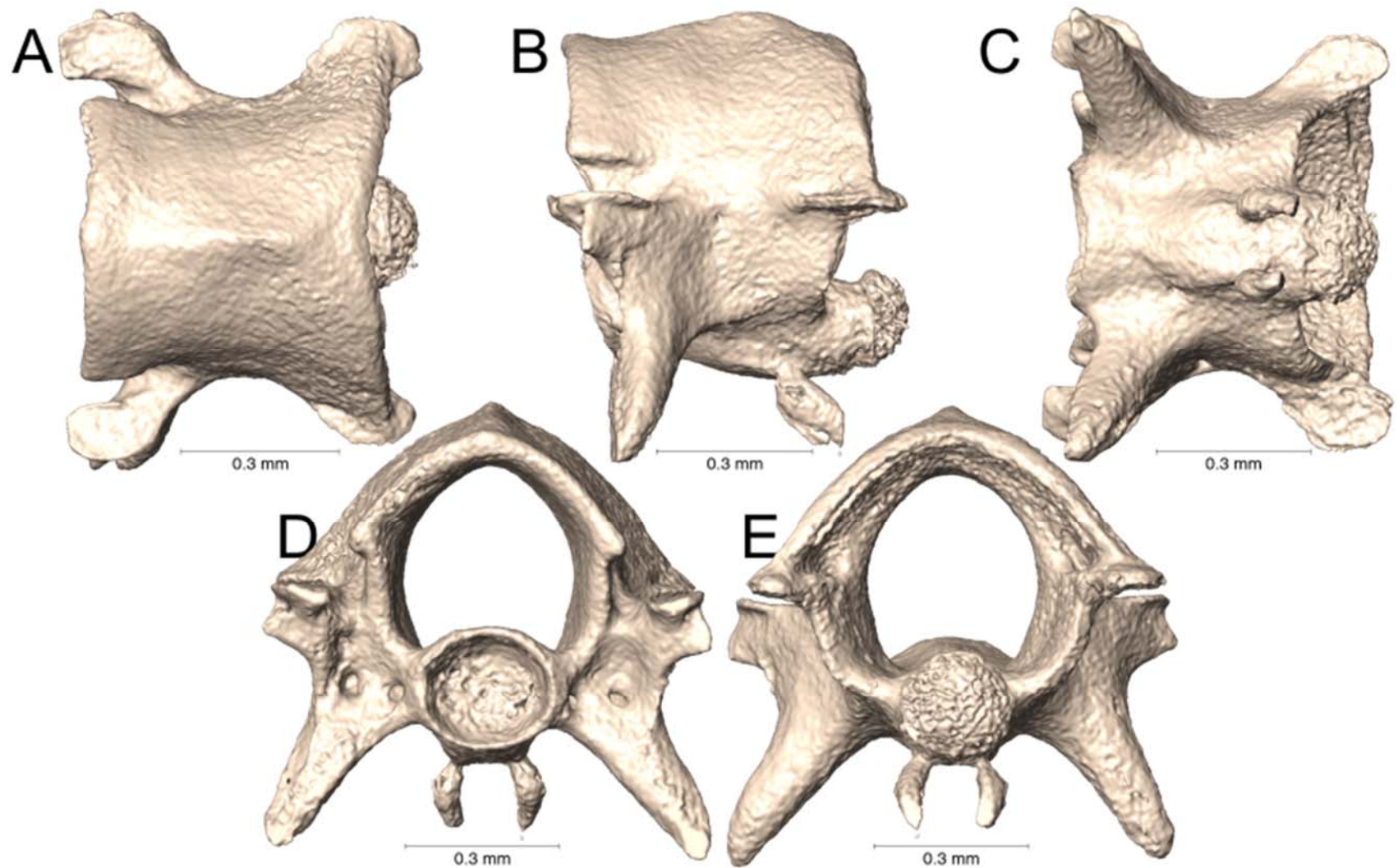
Supplemental Figure 5.38. Dorsal, lateral, ventral, anterior, and posterior views (A-E, respectively) of the caudal vertebra of *Micrurus elegans elegans* (MZFC 18819).



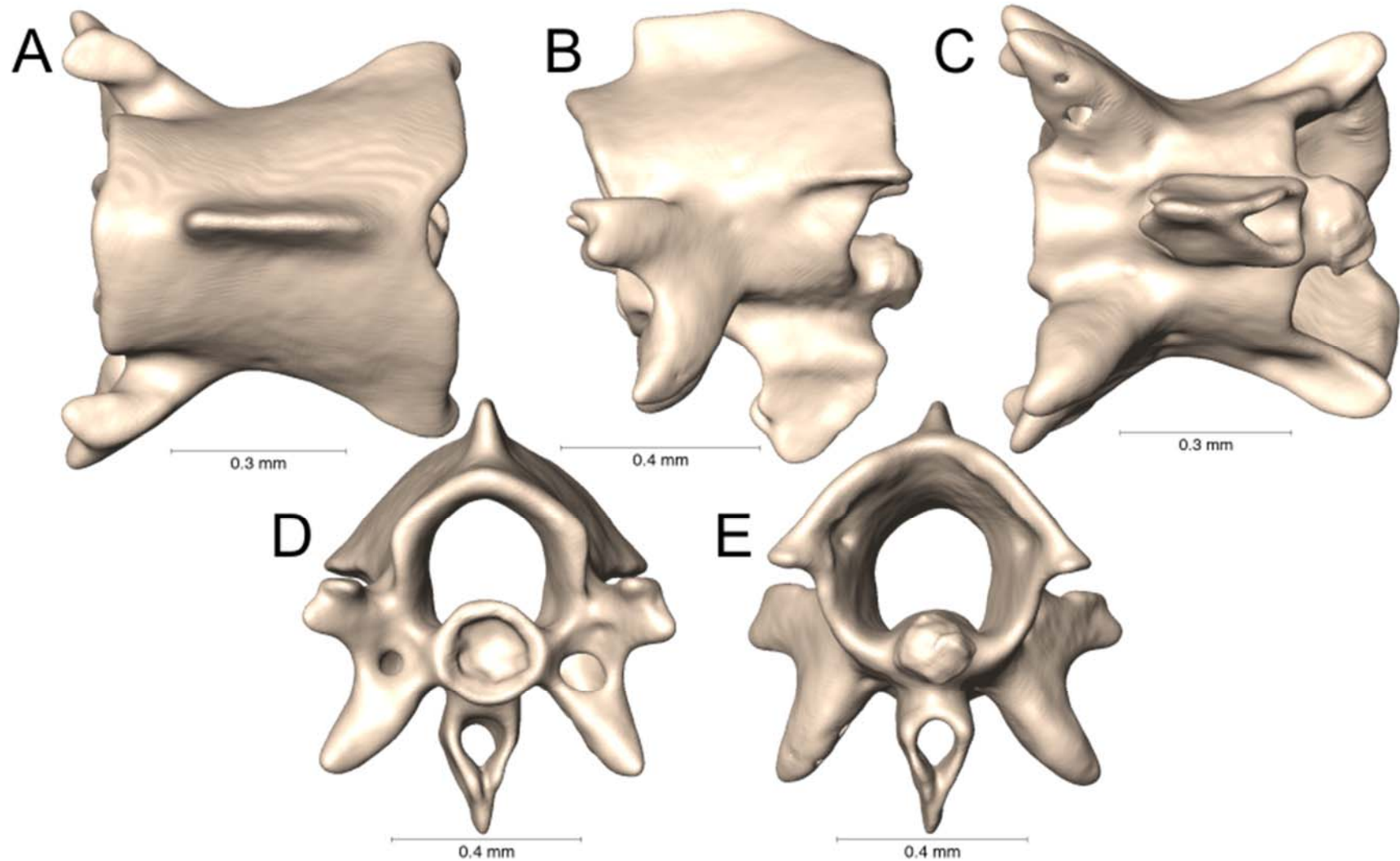
Supplemental Figure 5.39. Dorsal, lateral, ventral, anterior, and posterior views (A-E, respectively) of the caudal vertebra of *Micrurus elegans veraepacis* (UTA R-58869).



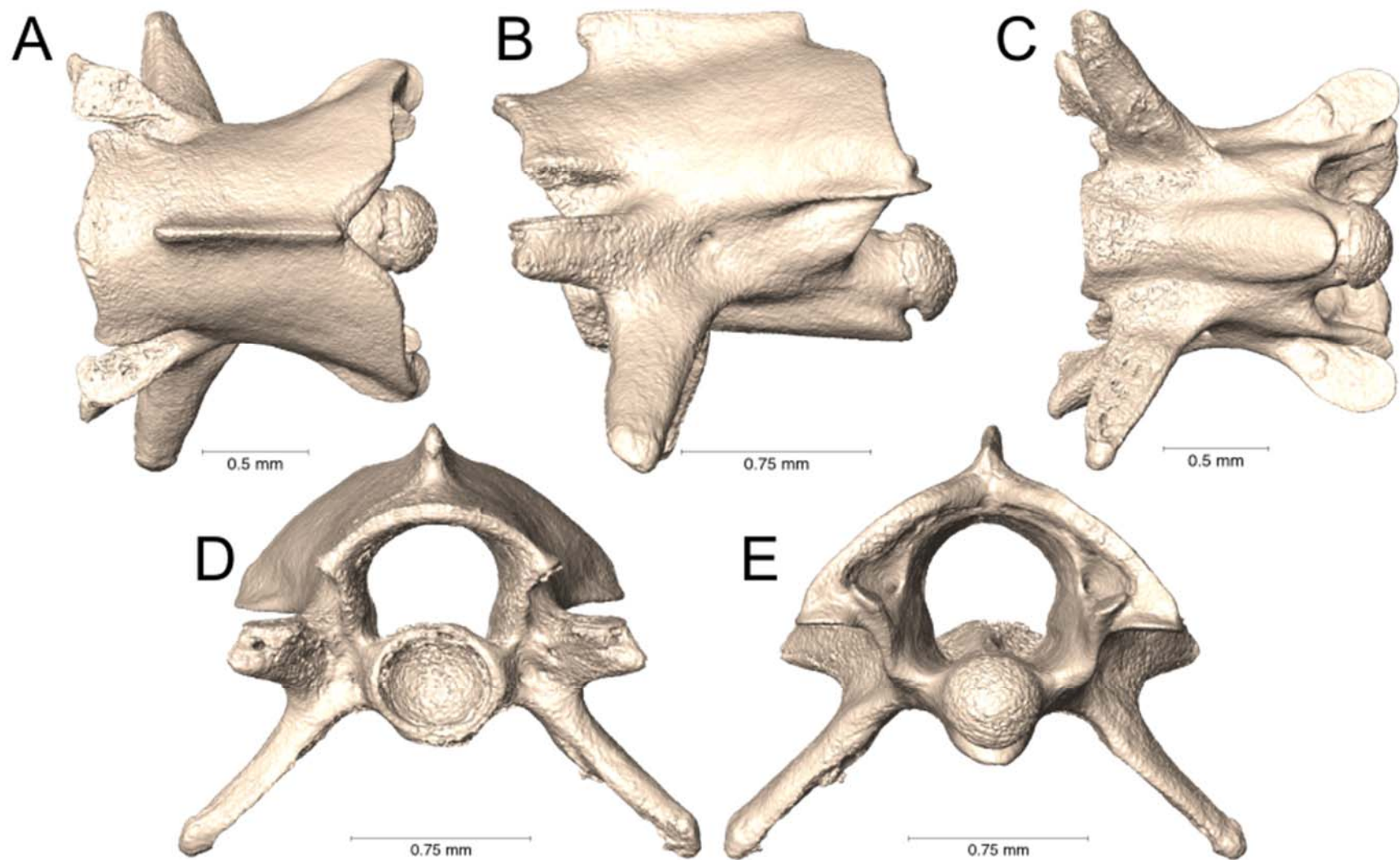
Supplemental Figure 5.40. Dorsal, lateral, ventral, anterior, and posterior views (A-E, respectively) of the caudal vertebra of *Micrurus ephippifer* (UTA R-64863).



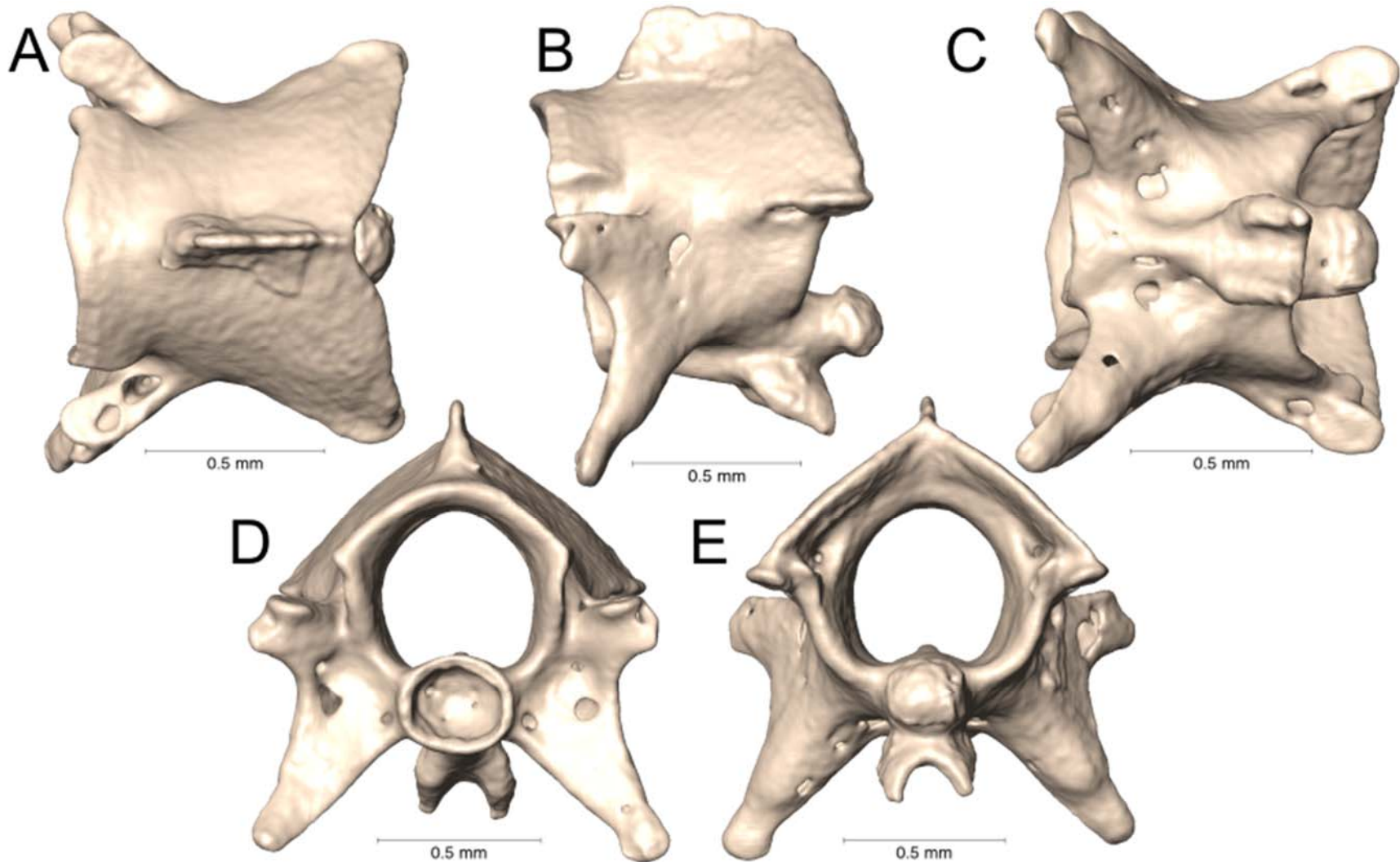
Supplemental Figure 5.41. Dorsal, lateral, ventral, anterior, and posterior views (A-E, respectively) of the caudal vertebra of *Micrurus filiformis* (UTA R-3423).



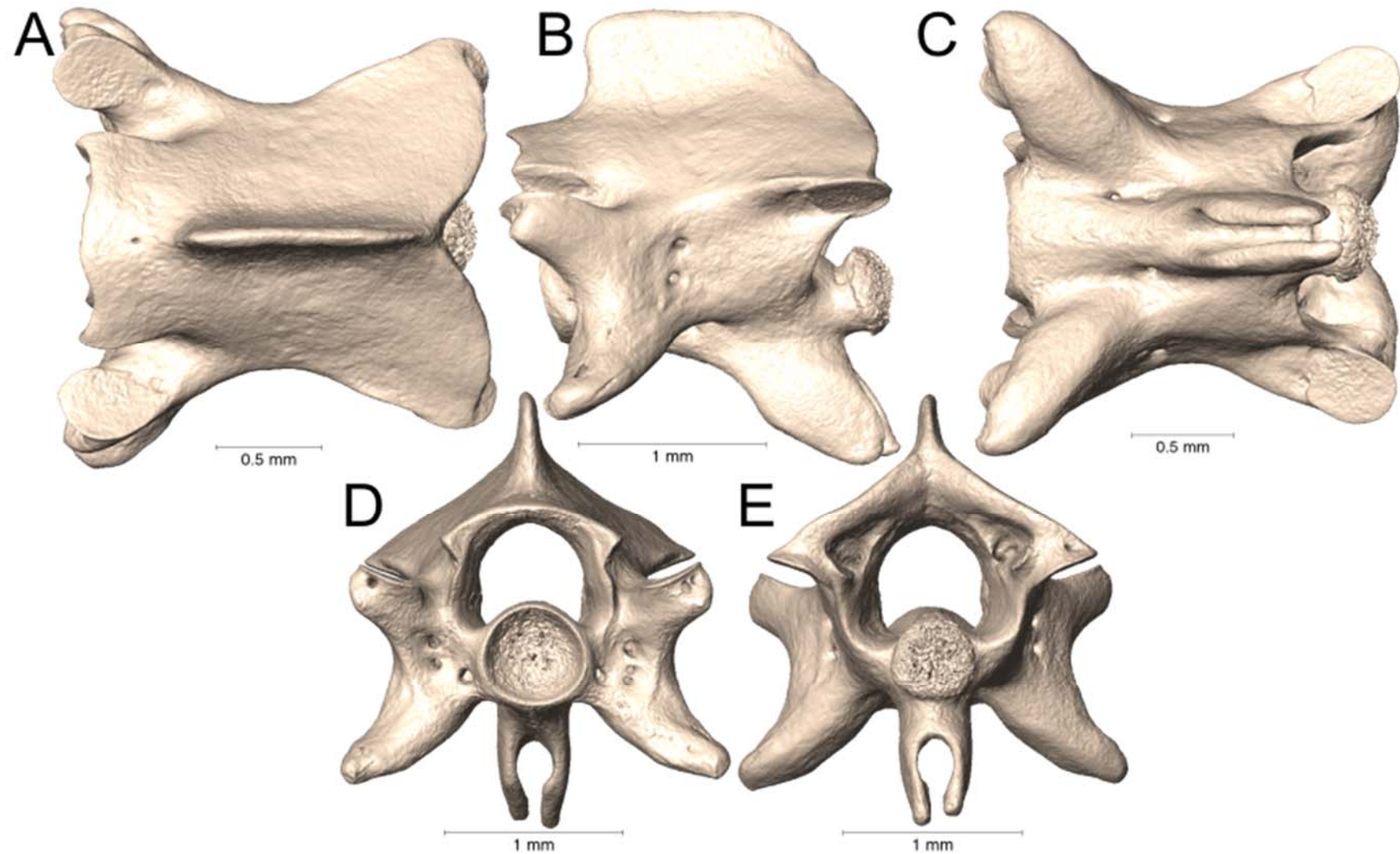
Supplemental Figure 5.42. Dorsal, lateral, ventral, anterior, and posterior views (A-E, respectively) of the caudal vertebra of *Micrurus filiformis* (UTA R-65836).



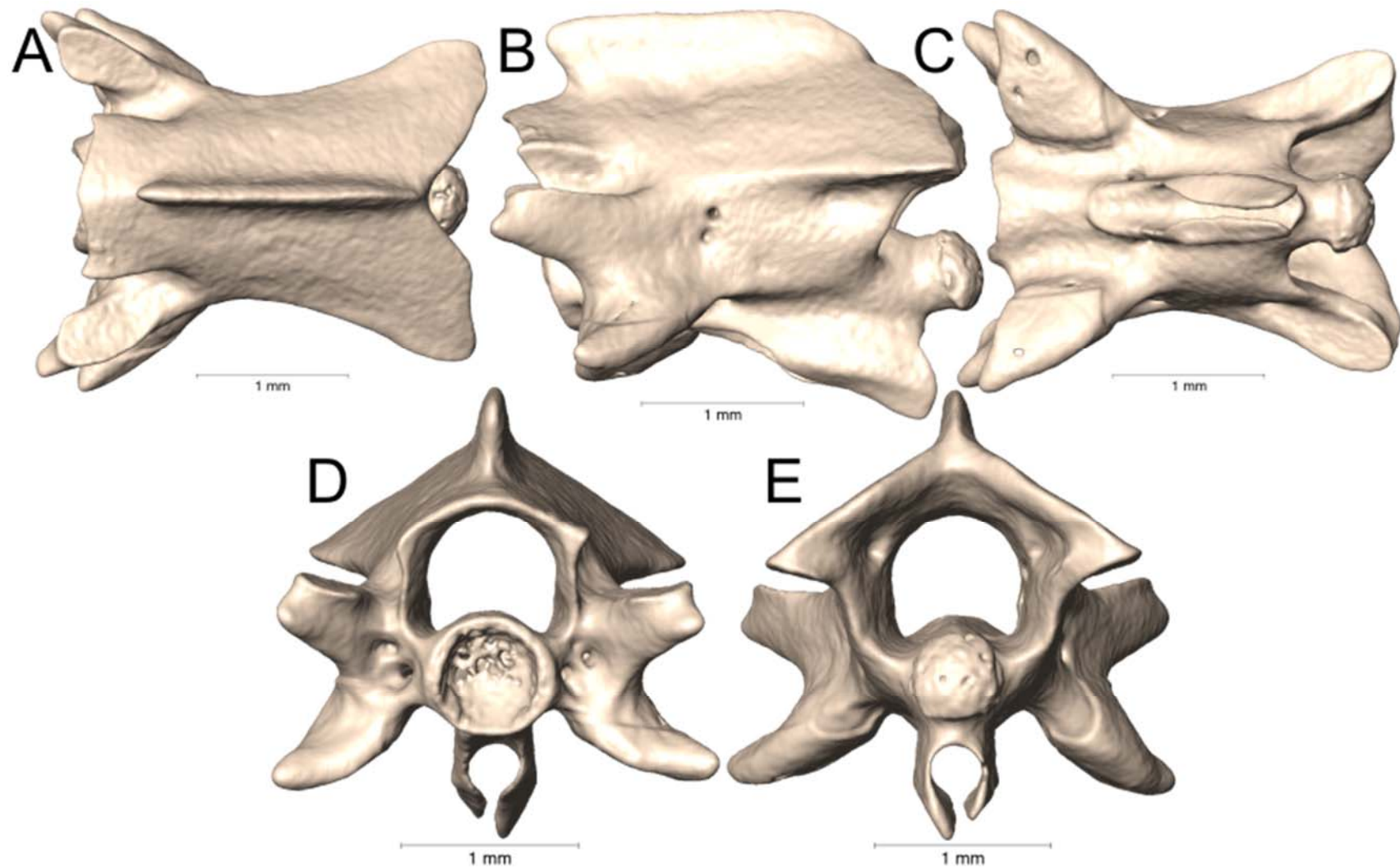
Supplemental Figure 5.43. Dorsal, lateral, ventral, anterior, and posterior views (A-E, respectively) of the caudal vertebra of *Micrurus fulvius* (UTA R-61632).



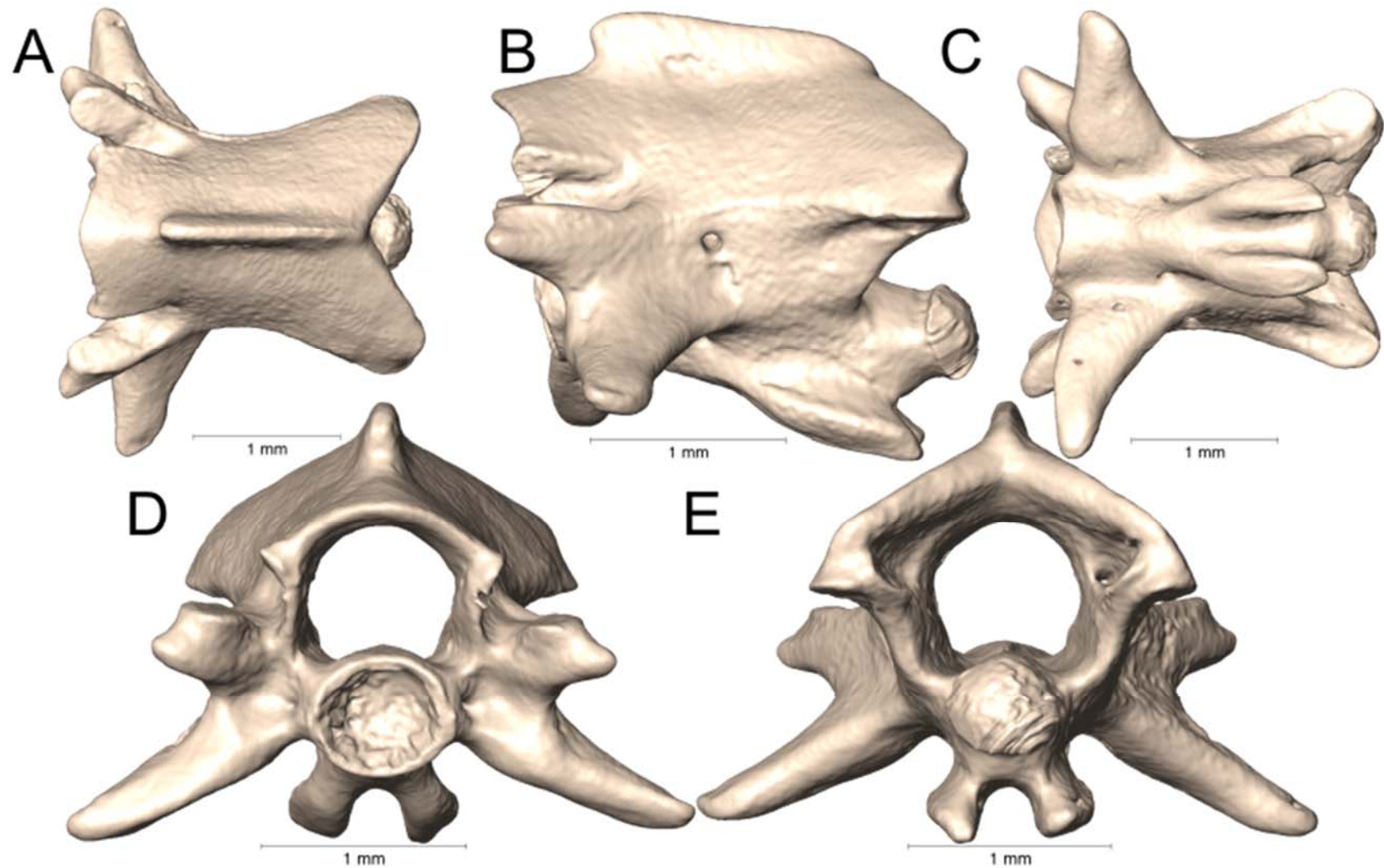
Supplemental Figure 5.44. Dorsal, lateral, ventral, anterior, and posterior views (A-E, respectively) of the caudal vertebra of *Micrurus helleri* (UTA R-38005).



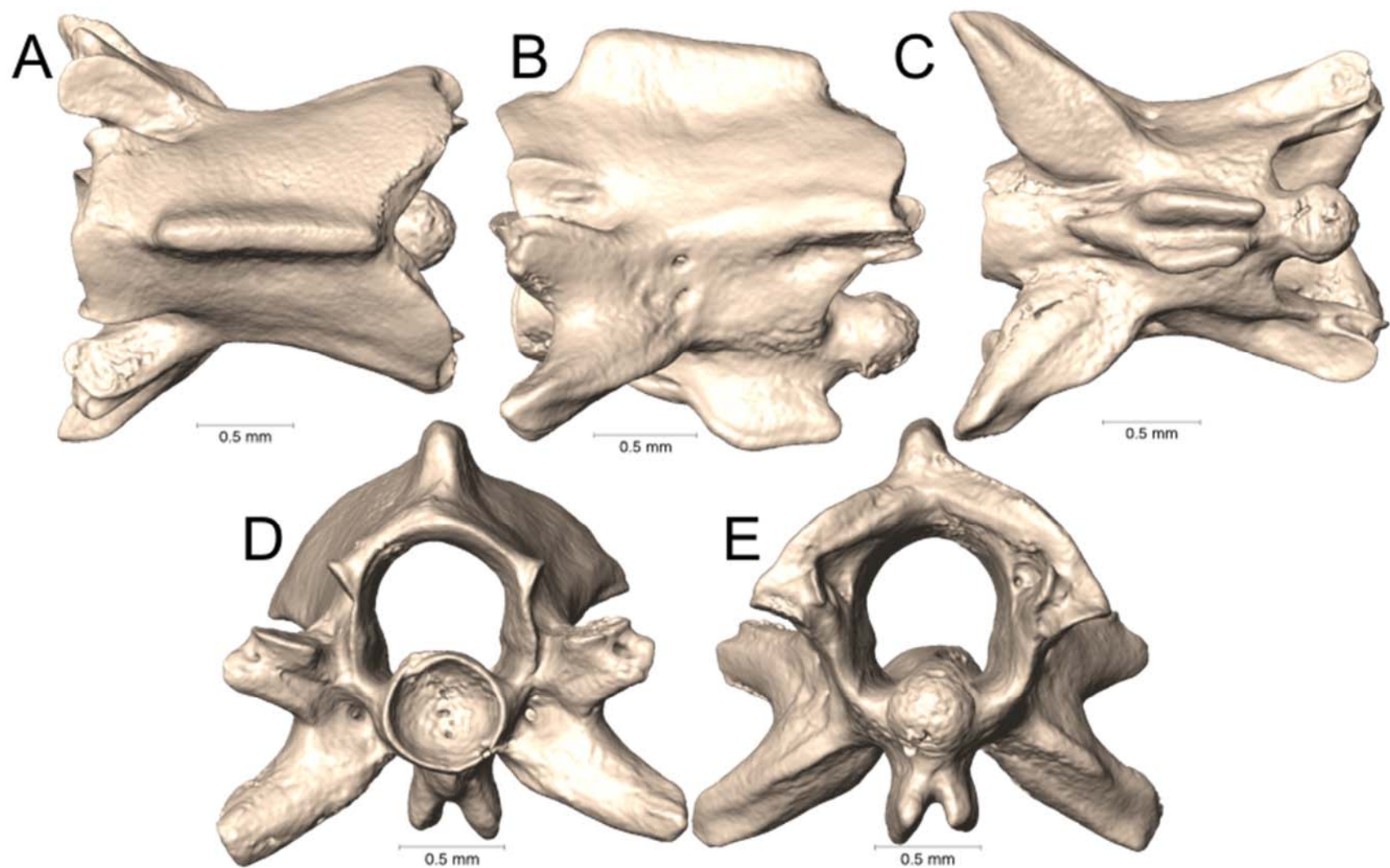
Supplemental Figure 5.45. Dorsal, lateral, ventral, anterior, and posterior views (A-E, respectively) of the caudal vertebra of *Micrurus helleri* (UTA R-55977).



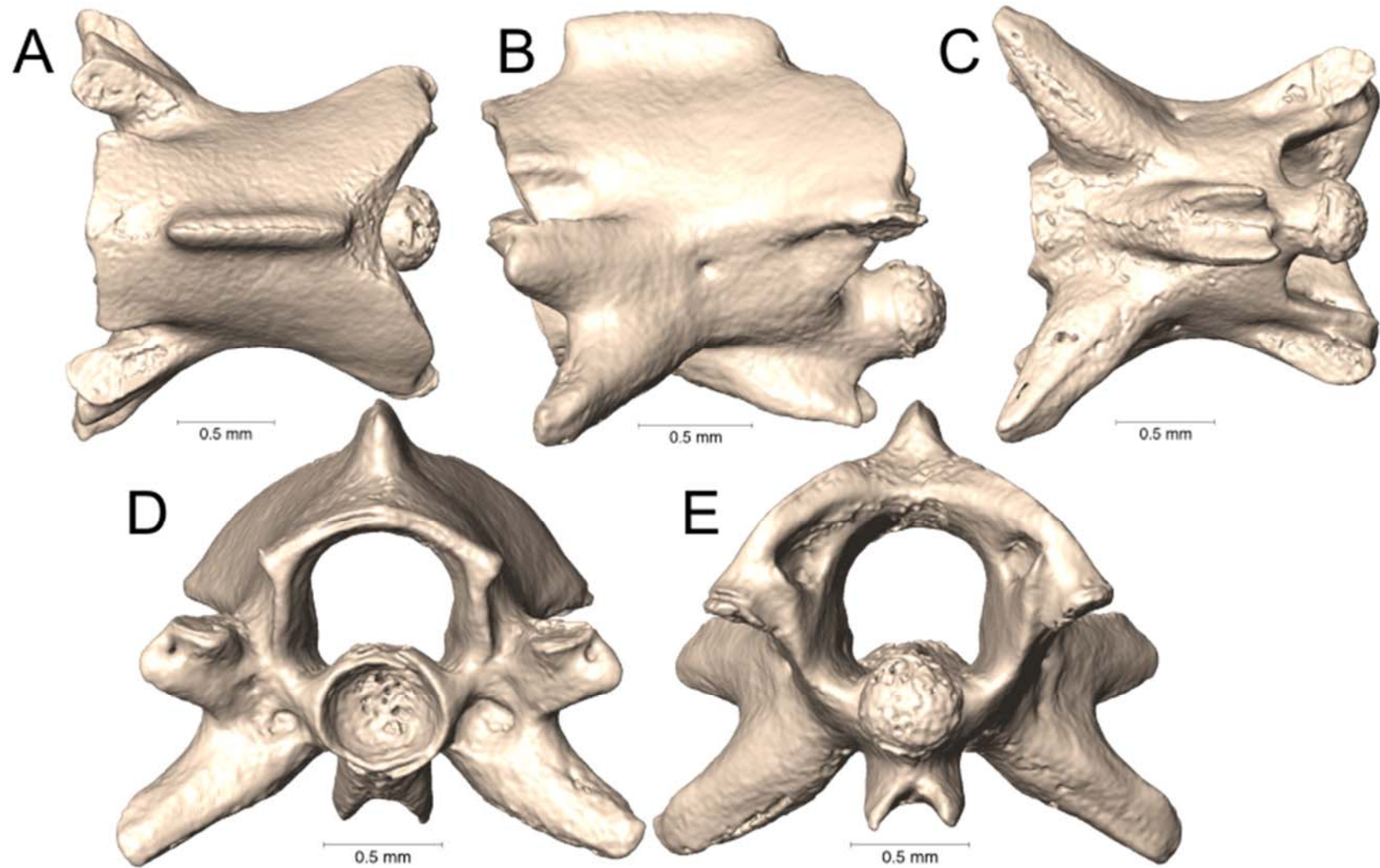
Supplemental Figure 5.46. Dorsal, lateral, ventral, anterior, and posterior views (A-E, respectively) of the caudal vertebra of *Micrurus hemprichii* (UTA R-9683).



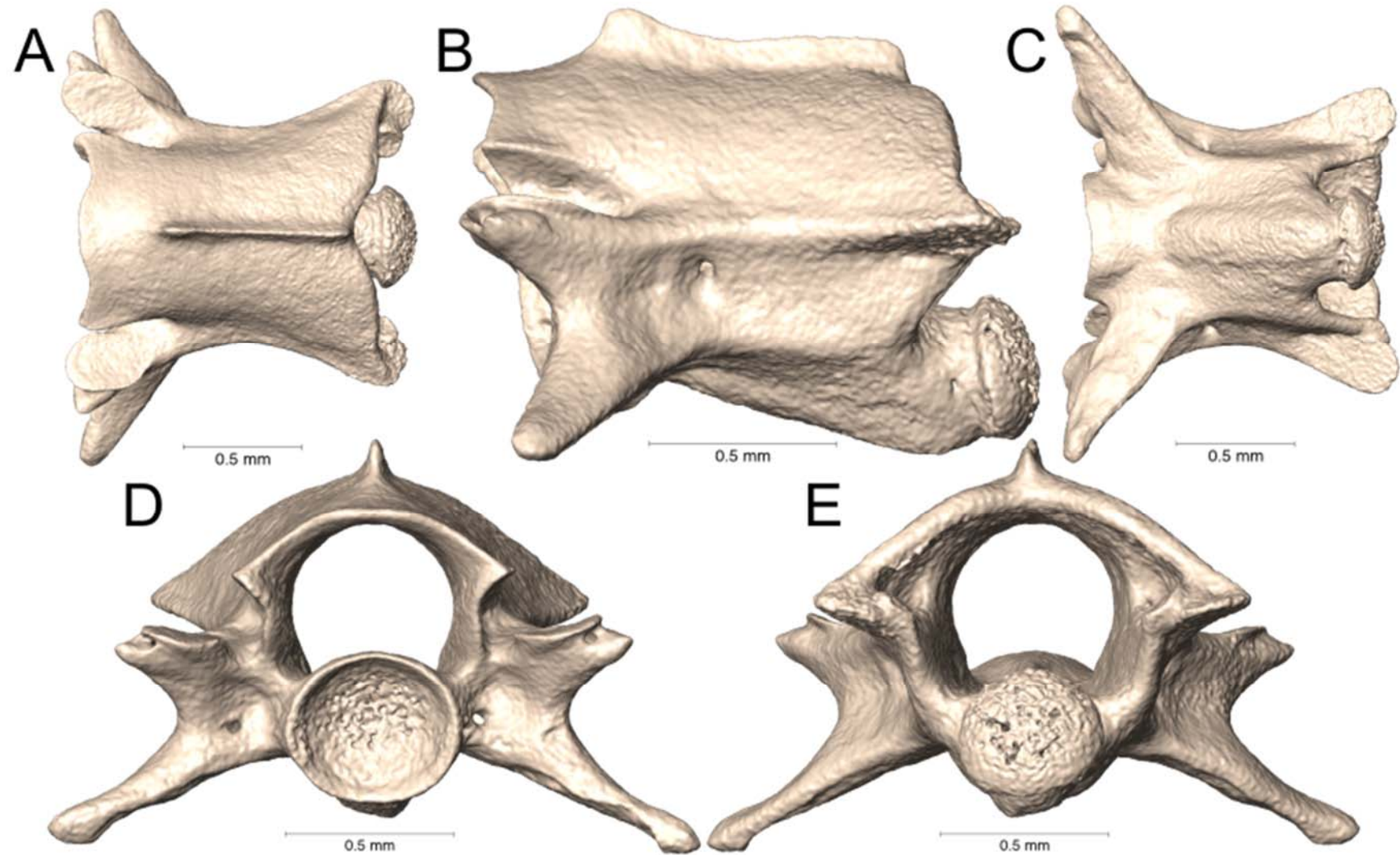
Supplemental Figure 5.47. Dorsal, lateral, ventral, anterior, and posterior views (A-E, respectively) of the caudal vertebra of *Micrurus hemprichii* (UTA R-29997).



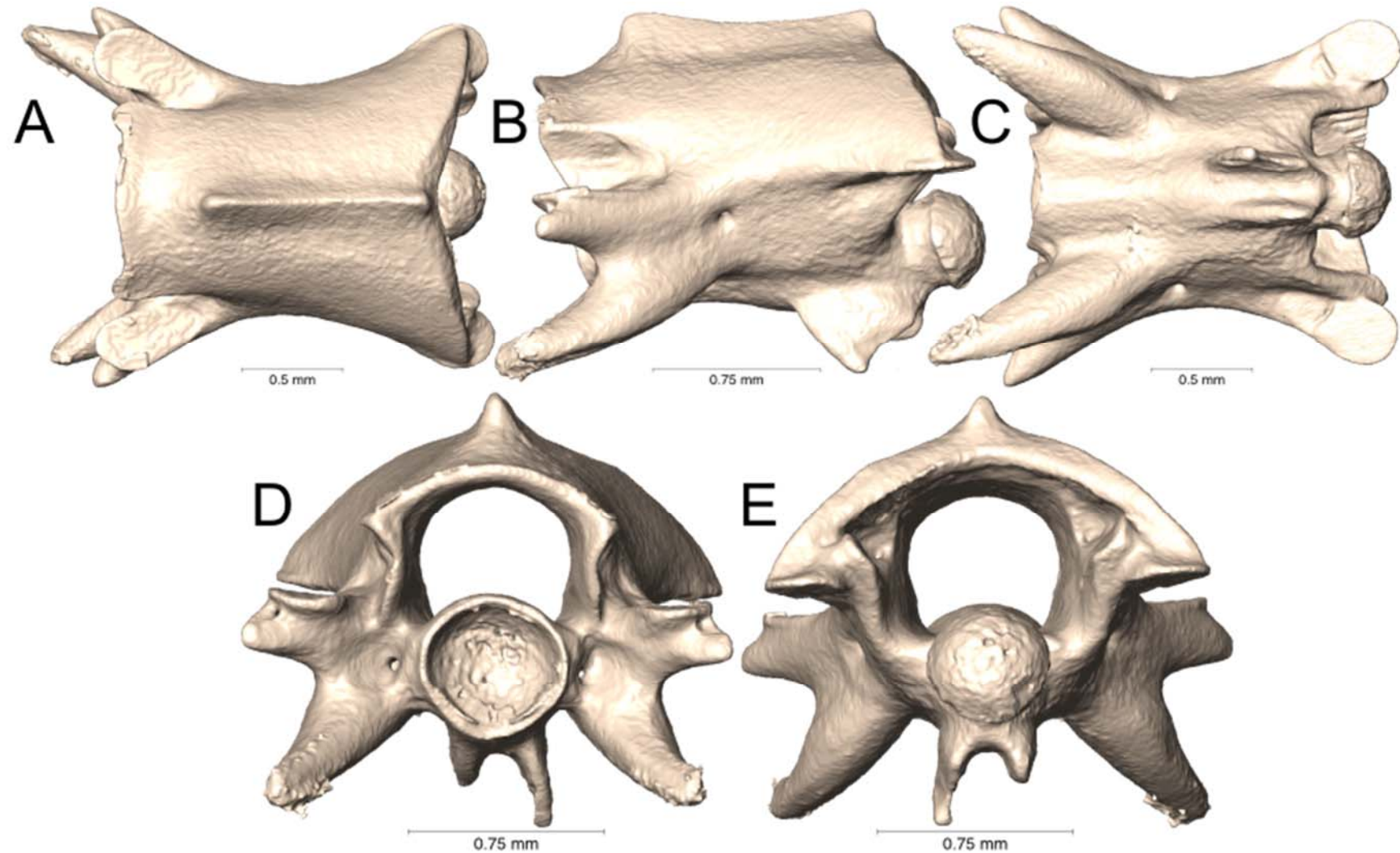
Supplemental Figure 5.48. Dorsal, lateral, ventral, anterior, and posterior views (A-E, respectively) of the caudal vertebra of *Micrurus isozonus* (UTA R-3951).



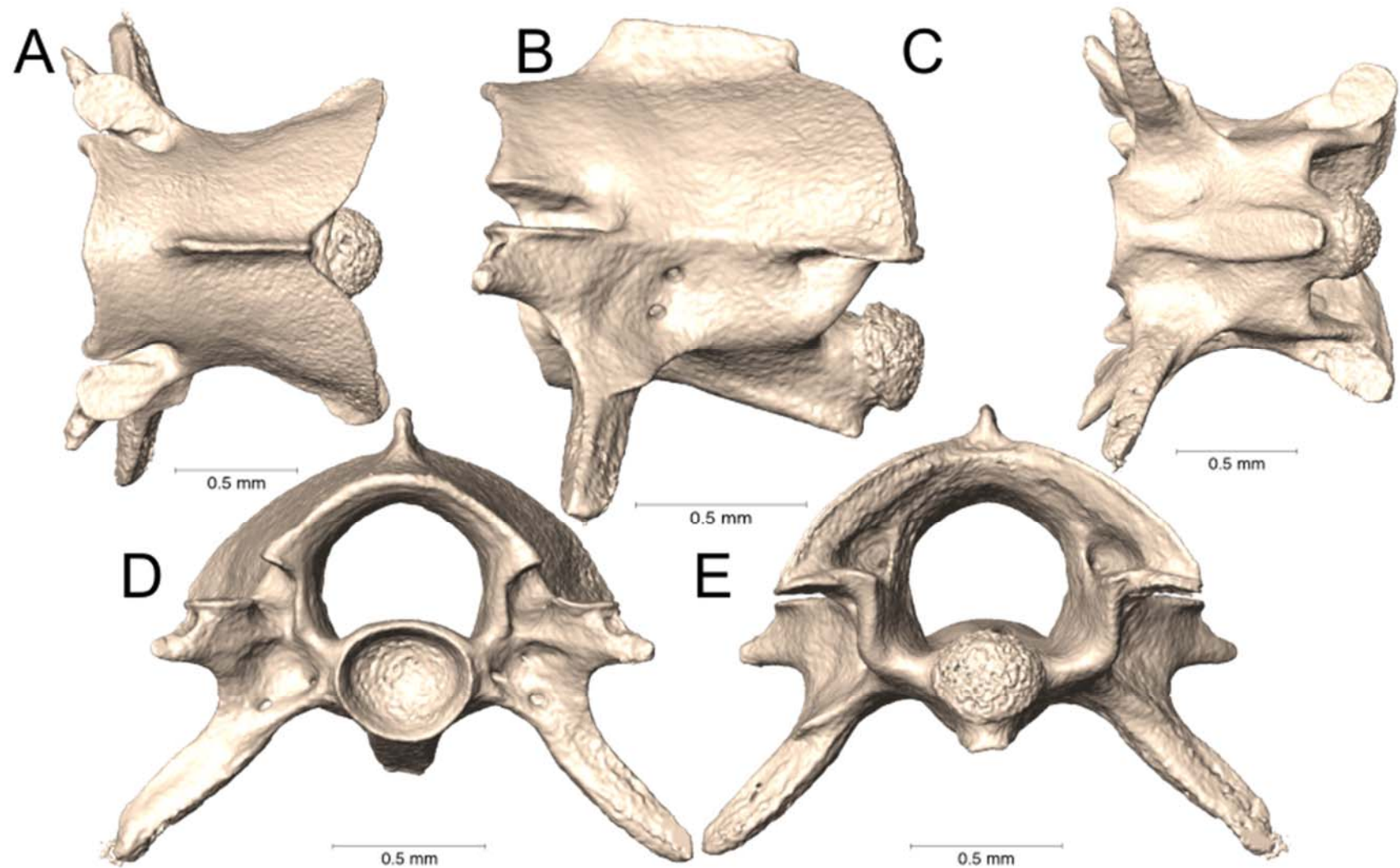
Supplemental Figure 5.49. Dorsal, lateral, ventral, anterior, and posterior views (A-E, respectively) of the caudal vertebra of *Micrurus isozonus* (UTA R-22589).



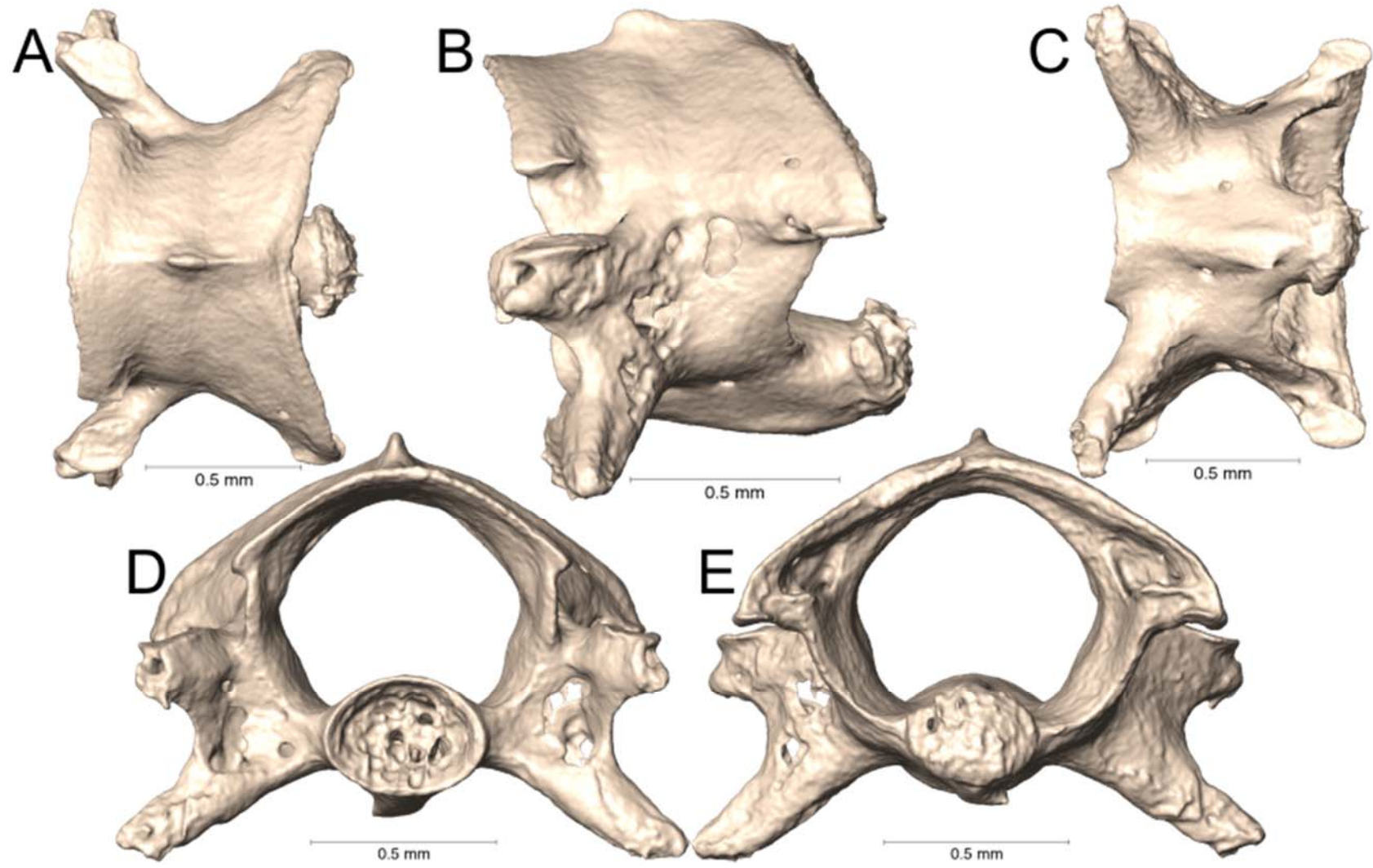
Supplemental Figure 5.50. Dorsal, lateral, ventral, anterior, and posterior views (A-E, respectively) of the caudal vertebra of *Micrurus laticollaris* (UTA R-52559).



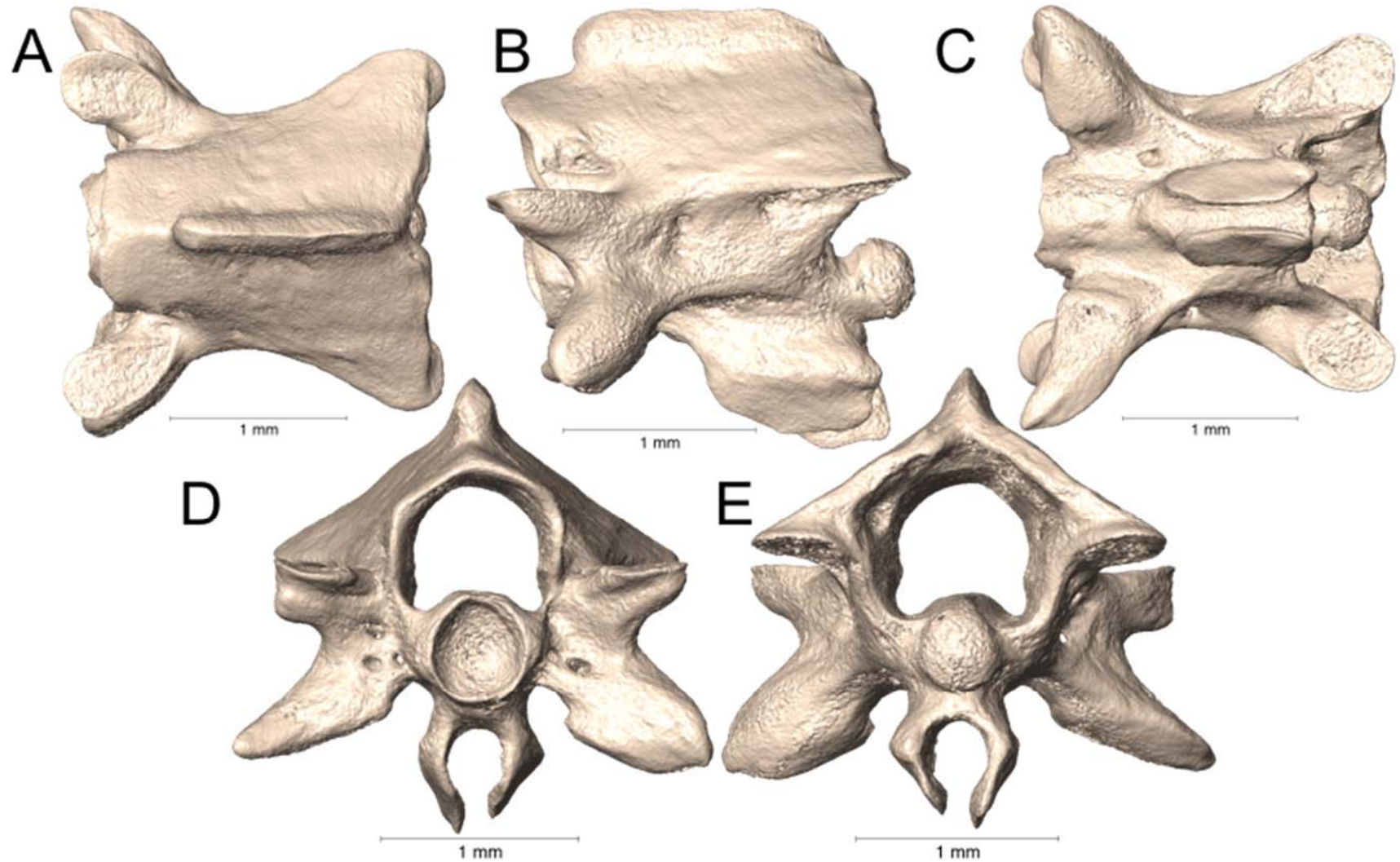
Supplemental Figure 5.51. Dorsal, lateral, ventral, anterior, and posterior views (A-E, respectively) of the caudal vertebra of *Micrurus laticollaris* (UTA R-57562).



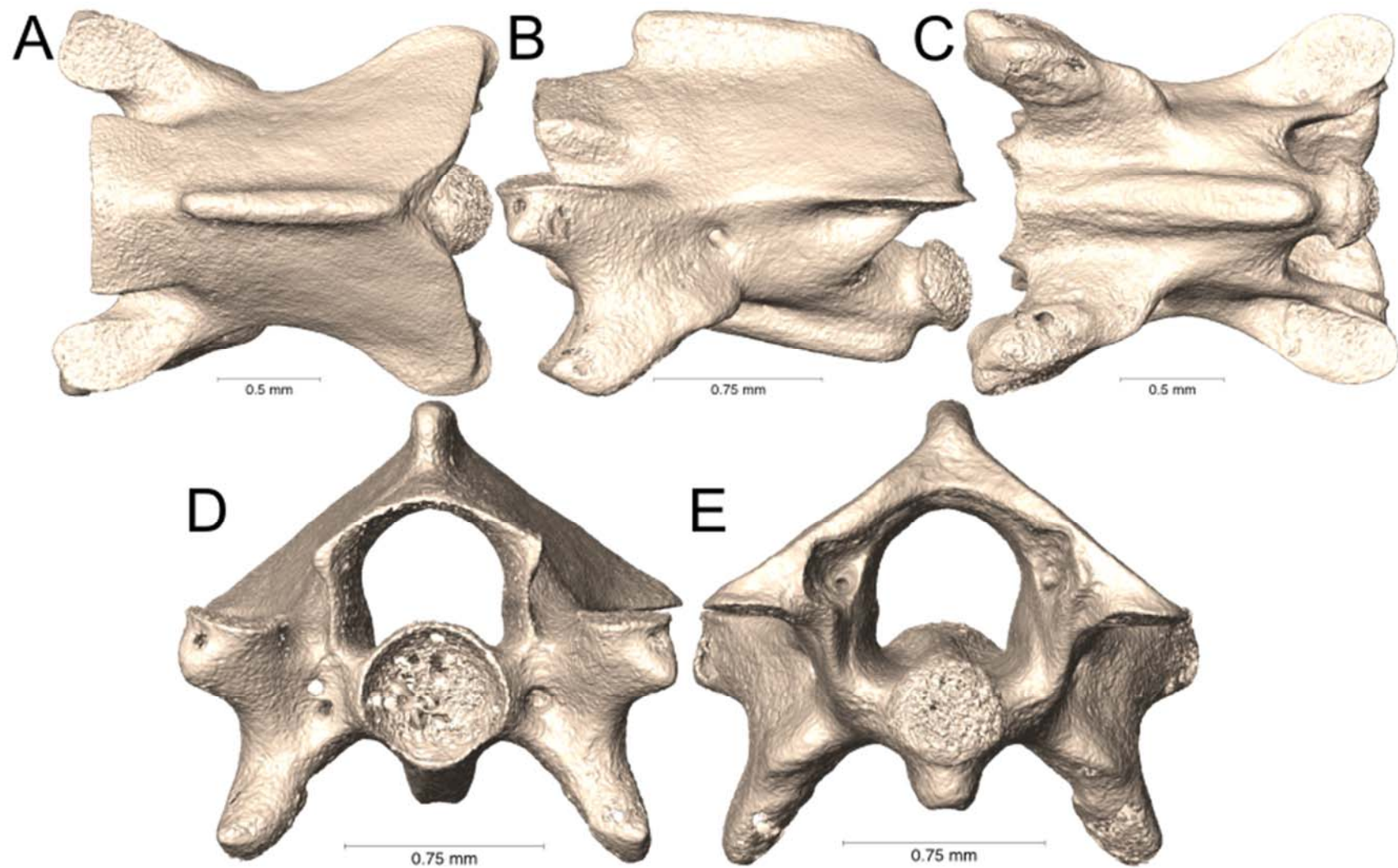
Supplemental Figure 5.52. Dorsal, lateral, ventral, anterior, and posterior views (A-E, respectively) of the caudal vertebra of *Micrurus latifasciatus* (UTA R-4606).



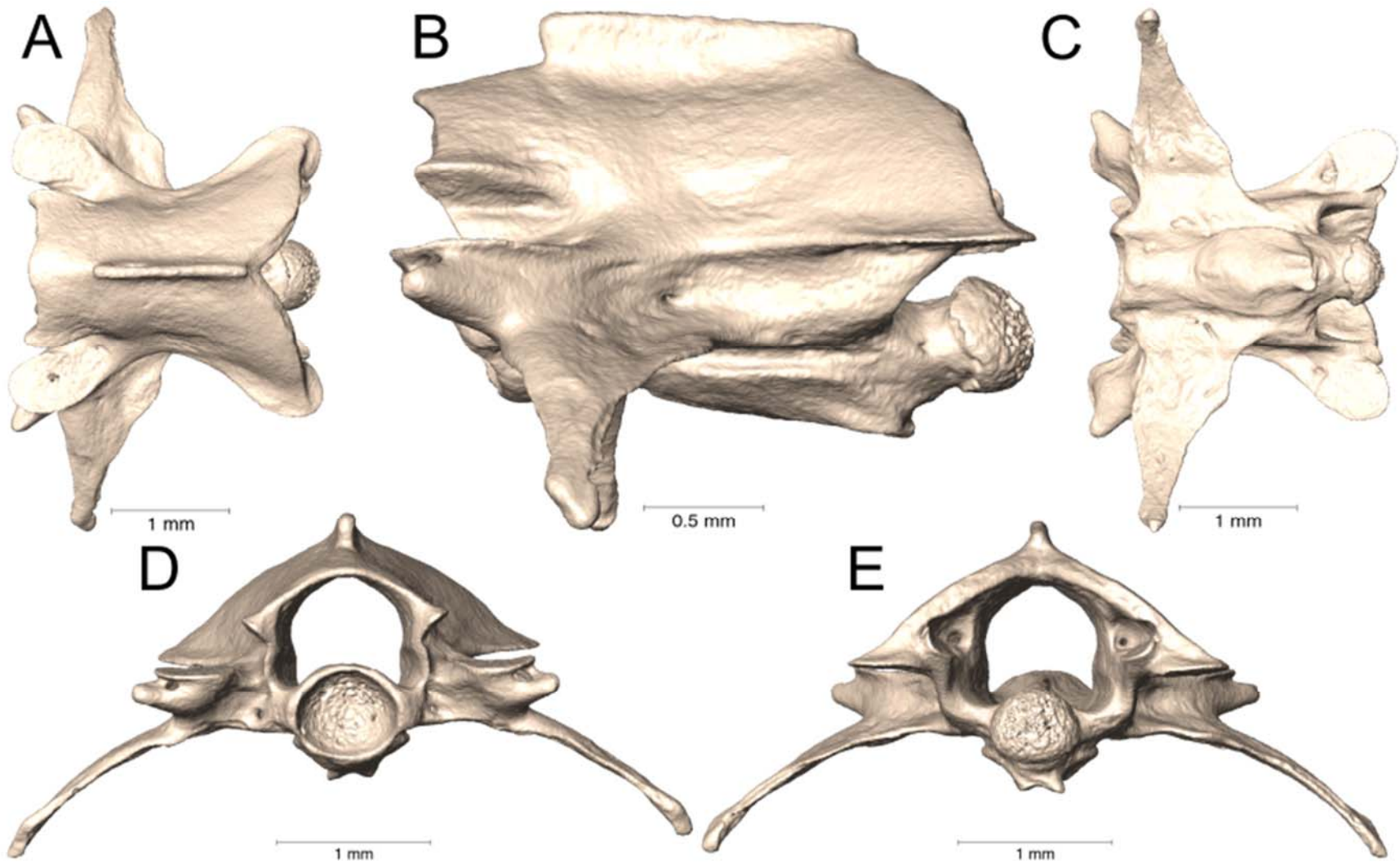
Supplemental Figure 5.53. Dorsal, lateral, ventral, anterior, and posterior views (A-E, respectively) of the caudal vertebra of *Micrurus lemniscatus* cf. *helleri* (UTA R-34563).



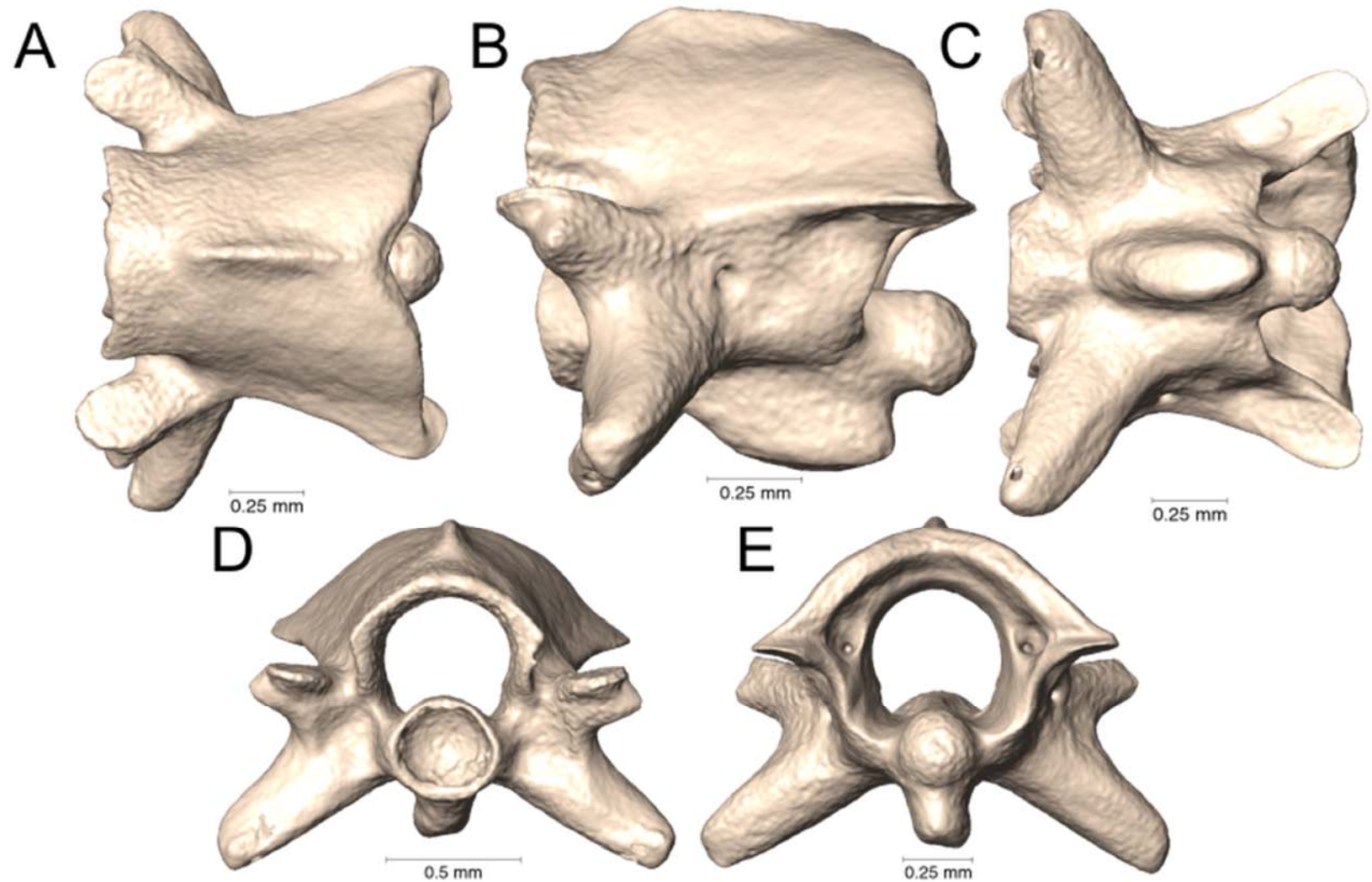
Supplemental Figure 5.54. Dorsal, lateral, ventral, anterior, and posterior views (A-E, respectively) of the caudal vertebra of *Micrurus lemniscatus* cf. *helleri* (UTA R-65803).



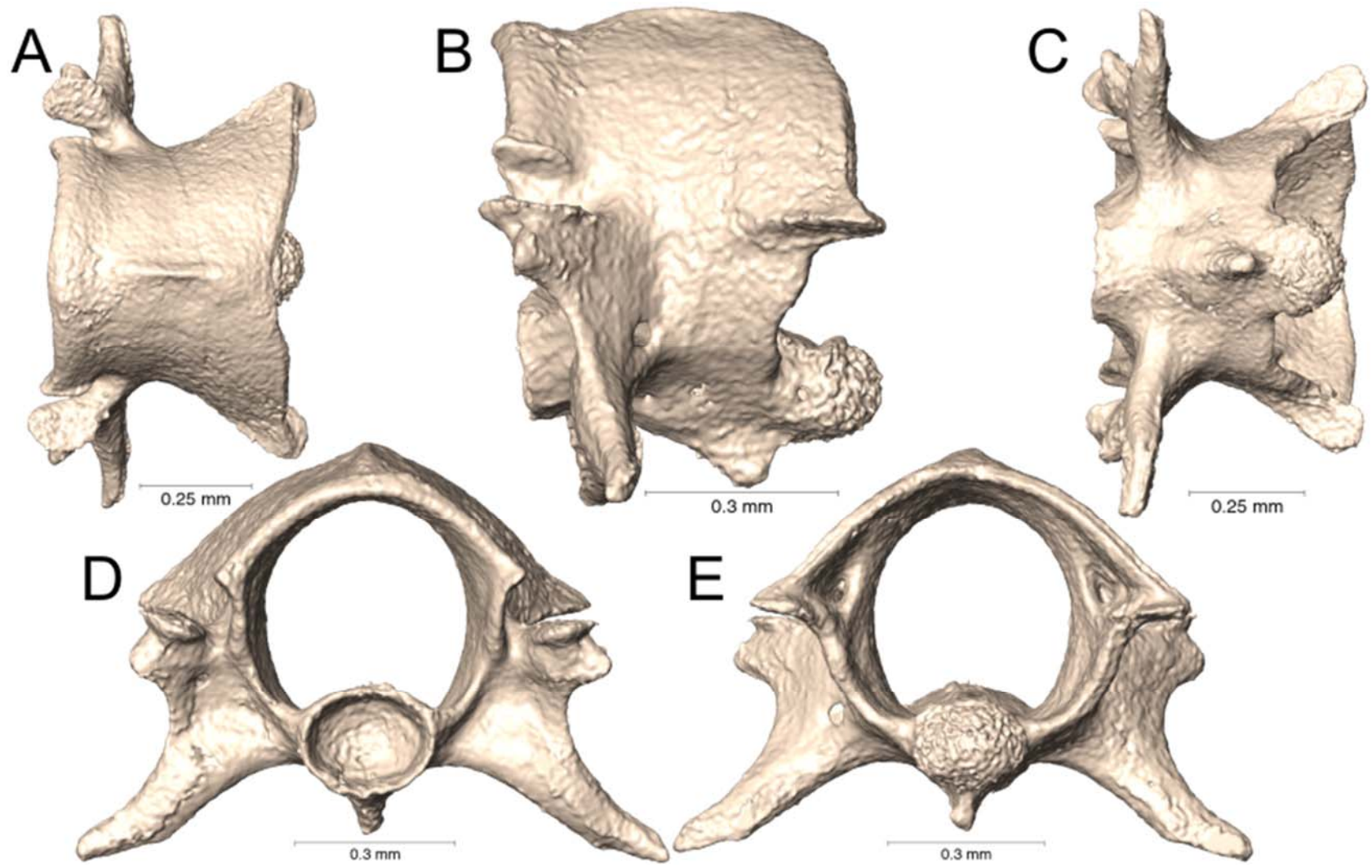
Supplemental Figure 5.55. Dorsal, lateral, ventral, anterior, and posterior views (A-E, respectively) of the caudal vertebra of *Micrurus limbatus* (UTA R-64852).



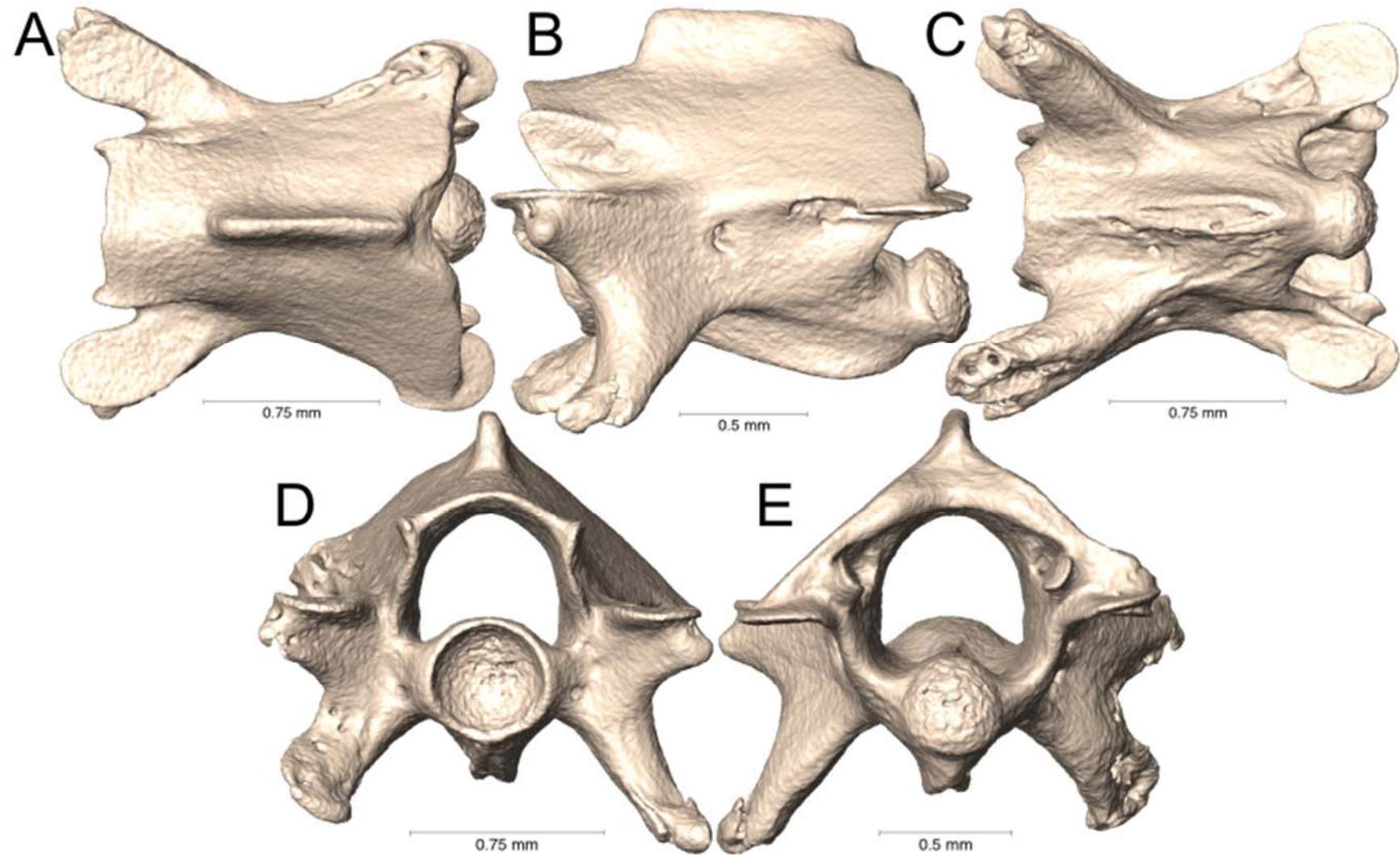
Supplemental Figure 5.56. Dorsal, lateral, ventral, anterior, and posterior views (A-E, respectively) of the caudal vertebra of *Micrurus limbatus* (UTA R-64899).



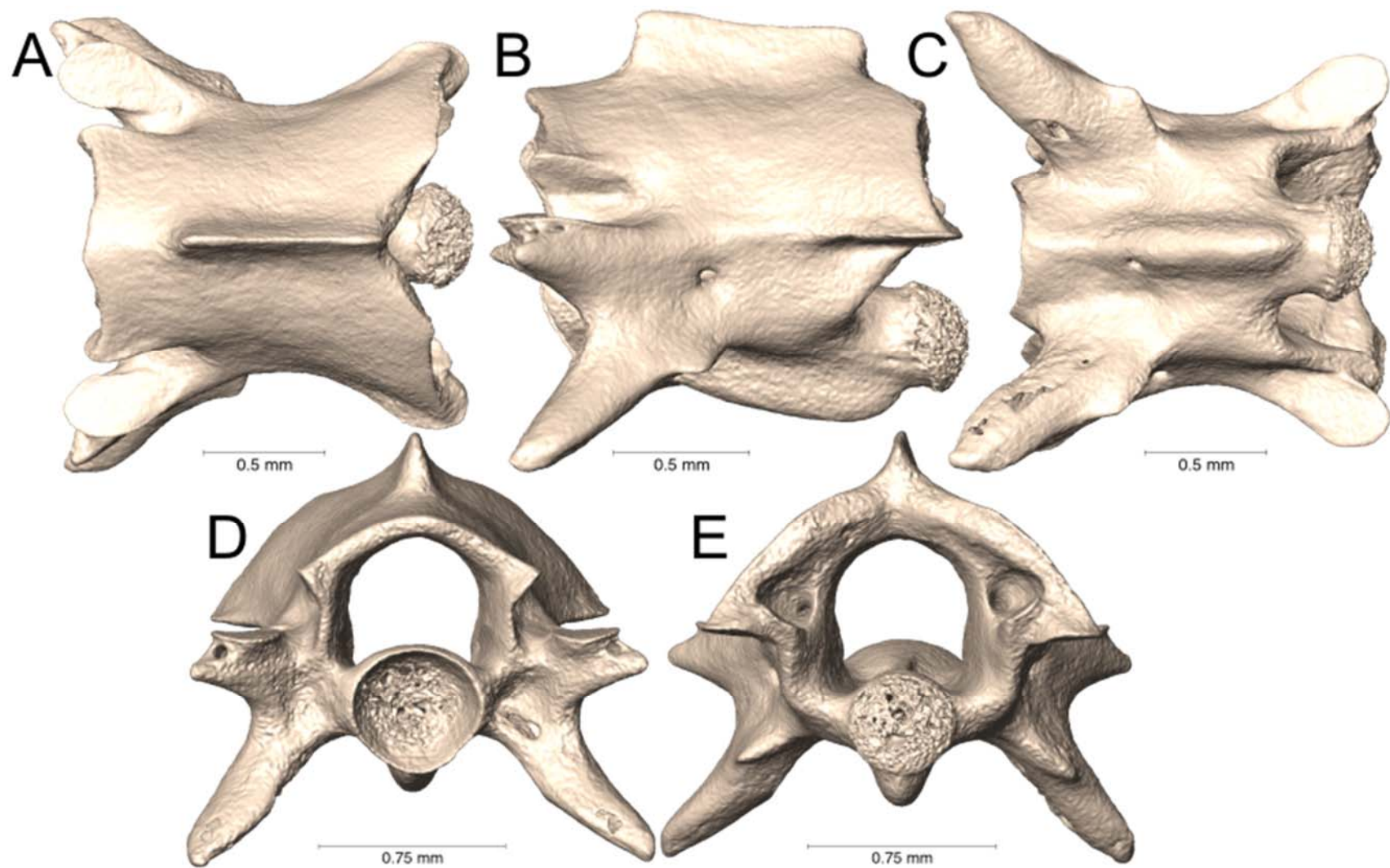
Supplemental Figure 5.57. Dorsal, lateral, ventral, anterior, and posterior views (A-E, respectively) of the caudal vertebra of *Micrurus melanotus* (AMNH 35934).



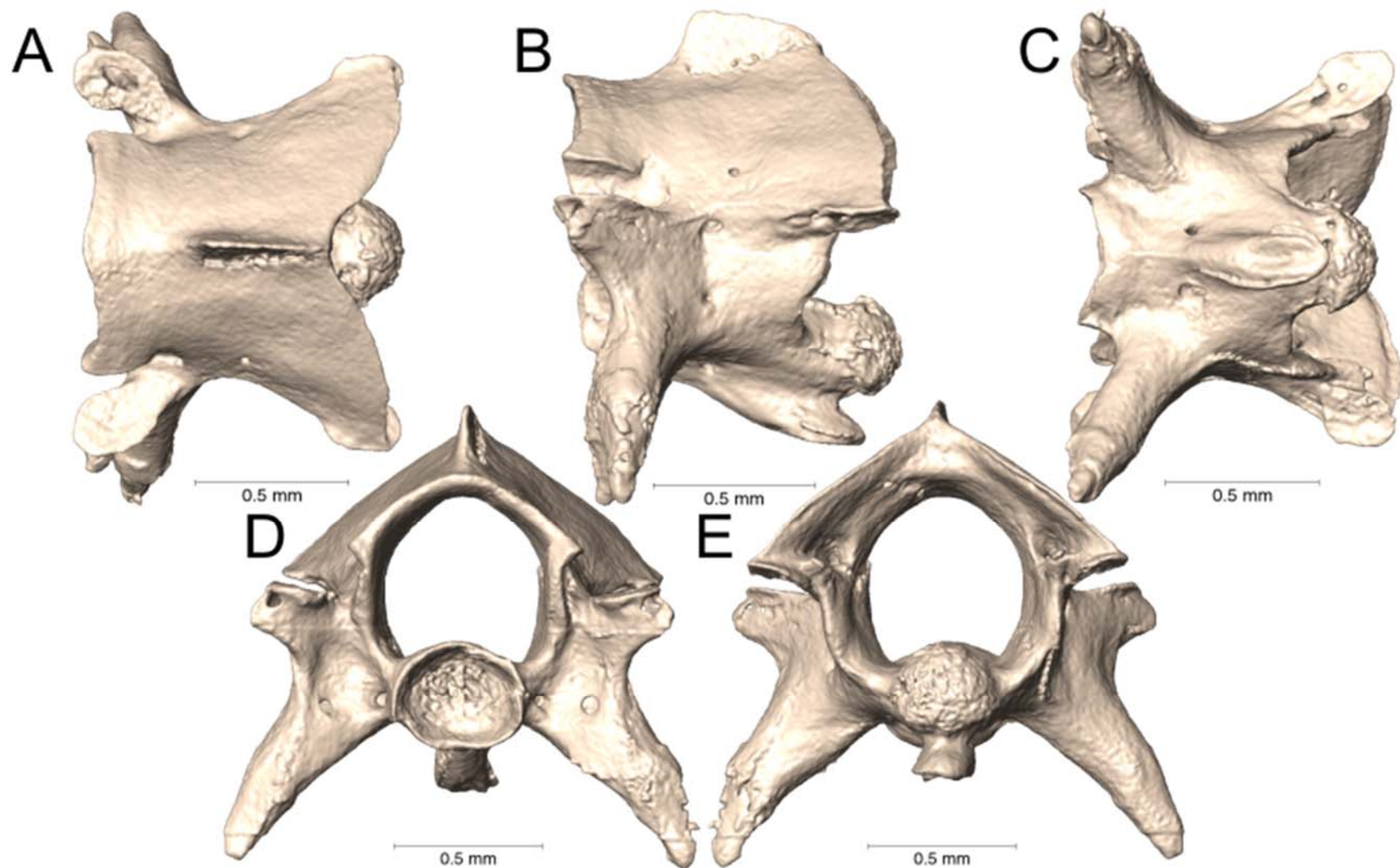
Supplemental Figure 5.58. Dorsal, lateral, ventral, anterior, and posterior views (A-E, respectively) of the caudal vertebra of *Micrurus melanotus* (UTA R-22582).



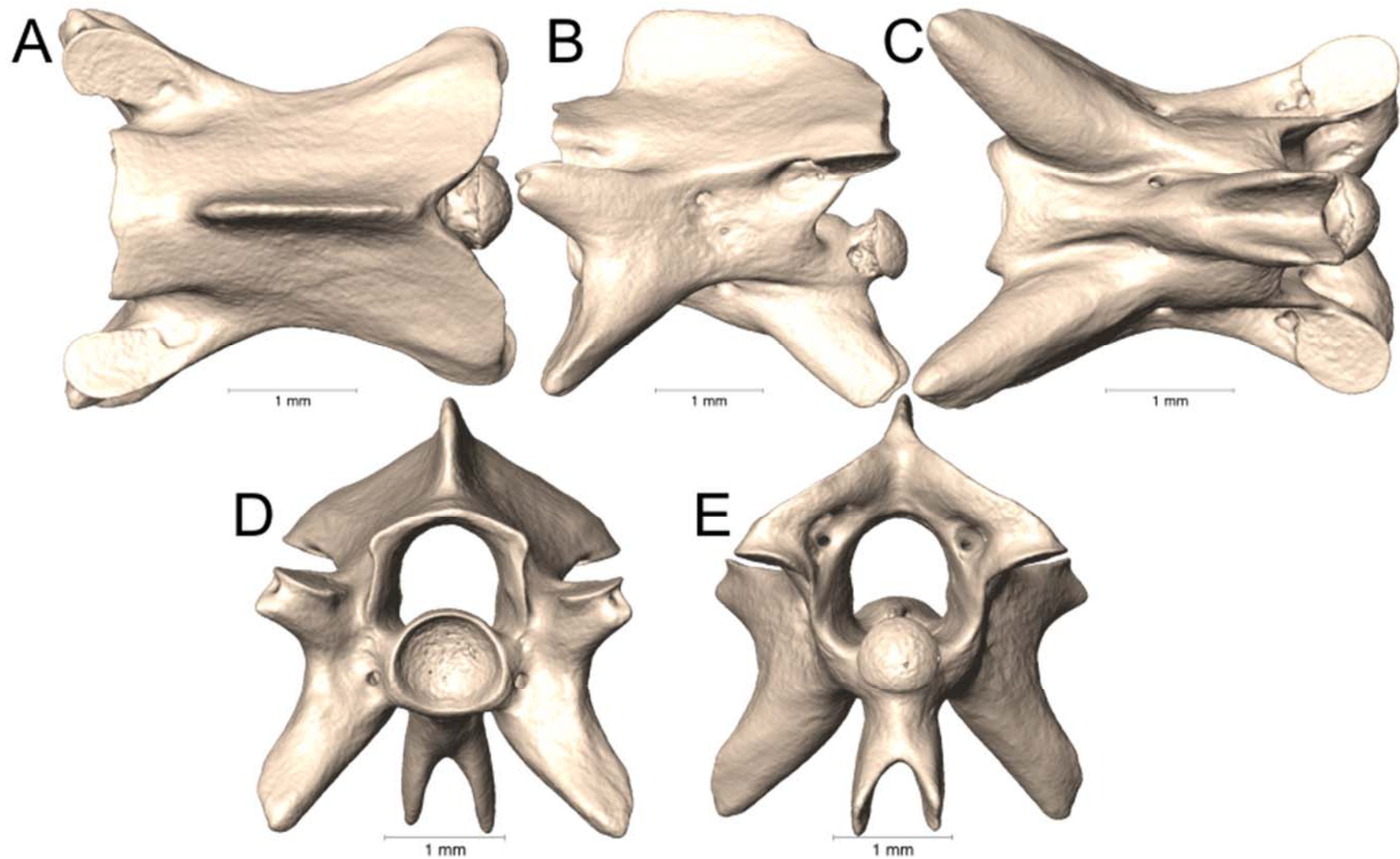
Supplemental Figure 5.59. Dorsal, lateral, ventral, anterior, and posterior views (A-E, respectively) of the caudal vertebra of *Micrurus mipartitus* (UTA R-54187).



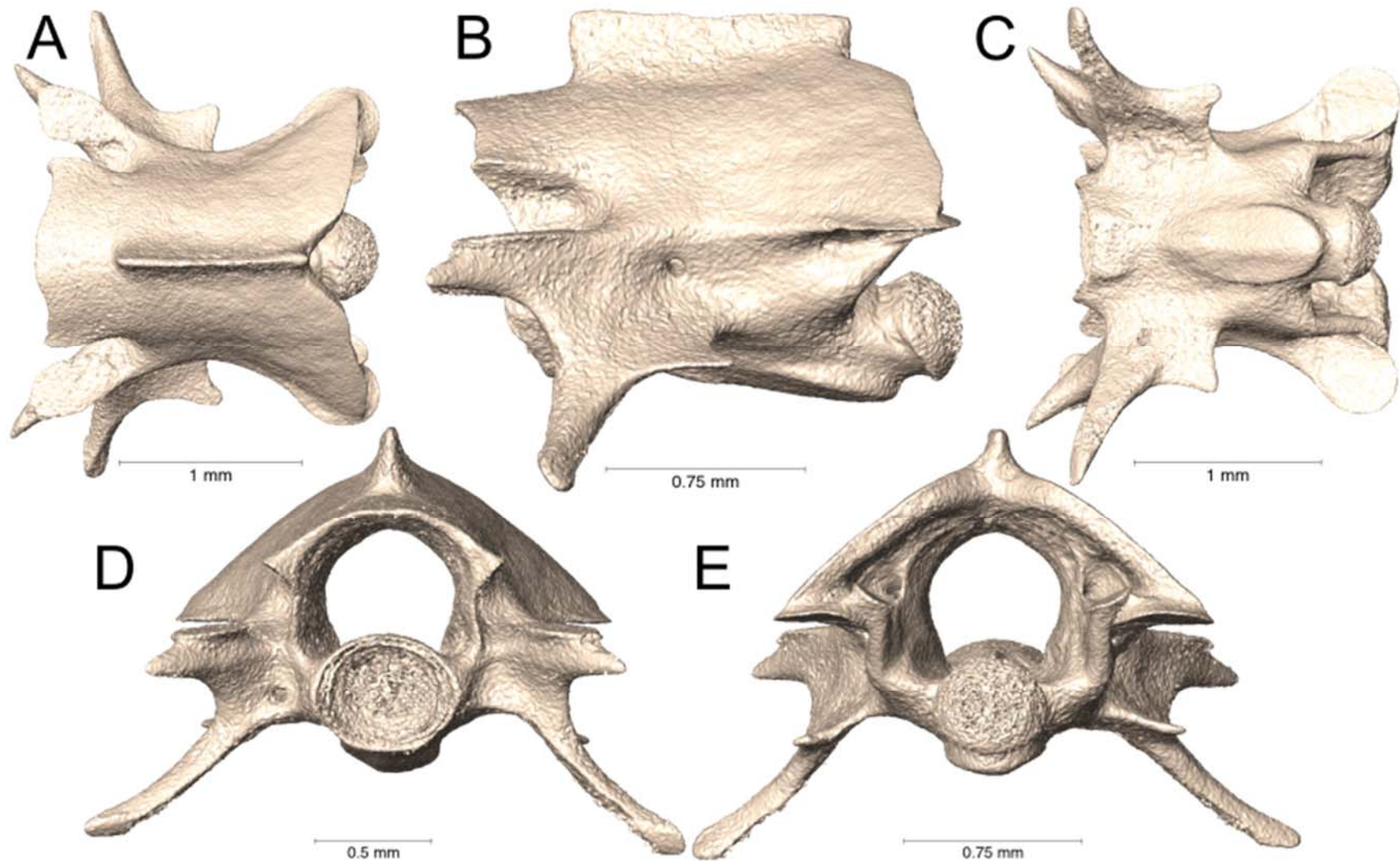
Supplemental Figure 5.60. Dorsal, lateral, ventral, anterior, and posterior views (A-E, respectively) of the caudal vertebra of *Micrurus mosquitensis* (UTA R-12919).



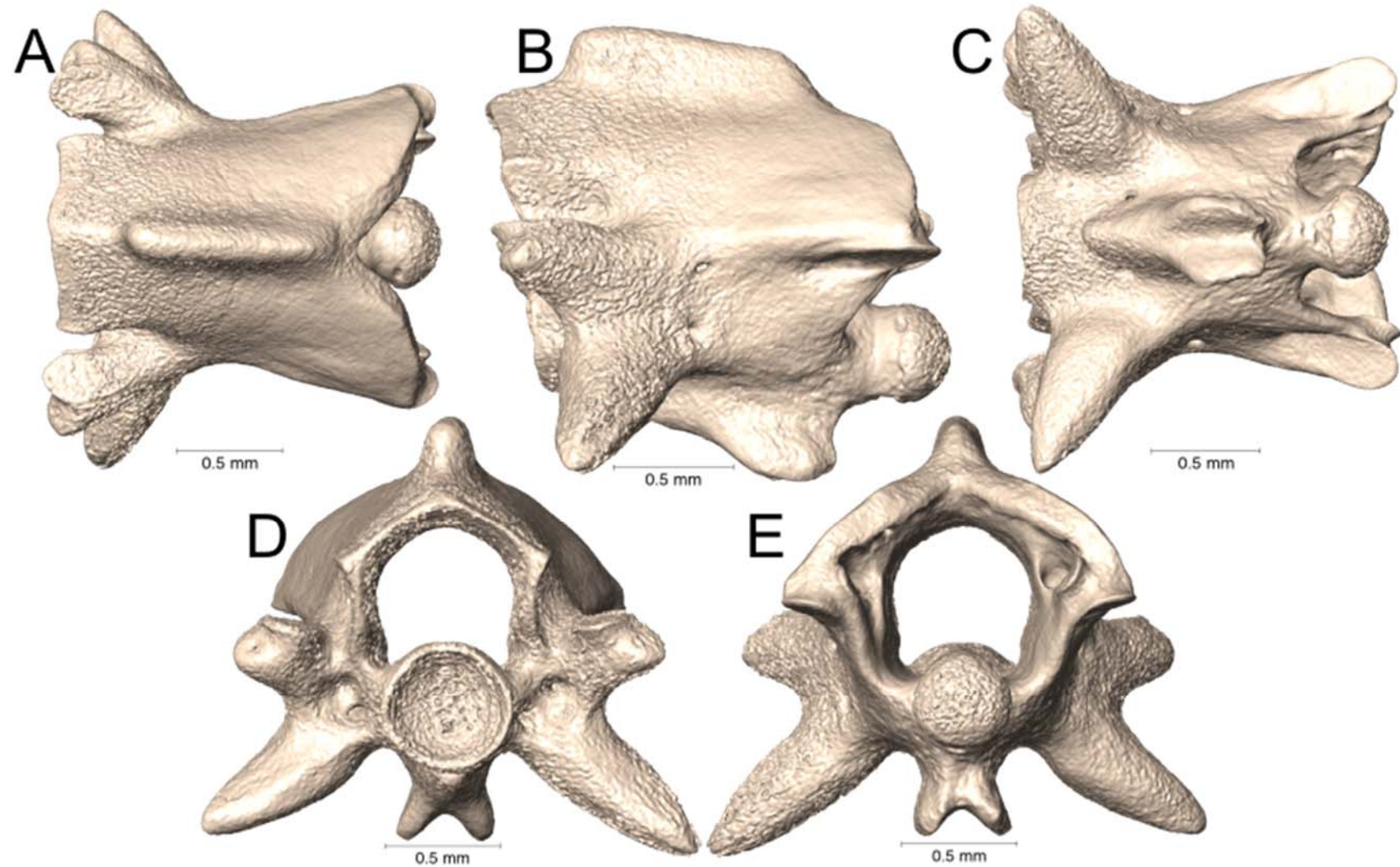
Supplemental Figure 5.61. Dorsal, lateral, ventral, anterior, and posterior views (A-E, respectively) of the caudal vertebra of *Micrurus nattereri* (UTA R-3594).



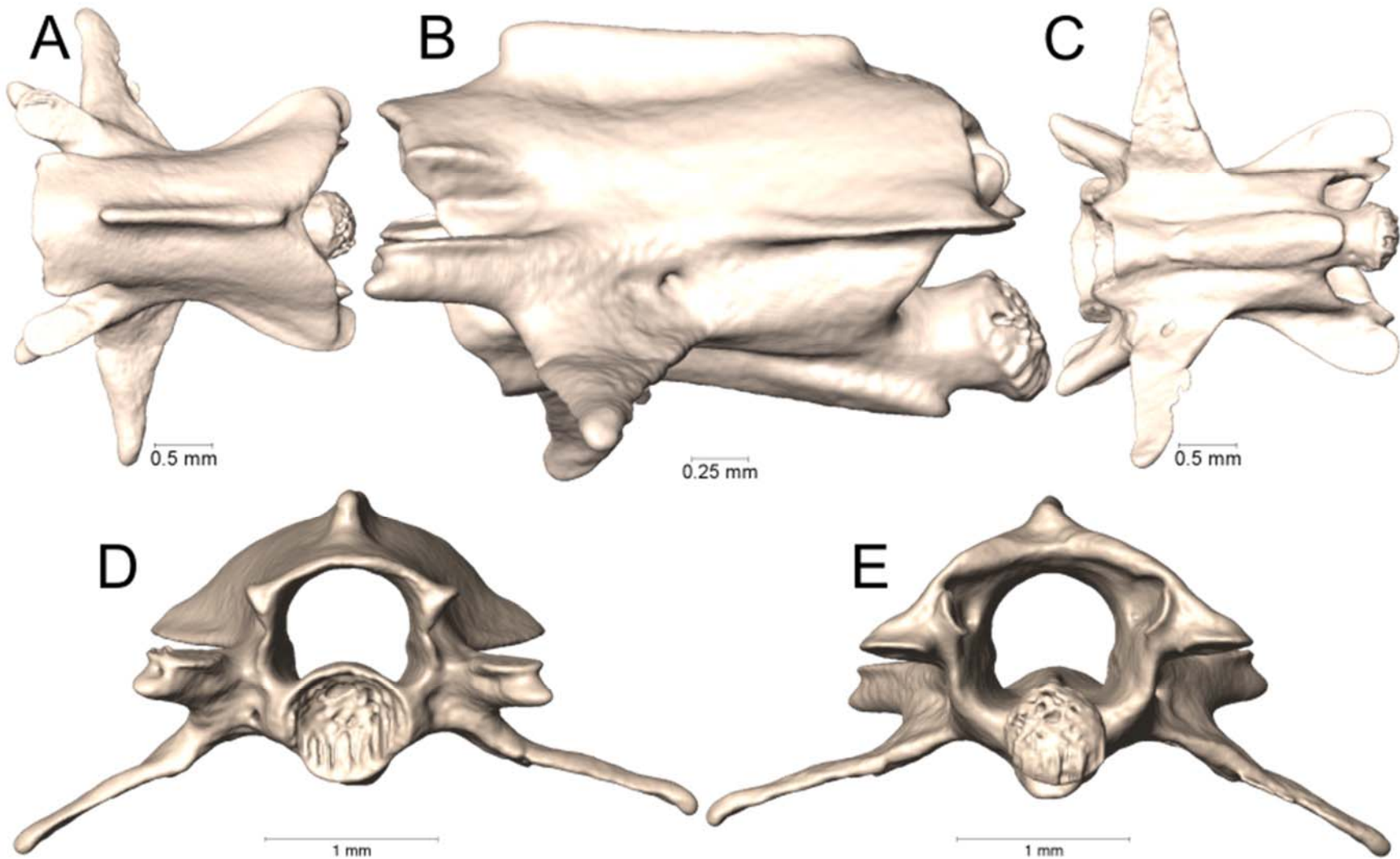
Supplemental Figure 5.62. Dorsal, lateral, ventral, anterior, and posterior views (A-E, respectively) of the caudal vertebra of *Micrurus nattereri* (UTA R-60727).



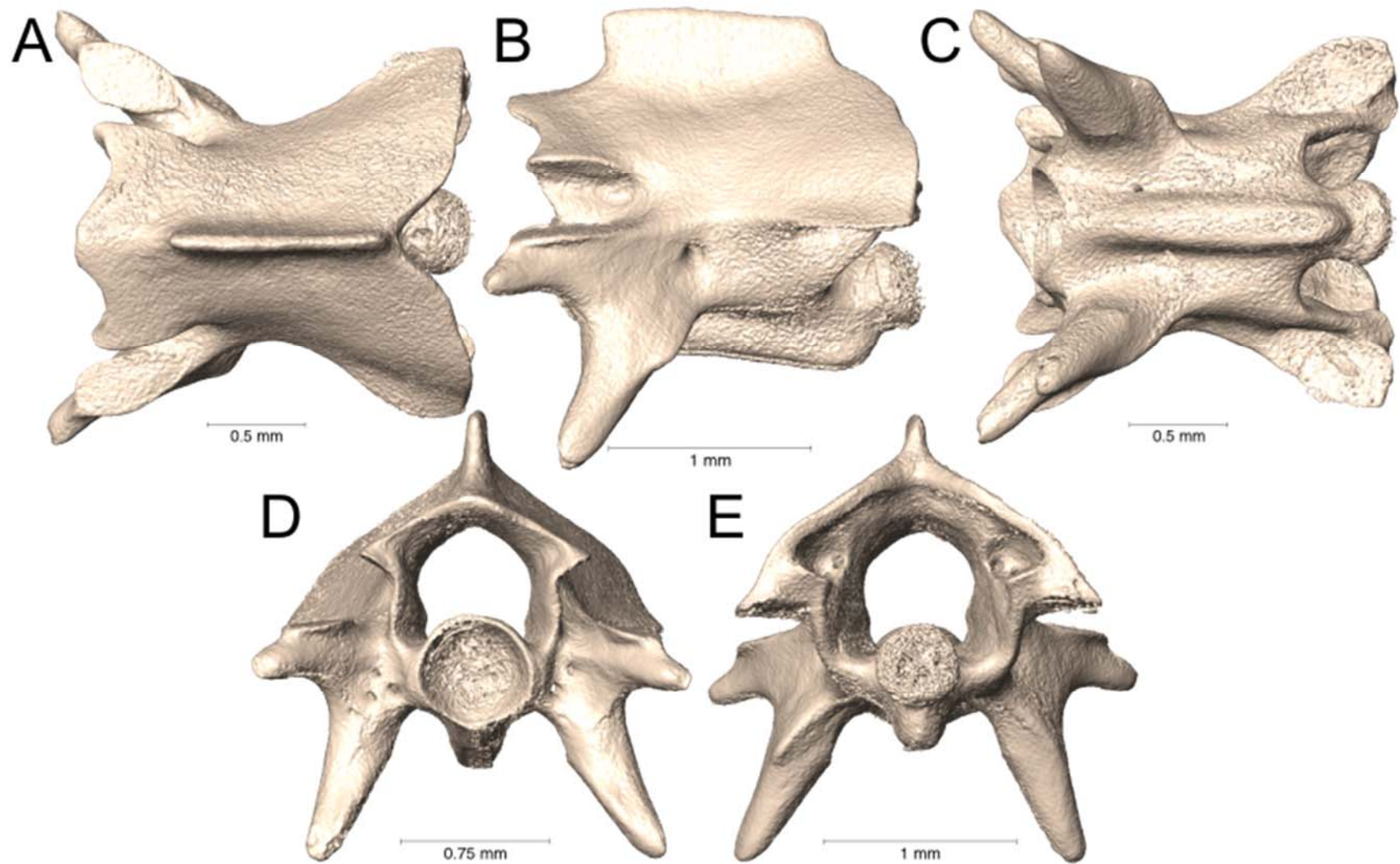
Supplemental Figure 5.63. Dorsal, lateral, ventral, anterior, and posterior views (A-E, respectively) of the caudal vertebra of *Micrurus nigrocinctus zunilensis* (UTA R-64858).



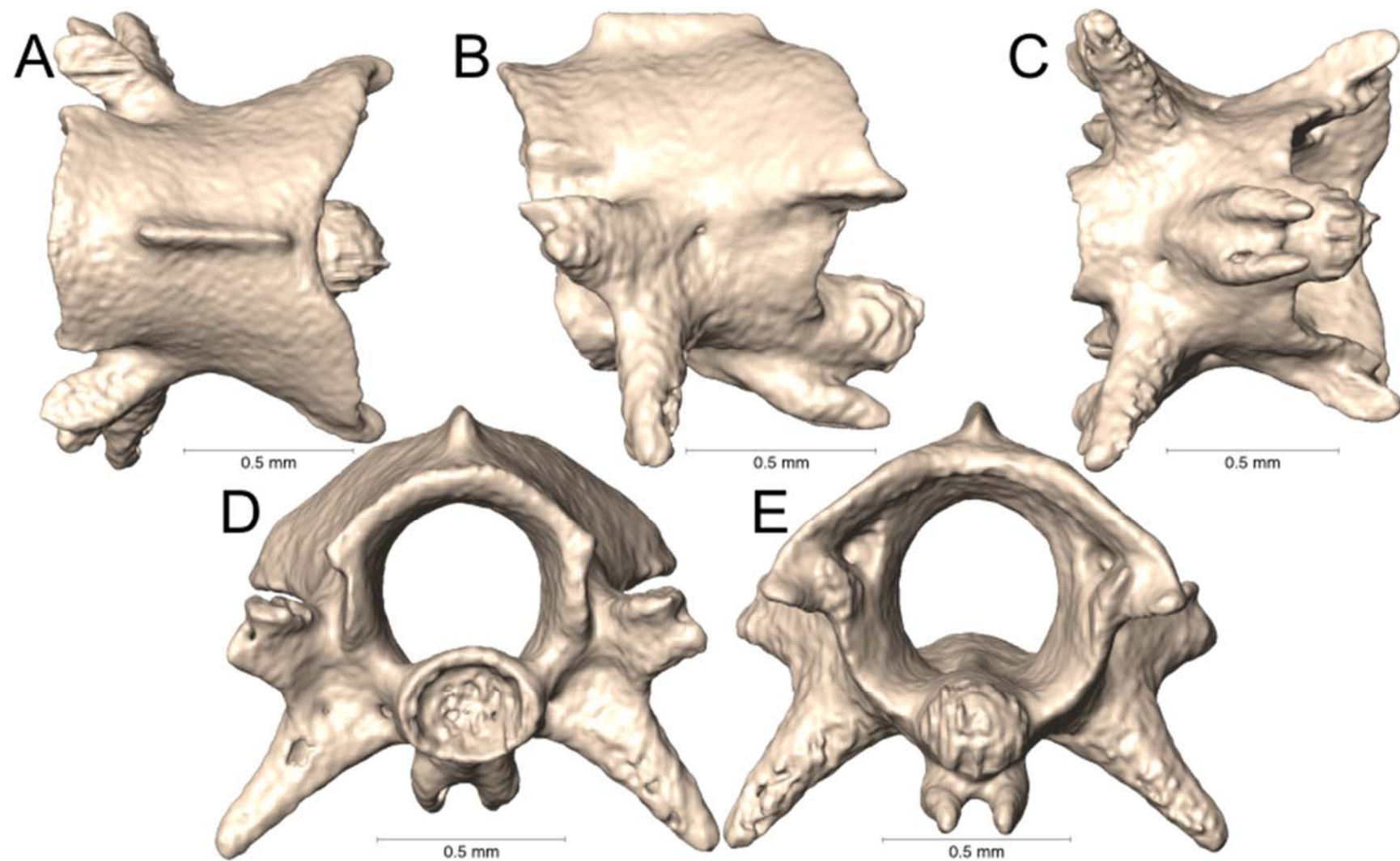
Supplemental Figure 5.64. Dorsal, lateral, ventral, anterior, and posterior views (A-E, respectively) of the caudal vertebra of *Micrurus obscurus* (UTA R-3840).



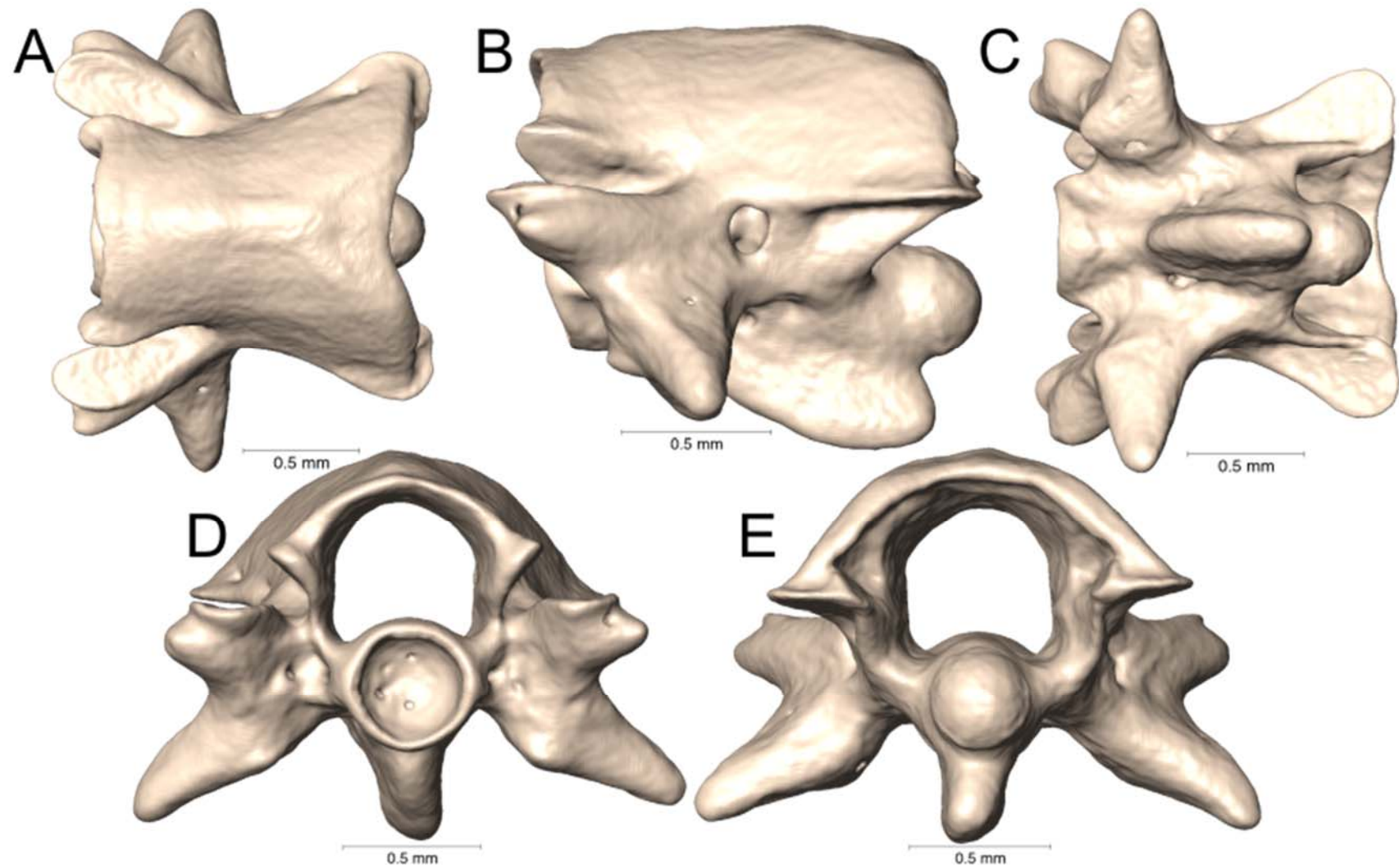
Supplemental Figure 5.65. Dorsal, lateral, ventral, anterior, and posterior views (A-E, respectively) of the caudal vertebra of *Micrurus oliveri* (UTA R-64893).



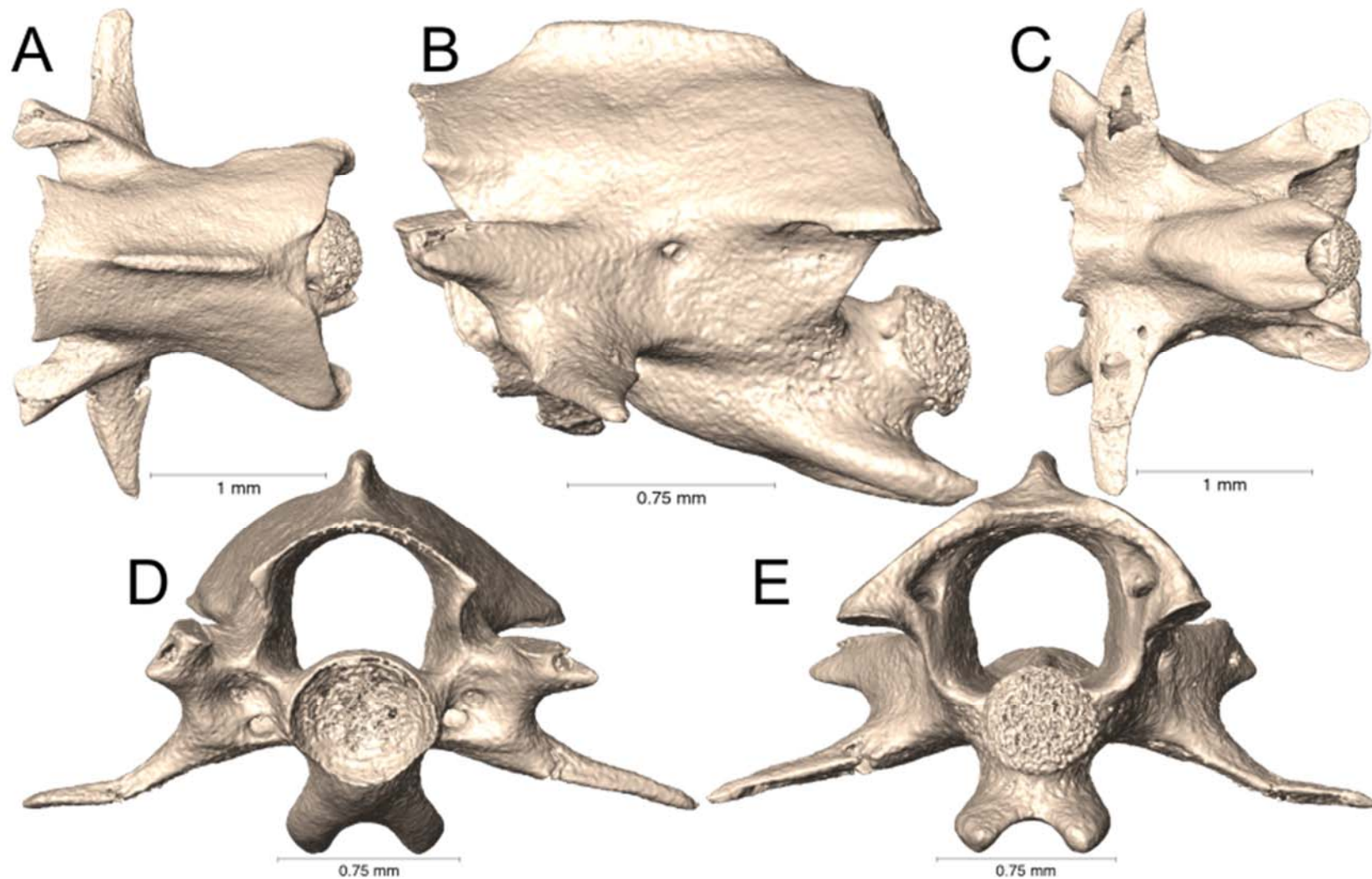
Supplemental Figure 5.66. Dorsal, lateral, ventral, anterior, and posterior views (A-E, respectively) of the caudal vertebra of *Micrurus ornatissimus* (UTA R-60724).



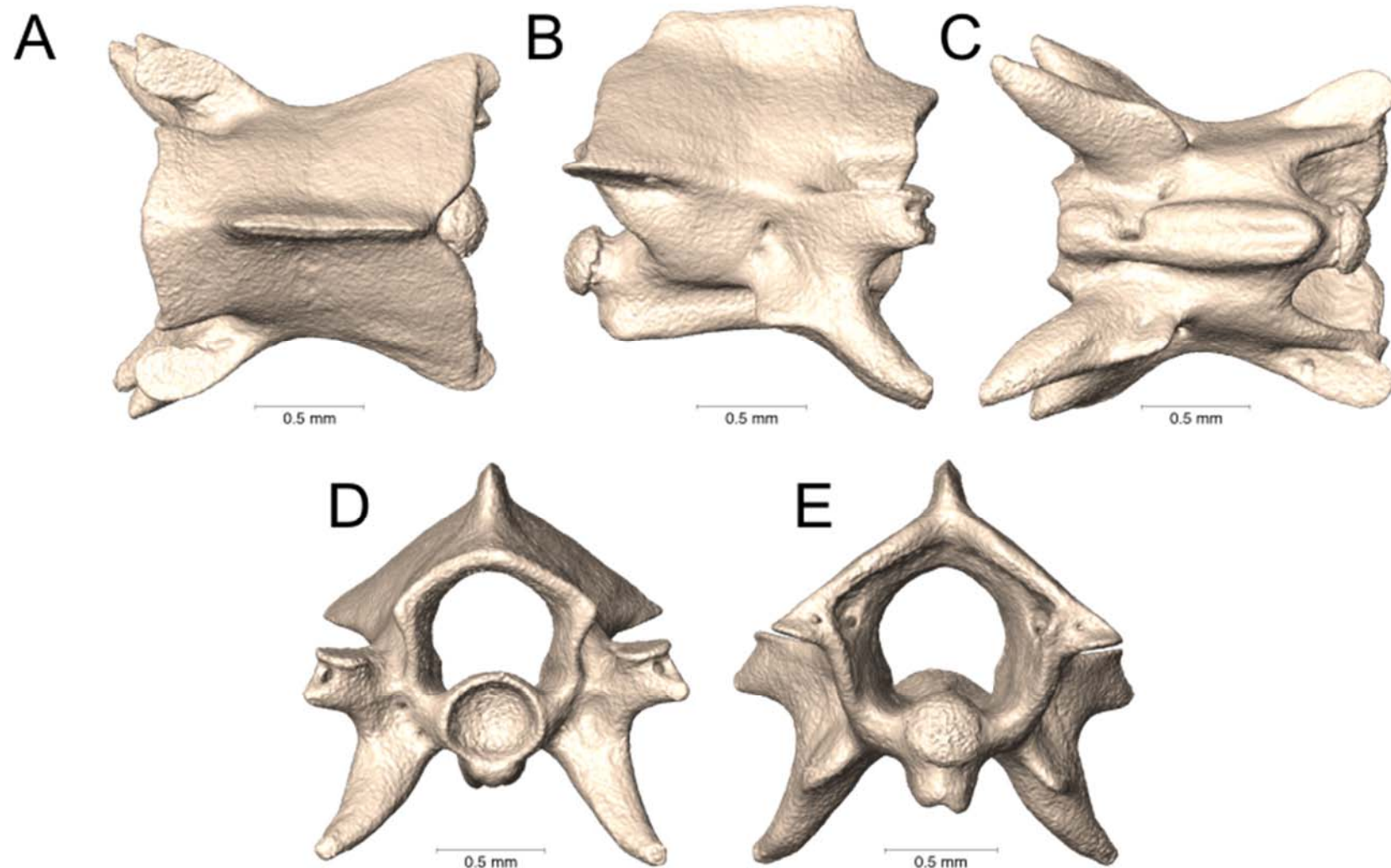
Supplemental Figure 5.67. Dorsal, lateral, ventral, anterior, and posterior views (A-E, respectively) of the caudal vertebra of *Micrurus pyrrhocryptus* (UTA R-51404).



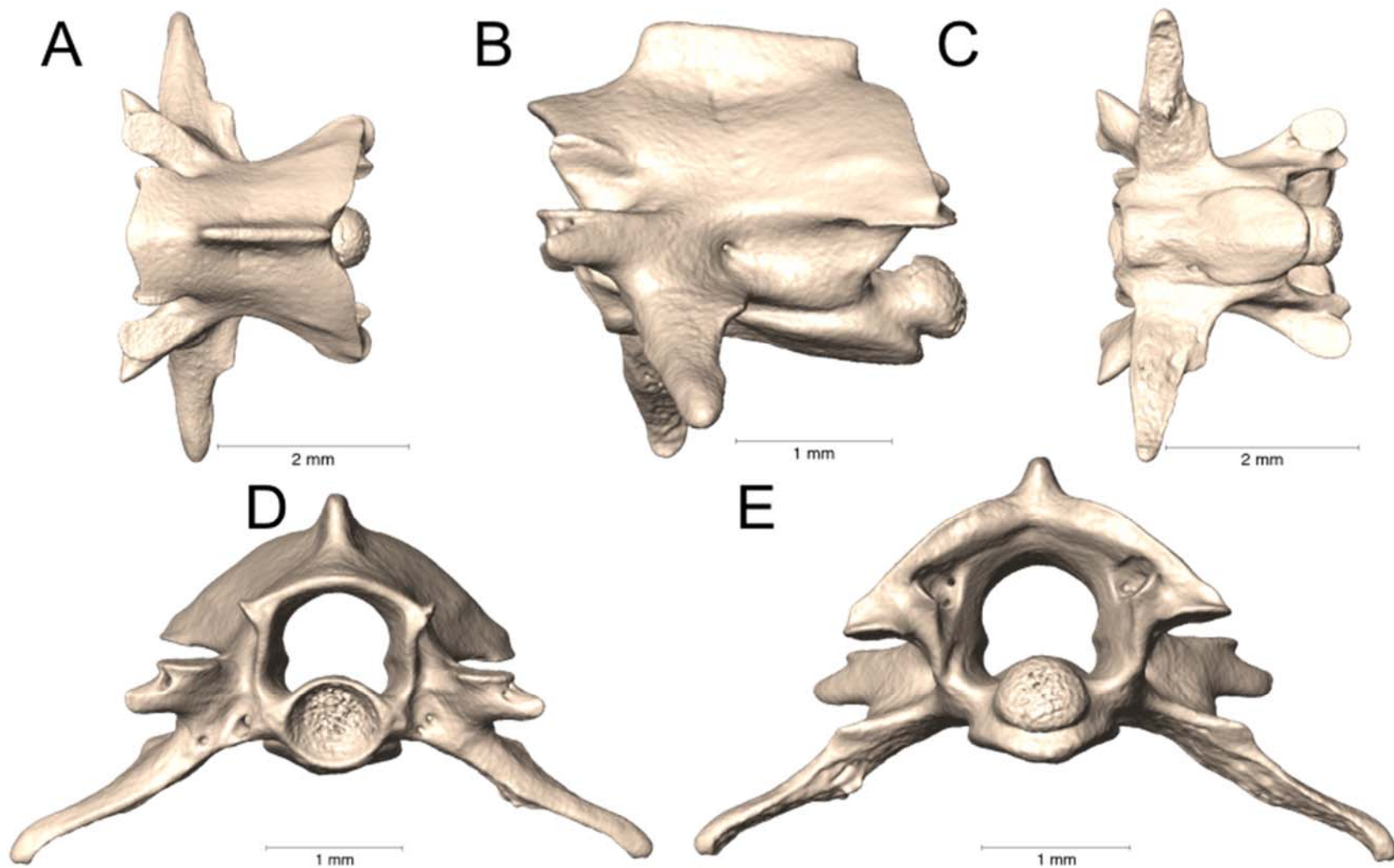
Supplemental Figure 5.68. Dorsal, lateral, ventral, anterior, and posterior views (A-E, respectively) of the caudal vertebra of *Micrurus renjifoi* (UTA R-3490).



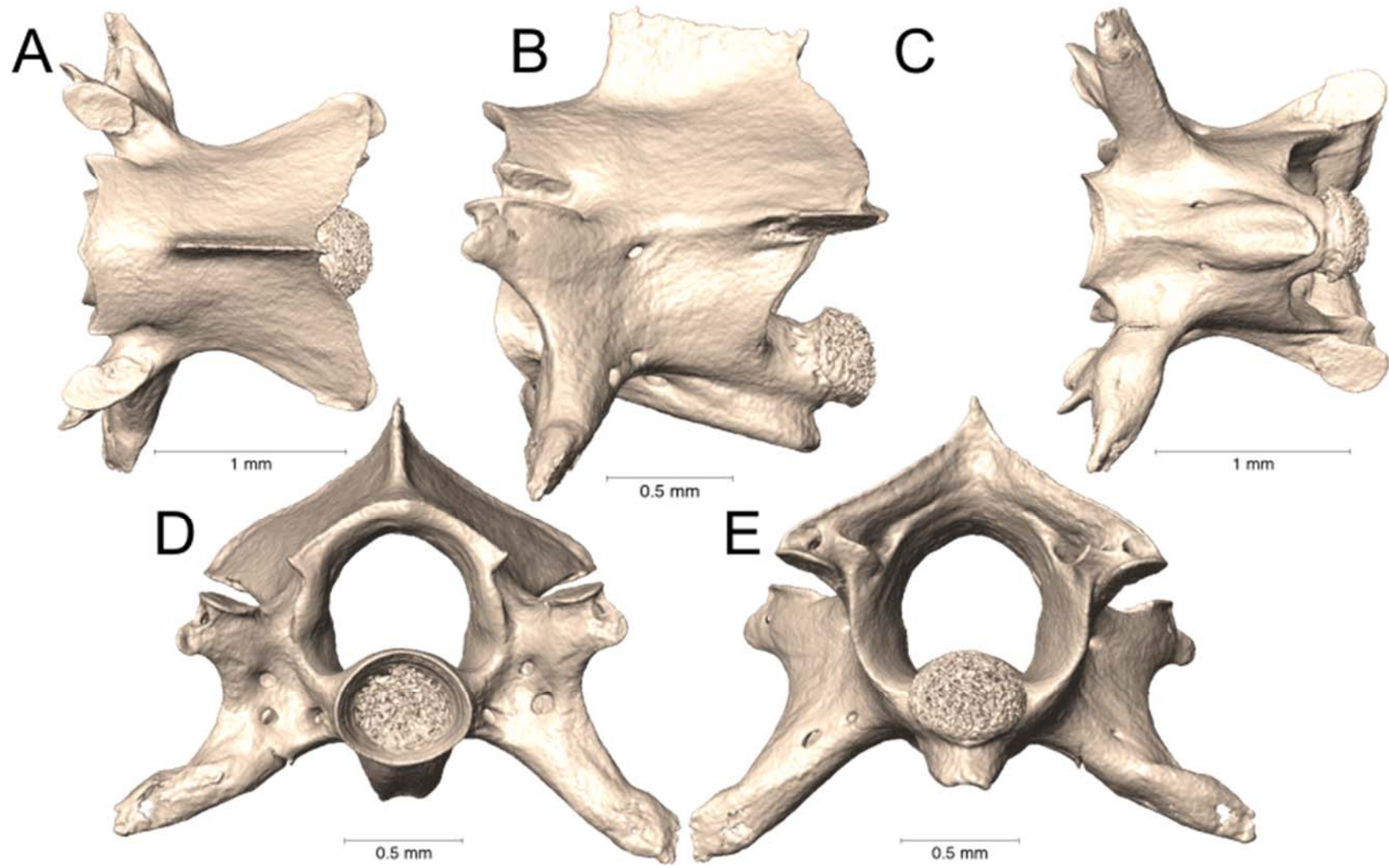
Supplemental Figure 5.69. Dorsal, lateral, ventral, anterior, and posterior views (A-E, respectively) of the caudal vertebra of *Micrurus serranus* (UTA R-34561).



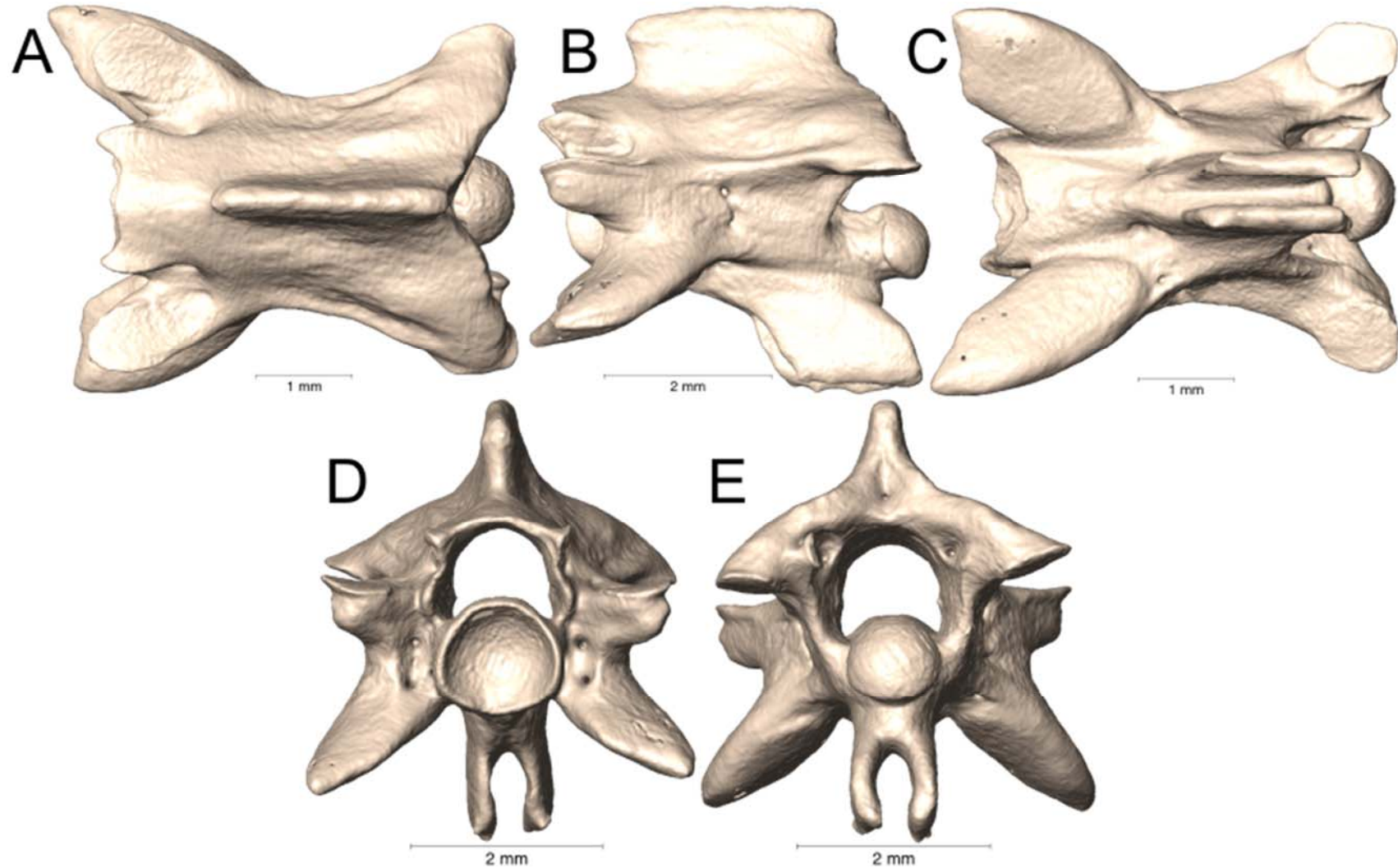
Supplemental Figure 5.70. Dorsal, lateral, ventral, anterior, and posterior views (A-E, respectively) of the caudal vertebra of *Micrurus steindachneri* (AMNH 28846).



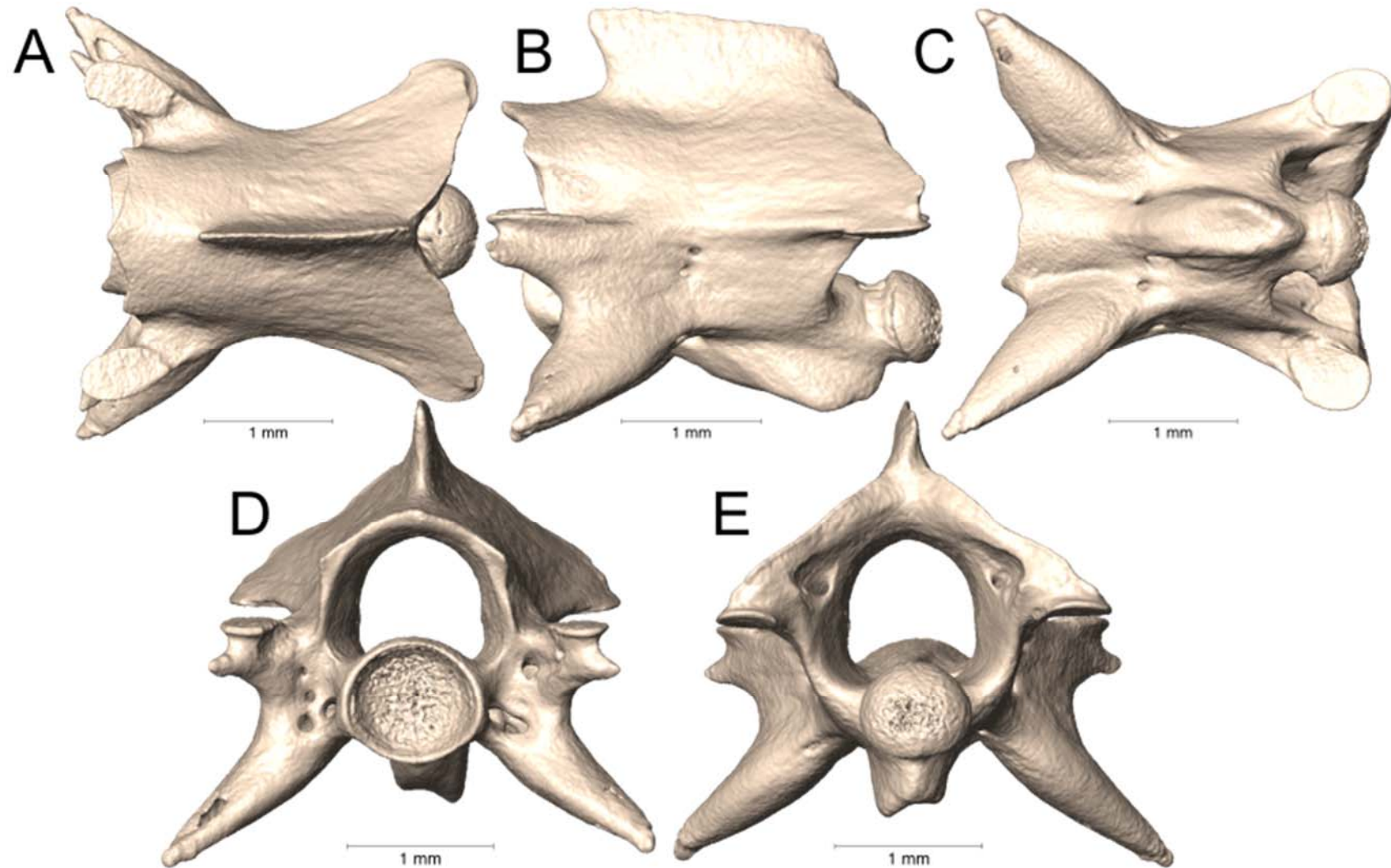
Supplemental Figure 5.71. Dorsal, lateral, ventral, anterior, and posterior views (A-E, respectively) of the caudal vertebra of *Micrurus steindachneri* (AMNH 35819).



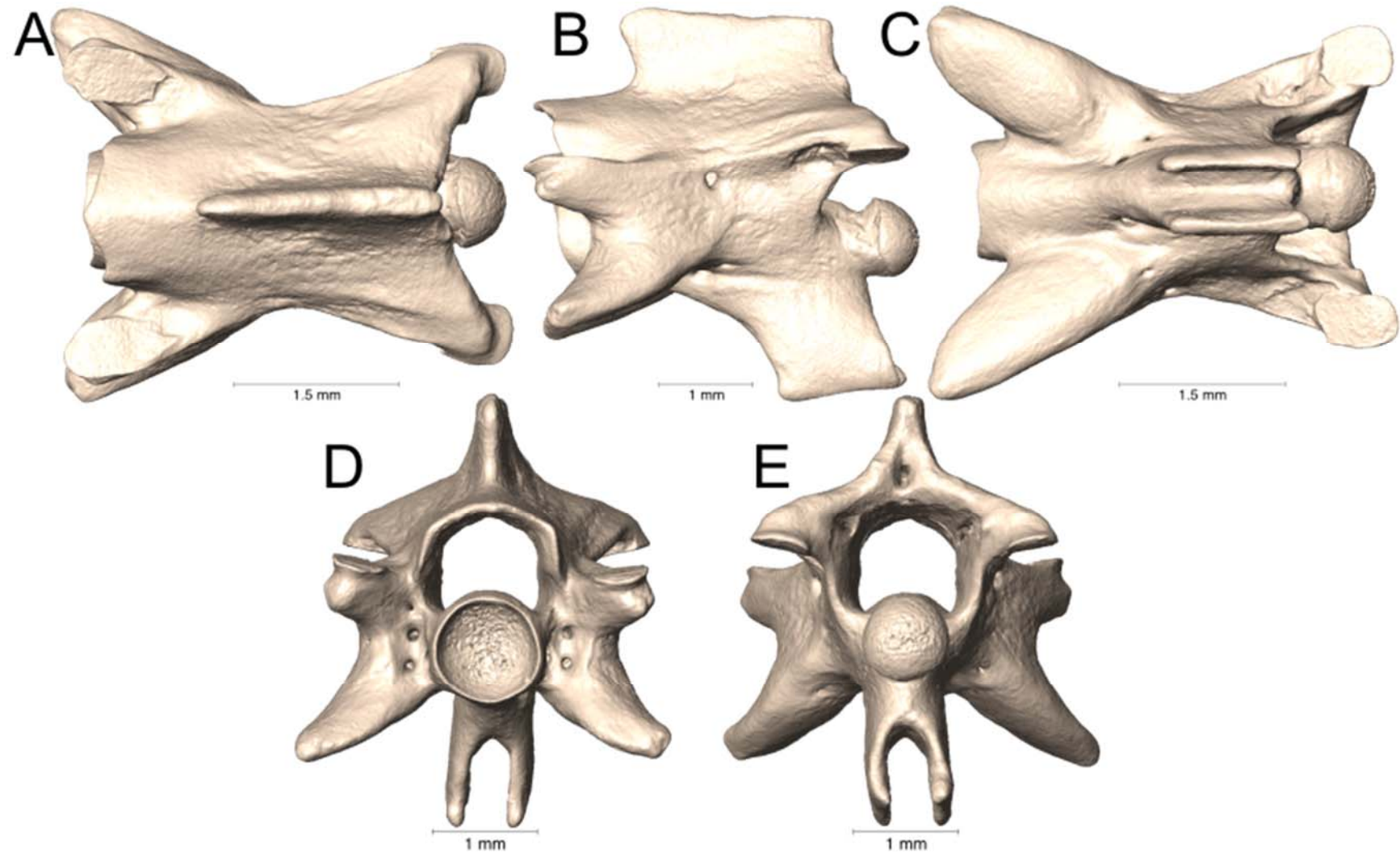
Supplemental Figure 5.72. Dorsal, lateral, ventral, anterior, and posterior views (A-E, respectively) of the caudal vertebra of *Micrurus surinamensis* (UTA R-5849).



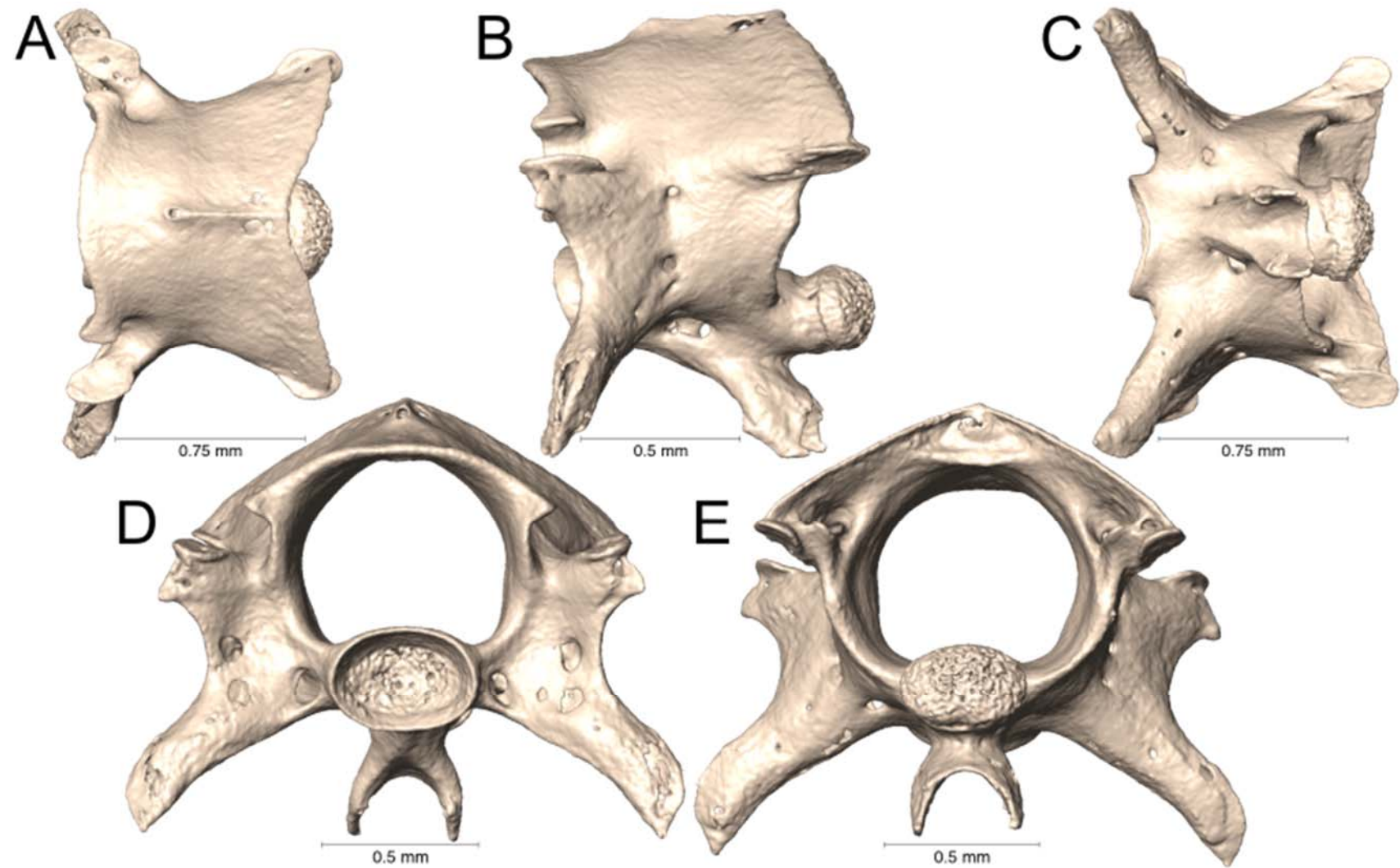
Supplemental Figure 5.73. Dorsal, lateral, ventral, anterior, and posterior views (A-E, respectively) of the caudal vertebra of *Micrurus surinamensis* (UTA R-15679).



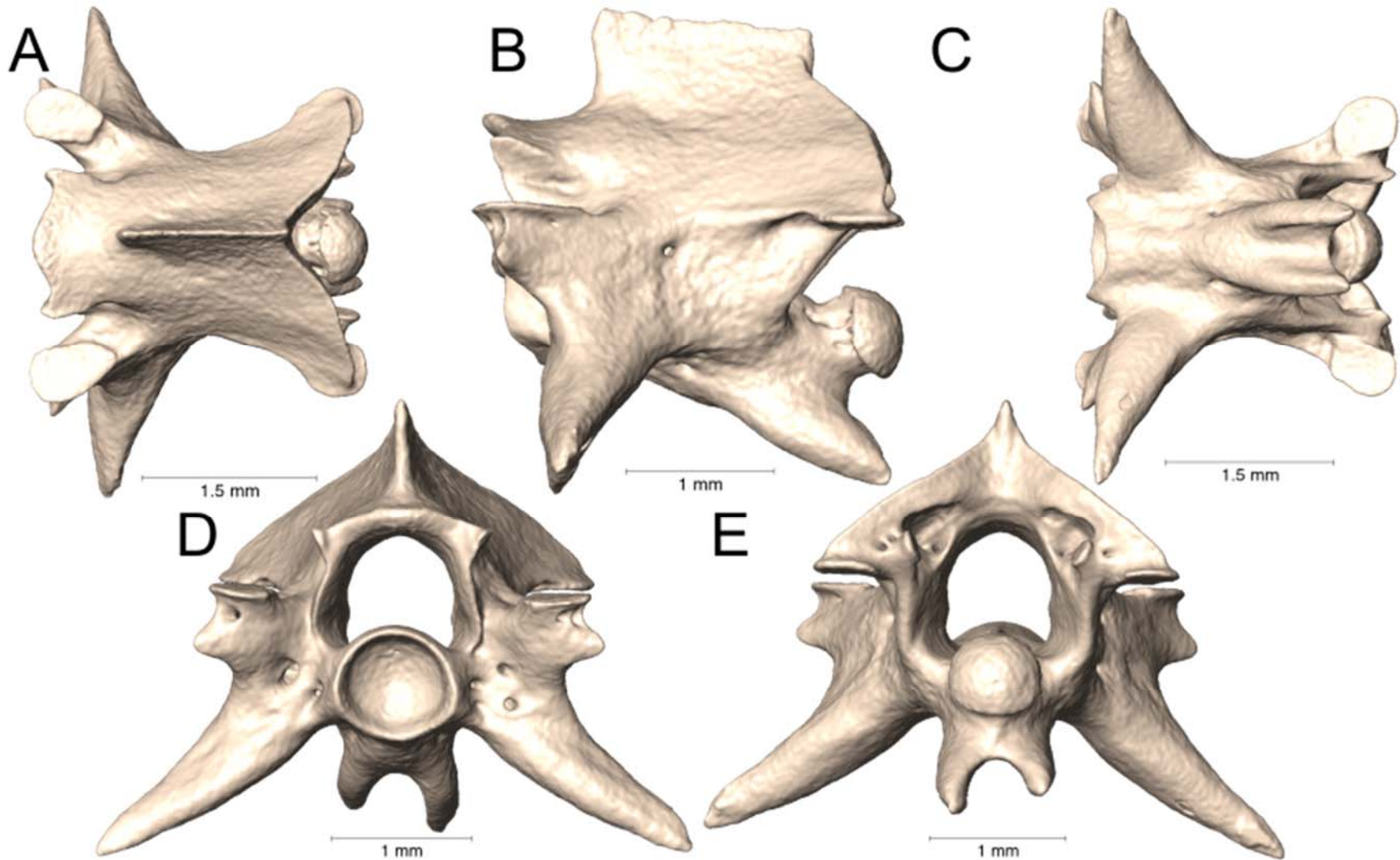
Supplemental Figure 5.74. Dorsal, lateral, ventral, anterior, and posterior views (A-E, respectively) of the caudal vertebra of *Micrurus surinamensis* (UTA R-50173).



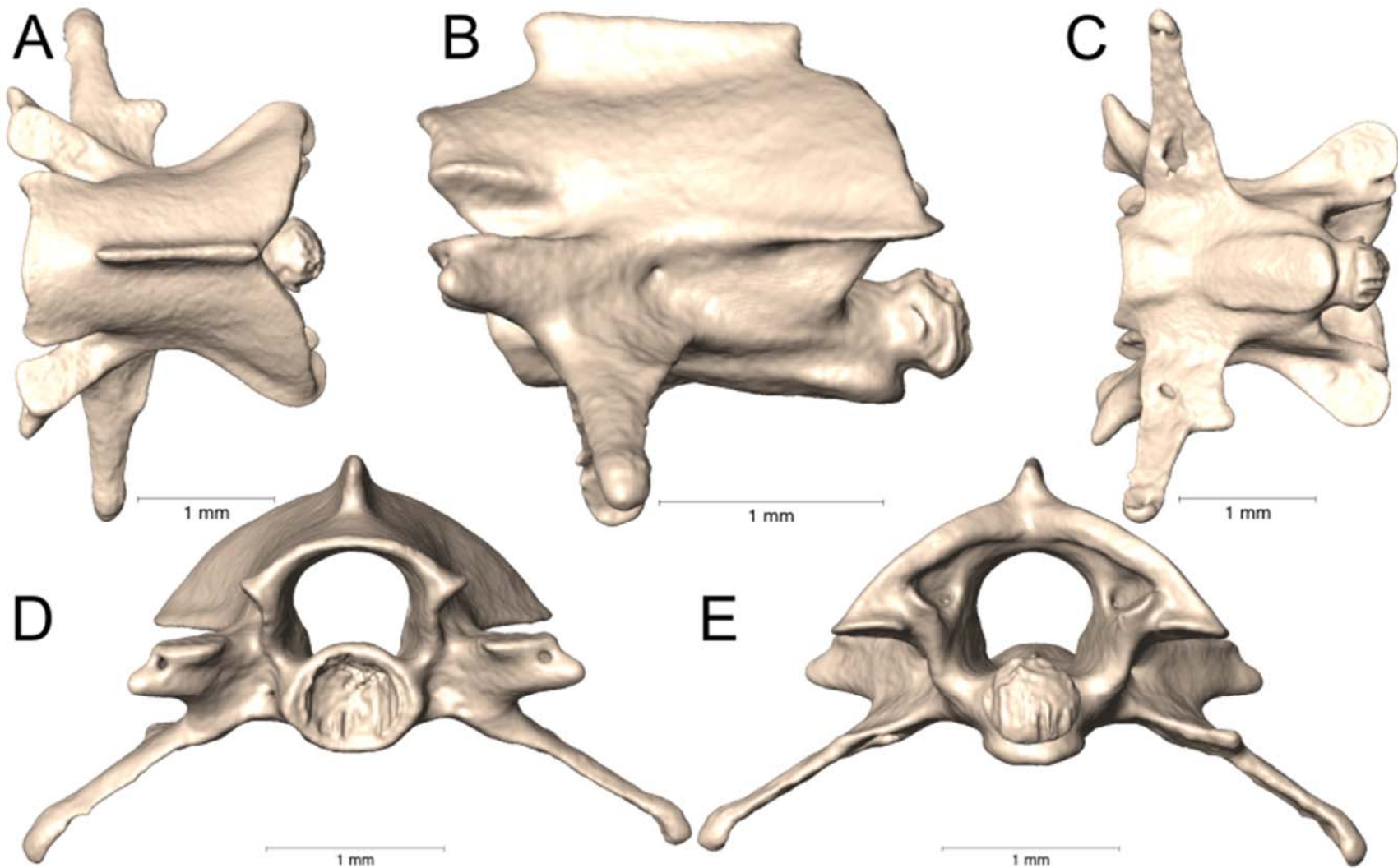
Supplemental Figure 5.75. Dorsal, lateral, ventral, anterior, and posterior views (A-E, respectively) of the caudal vertebra of *Micrurus surinamensis* (UTA R-54378).



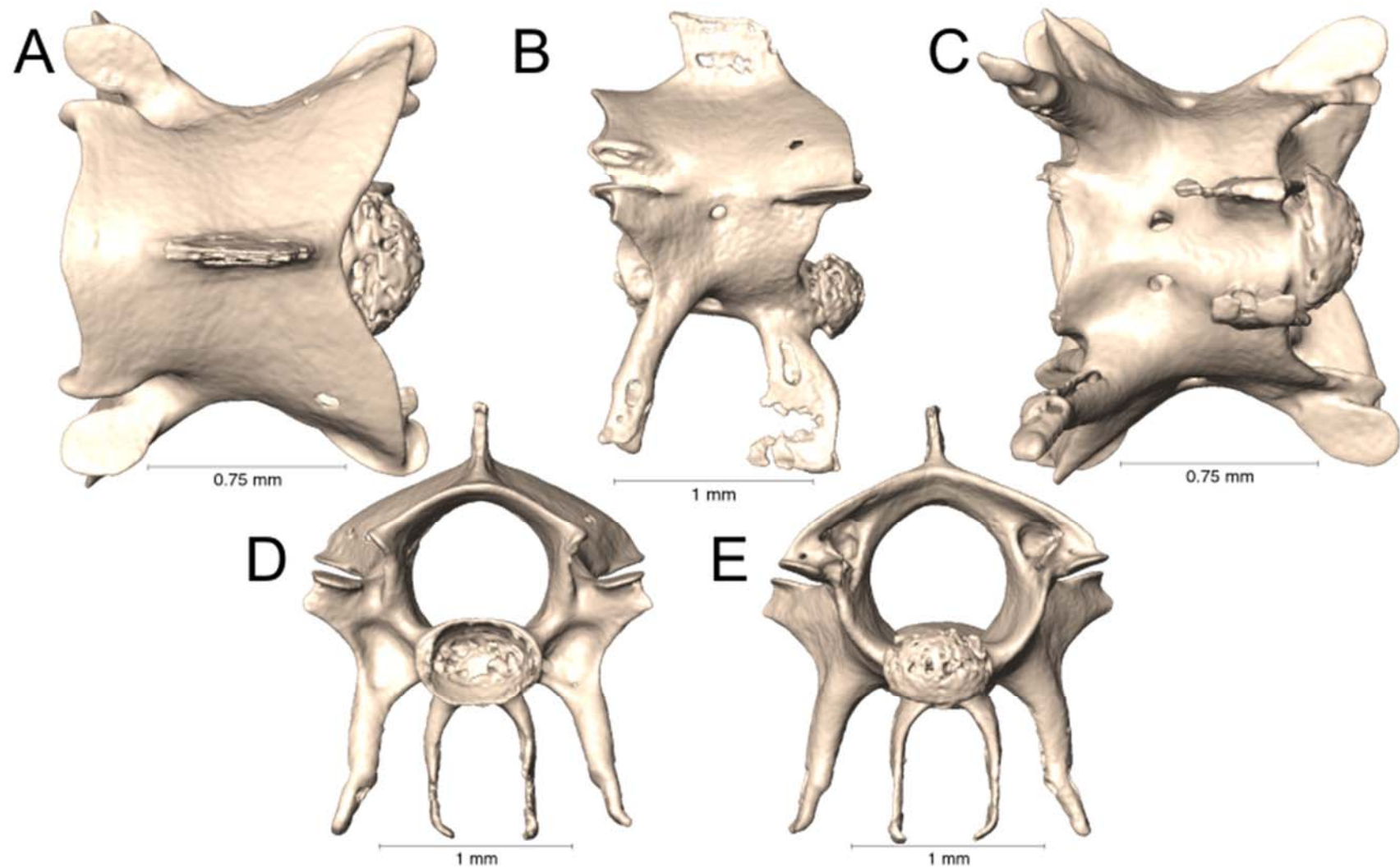
Supplemental Figure 5.76. Dorsal, lateral, ventral, anterior, and posterior views (A-E, respectively) of the caudal vertebra of *Micrurus surinamensis* (UTA R-65798).



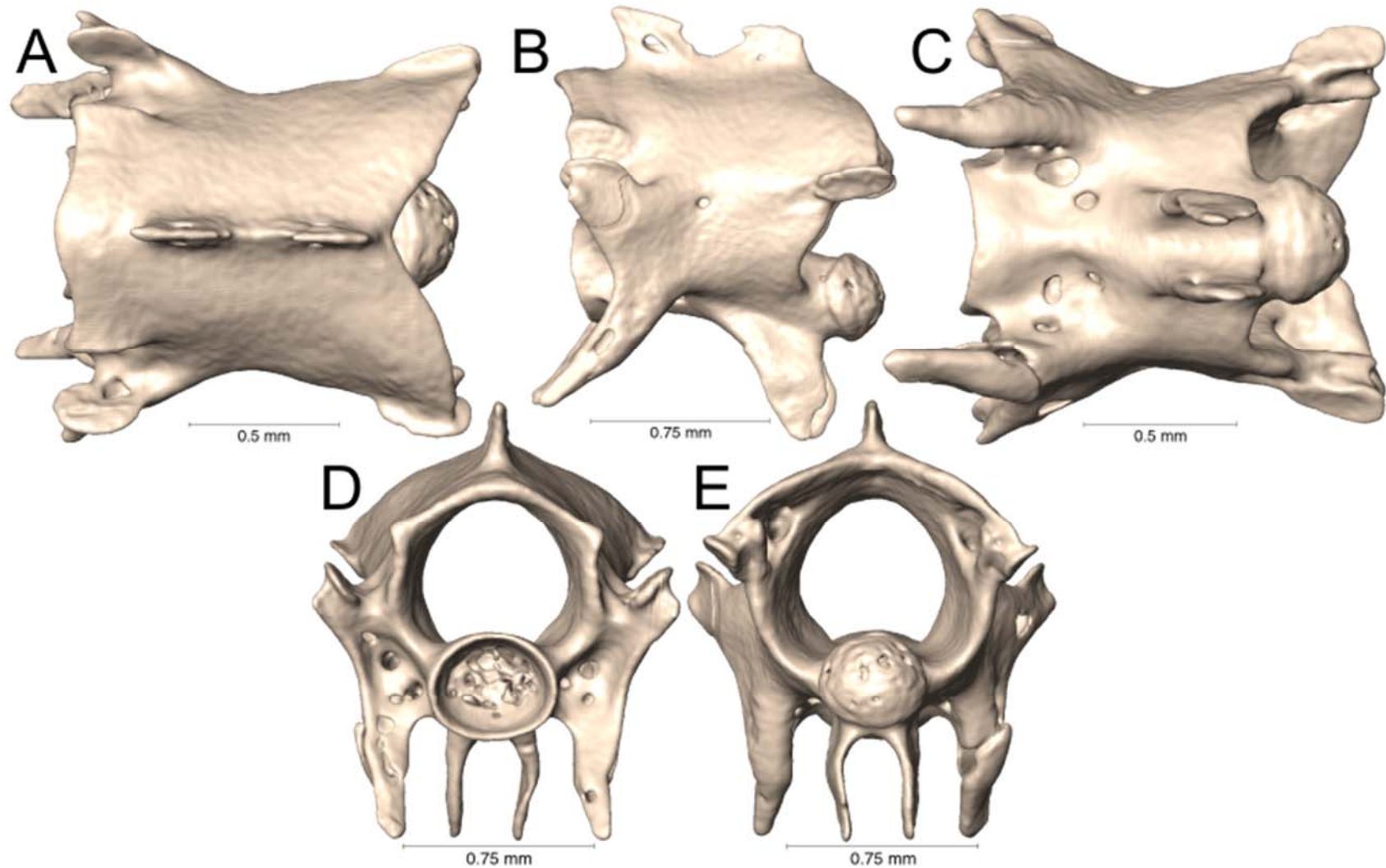
Supplemental Figure 5.77. Dorsal, lateral, ventral, anterior, and posterior views (A-E, respectively) of the caudal vertebra of *Micrurus surinamensis* (UTA R-65844).



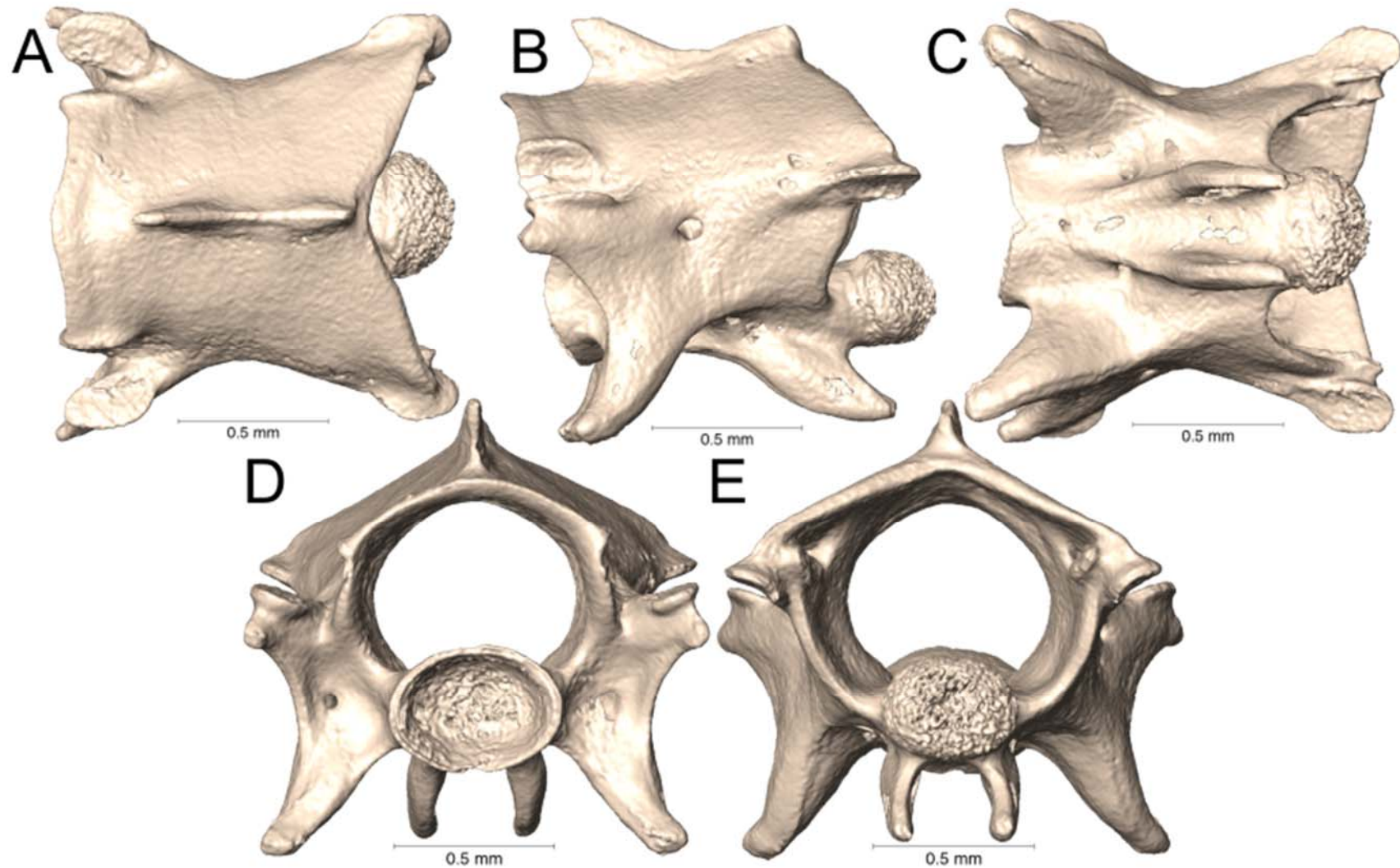
Supplemental Figure 5.78. Dorsal, lateral, ventral, anterior, and posterior views (A-E, respectively) of the caudal vertebra of *Micrurus tener* (UTA R-63282).



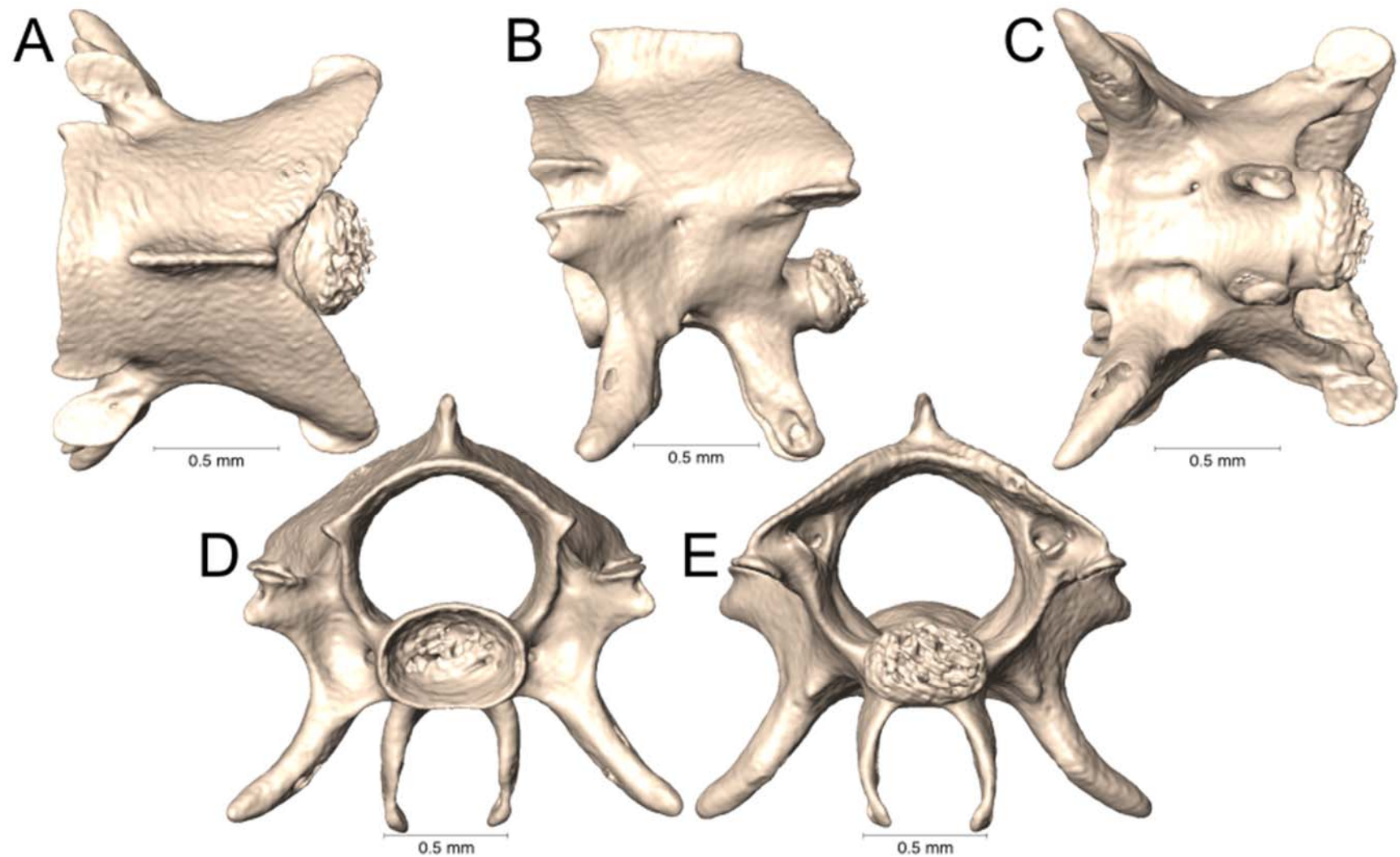
Supplemental Figure 5.79. Dorsal, lateral, ventral, anterior, and posterior views (A-E, respectively) of the caudal vertebra of *Naja annulata* (UTA R-18199).



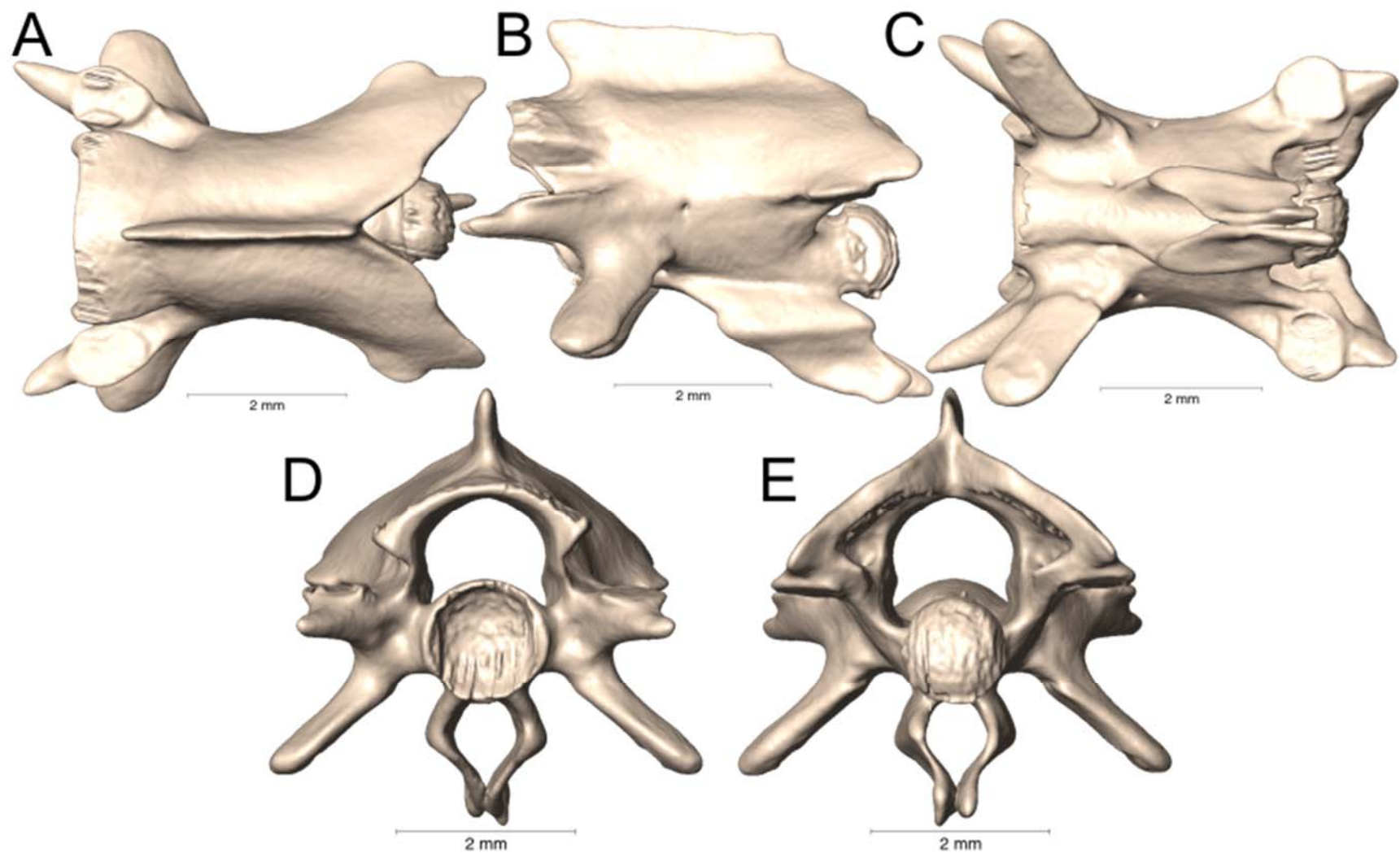
Supplemental Figure 5.80. Dorsal, lateral, ventral, anterior, and posterior views (A-E, respectively) of the caudal vertebra of *Naja christyi* (UTA R-18200).



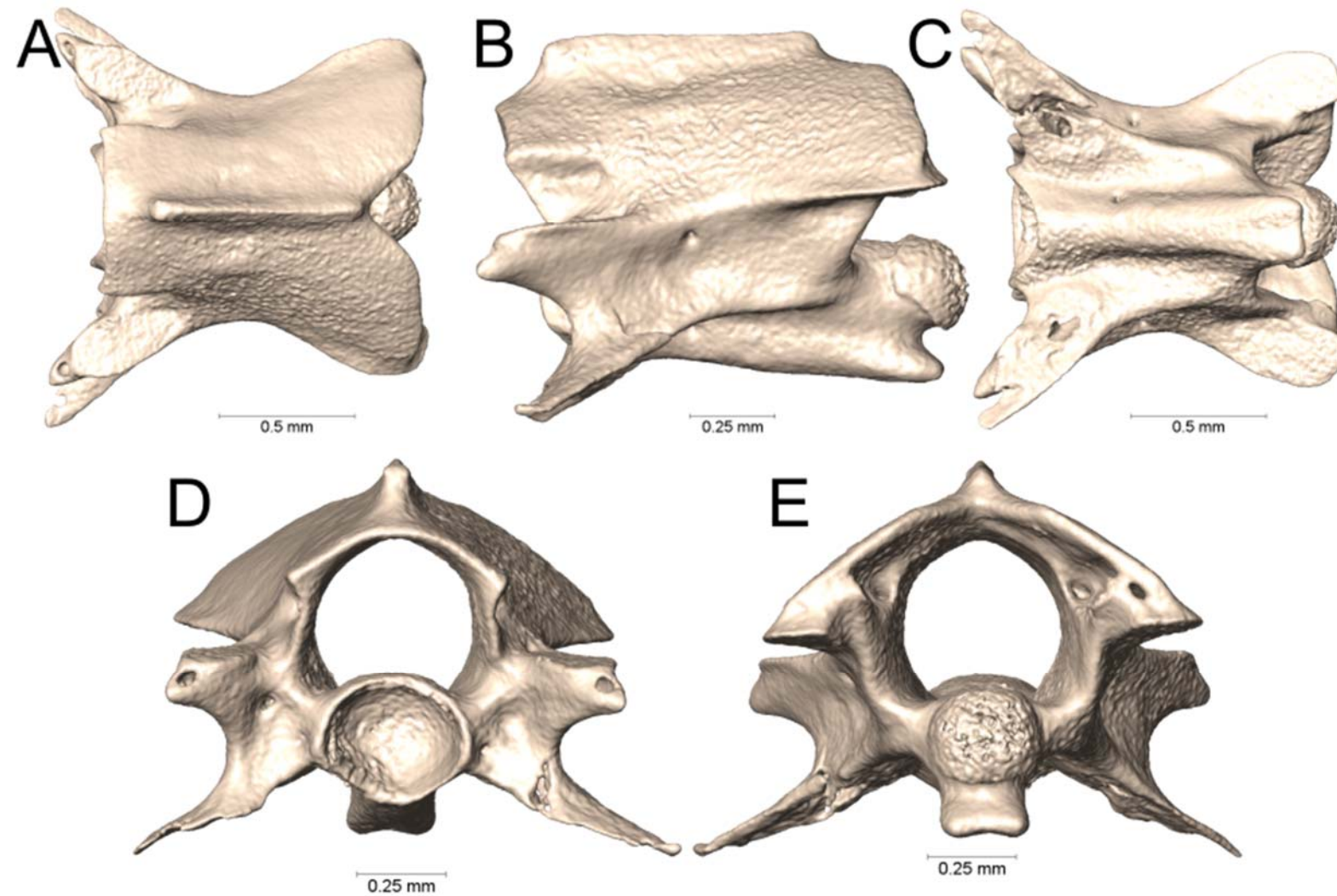
Supplemental Figure 5.81. Dorsal, lateral, ventral, anterior, and posterior views (A-E, respectively) of the caudal vertebra of *Naja siamensis* (UTA R-16872).



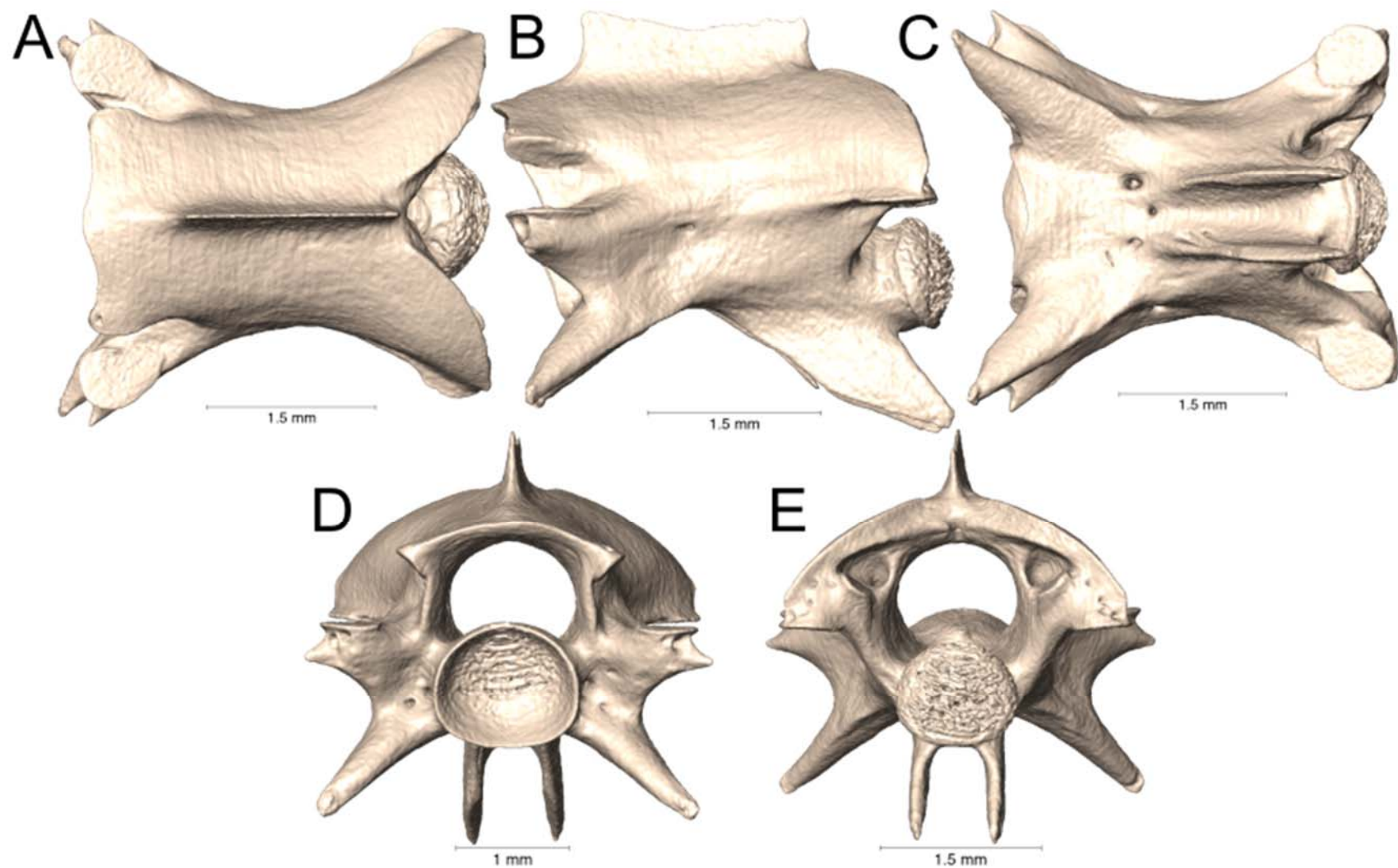
Supplemental Figure 5.82. Dorsal, lateral, ventral, anterior, and posterior views (A-E, respectively) of the caudal vertebra of *Ophiophagus hannah* (UTA R-60836).



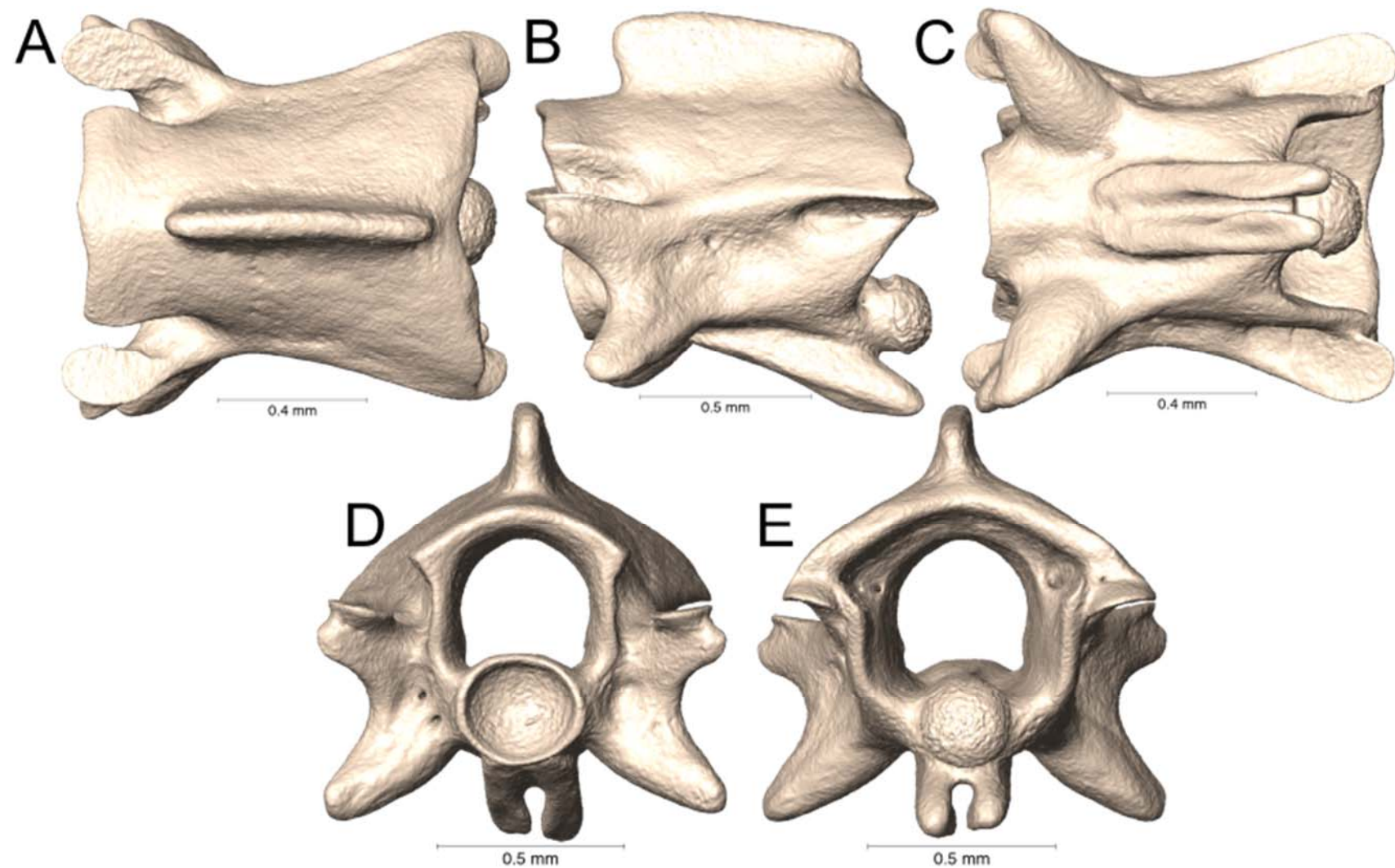
Supplemental Figure 5.83. Dorsal, lateral, ventral, anterior, and posterior views (A-E, respectively) of the caudal vertebra of *Oxyuranus scutellatus* (UTA R-60839).



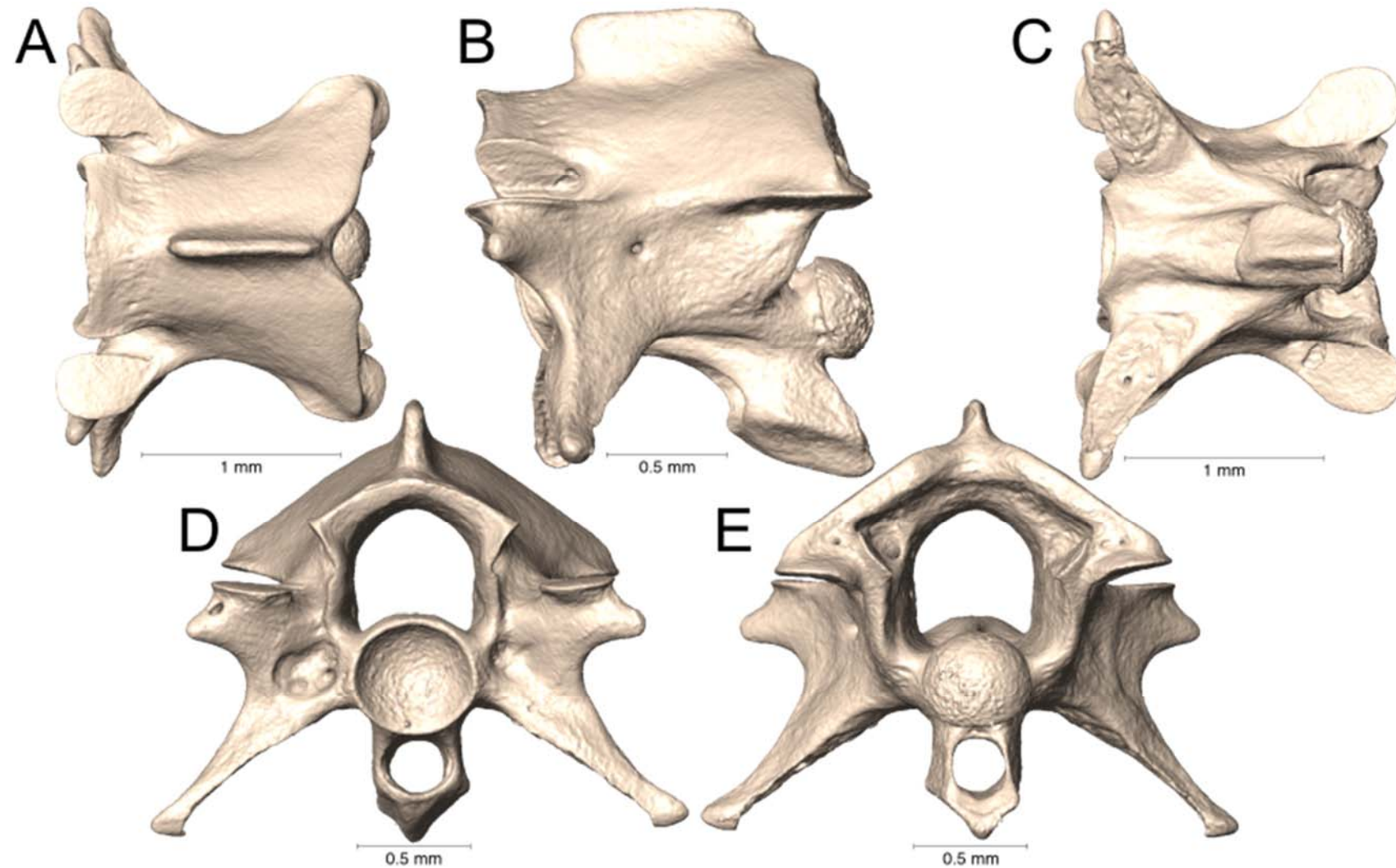
Supplemental Figure 5.84. Dorsal, lateral, ventral, anterior, and posterior views (A-E, respectively) of the caudal vertebra of *Prosymna stuhlmanni* (UTA R-64493).



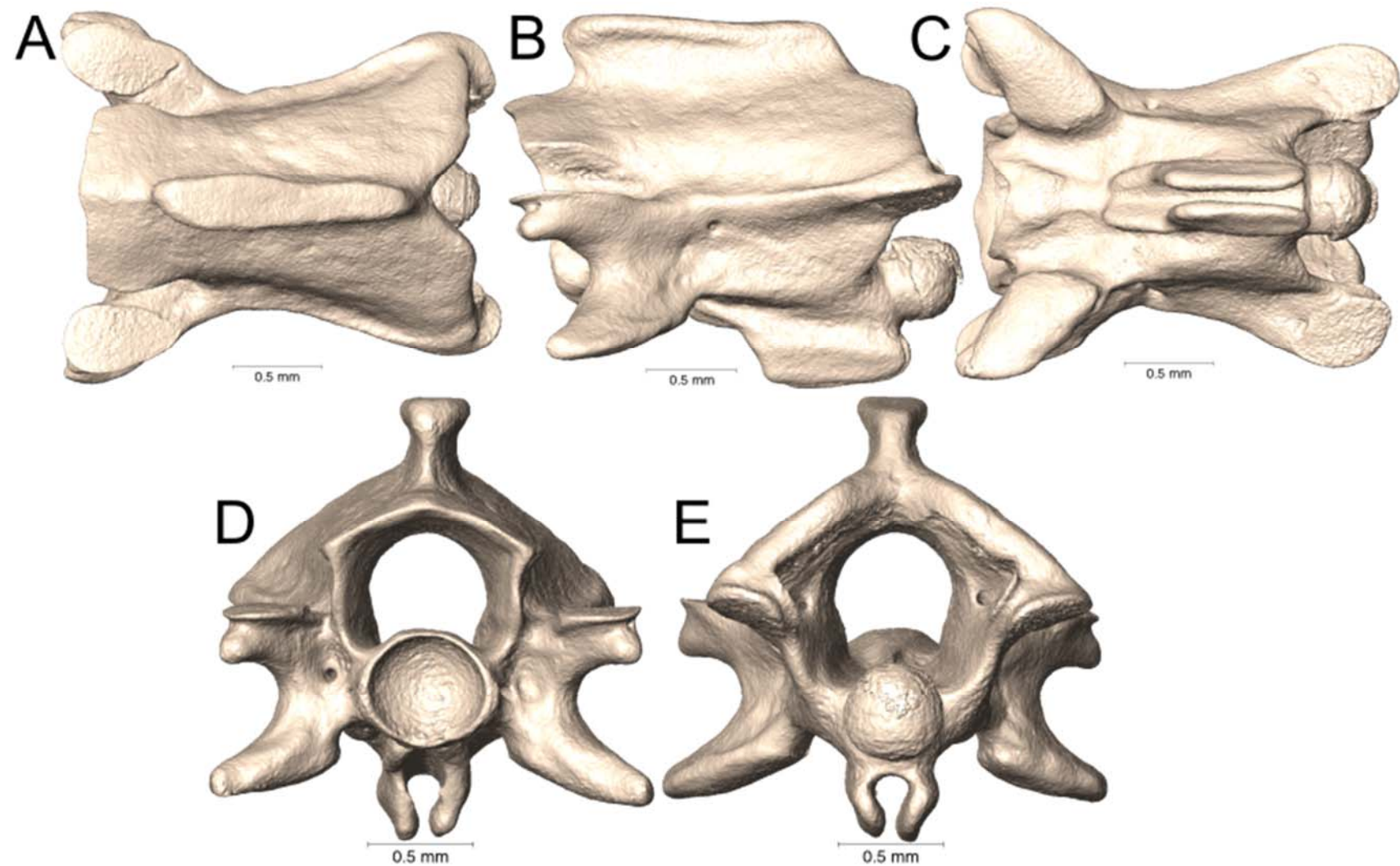
Supplemental Figure 5.85. Dorsal, lateral, ventral, anterior, and posterior views (A-E, respectively) of the caudal vertebra of *Pseudohaje goldii* (UTA R-63636).



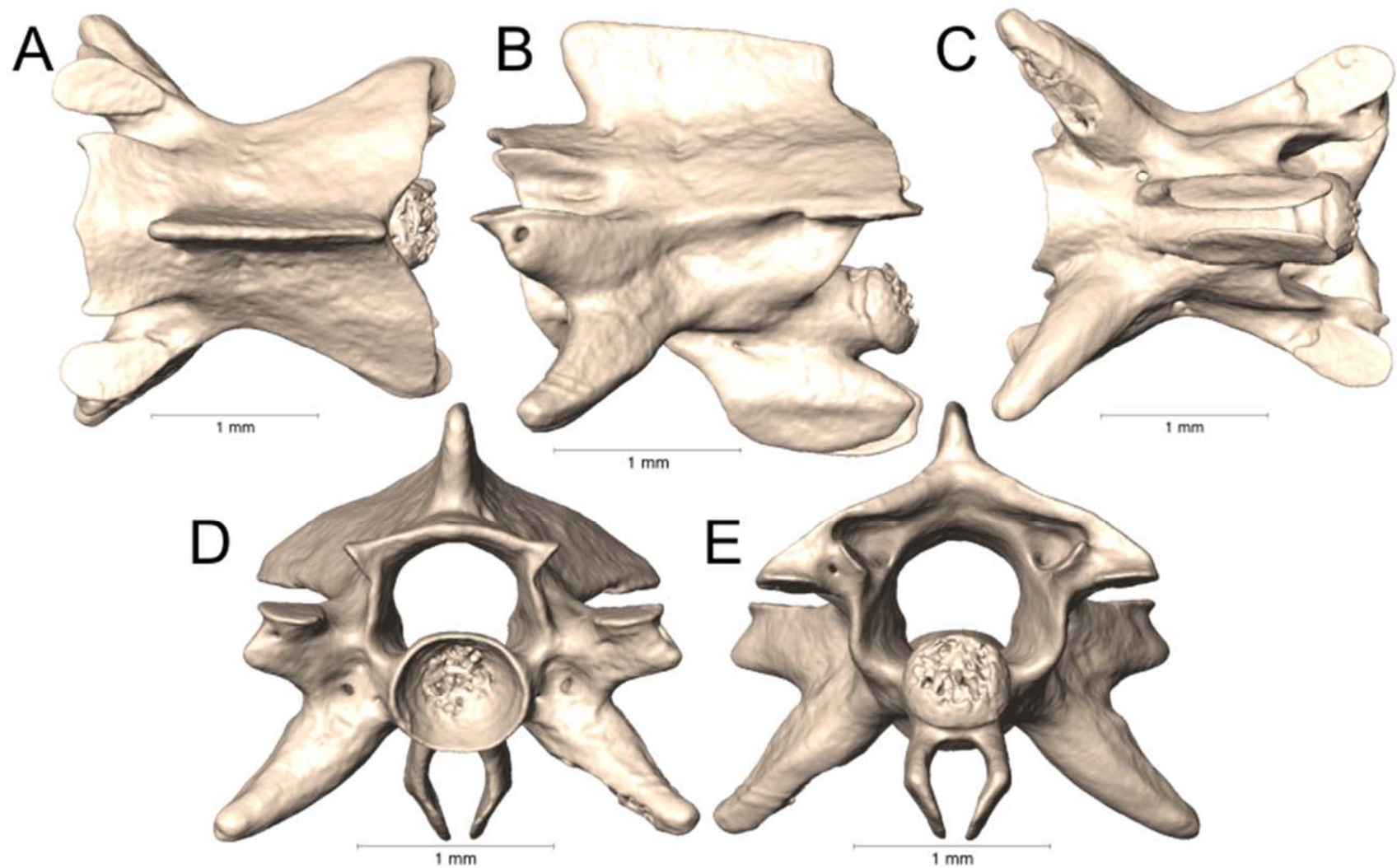
Supplemental Figure 5.86. Dorsal, lateral, ventral, anterior, and posterior views (A-E, respectively) of the caudal vertebra of *Sinomicrurus annularis* (ROM 31158).



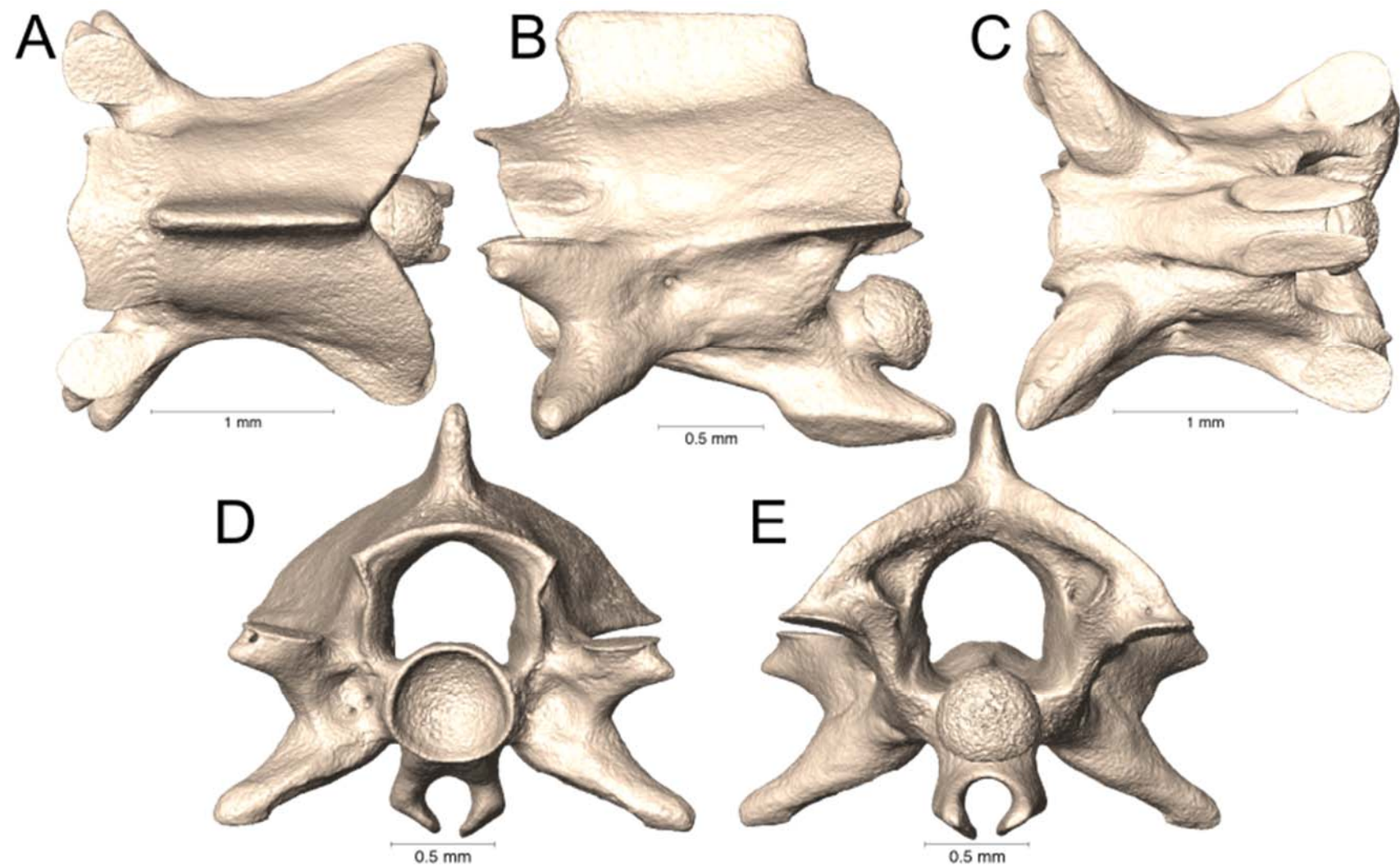
Supplemental Figure 5.87. Dorsal, lateral, ventral, anterior, and posterior views (A-E, respectively) of the caudal vertebra of *Sinomicrurus boettgeri* (UTA R-58837).



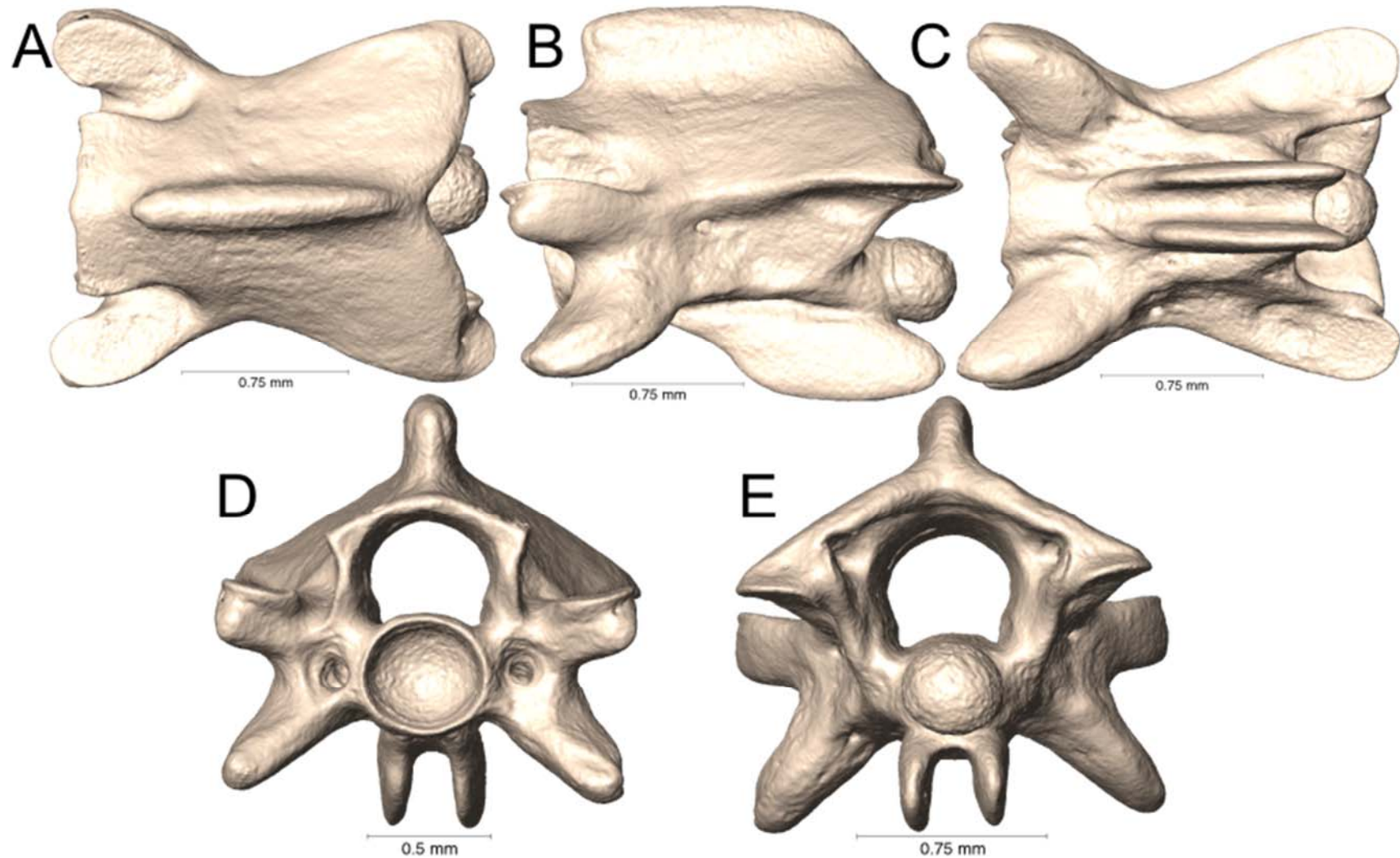
Supplemental Figure 5.88. Dorsal, lateral, ventral, anterior, and posterior views (A-E, respectively) of the caudal vertebra of *Sinomicrurus kelloggi* (ROM 37079).



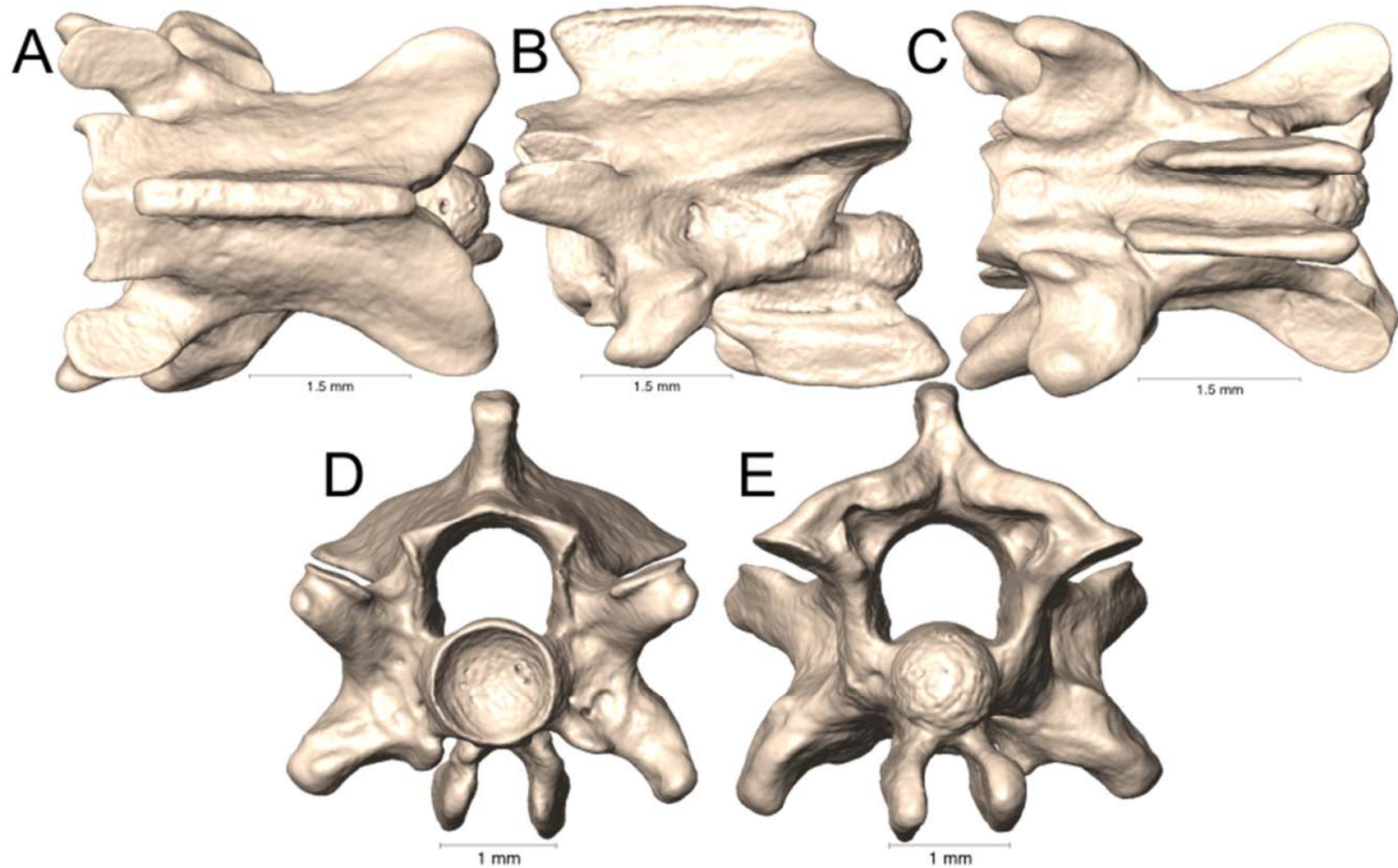
Supplemental Figure 5.89. Dorsal, lateral, ventral, anterior, and posterior views (A-E, respectively) of the caudal vertebra of *Sinomicrurus macclellandi* (CAS 17267).



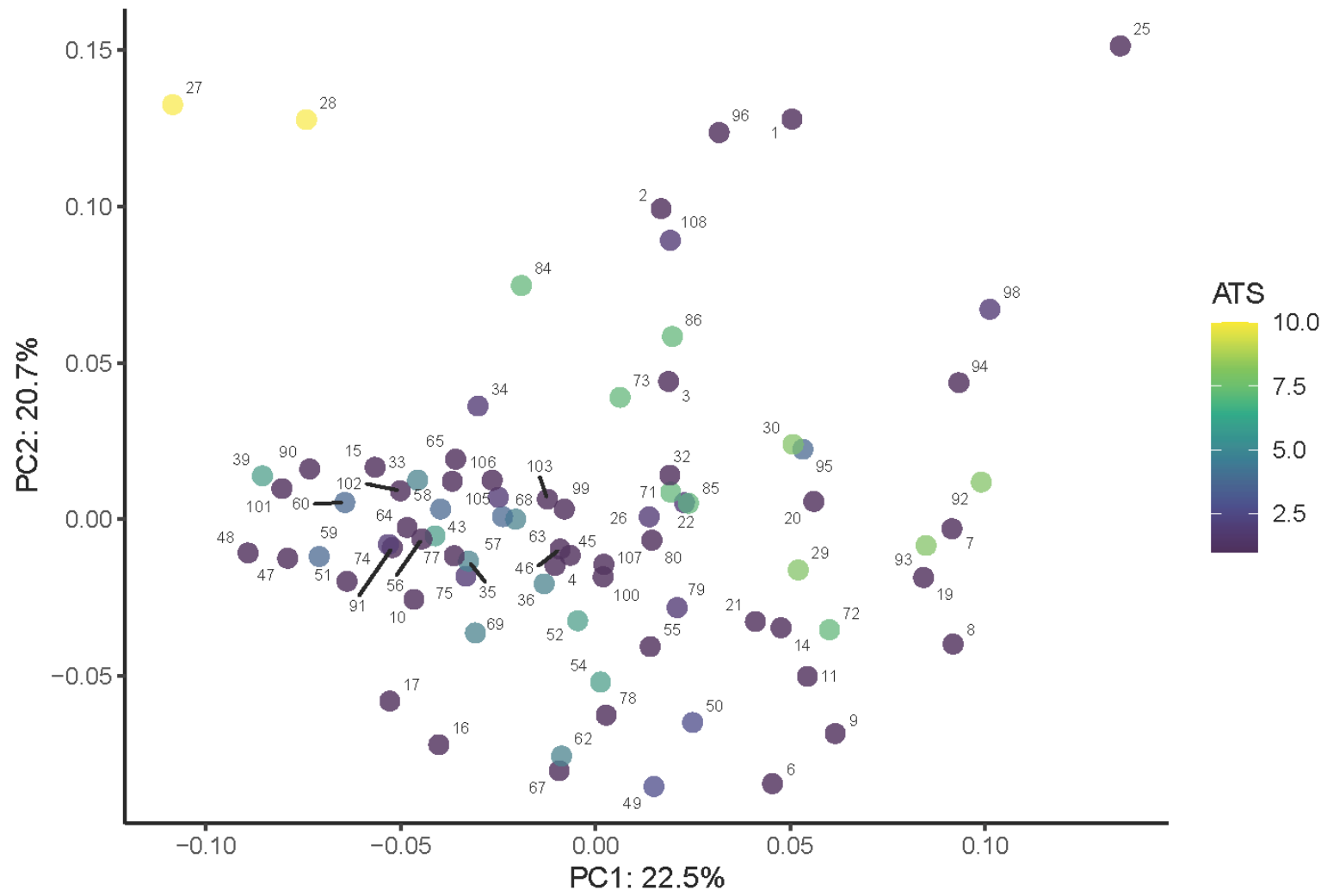
Supplemental Figure 5.90. Dorsal, lateral, ventral, anterior, and posterior views (A-E, respectively) of the caudal vertebra of *Sinomicrurus peinani* (ROM 37109).



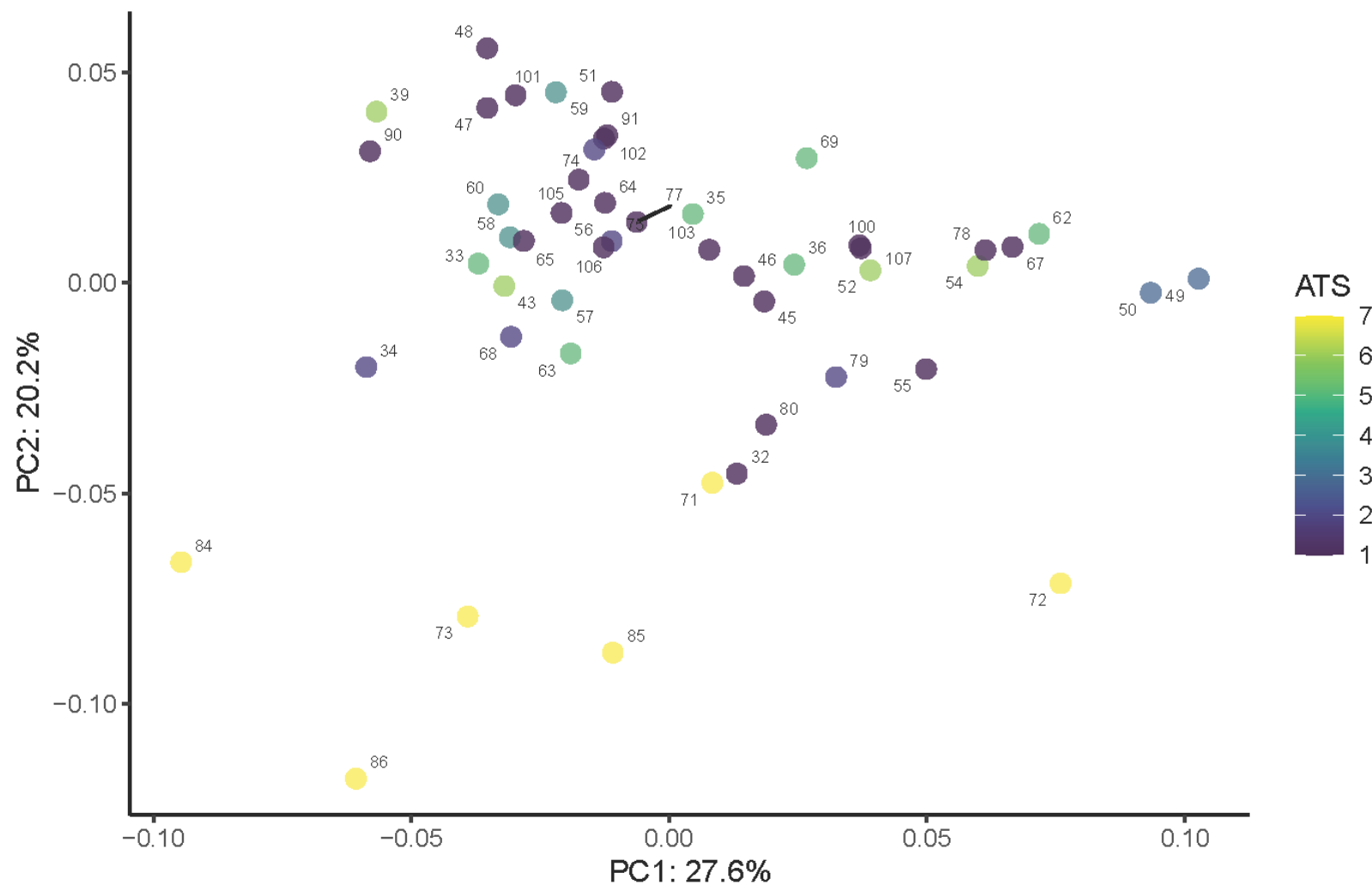
Supplemental Figure 5.91. Dorsal, lateral, ventral, anterior, and posterior views (A-E, respectively) of the caudal vertebra of *Sinomicrurus swinhoei* (MVZ 23876).



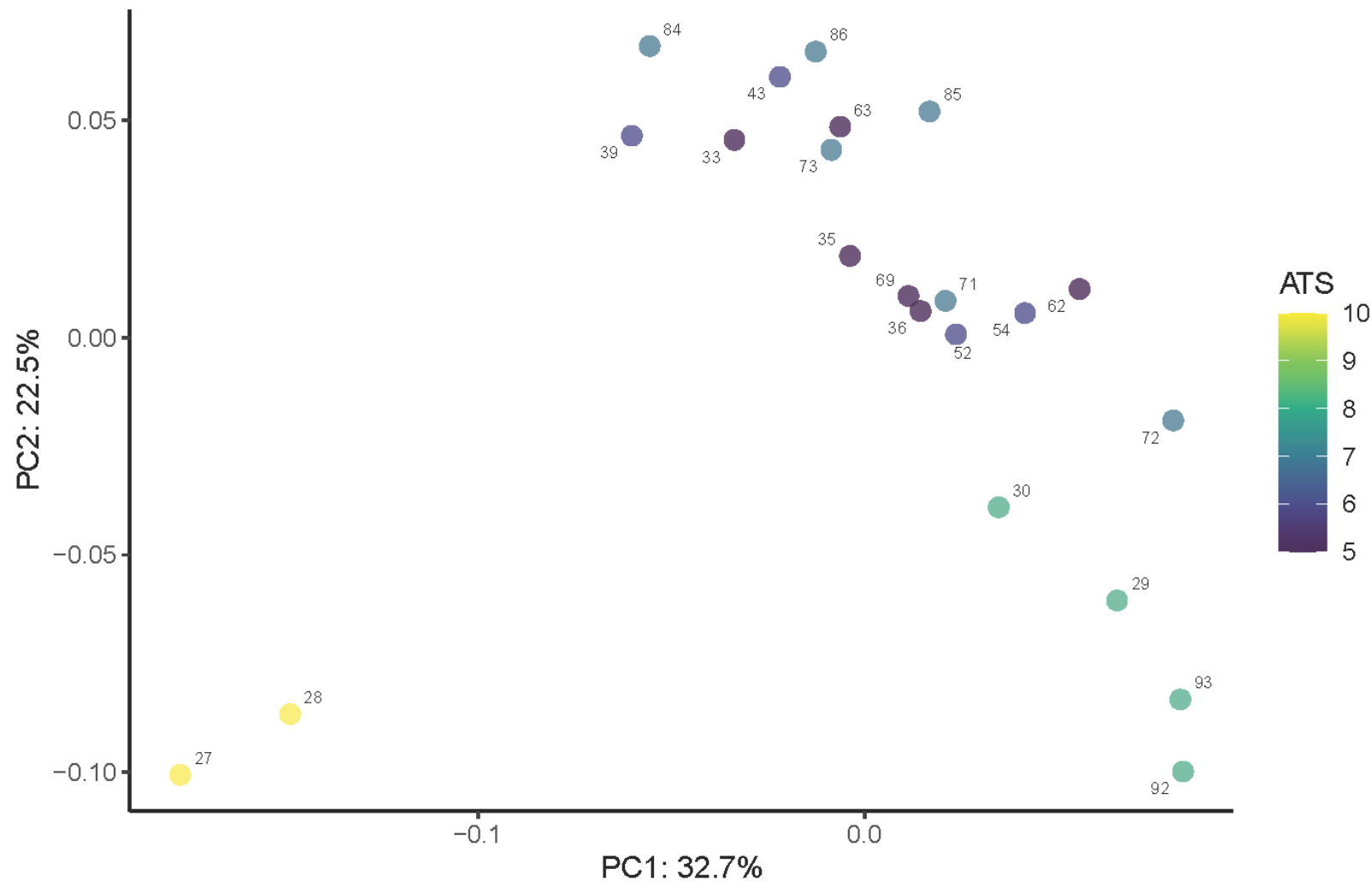
Supplemental Figure 5.92. Dorsal, lateral, ventral, anterior, and posterior views (A-E, respectively) of the caudal vertebra of *Walterinnesia aegyptia* (UTA R-13021).



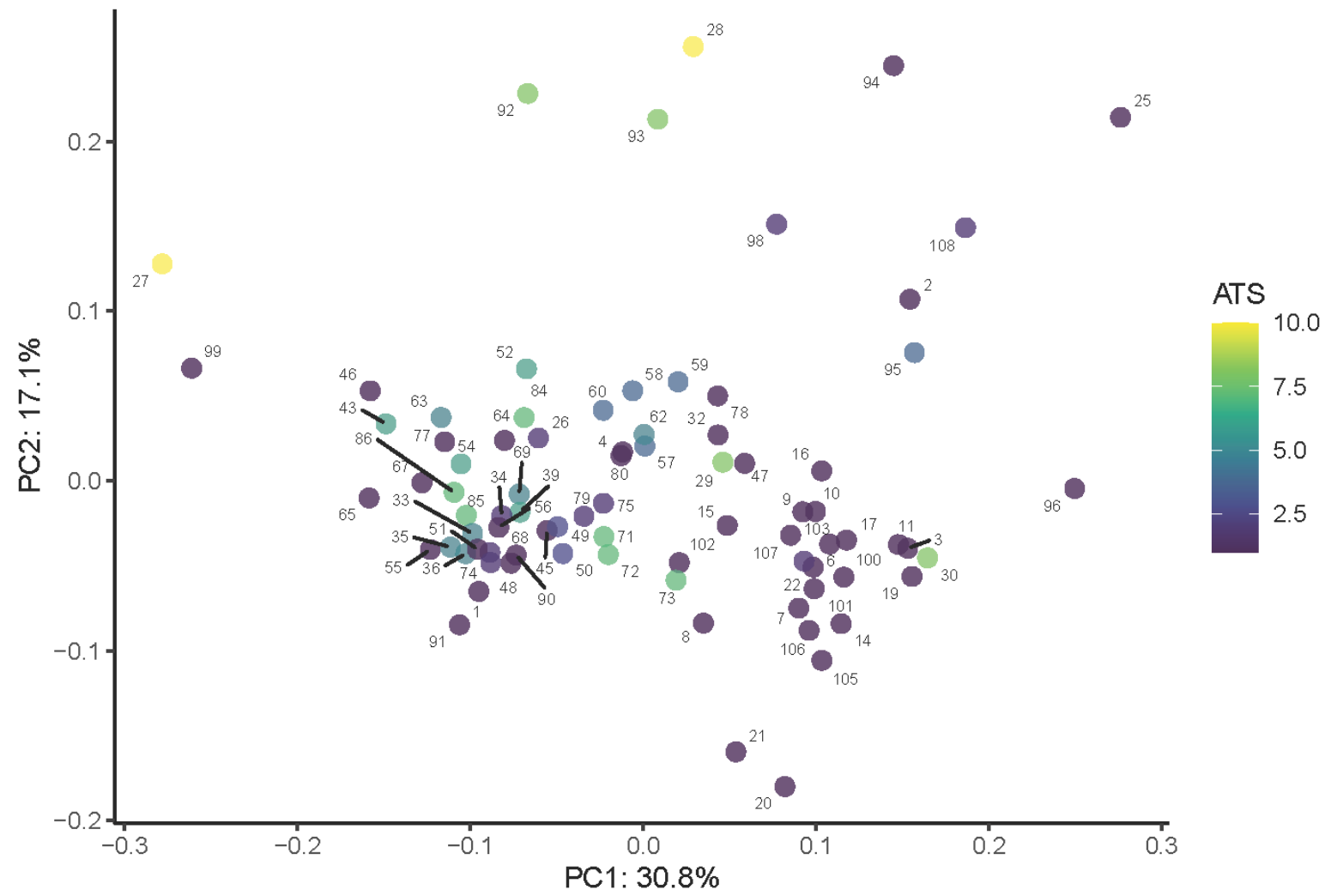
Supplemental Figure 6. PCA of the skull, utilizing all specimens, colored by ATS. Numbering corresponds with Table 2.1.



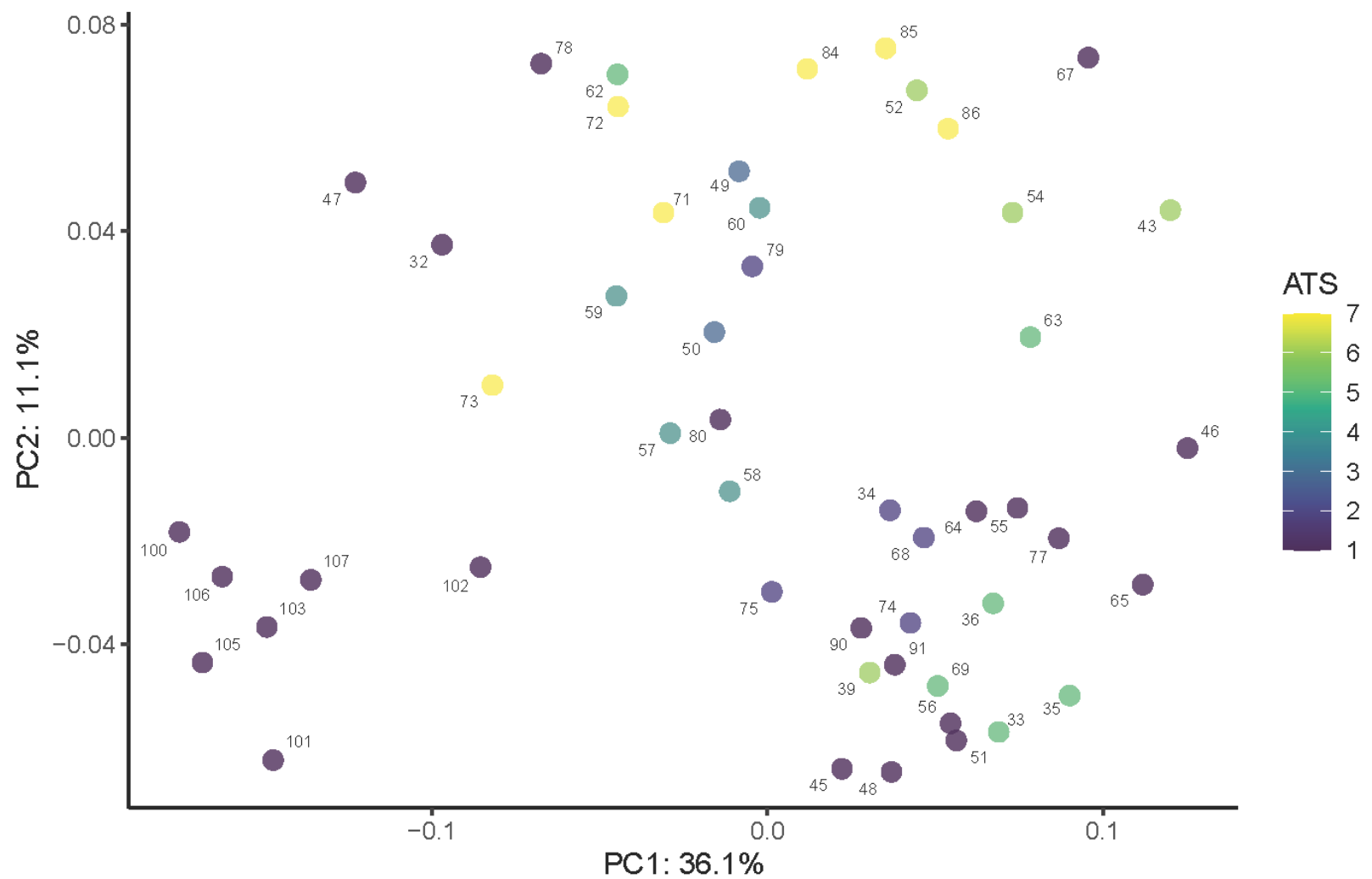
Supplemental Figure 7. PCA of the skull conducted on the coralsnake subset, colored by ATS. Numbering corresponds with Table 2.1.



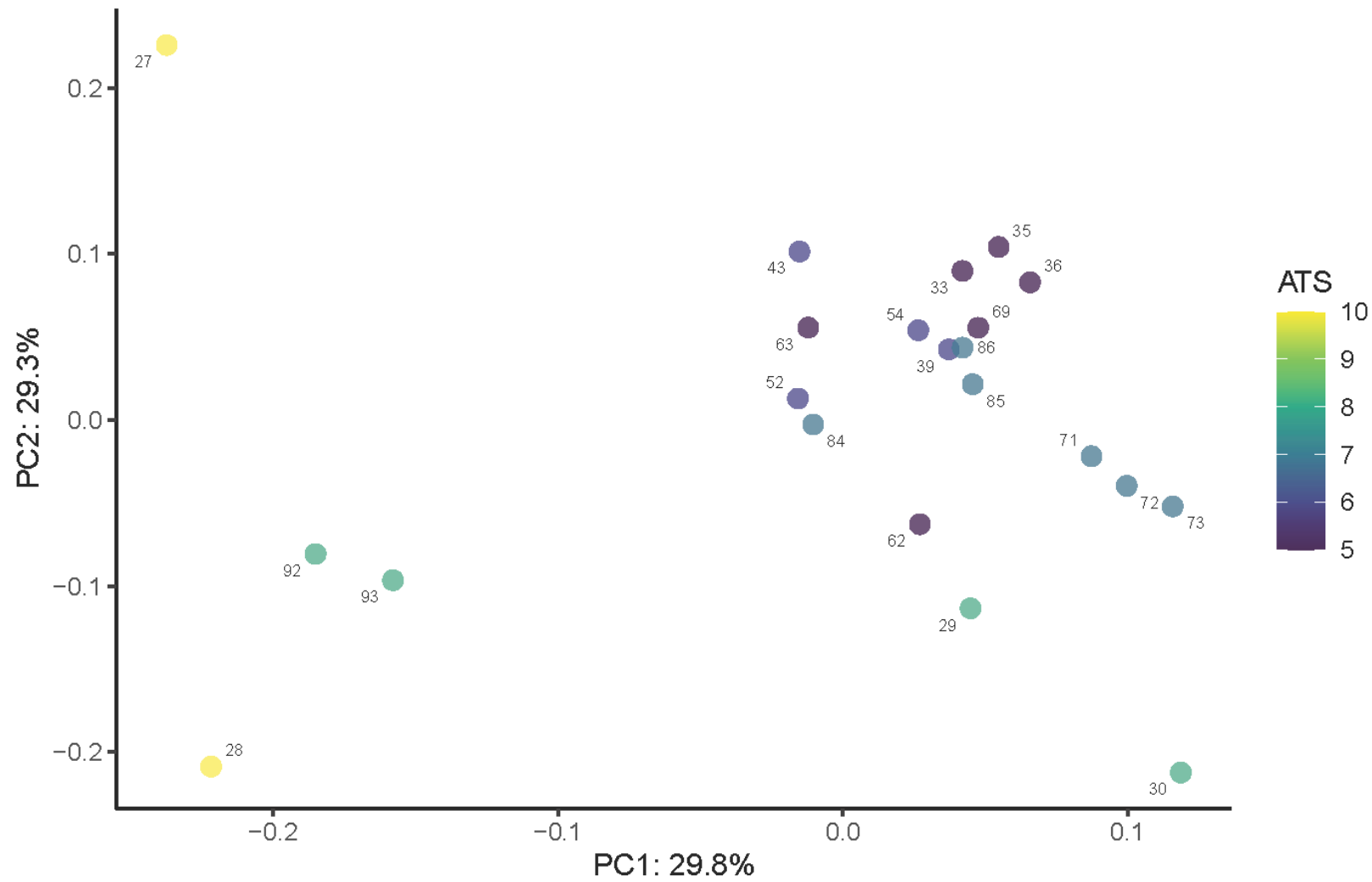
Supplemental Figure 8. PCA of the skull of the semi-aquatic and aquatic subset (>5 ATS), colored by ATS. Numbering corresponds with Table 2.1.



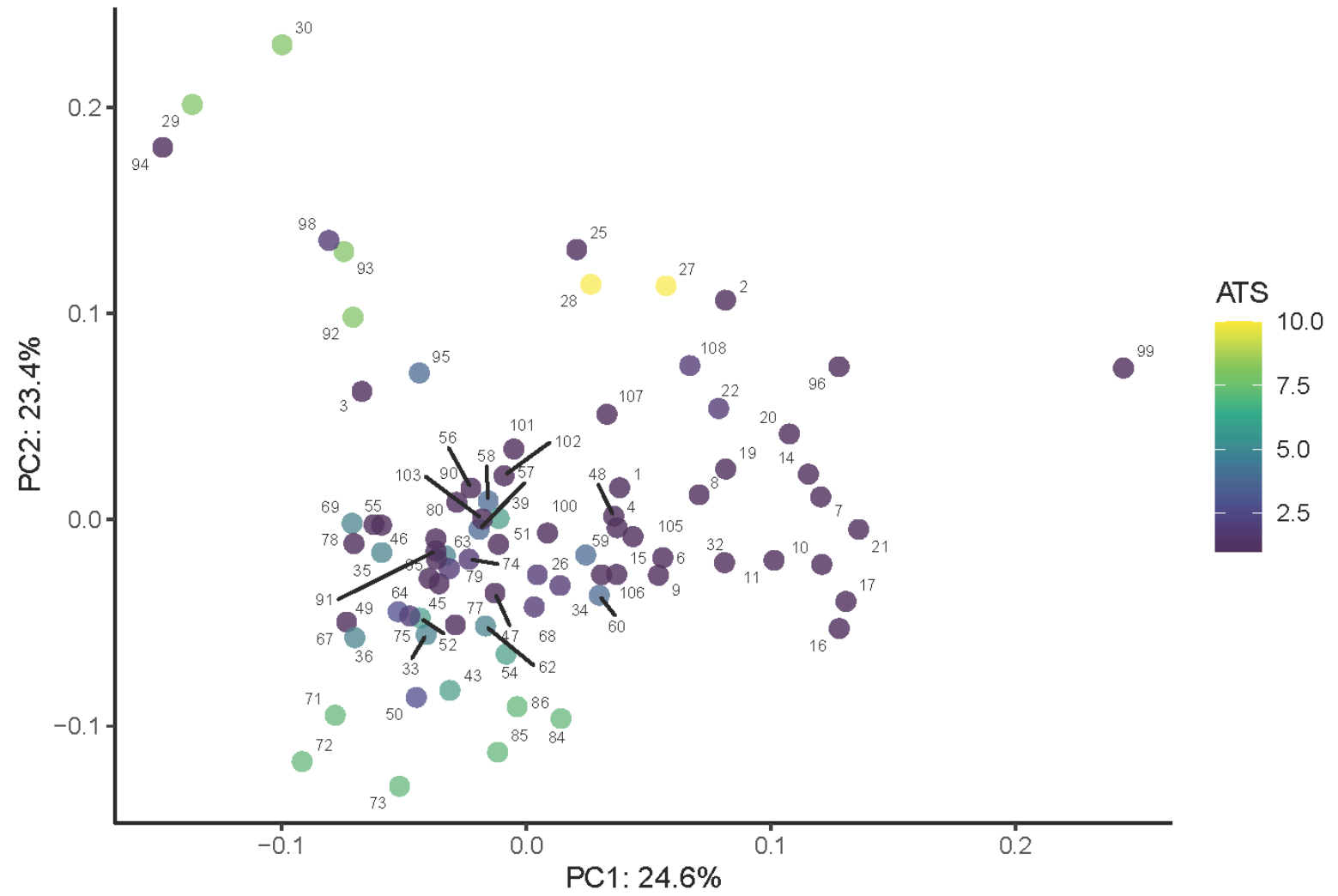
Supplemental Figure 9. PCA of the premaxilla module, utilizing all specimens, colored by ATS. Numbering corresponds with Table 2.1.



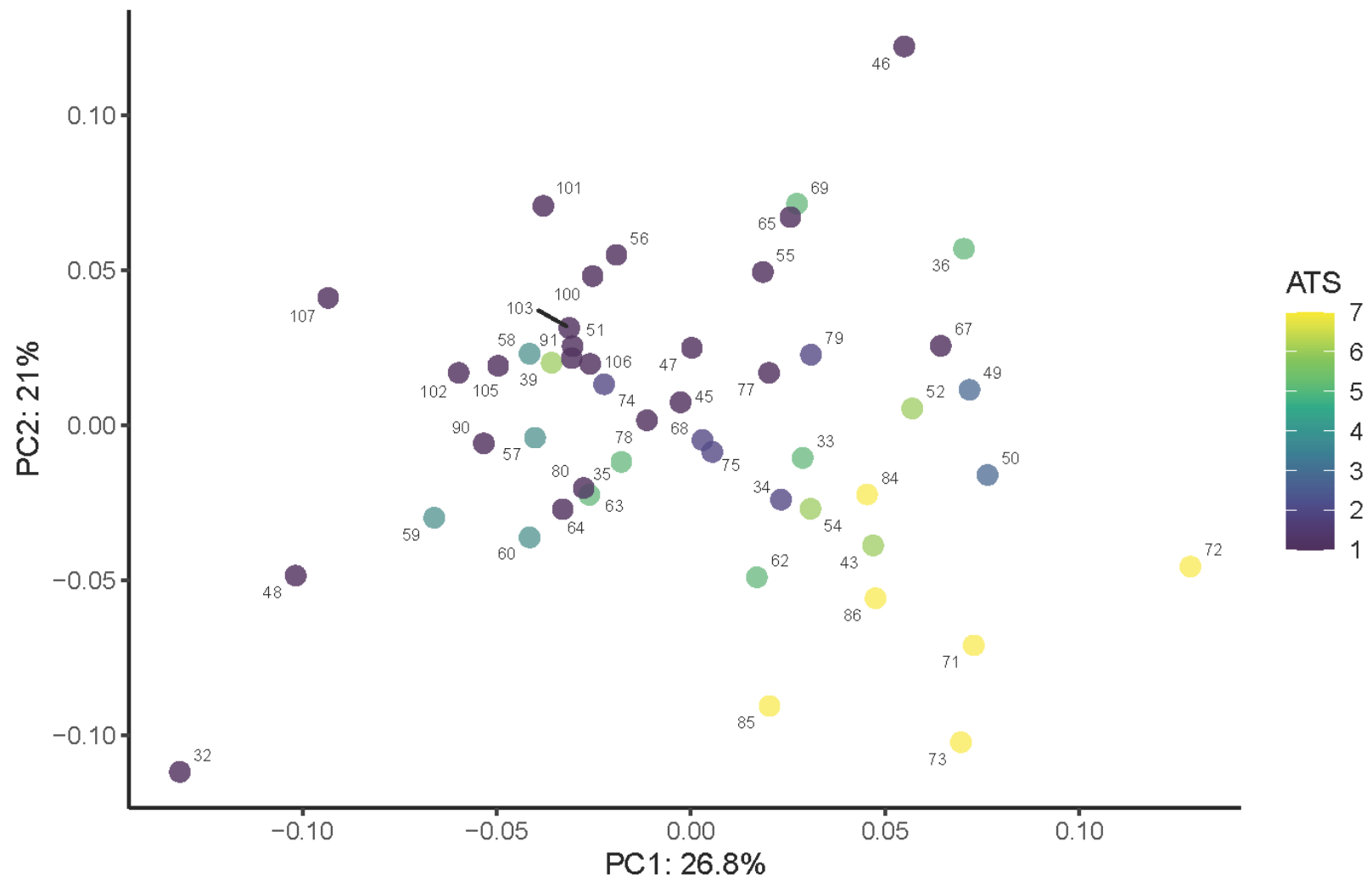
Supplemental Figure 10. PCA of the premaxilla module conducted on the coralsnake subset, colored by ATS. Numbering corresponds with Table 2.1.



Supplemental Figure 11. PCA of the premaxilla module conducted on the semi-aquatic and aquatic subset (>5 ATS), colored by ATS. Numbering corresponds with Table 2.1.

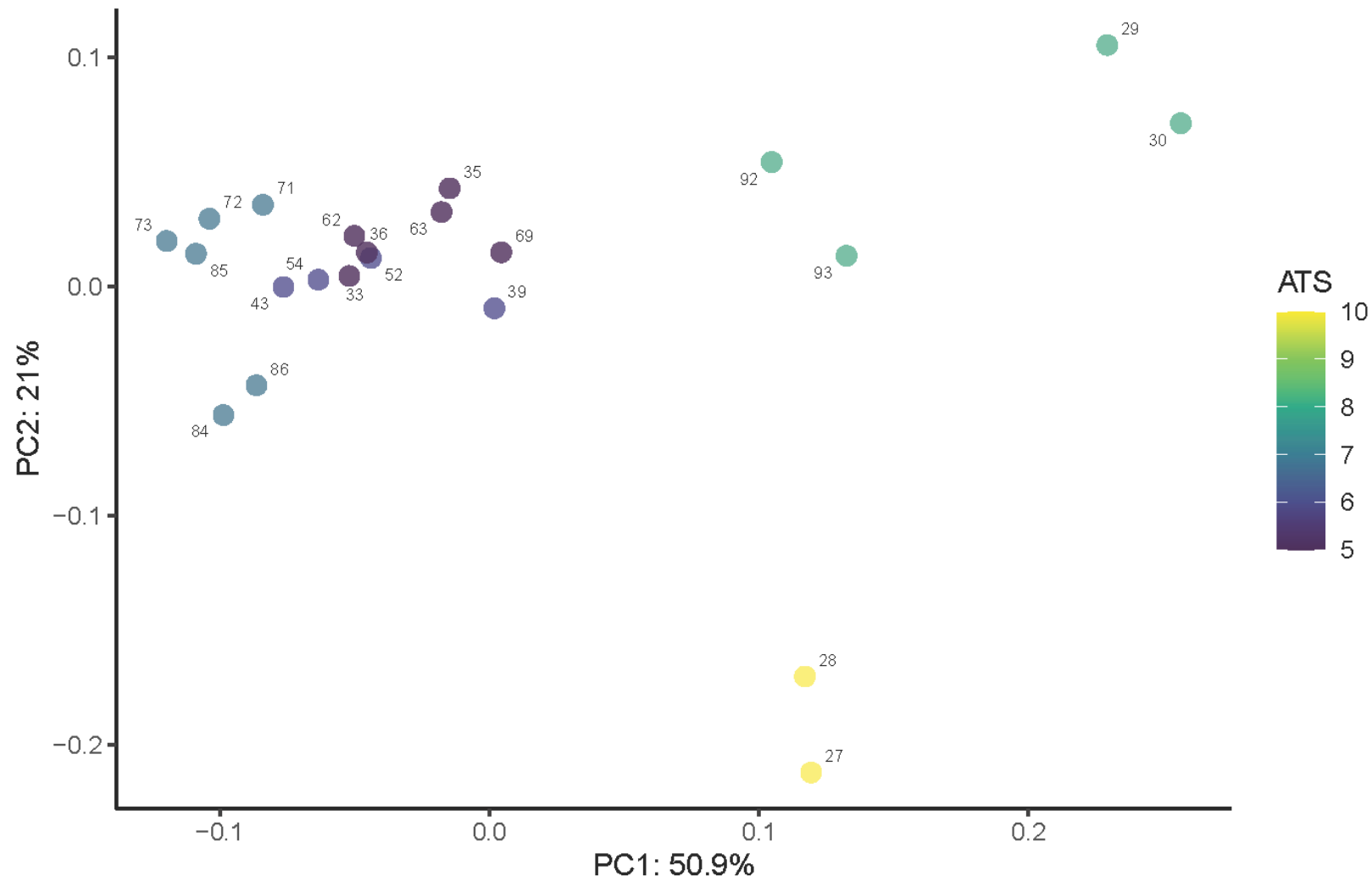


Supplemental Figure 12. PCA of the septomaxilla and vomer module, utilizing all specimens, colored by ATS. Numbering corresponds with Table 2.1.

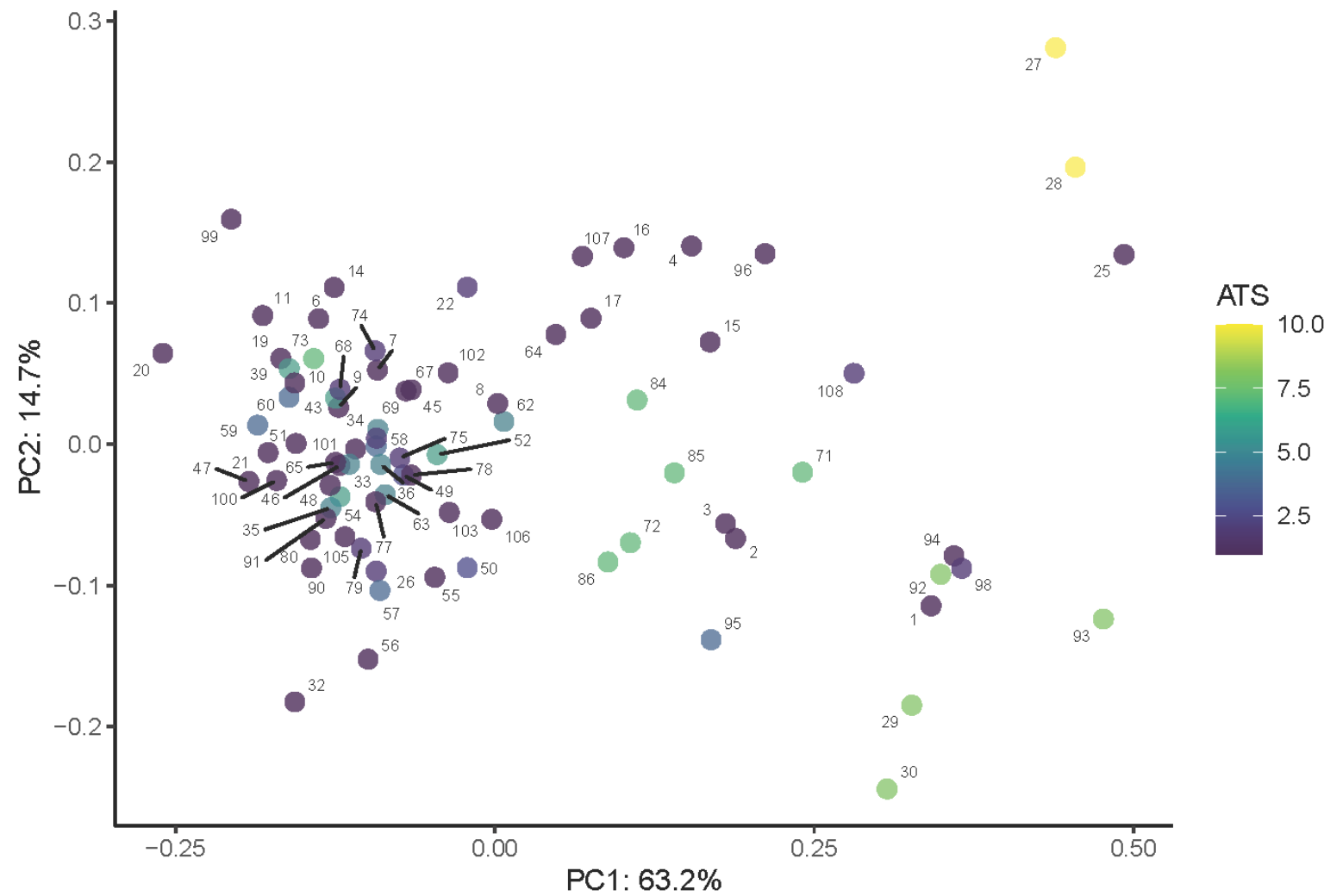


Supplemental Figure 13. PCA of the septomaxilla and vomer module conducted on the coralsnake subset, colored by ATS.

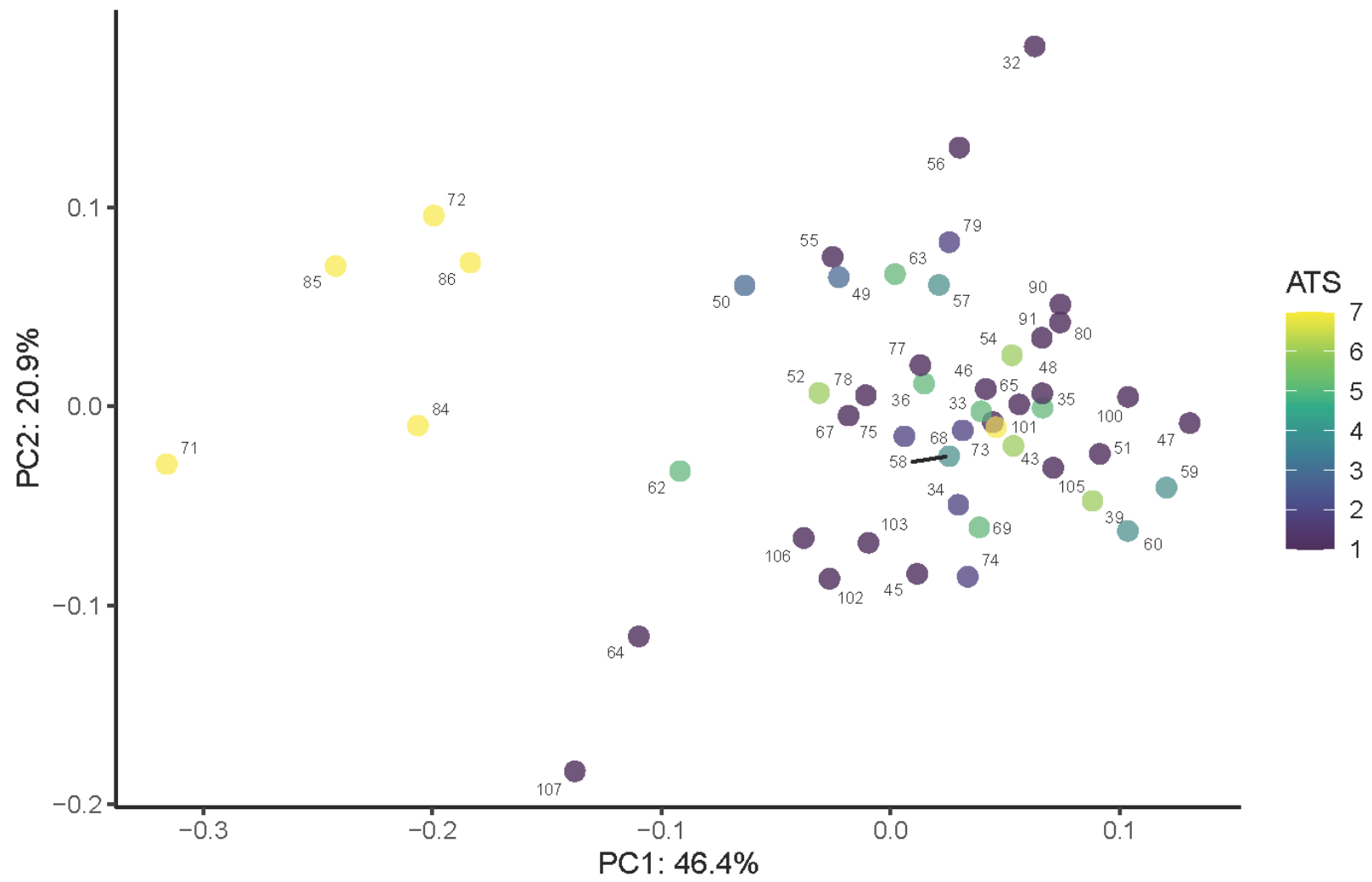
Numbering corresponds with Table 2.1.



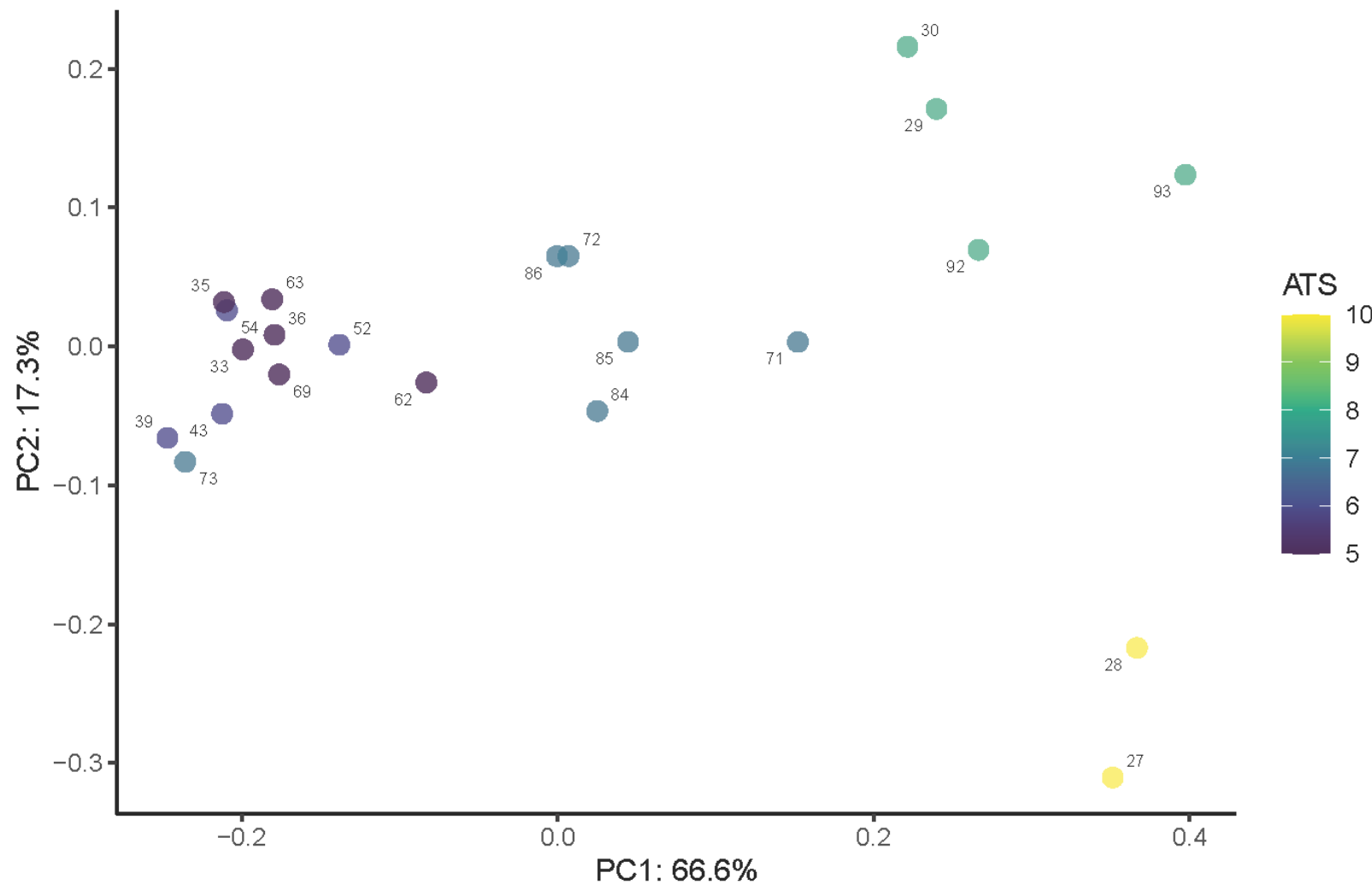
Supplemental Figure 14. PCA of the septomaxilla and vomer module conducted on the semi-aquatic and aquatic subset (>5 ATS), colored by ATS. Numbering corresponds with Table 2.1.



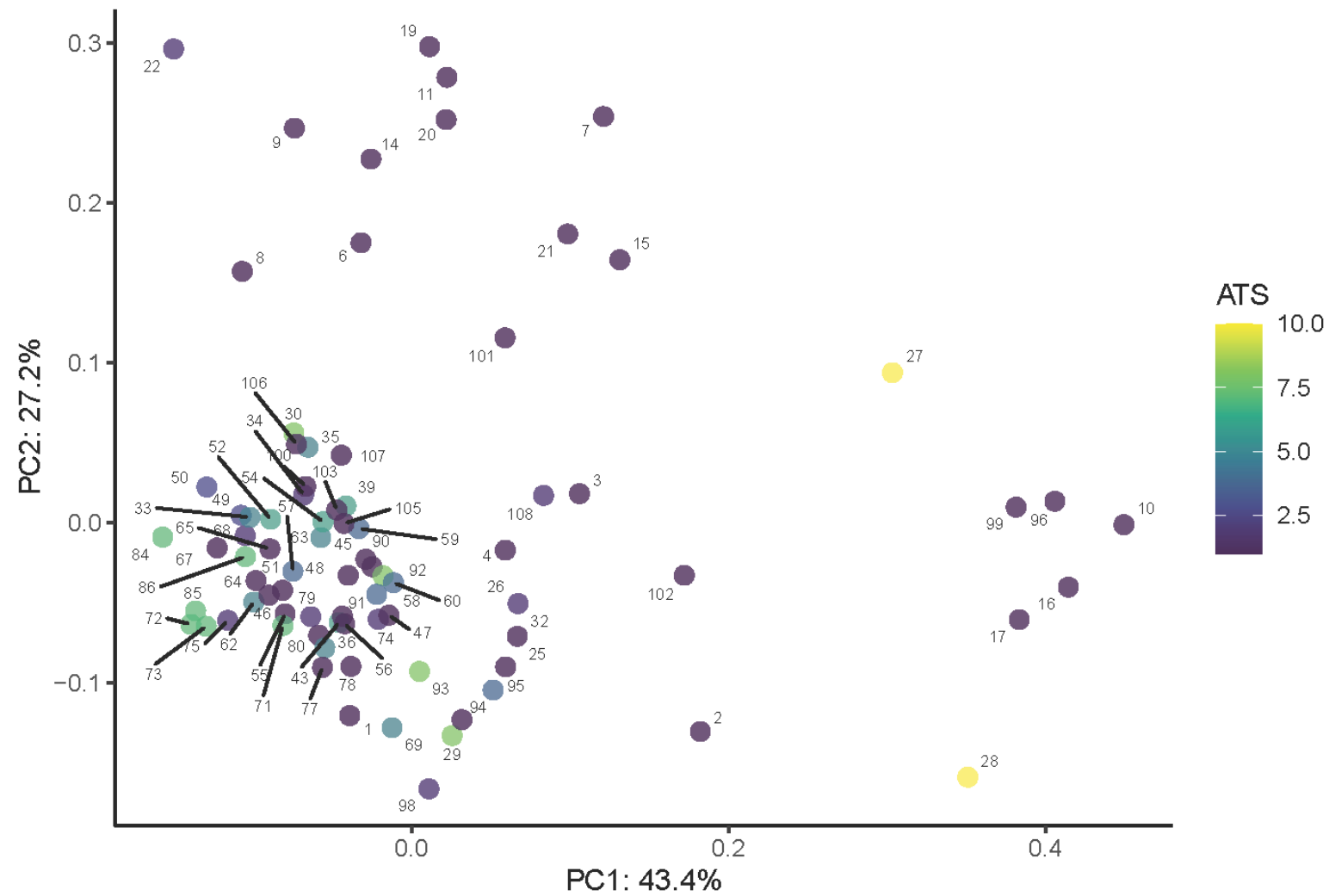
Supplemental Figure 15. PCA of the nasal module, utilizing all specimens, colored by ATS. Numbering corresponds with Table 2.1.



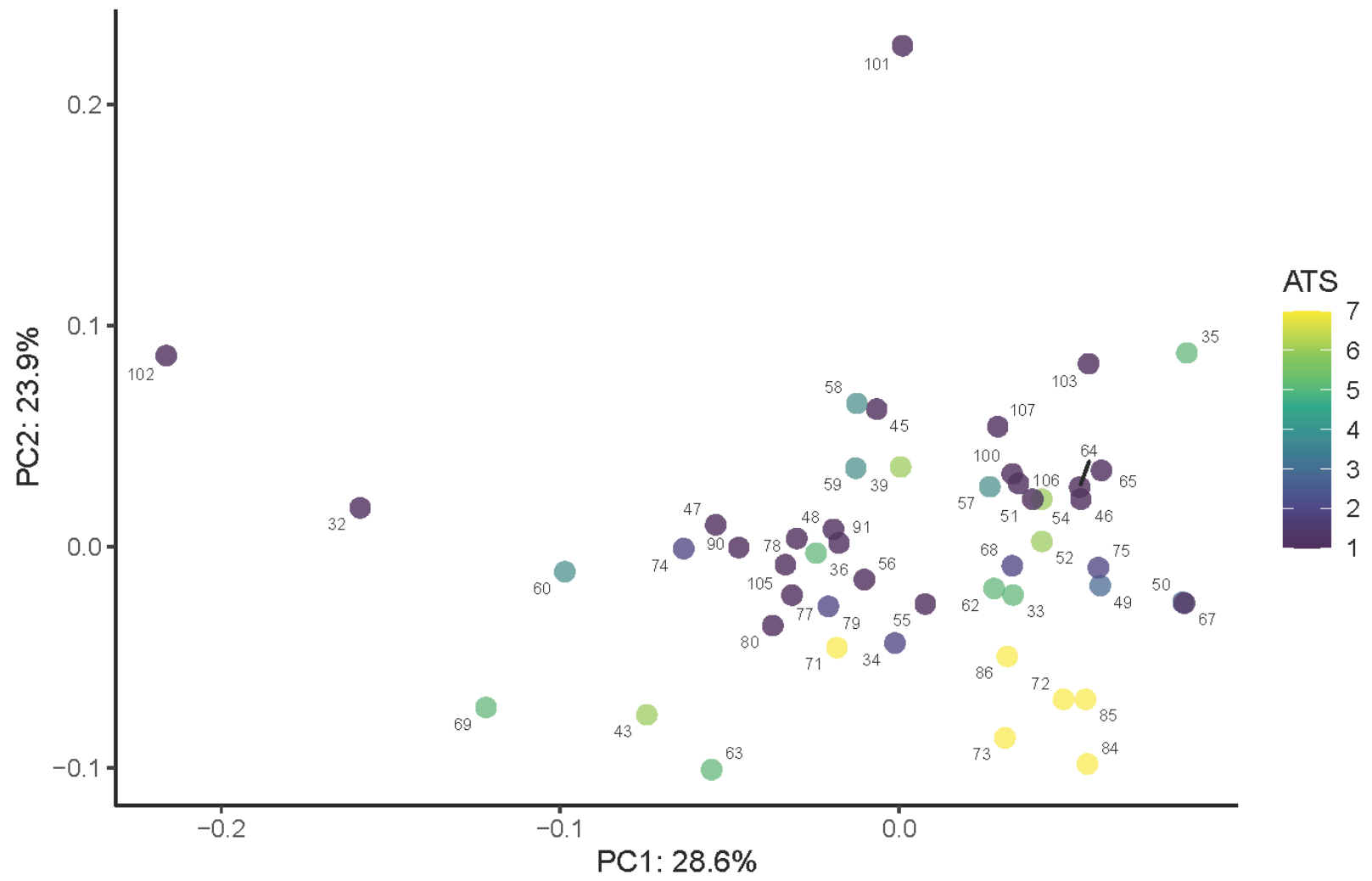
Supplemental Figure 16. PCA of the nasal module conducted on the coralsnake subset, colored by ATS. Numbering corresponds with Table 2.1.



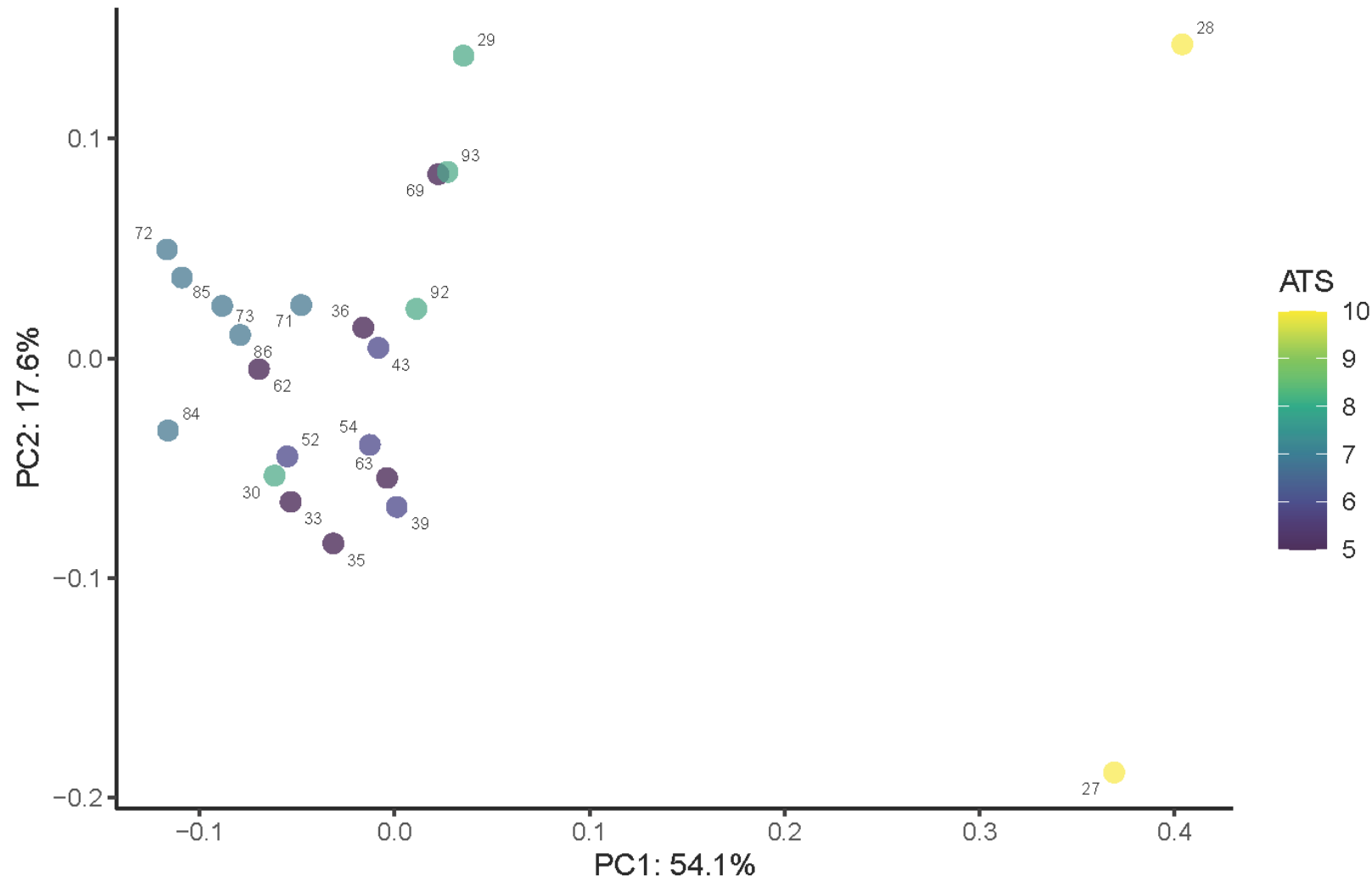
Supplemental Figure 17. PCA of the nasal module conducted on the semi-aquatic and aquatic subset (>5 ATS), colored by ATS. Numbering corresponds with Table 2.1.



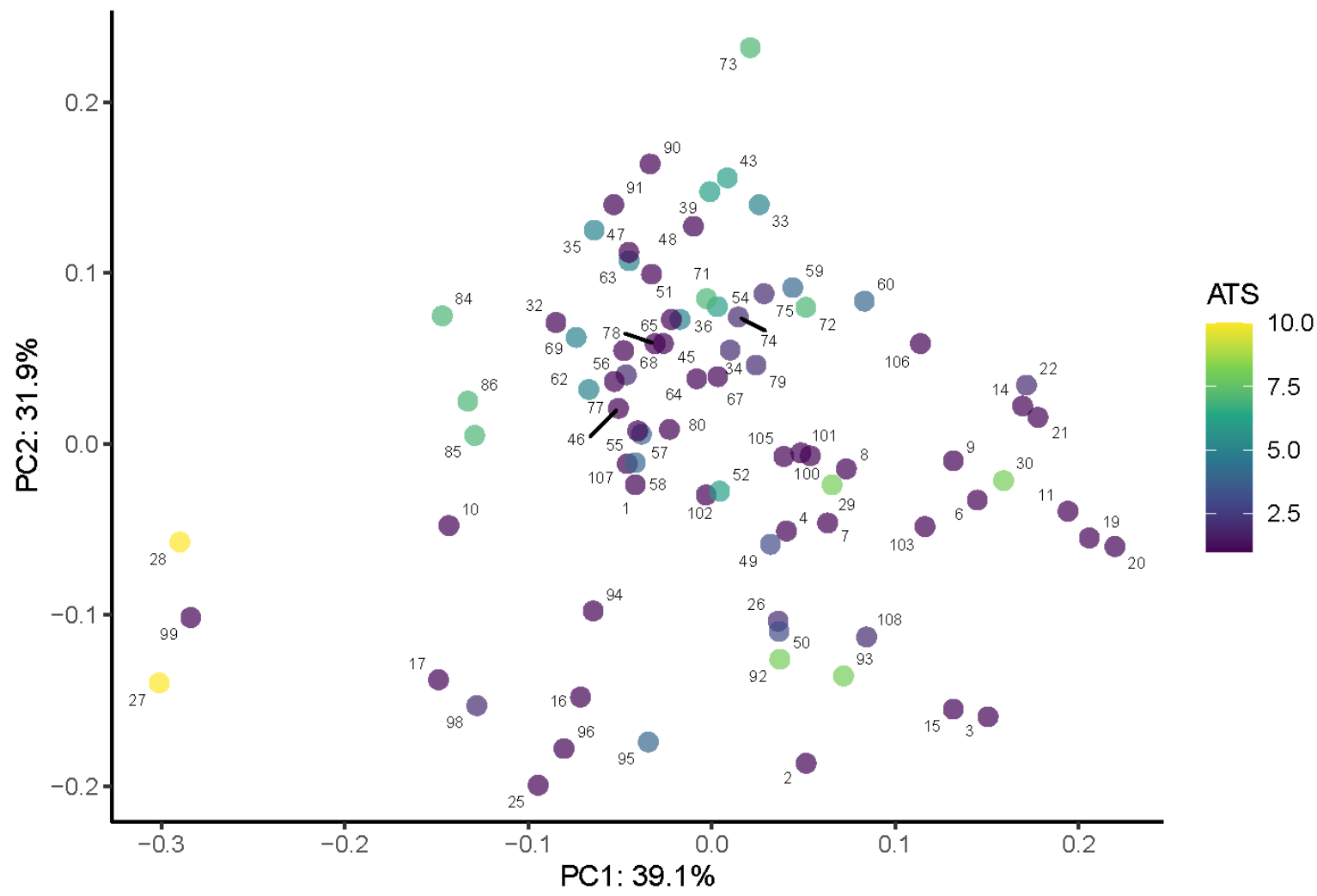
Supplemental Figure 18. PCA of the prefrontal module, utilizing all specimens, colored by ATS. Numbering corresponds with Table 2.1.



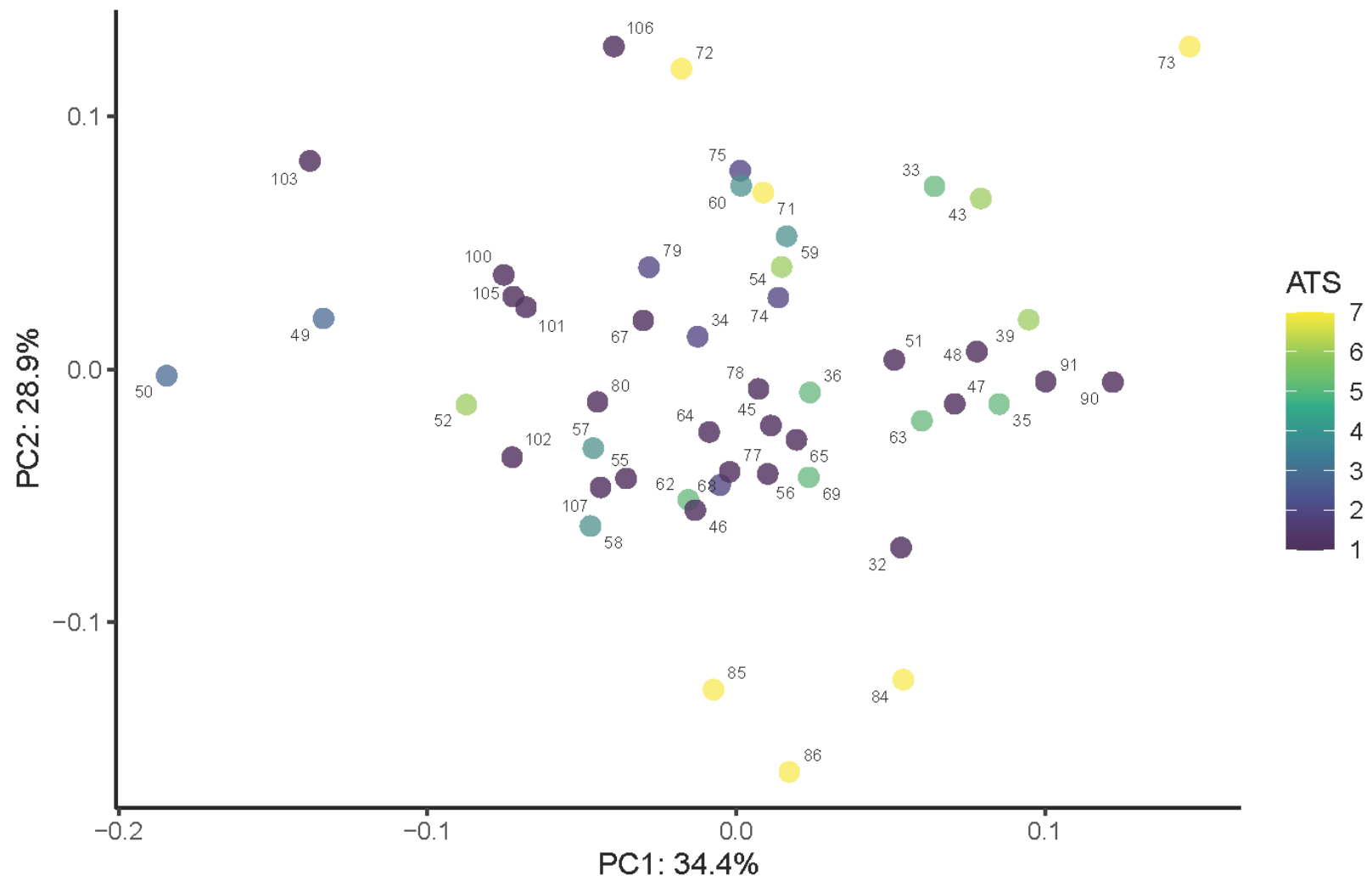
Supplemental Figure 19. PCA of the prefrontal module conducted on the coralsnake subset, colored by ATS. Numbering corresponds with Table 2.1.



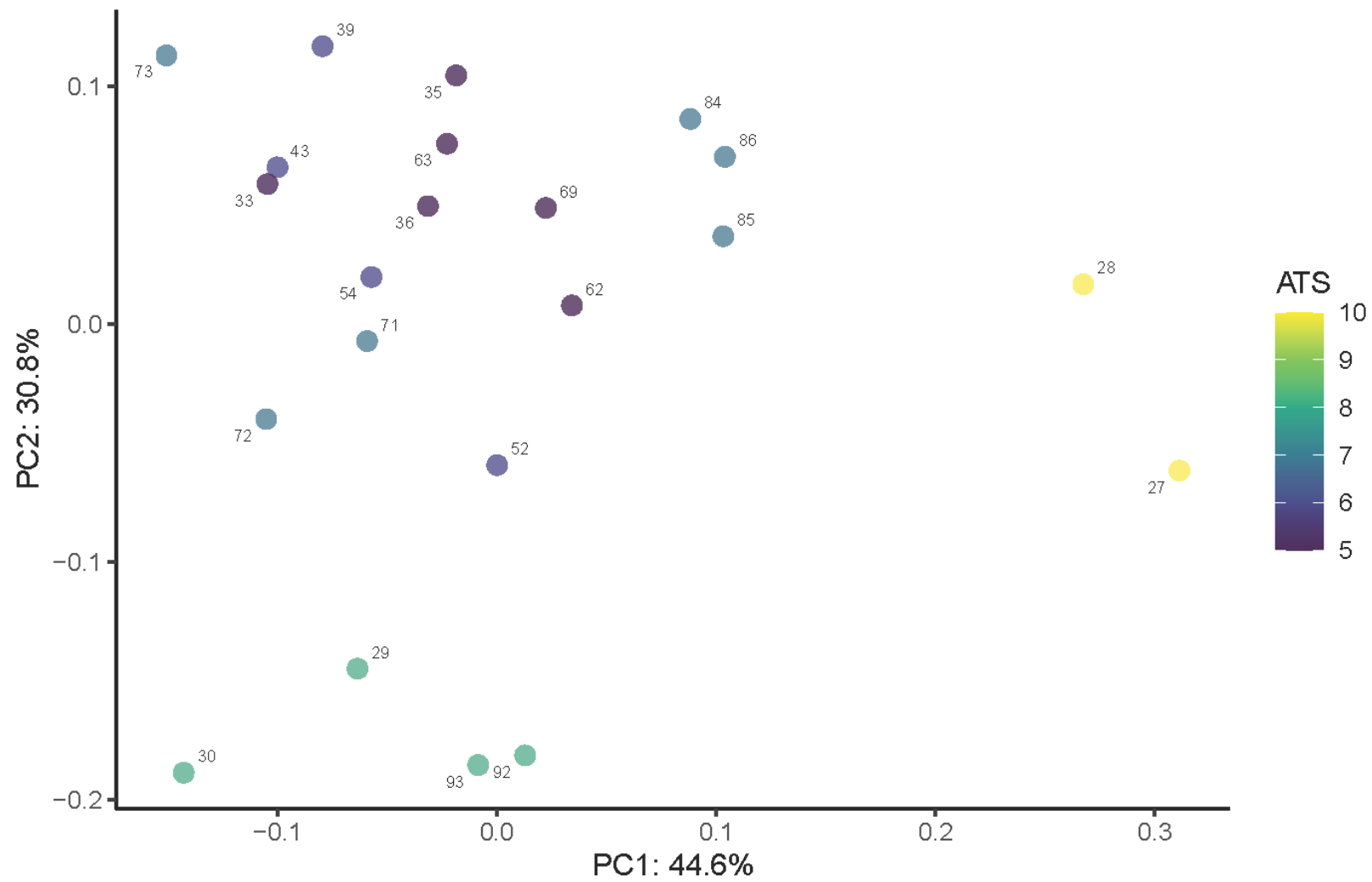
Supplemental Figure 20. PCA of the prefrontal module conducted on the semi-aquatic and aquatic subset (>5 ATS), colored by ATS. Numbering corresponds with Table 2.1.



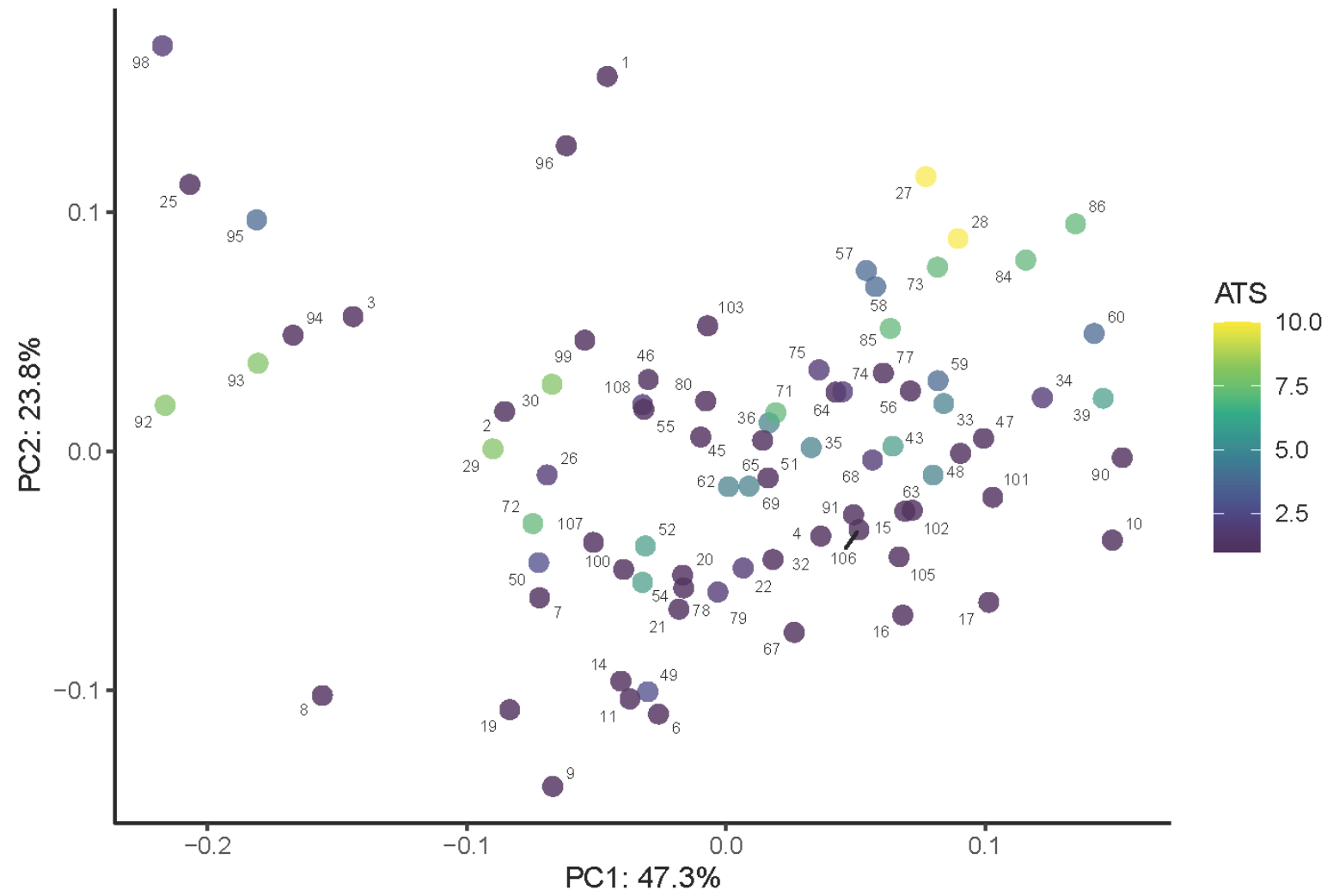
Supplemental Figure 21. PCA of the frontal module, utilizing all specimens, colored by ATS. Numbering corresponds with Table 2.1.



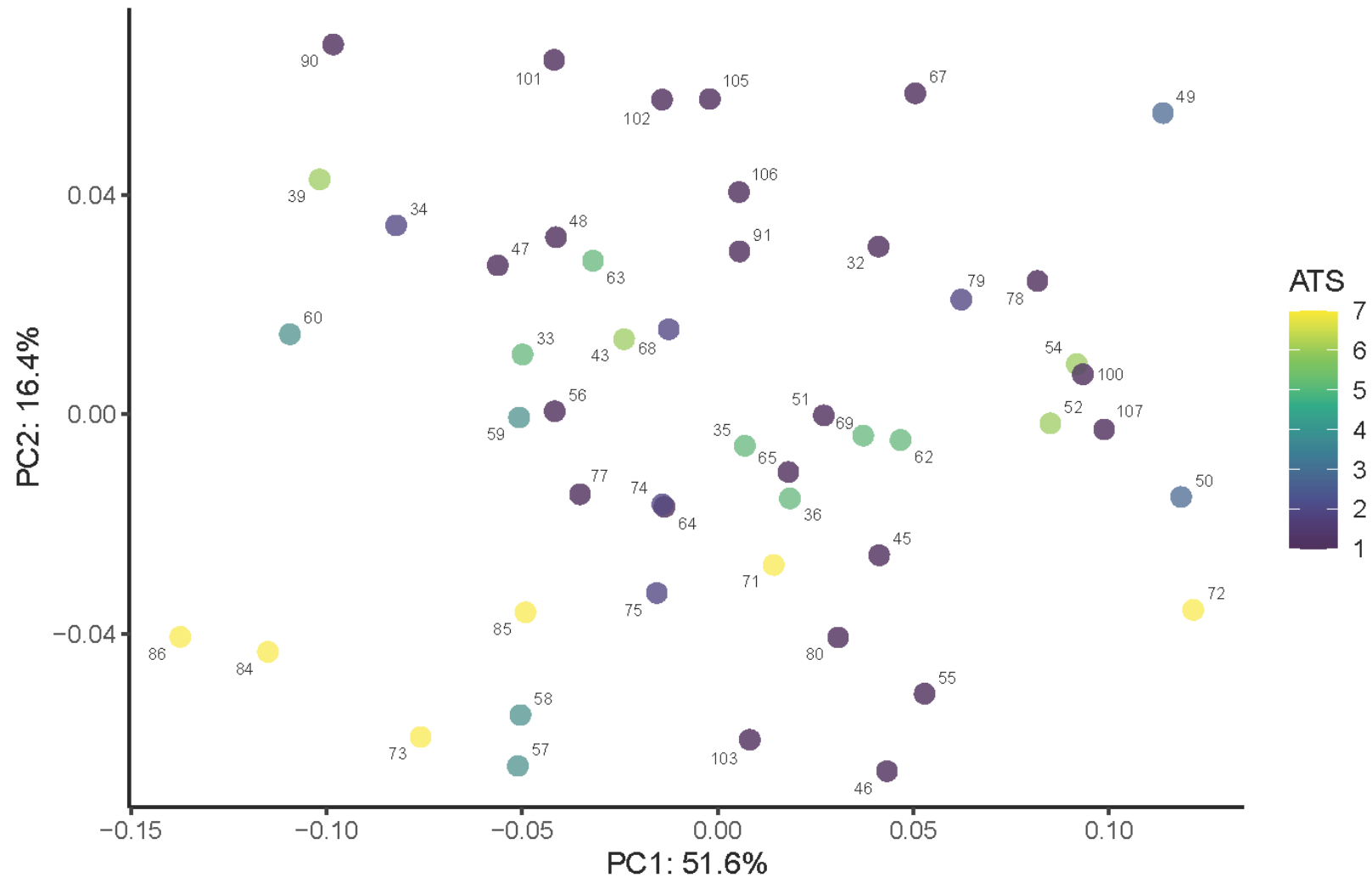
Supplemental Figure 22. PCA of the frontal module conducted on the coralsnake subset, colored by ATS. Numbering corresponds with Table 2.1.



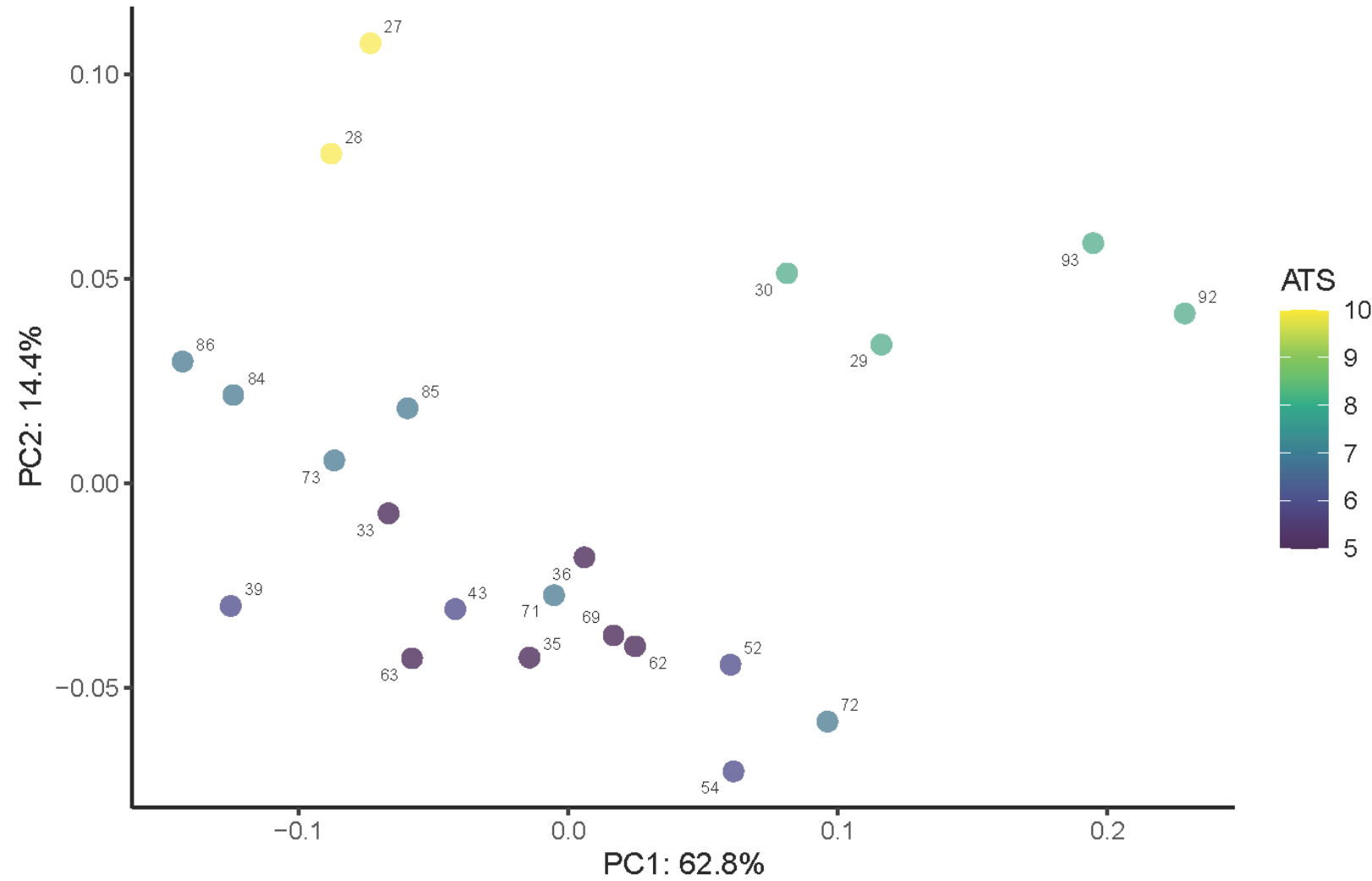
Supplemental Figure 23. PCA of the frontal module conducted on the semi-aquatic and aquatic subset (>5 ATS), colored by ATS. Numbering corresponds with Table 2.1.



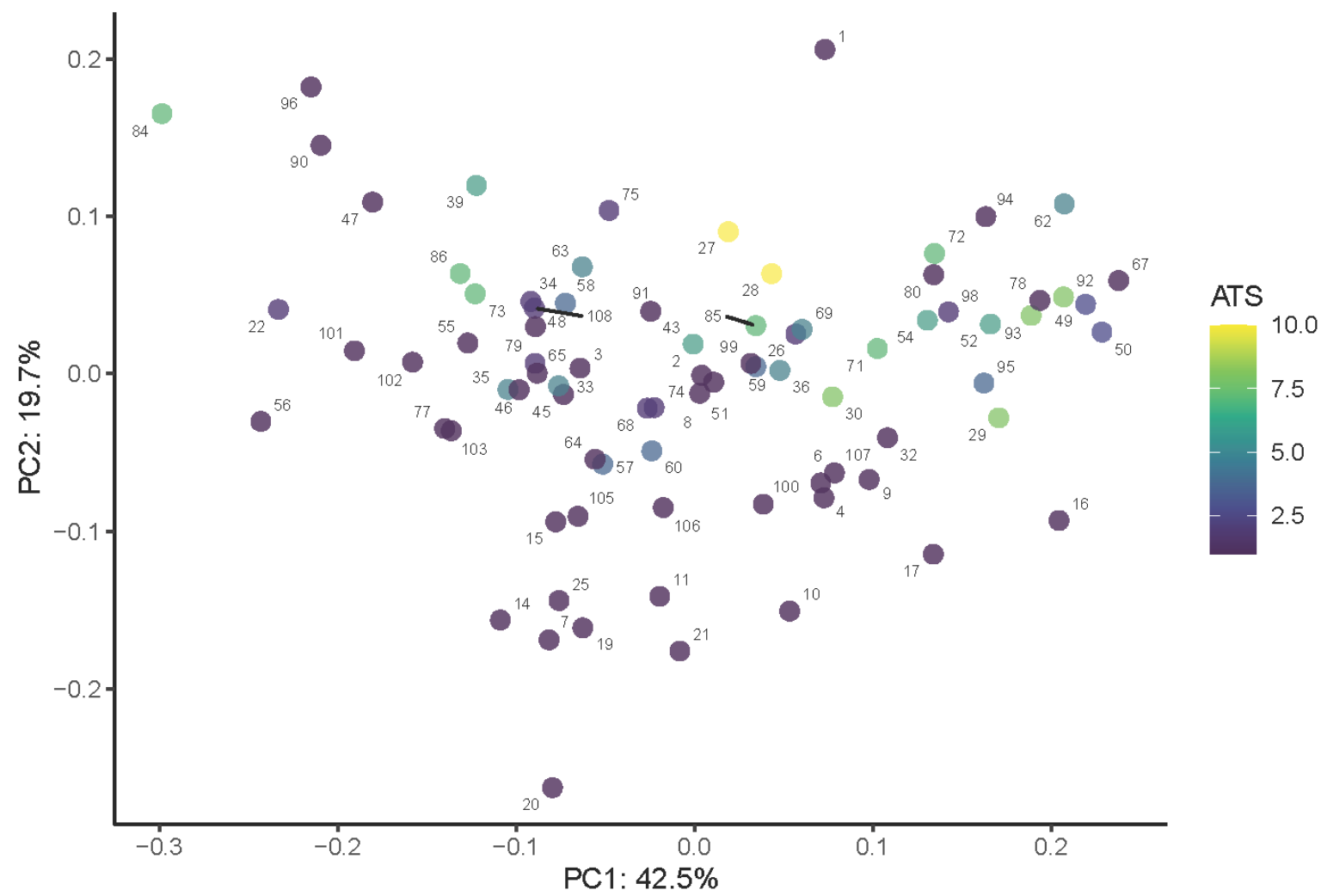
Supplemental Figure 24. PCA of the parietal module, utilizing all specimens, colored by ATS. Numbering corresponds with Table 2.1.



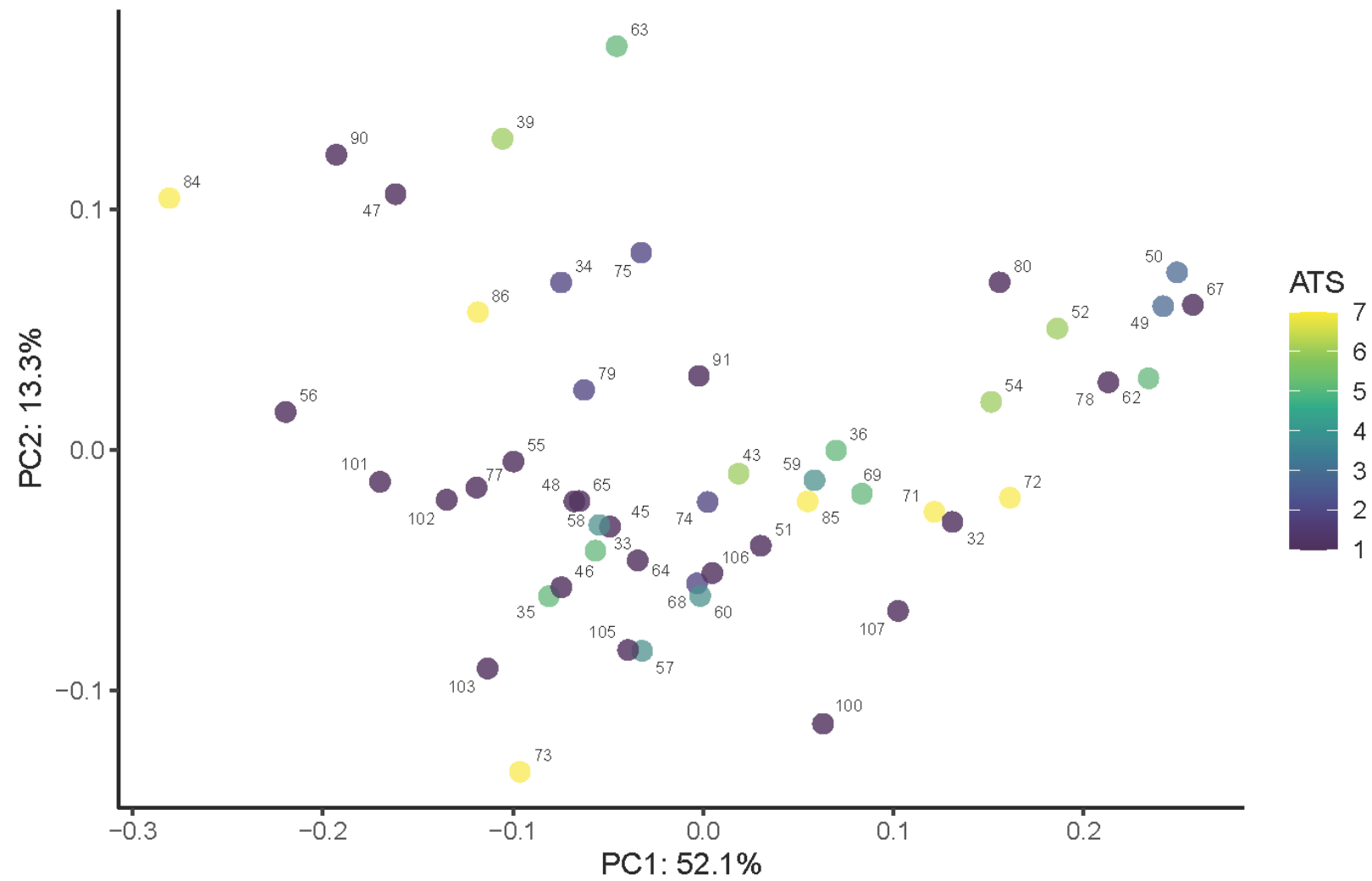
Supplemental Figure 25. PCA of the parietal module conducted on the coral snake subset, colored by ATS. Numbering corresponds with Table 2.1.



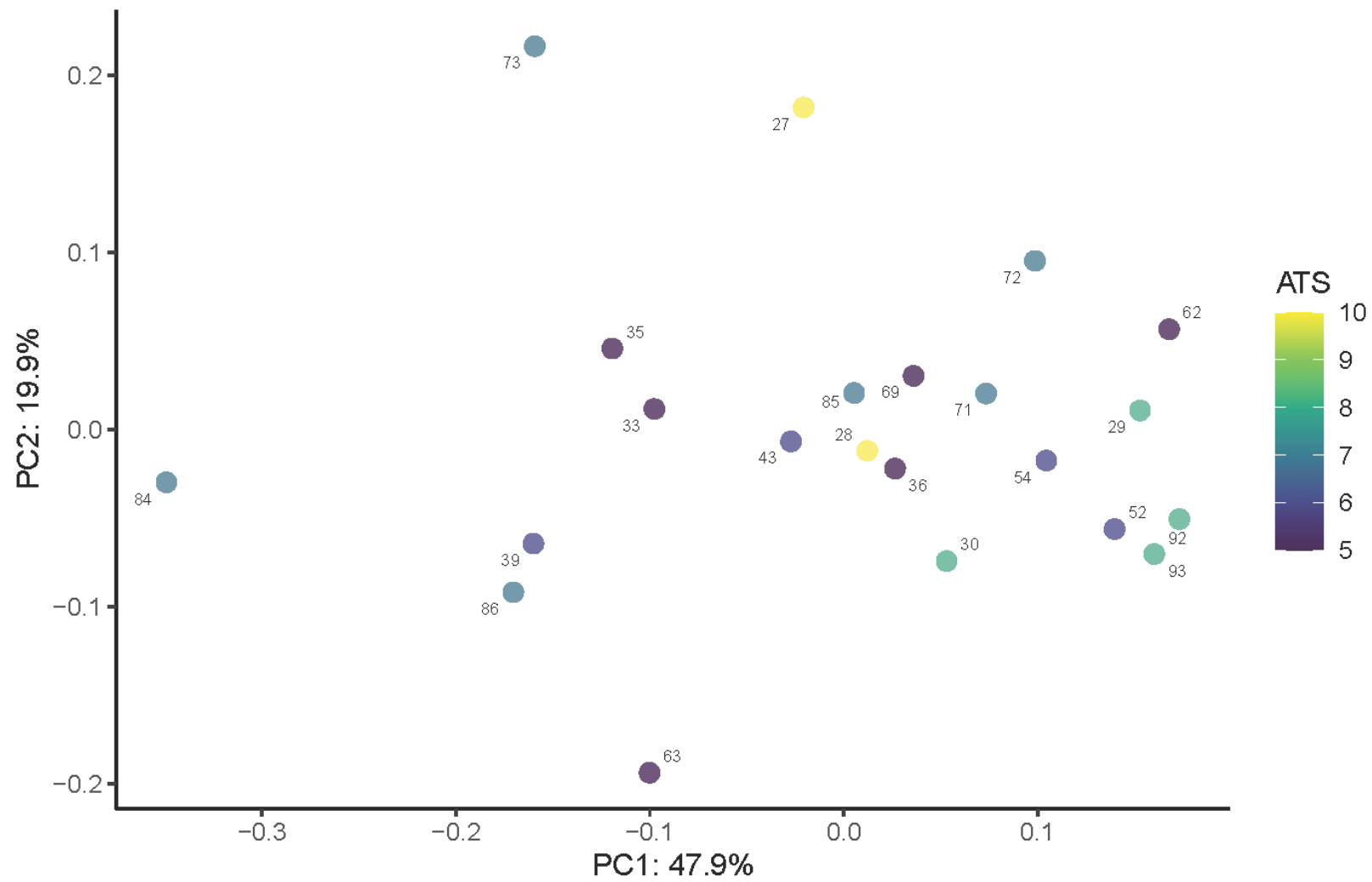
Supplemental Figure 26. PCA of the parietal module conducted on the semi-aquatic and aquatic subset (>5 ATS), colored by ATS. Numbering corresponds with Table 2.1.



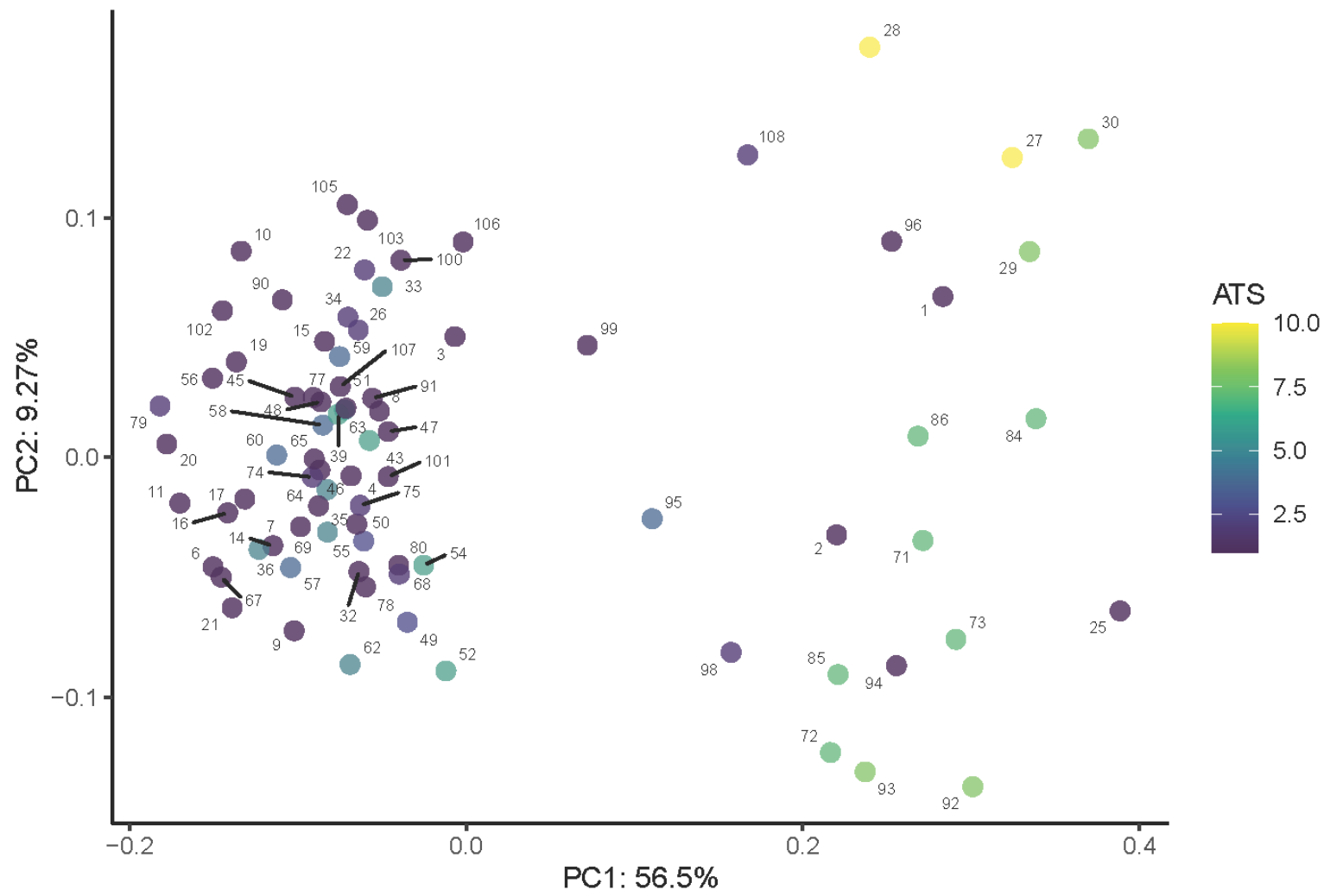
Supplemental Figure 27. PCA of the supraoccipital module, utilizing all specimens, colored by ATS. Numbering corresponds with Table 2.1.



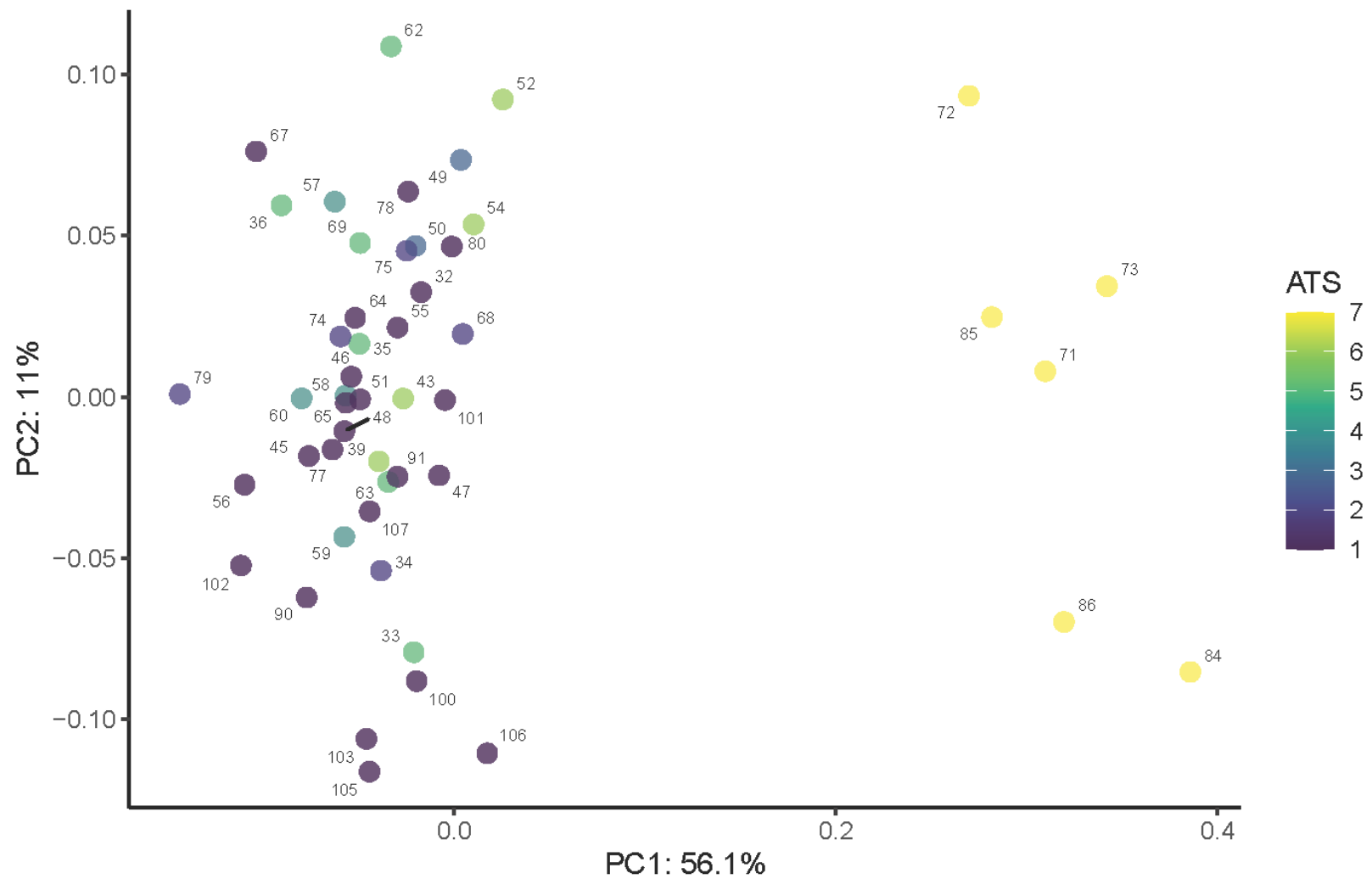
Supplemental Figure 28. PCA of the supraoccipital module conducted on the coralsnake subset, colored by ATS. Numbering corresponds with Table 2.1.



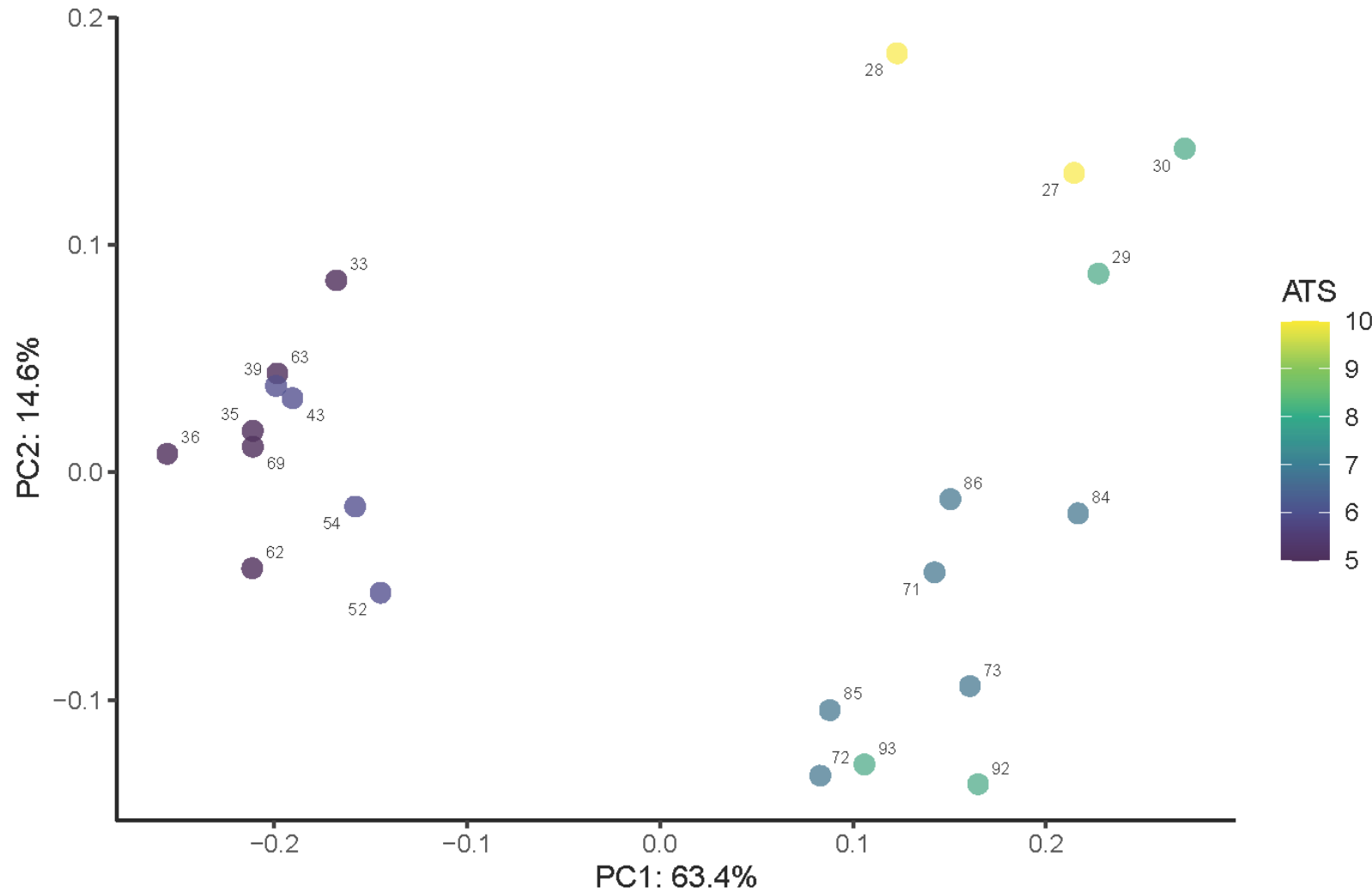
Supplemental Figure 29. PCA of the supraoccipital module conducted on the semi-aquatic and aquatic subset (>5 ATS), colored by ATS. Numbering corresponds with Table 2.1.



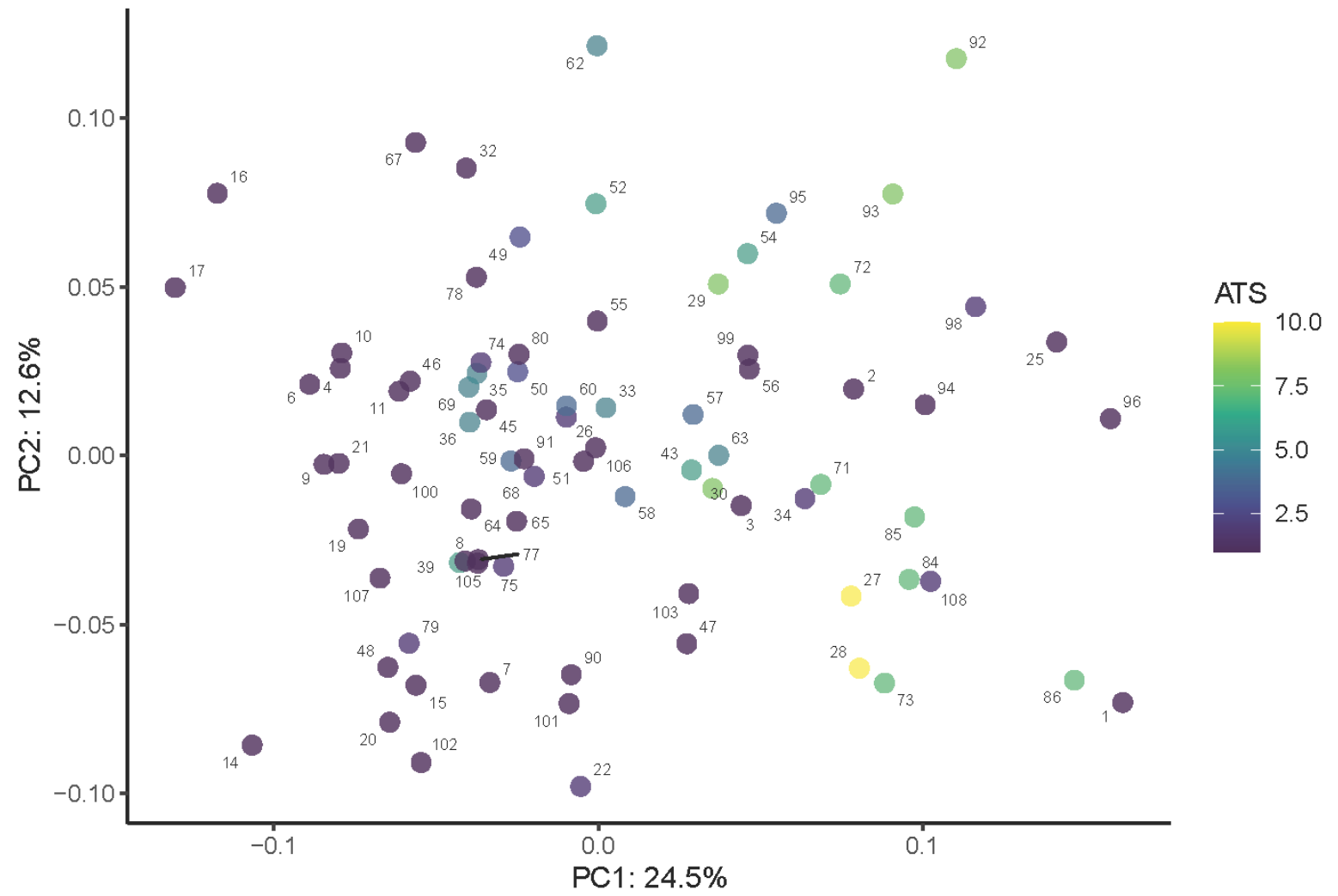
Supplemental Figure 30. PCA of the prootic module utilizing all specimens, colored by ATS. Numbering corresponds with Table 2.1.



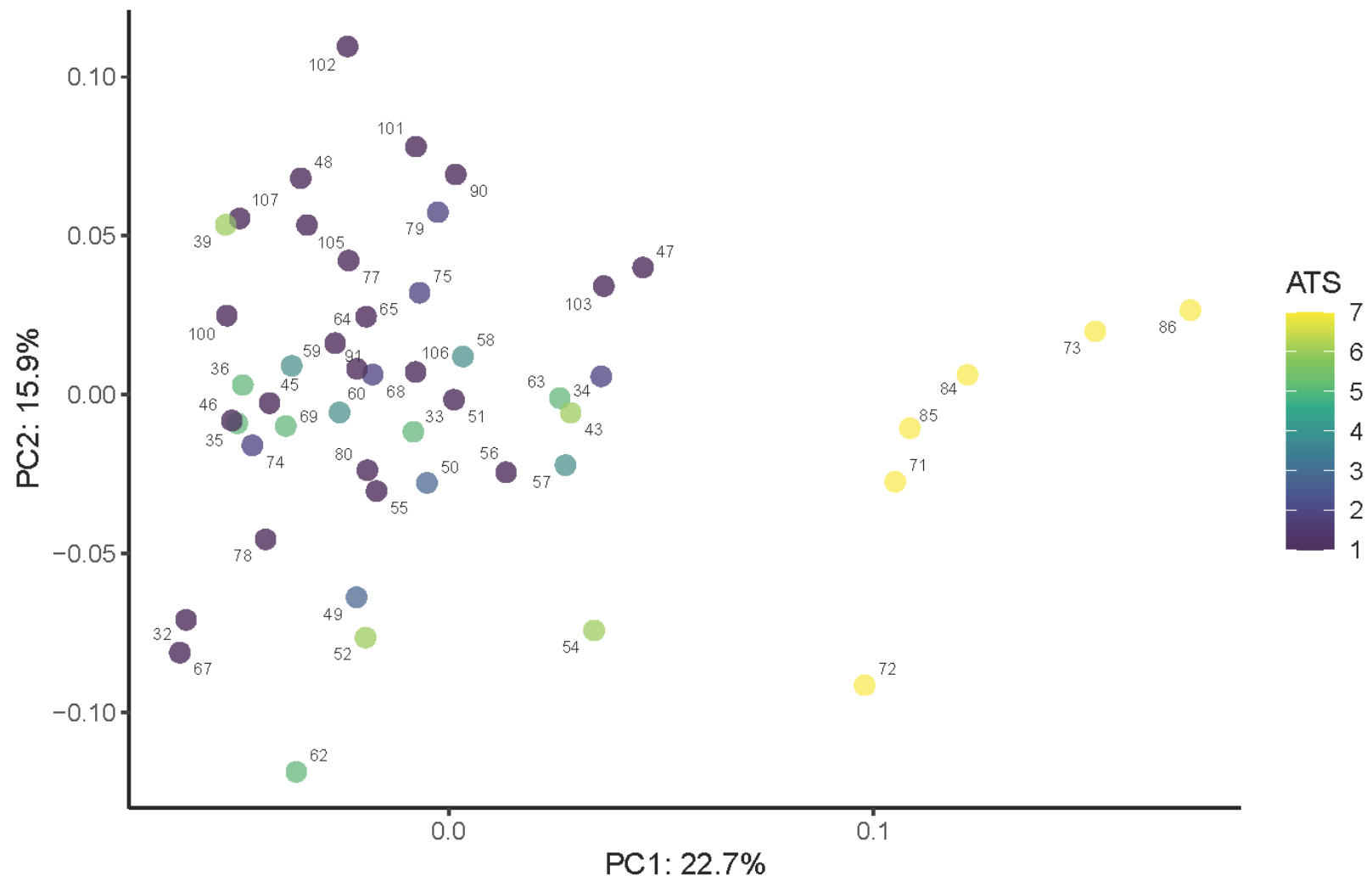
Supplemental Figure 31. PCA of the prootic module conducted on the coralsnake subset, colored by ATS. Numbering corresponds with Table 2.1.



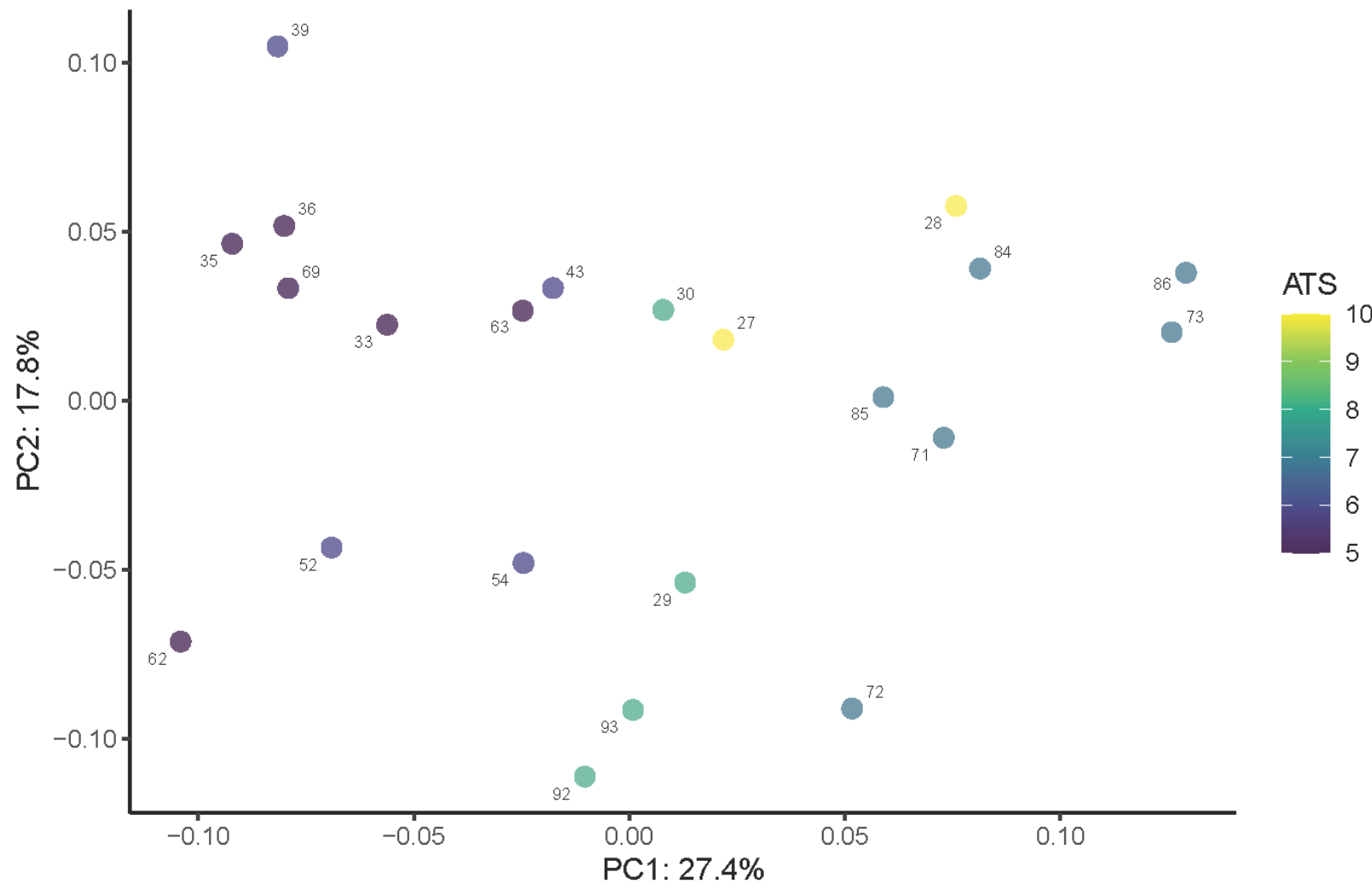
Supplemental Figure 32. PCA of the prootic module conducted on the semi-aquatic and aquatic subset (>5 ATS), colored by ATS. Numbering corresponds with Table 2.1.



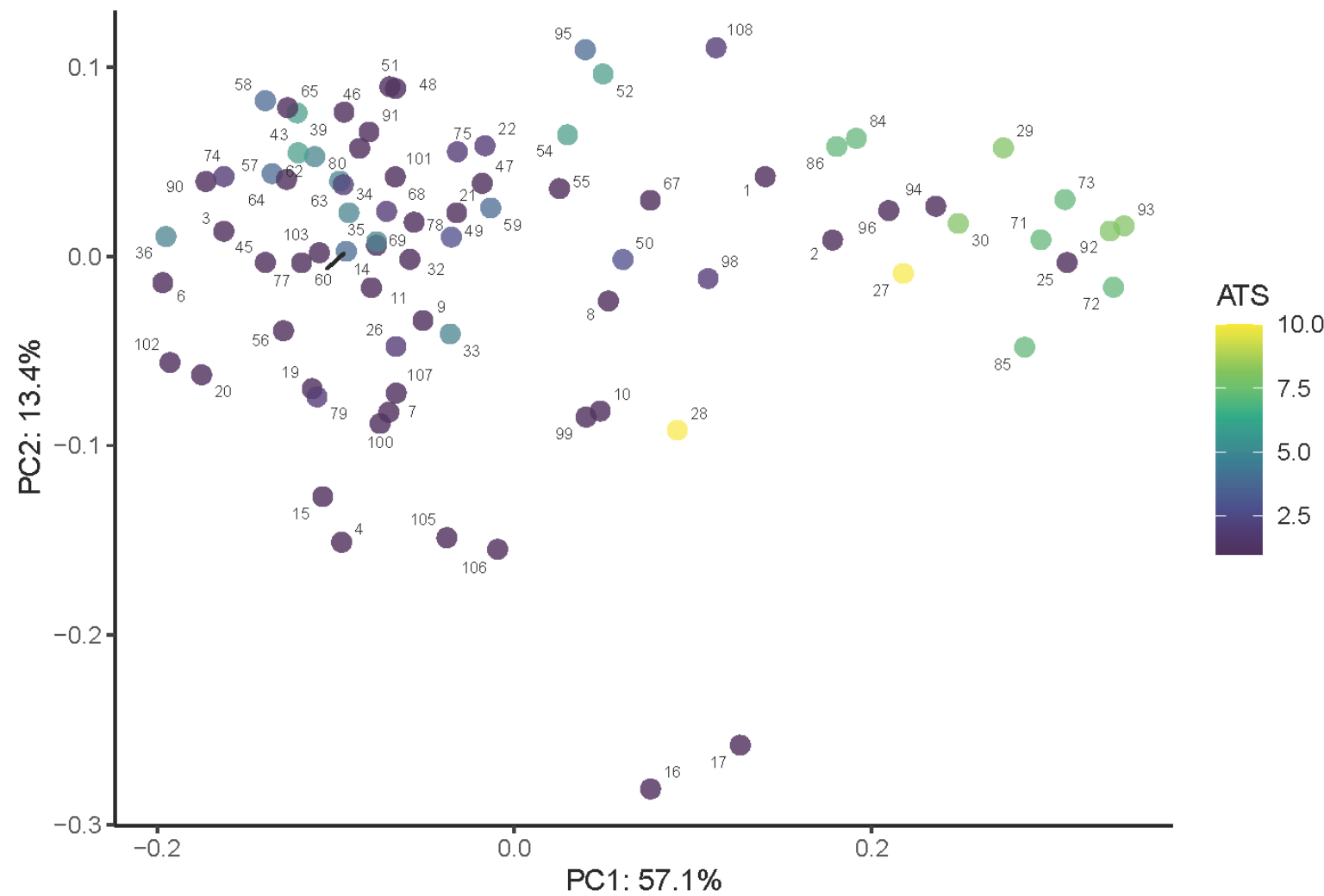
Supplemental Figure 33. PCA of the exoccipital module utilizing all specimens, colored by ATS. Numbering corresponds with Table 2.1.



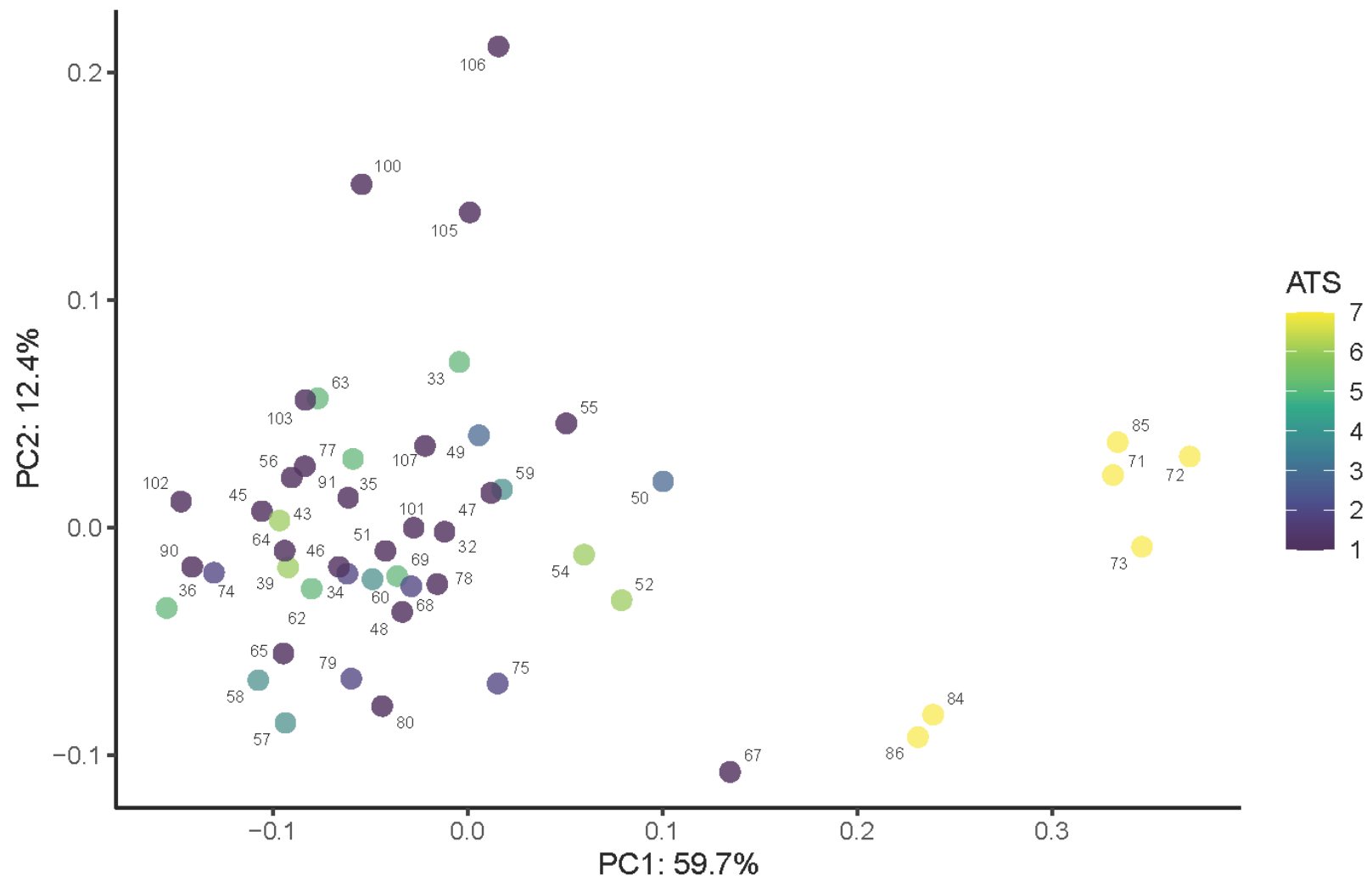
Supplemental Figure 34. PCA of the exoccipital module conducted on the coralsnake subset, colored by ATS. Numbering corresponds with Table 2.1.



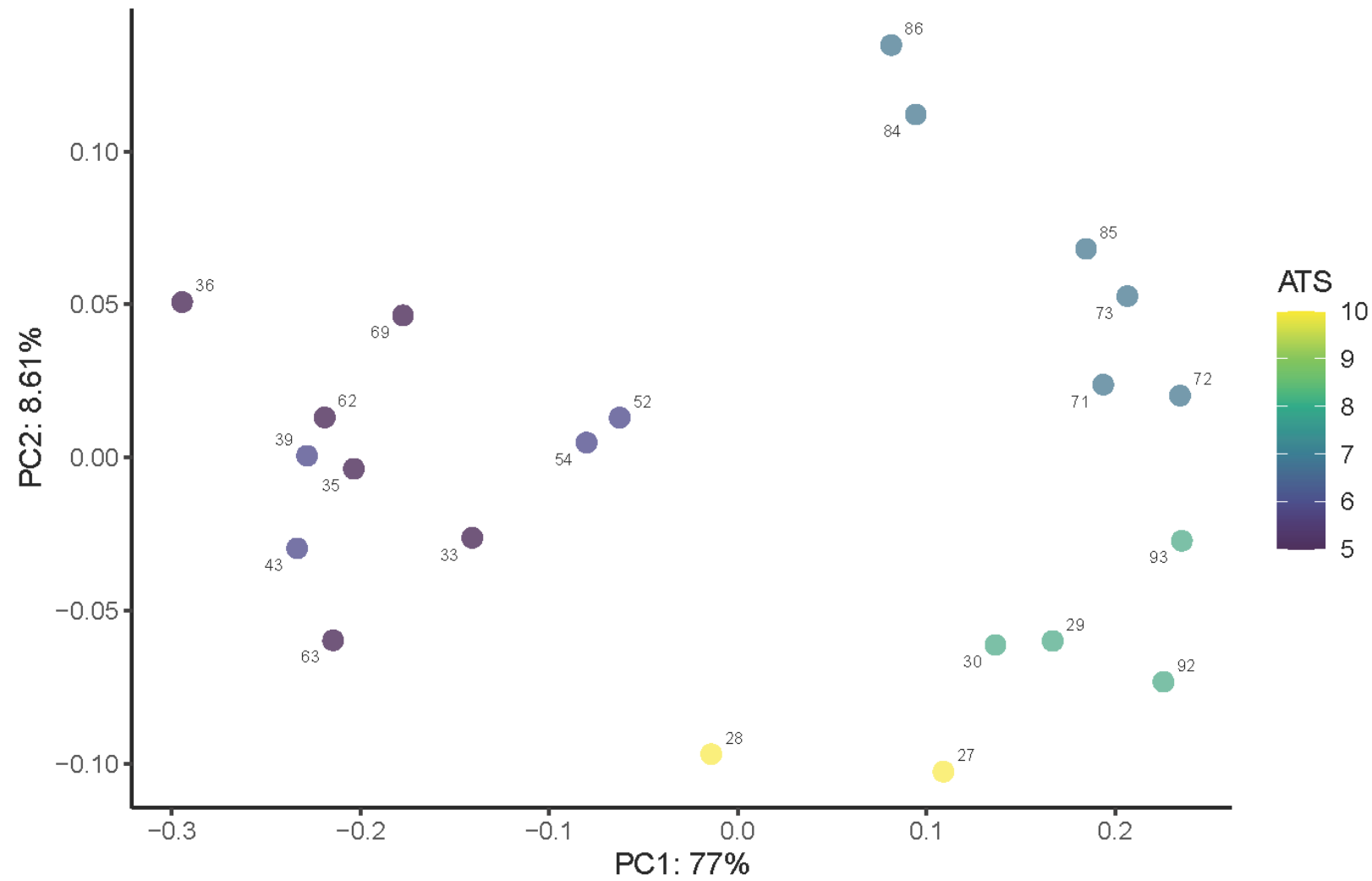
Supplemental Figure 35. PCA of the exoccipital module conducted on the semi-aquatic and aquatic subset (>5 ATS), colored by ATS. Numbering corresponds with Table 2.1.



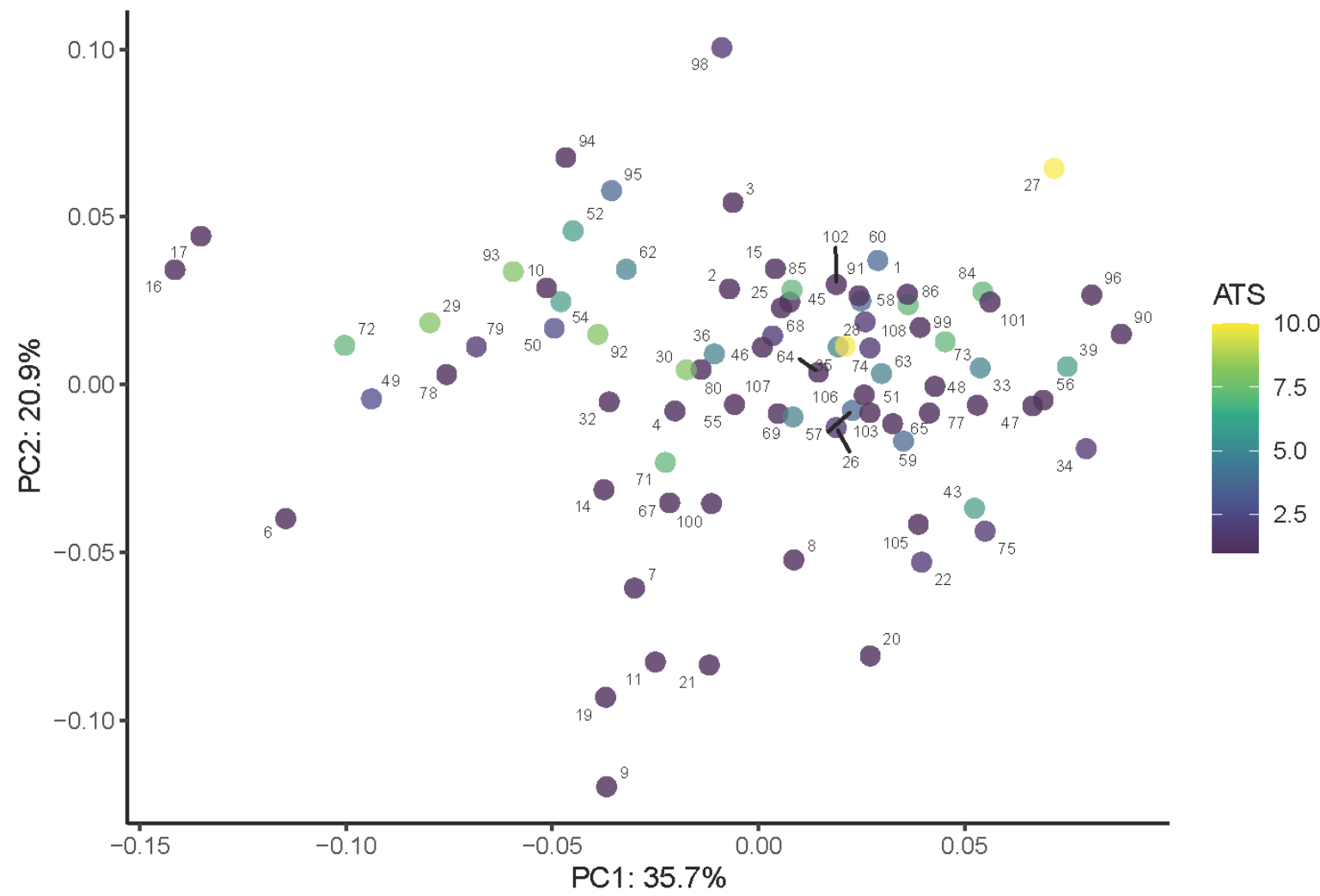
Supplemental Figure 36. PCA of the supratemporal module utilizing all specimens, colored by ATS. Numbering corresponds with Table 2.1.



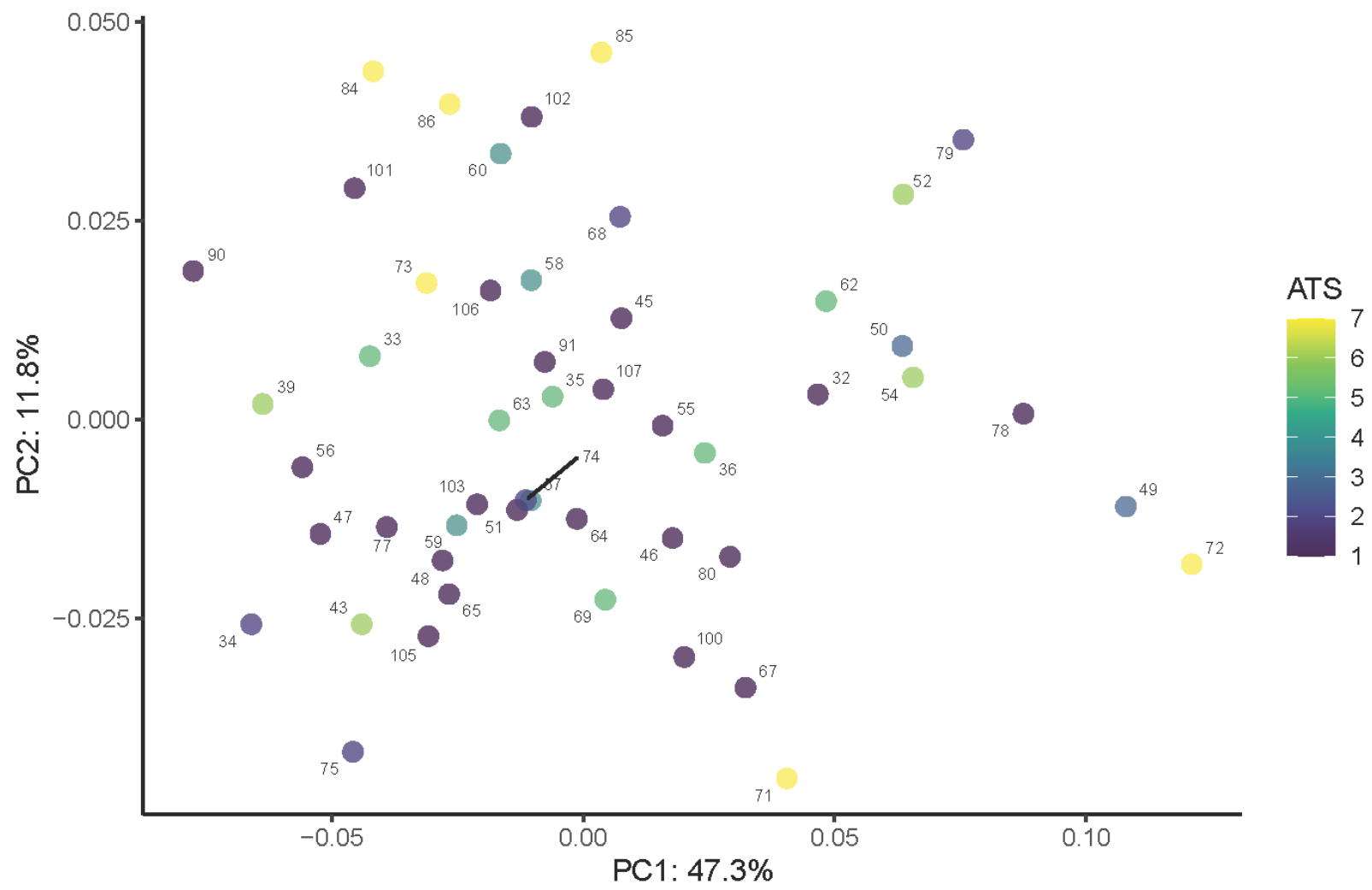
Supplemental Figure 37. PCA of the supratemporal module conducted on the coralsnake subset, colored by ATS. Numbering corresponds with Table 2.1.



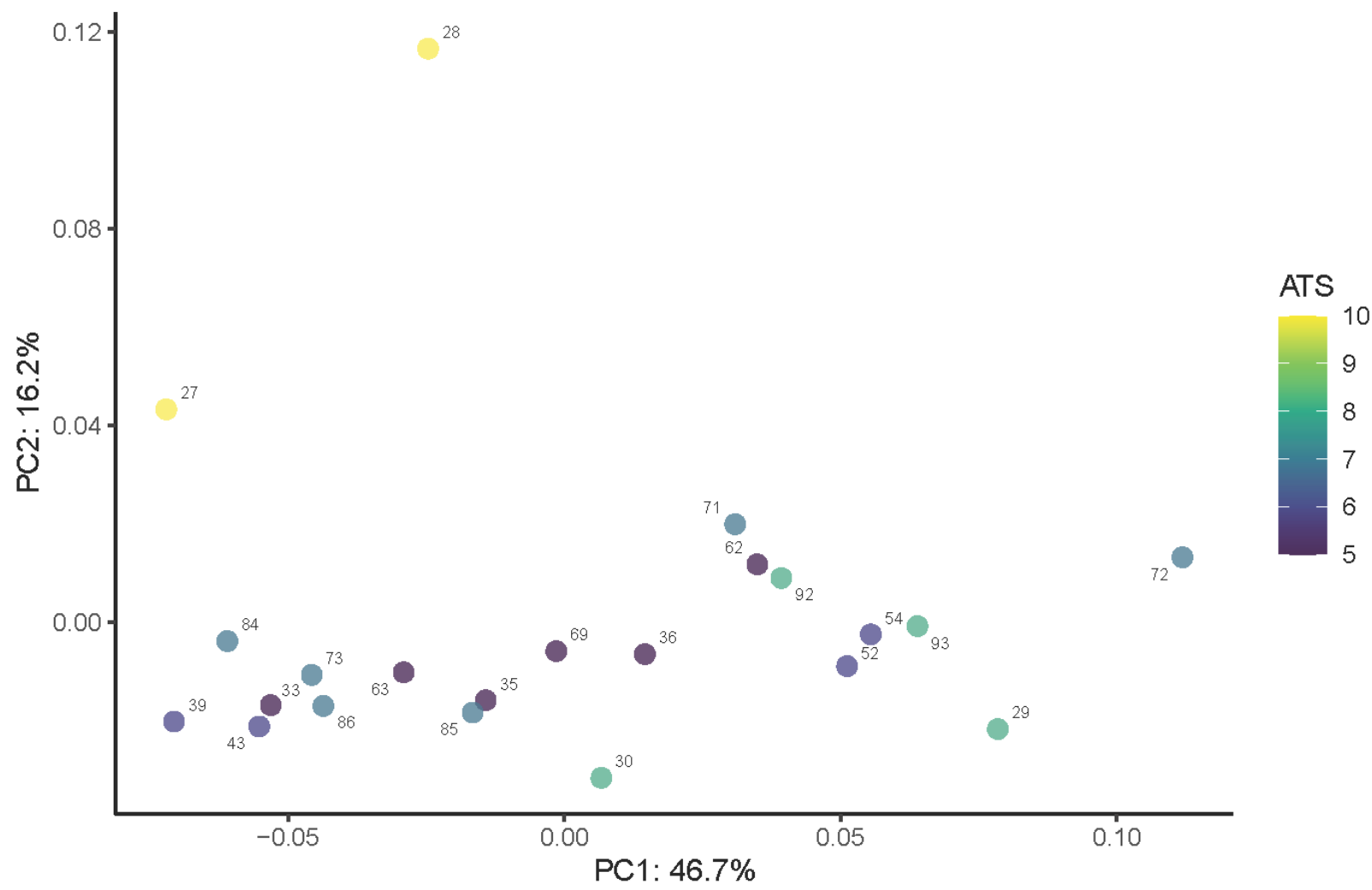
Supplemental Figure 38. PCA of the supratemporal module conducted on the semi-aquatic and aquatic subset (>5 ATS), colored by ATS. Numbering corresponds with Table 2.1.



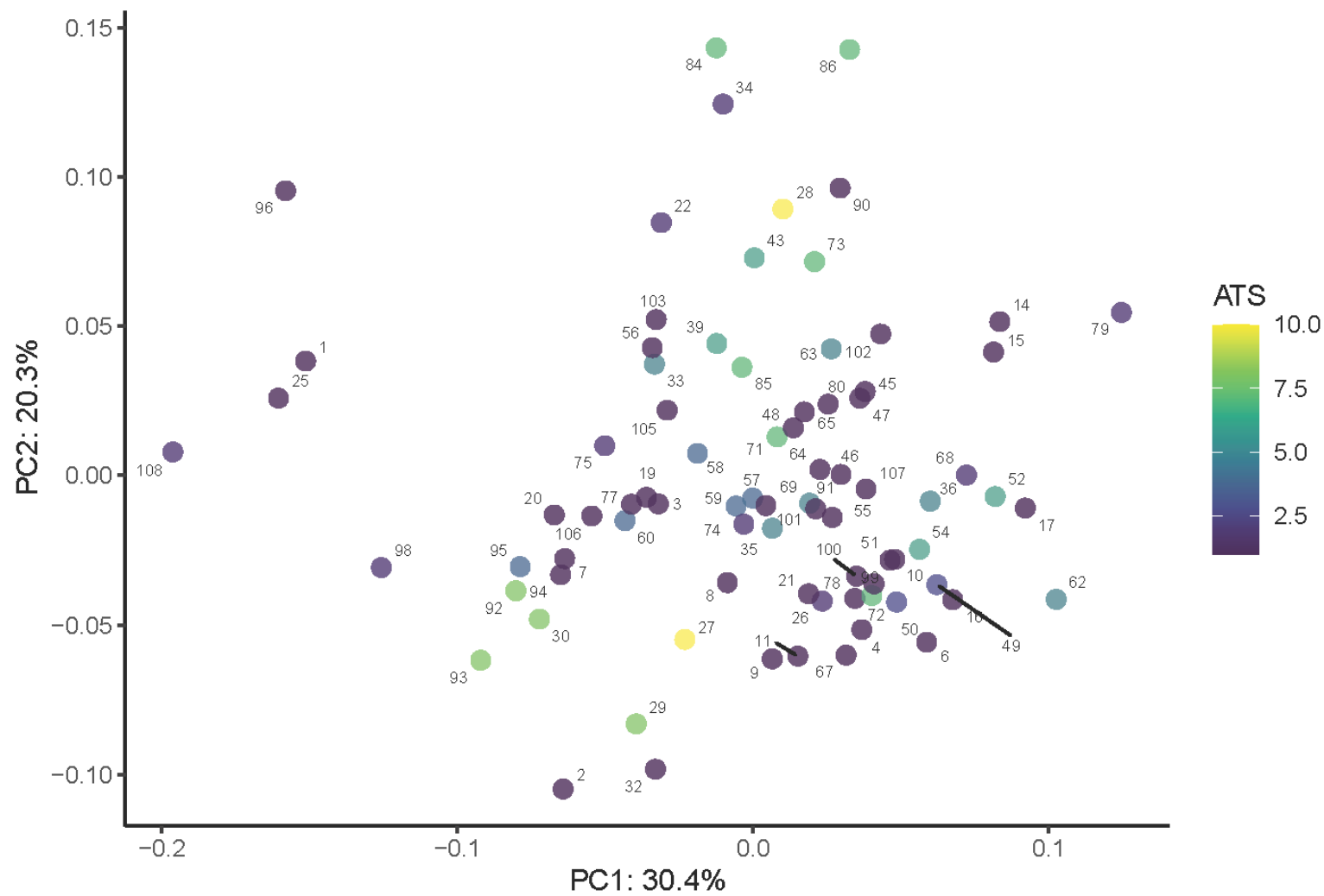
Supplemental Figure 39. PCA of the basisphenoid module utilizing all specimens, colored by ATS. Numbering corresponds with Table 2.1.



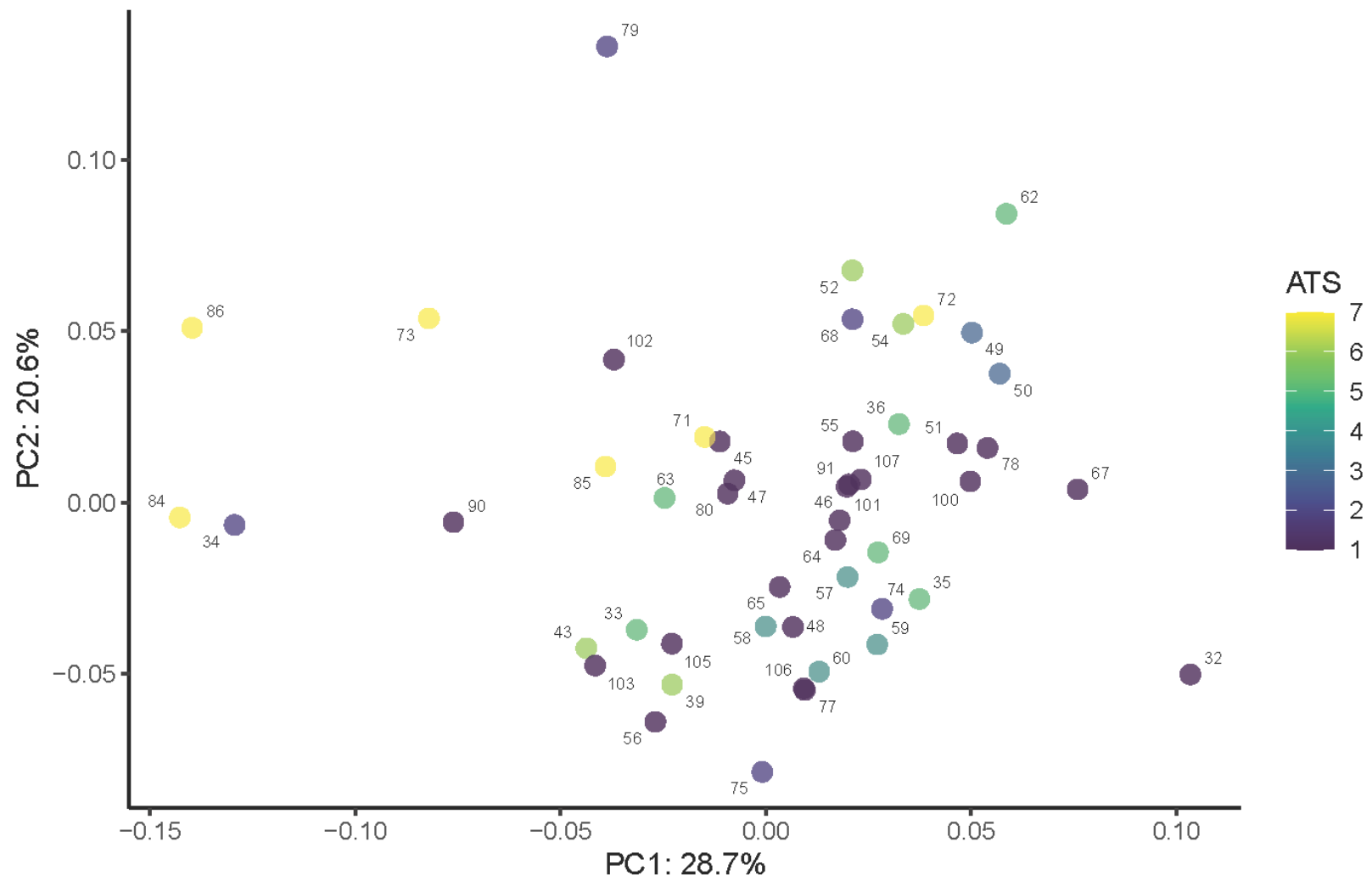
Supplemental Figure 40. PCA of the basisphenoid module conducted on the coralsnake subset, colored by ATS. Numbering corresponds with Table 2.1.



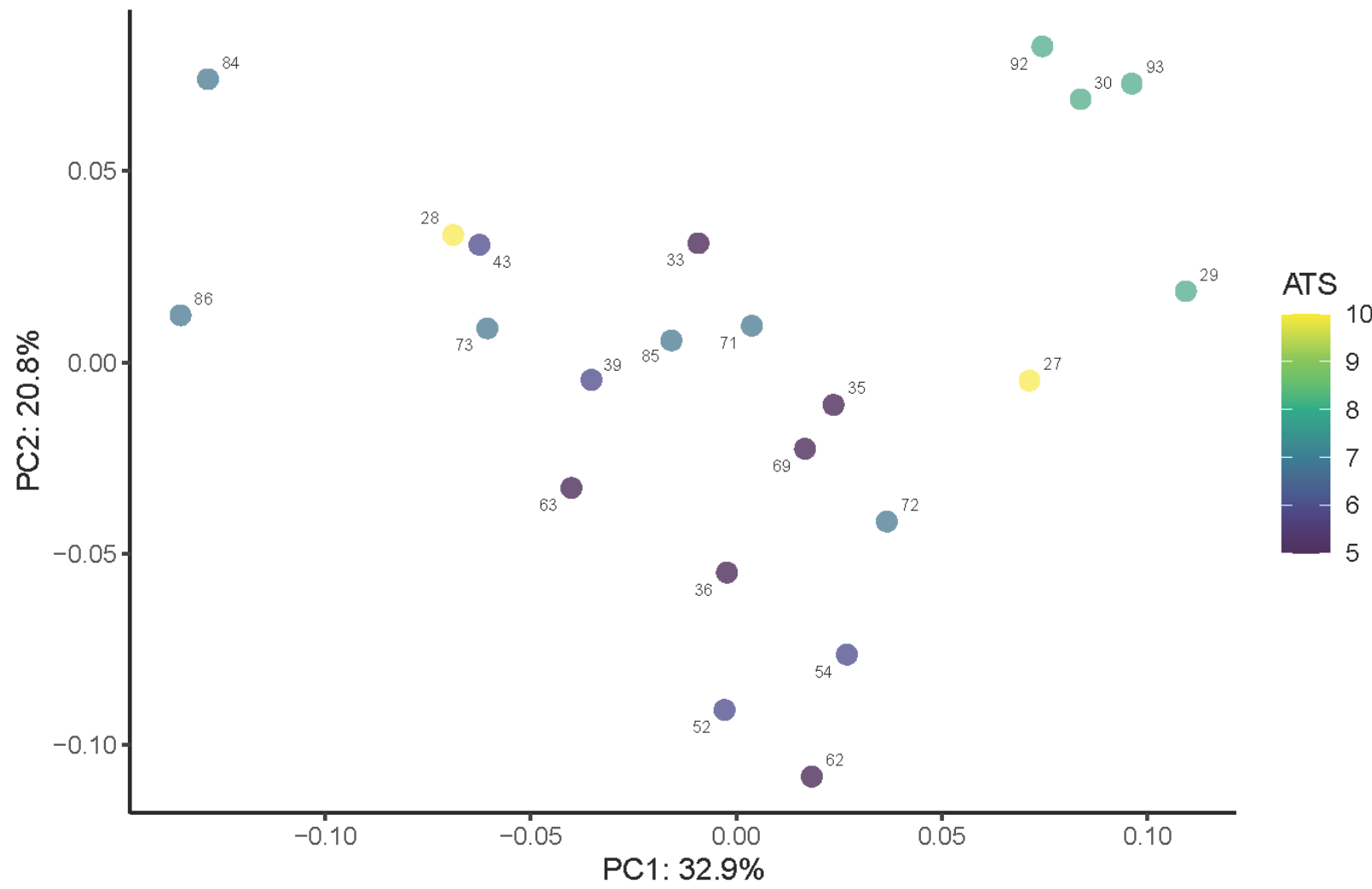
Supplemental Figure 41. PCA of the basisphenoid module conducted on the semi-aquatic and aquatic subset (>5 ATS), colored by ATS. Numbering corresponds with Table 2.1.



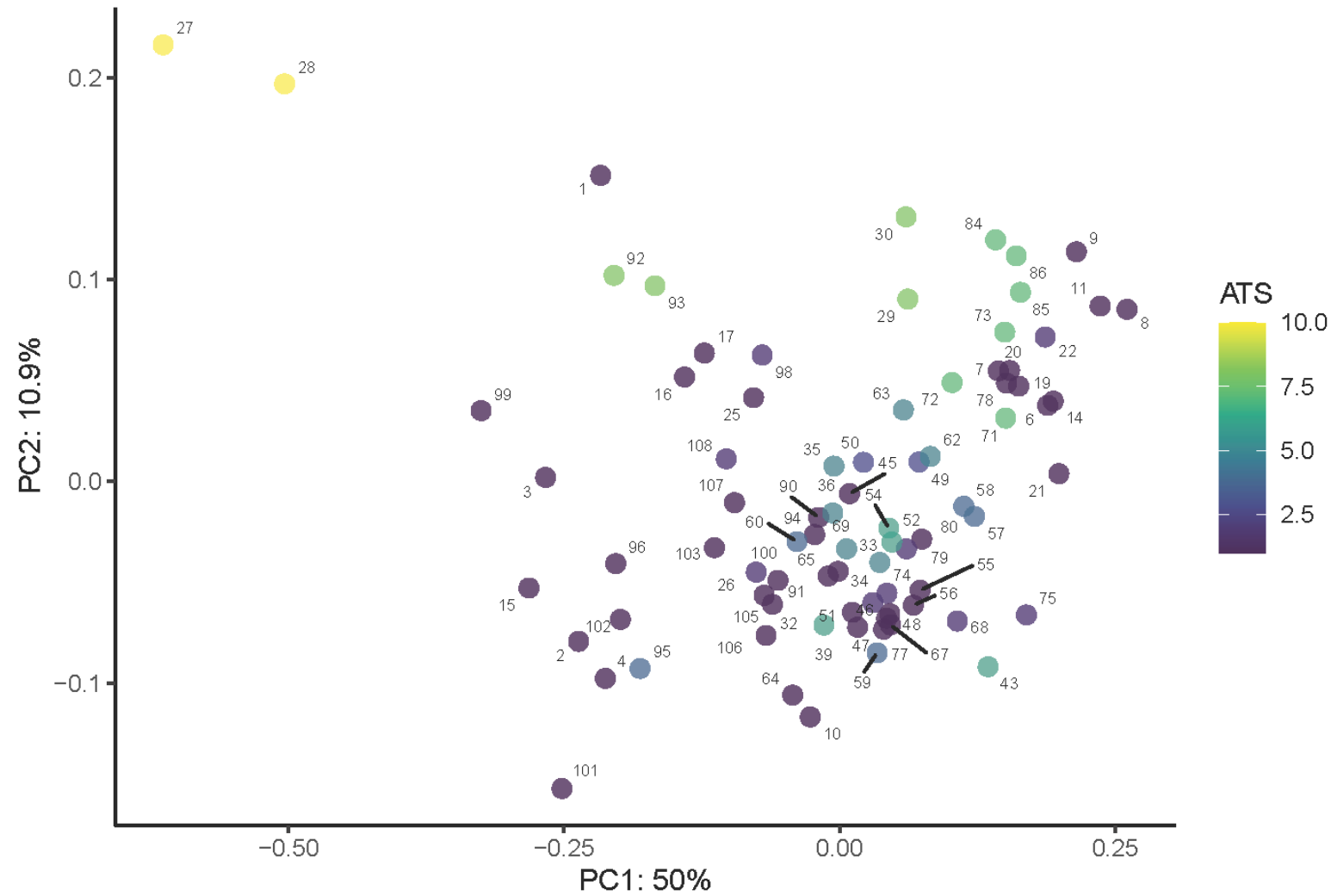
Supplemental Figure 42. PCA of the basioccipital module utilizing all specimens, colored by ATS. Numbering corresponds with Table 2.1.



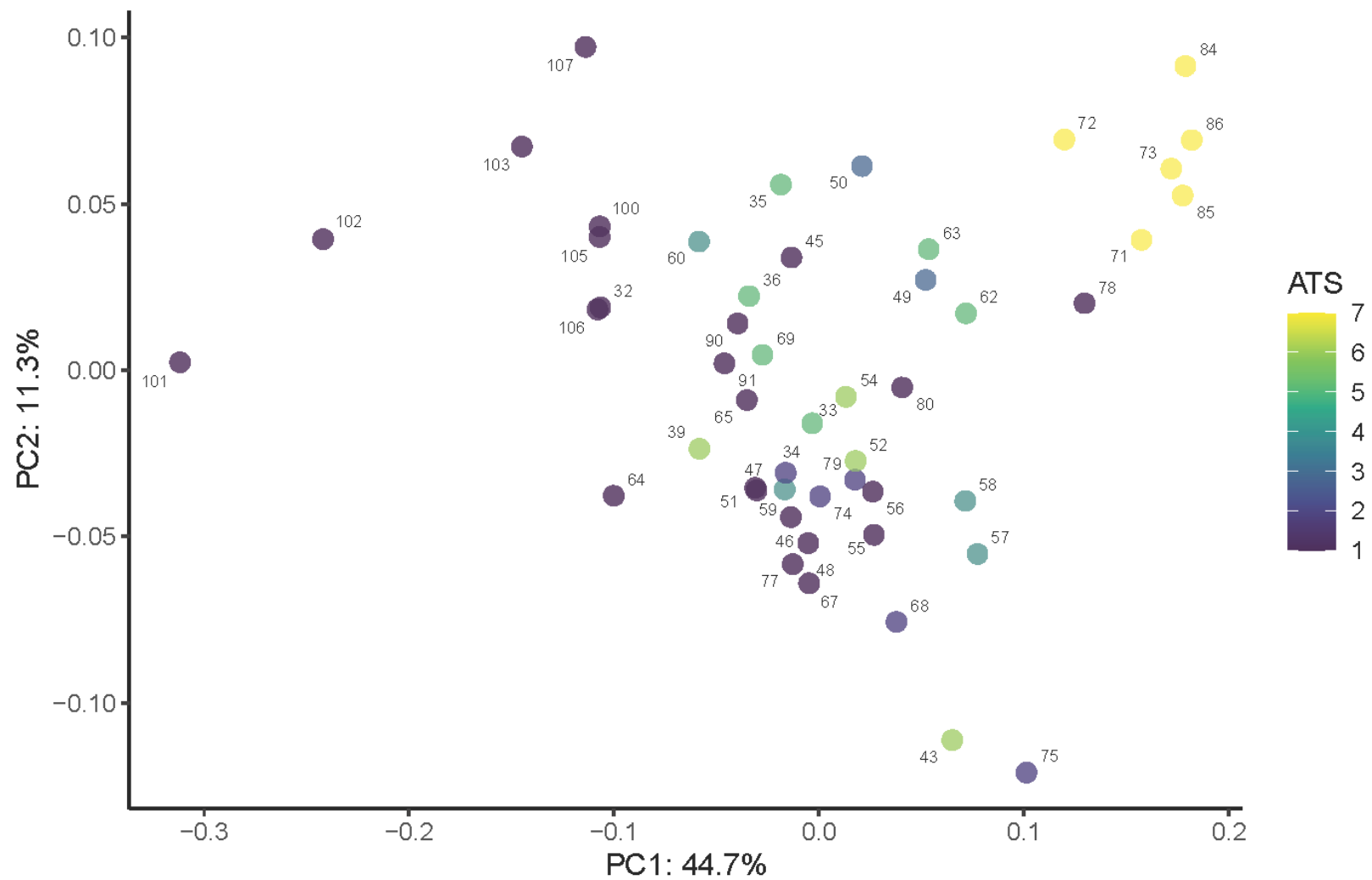
Supplemental Figure 43. PCA of the basioccipital module conducted on the coralsnake subset, colored by ATS. Numbering corresponds with Table 2.1.



Supplemental Figure 44. PCA of the basioccipital module conducted on the semi-aquatic and aquatic subset (>5 ATS), colored by ATS. Numbering corresponds with Table 2.1.

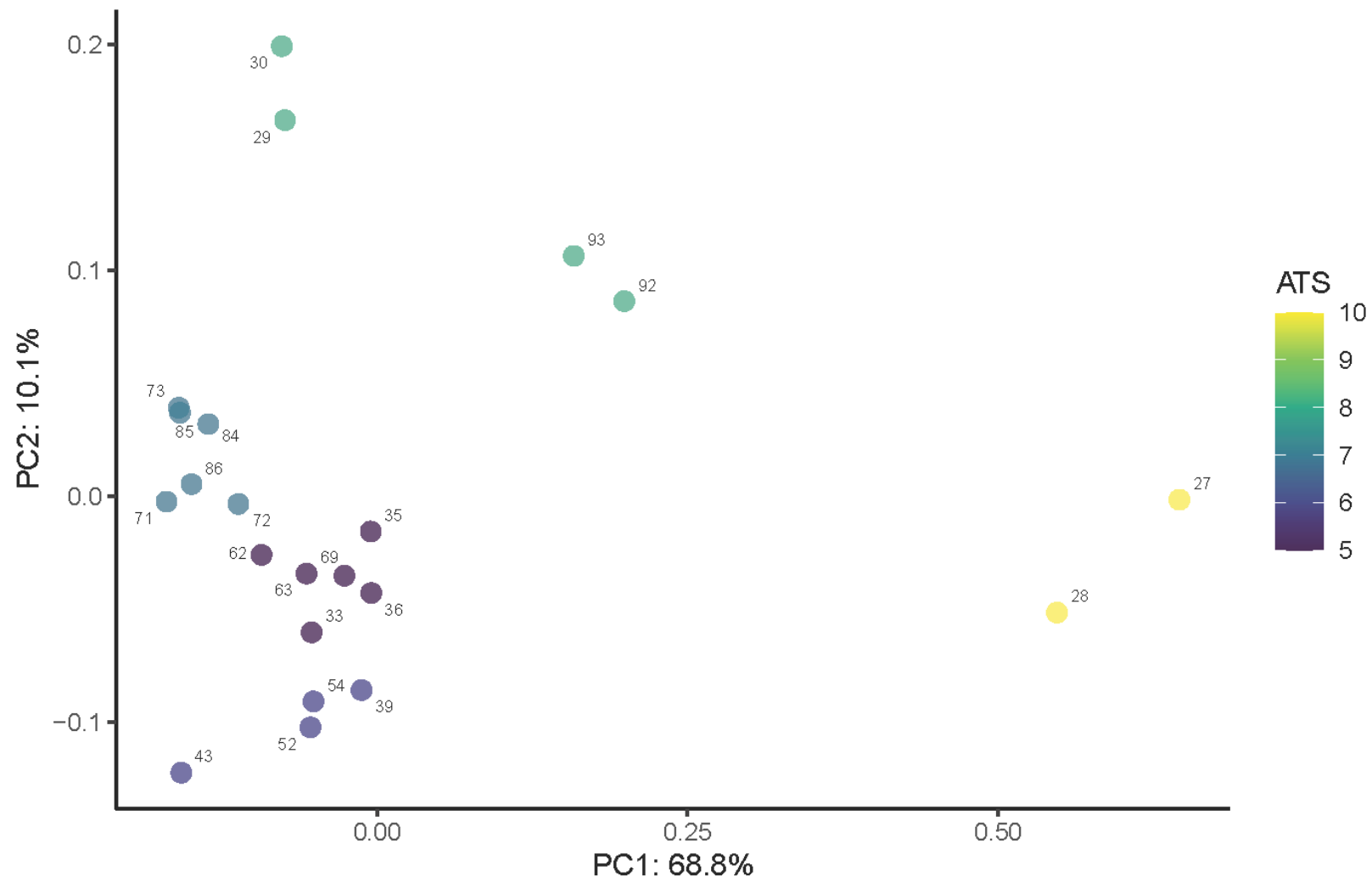


Supplemental Figure 45. PCA of the maxilla and palatine module utilizing all specimens, colored by ATS. Numbering corresponds with Table 2.1.

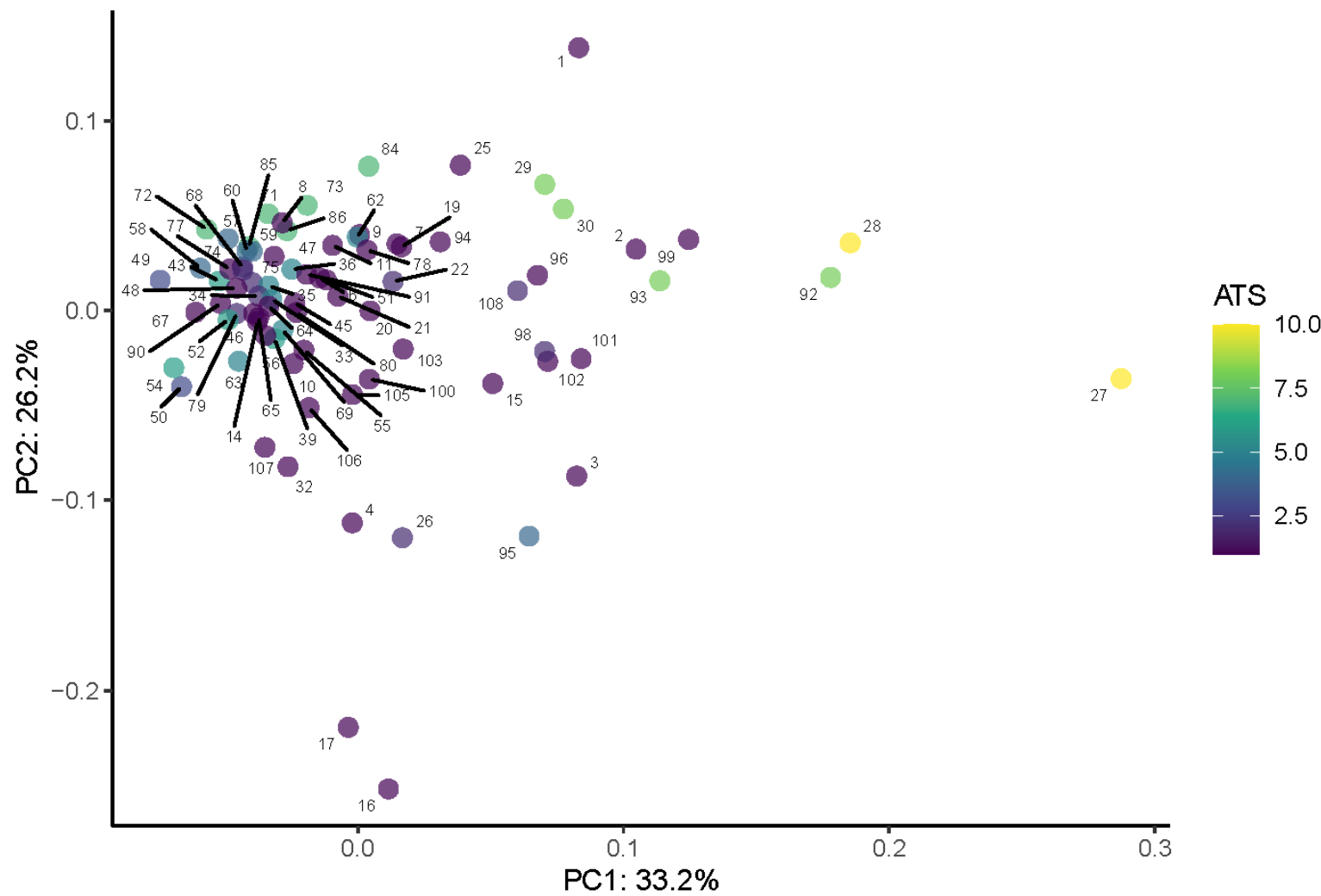


Supplemental Figure 46. PCA of the maxilla and palatine module conducted on the coralsnake subset, colored by ATS.

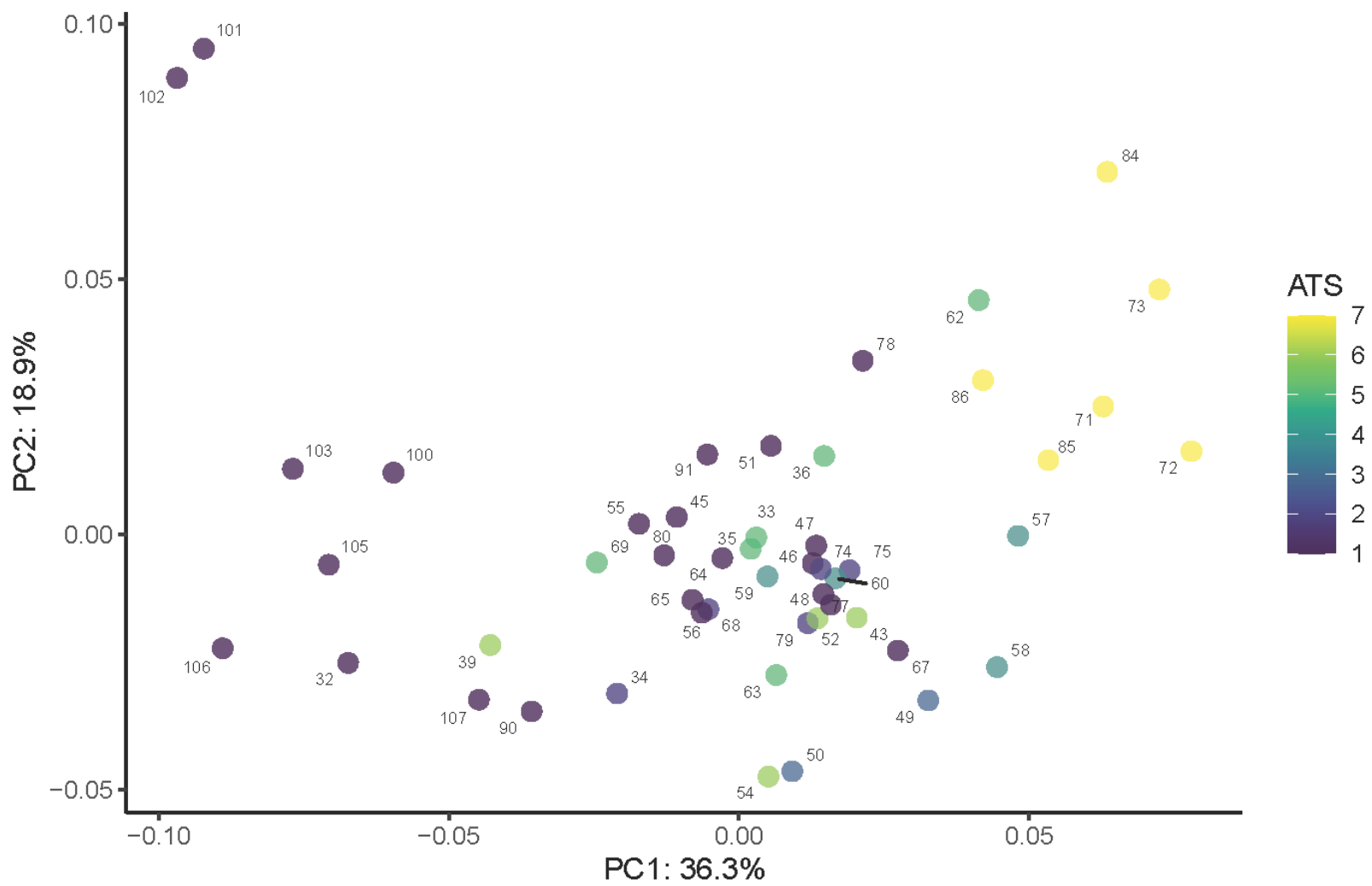
Numbering corresponds with Table 2.1.



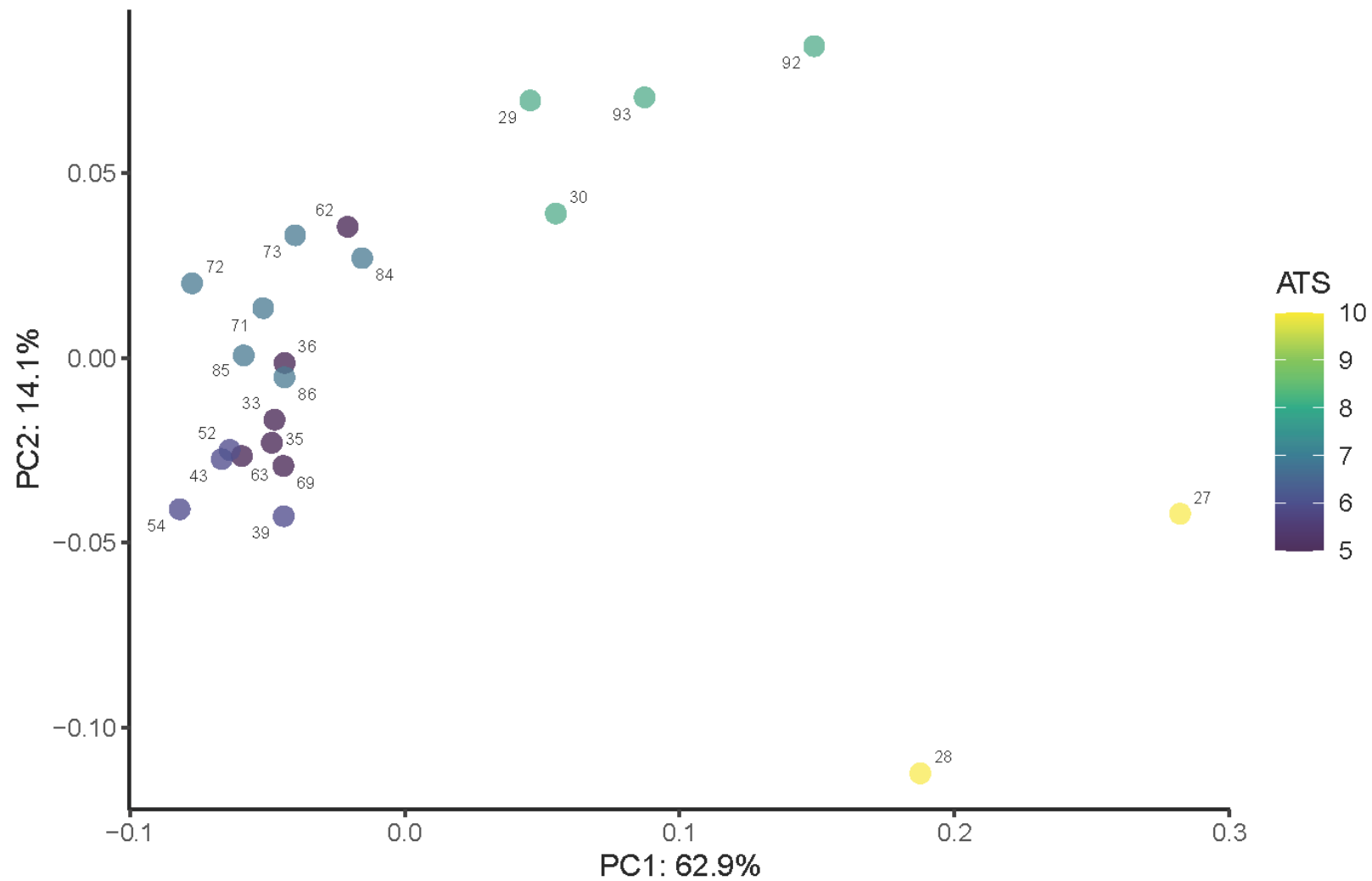
Supplemental Figure 47. PCA of the maxilla and palatine module conducted on the semi-aquatic and aquatic subset (>5 ATS), colored by ATS. Numbering corresponds with Table 2.1.



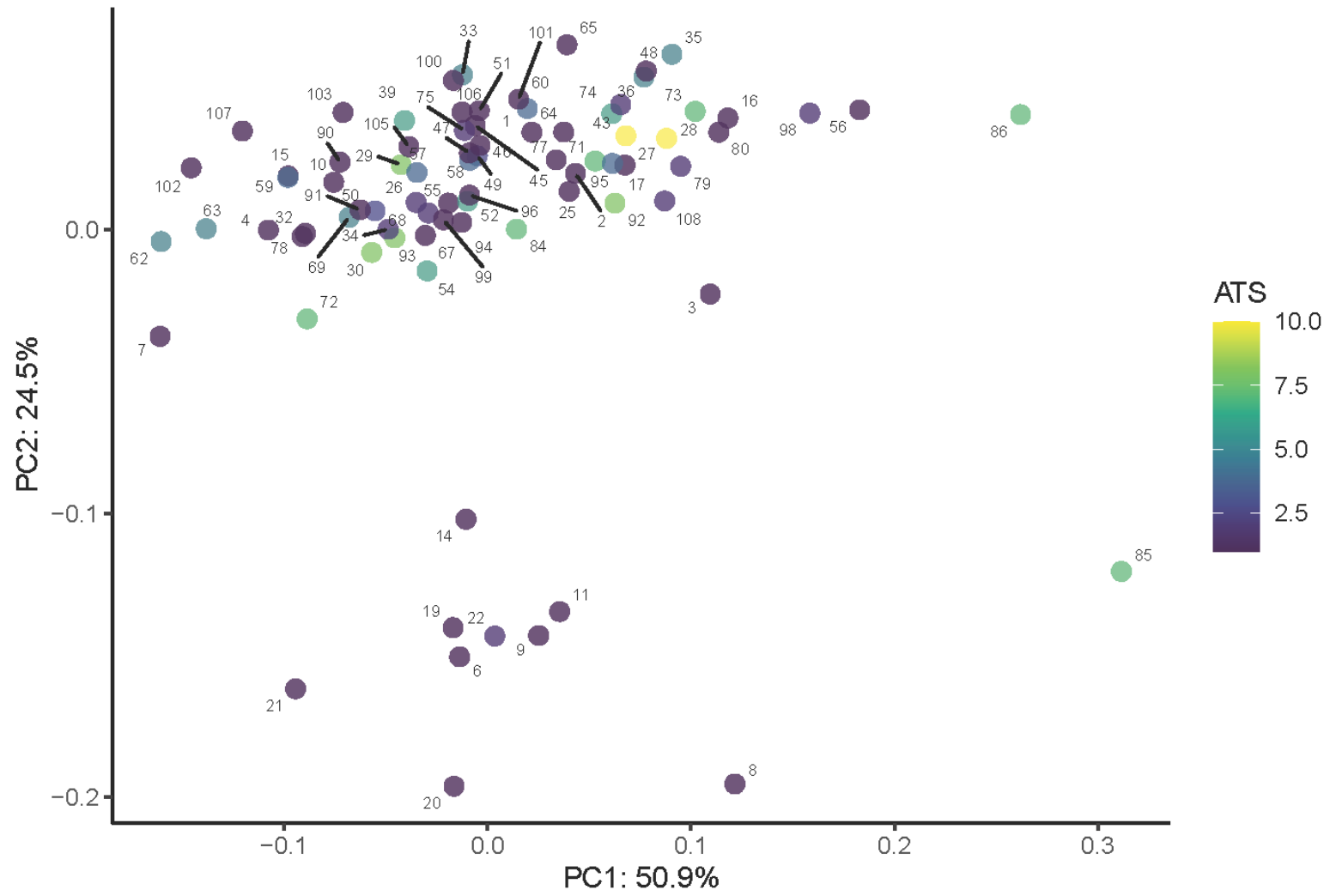
Supplemental Figure 48. PCA of the ectopterygoid module, utilizing all specimens, colored by ATS. Numbering corresponds with Table 2.1.



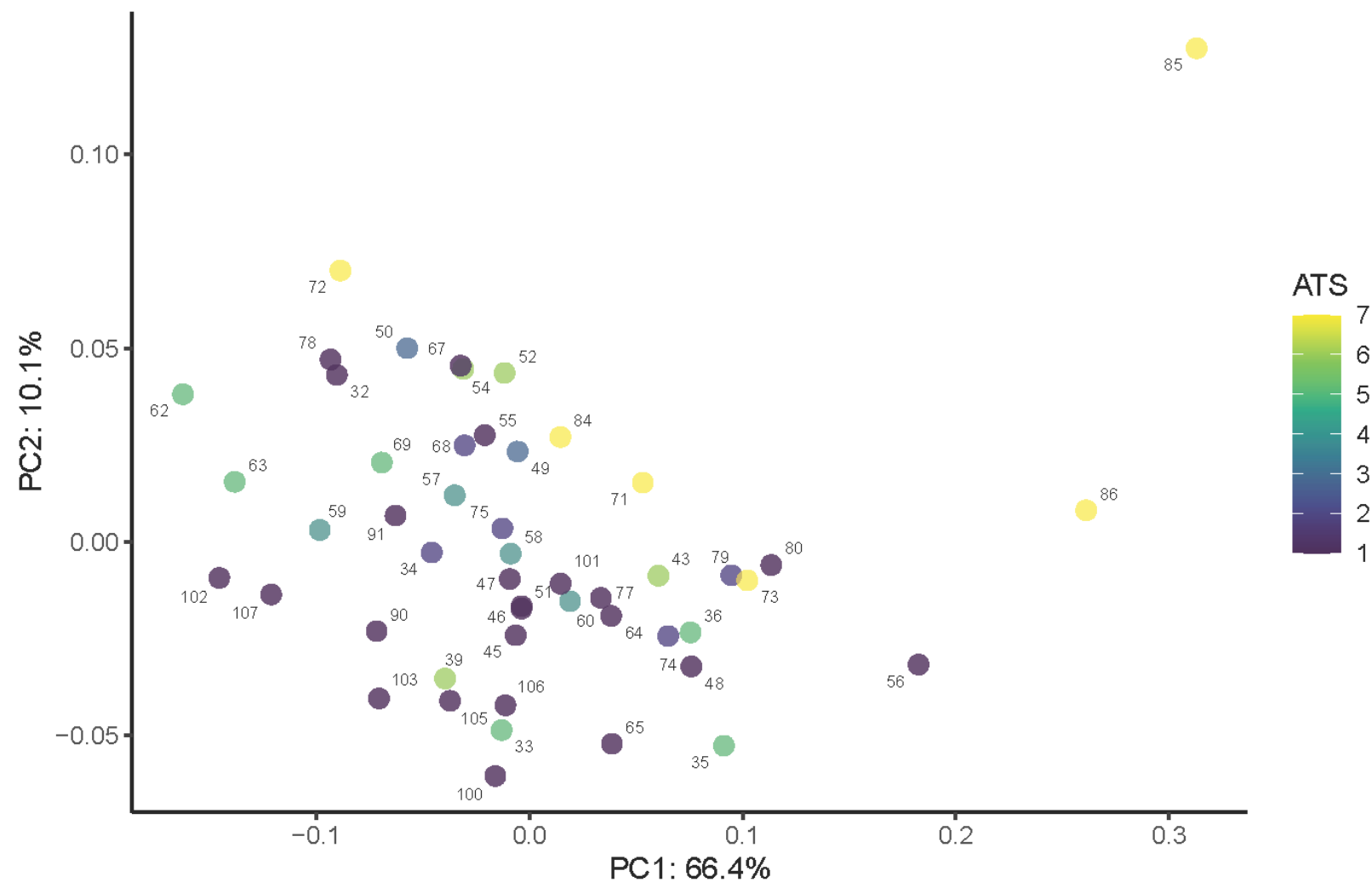
Supplemental Figure 49. PCA of the ectopterygoid module conducted on the coralsnake subset, colored by ATS. Numbering corresponds with Table 2.1.



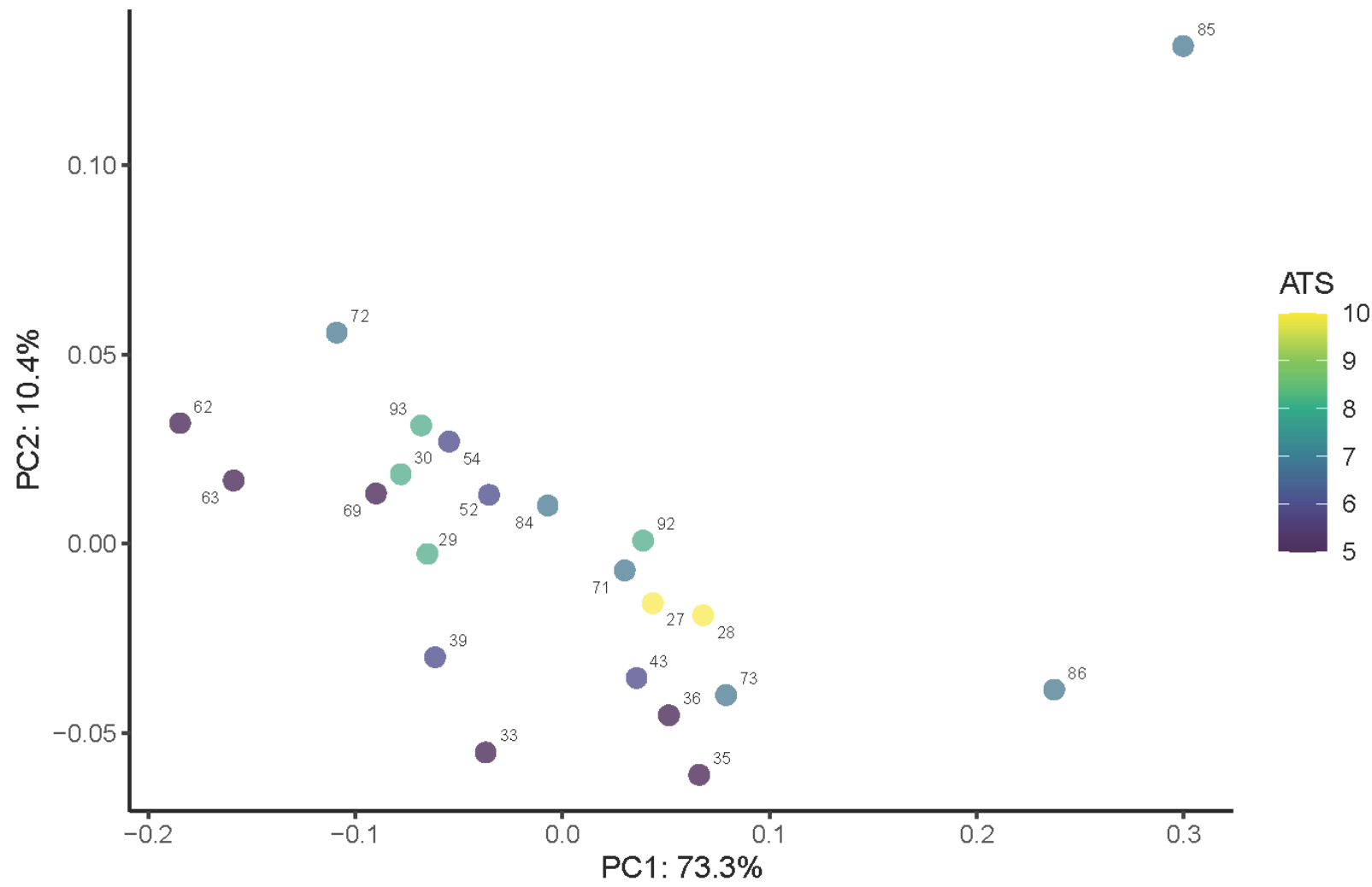
Supplemental Figure 50. PCA of the ectopterygoid module conducted on the semi-aquatic and aquatic subset (>5 ATS), colored by ATS. Numbering corresponds with Table 2.1.



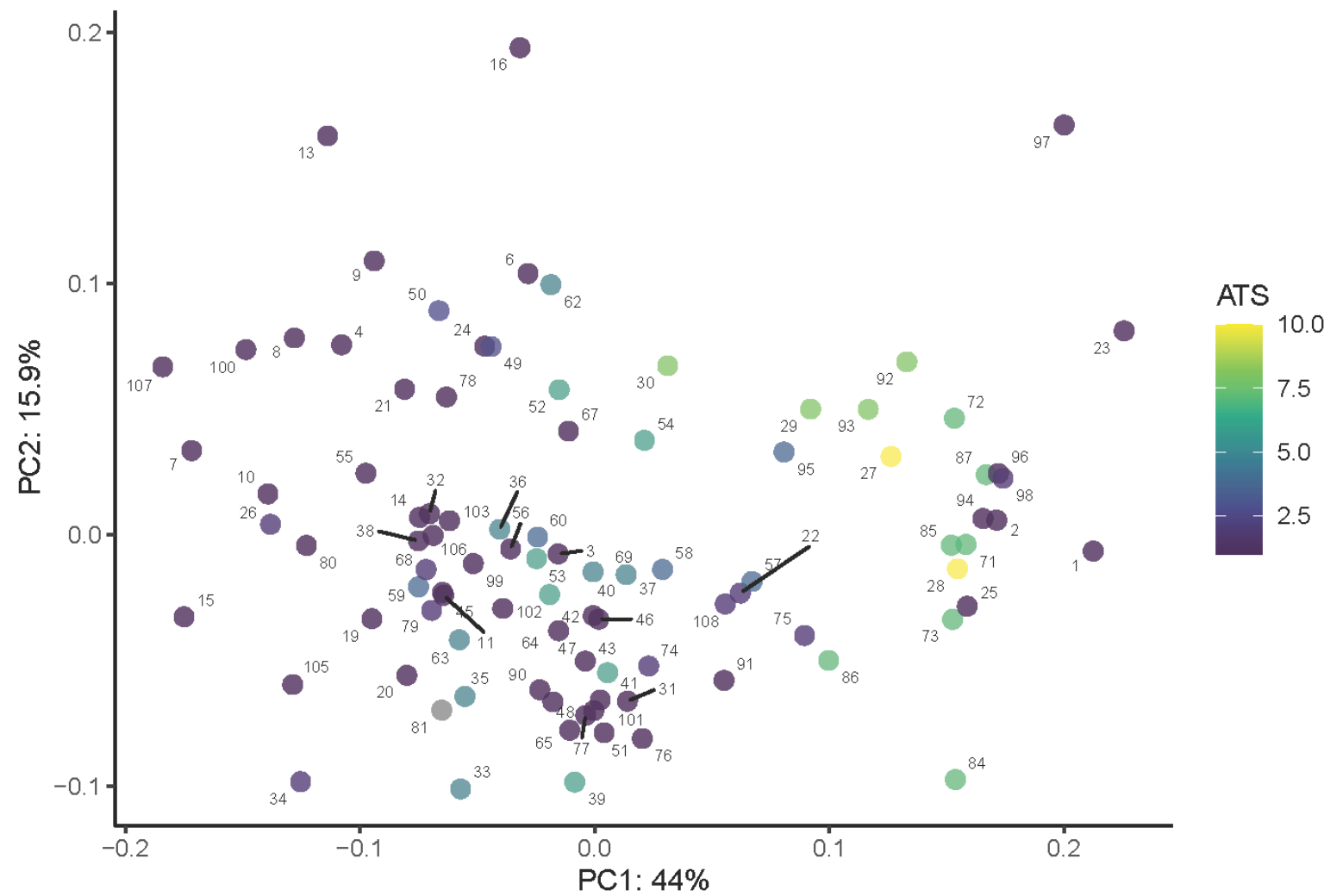
Supplemental Figure 51. PCA of the pterygoid module utilizing all specimens, colored by ATS. Numbering corresponds with Table 2.1.



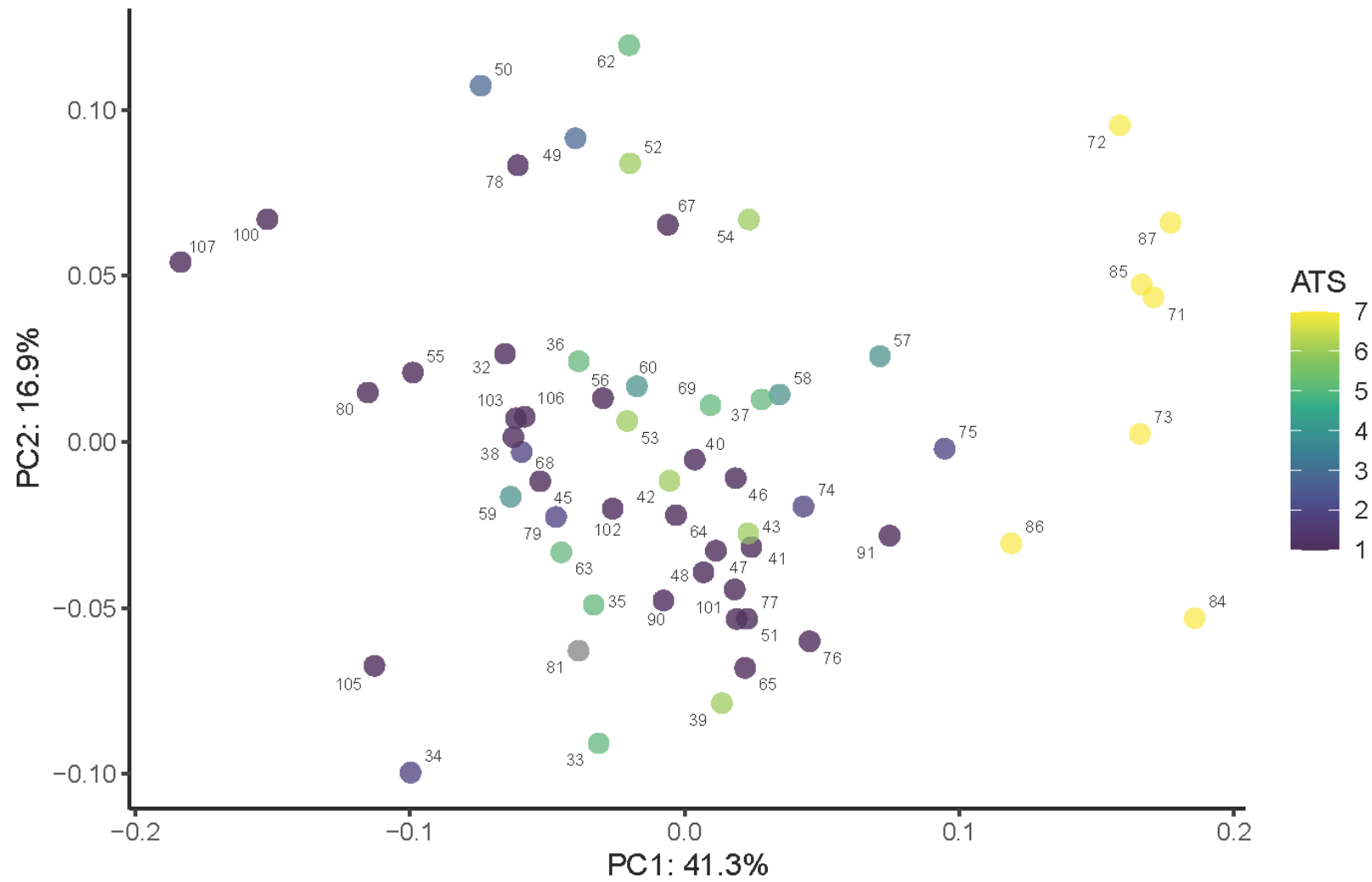
Supplemental Figure 52. PCA of the pterygoid module conducted on the coralsnake subset, colored by ATS. Numbering corresponds with Table 2.1.



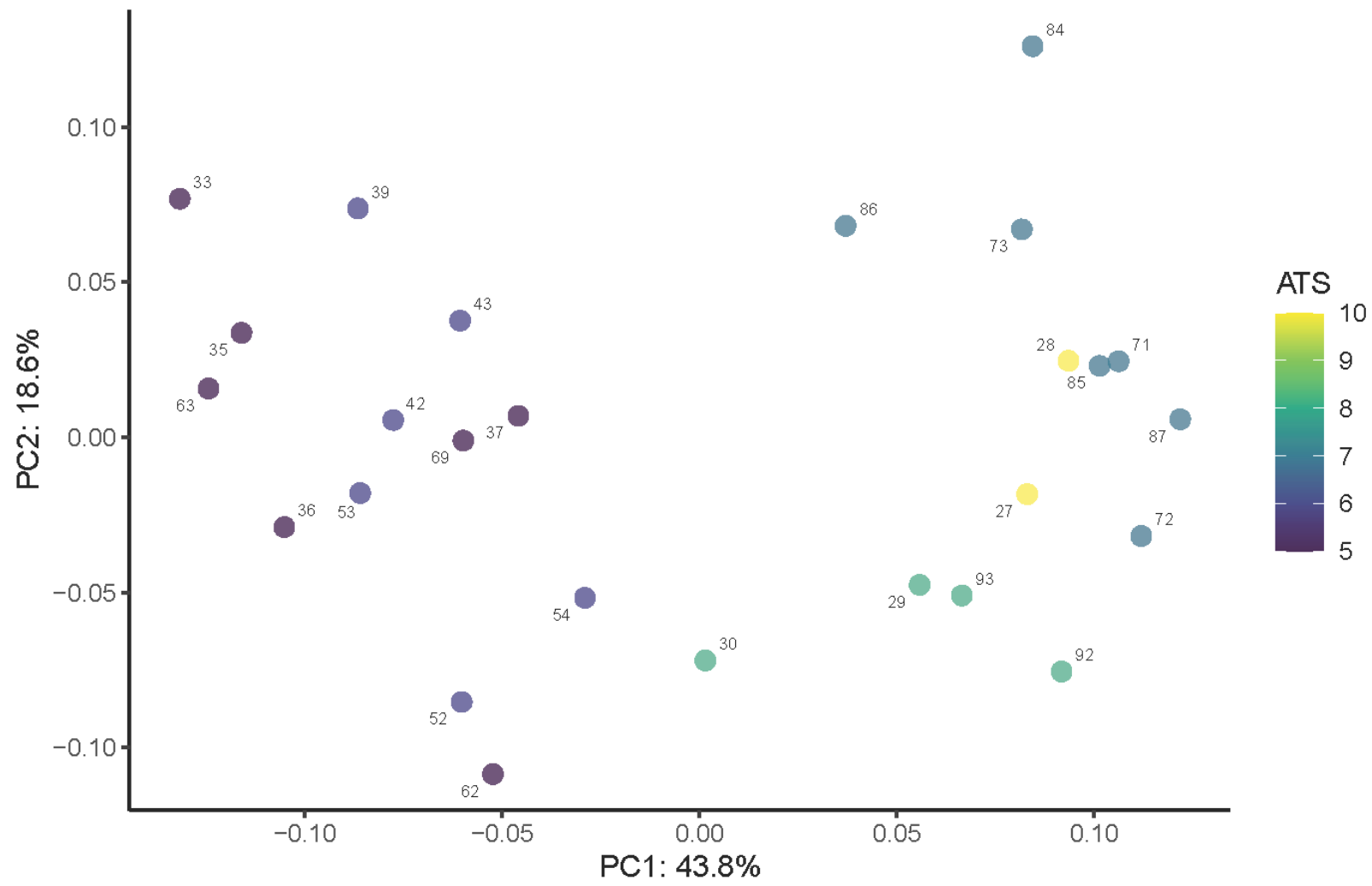
Supplemental Figure 53. PCA of the pterygoid module conducted on the semi-aquatic and aquatic subset (>5 ATS), colored by ATS. Numbering corresponds with Table 2.1.



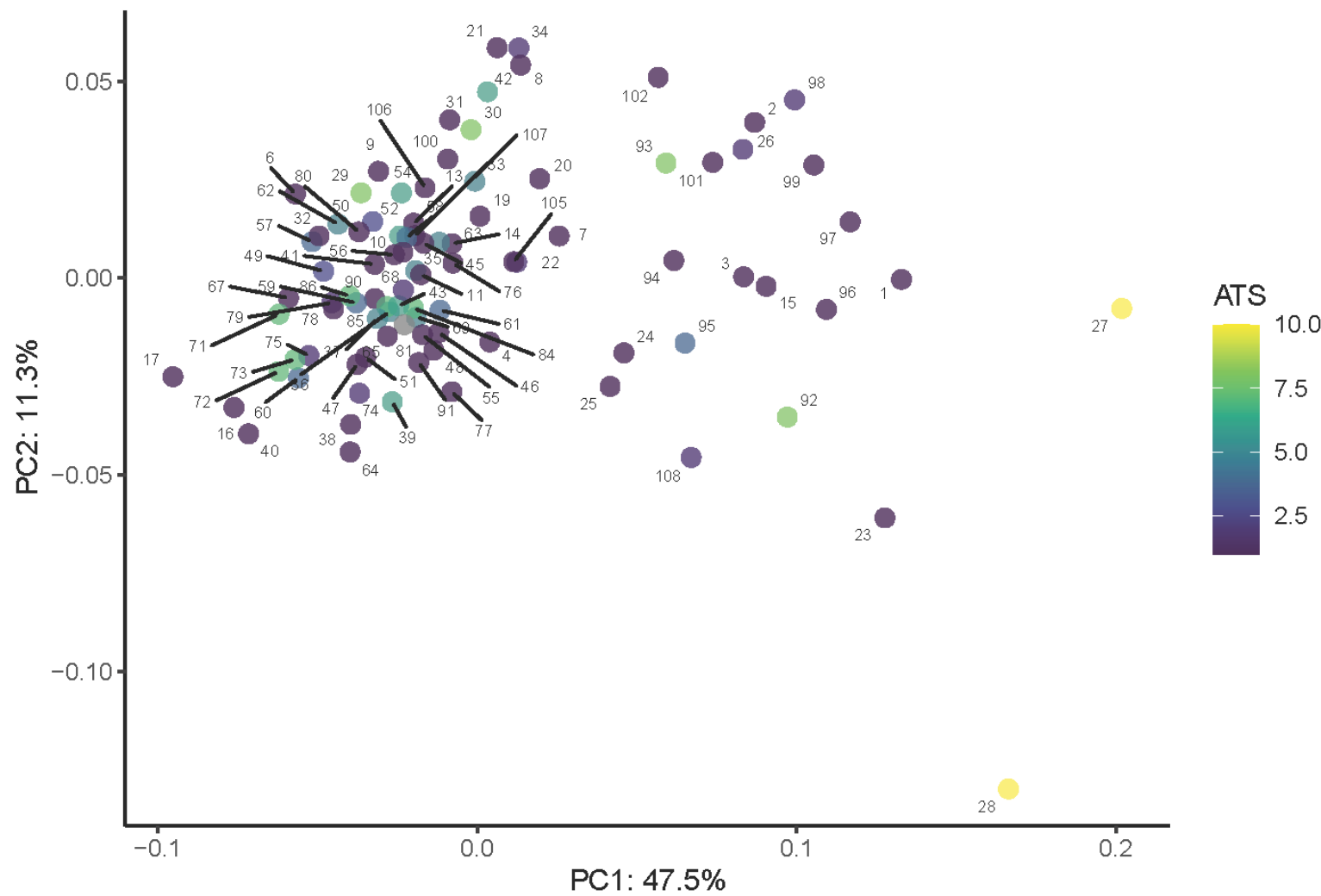
Supplemental Figure 54. PCA of the quadrate dataset utilizing all specimens, colored by ATS. Numbering corresponds with Table 2.1.



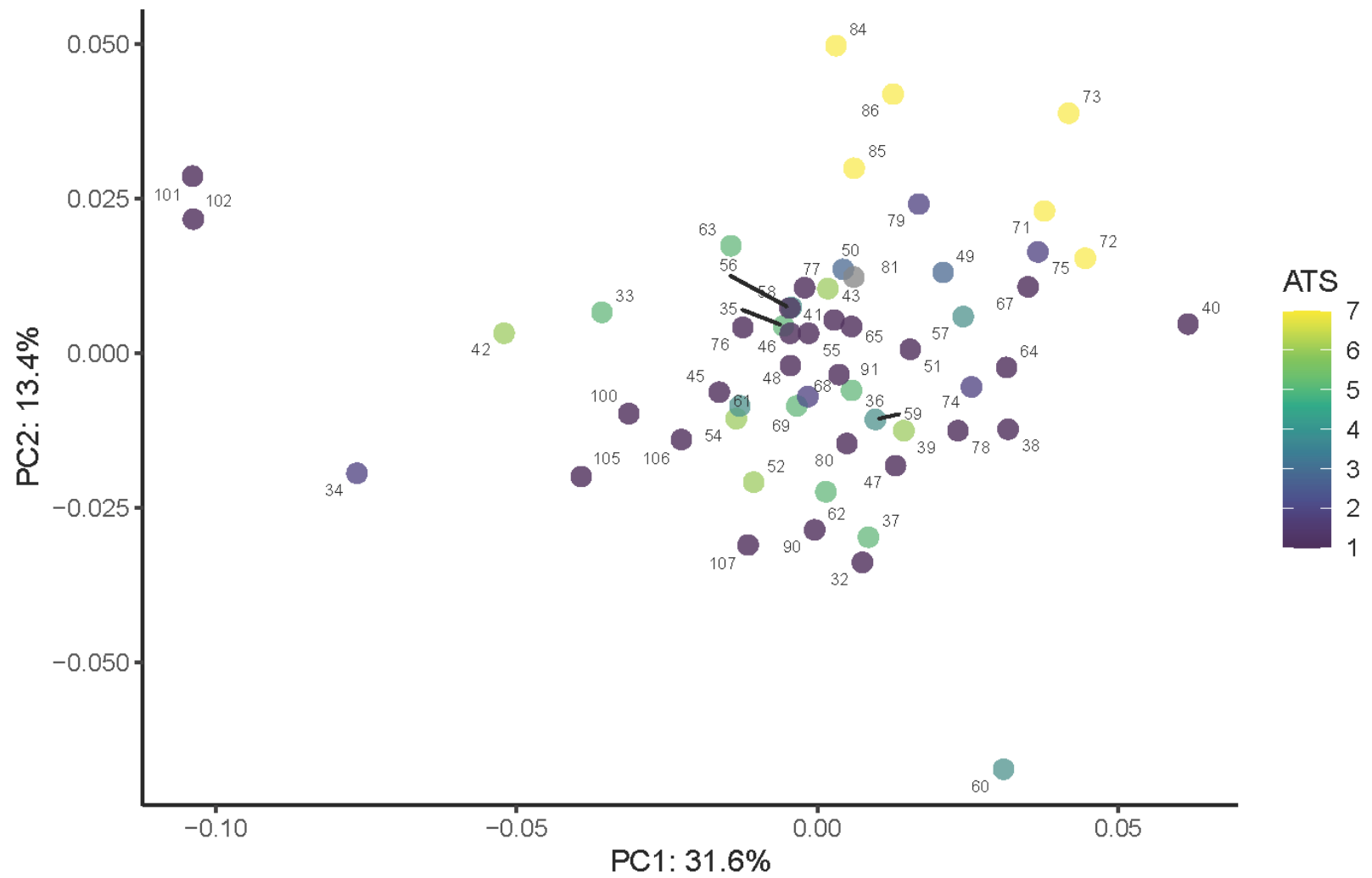
Supplemental Figure 55. PCA of the quadrat dataset conducted on the coralsnake subset, colored by ATS. Numbering corresponds with Table 2.1.



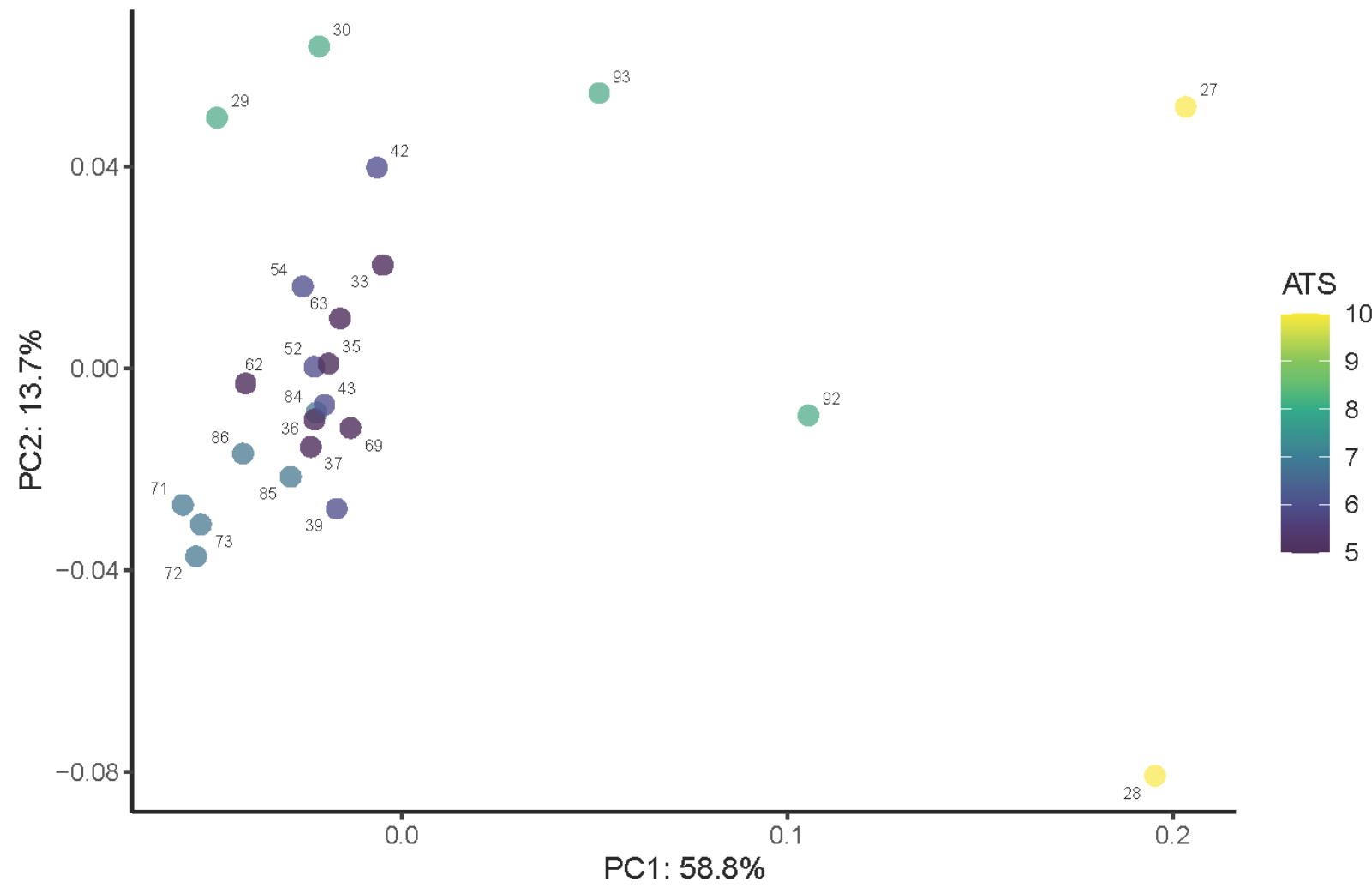
Supplemental Figure 56. PCA of the quadrat dataset conducted on the semi-aquatic and aquatic subset (>5 ATS), colored by ATS. Numbering corresponds with Table 2.1.



Supplemental Figure 57. PCA of the jaw utilizing all specimens, colored by ATS. Numbering corresponds with Table 2.1.

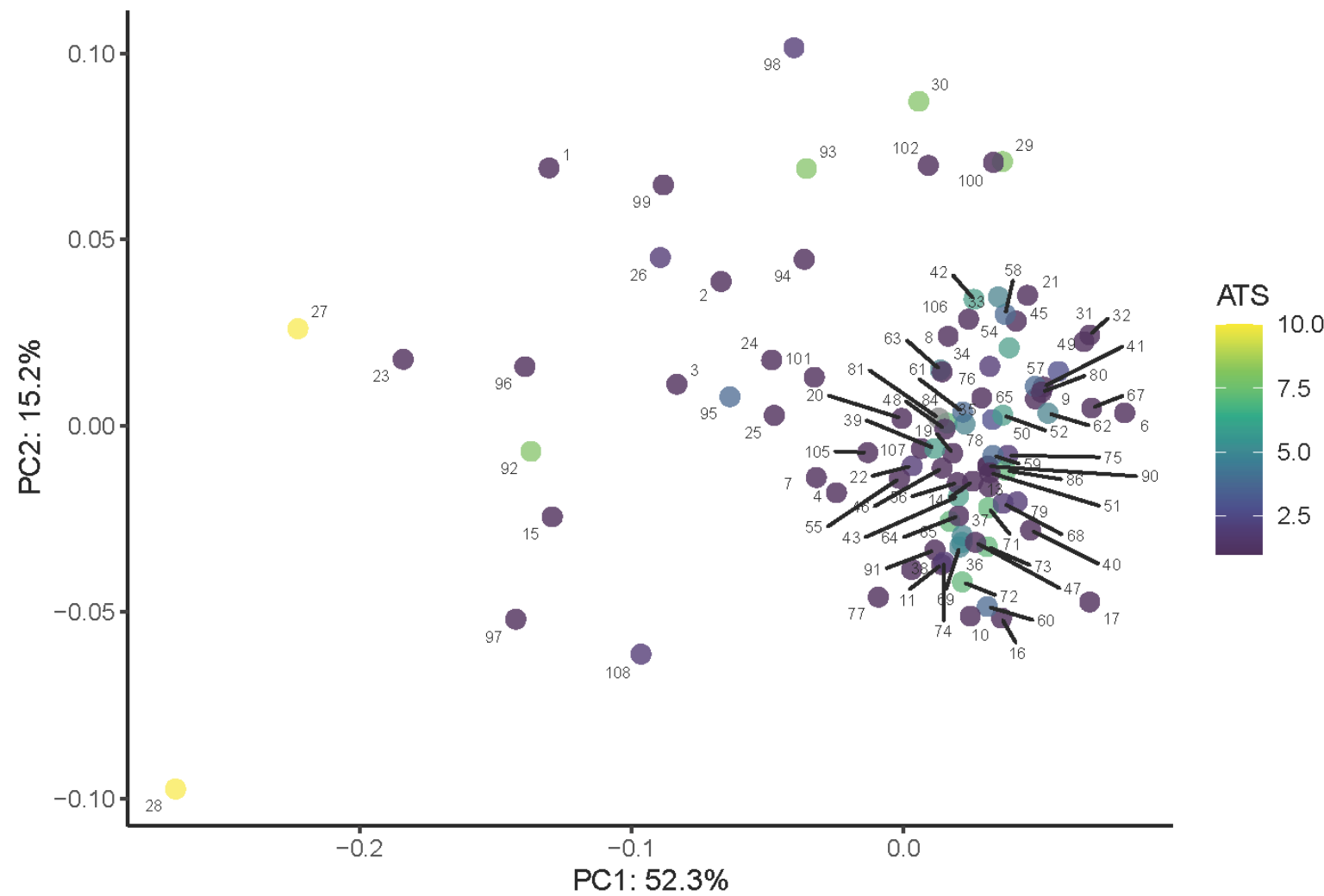


Supplemental Figure 58. PCA of the jaw conducted on the coralsnake subset, colored by ATS. Numbering corresponds with Table 2.1.

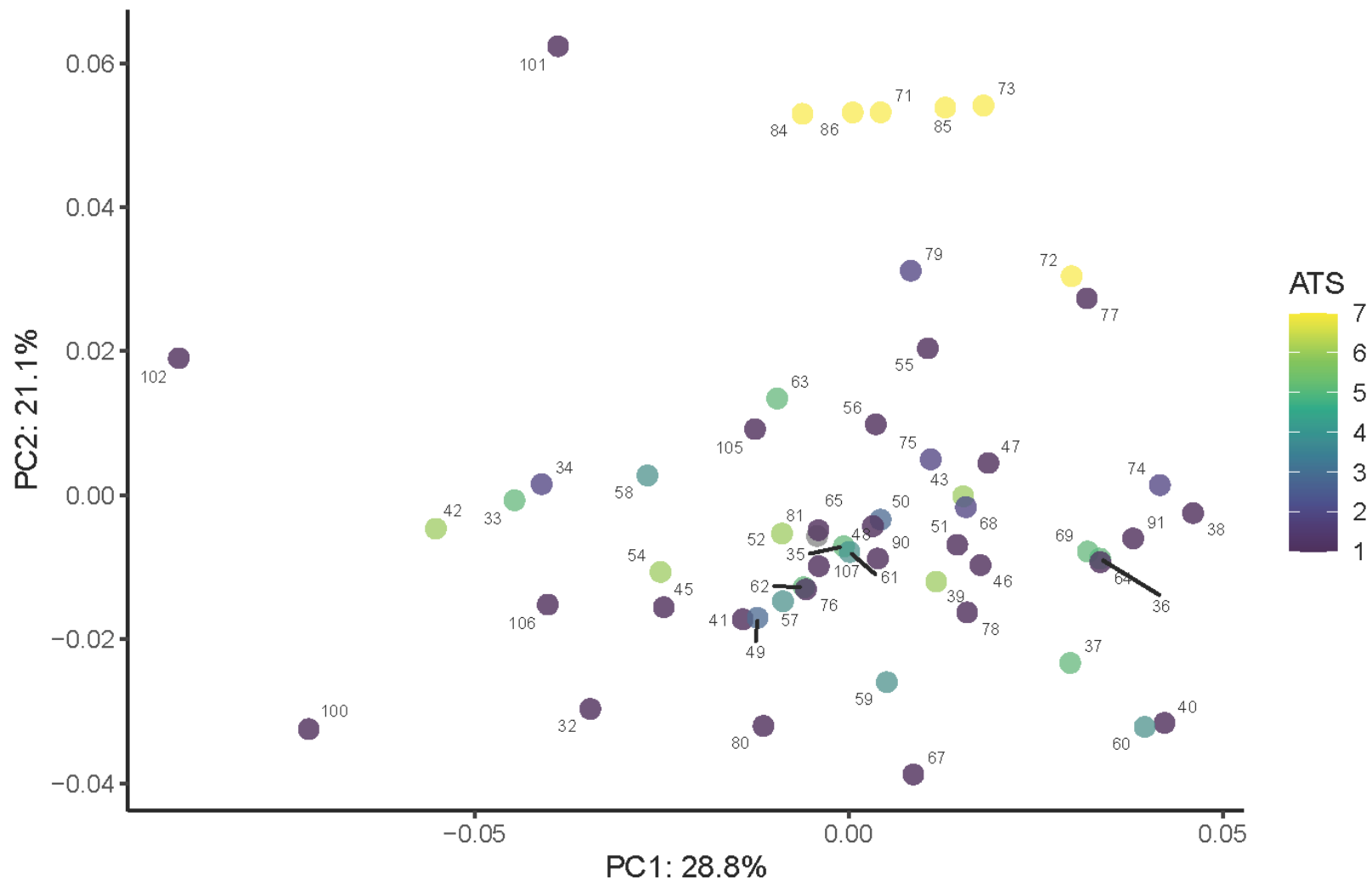


Supplemental Figure 59. PCA of the jaw conducted on the semi-aquatic and aquatic subset (>5 ATS), colored by ATS.

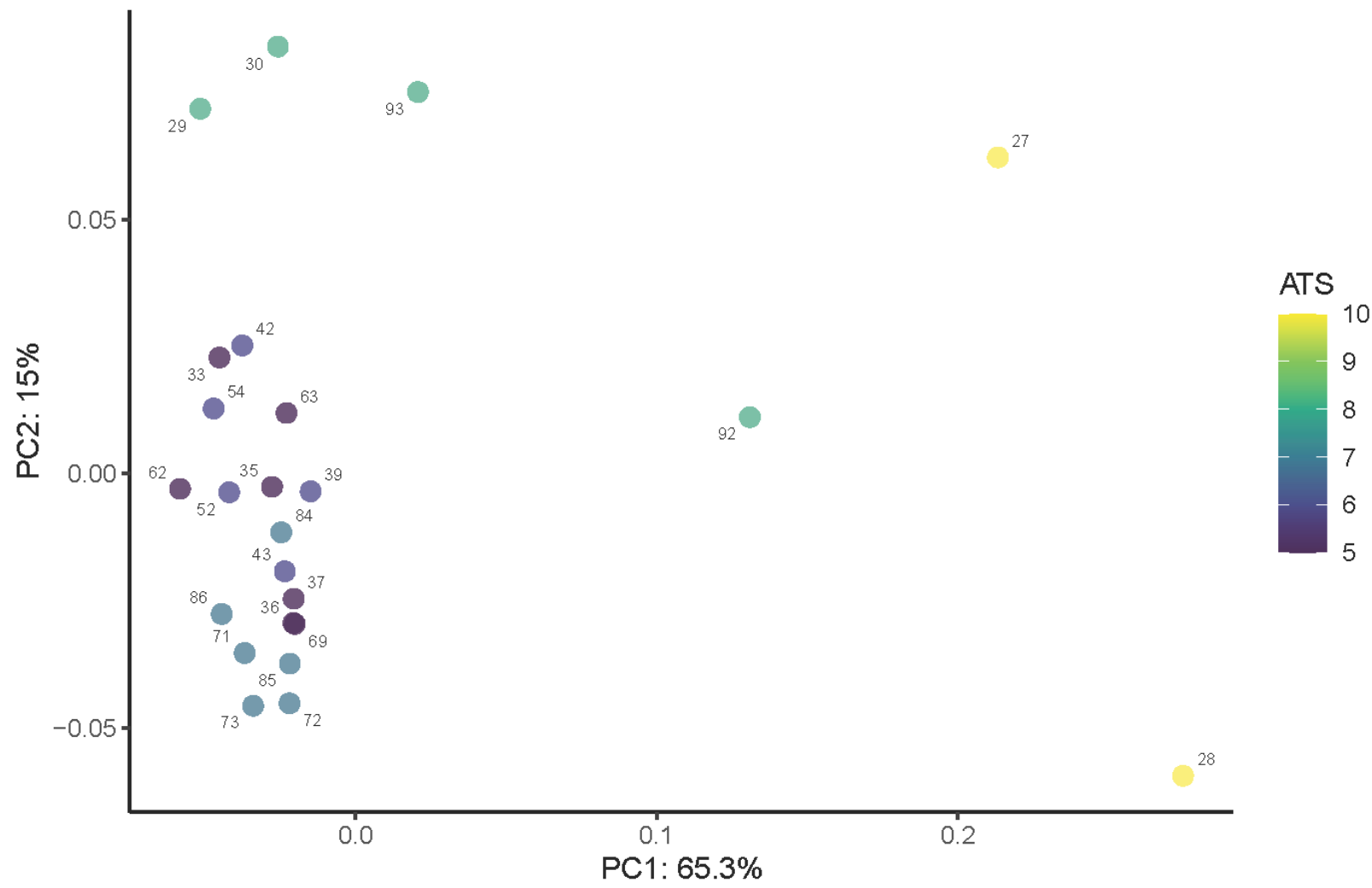
Numbering corresponds with Table 2.1.



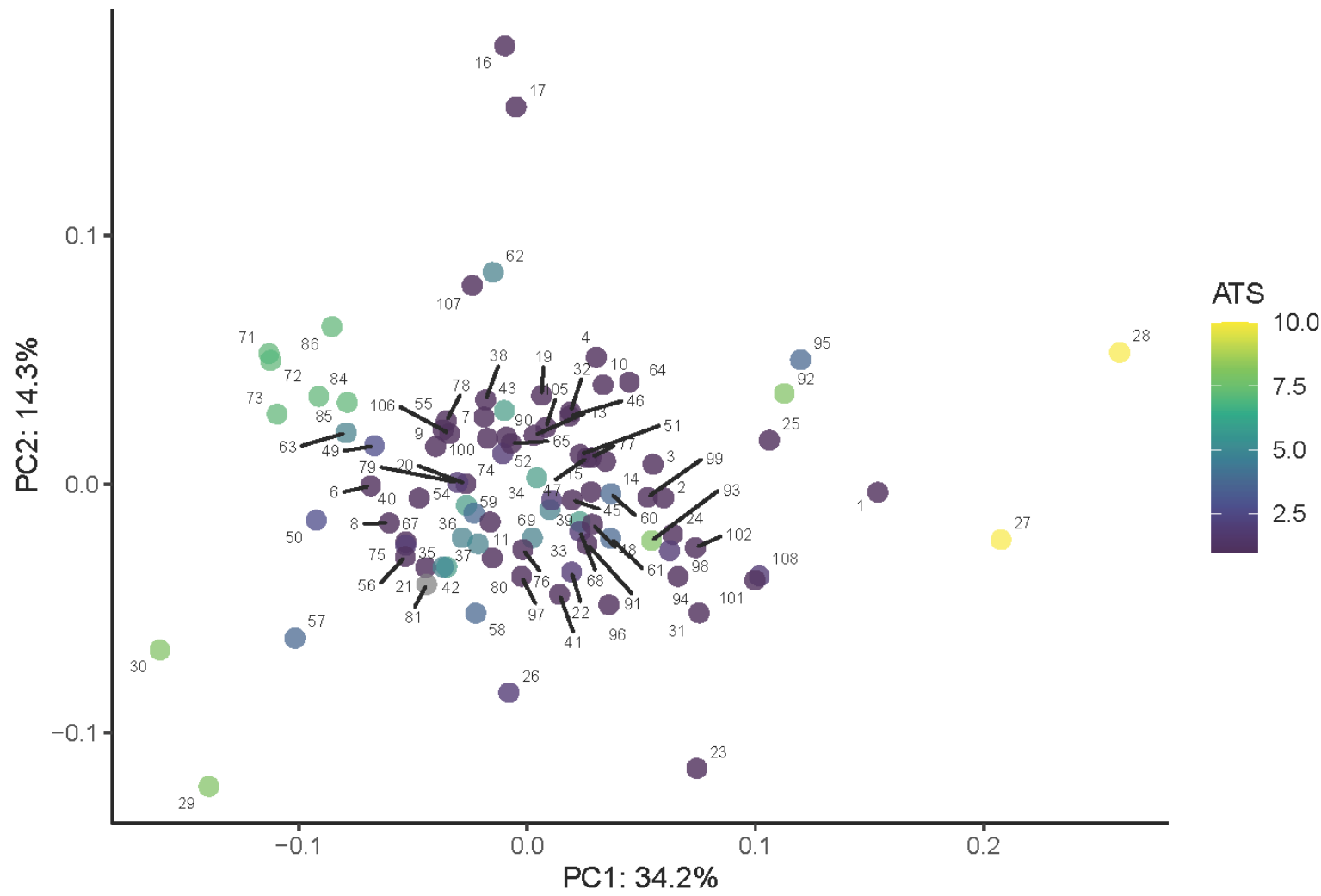
Supplemental Figure 60. PCA of the compound module utilizing all specimens, colored by ATS. Numbering corresponds with Table 2.1.



Supplemental Figure 61. PCA of the compound module conducted on the coralsnake subset, colored by ATS. Numbering corresponds with Table 2.1.

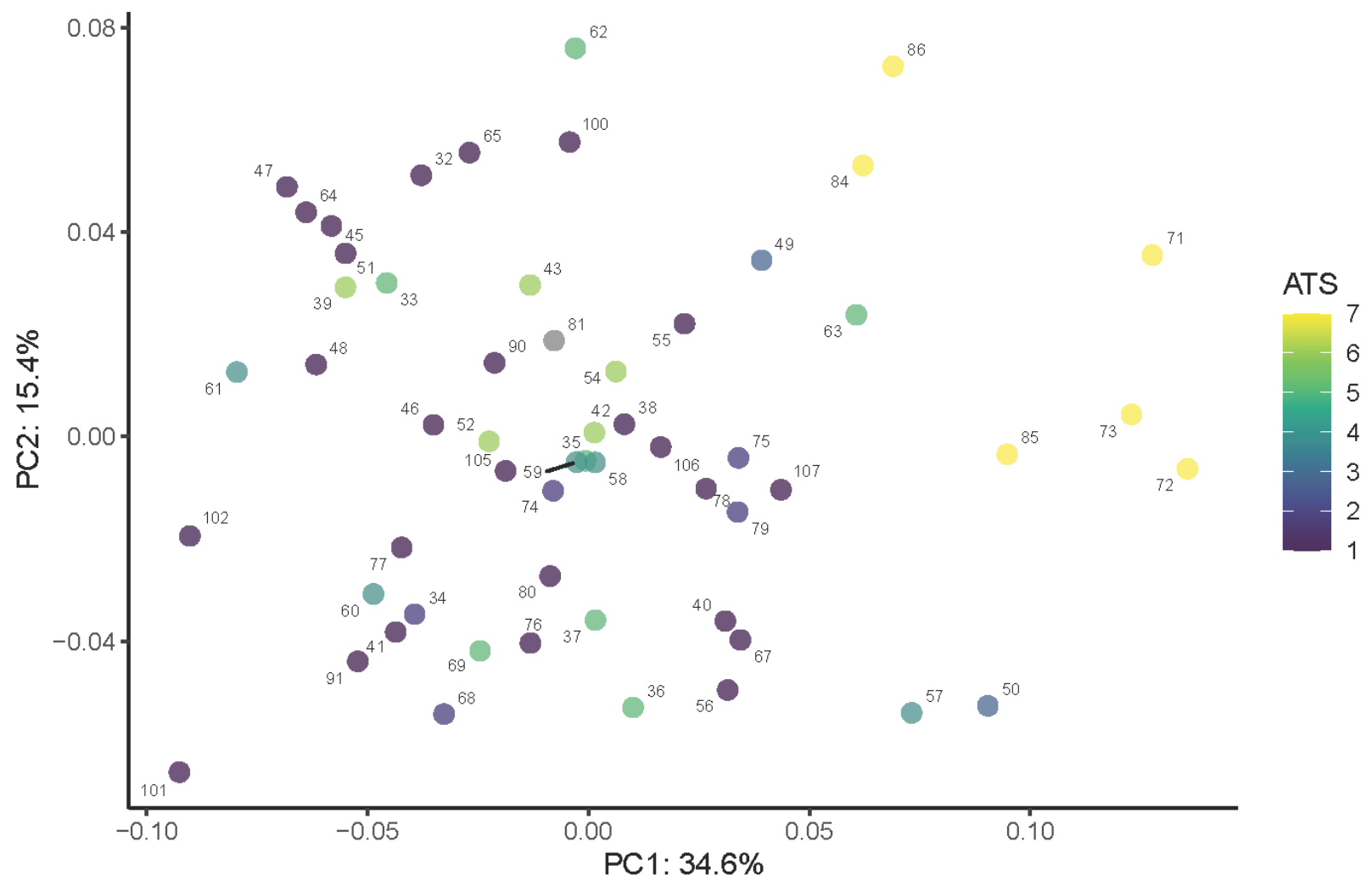


Supplemental Figure 62. PCA of the compound module conducted on the semi-aquatic and aquatic subset (>5 ATS), colored by ATS. Numbering corresponds with Table 2.1.

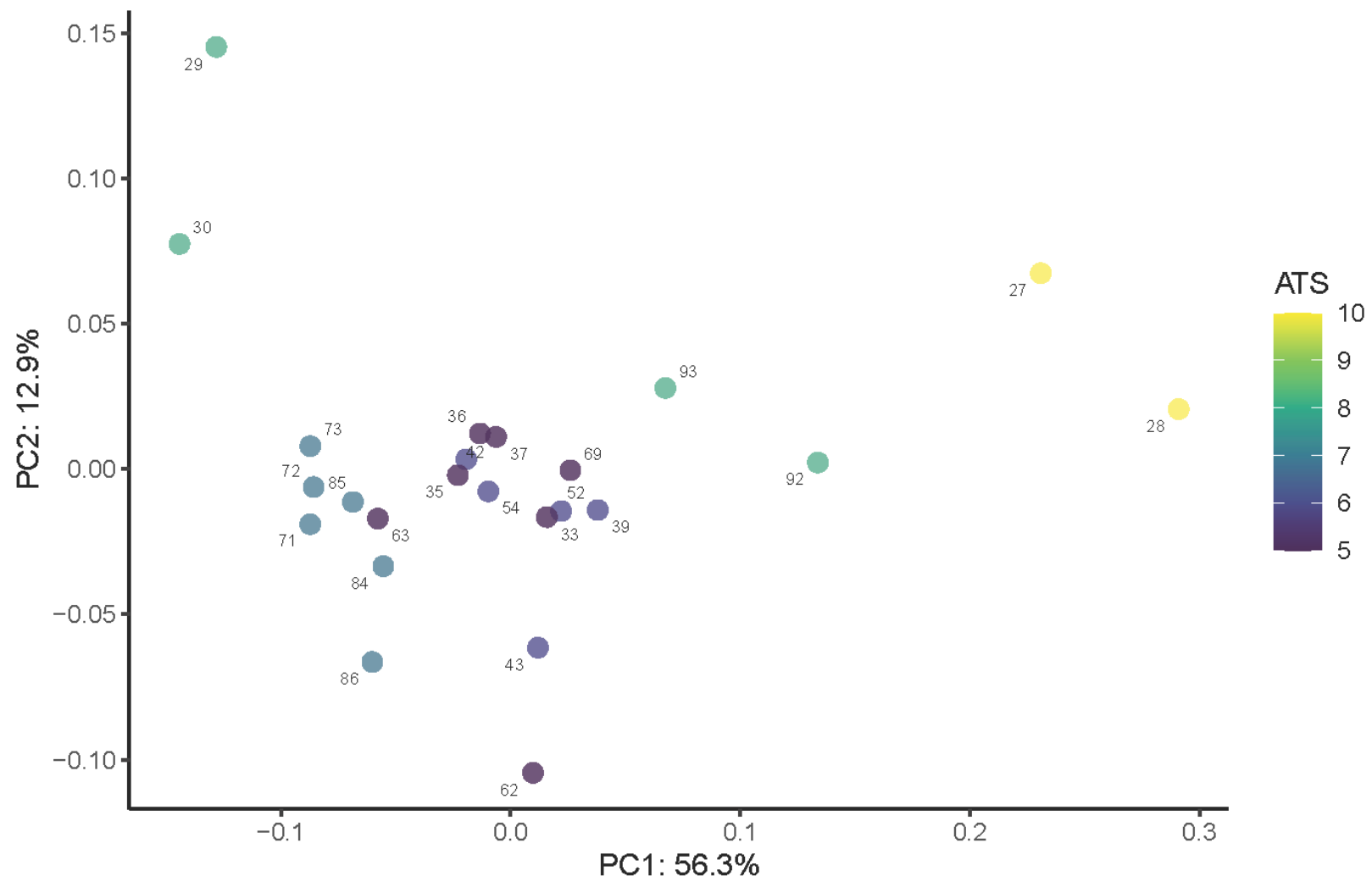


Supplemental Figure 63. PCA of the dentary, angular, and splenial module utilizing all specimens, colored by ATS.

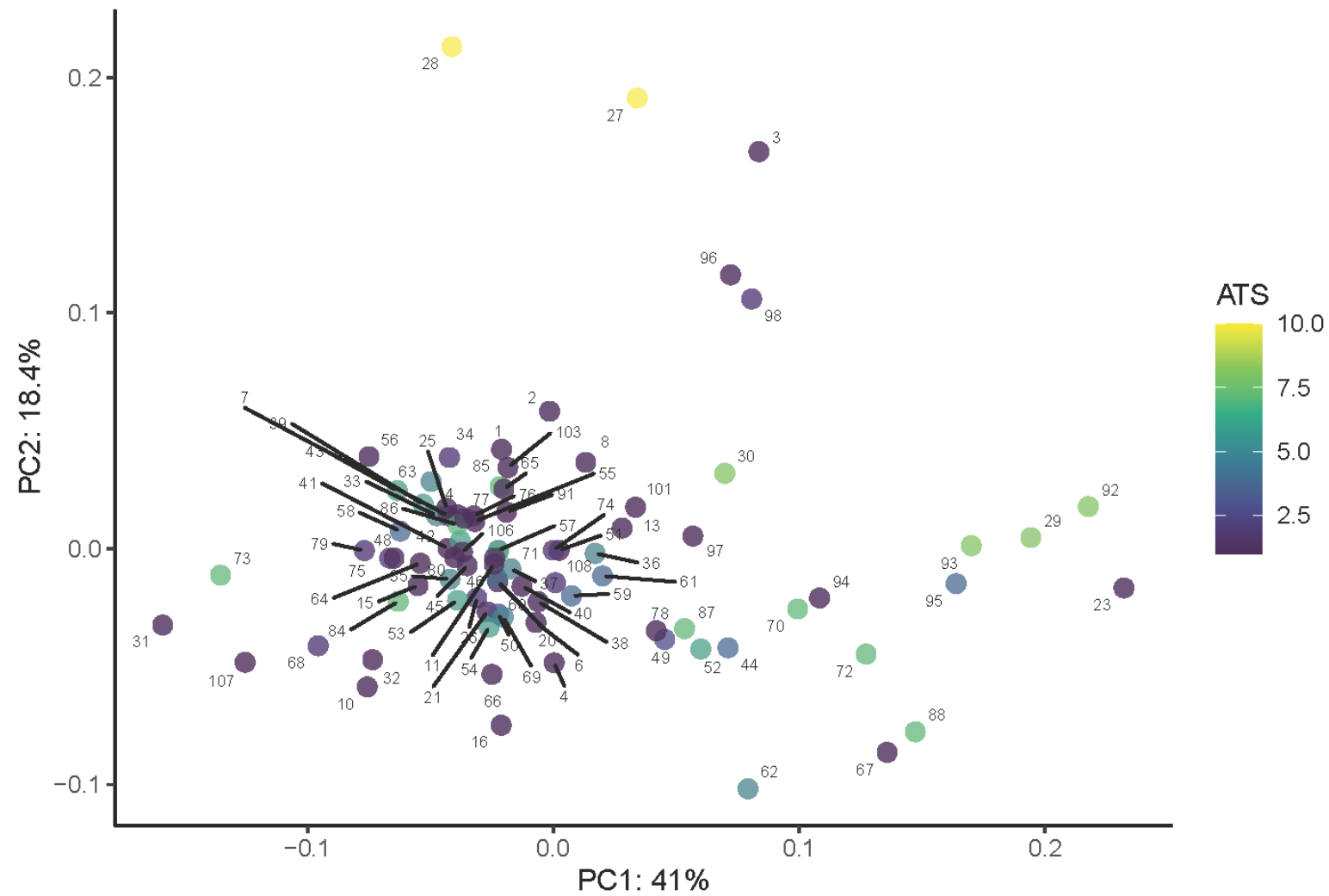
Numbering corresponds with Table 2.1.



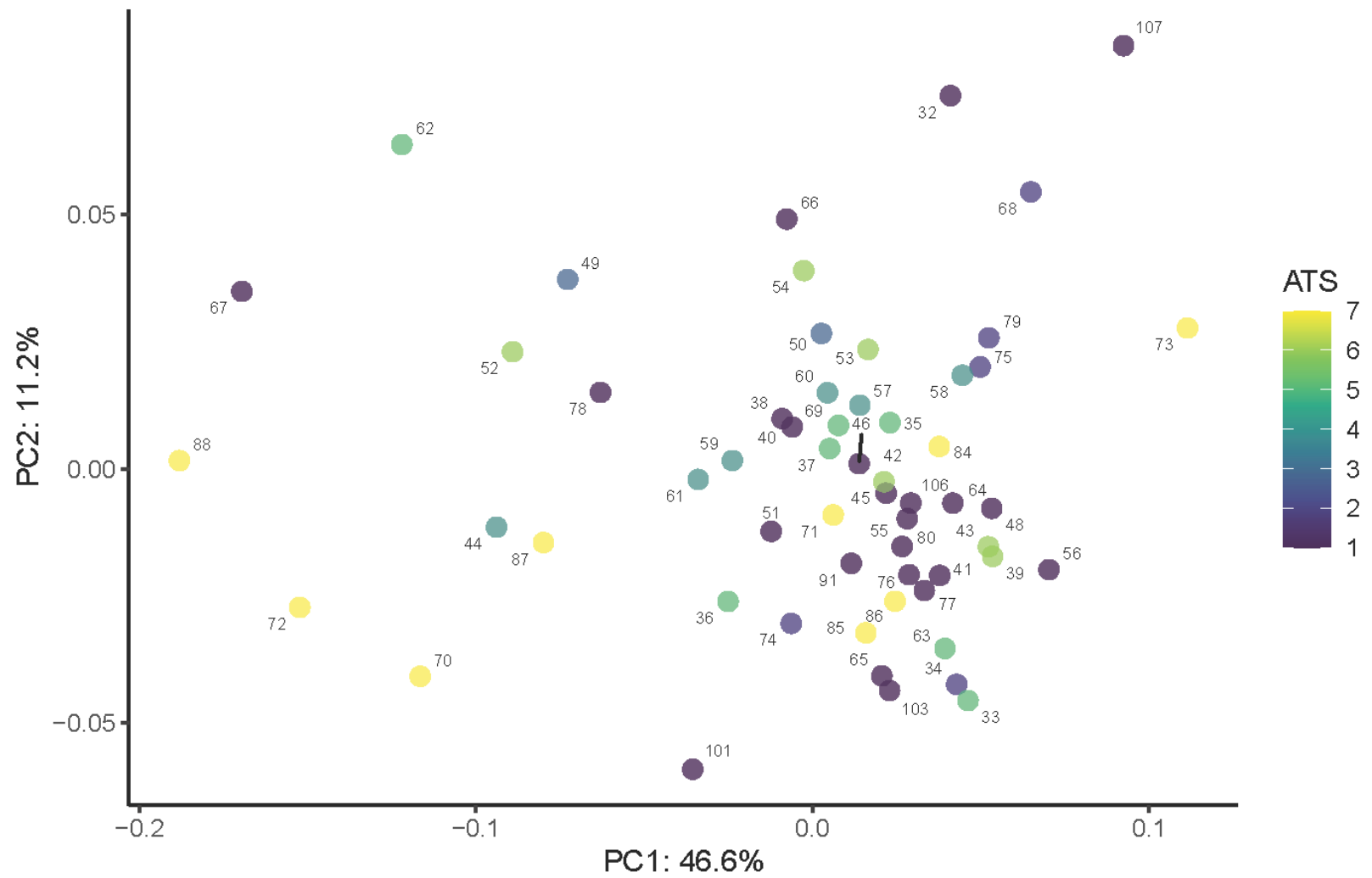
Supplemental Figure 64. PCA of the dentary, angular, and splenial module conducted on the coralsnake subset, colored by ATS. Numbering corresponds with Table 2.1.



Supplemental Figure 65. PCA of the dentary, angular, and splenial module conducted on the semi-aquatic and aquatic subset (>5 ATS), colored by ATS. Numbering corresponds with Table 2.1.

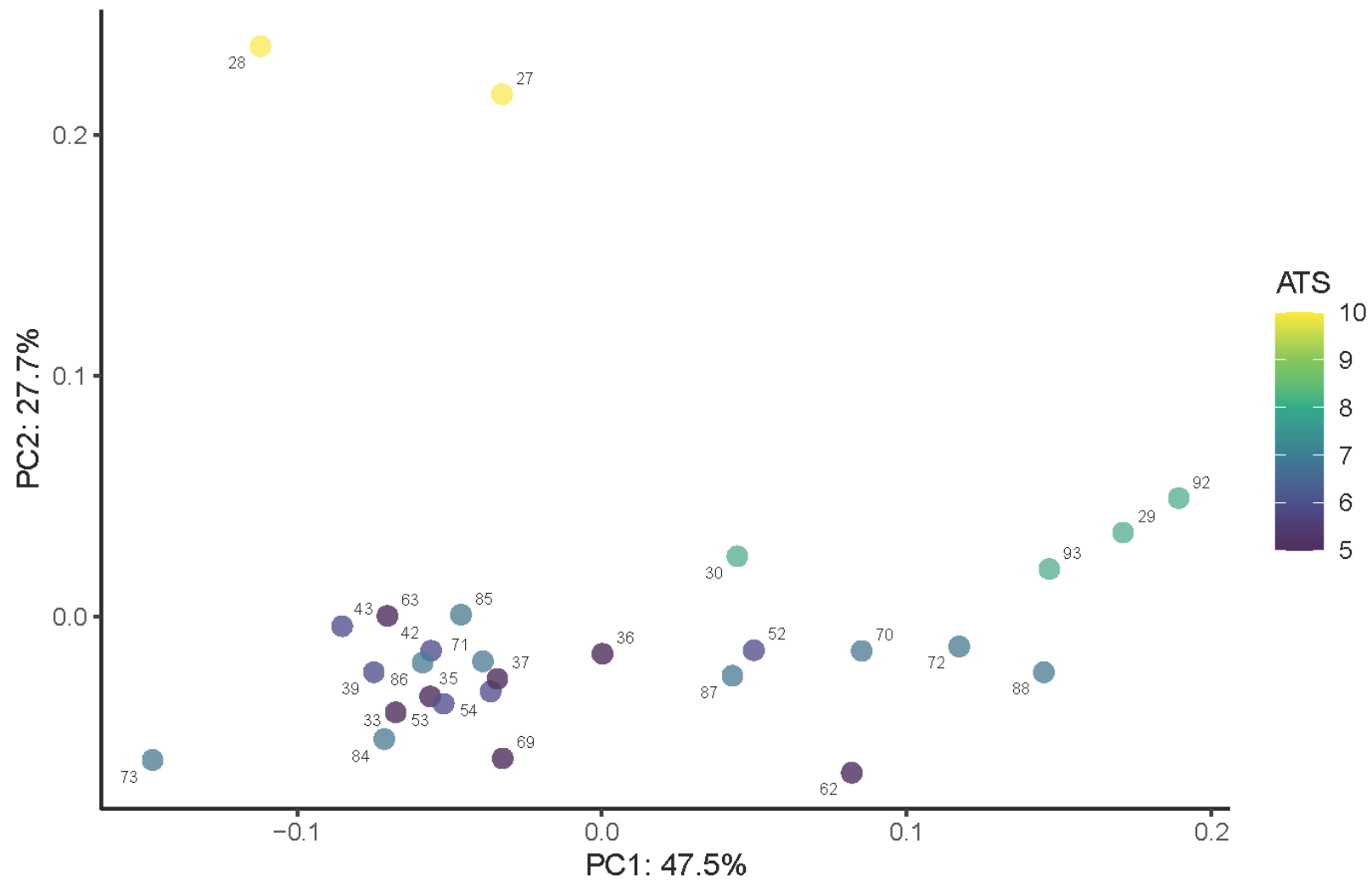


Supplemental Figure 66. PCA of the midbody vertebra dataset, utilizing all specimens, colored by ATS. Numbering corresponds with Table 2.1.

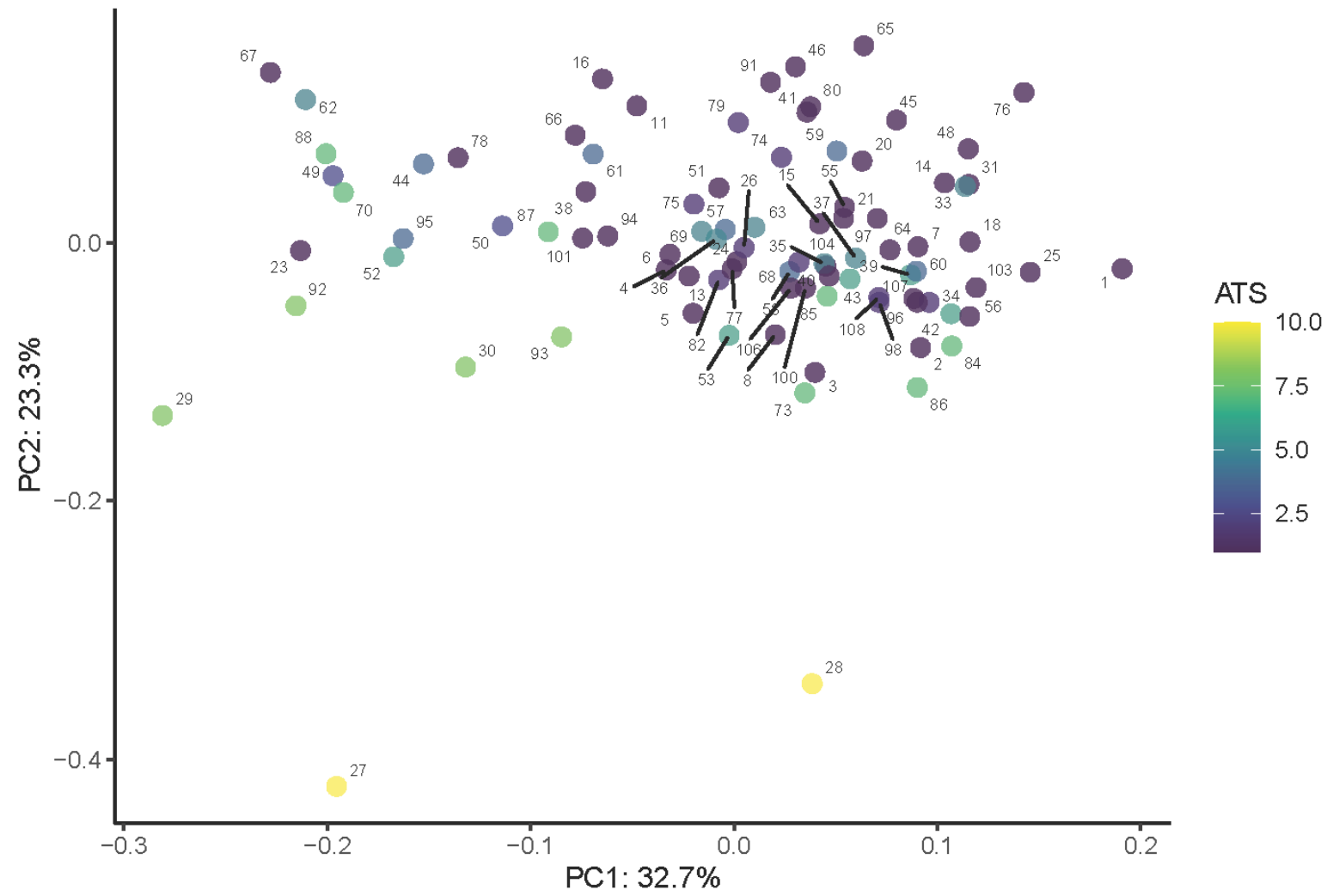


Supplemental Figure 67. PCA of the midbody vertebra dataset conducted on the coralsnake subset, colored by ATS.

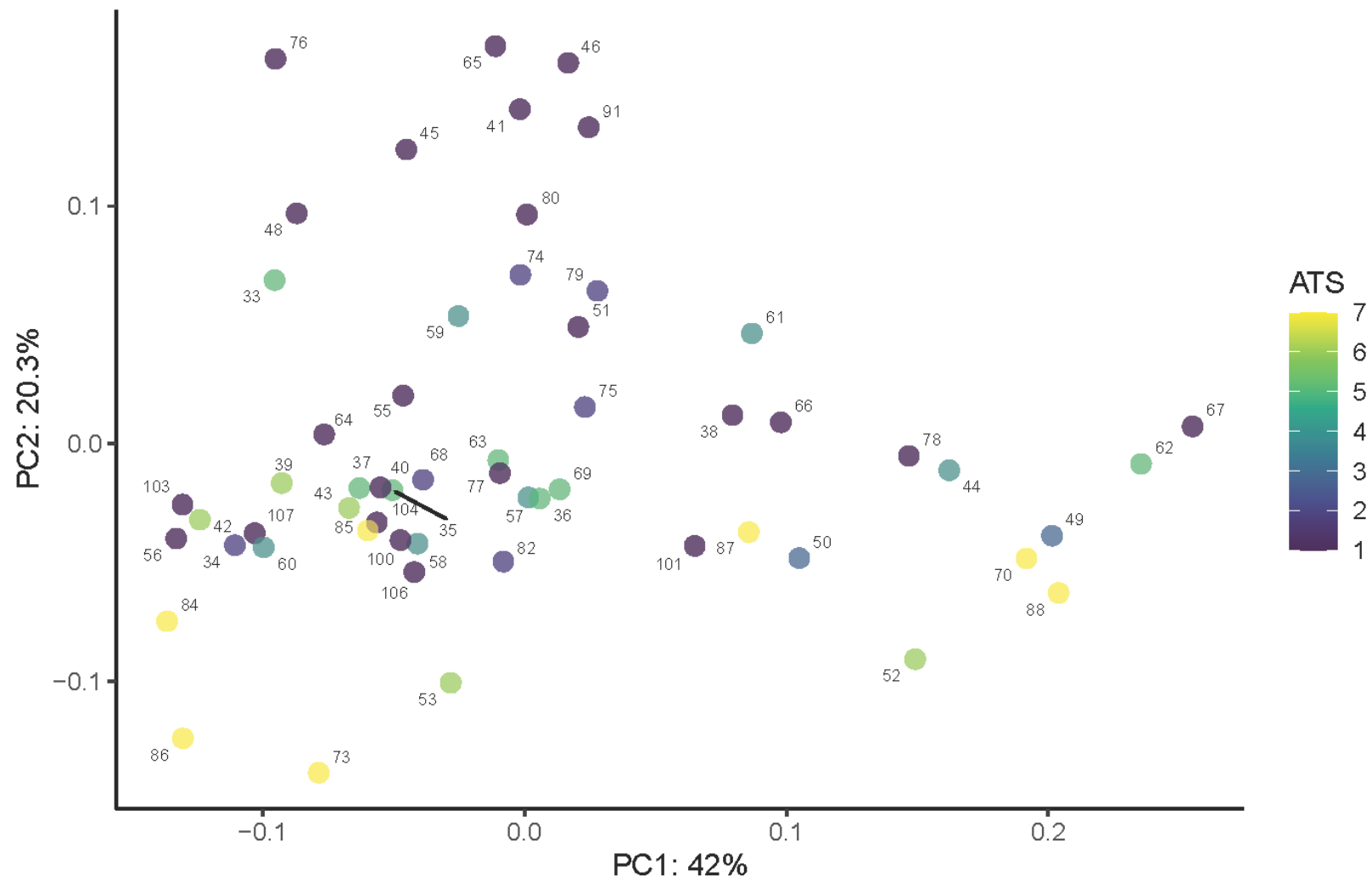
Numbering corresponds with Table 2.1.



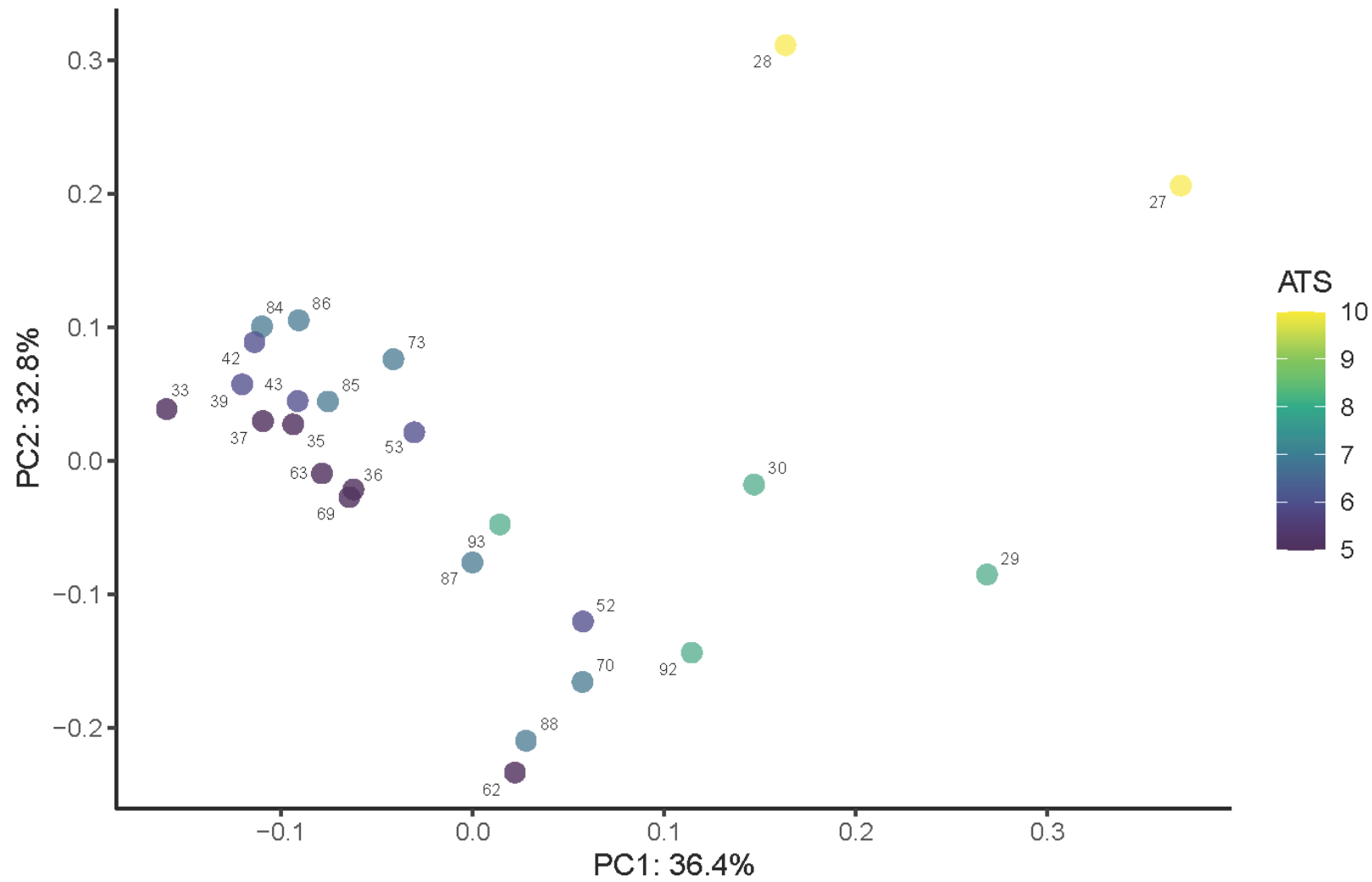
Supplemental Figure 68. PCA of the midbody vertebra dataset conducted on the semi-aquatic and aquatic subset (>5 ATS), colored by ATS. Numbering corresponds with Table 2.1.



Supplemental Figure 69. PCA of the caudal vertebra dataset, utilizing all specimens, colored by ATS. Numbering corresponds with Table 2.1.



Supplemental Figure 70. PCA of the caudal vertebra dataset conducted on the coralsnake subset, colored by ATS. Numbering corresponds with Table 2.1.



Supplemental Figure 71. PCA of the caudal vertebra dataset conducted on the semi-aquatic and aquatic subset (>5 ATS), colored by ATS. Numbering corresponds with Table 2.1.

Supplemental Tables

Supplemental Table 1. GenBank accession numbers of specimens used in phylogenetic tree creation.

Accession #	Species	Tag/identifier			
NC15812.1	<i>Python molurus molurus</i>		KC014504.1	Hydrophis obscurus	ZMUCR661171
DQ305477.1	<i>Daboia russellii</i>	CAS-205253	JX002985.1	Hydrophis mcdowellii	ABTC101326
DQ486323.1	<i>Prosymna ruspolii</i>	CMRK-316	KC014515.1	Leioselasma spiralis	MZBOPhi3896
FJ404389.1	<i>Prosymna janii</i>		JQ217216.1	Hydrophis atriceps	MZBOPhi4138
FJ404350.1	<i>Buhoma procterae</i>		KC014490.1	Hydrophis fasciatus	MZBOPhi3958
NC7398.1	<i>Boa constrictor</i>		KC014523.1	Kerilia jerdonii	ZMUCR661329
FJ404383.1	<i>Psammodynastes sp.</i>	NNV-2008	KC014472.1	Hydrophis belcheri	CM1677
FJ606538.1	<i>Laticauda laticaudata</i>		JQ217217.1	Hydrophis coggeri	MZBOPhi4228
FJ606530.1	<i>Laticauda laticaudata</i>		FJ593213.1	Hydrophis cyanocinctus	FMNH249391
FJ593191.1	<i>Laticauda laticaudata</i>	AM-EBU13932	KC014513.1	Hydrophis parviceps	ZMUCR661279
FJ606504.1	<i>Laticauda saintgironsi</i>		FJ593226.1	Hydrophis pacificus	QMJ83613
FJ593190.1	<i>Laticauda frontalis</i>	AM-EBU13918	JQ217213.1	Hydrophis donaldi	SAMAR65216
AY058977.1	<i>Laticauda colubrina</i>	CAS-HERP-220643	KC014511.1	Hydrophis pachycercos	ZMUCR661230
EU546998.1	<i>Laticauda colubrina</i>		KC014502.1	Disteira major	WAM154749
FJ606516.1	<i>Laticauda guineai</i>		FJ593208.1	Disteira kingii	QMJ80500
GQ397209.1	<i>Demansia psammophis</i>	NR-3389	JQ217209.1	Hydrophis peronii	MZBOPhi4257
EU547002.1	<i>Demansia papuensis</i>		KC014496.1	Hydrophis lamberti	MZBOPhi4240
AY058973.1	<i>Demansia vestigiata</i>		FJ593222.1	Hydrophis ornatus	QMJ82080
EU547001.1	<i>Toxicocalamus preussi</i>		KC014507.1	Hydrophis ocellatus	ABTC55606
GQ397211.1	<i>Toxicocalamus loriae</i>	FK-7523	JQ217218.1	Hydrophis caerulescens	MZBOPhi4145
AY340173.1	<i>Pseudechis papuanus</i>		FJ593212.1	Hydrophis brookii	FMNH252511
AJ830284.1	<i>Pseudechis guttatus</i>		FJ593205.1	Astrotia stokesii	QMJ83580
AJ830281.1	<i>Pseudechis colletti</i>		JX002986.1	Praescutata viperina	MZBOPhi4065
DQ098433.1	<i>Pseudechis australis</i>	ABTC-756	JX987173.1	Hydrophis zweifeli	SAMAR67201
AY340180.1	<i>Pseudechis butleri</i>		FJ593233.1	Pelamis platurus	NR8918
EU547009.1	<i>Furina ornata</i>		FJ593234.1	Pelamis platurus	NR8922
EU547008.1	<i>Furina diadema</i>		FJ593216.1	Hydrophis elegans	
EU546999.1	<i>Aspidomorphus muelleri</i>		FJ593232.1	Lapemis curtus	QMJ82553
GQ397204.1	<i>Aspidomorphus schlegeli</i>	FK-11616	FJ593218.1	Hydrophis lapemoides	FMNH249584
GQ397205.1	<i>Aspidomorphus lineaticollis</i>	FK-6220	FJ593201.1	Parahydrophis mertoni	NTM13607, ABTC28239
EU547000.1	<i>Micropechis ikaheka</i>		FJ593198.1	Ephalophis greyae	
EU547026.1	<i>Hemiaspis signata</i>		KC014494.1	Microcephalophis gracilis	MZBOPhi4169 NTM16471, ABTC28875
FJ593193.1	<i>Hemiaspis damelii</i>		FJ593199.1	Hydrelaps darwiniensis	
EU547038.1	<i>Emydocephalus annulatus</i>		EF210832.1	Oxyuranus scutellatus	
JX423417.1	<i>Aipysurus mosiacus</i>	BGF04498	DQ098438.1	Oxyuranus scutellatus	AMS-R119562
EF506636.1	<i>Aipysurus eydouxi</i>		MT346947.1	Oxyuranus scutellatus	
EF506634.1	<i>Aipysurus fuscus</i>		EU547005.1	Oxyuranus microlepidotus	
EF506658.1	<i>Aipysurus laevis</i>		EF210821.1	Oxyuranus temporalis	
EF506655.1	<i>Aipysurus laevis</i>		DQ098490.1	Pseudonaja modesta	SAMA-R35874
FJ593194.1	<i>Aipysurus apraefrontalis</i>	QMJ80569	DQ098470.1	Pseudonaja guttata	ABTC-32082
EF506633.1	<i>Aipysurus duboisii</i>		DQ098488.1	Pseudonaja ingrami	
EF210842.1	<i>Vermicella intermedia</i>				

Accession #	Species	Tag/identifier				
DQ098508.1	Pseudonaja nuchalis	BT23	KX130761.1	Calliophis intestinalis	MZB-6108	
DQ098644.1	Pseudonaja textilis	SAMA-R56770	KX130760.1	Calliophis intestinalis	PSGV89	
DQ098465.1	Pseudonaja affinis	WAM-R121141	LC543964.1	Calliophis intestinalis	KU-311415	
DQ098476.1	Pseudonaja inframacula	SAMA-R24757	KX130759.1	Calliophis intestinalis	KUHE-53910	
AY340168.1	Acanthophis pyrrhus		FJ404333.1	Atractaspis bibronii	KU-314913	
AY340169.1	Acanthophis wellsei		MK621531.1	Atractaspis duerdenii	MBUR-229	
AY340158.1	Acanthophis rugosus		JQ282155.1	Calliophis castoe		
AY340163.1	Acanthophis antarcticus		JQ282156.1	Calliophis nigrescens		
AY340163.1	Acanthophis antarcticus		KC347502.1	khandallensis		
AY340164.1	Acanthophis praelongus		KX130762.1	Calliophis melanurus		
EU547011.1	Brachyurophis semifasciata		AY058975.1	Calliophis melanurus	BNHSn03	
EU547010.1	Brachyurophis australis		JF357928.1	Elapsoidea nigra	LSUMZ-56273	
EU547013.1	Neelaps bimaculatus		AJ830250.1	Elapsoidea semiannulata		
EU547015.1	Simoselaps bertholdi		EU579523.1	Bungarus slowinskii		
EU547014.1	Simoselaps anomalus		KX130763.1	Bungarus fasciatus	MZB.Ophi.3576	
AJ830256.1	Pseudechis porphyriacus		KC347501.1	Bungarus ceylonicus		
EF210841.1	Neelaps calonotus		AJ830220.1	Bungarus caeruleus		
EU547007.1	Cacophis squamulosus		AJ830242.1	Bungarus sindanus		
EU547016.1	Suta fasciata		AJ830241.1	Bungarus niger		
EU547018.1	Suta suta		NC11392.1	Bungarus multicinctus		
EU547017.1	Suta spectabilis		AJ830228.1	Bungarus candidus		
EU547019.1	Suta monachus		AJ830239.1	Bungarus candidus		
EU547022.1	Rhinoplocephalus nigrescens		EF137408.1	Micruroides euryxanthus		
EU547020.1	Rhinoplocephalus bicolor		AY058969.1	Aspidelaps scutatus	LSUMZ-56251	
GU062884.1	Drysdalia rhodogaster	EBU39042	KX130764.1	Hemibungarus calligaster	KU-307474	
EU547028.1	Drysdalia mastersii		EF137403.1	Calliophis calligaster		
GU062882.1	Drysdalia coronoides		AY058971.1	Sinomicrurus japonicus	CAS-HERP-204980	
AY058972.1	Elapognathus coronata	SAM-R22966	AJ830251.1	Bungarus flaviceps		
EU547023.1	Denisonia devisi		AJ830219.1	Bungarus flaviceps		
EU547024.1	Echiopsis curta		EF137404.1	Leptomicrurus narduccii		
EU547029.1	Austrelaps labialis		KU754446.1	Micrurus laticollaris	M33	
EU547030.1	Austrelaps superbus		KX660567.1	Micrurus allenii		
EU547033.1	Tropidechis carinatus		KX660566.1	Micrurus allenii		
EU547034.1	Notechis ater		KU754449.1	Micrurus elegans	M22	
EU547031.1	Hoplocephalus bitorquatus		MG947663.1	Micrurus ephippifer		
EU547032.1	Echiopsis atriceps		AF228424.1	Micrurus corallinus		
FJ516687.1	Hoplocephalus bungaroides	NMV-AUS-Hb161	MK534175.1	Micrurus circinalis		
FJ404339.1	Homoroselaps lacteus	PEM-R17097	MK534170.1	Micrurus circinalis		
KM519694.1	Boaedon radfordi	UTEP-20995	MK534171.1	Micrurus circinalis		
HQ207158.1	Mchelya capensis		MK534172.1	Micrurus circinalis		
HQ207185.1	Lamprophis aurora		MK534173.1	Micrurus circinalis		
MG003042.1	Psammophis aegyptius		MK534174.1	Micrurus circinalis		
AF420196.1	Thamnophis sirtalis infernalis		JF308713.1	Micrurus psyches		
KX130755.1	Calliophis sp.	US-2016a	KP998035.1	Micrurus dumerilii transandinus	MECN-2881	
KX130756.1	Calliophis bivirgata	UTA-R60740	KP998036.1	Micrurus dumerilii transandinus	MECN-3862	
AY058979.1	Calliophis bivirgata	LSUMZ-37496	KP998029.1	Micrurus dumerilii transandinus	UTA-R55951	
KX130758.1	Calliophis bivirgata	FMNH-267967	KP998028.1	Micrurus ornatissimus	QCAZ-6094	
KX130757.1	Calliophis bivirgata	FMNH-273611	KP998033.1	Micrurus ornatissimus	FHGO-7137	

Accession #	Species	Tag/identifier	JF308708.1	Micrurus spixii obscurus	
KP998034.1	<i>Micrurus ornatissimus</i>	FHGO-7314	AF228443.1	<i>Micrurus spixii</i>	
JF308715.1	<i>Micrurus corallinus</i>		AF228442.1	<i>Micrurus hemprichii</i>	
JF308714.1	<i>Micrurus albicinctus</i>		JF308704.1	<i>Micrurus hemprichii ortoni</i>	
KP998030.1	<i>Micrurus bocourti</i>	UTA-R60726	AF228444.1	<i>Micrurus surinamensis</i>	
KP998031.1	<i>Micrurus bocourti</i>	MECN-2608	JF308709.1	<i>Micrurus surinamensis</i>	
KP998038.1	<i>Micrurus bocourti</i>	CORBIDI-4502	EF137407.1	<i>Micrurus surinamensis</i>	
KP998027.1	<i>Micrurus mertensi</i>	QCAZ-6692	JF308707.1	<i>Micrurus lemniscatus lemniscatus</i>	
KP998037.1	<i>Micrurus mertensi</i>	CORBIDI-14775	MK534176.1	<i>Micrurus diutius</i>	
KP998032.1	<i>Micrurus mertensi</i>	MHNC-11515	MK534177.1	<i>Micrurus diutius</i>	
JF308710.1	<i>Micrurus diastema diastema</i>		MK534178.1	<i>Micrurus diutius</i>	
MG947665.1	<i>Micrurus ephippifer</i>		AF228439.1	<i>Micrurus lemniscatus</i>	clone2
JF308712.1	<i>Micrurus mosquitensis</i>		MW662060.1	<i>Micrurus filiformis</i>	ICN11380
KU754421.1	<i>Micrurus nigrocinctus</i>	M13	JF308706.1	<i>Micrurus lemniscatus diutius</i>	
KU754457.1	<i>Micrurus nigrocinctus</i>	M28	MK534179.1	<i>Micrurus lemniscatus</i>	
KU754414.1	<i>Micrurus browni</i>	M15	AF228438.1	<i>Micrurus lemniscatus</i>	clone1
MG947648.1	<i>Micrurus diastema</i>		AF228435.1	<i>Micrurus lemniscatus lemniscatus</i>	
KU754434.1	<i>Micrurus diastema</i>	M50	JF308717.1	<i>Micrurus dissoleucus nigrirostris</i>	
MG947667.1	<i>Micrurus diastema</i>		JF308716.1	<i>Micrurus mipartitus decussatus</i>	
MG947657.1	<i>Micrurus diastema</i>		EF137406.1	<i>Micrurus mipartitus</i>	
KU754441.1	<i>Micrurus tener</i>	M230	EF137410.1	<i>Calliophis maclellandi</i>	
KU754401.1	<i>Micrurus tener</i>	M236	AY058974.1	<i>Dendroaspis polylepis</i>	CAS-HERP-220644
KU754402.1	<i>Micrurus tener</i>	M326	JF357927.1	<i>Dendroaspis angusticeps</i>	
JF308711.1	<i>Micrurus tener tener</i>		MT346816.1	<i>Dendroaspis angusticeps</i>	
KU754425.1	<i>Micrurus fulvius</i>	M314	EF137409.1	<i>Calliophis kelloggi</i>	
MG947653.1	<i>Micrurus sp.</i>		EU921899.1	<i>Ophiophagus hannah</i>	
KU754444.1	<i>Micrurus fulvius</i>	M175	AY058984.1	<i>Ophiophagus hannah</i>	CAS-HERP-206601
GU045453.1	<i>Micrurus fulvius</i>		AY058988.1	<i>Walterinnesia aegyptia</i>	
U49298.1	<i>Micrurus fulvius</i>		MT346838.1	<i>Hemachatus haemachatus</i>	
KU754440.1	<i>Micrurus fulvius</i>	M173	MT346952.1	<i>Pseudohaje goldii</i>	
KU754410.1	<i>Micrurus fulvius</i>	M176	MT346951.1	<i>Pseudohaje goldii</i>	
MG947728.1	<i>Micrurus distans</i>		AY058983.1	<i>Naja nivea</i>	
MG947641.1	<i>Micrurus distans</i>		GQ387080.1	<i>Naja senegalensis</i>	
MG947675.1	<i>Micrurus distans</i>		GQ387079.1	<i>Naja arabica</i>	
AF228441.1	<i>Micrurus decoratus</i>		GQ387062.1	<i>Naja haje</i>	
AF228434.1	<i>Micrurus pyrrhocryptus</i>		GQ387089.1	<i>Naja annulifera</i>	
JF308705.1	<i>Micrurus pyrrhocryptus</i>		GQ387085.1	<i>Naja anchietae</i>	
AF228433.1	<i>Micrurus baliocoryphus</i>		AY058985.1	<i>Naja multifasciata</i>	
AF228440.1	<i>Micrurus ibiboboca</i>		KX130765.1	<i>Naja melanoleuca</i>	CAS-207871
AF228437.1	<i>Micrurus lemniscatus carvalhoi</i>	clone2	DQ897689.1	<i>Naja melanoleuca</i>	
AF228436.1	<i>Micrurus lemniscatus carvalhoi</i>	clone1	MT346897.1	<i>Naja christyi</i>	
AF228429.1	<i>Micrurus altirostris</i>	clone1	AY058970.1	<i>Naja annulata</i>	HLMD-RA-1607
AF228430.1	<i>Micrurus altirostris</i>	clone2	MT346896.1	<i>Naja annulata</i>	
AF228432.1	<i>Micrurus altirostris</i>	clone4	MH337375.1	<i>Naja naja</i>	
AF228431.1	<i>Micrurus altirostris</i>	clone3	AY713378.1	<i>Naja naja</i>	
AF228428.1	<i>Micrurus brasiliensis</i>	clone2	DQ897691.1	<i>Naja sputatrix</i>	
AF228427.1	<i>Micrurus brasiliensis</i>	clone1	AY058982.1	<i>Naja kaouthia</i>	CAS-HERP-206602
AF228426.1	<i>Micrurus frontalis</i>	clone2	EU624209.1	<i>Naja kaouthia</i>	
AF228425.1	<i>Micrurus frontalis</i>	clone1	EU921898.1	<i>Naja atra</i>	CIB093931

Accession #	Species	Tag/identifier
DQ343648.1	<i>Naja naja</i>	
GQ359578.1	<i>Naja pallida</i>	
DQ897718.1	<i>Naja nubiae</i>	
GQ359576.1	<i>Naja katensis</i>	
DQ897724.1	<i>Naja mossambica</i>	
AY713377.1	<i>Naja nigricollis</i>	
GQ359575.1	<i>Naja ashei</i>	
DQ897709.1	<i>Naja nigricincta nigricincta</i>	
DQ897709.1	<i>Naja nigricincta nigricincta</i>	